



SECOND  
ANNUAL  
CONFERENCE

# Climate change: scenarios, impacts and policy

Venice  
September 29-30, 2014



#sisclima2014

## Proceedings

in collaborazione con



partners



con il patrocinio di







# PROCEEDINGS

SECOND  
ANNUAL  
CONFERENCE

## **Climate change: scenarios, impacts and policy**

Venice  
September 29-30, 2014

More information on the Italian Society for the Climate Sciences - SISC  
is available on the Internet: <http://www.sisclima.it>

ISBN 978 – 88 – 97666 – 04 – 2

© Società Italiana per le Scienze del Clima  
Venice, Italy - September 2014



# Contents

INTRODUCTION BY ANTONIO NAVARRA	xi
FOREWORD BY CARLO CARRARO AND SIMONA MASINA	xii
SISC AT A GLANCE	xiii
SCIENTIFIC COMMITTEE	xiv
ORGANIZING COMMITTEE	xv
ABOUT THE CONFERENCE	xvi

## MITIGATION POLICIES & STRATEGIES 1

<b>Climate change mitigation strategies</b>	<b>2</b>
Mitigating GHG emissions in subnational contexts: the case of the city of Rio de Janeiro	3
Sharing of Climate Risks across Macro Regions	11
Anthropic Emissions of greenhouse gas (GHG) and reference for mitigation policy of emissions in Mato Grosso (Brazil)	19
CO <sub>2</sub> emissions by a university campus: assessment, uncertainties and reduction strategies	35
<b>Low carbon finance</b>	<b>49</b>
The role of Public-Private Partnerships (PPPs) in scaling up financial flows in the Post-Kyoto Regime	50
The landscape of public Climate Finance in Indonesia	70
Public-Private Partnerships in green Energy Infrastructure Investments	78
The role of public finance in CSP: lessons from the ups and downs of CSP policies in Spain	92
<b>Energy technologies and policies</b>	<b>105</b>
Climate Change Mitigation and Energy Technology Costs: A Multi-model sensitivity analysis	106
Distributional impact of reducing fossil fuel subsidies in Indonesia	107
Banning Non-Conventional Oil Extraction: Would a unilateral move of the EU really work?	108
Oil market and long-term scenarios: a Nash-Cournot approach	109
<b>Air quality and carbon reduction policies</b>	<b>132</b>
Can Nigeria pursue low carbon development?	133
Synergies and Interactions Between Climate Change Policies and Air Pollution Control Strategies — Results of the WITCH Integrated Assessment Mode	154

Design, Process, and Performance Criteria Provide Structure to Climate Policy	166
Mirages in climate policy evaluation: how model assumptions may drive policy costs	176
Selection of carbon budgets under current knowledge of uncertainties	191
<b>Old and new market mechanisms</b>	<b>209</b>
Impacts of tradable emission allowances on investment and economic growth	210
Climate Changes: liability and insurability of risks in various legislative and institutional settings in light of the latest scientific knowledge	226
Community Managed Forest Groups and Preferences for REDD+ Contract Attributes: A choice experiment survey of communities in Nepal	235
Loss & Damage: a critical discourse analysis	254

## **ADVANCES IN CLIMATE SCIENCE** **266**

<b>Climate variability &amp; climate change I</b>	<b>267</b>
A simple explanation for climate variations in the Sahel	268
Projected daily precipitation characteristics change in the early 21st century in Southern Africa	273
Linking South Asian summer monsoon and eastern Mediterranean climate in CMIP5 simulations: performance and 21st century projections	287
A Zonal View of Atmospheric Heat Transport Variability	300
<b>Climate variability &amp; climate change II</b>	<b>312</b>
Turbulence regimes deduced from the analysis of observed and modeled global ocean data	313
Storm classification for Tyrrhenian Sea and wave conditions changes over last thirty years	326
Regional climate simulations with COSMO-CLM over the Mediterranean area	338
Tropical cyclone rainfall changes in response to a warmer climate and increased CO <sub>2</sub>	352
<b>GHG &amp; solar variability: past and future</b>	<b>365</b>
Influence of forcings and variability on recent global temperature behavior: A neural network analysis	366
Impact of greenhouse gases and insolation on the threshold of glacial inception	382
Past and future solar radiation variability and change over Sicily	397
Top down emission estimates of radiatively active F-gases vs bottom up inventories	416
<b>Climate data: management &amp; analysis</b>	<b>423</b>
The contribution of the homogenization in the extreme precipitation events	424
CLIME: analysing climate data in GIS environment	434
The Ophidia framework: toward big data analytics for climate change	448
Levels and particle size distribution of water-soluble organic compounds in the Antarctic particulate matter	454

<b>Data analysis &amp; modelling over Italy</b>	<b>457</b>
Extreme events in a Warmer Climate over Mediterranean Basin with focus over Italy	458
Evaluating the effects of changes in observational sites position and surrounding urbanisation on the historical temperature time series of the City of Trento in the Alps	467
High resolution hindcast simulations over Italy with COSMO-CLM model	487
Carbon flux and climate change on Capo Caccia karst ecosystem (Sardinia, Italy)	509
<b>Poster session</b>	<b>522</b>
Global scale energy budget variations in the outputs of the ERA-20CM experiment	523
Climate Models Performance Optimization through Min-Apps	540
The response of the mean meridional circulation to global warming and its relationship with precipitation	547
Downscaled temperature scenarios for 5 sites in the Basilicata region	557
An uncertainty monster: advances in addressing model uncertainty	570

## **VULNERABILITY, RISK ASSESSMENT AND ADAPTATION TO CLIMATE CHANGE** **581**

<b>Economic value of adaptation strategies</b>	<b>582</b>
Climate change impacts and market driven adaptation: The costs of inaction including market rigidities	583
Adapting natural capital: cost-benefit challenges and indicative net present values	604
The value of protecting Venice from the acqua alta phenomenon under different local sea level rises	623
A Choice Experiment application for valuing adaptation of river services to climate change	639
<b>Risk assessment</b>	<b>640</b>
Developing climate risk and adaptation services in coastal zones: an integrated bottom-up approach applied in the North Adriatic coast	641
Changing meso level response to extreme climate events in Viet Nam	642
Assessing the impacts of climate change on marine water quality through a spatially resolved risk assessment approach: the North Adriatic sea (Italy) as case study	653
<b>Adaptation policies and strategies</b>	<b>654</b>
Do political systems matter? Differences and similarities in institutional settings that support national adaptation strategies across European States	655
A national adaptation strategy to climate change in Italy: can the right stakeholders be engaged?	682
A methodological approach for stakeholder engagement at regional level in Climate Change Adaptation Policies	699

Adapting to Climate Change: Bologna as Resilient City	719
<b>Water Management</b>	<b>727</b>
Experience in water modelling in agriculture considering climate and policy change	728
Water security issue in the Caribbean Windward Islands	745
The Water Abstraction Licence Regime in Italy: a case for reform?	759
<b>Poster session</b>	<b>773</b>
Forest management in water protection areas under climate change	774
An online platform for supporting the analysis of Water Adaptation Measures in the Alps	779
Statistical downscaling method applied for a future climate profile at local level - Bologna case study as resilient city	780
Risk assessment on coastal environments under climate change: Southern Brazil	781

## **IMPACTS & IMPLICATIONS OF CLIMATE CHANGE** **792**

<b>Methods for assessment/quantification of climate change impacts</b>	<b>793</b>
Fire in ice and sediments: looking for early human impacts	794
Could Temperature Affect the Geospeciation of Trace Elements in sediments? LATECC Project (LAgoon, TEmpérature and Chemical Contamination) in the Venice Lagoon	812
The impacts of a changing climate on the human environment	825
Assessing the economic general equilibrium effects of sea level rise in the Italian Regions	838
<b>Hydrological Risk</b>	<b>857</b>
Assessing indirect expected annual loss of flooding in Italy under current and future climate	858
Climate Change Effects on Seawall Stability	870
Delta change variations in extreme values of precipitation for the next century in Central Campania	878
Climate change impacts on the flow regime of snow-dominated rivers: case study in Lebanon	897
<b>Impacts on energy, health and cultural heritage</b>	<b>922</b>
Results of the EU Project Climate For Culture: Future Climate-induced Risks to historic buildings and their interiors	923
Nature-based urban planning: a framework to assess the impact of green infrastructure design on ecosystem services ameliorating climate change	944
Future impacts of climate change on sectoral electricity demand	960
A preliminary approach to estimate the impact of climate change on electricity demand in Italy	977
Impact of climate change on historic architectural surfaces of the Venetian area	991
<b>Impacts on ecosystems, food and agriculture</b>	<b>1004</b>

Fires in the perspective of future changes: the contribute of CMCC to FUME Project	1005
Vulnerability of the Northern Adriatic Sea Fishery to Climate Change	1021
Assessing multiple climate change impacts in coastal zones: the North Adriatic case study	1036
The effects of climate change on agricultural sustainability in MENA Countries: implications for food security	1037
<b>Poster session</b>	<b>1038</b>
Forecasting bioclimatical trends from recent times until the end of the twenty-first century in Andalusia (South of Spain)	1039
Investigation on the reference Evapotranspiration Distribution at regional scale by alternative methods to compute the FAO Penman-Monteith equation	1050
Spatiotemporal changes in wildfire patterns in Sardinia	1067
Using regional climate models for food-security scenarios in Africa	1085
<b>AUTHOR INDEX</b>	<b>1099</b>

# Introduction

This book is both a success and a challenge.

It is a success because these pages, gathering the contributions to the SISC Second Annual Conference, are evidence of a continuing dialogue that began last year and show that the spirit of last year is very alive. It can be summed up in the desire and the need to give voice to the interdisciplinary approach that cannot be overlooked in climate change research.

The papers that are presented here, the authors who write them, and their contents and topics are proof that there is a reality of research in Italy that deserves to be appreciated and that is making a strenuous effort to meet the needs of innovation. It is a research reality that has been born in our country, but has an obvious international scope that, as perhaps few other disciplines have, expresses a strong demand for interdisciplinary integration, a dialogue between different skills and know-how, and opportunities for discussion and exchange. This book represents a continuation of work that began in 2013: it picks up the threads and carries them forward towards new frontiers in building something completely new that we call Climate Science.

In doing so, the papers published in the pages that follow express an integrated outlook on Climate Change, capable of holding together the methods, strategies, and knowledge from different areas and research communities which show that they are capable of talking to multiple stakeholders, involving complex issues such as advances in scientific research, mitigation, adaptation, risk assessment, and the impacts of climate change on various areas of environmental systems and socio-economic factors. And therein lies the open challenge: this book can in no way be considered a point of arrival, but once again is a starting point.

Scientific progress grows around young, hungry minds, and their sense of placement in history that too often is a disciplinary history, caught in the silos of XIX divisions of science. SISC believes that it is necessary to break down the barriers between the different disciplines as much as possible, raising the awareness that scientific research, especially climate change research, should be plural, inclusive, cross over national boundaries, and embody international collaboration. In other words, a spirit that is reflected in the values and mission that led to the foundation and the drive of the Italian Society for Climate Sciences.

**Antonio Navarra**

President of the Italian Society for Climate Sciences

# Foreword

Carrying out the second appointment of an innovative and unique reality, at least in the field of climate research such as SISC, has been an intriguing and compelling challenge for several reasons. It is impossible not to compare the second event with the first one, which was particularly positive given its participation. It is impossible not to look at last year as a starting point from which to proceed forward, integrating past experience with the needs and questions that have emerged in the last twelve months on the subject of climate change within the scientific community, the society, and the public sphere.

During 2014, these questions have been amplified due to the fact that the SISC Conference has come between two events that put some spotlights on climate science and on the interactions between climate change and environmental and socio-economic systems. On the one hand, in fact, there was the presentation of the three volumes of the Fifth Assessment Report of the IPCC on Climate Change, which has its own dimension of media and brings an attention to the climate sciences that they are not accustomed to receiving frequently. On the other hand, we cannot deny that the COP21, which will take place in the last months of 2015 in Paris will be a new moment in which the eyes of many will turn to those who study climate change to understand more of the research in the field, of the knowledge acquired and how policy makers are aware of the support that science can offer.

The pages that follow are the answer to this challenge. An answer that, faced with an increased number of proposals for papers, required a particularly challenging job for selection. The result is a collection of research, which manages to touch on a wide variety of topics and disciplines, and which are grouped here in four thematic areas. One of these is about the advances in climate science, with particular attention on climate variability, production and analysis of climate data. The mitigation of climate change, with its strategies and policies, is the main topic of a group of works that discuss the tools (from technologies to markets) to reduce emissions of greenhouse gases. And if, on the one hand, a session is devoted to adaptation strategies and topics such as vulnerability and risk assessment, there is also space in the collection for the issue of climate change impacts on many aspects (ecosystems, food, agriculture, energy, health, and even cultural heritage) of environmental and social systems.

Whether the challenge was met or not is not for us to determine, but certainly this volume attests the vitality that runs through the Italian research on climate which proves to be capable of attracting interest from many parts of the world and is growing year by year, according to the multidisciplinary vocation of SISC.

**Carlo Carraro / Simona Masina**

Presidents of the Scientific Committee of the Annual SISC Conference 2014

# SISC at a glance

*“From the integration of scientific disciplines,  
research and innovation to face climate change”*

The **Italian Society for Climate Sciences (SISC)** was created in 2013 to serve as a meeting point for scientists from different disciplines, who use climate information for their research: from climatologists to physicists and chemists, geographers to agronomists, economists to political scientists, and all scholars that deal with climate-related sciences and their applications.

**SISC** aims at contributing to scientific progress and innovation of climatic sciences in Italy by promoting the convergence of disciplines and multidisciplinary research.

The institutional purposes of SISC are:

## **To the world of research:**

- to foster the exchange of ideas, the creativity and the development of new interdisciplinary research;
- to promote communication and cooperation between universities and research institutions in Italy, strengthening the presence of climatic sciences in both Italian universities as well as higher education systems;
- to attract young talents to build a new interdisciplinary scientific community and increase overall productivity;
- to stimulate and coordinate the Italian contributions to the International programs in the field of climate sciences;
- to become the reference point and the meeting place for Italian scientists living abroad.

## **To the society:**

- to increase the impact of the studies and of the debate on climate issues, giving scientific rigor to the analysis of climate policies for mitigation and adaptation;
- to promote the dialogue among scientists, policy makers, businesses and citizens;
- to support actions in the interest of the society and the environment;
- to provide research results to institutions, businesses and citizens.

## **SISC's aims are pursued in particular through:**

- the organization of conferences and debates addressed to the scientific and policy communities;
- the implementation of web-communications;
- the promotion of training courses for young graduates;
- collaboration with multidisciplinary doctoral courses on climate sciences.

The SISC association is non-profit and non-advocacy, acts according to ethical principles and promotes policies for equal opportunities.

## **GOVERNANCE**

Antonio Navarra – President

Carlo Carraro - Vice-President

Donatella Spano – Elected President (in charge as President in 2015-16 period)

Simona Masina – Ordinary Member of the Executive Board

Riccardo Valentini – Ordinary Member of the Executive Board

Martina Marian – Secretary General / Ordinary Member of the Executive Board

# Scientific Committee

**Prof. Carlo Carraro (co-chair)**

Ca' Foscari University of Venice/ Fondazione Eni Enrico Mattei

**Dr. Simona Masina (co-chair)**

Istituto Nazionale di Geofisica e Vulcanologia/ Euro-Mediterranean Center on Climate Change

**Prof. Antonio Ballarin Denti**

Fondazione Lombardia per l'Ambiente (FLA)

**Prof. Francesco Bosello**

Università Statale di Milano

**Prof. Valentina Bosetti**

Università Bocconi

**Prof. Renato Casagrandi**

Politecnico di Milano

**Dr. Fabio Eboli**

Fondazione Eni Enrico Mattei (FEEM)

**Dr. Paola Faggian**

RSE SpA – Ricerca sul Sistema Energetico

**Dr. Riccardo Farneti**

International Centre for Theoretical Physics (ICTP)

**Prof. Marzio Galeotti**

Università Statale di Milano

**Prof. Alessandra Giannini**

Columbia University

**Dr. Silvio Gualdi**

Centro Euro-Mediterraneo sui Cambiamenti Climatici (CMCC)

**Prof. Sari Kovats**

London School of Hygiene and Tropical Medicine

**Dr. Mita Lapi**

Fondazione Lombardia per l'Ambiente

**Dr. Emanuele Massetti**

Georgia Institute of Technology

**Dr. Renzo Mosetti**

Istituto Nazionale di Oceanografia e di Geofisica Sperimentale (OGS)

**Prof. Luciano Picarelli**

Seconda Università degli Studi di Napoli

**Dr. Guido Rianna**

CIRA-Centro Euro-Mediterraneo sui Cambiamenti Climatici (CMCC)

**Dr. Guido Santini**

Food and Agriculture Organization (FAO – NRL)

**Dr.ssa Monia Santini**

Centro Euro-Mediterraneo sui Cambiamenti Climatici (CMCC)

**Prof. Roger Street**

UKCIP, University of Oxford

# Organizing Committee

**SCIENTIFIC SECRETARY** - [scientific.program@sisclima.it](mailto:scientific.program@sisclima.it)

**Annalisa Cherchi**

Euro-Mediterranean Center on Climate Change (CMCC), ANS Division

**Marinella Davide**

Fondazione Eni Enrico Mattei (FEEM)/ Euro-Mediterranean Center on Climate Change (CMCC), CIP Division

**Martina Marian**

Fondazione Eni Enrico Mattei (FEEM)/ Euro-Mediterranean Center on Climate Change (CMCC), CIP Division

**ORGANISING SECRETARY** - [sisc.conference2014@unive.it](mailto:sisc.conference2014@unive.it)

**Stefania Amerighi**

Fondazione Università Ca' Foscari Venezia

**Consuelo Puricelli**

Fondazione Università Ca' Foscari Venezia

**Martina Sguazzin**

Fondazione Università Ca' Foscari Venezia

**COMMUNICATION** - [press@sisclima.it](mailto:press@sisclima.it)

**Mauro Buonocore**

Euro-Mediterranean Center on Climate Change (CMCC), Communication Office

**Renato Dalla Venezia**

Università Ca' Foscari Venezia

Euro-Mediterranean Center on Climate Change (CMCC)/Fondazione Eni Enrico Mattei (FEEM)

**Lucia Luperto**

Euro-Mediterranean Center on Climate Change (CMCC), Communication Office

**Alessandra Mazzai**

Fondazione Eni Enrico Mattei (FEEM)/ Euro-Mediterranean Center on Climate Change (CMCC), CIP Division

**Carlo Palma**

Euro-Mediterranean Center on Climate Change (CMCC), Communication Office

# About the conference

The **Second Annual Conference of the Italian Society for Climate Sciences**, entitled **Climate Change: Scenarios, Impacts and Policy**, aims to involve scientists, researchers and policy makers, whose activities are focused on different aspects of climate change, its impacts and related policies.

The Conference aims to:

- **Develop** a platform for sharing and discussing between the different disciplines that study climate dynamics and their interactions with the environment and society;
- **Promote** a constructive and transdisciplinary dialogue between scientists, policy makers, service providers and the general public;
- **Foster** scientific dialogue on mitigation policies and sustainable growth;
- **Deepen** the understanding of climate change impacts and the best adaptation strategies.

The program of the Conference includes plenaries, parallel sessions, a poster session and special events.

The scientific program of the Second Annual SISC Conference is enriched by events aimed at pointing out that the issues of climate research can be communicated to a more general and broader public and not only to the scientific community. Besides activities with schools, SISC will host a dialogue among climate scientists and media experts to understand how the vast and complex mine of scientific data can be translated into a language understandable and interesting to the public and policymakers.



# Mitigation Policies & Strategies

**Mitigation Policies & Strategies**

**Climate change  
mitigation strategies**

# Mitigating GHG emissions in subnational contexts: the case of the city of Rio de Janeiro

La Rovere, E.L.<sup>1\*</sup>, Carloni, F.B.B.A.<sup>2</sup>

<sup>1</sup>Professor, Federal University of Rio de Janeiro (UFRJ), Institute for Postgraduate Studies and Research in Engineering (COPPE), Energy and Environmental Planning Program (PPE) - Brazil, <sup>2</sup>Researcher, Centre for Integrated Studies on Climate Change and the Environment, CentroClima/COPPE/UFRJ - Brazil

\*Corresponding Author: emilio@ppe.ufrj.br

## Abstract

This paper summarizes the main findings of a study carried out by the CentroClima/COPPE/UFRJ for the Environmental Secretariat of the City of Rio de Janeiro. The results of the city's GHG emissions inventories for 2005 and 2012 as well as its performance in terms of avoided GHG emissions are compared to the voluntary targets established by the municipality. The update of the city's Mitigation Action Plan was designed to meet the mitigation goals for 2016 and 2020.

**Keywords:** cities, GHG emissions, inventories, mitigation, urban policy

## 1. MITIGATION OF THE GHG EMISSIONS OF THE CITY OF RIO DE JANEIRO

The greenhouse gas (GHG) emissions of a city, region or country arise from burning fossil fuels (oil products, natural gas and coal), waste treatment, industrial processes and changes in plant cover, among others. Practically all economic sectors of modern society (industry, services, transports, farming, and construction) produce carbon dioxide (CO<sub>2</sub>), methane (CH<sub>4</sub>) and nitrous oxide (N<sub>2</sub>O) emissions, the main GHG gases, to a greater or lesser extent. Estimates of GHG emissions have an inbuilt uncertainty because of the difficulty in obtaining data on all these activities and emission factors. This is even more so when dealing with cities, where delimiting the boundaries of the activities is more complex. Nevertheless, the City Government of Rio de Janeiro was one of the first cities to carry out a GHG emissions inventory on a municipal scale. In 2000, the City Government presented the inventory of the emissions of the three main GHG gases in the City of Rio de Janeiro for the years 1990, 1996 and 1998; and in 2010, it did it for the year 2005, in addition to developing Scenarios and a Plan of Action to mitigate its GHG emissions, always with the technical support of CentroClima/COPPE/UFRJ. This paper summarizes now the results of the third GHG emissions inventory of the city of Rio de Janeiro, which amounted to 22.6 million tonnes of CO<sub>2</sub> equivalent (Mt CO<sub>2</sub>e) in 2012, in addition to revising the estimates for 2005 (11.6 Mt CO<sub>2</sub>e).

The reduction of GHG emissions in Rio de Janeiro is one of the strategic projects of the City Government. Emissions reduction targets were defined and consolidated in the Municipal Climate Change and Sustainable Development Law, enacted in January 2011. Targets were set using the total emissions verified in 2005 as reference. Reduction targets were defined as follows: avoid 8% of the 2005 emissions in 2012 (0.93 Mt CO<sub>2</sub>e), 16% in 2016 (1.86 Mt CO<sub>2</sub>e) and 20% (2.32 Mt CO<sub>2</sub>e) in 2020.

Targets were established while many City Government projects for emissions reductions were being defined and detailed. Large-scale works and interventions such as the inauguration of the Waste Treatment Center in Seropédica and the operation of large high-capacity express bus lanes (BRTs) are leading to a significant reduction of GHG emissions.

On the other hand, GHG emissions avoided by the actions of the City Government were not enough to ensure an overall reduction of the level of GHG emissions in the city, which almost doubled from 2005 to 2012. Population growth and economic development of a city induce a rise in GHG emissions. While the city's population has been increasing slowly over the past few years (growth of 3.6% from 2005 to 2012), the economic dynamics began to accelerate in November 2009, when Rio de Janeiro was chosen as the host city for the 2016 Olympic and Paralympic Games (45% growth in the municipal GDP from 2005 to 2012). Deployment of a large-scale steel mill using coke (manufactured from coal) within the boundaries of the city at the end of 2010 also contributed to increase GHG emissions. The Companhia Siderúrgica do Atlântico (TKCSA) had gross on-site emissions of 8.8 Mt CO<sub>2</sub>e (scope 1), even though attenuated by the company's major efforts, resulting in net GHG emissions estimated by the company to be around 6.3 Mt CO<sub>2</sub>e in 2012. Changes in the country's energy policy, arising from decisions made beyond the responsibility of the city, such as the increased use of thermopower for electricity generation, increase use of gasoline due to price subsidies and growth in the number of private vehicles, in addition to the crisis in ethanol production, also contributed to the increase of GHG emissions in the City of Rio de Janeiro from 2005 to 2012.

As a result, the Rio de Janeiro City Government decided to steer public policies towards a low-carbon urban development. Investments and interventions must have a climate component in their priorities, demonstrating to economic agents and civil society that it is indeed a priority. Moreover, the main guideline of the City's Strategic Plan is to promote sustainable development. The option of the City Government, with the support from the City Council, was to adopt realistic and transparent GHG emission reduction targets, in accordance with the public policies of City Government. This decision allowed Rio de Janeiro to preside with New York the meeting of the cities participating in the C40 Climate Leadership Group, an entity bringing together 58 megacities of the world, during Rio+20. The C40 mayors made the commitment to reduce global greenhouse gas emissions by 1.3 billion tonnes by 2030, according to the policies being implemented in their

respective cities. The commitment contrasted with the difficulty of achieving consensus in the multilateral area and with the absence of climate change debate during the United Nations Conference on Sustainable Development, Rio +20, promoted by national governments. Notwithstanding the leadership and autonomy of the cities, the perspectives and goals of national, regional and local governments, including the city of Rio de Janeiro, also suffer the direct consequences of these negotiations.

Within this context, the Government of the City of Rio de Janeiro has updated the Municipal Plan of Action for Emissions Reduction in order to meet the voluntary mitigation targets established for 2016 and 2020.

### **Consolidated Results of City of Rio de Janeiro Emissions in 2012**

Table 1 shows the total amounts obtained in the Greenhouse Gas Emissions Inventory of the City of Rio de Janeiro. The amounts are tabled per emission source and per gas, including carbon dioxide (CO<sub>2</sub>), methane (CH<sub>4</sub>) and nitrous oxide (N<sub>2</sub>O) emissions, and the total amount is in carbon dioxide equivalent. Scope 1 emissions include the direct GHG emissions within the city geographical boundaries. Scope 2 emissions correspond to the electricity imported from the grid (National Interconnected System). Scope 3 emissions correspond to the balance of emissions from the ethanol production chain; the fugitive emissions of the coal consumed by the city, but which is mined outside its borders; and the wastes generated by the city, but taken for disposal in landfills outside its borders.

### **Analysis of Indicators**

With respect to the carbon content of the GDP of the City of Rio de Janeiro, there is an increase in this indicator, as in the emission per capita, as shown by Table 2. However, as the population of the city did not grow significantly, the emission per capita almost doubled. However, the economic growth of the city from 2005 to 2012 occurred in activities that are more intense in their use of energy and their GHG emissions. The intensity of emissions per GDP unit increased by 34% in the period.

## Updated Mitigation Plan

A Plan of Action including the measures that the City Government must undertake to achieve the greenhouse gas emissions reduction targets has been updated.

According to the updated 2005 inventory results, the total city emissions in 2005 amounted to 11,613 tonnes CO<sub>2</sub>e. Thus, emission reduction targets provided for in law correspond to 929,000 tonnes CO<sub>2</sub>e (8% of 2005 emissions) in 2012. For 2016, the 16% would mean 1,858,000 tonnes CO<sub>2</sub>e.

Due to the delay in the construction of the new Waste Treatment Centre and of the methane capture facilities in the main landfill, the estimates of the current study show that the actions carried out by the City Government until 2012 were not enough to achieve the 8% target. However, for 2016, the projected actions, if actually implemented, will be close to achieving the 16% target, as shown by Table 3.

It should be stressed that the city is thriving and it is necessary to consider that the huge steel mill recently built in the city (Complexo Siderúrgico do Atlântico), which is not yet operating at its full capacity, should achieve it by 2016. Given that for production of 3.5 million tonnes of crude steel, gross emissions for the complex amounted to 8.8 million tonnes CO<sub>2</sub>e, and net emissions 6.3, in 2012; with a full load of 5 Mt of crude steel, these emissions will be greater and will probably overshoot the reductions foreseen by the city's mitigation actions.

## **2. ACKNOWLEDGMENTS**

The authors thankfully acknowledge the institutional support from the Environmental Secretariat of the City of Rio de Janeiro and the financial support from TKCSA.

## **3. REFERENCES**

1. La Rovere, E.L.; Carloni, F.B.B.A. et al; Greenhouse Gas Emissions Inventory of the City of Rio de Janeiro in 2012 and Updating of the Municipal Plan of Action for Emissions Reduction, Technical Summary, Environmental Secretariat of the City of Rio de Janeiro & CentroClima/COPPE/UFRJ, December 2013.

## 4. TABLES

Tab. 1 Total GHG emissions in the City of Rio de Janeiro, in 2012, by scope (Gg CO<sub>2</sub>e)

	Scope 1	Scope 2	Scope 3	Total
<b>ENERGY</b>	16,346.49	1,413.43	-133.37	17,942.41
<b>Energy sector consumption</b>	<b>2,702.10</b>	<b>469.83</b>		<b>3,171.93</b>
Losses	1,614.57	469.83		2,084.40
Coke production	1,087.53			1,087.53
<b>Residential</b>	<b>1,574.94</b>	<b>314.71</b>		<b>1,889.65</b>
Commercial/services	1,283.32	343.56		1,626.88
Public sector	436.44	126.36		562.80
Farming	0.54	0.14		0.68
<b>Transports</b>	<b>6,733.68</b>	<b>20.09</b>	<b>-315.86</b>	<b>6,753.77</b>
Road	5,301.37		-315.86	4,985.51
Rail	72.96	20.09		93.05
Air	1,664.87			1,664.87
Water	10.34			10.34
<b>Industry</b>	<b>2,361.05</b>	<b>138.74</b>		<b>2,499.79</b>
Fugitive emissions	1,254.42		182.49	1,436.91
<b>IPPU</b>	<b>2,355.33</b>	<b>0.00</b>	<b>0.00</b>	<b>2,355.33</b>
<b>Industrial processes</b>	<b>2,286.59</b>			<b>2,286.59</b>
Product Use	68.74			68.74
<b>AFOLU</b>	<b>8.57</b>	<b>0.00</b>	<b>0.00</b>	<b>8.57</b>
Land Use Change	-11.66			-11.66
Livestock	10.11			10.11
Agriculture	10.12			10.12
<b>WASTES</b>	<b>634.42</b>	<b>0.00</b>	<b>1,696.41</b>	<b>2,330.83</b>
Solid Wastes	10.17		1,696.41	1,706.58
Urban Solid Wastes	9.72		1,637.98	1,647.70
Healthcare Wastes			6.33	6.33
Incineration	0.44			0.44
Industrial Wastes			52.10	52.10
<b>Sewage and Effluents</b>	<b>624.26</b>			<b>624.26</b>
Res + Com Sewage	526.97			526.97
Industrial Effluents	97.28			97.28
<b>TOTAL</b>	<b>19,344.81</b>	<b>1,413.43</b>	<b>1,563.04</b>	<b>22,637.14</b>

Source: La Rovere, E.L.; Carloni, F.B.B.A. et al, 2013 [1]

Tab. 2 GHG emissions, GDP and population of the City of Rio de Janeiro, 2005 and 2012

	2005	2012	2012/2005 Increase (%)
<b>Total emissions (million tonnes CO<sub>2</sub>e)</b>	11.61	22.64	95%
<b>GDP (billion Reals at 2012 prices)*</b>	167.00	242.50	45%
<b>Population (million inhabitants)</b>	6.10	6.32	4%
<b>Total emissions/GDP (t CO<sub>2</sub>e/million 2012 Reals)</b>	69.54	93.35	34%
<b>Total emissions per capita (t CO<sub>2</sub>e/inhabitant)</b>	1.90	3.58	88%

Source: La Rovere, E.L.; Carloni, F.B.B.A. et al, 2013 [1]

\*Amount estimated from the 2010 amount.

Tab. 3 Estimated emissions reductions for 2012 and for the Strategic Plan period (2013-2016) in the City of Rio de Janeiro (thousand tonnes CO<sub>2</sub>e)

Reduced emissions	2012	2016
Energy – stationary sources	0.7	0.7
Energy – fugitive emissions	5.7	17
Replacement of gas distribution network (CEG )		
Energy – transports	79.6	525
BRTs (1 in 2012, 4 in 2016)	7.7	211.1
Copacabana BRS	17.6	17.6
Subway expansion	51.1	289.9
Expansion of bicycle lanes network (300km)	3.2	6.4
Agriculture, Forests and Land Use – AFOLU	36.3	49.7
Urban Solid Wastes	243.8	1,240
Capture and burning of biogas in Gramacho Landfill	235.1	329
Capture and burning of biogas in Seropédica Landfill	8.7	911
Liquid effluents	11.9	–
<b>Total Emissions Reductions</b>	<b>378.00</b>	<b>1,832.40</b>
<b>Targets of the City Climate Change Policy</b>	<b>929</b>	<b>1,858</b>

Source: La Rovere, E.L.; Carloni, F.B.B.A. et al, 2013 [1]

# Sharing of Climate Risks across World Regions

Emmerling J.<sup>1</sup>

<sup>1</sup>Fondazione Eni Enrico Mattei (FEEM) and Centro Euro-Mediterraneo sui  
Cambiamenti Climatici (CMCC)

\*Corresponding Author: johannes.emmerling@feem.it

## Abstract

Uncertainty is prevalent in the context of climate change impacts. Moreover, the distribution across the globe is not uniform. We analyze how climate risks could be reduced via an insurance scheme at the global scale across regions and quantify the potential welfare gains from such a scheme. Starting from the standard welfare analysis in Integrated Assessment Models (IAMs), which assumes no risk sharing across region, we introduce global risk sharing via a market for state-dependent Arrow-Debreu securities. We show that this allows equalizing relative consumption differences between states of the world across regions. We estimate that such risk sharing scheme of climate risks could lead to welfare gains reducing the global costs of climate change by up to one third, while the amount of transfers required is substantial. This provides arguments for considering risk sharing in IAMs, but also for potentially welfare increasing negotiations about sharing risks of climate change at the global level.

**Keywords:** uncertainty, risk sharing, insurance, climate change, risk aversion

## 1. TEXT

Uncertainty is prevalent in the context of climate change impacts. Moreover, the distribution across the globe is not uniform. We study how different welfare functions and discount rates affect the optimal climate policy when such uncertainties are taken into account notably taken into consideration the regional pattern of risks and their correlation across countries. We then analyze how climate risks could be reduced via an implicit insurance scheme at the global scale across regions and quantify the potential welfare gains from such a scheme. Starting from the standard welfare analysis in Integrated Assessment Models (IAMs), we study how different welfare functions and discount rates affect the optimal climate policy when such uncertainties are taken into account notably taken into consideration the regional pattern of risks and their correlation across countries. We use a disentangled welfare function between risk and time preferences and introduce global risk sharing via a market of state-dependent Arrow-Debreu securities.

This framework in particular allows to evaluate risks associated to impacts from climate change, including per se stochastic events such as extreme events but also long term trends that potentially include severe damages in the most vulnerable regions of the world. These uncertainties have led to increasing concerns also by policy makers to not only mitigate climate change as such, but also to address issues of equity such as the compensation of the worst hit regions or countries. For instance, the “Warsaw international mechanism for loss and damage associated with climate change impact decided at COP19 end of 2013 aimed at creating an insurance scheme to provide compensations for developing countries being severely affected by such random climate change impacts. Therefore, the idea of insurance on a global scale against climate impacts could provide a way of mitigating the economic costs of global warming. While on a smaller scale the role of insurance, risk sharing, transfer schemes, and even micro-insurance in times of global warming are widely discussed (e.g., Mills (2005); Mills (2009); Munich Climate Insurance Initiative (2013)), this approach is quite different in that insurance or other risk transfer schemes based on the global scale contingent to certain impacts or extreme events cannot rely on a law of large numbers to achieve an efficient risk sharing across agents. Rather, an idea of risk transfers can be established in cases where the impacts of global warming are not perfectly correlated across world regions. This

gives rise to a global possibility to share risk efficiently in order to reduce the global risk exposure by a risk sharing mechanism, which is what we study in this paper.

While the uncertainty about the future climate and associated socioeconomic impacts has received increasing attention in recent years, still, in many integrated assessment models (IAMs), the effect of uncertainty is frequently found to be of minor importance confirming that uncertainty is a second order effect. The discussion of catastrophic, fat-tailed risk on the other hand found a much stronger effect (Weitzman, 2009). More recently, the role of risk aversion and appropriately parameterizing this preference characteristic has somewhat allowed to obtain more significant effects of uncertainty (Croston and Traeger, 2011; Traeger, 2009; Ackerman et al., 2013; Cai et al., 2013). However, their analysis has exclusively relied on globally aggregated models. If rather than a single representative agent multiple regions or countries are considered, the distribution of income, damages from climate change, and mitigation costs becomes relevant. Notably, the assumptions about how the uncertainty is distributed and correlated across regions, becomes relevant. Moreover, assumptions about how risk might or not be shared across regions are needed. Intuitively speaking, the question can be framed as whether risk aversion is considered at the global or regional level. Intuitively, this results in different evaluations based on whether the social planner exhibits different degrees of risk and inequity aversion, which is very plausible, see Atkinson et al. (2009). Moreover, the way risks are able to be shared across agents or countries, or risk transfers are allowed for, will impact the evaluation of climate change in globally disaggregated IAM models.

In this paper, we explicitly introduce the possibility of risk sharing of climate risks across macro regions. This addresses the role of risk sharing of, e.g., extreme events where within a region, individual risky damages are able to be reduced via different types of insurance or risk sharing schemes. Only if all risks were perfectly correlated, risk sharing cannot lead to a welfare improvement. Otherwise, however, all idiosyncratic risk could be in theory removed Ligon (1998). In reality, there are however several obstacles to insure all idiosyncratic risks, namely transaction costs, limited liability, asymmetric information, and ambiguity. Notably ambiguity provides a serious hindrance to insurance in the context of climate change where the scientific

uncertainty is hard to assess with probability estimates (Kunreuther et al., 1993). As a result, insurance is far from covering all climate change damages.

While standard Integrated Assessment Models assume no risk sharing across regions, we explicitly allow for this possibility introducing a market for contingent claims. We show that this allows equalizing relative consumption differences between states across regions leading to potential welfare gains reducing the welfare costs of climate change. Optimal climate risk sharing could therefore lead to a more equally distributed impact of climate change on consumption. Figure [1] shows the estimated climate change impacts (as per cent of consumption compared to the case where no climate change impacts occur across regions with (red) and without (blue) the risk sharing scheme.

Our estimates suggest that the welfare costs of climate change could be reduced by up to 30-40% via such an insurance scheme. This estimate is surprisingly high but is due to the relatively unequal distribution of climate impacts. Measured by the “certainty, equity, and balanced growth equivalent” level of consumption, climate impacts lead to a global loss of 4.5% of consumption in our model. Allowing for risk sharing reduces this global consumption loss to 2.3% or by about 38% from the original welfare loss. Based on the regional damage estimates, we can also compute the amount of contingent claims that each region would buy or sell. Notably, China will be the biggest insuring party due to its lower-than-average impacts, see Figure [2].

How such an insurance scheme could work is not trivial. However, risk sharing at the global scale can comprise relocation of capital and labor (migration), international trade, financial markets, and--potentially most relevant in this context--an explicit risk transfer scheme between regions or countries. While the residual damages remain an important welfare loss, the results suggest that indeed compensating particularly hard hit countries from climate change impacts could reduce global welfare loss significantly; in particular, such a scheme can--and should-- be implemented ex-ante and would benefit all participating countries. Based on our model we can compute the volume of such a scheme necessary to achieve the welfare gains from risk sharing. Based on the market outcome on the market for contingent claims, we find that for a moderate degree of risk aversion of 1.5 a total market volume of 240 billion USD in 2015 or 0.18% of global GDP and increasing with GDP growth over time.

This amount is substantial and would imply significant institutional and governance challenges. Still, compared to, e.g., the 359 billion USD of total global climate finance as estimated by the Climate Policy Initiative (2013) for 2012, the magnitude seems reasonable, even if this risk sharing/transfer scheme does not contain any mitigation or adaptation measures but only looks at the welfare maximizing risk sharing across world regions.

Finally, while the public good nature of climate change renders global cooperation hard to achieve, this should be substantially less difficult to achieve global welfare gains from insuring against idiosyncratic uncertain climate impacts. The use of an extended welfare framework based on Epstein-Zin (1989) preferences allows to further improve the realism of an integrated assessment model such as the one used to better evaluate the cost of uncertainty on climate impacts. In particular, for more reasonable degrees of risk aversion, the insurance scheme becomes more costly for the regions expected to bear higher damages, and the volume of the transfer scheme increases slightly. Still, ex-post equalization of consumption differences are achieved as predicted by the proposition and the insurance scheme is incentive-compatible. For future research, it would be interesting to consider differing risk attitudes across regions or countries. In this case, one can solve for the equilibrium allocation as we did to find the optimal risk sharing allocation, even though the main result does not hold anymore.

## **2. ACKNOWLEDGMENTS**

I would like to thank Valentina Bossetti, Per Krusell, Simon Dietz, and participants at the FEEM/CMCC Convention 2013 in Venice, at the IAERE Annual Conference 2014 in Milan, and at IEW2014 in Beijing for very helpful comments. The usual caveat applies. The research leading to these results has received funding from the European Union Seventh Framework Programme FP7/2007-2013 under grant agreement No. 266992 (GLOBAL-IQ) and No. 282846 (LIMITS).

## **3. REFERENCES**

1. Ackerman, Frank and Charles Munitz, "Climate damages in the FUND model: A disaggregated analysis," *Ecological Economics*, May 2012, 77, 219–224.

2. Atkinson, Giles D., Simon Dietz, Jennifer Helgeson, Cameron Hepburn, and Håkon Sælen, “Siblings, not triplets: social preferences for risk, inequality and time in discounting climate change,” *Economics - The Open Access, Open Assessment E-Journal*, 2009, 3 (26), 1–29.
3. Cai, Yongyang, Kenneth L. Judd, and Thomas S. Lontzek, “The Social Cost of Stochastic and Irreversible Climate Change,” NBER Working Paper 18704, National Bureau of Economic Research, Inc 2013.
4. Climate Policy Initiative, “The Global Landscape of Climate Finance 2013”, 2013.
5. Crost, Benjamin and Christian P Traeger, “Risk and aversion in the integrated assessment of climate change,” November 2011.
6. Epstein, Larry G. and Stanley E. Zin, “Substitution, Risk Aversion, and the Temporal Behavior of Consumption and Asset Returns: A Theoretical Framework,” *Econometrica*, July 1989, 57 (4), 937–969.
7. Gollier, Christian, “Some Aspects of the Economics of Catastrophe Risk Insurance,” in “Policy Issues in Insurance,” Organisation for Economic Co-operation and Development, July 2006, pp. 13–30.
8. Kunreuther, Howard, Robin Hogarth, and Jacqueline Meszaros, “Insurer ambiguity and market failure,” *Journal of Risk and Uncertainty*, August 1993, 7 (1), 71–87.
9. Ligon, Ethan, “Risk Sharing and Information in Village Economies,” *The Review of Economic Studies*, October 1998, 65 (4), 847–864.
10. Mills, Evan, “Insurance in a Climate of Change,” *Science*, August 2005, 309 (5737), 1040–1044.
11. Mills, Evan, “From Risk to Opportunity Insurer Responses to Climate Change,” Technical Report 2009.
12. Munich Climate Insurance Initiative, “Climate Risk Adaptation and Insurance: Reducing vulnerability and sustaining the livelihoods of low-income communities,” Technical Report No. 13, UNU-EHS, Bonn 2013.

## 4. IMAGES AND TABLES

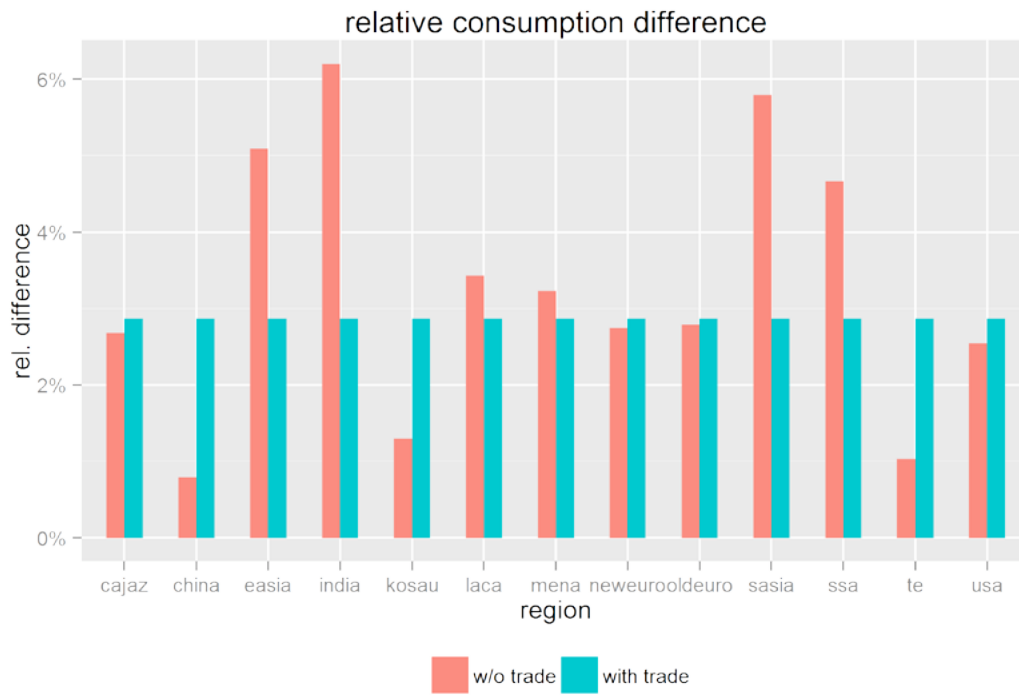


Fig. 1 Relative consumption differences with and without the risk-sharing scheme (in 2050)

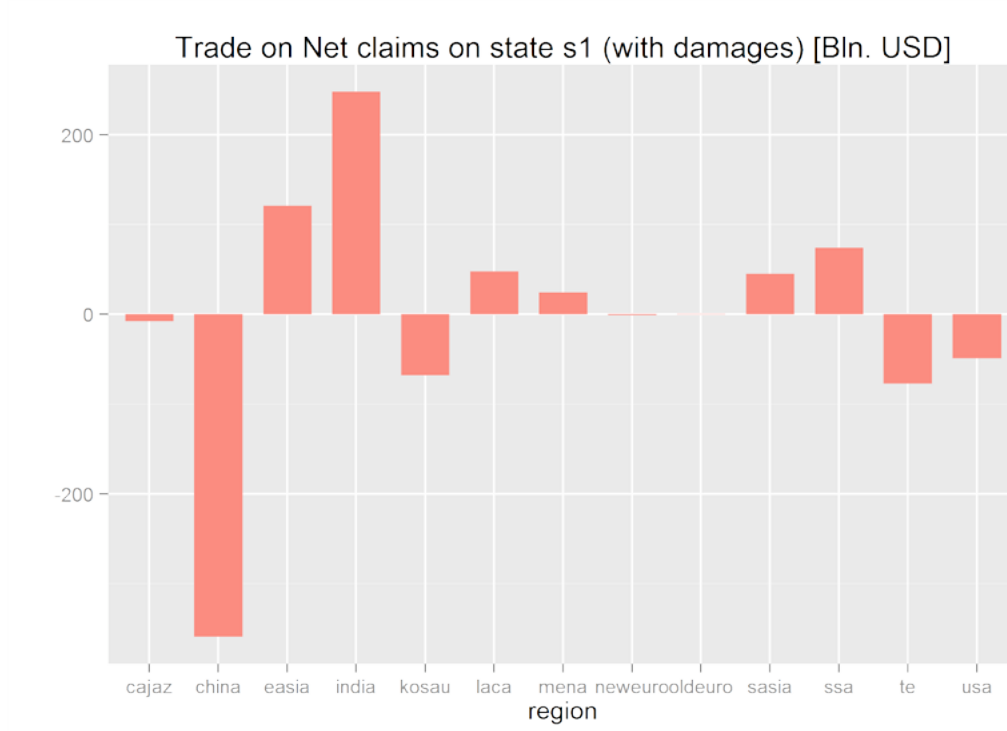


Fig. 2 Contingent claims bought and sold by different regions (for the year 2050, traded in 2015)

# **Anthropic emissions of Greenhouse Gas (GHG) and reference for mitigation policy of emissions in Mato Grosso (Brazil)**

**Teixeira Maria Daniele de Jesus<sup>1</sup>, Faria Alexandre Magno de Melo<sup>2</sup>, Zavala  
Arturo Alejandro Zavala<sup>3</sup> and Ferreira Raphael Pires<sup>\*4</sup>**

<sup>1</sup>University of Brasília – Brazil, mdani2827@gmail.com, <sup>2</sup>Federal University of Mato Grosso – Brazil, dr.melofaria@gmail.com, <sup>3</sup>Federal University of Mato Grosso – Brazil, arturoz@ig.com.br and <sup>4</sup>Federal University of Mato Grosso – Brazil

\*Corresponding Author: rapha.ufmt@gmail.com

## **Abstract**

The research deals with the increase in GHG emissions from anthropogenic activities and press estimate an overview of emissions of carbon dioxide equivalent (CO<sub>2</sub>e) of the state of Mato Grosso, as well as designing a scenario for the implementation of public policies. Emissions were estimated for the sectors of fuel, electricity, soybean production, cattle, pigs and deforestation, followed by a projection of emissions between 2010 and 2020 through a nonlinear regression model simple. The projections for 2020 showed increasing trends for all productive sectors, except deforestation, which before the representativity induced emission reduction overall condition. Despite the overall reduction, the Mato Grosso State should implement environmental regulatory instruments sector to achieve the goal of mitigating emissions in Mato Grosso.

**Keywords:** GHG emissions, Projection, Mato Grosso, National Policy on Climate Change.

## 1. TEXT

### INTRODUCTION

In face of the world dissemination concerning weather change information, we can note that some efforts has been done to mitigate the environmental damage. Considering the Brazilian government, some actions about sustainable growth can be noticed and also in GHG questions. In 2009 the National Policy about Weather Change was established – NPWC, that sets actions of greenhouse gases emissions mitigation, in sight to reduce between 36,1% and 38,9% [Table 2] the projected emissions in Brazilian grounds until 2020 – [4].

Some actions for this reduction have already been set in motion, and the goals are in its majority quantitative. However, one of the problems that have been found is the lack of information about the actual scenario, and the past years, the low numbers of specific methods that quantify and estimate those emissions. In this context, this research is about the GHG anthropic emissions, and given the calculation difficulty and scarce bibliography, especially on municipal, regional and state levels, it estimates the CO<sub>2</sub>e emissions of representative part on Mato Grosso state levels, looking for directing the possible implementation of public policies and environmental regulation instruments about emissions mitigation of greenhouse gases.

The specific objectives are: a) estimate the Greenhouse Gases anthropic emissions of CO<sub>2</sub> equivalent in Mato Grosso between 2000 and 2009; b) identify the activity sectors with the higher emissions percent; c) elaborate a emission projection by sector for 2020, which will sustain the implementation of appropriate policies that has the objectives converging to minimizing emissions.

In this paper methodology, calculations were used to estimate CO<sub>2</sub>e emissions by activity sector in the state of Mato Grosso and the nonlinear model of regression to estimate the projected quantity of CO<sub>2</sub>e emission in 2020, reference year set by NPWC as limits to reach the emission reduction goals. The detail of information required for this research and its sources that provide this information can be found on [Frame 1]. Highlight that the emissions and projections were estimated for Mato Grosso mesoregions and after were elaborated for the whole state.

## METHODOLOGY

The methodology is well detailed in [25]. Specific methodologies were utilized to estimate for each sector, the Top Down Methodology to estimate the fuel emissions, for electricity emissions a adapted methodology were utilized from emission inventory. To estimate the CO<sub>2</sub>e emission by the sectors of land change usage and forest, were used deforestation increment by emission factor hectare/year, for cattle sector were used animal emission factor/year, for agriculture the biological fixation factor in hectare/year.

Factors presented in the [Frame 2] were used to perform the calculation of greenhouse gases emissions by municipality, subsequently clustered up in mesoregion by sector like: deforesting (vegetal biomass burn), cattle ranching (enteric digestion and animals in pasture), swine culture (enteric digestion and decomposition of waste) and soy farming (nitrogen biological fixation). All data are presented in ton of equivalent CO<sub>2</sub>e.

The CO<sub>2</sub>e emissions projection for 2020 were established to give foundation to the law number 12.187 of 2009, on its article 12, which says:

To achieve the objectives of NPWC, the country will adopt as national voluntary commitment, actions to mitigate emissions of greenhouse gases, with a view to reducing by 36.1% (thirty-six point one percent) and 38 9% (thirty-eight and nine-tenths percent) their projected emissions by 2020 [4].

To make possible the CO<sub>2</sub>e emissions estimate from 2010 to 2020, the Simple nonlinear regression model were used for the whole state and its mesoregion by activity sector, this method is better detailed in [25].

$$y^* = \frac{\text{Ln}(y)}{\sqrt{t}} \quad (8)$$

$y^*$  is the variable that represents the CO<sub>2</sub>e emission quantity in tons by year and  $t$  is the variable time (year). In this way the regression model will be power type, that can be written like:

$$y^*_i = \beta_0 t^{\beta_1} e_i \quad (9)$$

$y^*$  is the variable that represents the CO<sub>2</sub>e emission quantity in tons by year;  $\beta_0$ ,  $\beta_1$  are simple nonlinear model coefficients;  $t_i$  it's the time variable (year) and  $e_i$  is the random mistake.

This method gets the studied parameters if the relationship between the dependent variable and the model parameters is of linear type, due to this equation (9) it should be linearized by applying the logarithmic transformation (Equation 10). For the calculations Excel 2007 ® software version was used. Once obtained the MQO estimators proceeded to extrapolations for the years 2010-2020, it was used for such conversion of the original units, the following procedure:

$$y_i = \exp(\hat{y}_i * \sqrt{t}) \quad (10)$$

Where  $y_i$  is the variable amount of CO<sub>2</sub>e emitted in original values;  $i$  is the amount estimated variable and  $t$  is the time variable (year). Once established this relationship by the regression model, according [8], we must evaluate the confidence that can be put on it, performing statistical tests on the setting and significance, which was performed and showed satisfactory statistical values.

## RESULTS AND DISCUSSION

As shown in [Figure 1], deforestation has issued more than 80% of CO<sub>2</sub>e of Mato Grosso between 2000 and 2005, with a reduction in 2006-2008 to about 60%. In the period 2009-2011 emissions related to deforestation dropped to about a third of CO<sub>2</sub>e emitted in Mato Grosso. On the other hand, the production of cattle has expanded continuously, generating methane gas emissions that have been established as industry leading emitter of greenhouse gas. It can be said that there was a substitution between emissions from deforestation emissions by cattle, which became the major economic sector emitter of CO<sub>2</sub>e.

Other two sectors that stand out are the fuels and soybeans. Fuels expanded its share of about 2% in 2000 to a share of around 7% from 2009-2011, influenced both by the reduction in total emissions as the expansion of domestic productive activity that requires large flows of diesel, as the transportation of inputs and export of final products to and out of Mato Grosso. Soybean expanded its emissions of around 1% in 2000 to 4% in 2009-2011, confirming the expectations of incorporation of new productive areas and becoming the largest producer of this oilseed in Brazil.

While illegal deforestation can be controlled with command and control actions from the existing legislation in the country, the difficulties of reducing other emitting sectors such as fuels, cattle, swine and soybeans reside in the complexity of the activities and the need for various technical studies to verify the best ways to mitigate the emission without cooling economic activities.

This way the optimal scale for ecological economics would not be reached, in which the physical increase in economic subsystem has to cost more than the benefit it can bring to the welfare of humanity, in other words, the point where the growth of productive activity becomes uneconomical (Daly and Farley, 2004 [6]). Therefore, in this line of thought, the state has a role to play, according to Romeiro, Rydon and Leonardi (2001) [23] placing limits on the use of the environment, usually through command and control policies.

However, unlike the illegal deforestation that can be contained with instruments of command and control, licit economic activities can't simply be prohibited. In this case should be preponderate economic instruments as auxiliary measures to mitigate emissions, since the trend of expansion of a sector and the possibility of generating pollution above the desired range is identified 2020 CO<sub>2</sub>e emissions projection

Comparing the target relative to the base (2005) year, the state already in 2006 would meet the reduction target, considering that about 57% reduced emissions from 2005 to 2006, which shows a very high baseline. That is, despite a considerable reduction, the values were still significant. As the NPWC was established in 2009, analyzing the results of the projections goals based on emissions this year (81.9 million tons of CO<sub>2</sub>e, according to [Table 1]), so the goal is considered that in 2020 the state should issue between 52.2 and 49.9 million tons of CO<sub>2</sub>e.

The regressions were run for each emission sector of the state, the estimated equations were significant, the coefficients of determination were greater than 80%. After analysis of the significance and tests to assess the quality of the adjustments proceeded to projection of the amount of CO<sub>2</sub>e emitted from the year 2010 to 2020, from the estimated equations. The results are shown in [Figure 2], where the emission from the fuel, energy, cattle, pigs and soybean sectors have increasing trend. Only the sector of deforestation show tendency of decrease by 2020.

The increasing projection of emissions by fuel sector can be explained by population increase, expansion of purchasing power in the state, the urban agglomeration as well as deployment of new industries and also the use by the agricultural sector, which has responded to exogenous demand within the country and the global economy. The information and projections show that there is a need to implement policies to reduce emissions from the fuel sector to achieve the reduction target. In particular, the replacement of fossil fuels with renewables like ethanol and biodiesel and creating a possible maximum quota of fossil fuel use.

Projections of CO<sub>2</sub>e emissions from the energy sector showed an increasing trend, issuing more than 150 tons of CO<sub>2</sub>e in 2020. This trend can be explained by the growth and development of urban spaces, along with the increase in population as well as the expansion income that is linked to the consumption of appliances. However, emissions from this sector, despite showing increasing trend, about 9% from 2010 to 2020, show no great need of attention of public policies, as would represent less than 1% of the emission target for the state in 2020.

As Allison (2012 [1]) scientists can contribute greatly through the expansion of knowledge of agricultural practices that can deliver multiple benefits and the link between agriculture and forestry. Several public policies indicate the direction of sustainable agriculture and eventually the sector will accelerate the introduction of new sustainable practices. In other words, increased productivity can happen with reduced emissions and greater ability to adapt to climate change with less environmental impact, especially on biodiversity.

Considering the need to summarize in a few words to fit the standards of the article, further discussions were withdrawn, as analysis for each sector, taking into account trends, explanations of the growth or decline and policy statements. However, the main conclusions are highlighted in the next section.

## CONCLUDING REMARKS

Agriculture, cattle creation and forest exploration are the most representatives' economics activities in Mato Grosso. Such activities aggregate many negativities externalities, GHG is one of them. Concerning the CO<sub>2</sub>e emissions, the state had presented elevated quantities, especially in 2003 when it emitted 377 million tons. In 2006 the CO<sub>2</sub>e emissions reduced about 60% in comparison with the estimated

emissions for the year of 2003. This reduction can be explain by the fall of the deforestation increment, recorded from 2006, and followed by subsequent years, result of instrument of environment regulation of control and command, besides restrictive economic vectors to productive expansionism. The greatest source of emission in Mato Grosso by the year of 2008 was the change of land use, but from that the emissions originated by the cattle sector started to become relevant, scoring since 2009 greater participation than deforesting.

For the year of 2020 the projections for the sectors revels that the majority of the sectors presents growth tendencies for the emissions. The fuel sector would increase 6% from 2010 to 2020, electric energy 9%, 12% for the cattle sector, swine 32%, soy farming 30% and the only one sector that presented decreasing tendencies was deforestation, with the reduction of 13%. These projections show that because of the weight of the deforestation sector in the state emissions, its reduction led to the aggregate contention of the state emissions, besides all the other sectors presented growth tendencies. In the sum of all, Mato Grosso emissions would reach about 119,5 million tons of CO<sub>2</sub>e in the 2020 [Figure 3].

Besides the decreasing tendency presented by the total emissions of CO<sub>2</sub>e in the state, it was found that projected quantities got higher values than the emissions goals of PNMC with 2009 as the base year, in other words, it's not sufficient to accomplishes the government reduction goals, estimated in this paper between 52,2 and 49,9 million tons of CO<sub>2</sub>e. Special attention is suggested to the cattle sector, land use change, fuel and soy farming.

In the case of land use change, the central question is the complete institutionalization of existing laws, in illegal deforestation and in acceptable handling practices. The implementation of laws is the basic instrument for emissions mitigation in this segment that can be complemented by economic instruments like REDD, PSA and MDL, which should conduct the liquid emissions closer to zero.

For cattle, we highlight the evolution of emission because of the intense growth tendencies for the next years. There are policies for emission reduction for this sector and the majority suggests change in the animals feeding components and change on the long term handling, acting in the final productive. Opens up a huge tecno-economic trajectory that needs to adjust technical parameters related to the GHG emission conjugate with the capacity of keeping the accumulation rate of the sector,

because reducing the ruminants objective capital rotational time, probably will be contention in methane emissions.

Another important sector to be planned is the fuel one. This sector also presents growth tendencies of emission for the next year, showing the need of substitution by cleaner sources of energy, like biodiesel and ethanol. Also suggest focusing on automotive industry that can develop low emission vehicles this innovation is more studied when encouraged by environmental regulation instrument like carbon credit that has been gain significant values, in countries that signed the emission reduction obrigatorities and the others.

The emissions coming from soy farming also occupy a highlighted place. Regarding the smallest representative against all other emissions, has been presented with values and growing tendencies, what may become exponential in face of it's importance and utility for for human and animal feeding, basic product for energy, lubes, plastics and others. On what has been exposed the suggested mitigation policy for the sector is the nitrogen biological fixation that reduces production costs and improves fertility. The percentage and efficiency of emission as emissions mitigation also must be researched.

Almost all the actions for emissions mitigation presented on the researched literatures comes from neoclassic foundations, specific environmental economic, on which there are studies to find techniques and means to reduce the negative externalities and the environmental impact giving the chance for optimum allocation and allow, at the same time, the activities expansion. The concern in this approach line is the search for equilibrium points that guarantee to the producer the maximum profit and to the consumer the maximum satisfaction, not caring about the acceptable pollution scale by the natural environment.

For ecological economy, above all, the studies should, prioritize researches to find the optimum scale, which would be the point that the system could support the expansion of the activities. In the case of "*Pacto Nacional pela Valorização da Floresta e Fim do Desmatamento na Amazônia*", some ecological economy foundations are presents which highlights the Amazonia zero deforestation. The sustainability is prioritize in this, focusing on long terms. As PNMC which limits the growth scale, setting reduction goals for the emissions.

Can be observed that there are some emissions mitigation policies in the state, but, the scientific framework still needs to evolve in technical aspects to make possible more GEE emissions reduction and enable to reach the PNMC goal that estimated in this 49 million. The environmental regulation instruments, applied as command and control and as economic incentives shows that are quite effective at emissions mitigation. Ecological economy presupposes, the state has a role to play, establishing boundaries on environmental usage, providing the foundations of sustainable development, meet the present needs without compromises the welfare of future generations.

## 2. ACKNOWLEDGMENTS

The author gratefully acknowledges support from the Federal University of Mato Grosso, University of Brasília, the National Center of Development Cientific and Technological (CNPQ), and all authors that contributed to this paper.

## 3. REFERENCES

1. ALISSON, E. Redução do desmatamento com aumento da produção agrícola. Agência FAPESP. 16/01/2012a. Disponível em: <<http://agencia.fapesp.br/15033>> Acesso em 16 jan. 2012a.
2. ÁVILA, Fabiano. NOAA: concentração de CO2 subiu rapidamente em 2012. Instituto Carbono Brasil, 06/03/2013. Disponível em: <http://www.institutocarbonobrasil.org.br/noticias2/noticia=733337>.
3. BAZANI, S. Araguaia é a nova fronteira agrícola. Jornal A Gazeta, Cuiabá, ano XXI, n.º7402, pág. 1C, 25 de março de 2012.
4. BRASIL, Presidência da República - Casa Civil -Subchefia para Assuntos Jurídicos. LEI Nº 12.187, DE 29 DE DEZEMBRO DE 2009. Disponível em: <[http://www.planalto.gov.br/ccivil\\_03/\\_ato2007-2010/2009/lei/l12187.htm](http://www.planalto.gov.br/ccivil_03/_ato2007-2010/2009/lei/l12187.htm)> Acesso em: 10 jan. 2011.
5. DALL'AGNOL, A. D. O complexo agroindustrial da soja brasileira. Circular Técnica 43, ISSN 1516 – 7860, EMBRAPA, Londrina, PR. 2007.

6. DALY, H. E. e FARLEY, J. C. Ecological economics: principles and applications. Island Press, 2004. 454p.
7. FARIA, A.M.M. Destramando o Tecido do Desenvolvimento: do campesinato à hegemonia do capital agrário na cotonicultura de Mato Grosso. 326 f. Tese de Doutorado, Belém, UFPA/NAEA, Programa de Pós-graduação em Desenvolvimento Sustentável do Trópico Úmido (Área de Concentração: Economia Regional e Desenvolvimento Sustentável), 2008.
8. FBDS – FUNDAÇÃO BRASILEIRA PARA O DESENVOLVIMENTO SUSTENTÁVEL. Práticas de gestão para redução da emissão de gases do efeito estufa e remoção de carbono na agricultura, pecuária e engenharia florestal brasileira. 2009. Disponível em: <<http://www.fbds.org.br/fbds/IMG/pdf/doc-496.pdf>> Acesso em: 08 nov. 2011.
9. GUJARATI, D. Econometria Básica. 4 ed. RJ: Campus Elsevier, 2006.
10. Instituto FNP. Análise do Mercado de Terras, Mai./Jun. 2007. Disponível em <[www.fnp.com.br](http://www.fnp.com.br)>. Acesso em 10 nov. 2011.
11. IBGE – INSTITUTO BRASILEIRO DE GEOGRAFIA E ESTATÍSTICA- SIDRA - Pesquisa Pecuária Municipal, Produção Agrícola Municipal. Séries PIB municipal. Disponível em: <<http://www.ibge.gov.br/>>. Acesso em: 26 jan. 2013.
12. INPE – INSTITUTO NACIONAL DE PESQUISAS ESPACIAIS. Projeto PRODES - Monitoramento da floresta amazônica brasileira por satélite. Disponível em: <<http://www.dpi.inpe.br/prodesdigital/prodesmunicipal.php>>. Acesso em: 15 jan. 2011.
13. ISA – INSTITUTO SOCIOAMBIENTAL – Desmatamento e Agronegócio. Novembro de 2006. Disponível em: <<http://www.socioambiental.org/esp/desmatamento/site/agronegocio>>. Acesso em: 30 out. 2011.
14. LINDOSO, D. “Pegada climática” do Uso da Terra: um diagnóstico do dilema entre o modelo de desenvolvimento agropecuário mato-grossense e mudanças climáticas no período 2001 – 2007. Universidade de Brasília -

- Centro de Desenvolvimento Sustentável. Dissertação de Mestrado. Brasília: 2009.
15. MAPA - MINISTÉRIO DA AGRICULTURA, PECUÁRIA E ABASTECIMENTO. Disponível em: <<http://www.agricultura.gov.br/desenvolvimento-sustentavel/programa-abc>> Acesso em: 30 out. 2011.
  16. MATTOS, L. B. A importância do setor de transportes na emissão de gases do efeito estufa – O caso do município do Rio de Janeiro. Rio de Janeiro, COPPE/ UFRJ, 2001.
  17. MCT - MINISTÉRIO DE CIÊNCIA E TECNOLOGIA. Primeiro inventário brasileiro das emissões e remoções antrópicas de gases de efeito estufa - Informações gerais e valores preliminares. 2004. Disponível em: <[www.mct.gov.br](http://www.mct.gov.br)>. Acesso em 20 nov. 2010.
  18. MCT - MINISTÉRIO DE CIÊNCIA E TECNOLOGIA. Inventário brasileiro das emissões e remoções antrópicas de gases de efeito estufa. 2010. Disponível em: <[www.mct.gov.br](http://www.mct.gov.br)>. Acesso em 20 nov. 2010.
  19. MICOL, L. ANDRADE, J. BORNER, J. Redução das Emissões do Desmatamento e da Degradação (REDD): potencial de aplicação em Mato Grosso. Alta Floresta - MT: ICV, 2008. 92 p. Disponível em: <[http://www.icv.org.br/w/library/redd\\_icv.pdf](http://www.icv.org.br/w/library/redd_icv.pdf)> Acesso em 11 nov. 2011.
  20. PREFEITURA DE BELO HORIZONTE, Inventário Municipal de emissões de gases de efeito estufa – Relatório Final. Dezembro de 2009.
  21. ROMEIRO, A.R. Economia ou economia política da sustentabilidade? Texto para Discussão. IE/UNICAMP, Campinas, n. 102, set. 2001.
  22. SEMA – SECRETARIA DE ESTADO DO MEIO AMBIENTE DE MATO GROSSO– Mudanças Climáticas. Disponível em: <[http://www.sema.mt.gov.br/index.php?option=com\\_content&view=article&id=261&Itemid=379](http://www.sema.mt.gov.br/index.php?option=com_content&view=article&id=261&Itemid=379)> Acesso em 21 set. 2011.
  23. ROMEIRO, A.R., REYDON, B.P, LEONARDI, M.L.A. Economia do meio ambiente: teoria, políticas e a gestão de espaços regionais. Campinas, SP: Unicamp. IE, 2001

24. SEPLAN – SECRETARIA DE ESTADO DE PLANEJAMENTO E COORDENAÇÃO GERAL - Superintendência de Estudos e Informações. Anuários. Disponível em: <<http://www.anuario.seplan.mt.gov.br/>>. Acesso em 10 fev. 2011
25. TEIXEIRA, Maria Daniele. Emissões Antrópicas de Gases de Efeito Estufa e Referenciais para Políticas de Mitigação das Emissões em Mato Grosso. Dissertação de Mestrado. Defendida na Universidade Federal de Mato Grosso em fevereiro de 2012.

## 4. IMAGES AND TABLES

Frame 1 – Necessary information description for research and source data.

Source	Activity Data	Data source
Fuel, stationary and mobile sources	Municipal sales	ANP
Electricity	Total consumption of electricity by City	SEPLAN/MT
Change in land usage	Deforesting increment	INPE
Livestock (cattle e swine)	Number of animals (cattle/swine)	IBGE
Agriculture	Soy farming area	IBGE

Source: Author made (2013).

Frame 2 – Sectors of land usage and change of land usage considered in this paper and its respective GHG emission factors.

Sector		Process	Emission factor (equivalent t CO <sub>2</sub> )
Livestock	Cattle	Enteric digest	1,34 t CO <sub>2</sub> animal/year
		Animals in pasture	0,39 t CO <sub>2</sub> animal/year
	Swine	Enteric digest	0,025 t CO <sub>2</sub> animal/year
		Waste	0,025 t CO <sub>2</sub> animal/year
Agriculture	Soy farming	BNF	0,59 t CO <sub>2</sub> ha/ano
Change of land usage	Deforesting	Transition forest biomass burn	302 t CO <sub>2</sub> ha/ano

Source: Adapted from Primeiro Inventário Brasileiro (2004), In Lindoso (2009).

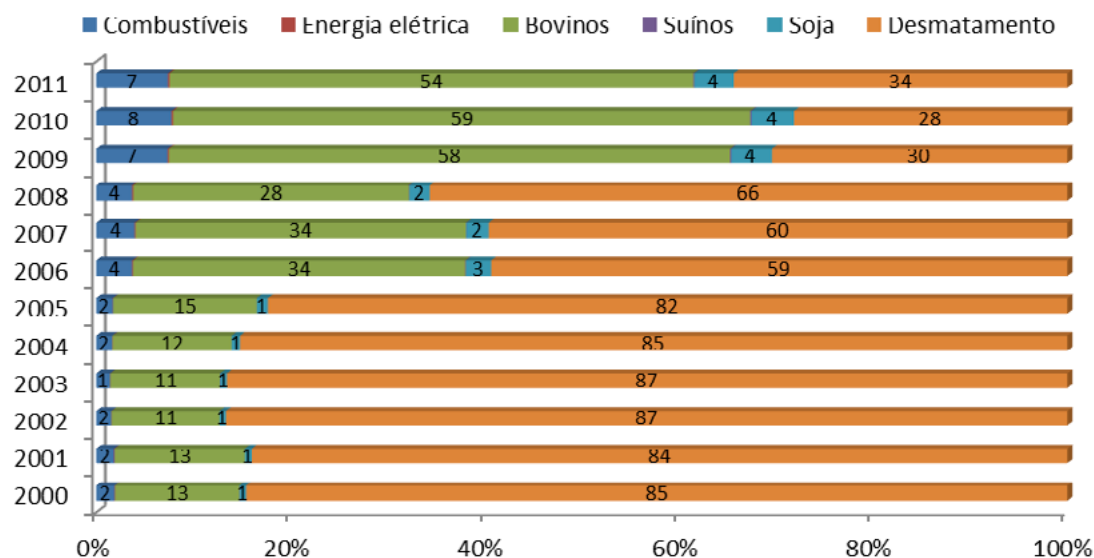
BNF: Biological Nitrogen Fixation.

Tab. 1 CO<sub>2</sub> emissions evolution by Mato Grosso sectors from 2000 to 2011 (thousand tons).

Setor	2000	2001	2002	2003	2004	2005	2006	2007	2008	2009	2010	2011
Combustível	4.801	4.745	5.305	5.361	6.048	5.325	4.876	5.156	5.828	6.020	6.470	6.934
Energia elétrica	123	137	125	101	134	138	128	127	230	122	143*	145*
Bovino	32.739	34.464	38.378	42.582	44.840	46.107	45.091	44.432	45.012	47.328	49.750	50.630
Suíno	42	47	52	56	66	68	72	70	81	93	105	98
Soja	1.715	1.842	2.253	2.605	3.115	3.612	3.435	2.994	3.339	3.441	3.674	3.809
Desmatamento	216.002	216.002	299.225	326.520	311.954	257.162	78.221	77.868	104.220	24.930	23.553	32.251
<b>Total</b>	<b>255.422</b>	<b>257.237</b>	<b>345.337</b>	<b>377.223</b>	<b>366.157</b>	<b>312.412</b>	<b>131.824</b>	<b>130.646</b>	<b>158.710</b>	<b>81.934</b>	<b>83.696</b>	<b>93.866</b>

Source: Research data (2011). \*Estimated data according to the projection methodology showed on the methodology.

Fig. 1 Evolution of percentage distribution of CO<sub>2</sub>e total emissions by Activity sector in Mato Grosso from 2000 to 2011 (%).



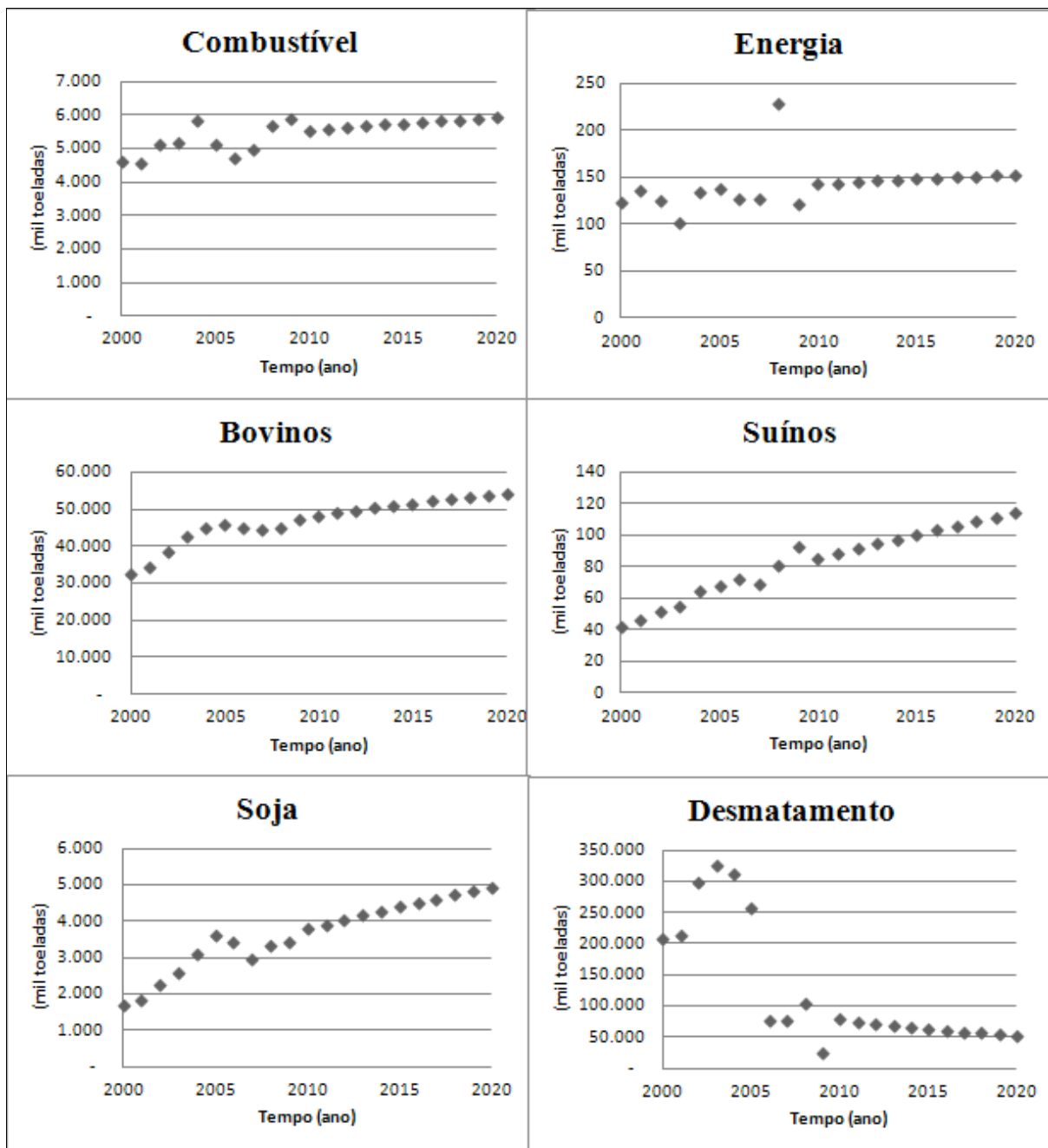
Source: Research data (2011).

Tab. 2 Goals for 2020 of CO<sub>2</sub>e emission mitigate according to NPWC (thousand tons).

Goals	Base year (2005)	Base year (2009)
<b>Reduction of 36,1%</b>	199.530	52.273
<b>Reduction of 38,9%</b>	190.786	49.983

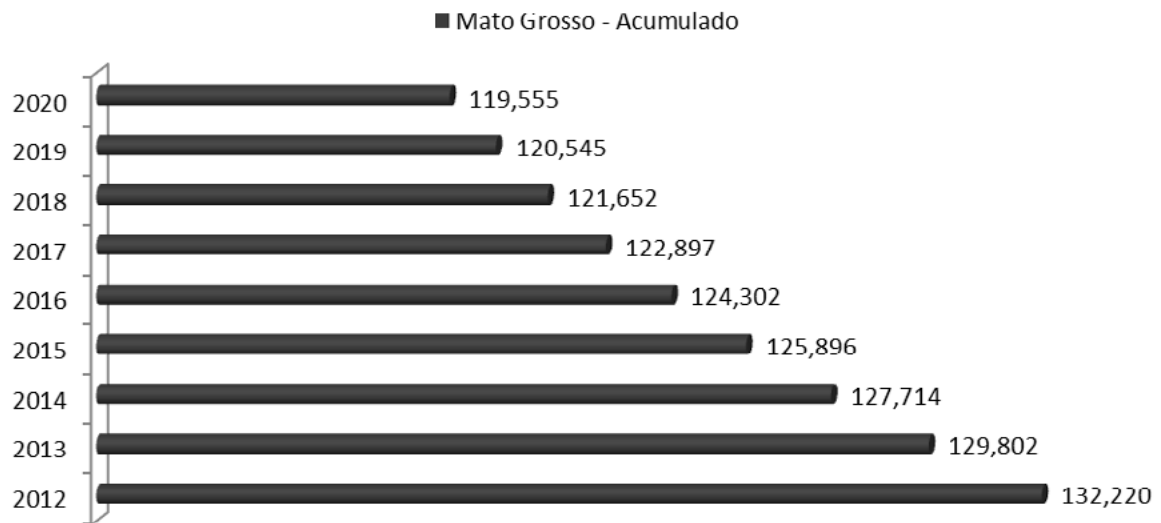
Source: Research data (2011).

Fig. 2 CO<sub>2</sub>e emissions projection by sector in Mato Grosso state (thousand tons).



Source: Research data (2011).

Fig. 3 General CO2e emissions projection in Mato Grosso state (thousand tons)..



Source: Research data (2011).

# CO<sub>2</sub> emissions by a university campus: assessment, uncertainties and reduction strategies

Caserini S.<sup>1\*</sup>, Scolieri S.<sup>1</sup> and Perotto E.<sup>2</sup>

<sup>1</sup>Politecnico di Milano, Department of Civil and Environmental Engineering - Environmental Section - Italia, <sup>2</sup>Politecnico di Milano, Servizio Sostenibilità di Ateneo -Italia

\*Corresponding Author: stefano.caserini@polimi.it

## Abstract

This paper shows the results of a detailed quantification of CO<sub>2</sub> emissions by the “Politecnico di Milano - Leonardo Campus”, one of the largest university campuses in Italy. The assessment considers all direct and the most important indirect emissions, and is based on a comprehensive collection of data provided by facilities of the University and by external companies handling some campus services, as well as CO<sub>2</sub> emission factors used in literature.

Total CO<sub>2</sub> emissions were 21.5 kt/y for the year 2011, with a per capita value of about 1 tCO<sub>2</sub>/person (students, professors and employees). The categories with the highest percentage of emissions are those related to electricity consumption (47%), motorized access to the campus (29%) and heating (15%). The uncertainty analysis, carried out with the error propagation method, allows quantification of the range of variation of the estimate (about  $\pm 4.2\%$  at 95% c.i.).

The results obtained were compared with those of other national and international universities; the comparison shows significantly lower emissions by Italian universities, as compared in particular to campuses in U.S.A.. Lastly, a number of reduction strategies have been identified, aiming to achieve a reduction target of 24% in comparison with emissions in 2011.

**Keywords:** CO<sub>2</sub>, emission, university, uncertainty, mitigation.

## INTRODUCTION

Following a widespread increase in awareness of the importance of the global warming issue, over recent years an increasing number of European and non-European universities have begun to monitor their energy consumption and assess their greenhouse gas emissions. In order to assess how to make their activities more sustainable, they have prepared greenhouse gas emissions inventories and established reduction targets (citare dei rapporti da mettere in biblio, es, Smith et al., 2011) e.g. Yale University, University of Texas at Austin).

In this context, in 2011 the “Politecnico di Milano” and “Università degli Studi di Milano” universities launched the "Città Studi Sustainable Campus" project [1] and joined the International Sustainable Campus Network [2], with the aim of making the Città Studi university district (a 5 km<sup>2</sup> area in the center of Milan) an example for quality of life and environmental sustainability.

Various initiatives have recently been undertaken by the Politecnico di Milano with the purpose of reducing energy consumption and related emissions into the atmosphere (in particular CO<sub>2</sub>). Various activities by the technical areas have begun to monitor and control energy consumption, while other projects addressed to students and staff (e.g. the publication of a behavior code - written in wiki mode) have been undertaken and aim to improve studies focused on the university itself. The work presented in this paper falls into this perspective, and is based on a master thesis that made the first inventory of CO<sub>2</sub> emissions by the Leonardo Campus and proposed a strategic portfolio of actions aiming to reduce CO<sub>2</sub> emissions [3].

### 1. METHODOLOGY AND DATA COLLECTION

The study focuses on the “Leonardo Campus” of the Politecnico di Milano, located in the Città Studi district of Milan, the historical and largest campus of the Politecnico di Milano, covering a floor area of 185,990 m<sup>2</sup> and attended by about 20,000 people, around 17,000 of whom are students. The various types of emissions are divided according to the "Scopes" and the categories defined by WRI/WBCSD GHG Protocol [4] and ISO 14064 [5]. Table 1 lists all the categories analyzed according to the WRI/WBCSD:

Scope 1	Emissions from sources owned or controlled by the university	Motor vehicles owned by Politecnico di Milano (Departments and Central Administration) Combustion in thermal power unit Motorized transport of Central Administration personnel (missions) Motorized transport of Department personnel (missions)
Scope 2	Emissions from energy sources purchased by the university	Electricity consumption
Scope 3	Emissions from sources that do not belong or are not directly controlled by the university	Motorized transport for commuting to the Campus Motorized transport of Erasmus students

Tab. 1 – Emission sources divided according to the GHG Protocol scopes.

In this study, emissions from waste disposal and wastewater, gas coolers and laboratories, and those resulting from the embodied energy in purchased goods and services have not been considered. Data collection in these areas is in fact difficult and inaccurate, and the estimation methodology is still under development. In fact, as shown by similar assessments made by other universities [6, 7, 8], the greatest uncertainties are attributable to these sources. However, a preliminary assessment shows that these emissions are of minor relevance in the case of the Politecnico di Milano.

CO<sub>2</sub> is the only greenhouse gas considered, as in many other similar papers; it accounts for 98% of the total emissions by a university, and its value increases further when analyzing emissions from fossil fuel combustion.

The methodology for estimating emissions is based on the following general formula:

$$E_{tot} = \sum_i (AD_i \cdot EFi) \quad (1)$$

where:

E<sub>tot</sub> = total emission

AD<sub>i</sub> = activity data concerning source i

EF<sub>i</sub> = emission factor concerning source i

Emission factor is defined as the amount of emissions of a given source for a unit of activity of the emitting source. Activity data is a quantity able to describe an emissive activity in the best way, e.g. fuel consumption in the case of combustion, km driven in

case of car use). This formula is thus usable for the various types of categories considered.

Although the study refers to the year 2011, the activity data were collected for previous years too, where possible, with a view to analyzing variability and the factors that most influenced their variations.

To build the emission inventory, it is necessary to find a substantial amount of information and data. It has been a very laborious task, due to the lack of integrated monitoring of consumption and information and due to the fact that it is sometimes impossible to know the real availability and reliability of the data.

The emission assessment is based primarily on detailed data collected from various offices of the university, as well as from external companies that handle some services, such as the biggest heating plants of the campus. Where such data were unavailable, proxy data closely correlated to the activity data were used; otherwise, data gathered from surveys or samples were used. For example, in the case of heating, for some small boilers it was necessary to infer their fuel consumption calculating it from the power of the thermal unit and the equivalent operating hours per year of the source.

For the transport sector, we processed data from a survey carried out in 2010 by the Mobility Management of the university, which made it possible to quantify the annual travel by the teaching staff, researchers, administrative staff and students.

To estimate the emissions due to business travel by teaching staff and researchers (e.g. to attend meetings or conferences), a sample analysis was also conducted in one department (DICA- Department of Civil and Environmental Engineering) and then extrapolated on the basis of the total numbers of permanent staff (including teachers and researchers) of the university.

Emission factors for each type of fuel and method of transportation (e.g., cars, trains, planes) were found in literature [9], in some cases specific for Italy [10] or for the Lombardy region [11].

## 2. RESULTS

The total CO<sub>2</sub> emissions by the Leonardo campus amounts to 21.5 kt/y for the year 2011, with a per capita value of 1.08 tCO<sub>2</sub>/person (considering the teaching staff, non-teaching staff, and students). As shown in Figure 1, the categories with the highest percentage of emissions are those relating to electricity consumption (47%), motorized access to the Campus (29%) and heating (15%).

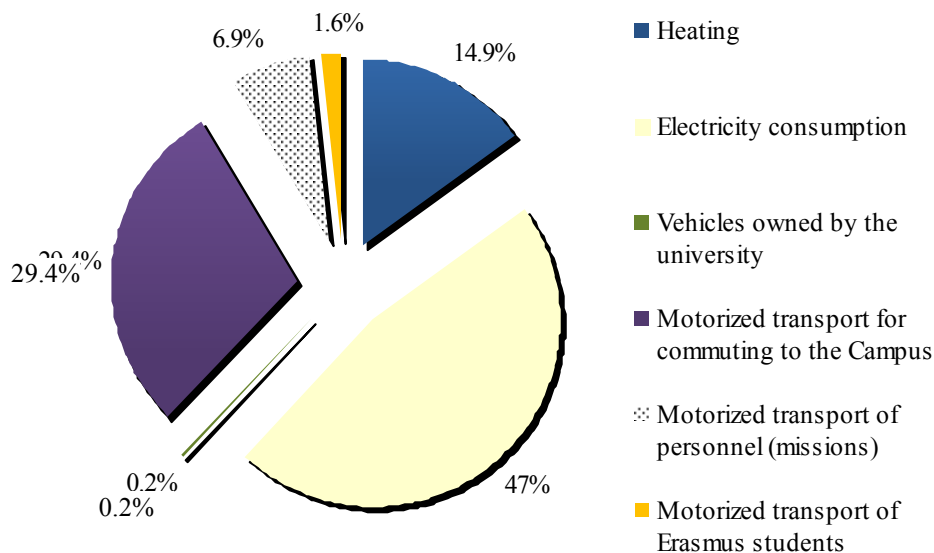


Fig. 1 - Breakdown of total CO<sub>2</sub> emissions by the Leonardo Campus by source.

97% of emissions for heating derive from the use of natural gas in heating plants, while 3% comes from the use of gas oil. These data have been substantially constant over the past 6 years. Of the total 8.2 ktCO<sub>2</sub>/y assessed for motorized access to the campus, 78% is contributed by students and 22% by lecturers, researchers and administrative staff. The largest contribution to emissions from transport [Fig. 2] results from the use of cars (55%) and travel by train (36%). Even though the train is more frequently used (45% of people commuting to the campus travel by train), cars contribute more to CO<sub>2</sub> emissions, due to their higher emission factor in terms of g/pass./km.

The greater part of emissions from business travel by university professors and staff derive from the use of aircraft (87%) and only a minor share is due to travel by car and train (9% and 4% respectively). Consumption of fuel used for vehicles owned by the campus is very limited, although growing, and derives from the use of gas oil (74%), gasoline (19%), methane (5%) and LPG (2%). Finally, total CO<sub>2</sub> emissions for

transport of 'Erasmus students derive mainly from "short haul" flights (routes with mileage less than 3,700 km).

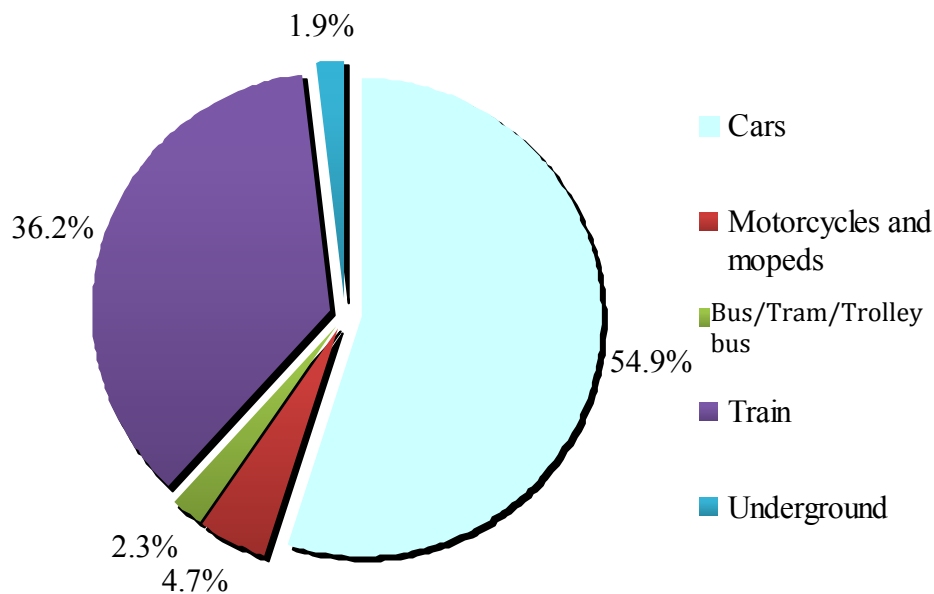


Fig. 2 CO<sub>2</sub> emissions due to differing means of transportation used to access the Leonardo Campus.

### 3. EMISSION UNCERTAINTY

Uncertainty in emission assessment arise from the uncertainties associated with emission factors and activity data. The first depends on how specific and accurate the emission factors are for the analyzed situation, while uncertainty of activity data is related to their availability, the type of procedure for their retrieval and how far these data represent the actual emission source.

Uncertainty associated with CO<sub>2</sub> emissions by Leonardo Campus was assessed using the methodology proposed by the IPCC and currently in use for GHG inventories, based on the error propagation theory [12]. The method is based on a semi-quantitative approach, in which the uncertainty of emission factors and activity data for each type of source is allocated to one of the following five categories:

- Very high uncertainty: ± 20%
- High uncertainty: ± 10%
- Average uncertainty: ± 5 %
- Low uncertainty: ± 3 %

- Very low uncertainty:  $\pm 1 \%$

The definition of these values, based on expert judgment, take into account the assessments of uncertainty of emission factors and activity data available in the National emissions inventory [13] and in the literature [14].

Activity data in the transport sector are more uncertain, while uncertainties due to the emission factors and parameters such as density and heating content of fuels are smaller. After assigning a category of uncertainty to each type of data used for the inventory, the error propagation law was used to estimate the uncertainty of emissions by each single source, and of the total emissions by the Campus. In this method, the uncertainty in absolute and relative terms of a variable E, deriving from the product of two variables AD and EF, can be obtained by the following formulas:

$$E_i = (AD_i \times EF_i)$$

$$u_{E_i} = \sqrt{EF_i^2 \times u_{AD_i}^2 + AD_i^2 \times u_{EF_i}^2}$$

$$u'_{E_i} = \sqrt{u'_{AD_i}^2 + u'_{EF_i}^2}$$

Where:

- Y,  $AD_i$ ,  $EF_i$  = uncertain variable
- $u_{E_i}, u_{AD_i}, u_{EF_i}$  = uncertainty as absolute values
- $u'_{E_i}, u'_{AD_i}, u'_{EF_i}$  = relative uncertainty, where  $u'_{E_i}$  is half of the 95% confidence interval of the total (average value), expressed as a percentage

The error propagation law provides the following formula to estimate the uncertainty of the total CO<sub>2</sub> emissions, that is the sum of emissions from all sources:

$$E_T = (E_1 + E_2)$$

$$u_{E_T} = \sqrt{u_{E_1}^2 + u_{E_2}^2}$$

$$u'_{E_T} = \sqrt{\frac{E_1^2 \times u'_{E_1}^2 + E_2^2 \times u'_{E_2}^2}{(E_1 + E_2)^2}}$$

The relative uncertainty of the total CO<sub>2</sub> emission on the campus is equal to 4.2%, and determines a 95% confidence interval for total emissions between 20.6 and 22.5 ktCO<sub>2</sub>/y [Tab. 2]. The largest contribution to uncertainty comes from the transport sector, in particular from motorized transport used for access to the campus. Overall, the low value of the uncertainty is due to the fact that, although some categories are characterized by high uncertainty, the activity data and emission factors of the two sectors that contribute most to the total emissions (electricity and heating) are quantified with a high accuracy.

	CO <sub>2</sub> emissions (t/year)		Relative uncertainty
	Average	95% c.i.	
Electricity consumption	10,115	9,972 - 10,258	1.4%
Combustion in thermal power units	3,211	3,052 - 3,369	4.9%
Motor vehicles owned by Politecnico di Milano (Departments and Central Administration)	41	40 - 42	2.4%
Motorized transport of Department personnel (missions)	25	22 - 28	10%
Motorized transport for commuting to the Campus	6,354	5,506 - 7,201	13%
Motorized transport of Central Administration personnel (missions)	1,455	1,198 - 1,713	18%
Motorized transport of Erasmus students	343	307 - 379	10%
<b>Total</b>	<b>21,544</b>	<b>20,098 - 22,990</b>	<b>4.2%</b>

Tab. 2 CO<sub>2</sub> emissions by the Leonardo Campus: average value, 95% confidence interval and relative uncertainty.

#### 4. COMPARISON WITH OTHER UNIVERSITIES

Estimated per capita and per unit area emissions from electricity consumption and heating of buildings, are compared with those of Italian and foreign universities. The data used for comparison were collected from literature sources and from information collected directly by the Energy Manager of the universities. The sample of 46 universities (29 in Italy, 10 in other European countries, 5 in U.S.A., 1 in Canada and 1 in Australia), was subjected to statistical analysis to study the variability of data and to identify the presence of outliers.

Electricity and heating consumption shows high variability, due to the influence of several factors such as the type of buildings and their year of construction, the fuel used, the type of installed heating and cooling systems. In addition, the type of university is important; as an example, if in the campus there are Departments of Physics, Chemistry, Engineering, and Medicine, energy consumption increases substantially, due to the presence of laboratories, fume hoods and air handling units for pre-heating.

The climate of the city where the university is located does not seem to be a relevant factor in determining energy consumption; in fact, no correlations were observed between climatic parameters (e.g. heating degree days) and consumption due to heating the university; only where universities in the U.S.A. are concerned is it possible to note a relationship between electricity consumption and the cooling degrees.

The comparison shows first of all that electricity and heating consumptions are higher in foreign universities than in those in Europe and in Italy, both when energy consumptions are expressed in per-capita terms (data available for 22 universities) and per m<sup>2</sup> of floor extension of the campus (data available for 33 universities).

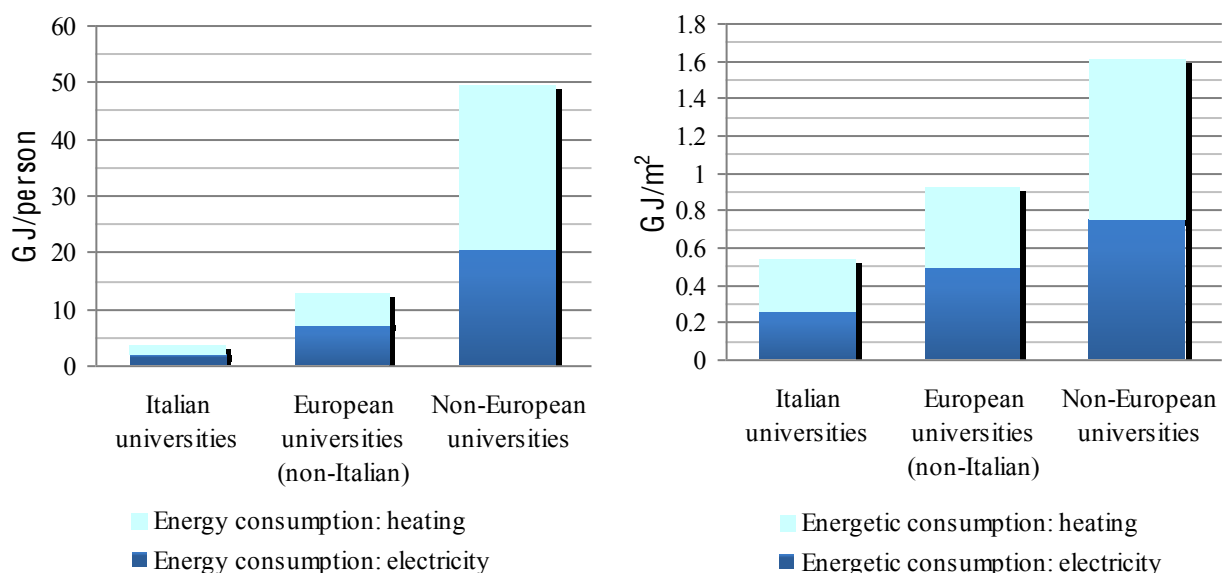


Fig. 3 Comparison of average energy consumption of universities in Italy, Europe and outside Europe.

The emissions of the Politecnico di Milano are placed at a medium/high level in the Italian university context, but are lower than emissions in Europe and significantly lower than those in non-European countries (Figures 4 and 5).

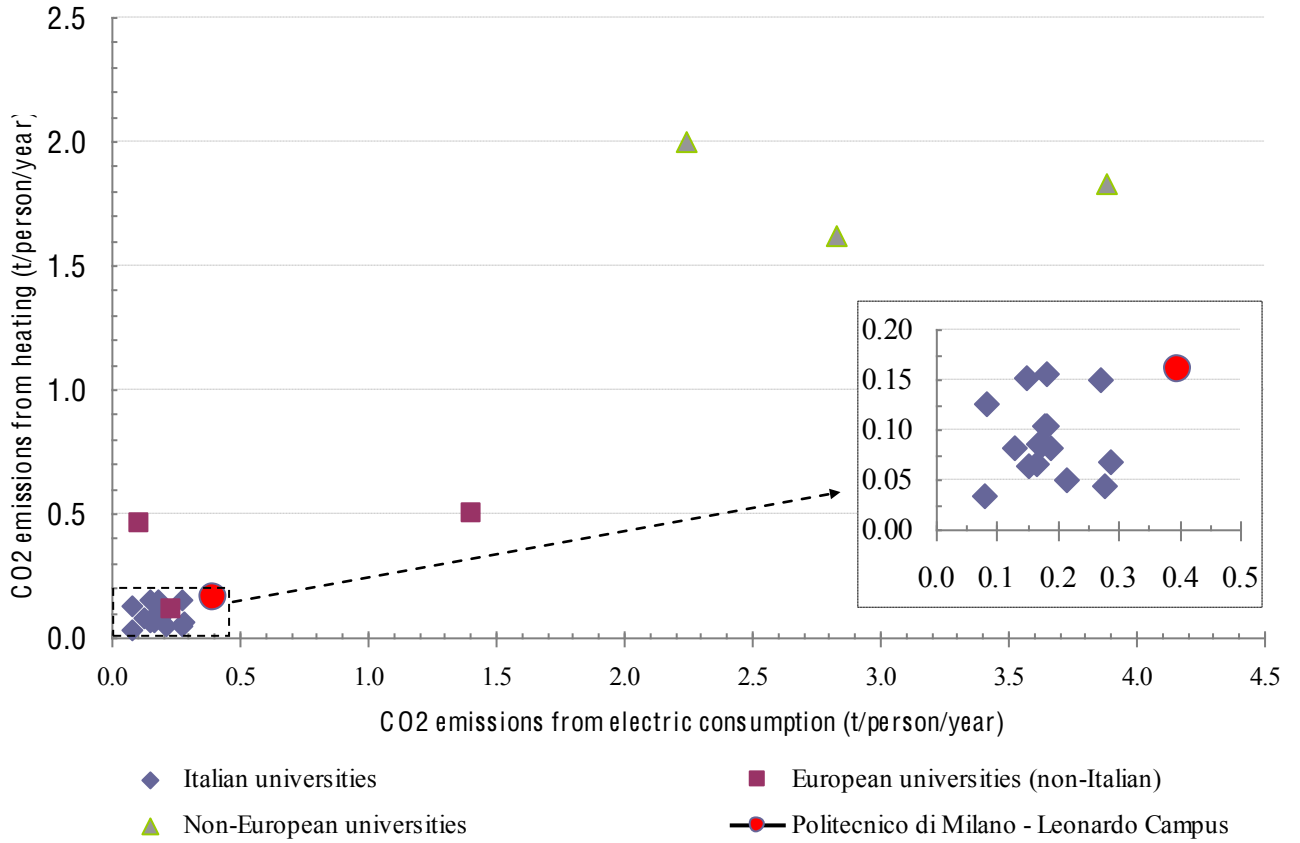


Fig. 4 Comparison of per capita CO<sub>2</sub> emissions from electricity consumption and heating of buildings (t/person/year).

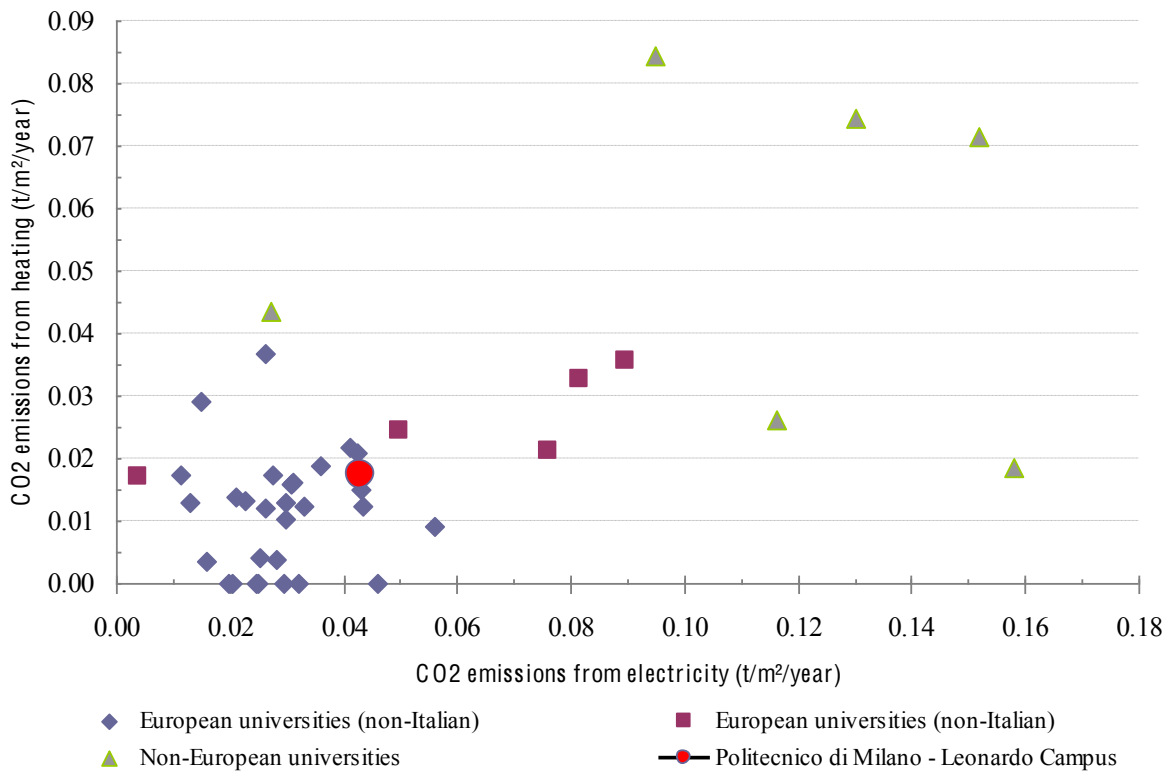


Fig. 5 Comparison of CO<sub>2</sub> emissions per unit area from electricity consumption and heating of buildings (t/m<sup>2</sup>/year).

The average values of CO<sub>2</sub> emissions per capita and per m<sup>2</sup> are shown in the Table 3 below.

	Emission tCO <sub>2</sub> /person			Emission tCO <sub>2</sub> /m <sup>2</sup>		
	min	average	max	min	average	max
Italian universities	0.11	0.29	0.49	0.02	0.05	0.07
European universities (non-Italian)	0.35	0.94	4.45	0.02	0.09	0.13
Non-European universities	4.24	4.80	5.71	0.07	0.17	0.22

Tab. 3. Average value of CO<sub>2</sub> emissions for the sample of Italian, European and non-European universities.

## 5. REDUCTION STRATEGIES

Based on the results, it is possible to make an initial assessment of strategies to reduce energy consumption and motorized travel, and consequently their emissions. The main options considered are measures for energy saving, energy efficiency and operational improvement, as well as minimization of motorized travel.

The main actions focus on plant overhaul, aimed at reducing waste electrical and thermal energy (such as use of window opening sensors, installation of occupancy sensors, diversified curtain opening sensors, installation of daylighting sensors, better distribution of light switches, local regulation of air conditioning terminals, installation of timers), as well as the introduction of a trigeneration plant to produce hot water for central heating, chilled water for air conditioning and electricity.

New measures to reduce business travel by air are provided including the use of video conferencing and increased use of travel by train.

Strong communications and marketing campaigns are planned to reduce the number of people (students, professors, staff) who travel by car to reach the campus. Given that actions that require coordination with other bodies managing transport policies on urban or regional scale are not taken into consideration, it has been assumed that it would be possible to shift 20% of car travel to / from the campus originating from suburban areas, and 30% of that originating in urban areas to train or subway.

Overall, the established emission reduction scenario shows that the actions identified would be able to achieve a 24% reduction in the emissions by the Campus previously

assessed for the year 2011. The action aiming to increase energy efficiency and use of renewable sources provide the largest contribution (73% of the total reduction), while the contribution of plans to cut electricity and heating consumption is smaller. The measures identified in the transport sector lead to a limited reduction, equal to 12% of the total reduction (Tab. 4).

Based on the timeframe for the action, the analysis considers the reductions to be achievable by 2020. In this case, it will be possible to achieve and exceed the emissions target of “-20%”, identified in the “2020 European Energy and Climate Package” and in many commitments by other universities with reference to the year 2020 (e.g.: Yale Univ -43% compared to 2005, Brown Univ -42% compared to 2007, Oxford -33% compared to 2005; Harvard -30% compared to 2006 by 2016).

It may be possible to increase reductions in emissions by the Leonardo Campus by introducing new categories of emissions, such as those included in Scope 3, arising from the life cycle CO<sub>2</sub> emissions of goods and services purchased by the university and from waste disposal.

However, the possibility of easily measuring the electric power consumption, which represents the largest source of CO<sub>2</sub> emissions (even if it is an indirect source), has clear advantages, and will allow monitoring of the achievement of reduction targets in a more accurate and timely manner.

	Reference (2011) kt/year	Scenario with actions kt/year	Change kt/year	% change per sector %	% change of total %
Motorized transport for commuting to the Campus	6.4	6.1	-0.3	-4.0%	5%
Motorized transport of Department personnel (missions)	1.5	1.1	-0.4	-25%	7%
Electricity consumption	10.1	6.3	-3.8	-37%	73%
Heating	3.2	2.4	-0.8	-25%	16%
<b>Total</b>	<b>21.1</b>	<b>15.9</b>	<b>-5.2</b>	<b>-25%</b>	<b>100%</b>

Tab. 4 – Leonardo Campus CO<sub>2</sub> emissions in 2011 and in the scenario with interventions

## 6. CONCLUSIONS

The work shows that it is possible to make a detailed estimate of the CO<sub>2</sub> emissions of a large university with a low level of uncertainty, identifying the sector most responsible for the emissions, in order to define an effective mitigation strategy. CO<sub>2</sub> emissions by the Politecnico di Milano – Leonardo Campus are estimated at about 21.5 kt/y for the year 2011, with an uncertainty of about 4.3%. Per capita and per unit of floor area emissions are aligned with middle-high values of many other Italian universities (of which it has been possible to obtain emission values), but considerably lower than those of non-European universities.

In order to reach a more complete, accurate and updated assessment of CO<sub>2</sub> emissions by all the Politecnico di Milano campuses, it is considered necessary to systematize energy consumption monitoring, creating an integrated database that provides a direct and periodic flow of data. This will also allow us to monitor the effect of the action implemented on CO<sub>2</sub> emissions and the distance from the emission target that could be adopted by the University in the future.

In this context, problems may arise mainly from the monitoring of the data needed for the assessment of CO<sub>2</sub> emissions from motorized travel to the campus, i.e. modal split of student and travel distances. These data are characterized by significantly higher margins of uncertainty, which could only be reduced by specific surveys. Nevertheless, the analysis carried out on the possible reduction strategies shows that this sector, which accounts for about 29% of total emissions, may provide a limited contribution to reducing overall emissions, while more substantial reductions are expected from energy efficiency measures.

## 7. ACKNOWLEDGMENTS

The authors would like to thank Manuela Grecchi for her support and all the staff of the Politecnico di Milano who have provided data and suggestions.

## 8. REFERENCES

1. Città Studi Campus Sostenibile. [www.campus-sostenibile.polimi.it/web/guest](http://www.campus-sostenibile.polimi.it/web/guest).
2. The International Sustainable Campus Network (ISCN). [www.international-sustainable-campus-network.org](http://www.international-sustainable-campus-network.org).

3. Scolieri S. (2012), *Stima delle emissioni di CO<sub>2</sub> delle università: il caso del Politecnico di Milano, Campus "Città Studi*, Politecnico di Milano, A.A. 2011/2012. Relatore: S. Caserini; Correlatori: E. Perotto, M. Grecchi.
4. WRI/WBCSD, *GHG Protocol*. [www.wbcsd.org](http://www.wbcsd.org).
5. ISO 14064:2006, *Greenhouse gases - Part 1, Part 2 and Part 3*.
6. Buttazoni et al., (2005) Inventory and Analysis of Yale University's Greenhouse Gas Emissions
7. Skov J., Toney A., (2009) 2009 Greenhouse Gas Inventory-University of Texas at Austin.
8. Ozawa-Meida L., Brockway P., Letten K., Davies J., Fleming P.,(2011) Measuring carbon performance in a UK University through a consumption-based carbon footprint: De Montfort University case study. *Journal of Cleaner Production*, 3, 1-14.
9. IPCC (2006) Volume 2: Energy, In: 2006 IPCC Guidelines for National Greenhouse Gas Inventories (eds Eggleston S, Buendia L, Miwa K, Ngara T, Tanabe K).
10. ISPRA, (2011) Fattori di emissione per la produzione ed il consumo di energia elettrica in Italia.
11. ARPA LOMBARDIA (2008) Fattori di emissione medi da traffico in Lombardia nel 2008. [www.inemar.eu](http://www.inemar.eu)
12. IPCC (2000) Good Practice Guidance and Uncertainty Management in National Greenhouse Gas Inventories, Intergovernmental Panel on climate Change, Task Force on National Greenhouse Emission Inventories.
13. ISPRA (2011) National Inventory Report. Istituto Superiore per la Ricerca Ambientale, Roma,
14. Romano D. (2005) Evaluating uncertainty in the Italian GHG Inventory. In. IN EEA, 2005, Proceedings of the EU workshop on uncertainties in greenhouse gas inventories. 5 - 6 September 2005, Helsinki, Finland

**Mitigation Policies & Strategies**

**Low carbon finance**

# The Role of Public-Private Partnerships (PPPs) in Scaling Up Financial Flows in The Post-Kyoto Regime

Galluccio G.<sup>1</sup>

<sup>1</sup> Centro Euro-Mediterraneo sui Cambiamenti Climatici – Italy

\*giulia.galluccio@cmcc.it

## Abstract

The climate change agenda requires in the near future adequate financial flows in order to support mitigation and adaptation efforts and the low –carbon development of emerging and new economies. The potentials of Public-Private Partnerships (PPPs) - as a risk sharing structure in order to bring private funds on the table - are presented in the new climate change context, offering a fresh contribute to the discussion of climate finance and public finance practitioners.

The paper, based on the analysis of a panel data of two decades (1990-2011), first presents global evidence that international climate agreements are among the key drivers of PPP renewable energy investments in developing countries, second it discusses and provides recommendations on PPPs as a good financing model to mainstream climate change into the development agenda of emerging and less-developed economies.

**Keywords:** Public-Private Partnership, PPP, climate change finance, infrastructure

## 1. INTRODUCTION

The 17th UNFCCC Conference of the Parties (COP) held in Durban in 2011 reaffirmed the urgency of adequate financial flows in order to support both mitigation and adaptation efforts. In this occasion, convened Parties confirmed the commitment to reach the financial goal of 100 billion USD investments per year by 2020 from developed to developing countries.

For the first time, this year, IPCC in its Fifth Assessment Report includes a specific chapter on Cross cutting investment and finance issues and states, with medium evidence and high agreement, that: *Resources to address climate change need to be scaled up considerably over the next few decades both in developed and developing countries*<sup>1</sup> [28]

Recognizing that a global effort is needed to enhance ambition and close the current gap effectively, participants to the COP highlighted several ways in which this could be achieved, including the role of national governments, international cooperation, the private sector and how to mobilize resources.

In a period of shrunk public resources, the emphasis given to the potential role of the private contribution appears obvious.

As a form of cooperation between the private and public sector, the public-private partnerships are not a new phenomenon or a new way of doing public policy. To incorporate the technical expertise, innovation, the financial capability, cost-effectiveness and economic efficiency of the private sector when providing public goods and services is not an idea of the last century.

The involvement of private sector in the traditional public policy investment has met with different degree of acceptance and resistance during the world development history. There has been a golden age of concessions contracts in Europe during the century following the industrial revolution; it was the time of the expansion of cities, of the development of public services for the water and energy supply and of the construction of big transport networks. Private entrepreneurs were deeply involved in

---

<sup>1</sup> Chapter 16, Working Group III contribution to the IPCC 5th Assessment Report "Climate Change 2014: Mitigation of Climate Change

the creation of railways at that time and the concept of involving and promoting the private enterprise was well supported by the new ideals brought by the French Revolution. [5]

In particular, PPPs are connected to the infrastructural development of countries. Countries like Italy, Spain and France, they all have utilised the PPP model in order to develop their national transport system<sup>2</sup>, the quality of which is often used as criterion to judge the country's competitiveness. Data from the Private Participation in Infrastructure (PPI) project database of the World Bank and the Public-Private Infrastructure Advisory Facility (PPIAF) shows a steadily growth of investments in infrastructures in the developing countries [Fig. 1] and national PPP programs account for a large share of investment<sup>3</sup>.

Notwithstanding the low recovery faced by the developed countries, developing nations are expected to continue to grow and will need massive investments in energy, urban systems, transport, agriculture. There is scope for developing countries to invest in a low-carbon future without sacrificing their growth.

## 2. AIM OF THE STUDY

The present work focuses on PPPs opportunities in developing countries and on the role that PPPs can play in meeting their development goals.

Existing literature on this issue is in fact very limited. International Finance Corporation (IFC), the "private" arm of the World Bank has dedicated the second issue of its quarterly journal on PPPs "Handshake" to climate change. Other studies include the work done by PPIAF in its role of disseminating PPPs knowledge. Three years ago PPIAF introduced climate change among its strategic themes. Since then, the activities conducted on PPPs and climate change seem to be limited in numbers and mainly related to pilot studies. Furthermore, despite the PPIAF PPI project database represents a unique and well-acknowledged web resource on PPPs, the

---

2 In 2011 68,8% (in terms of value) of PPP calls published in Italy is related to the transport sector (Presidenza del Consiglio dei Ministri, 2011)

3 According to a published IMF Working Paper, the total capital value of PPP in Korea was equal to the 6.7% of GDP at the end of 2008, while in Portugal was equal to the 5.6% at the end of 2007. For South Africa, Peru, and Canada the figures for 2008 are smaller: respectively 1.7%, 2.6% and 1.4% of GDP. (IMF, 2009)

climate change aspect of those projects is either not evaluated, or highlighted to a limited extent.

The present study aims to offer a contribution to this research area, providing advice to PPP facilities and practitioners on the investment needs generated by the climate agenda on the one hand, and advising the climate policy circle on a concrete instrument to support the climate action through private participation.

### **3. METHODOLOGY**

The study provides an in-depth analysis of the existing PPPs activities and an evaluation of their role in the climate change affected sectors.

The most comprehensive is the PPIAF database, a collection of more than 6000 projects in developing countries.

An “internal” version of the PPI project database (last update on August 15th 2012) has been kindly provided by the PPIAF to the author. For the first time, data from 1990 to 2011 are used and analysed according to several dimensions. The availability of this updated dataset, allowed an evaluation of the very recent trends registered in the energy, water and transport sectors, tracking the immediate effects of the 2008 and still on-going financial crisis.

After having analysed and assessed the dimension of the overall phenomenon, the study focuses on some selected case studies of PPPs project “climate change labelled”.

In order to select the most representative case studies, we reviewed the publicly available project portfolios of PPIAF, IFC Climate Change Group and the Climate Investment Funds, including Climate Investment Fund (CIF) programmes like the Clean Technology Fund (CTF) and the Scaling Up Renewable Energy Program in Low Income Countries (SREP).

All of the selected projects can be viewed as “best practices”. We attempted to identify key elements of success along the projects development cycle: PPPs policy framework and governance, financing mechanism, role of advisers, procurement management, contract management, climate change co-benefits.

#### 4. THE PPPs DATA ANALYSIS

The aim of this section is to assess the magnitude of the overall PPPs phenomenon, more particularly to assess whether and in which sectors the PPP model has been used in order to realize projects with a climate change mitigation or adaptation co-benefit.

In order to present the current evolution of PPPs we used the most comprehensive database available, the Private Participation in Infrastructure (PPI) Database<sup>4</sup>. The PPI Database is managed by the World Bank and the Private-Public Infrastructure Advisory Facility (PPIAF). The PPI database offers a collection of more than 6000 infrastructure projects in developing countries. Its purpose is to identify and disseminate information on private participation in infrastructure projects in low- and middle-income countries, as classified by the World Bank, recording data on the contractual arrangements used to attract private investment, the sources and destination of investment flows, and information on the main investors<sup>5</sup>.

The PPI Database we used for this work is the version updated on August 15<sup>th</sup> 2012 kindly provided by the PPIAF Team<sup>6</sup>. The database records 5598 infrastructure projects from 1990 to 2011 with a total investment commitments equal to around US\$ 2,260 billion.

We analysed a representative sample of 4324 PPP projects operating in sectors that are affected by climate mitigation and adaptation policies, such as the energy, water and transport sector.

Tables below illustrate the selection we performed on the PPI database according to the well defined criteria and give a first outlook to the existing PPP projects in climate affected sectors. [Tab. 1, Tab. 2, Tab. 3]

The selected sample include 4,324 projects for total investment commitments of 1,212,935 millions of US\$. Out of these projects, 352 projects have been classified in

---

4 <http://ppi.worldbank.org/index.aspx>

5 See PPI Database Expanded methodology available at [http://ppi.worldbank.org/resources/ppi\\_methodology.aspx](http://ppi.worldbank.org/resources/ppi_methodology.aspx)

6 The August 15<sup>th</sup> 2012 version contains further details on renewable energy projects. Those data have been gathered in a separate database made publicly available on September 2012 at <http://ppi-re.worldbank.org>

the pipeline since they haven't reached the financial closure yet, but are in an advanced development stage<sup>7</sup>.

As expected, the energy sector still represents by far the largest share of the sample, followed by the transport sector, both in terms of numbers of projects (respectively 54% and 30%) and investment values (respectively 63% and 30%). [Fig. 2]

Concerning the types of contract, 60% of the projects follow under the greenfield category (55% in terms of investment value), while another 30% are concession contracts (more than 31% in terms of investment value), the remaining being lease contracts and partial divestiture. [Tab.1 ]

Concerning the geographical coverage, the East Asia and Pacific region registers the largest share in terms of number of projects (almost 35%), while the Latin America and the Caribbean has the largest share in terms of investment commitment value (36%). The two African regions together with Middle East, North Africa and Middle East and Sub-Saharan Africa remain last, attracting in the area only the 0.07% of the total number of projects and investments. [Tab. 2]

The largest share of the number of projects is related to operational and under construction projects (respectively 63% and 20%). Another 8% of project numbers are currently under development since they haven't reached the financial closure in 2011 but they are in advanced stage of development. Only the 5% are related to project cancelled or distressed<sup>8</sup>, while the 3% of the sample is related to concluded projects. [Tab. 3]

The in-depth analysis of trends and characteristics of the selected sample provided us with the following main findings:

- The analysis performed of the two decades panel data presented global evidence that international climate agreements are among the key drivers of PPP energy investments in developing countries.
- In particular, the energy sector represents an important arena for the PPP private players; these, in turn, can represent an important resource for the

---

<sup>7</sup> All projects in the pipeline follow under the energy sector and they account for around 54,700 millions of US\$ (constant 2011 US\$).

<sup>8</sup> A project is categorised as distressed when the exit of the private sector has been formally requested or a major dispute is ongoing. ([http://ppi.worldbank.org/resources/ppi\\_methodology.aspx](http://ppi.worldbank.org/resources/ppi_methodology.aspx).)

policy makers involved in the deployment or in the definition of a developing country climate agenda.

- Future energy investments electricity generation segment in the renewable sector will exceed the investment in the fossil fuels energy sectors, thus showing the evidence of a progressive switch toward low-carbon sources of energy. [Fig 3]
- PPPs in renewable energy have been traditionally used for the construction of large hydro projects (>50MW), looking at future trend [Fig 4], private investors in pipelines projects seems to prefer to be engaged in PPPs in the wind power sector, followed by large hydropower plants. Results are consistent with IEA [21], which foresees a shift from hydro to wind in the renewable sources development in non-OECD countries.
- The presence of PPP CDM projects shows the role played by the carbon market in stimulating private investments in the renewable sector [Fig 5]
- On the contrary, PPP investments in water and transport infrastructures appeared not stimulated by the implementation of the Kyoto Protocol and by the international discussion on climate change policies [Fig 6].

## 5. THE CASES STUDIES ANALYSIS

As a complement to the numerical analysis for each sector we selected a best case study, each of them highlighting specific features leading to success. We then added a worst-case analysis in the water sector, which nevertheless turned out after few years in a learning platform for the local authorities.

More in particular the following case studies were analysed:

- Manila Water Company (Manila East), Philippines, Concession for build, rehabilitate, operate and transfer (BROT), Philippines, year of financial closure 1997
- Maynilad Water Services (Manila West), Philippines, Concession for build, rehabilitate, operate and transfer (BROT), year of financial closure 1997
- Ouarzazate Concentrated Solar Power Station, Morocco, Concession for build, own, operate and transfer (BOOT), year of financial closure 2012

- Kuala Lumpur Stormwater Management and Road Tunnel (SMART), Malaysia, Concession for build, operate and transfer (BOT), year of financial closure 2003
- Cochabamba Aguas del Tunari concession, Bolivia, year of financial closure 1999 (project cancelled in 2000)

The case studies in the respective sectors showed the unlocked potentials of well-managed PPP projects in terms of contributing to climate adaptation objectives and they further relevant thoughts to the data analysis helping us to formulate the following recommendations:

#### *Mainstreaming the climate change issue*

The PPP model is already part of the adopted solution when referring to infrastructure investments. In an ideal context, climate change issues should be simply mainstreamed in the decision making process. Long-term investment policies such as national infrastructure investment plans or national development policies may effectively incorporate climate change considerations within the decision-making variables – as it is already happening in some developed country, like UK. Nevertheless, especially when referring to the developing countries, the “perfect” mainstreaming could conceal the climate change objectives, thus risking to lose the capacity to attract financial resources locked for the climate agenda.

#### *Integration of climate and PPP practices*

MDBs, development finance institutions and PPP expertise centres play an important “marketing” role in implementing PPPs in developing and emerging nations. They are also at the front-line in their role of advisers, long-term finance provider and promoters of a sound investment environment for climate related activities, directly or through their participation in climate funds. Still, there is small emphasis on the contribution to climate change adaptation and mitigation policies that can be provided through the adoption of a PPP model. More integration among the climate and PPP practices already existing would be desirable.

#### *Implementation of databases*

Following the adoption of transparency principles, a number of databases are today available tracking the development finance institutions activities, highlighting either their role as private investment stimulus, or as climate investment stimulus. A better integration of databases, and the creation of a specific climate PPPs focus would help future research and dissemination of lessons learned.

### *Ad-hoc climate change PPPs*

Policy makers shall promote the right investment for the right objective. In general focusing investment promotion on a few sectors attracts more resources. Policy makers shall work out the ultimate objectives they want to achieve bearing in mind that one cannot serve all. Ad hoc sector oriented climate change PPPs promotion should be adopted by governments and PPPs focal points in order to take advantage of most promising sectors. Furthermore, the formal development of climate change action plans can help in identifying and prioritizing the climate objectives per sector that can be achieved through the PPP model. The development of National Adaptation Plans (NAPs) or National Appropriate Mitigation Actions (NAMAs) can be the right actions for calling the private sector's contribution to the public interest, providing them with a portfolio of possible PPP projects.

### *Targeting success areas*

The climate action is calling developed and developing countries to change their development model, adopting new and sometimes innovative solutions. If mitigation recalls the adoption of new technologies, adaptation recalls a pure sense of ingenuity. In both cases the private party can bring in the partnership the right skills and expertise to put needs into reality.

The case studies reinforced the evidence on the PPP ability to catalyse the private investment in high technology projects. However, the sustainability of a business model largely depends on the ability to demonstrate benefits on-the-ground. When prioritizing a list of actions it is important to first target those areas that will quickly and easily demonstrate success. This will help to build the right investment environment for the future more innovative initiatives. CDMs can serve as example in the climate context.

### *Climate does not change PPPs governance rules*

Pursuing climate change objectives through the adoption of a PPP, will not alter the PPP good governance rules. Setting an effective PPP framework made of a sound, legal, regulatory and institutional environment remain essential. The private party is traditionally able to pick the business opportunities, as soon as they appear available, nevertheless building the right perception is crucial: the proposed climate PPP project shall be perceived as part of a formal, transparent and predictable selection, evaluation, implementation and monitoring process.

## 6. CONCLUSION

There is a vast literature on PPP's management principles on one side, and a huge literature is emerging on the climate finance needs. However, if we exclude the today mature discussion on the Kyoto Protocol market based mechanisms, only limited efforts have been made to investigate existing business models capable to attract the private party into investment activities, characterised by high public interest and higher business risk, like the climate mitigation and adaptation projects.

The PPP business model, by its nature, brings private and public parties together in a long-term formal union, where both parties cooperate during the whole life of the project. Such form of cooperation therefore represents a good framework in order to involve the private sector (usually acting with a shorter time frame) in climate related investments that require a long-term perspective.

PPPs, which have been extensively used in the past to promote the countries infrastructure development, today represent an interesting business model that need to be more extensively explored in its capacity to serve the implementation of the climate mitigation and adaptation agenda of developing nations. In the near future, policy makers will take more and more into account the opportunities offered by PPPs to best combine the public and private interest, while the climate action plans will represent for the private investors a new "good business" opportunity to bring their ingenuity and innovation.

## 7. ACKNOWLEDGMENTS

Insert your acknowledgments here; do not place them on the first page of your paper or as a footnote.

## 8. REFERENCES

1. AfDB. (2012). Ouarzazate Solar power Station - Phase I. Project Appraisal Report.
2. AfDB, ADB, EBRD, EIB, IDB, WB, et al. (2012). Joint MDB Report on Adaptation Finance 2011.
3. AfDB, ADB, EBRD, EIB, IDB, WB, et al. (2012). Joint MDB Report On Mitigation Finance 2011.
4. Bechtel. (2005, 03 16). Tratto il giorno 01 30, 2013 da [http://www.bechtel.com/2005-03-16\\_38.html](http://www.bechtel.com/2005-03-16_38.html)
5. Bezançon, X. (2004). 2000 ans d'histoire du partenariat public-privé: Pour la réalisation des équipements et services collectifs. Paris: Presses de l'École Nationale des Ponts et Chaussées.
6. Bonnardeaux, D. (2009). The Cochabamba "Water War": An Anti-Privatisation Poster Child? .
7. Buchner, B., Falconer, A., Hervé-Mignucci, M., Trabacchi, C., & Brinkman, M. (2011). The Landscape of Climate Finance. Venice: Climate Policy Initiative.
8. Climate Change Commission. (2011). National Climate Change Action Plan: 2011-2028. Metro Manila: Climate Change Commission.
9. Climate Investment Funds. (2011). Climate Investment Funds: Lessons Learned from Private Sector Interventions through MDB Intermediaries. Joint Meeting of the CTF and SCF Trust Fund Committees, Washington DC.
10. Delmon, J. (2011). Public-Private Partnership Projects in Infrastructure. New York: Cambridge University Press.
11. Delmon, J. (2010). Understanding Options for Public-Private Partnerships in Infrastructure Sorting out the forest from the trees: BOT, DBFO, DCMF, concession, lease... (Policy Research Working Paper 5173 ed.). Washington DC: The World Bank.

12. Dumol, M. (2000). *The Manila Water Concession. A Key Government Officials Diary of the Worlds Largest Water Privatization.* Washington DC: The World Bank.
13. Dutz, M., Harris, C., Dhingra, I., & Shugart, C. (2006). *Public-Private Partnership Unit. What are They, and What do They Do? Public Policy for the Private Sector (Note 311) .* Washington DC: The World Bank.
14. Economic Planning Unit. (2010). *Tenth Malaysia Plan.* Prime Minister's Department, Putrajaya.
15. Farquharson, E., Torres de Mästle, C., Yescombe, E., & Encinas, J. (2011). *How to Engage with the Private Sector in Public-Private Partnerships in Emerging Markets.* Washington DC: The World Bank.
16. Farrugia, C., Reynolds, T., & Orr, R. J. (2008). *Public-Private Partnership Agencies: A Global Perspective.* Collaboratory for Research on Global Projects. Stanford: Stanford Univeristy.
17. Forrer, J., Kee, J. E., Newcomer, K. E., & Boyer, E. (2010). *Public–Private Partnerships and the Public Accountability Question.* *Public Administration Review* (May-June), 475-484.
18. Gusztáv Klados, Y. H. (2007). *Stormwater management and road tunnel (SMART).* In H. R. Barták (A cura di), *Underground Space – the 4th Dimension of Metropolises.* London: Taylor & Francis Group.
19. IEA. (2012). *Energy Technology Perspectives 2012 Pathways to a Clean Energy System.* Paris: OECD/IEA.
20. IEA. (2011). *World Energy Outlook 2011.* Paris: OECD/IEA.
21. IEA. (2012). *World Energy Outlook 2012.* Paris: OECD/IEA.
22. IFC. (2011). *Handshake. Issue #1.* Washington DC: International Finance Corporation.
23. IFC. (2011). *Handshake. Issue #2.* Washington DC: International Finance Corporation.
24. IFC. (2010). *IFC Advisory Services in Public Private Partnerships. Lessons from Our Work in Infrastructure, Health and Education.* Washington DC.

25. IMF. (2006). Determinants of Public-Private Partnerships in Infrastructure. (M. Hammami, J.-F. Ruhashyankiko, & E. Yehoue, A cura di) Washington DC: International Monetary Fund.
26. IMF. (2004). Public-Private Partnerships. [www.imf.org/external/np/fad/2004/pifp/eng/031204.pdf](http://www.imf.org/external/np/fad/2004/pifp/eng/031204.pdf), Fiscal Affairs Department. Washington DC: International Monetary Fund.
27. IMF. (2009). The Effects of the Financial Crisis on Public-Private Partnerships. Fiscal Affairs Department. Washington DC: International Monetary Fund.
28. IPCC. (2014). Contribution of Working Group III to the Fifth Assessment Report of the Intergovernmental Panel on Climate Change, 2014. (O. Edenhofer, et al.) Cambridge, United Kingdom: Cambridge University Press,.
29. Leitman, J., & Bishop, V. (2011). Concessional Climate Finance: MDB Experience and Opportunities. Washington DC: The World Bank.
30. Marin, P. (2009). Public-Private Partnerships for Urban Water Utilities. Washington DC: The World Bank.
31. Ministry of Natural Resources and Environment Malaysia. (2011). Malaysia's Second National Communication. Putrajaya.
32. Nickson, A., & Vargas, C. (2002). The Limitations of Water Regulation: The Failure of the Cochabamba Concession in Bolivia. *Bulletin of Latin American Research*. Society for Latin American Studies , 21 (01), 99-120.
33. OECD-DAC. (2012, June). Factsheet: OECD DAC statistics on climate-related aid (pdf). Tratto il giorno September 10, 2012 da OECD: <http://www.oecd.org/dac/aidstatistics/FactsheetRio.pdf>
34. PPIAF. (2011). 2011 Annual Report.
35. PPIAF. (2012). Government Support to Public Private Partnerships: 2011 Highlights (PPI data update note 78 ed.).
36. PPP Center. (2012). Developing Public Private Partnerships in Local Infrastructure and Development Projects A PPP Manual for LGUs. Quezon City.

37. Presidenza del Consiglio dei Ministri. (2011). Relazione al CIPE sull'attività svolta nel 2011 dall'Unità Tecnica Finanza di Progetto (UFTP). Dipartimento per la programmazione e il coordinamento della politica economica, Roma.
38. Sanghi, A., Sundakov, A., & Hankinson, D. (2007). Designing and Using Public-Private Partnership Unit in Infrastructure: Lessons from Case Studies around the World. Washington DC: PPIAF.
39. Savas, E. S. (2000). Privatization and Public-Private Partnerships. New York: Chatam House.
40. UNECE. (2008). Guidebook on Promoting Good Governance in Public-Private Partnerships. Geneva: United Nations.
41. UNICEF, & WHO. (2012). Progree on Drinking Water and Sanitation 2012. New York: UNICEF and World Health Organization.
42. UNISDR. (2009). The Development of a Public Partnership Framework and Action Plan for Disaster Risk Reduction (DRR) in Asia. Bangkok: UNISDR Secretariat Asia and the Pacific.
43. United Nations. (2010). Report of The Secretary-General's High-Level Advisory Group on Climate Change Financing . New York: United Nations.
44. UNSSC and NCPPP. (2008). Examples of Successful Public-Private Partnerships. Volume 15 of series Sharing Innovative Experiences. United Nations Office for South-South Cooperation and the National Council for Public-Private Partnerships. New York: UNDP.
45. URS. (2010). Adapting Energy, Transport and Water Infrastructure to the Long-term Impacts of Climate Change (Vol. Ref. No RMP/5456). URS Corporation Ltd.
46. Vagliasindi, M. (2012). Key Drivers of PPPs in Electricity Generation in Developing Countries (Policy Research Working Paper 6118 ed.). Washington DC: The World Bank.
47. Waterlinks - News and Events. (2011, June 3). Tratto il giorno January 30, 2013 da Waterlinks: <http://www.waterlinks.org/news/palm-beach-county-and-manila-water-operators-initiate-twinning-partnership-climate-change-adapt>

48. WBI and PPIAF. (2012). Public-Private Partnerships. Reference Guide. Washington DC: The World Bank.
49. World Bank. (2008). Development and Climate Change: A Strategic Framework for the World Bank Group. Washington DC: The World Bank.
50. World Bank. (2011). Project Appraisal Document on a proposed loan in the amount of US\$200 million and a proposed Clean Technology Fund loan in the amount of US\$97 million to the Moroccan Agency for Solar Energy (MASEN) with the guarantee of the Kingdom of Morocco for the Ouarzazate I Concentrated Solar Power plant project. Report No: 64663-MA.
51. World Bank. (2010). World Development Report 2010. Washington DC: The World Bank.

## 9. IMAGES AND TABLES

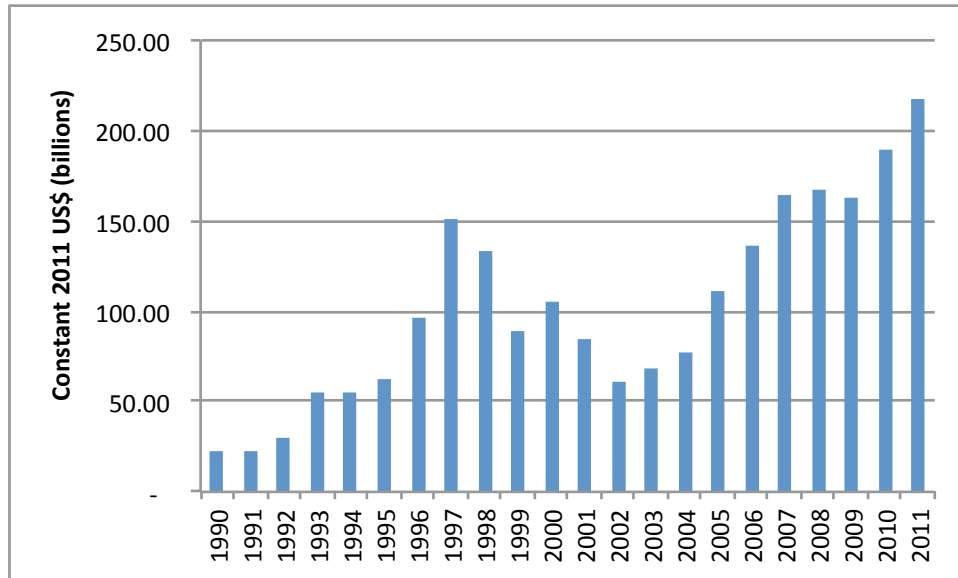
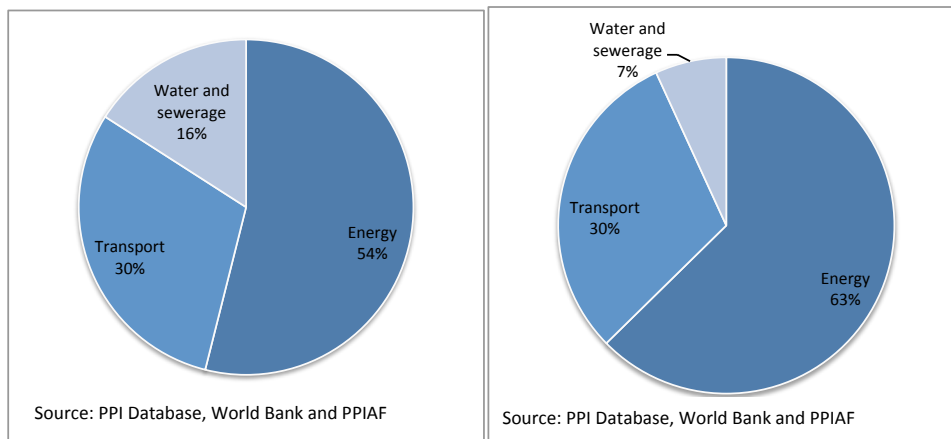


Fig. 1 Investment commitments to PPI in developing countries, 1990-2011  
 Source: PPI Database, World Bank and PPIAF



a) number of new projects

b. total investments commitments

Fig. 2 Total PPPs sample by sector

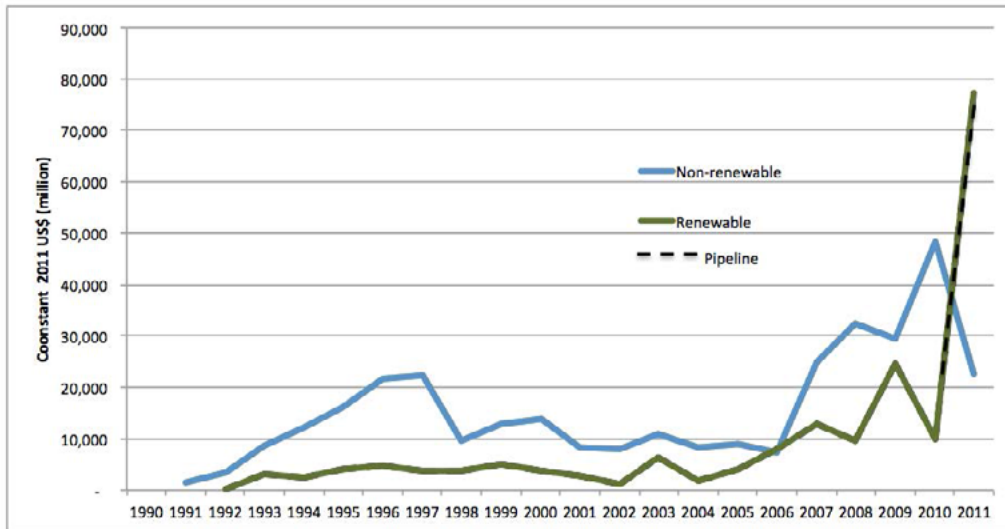


Fig. 3 Renewable and non-renewable PPP energy projects in the electricity generation segment (total annual investment commitments -including pipeline)

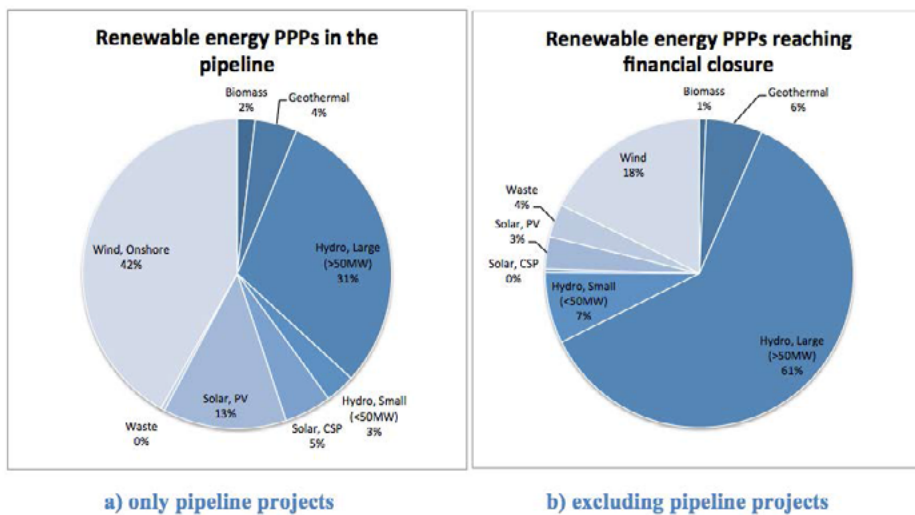


Fig. 4 PPPs investments in renewable energy generation by energy sources

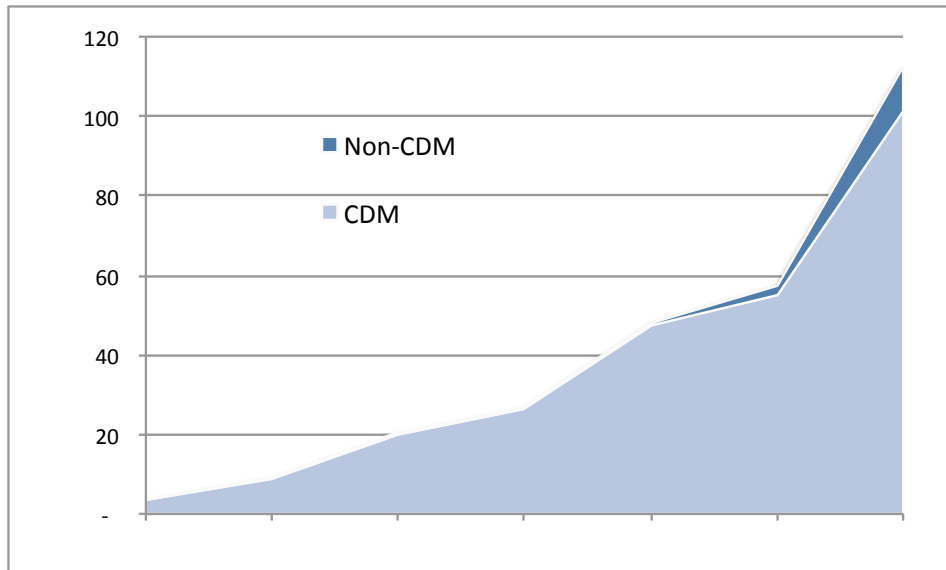


Fig. 5 Installed capacity (GW) of PPP and CDM projects in renewable energy in the period 2005-2011

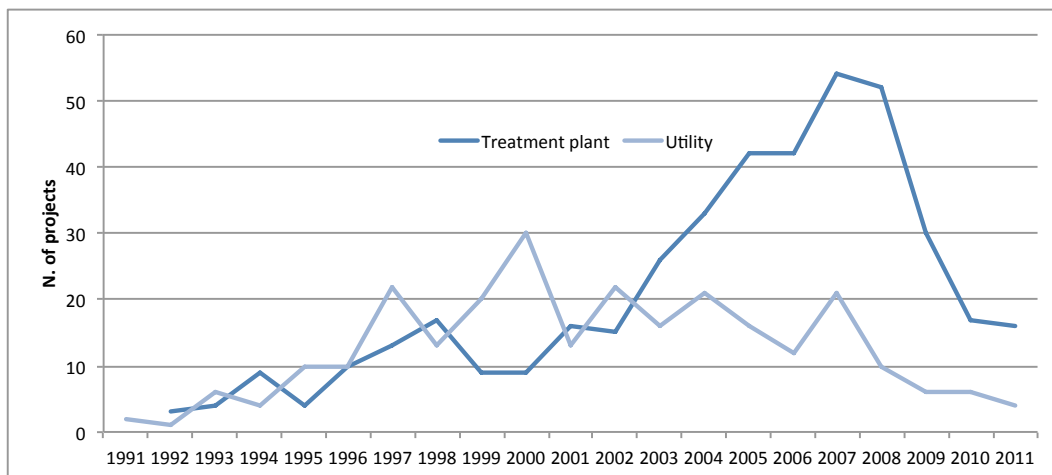


Fig. 6 Water PPPs trends by main sub-sector

PPP contract type	Energy		Transport		Water and sewerage		Total	
	N. of projects	Total Investment commitment	N. of projects	Total Investment commitment	N. of projects	Total Investment commitment	N. of projects	Total Investment commitment
Concession	202	125,406	792	204,082	295	52,943	1,289	382,431
Partial divestiture	290	116,420	57	18,909	24	11,203	371	146,532
Greenfield project	1,823	517,548	428	141,191	318	17,425	2,569	676,164
Lease contract	17	494	26	5,760	52	1,554	95	7,807
<b>Total</b>	<b>2,332</b>	<b>759,867</b>	<b>1,303</b>	<b>369,941</b>	<b>689</b>	<b>83,126</b>	<b>4,324</b>	<b>1,212,935</b>

Table 1 Selected PPPs projects by contract type and sector (number of projects and total investment commitments in constant 2011 US\$ million)

Region	Energy		Transport		Water and sewerage		Total	
	N. of projects	Total Investment commitment	N. of projects	Total Investment commitment	N. of projects	Total Investment commitment	N. of projects	Total Investment commitment
East Asia and Pacific	745	182,100	352	102,184	410	39,159	1,507	323,443
Europe and Central Asia	408	113,710	58	23,418	33	4,170	499	141,299
Latin America and the Caribbean	631	249,786	461	151,200	212	35,046	1,304	436,032
Middle East and North Africa	38	28,520	27	7,873	13	4,033	78	40,426
South Asia	377	153,755	315	68,309	7	391	699	222,455
Sub-Saharan Africa	133	31,995	90	16,958	14	327	237	49,280
<b>Total</b>	<b>2,332</b>	<b>759,867</b>	<b>1,303</b>	<b>369,941</b>	<b>689</b>	<b>83,126</b>	<b>4,324</b>	<b>1,212,935</b>

Table 2 Selected PPPs projects by region and sector (number of projects and total investment commitments in constant 2011 US\$ million)

Status	Energy		Transport		Water and sewerage		Total	
	N. of projects	Total Investment commitment	N. of projects	Total Investment commitment	N. of projects	Total Investment commitment	N. of projects	Total Investment commitment
Canceled	63	17,402	61	26,132	47	23,464	171	66,998
Concluded	39	6,633	46	3,712	15	705	100	11,050
Construction	447	194,694	242	82,161	169	8,756	858	285,611
Distressed	27	24,560	12	4,183	12	5,731	51	34,474
Merged	55	149	-	-	-	-	55	149
Operational	1,349	461,551	942	253,752	446	44,470	2,737	759,774
Under development	352	54,878	-	-	-	-	352	54,878
<b>Total</b>	<b>2,332</b>	<b>759,867</b>	<b>1,303</b>	<b>369,941</b>	<b>689</b>	<b>83,126</b>	<b>4,324</b>	<b>1,212,935</b>

Table 3 Selected PPPs projects by status and sector (number of projects and total investment commitments in constant 2011 US\$ million)

# The Landscape of Public Climate Finance in Indonesia

Ampri I.<sup>1</sup>, Falconer A.<sup>2\*</sup>, Wahyudi N.<sup>1</sup>, Rosenberg A.<sup>2</sup>, Ampera B.<sup>1</sup>, Tuwo A.<sup>3</sup>,  
Glenday S.<sup>3</sup>, Wilkinson J.<sup>2</sup>

<sup>1</sup>Ministry of Finance - Indonesia, <sup>2</sup>Climate Policy Initiative - Italy, and <sup>3</sup>Climate Policy Initiative - Indonesia

\*Corresponding Author: [angela.falconer@cpivenice.org](mailto:angela.falconer@cpivenice.org)

## Abstract

Public policy and finance will play a crucial role in meeting Indonesia's economic growth and greenhouse gas emissions reduction targets. International and domestic public actors are now scaling up investment, and different levels of Indonesian government are setting up frameworks to incentivize the private finance that will undoubtedly also be required. Understanding which public actors are investing, through which instruments, what they are investing in, and for what reasons, is therefore essential. By identifying what is already happening on the ground, we provide a baseline against which to measure progress and plan scale up. We also reveal investment patterns that allow us to pinpoint where the biggest barriers and opportunities exist.

We identify at least IDR 8,377 billion (USD 951 million) of climate finance from public sources disbursed in Indonesia in 2011. This falls below Indonesian government estimates of the level of annual finance required by 2020 to meet emission reduction targets. However, both domestic and international public and private flows are expected to grow in the next few years as comprehensive national policies on climate change are fully implemented.

The study also provides an insight into the significant methodological challenges in tracking and collecting climate finance data in Indonesia.

**Keywords:** climate finance, Indonesia, public finance

## 1. TEXT

Indonesia's desire to drive economic growth and reduce climate risk is reflected in the sweeping policy reforms it has introduced in recent years to meet targets announced in 2009 to reduce greenhouse gas emissions. It is aiming for a reduction of 26% on business as usual levels by 2020, or of 41% with international support.

Public policy and finance will play a crucial role in meeting these targets. International and domestic public actors are now scaling up investment, and different levels of Indonesian government are setting up frameworks to incentivize the private finance that will undoubtedly also be required. Understanding which public actors are investing, through which instruments, what they are investing in, and for what reasons, is therefore essential. By identifying what is already happening on the ground in Indonesia through this report, we provide a baseline against which to measure progress and plan scale up. We also reveal investment patterns that allow us to pinpoint where the biggest barriers and opportunities are.

The Landscape of Public Climate Finance in Indonesia, conducted by the Indonesian Ministry of Finance's Fiscal Policy Agency and Climate Policy Initiative (CPI) breaks new ground. It is the first time CPI has undertaken a landscape in a developing country. It is valuable both as an overview of public climate flows in Indonesia, and an insight into the significant methodological challenges in tracking and collecting this information.

At least IDR 8,377 billion (USD 951 million) of climate finance from public sources was disbursed in Indonesia in 2011. This figure of 2011 expenditure falls below Indonesian government estimates of the level of annual finance required by 2020 to meet emission reduction targets. However, both domestic and international public flows are expected to grow in the next few years as comprehensive national policies on climate change mitigation (RAN-GRK) and adaptation (RAN-API) are fully implemented.

### **Domestic Public Climate Finance**

National public resources sit at the center of Indonesia's climate finance landscape. In 2011, the Government of Indonesia contributed by far the largest share, disbursing

at least IDR 5,526 billion (USD 627 million) or 66% of public climate finance, through budget transfer instruments.

The bulk of domestic climate finance (almost 75%) supported essential “indirect” activities, such as policy development, research and development, establishment of measuring, reporting and verification systems, and other enabling environments. These activities will drive the future scale up and effective allocation of finance by laying the foundation for “direct” mitigation projects. The Government of Indonesia’s focus on indirect activities makes sense given its role in developing and implementing policies and frameworks to stimulate direct investments. With the RAN-GRK framework only introduced in late 2011, high spending rates on indirect activities was to be expected in this period while national policy frameworks were established, but could be expected to reduce in the medium term.

In terms of indirect activities, most support was targeted at the forestry sector (73%), with another 10% targeted at agriculture and 7% focused on energy. This focus aligns with the fact that a high percentage of Indonesia’s emissions come from the land sector. Finance for direct mitigation was also targeted to some of the highest emitting sectors, including transport (35%), waste and waste-water (26%), agriculture and livestock management (27%), and energy (10%). However, to date, little finance for direct mitigation has flowed to forestry and land use. Direct adaptation finance went mostly to disaster risk management.

In 2011, the principal instrument used to transfer money from the state budget was budget expenditures (IDR 5,975 billion or USD 678 million). This amount included international money received by central government and channeled directly into the state budget. These flows were disbursed mainly to central government ministries and agencies (97%), with expenditures to local governments making up a very small proportion. Despite the fact that most climate actions will need to be implemented at the local level, available information indicates that there are blockages to the smooth flow of domestic climate finance to local government. Urgent work is needed to understand how to support timely, efficient and effective scale up of public climate finance at the provincial and district level.

In addition to budget transfers, the central government made investments, mostly through equity participation in state-owned enterprises (not estimated in this study) and revolving funds (IDR 1,266 billion or USD 144 million) to support projects and

activities that generated revenues. However, only IDR 30 billion were disbursed out of the revolving funds to project activities in 2011. This gap between financial transfers into the revolving funds and realized disbursements suggest they are not currently operating as intended. Further work is needed to understand why, and what improvements might unlock flows.

### **International Public Climate Finance**

International development partners added significantly to domestic public resources by contributing an estimated IDR 2,851 billion (USD 324 million) to public climate finance flows. The majority (68%) of international climate finance went to fund direct mitigation and adaptation projects happening on the ground. A large share of this (55%) went directly to state-owned enterprises and the private sector (mostly in the form of loans). The remaining 32% of international public climate finance went to support indirect activities by central and local governments (e.g. policy development) and organizations involved in capacity and knowledge building, including private consultancies, international organizations and NGOs.

International resources were split almost evenly between grants and loans. Loans went to support infrastructure projects with direct mitigation and adaptation benefits (e.g. a geothermal power plant, and a drainage rehabilitation project), while grants were directed to building enabling environments and other forms of readiness. Disbursements were lower than commitments reflecting challenges for development partners operating in Indonesia and for the Government of Indonesia to absorb resources at scale or pace.

### **Alignment of Climate Finance with National Priorities**

Overall, domestic and international public finance resources appeared to be well aligned with Indonesia's future policy needs and priority sectors. The sectoral focus of mitigation activities in 2011 was already closely aligned with emerging national level plans, such as the RAN-GRK. Some of the most emission intense sectors benefit from the highest share of direct and indirect climate finance, including forestry (41%), energy (19%), agriculture and livestock management (10%), transport (9%), and waste and waste water (7%). As early finance flows favor indirect actions such

as policy development and enabling environments, this preference suggests Indonesia is positioning itself well to scale up action in the most important sectors.

## **Recommendations**

Taking into account these high-level findings, we offer the following recommendations:

### **Opportunities to increase the flow of climate finance into projects**

Designing a dedicated instrument to link national government climate plans and sub-national expenditures may accelerate delivery of flows to Indonesia's regions. National public resources have the potential to drive and impact the future effectiveness of the overarching system. Central and local governments can play complementary roles - policy is decided at the national level, while outcomes are delivered and tracked locally. In this respect, readiness at subnational level is an important issue. The bulk of future climate actions will need to be implemented at the local level, but there are challenges in disbursing funding to regions to support climate activities, and currently, no dedicated instrument or mechanism.

Indonesia's public financial management framework provides a foundation for ensuring that international public grants and loans support country-led priorities. In 2011, international development partners directed the bulk of their spending at priority sectors, clearly trying to align support with Indonesia's priorities. However, most international climate finance was disbursed through non-government actors (68%) and was often not reported appropriately within the Ministry of Finance system. As such, the Indonesian Government had limited scope to oversee how and where international climate finance was directed. Reporting international climate finance through the existing governance framework would enable the Ministry of Finance to better direct international finance to support priority sectors.

Designing emerging multilateral funds to effectively link both developing countries' climate change priorities (including Indonesia's) on one side and funders' objectives on the other may help to scale up multilateral flows. Our analysis shows that in 2011,

bilateral finance (which made up 90% of international flows) flowed more readily in Indonesia than multilateral finance, suggesting partner countries' respective interests were better aligned. Ongoing efforts to finalize governance arrangements for the Green Climate Fund (GCF) may benefit from a closer examination of bilateral governance frameworks and lessons they may offer for the new international climate funding framework.

### **Opportunities to Improve Climate Finance Tracking**

There are multiple opportunities to improve how climate finance is tracked and reported in most sectors and at most levels of activity. Efforts are already underway to strengthen current reporting systems. Based on our experience with tracking climate finance in Indonesia we highlight the following measures that could support efforts to raise the level and standard of reporting, and help to more comprehensively track flows:

Detailed guidance on how to determine what activities are climate specific, particularly in relation to adaptation. This challenge is not unique to Indonesia. However, urgent work is required to clarify definitions and how they should be applied at the activity level in Indonesia. In the absence of such guidance, our study showed that key actors were unable to verify potentially large amounts of climate specific finance.

A single national system or database for systematically collating comparable information from the full spectrum of actors. Such a system would greatly increase the comparability of information on climate finance, and also enable the Ministry of Finance to direct different finance flows more effectively.

Clearer, more detailed, and more readily accessible guidelines to explain existing and emerging reporting requirements, including simplified and consistent reporting templates. Further simplification and training on reporting requirements for all actors would lower barriers to accurate reporting. Tailored guidelines would be especially beneficial for international development partners and local government, where it is currently most challenging to track expenditure and its impacts.

## Methodological Issues

Understanding the significance of our findings on public finance flows in Indonesia we must also highlight three crucial limitations:

We anticipate the introduction of the national action plan for climate change in late 2011 and roll out to the sub-national level will stimulate an increase in climate-specific finance in the coming years. Our study is focused on the year 2011 because it was the most recent year for which a comparatively comprehensive data set on public spending was available for all actors, and as such also provides a useful baseline for future similar studies.

The scope of our study captures only the public part of the overarching climate finance and hence, only part of total climate finance flows in Indonesia. CPI's Global Landscape of Climate Finance reports confirm that private finance contributes a majority of total climate finance flows, a situation that may also be the case in Indonesia. One study by the Pew Environment Centre estimated more than USD 1,000 million of investment in clean energy assets in Indonesia in 2011.

Although this study makes significant inroads in coding state budget for climate action, building on and expanding the Ministry of Finance's Mitigation Fiscal Framework (MoF, 2012) [2], we were unable to verify a large volume of public climate flows that may be highly relevant. This was largely due to challenges in classifying certain development activities as climate specific. In particular, the uncertainty regarding adaptation activities is very significant, reflective of a larger global issue in tracking adaptation versus development finance. In total, we identified, but were unable to verify, approximately IDR 10,008 billion (USD 1,136 million) that may be contributing to climate outcomes.

## 2. REFERENCES

1. Ampri I, Falconer A., Wahyudi N., Rosenberg A., Ampera B., Tuwo A., Glenday S. & Wilkinson J. (2014), *The Landscape of Public Climate Finance in Indonesia*. An Indonesian Ministry of Finance and CPI report (forthcoming). Executive Summary at: <http://climatepolicyinitiative.org/publication/landscape-of-public-climate-finance-in-indonesia-3/>.

- MoF (Indonesian Ministry of Finance) (2012), *Indonesia First Mitigation Fiscal Framework*. In support of the National Action Plan to Reduce Greenhouse Gas Emissions. Jakarta: Government of Indonesia, Ministry of Finance. Available from: [http://www.climatefinance-developmenteffective-ness.org/images/stories/Indonesia\\_MFF\\_report.pdf](http://www.climatefinance-developmenteffective-ness.org/images/stories/Indonesia_MFF_report.pdf)

### 3. IMAGES AND TABLES

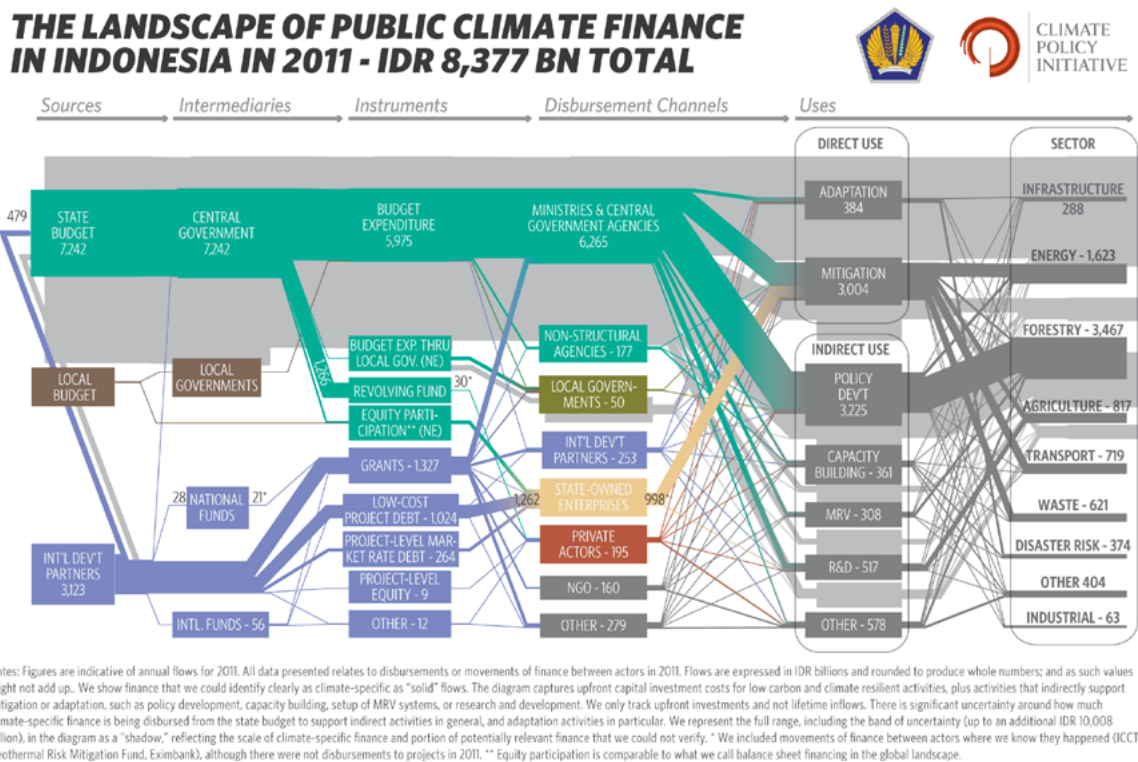


Fig. 1 The Landscape of Public Climate Finance in Indonesia in 2011

# Public-Private Partnerships in Green Energy Infrastructure Investments

Alloisio I.<sup>1</sup>

<sup>1</sup>FEEM, ICCG, CMCC - Italy

\* isabella.alloisio@feem.it

## Abstract

The potential of Private Public Partnerships (PPPs) for accessing finance and reducing capital expenditure (capex costs) of energy infrastructure projects becomes more and more important in a time of shrinking financial resources, which have widened the gap between public and private funding. Economic recession has limited national budget spending and the lending capacities of commercial banks for the realization of infrastructure projects in the field of energy generation, transmission and distribution. These, as capital intensive projects, require high up-front investment and long-term commitment with variable returns into the future. The private and public sectors can reach a mutually beneficial agreement through a PPP: the private sector needs guarantees to face risks entailed in the time gap between the project's planning phase and its actual implementation, whereas the public sector needs capital investment and management expertise. According to the IEA New Policies Scenario, world's projected energy consumption will require more than \$40 trillion in cumulative investment in energy supply over the period from 2014 to 2035, where \$6.8 trillion in power transmission and distribution lines, and \$5.8 trillion of investments in renewable energy generation. With approximately \$71 trillion in managed assets in OECD in the end of 2010, institutional investors such as pension funds and insurance companies are a very promising source of funding.

**Keywords:** Public-Private Partnerships, Energy Infrastructure, Risk Sharing, Internal Rate of Return, Value-for-Money

## 1. INTRODUCTION

The 2008 financial crisis significantly restrained the capacity of banks to lend financial resources in terms of volume, cost, and duration across many sectors, including the power sector, a situation which caused many renewable energy projects to be postponed until market conditions improved. The subsequent economic crisis also endured a series of consequences on the energy market, ranging from lower commodity prices to reduced demand forecasts. Nevertheless, renewable energy has maintained its attractiveness for banks and equity investors, and new funds have been raised throughout the whole crisis period. While in late 2008 and early 2009 investments in renewable generation fell much lower than those for other types of generating capacity [1], and global investment in renewable energy fell 3% during 2009, it rebounded strongly in 2010 and 2011, when it reached \$260-290 billion [2]. Interestingly, in the developed countries, where the financial crisis hit hardest, investment generally dropped 14%, while renewable energy investment continued to grow in developing countries [3]. In 2012, 25,954 MW of renewable energy projects with private participation reached financial closure in developing countries, with total project costs of \$46,390 million [4]. In this economic and financial framework, Public-Private Partnership (PPP) becomes the most valuable instrument for green energy projects financing capable of overcoming the shrinkage of available financial resources. Cooperation between private and public actors is pivotal in an investment decision, since they compensate each other to their mutual advantage: the private sector needs guarantees to face the risks entailed in the time gap between a project's planning phase and its actual implementation, and the public sector needs capital investment and management expertise. Debt and equity are the two major sources for investments in renewable energy projects and a well-structured combination of these two is the key to a healthy investment climate. This is true especially with regard to the financing of energy infrastructure projects, where challenges for access to capital can be greater, given the large investment requirements and the long-term investment horizon. This paper attempts to answer the following research questions: which financial instruments are best for tackling the credit crunch and fostering the development of energy infrastructure? Would equity come from infrastructure funds or institutional investors, such as pension funds or insurance companies?

## 2. PUBLIC-PRIVATE PARTNERSHIPS: A DEFINITION

Although there is no broad international consensus about what constitutes a PPP, this can be defined as an organizational form that originated from the rapprochement between governments and private enterprises. It involves contractual arrangements for designing, financing, producing or operating public projects [5]. Although these organizational forms vary with national governance systems, PPPs present common features that allow them to be defined as follows: any long-term association between distinct legal and administrative entities in the public and private sectors for the pursuit of ends they would not be able to attain efficiently, effectively, economically, or equitably on an individual basis [6]. The World Bank has provided a similar definition: a long-term contract between a private party and a government agency, for providing a public asset or service, in which the private party bears significant risk and management responsibility [7].

This definition encompasses a PPP that provides new assets and services (greenfield), and one that is structured for existing assets and services (brownfield). PPP includes many contracts in many sectors and for many services, provided that there is a public interest in the provision of the service, and that significant risk and management responsibility have been transferred to a private party. The distinctive characteristic of a PPP is that it builds on a long-term relationship and an extensive series of agreements between the public and private sectors with the aim of realizing a project of public interest. Thus, public services provided entirely by the public sector, or passed on to the private sector through full divestiture (privatization), cannot be considered a PPP.

Public-Private Partnerships can take a wide range of forms varying in the degree of involvement of the private entity in a traditionally public infrastructure [8]. A PPP generally takes shape as a contract or agreement outlining the responsibilities of each party and clearly allocating risk. If risk is the main driver of supply and demand for finance, risk sharing is the fundamental characteristic of a PPP agreement because it facilitates the commitment of the public actors and at the same time the attractiveness of investment by the private actors. Risk sharing is even more important in green infrastructure investments, which are typically characterized by higher risk perception because of the relative immaturity of technologies, markets, and industries, and uncertainty about public policy. Therefore, policy and regulatory

risks (certainty over long-term infrastructure planning, risk of corruption in the budding process), market risks (business risks due to more competitors, change in consumer preferences), and technological risks (the risk of technology failure, obsolescence, under-performance) add to already existing financing and liquidity risks (luck of funding and the variation of the cost of capital). On top of that there is also a country risk, especially in the case of developing countries, where the perception of risk is higher than in developed countries and financing risks are higher because of immature financial institutions and markets.

The graph below [Fig. 1] depicts the spectrum of PPP agreements and the entire range of ownership structure and investment responsibility, which is a very important factor that needs to be clearly determined in advance of a PPP agreement.

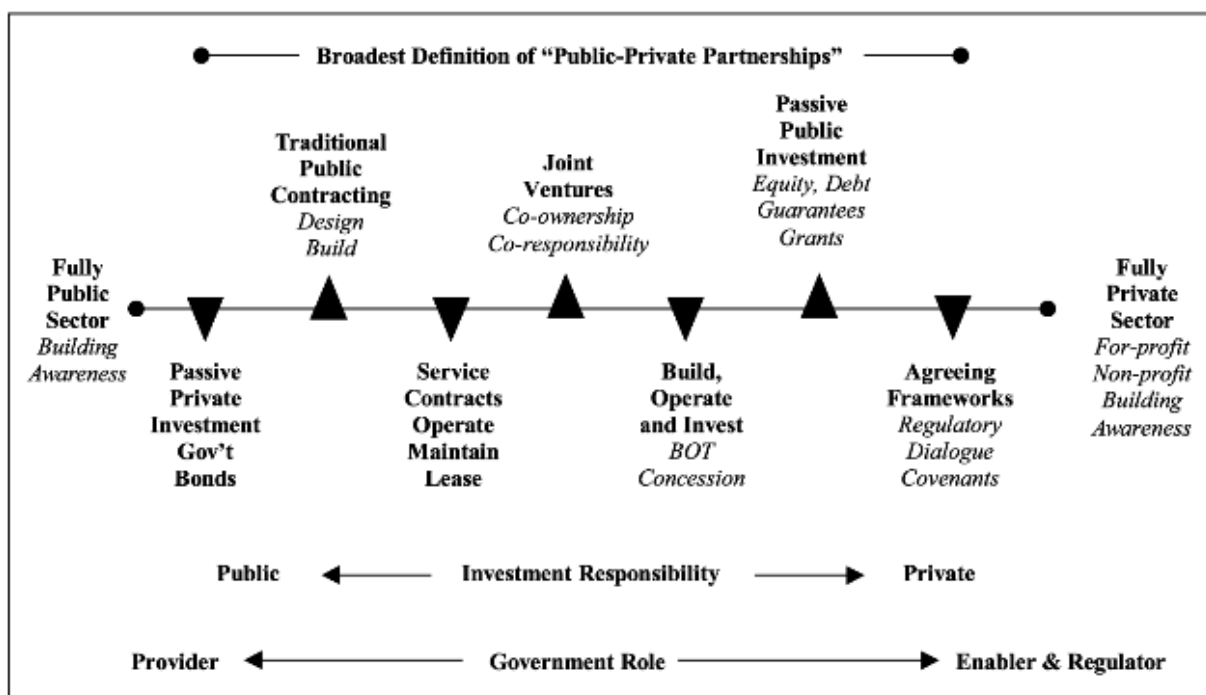


Fig. 1 PPP agreements, ownership structure and investment responsibility [9]

When discussing brownfield and greenfield investments, the crucial issue is the balance between the pre-existing shareholders' interests and the need to make new investments and attract new investors. Another important factor is effective regulation whose stability and straightforwardness are essential for the well-being of PPP agreements. In the energy sector, Italy, for example, has been able for a certain

period of time to attract foreign investments to invest in Italian utilities, especially in renewable energy projects. Nevertheless, the uncertainty in the policy framework and the fear of retroactive measures, put a lot of strains in renewable energy investments in Italy, and in particular in the photovoltaic sector. Last but not least, the issue of the quality of the project, which needs to be useful for the whole community and to have a long-run strategy. Because of the higher political instability in developing countries, investors are particularly reluctant to invest in projects with a long-term investment horizon, such as those in energy infrastructures. Indeed, financing low carbon infrastructure in economies lacking a good track record in low carbon technologies requires long-term financing and therefore faces significant risks.

### **3. BENEFITS AND CHALLENGES OF INFRASTRUCTURE PUBLIC-PRIVATE PARTNERSHIPS**

A growing number of governments from development and developing countries are using PPPs as a way to supplement limited public sector funding and in order to meet the growing demand for infrastructure development. But fiscal leveraging is not the only reason why governments look to the private sector to help them fostering infrastructure development. There are a number of other reasons [Fig. 2]:

1. Exploring PPPs with the aim of bringing additional sources of knowledge and technology solutions for innovation by the private sector and thus providing better public services through improved operational efficiency.
2. Using PPPs as a way of gradually exposing governments and state-owned enterprises to increasing levels of private sector participation (especially from foreign direct investments - FDI).
3. Achieving long-term value-for-money through delivering a service to the private sector in the most efficient way commensurate with acceptable cost limits and meeting an effective demand for services.
4. Ensuring budgetary certainty of the infrastructure projects' costs over time from its design to its operations and maintenance, thus incentivizing appropriate and gradual risk transfer to the private sector and on time and within budgets delivery of projects.

5. Making PPPs conducive to developing local private sector capabilities through joint ventures with large international firms.

6. Contributing to remove barriers to infrastructure innovation as infrastructure markets are monopolistic by nature and tend not to stimulate investments by new incumbents [10].

On the other hand, there are a number of potential challenges associated with PPPs [Fig. 2]:

1. A clear and stable legal and regulatory framework is pivotal for enabling private investors to enter into PPPs, and defining the rules and boundaries for how PPPs are to be implemented.

2. Private sector financing will depend upon expectations of a reasonable Return on Investment (ROI) by the operating cash flows of the project company.

3. The principle adopted is that a service should be delivered in the most efficient way commensurate with acceptable cost limits and meeting an effective demand for services. Either the public authority is able to show that it can deliver a service to an acceptable quality and within a reasonable cost ceiling or the delivery of the service could be partly or wholly transferred to the private sector.

The concept of value-for-money in service delivery is therefore very relevant [11]. It is reflected in the principle of effectiveness: the service meets the objectives expected, i.e. the different groups of service users receive the services they require and are willing and able to pay for them; and in the principle of efficiency: the service is provided at minimal cost possible in most responsive manner to user effective demand.

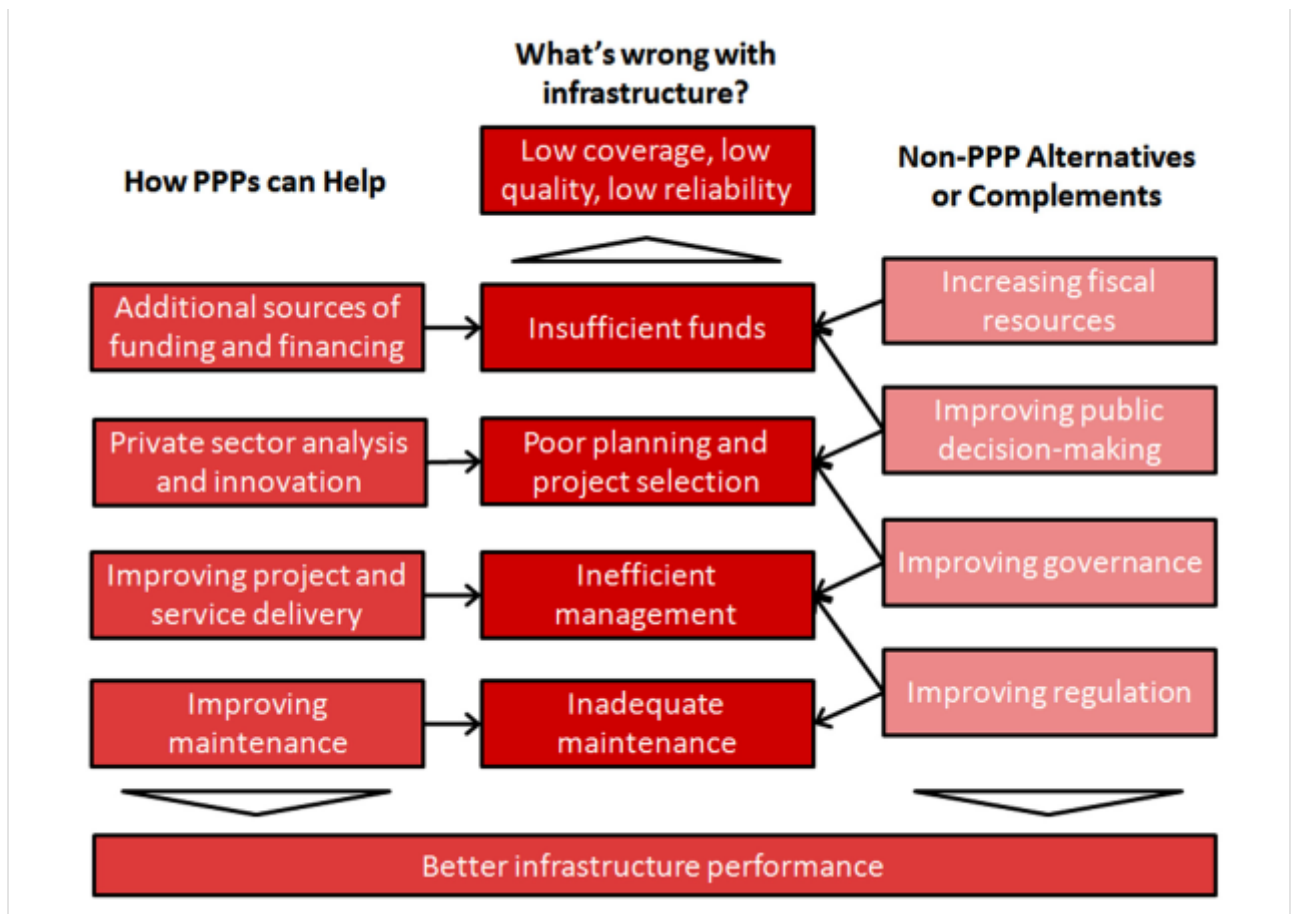


Fig. 2 Public-Private Partnerships for a better infrastructure performance [12]

#### 4. PUBLIC-PRIVATE PARTNERSHIPS FOR GREEN ENERGY INVESTMENTS

Risk and return are crucial factors in any investment decision, including renewable energy investments. The higher the perceived risk, the higher the internal rate of return (IRR) will be. The risk-return profile that is acceptable for an investor or lender depends on the type of capital. Public sector funds flow through government budgets and development banks while private sector funds originate from private and public finance institutions, institutional investors, capital markets, and corporate cash flow.

Debt financiers, like banks, have an interest in ensuring that their loans are paid back and hence provide funds to less risky, proven technologies and established companies. On the opposite side, early venture capitalists typically invest in new companies and technologies, and are therefore willing to take higher risks while expecting much higher returns. Venture capitalists may require an IRR of 50% or higher because of the high chances that individual projects will fail [Tab. 1]. Private

equity funds that invest in more established companies and technologies may still require an IRR of about 35% [Tab. 1]. However, other factors are figured into the IRR calculation, such as the perceived risks of the investment category, which vary significantly from project to project, technology to technology, industry to industry, and country to country, the availability of alternative investment opportunities, and prevailing basis interest rates (i.e. the current LIBOR).

Many energy projects, especially in developing countries where additional risk margins are added, are struggling to achieve high returns that satisfy the expectations of financiers of equity and debt. For renewable energy projects, higher costs of capital will increase start-up costs, which are generally front-loaded. Lenders require a higher equity share if a project is perceived as risky. A typical project finance structure in an industrialized country consists of 10-30% equity, whereas in developing countries this share tends to be higher. However, equity tends to be scarce in many developing countries [13].

One of the most relevant outcomes of the financial crisis was that banks were reluctant to lend money for more than 6 or 7 years, a situation which forced projects requiring longer-term loans, such as those in the energy sector, to run the risk of what financial conditions will be like at that point in the future. It is estimated that in 2009 debt financiers (both bank senior debt and bank mezzanine debt) required an average IRR of around 300-700 basis points above the LIBOR rate for RE projects in industrialized countries [Tab. 1]. On the other hand, private equity generally expects to make their return and exit the investment in a 3 to 5 year timeframe, whereas venture capital funds have an investment horizon of around 4 to 7 years. In this framework, institutional investors look like those best suited for renewable energy investment thanks to their longer time investment horizon and larger amounts of money to invest, with lower expectation of returns (IRR) [14].



Source of capital						
	Venture capital	Private equity	Infrastructure funds	Pension funds	Bank mezzanine debt	Bank senior debt
Deployment	Equity investments in start ups New technology Prototypes	Equity investments prior to initial public offering Demonstrator technologies	Equity investments in private companies Proven technology	Equity investments in private companies and projects Proven technology	Loans for emerging technology New and poorly capitalised companies and projects	Loans for Proven technology Established and well capitalised companies and projects
IRR	>50 %	35%	15%	15%	LIBOR + 700 bps	LIBOR + 300 bps

Tab. 1 Sources of capital, typical deployment and IRR for renewable energies [14]

In response to the financial crisis, stimulus packages focused on getting credit flowing again, although the impact on banks and equity actors took long time to recover. A redefinition of the role of public financing and of relevant issues in the operation of financial markets and institutions characterized the post financial crisis period. G20 governments implemented economic stimulus packages amounting to \$2.6 trillion. Of that amount, \$180 to 242 billion were allocated to low-carbon funding [1]. The stimulus spending supported the rapid recovery of renewable energy investment by compensating for reduced financing from banks. Some countries facing large public sector deficits scaled down green spending when the economy started recovering [15]. Other governments responded to this challenge by introducing specific measures to support PPP through the crisis, e.g. in the United Kingdom, the Treasury established an Infrastructure Finance Unit (TIFU).

Often, the lack of debt available in the market meant difficulty for private investors to complete long-term energy projects where debt was required to complement the available equity, or to spur equity returns to an acceptable IRR. Institutional investors, such as pension funds and insurance companies, have long-term investment horizon which is diversified across asset classes with varying risk return profiles and investment duration, sectors and geographies. Although they may have a cap set on the amount of renewable energy as a proportion of the allocation within wider infrastructure funds, at least they have a large amount of money to invest and

the ability to accept some illiquidity, thus potentially lowering the cost of capital for renewable energy. According to the OECD, institutional investors have an important role to play in financing green growth projects with \$71 trillion in assets in 2010, with \$19,3 trillion and \$22.4 trillion from pension funds and from insurance companies respectively [Fig. 3] [16].

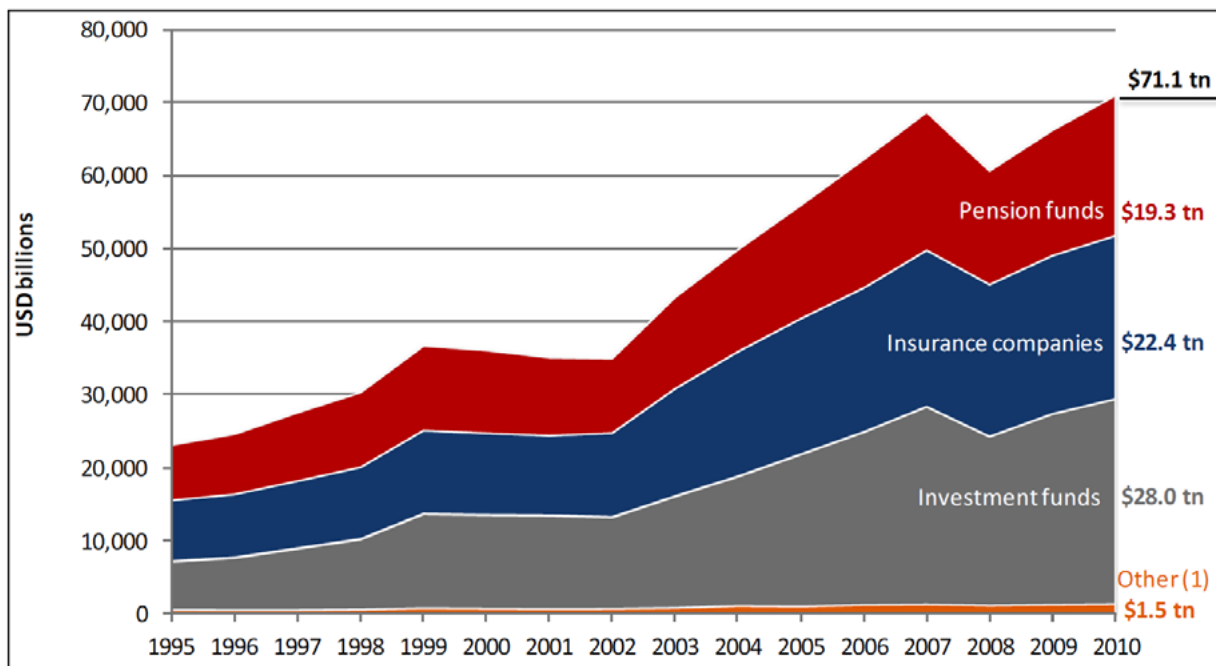


Fig. 3. Share and total assets by type of institutional investors in OECD (1995-2010) [17]

Institutional investors could meet, under particularly good circumstances with no policy barriers, 24% of project finance equity needs, and 49% of project finance debt needs. Therefore, the potential for insurance companies is higher, considering that their assets are highly invested in corporate debt securities, whereas pension funds maintain currently large allocations to corporate, publicly traded equity [18]. Nevertheless, within insurance companies a distinction needs to be made between non-life insurance assets requiring more liquidity, and life insurance assets that are more suitable for renewable project finance markets.

If we compare potential annual institutional investment against estimates for renewable energy annual investment required in OECD countries, segmented by asset classes, we can observe that insurance companies invest \$25.1 billion in corporate debt securities covering almost 40% of the total annual investment need,

whereas pension funds invest \$5 billion, corresponding to around 9% of the total annual investment need in OECD projects [Fig. 4].

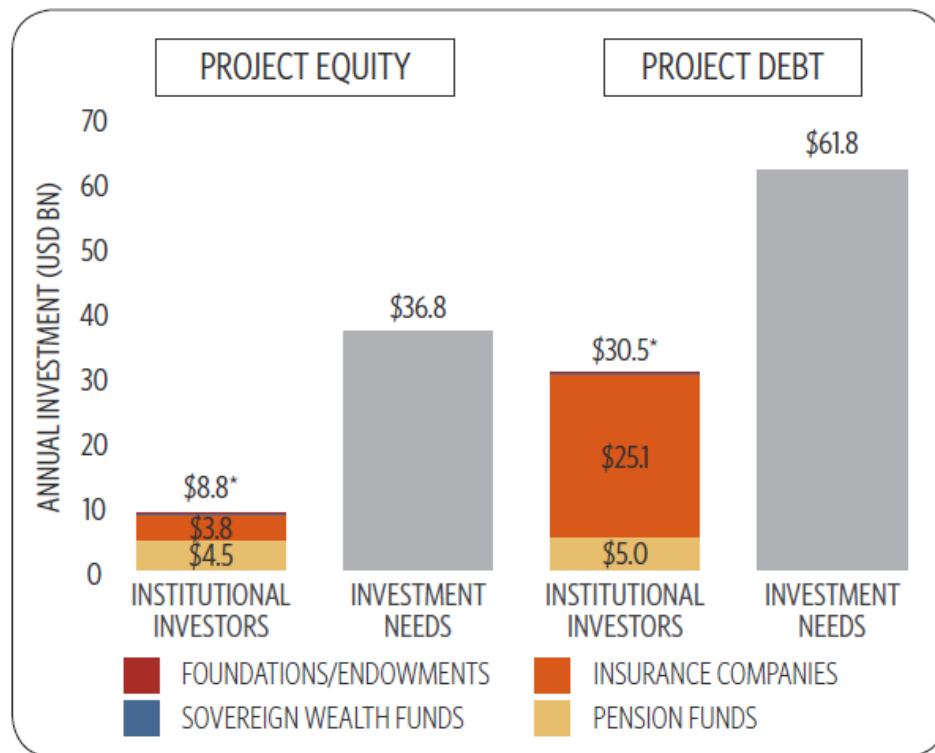


Fig. 4. Potential annual pension funds and insurance companies investment versus OECD project investment needs [18]

Nevertheless, institutional investors' direct asset allocations to green investments remain low. This could be due to lack of environmental policy support, lack of appropriate investment vehicles and market liquidity, regulatory disincentives, lack of knowledge and expertise, and scale issues [19]. For instance, pension funds usually require a sizeable investment of around \$250 million or more equity investment, with debt taken on to support the investment. Also, it is important to take note that there are about 45 pension funds worldwide large enough for direct investment in renewable energy projects and that they are unlikely to make up more than 1% of an investor's total portfolio, due to liquidity constraints and the need to diversify among different classes of illiquidity investments. [18].

In this framework, where debt financing is scarce and equity investment alone is not self-sustainable, it is evident how a combination of debt and equity financing through

a Public-Private Partnership long-term agreement can be the key driver to investment in energy infrastructures and green growth.

## 5. CONCLUSIONS

The current economic climate has posed a serious challenge to huge investment needs in energy infrastructure development. A new financial paradigm based on innovative approaches to fund raising that can improve bankability and enhance value for investors and governments needs to be implemented. The public sector has a major role in establishing an enabling environment for green technologies deployment, especially in reducing political and policy uncertainty. The pivotal role of straightforward national policy and regulation, its stability, and the importance of being embedded in a wider energy policy are conditions for scaling investment in renewable energy projects.

The need for smart grids' infrastructure for delivering renewable energy is a key part of the overall energy system. Optimizing transmission infrastructure to support the integration of renewable energy sources should not be perceived as a cost but as a significant economic opportunity. In Europe, a roughly \$1.5 billion annualized investment in transmission expansion could lead to electricity savings of roughly \$11 billion annually by 2030 [20]. This is just a small share if compared to IEA forecasts of \$260 billion of investments in new transmission and distribution lines up to 2035, but it gives a clear measure of the potential economic benefits to be derived from energy infrastructure development in the power sector [21].

A well-designed Private Public Partnership structure that reaps private sector advantages in terms of innovation and knowledge transfer, efficient management and mobilization of funds is a key factor in energy infrastructure investments. The creation of a conducive investment environment for private sector participation in large infrastructure investments, by eradicating barriers in the bidding process and by implementing and enforcing competition law, is fundamental for the success of infrastructure PPPs. The creation of new financial instruments, like international equity funds, long-term projects bonds and guarantee schemes will allow to get back capital markets into financing of green infrastructure. The Project Bond initiative of the EIB, designed to enable eligible infrastructure projects promoters, usually public

private partnerships (PPP), is fundamental to attract additional private finance from institutional investors such as insurance companies and pension funds [22].

## 6. REFERENCES

1. IEA (2009), *World Energy Outlook*. OECD/IEA
2. REN21 (2013), *Renewables Global Futures Report*. REN21
3. UNEP (2012), *Global Trends in Renewable Energy Investment 2012*. UNEP
4. World Bank (2014), *Private Participation in Renewable Energy Database*, at <http://ppi-re.worldbank.org/Snapshots/Global>
5. Mazouz, B. (2009), *Les aspects pratiques des PPP. De la rhétorique néolibérale aux enjeux, défis et risques de gestion des PPP*. Revue française d'administration publique, no. 130: 215-232
6. Mazouz, B., J. Facal and J. M. Viola (2008), *Public-Private Partnership: Elements for a Project-Based Management Typology*. Project Management Journal, vol. 39, no. 2: 98-110
7. World Bank (2012), *Public-Private Partnerships: Reference Guide*. World Bank Institute and Public-Private Infrastructure Advisory Facility (PPIAF)
8. Caselli S., Sattin F.L. (2011), *Private Equity e Intervento Pubblico*. Egea: 104-110
9. Singaravelloo K. (2010), *PPP: The Right Marriage between Local Government and the Private Sector in Malaysia?*. International Journal of Institutions and Economies, Vol. 2, No. 2: 142-166
10. Corfee-Morlot J., et al (2012), *Towards a Green Investment Policy Framework, The Case of Low-Carbon, Climate-Resilient Infrastructure*, OECD Staff consultation draft
11. World Bank (2013), *Value-for-Money Analysis - Practices and Challenges: How Governments Choose When to Use PPP to Deliver Public Infrastructure and Services*. Report from World Bank Global Round-Table 28 May, 2013

12. Alloisio, I. (2014), "Public-Private Partnerships: a focus on Energy Infrastructures and Green Investments". International Center for Climate Governance, Reflection No. 22/April 2014 at [http://www.iccgov.org/FilePagineStatiche/Files/Publications/Reflections/22\\_Reflection\\_\\_April%202014.pdf](http://www.iccgov.org/FilePagineStatiche/Files/Publications/Reflections/22_Reflection__April%202014.pdf)
13. IEA (2014), *World Energy Investment Outlook. Special Report*. OECD/IEA
14. Justice S. (2009), *Private Financing of Renewable Energy: A Guide for Policy Makers*. UNEP SEFI, Bloomberg Renewable Energy Finance. Chatham House
15. Eyraud L., Wane A.A., Zhang C., and Clements B. (2011), *Who's Going Green and Why? Trends and Determinants of Green Investment*. International Monetary Fund
16. Inderst, G., Kaminker, Ch., Stewart, F. (2012), *Defining and Measuring Green Investments: Implications for Institutional Investors' Asset Allocations*, OECD Working Papers on Finance, Insurance and Private Pensions, No.24, OECD Publishing
17. *OECD Global Pension Statistics and Institutional Investor databases and OECD estimates*,  
at <http://www.oecd.org/finance/private-pensions/globalpensionstatistics.htm>
18. Nielsen, D., Pierpont B. (2013), *The Challenge of Institutional Investment in Renewable Energy*. CPI Report
19. Della Croce, R. D., Kaminker C., Stewart F. (2011), *The Role of Pension Funds in Financing Green Growth Initiatives*, OECD Working Papers on Finance, Insurance and Private Pensions, No. 10, OECD Publishing
20. The Global Green Growth Forum (2012), *Report on Accelerating Green Growth through Public-Private Partnerships*. 3GF
21. IEA (2013), *World Energy Outlook*. IEA
22. EIB (2012), *An outline guide to Project Bonds Credit Enhancement and the Project Bond Initiative*, EIB

# The role of public finance in CSP: lessons from the ups and downs of CSP policies in Spain

Frisari G.<sup>1,2\*</sup>, and Feás J.<sup>3</sup>

<sup>1</sup>Ca' Foscari University of Venice - Italy, <sup>2</sup>Climate Policy Initiative - Italy, and

<sup>3</sup>University of Santiago de Compostela - Spain

\*Corresponding Author: gianleo.frisari@cpivenice.org

## Abstract

In a low carbon energy system, concentrated solar power is of particular interest for its ability to store solar energy as heat. This allows the delivery of power even when the sun sets, so to complement and compensate other intermittent clean sources of power. However, CSP investment costs are high compared to other options such as fossil fuel generation and mature renewable energy technologies, calling upon public support to make investments profitable and appealing to private investors.

This work looks at the evolution of CSP support policies and their impact on financial returns for the industry in Spain, historically the largest market for the technology. We analyze the key features that made the development of the domestic CSP industry possible in a very short time, and measure their impact on investments' profitability and other relevant measures (e.g. incentives for storage). We then identify and measure the impact of policy changes (aimed at containing policy costs) on investments and the implication of a higher risk aversion and lower investors' confidence on the outlook for the industry in the country. We derive our conclusions by simulating projects' financial profiles with a cash-flow modeling of a "representative" CSP plant whose investment costs, capital structure and production estimates equal the national averages of all the plants. We find that policy changes have now significantly increased risk aversion, so that any new eventual investment would require a support higher than before, even assuming a significant reduction in technology costs. Policy uncertainty has ultimately made the country much less attractive for CSP investors than many other developed and emerging ones. We conclude that policy uncertainty and investor confidence should be the first barriers to be tackled if Spain were to reach renewable energy (and CSP) 2020 targets.

**Keywords:** concentrated solar power; Feed-in-tariff; policy risk

## 1. THE SPANISH CSP POLICY AND INDUSTRY

Among renewable energy technologies, concentrated solar power (CSP) is of particular interest because its ability to store solar energy as heat allows the delivery of power even when the sun sets. This technology can help overcome gaps from balancing supply and demand, including those arising from other (intermittent) renewable energy sources, and helps to maintain a stable yet low-carbon energy supply. However, CSP investment and production costs are high compared to other more established conventional options such as fossil fuel generation and mature renewable energy technologies, calling upon public support to make investments profitable and risks appealing to private investors. Despite having been deployed for years, yet there is still potential for bringing down the technology learning curve and the cost of the technology. Projects around the world show that almost all CSP projects have needed some sort of public support, and that, at the same time, there's been a high dispersion of both policy tools and their results on capacity installed and costs [18]. In some context, policies have resulted in significant installations but have led to higher costs of supports than what had been budgeted for; in others, costs have been reduced but the capacity deployed has met expectations only partially. This work looks at the evolution of CSP support policies and their impact on financial returns for the industry in Spain, historically the largest market for the technology. We first analyze the key features that made the development of the CSP industry in the country possible in a very short space of time, and measure their impact on investments' profitability and other relevant measures (e.g. incentives for storage). We then identify and measure the impact of the policy changes (aimed at containing the costs of the policy) on existing investments and the implication of a higher risk aversion and lower investors' confidence on the outlook for the industry in the country. The following findings are based on a literature review, financial modelling and interviews with stakeholders (investors, developers, and policymakers).

## 2. THE POLICY FRAMEWORK

The Spanish support to CSP, and renewable energy overall, has been part of a broader national effort to liberalize the national energy market. It began in 1997 with the Electricity Act 54/1997 and continued in the following years with several pieces of legislation [Figure 1]. This first act established the "special regime" for facilities based

on renewable, cogeneration and waste energy and set capacity targets for energy efficiency, environment protection and energy production from renewable sources. The remuneration system for the special regime was introduced in 2004 with the Royal Decree (RD) 436/2004 – though most plants were announced and, later, commissioned under the RD 661/2007 system that replaced the variable “reference price” as base for the incentive with a fixed amounts for both the tariff and the premium over the negotiated market price (the “pool price”<sup>1</sup>). In 2011, in slightly less than 5 years, the CSP industry was estimated to employ more than 20 thousand people and generating an annual contribution to the Spanish GDP of 1.65 billion Euros [6]. The 2.3GW of plants commissioned under the 661/2007 policy contributed 700 GWh of electricity in 2010 (0.25% of total national demand) and more than 4,000 GWh in 2013 (1.70%) [2] – saving 361,250 tons of CO<sub>2</sub> in 2010 and more than 2 million tons of CO<sub>2</sub> in 2013 (authors’ estimations on parameters from [6]). From an industrial economic perspective, Spanish companies owned more than 75% of the national solar thermal market, with one third of the plants being financed by foreign equity investors. Interestingly, the same companies have developed (as sponsors or contractors) more than 55% of the global CSP capacity installed outside Spain in the last 10 years. These several benefits of the policy framework have to be put in context with the financial burden on the electricity rate-payers budget: under the 661/2007 incentive system, all Spanish CSP plants required a financial incentive of EUR 185 million in 2010 and up to EUR 1.1 billion in 2013 (authors’ estimations on parameters from [2]).

### 3. METHODOLOGY AND DATA

The analysis in this brief is supported by data collected by publicly available databases (Bloomberg New Energy Finance – BNEF; and the National Renewable Energy Laboratory - NREL), literature review and direct interviews with key stakeholders in the local CSP industry.<sup>2</sup> Within a project finance model, we have

---

<sup>1</sup> The electricity market sets the pool price by adjusting the supply and demand of energy scheduled for the next day. The first offers come from nuclear power and renewable energy. Both offer energy at zero prices to give them priority. Then the most expensive (gas and coal) energy offered to meet the demand, thus setting the marginal price that becomes the “pool price”. All other sources offered are also paid at this price, even if they were offered initially at lower prices.

<sup>2</sup> Interviews conducted: one policymaker from a regional government, two project sponsors, two project developers, two lenders and one representative from the European trade association.

simulated projects' financial profiles with a cash-flow modelling of a "representative" CSP plant whose investment costs, capital structure and production estimates are the national averages of all the plants (categorized by homogenous technology types) commissioned during the period in analysis (2007-2013). The analysis then focuses on three main outputs of these cash flow models:

- the *internal rate of return* as the key measure of the project's profitability for the project sponsors. In order for a project to be viable, this value needs to be larger than the sponsors' cost of capital, and also higher than benchmark returns from comparable investments and, obviously, than the "risk-free" rate offered by the country's government bonds. While the internal rate of return is typically an output of the cash-flow model; here we also use it as an input as, for a given set of technology costs and financing terms available from lenders, it ultimately drives the amount of public support needed to make a project attractive to private investors.
- the *levelized cost of electricity* as a key measure of project costs for each unit of power produced. It's a measure of the cost of the power after all resources (including financial ones) are remunerated.
- The *debt service coverage ratio* (DSCR) as an indication of a project's ability to repay its financial liabilities. Lenders set a minimum threshold for this ratio to be kept at all times. A DSCR below 1, it indicates that the project is not generating enough financial resources to repay its debt and might soon encounter financial stress.

### **Plants profitability and market alternatives under the RD 661/2007**

Under the incentive framework set out in the RD 661/2007, project sponsors could choose (annually) between a 26.9 €cents/kWh fixed regulated rate (feed-in tariff) and a 25.4 €cents/kWh premium over the market price (feed-in premium).<sup>3</sup> While, at market rates without the revenue support, a CSP project would have not achieved a positive rate of return;<sup>4</sup> we estimate that these incentives allowed a generic CSP project to reach a rate of return of 10%, and its equity sponsors to enjoy a levered

---

<sup>3</sup> Both options had a fixed life of 25 years with a marginal reduction for a further 15 years (to 21.5 €cents/kWh for the tariff and 20.3 €cents/kWh for the premium) and included the option of using a back-up fuel (e.g. gas) for a maximum of 15% of power produced.

<sup>4</sup> Without any tariff incentive, our simulated rate of returns would be -2%.

12.5% return (after taxes). Bearing in mind the higher risks associated with an innovative technology such as CSP, these returns appear favorable if compared with an estimated cost of capital for the utilities in the country at around 8%, and rate of returns offered by wind investments in Europe - 8/16% [14]; however they appear in line if not below with those offered by solar PV installations in Europe, estimated at 15-18% for equity owners in the year 2011 [20].

Interestingly, despite not featuring any specific incentive for it, the FIT encouraged investments in the less proven thermal storage technology.<sup>5</sup> Storage helped plants to reach significantly higher capacity factors (increasing from 24% without storage to 38% in our estimation) and resulted in much lower levelized costs of electricity (from 0.27 Eur/kWh to 0.24 Eur/kWh). Lower levelized costs coupled with the possibility to earn a premium over the market price and favorable financing terms from lenders, allowed plants to achieve higher internal rate of returns (close to 11.5%) and their sponsors levered returns of 14.5% (after tax). Very interestingly, despite the typical perception of higher risk related to thermal storage technology, banks and lenders did not demand a premium for the loans and the financing terms were basically the same for the plants without any storage.<sup>6</sup>

### **Inefficient policy features: plant size, technology costs and impact on deficit**

Several features of the policy framework proved inefficient and, ultimately, led a much higher cost of the policy than expected (and politically acceptable), prompting the government to amend the framework with severe effects on projects' financial performance and the overall market.

The incentivized tariff in the RD 661/2007 was conditional to a maximum plant capacity of 50MW, far below the optimal scale for the technology between 100 and 250MW [9]; even if many of them were built in adjacent 50MW modules for a total of 100-150 MW.<sup>7</sup> Considering many parts of a generic CSP plant do not depend on scale (such as the conventional power block and project development costs), we

---

<sup>5</sup> Almost half of the plants commissioned in the country featured storage facility with an average seven hours of capacity.

<sup>6</sup> This is also explained by the willingness - reported by stakeholders - of project developers and sponsors to offer banks comprehensive guarantees from their corporate assets, making project finance deals more similar to balance sheet financing.

<sup>7</sup> This was attributed to concerns from the grid operator about connecting large plants generating renewable power, and the preference from policymakers to keep the approval of renewable energy projects under the regional governments' sphere.

estimate that a large plant with 150MW capacity could produce power at a 15% lower levelized cost and a 20% lower investment cost per MW installed. Furthermore, the incentive mechanism had no systematic link to the cost of the technology of the single plant, and no periodic price revision system.<sup>8</sup> While it is true that project developers could increase project profitability by reducing the plant costs, the large number of installed projects coupled with a limited number of suppliers meant that competition was not sufficient [4]. Policymakers struggled to exert any downward pressure to the plants' costs as capacity was being deployed and, by policy design, they would have not benefitted from any cost reduction. Looking at both investments costs per capacity installed and levelized investment costs for all plants financed between 2006 and 2012, no downward trend emerges [Figure 2].

As CSP installations (alongside other REs) increased, the impact of their premium on energy production costs grew and, given the government decision not to pass them fully on ratepayers, it started to contribute to the national tariff deficit, becoming a political issue despite its rather limited absolute size.<sup>9</sup> The contribution of renewable energy installations to the evolution of the tariff deficit is a very debated and complex matter, whose precise treatment goes beyond the scope of this brief. On one side, renewable energy installations (as a whole) exceeded initial expectations and national targets, with their premia clearly contributing to higher production costs and a widening of the deficit. On the other side, this view both ignores the impact of higher penetration of renewable energy on reducing the average market price, via the "merit order" effect given their null marginal costs of production. [Figure 3] shows at the same time the relative size of the premium directly linked to CSP deployment compared with the total premia for the Special Regime, and the annual deficit, whose evolution especially in the last years appears actually un-correlated with the support to renewables.

---

<sup>8</sup> Differently for the solar photovoltaic project, the RD 1578/2008 introduced in 2008 a "quota" system that aimed to control costs as capacity grew: installations were staggered in annual quotas that, once reached, would proportionally reduce the FIT for the following year [5].

<sup>9</sup> The tariff deficit emerged soon after the process of electricity market liberalization started (hence before renewables began to be installed) and was the result of the final consumer rates set by the government failing to cover the whole energy production cost, which included wholesale market price and regulated access costs to be paid to distribution companies.

## Retroactive policy changes: impact on returns and installations

With the aim to reduce the cost of renewable energy support and to reduce the large tariff deficit, national policies switched from supporting installations to limit connections. The introduction of the new income tax on power, the curtailment of operating hours and the reduction of the FiT for power generated by backup fossil fuel has severely reduced the profitability of projects' sponsors and, in our estimation, has deteriorated significantly their ability to repay debt and interest due. New policies first limited the amount of power eligible for the incentives (operating hours curtailment and non-eligibility of gas-fired back-up power for beneficial tariffs); then introduced new taxation to help finance the tariff deficit (RDL 15/2012), and finally removed the "premium over market-price option" to make the overall renewable expenditure less variable. These policy changes amended the RD 661/2007 and applied retroactively to plants already in operation. Our simulations for a plant with parabolic trough without storage show that policy changes seem to have reduced plants' profitability from 12% to 7% rate of return and, more worryingly, project's ability to repay their loans becomes very limited.<sup>10</sup> Plants' profitability and financial health deteriorate further when the remuneration profile and the limitation in operating hours anticipated in the proposed energy sector reform are introduced in the simulation. With the moratorium on renewable energy plants introduced with the Law 1/2012, no new plants have been announced since 2010 and the ones that did not qualify for the register have been put on hold or abandoned until regulatory stability is achieved. After controlling CSP deployment to be within the target of 500MW for 2010 in Spain's Renewable Energy Plan [11] Spanish policymakers are now at the opposite risk of missing the 5GW target set for CSP for 2020 [12].

Given the lack of projects seeking financing and the lack of investors willing to commit resources in the renewable energy sector in the country, it is difficult to estimate which financing terms a project developer could find in the market today. However, stakeholder interviews suggest that risk aversion has significantly increased, leading to expectations of much lower debt/equity ratios (from 75/25 to now 60/40), much higher debt service coverage ratios (from 1.3 to now 1.5) and increased financing spreads on shorter maturities. Even assuming a significant

---

<sup>10</sup> In our simulations, following changes in remuneration profiles, projects show debt service coverage slightly below the thresholds that lenders typically require in project finance.

reduction of investment costs<sup>11</sup>, these new financing terms would decrease plant profitability to such a level that even the RD 661/2007 feed-in tariff would still not be enough to make the investment appealing for interested sponsors. In our simulation, a 50MW plant with storage and 30% less investment costs and the RD 661/2007 tariff would now yield a 7% rate of return – significantly lower than returns estimated for similar projects in emerging markets (closer to 10% for recent plants in Morocco and India CPI [7; 19] and that would hardly appeal risk-averse project developers in the uncertain policy framework in the country. The financial simulations show how increased financing costs due to a higher perception of risk in the sector would make it impossible for the government to reduce the value of the incentive scheme if the 2020 renewable energy targets are to be met and almost 2 GW of CSP capacity needs to be commissioned.

#### 4. CONCLUSIONS

The 2007 incentive framework based on a feed-in tariff/premium system was very effective in prompting installation of CSP plants and the development of a Spanish CSP industry that became a world-leader not only in the domestic but also foreign markets.

However, the lack of policy control over the level of capacity deployed and the overall public support required led to the announcement of a greater number of projects than initially targeted, and the potential of support costing much more than planned.

Further, the inability of the policy to stimulate cost reductions and foster market competition meant investment costs didn't decrease as installed capacity increased.

To fight excessive installations and costs to the public, the government first introduced a project approval process that staggered connections on an annual basis; then added several retroactive changes that aimed to reduce the amount of support CSP investments were receiving. These measures directly hurt the financial performance of operating plants and brought the domestic market to a complete standstill.

---

<sup>11</sup> In the simulation we assume investment costs in line with the more recent installations in the MENA region and United States.

Further, as a significant side effect, policy changes have now significantly increased risk aversion and financing costs for the technology in the country. Our financial simulations show that, if investors' confidence is not restored and risk perception mitigated, any new eventual investment would need more public support than before, even assuming a significant reduction in technology costs.

Policy uncertainty has ultimately made Spain much less attractive for CSP than many other developed and emerging countries, despite the significant national expertise of Spanish CSP companies. Therefore, we recommend, going forward, that establishing a transparent and stable support framework that can address this policy uncertainty should be a higher priority in Spain than setting a different level for the support or a new feed-in tariff.

For all countries looking to support CSP installations, several other lessons also emerge from the Spanish example:

- CSP support policies need to foster competition and cost reduction alongside deployment, while also systematically and transparently reducing subsidy levels as technology costs decrease;
- CSP support policies need to introduce differentiated remuneration profiles to stimulate innovation and investments in the technologies with the highest system benefits;
- Policymakers need to be able to control the amount of support that public budget or rate payers are liable to pay as a result of the capacity installed, plan these liabilities in advance and avoid late and retroactive cut-backs;
- Policymakers need to avoid retroactive changes to policy as they add significantly to policy support costs by damaging investors' perception of policy risk and increasing their overall risk aversion meaning they demand a greater return.

## 5. REFERENCES

1. CNMC 2013a. *Note summary outstanding debt of the electric system*. November 2013. Madrid: National Markets and Competition Commission.
2. CNMC. 2013b. *Monthly statistical information about sales of special regime*. December 2013. Madrid: National Markets and Competition Commission.
3. Crespo. 2013. *Reflections on the Spanish Regulation Framework*. Presentation held at the CSP Today Sevilla 2013, 7th International Concentrated Solar Thermal Power Summit, 12-13 November 2013. Madrid: Protermosolar
4. CSP Today. 2009. *CSP policy: Not always the right FiT*. Posted on November 2009, Accessed on March 2014. CSP Today: London.
5. Del Rio P., Mor-Artigues P. 2012. *Support for solar PV deployment in Spain: Some policy lessons*. Renewable and Sustainable Energy Reviews 2012; 16: 5557-5566.
6. Deloitte-ProtermoSolar. 2011. *Macroeconomic impact of the Solar Thermal Electricity Industry in Spain*. October 2011. Madrid: Deloitte; Madrid: Protermosolar.
7. Falconer A., Frisari G. 2012. *San Giorgio Group Case Study: Ouarzazate I CSP*. Venice: Climate Policy Initiative. Available from: <http://climatepolicyinitiative.org/our-work/publications/>
8. KPMG. 2013. *Taxes and incentives for renewable energy*. September 2013. KPMG International. Available at: <http://www.kpmg.com/Global/en/IssuesAndInsights/ArticlesPublications/taxes-and-incentives-for-renewable-energy/Documents/taxes-and-incentives-for-renewable-energy-2013.pdf>
9. IEA. 2010. *Technology Roadmap. Concentrating Solar Power*. Paris: International Energy Agency.
10. Gelabert L., Labandeira X., Linares P. 2011. *Renewable Energy and Electricity Prices in Spain*. Economics for Energy, 2011; WP 01/2011

11. GoE. 2005. *Plan de Energías Renovables en España 2005-2010*. August 2005. Madrid : Gobierno De España.
12. GoE. 2010. *Plan de Energías Renovables en España 2010-2020*. June 2010. Madrid : Gobierno De España.
13. IRENA. 2012. *Concentrating Solar Power. IRENA Working Paper, Volume 1: Power Sector*. Issue 2/5 June 2012. Abu Dhabi: International Renewable Energy Agency.
14. Macquarie 2011, *Global Wind Sector: Approaching Grid Parity*. Equities Research, July 2011.
15. Perez I., Lopez A., Briceño S., Relancio J. 2013. *National Incentive Programs for CSP – Lessons learned*. SolarPACES 2013. Energy Procedia 00 (2013) 000–000
16. REE, 2013. *The Spanish Electricity System PRELIMINARY REPORT 2013*. Madrid: Red Eléctrica De España. Available at:  
[http://www.ree.es/sites/default/files/downloadable/preliminary\\_report\\_2013.pdf](http://www.ree.es/sites/default/files/downloadable/preliminary_report_2013.pdf)
17. Solar Millennium, 2008. *The parabolic trough power plants Andasol 1 to 3*. Erlangen: Solar Millennium
18. Stadelmann M, Frisari G, Boyd R, Feas, J. 2014a. *The Role of Public Finance in CSP: Background and Approach to Measure its Effectiveness*. Venice: Climate Policy Initiative. Available at:  
<http://climatepolicyinitiative.org/publication/san-giorgio-group-brief-the-role-of-public-finance-in-csp-background-and-approach-to-measure-its-effectiveness/>
19. Stadelmann M, Frisari G, Konda C. 2014b. *The Role of Public Finance in CSP: Rajasthan Sun Technique 100MW CSP plant, India*. Venice: Climate Policy Initiative. Available at: <http://climatepolicyinitiative.org/publication/san-giorgio-group-case-study-the-role-of-public-finance-in-csp-india-rajasthan-sun-technique/>
20. Varadarajan U., Nelson D., Pierpont B., Hervé-Mignucci M. 2011. *The Impacts of Policy on the Financing of Renewable Projects: A Case Study Analysis*. October 2011. San Francisco: Climate Policy Initiative. Available at

<http://climatepolicyinitiative.org/publication/the-impacts-of-policy-on-the-financing-of-renewable-projects-a-case-study-analysis/>

21. Würzburg K., Labandeira X., Linares P. 2013. *Renewable Generation and Electricity Prices: Taking Stock and New Evidence for Germany and Austria*. Economics for Energy, 2013; WP FA03/2013

## 6. IMAGES AND TABLES

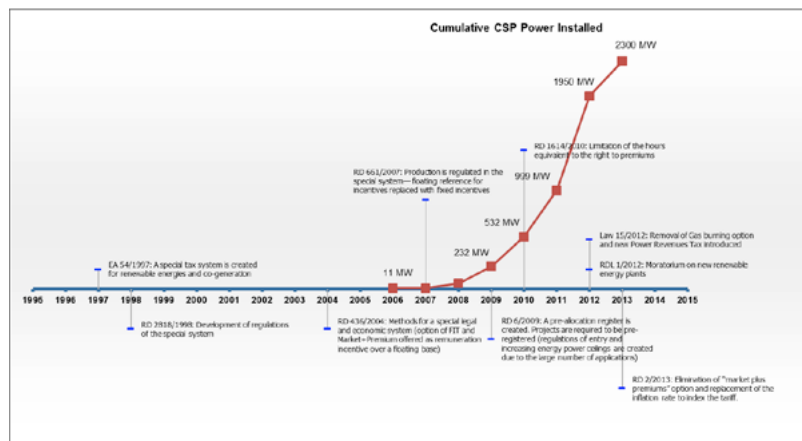


Fig. 1 History of regulations for thermal solar energy in Spain and cumulative capacity installed

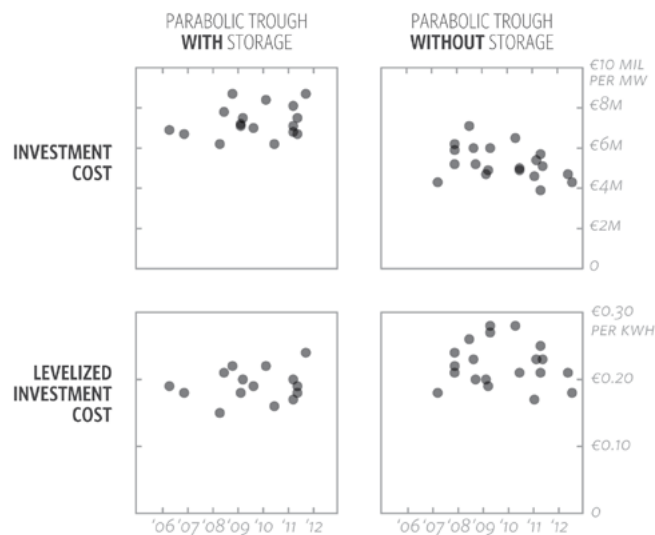


Fig. 2 Investment costs and levelized costs evolution for parabolic trough plants, <sup>12</sup> 2006 and 2012 - Source BNEF

<sup>12</sup> For solar tower and Fresnel plants there is not enough data to infer any conclusions on cost reductions.

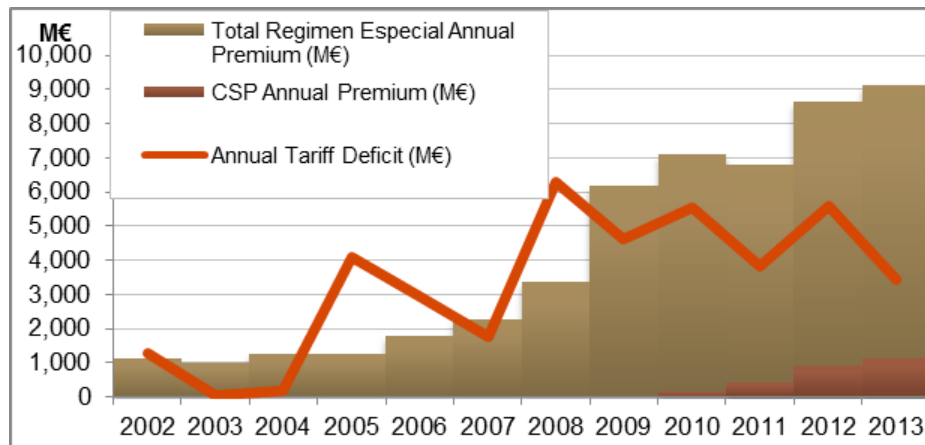


Fig. 3 Annual tariff deficit, RE premium and CSP premium – [2]

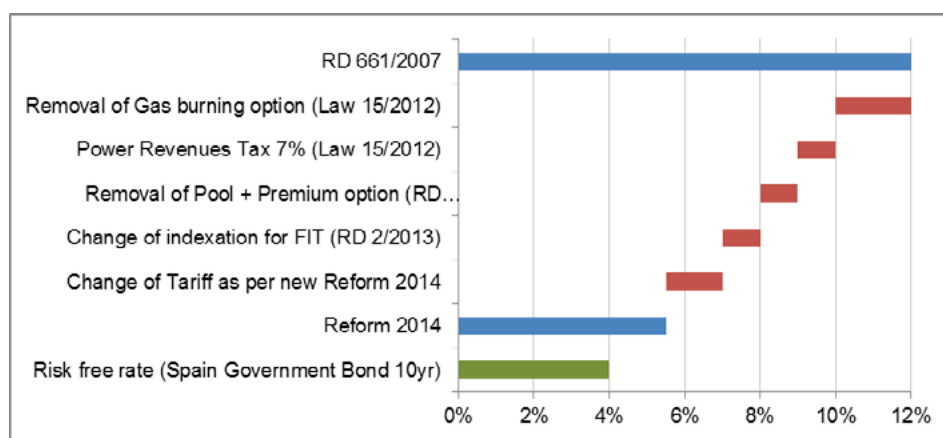


Fig. 3: Policy changes impact on projects' equity rate of return

Tab. 1 Effect of policy changes on plants' rate of returns and debt coverage

Plant: 50MW Parabolic Trough without Storage	Equity IRR (after tax)	DSCR
RD 661/2007	12%	1.65
Hours curtailment (RD 1614/2010)	12%	1.65
Removal of Gas burning option (Law 15/2012)	10.4%	1.5
Power Revenues Tax 7% (Law 15/2012)	9.4%	1.4
Removal of Pool + Premium option (RD 2/2013)	7.9%	1.3
Change of indexation for FIT (RD 2/2013)	7.2%	1.28
Change of Tariff as per new Reform 2014	5.7%	1.12
Risk free rate (Spain Government Bond 10yr)	4%	

**Mitigation Policies & Strategies**

**Energy technologies and  
policies**

# Climate change mitigation and energy technology costs: A Multi-model Sensitivity Analysis

**Bosetti V.<sup>1,2</sup>, Marangoni G.<sup>2,3\*</sup>, Borgonovo E.<sup>1</sup>, Anadon D. L.<sup>4</sup>, Barron R.<sup>5</sup>,  
McJeon C. H.<sup>6</sup>, Politis S.<sup>7</sup>, Friley P.<sup>7</sup>**

<sup>1</sup>Bocconi University – Italy, <sup>2</sup>Fondazione Eni Enrico Mattei and CMCC – Italy,  
<sup>3</sup>Politecnico di Milano – Italy, <sup>4</sup>Harvard Kennedy School, Harvard University – USA,  
<sup>5</sup>University of Massachusetts Amherst – USA, <sup>6</sup>Pacific Northwest National Laboratory  
- USA, <sup>7</sup>Brookhaven National Laboratory – USA

\*Corresponding Author: [giacomo.marangoni@feem.it](mailto:giacomo.marangoni@feem.it)

## Abstract

In the present paper we use the output of multiple expert elicitation surveys on the future cost of key low-carbon technologies and use it as input of three Integrated Assessment models. By means of a large set of simulations we aim at assessing the implications of these subjective distributions of technological costs over key model outputs. We are able to detect what sources of technology uncertainty are more influential, how this differs across models and whether and how results are affected by the time horizon, the metric considered or the stringency of the climate policy.

**Keywords:** Sensitivity Analysis, Integrated Assessment models, Expert elicitation, Technology Cost

# Distributional impact of reducing fossil fuel subsidies in Indonesia

Campagnolo L.<sup>1</sup>, Chateau J.<sup>2\*</sup>, Dellink R.<sup>3\*</sup> and Durand-Lasserve O.<sup>4\*</sup>

<sup>1</sup>Feem and University of Venice - Italy, <sup>2</sup>OECD - France, <sup>3</sup>OECD and Wageningen University and Research Center – France/Holland, and <sup>4</sup>OECD - France

Corresponding Author: [lorenza.campagnolo@feem.it](mailto:lorenza.campagnolo@feem.it)

## Abstract

This paper studies the distributional impacts of fossil fuel consumption subsidy reforms in Indonesia. The analysis highlights how the rebate of the saved expenditures on fuel subsidies (i.e. the recycling scheme) is crucial for assessing the equity of the reform. The evaluation method combines in a top-down fashion a CGE model (ENV-Linkages), with a micro-simulation model built upon Indonesia IFLS 2007 household survey data. Two scenarios portraying a marginal decrease of the subsidy rates on electricity and other fuels are simulated. In the “cash transfer” scenario the reform is accompanied by a full unconditional cash transfer to the households, in the “government expenditures” scenario, the expenditures saved by the reform are used to increase government consumption. The “cash transfer” policy is overall welfare improving, beneficial to all the income decile categories and very progressive. The progressive effect of the cash transfers dominates the slightly regressive effect due the changes in expenditures and primary incomes. When considering only the short-term impact through expenditures and primary incomes, the “government expenditure” policy is regressive.

**Keywords:** microsimulation, fossil fuel subsidy, CGE model

\*The views of the authors do not necessarily represent the views of the OECD or of its member countries.

# Banning Non-Conventional Oil Extraction: Would a Unilateral Move of the EU Really Work?

Carrara S.\* and Massetti E.

Fondazione Eni Enrico Mattei (FEEM) and Centro Euro-Mediterraneo sui Cambiamenti Climatici (CMCC), Italy

\*Corresponding Author: [samuel.carrara@feem.it](mailto:samuel.carrara@feem.it)

## Abstract

The extraction and processing of oil shales and oil sands – commonly defined as non-conventional oil resources – is more energy intensive than the extraction of conventional oil resources. The European Union (EU) estimates that oil sands lead to 22% more emissions than conventional oil. The EU is very concerned by this prospects and advocates a tax on non-conventional oil in order to discourage its production.

This study shows that a global ban on the use of non-conventional oil substantially reduces global carbon dioxide emissions, but the policy is not efficient as other tools (e.g. a global carbon tax) may achieve the same environmental goal at lower cost. A unilateral ban of the EU on non-conventional oil has no environmental benefits (global oil demand does not significantly change) and it is expensive for Europe. The EU should not focus on contrasting a specific technology, but rather on promoting the implementation of economy-wide policies to penalize GHG emissions.

**Keywords:** non-conventional oil, climate mitigation, EU

# Oil Market and Long-term Scenarios: a Nash-Cournot Approach

Sferra F.<sup>1</sup>

<sup>1</sup>Climate Analytics and CMCC - Italy

\*Corresponding Author: [fabio.sferra@gmail.com](mailto:fabio.sferra@gmail.com)

## Abstract

Integrated Assessment Models (IAMs) are widely used by the scientific community to evaluate long-term scenarios. Yet, these models commonly assume perfect competition in fuel markets. Therefore, the aim of this paper is to introduce strategic behaviour in IAMs and to provide more reliable portrays of future long-term scenarios for the oil market. Results confirm that a Nash-Cournot equilibrium leads to higher oil price and lower extraction compared to a price-taker equilibrium. This entails a higher payoff for the oil-exporting countries. Under a climate policy scenario, oil producers retain their ability to set the price for many years, due to a more inelastic demand. In fact, the long-run oil price elasticity will be in the range of -0.25 and -0.50 (compared to -0.5 and -0.75 in the BaU scenario). Stabilisation costs do not change substantially.

**Keywords:** Oil, Nash-Cournot, Integrated Assessment Models

## 1. INTRODUCTION

The aim of this paper is to introduce Nash-Cournot in Integrated Assessment Models (IAMs), in order to provide a better representation of the fuel market structure. In fact, IAMs provide scenarios based on perfect competition or price-taker assumption regarding the fossil fuels market (Edenhofer et al. 2010, Huntington et al. 2013). This assumption is unrealistic for energy markets (Holz et al. 2007, Trüby 2013) and in particular for the oil extraction sector (Brémond 2012, Huppmann 2009, Böckem 2004, Danielsen and Kim 1988). Indeed, OPEC countries exert market power in the oil market (Dées et al. 2007, Kaufmann et al. 2008), even though their influence can vary over time (Fattah and Mahadeva 2013) and reportedly, it decreased in recent years (Huppmann 2012). The literature also clarifies that OPEC is not a friction-less cartel (Loderer 1985, Smith 2005, Reynolds and Pippenger 2010) and recognised the presence of a dominant producer within the cartel, represented by Saudi Arabia (Alhajji and Huettner 2000, De Santis 2003, Cairns and Calfucura 2012).

The literature on strategic behaviour started with the seminal paper of Cournot (1838) who first devised the oligopolistic competition as a simultaneous game in which firms compete in quantity. Then, other types of strategic behaviour have been formulated, such as the Bertrand (1883) equilibrium, where firms compete in price instead of quantity; and the Stackelberg (1934) model, which is a sequential game where two types of firms can be distinguished: the leader firm (which moves first) and follower firms (which move sequentially).

This study employs an Integrated Assessment Model where oil is considered as a homogenous good. In this regard, the assumption of a Nash-Cournot equilibrium is probably the most suitable to model strategic behaviour, as it is a simultaneous game – which is in line with the classic game-theory setup used in IAMs.

## 2. METHODOLOGY

The purpose of IAMs is to provide long-term scenarios by taking into account three different but interrelated aspects: climate change, the economy and the energy sector. To this end, Gross Domestic Product (Y) is usually governed by a constant elasticity of substitution (CES) function. Typically, it considers Capital (K), Labour (L) and Energy Consumption (EN) as factors of production.

There exist two ways of implementing a Nash-cournot equilibrium in IAMs: the standard approach or the Orbay approach (Orbay 2009). The standard approach requires the derivation of the inverse demand functions. This approach is not applicable if the demand functions can not be derived in an analytical form.

Instead, the Orbay approach describes a Nash-Cournot equilibrium by means of the first-order conditions. This approach is relevant in case of homogenous goods and presents major advantages from the computational point of view. In particular, Orbay (2009) showed that a Cournot equilibrium can be computed through prices as instruments to maximize profit functions. This simply means that oil producers use market prices (instead of quantities) as if they are strategic variables. This papers employs the Orbay approach, which has been applied in the Integrated Assessment Model WITCH.

### 3. THE WITCH MODEL

WITCH – World Induced Technical Change Hybrid Model – is a Ramsey-type model with a top-down representation of the economy and a compact representation of the energy sector. The world is divided in thirteen macroeconomic regions, which compete strategically to maximise social welfare (defined as the logarithm of discounted consumption per capita).

When deciding the optimal investment paths, each region is forward-looking (perfect foresight assumption). An important feature of the WITCH model is the endogenous technical change, which can be increased via dedicated investment in R&D. Another important characteristic is the prominent role of technological spillovers among regions.

Gross Domestic Product (GDP) is determined by a nested sequence of CES functions. The CES functions provide flexibility to the model by allowing for factors substitution, and at the same time limiting extreme changes in the shares. The energy sector (EN) is divided in the electric (EL) and non-electric (NEL) sector, by assuming an elasticity of substitution of 0.5 (Bosetti et al. 2007).

Besides, the WITCH model takes into account two non-tradable backstop technologies either for the electric and non-electric sectors, which are supplied competitively. It is relevant for this study, to focus on the backstop technology of the

non-electric sector, as it enters linearly with consumption of oil. The price of the backstop technology in 2005 is ten times higher than the price of oil. Then, the future price of the backstop technology is driven by a two-factor learning curve. On one hand, investment in R&D raises the amount of domestic knowledge that lowers the price of the backstop, and on the other hand, investment in backstop technology propels the learning-by-doing effect.

Regarding the oil extraction sector, each region is endowed with a given amount of oil resources, which are distinguished in eight different categories (stretching from conventional to unconventional oil). Oil capacity is built cumulatively over time. It can be increased by means of dedicated investments in the extraction sector and it is subjected to depreciation rate (10% annual, to reflect an average economic lifetime of ten years).

An important caveat to this study, is that I assume absence of market power in the carbon market (emission trading scheme) since each region plays as price taker. Certainly, it would be interesting to explore the interaction among the oil and carbon market both in a Cournot equilibrium framework and I deserve this for future work.

#### **4. RESULTS**

Baseline projection from the WITCH model envisages a growing price of oil over time, as depicted in Figure 2. In such a context, the assumption of a Nash-Cournot competition in the oil market, will lead to an upshift in the international price of oil (up to 14% compared to price taker solution). This result is driven by lower investments in the oil extraction sector, as shown in table 1. The higher oil price holds down global consumption of oil (figure 3).

Under a 450 scenario, the difference in oil prices is even larger across the two scenarios (450\_Cournot and 450\_PT). In fact, a competition à la Cournot, will anchor the oil price to a trend similar to that of the business-as-usual benchmark, for many years. Only in the second half of the century, the deployment of a backstop technology at large scale will inevitably decouple them.

From a global standpoint, the higher price curbs the rise in world trade of oil. At the regional level, a Cournot competition reshapes the oil trade flows (as shown in figures 4-7). In fact, the largest oil producer (MENA) tends to pursue a more

“conservative” extraction strategy compared to the competitive equilibrium (as mentioned in Solow 1974, Stiglitz 1976, Malueg and Solow 1990), leading to both reduced oil exports and revenues. This is because a strategic competition dampens the incentive to invest in the oil extraction (as shown in table 1). Accordingly, MENA countries deter investments, which are displaced by higher consumption of final goods in the short term. As a result, oil production, and thus oil revenues, is diverted from MENA countries to other regions (Salant 1976, Ulph and Folie 1980, Loury (1986). Consequently, a Nash-Cournot equilibrium tends also to ease the oil dependency of oil importing countries throughout the century (as shown in Figure 8 and 9). However, the outcome of the Nash-Cournot equilibrium is still beneficial for MENA countries: a sustained oil price and higher consumption of final goods in the short term will overcome the detrimental effect of ailing market shares, both in the BaU and 450 scenarios. Hence, a Nash Cournot competition will enhance the welfare of MENA countries in both a BaU and 450 scenario (Table 2).

A Cournot competition in the oil market will also tamper with the carbon market, as it reduces the price of permits up to 20% (depending on the time period), compared to the price-taker solution (Figure 10). This is simply because a lower consumption of oil entails lesser GHG emissions.

Regarding the climate policy cost, Latin American Countries are the sole major oil exporting regions able to cope with a low carbon world, without incurring in grievous economic losses. In fact, the loss in oil revenues can be retrieved by means of the carbon market. LACA, in particular, has a significant technical potential of biomass resources (up to 60 EJ per year) that, combined with CCS (carbon capture and sequestration), allows for negative carbon emissions. Therefore, Latin American countries are able to restructure their economies by switching from oil revenues to carbon revenues. This will set LACA countries on a path to carbon-credits export-led growth. Consequently, LACA will bear a climate policy cost lower than the world average, as shown in table 2.

A similar conclusion can be drawn for Sub-Saharan African countries (in the SSA aggregate), as they are the biggest potential beneficiaries of a stringent climate agreement. In fact, according to the WITCH model, SSA is the only region incurring in GDP gains, in a low carbon world, as it is both a large seller of carbon permits and minor exporter of oil – so its economy is not gravitating much to the oil industry.

On the contrary, the economy of MENA and TE (Transition Economies, including Russia), is largely skewed towards the oil sector, as their share in the GDP accounts for 40% and 36% at the base year (2005), respectively. The climate policy cost in MENA and TE accounts for 15.89% and 10.54% respectively, under Nash-Cournot competition.

At the global scale, a competition à la Cournot would slightly soothe the global GDP losses compared to the price taker equilibrium: 3.54% against 3.64%.

In order to better comprehend the underlying process leading to these results; it is useful to analyze the pattern of marginal costs, which are the starting point for the measurement of the market power. Under a price-taker equilibrium, marginal revenues are equal across regions and coincide with the international price of oil. Conversely, under a Cournot competition, marginal revenues equal the full marginal social costs (Pindyck 1985). For this reason, I will focus on the marginal social costs only for the Nash-Cournot scenarios (figure 11 and 12). Large oil exporting countries (in particular MENA) enjoy lower marginal social costs, both in a BaU and 450 scenarios.

At this point, we can also compute the Lerner Index, which is a price-cost margin indicator useful to evaluate the market power both at a regional or global level. The Lerner Index can vary between zero (absence of market power) and one (monopoly power). It is defined as the difference between one and the full marginal social costs divided by the price. Interestingly, under a Cournot equilibrium the global Lerner Index is also linked with the Herfindahl-Hirschman (HHI) index – which measures the level of concentration of supply – along with the global elasticity of demand.

Figure 13 and 14 show the regional (dashed lines) and global (solid line) Lerner index and compare with the global HHI index (solid line, in red).

By comparing figures 13 and 14, we can notice that MENA countries enhance their market power under a 450 ppm scenario. At a first glance, this seems to be beneficial for MENA countries. Instead, a stringent policy backdrop (450 ppm) will have sweeping implications for the oil extraction industry. In fact, the value of the oil market will gradually wane during the century, from roughly \$700 Billion in 2005 (1.6% of world GDP) to \$100 Billion in 2100 (0.03% of global GDP). This will cause a drop in oil revenues, as reported in table 1.

Also at the global level, the Lerner Index (solid line in black) exhibits a noticeable growth in the 450-ppm scenario, albeit the global HHI index – which measures the concentration of oil supply – is roughly in line with the BaU scenario. This suggests that the escalation in the monopoly power in the 450 scenario is mainly due to a shift in the elasticity of demand, rather than to a gain in the market shares of large oil producers (as shown in table 1). Indeed, demand of oil is not iso-elastic in WITCH as shown in figure 14 and 15.

The long-run price elasticity of oil, in the WITCH model, appears to be in line with many empirical studies and surveys (Brons et al. 2008, Espey 1998, Burke and Nishitateno 2013, Graham and Glaister 2004, Havranek et al. 2012, Scott 2012, Baranzini and Weber 2013, Cynthia Lin and Zeng 2013, Seale and Solano 2012, Agnolucci 2009), which found that the long-run price elasticity falls in the range of -0.84 and -0.31.

Results from the WITCH model suggest that, in a BaU scenario, future price elasticities of oil tend to converge across regions to the range of -0.51 (WEURO) and -0.63 (TE) in 2100, as shown in Figure 14. Conversely, in a 450-ppm scenario (Figure 15), the introduction of a carbon price (from 2015 onwards), will cause an abrupt shift in the long-run price elasticities of oil. In fact, they will become more inelastic, until the backstop will replace oil, causing a sharp rebound in regional elasticities.

Interestingly, when the price of carbon will reach 100 \$ per tonne of CO<sub>2</sub> – which will occur in 2030 – the regional elasticities will be in the range of -0.33 (SASIA) and -0.5 (MENA). Then, after 2030, the regional elasticities will start to diverge over time. This is due to the different regional patterns of diffusion of the backstop technology.

However, the key issue for the oil extraction industry is the trend of the price elasticity at the global level. If we consider the world price elasticity (black solid line), it will become consistently less elastic compared to the BaU scenario and this explains the associated uptick in the monopoly power in the 450 scenario.

## 5. CONCLUSION

This paper has investigated the outcome of a Nash-Cournot equilibrium in the oil extraction sector using an Integrated Assessment Model. Two scenarios have been

considered: a Business as Usual scenario and a stringent climate policy (consistent with a 450-ppm target in 2100). They have been run using both a price equilibrium setting and a Cournot competition. The main conclusions of this study can be summarised as follow:

- a) In all scenarios, the international price of oil turns out to be higher under a Nash-Cournot competition compared to the price taker solution. This result is driven by a restrained oil extraction, triggered by weaker investments. The largest oil producer tends to behave more conservatively. Oil importing countries tend to accelerate their extraction rate. Consequently, the growth in world trade of oil slows down.
- b) At the regional level, investments are diverted towards smaller producers. This will cause ailing market shares for large oil-exporting countries. Nonetheless, a Nash-Cournot competition will enhance the payoff of oil-exporting countries. This result is driven by sluggish investments in the oil extraction sector, which are displaced by a prompt rise in consumption of final goods.
- c) In a low-carbon world, a Cournot competition in fuel markets reduces the price of permits, under the hypothesis of a competitive carbon market.
- d) In the short term, the introduction of carbon price hinders the responsiveness of oil demand to a change in the oil price. Oil producers enhance their market power due to a less elastic demand. Consequently, oil producers retain their ability to set the price for many years, until a backstop technology will replace oil.
- e) A low carbon world increases the monopoly power of oil producers. Nonetheless, a stringent will lead to flagging oil demand and shrinking revenues, which will strain the economy of large exporting countries. In particular, the largest oil producer (MENA) will bear the highest climate policy cost (15.89%).
- f) Finally, under a Nash-Cournot competition, global mitigation costs are slightly reduced (3.54% instead of 3.64%).

## 6. ACKNOWLEDGMENTS

Insert your acknowledgments here; do not place them on the first page of your paper or as a footnote.

## 7. REFERENCES

1. Agbeyegbe, T.D. (1989). "Interest rates and metal price movements: Further evidence". *Journal of Environmental Economics and Management*, Volume 16, Issue 2, March 1989, Pages 184-192.
2. Agnolucci, P. (2009). "The energy demand in the British and German industrial sectors: Heterogeneity and common factors". *Energy Economics*, Volume 31, Issue 1, January 2009, Pages 175-187.
3. Alhajji, A.F., D. Huettner (2000). "OPEC and other commodity cartels: a comparison". *Energy Policy*, Volume 28, Issue 15, December 2000, Pages 1151-1164.
4. Amir, R., I. Grilo (1999). "Stackelberg versus Cournot Equilibrium". *Games and Economic Behavior* 26, 1–21 (1999).
5. Baranzini, A., S. Weber (2013). "Elasticities of gasoline demand in Switzerland". *Energy Policy*, Volume 63, December 2013, Pages 674-680.
6. Barnett, J., S. Dessai, M. Webber (2004). "Will OPEC lose from the Kyoto Protocol? ". *Energy Policy*, Volume 32, Issue 18, December 2004, Pages 2077-2088.
7. Berg, E., S. Kverndokk, K.E. Rosendahl (1997). "Gains from cartelisation in the oil market". *Energy Policy*, Volume 25, Issue 13, November 1997, Pages 1075-1091.
8. Bertrand, J. (1883). " Review of *Théorie Mathématique de la Richesse Sociale* and *Recherches sur les Principes Mathématique de la Théorie des Richesses*". *Journal des Savants* 68, 499–508. English translation reprinted in Daughety, A.F., 1988. *Cournot Oligopoly: Characterizations and Applications*. New Cambridge University Press, New York.

9. Böckem, S. (2004). "Cartel formation and oligopoly structure: a new assessment of the crude oil market". *Applied Economics* 2004(36)-12, Pages 1355-1369.
10. Bosetti, V., E. Massetti, M. Tavoni (2007). "The WITCH model: Structure, Baseline and Solutions". Working Paper 10-2007.
11. Bosetti, V., C. Carraro, M. Galeotti, E. Massetti, M. Tavoni (2006). "WITCH: A World Induced Technical Change Hybrid Model". *The Energy Journal*, Special Issue on Hybrid Modeling of Energy-Environment Policies: Reconciling Bottom-up and Top-down, 13-38.
12. Bosetti, V., M. Tavoni, E. De Cian, A. Sgobbi. (2009). "The 2008 WITCH Model: New Model Features and Baseline". FEEM Working Paper 2009.085.
13. Boyce, J.R., L. Vojtassak (2008). "An 'Oil'igopoly Theory Of Exploration". *Resource and Energy Economics* - 30(3) (2008), 428–454.
14. Braten, J., R. Golombek (1998). "OPEC's Response to International Climate Agreements". *Environmental and Resource Economics* 12: 425–442, 1998.
15. Brémond, V., E. Hache, V. Mignon (2012). "Does OPEC still exist as a cartel? An empirical investigation". *Energy Economics*, Volume 34, Issue 1, January 2012, Pages 125-131.
16. Brons, M., P. Nijkamp, E. Pels, P. Rietveld (2008). "A meta-analysis of the price elasticity of gasoline demand. A SUR approach". *Energy Economics*, Volume 30, Issue 5, September 2008, Pages 2105-2122.
17. Burke, P.J., S. Nishitateno (2013). "Gasoline prices, gasoline consumption, and new-vehicle fuel economy: Evidence for a large sample of countries". *Energy Economics*, Volume 36, March 2013, Pages 363-370.
18. Cairns, R.D., E. Calfucura (2012). "OPEC: Market failure or power failure?". *Energy Policy*, Volume 50, November 2012, Pages 570-580.
19. Chermak, J.M., R.H. Patrick (2002). "Comparing tests of the theory of exhaustible resources". *Resource and Energy Economics*, Volume 24, Issue 4, 1 November 2002, Pages 301-325.

20. Chilton, J. (1984). "The Pricing of Durable Exhaustible Resources: Comment". *The Quarterly Journal of Economics*, Vol. 99, No. 3 (Aug., 1984), pp. 629-637.
21. Colombo, L., P. Labrecciosa (2008). "When Stackelberg and Cournot Equilibria Coincide". *The B.E. Journal of Theoretical Economics*, De Gruyter, vol. 8(1), pages 1-7, January.
22. Cournot, A. (1838). "Researches into the Mathematical Principles of the Theory of Wealth". New York, Transl. by Nathaniel T. Bacon (1897).
23. Cynthia Lin C.Y., J. Zeng (2013). "The elasticity of demand for gasoline in China ". *Energy Policy*, Volume 59, August 2013, Pages 189-197.
24. Dahl, C.A. (2012). "Measuring global gasoline and diesel price and income elasticities". *Energy Policy*, Volume 41, February 2012, Pages 2-13.
25. Danielsen, A.L., S. Kim (1988). "OPEC stability: An empirical assessment ". *Energy Economics*, Volume 10, Issue 3, July 1988, Pages 174-184.
26. De Santis, R.A. (2003). "Crude oil price fluctuations and Saudi Arabia's behaviour". *Energy Economics*, Volume 25, Issue 2, March 2003, Pages 155-173.
27. Déés, S., P. Karadeloglou, R.K. K. Kaufmann, M. Sánchez (2007). "Modelling the world oil market: Assessment of a quarterly econometric model". *Energy Policy*, Volume 35, Issue 1, January 2007, Pages 178-191.
28. Edenhofer, O., B. Knopf, T. Barker, L. Baumstark, E. Bellevrat, B. Chateau, P. Criqui, M. Isaac, A. Kitous, S. Kypreos, M. Leimbach, K. Lessmann, B. Magné, S. Scriciu, H. Turton, D. P. Van Vuuren (2010). "The Economics of Low Stabilization: Model Comparison of Mitigation Strategies and Costs". *Energy Journal*. Jan2010 Special Issue, Vol. 31, p11-48. 38p.
29. Espey, M. (1998). "Gasoline demand revisited: an international meta-analysis of elasticities". *Energy Economics* 20 (1998),pp. 273-295.
30. Eswaran, M., T.R. Lewis, T. Heaps (1983). "On the Nonexistence of Market Equilibria in Exhaustible Resource Markets with Decreasing Costs". *Journal of Political Economy*, Vol. 91, No. 1, Feb., 1983 .

31. Fattouh, B., L. Mahadeva (2013). "OPEC: What Difference has it Made?". Oxford Institute for Energy Studies, January 2013, MEP3.
32. Gaudet, G., S.W. Walter Salant (1991). "Uniqueness Of Cournot Equilibrium: New Results From Old Methods". *Review of Economic Studies*, Wiley Blackwell, vol. 58(2), pages 399-404.
33. Gerlagh, R., M. Liski (2011). "Strategic resource dependence ". *Journal of Economic Theory*, Volume 146, Issue 2, March 2011, Pages 699-727.
34. Graham , D.J., S. Glaister (2004). "Road Traffic Demand Elasticity Estimates: A Review". *Transport Reviews: A Transnational Transdisciplinary Journal* Volume 24, Issue 3, 2004, pages 261-274.
35. Halvorsen, R., T.R. Smith (1991). "A Test of the Theory of Exhaustible Resources". *The Quarterly Journal of Economics* (1991) 106 (1): 123-140.
36. Havlík, P., U.A. Schneider, E. Schmid, H. Böttcher, S. Fritz, R. Skalský, K. Aoki, S.D. Cara, G. Kindermann, F. Kraxner, S. Leduc, I. McCallum, A. Mosnier, T. Sauer, M. Obersteiner (2011). "Global land-use implications of first and second generation biofuel targets". *Energy Policy*, Volume 39, Issue 10, October 2011, Pages 5690-5702.
37. Havranek, T., Z. Irsova, K. Janda (2012). "Demand for gasoline is more price-inelastic than commonly thought". *Energy Economics* 34 (2012),pp. 201–207.
38. Heal, G. (1976). "The Relationship between Price and Extraction Cost for a Resource with a Backstop". *The Bell Journal of Economics*, Vol. 7, No. 2 (Autumn, 1976), pp. 371-378.
39. Heal, G., M. Barrow (1980). "The Relationship between Interest Rates and Metal Price Movements". *The Review of Economic Studies* , Vol. 47, No. 1, Jan., 1980 .
40. Hoel, M. (1978). "Resource extraction, substitute production, and monopoly". *Journal of Economic Theory*, Volume 19, Issue 1, October 1978, Pages 28-37.
41. Holz, F., C. von Hirschhausen, C. Kemfert, A. Kanudia (2007). "A strategic model of European gas supply (GASMOD)". *Energy Economics*, Volume 30, Issue 3, May 2008, Pages 766-788.

42. Hotelling, H. (1931). "The Economics of Exhaustible Resources". *Journal of Political Economy*. 39(2), April 1931, pages 137-75.
43. Huck, S., W. Müller, H.T. Normann (2001). "Stackelberg Beats Cournot: On Collusion and Efficiency in Experimental Markets". *The Economic Journal*, Vol. 111, No. 474 (Oct., 2001), pp. 749-765.
44. Huntington, H., S. M. Al-Fattah, Z. Huang, M. Gucwa, A. Nouri (2013). "Oil Markets and Price Movements: A Survey of Models". USAEE Working Paper No. 13-129.
45. Huppmann, D., F. Holz (2012). "Crude Oil Market Power—A Shift in Recent Years?". *Energy Journal*; 2012, Vol. 33 Issue 4, p1.
46. Huppmann, D., F. Holz (2009). "A Model for the Global Crude Oil Market Using a Multi-Pool MCP Approach". DIW Berlin, German Institute for Economic Research.
47. Kalkuhl, M., R.J. Brecha (2013). "The carbon rent economics of climate policy". *Energy Economics* 39 (2013) 89–99.
48. Karp, L. (1996). "Monopoly Power can be Disadvantageous in the Extraction of a Durable Nonrenewable Resource". *International Economic Review*, Vol. 37, No. 4, Nov., 1996.
49. Karp, L., D.M. Newbery (1991). "OPEC and the U.S. Oil Import Tariff". *The Economic Journal*, Vol. 101, No. 405 (Mar., 1991), pp. 303-313.
50. Kaufmann, R.K., A. Bradford, L.H. Belanger, J.P. McLaughlin, Y. Miki (2008). "Determinants of OPEC production: Implications for OPEC behavior". *Energy Economics*, Volume 30, Issue 2, March 2008, Pages 333-351.
51. Kolstad, C.D., L. Mathiesen (1987). "Necessary and Sufficient Conditions for Uniqueness of a Cournot Equilibrium". *The Review of Economic Studies*, Vol. 54, No. 4, Oct., 1987.
52. Kreps, D.M., J.A. Scheinkman (1983). "Quantity Precommitment and Bertrand Competition Yield Cournot Outcomes". *The Bell Journal of Economics*, Vol. 14, No. 2 (Autumn, 1983), pp. 326-337.

53. Kriegler et al. (2013). "Overview of the EMF 27 Study on Energy System Transition Pathways Under Alternative Climate Policy Regimes.". *Climatic Change*, in press. doi:10.1007/s10584-013-0953-7.
54. Levhari, D., R.S. Pindyck (1981). "The Pricing of Durable Exhaustible Resources". *The Quarterly Journal of Economics*, Vol. 96, No. 3 (Aug., 1981), pp. 365-378.
55. Lewis, T.R., S.A. Matthews, H.S. Burness (1979). "Monopoly and the Rate of Extraction of Exhaustible Resources: Note". *The American Economic Review*, Vol. 69, No. 1, Mar., 1979.
56. Loderer, C. (1985). "A Test of the OPEC Cartel Hypothesis: 1974-1983". *The Journal of Finance*, Vol. XL, no. 3, July 1985.
57. Loulou, R., M. Labriet, A. Haurie, A. Kanudia (2008). "OPEC Oil Pricing Strategies in a Climate Regime: a Two-Level Optimization Approach in an Integrated Assessment Model". *lea-Etsap*.
58. Loury, G.C. (1986). "A theory of 'oil'igopoly: Cournot equilibrium in exhaustible resource markets with fixed supply". *International Economic Review*, Vol. 27, No. 2 (Jun., 1986), pp. 285-301.
59. Malueg, D.A., J.L. Solow (1990). "Monopoly Production of Durable Exhaustible Resources". *Economica, New Series*, Vol. 57, No. 225 (Feb., 1990), pp. 29-47.
60. Massetti, E., F. Sferra (2010). "A Numerical Analysis of Optimal Extraction and Trade of Oil Under Climate Policy". *Fondazione Eni Enrico Mattei, Working Paper No. 2010.113*.
61. Newbery, D. M. G. (1981). "Oil Prices, Cartels, and the Problem of Dynamic Inconsistency". *The Economic Journal*, Vol. 91, No. 363 (Sep., 1981), pp. 617-646.
62. Nordhaus, W.D., H. Houthakker, R. Solow (1973). "The Allocation of Energy Resources". *Brookings Papers on Economic Activity*, Vol. 1973, No. 3 (1973), pp. 529-576.
63. Orbay, H. (2009). "Computing Cournot Equilibrium through Maximization over Prices". *Economics Letters*, Volume 105, Issue 1, October 2009, Pages 71-73.

64. Pindyck, R.S. (1978). "The Optimal Exploration and Production of Nonrenewable Resources". *Journal of Political Economy*, Vol. 86, No. 5 (Oct., 1978), pp. 841-861.
65. Pindyck, R.S. (1978b). "Gains to producers from the cartelization of exhaustible resources". *The Review of Economics and Statistics* 60 (2), 238–251.
66. Pindyck, R.S. (1985). "The measurement of monopoly power in dynamic markets". *Journal of Law and Economics* Vol. 28, No. 1, Apr., 1985 .
67. Reynolds, D.B., M.K. Pippenger (2010). "OPEC and Venezuelan oil production: Evidence against a cartel hypothesis". *Energy Policy*, Volume 38, Issue 10, October 2010, Pages 6045-6055.
68. Salant, S.W. (1976). "Exhaustible Resources and Industrial Structure: A Nash-Cournot Approach to the World Oil Market". *The Journal of Political Economy*, Volume 84, Issue 5 (Oct., 1976), 1079-1094.
69. Scott, K.R. (2012). "Rational habits in gasoline demand". *Energy Economics* 34 (2012) 1713–1723.
70. Seale J.L. Jr., A.A. Solano (2012). "The changing demand for energy in rich and poor countries over 25 years". *Energy Economics*, Volume 34, Issue 6, November 2012, Pages 1834-1844.
71. Sferra, F., M. Tavoni (2013). "Endogenous participation in a Partial Climate Agreement with open entry: a numerical assessment". *Fondazione Eni Enrico Mattei Working Paper No. 2013.060* .
72. Smith, J.L. (2005). "Inscrutable OPEC? Behavioral Tests of the Cartel Hypothesis". *The Energy Journal* 26 (1), 51–82.
73. Solow, R.M. (1974). "The Economics of Resources or the Resources of Economics". *The American Economic Review* , Vol. 64, No. 2, Papers and Proceedings of the Eighty-sixth Annual Meeting of the American Economic Association. (May, 1974), pp. 1-14.
74. Stackelberg, H. Von (1934). "Marktforn und Gleichgewicht". Springer-Verlag, Berlin-Wien.

75. Stiglitz, J. (1976). "Monopoly and the rate of extraction of Exhaustible Resources". *The American Economic Review*, Vol. 66, Issue4, (Mar., 1976), 655-661.
76. Stiglitz, J., P. Dasgupta (1981). "Market structure and resource extraction under uncertainty". *The Scandinavian Journal of Economics*, 1981 - JSTOR.
77. Tremblay, C.H., V.J. Tremblay (2011). "The Cournot–Bertrand model and the degree of product differentiation". *Economics Letters*, Volume 111, Issue 3, June 2011, Pages 233-235.
78. Tremblay, C.H., M.J. Tremblay, V.J. Tremblay (2011b). "A General Cournot-Bertrand Model with Homogeneous Goods". *Theoretical Economics Letters*, 2011, 1, 38-40.
79. Trüby, J. (2013). "Strategic behaviour in international metallurgical coal markets ". *Energy Economics*, Volume 36, March 2013, Pages 147-157.
80. Ulph, A.M., G.M. Folie (1980). "Exhaustible Resources and Cartels: An Intertemporal Nash-Cournot Model". *The Canadian Journal of Economics / Revue canadienne d'Economie*, Vol. 13, No. 4(Nov., 1980), pp. 645-658.
81. Waisman, H., J. Rozenberg, J.C. Hourcade (2013). "Monetary compensations in climate policy through the lens of a general equilibrium assessment: The case of oil-exporting countries". *Energy Policy*, In Press, Corrected Proof, Available online 13 September 2013.
82. Wang, M., J. Zhao (2013). "Monopoly extraction of a nonrenewable resource facing capacity constrained renewable competition". *Economics Letters*, Volume 120, Issue 3, September 2013, Pages 503-508.
83. Yang, Z. (2008). "How Does ANWR Exploration Affect OPEC Behavior? —A Simulation Study of an Open-loop Cournot-Nash Game". *Energy Economics* 30 (2008) 321–332.
84. Zhihao, Y. (2007). "Strategic Trade Policy Aspects of the Kyoto Protocol: Extracting Oil Rents". *Asia-Pacific Journal of Accounting & Economics* 14 (2007) 219–234.

## 8. IMAGES AND TABLES

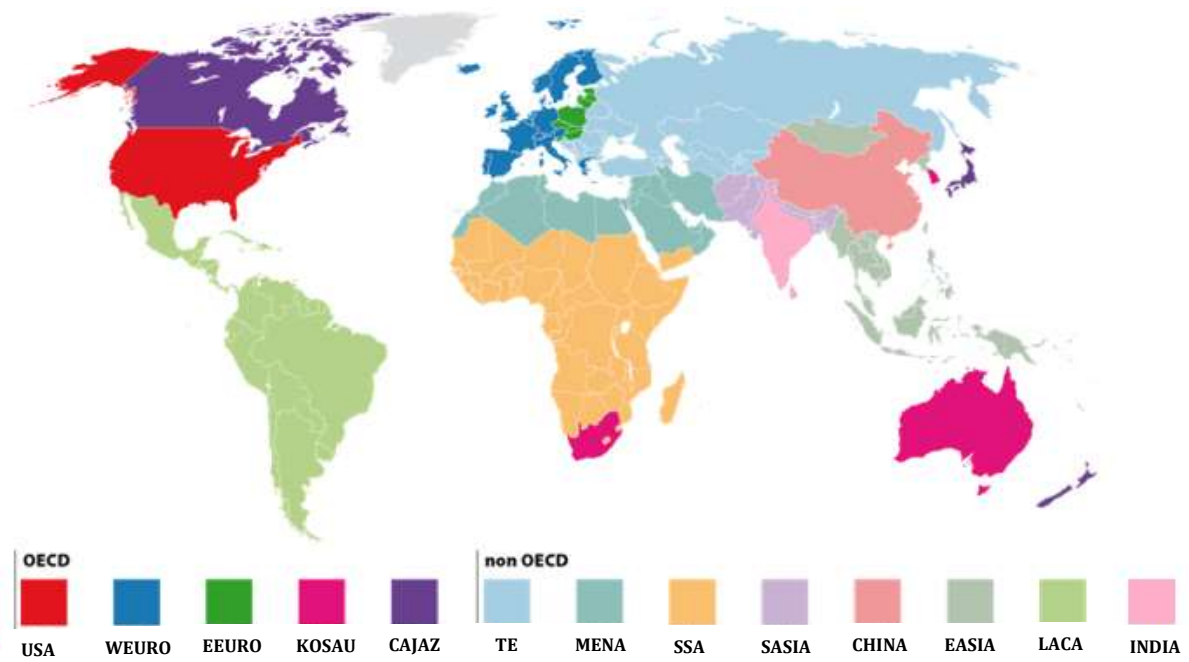


Fig. 1 Regional description.

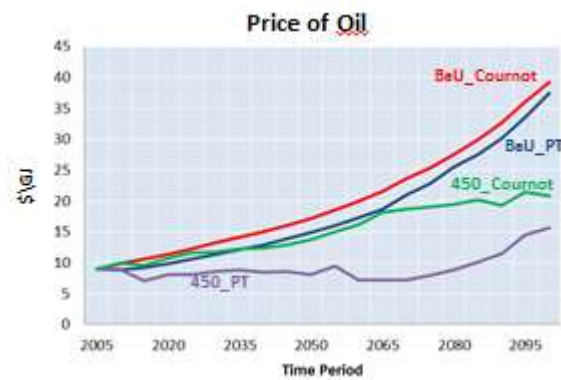


Fig. 2 Price of Oil

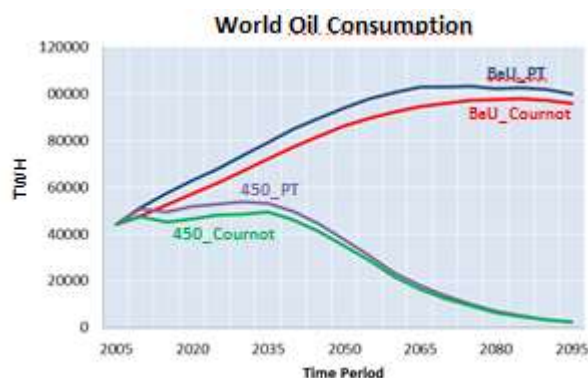


Fig. 3 Oil Demand

	<i>Business as Usual Scenario</i>				<i>Stabilisation Scenario</i>			
	<i>BaU_PT</i>		<i>BaU_Cournot</i>		<i>450_PT</i>		<i>450_Cournot</i>	
	<i>2005-2030</i>	<i>2035-2100</i>	<i>2005-2030</i>	<i>2035-2100</i>	<i>2005-2030</i>	<i>2035-2100</i>	<i>2005-2030</i>	<i>2035-2100</i>
<b>Cumulative Oil Investments (T\$)</b>								
MENA	4.6	36.8	2.0	22.4	3.3	4.4	1.1	0.9
LACA	2.2	26.8	1.8	22.6	1.3	0.9	1.1	1.2
TE	2.0	18.7	1.6	16.4	1.2	0.6	1.0	1.0
WORLD:	15.7	141.6	13.7	124.2	10.1	8.0	9.4	9.7
<b>Cumulative Oil Revenues (T\$)</b>								
MENA	18.4	161.8	15.9	148.7	14.7	31.5	12.5	20.6
LACA	6.4	89.3	6.7	89.9	4.7	5.5	5.5	10.3
TE	6.9	70.3	7.1	73.2	5.2	4.9	5.9	9.9
WORLD:	49.4	556.5	51.5	580.2	37.3	55.2	43.0	84.2
<b>Oil Market Shares:</b>								
MENA	37%	31%	31%	26%	39%	57%	29%	25%
LACA	13%	15%	13%	15%	13%	10%	13%	12%
TE	14%	12%	14%	12%	14%	9%	14%	12%
WORLD:	100%	100%	100%	100%	100%	100%	100%	100%
<b>Average Return on Investment (ROI)</b>								
MENA	3.2	4.0	4.6	6.2	2.6	3.4	4.8	8.1
LACA	2.5	3.0	2.9	3.5	2.0	1.9	2.9	3.3
TE	2.9	3.2	3.5	3.7	2.4	1.8	3.4	3.2
WORLD:	2.5	3.3	2.9	3.6	2.1	1.9	2.8	3.0

Tab. 1 Large oil producers: overview

	Social Welfare				Discounted (5%) GDP losses			
	BaU_PT	BaU_Cournot	450_PT	450_Cournot	BaU_PT	BaU_Cournot	450_PT	450_Cournot
USA	-8413.0	-8418.3	-8500.5	-8506.3	-	-	2.80%	2.81%
WEURO	-9985.6	-9989.0	-10029.5	-10031.0	-	-	1.35%	1.28%
EEURO	-3032.3	-3033.0	-3057.0	-3055.9	-	-	3.30%	2.54%
KOSAU	-3485.0	-3486.6	-3491.1	-3493.2	-	-	1.51%	1.69%
CAJAZ	-3807.2	-3806.9	-3829.2	-3828.7	-	-	1.99%	2.03%
TE	-13380.4	-13360.3	-13699.1	-13659.1	-	-	11.41%	10.54%
MENA	-17953.3	-17934.8	-18538.1	-18528.7	-	-	16.35%	15.89%
SSA	-61488.7	-61413.3	-61063.9	-61051.4	-	-	-0.24%	-0.36%
SASIA	-27002.8	-27014.9	-27040.7	-27063.1	-	-	2.08%	2.04%
CHINA	-52168.7	-52203.9	-52853.5	-52877.9	-	-	7.16%	7.11%
EASIA	-29364.9	-29382.0	-29362.8	-29397.0	-	-	3.07%	2.99%
LACA	-22800.4	-22790.6	-22791.6	-22793.9	-	-	2.82%	2.72%
INDIA	-61439.0	-61483.2	-61339.1	-61425.7	-	-	0.40%	0.66%
world	-	-	-	-	-	-	3.64%	3.54%

Tab. 2 Social Welfare and Policy Cost

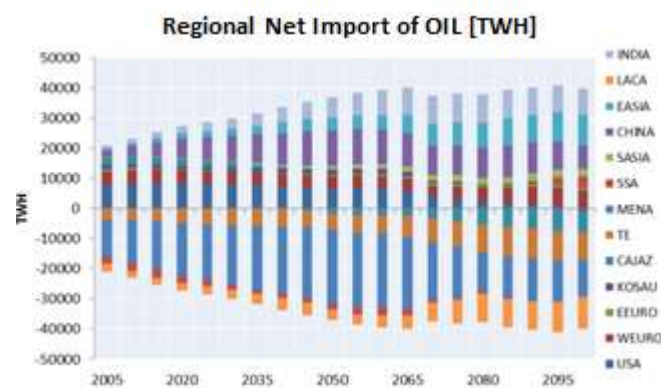


Fig. 4 Trade of Oil: BaU\_PT

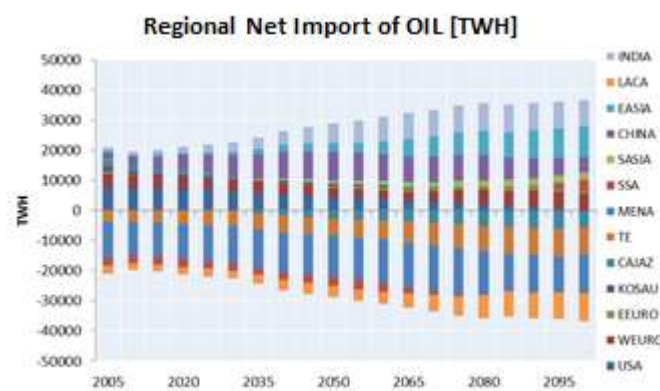


Fig. 5 Trade of Oil: BaU\_Cournot

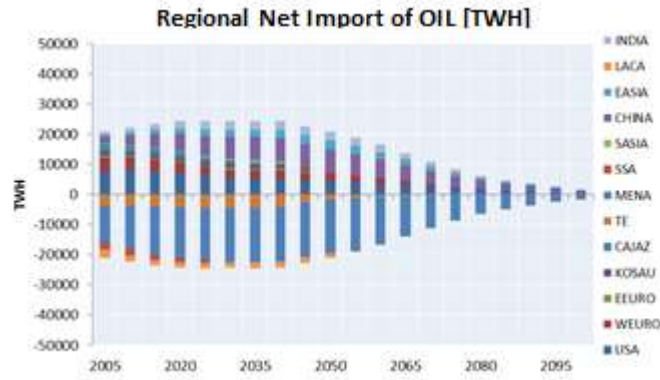


Fig. 6 Trade of Oil: 450\_PT

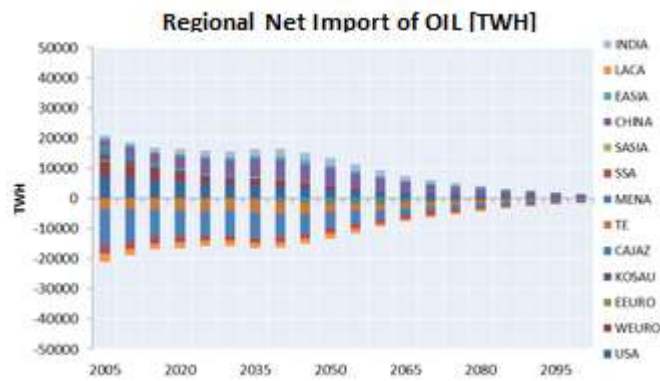


Fig. 7 Trade of Oil: 450\_Cournat

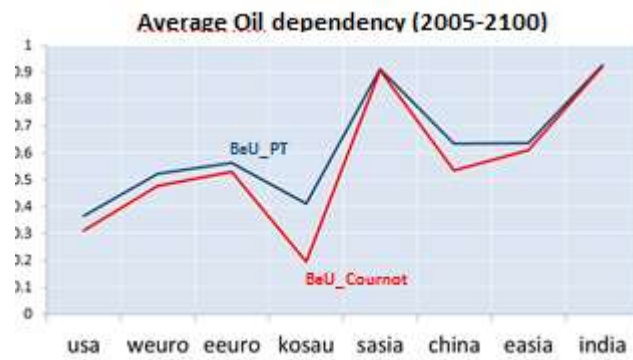


Fig. 8 Oil Dependency - BaU

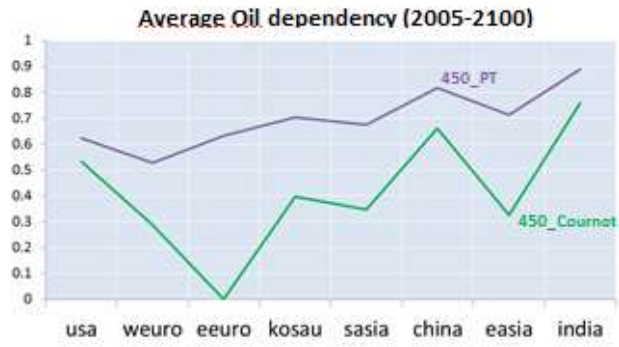


Fig. 9 Oil Dependency - Stab 450 ppm

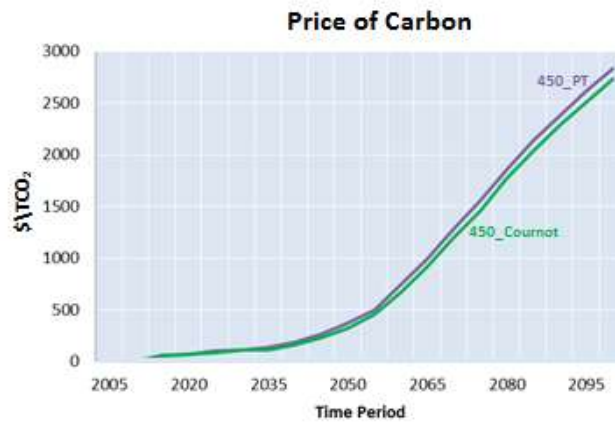


Fig. 10 Price of carbon permits (450 ppm)



Fig. 11 Marginal Costs: BaU\_Cournot



Fig. 12 Marginal Costs: 450\_Cournot

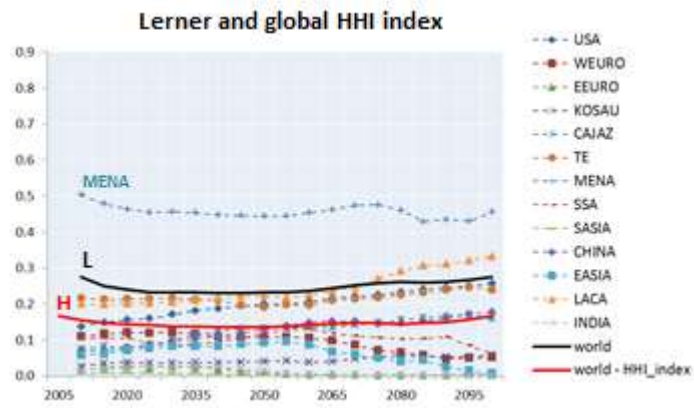


Fig. 13 Lerner Index: BaU\_Cournot

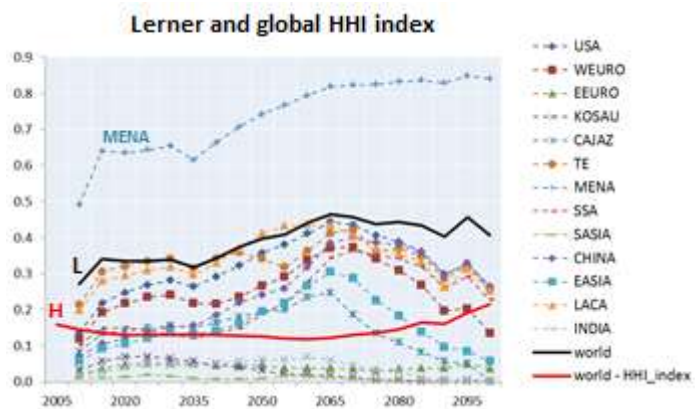


Fig. 14 Lerner Index: 450\_Cournot

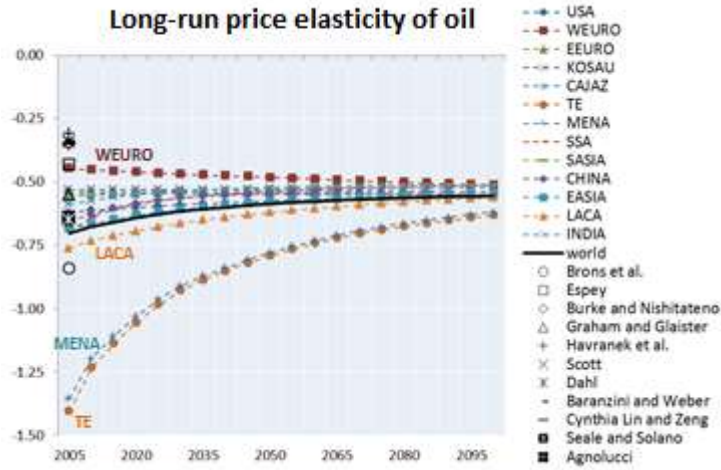


Fig. 14 Price Elasticity of oil: BaU\_Cournot

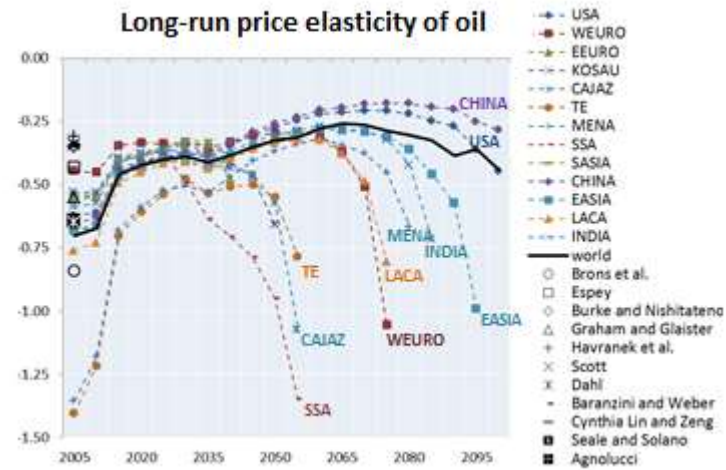


Fig. 15 Price Elasticity of oil: 450\_Cournot

**Mitigation Policies & Strategies**

**Air quality and carbon  
reduction policies**

## Can Nigeria pursue low carbon development?

Cervigni, R\*.<sup>1</sup>, Rogers, J.A.<sup>2</sup>, and Henrion, M.<sup>3</sup>

<sup>1</sup>The World Bank - USA, <sup>2</sup>The World Bank - USA, and <sup>3</sup>Lumina Decision Systems - USA

\*Corresponding Author: rcervigni@worldbank.org

### Abstract

This paper argues that Nigeria can achieve its national development goals with up to 32 percent lower carbon emissions than in a business-as-usual growth scenario. A lower carbon path offers not only the global benefits of reducing contributions to climate change, but also net economic benefits to Nigeria, estimated at about 2 percent of GDP. These national benefits include cheaper and more diversified electricity sources, with savings of the order of 7 percent or US\$12 billion; more efficient operation of the oil/gas industry, with discounted net benefits of US\$7.5 billion more productive and climate-resilient agriculture; and better transport services, resulting in fuel savings, better air quality, and reduced congestion. These domestic benefits would be accompanied by a global benefit of avoiding some 2.3 billion tons of CO<sub>2</sub>e (carbon dioxide equivalent) emissions over 25 years. An additional 1.4 billion tons of emission reductions are technically viable, but would require extra financial incentives to be economically viable for Nigeria.

**Keywords:** Low Carbon Development, Sub-Saharan Africa, climate change mitigation, Nigeria

## 1. INTRODUCTION

The Federal Government of Nigeria (FGN) has formulated an ambitious strategy, known as Vision 20:2020, which aims to make Nigeria the world's 20th largest economy by 2020. Sustaining such a pace of growth over a longer term implies that by 2035 Nigeria would increase electricity generation by a factor of 9, road freight transport by a factor of 18, and private car ownership by a factor of 3.5. Domestic agricultural production would need to increase six-fold to meet the food requirements of a growing population while decreasing dependency on food imports—an important FGN priority.

Assuming conventional approaches to oil and gas production, electricity generation and use, transportation, and agriculture, achieving these goals could mean a doubling of greenhouse gas (GHG) emissions by 2035. Cumulative emissions over this period (2010–35) might add up to 11.6 billion tons of CO<sub>2</sub> (Gt CO<sub>2</sub>) to the atmosphere—five times the estimated historical emissions between 1900 and 2005.

This paper<sup>1</sup> argues that there are many ways that Nigeria can achieve the Vision 20:2020 development objectives to 2020 and beyond, which include up to 32 percent lower carbon emissions. A lower carbon path offers not only the global benefits of reducing contributions to climate change, but also net economic benefits to Nigeria, estimated at about 2 percent of GDP. These national benefits include cheaper and more diversified electricity sources, with savings of the order of 7 percent or US\$12 billion; more efficient operation of the oil/gas industry, with discounted net benefits of US\$7.5 billion more productive and climate-resilient agriculture; and better transport services, resulting in fuel savings, better air quality, and reduced congestion. These domestic benefits would be accompanied by a global benefit of avoiding some 2.3 billion tons of CO<sub>2</sub>e (carbon dioxide equivalent) emissions over 25 years. An additional 1.4 billion tons of emission reductions are technically viable, but would require extra financial incentives to be economically viable for Nigeria.

---

<sup>1</sup> This paper summarizes the finding of a broader analytical effort: see Cervigni, Rogers and Henrion (2013) and Cervigni, Rogers and Dvorak (2013).

## 2. METHODOLOGY

The analysis of each of the four economic sectors is based on a comparison between a reference scenario and one or more low-carbon scenarios.

The reference scenario was designed as a plausible representation of how the country's economy might evolve in the period up to 2035 on the basis of historical trends and current government plans. It describes a reasonable trajectory for growth and structural change of the economy in the absence of targeted interventions to reduce carbon emissions. It assumes that future sector development decisions would be made without any specific focus on their climate change impacts or on their long-term resilience to a changing climate. It uses historic data to define the activity and resulting emissions in the base year. It takes into account existing, concrete, feasible investment plans (for example, power stations that are in the process of being built or are under firm commitment) and attempts to include the "best-business-decision" investments that could be made in future years within the constraints and barriers that are present in the economy.

Thus, the reference case is not a mere continuation of current practice, nor is it always the scenario with the highest GHG emissions. Sometimes the "best-business-decision" investments will lead to higher energy efficiency, greater productivity per unit of energy used, or cleaner energy sources, even within current constraints and barriers. It follows existing policies and plans adopted by the government. For example, the reference scenario for oil and gas assumes significant reduction in gas flares following flare-reduction agreements and programs already in place. The reference scenario for electric power assumes building nuclear power and coal-fired power plants according to current government policy.

The low-carbon scenarios include technological, institutional, organizational, or management interventions designed to achieve at least the same development objectives of the reference scenario, but with lower GHG emissions and sometimes also additional benefits in other areas. Adoption of low-carbon solutions often will require policy changes to remove constraints and barriers. This process will necessitate making project financing available to enable changes that would not otherwise be practical.

Different stakeholders may approach the search for a realistic low-carbon development pathway from a different angle, illuminating important aspects of the economics of GHG mitigation and implementation strategies. Choosing which interventions or policy changes to include in the reference scenario and which to leave to the low-carbon scenarios is a delicate task crucial to the credibility of the strategy. It is very difficult to get buy-in from a wide range of stakeholders around an excessively “dirty” reference scenario that is unlikely to happen in reality.

### Selecting Low-Carbon Technologies and Interventions

The low-carbon scenario provides a list of low-carbon technologies, also termed mitigation options or interventions, designed to reduce carbon emissions relative to the reference scenario. Examples are: for agriculture, conservation agriculture, agro-forestry, and sustainable rice intensification; for the oil and gas sector, reducing flaring of natural gas and using more efficient pumps for oil extraction; for the power sector, promoting energy-efficient lighting and generating power from renewables such as photovoltaics and wind; and for transport, expanding bus rapid transit and tightening standards of fuel efficiency for road vehicles.

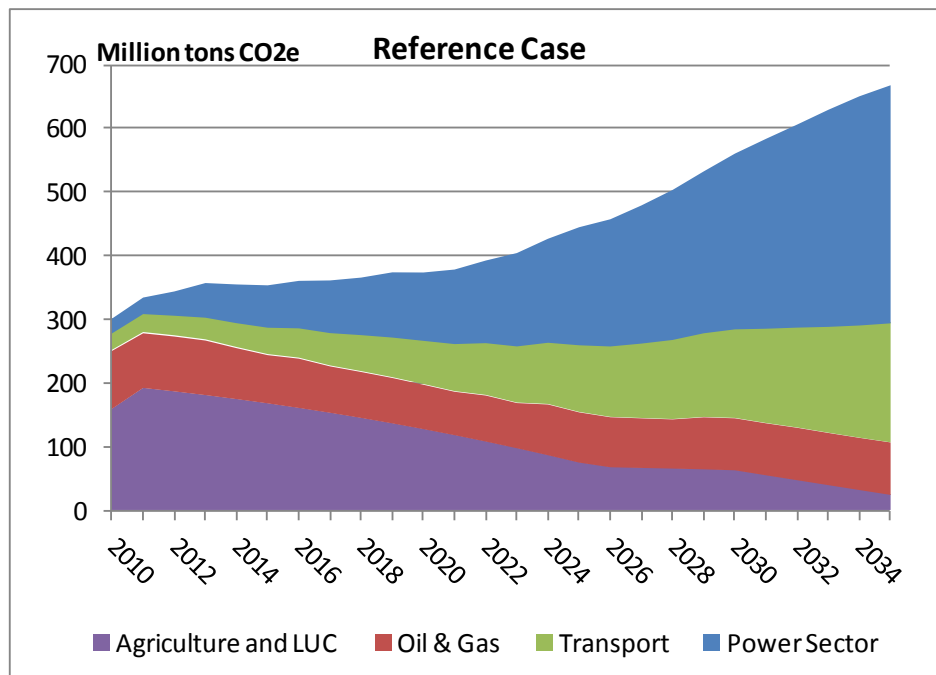
The study team considered a wide range of such mitigation options for each of the four sectors. They then evaluated each candidate option using the following criteria:

- Potential resource availability, such as the area of land affected or solar intensity for photovoltaics, in order to provide a rough estimate of the magnitude of the potential emissions reduction. The study selected only those options with the potential to have a substantial overall effect in Nigeria, ignoring some that, though beneficial, have only modest or local effects.
- Technical-economic analysis to estimate the technical and economic feasibility, comparing costs and emissions of each low-carbon option to a reference technology that it replaces or supplements.
- Implementation feasibility in institutional, market, and policy terms, which took into account feedback of sectoral experts, public and private sector stakeholders, and members of civil society. It entailed identifying potential barriers to implementation and measures and policies to remove those barriers.

### 3. THE REFERENCE SCENARIO

The reference scenario projects a doubling of emissions from the four sectors from 2010 to 2035 [Figure 1]. Over the same period, the population is projected to grow by 82 percent and the real GDP is projected to increase 6.5 times.

Fig. 1 Annual CO<sub>2</sub>e Emissions in the Reference Scenario



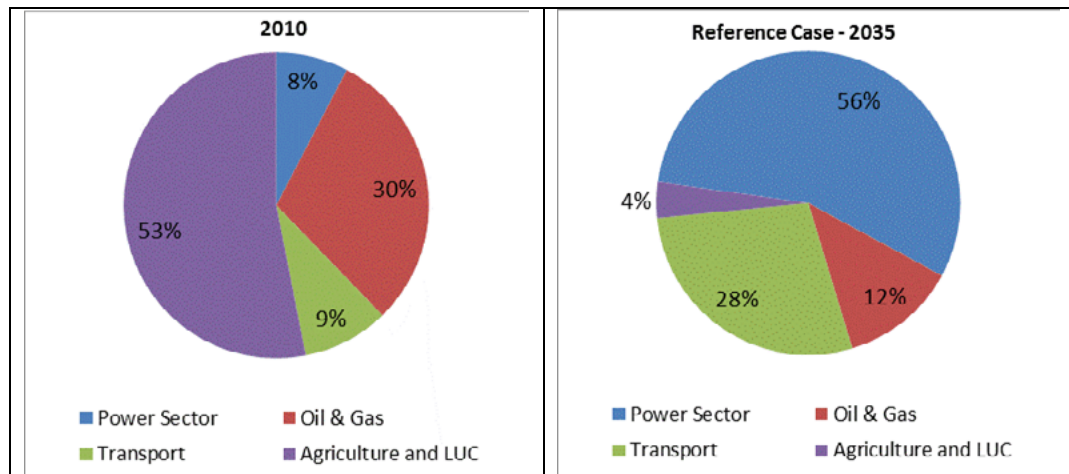
This doubling of GHG emissions results from an important structural change: In 2010, over half of the nation's emissions originated from agriculture and land-use change (53 percent), with oil and gas contributing 30 percent of the total. The power and road transport sectors added 8 percent and 9 percent, respectively.

By 2035, in the reference scenario, the mix is projected to be radically different: Agriculture, forestry, and land-use change constitute only 4 percent of the total. Oil and gas drop from 30 to 12 percent. The power sector becomes the largest contributor at 56 percent, followed by road transport at 28 percent (Figure 2). The principal causes of these structural changes are as follows:

- For the agriculture sector, a dramatic reduction in net emissions is due to a slow-down in land-use changes and to negative emissions from changes in annual, perennial, and wet rice crops
- For the oil and gas sector, increased emissions from on-site gas combustion are counterbalanced by a reduction in emissions from flaring

- For the electricity and transport sectors, dramatic growth in emissions reflects growing electricity generation and volume of road transport as a result of increases in population and income per capita.

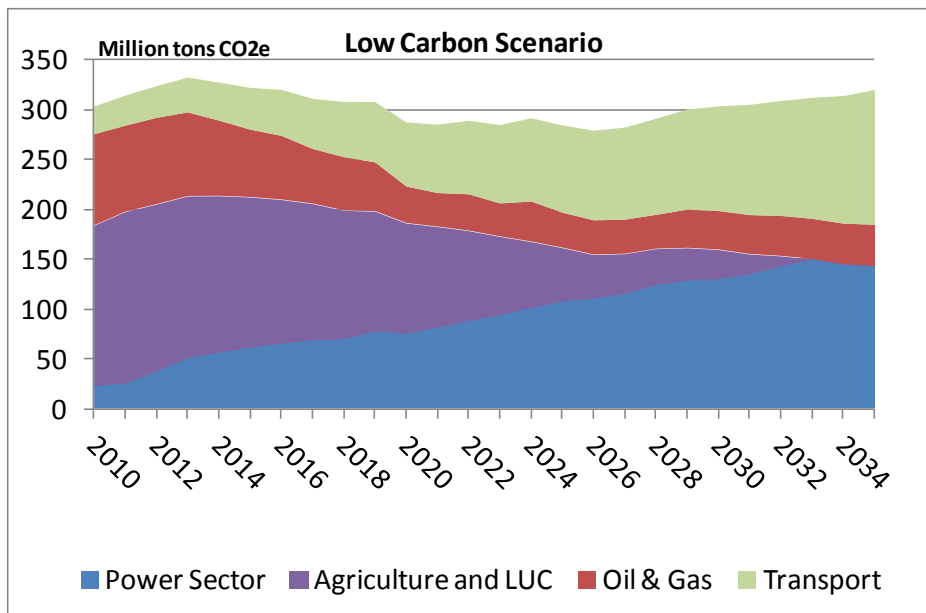
Fig. 2 Reference Scenario: Sector Composition of GHG Emissions in 2010 and 2035



#### 4. EMISSIONS AND MITIGATION POTENTIAL FOR THE LOW-CARBON SCENARIO

The study team for each sector identified a set of low-carbon interventions (mitigation options.) As indicated above, interventions were evaluated according to a series of criteria, including the magnitude of potential emission reductions, technical feasibility, economic feasibility, and institutional practicality. The goal was to assess whether each option can help reduce carbon emissions while meeting Nigeria's ambitious goals for economic development.

Fig. 3 Annual CO<sub>2</sub>e Emissions in the Low-Carbon Scenario



As result of this process, the teams selected some 30 options for inclusion in the low-carbon scenario. These measures would allow the Vision 20:2020 development goals to be reached with minimal change in annual GHG emissions, increasing from 303 Mt CO<sub>2</sub>e/y in 2010 to 320 Mt CO<sub>2</sub>e 2035 [Figure 3].

The low-carbon scenario would result in a 50 percent reduction of emissions in the terminal year relative to the reference scenario. The reduction in cumulative emission over the whole simulation period would be some 3.7 billion tons of CO<sub>2</sub>e (Table 1).

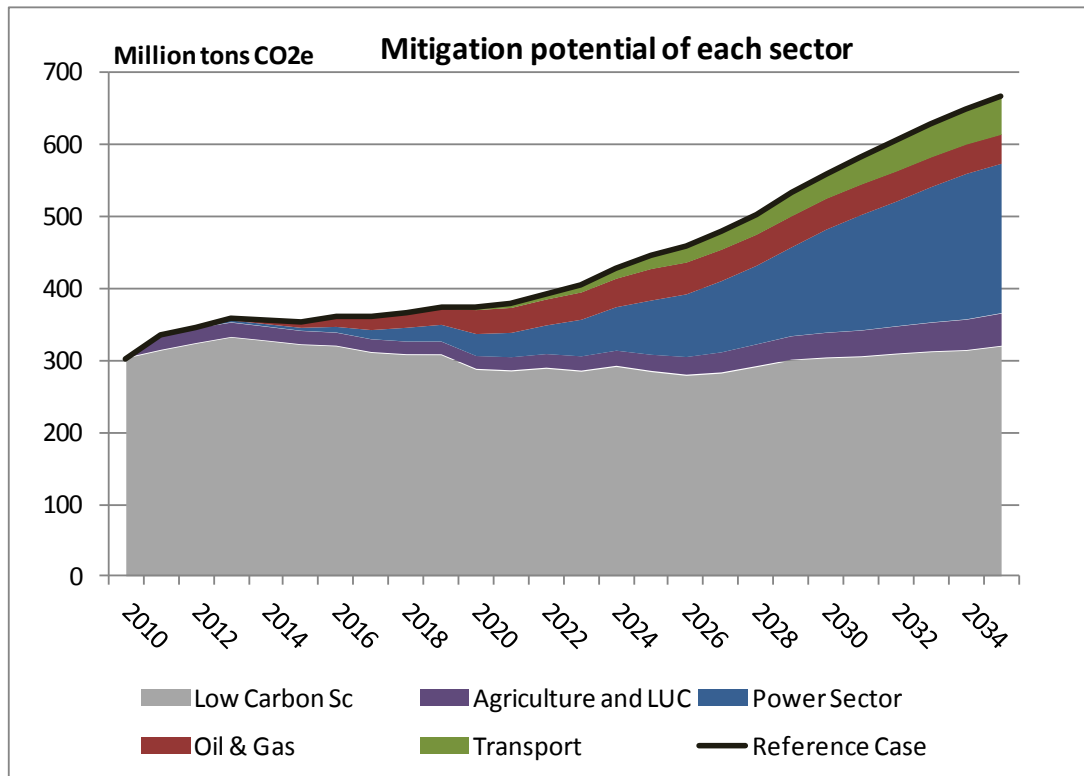
Tab. 1 Low-Carbon Scenario: End-Year Emission and Cumulative Emissions Abatement by Sector

Sector	GHG emissions Billion tons CO <sub>2</sub> e/y in 2035		Emission reduction 2010–35 Billion tons CO <sub>2</sub> e
	Reference	Low-carbon	
Power sector	0.37	0.16	1.92
Oil and gas sector	0.08	0.04	0.75
Road transport	0.19	0.14	0.45
Agriculture and LUC	0.03	(0.02)	0.65
<b>Total</b>	<b>0.67</b>	<b>0.32</b>	<b>3.77</b>

The largest contribution to the total mitigation potential comes from the power sector (some 1.9 billion tons), with smaller but significant contributions from oil and gas (0.7 billion tons), agriculture (0.6 billion), and transport (0.5 billion tons). The differences over time between the emissions in the reference scenario and in the low-carbon

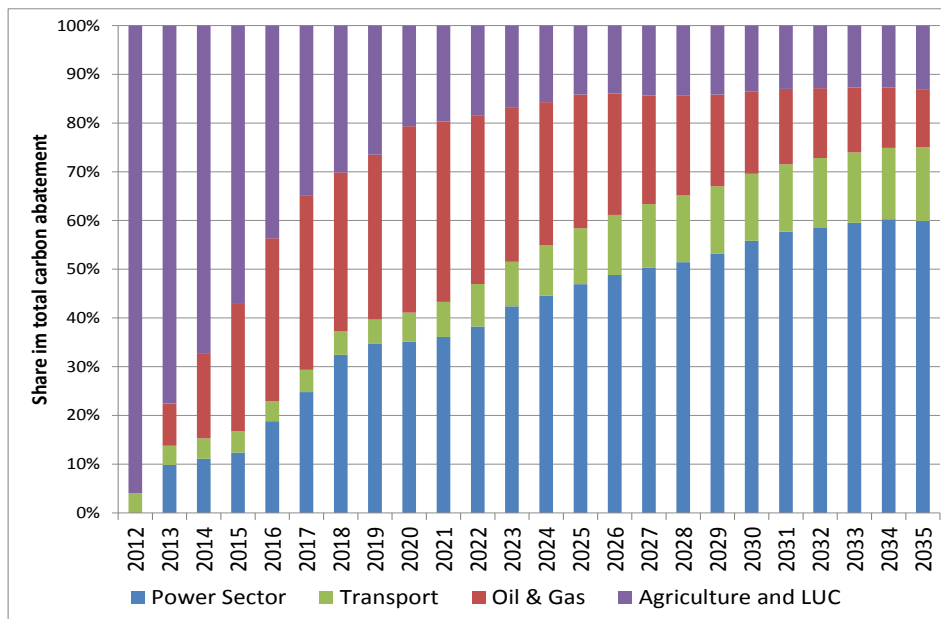
scenario are shown in figure 4 as the “mitigation wedges,” reducing emissions from the reference case (top black line) to low-carbon case (top of gray area).

Fig. 4 Mitigation Wedges for the Four Sectors



Sectors differ significantly in time distribution of their abatement potential [figure 5]: Agriculture and land use account for the largest share of emissions abatement in the earlier years, when most of the changes in land use changes might take place. In the middle of the period, the oil and gas sector provides considerable abatement opportunities. In the second part of the simulation period, land-use changes slow down, and opportunities for expanding renewable energy generation increase. This reflects in part, projections that costs of renewable technologies will become economically competitive with fossil fuel in terms of levelized cost. By the end of the period, the power sector offers 60 percent of the total abatement potential.

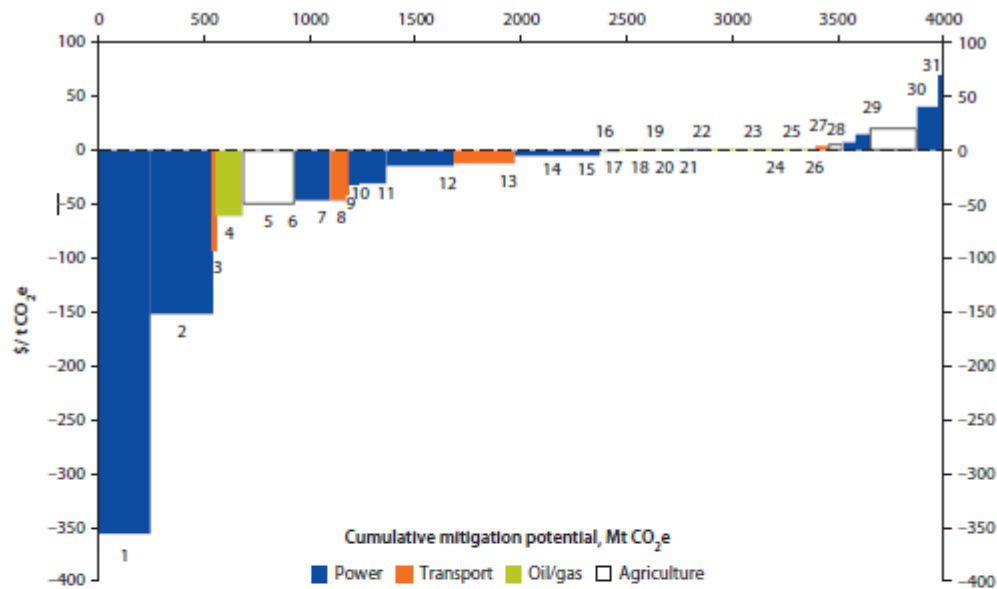
Fig. 5 Percent Shares by Sector of Mitigation Potential over Time



## 5. COSTS AND BENEFITS OF THE LOW-CARBON SCENARIO

Much of the low-carbon scenario appears economically attractive from Nigeria's point of view, even ignoring GHG abatement. Figure 6 shows the marginal abatement cost (MAC) of each intervention (in US dollars per ton of carbon dioxide equivalent, \$/t CO<sub>2</sub>e), plotted against the accumulated potential mitigation in Mt CO<sub>2</sub>e from 2010 to 2035. The main interventions are ordered from lowest to highest MAC. Some 62 percent of the total mitigation potential (2.3 Gt CO<sub>2</sub>e) can be achieved at negative cost—that is, at a net social benefit. An additional 25 percent or 0.9 Gt CO<sub>2</sub>e has a MAC of \$5/t CO<sub>2</sub>e or less. The remaining 14 percent (0.5 t CO<sub>2</sub>e) has MAC values in excess of \$5/ ton. The average MAC of all 31 interventions (weighted by abatement potential) is a net social benefit of \$42/t CO<sub>2</sub>e.

Fig. 6 MAC for Nigeria for Selected Low-Carbon Interventions



Code	Sector	Intervention	Mitigation potential (Mt CO <sub>2</sub> e)	Average cost of mitigation (\$/t CO <sub>2</sub> e)
1	P	EE lighting off-grid	233	-356
2	P	EE lighting on-grid	279	-152
3	T	Large bus	11	-93
4	O	Flaring	120	-61
5	A	Perennials	38	-50
6	A	Annuals	192	-49
7	P	Off-grid photovoltaics	158	-46
8	T	Freight efficiency improvements	73	-46
9	T	BRT	14	-41
10	P	Small hydro power	44	-32
11	P	Off-grid PV/diesel hybrid	124	-31
12	P	Gas combined cycle	300	-15
13	T	Fuel efficiency	269	-12
14	P	Expanded hydropower	382	-5
15	O	Glycol dehydration	19	-1
16	P	Transmission	65	0
17	T	Rail freight	10	0
18	O	Crude storage	131	0
19	T	Freight training	22	0
20	A	Agroforestry	145	1
21	P	Concentrated solar power	92	1
22	A	SRI	3	1
23	O	Gas used for on-site powergen	388	2
24	O	Fugitives	88	2
25	T	CNG adoption	53	4
26	A	Livestock and pasturelands improvements	61	5
27	P	Solar PV (grid)	61	7
28	P	Biomass	64	15
29	A	Avoided deforestation	207	20
30	P	Wind turbines	104	41
31	P	Supercritical coal with CCS	17	70

P = power; T = transport; A = agriculture; O = oil/gas

Reviewing interventions using MAC shows that the benefits of the low-carbon scenario vary by sector: In power and transport, interventions with more than 80 percent of the abatement potential have net social benefits (Table 8.2). In agriculture, the corresponding share is over 35 percent; however in agriculture, and oil/ gas, a significant share of total mitigation potential can be attractive for a relatively modest carbon price of US\$5/t CO<sub>2</sub>e or less; this is about 80% of the total the case of oil and gas.

Tab. 2 Shares of Sector Mitigation Potential by Class of Marginal Abatement Cost

Sector	Marginal Abatement Cost			Total (%)
	Negative (%)	< \$5/t CO <sub>2</sub> e	> \$5/t CO <sub>2</sub> e	
Agriculture	36	23	41	100
Oil and gas	19	81	0	100
Power	82	5	13	100
Transport	81	19	0	100
<b>Total</b>	<b>62</b>	<b>25</b>	<b>14</b>	<b>100</b>

Emissions abatement often requires higher capital expenditures, with lower fuel and operating costs over time, resulting in substantial long-run national benefits. In the agriculture sector, an additional public investment over the study period of \$7 billion (0.04 percent of GDP) would result in additional cash flow to farmers and landowners of \$37.3 billion (0.23 percent of GDP) while reducing GHG emissions by 646 Mt CO<sub>2</sub>e.

For the oil and gas sector, a capital expenditure over the study period of \$17 billion (0.11 percent of GDP) would generate net revenue (gross revenues minus gross expenditures) of \$42 billion (0.26 percent of GDP). In the power sector, the capital expenditure of \$118 billion (0.7 percent of GDP) is projected to reduce net expenditures (capital, fuel, and operating) by \$225 billion (1.4 percent of GDP).

Tab. 3 National Costs and Benefits of Low-Carbon Scenario

Sector	National Costs			National Benefits			Cumulative GHG abatement 2010–35, Billion Tons CO <sub>2</sub> e
	Indicator	US\$Billion 2010–35	% of GDP	Indicator	US\$Billion 2010–35	% of GDP	
<b>Agriculture</b>	Cumulative public additional capital expenditure	7	0.04	Net social additional cash flow	37	0.22	0.65
<b>Oil and gas</b>	Cumulative additional capital expenditure	17	0.10	Net additional cash flow	42	0.26	0.75
<b>Power</b>	Cumulative capital additional expenditure	118	0.72	Savings on cumulative capital, operating and fuel expenditure	225	1.37	1.92
<b>Transport</b>	Additional public capital expenditure	(a)	(a)	Reduced congestion, improved air quality, etc.	(a)	(a)	0.45
<b>TOTAL</b>		<b>142.4</b>	<b>0.85</b>		<b>267.5</b>	<b>1.89</b>	<b>3.77</b>

Notes: a. values not quantified

In the transport sector, further work is required to quantify the public and private expenditures and savings. They will include important health benefits from reduced pollution (particularly in urban areas), reduced traffic congestion leading to time savings in travel and improved quality of life, and increased productivity and competitiveness in the manufacturing and service sectors.

In summary, there is the potential of abating some 3.7 billion tons of GHG emissions (CO<sub>2</sub>e) with a net financial benefit close to 1.9 percent of GDP, over the study period.

## **6. CONCLUSIONS AND RECOMMENDATIONS**

While possible and often economically attractive, low-carbon development is by no means easy, in Nigeria or elsewhere. Barriers, including information needs, technologies, institutions, regulations, and financing, stand in the way of making low-carbon development a reality. Key recommendations to overcome these obstacles and promote low-carbon development are discussed in this section.

**Cross-cutting: Elevate decision making on low-carbon strategies to the Economic Management Team level**

An entity with a cross-sector policy mandate should be charged with the task of defining climate action policies that will require the concurrence of several line agencies. Pending a final decision on the proposed National Climate Change Commission, the FGN might consider assigning to the Economic Management Team (EMT) the role of overall coordination on policies for low-carbon, climate-resilient development. Such action would make the technical leadership exerted so far by the Federal Ministry of the Environment (FME) more effective; the FME would continue exerting a role of stimulus and liaison with international climate discussions.

**Recommendations for the Agriculture Sector**

**Promote research and extension on climate-smart agriculture**

The Federal Ministry of Agriculture and Rural Development (FMARD) could launch a dedicated program on climate-smart agriculture (CSA), with individual research lines to be awarded competitively to institutions included in the National Agricultural Research System. The program could focus on both development of planning tools (for example, a CSA atlas) to define and prioritize opportunities for adopting "triple-win" agricultural options (higher yields, higher climate resilience, reduced carbon

emissions), as well as on the definition of solutions on the ground that farmers can adopt. Strengthening of research should be accompanied by suitable measures to improve the effectiveness of extension services, including through a larger involvement of state governments.

#### Support demonstration projects on CSA technologies

The government could include in the Agriculture Transformation Agenda (ATA) a dedicated program to support projects aimed at demonstrating and scaling up climate-smart production and land management technologies. The proposed program should focus on a range of areas wide enough to represent Nigeria's different agro-climatic conditions, including regions particularly vulnerable (in the north, but also in the southwest), and on strategic crops and supply chains.

#### Recommendations for the Oil and Gas Sector

##### Launch a program to facilitate the cluster-based collection of gas from flare sites

Because of the high cost of installing gas gathering and processing facilities at small flare sites, it is recommended that consideration be given to collecting the small volumes of associated gas (AG) in clusters for processing and export of the dry gas and liquefied petroleum gases (LPGs). Opportunities for financing the initiative through a carbon-finance program of activities should be explored.

#### Recommendations for the Power Sector

##### Support grid and off-grid renewable energy technologies

The Federal Ministry of Power (FMP) could actively develop large-scale renewable energy projects. Hydropower could be an immediate priority, with a possible goal being of having three major hydro projects ready for construction within 18 to 24 months, with completed feasibility studies (including resettlement, environmental and social impact assessments). Feasibility studies for large-scale wind and concentrated solar power (CSP) plants should also be considered.

##### Promote demonstration projects for grid and off-grid low-carbon technologies

The FMP could launch a series of demonstration projects to test in different geographic contexts the viability of both small-scale, off-grid low-carbon power systems (including PV, small hydro, wind, and hybrid generator set/renewables) and larger scale renewable energy plants, such as wind and CSP.

Both the feasibility studies for large-scale renewable energy projects, as well as the financing for the demonstration off-grid projects, could be supported by seed resources already earmarked for this purpose under the World Bank NEWMAP project (Nigeria Erosion and Watershed Management Project) as well through mobilization of additional resources.

#### Recommendations for the Transport Sector

Define an action plan to improve fuel efficiency and the effectiveness of the vehicle inspection system

The FGN could develop an action plan to gradually close the gap between Nigerian and European standards on vehicle efficiency and emissions. In parallel, the application of an effective vehicle inspection and maintenance system in major cities could be considered to improve vehicle maintenance and reduce tailpipe and GHG emissions.

Define an action plan to improve the efficiency of freight handling and transport

The FGN could define an action plan for improving freight handling and transport. Such a plan could involve an effective expansion of rail services, road infrastructure, vehicle technology, logistical planning, and fleet management. Significant savings (and a reduction in GHG emissions) can be achieved by leapfrogging into solutions that have proven effective in higher income countries.

## 7. REFERENCES

1. Cervigni, R, Rogers, J A and Henrion, M (editors) (2013) “Low-Carbon Development: Opportunities for Nigeria” Directions in Development The World Bank, Washington DC. <http://elibrary.worldbank.org/doi/book/10.1596/978-0-8213-9925-5>
2. Cervigni, R, Dvorak, I and Rogers, J A (editors) (2013) “Assessing Low-Carbon Development in Nigeria: An Analysis of Four Sectors” The World Bank, Washington DC. <http://elibrary.worldbank.org/doi/book/10.1596/978-0-8213-9973-6>
3. Chivengea, P. P., H. K. Murwiraa., K.E. Gillerc, P. Mapfumod J. Sixb. 2007. “Long-term Impact of Reduced Tillage and Residue Management on Soil

- Carbon Stabilization: Implications for Conservation Agriculture on Contrasting Soils.” *Soil and Tillage Research* 94: 328–37.
4. CGIAR-CSI (Consultative Group on International Agricultural Research Consortium for Spatial Information). Washington DC. <http://srtm.csi.cgiar.org/>
  5. Doppler, W., and S. Bauer (eds). 2001–09. *Farming and Rural System Economics*. Weikersheim, Ger.: Margraf Verlag.
  6. FAO. 2010. *Global Forest Resources Assessment 2010*. Food and Agriculture Organization of the United Nations, Rome.
  7. FAO GeoNetwork Database. <http://www.fao.org/geonetwork/srv/en/main.home>
  8. FAOStat. <http://faostat.fao.org/>
  9. FGN (Federal Government of Nigeria). 2010a. *Nigeria Vision 20: 2020: The First National Implementation Plan, (2010–2013), Volume II: Sectoral Plans and Programmes*. FGN, Abuja, Nigeria.
  10. ———. 2010b. *Nigeria Vision 20: 2020 The First NV20:2020 Medium Term Implementation Plan (2010 –2013)*. FGN, Abuja, Nigeria.
  11. FMARD (Federal Ministry of Agriculture and Rural Development). 2005. *National FADAMA Development Office*. Abuja, Nigeria.
  12. ———. 2010a. *National Agricultural Investment Plan (NAIP): 2011–2014—ECOWAP/CAADP Process*. FMARD, Abuja, Nigeria.
  13. ———. 2010b. “Nigeria: Global Agriculture and Food Security Program (GAFSP): A Proposal to Global Agriculture and Food Security Program (GAFSP) Trust Fund.” FMARD, Abuja, Nigeria.
  14. Global Administrative Areas database. <http://www.gadm.org/>
  15. Global Land Cover Network [http://www.glcn.org/dat\\_0\\_en.jsp](http://www.glcn.org/dat_0_en.jsp) and <http://www.fao.org/geonetwork/srv/en/metadata.show?id=37204&currTab=simple>. FAO. Rome, Italy.
  16. Guo, R., and K. Hanaki. 2010. “Potential and Life Cycle Assessment of Biodiesel Production in China.” *Journal of Renewable Sustainable Energy* 2: 033107; doi: 10.1063/1.3449298.

17. Henry, M. 2010. "Carbon Stocks and Dynamics in Sub-Saharan Africa." PhD dissertation. Paris Institute of Technology for Life, Food and Environmental Sciences (AgroParisTech), Paris, and University of Tuscia, Italy.
18. IIASA (International Institute for Applied Systems Analysis). Harmonized World Soil Database. Laxenburg, Austria.  
<http://www.iiasa.ac.at/Research/LUC/External-World-soil-database/HTML/SoilQuality.html?sb=10>.
19. Intergovernmental Panel on Climate Change (IPCC). 2006. "IPCC Guidelines for National Greenhouse Gas Inventories." Prepared by the National Greenhouse Gas Inventories Programme. In Agriculture, Forestry and Other Land Use, vol. 4. Edited by, H. S. Eggleston, L. Buendia, K. Miwa, T. Ngara, K. Tanabe. Institute for Global Environmental Strategies, Japan.
20. Leite, L. F., P. C. Doraiswamy, H. J. Causarano, H. T. Gollany, and E. S. Mendonca. 2008. "Modeling Organic Carbon Dynamics under No-tillage and Plowed Systems in Tropical Soils of Brazil Using CQESTR," Soil and Tillage Research 102: 118–25.
21. National Bureau of Statistics (NBS). <http://www.nigerianstat.gov.ng/index.php/>. Federal Government of Nigeria. Abuja, Nigeria.
22. National Food Reserve Agency (NFRA) and Japan International Cooperation (JICA). 2009. "National Rice Development Strategy—Federal Republic of Nigeria." Prepared for the Coalition for African Rice Development (CARD). Tokyo.
23. United Nations Collaborative Programme on Reducing Emissions from Deforestation and Forest Degradation in Developing Countries. Publications and Resources from <http://www.un-redd.org/>. Geneva, Switzerland
24. World Bank. 2006. Getting Agriculture Going in Nigeria: Framework for a National Growth Strategy, Report 346180NG. Washington DC.: World Bank.
25. ———. 2007. World Development Indicators. World Bank, Washington, DC.  
<http://data.worldbank.org/indicator/NV.AGR.TOTL.ZS>
26. Adamson, B. 2008. "FPSO Vapor Recovery for HSEE Benefits." Refrigeration Engineering, Offshore South-East Asia Conference, Singapore, December.

27. API (American Petroleum Institute). 2009. Compendium of Greenhouse Gas Emissions Methodologies for the Oil and Gas Industry. American Petroleum Institute, Washington, DC.
28. Black, A. 2011 "Knowing Life Cycle Costs Aids Power Plant Investment Decisions." Wartsila Technical Journal Jan. 2011.
29. BP (British Petroleum). 2010. BP Statistical Review of World Energy 2010. London: British Petroleum [www.bp.com/statisticalreview](http://www.bp.com/statisticalreview) (August 20, 2011).
30. Brook, F. J. 2000. "GE Gas Turbine Performance Characteristics." In Gas Processing, Vols. 1 and 2. GE Power Systems, edited by J. M. Campbell, October 2000. GE Power Systems, Schenectady NY.
31. Clearstone Engineering 2002. "Identification and Evaluation of Opportunities to Reduce Methane Losses at Four Gas Plants." Clearstone Engineering Ltd., prepared for the Gas Technology Institute, Calgary, Alberta, Canada. June 2002.
32. Cleaver-Brooks, 2010. Boiler Efficiency Guide, Technical guide, Cleaver-Brooks, [www.cleaver-brooks.com](http://www.cleaver-brooks.com)
33. Cleaverbrooks, 2010: Cleaverbrooks Boiler Efficiency Guide, Technical Guide, 2010. Cleaver-Brooks Inc., Thomasville, GA..
34. Department of Petroleum Resources. 2011. Ministry of Petroleum Resources, Federal Government of Nigeria. "Gas Flare-down Updates: DPR Perspective." Oil & Gas sector Low Carbon workshop, Abuja, 14 June 2011.
35. Eastern Research. 1996. "Preferred and alternative methods for estimating fugitive emissions from equipment leaks." "Final Report for Point Source Committee Emissions Inventory Improvement Program." Vol. 2, chapter 4. Point Sources Committee Emission Inventory Improvement Program, Washington, DC.
36. Energy Redefined (2012). White-papers and presentations on [www.energy-redefined.com](http://www.energy-redefined.com). Glasgow, UK.
37. Energy Resources. 2000. "Activities to Reduce Greenhouse Gas Emissions from Natural Gas Operations." Energy Resources Inc. and Interstate Natural Gas Association of America, Washington, DC.

38. Finkenrath, M. 2011. "IEA Cost and Performance of Carbon Dioxide Capture from Power Generation." International Energy Agency, U.S. Environmental Protection Agency, Washington DC. [www.iea.org/publications/freepublications/publication/name,3950,en.html](http://www.iea.org/publications/freepublications/publication/name,3950,en.html)
39. Howorth, G. 2012. "Nigerian Oil and Gas Industry Low-carbon Options Methodology." Unpublished study for this book.
40. Hoefft, R.E., J. Janowitz, and R. Keck. 2003. "Heavy-duty Gas Turbine Operating and Maintenance Considerations." GE Energy Services, Atlanta, GA. [www.ge-energy.com/content/.../GER3620L\\_1\\_Oct\\_19\\_2010\\_1.pdf](http://www.ge-energy.com/content/.../GER3620L_1_Oct_19_2010_1.pdf)
41. Hanlon, P. C. 2001. Compressor Handbook. New York: McGraw-Hill.
42. INGAA (Interstate Natural Gas Association of America). 2005. "Greenhouse Gas Emission Estimation Guidelines for Natural Gas Transmission and Storage (vol. 1). INGAA, Washington, DC. <http://www.ingaa.org/cms/33/1060/6435/5485.aspx>
43. Latour, P.L., J. H. Sharpe, and M.C. Delaney. 1986. "Estimating Benefits from Advanced Control." Emerson Controls, ISA Transactions 25 (4).
44. McCarrick, M.T., and K. Mackenzie. 2011. "GE Power and Water LM2500 to LM2500+DLE Gas Turbine Combined Cycle Plant Repowering." GE Power and Water, GE Energy. Atlanta, GA.
45. NNPC (Nigerian National Petroleum Corporation). 2011. NNPC Annual Statistical Bulletin, NNPC, Abuja, Nigeria. <http://www.nnpcgroup.com/PublicRelations/OilandGasStatistics/AnnualStatisticsBulletin.aspx>
46. ———. 2011a. "Growth Projections in Nigeria's Oil and Gas Sector." Oil & Gas sector LC workshop, Abuja, 14 June 2011.
47. ———. 2011b "Nigerian Gas Master Plan Status Update." Oil & Gas sector LC workshop, Abuja, 14 June 2011.
48. Rahmen, M.M., T.K. Ibrahim, and A.N. Abdalla. 2011. "Thermodynamic Performance Analysis Of Gas-Turbine Power-Plant." International Journal of Physical Sciences 6 (14): 3539–50.

49. USDOE (U.S. Department of Energy). 2012. Annual Energy Outlook 2011. Energy Information Administration, U.S. Department of Energy, Washington, DC.
50. USEPA (U.S. Environmental Protection Agency). 1996. Methane Emissions from the Natural Gas Industry, vol. 9: "Underground Pipelines." Natural Risk Management Research Laboratory, USEPA, Washington, DC.
51. ———. 1996. Methane Emissions from the Natural Gas Industry, vol. 7: "Blow-down and Purge." Environmental Protection Agency, Research and Development, 1996. USEPA, Washington, DC.
52. ———. 1999. "US Methane Emissions 1990–2010: Inventories, Projections, and Opportunities for Reductions." U.S. Environmental Protection Agency, Washington, DC.
53. ———. 2003. "Lesson Learned: Directed Inspection and Maintenance at gas Processing Plants and Booster Stations." Natural Gas STAR Partners, USEPA, Washington, DC.
54. ———. 2005. "Methane Losses from Compressors." Producers Technology Transfer Workshop, Houston Texas, , [www.ontime.methanetomarkets.org/m2mtool/files/docs/methloss.pdf](http://www.ontime.methanetomarkets.org/m2mtool/files/docs/methloss.pdf)
55. ———. 2010. "Greenhouse Gas Emissions Reporting from the Petroleum and Natural Gas Industry: Background and Support Document—Revised Factors of Prior Studies." USEPA, Washington, DC.
56. Wood Mackenzie. 2011., "A Domestic Challenge to Nigerian LNG Projects." Wood Mackenzie Upstream Insight August 2011. <http://www.woodmacresearch.com/cgi-bin/wmprod/portal/energy/productMicrosite.jsp?productOID=664070>
57. Ziegler, Urban T. (2005). "Gas turbine efficiency in project development", Presented at 17th symposium, Industrial Application of Gas Turbines (IAGT), Banff, Alberta, Canada, October 12–14, 2005
58. de Gouvello, Christophe, Felix B. Dayo, and Massamba Thioye. 2008. Low-carbon Energy Projects for Development in Sub-Saharan Africa: Unveiling the

- Potential, Addressing the Barriers. Norwegian Trust Fund for Private Sector and Infrastructure, Washington, DC: World Bank.
59. DECC (UK Department of Energy and Climate Change). 2011: DECC Fossil Fuel Price Projections: Summary. UK Department of Energy and Climate Change, London, UK.
60. FRN (Federal Republic of Nigeria). 2010. Roadmap for Power Sector Reform. The Presidency, Presidential Action Committee on Power, Abuja, Nigeria, August, 2010.
61. Hearps, P., and McConnell, D., 2011. Renewable Energy Technology Cost Review. Energy Research Institute (ERI), 2011. The University of Melbourne, Melbourne, Australia. March 2011.
62. IEA (International Energy Agency). 2010a: International Energy Agency World Energy Outlook 2010. IEA, Paris.
63. Lowbeer-Lewis, Nathaniel. 2010. Nigeria and Nuclear Energy: Plans and Prospects. Nuclear Energy Futures Papers 11. Centre for International Governance Innovation, Waterloo, Ontario, Canada. [www.cigionline.org](http://www.cigionline.org) (January 2010).
64. NERC (Nigerian Electricity Regulatory Commission). 2011. "Consultation Paper for the 2011 Major Review of the Multi Year Tariff Order (MYTO)." NERC, Abuja, Nigeria. May, 2011
65. NREL & UNDP. (NREL and United Nations Development Programme). 2005. "Africa Direct Normal Solar Radiation 40km Resolution Map.) National Renewable Energy Laboratory (NREL), Global Environment Facility (GEF), and United Nations Environment Program (UNEP), Golden, CO. [http://www.nrel.gov/gis/pdfs/swera/africa/africa\\_dir.pdf](http://www.nrel.gov/gis/pdfs/swera/africa/africa_dir.pdf) November, 2005. (Sep. 2009).
66. UN (United Nations). 2010. UN World Population Prospects, 2010 rev. New York: United Nations. <http://esa.un.org/unpd/wpp/index.htm> (October 5, 2011).
67. USDOE (U.S. Department of Energy). 2011. Annual Energy Outlook 2011. DOE/EIA-0383, USDOE, Energy Information Administration, Washington, DC.

68. USEPA (United States Environmental Protection Agency). 2010. Landfill Recovery and Use in Nigeria (Pre-Feasibility Studies of Using Landfill Gas To Electricity Project (LFGE)). Methane-To-Markets Program, USEPA, Washington, DC.
69. World Bank. 2011. World Bank Development Indicators. World Bank, Washington, DC. <http://data.worldbank.org/indicator/EP.PMP.DESL.CD> (October 20, 2011).
70. Zarma, I. H. 2006. "Hydropower Resources in Nigeria." Energy Commission Of Nigeria. Country position paper presented at 2nd Hydro Power for Today Conference, International Centre on Small Hydro Power (IC-SHP), Hangzhou, China.
71. FGG (Federal Government Gazette). 2011. "National Environmental (Control of Vehicular Emissions Petrol and Diesel Engines) Regulations." Federal Government Gazette 47, May 17, 2011.
72. FGN (Federal Government of Nigeria). 2009. "Nigeria Vision 2020 National Technical Working Group on Transport, Report of the Vision 2020." FGN, Abuja, Nigeria. <http://www.npc.gov.ng/vault/files/transport%20ntwg%20report.pdf>
73. GeoNames geographical database. <http://www.geonames.org/>
74. *Thomas Brinkhoff: City Population*. 2012. <http://www.citypopulation.de/Nigeria-Cities.html>
75. SLA (State Licensing Authority). 2005. "Newly Registered Motor Vehicles by Type of Vehicle and by Year of Registration: 1990-2005. Lagos State Licensing Office and Lagos State Central Statistics Office, Lagos, Nigeria.
76. UITP/UATP (Union Internationale des Transports Publics and Union Africaine des Transports Publics). 2010. Report on Statistical Indicators of Public Transport Performance in Africa. Brussels, Belgium. [http://www.uitp.org/knowledge/pdf/Report\\_on\\_statistical\\_indicators\\_of\\_publictransportperformanceinS-SA.pdf](http://www.uitp.org/knowledge/pdf/Report_on_statistical_indicators_of_publictransportperformanceinS-SA.pdf)

# Synergies and Interactions Between Climate Change Policies and Air Pollution Control Strategies — Results of the WITCH Integrated Assessment Model

Reis A L.<sup>1,2\*</sup>, Drouet L.<sup>1,2</sup> and Tavoni M.<sup>1,2</sup>

<sup>1</sup>Fondazione Eni Enrico Mattei - Italy, and <sup>2</sup>Euro-Mediterranean Center on Climate Change CIP Division -Italy

\*Corresponding Author: lara.aleluia@feem.it

## Abstract

Climate change and air pollution are two major topics in international policy. Scientific evidence points to the need of integrating both fields in integrated assessment studies. Climate change mitigation policies are based on restructuring the energy system in order to reduce the emissions of greenhouse gases. These actions have impacts beyond the climate change policy framework, namely in air quality policies. In this context, we use the WITCH integrated assessment model to account for the impacts of climate change mitigation actions on the air pollution strategies. We consider a set of scenarios where both types of policies are combined, to analyze the magnitude of the interactions between the climate change mitigation policies and air pollution abatement strategies focusing on the energy sector. The results show the benefits of the application of integrated emission abatement strategies, and reveal the undesirable consequence that arises from reducing the aerosol concentration in the atmosphere.

**Keywords:** WITCH, air pollution, climate change, trade-offs

## 1. INTRODUCTION

Climate change is a phenomenon mainly driven by the emissions of carbon dioxide (CO<sub>2</sub>) and other Greenhouse Gases (GHG), such as methane (CH<sub>4</sub>) and nitrous oxide (N<sub>2</sub>O) [12]. However connections between some air pollutants and climate exist and became an independent branch of research [13]. Aerosols are known to play an important role in the earth net radiative forcing, directly by changing the absorbing properties of the atmosphere and indirectly interfering with properties of the clouds. Organic Carbons (OC) and sulfur dioxide (SO<sub>2</sub>) aerosols scatter the sunlight therefore cooling the earth's atmosphere. Moreover they increase cloud droplet concentration augmenting the cloud's albedo and lifetime by retarding precipitation. This effect is considered as a significant "mask" of the warming effects of the GHG emissions [13].

On the other hand, anthropogenic emissions of Black Carbon (BC) aerosols, also called soot, have absorbing properties and thus contribute to a warming effect. This type of particles has a characteristic black color which absorbs light. Another effect of BC is the reduction of surface albedo when deposited, especially on ice and snow. The reduction of the ice albedo reduces the reflection of light and increases the melting of the ice due to a higher absorption [15]. Moreover, the temperature increase caused by the climatic change has consequences on the reaction rates of the pollutants in the atmosphere. Likewise the changes in global circulation and weather patterns influence the concentration and spatial distribution of the pollutants. Additionally, climate change can affect the biogenic emissions and photochemical smog [7, 6].

The relation between air pollution and climate change goes beyond the physical interplay of aerosols and the radiative forcing. The emission sources of GHG and of air pollutants are often identical, thus mitigation policies on climate change may also contribute to local air quality control policies [16, 10]. Contrarily air pollution control policies will, most probably, lead to increased efforts of climate change mitigation policies, due to the decrease in cooling aerosol emissions.

The negative effects, on human health and society, of both climate change and air pollution are well known and both topics have great influence on the implementation and design of policies. The international policy deals with both topics separately, examples of that are the UN Framework Convention on Climate Change and the Convention on Long-Range Transboundary Air Pollution [11]. Despite the links between these two environmental issues and their importance, integrated assessment models tended to treat them separately, using different methodologies and focuses [16]. Historically, air pollution management tends to be based on End Of Pipe (EOP) measures which normally are pollutant specific. Climate change mitigation, on the other hand,

focuses on the management of fuels shares and energy technological options [1]. Additionally climate change mitigation policies are often in contrast with local and regional policy objectives, due to the global and long term objectives characteristic of climate change. In this context the success of climate change policies would benefit greatly from a deeper knowledge of the economic and environmental implications of climate change policies in air quality. Accordingly, integrated assessment models are evolving towards the integration of air pollutants' emissions, impacts and benefits. In this context, we developed an air pollution module to account for this relationship within the World Induced Technical Change Hybrid (WITCH) model [4].

The main goal of this study is to study the contribution of climate change mitigation to the achievement of air pollution goals. As previously mentioned, the relationship between climate and aerosols can generate conflicts between air quality objectives and climate targets. This happens due to the possible trade-offs between the cooling effects of some air pollutants and the temperature targets of the climate global policies. These trade-offs are still uncertain and should be better evaluated and analyzed.

## 2. METHODOLOGY

We have developed an air quality module for the WITCH energy-economic-climate model, on the framework of the project LIMITS [8]. The module calculates the air pollution emissions which are relevant for climate change interactions and allows for the quantification of the air pollution abatements caused by stringent climate mitigation. This model configuration permits to explore which are the climate policies that lead to the greatest synergies with air quality policies which ultimately will lead to an increase in human health. Thus providing a picture of the importance of integrated policies in achieving air pollution reductions.

**The WITCH model** The WITCH model is an economic growth model designed to study optimal economic and climate change policies [4]. The energy-economic system covers the whole world, grouping the countries into sub-regions which share economic, energetic and/or geographical characteristics. The energy sector is well represented and it includes electric and non-electric use, six types of fuels and seven electricity generation technologies. The climate module is connected to the economic system using a damage function. The GHG emissions generated by the economy are translated into temperature and economic impacts, which in turn feeds back the model as an economic gain or loss of a given region. Additionally, the model accounts for acquired technological knowledge due to experience and also for research and development investments to increase energy efficiency and reduce costs of biofuels. The

model has been used in several economic and climate change policy studies [5, 3, 2]. For this study we have incorporated the air pollutants (OC, BC, SO<sub>2</sub>, Nitrogen oxides (NO<sub>x</sub>), Particulate Matter (PM), Non-Methane Volatile Organic Compounds (NMVOC) and carbon monoxide (CO)) into the WITCH model endogenously, in addition to the GHG already taken into account by the climate module.

The air pollutants' emissions are calculated according to the following equation:

$$E_{p,n} = \sum_j A_{j,n} e_{f_{p,j,n}}, \quad (1)$$

where  $E$  are the emissions,  $A$  is the sectoral activity and  $ef$  is the emission factor for every pollutant  $p$ , region  $n$  and sector  $j$  (energy related sectors). The sectoral activity is calculated by the WITCH model and the emission factors are adapted from the LIMITS database. Moreover, the model exogenously accounts for the non energy related emissions, using the RCP 8.5 scenario [14], adjusted to the population growth.

The additional radiative forcing, by non-Kyoto gases, are provided, in a subsequent step, by the MAGICC model [9].

### 3. RESULTS AND DISCUSSION

In this analysis we have chosen two air quality policies and two climate change mitigation scenarios:

- business as usual climate scenario with a current legislation air pollution scenario — *bauCcleA*
- business as usual climate scenario with a stringent legislation air pollution scenario ( $\approx 75\%$  of the technical frontier) — *bauCslA*
- mitigation climate scenario (equivalent to a radiative forcing of 2.8 W/m<sup>2</sup> by the end of the century) with a current legislation air pollution scenario — *mitCcleA*
- mitigation climate scenario (equivalent to a radiative forcing of 2.8 W/m<sup>2</sup> by the end of the century) with a stringent legislation air pollution scenario ( $\approx 75\%$  of the technical frontier) — *mitCslA*

The first policy *bauCcleA* refers to a policy baseline scenario, to which all other are compared and that involves the lowest costs. The fourth scenario *mitCslA* represents a simultaneous climate and air pollution policy, thus it is the one from which better outcomes are expected and with higher costs associated. Scenario *bauCslA* highlights the impacts of air pollution policies alone, while scenario *mitCcleA* the effects of climate mitigation policies.

The four Policy scenarios have been run and the comparison between them shows the impacts of both types of policies. Figure [Fig. 1] shows the results for all the policy scenarios and all the air pollutants. The *bauCcleA* scenario results show stable or decreasing pollutants' levels due to the current legislation emission factors which imply the complete application of the existing air pollution laws. The results show a significant impact of the climate change mitigation policy on all of the air pollutants, specially important on SO<sub>2</sub> and NO<sub>x</sub>. Likewise these are the pollutants that show the highest effect of the air pollution control strategies. We observe that for the cases of OC and BC the climate mitigation alone converge to similar results by the end of the century as when applying both policies simultaneously. The same is not true when one considers the early century period where air pollution policies are more important in air pollutants' emissions control than climate mitigation.

[Figure 1 about here.]

This is crucial for the particular case of china [Fig. 2], where climate mitigation policies only start to be effective in the mid century, as for the case of BC, CO and OC. China is a region of the world that would benefit greatly from the application of a simultaneous climate and air pollution policy.

[Figure 2 about here.]

The emission reductions are achieved both by changes in the structure of the energy system (mainly climate mitigation policies) and by introducing EOP measures (air quality policies). Figure [Fig. 3] shows the impact of the mitigation policies on the pollutants' activities.

[Figure 3 about here.]

We observe that by the end of the century almost all the coal and gas for electricity has been replaced by electricity with IGCC biofuels and renewable energy sources<sup>1</sup>. The shift to electricity with Integrated gasification combined cycle (IGCC) with biofuels is mainly important in USA, Eastern EU countries, sub Saharan Africa, Central and Latin America, Southeast Asia, Australia, South Korea and south Africa. This structural change drives important reductions in the air pollutants specially in SO<sub>2</sub>, however it leads to small increases mainly in NO<sub>x</sub>. Additionally important reductions in non electricity gas and oil energy sources are observed.

However, the energy sector is not the only driver of air pollution emissions, and some pollutants are highly affected by sectors which are not controlled by the WITCH model.

---

<sup>1</sup>Not shown in [Fig. 3].

It is shown that for OC, CO and BC the non energy related sectors represent a major share of the total emissions, also VOC present a significant share from the solvents sector. These emissions can not be reduced directly with climate and/or air control policies, however they also open space to additional policies that can relax the constraints in the energy system and in the air pollution control structures. On the other hand, energy related emissions are rapidly cut down by climate mitigation policies, namely energy generation, transport, industry and residential and commercial sectors.

Finally, we look at the physical interactions between climate and air pollution. Figure [Fig. 4] depicts the impact of the policy scenarios on the total radiative forcing. The results show a higher forcing for the air pollution stringent policies, this is according to the expected since there is a higher reduction of the aerosols in these scenarios thus reducing the scattering in the atmosphere, ultimately leading to an increase in the radiative forcing and in the global warming [13].

[Figure 4 about here.]

#### **4. CONCLUSION**

We have calculated the impacts of a set of combinations of policies both related to climate change mitigation and air pollution control using the WITCH integrated assessment model. The analysis of the results shows that, in general, climate change mitigation policies can achieve similar or even more effective influence in air pollutant emissions by the end of the century than air pollution strategies. However the same is not true for the beginning of the century (until  $\approx 2030$ ) where air pollution policies proved to be more effective in the fast reduction of emissions. Specifically, the results for China show that a greater benefit would come from the simultaneous application of both policies. Additionally, we have verified the unwanted consequence of the increased radiative forcing due to the reduction of aerosol emissions induced by the air pollution policies. This will ultimately lead to an increasing effort for reduction of GHG, however leading to a more healthy environment. The results of this work generally conclude that climate change policies are able to reduce a major share of the air pollutant emissions by the mid-end of the century, however a lot is still to tell about the costs of these policies and their possible economic co-benefits.

#### **5. ACKNOWLEDGMENTS**

The research leading to these results has received funding from the Italian Ministry of Education, University and Research and the Italian Ministry of Environment, Land and

Sea under the GEMINA project. Additionally, this research has received funding from the European Union Seventh Framework Programme (FP7/2007-2013) under grant agreement n° 282846(LIMITS).

## 6. REFERENCES

- [1] Bollen, J., van der Zwaan, B., Brink, C., & Eerens, H. (2009). Local air pollution and global climate change: A combined cost-benefit analysis. *Resource and Energy Economics*, 31(3), 161 – 181.  
URL <http://www.sciencedirect.com/science/article/pii/S092876550900013X>
- [2] Bosetti, V., Carraro, C., De Cian, E., Massetti, E., & Tavoni, M. (2013). Incentives and stability of international climate coalitions: An integrated assessment. *Energy Policy*, 55, 44–56.
- [3] Bosetti, V., Carraro, C., & Tavoni, M. (2012). Timing of mitigation and technology availability in achieving a low-carbon world. *Environment and Resource Economics*, 51, 353–369.
- [4] Bosetti, V., Massetti, E., & Tavoni, M. (2007). The witch model. structure, baseline, solutions. Tech. rep., FEEM, Fondazione Eni Enrico Mattei.
- [5] Hohne, N., Taylor, R., C. and Elias, den Elzen, M., Riahi, K., Chen, C., Rogelj, J., Grassi, G., Wagner, F., Levin, K., & Massetti, E. (2012). National greenhouse gas emissions reduction pledges and 2c — comparison of studies. *Climate Policy*, 12, 356–377.
- [6] Jacob, D., & Winner, D. A. (2009). Effect of climate change on air quality. *Atmospheric Environment*, 43, 51–63.
- [7] Kelly, J., Makar, P., & Plummer, D. A. (2012). Projections of mid-century summer air-quality for north america: effects of changes in climate and precursor emissions. *Atmospheric Chemistry and Physics*, 12, 5367–5390.
- [8] LIMITS (2014). Low climate impact scenarios and the implications of required tight emission control strategies. <http://www.feem-project.net/limits/>.
- [9] Meinshausen, M., Raper, S. C. B., & Wigley, T. M. L. (2011). Emulating coupled atmosphere-ocean and carbon cycle models with a simpler model, magicc6 part

- 1: Model description and calibration. *Atmospheric Chemistry and Physics*, 11(4), 1417–1456.  
URL <http://www.atmos-chem-phys.net/11/1417/2011/>
- [10] Muller, N. (2012). The design of optimal climate policy with air pollution co-benefits. *Resource and Energy Economics*, 34, 696–722.
- [11] Nemet, G. F., Holloway, T., & Meier, P. (2010). Implications of incorporating air-quality co-benefits into climate change policymaking. *Environ. Res. Lett.*, 5, 014007 (9pp).
- [12] Intergovernmental Panel on Climate Change, I. P. (2007). *Fourth Assessment Report: Climate Change 2007: The AR4 Synthesis Report*. Geneva: IPCC.  
URL <http://www.ipcc.ch/ipccreports/ar4-wg1.htm>
- [13] Ramanathan, V., & Feng, Y. (2009). Air pollution, greenhouse gases and climate change: Global and regional perspectives. *Atmospheric Environment*, 43, 37–50.
- [14] Riahi, K., Gruebler, A., & Nakicenovic, N. (2007). Scenarios of long-term socio-economic and environmental development under climate stabilization. *Technological Forecasting and Social Change*, 74(7), 887–935.
- [15] UNEP (2011). Near-term climate protection and clean air benefits: Actions for controlling short-lived climate forcers. Tech. rep., United Nations Environment Programme, Nairobi, Kenya.
- [16] van Vuuren, D., Cofala, J., Eerens, H., Oostenrijk, R., Heyes, C., Klimont, Z., & den Elzen, M., M. and Amann (2004). Exploring the ancillary benefits of the kyoto protocol for air pollution in europe. Tech. rep., EEA.

## 7. IMAGES AND TABLES

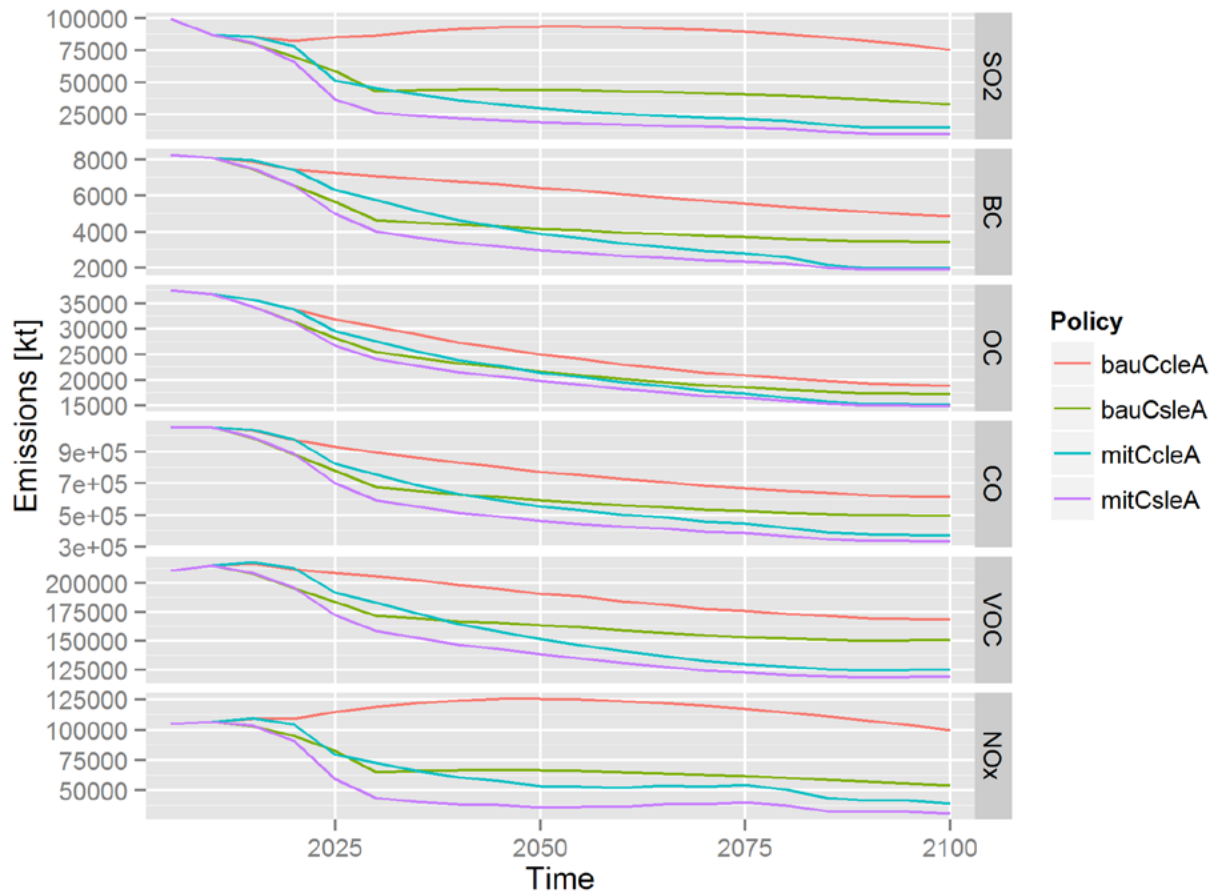


Fig. 1 WITCH world emissions for the different pollutants and policy scenarios, excluding the non country based emissions (e.i. international shipping and aviation).

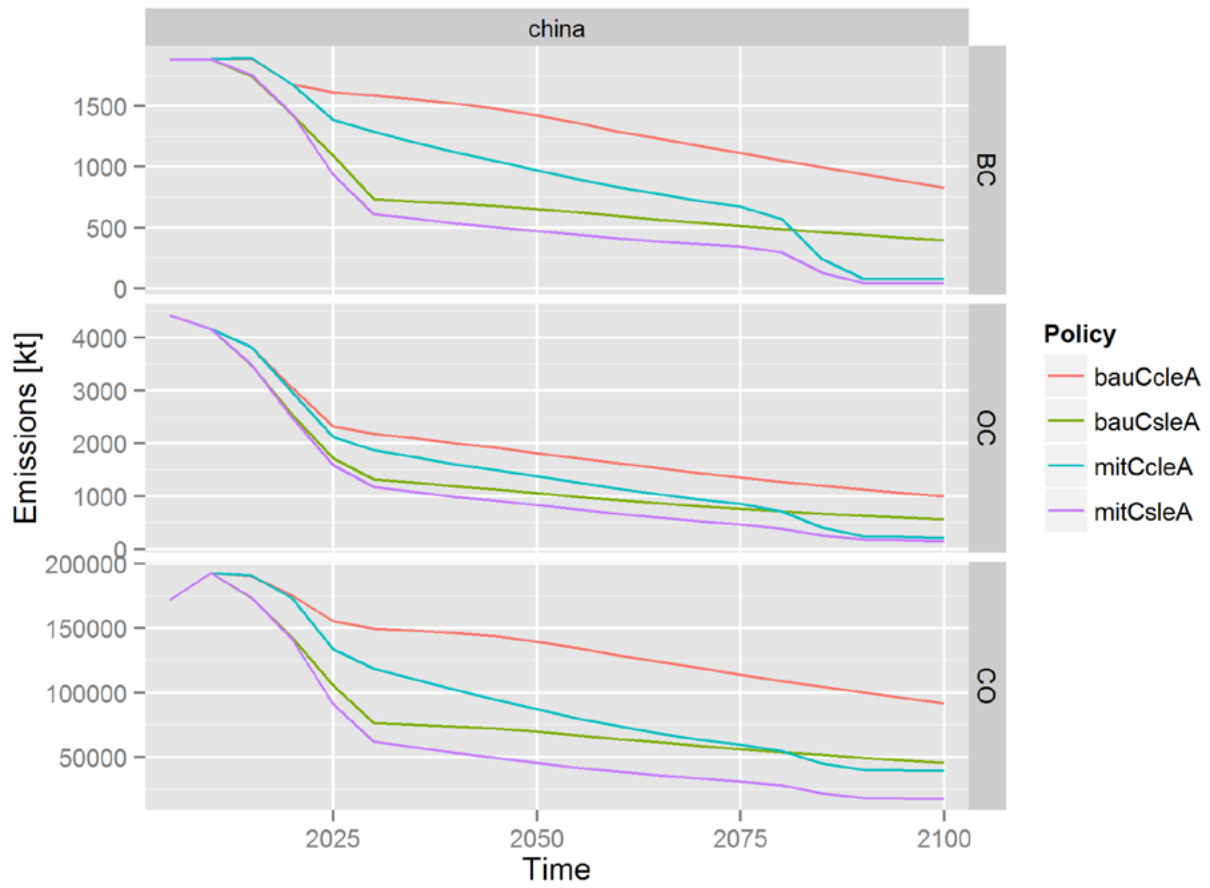


Fig. 2 WITCH China emissions for the different pollutants and policy scenarios.

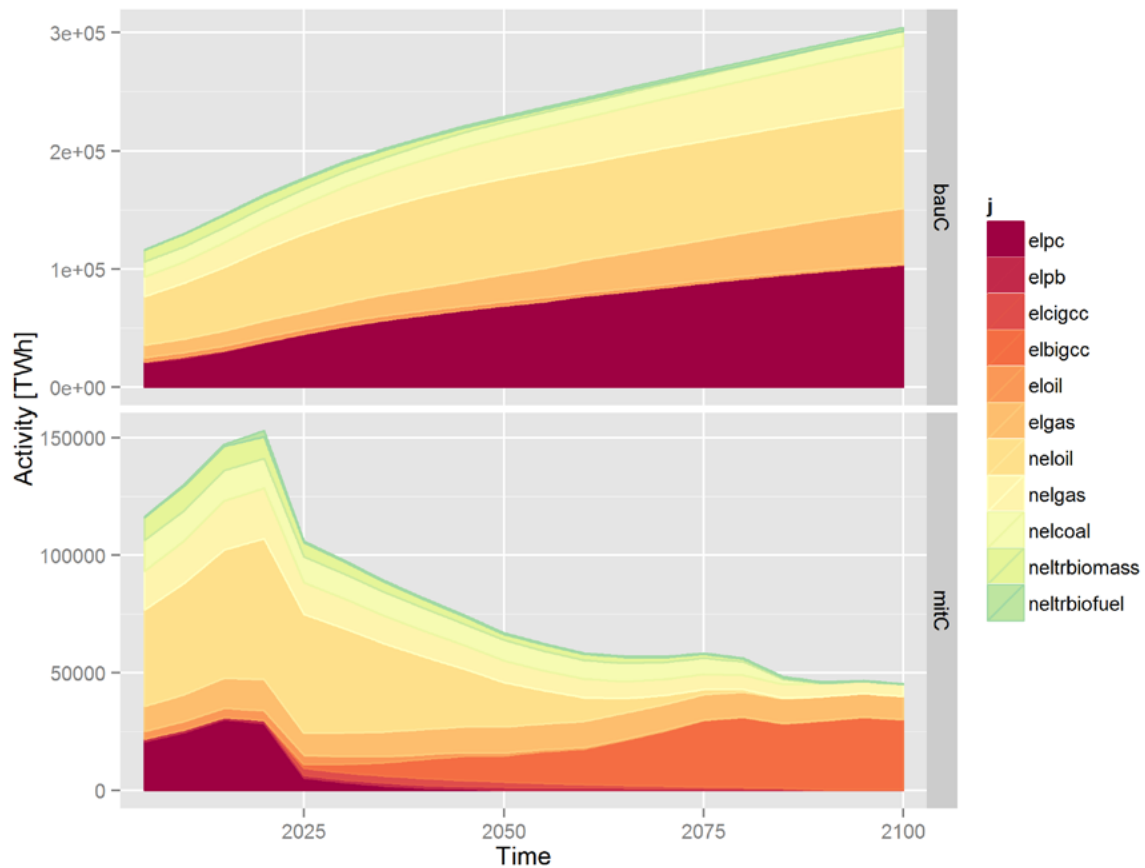


Fig. 3 WITCH world sectoral energy activities for the both energy scenarios (business as usual (*bauC*) and mitigation scenario (*mitC*,  $2.8 \text{ w/m}^2$ )), excluding the non-pollutant and non-energy related sectors. Legend: elpc = electric pulverized coal, elpb = electricity from biomass, elcigcc = electricity IGCC coal, elbigcc = electricity IGCC biofuels, eloil = electricity from oil, elgas = electricity from gas, neloil = non-electric energy from oil, nelgas = non-electric energy from gas, nelcoal = non-electric energy from coal, neltrbiomass = non-electric energy from traditional biomass, neltrbiofuel = non-electric energy from traditional biofuels.

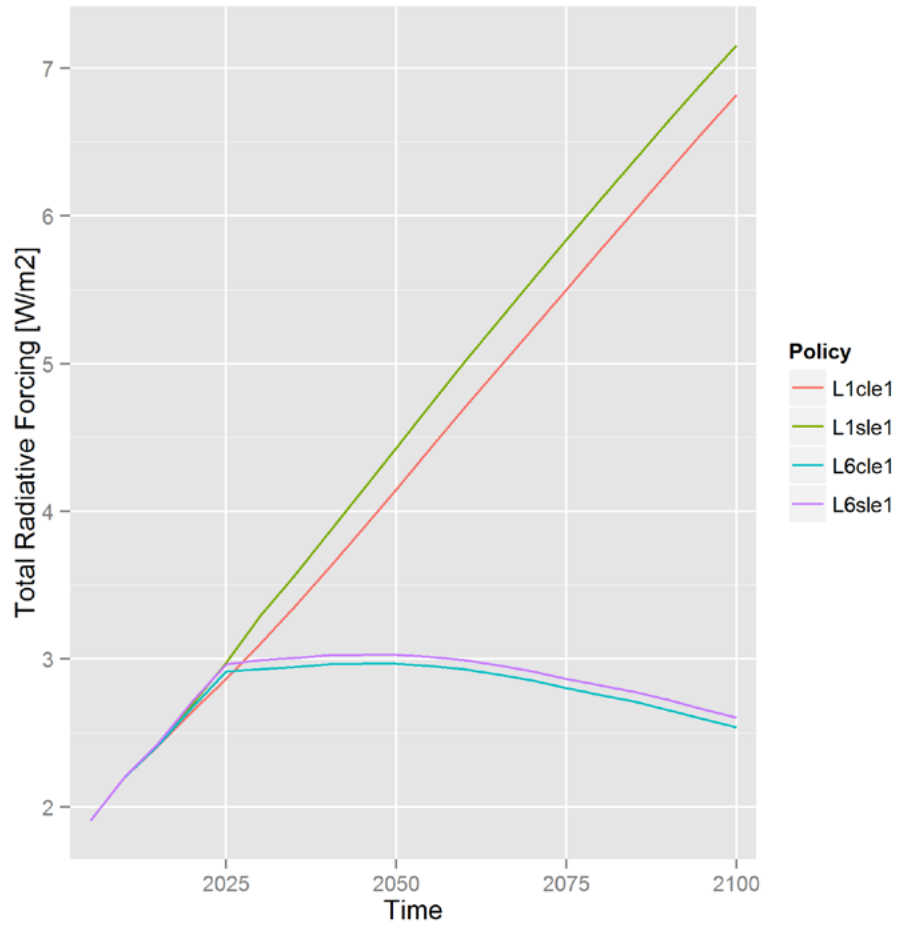


Fig. 4 Total radiative forcing shown for all the policy scenarios.

# Design, Process, and Performance Criteria<sup>1</sup>

## Provide Structure to Climate Policy

Verbruggen A.

University of Antwerp – Belgium

aviel.verbruggen@uantwerpen.be

### Abstract

While the calls for urgent and drastic climate action at all levels of the global society multiply, climate policy development has significantly receded on the political priorities list. Proponents of the Kyoto protocol approach are rather silent since the 2009 COP at Copenhagen, but hope one day “the only game in town” will play music. The opponents seem breeding a wide variety of alternative approaches, with little interaction and unifying proposals and initiatives. This article is not another variant architecture of global climate policy. Here is specified and elaborated a set of ten criteria for supporting the development of climate policy architecture. The ten criteria are classified under – climate policy – design, process, and performance. It is discussed what kind of attributes climate policy has to avoid, or contrary, has to own for meeting the criteria. The analysis is open for comments, amendments, and completion. Its main purpose is to show how rather simple analytical frameworks (like a set of criteria) can provide functional scaffolds for constructing the proper climate policy regimes.

**Keywords:** climate policy design criteria, process criteria, performance criteria

---

<sup>1</sup> A criterion is “a standard on which a judgment or decision may be based” (Webster’s Collegiate Dictionary). Here standards are attributes to own or results to obtain by climate policies or policy makers at various levels (from local to global).

## 1. TEXT

A multitude of ideas about better climate policy architecture have been around for many years [1], [2], [3], [4], [5]. The criticism on the 1997 Kyoto protocol has been vivid since its approval and has grown over time [1], [6]. Next to academics, world leaders sidelined the protocol at the 2009 COP in Copenhagen. But no alternative policy architecture emerged for strengthening the credibility of the agreed +2°C global temperature ceiling. In the debate the pendulum switched from UN steered global prescriptions [7] to expectations about delivering bottom-up initiatives [5], [8], eventually dressed in pledged actions. This contribution identifies ten climate policy criteria and shows what kind of policy attributes and results may meet the criteria. The approach is open for comments and additions.

In a few publications on climate policy regimes, criteria are suggested or applied [8], [9]), for evaluating (proposed) climate policy regimes and their (expected) results. Here is specified and elaborated a set of ten criteria for supporting the development of climate policy architecture. The ten criteria are classified under – climate policy – design (structure), process (action, procedure), and performance (outcome). [Fig. 1] They are discussed one by one, although their interactions are many and some intense and significant.

**POLICY DESIGN.** COHERENCE (also called: consistency) is a common quality standard, but difficult to preserve when a policy covers many items, addresses a diversity of constituencies, requests contributions from almost all scientific disciplines, and operates at different levels. Nested polycentric and multilevel institutions are recommended but submitted to “eight underlying design principles that characterize robust common-property institutions” [10]. Despite the wide awareness about the multilevel reality of climate policy, conflict between top-down policy command [7] and bottom-up endeavors [8] delays progress in designing workable policies. COMPREHENSIVENESS, reflecting the scope of the policy design, is also contentious. The minimum scope is imposed by the policy problem itself, but additional ambition may irresponsibly extend the scope. At minimum scope, global climate policy encompasses mitigation and adaptation, respectively upstream (drivers and pressures) and downstream (impacts) the atmospheric state of global CO<sub>2</sub>-eq concentration, building up by emissions of long-term potent greenhouse gases (GHG). Mitigation reduces the GHG emissions, caused by fossil energy use, land-use

changes, and industrial processes. GHG emissions daily result from trillions of decisions by billions of people. Adaptation plows through major human activities and natural assets (settlements, agriculture, water, biodiversity). Both mitigation and adaptation address all centers of human activity: individuals and households – local organizations and authorities – state, provincial, national – regional, global. Specific polycentric approaches at the proper level are due [10], with “a wide array of institutions rather than a single hierarchy” [8]. Already the minimum scope of global climate policy is extremely challenging to cover politically and administratively in a proper way. Yet, the policy tasks are a manifold heavier when global climate policy mainstreams in sustainable development, as preferred by many e.g. IPCC. Blending positions is understandable: since decades the development agenda is in limbo, and at the 1992 Rio Summit on Sustainable Development the UNFCCC treaty was born, receiving intense political and media attention up to the 2009 Copenhagen COP. Blending is, however, not helpful because it overloads the climate policy train in a way that it remains blocked in the station of departure. Mapping the comprehensive area covered by global climate policy is necessary, but should be followed by rigorous selection of the few paths that lead to emissions levels that guarantee a high likelihood of staying below 2°C warming. A strategy of spearheading climate policy along an urgent and drastic turnover of the global to local energy supply systems, may better realize climate and development goals [3], [11]. SPECIFICITY is a crucial attribute of policy designs. Different degrees of specificity are related to multilevel and polycentric structuring, referring to the diversity of issues and actors, causes and solutions. Policy designers pursue optimal specificity by finding out what issues and which actors belong to a similar class, i.e. a class that can be treated similarly. The policy for one class is designed specific, differing more or less from policies for other classes [12]. Optimal policy design opens suitable degrees of freedom to the regulated actors in constituting their personal state and processes that align with the rules and goals of the policy. Such freedom permits a broadening of the classes, to end with a limited and comprehensible set of classes that are manageable. This accords with Simon’s analysis of complex systems as hierarchically organized, decomposable in subsystems with a high degree of redundancy supporting practical state and process descriptions [13]. But it does not accord with one-size-fits-all mirages by imposing “uniform rules and large boundaries on systems so they are more comprehensible to academics and policymakers” [10]. Many economists adhere

the belief that a global uniform carbon price obtained via emissions trading or via harmonized carbon taxes, could be created. They assume it would be superior to the patchwork of effectively functioning regulations and instruments. They label the policies that today function as preliminary and inferior, and recommend no further development while expecting the messiah of uniformity. Such trials in superseding optimal specificity mostly end in clumsy stapling of rules with exceptions and exemptions agreed in comitology arenas, derailing or blocking policy process and performance. At the other end of the spectrum, unlimited reliance on daily governmental wisdom and power is even imprudent. Markets and states (or global treaties in the case of global climate policy) are established and necessary, as are, evidently decomposed, institutions and organizations. None are full substitutes for coherent, comprehensive and specific designs; they are all valid parts of it.

**POLICY PROCESS.** The URGENT & DRASTIC criterion bridges the design to the process phase in climate policy. [Fig. 1] N. Stern [14] emphasized both attributes, although they imply contradictory policy directions. On the one hand, a state of urgency leaves no time for planting and fostering new institutions and organizations, for experimenting unproven instruments, and for repeating policy failures. Established and experienced institutes can deliver urgent responses by applying with agility and creativity their know-how on new problems, eventually adapting or extending their mission, methods and practices. It aligns with enhanced cooperation between UNFCCC and other multinational organizations, and with authorities at lower levels assuming the utmost share of climate policy design, investment and operation by the Parties of the convention. On the other hand, drastic change requests novel perspectives, analysis, proposals, directions, leadership, etc. And more is required for a spearheading turnover of the energy systems worldwide, that should come first in the industrialized countries, heavily locked in energy and carbon intensive infrastructures, technologies, and practices. Revolutionary novelty is not the landmark of powerful states, established organizations, vested companies, or acquainted privileges. The stalemate positions hint that peaceful transitions to a low-carbon global society are elusive. Which policy designs and processes are hitting the balance between “stop losing valuable time” and “reckless storming into the minefield”? FLEXIBLE & ADAPTABLE, generally lauded attributes for facing uncertainty and evading lock-in (and its ultimate version: absolute irreversibility [15]). Flexibility across issues

and adaptability over time are considered as “distinct advantages” by Keohane and Victor [8], but should come evenhanded with responsibility and accountability. Flexible is not “everything goes and is allowed”, but evolves within demarcated deviations from a “normal” standard. It remains the task of policymakers to establish the normal standards, and to assign deviation margins for flexibility. Adaptability is an attribute of good policy, as brought up by decision analysis and by option value in environmental policy [16]. One decides whether buying time, use of upcoming knowledge (innovations), and preserving adaptability space, outweigh immediate irrevocable (lock-in) investment. However, “wait and learn” may be replaced by “choose or lose” in case irrevocable attributes are forgone forever when not adopted now [15]. In climate policy both opposite poles are relevant. The time-sequential partitioning of the climate policy cycle [3] completes the decomposability of the hierarchical complexity (see criterion specificity). “Complex adaptable systems” stay in the centre of discussing the meaning and evolvement of complexity [13]. RESPONSIBLE & ACCOUNTABLE is connected to, often personal, actors. Responsibility refers to the effects and consequences of past and present behavior, but also to future engagement or obligations to lead, execute, care, etc. Accountable is almost synonymous, adding the notion of payments in kind or in money when responsibilities are not fulfilled. For environmental problems the “polluter pays principle” is established since 1972, when OECD convened to make the companies pay the expenses of abating pollution. The enlarged concept of polluters also paying damage costs of residual pollution is not broadly applied. Proposals to charge countries for historical GHG emissions [17] [18] are popular among developing countries, but difficult to realize practically and politically. When precluding progress in common resolve to address climate change by the most responsible nations, the idea is moreover counterproductive. The polluter pays principle remains a beacon in implementing equity principles [19]. Allocation of responsibility & accountability duties over nations, organizations, and individuals, should respect fairness, their execution be monitored, with graduated sanctions and procedures to enforce [10]. In discussing polycentrism, Mansbridge [20] highlights four roles for the higher level authority (mostly the state): “threaten to impose other solutions, provide neutral information, provide venues and support for the local negotiation, and, crucially, sanction non-compliance”. Enforcement is the linchpin of climate policies. Starting point is that sovereign nations cannot be enforced; they have to commit or “bind” themselves [1]. No pledge is

directly enforceable whether or not it is embellished with a tag “binding”. The arsenal of softer pressures to engage Parties and keep them complying is broad but shallow, such as: conviction, respected partnership in the world community, loss of status and related benefits in other fields, exposure to eventual penalties, etc. Most convincing are agreements that are mutually beneficiary [3]. Global benefits from urgent and drastic emissions reductions are tremendously large [14], such as a little polluted atmosphere, a stable climate, escaping the absolute irreversibility of a highly turbulent and unreliable atmosphere and climate [15]. More and more the climate risks and impacts shift from long-term and distant to short-term and nearby. The more people live with nature and down to earth, the more they are exposed, also the more concerned. The constituencies’ demand for responsible care by politicians will presumably increase in the nearby future. The height of ADMINISTRATIVE & TRANSACTION COSTS is of concern to every real-life policy. In 2007, IPCC [9] added administrative feasibility as a performance criterion to the three standard ones [Fig. 1]. The literature on climate policy reveals an uneasy debate among (neo-classical trained) economists and social scientists that want institutions and organizations to be considered as even (or more) important as markets. Neo-classical economics prevail in Anglo-Saxon academia, and strongly represented in the EU Commission’s climate directory and in IPCC. Their uniform recipes are attractively simple, but humdrum, and attract criticism. “Much study has focused on uniform cap and trade systems. Events have shown this assumption to be unrealistic. The root of the problem with climate policy analysis has been that the Integrated Assessment Models that it uses ignore both transaction costs and institutions”. Rational Choice Institutionalism states “transaction costs are positive and important” [21]. Where administrative and transaction costs are assumed irrelevant, there is little interest in their identification and measuring. But real policy is confronted with institutions and transactions, e.g. the UNFCCC program on Monitoring – Reporting – Verification (MRV) of mitigation actions pledged by the Parties. When effective control and sanctioning by higher-level authorities occurs at the end of policy processes, the processes will be conceived more carefully and realistically for making MRV feasible and affordable.

**POLICY PERFORMANCE.** EFFECTIVENESS in mitigation is measured by the quantity of emitted GHG over time, expecting that today’s growth in emissions bend of in the next few years on a downward slide to low volumes around mid of this century [22].

However, the date of arrival at the top of the emissions curve seems continuously receding in time. Within UNFCCC, Annex-I countries have set distant GHG emissions reduction targets as their mitigation goals. This approach has not proven to be effective, and substitutes like other indicators of progress in emissions reduction, pledged actions, and technology pushes, are suggested and some implementation is going on [3] [1] [8]. When no quantitative indicators identifiable and measurable by participant (Parties of the UNFCCC) are adopted, probably MRV turns out as a bureaucratic mess. Identifiable mitigation effectiveness by participant is necessary for incentivizing progress in a polycentric architecture. If not, leakage is abandoning and robust emission reductions are unlikely. Effectiveness in adaptation is measured by assessed risks of human, ecological, and economic losses. The already noted and further expected losses are highly diverse and spread over the globe. MRV of adaptation actions and results at many levels demands significant resources. EFFICIENCY is the division of obtained results (physical effectiveness, eventually monetized) by costs spent to realize the results. Costs should include monetized externalities and other non-pecuniary uses of resources. In the best of all worlds, the socially optimal results (wanted by people) are delivered at least costs. Because the numerator of the efficiency ratio is very difficult to know, surrogates are (democratically) declared policy objectives, and efficiency (then also called: cost-effectiveness) boils down to realizing the objectives at least costs. This aspect of efficiency is worshipped a lot in the appearance of global emissions trading or of harmonized carbon taxes. Mathematically, total reduction costs from  $N$  emission sources are minimized when every source reduces to the point where every marginal reduction cost price is equal. The mathematical formula ticks higher gains when more emission sources are included (ultimately all sources on earth). Economically and politically, it is not possible, nor desirable, to amalgamate all sources on a single (anyhow imaginary) market floor. Real institutions, diverse technologies and practices, diverse preferences require the search for optimal specificity, with respect to other design and process criteria. Also, dynamic efficiency (least costs over future periods by induced innovation in selected technologies and practices) should prevail over a static mathematical formula. The realities of cost minimizations exceed the simplicity of a simple formula. This finding is opposite to the repetitive quoting of the amalgamation mess as the “heavenly ideal the world should continue to strive for, yet it may not be accessible by the human race”. Actually, the world should count on the

specificity of incentives and institutions, and on multiple governing authorities at differing scales [10] [21]. This realistic road is not simplistic and conflicts and failures will be a part of it, but progress is feasible and the outcome will pay off the effort. EQUITY is the last of the ten criteria, but not the least. Equity is an essential component of sustainable development [22], and stays high on the UNFCCC agenda. The atmosphere and embedded climate as global, long-term commons trigger intra- and intergenerational equity questions beyond the answering capacity of theorists and of practitioners. Let me single out a few issues. First, a proper application of the enlarged “polluter pays principle” on GHG emitters. This starts by applying fossil energy use and carbon emission levies in all corners of the world, imposed by there governing public authorities. Public levies on energy differ from rents cashed by energy corporations: the money is available for the public interest, also for relieving the living conditions of the poorest citizens. Levies based on present and future GHG emissions are recommended. The GDP height of a country is proposed as proxy metrics for the country’s historical emissions responsibility. Second, transfers from donor to recipient Parties is a redistribution aspect of global climate policy. Transfers may include technology, goods, finance, services e.g. to strengthen governance capability. The size and direction of the transfers between parties depend on the classification of the countries as donor or recipient. The Rio 1992 Annexes are outdated and not enough specific to house a responsible and adaptable classification. Better is the yearly ranking of all countries on a GDP/capita scale. Countries above average income are donors to countries below average income. Gifts and receipts are graduated over the scale, and adjusted by every country’s yearly performances on mitigation and adaptation progress indicators. This will not solve all the world’s development and inequity problems, but in this way operational climate policy contributes to sustainable development.

## 2. REFERENCES

1. Aldy E.J. & Stavins R.N., eds. (2007), *Architectures for Agreement. Addressing Global Climate Change in the Post-Kyoto World*, Cambridge University Press
2. Kuik O., Aerts J., Berkhout F., Biermann F., Bruggink J., Gupta J. & Tol R.S.J. (2008), *Post-2012 climate policy dilemmas: a review of proposals*, Climate Policy, No. 8, pp. 317-336

3. Verbruggen A. (2009), *Beyond Kyoto, plan B: A climate policy master plan based on transparent metrics*, Ecological Economics, No. 68, pp.2930-2937
4. Bosetti V., Carraro C. & Tavoni M. (2009) *Climate policy after 2012. Technology, Timing, Participation*, Cesifo Economic Studies, No. 55(2), pp. 235-254
5. Hahn R. & Ulph A., eds. (2012) *Climate Change and Common Sense. Essays in Honour of Tom Schelling*, Oxford University Press
6. Prins G. & Rayner S. (2007) *Time to ditch Kyoto*, Nature, No. 449, pp. 973-975
7. Hare W., Stockwell C., Flachsland C. & Oberthür S. (2010) *The architecture of the global climate regime: a top-down perspective*, Climate Policy, No. 10, pp. 600-614
8. Keohane R.O; & Victor D.G. (2011) *The Regime Complex for Climate Change*, Perspectives on Politics, No. 9(1), pp. 7-23
9. Gupta S., Tirpak D.A., et al. (2007) *Policies, Instruments and Co-operative Agreements*, Chapter 13 in IPCC Climate Change 2007, Fourth Assessment Report, Mitigation of Climate Change, Cambridge University Press
10. Ostrom E. (2005) *Understanding Institutional Diversity*, Princeton University Press
11. Dubash N.K. & Florini A. (2011) *Mapping Global Energy Governance*, Global Policy, No. 2, pp. 6-18
12. Ostrom E. (1990) *Governing the Commons. The Evolution of Institutions for Collective Action*, Cambridge University Press
13. Simon H. (1996), *The Sciences of the Artificial*, The MIT Press
14. Stern N. (2006), *The Economics of Climate Change. Executive Summary*
15. Verbruggen A. (2013), *Revocability and reversibility in societal decision-making*, Ecological Economics, No. 85, pp. 20-27
16. Arrow K.J. & Fisher A.C. (1974), *Environmental preservation, uncertainty, and irreversibility*, Quarterly Journal of Economics, No. 88, pp. 312-319

17. Ngwalda X. (2013), *An operational framework for equity in the 2015 Agreement*, *Climate Policy*, No. 14(1), pp. 8-16
18. Klinsky S. & Winkler H. (2013), *Equity, sustainable development and climate policy*, *Climate Policy*, No. 14(1), pp.1-7
19. Heyward M. (2007), *Equity and international climate change negotiations: A matter of perspective*, *Climate Policy*, No. 7, pp. 518-534
20. Mansbridge J. (2014) *The role of the state in governing the commons*, *Environmental Science & Policy*, No. 36, pp. 8-10.
21. Lane L. & Montgomery W.D. (2014), *An institutional critique of new climate scenarios*, *Climatic Change*, No. 122, pp. 447-458.
22. IPCC (2014), *Mitigation of Climate Change. Summary for Policymakers*, Intergovernmental Panel on Climate Change, Fifth Assessment Report,
23. WCED (1987), *Our Common Future*, The World Commission on Environment and Development, Oxford University Press

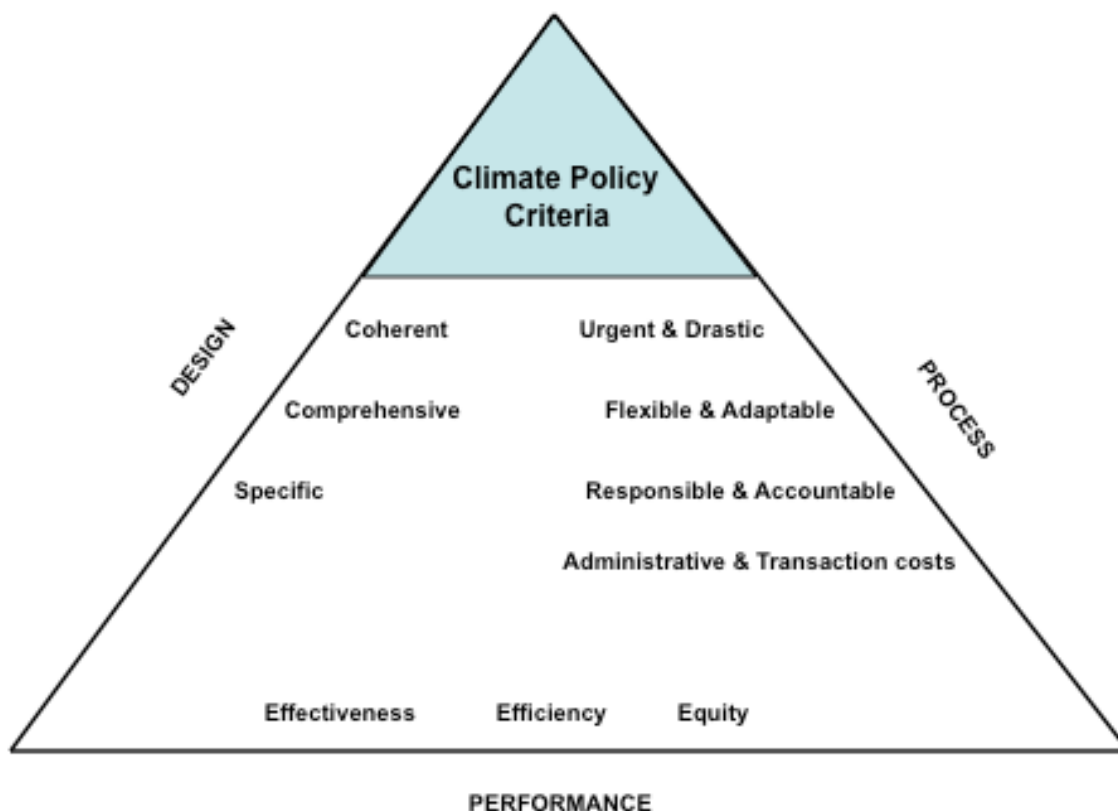


Fig. 1 Overview of ten criteria for climate policy design, process, performance

# Mirages in climate policy evaluation: how model assumptions may drive policy costs

Michetti M.<sup>1\*</sup>, Parrado R.<sup>1,2</sup>

<sup>1</sup> Centro Euro-Mediterraneo sui Cambiamenti Climatici - Italy

<sup>2</sup> Fondazione Eni Enrico Mattei– Italy

\* Corresponding Author: melania.michetti@cmcc.it

## Abstract

Within climate and energy policy evaluations, computable general equilibrium models are amongst the most used tools to assess and quantify climate mitigation costs. While key model parameters have been recently downward revised, few attempts have proposed an extensive sensitivity analysis on policy costs and related effects, explicitly comparing old with new elasticity values. Employing the widely used GTAP-E model in its existing two model versions, this paper intends to bridge this gap. We disentangle the role played by each distinct parameter category in affecting policy cost, carbon price, and leakage effects. An increased rigidity of the GTAP-E model is generated when key substitution parameters are replaced with a set of validated elasticities. We show that the most important assumption, driving results on policy costs and carbon price, is the substitution flexibility between capital and energy inputs. This, shows to be the most relevant elasticity component to address the carbon leakage concern too. A lower capital-energy substitution generates a structural rigidity in the system such that leakage also applies when more favorable trade settings are assumed.

**Keywords:** climate change, climate mitigation, General Equilibrium Modelling, elasticity parameters

## 1. INTRODUCTION AND MOTIVATION

Quantifying climate mitigation costs has been the scope of many analyses since the Kyoto Protocol agreement was sealed, and many methods and models have been implemented to this aim. Several simplifications and assumptions are needed in order to deal with difficulties in evaluating policy impacts and costs. This paper proposes a sensitivity analysis on models assumptions that are expected to influence policy costs and implications.

Amongst the tools used for policy evaluation, Computable General Equilibrium (CGE) models have recently gained much attention in the context of climate policy cost assessment and energy policy analysis. A big number of CGE studies base their results on a widely used model, GTAP-E [1, 2]. GTAP-E improves the production structure of the well-known GTAP standard model [3] introducing inter-fuel substitution and combining energy with capital.

In spite of its extensive use, only recently there has been a validation of the values adopted in GTAP-E for key elasticity parameters; this has been proposed by Beckman et al. [4, 5], which acknowledge that the model's energy demand is too price elastic (i.e., original substitution parameters are overestimated), leading to a substantial underestimation of climate abatement efforts. Hence, a set of new validated parameters is proposed, which has been already extensively used within CGE literature [6-11].

However, only a couple of attempts have proposed a sensitivity analysis of mitigation costs, explicitly comparing the outcomes resulting from using original versus revised parameter values. A first effort is that of Michetti and Parrado [12] which focusing on the forestry sector modelling propose a sensitivity analysis confirming that the lower the factor demand elasticities, the higher the abatement effort required to achieve emissions reduction targets. A second study by Golub [13] centered on the modeling of the capital adjustment mechanism across markets and on decomposing the impact of energy and non-energy channels on carbon leakage, substantiates that the costs of achieving abatement targets are much higher when a low degree of technological flexibility is assumed.

Both studies produce their outcomes using models based on, but far different from, GTAP-E. This makes difficult disentangling the effects of a change in the elasticities for the carbon supply and the level of technological flexibility.

Considering original and new parameters, the present study offers a sensitivity analysis specifically focusing on the supply side of the GTAP-E model, accounting for its two existing model versions.

## **2. PRODUCTION STRUCTURE, ELASTICITY PARAMETERS AND POLICY COSTS IN A GENERAL EQUILIBRIUM FRAMEWORK**

Typically, CGEs model the level of available technology and agents' responses to changes in relative input prices, with a nested production structure involving different constant elasticity of substitution (CES) functions. CES aggregators, used to reproduce the response of the economic system, represent a parsimonious and elegant way to adopt different assumptions about the substitutability between diverse pairs of inputs.

The extent to which the input mix can change (i.e., the responsiveness of the production to variations in relative input prices following a climate policy) is determined by substitution or elasticity parameters ( $\sigma$ ) in the production function. Thus, the size of substitution parameters in each nest is central for climate policy analysis as it determines the dimension of the abatement effort. The magnitude of corresponding elasticities drives the policy burden in such a way that with a higher substitution flexibility, policy costs will turn out to be lower.

Graphically the GTAP-E production function can be represented as a nested tree [Fig. 1]. Starting from lower to higher nests, the production structure involves initial inputs, intermediate aggregates and final outputs. The upper-level describes the final output of a generic sector  $j$ , which can be expressed as a function of the aggregate value added-energy (VAE), and the other intermediate inputs purchased from the remaining sectors. Lower levels are represented by CES functions allowing for some degree of substitutability ( $\sigma_{VAEN}$ ) between primary production factors (land, labor, natural resources), and a capital-energy composite (KE), produced, in its turn, by combining capital (K) and energy (E) with an elasticity of substitution  $\sigma_{KE}$ . Then,

energy (E) is modelled as a mix of all energy vectors, combining a single type of energy with a composite in pairs, according to their particular features. The first energy mix compounds electric (EL) with non-electric energy (NEL) with the elasticity of substitution  $\sigma_{ENER}$ . Then, the Non-electric composite (NEL) results from combining coal and non-coal energy, assuming an elasticity of substitution of  $\sigma_{NELY}$ . The rest of liquid fossil fuels (oil, gas, oil products) are pooled in a composite (NCOAL) also following a CES production function with the elasticity of substitution  $\sigma_{NCOAL}$ .

Comparing original with parameters revised by Beckman et al. [11] we aim to evaluate the effects exerted by changes in elasticity values. We make assumptions on the capital and inter-fuel substitution parameters for each nest of the production structure [Tab. 1]. In addition, we recalibrate the original  $\sigma_{VAE}$  values, using new supply elasticity values (assumed the same across regions) for coal, oil, and gas sectors (coal = 1; oil = 0.25; gas = 0.60) [Tab. 2].

### 3. EVALUATION OF CLIMATE POLICY EFFECTS IN GTAP-E

The GTAP-E model links a more detailed representation of the energy supply compared to the standard GTAP framework [3], considering inter-fuel and fuel-factor substitution, with a top-down (economic) approach. Such specification is also enhanced with a carbon tax and an emission trading system, which allows imposing regional reduction quotas on CO<sub>2</sub> emissions and simulating the trading of emission permits among countries participating in a coordinated mitigation effort. This formulation reproduces a carbon market where the allocation of emissions permits among participating countries results from equalizing the marginal climate abatement costs across the trading areas (equaling the common price at which the quotas are traded).

We use the GTAP-E model in the two existing versions: the original by Burniaux and Truong [1], and the framework revised by McDougall and Golub [2], respectively B-T and McD-G from now on. The comparison of the corresponding results functions as a robustness check. Although both versions share the same core structure and initial parameters, there are some differences such as the way the emissions are modelled

along with the carbon taxation, the emissions trading system, as well as the formulation of the inter-fuel and energy substitution. We use the GTAP 8 database for 2007 as reference year with a specific regional and sectoral aggregation [Tab. 3].

#### **4. BASELINE AND POLICY SCENARIO**

The baseline scenario for 2020 has been calibrated following major assumptions for population and GDP from the Shared Socioeconomic Pathways, considering the Middle of the Road scenario (SSP2). This setting envisages the continuation of current trends with some achievements of development goals and a slow reduction in fossil fuels use [14-16]. As for coal, oil and gas prices, they have been calibrated to closely reproduce the trends proposed by the International Energy Agency [17].

We simulate a climate policy where major emitting EU countries agree to curb their carbon emissions in 2020 as proposed in the Copenhagen Accord, low pledges [18, 19]. For the sake of simplicity, we include only CO<sub>2</sub> emissions in this analysis. By allowing European regions to exchange emissions permits on the carbon market, we replicate the European Emissions Trading System (EU-ETS).

#### **5. SENSITIVITY ANALYSIS AND BASELINE RECALIBRATION**

Considering recently revised parameter values [Tables 1, 2], we evaluate the overall sensitivity of policy costs to changes in elasticities as well as the individual contributions of each parameter category ( $\sigma_{KE}$ ,  $\sigma_{ENER}$ ,  $\sigma_{NELY}$ ,  $\sigma_{NCOAL}$ , and  $\sigma_{VAEN}$ ) to the total cost variation. In the following sub-sections, illustrative figures are presented for both GTAP-E model versions for which we highlight differences expressed in terms of mitigation cost as percentage of GDP, carbon market price, and leakage effects.

##### **a. POLICY COSTS**

A mitigation target of 20% emissions reduction by 2020 would imply for the EU an indirect cost in terms of real GDP in the range 0.25% and 0.63% [Fig. 2]. When the old elasticities are in place the difference between the two model versions is indiscernible. In this case, policy cost is around 50 USD bn

corresponding to a 0.25% decline in GDP compared to 2020 baseline values. Using all new parameters, policy costs attain 132 (B-T) and 114 (McD-G) USD bn. In relative terms, these are 158% (B-T) and 128% (McD-G) higher than those reported using old elasticity values. Hence, we confirm that the lower the flexibility in substituting energetic-inputs the higher the policy cost [Fig. 3]. In general, differences between models, across elasticity scenarios and regions, are negligible and below |0.2| percentage points (results are robust).

The variation of the supply elasticity for coal, oil and gas sectors (and therefore the corresponding variation of  $\sigma_{VAEN}$ ) maintains policy costs almost unaltered. The larger impact in raising the mitigation cost is produced by the elasticity  $\sigma_{KE}$ , followed by  $\sigma_{ENER}$  and  $\sigma_{NELY}$ .

In opposition to what occurs with the other parameters (higher rigidity increases policy costs), by lowering the  $\sigma_{NCOAL}$  elasticity a cost reduction occurs. Although this may appear counterintuitive, the explanation is rather simple. Specifically, the  $\sigma_{NCOAL}$  elasticity belongs to the lower nest where only fossil fuels (oil, and oil products, in addition to gas) are combined. When a climate policy applies and increases fossil fuel prices, an industry, such as electricity generation, can switch to less carbon-intensive fuels (from coal to gas). However, a reduced inter-fuels substitution (lower  $\sigma_{NCOAL}$  value) leads to abandon the increased-cost inputs (and the composite in which they are used for) in favor of other inputs or factors in the upper nests, which are less carbon-intensive (non-electric, energy, capital-energy, and value added). This explains the decline in the final policy cost. Whereas the size of the effect is contained because the cost share of the lower nest inputs is much smaller compared to that of the upper nests, where more possibilities for substitution exist. Shifting from the original to the new values for all substitution elasticities simultaneously generates a compound effect due to the interaction of all the nests at the same time. For all the regions, costs are more than doubled compared to the original scenario. The updated formulation reduces the flexibility of the whole system where it is more difficult to substitute energy commodities with capital, and the most valuable alternatives to deal with an increased carbon price are mostly located in the upper value-added-energy nest.

## **b. CARBON PRICE**

The price pattern is symmetric to the policy cost in terms of GDP, and the prices in both model versions are close for each scenario [Fig. 4]. The set of new parameters produce a price increase of 179% (B-T) and 151% (McD-G) compared to the original set of values. The relative rise in the carbon price is much higher than that of the indirect policy cost, measured as percentage of GDP.

## **c. CARBON LEAKAGE**

Carbon leakage is one of the measures that allows synthetizing the real policy success by looking at the mitigation effort offset by the increase on emissions outside the agreement. Leakage depends on the rest of countries that do not face an emission constraint and, therefore, are free to adjust to changes in import demands from regions enforcing a climate agreement.

We compute leakage rates as emissions increases outside the EU policy boundaries divided by the reduced emissions following the EU mitigation target [Fig. 5]. Variations in the substitution elasticity at different nests produce changes in leakage rates, confirming the importance of the substitution elasticity for the capital-energy composite: the only parameter able to shrink the magnitude of leakage in all cases. Reducing the substitution elasticities in the rest of the lower nests, below the capital-energy composite enlarges the leakage effect. The carbon price signal in countries implementing the climate policy translates in a reduction of world prices, which benefit the rest of the world. This effect is more evident when the supply elasticity of fossil fuels is reduced. Indeed, with an inelastic supply, given that shifts in demand will produce higher price variations, the price of fossil fuels in the international market would be even lower, therefore amplifying leakage. In this case, the combination of all rigidities imposed with the new set of parameters shows a leakage rate that is around three times higher vis-à-vis original values.

In terms of distributional leakage effects North\_EU15 would pay the most in absolute values, (more than 22 and 50 USD bn, respectively, for the original and new set of parameters). However, East\_EU12 and Med\_EU12 are the most affected regions in terms of climate policy impact on GDP in percentage values [Fig. 6]. Indeed, an emissions reduction of 20%, of their 1990 values, corresponds to a reduction of their GDP between 0.5% and 1.1% for the original and new set of values, respectively. Remaining European regions' effort is between 0.17% and more than 0.63% for the new set of elasticities. As for the rest of countries not participating in climate mitigation, impacts on GDP are dissimilar across regions and elasticity scenarios. To a lower flexibility in energy inputs substitution corresponds, as expected, larger leakage gains for regions remaining outside the policy agreement. Benefiting the most from the EU's climate policy is the Rest of Europe and the Rest of Former Soviet Union showing a relevant increase in their GDP.

## 6. CONCLUSION

This paper analyses the flexibility of CES nested production structure, widely used in CGE models and in the context of climate policy evaluation. We use the well-known GTAP-E model in a climate policy context to investigate the sensitivity of policy costs, carbon price, and leakage effects to changes in elasticity parameters.

The most important elasticity driving results is the capital-energy substitution. Changes in this elasticity can affect not only policy costs but also the leakage rate, which is a measure of the effectiveness of a unilateral mitigation effort. Reducing only this elasticity could decrease leakage outside the EU coalition on climate change. Moreover, a lower substitution between capital and energy together with reduced elasticities in the lower nests of the production function generate a structural rigidity in the system so that leakage also applies in different trade settings, simulated by changing assumptions on Armington elasticities.

All policy evaluations, performed with any kind of model, are subject to their own limitations due to the simplifications made to simulate the complexity of the real world with, unfortunately, insufficient data resources. We have shown that, within CGE

models, downward revising elasticity values provides costs and leakage rates much higher than those normally presented by the CGE literature on climate policy costs. With our exercise, we have tried to understand the magnitude of these numbers and the assumptions driving these outcomes.

## 7. REFERENCES

1. Burniaux, J., T. Truong, (2002). *GTAP-E: An Energy-Environmental Version of the GTAP Model*. GTAP Technical Paper No. 16, Center for Global Trade Analysis. Purdue University, West Lafayette, IN.
2. McDougall, R., A. Golub, (2007). *GTAP-E: A Revised Energy-Environmental Version of the GTAP Model*. GTAP Research Memorandum No. 15, Center for Global Trade Analysis, Department of Agricultural Economics, Purdue University, West Lafayette.
3. Hertel T.W., Tsigas, M. (1997), *Structure of GTAP*, in Hertel, T.W., 1997 (ed). *Global Trade Analysis: Modeling and applications*. Cambridge University Press, Cambridge.
4. Beckman J., Hertel T., Tyner W., (2011). *Validating energy-oriented CGE models*. *Energy Economics*. Elsevier, Vol. 33 No.5: 799-806.
5. Beckman J.F., T.W. Hertel, (2009). *Why previous estimates of the cost of climate mitigation are likely too low*. GTAP Working Paper No. 54, Center for Global Trade Analysis. Purdue University, West Lafayette, IN.
6. Golub, A., T.W Hertel, F. Taheripour and W. Tyner, (2010). *Modeling Biofuels Policies in General Equilibrium: Insights, Pitfalls and Opportunities*. GTAP Working Paper No. 61.
7. Kuik O., M. Hofkes, (2010). *Border adjustment for European emissions trading: Competitiveness and carbon leakage*. *Energy Policy* No. 38:1741-1748.
8. Hertel T.W., J. Beckman (2011). *Commodity Price Volatility in the Biofuel Era: An Examination of the Linkage between Energy and Agricultural Markets*. NBER Working Paper No. 16824
9. Golub A., T.W. Hertel. (2012). *Modeling land-use change impacts of biofuels in the GTAP-bio framework*. *Climate Change Economics*. Vol. 03, No. 03

10. Zhang et al. (2013). *Effects and mechanism of influence of China's resource tax reform: A regional perspective*. Energy Economics, No. 36: 676-685.
11. Antimiani A., et al., (2013). *Assessing alternative solutions to carbon leakage*. Energy Economics, No. 36: 299-311.
12. Michetti, M., Parrado, R., (2012). *Improving land-use modeling within CGE to assess forest-based mitigation potential and its costs*. CMCC Research Papers Series, N. 126 & FEEM Working Paper N. 19.2012.
13. Golub, A., (2013). *Analysis of Climate Policies with GDyn-E*. GTAP Technical Paper No. 32.
14. Moss et al., (2010). *The next generation of scenarios for climate change research and assessment*. Nature 463, 747-756.
15. van Vuuren et al.,(2012). *A proposal for a new scenario framework to support research and assessment in different climate research communities*. Global Environmental Change, Volume 22(1):21-35
16. Kriegler et al., (2010). *Socio-economic Scenario Development for climate change analysis*. CIRED Working Paper DT/WP N2010-23
17. IEA, (2011). World Energy Outlook:  
<http://www.worldenergyoutlook.org/publications/weo-2011/#d.en.25173>
18. UNFCCC (2011a). *Compilation of economy-wide emission reduction targets to be implemented by Parties included in Annex I to the Convention*.
19. UNFCCC (2011b). *Compilation of information on nationally appropriate mitigation actions to be implemented by Parties not included in Annex I to the Convention*.

## 8. IMAGES AND TABLES

Substitution elasticity	Original	New
Capital & Energy ( $\sigma_{KE}$ )	0.5	0.25
Energy composite ( $\sigma_{ENER}$ )	1	0.16
Non-electric Energy ( $\sigma_{NELY}$ )	0.5	0.07
Non-coal energy ( $\sigma_{NCOAL}$ )	1	0.25

Tab. 1 Elasticities for energy and inter-fuel substitution.

Region	Coal		Oil		Gas	
	Original	New	Original	New	Original	New
<b>Supply elasticity</b>	<b>10</b>	<b>1</b>	<b>1</b>	<b>0.25</b>	<b>4</b>	<b>0.6</b>
<b>Value Added elasticities (<math>\sigma_{VAEN}</math>)</b>						
USA	3.8	0.38	0.39	0.1	0.2	0.03
North Europe	3.7	0.37	0.4	0.1	1.55	0.23
North EU15	3.8	0.38	0.4	0.1	0.53	0.08
Mediterranean EU15	3.5	0.35	0.38	0.1	0.01	0.00076
Mediterranean EU12	3.4	0.34	0.35	0.09	0.19	0.03
Eastern EU12	3.3	0.33	0.35	0.09	0.07	0.01
Rest of Europe	3.7	0.37	0.36	0.09	0.35	0.05
Russia	3.3	0.33	0.39	0.1	0.58	0.09
Rest of FSU	3.2	0.32	0.37	0.09	0.68	0.1
South Korea	3.8	0.38	0.26	0.06	0.00011	0.00002
Australia	3.7	0.37	0.39	0.1	1.08	0.16
South Africa	3.9	0.39	0.4	0.01	0.97	0.15
Canada	3.9	0.39	0.39	0.01	1.36	0.2
Japan	4	0.4	0.4	0.01	0.01	0.0011
New Zealand	3.9	0.39	0.4	0.01	0.68	0.1
North Africa	3.6	0.36	0.4	0.01	1.31	0.2
Middle East	3.8	0.38	0.39	0.01	1	0.15
Sub Saharan Africa	3.1	0.31	0.39	0.01	1.19	0.18
South Asia	3.8	0.38	0.4	0.01	0.26	0.04
India	4	0.4	0.39	0.01	0.28	0.04
China	3.6	0.36	0.37	0.09	0.28	0.04
East Asia	3.9	0.39	0.39	0.1	0.79	0.12
Rest of Latin America	4	0.4	0.4	0.1	0.92	0.14
Brazil	4	0.4	0.39	0.1	0.75	0.11
Mexico	4	0.4	0.36	0.09	0.51	0.08

Tab. 2 Value added nest Substitution elasticities for fossil fuels.

<b>N</b>	<b>Regions</b>	<b>Description</b>	<b>Sectors</b>
1	USA	United States	Agriculture
2	North_Europe	North Europe	Forestry
3	North_EU15	North Europe_15	Fishing
4	Med_EU15	Mediterranean Europe_15	Coal
5	Med_EU12	Mediterranean Europe_12	Oil
6	East_EU12	Eastern Europe_12	Gas
7	RoEurope	Rest of Europe	Oil products
8	Russia	Russia	Electricity
9	RoFSU	Rest of Former Soviet Europe	Energy Intensive Industries
10	SouthKorea	South Korea	Other Industries
11	Australia	Australia	Transport
12	SouthAfrica	South Africa	Market Services
13	Canada	Canada	Public Services
14	Japan	Japan	
15	NewZealand	New Zealand	
16	NAF	North African Countries	
17	MDE	Middle East	
18	SSA	Sub-Saharan Africa	
19	SASIA	South Asia	
20	India	India	
21	China	China	
22	EASIA	East Asia	
23	RoLACA	Rest of Latin American Countries	
24	Brazil	Brazil	
25	Mexico	Mexico	

Tab. 3 Regional and sectoral aggregation.

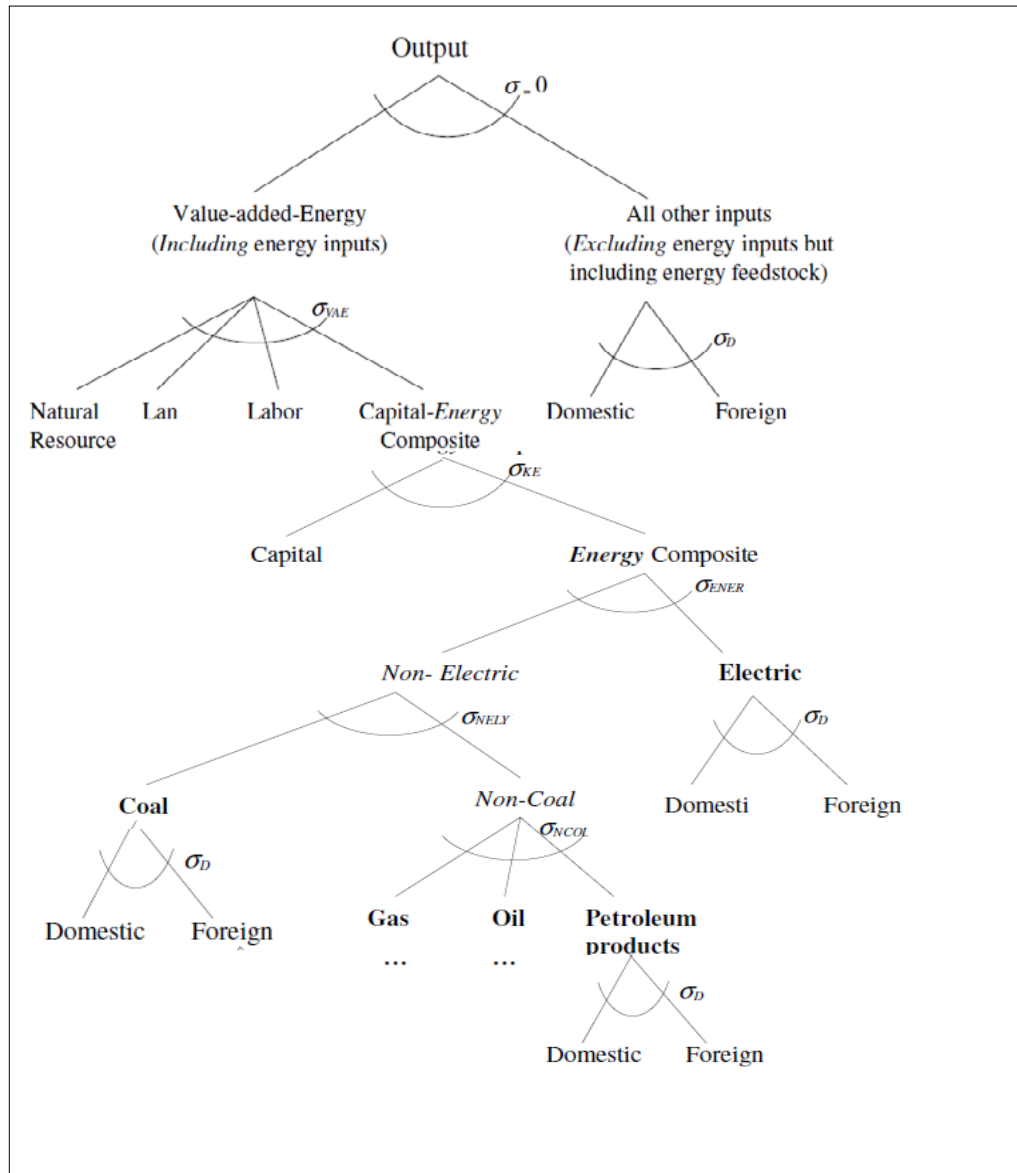


Fig. 1 GTAP-E production function for sector  $j$ .

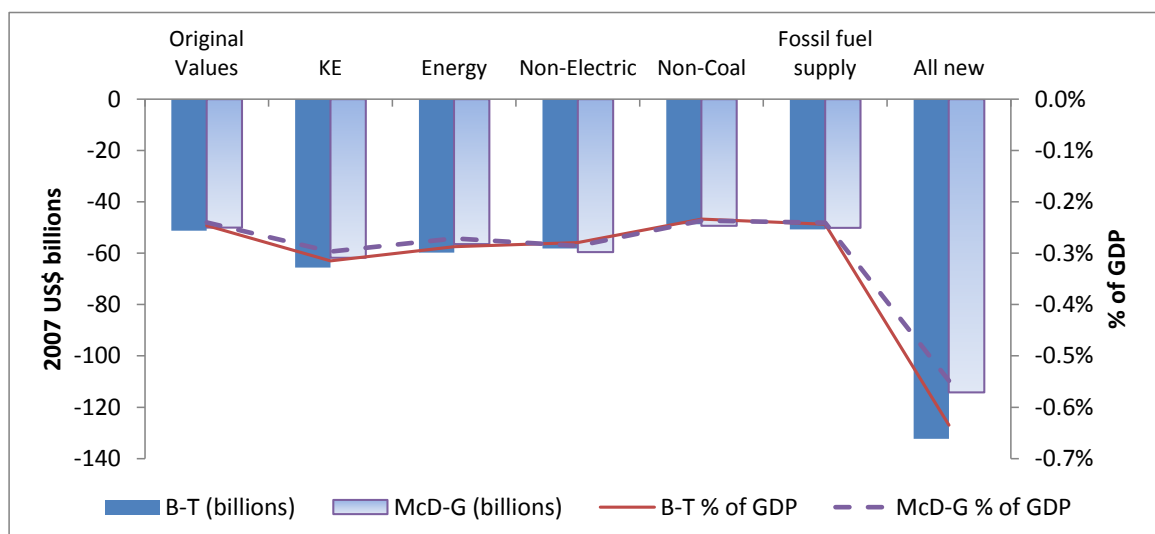


Fig. 2 EU Policy costs in 2020 corresponding to a 20% mitigation target.

1

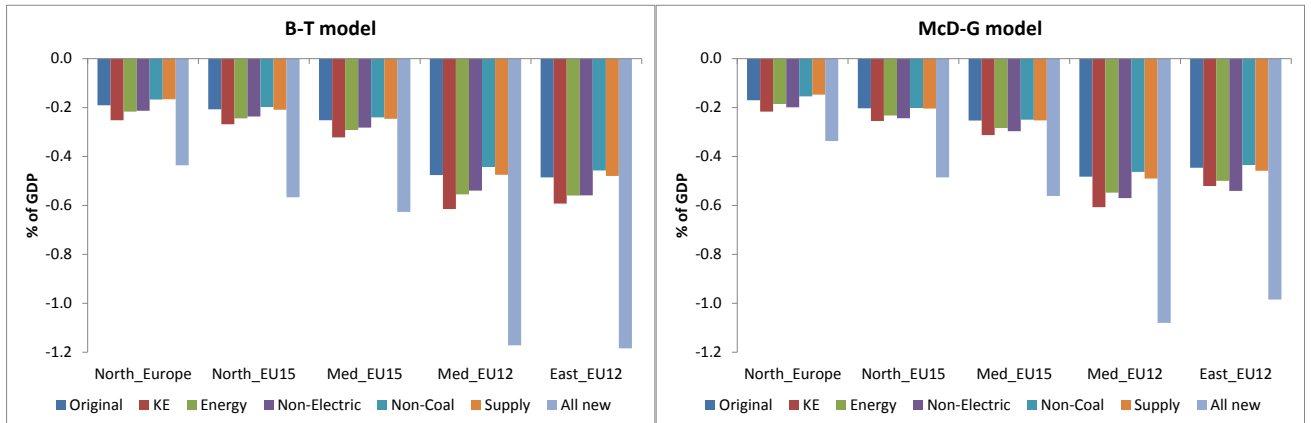


Fig. 3 Policy costs by elasticity, region and model version in percentage of GDP.

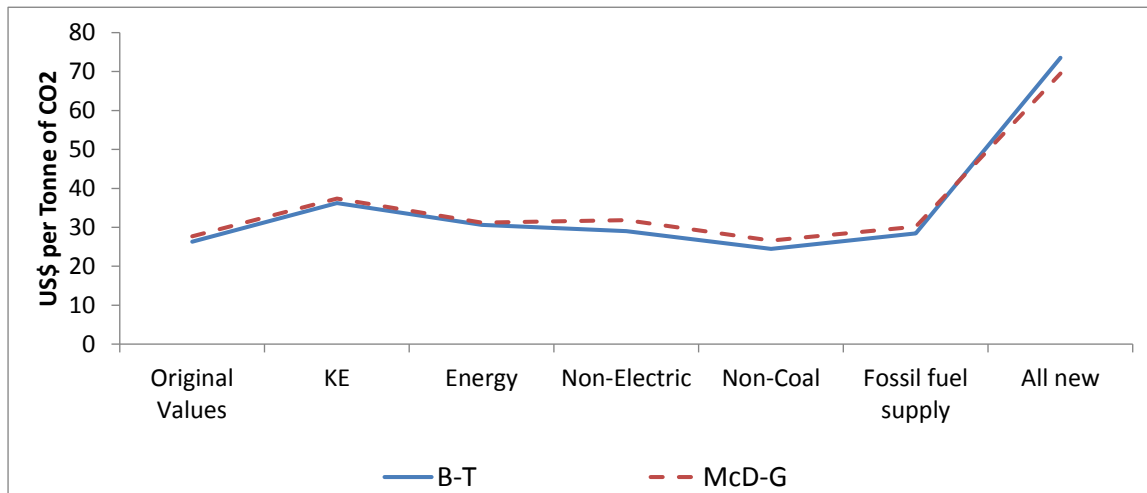


Fig. 4 Carbon price for a 20% emission reduction target.

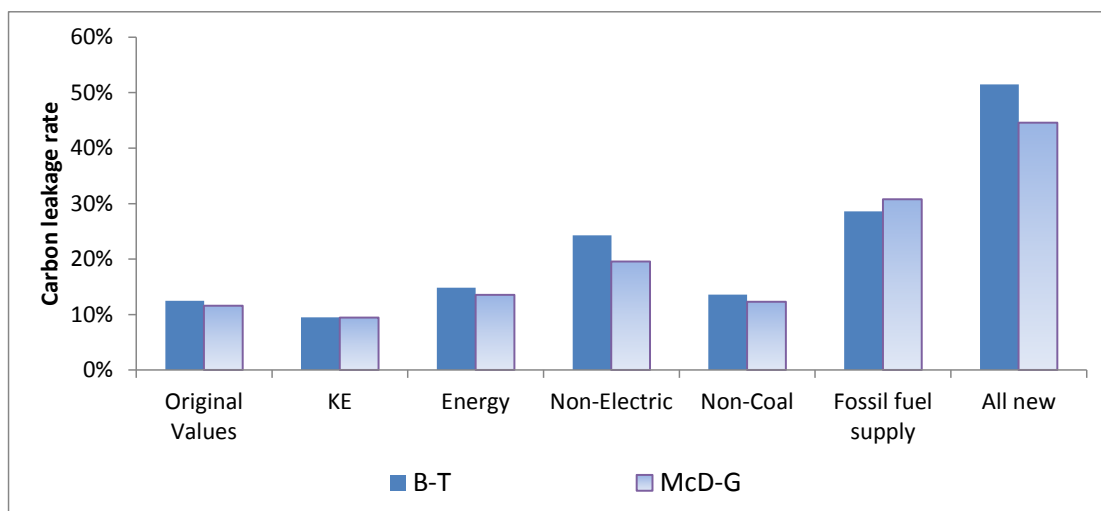


Fig. 5 Carbon leakage rates.

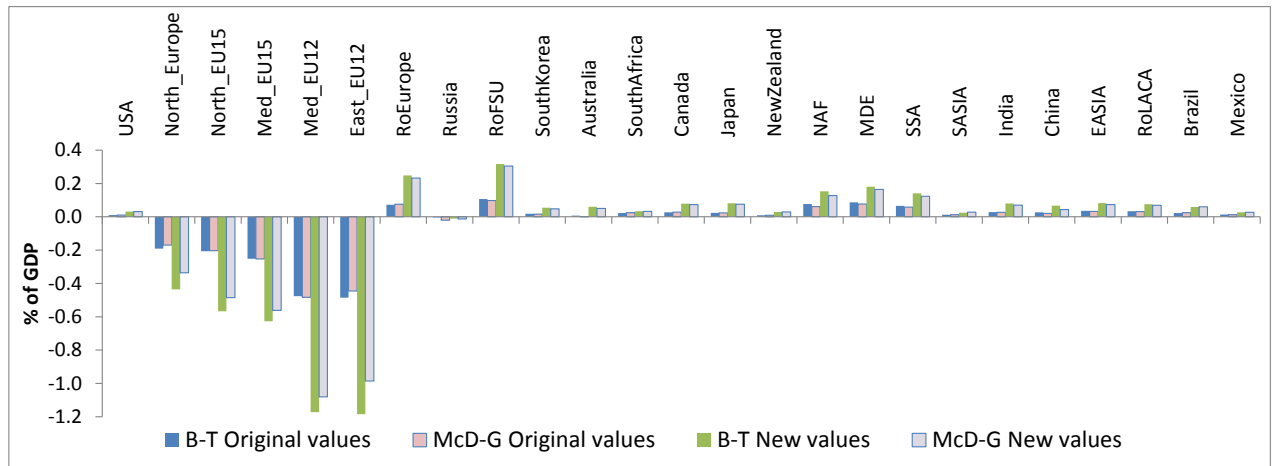


Fig. 6 Climate policy impacts on GDP by elasticity and for all regions.

# Selection of carbon budgets under current knowledge of uncertainties

Drouet L.<sup>1,2\*</sup>, Bosetti V.<sup>1,2</sup> and Tavoni M.<sup>1,2</sup>

<sup>1</sup>Centro Euro-Mediterraneo sui Cambiamenti Climatici - Italy, and <sup>2</sup>Fondazione Eni

Enrico Mattei - Italy

\*Corresponding Author: laurent.drouet@cmcc.it

## Abstract

Policy making in the face of climate change is a process that has to take into account and incorporate several sources of uncertainties, as well as the normative models societies decide to adopt to cope with those uncertainties. In the present paper we use best available knowledge, produced for the fifth IPCC assessment report, to account for uncertainties affecting future climate change, its economic impact on societies and the cost of mitigating climate change. This knowledge comes from inter-model comparison datasets: the fifth phase of the Coupled Model Intercomparison Project for the climate and the AR5 Scenario database involving many integrated assessment models for the mitigation costs. We then identify robust climate policies by means of a set of selection rules representing the different attitude towards uncertainty and ambiguity. The results show a trade-off between the uncertainties on mitigation costs and on the economic impacts from climate change.

**Keywords:** uncertainty, mitigation, economic impacts, decision making frame-work

## 1. INTRODUCTION

The assessment and the selection of climate policies is hampered by uncertainties. Indeed, while many efforts have been carried out in recent years, there is still an incomplete understanding of climate change in many aspects. These uncertainties have to be taken into account during the evaluation process, they have to be quantified and reported. And, in case of incomplete information which prevents a consensus on the quantification, the decision maker must also be informed as mentioned in the IPCC's recommendations on uncertainties [13]. It is also important to provide for decision support in this context of uncertainty and ambiguity.

Heal and Millner [8] classify the uncertainties in two major categories: the scientific uncertainty and the socio-economic uncertainty. On the one hand, some phenomena are known to be highly uncertain (e.g. long-term climate sensitivity or the aerosol radiative forcing) and, while parameters describing the internal climate variability may be less uncertain in the future, the improvement in the understanding of the climate system is creating new research questions and may raise the overall climate uncertainty [7]. Additionally, many climate models coexist which are based on different modeling assumptions and geophysical process descriptions. Inter-model comparison projects, such as the fifth phase of the Coupled Model Intercomparison Project (CMIP), aim at capturing this variability and provide range of climate outcomes [19]. On the other hand, the socio-economic uncertainties are linked to human development, on future human decisions and on the interaction human-nature. Recently, the integrated assessment community put some efforts to provide range of socio-economic outcomes from their integrated assessment models (IAM).

The standard approach to select the best policy action is the expected utility framework [22], enhanced by [17]. This framework requires that the decision maker is rational and has a complete knowledge of the uncertainty, so he can rank possible futures and choose the one which provides him the maximum expected utility. However, this knowledge of uncertainty can be ambiguous and other decision frameworks have to be considered [11]. Thus, selection rules of optimal policies can be based on probabilities or degrees of belief, on the existence of multiple priors or can be based on non-probabilistic criteria [8].

In this paper, we use best available knowledge to account for uncertainties affecting future climate change, its economic impact on societies and the cost of mitigating climate change. We then select robust climate policies by means of a set of selection rules that reflect the attitude of the decision maker facing uncertainty. The paper is organized as follows. Section 2 presents the adopted methodology to perform the policy

assessment. Section 3 presents the selection rules and the results. We conclude with Section 4 with a discussion on the approach and on the forthcoming studies.

## 2. METHODOLOGY

[Figure 1 about here.]

The integrated assessment is decomposed in three components: the socio-economic scenarios, the climate system and the global economic impacts. We use the best available knowledge to account for uncertainties in each of this component. First, Emissions profiles and mitigation costs are coming from inter modeling comparisons projects, from the IAMC dataset. A climate model, SNEASY [21], is producing probabilistic temperature projections, calibrated on the CMIP5 outcomes. Three probabilistic damage prior functions, fitted with estimates from literature, compute the economic impact of climate change. These costs are aggregated in a discounted utility function and a set of policy selection rules are applied (see Figure 1).

A policy action is characterized by a carbon budget, defined as the cumulative CO<sub>2</sub> emissions over the 21st century. Meinshausen et al. [12] established a robust relation between these emissions and the temperature increase. In this context, the carbon budget can be used as a policy decision determining the foreseen warming occurring during the next decades. The decision is taken now ( $t = t_0$ ) and there is no resolution of the uncertainty over time. This last assertion can be supported by the fact that between the third and the fifth CMIP, the spread in climate outcomes didn't diminish [10]

We denote the carbon budget  $c \in \mathbf{R}^+$  and the states of the world  $s$ . The prior on damage function is denoted  $p$ . The net present welfare is computed as

$$W_t(c; s, p) = \sum_{j \geq 0} \beta^{j-t} Y_{t+j}(c; s, p) \quad (1)$$

where  $\beta$  is the discount factor and

$$Y_t(c; s, p) = \tilde{Y}_t \times M_t(c; s) \times I_t(c; s, p). \quad (2)$$

$M_t(c; s)$  are the mitigation costs and  $I_t(c; s, p)$  are the economic impacts from climate change, expressed in % GWP change.  $\tilde{Y}$  is a reference GWP trajectory.

To introduce the risk aversion, we use a recursive utility function [4] is expressed as

$$V_t(c; p) = [(1 - \beta) Y_t^{1-\rho}(c)] + \beta \left( \mathbf{E}_s V_{t+1}^{1-\alpha}(c; p) \right)^{\frac{1-\rho}{1-\alpha}} \frac{1}{1-\rho}, \quad (3)$$

where  $\alpha$  is the relative risk aversion and  $\rho$ , the inverse of the intertemporal elasticity of substitution.  $\mathbf{E}_s$  is the expectation operator, which allows us to compute a certainty equivalent across all states of the world.

**Mitigation costs** The mitigation cost estimates come from a set of IAMs which have participated to inter model comparison projects. Using a common protocol describing the policy scenarios to be run, the models provided the same outputs in order to ease the comparisons. We use the outcomes from 5 modeling comparison projects: EMF-22, EMF-27, AMPERE, LIMITS and ROSE, and 289 different scenarios are considered. 10 models are considered: GCAM, GRAPE, IMAGE, MERGE, MESSAGE, MiniCAM, REMIND, SGM, TIAM and WITCH. Only long-term model, with a time horizon up to or beyond 2100, have been retained. The selected models show different characteristics. Some have a bottom-up approach, while others have a top-down approach. They have different representations in space (numbers of regions), in time (period length) or in type of usage (optimization or simulation mode). Such a heterogeneity makes the comparison of mitigation costs difficult, but, given the large number of scenarios, the dataset allows us to obtain a large number of possible socio-economic futures.

In the top-down models, the mitigation costs is provided in terms of percentage of gross world product, so the values are taken directly. In the bottom-up model, the mitigation costs are available either as additional energy sector cost or as the area located to the marginal abatement curve. These values are absolute and are translated in percentage change in comparison with the baseline scenario. In the case of additional energy sector cost, the mitigation cost is underestimated, as the others sectors costs are ignored, but the energy sector remains the most costly sector.

**CMIP5 emulation** To compute the climate response to climate policies, we use the climate model of reduced complexity SNEASY, which is composed of a climate module, a carbon cycle model including feedbacks from the atmospheric CO<sub>2</sub> concentration and temperature, and an Atlantic meridional overturning circulation box model [21]. In this study, we don't consider tipping points, thus the slowdowns of the Atlantic meridional overturning circulation are not explored, while it is featured in the model. SNEASY is enough fast to perform data assimilation and to run in probabilistic mode. To emulate the CMIP5 temperature projections, the model parameters are estimated using a Bayesian inversion technique based on the Markov Chain Monte Carlo (MCMC) algorithm. This procedure has been similarly applied to an older version of the model and describe in [21]. However, in this case, the model was constrained with with past observations.

Other climate models have also been run in a similar framework: the "Bern model"[9], MAGICC [15], with a version including a probabilistic carbon-cycle [2] and the intermediate complexity model EMIC [18]. In all cases, they all use an observation-informed Bayesian approach to estimate the joint probability distribution of the parameters.

Precisely, in our climate model, the estimated climate parameters are the climate sensitivity, the vertical diffusivity of heat in the ocean and the aerosol scaling factor to the radiative forcing. The carbon-cycle estimated parameters are the carbon fertilization from living plants, the respiration sensitivity related to temperature and the thermocline carbon transfer rate in the ocean. Additionally, initial conditions of atmospheric temperature and CO<sub>2</sub> concentration are also estimated.

In the MCMC, 10'000 parameters' combinations out of 1 million are retained. Each column vector of the chain can be considered as a different state of the "climate" world. To produce probabilistic temperature projections, CO<sub>2</sub> emissions are taken from the dataset, together with the CH<sub>4</sub>, N<sub>2</sub>O emissions. The radiative forcing from the aerosols is taken from the RCP scenarios.

**Economic impacts of climate change** Tol [20] reviews from the literature 17 estimates of total economic effects of climate change. These estimates have been calculated using various methods, but they usually aggregate one by one the economic costs of individual global and local impacts. For each study, the study reports the mean estimates of the economic impact for a given increase of the global temperature. Five of them also include a measure of uncertainty under the form of standard deviation (normal distribution) or a confidence interval (skewed distribution). In the case of the skewed distributions, we estimate the parameters of displaced Gamma distribution that match the confidence interval and the mean. We adopt three priors of economic impact function, as there is no consensus on it. Let  $D_p$  are the economic impacts expressed in % of GWP,  $T$  is the temperature increase and  $\beta_j$  are the regression coefficients.

1. A *quadratic* impact function  $D_1 = \beta_1 T + \beta_2 T^2$ , as proposed by Tol [20] and has been used in the DICE integrated model Nordhaus and Boyer [14]. This function allows for benefits at low temperatures.
2. A *exponential* impact function  $D_2 = \exp(-\beta_3 T^2) - 1$ , as introduced by Weitzman [24], without the possibility of benefits and with greater losses at high warming.
3. A *catastrophic* impact function  $D_3 = \beta_4 T^2 + \beta_5 T^6$ , adapted from Weitzman [25], which highlights catastrophic outcomes at extreme temperatures.

[Figure 2 about here.]

We compute the distribution of the regression coefficients of the quadratic damage function, by performing Monte Carlo quantile regressions. In Figure 2 (a,b and c), we present the probabilistic economic *quadratic*, *exponential* and *catastrophic* impact function as a function of the global warming. The range of uncertainty become larger

for high warming, mainly because the impact estimates from the studies are given for temperature increase from 1°C to 5°C.

The economic impacts  $I_t(c; s, p)$  are evaluated for each model-scenario combination and for each state of the world, which is also a combination of the climate states, as described in the last section, of the location within the probabilistic impact function (quantile). And, the impacts are also computed for the three prior functions.

**Policy selection** We apply several decision making frameworks in order to select the best climate policies according to their respective formulation (Table 1).

[Table 1 about here.]

First, we use a set of rules based on the standard expected utility framework. Here, the knowledge of the decision maker is represented as subjective probability distribution of the states of the world. We apply the *subjective expected utility* framework [17]. In this framework, the prior impact functions are equally reputable — no ambiguity is considered. Then, we consider the *maxmin expected utility* framework [6] which introduces the notion of multiple priors and full ambiguity aversion. The expected utilities of each prior is computed and, only the minimum of them is used for the assessment. We also apply the  $\alpha$ -*maxmin expected utility* criterion [5] which is an extension of the precedent rule, introducing uncertainty aversion. Within this rule, the lowest expected damage from climate change (maxmax) is retain for each policy strategy as opposed to the highest expected damage (maxmin), amongst the priors. These three rules can be visualize in Figure 3. Practically, the mean temperature projections are translated into economic impacts for each model/scenario co and for each priors, and the mitigation cost is added. The resulting expected utilities are transformed as expected losses to be minimized.

[Figure 3 about here.]

We also consider non-probabilistic approaches. First, the *maxmin* framework [23] is looking for the best amongst the set of worst-case outcome of each policy action. Secondly, the  $\alpha$ -*maxmin* criterion from Arrow and Hurwicz [1] is also considered. Finally, we apply the *minimax* regret criterion [16] which minimizes the max regret corresponding to the difference between the worst and the best outcome of each policy. Practically, we approximate the maximum by the 99th percentile and the minimum by the 1st percentile, as a strict application of the criteria would imply the use of infinite values.

### 3. RESULTS

**Utility values distribution** There is a trade-off between mitigation costs and economic impacts (see Figure 4). Low carbon budget policies have benefits or no impacts from climate change but may suffer high mitigation costs. At the opposite, high carbon budget policies have very low mitigation costs but the risk of very high damage is not negligible, as the probability distribution of the damage costs has a very long tail. In consequence, there is a range of carbon budget, located in the middle, where the distribution spread of the utility values is smaller. This

An important issue is the value of the discount rate  $r$  which reflects the attitude towards time preference, we then vary the value of  $r = \{2\%, 3\%, 4\%, 5\%\}$ . Very low discount rates see damage costs higher than mitigation costs, while increasing the value of the discount rate reverses this relation. When the discount rate is enough high ( $\geq 5\%$ ). The damage costs become negligible in comparison with the mitigation costs. Looking at the shape of the tail of the distribution of the utility values gives an insight of the risk of high costs. The tail is much longer for utilities with high damages than for high mitigation costs. This means that the risk of high costs is driven by the damage costs.

[Figure 4 about here.]

**Selection of policies** Using the integrated assessment framework presented in the last section, we select the best policy according to the set of rules of Table 1. As the number of models/scenarios of the dataset is limited to 289, there is hardly a continuity in the outcomes. We then have to apply the rules over ranges of carbon budgets. Many definitions of range have been tested, based on the interval size or on the number of observations, and they lead to the same conclusions presented later, but the smaller are the ranges the more artifacts appears due to the discontinuities. In Table SPM.3 of the fifth assessment report of the IPCC, the 4 RCPs are associated with compatible ranges of cumulative CO<sub>2</sub> emissions. These ranges have a similar size of about 1500 GtCO<sub>2</sub>. From this table, we distinct five carbon budget intervals: [500,1500), [1500,3000), [3000,4500), [4500,6000) and [6000,7500).

Figure 5 show the relation between cumulative CO<sub>2</sub> emissions and probability to stay below 2°C, 3°C and 4°C of warming. Retained carbon budget ranges are represented over the x-axis. No scenario has a probability higher than 75% to stay below 2°C., while the budget lower than 4500 GtCO<sub>2</sub> are likely to stay below a temperature increase of 4°C. The spread of the different is quite large because the non-CO<sub>2</sub> greenhouses gases have different trajectories depending on the scenarios. A more direct

relation can be established between these probabilities and the Kyoto greenhouse gases budget.

[Figure 5 about here.]

The selected ranges of carbon budget per rule and discount rate are reported in Table 2. The first observation is related to the discount rate. The size of the selected carbon budget remains the same or is increasing with the value of the discount rate. Indeed, when the discount rate is increasing, the importance of the damage costs is decreasing. Secondly, Expected utility-based rule carbon budgets are higher than the non probabilistic rules, which is consistent as the latter grant more precautionary.

Concerning the EU-based rules, varying the attitude towards uncertainty and ambiguity does not modify the solutions. When using smaller carbon budget ranges, we observe that the carbon budgets tend to be smaller with the level of ambiguity. But, in these tests, the differences between the carbon budgets (*EU* and *maxmin EU*) are lower than 500 GtCO<sub>2</sub>, and thus not visible with the retained intervals.

The results with the non-probabilistic rules give the lowest carbon budget for the *maxmin* criteria and 2% of discount rate. The *maxmax* criteria (when  $\alpha=1$  in the  $\alpha$ -maxmin rule) does not depend on discount rate and a low carbon budget is selected. This is due to the *quadratic* function which gives benefits on the economy for low warming. So surprisingly, in the case, the discount rate is 5% *maxmax* budget is lower than the *maxmin* budget.

[Table 2 about here.]

#### 4. CONCLUSIONS

We build up a integrated framework based on datasets of outcomes coming from many climate models and integrated assessment models. This integrated assessment is able to represent uncertainty when it is possible to quantify it. A number of decision rules has been applied to the resulting outcomes. There is a trade-off between the range of potential mitigation costs and the scientific uncertainty strongly linked to the impacts of climate change. This new approach informs the decision makers on the level of uncertainty they are facing but also on the ambiguity related to the knowledge of this uncertainty.

More finer results would be possible with a larger number of IAMs' outcomes, or with outcomes produced in order to perform this type of analysis. Especially, very low carbon budgets have been well explored but simulations with medium carbon budgets

are less numerous. Current developments are carried out with the WITCH integrated assessment model [3] to systematically produce distribution of outcomes for the whole range of carbon budgets, but, of course, losing the advantage of a multi-model study as it is the case in this paper.

## 5. ACKNOWLEDGMENTS

The research leading to these results has received funding from the Italian Ministry of Education, University and Research and the Italian Ministry of Environment, Land and Sea under the GEMINA project. We thank K. Keller from the Pennsylvania State University for supplying the SNEASY code.

## 6. REFERENCES

- [1] K. Arrow and L. Hurwicz. An optimality criterion for decision-making under ignorance. In C. Carter and J. Ford, editors, *Uncertainty and Expectations in Economics*, pages 1–11. 1972.
- [2] Roger W. Bodman, Peter J. Rayner, and David J. Karoly. Uncertainty in temperature projections reduced using carbon cycle and climate observations. *Nature Climate Change*, advance online publication, May 2013. ISSN 1758-678X, 1758-6798.
- [3] V. Bosetti, C. Carraro, M. Galeotti, E. Massetti, and M. Tavoni. WITCH: A world induced technical change hybrid model. *The Energy Journal*, 2:13–38, 2006. Hybrid Modeling, Special Issue.
- [4] Larry G. Epstein and Stanley E. Zin. Substitution, risk aversion, and the temporal behavior of consumption and asset returns: A theoretical framework. *Econometrica*, 57(4):937, Jul 1989. ISSN 0012-9682.
- [5] Paolo Ghirardato, Fabio Maccheroni, and Massimo Marinacci. Differentiating ambiguity and ambiguity attitude. *Journal of Economic Theory*, 118:133–173, 2004.
- [6] I. Gilboa and D. Schmeidler. Maxmin expected utility with non-unique prior. *Journal of Economic Persp*, 18(2):141–153, 1989.

- [7] Alexis Hannart, Michael Ghil, Jean-Louis Dufresne, and Philippe Naveau. Disconcerting learning on climate sensitivity and the uncertain future of uncertainty. *Climatic Change*, 119(3–4):585–601, August 2013. ISSN 0165-0009, 1573-1480.
- [8] G. Heal and A. Millner. Uncertainty and decision in climate change economics. NBER Working Paper Series 18929, National Bureau of Economic Research, March 2013.
- [9] R. Knutti, T. F. Stocker, F. Joos, and G.-K. Plattner. Probabilistic climate change projections using neural networks. *Climate Dynamics*, 21(3-4):257–272, September 2003. ISSN 0930-7575, 1432-0894.
- [10] Reto Knutti and Jan Sedláček. Robustness and uncertainties in the new cmip5 climate model projections. *Nature Climate Change*, 3:369–373, 2013.
- [11] Howard Kunreuther, Geoffrey Heal, Myles Allen, Ottmar Edenhofer, Christopher B. Field, and Gary Yohe. Risk management and climate change. *Nature Climate Change*, 3(5):447–450, Mar 2013.
- [12] M. Meinshausen, N. Meinshausen, W. Hare, S. C. B. Raper, K. Frieler, R. Knutti, D. J. Frame, and M. R. Allen. Greenhouse-gas emission targets for limiting global warming to 2°. *Nature*, 458(7242):1158–1162, April 2009.
- [13] R.H. Moss and S.H. Schneider. *Guidance Papers on the Cross Cutting Issues of the Third Assessment Report of the IPCC*, chapter Uncertainties in the IPCC TAR: Recommendations to lead authors for more consistent assessment and reporting, pages 33–51. World Meteorological Organization, Geneva, 2000.
- [14] Nordhaus and Boyer. *Warming the World: economic MModel of Global Warming*. MIT Press, Cambridge, Mass., 2000.
- [15] Joeri Rogelj, David L. McCollum, Andy Reisinger, Malte Meinshausen, and Keywan Riahi. Probabilistic cost estimates for climate change mitigation. *Nature*, 493(7430):79–83, January 2013. ISSN 0028-0836, 1476-4687.
- [16] L. J. Savage. The theory of statistical decision. *Journal of the American Statistical Association*, 46(253):55–67, Mar 1951.
- [17] Leonard J. Savage. *The Foundations of Statistics*. Dover Publications, 1954. ISBN 0486623491.

- [18] Marco Steinacher, Fortunat Joos, and Thomas F. Stocker. Allowable carbon emissions lowered by multiple climate targets. *Nature*, 499:197–201, July 2013. ISSN 0028-0836, 1476-4687.
- [19] Karl E. Taylor, Ronald J. Stouffer, and Gerald A. Meehl. An overview of cmip5 and the experiment design. *Bulletin of the American Meteorological Society*, 93(4):485–498, Apr 2012.
- [20] Richard S.J. Tol. Targets for global climate policy: An overview. *Journal of Economic Dynamics and Control*, 37(5):911–928, May 2013.
- [21] N. M. Urban, , and K. Keller. Probabilistic hindcasts and projections of the coupled climate, carbon cycle and atlantic meridional overturning circulation system: a bayesian fusion of century-scale observations with a simple model. *Tellus A*, 62: 737–750, 2010.
- [22] J. von Neumann and O. Morgenstern. *Theory of Games and Economic Behavior*. (Commemorative Edition) Princeton University Press, 1944.
- [23] Abraham Wald. Statistical decision functions which minimize the maximum risk. *Annals of Mathematics*, 46(2):265–280, Apr 1945.
- [24] M. Weitzman. *Handbook of Environmental Accounting*, chapter Some Dynamic Economic Consequences of the Climate Sensitivity Inference Dilemma, pages 187–207. Edward Elgar, 2010.
- [25] Martin L. Weitzman. Targets as insurance against catastrophic climate damages. *Journal of Public Economic Theory*, 14(2):221–244, 2012.

## 7. IMAGES AND TABLES

Rule	Formulation
Subjective Expected Utility (EU)	$\max_{c \in \mathcal{C}} \mathbf{E}(U(c; s))$
Maxmin EU	$\max_{c \in \mathcal{C}} (\min_{\pi \in \Pi} \mathbf{E}(U(c; s)))$
$\alpha$ -maxmin EU	$\max_{c \in \mathcal{C}} (\alpha \min_{\pi \in \Pi} \mathbf{E}(U(c; s)) + (1 - \alpha) \max_{\pi \in \Pi} \mathbf{E}(U(c; s)))$
Maxmin	$\max_{c \in \mathcal{C}} (\min_{s \in \mathcal{S}} U(c; s))$
$\alpha$ -maxmin	$\max_{c \in \mathcal{C}} (\alpha \min_{s \in \mathcal{S}} U(c; s) + (1 - \alpha) \max_{s \in \mathcal{S}} U(c; s))$
Minimax regret	$\min_{c \in \mathcal{C}} (\max_{s \in \mathcal{S}} [(\max_{c' \in \mathcal{C}} U(c'; s)) - U(c; s)])$

Tab. 1 Selection rules

Decision rule	Discount rate			
	2%	3%	4%	5%
Expected Utility	3000–4500	3000–4500	4500–6000	4500–6000
Maxmin EU	3000–4500	3000–4500	4500–6000	4500–6000
Maxmax EU	3000–4500	3000–4500	4500–6000	4500–6000
Maxmin	500–1500	1500–3000	1500–3000	3000–4500
Maxmax	1500–3000	1500–3000	1500–3000	1500–3000
Minimax regret	500–1500	1500–3000	1500–3000	3000–4500

Tab. 2: Selected cumulative CO<sub>2</sub> emissions, in GtCO<sub>2</sub>, according to decision rules.

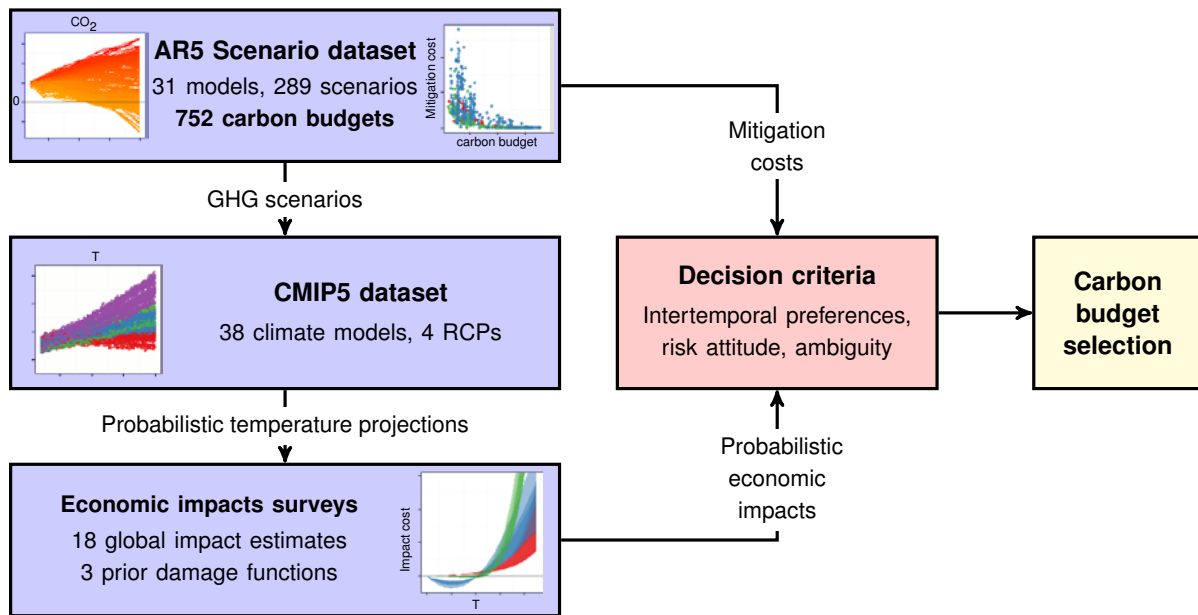


Fig. 1: Methodology

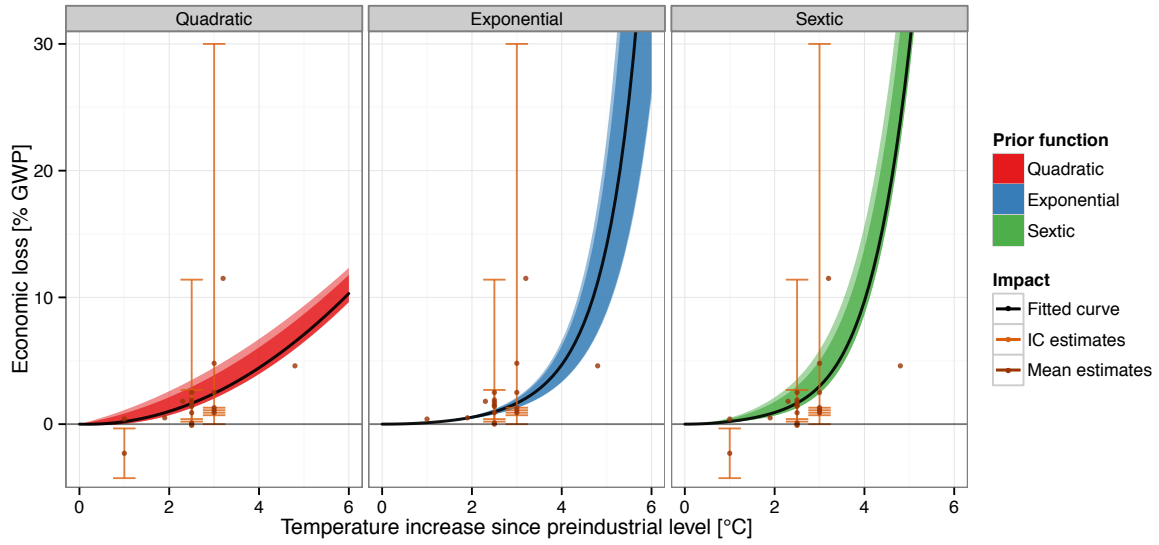


Fig. 2 Probabilistic impact function of temperature increase. Mean estimates from the survey. The black error bars represent the confidence intervals of the mean estimates.

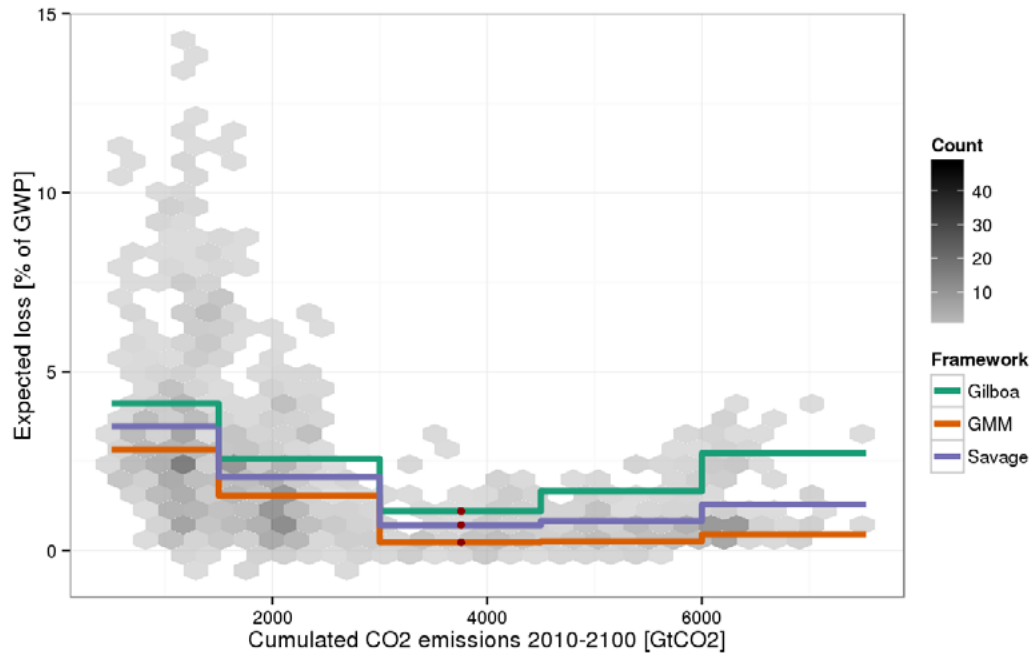


Fig. 3 Search paths and solutions for the 3 selection rules based on expected utility. Expected losses as a function of cumulative CO2 emission are binned. Discount rate=3%.

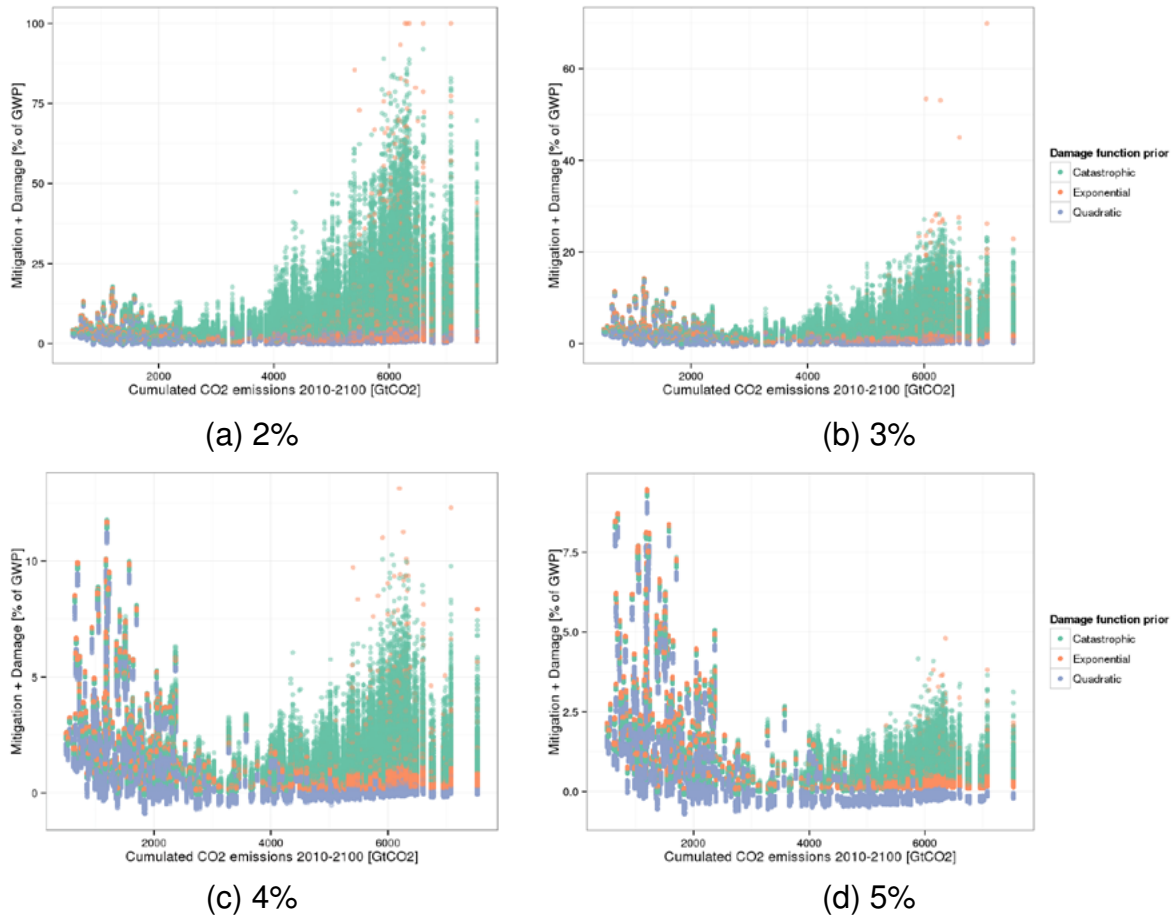


Fig. 4 Utility as a function of cumulative CO<sub>2</sub> emissions 2010–2100 per discount rate.

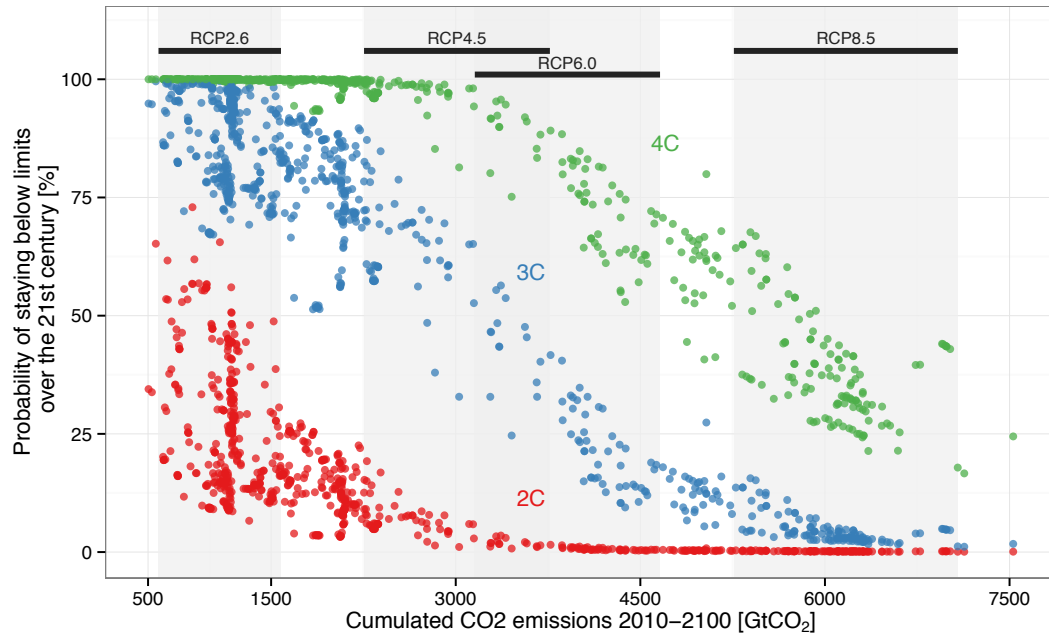


Fig. 5 Probability that the temperature increase from pre-industrial stays below 2°C, 3°C and 4°C over the 21st century as a function of cumulative CO<sub>2</sub> emissions during the period 2010-2020.

**Mitigation Policies & Strategies**

**Old and new market  
mechanisms**

# Impacts of Tradable Emission Allowances on Investment and Economic Growth

Huang Chung-Huang<sup>1\*</sup>, Lee Chien-Ming<sup>2</sup>, Su Han-Pang<sup>3</sup> and Yang Chin-Wen<sup>4</sup>

<sup>1</sup>Taiwan Research Institute - Taiwan, <sup>2</sup>National Taipei University - Taiwan,

<sup>3</sup>Taiwan Research Institute – Taiwan, and <sup>4</sup>Taiwan Research Institute – Taiwan

\* Corresponding Author: [chhuang@tri.org.tw](mailto:chhuang@tri.org.tw)

## Abstract

We develop a dynamic model to examine the firm's investment behavior under emission trading and evaluate the impact of the initial allocation of emission allowance on economic growth as well as on the firm's profit. With perfect foresight about the permit price, the firm's productive investment responds to interest rate in different manner from the abatement investment. Although the lenient initial allocation of permits is not favored by environmentalists, we shown that it plays important role not only in dictating the time path of permit price toward steady state, but also in generating incentives for the firm to invest more for pollution control. Given the lenient initial allocation, the initial permit price tends to be low but may increase over time toward steady-state equilibrium. Whether or not the firm will gain from lower permit price depends on its status as a demander or supplier in the permit market. The firm, however, always gains from more lenient initial allocation. The effect of the initial allowance on the economic growth rate is indeterminate, depending on the value of the coefficient of relative risk aversion.

**Keywords:** emission trading, economic growth, climate change, carbon price, abatement investment

## 1. INTRODUCTION

The role of emission trading as one of the policy instruments for global warming mitigation has attracted extensive attention worldwide, particularly after the Kyoto Meeting of 1997. Theoretically speaking, the tradable emission approach (TEA) is favored for several reasons. It is characterized, for example, by cost effectiveness (3, 11, 12, 16) and the advantages with mass control. It also could be exempt from critics against emission charge. More importantly, it creates less implementation obstacle than emission charge since, to all polluters, allocation of emission allowance sounds like a property giving while the charge like a financial burden.

There were extensive discussions in the literature trying to identify plausible sources that explain the low price of permit in the early stage. Among others, such factors as high transaction cost ([5, 14]), uncertainty over transaction benefits ([2, 4]), additional allowance in response to political pressure ([13]), stringent regional standards ([5, 6]), deregulation of energy industries ([5, 9]), and permit banking were considered relevant. Nevertheless, the phenomenon that permit price has been increasing since 1997 was not explained. The firm's expectation about the permit price was often ignored. Some interesting questions regarding the impacts of initial allocation on abatement investment and economic growth remain unexplored.

In this paper we develop a dynamic model with perfect foresight about permit price to examine the firm's investment behavior under emission trading. The comparative dynamics of permit price indicates that, given the lenient initial allocation, the initial price of permit tends to be low but may increase over time toward steady-state equilibrium. The model also reveals that the initial low price could be attributable to the increase in abatement investment induced by the lenient initial allocation. Such an allocation-induced investment hypothesis provides an economic rationale to justify the lenient initial allocation. The impact of the initial allocation of emission allowance on economic growth is also addressed.

The paper is organized as follow. An investment decision model under the emission trading system is formulated in Section 2. The comparative statics of production and abatement investments as well as the comparative dynamics of permit price toward steady-state equilibrium are analyzed in section 3. In section 4, the impact of initial allocation on economic growth is addressed on the basis of an

endogenous growth model that incorporates the firm's investment decisions. Section 5 concludes our paper.

## 2. THE INVESTMENT DECISION

The advantages of emission trading had been discussed extensively in the literature ([1, 14, 15]). Very few, however, tried to investigate the firm's investment decision under emission trading system. Kort (1996) [10] and Xepapadeas (1997) [17] pioneered the analysis of this subject. Although they established rigorous frameworks to elicit the firm's optimal investment decision rules under the assumption of perfect competition in permit market, neither the comparative dynamics of permit price was described nor the reasons contributing to the initial low price were provided.

We develop the model here for the following purposes: (1) To develop a dynamic model to describe the comparative dynamics of permit price that could possibly explain the price path in reality. (2) To verify our hypothesis that the initial low price of permit could be attributable to the increase in abatement investment induced by the lenient initial allocation. (3) To evaluate the impact of the initial allocation on economic growth, a subject so far not satisfactorily treated.

Let's consider a heterogeneous firm  $i$  that applies capital and labor at time  $t$  for production and receives an initial allowance equal to  $\bar{e}_i$  throughout the emission reduction planning horizon.<sup>1</sup> The underlying allowance path and reduction path are presented, respectively, by the curves  $ac$  in the upper panel of Figure 1 and  $AC$  in the lower panel, where the curves  $de$  and  $DE$  represent, respectively, the more likely allowance path and reduction path as in ARP. The emission is solely generated by productive capital ( $k_{pit}$ ) and could be removed by abatement capital ( $k_{ait}$ ). The actual emission discharge to the environment by firm  $i$  at time  $t$  is, therefore, defined as:

$$e_{it} = s_{it}(k_{pit}) - h_{it}(k_{ait}) \geq 0 \quad \forall t = 0, 1, 2, \dots, \quad (1)$$

where  $s' = \partial s_{it} / \partial k_{pit} > 0$  and  $h' = \partial h_{it} / \partial k_{ait} < 0$ .

Typically the firm is assumed to be price taker in the permit market. However, just as its production investment is sensitive to the expected output price, so is the firm sensitive to the expected price of permits when making abatement decision. The

---

<sup>1</sup> This assumption simplifies our analysis to a great extent without loss of generosity. It could be relaxed so that the allowance decreases over time as the curve  $de$  in the upper panel. As it will be shown later, this will not reverse our major hypothesis.

price-taker assumption, therefore, should not deprive the firm of its expectations about future prices. Here we assume that the firm has perfect foresight about the rate of change of the permit price (denoted by  $\dot{P}_t^T$ ) such that:

$$\dot{P}_t^T = \theta \cdot g(ED), \quad (2)$$

where  $\theta > 0$  is the adjustment coefficient;  $g(\cdot)$  is a function of the market excess demand of permits, denoted by  $ED \equiv \sum_{i=1}^n (e_{it} - \bar{e}_i)$ , with the following properties:  $g' > 0$ , and  $g'' < 0$ . A graphical representation of equation (2) is illustrated by Figure 2, where the permit price increases at a decreasing rate with excess demand and the curve tilts as the parameter  $\theta$  changes. In steady state,  $\dot{P}_t = 0 \forall t$ .

Following Xepapadeas (1997)[16], we assume that the firm chooses its optimal production investment ( $I_{pit}$ ) and abatement investment ( $I_{ait}$ ) to maximize the net present value of profit under the emission trading system, in which the firm could sale or purchase permits in the permit market at a price  $P^T$ . Thus, the firm is to solve the following problems:

$$\begin{aligned} \{I_p, I_a, I_p\} \quad \text{Max} \quad PV_t &= \int_0^{\infty} e^{-rt} \pi_{it} dt \\ \text{S.T.} \quad \pi_{it} &= B_{it}(k_{pit}, l_{pit}) - \sum_j [w_p l_{pit} + v_j I_{jit} + A_{ji}(I_{jit}) + P^T \cdot (e_{it} - \bar{e}_i)], \end{aligned} \quad (3)$$

Equations (1) and (2),

$$\dot{k}_{jit} = I_{jit} - \delta_{ji} k_{jit}, j = p, a \quad (4)$$

$$I_{jit} \geq 0 \quad \forall j = p, a \quad (5)$$

$\bar{e}_i, e_{i0}, k_{ji0}$ , and  $I_{ji0}$  are given.

$B_{it}(k_{pit}, l_{pit})$  in equation (3) is the production revenue of the firm  $i$  at time  $t$ , as a strictly concave function of the productive capital stock ( $k_p$ ) and labor ( $l_p$ ) with market price  $v_p$  and  $w_p$ , respectively.  $A_j$  ( $j = p, a$ ) is the adjustment cost of capital stocks with the following properties:  $A_j(0) = 0$ ,  $A_j'(I_j) > 0$ , and  $A_j''(I_j) \geq 0$ . The firm is said to be a buyer (seller) in the permit market if  $e_{it} - \bar{e}_i > 0$  ( $< 0$ ). Equation (4) represents the capital accumulation of production and abatement with depreciation rate  $\delta$ . Equation (5) implies that all types of investments are irreversible.<sup>2</sup>

<sup>2</sup> Our model here differs from Xepapadeas's in two ways. First, the charge base is different. The charge base defined by Xepapadeas is the rate of change in emission,  $\dot{e}_{it}$ , since he assumes the permit is good for lifetime. This assumption is discarded here in

The Hamiltonian and Lagrangean equations of the above problem are given, respectively, as follow:

$$H_{it} = B(k_{pit}, l_{pit}) - w_p l_{pit} - \sum_j [v_j I_{jit} + A_{jit}(I_{jit})] - P^T \cdot [s(k_{pit}) - h(k_{ait}) - \bar{e}_i] \\ + \sum_j \phi_j \cdot (I_{jit} - \delta_j k_{jit}) + \mu \theta g(ED),$$

$$L_{it} = H_{it} + \sum_j \eta_j I_{jit} + \lambda \cdot (s(k_{pit}) - h(k_{ait})),$$

where  $\phi_j$  ( $j = p, a$ ) and  $\mu$  represents, respectively, the Hamiltonian multiplier of equations (2) and (4), while  $\eta_j$  and  $\lambda$  represents, respectively, the Lagrangean multiplier of equations (1) and (5).

The necessary conditions of the above maximization problem are as follow:<sup>3</sup>

$$\frac{\partial \mathcal{L}}{\partial w_p} = 0 \Rightarrow w_p = \frac{\partial B}{\partial l_p} \quad (6a)$$

$$\frac{\partial \mathcal{L}}{\partial I_p} = 0 \Rightarrow v_p + A'_p(I_p) = \phi_p + \eta_p \quad (6b)$$

$$\frac{\partial \mathcal{L}}{\partial I_a} = 0 \Rightarrow v_a + A'_a(I_a) = \phi_a + \eta_a \quad (6c)$$

$$\dot{\phi}_p = (r + \delta_p)\phi_p - \frac{\partial B}{\partial k_p} + (P^T - \mu \theta g' - \lambda)s' \quad (6d)$$

$$\dot{\phi}_a = (r + \delta_a)\phi_a - (P^T - \mu \theta g' - \lambda)h' \quad (6e)$$

$$\dot{\mu} = r\mu + (s(k_p) - h(k_a) - \bar{e}_i) \quad (6f)$$

$$\eta_j \geq 0, \quad \eta_j I_j = 0 \quad (j = p, a) \quad (6g)$$

$$\lambda \geq 0, \quad \lambda \cdot (s(k_{pit}) - h(k_{ait})) = 0 \quad (6h)$$

To investigate the conditions under that abatement investment will be made, we assume that the initial productive capital stock is positive (i.e.,  $k_{pi0} > 0$ ) and no abatement capital stock exists (i.e.,  $k_{ai0} = 0$ ). This implies emission is positive and, therefore,  $\lambda = 0$ . Differentiating equations (6b) and (6c) with respect to time, and then plugging in equations (6d) and (6e), one obtains equations (7a) and (7b):

$$A''_p \dot{I}_p = (r + \delta_p)\phi_p - \partial B / \partial k_p + (P^T - \mu \theta g')s' + \dot{\eta}_p \quad (7a)$$

$$A''_a \dot{I}_a = (r + \delta_a)\phi_a - (P^T - \mu \theta g')h' + \dot{\eta}_a \quad (7b)$$

light of RECLAIM. The optimal life span of the permit is a policy issue deserving further investigation. Second, the firm's expectations about permit price is not taken into account by Xepapadeas.

<sup>3</sup> For any feasible solution  $(\tilde{k}_p, \tilde{k}_a)$ , if the transversality condition

$\lim_{t \rightarrow \infty} e^{-rt} \phi_j (\tilde{k}_j - k_j) = 0$  holds  $\forall j (= p, a)$ , the following conditions are also sufficient.

Together with the steady-state equilibrium conditions (i.e.,  $\dot{I}_p = \dot{I}_a = \dot{k}_p = \dot{k}_a = \dot{P}^T = 0$ ) and equations (6b) and (6c), equations (7a) and (7b) can be expressed as following investment decision rules:

$$\partial B / \partial k_p = (r + \delta_p)[v_p + A'_p(I_p) - \eta_p] + (P^T - \mu\theta g')s'(k_p) + \dot{\eta}_p \quad (8a)$$

$$(r + \delta_a)[v_a + A'_a(I_a)] = (P^T - \mu\theta g')h'(k_a) + \eta_a \cdot (r + \delta_a) \quad (8b)$$

Equations (8a) and (8b) indicate that the effects of the firm's expectation about the permit price on its optimal investment are represented by such terms as  $\mu\theta g' \cdot s'(k_p)$  and  $\mu\theta g' \cdot h'(k_a)$ .

To get explicit solutions of investments, we assume, without loss of generality, that productive investment is positive (i.e.,  $I_{pit} > 0$ , implying  $\eta_p = \dot{\eta}_p = 0$ ) and adjustment cost functions are quadratic (i.e.,  $A_j = (c_j / 2)I_j^2 \forall j = a, p$ ). As such, the productive investment and abatement investment are given, respectively, by  $I_p^*$  and  $I_a^*$  as follow:

$$I_p^* = \frac{M}{c_p(r + \delta_p)} - \frac{v_p}{c_p} > 0, \quad (9a)$$

$$I_a^* = \frac{N}{c_a(r + \delta_a)} - \frac{v_a - \eta_a}{c_a} \geq 0, \quad (9b)$$

where  $M = (\partial B / \partial k_p) - (P^T - \mu\theta g')s' > 0$ ;  $N = (P^T - \mu\theta g')h'$ .

Equation (9) reveals that the firm might not make any abatement investment under certain circumstance. To derive the conditions for zero abatement investment, we need to prove Proposition 1.

**Proposition 1.** Equation (9b) implies  $\mu = g / rg'$ .

Given Proposition 1 and equation (9b), the conditions under that the firm will not make abatement investment is stated in Proposition 2.

**Proposition 2.**  $I_a^* = 0$  only if the growth rate of permit price follows  $G_p = r - \Omega$ ,

$$\text{where } \Omega = (v_a - \eta_a)(r + \delta_a)r / h'P^T > 0.$$

Proposition 2 implies that zero abatement investment requires that the growth rate of the permit price sufficiently lower than the rate of time preference. The set  $\{(G_p, r) \mid I_a^* = 0\}$  is depicted in Figure 3 as the shaded area. Notice that Figure 3

also reveals there exists a threshold of interest rate above that permit price will decrease and increase otherwise.

### 3. COMPARATIVE STATICS AND PERMIT PRICE

In this section, we report the comparative static analysis of the productive and abatement investments, as well as the comparative dynamics of the permit price.

#### *The productive and abatement investments*

The comparative statics of the productive and abatement investments can be derived by totally differentiating equations (9a) and (9b) and solving the simultaneous equations. As expected, the productive investment varies in opposite direction with such factors as rate of time preference ( $\gamma$ ), rate of capital depreciation ( $\delta_p$ ), unit price of investment ( $v_p$ ), and marginal adjustment cost ( $c_p$ ). Similar relationship holds for abatement investment with respect to  $\delta_a$ ,  $v_a$ , and  $c_a$ . In contrast, the effect of the time preference rate on the abatement investment is indeterminate since  $\gamma$  affects not only the interest cost of the investment but also the interest cost of the expenditure on permits. The sign of  $\partial I_a / \partial \gamma$  depends, therefore, on the difference between the two effects.

The effects of the initial allowance ( $\bar{e}$ ) on the firm's investments have the same sign, that, in turns, depends on whether the firms is a seller or a buyer in the permit market. Proposition 3 summarize their relationships.

**Proposition 3.** If the firm with perfect foresight is a seller in the permit market, its productive investment (abatement investment) will increase (decrease) with the initial allocation of emission allowance. The reverse prevails for a buyer in the permit market.

The reason why a seller's abatement investment varies oppositely with  $\bar{e}$  is because the more is the initial allocation, the more likely will be the initial permit price lower than the steady state equilibrium price. Given perfect foresight, the seller then expects the market price to increase over time, as it will be shown later. This would induce the firm to postpone its investment so as to reap the profits later by selling permits at higher price. Under the same circumstance, the buyer has the incentive to invest more on abatement in the hope of reducing its purchase in later periods at higher price.

Generally speaking, the firm with inadequate abatement technology is more likely to be a buyer in the permit market. The more lenient initial allocation of allowance may create incentives for the inefficient firm to invest more on pollution control. Incentive of this type was never recognized in the literature and provides an economic rationale for more lenient initial allocation as it was under ARP and RECLAIM.

Given the linkage between  $\dot{P}_t^T$  and  $\theta$ , the explanation of the sign of  $\partial I_a / \partial \theta$  is straightforward. The firm as a seller will expect the price to increase faster when  $\theta$  takes greater value, provided that the market price increases over time. Therefore, the firm will postpone its investment in the earlier stage. On the contrary, the buyer's abatement investment will increase with  $\theta$ .

Equations (9a) and (9b) also shed some light on the effects of permit price on the production and abatement investments. As expected, abatement investment increases with permit price, while the reverse is true for production investment. This is because higher permit price implies higher opportunity cost of production and emission.

### **Demand for emission**

In order to further investigate the emission in steady state (i.e.,  $e_{it}^*$ ), we assume, for simplicity, the emission function linear and the abatement technology concave; that is,  $s(k_p) = \alpha k_p$  and  $h(k_a) = \beta_0 k_a - (1/2)\beta_1 k_a^2$ . Using equations equilibrium investments (i.e., equations (9a) and (9b)), it can be shown that equilibrium capital stocks for production and abatement are, respectively, given by equations (10a) and (10b), and the equilibrium emission by equation (11):

$$k_p^* = \frac{\frac{\partial B}{\partial k_p} - \alpha(P^T - \mu\theta g') - (r + \delta_p)v_p}{\delta_p c_p (r + \delta_p)} \quad (10a)$$

$$k_a^* = \frac{\beta_0 (P^T - \mu\theta g') - (r + \delta_a)v_a}{c_a \delta_a (r + \delta_a) + \beta_1} \quad (10b)$$

$$e_{it}^* = \alpha \cdot \left[ \frac{\frac{\partial B}{\partial k_p} - \alpha(P^T - \mu\theta g') - (r + \delta_p)v_p}{c_p (r + \delta_p)} - \beta_0 \cdot \frac{\beta_0 \cdot (P^T - \mu\theta g') - (r + \delta_a)v_a}{\delta_p c_p (r + \delta_p) + \beta_1} \right] - \beta_1 \left[ \frac{\beta_0 \cdot (P^T - \mu\theta g') - (r + \delta_a)v_a}{c_a \delta_a (r + \delta_a) + \beta_1} \right]^2 \quad (11)$$

### Comparative dynamics of permit price

Given the rate of change of permit price,  $\dot{P}^T = \theta \cdot g(Z_t)$ , its Taylor expansion around the steady state equilibrium price,  $\tilde{P}^T$ , can be expressed as follows:

$$P^T(t) = \tilde{P}^T + (P^T(0) - \tilde{P}^T)e^{g'Z't}, \quad (12)$$

where  $P^T(0)$  is the initial permit price,  $Z_t = \sum_i^n (e_{it} - \bar{e}_i)$ , and  $Z' = \partial Z / \partial P^T$ .

Since  $e_{it} = s(k_{pit}) - h(k_{ait})$ , it can be shown that  $Z' < 0$ ,<sup>4</sup> implying that the dynamic stability condition of the permit price is satisfied. Accordingly, the time paths of the permit price are illustrated by Figure 4, indicating that the price may either increase or decrease over time toward steady state. The realized path depends on the initial permit price. The lenient initial allocation as it is under ARP and RECLAIM is likely to result in the increasing path that is quite consistent with actual price trend of ARP. The increasing velocity depends on various parameters such as  $\delta_p$ ,  $\delta_a$ ,  $c_p$ ,  $c_a$ ,  $\alpha$ , and  $\beta_0$ .

### Profit

The profit function of the firm is defined as follows:

$$\begin{aligned} \pi_{it}^*(P^T, \bar{e}) = \text{Max}_{\{I_j, I\}} & \int_0^\infty e^{-rt} [(B(k_{pit}^*, l_{pit}^*) - \sum_j (w_j l_{jt}^* + v_j I_{jt}^* + A_j(I_{jt}^*))) \\ & - P^T \cdot (e_{it} - \bar{e}_i)] dt \end{aligned} \quad (13)$$

By Envelope theorem, it can be shown that

$$\frac{\partial \pi_{it}^*}{\partial P^T} = - \int_0^\infty e^{-rt} \cdot (e_{it} - \bar{e}_i) dt \begin{cases} > 0 \\ < 0 \end{cases}, \text{ and} \quad (14a)$$

$$\frac{\partial \pi_{it}^*}{\partial \bar{e}} = \int_0^\infty e^{-rt} P^T dt > 0. \quad (14b)$$

Equation (14a) indicates that the impact direction of the permit price on the firm's profit depends on whether it is a seller or a buyer. As a buyer at time  $t$  (i.e.,  $e_{it} - \bar{e}_i > 0$ ), the firm's profit will decrease with permit price, and vice versa for a seller. In contrast, the firm's profit will increase with initial allowance. This partly explains the difference between emission trading and emission charge in gaining support from the regulated firms.

<sup>4</sup> Here we use the results from equations (10a) and (10b), i.e.,  $\partial k_p^* / \partial P^T = -\alpha / (c_p \delta_p \cdot (r + \delta_p)) < 0$ ,

$\partial k_a^* / \partial P^T = \beta_0 / c_a \delta_a \cdot (r + \delta_a) + \beta_1 > 0$ .

#### 4. IMPACT ON ECONOMIC GROWTH

The impact of initial allocation on economic growth did not receive adequate attention in the literature. A growth model is presented in this section that integrates the firm's investment decision in the previous section. To simplify the model, it is assumed that the growth rate of population is zero and the consumer, who is also the producer, is characterized by constant relative risk aversion. The social planning problem is formulated as follows:

$$\underset{\{C_t, \bar{E}_t\}}{\text{Max}} U = \int_{t=0}^{\infty} \exp(-\rho t) \left[ \frac{(C_t / \psi_t^\sigma)^{1-\sigma} - 1}{1-\sigma} \right] dt \quad (15)$$

$$\begin{aligned} \text{S.T.} \quad \sum_{i=1}^n \dot{k}_{pit} &= \sum_i \{ \pi_{it} + v_p I_{pit} + v_a I_{ait} + \sum_j T_{ji} (I_{jit}) + P^T \cdot (e_{it} - \bar{e}_i) - c_{it} \} \\ &\quad - I_a - \delta_p K_p = \sum_i A_i k_{pi} - C_t - I_a - \delta_p K_{pt} \end{aligned} \quad (16a)$$

$$\dot{P}_t = b_0 E_t - b_1 P_t, \quad b_0, b_1 > 0 \quad (16b)$$

$$E_t = \sum_i e_{it} = \sum_i (s(k_{pit}) - h(k_{ait})), \quad (16c)$$

$$E_t \equiv \sum_i e_{it} = \sum_i \bar{e}_i \equiv \bar{E}, \quad \forall t \quad (16d)$$

$$\psi_t = \psi(P_t), \quad (16e)$$

where the subscript  $t$  is depressed for convenience.  $\rho$  = the social rate of time preference;  $1/\sigma$  = the intertemporal elasticity of substitution. The production is assumed AK-type (i.e.,  $y_{it} = A_i k_{pit}$ ) and, therefore, the production revenue is given by  $B_{it} = A_i k_{pit}$  with normalized output price. The aggregate capital stock for production is denoted by  $K_{pt} \equiv \sum_i k_{pit}$ . The total flow and stock of emission are represented by  $E_t$  and  $P_t$ , respectively. Hence, equation (16b) represents the pollution accumulation in the environment. Equation (16d) assures that the total emission meet the emission target set by the authority. Equation (16e) represents the damage caused by the pollution stock such that  $\psi' > 0$ , that in turns reduces utility.

Let  $\lambda_1$  and  $\lambda_2$  be the Hamiltonian multipliers of equations (16a) and (16b). Solving the above problem, one gets the economic growth rate in steady state as follows (see Appendix A):<sup>5</sup>

$$g_C = [A - \delta_p - \rho - \varphi \cdot (1 - \sigma) g_\psi] / \sigma \quad (17)$$

Furthermore, it can be shown that the growth rate of the damage is given by (see Appendix B):

$$g_\psi \equiv \varepsilon_{\psi P} \cdot g_P = \varepsilon_{\psi P} \cdot \left\{ \frac{b_0 \bar{E}}{(b_0 \bar{E} / b_1) + [P_0 - (b_0 \bar{E} / b_1)] \cdot (1 - b_1)^t} - b_1 \right\}, \quad (18)$$

where  $\varepsilon_{\psi P} = (\partial \psi / \partial P) \cdot (P / \psi)$  represents the pollution elasticity of environmental damage.

Substituting equation (18) into equation (17), one gets the economic growth rate that links to the initial allocation:

$$g_C = \{A - \delta_p - \rho - \varphi \cdot (1 - \sigma) \cdot \varepsilon_{\psi P} \cdot (b_0 \bar{E} / b_1) + [P_0 - (b_0 \bar{E} / b_1)] \cdot (1 - b_1)^t - b_1\} / \sigma \quad (19)$$

Equation (19) allows us to examine the marginal effects of various parameters on economic growth rate with transitional dynamics. The comparative statics are reported in Table 3, where the sign of marginal effect of the parameters such as  $A$ ,  $\delta_p$ ,  $\rho$ ,  $\delta$ , and  $\sigma$  is consistent with what is expected in most endogenous growth models. What is of most concern here is that the effect of the initial allowance ( $\bar{E}$ ), identical in all periods in our model, on the growth rate. As shown by equation (20), the sign is indeterminate, depending on the value of the coefficient of relative risk aversion ( $\sigma$ ), and the size is decreasing over time even if the allowances identical throughout the planning horizon (see equation (21)). In other words, the impact of allowance cap on the growth rate may be more significant in the earlier phase than the later.

$$\frac{\partial g_C}{\partial \bar{E}} = \frac{-\theta(1 - \sigma)\varepsilon_{\psi P}}{\sigma} \cdot \frac{b_0 P_0 (1 - b_1)^t}{\Delta'} \begin{matrix} > 0 & \text{if } \sigma > 0 \\ < 0 & \text{if } \sigma < 0 \end{matrix} \quad (20)$$

where  $\Delta' = (b_0 \bar{E} / b_1) + [P_0 - (b_0 \bar{E} / b_1)](1 - b_1)^t > 0$ .

<sup>5</sup> The proof is available from the author.

$$\frac{\partial^2 g_C}{\partial E_t \partial t} = -\frac{\varphi \cdot (1 - \sigma) \varepsilon_{\psi P} t b_0^2 P_0 \cdot \bar{E} \cdot (1 - b_1)^{t-1}}{b_1 \sigma (\Delta')^2} \quad \text{if } \sigma \begin{matrix} < \\ > \end{matrix} 0 \quad (21)$$

## 5. CONCLUDING REMARKS

We develop a dynamic model to examine the firm's investment behavior under emission trading and evaluate the impact of the initial allocation of emission allowance on economic growth as well as on the firm's profit. With perfect foresight about the permit price, the firm's productive investment responds to interest rate in different manner from the abatement investment. Although the lenient initial allocation of permits is not favored by environmentalists, we shown that it plays important role not only in dictating the time path of permit price toward steady state, but also in generating incentives for the firm to invest more for pollution control. Given the lenient initial allocation, the initial permit price tends to be low but may increase over time toward steady-state equilibrium. Whether or not the firm will gain from lower permit price depends on its status as a demander or supplier in the permit market. The firm, however, always gains from more lenient initial allocation. The initial low price could be attributable to the increase in abatement investment induced by the lenient initial allocation. The effect of the initial allowance on the economic growth rate is indeterminate, depending on the value of the coefficient of relative risk aversion. The impact of allowance cap on the growth rate may be more significant in the earlier phase than the later.

## 6. ACKNOWLEDGMENTS

Financial support from the Ministry of Science and Technology in Taiwan is greatly appreciated. Constructive comments on earlier draft from Professor Chien-Ming Lee and C.K. Lee are also acknowledge.

## 7. REFERENCES

1. Baumol, W. J. and W.E. Oates (1988). *The Theory of Environmental Policy*. Cambridge University Press.
2. Bohi, D. and D. Burtraw (1992). "Utility Investment Behavior and the Emission Trading Market." *Resources and Energy* 14(1/2): 129-156.

3. Bohm, P. and B. Larsen (1994). "Fairness in a Tradable Permit Treaty for Carbon Emissions Reductions in Europe and the Former Soviet Union." *Environmental and Resource Economics* 4: 219-239.
4. Burtraw, D. (1996). "The  $SO_2$  Emissions Trading Program: Cost Saving without Allowance Trades." *Contemporary Economic Policy* 14(2): 177-95.
5. Coggins, J. S. and J. R. Swinton (1996). "The Price of Pollution – a Dual Approach to Valuing  $SO_2$  Allowances." *Journal of Environmental Economics and Management* 30(1): 133-160.
6. Conrad, K. and R. E. Kohn (1996). "The US Market for  $SO_2$  Permits: Policy Implications of the Low Price and Trading Volume." *Energy Policy* 24(12): 1051-1059.
7. Doucet, J. A. and T. Strauss (1994). "On the Bundling of Coal and Sulfur Dioxide Emissions Allowances." *Energy Policy* 22: 764-770.
8. Egteren H., and Weber M. (1996). "Marketable Permits, Market Power, and Cheating." *Journal of Environmental Economics and Management* 30: 161-173.
9. Ellerman, A. D., and J.P. Montero (1996). "Why Are Allowance Prices So Low? An Analysis of the  $SO_2$  Emissions Trading Program." Working Paper 96-001. MIT CEEPR.
10. Kort, P. M. (1996). "Pollution Control and the Dynamics of the Firm- the Effect of MarketBase Instruments on Optimal Firm Investment." *Optimal Control Application & Methods* 17(4): 267-279.
11. Maluge D. A. (1989). "Emission Credit Trading and the Incentive to Adopt New Pollution Abatement Technology." *Journal of Environmental Economics and Management* 16: 52-57.
12. Montgomery, W. D. (1972), "Markets in Licenses and Efficient Pollution Control Programs." *Journal of Economic Theory* 5: 395-418.
13. Rico, R. (1995). "The U.S. Allowance Trading System for Sulfur Dioxide: An Update on Market Experience." *Environmental and Resource Economics* 5(2): 115-129.
14. Stavins R. N. (1995). "Transaction Costs and Tradable Permits." *Journal of Environmental Economics and Management* 29: 133-148.
15. Tietenberg, T. (1998). "Tradable Permits and the Control of Air Pollution in the United States." Written for the 10<sup>th</sup> Anniversary Jubilee Edition of the ZEITSCHRIFT FÜR ANGEWANDTE UMWELTFORSCHUNG.
16. Tietenberg, T. (1995). "Tradable Permits for Pollution Control When Emission Location Matters: What Have We Learned?" *Environment and Resource Economics* 5(2): 95-113.
17. Xepapadeas, A. (1997). *Advanced Principles in Environmental Policy*, UK: Edward Elgar Publishing Ltd..

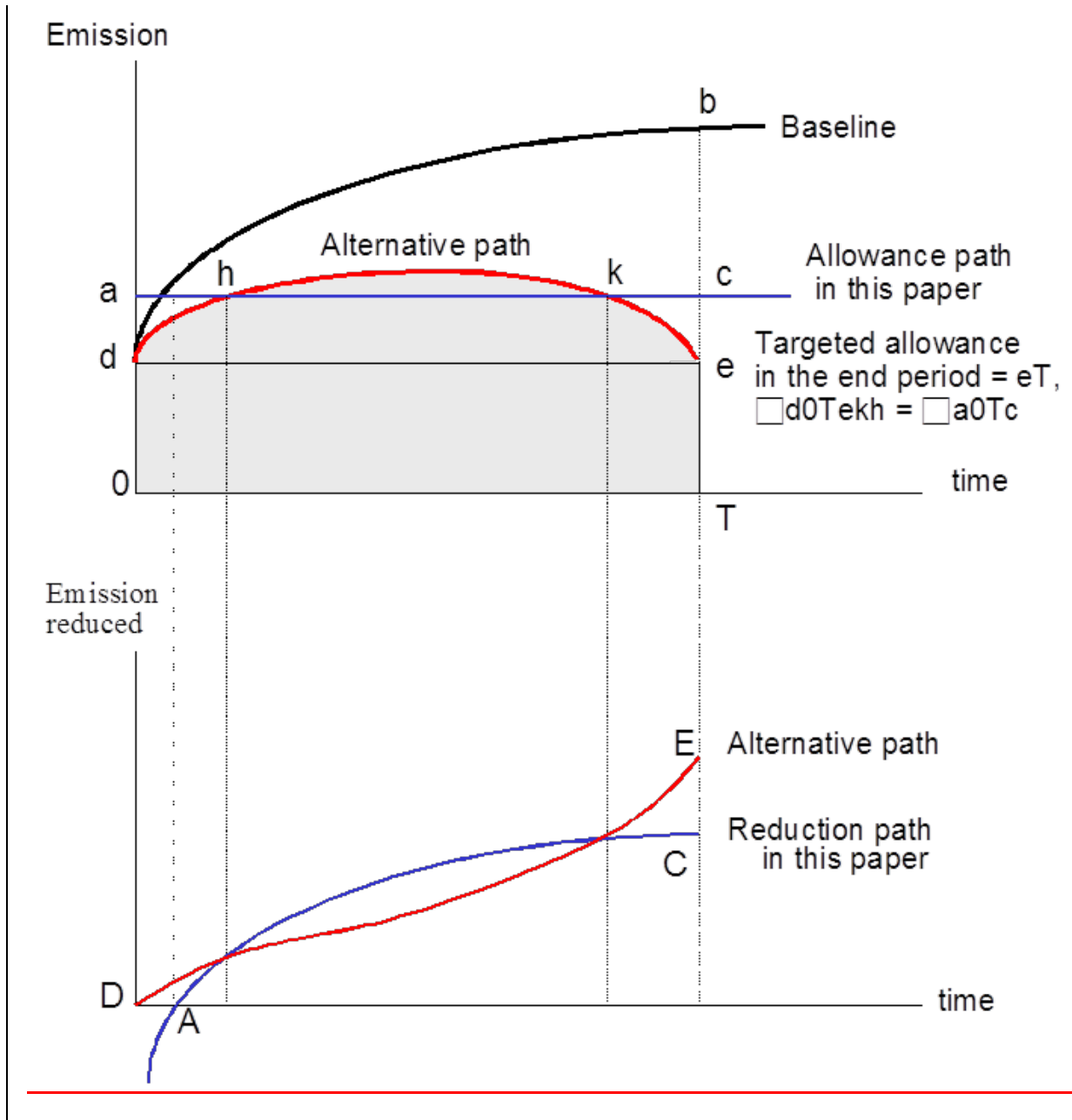


Fig. 1 Illustration of the allowance and reduction paths of emission

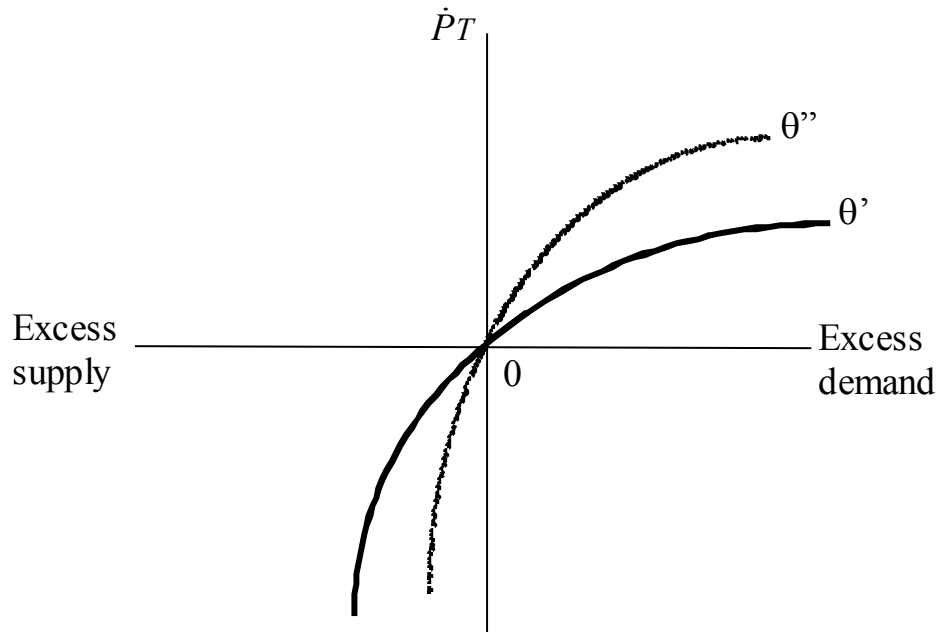


Fig. 2 Rate of change of permit price:  $\theta'' > \theta'$

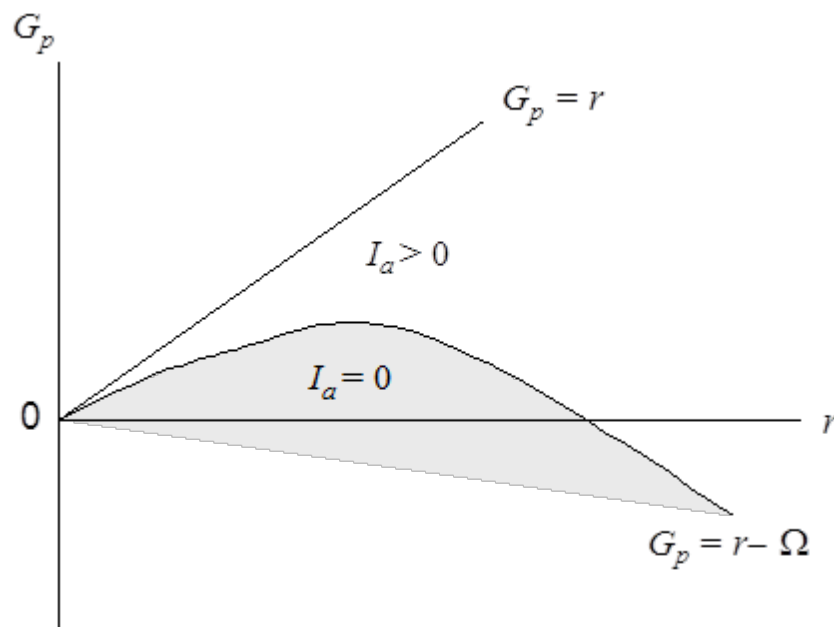


Fig. 3 The set  $\{(G_p, r) \mid I_a^* > 0\}$

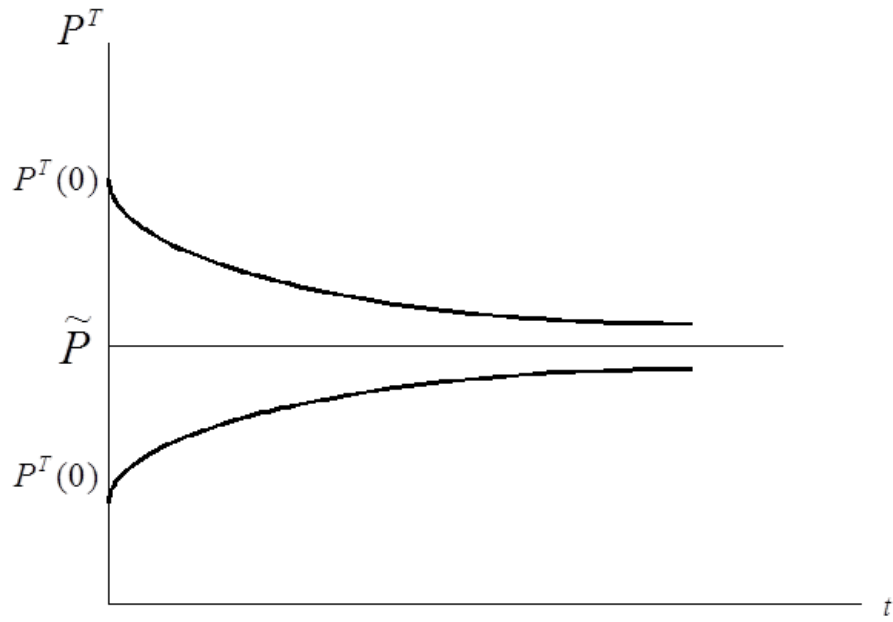


Fig. 4 Time path of the permit price toward steady state

# Climate Changes: liability and insurability of risks in various legislative and institutional settings in light of the latest scientific knowledge

Pozzo B.<sup>1</sup>

## Abstract

The article aims at providing a first inquiry on the various legal approaches that have been developed in order to cope with the peculiar problems connected with climate changes, that need a collaboration between scientists and lawyers in order to provide efficient tools. Whatever the background of the legal system foresees in this ambit, it appears clear that insurance will play a major role.

**Keywords:** climate changes, liability, insurability, interdisciplinary work

---

<sup>1</sup> Full Professor of Comparative Law – Department of Law, Economics and Culture, University of Insubria – Como; Coordinator Legal Researches Fondazione Lombardia per l’Ambiente – Seveso; Director Postgraduate Course in Environmental Law, University of Milan - Milan.

## 1. THE INTERNATIONAL SETTING

The Intergovernmental Panel on Climate Change has allowed to reach a very wide comprehension of the scientific dimension of climate changes, especially with its last 5<sup>th</sup> Report that provides a clear and up to date view of the current state of scientific knowledge relevant to climate change.

From a legal point of view, on the other side, climate changes have undergone a process of international regulation which has experienced its ups and downs.

From the 1992 United Nations Framework Convention on Climate Changes (UNFCC) to the Kyoto Protocol which came into force in February 2005, the alternating phases of the institutional debate have established an international binding legislative framework for action setting the objectives (mitigation and adaptation) and the tools (emissions trading, clean development mechanism, joint implementation) for facing the challenge of climate changes.

It should also be noted that, within the framework of the UNFCC and the principle of common but diversified responsibility, industrialised, newly industrialised and developing countries are all called upon to play an active role in climate protection.

After December the 8th, with the closing of the 18th Conference of the Parties (COP) held in Doha, Qatar, the complex structure taken on by international negotiations has become self evident.

The idea of a single binding international agreement which would have favoured the prorogation and extension of the Kyoto Protocol has been given up. After that, an attempt has been made to cope with the various problems arising out of climate changes on the different working tables but the outcome of these efforts is not easily assessed.

International negotiations have very likely become so complex because of the will to encourage the participation and involvement of all the industrialised and newly industrialised countries as much as possible.

After the COP held in Bali in 2007, it became evident that the United States were to be taken back to the negotiating table and newly industrialised countries were to be induced to make mitigation efforts worldwide, including with tools other than the

Kyoto Protocol under the auspices of the United Nations Framework Convention on Climate Changes.

However, countries found it hard not to carry on heading down the path set by the Kyoto Protocol, which was felt by most of the Parties concerned as a sort of *acquis* of the international legislation on climate changes.

In order to lead the United States back to higher participation, the parties decided to launch a second round of negotiations, always within the Framework Convention, by setting up a second working table, the so called *Ad Hoc Working Group on Long-term Cooperative Action under the Convention (AWG-LCA)*.

As set out in section 3.9 of the Kyoto Protocol, the AWG-LCA was supposed to prepare the first meeting of the parties to the Protocol held in Montreal in 2005, in parallel with the so called *Ad Hoc Working Group on Further Commitments for Annex I Parties under the Kyoto Protocol (AWG-KP)*, so as to identify the obligations of the Parties after 2012.

Hence, the complexity of the negotiations held in parallel, sometimes with different parties, which inevitably results in a lack of transparency of the outcome of the negotiations themselves.

## **2. THE DIFFERENT REGIONAL SETTINGS: REGULATION V. LITIGATION**

Independently from the availability of scientific data that are nowadays worldwide shared, such complexity has led to a very heterogeneous legislative framework in the various contexts<sup>2</sup>.

### **I. The European Union**

The European Union is playing an increasingly active role in pursuing an energy policy which is strictly connected with climate changes regulations both on a national and international level, where it is one of the most enthusiastic supporters of an international binding treaty.

---

<sup>2</sup> Blomquist, R. F., *Comparative Climate Change Torts*, 46 Val. U. L. Rev. 1053 (2012).

This has given rise to a number of concrete European initiatives in favour of power savings, renewable sources, emission reductions and green economy.

Therefore, the European Union is intensively regulating the sector.

If the EU is passing legislation aimed at mitigating the effects of climate changes, the Commission is pursuing a strategy of adaptation to climate change. Within this new framework, a key role will be played by the new standards of liability for the damages resulting from climate changes, including the possibility to take out a specific insurance policy.

## II. The United States

As is well known, the United States have never ratified the Kyoto Protocol nor do they intend to enter into any binding international treaty regarding climate changes.

United States have adopted a very different approach from the European one.

However, a number of actions aimed at facing climate changes have been taken in the country to make up for the gaps and defects of federal regulations.

**Industries have been the first to take action** with their “greener” styles and attitudes. Various groups of undertakings, including the Climate Group, an independent NGO, have taken a number of initiatives for a new Clean Revolution and a future based on low carbon.

In this respect, the idea is often to take measures aimed at a “voluntary, legally binding, rules-based greenhouse gas emission reduction and trading system<sup>3</sup>”.

**The second kind of action has been a local one.** In spite of the lack of specific federal regulations, local initiatives have been remarkable.

The first example is the Regional Greenhouse Gas Initiative (RGGI): in December 2005, the governors from seven states entered into an agreement on a system of *cap and trade* for carbon dioxide<sup>4</sup>. These States undertook to reduce their CO<sub>2</sub> emissions from electric plants by 10% by the end of 2018.

---

<sup>3</sup> Hunter D. and Salzman J., *Negligence In The Air: The Duty Of Care In Climate Change Litigation*, 155 U. Pa. L. Rev. 1741 (2007).

<sup>4</sup> The agreement has been entered into by 9 countries so far: Connecticut, Delaware, Maine, Maryland, Massachusetts, New Hampshire, New York, Rhode Island, and Vermont.

The Parties to this agreement auction off their emission credits and invest the proceeds for the benefit of consumers through energetic efficiency policies, renewable energy and other clean energy technologies.

Another interesting initiative has been taken by 22 States and the District of Columbia, who ask their municipal utilities to develop part of their electricity from renewable sources, while Washington and Oregon ask for a compensation for Greenhouse gases (GHG)

**The third and last kind of action** concerns the development of a “climate change litigation” movement which – as already underlined – may be not so much aimed at damage compensation but rather at “regulation through litigation<sup>5</sup>”.

Actually, climate change litigation concerns a series of proceedings started by different parties for very heterogeneous claims.

- I. The first group of cases concerned actions from various States against public authorities. In *Massachusetts et al., v. Environmental Protection Agency*<sup>6</sup>, for example, certain States sued the EPA under the Clean Air Act to order the agency to regulate carbon dioxide as a pollutant.
- II. The second group of cases is exemplified by the action started by some towns and environmental associations against the Overseas Private Investment Corporation (OPIC), the financial institution of the Government of the United States which promotes US private investments in newly industrialised countries, within the wider framework of US foreign policy promotion. The plaintiffs in this action claimed that the OPIC should start conducting environmental impact assessments regarding its investment procedures, taking into account any possible climate impact of the infrastructures financed by the OPIC itself.  
*Friends of the Earth, Inc. v. Watson*, No. C 02-4106 JSW, 2005 U.S. Dist. LEXIS 42335 (N.D. Cal. Aug. 23, 2005).
- III. The third group of cases is exemplified by the action brought by the representatives of the Inuit peoples against the United States before the Inter-American Commission on Human Rights.

---

<sup>5</sup> Hersch J. and Viscusi W., *Allocating Responsibility for the Failure of Global Warming Policies*, 155 U.Pa.L.Rev. 1657.

<sup>6</sup> Supreme Court, 2 April 2007.

Petition to the Inter-American Commission on Human Rights Seeking Relief from Violations Resulting from Global Warming Caused by Acts and Omissions of the United States.

- IV. However, there has been an increase in civil liability actions against private individuals for compensation of damages resulting from climate changes. These actions are hard to tackle because of the difficulties in establishing their clear causal connection, quantifying and distinguishing the damages resulting from anthropical events from those caused by natural events, identifying and attributing liability. The development of scientific knowledge will definitively help law experts with their theorization efforts<sup>7</sup>.

Tort litigation as developed so far in the United States shows, on the one hand, the nature of its possible claims and, on the other, the unquestionable difficulties of this kind of lawsuits.

In *Connecticut v. American Electric Power*, eight States and the city of New York brought an action against five important fuel manufacturers, allegedly the main responsible for CO<sub>2</sub> emissions in the United States. The lawsuit was based in the tort of public nuisance<sup>8</sup>, which can be defined as a behaviour which obstructs the exercise of rights common to all<sup>9</sup>. In the case at issue, the breach of the duty of care against defendants was described as follows: “*Defendants, by their emissions of carbon dioxide from the combustion of fossil fuels at electric generating facilities, are knowingly, intentionally or negligently creating, maintaining or contributing to a public nuisance - global warming - injurious to the plaintiffs and their citizens and residents*”.

The suit was never decided at first instance because the Court turned down the claim on the grounds that it was a “nonjusticiable political question”. The plaintiffs appealed.

In an ensuing lawsuit, *Korsinski v. United States EPA*, Mr Korsinski sued the Environmental Protection Agency for tort of public nuisance. The plaintiff’s claims,

---

<sup>7</sup> Grossmann D. A., *Warming Up To A Not-So-Radical Idea: Tort-Based Climate Change Litigation*, 28 Colum. J. Envtl. L. 1 (2003), p. 9: “Any climate change lawsuit will be inextricably linked to the science of global warming”

<sup>8</sup> See Prosser W.L., *Private Actions for Public Nuisance*, op.cit., p. 1001 ff.

<sup>9</sup> As concerns tort of public nuisance regulations, see Restatement Second of Torts (1977); Christie G.C. and Meeks J.E., *Cases and Materials on the Law of Torts*, St. Paul, Minnesota, 1990, p. 874.

which were mainly based on the same demands made in *Connecticut v. American Electric Power*, were turned down for inability to prove a specific injury.

In *Comer v. Murphy*, which went down in history as “the first climate change liability damages suit”, some citizens victims of hurricane Kathrina sued nine fuel manufacturers, thirty-one coal producers and four chemical companies on the basis of the following torts: tort of negligence, unjust enrichment, civil conspiracy, fraudulent misrepresentation, concealment and trespass. The Court turned down the claim both at first instance and appeal.

In *California v. General Motors Corp.*, the Attorney General of California started proceedings against General Motors and 5 other big car manufacturers for tort of public nuisance. According to the statistics shown during the trial, the emissions of the cars manufactured by the defendants account for 9% of CO<sub>2</sub> emissions worldwide. As specified by the Attorney General: “*by manufacturing products defendants knew would contribute to climate change, they have breached a duty not to unreasonably interfere with public welfare*”. In this case too, the Court turned down the claim both at first instance and appeal.

Independently from these efforts in order to create a regulation through litigation, American scholars<sup>10</sup> recognize by now the leading role that insurance will play in the American context. It has been - in fact - underlined that climate change will increase risks significantly in many areas of society, and will make many risks more uncertain and harder to measure. In order to face climate change without significant human costs, it is therefore necessary to develop robust institutions and practices to manage these risks. The insurance industry may play the role of society’s primary financial risk manager and needs to play a leading role in developing these institutions and practices.

The American market has already in the past developed instruments in order to cope with uncertain weather conditions. This is the case of so-called “Weather derivatives”, that are financial instruments that can be used by organizations or individuals as part of a risk management strategy to reduce risk associated with adverse or unexpected weather conditions.

---

<sup>10</sup> Hecht S.B. , *Climate Change And The Transformation Of Risk: Insurance Matters*, 55 UCLA LAW REVIEW 1559 (2008).

### III. China

For a few years now, China has adopted a new environmental and energy policy which is more aware of climate changes. After being introduced by Hu Jintao in his speech at the 2009 United Nations Summit on Climate Change, the policy was fully included in the Twelfth Five-Year Plan (2011-2015).

This policy has given rise to various regulatory and institutional initiatives by the Chinese government in favour of power savings, renewable resources, emission reductions and incentives for a green economy.

These massive regulation efforts also concern environmental litigation, which is undergoing extensive transformation with the setting up of a system of environmental courts within the country.

The process briefly outlined so far is also an expression of the increasingly active role played by China in the struggle against climate change worldwide: on the one hand, its regulatory efforts and institutional reforms are only made within the framework of international cooperation programmes, especially with the EU, which is becoming the first partner of the Chinese government in this respect. On the other hand, China itself is taking up a new active role as one of the countries which are identifying economic sustainability and free international transactions patterns.

Just consider the recent initiative taken by China in favour of a reading of the World Health Organisation (WHO) law as aimed at achieving a constantly sustainable development, i.e. one which is not based on an uncritical removal of barriers to trade, but rather capable of identifying and justifying measures that, though preventing the full liberalisation of international trade, are all the more necessary for protecting the health and the environment, and for preserving natural resources (see, in particular, the strategy defined by China in the proceedings WHO China - Raw Materials and China - Rare Earths).

### IV. India

The Indian Minister of Environment **Jairam Ramesh** has recently published a report titled "Climate Change Assessment for 2030", which contains the forecasts on

climate changes in India up to 2030. The research has been carried out by the *Indian National Confederation and Academy of Anthropologists* (INCAA) with the participation of over 220 scholars from 120 different institutions, including the *Indian Institute of Tropical Metereology (IITM)*. Moreover, in 2008 the *National Climate Change Action Plan* was launched and the Indian Government promoted a “Roadmap for low carbon development”, aimed at decarbonising the Indian industries<sup>11</sup>.

According to recent studies and analysis<sup>12</sup>, it appears that the potential impacts of climate change on insurance demand may be considered small relative to those of the baseline economic growth expected over the coming decade. The most significant impacts are expected in China and India. These countries have the greatest potential impacts across all of the pathways. Beyond 2030, the impacts of climate change and therefore, the implications for insurance demand, are expected to increase significantly<sup>13</sup>

---

<sup>11</sup> Chitre S. P., *India's Role In An International Legal Solution To The Global Climate Change Problem*, (April 4, 2011), Available at SSRN: <http://ssrn.com/abstract=1802862> or <http://dx.doi.org/10.2139/ssrn.1802862>.

<sup>12</sup> Parry M.L., Canziani O.F. et al. *Technical summary. Climate change 2007: impacts, adaptation and vulnerability. Contribution of working group II to the fourth assessment report of the intergovernmental panel on climate change* [ML Parry, OF Canziani, JP Palutikof, PJ van der Linden, CE Hanson, editors]. Cambridge, UK: Cambridge University Press; 2007; p. 23–78.

<sup>13</sup> Ranger N., Surminski S., *A preliminary assessment of the impact of climate change on non-life insurance demand in the BRICS economies*, International Journal of Disaster Risk Reduction Volume 3, March 2013, Pages 14–30.

# Community Managed Forest Groups and Preferences for REDD+ Contract Attributes: A choice experiment survey of communities in Nepal

Dissanayake S.T. M.<sup>1</sup>, Jha P.<sup>2</sup>, Adhikari B.<sup>3</sup>, Bista R.<sup>4</sup>, Bluffstone R.<sup>5</sup>, Luintel H.<sup>6</sup>, Martinsson P.<sup>7</sup>, Paudel N. S.<sup>8</sup>, Somanathan E.<sup>9</sup> and Toman M.<sup>10</sup>

<sup>1</sup>Colby College, and Portland State University-USA; <sup>2</sup>University of Venice Ca Foscari-Italy, IDRC-Canada; ForestAction-Nepal; Portland State University-USA; <sup>6</sup>Portland State University-USA; <sup>7</sup>University of Gothenburg-Sweden; <sup>8</sup>ForestAction-Nepal; <sup>9</sup>Indian Statistical Institute; <sup>10</sup>The World Bank

\*Corresponding Author: jprakash23@yahoo.com

## Abstract

A significant portion of the world's forests that are eligible for REDD+ payments are community managed forests. At the same time there is little knowledge in the existing literature about preferences of households in communities with community managed forests for REDD+ contracts and the opportunity costs of accepting REDD+ contracts for these communities. We use a choice experiment survey of rural communities in Nepal to understand respondent's preferences towards the institutional structure of REDD+ contracts. We split our sample across communities with community managed forests groups and those without to see how prior involvement in community managed forest groups impact preferences. Preliminary results show that respondents care about how the payments are divided between the households and the communities, the restrictions on firewood use, the restrictions on grazing and the level of payments. We analyze the preferences in more detail using specifications with attribute interactions terms and by including information about respondents' beliefs about REDD and community forestry. We find that the payment level and the values of the other attributes affect the respondents' preferences for each attribute. We also find that good governance and ensuring equitable access to CF resources increases the likelihood of respondents participating in the REDD+ program. We find that the preferences for REDD contracts are in general similar between CF and non-CF respondents, but there are differences particularly with regard to how beliefs influence the likelihood of accepting the contracts.

**Keywords:** REDD+, Community Forestry, Nepal, Choice Experiment, Interaction Terms

## 1. INTRODUCTION

The objective of the paper is to inform policy dialogue in the areas of REDD+(Reducing Emission from Deforestation and Forest Degradation) in the context of community forest management (CFM). REDD+ is a payment for ecosystem services (PES) system created under the United Nation's Framework Convention on Climate Change (UNFCCC) that tries to reduce deforestation and degradation in countries not subject to requirements under the convention (non-Annex 1 countries) and, therefore, release less and sequester more carbon. The '+' in REDD+ stands for other co-benefits that have been added to the original REDD program (that was focused solely on carbon) to address potentially negative, unintended effects on non-carbon ecosystem services and to take account of effects on those who currently have claims to forests.

REDD+ is important because the loss of forest biomass through deforestation and forest degradation accounts for 11–20 per cent of annual greenhouse gas emissions (Saatchi et al. 2011; van der Werf et al. 2009; UNEP 2012). Due to the increasing<sup>1</sup> trend of decentralization of forest management under community forest management, the success of REDD+ would depend on how CFM would be included in REDD+ program (World Bank 2009, Agrawal et al. 2008).

The effectiveness and decision to adopt REDD in CFM depends on incentives, benefit sharing arrangements, the opportunity costs of carbon sequestration, allocation of forest management decision making rights, and community interactions (McKinsey & Company, 2010; Gregorsen et al. 2011) but there is a lack of clear picture on the opportunity costs in case of the CFM. For example, some says REDD+ is a cheaper mitigation option (Angelsen 2008; McKinsey and Company 2010; Kindermann et al. 2008; Strassburg et al. 2009); while others find REDD+ as costly (Dyer and Counsel 2010; Gregorsen et al. 2011; Yesuf and Bluffstone 2009).

In this paper we use choice experiment (CE) survey in rural Nepali communities to understand people's preference toward the structure of REDD+ contracts and the opportunity costs they face. The reason for selecting Nepali Community Forests

---

<sup>1</sup> The forest decentralization is rapidly increasing over time and therefore the area of community forests roughly doubled to 250 million hectares during the period 1997–2008 (World Bank 2009).

(CFs) for the study is because of Nepal's long history of CFs, larger forest areas and population under CFs management.

CFs in Nepal are patches of national forest area handed over to the local user group for management, conservation and utilization according to the Forest Act 1993 and subsequent Forest Regulation 1995 (HMGN, 1993, HMGN, 1995). CF policy in Nepal emerged after an urgent need to stop forest degradation in Nepalese Himalays (Ives and Messerli, 1989) and failure of the government approach to protect forests (Kanel, 2004a). Until 2014 January there are 18133 forest user groups, managing 1.7 million hectares of forest area (DOF, 2014). Gradually CFUGs developed as an institution not only implementing forest management activities but also various community development activities (Kanel, 2004b).

Results show that respondents care about how REDD+ programs are structured with regard to the manner in which the payments are divided between the households and the communities, the restrictions on using grazing land, the restrictions on firewood collection and the level of payments received for the program. We find that respondents prefer that more of the REDD+ payments go to communities rather than households, which indicate trust in community level institutions. At the same time we find that that corruption and unequal access to CF resources decreases the likelihood of accepting the contracts.

We also find that preferences for REDD+ contract attributes depend on the levels of other attributes. One particularly interesting finding is that when REDD+ payment levels are high, the estimated additional REDD+ payment required to further tighten firewood collection restrictions or impose grazing closures is lower.

## **2. METHODOLOGY**

### **2.1 Choice Experiment Surveys**

We use choice experiment (CE) surveys for this study. CE surveys are based on Lancaster's (1966) consumer theory and are used to elicit preferences for environmental goods and policies (Boxall et al. 1996, Louviere et al. 2000). This was used because we are interested in understanding how different characteristics of the REDD+ contracts influence adoption of contracts. In a typical CE survey, the respondent repeatedly chooses the best bundle/choice from several hypothetical

bundles/choices. The attribute values appearing in each bundle/choice are identified using experimental design techniques to ensure a balanced representation of values across choices. Hanley et al. (2001), Hensher et al. (2005), and Hoyos (2010) provide reviews of the choice experiment methodology.

## 2.2 Survey Instruments

The survey for this particular study presents respondents with opportunities to express preferences over hypothetical REDD+ contracts. The attributes of costs and benefits and their levels, presented in Table 1, were selected through the focus group discussions in nine CFUGs and nine non-CFUGs. These CFUGs were purposively represented in Hill and Terai regions. In each region, these CFUGs were selected randomly from the random set of sites from a previous CF impact study (MFSC, 2013). The surveys given out to communities that do not have CFGs had four attributes; while communities with CFs do not contain grazing restriction attributes because they already have grazing restrictions in place. The exact list of attributes was refined after studying the REDD+ literature and analyzing results from focus groups in multiple communities.

Once an initial list of attributes was developed, we conducted focus groups with potential survey respondents. The final survey instrument contains background information about the REDD+ program, a description of the attributes and the levels, seven sets of binary choice question sets, and a small demographic questionnaire. These documents were pretested in the field before launching full implementation. For each of the choice sets the respondents choose between the two given alternatives and the status quo option.

## 2.3 Experimental Design

We follow standard practice in the choice modeling literature (Adamowicz et al. 1997, Adamowicz et al. 1998, Louviere et al. 2000) and create an efficient experiment design that will allow both main effects and interaction effects to be estimated. The designs for the choice experiments were generated following Kuhfeld (2010)<sup>2</sup> and achieve a 100% D-efficiency<sup>3</sup>.

---

<sup>2</sup>The experiment design was conducted using the SAS experiment design macro (Kuhfeld 2010).

<sup>3</sup>D-efficiency is the most common criterion for evaluating linear designs. D-efficiency minimizes the generalized variance of the parameter estimates given by  $D = \det [V(X, \beta)]/k$  where  $V(X, \beta)$  is the

## 2.4 Model and Estimation

We use a mixed multinomial logit model (MMNL)<sup>4</sup> that incorporates heterogeneity of preferences (Hensher and Greene 2003, Carlsson et al. 2003) as the respondents might not be homogenous. Assuming a linear utility, the utility gained by person  $q$  from alternative  $i$  in choice situation  $t$  is given by

$$U_{qit} = \alpha_{qi} + \beta_q X_{qit} + \varepsilon_{qit} \quad (1)$$

where  $X_{qit}$  is a vector of non-stochastic explanatory variables. The parameter  $\alpha_{qi}$  represents an intrinsic preference for the alternative (also called the alternative specific constant). Following standard practice for logit models we assume that  $\varepsilon_{qit}$  is independently and identically distributed extreme value type I. We assume the density of  $\beta_q$  is given by  $f(\beta/\Omega)$  where the true parameter of the distribution is given by  $\Omega$ . The conditional choice probability of alternative  $i$  for individual  $q$  in choice situation  $t$  is logit<sup>5</sup> and given by

$$L_q(\beta_q) = \prod_t \frac{\exp(\alpha_{qi} + \beta_q X_{qit})}{\sum_{j \in J} \exp(\alpha_{qj} + \beta_q X_{qjt})}. \quad (2)$$

The unconditional choice probability for individual  $q$  is given by

$$P_q(\Omega) = \int L_q(\beta) f(\beta | \Omega) d\beta. \quad (3)$$

The above form allows for the utility coefficients to vary among individuals while remaining constant among the choice situations for each individual (Hensher et al. 2005, Carlsson et al. 2003, Train 2003). There is no closed form for the above integral; therefore  $P_q$  needs to be simulated. The unconditional choice probability can be simulated by drawing  $R$  random drawings of  $\beta$ ,  $\beta_r$ , from  $f(\beta/\Omega)$ <sup>6</sup> and then averaging the results to get

---

variance-covariance matrix and  $k$  is the number of parameters. Huber and Zwerina (1996) identify four criteria (orthogonality, level balance, minimum overlap, and utility balance) which are required for a D-efficient experiment design.

<sup>4</sup>This approach is also referred to as the mixed logit, hybrid logit, random parameter logit, and random coefficient logit model.

<sup>5</sup>The remaining error term is IID extreme value.

<sup>6</sup>Typically  $f(\beta | \Omega)$  is assumed to be either normal or log-normal but it needs to be noted that the results are sensitive to the choice of the distribution.

$$\tilde{P}_q(\Omega) = \frac{1}{R} \sum_{r \in R} L_q(\beta_r). \quad (4)$$

In the choice experiment questions, option A and option B are both restoration options that can be viewed as being closer substitutes with each other than with option C, the status quo option (Haaijer, et al. 2001; Blaeij et al. 2007). One method to incorporate this difference in substitution between options is to use an econometric specification for the mixed multinomial logit model that contains an alternative specific constant (ASC) that differentiates between the status quo option and choices that represent deviations from the status quo. We do so by using a constant that is equal to one for alternative A or alternative B.

The coefficient estimates for the mixed multinomial logit model cannot be interpreted directly. Therefore, following the standard practice in the literature we calculate average marginal WTA for a change in each attribute by dividing the coefficient estimate for each attribute with the coefficient estimate for the payment term, as given in (5).

$$MWTA_i = \frac{\beta_i}{\beta_{cost}} \quad (5)$$

## 2.5 Econometric Specification

We present main effects (no interactions) specification and specifications with attribute interaction terms and regional interaction terms. The specifications are given in Equation 7 – Equation 8:

$$V_{ni} = \beta_{1n}ASC + \beta_{2n}X_{payment\_to\_community} + \beta_{3n}X_{duration} + \beta_{4n}X_{firewood} + \beta_{5n}X_{grazing} + \beta_{6n}X_{payment} + \varepsilon_{ni} \quad (6)$$

$$V_{ni} = (6) + \beta_{7n}X_{firewood} * X_{cost} + \beta_{8n}X_{grazing} * X_{cost} + \beta_{9n}X_{firewood} * X_{payment\_to\_community} + \beta_{8n}X_{grazing} * X_{payment\_to\_community} + \beta_{9n}X_{payment\_to\_community} * X_{cost} \quad (7)$$

$$V_{ni} = (6) + \beta_{sn}ASC * Z_s \quad (8)$$

where  $Z_s$  denotes the socio-demographic variables. The data was analyzed using the clogit and mixlogit commands in STATA for the Conditional Logit and MMNL specifications.

### 3. DATA

Data were collected from 1300 randomly selected households in both the hill areas and plains (Terai) in Nepal. Of the households 650 were from 65 communities that currently have CFGs and 650 were from 65 communities that currently do not have CFs. The location of the sites is shown in Figure 1. The sampling design for CFGs was adopted from the data set of the CF impact study (MFSC, 2013). For each CFG, the matching communities not having CFs were selected based on criteria such as the socioeconomic characteristics, forest types and accessibility.

#### 3.1 Household characteristics

A summary of the household characteristics is provided in Table 2 for both CF and non-CF households. On average the CF and non-CF households were very similar. For CF households, 81.2% of the respondents were male, 38.9% of the households were categorized as “poor” and 52% of the households were categorized as “medium” with regards to social status. For non-CF households 86.3% of the respondents were male, 37.5% of the households were categorized as “poor” and 51.4% of the households were categorized as “medium” with regards to social status. Both groups were similar in educational achievements; for CF households 21.6% was illiterate, 33.8% had only a primary education, and 17.3% didn’t finish secondary school and 11.4% finished secondary school. For non-CF households 20.4% was illiterate, 37.1% had only a primary education, and 16.2% didn’t finish secondary school and 11.4% finished secondary school.

### 4. RESULTS AND DISCUSSION

Given that the choice experiment surveys for the two respondent groups (CF and non-CF) have different attributes, we analyze the two groups separately and compare findings. We present four sets of results that correspond to specification (6) - (8). Tables 3 and 4 present results for the main effects specifications analyzed using a conditional logit model (column 1), the main effects specification analyzed using a MMNL model (column 2), the attribute interactions effects specification analyzed using a MMNL (column 3), and the beliefs and attitude interactions effects specification analyzed using a MMNL (column 4) for the non-CF and CF communities respectively. The significance of the standard deviation estimates for random

coefficients from the MMNL is indicated with a “SD” next to the standard errors. As can be seen many of the variables exhibit individual heterogeneity and therefore it is necessary to account for this in the analysis by using a MMNL model.

The overall results from the three specifications indicate that the percentage of the payment going to the community, the required firewood reduction, the required grazing reduction (for non-CF households) and the payment amount are all significant variables in determining the respondent s’ willingness to adopt REDD+ contracts. The significant coefficient results are robust across the econometric specifications and have expected signs. The significant results indicate the following:

1. As the required firewood reduction increases, respondents are less likely to choose that option;
2. For non-CF households as the required grazing reduction increases, respondents are less likely to choose that option;
3. As the percentage of the payment going to the community increases, respondents are more likely to choose that option;
4. As the payment values (amount) increases, respondents are more likely to choose that option

We find that for non-CF households (Table 3) the interaction terms among some variables are significant. This indicates that

5. The implicit opportunity cost of firewood reduction and grazing reduction is non-linear and is dependent on the payment amount.

Since this variable is positive it indicates that at higher payment levels the implicit opportunity cost is lower.

6. The preferences for the distribution of the payment between the households and the community are influenced by the required amount of firewood reduction.

Since this variable is negative it indicates that when the required firewood reduction is high, respondents are less likely to support a larger portion of the payment going to the community.

7. For CF households we find that the interaction term for the firewood reduction variable and the payment % to community variable is significant.

This indicates that as the payment level increases respondent would want more of the payment to go towards the households (as opposed to the community).

We finally analyze how the institutional arrangements, and beliefs about climate change and the benefits from the REDD program influence the REDD contract adoption decisions. For CF households to adopt REDD+ contracts we find that respondents that

- 8.a. believe they have equitable access to forest funds are willing accept smaller payments.
- 8.b. are migrants requires higher payments.
- 8.c. believe climate change is serious for Nepal require higher payments while respondents that believe climate change is serious for their community require smaller payments.
- 8.d. believe that the REDD program will benefit them personally require higher payments.
- 8.e. believe village authorities monitor forest use require higher payments.
- 8.f. believe that authorities support rule breakers require higher payments.

For non-CF households to adopt REDD+ contracts we find that respondents that

- 9.a. believe climate change is serious for Nepal require higher payments
- 9.b. believe rules of forest access are clear require smaller payments
- 9.c. believe village authorities monitor forest use require smaller payments
- 9.d. believe that authorities support rule breakers require higher payments.

We find that there are no significant differences in the payment amounts necessary to initiate REDD+ contracts between the CF and non-CF respondent groups but we find that respondent groups differ in their beliefs about REDD payments and the institutional arrangements. In general we find ensuring equitable access to forest resources, preventing corruption and ensuring proper monitoring of forest use can result in contracts being adopted for lower payments.

## 5. CONCLUSIONS AND POLICY IMPLICATIONS

In this paper we present results from a choice experiment survey conducted in Nepal in 2013 as part of a collaborative effort to analyze the preference for REDD+ contracts in Nepal. In both CF and non-CF communities we find, for example, that households prefer higher REDD+ payments and would rather not take on REDD+ obligations without adequate compensation. For example, CF and non-CF respondents generally are not likely to choose options with high levels of firewood reductions and low REDD+ payments. Non-CF households also have the option to reduce grazing in exchange for payments. We find that those respondents are less likely to choose options with grazing restrictions than options without such restrictions. Such results are consistent with individuals making choices that are in their own interests.

A key REDD+ policy question is how to divide up REDD+ payments. Should they go to the community? To households? Part to households and part to communities? We find that respondents prefer that more of the payments go to communities rather than to households. This result indicates a high degree of trust in forest user group communities, because pure self-interest would likely have suggested a preference for payments to go to households where they can be fully controlled. This result mirrors our focus group findings.

We also find that preferences for REDD+ contract attributes depend on the levels of other attributes. One particularly interesting finding is that when REDD+ payment levels are high, the estimated additional REDD+ payment required to further tighten firewood collection restrictions or impose grazing closures is lower. Preferences for payments to be made to communities rather than households are found to be influenced by the required level of reduction in firewood collection. For example, when the required firewood reduction is high, respondents are less likely to support a larger portion of payments going to their communities. This finding suggests that as REDD+ contract requirements become very stringent, respondents would like to be sure their households get direct benefits in exchange for those sacrifices. Similarly, for CF households, at higher REDD+ payment levels respondents prefer that more of their payments go to households rather than communities, perhaps reflecting concerns with community level management of large sums.

Besides payment levels good governance and equity are also important in REDD+ contracts. We find that people are willing to accept smaller payments if equitable access to forest resources, preventing corruption and ensuring proper monitoring of forest use are ensured. Overall our results show that there is a strong willingness to accept REDD+ contracts from community members of both CF and non-CF communities.

## 6. ACKNOWLEDGMENTS

Financial support for this work was provided by the World Bank. We would like to thank participants at the Economics Department Seminar Series at the University of New Hampshire for valuable feedback and suggestions on this work.

## 7. REFERENCES

1. Adamowicz, W., Boxall, P., Williams, M. and Louviere, J., 1998. *Stated preference approaches for measuring passive use values: choice experiments and contingent valuation*. *Am.J.Agric.Econ.* 80, 64-75.
2. Adamowicz, W., Swait, J., Boxall, P., Louviere, J. and Williams, M., 1997. *Perceptions versus objective measures of environmental quality in combined revealed and stated preference models of environmental valuation*. *J.Environ.Econ.Manage.* 32, 65-84.
3. Agrawal, A. Chhatre, A. and Hardin, R. 2008. *Changing Governance of the World's Forests*. *Science*, 320: 1460-1462.
4. Angelsen A (Ed). 2008. *Moving Ahead with REDD: Issues, Options and Implications*. CIFOR, Bogor, Indonesia.
5. Blaeij A, Nunes P and van den Bergh J (2007) *Modeling "no-choice" options in attribute nased valuation experiments: is one model is sufficient?*. *Appl Econ* 39:1245–1252
6. Boxall, P.C., Adamowicz, W.L., Swait, J., Williams, M. and Louviere, J., 1996. *A comparison of stated preference methods for environmental valuation*. *Ecol.Econ.* 18, 243-253.

7. Carlsson, F., Frykblom, P. and Liljenstolpe, C., 2003. *Valuing wetland attributes: an application of choice experiments*. *Ecol.Econ.* 47, 95-103.
8. DOF 2014. *CF database*. Babarmahal, Kathmandu: Community Forestry Division, Department of Forest.
9. Dyer, N. and Counsel, S.2010.McREDD: *How McKinsey 'Cost Curves' are Distorting REDD,*" Rainforest Foundation UK Climate and Forests Policy Brief.November 2010.
10. Gregorsen, H, Lakany, H., Karsenty, A. and White, A. 2011. *Does the Opportunity Cost Approach Indicate the Real Cost of REDD+?* Rights and Realities of Paying for REDD+ at Washington, DC: Rights and Resources Initiative.
11. Haaijer, R., Kamakura, W., Wedel, M. (2001). *The 'no-choice' alternative in conjoint choice experiments*. *International Journal of Market Research*, 43(1), 93-106
12. Hanley, N., Mourato, S. and Wright, R.E., 2001. *Choice Modelling Approaches: A Superior Alternative for Environmental Valuation?* *Journal of economic surveys*. 15, 435-462.
13. Hensher, D.A. and Greene, W.H., 2003. *The mixed logit model: the state of practice*. *Transportation*. 30, 133-176.
14. Hensher, D. A., Rose, J.M. and Greene, W.H., 2005. *Applied choice analysis: a primer*. Cambridge UnivPr,
15. HMGN 1993. *Forest Act*. Kathmandu: His Majesty's Government of Nepal, Law Books Management Board/HMGN.
16. HMGN 1995 *Forest Regulation* 1995. Kathmandu, Nepal: Law Books Management Board, His Majesty's Government of Nepal, Ministry of Forest and Soil Conservation.
17. Hoyos, D., 2010. *The state of the art of environmental valuation with discrete choice experiments*.*Ecol.Econ.* 69, 1595-1603.
18. Ives, J. & Messerli, B. 1989. *The Himalayan Dilemma*, London, Routelodge.
19. Kanel, K. 2004a. *Current Status of Community Forestry in Nepal*. Regional

Community Forestry Training Center for Asia and the Pacific (RECOFTC)  
Bangkok, Thailand

20. Kanel, K. R. 2004b. *Twenty Five Years of Community Forestry: Contribution to Millennium Development Goals*. In: Kanel, K. R., Mathema, P., Kandel, B. R., Niraula, D. R., Sharma, A. R. & Gautam, M., eds. Fourth National Community Forestry Workshop, Kathmandu Community Forestry Division, Department of Forest, Government of Nepal.
21. Kindermann, G, Obersteiner, M., Sohngen, B., Sathaye, J., Andrasko, K., Rametsteiner, E., Schlamadinger, B., Wunder, S. and Beach, R. 2008. *Global Cost Estimates of Reducing Carbon Emissions through Avoided Deforestation. Proceedings of the National Academy of Science*, 105: 10302–10307
22. Kuhfeld, W.F., 2010. *Marketing research methods in SAS experimental design, choice, conjoint, and graphical techniques*.
23. Lancaster, K.J., 1966. *A new approach to consumer theory. The Journal of Political Economy*. 74, 132-157.
24. Louviere, J.J., Hensher, D.A. and Swait, J.D., 2000. *Stated choice methods: analysis and applications*. Cambridge University Press.
25. McKinsey and Company. 2010. *Impact of the Financial Crisis on Carbon Economics: Version 2.1 of the Global Greenhouse Gas Abatement Cost Curve*. ([http://www.mckinsey.com/clientservice/sustainability/pdf/Impact\\_Financial\\_Crisis\\_Carbon\\_Economics\\_GHGcostcurveV2.1.pdf](http://www.mckinsey.com/clientservice/sustainability/pdf/Impact_Financial_Crisis_Carbon_Economics_GHGcostcurveV2.1.pdf) accessed on January 8, 2011).
26. MFSC 2013. *Persistence and change: Review of 30 years of community forestry in Nepal*. Kathmandu: Ministry of Forest and Soil Conservation, Government of Nepal.
27. Saatchi, S, Harris, M., Brown, S., Lefsky, M., Mitchard, E., Salas, W., Zutta, B., Buermann, W., Lewis, S., Hagen, S., Petrova, S., White, L., Silman, M. and Morel, A. 2011. *Benchmark Map of Carbon Forest Carbon Stocks in Tropical Regions across Three Continents. Proceedings of the National Academy of Sciences*, 108(24): 9899-9904.
28. Strassburg, B., Turner, R. K., Fisher, B., Schaeffer, R. and Lovett, A. 2009.

*Reducing Emissions from Deforestation – The “Combined Incentives” Mechanism and Empirical Simulations. Global Environmental Change, 19: 265-278.*

29. Train, K.E., 2003. *Discrete choice methods with simulation*. Cambridge university press.
30. UNEP. 2012. “*The Emissions Gap Report 2012: A UNEP Synthesis Report,*” Available at <http://www.unep.org/pdf/2012gapreport.pdf>
31. Van der Werf, G.R., Morton, D.C., DeFries, R.S., Olivier, J.G.J., Kasibhatla, P.S., Jackson, R.B., Collatz, G.J. and Randerson, J.T. 2009. *CO2 Emissions from Forest Loss. Nature Geoscience, 2: 737 – 738.*
32. World Bank. 2009. *Forests Sourcebook: Practical Guidance for Sustaining Forests in International Cooperation*. Washington D.C.: The World Bank
33. Yesuf, M. and Bluffstone, R. 2009. *Poverty, Risk Aversion and Path Dependence in Low Income Countries: Experimental Evidence from Ethiopia. American Journal of Agricultural Economics, 91(4): 1022-1037*

## 8. IMAGES AND TABLES

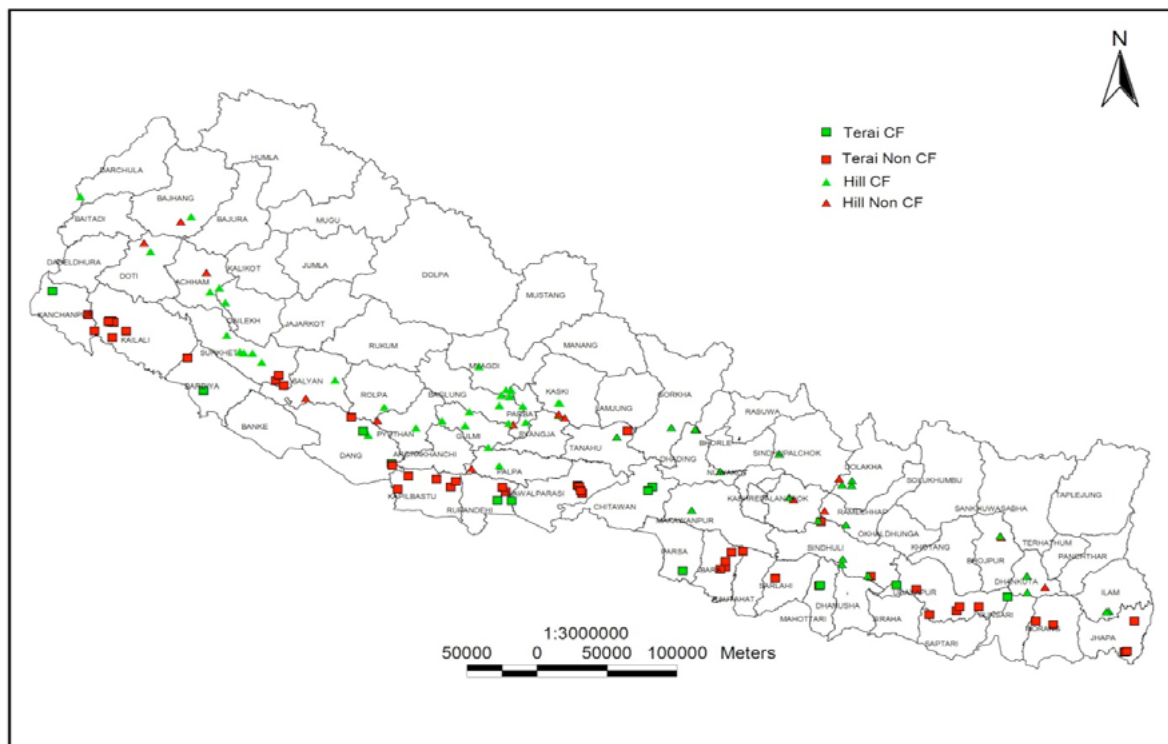


Fig. 1 Study sample sites

Attributes		Levels
REDD + payments (Rs. per household per year)	Annual total REDD+ payment to your community.	1000 2000 3000 4000 5000
Portion of the REDD+ payment going to the <u>household</u> .	The portion of REDD+ payments that go to communities for community projects and /or equally divided between households in your group.	100% community 50% community and 50% household 100% household
Reduction in amount of fuel wood collected	Required fuelwood reduction measured as a portion of your current use.	25% 50% 75% 100%
Grazing restrictions	Required reduction of grazing measured as a portion of your current use.	Yes No

Tab. 1 Attributes and levels for the REDD+ Survey Instrument

SN	Variable	CF HH %	Non-CF HH %	p-value
<b>A</b>	<b>Gender</b>			
1	Women headed households (WHH)	18.77	13.69	0.01306
2	WHH due to temporary migration of men	4.15	3.69	0.6682
3	WHH due to men's death	6.77	4.92	0.156
<b>B</b>	<b>Wellbeing class</b>			
1	Rich	9.08	11.08	0.231
2	Medium	52	51.38	0.8243
3	Poor	38.92	37.54	0.6075
<b>C</b>	<b>Caste groups</b>			
1	Dalit	14.46	17.69	0.1128
2	Janajati	43.69	39.38	0.1151
3	BC	39.54	41.08	0.5718
4	Others	2.31	1.85	0.5596
<b>D</b>	<b>Age of HH head (in years)</b>	52.46	48.77	4.297e-06
<b>E</b>	<b>Total population</b>	50.58	49.72	0.2879
	Men	51.91	52.80	0.4315
	Married	54.24	52.20	0.07231
	Immigrated	15.08	35.85	2.20E-16
<b>F</b>	<b>Main occupation</b>			
1	Agriculture	34.48	30.80	0.0005527
2	Skilled worker	1.26	1.69	0.1093
3	Services in GO, NGO, private sector	3.69	3.34	0.3984
4	Services in foreign country	7.38	6.75	0.2804
5	Household chores	6.18	7.48	0.02278
<b>G</b>	<b>Land holding and food security</b>			
1	Land holding by family	95.85	0.92	0.003704
2	Food sufficiency from own land	26.46	35.69	0.000324
<b>H</b>	<b>Income fluctuation in last ten years due to agriculture and livestock</b>			
	Increased	24.31	24.00	0.8969
	No change	57.08	60.15	0.2601
	Decreased	18.62	15.85	0.1862
<b>I</b>	<b>Income fluctuation in last ten years due to off-farm activities</b>			
1	Increased	37.69	37.08	0.8186
2	No change	53.69	54.00	0.9114
3	Decreased	8.62	8.92	0.8445

Tab. 2 Household Characteristics in CFs and Non-CFs

	(1) CL Main Effects	(2) MMNL Main Effects	(3) MMNL Attribute Interactions	(4) MMNL Demographic Interactions
ASC	2.776*** (0.102)	7.512*** (0.526), SD	9.173*** (0.779), SD	9.407*** (1.688), SD
Payment % to Community	0.0329*** (0.00507)	0.0733*** (0.0153), SD	0.101* (0.0567), SD	0.0989*** (0.0210), SD
Firewood Reduction	-0.171*** (0.00815)	-0.380*** (0.0235), SD	-0.516*** (0.0629), SD	-0.299*** (0.0266), SD
Grazing Restriction	-0.299*** (0.0360)	-0.668*** (0.101), SD	-1.481*** (0.368), SD	0.255** (0.122), SD
Payment	0.141*** (0.0159)	0.263*** (0.0273)	-0.0660 (0.122)	-0.296*** (0.0357)
Community X Payment			0.0136 (0.0103), SD	
Firewood X Payment			0.0389** (0.0155)	
Grazing X Payment			0.195** (0.0855), SD	
Firewood X Community			-0.00963* (0.00565), SD	
Grazing X Community			0.0165 (0.0369)	
ASC X Equitable access to forest fund				-0.919 (0.863)
ASC X Respondent migrated				0.764 (0.866)
ASC X CC serious for Nepal				2.865** (1.144)
ASC X CC serious for community				-1.040 (1.030)
ASC X CC serious personally				-0.840 (1.012)
ASC X REDD likely to benefit community				0.988 (0.980)
ASC X REDD likely to benefit personally				-0.215 (1.014)
ASC X Community members trustworthy				0.129 (1.096)
ASC X Community members follow rules				-0.271 (0.821)
ASC X Rules of access and forest use				-3.717***

are clear				(1.364)
ASC X Forest access decisions are fair				1.377 (1.081)
ASC X Village authorities monitor forest use				-1.389* (0.831)
ASC X Villages monitor forest use				1.162 (0.886)
ASC X Authorities support rule breakers				1.537* (0.849)
Observations	11694	11694	11694	7122
Log likelihood	-3027.4	-2473.3	-2446.7	-1454.8
Chi-squared	2510.0	1108.1	1149.0	581.6

Standard errors in parentheses \* $p < 0.1$ , \*\* $p < 0.05$ , \*\*\* $p < 0.01$

Tab. 3: Regression Results for the REDD+ CE Survey for Non-CF Communities

	(1) CL Main Effects	(3) MMNL Main Effects	(5) MMNL Attribute Interactions	(X) MMNL Demographi c Interactions
ASC	3.322*** (0.108)	7.647*** (0.479), SD	6.978*** (0.563), SD	7.179*** (0.899), SD
Payment % to Community	0.0416*** (0.00542)	0.0640*** (0.0118), SD	0.182*** (0.0308), SD	0.0590*** (0.0121), SD
Firewood Reduction	-0.260*** (0.00913)	-0.454*** (0.0239), SD	-0.431*** (0.0438), SD	-0.462*** (0.0253), SD
Payment	0.135*** (0.0170)	0.255*** (0.0250)	0.594*** (0.0909)	0.250*** (0.0260)
Firewood X Payment			-0.0191 (0.0117)	
Community X Payment			-0.0397*** (0.00762), SD	
Firewood X Community			0.00118 (0.00367)	
ASC X Equitable access to forest fund				-1.031* (0.579)
ASC X Respondent migrated				3.029** (1.430)
ASC X CC serious for Nepal				1.647** (0.800)
ASC X CC serious for community				-2.117** (0.824)
ASC X CC serious personally				-0.634 (0.654)
ASC X REDD likely to benefit community				0.349 (0.631)

ASC X REDD likely to benefit personally				2.095*** (0.681)
ASC X Community members trustworthy				-0.463 (0.798)
ASC X Community members follow rules				-0.591 (0.675)
ASC X Rules of access and forest use are clear				-1.191 (0.816)
ASC X Forest access decisions are fair				1.038 (0.663)
ASC X Village authorities monitor forest use				1.592*** (0.545)
ASC X Villages monitor forest use				0.516 (0.537)
ASC X Authorities support rule breakers				1.814** (0.713)
Observations	11697	11697	11697	10851
Log likelihood	-2702.3	-2316.4	-2298.4	-2140.5
Chi-squared	3162.3	771.9	783.5	632.7

Standard errors in parentheses \*p< 0.1, \*\*p< 0.05, \*\*\*p< 0.01  
 Tab. 4 Regression Results for the REDD+ CE Survey for CF Communities

MWTA - Main Effects			
Attribute	Conditional Logit	MMNL	
Payment to Community (Rs per 1%)	32.89	27.84	
Reduction in Firewood (Rs per 1%)	-120.80	-144.45	
Reduction in Grazing (Rs for restriction)	-2114.90	-2536.28	

Table 5a: Marginal Willingness to Accept for REDD+ Attributes for non-CF

MWTA - Main Effects			
Attribute	Conditional Logit	MMNL	
Payment to Community (Rs per 1%)	30.85	25.09	
Reduction in Firewood (Rs per 1%)	-193.13	-178.28	

Tab. 5b Marginal Willingness to Accept for REDD+ Attributes for CF

# Loss & Damage: a Critical Discourse Analysis

Calliari E.<sup>1,2</sup>

<sup>1</sup>Fondazione Eni Enrico Mattei – Italy

<sup>2</sup>Euro-Mediterranean Center on Climate Change - Italy

\*Corresponding Author: elisa.calliari@feem.it

## Abstract

The years-long negotiations on an international mechanism for loss and damage (L&D) associated with climate change impacts got to a milestone during the nineteenth session of the UNFCCC Conference of the Parties (COP-19), held in Warsaw in November 2013. The COP established the Warsaw international mechanism, aiming to address L&D associated with the adverse effects of climate change, including extreme events and slow onset events, in vulnerable developing countries (Decision 2/CP.19). The paper performs a Critical Discourse Analysis (CDA) of COP decision 2/CP.19 in order to evaluate its content and reflect on how the mechanism will be implemented. The analysis builds on Fairclough's (1992) three-dimensional model for CDA, and makes use of a wide range of materials including previous COP decisions, High Level Segment statements and Parties submissions to COP 19, press releases and other relevant documents. The analysis highlights the lack of a common understanding and representation of L&D by developed and developing countries, with this fact ultimately hampering the possibility to define actual tools to address the issue within the mechanism. The difficulty to come to a shared meaning on L&D is due to its connection to other controversial discourses under the UNFCCC: those of attribution, liability and compensation.

**Keywords:** Loss and Damage, limits and constraints to adaptation, liability, attribution, climate change negotiations

## 1. INTRODUCTION

The years-long negotiations on an international mechanism for loss and damage (L&D) associated with climate change impacts got to a milestone during the nineteenth session of the UNFCCC Conference of the Parties (COP-19), held in Warsaw in November 2013. The COP established the so-called Warsaw international mechanism (WIM) [1], aiming to address L&D associated with the adverse effects of climate change, including extreme events and slow onset events, in particularly vulnerable developing countries. Discussion on L&D, formally initiated with the 2007 Bali Action Plan [2] and later embedded in the Cancun Adaptation Framework (2010) [3], has been campaigned by the Alliance of Small Island States (AOSIS) since the early 1990s. AOSIS' claims have mainly focused on the establishment of a compensation mechanism, able to refund developing countries for those unavoidable impacts materializing when both mitigation and adaptation efforts fall short. However, the WIM does not recognize any liability of the most advanced economies for past and ongoing human induced climate change, nor makes any tangible commitment for helping low income and small developing island states to cope with L&D. Rather, it outlines a partnership for a better knowledge gathering, coordination and support, "including finance, technology and capacity building".

Up to date, L&D attracted little academic research [4] [5]. The existing body of literature is primarily composed by advocacy groups [6] [7] [8] and has mainly been produced in preparation of international meetings and with the aim of supporting developing countries' negotiating position. Interestingly, a recent branch of literature has been concentrating on a topic which is directly linked to that of L&D, i.e. the limits to adaptation [9] [10] [11] [12]. The IPCC AR5 has also devoted attention to the concept of "constraints and limits to adaptation" (Working Group II, Chapters 16 and 17) [13], where the first are those factors which make it difficult to implement adaptation actions, while the latter are insurmountable barriers to adaptation [10] [14]. Nevertheless, the connection between L&D and the constraints/limits to adaptation is not always made explicit, leaving the integration of the two branch of literature at an embryonic stage.

As a result, no commonly agreed definition is available for the concept yet. In the literature review prepared by the Work programme on L&D under the Subsidiary Body for Implementation (SBI) to the UNFCCC, L&D is very broadly referred to as

“the actual and/or potential manifestation of impacts associated with climate change in developing countries that negatively affect human and natural systems” [15]. Such definition, however, does not clarify why L&D should be regarded as a different category within climate change impacts and should be therefore addressed with an *ad hoc* instrument. Other definitions make a step ahead, explicitly linking L&D with the inability to cope and adapt to climate change impacts [4]. However, this does not allow for precisely setting the boundaries of the concept: is such inability to adapt stemming from institutional barriers, prohibitive costs or technical impossibility? All these cases holding true, what the difference with the concept of residual impact would be then?

The fluidity in the way L&D is conceptualized, also shows up at the negotiations level. While consensus around core concepts like mitigation and adaptation has been reached, this does not hold true for L&D. Discourses around the concept are still characterized by a strong juxtaposition between developing and developed countries, with the former claiming L&D to be something beyond adaptation and thus requiring additional instruments besides mitigation and adaptation, and the latter including L&D within the scope of adaptation.

The paper employs a Critical Discourse Analysis (CDA) to investigate how different discourses, i.e. way of understanding and representing the issue of L&D, have been endorsed by developed and developing countries and the possible reasons for their divergence. It also reflects on the consequences this had on the definition of appropriate and concrete actions to address L&D through the WIM. The first section provides an overview of the theory and method of discourse analysis: particular attention is drawn on the CDA approach and its theorization by Norman Fairclough. Making use of Fairclough’s three-dimensional model for CDA, the analysis carried out in section 3 highlights the lack of a common understanding and representation of L&D by developed and developing countries, with this fact ultimately hampering the definition of actual tools to address the issue within the mechanism. The difficulty to come to a shared meaning on L&D is due to its connection to other controversial discourses under the UNFCCC: those of attribution, responsibility/liability and compensation. The paper concludes with some considerations on the possible developments of the L&D issue and on the near future implementation of the WIM.

## 2. THEORY AND METHOD: CRITICAL DISCOURSE ANALYSIS

Being aware that there is no generally accepted definition of *discourse* in social science [14], I adhere to its interpretation as a particular way of talking about and understanding the world, or an aspect of the world [16]. Therefore, discourse analysis becomes a strategy to reveal how the understanding of the world is built through language and how, conversely, the latter contributes to change social reality. It draws attention on the way discourse is produced, what it excludes, how some knowledge becomes significant and some other does not, and how power relations are reflected in language [17] [18].

Discourse analysis is rooted in a social constructionist approach within social sciences and humanities [14]. Despite the common epistemological premises, approaches to discourse analysis vary, differing *inter alia* with respect to the role of discourse in the construction of the world and the analytical focus [19]. In this paper, I employ a CDA as mainly concerned with social problems and political issues and for its attempt not only to interpret but also to explain discourse structures [20]. In particular, CDA focuses on the ways discourse structures enact, confirm, legitimate, reproduce, or challenge relations of power and dominance in society [19]. As negotiations under the UNFCCC are characterized by pronounced power asymmetries, CDA turns out to be useful in detecting whether the latter are reflected in the discussion on L&D.

Within the CDA approaches, I focus on Norman Fairclough's work and adopt his three-dimensional model for CDA [21]. According to it, the starting point of any analysis should be the consideration of two important elements of the discourse: i) the *communicative event* (for example, a newspaper article or any other text or speech); ii) the *order of discourse*, i.e. the configuration of all discourse types used in a specific field. The communicative event has three dimensions, each of which should be covered by a specific analysis:

- I. it is a *text*, and should be subject to a linguistic analysis (vocabulary, grammar, syntax);
- II. it is a *discursive practice*: attention should be drawn on how the text is produced and consumed, focusing on the way power relations are enacted.

The underlying hegemonic processes, through which consensus around meanings emerges, should be explored;

- III. it is a *social practice*, with this implying considering how the discursive practices reproduces or restructures the existing order of discourse and how this translates into social change.

Hence, Fairclough proposes three levels of analysis: at *micro*, *meso* and *macro* scales. Accordingly, the analysis of COP Decision 2/CP.19 (*communicative event*) in section 3 is carried out considering these dimensions. Although the text of 2/CP.19 constitutes the core of the analysis, it is examined in connection with other relevant documents, including previous COP decisions (1/CP 16, 7/CP 17, 3/CP 18), High Level Segment statements made by Heads of States and Governments at COP 19/CMP 9, Parties submissions in preparation of COP 19, press releases and other relevant documents available on the UNFCCC website. This is functional to reconstruct in an organic way the different discourses adopted by developed and developing countries on L&D.

### 3. ANALYSIS OF THE DECISION (2/CP.19) AND DISCUSSION

I start from the analysis of the discursive practice (*meso scale* in Fairclough's model) as crucial to understand how the authors of Decision 2/CP.19 draw on existing discourses when producing the text. It entails eliciting the particular ways in which authors understand and represent the issue, and detecting how such views interact, eventually reproducing or transforming the order of discourse. I have already recalled in the introduction how developing and developed countries frame L&D in two conflicting way, the former claiming L&D to be something *beyond* adaptation and thus requiring additional instruments besides mitigation and adaptation, and the latter including L&D *within* the scope of adaptation. The reasons behind such juxtaposition lie in the strong reference made by developing countries to the concept of compensation: in their view, developed countries should refund them for the unavoidable impacts already materializing as a consequence of past and ongoing greenhouse gases (GHG) emissions. Talking about compensation, however, ultimately links the discourse on L&D to another controversial issue under the UNFCCC, i.e. that of historical responsibility for GHG emissions. Although the

UNFCCC recognized industrialized countries as historically responsible for having emitted a larger share of GHG compared to developing countries (art. 3, §1 UNFCCC), the implications of such “common but differentiated responsibilities” have been interpreted more in terms of voluntary aid and differentiation on grounds of capacity [18]. A step ahead in this discussion has been recently made, with some scholars [22] endorsing the possibility of holding a state generally responsible for climate change damages for breaching the *no harm rule* under international customary law. This argument, however, does not appear to be based on solid ground. Before holding a state responsible, it is necessary to prove the causal link between the damage and the act/omission attributable to the state. This is particularly challenging for the current state of scientific knowledge. As highlighted by the 2012 *Special Report on Managing the Risks of Extreme Events and Disasters to Advance Climate Change Adaptation* [23], while some slow-onset events are direct consequences of large-scale warming and can therefore be linked directly to past emissions, extreme weather events (which are also associated with greater loss and damage) cannot still be entirely attributed to climate change. Lacking the full causal link of L&D with climate change, claims for compensations become ultimately arduous to rise. Not least, it is difficult to distinguish the contribution and the sign of other factors, like exposure and vulnerability, to L&D. Within international law, talking about state liability, i.e. responsibility for acts not prohibited by international law, would provide a better framework for the issue. Indeed, liability is a form of more sophisticated and solidaristic responsibility [24], aiming at regulating certain socially useful but hazardous activities so that to guarantee their economic viability while providing prompt reparation in case of transboundary damages to the environment or the society [25]. No international obligations has to be breached and no fault has to be proved: only causation is relevant [25]. However, the concept has been rarely activated and is envisaged by the *Convention on International Liability for Damage Caused by Space Objects* (1972) only. Moreover, being causation the only parameter to matter, the same difficulties observed as for the traditional view of state responsibility would apply in proving the causal link between (lawful) activities and damages.

The analysis of the text of Decision 2/CP.19 (*micro scale* in Fairclough’s model) confirms the presence of such Gordian knots. Firstly, the relationship between L&D

and adaptation is defined in two clashing ways. According to line 6 of the Decision L&D “includes, and in some cases involve more than, that which can be reduced by adaptation”, while at line 13 the WIM is placed “under the Cancun Adaptation Framework”. The first statement recognizes L&D as something which, in some cases, can go beyond adaptation and thus recognizes developing countries’ claims. On the contrary, the second statement –placing L&D under the *Cancun Adaptation Framework*- suggests a relation of subordination between the concepts, with L&D being a part of adaptation as argued by developed countries. From a rhetoric point of view, this is a case of “constructive ambiguity”, a tool often employed in diplomacy to get over situations of impasse [26]. It is a strategy used when parties have strong and contradictory interests and views and/or the negotiations are running short of time [27]. The incapacity to get to a shared definition of the concept is also shown by the provision requiring a review of the mechanism “including its structure, mandate and effectiveness” at COP 22 in 2016 (§1 and §15 of the Decision).

As for the attribution of L&D to climate change, in Decision 2/CP.19 (as well as in the decisions adopted since the Cancun Agreements), L&D is referred to as being *associated* with climate change impacts, including extreme weather events and slow onset events. Again, this could be seen as an example of constructive ambiguity in its lexical form. The verb “associate” implies a connection between two things either because they occur together or because one produces the other [28]. Thus, the verb can entail different relationships linking the concepts: they can be on the same level, being simply connected, or one can be subordinated to the other, as caused by the latter. More research should be done in understanding whether this expression has been used in the decisions as a compromise on the different views on attribution of L&D to climate change, or simply because of the uncertainty that still lingers in science on the relationship between climate change and extreme events. However, it is interesting to note that developing countries, and AOSIS in particular, are more inclined in adhering to the second meaning of the verb, i.e. implying causality. Taking as an example Nauru’s submission to COP 19 (“Views and information on elements of an international mechanism to address loss and damage from the adverse effects of climate change” [29]), the alleged causal link between L&D and climate change impacts is made explicit by the same title. Indeed, the preposition “from” indicates the source or cause of something [28].

Drawing together the threads of the above arguments, it is hard to say whether during COP 19 negotiations the order of discourse on L&D has been truly transformed (*macro scale* within Fairclough's model). It is true that power relations among developed and developing countries slightly changed, as the latter were able to introduce a "new" discourse on L&D in the final text of Decision 2/CP.19, referring to it as something beyond adaptation. For the time being, however, it is still uncertain whether this will actually correspond to a new way of representing the issue and, most importantly, to a change in the way L&D has been addressed in the practice so far. In fact, as Fairclough notes [30], a new discourse may come into an institution without being enacted or inculcated, or it may be enacted but never fully inculcated. Inculcation means that people own the discourse. What more reasonably happened in Warsaw is that developed countries have "learnt" this new discourse for the purpose of closing the negotiation process, but at the same time they beware of internalizing it.

#### 4. CONCLUSIONS

One of the aim of discourse analysis is to investigate the relations of power and their possible changes through language. The insertion of the expression of L&D going beyond adaptation in the final text of Decision 2/CP.19 reflects a small but not negligible result for developing countries. It is actually expected that this point will be used in 2016 as a lever to move the issue of L&D out of the adaptation pillar and position it as a new field in the battle against the adverse impacts of climate change, subsequent to the "preventive" phase of mitigation and the "managing" phase of adaptation [31]. Negotiating power on the issue can be therefore deemed to have somewhat increased for developing countries. Yet, the use of constructive ambiguity in the text reminds us that developed and developing countries have failed to come to a shared meaning and representation of L&D and that many unresolved issues remain on the table. The crux of the matter can be depicted as a "triangle of discord" at whose vertex are the concepts of attribution, liability and compensation. Without untying such Gordian knots, it will not be possible to be of the same mind on what L&D is and therefore arrange precise and concrete activities to address it.

Nevertheless, it would not be fair to depict the WIM as meaningless. It offer a set of tools, mostly related to knowledge and expertise sharing, data distribution and

collection, technological support and international dialogue enhancement, that have the potential to tackle some important dimensions of L&D which cannot be addressed financially, like the loss of biodiversity, culture and statehood are. As recently stated by developing countries' negotiators on L&D at COP 19, "financial compensation may represent a normative solution to the perils of vulnerable countries, but does not necessarily mean that the underlying needs are addressed" [32]. The establishment of the mechanism will therefore allow for further confrontation and advancement in the understanding of this complex and multifaceted issue. Nevertheless, its performance will need to be judged on the basis of its actual implementation, expected by the end of 2014.

## 5. ACKNOWLEDGEMENTS

The research leading to this paper has received funding from the European Union under the CASCADE Action (*Climate change adaptation strategies for water resources and human livelihoods in the coastal zones of Small Island Developing States*, Grant contract id number FED/2011/281-147) implemented by the ACP Caribbean & Pacific Research Programme for Sustainable Development, 10<sup>th</sup> European Development Fund.

The author also gratefully thanks Dr. Jaroslav Mysiak for the valuable suggestions and assistance in this research.

## 6. REFERENCES

- [1] UNFCCC Secretariat, "2/CP.19 Warsaw international mechanism for loss and damage associated with climate change impacts," United Nations Office at Geneva, Geneva, 2012.
- [2] UNFCCC Conference of the Parties (COP), "Report of the Conference of the Parties on its thirteenth session, held in Bali from 3 to 15 December 2007," United Nations Office at Geneva, Geneva, 2008.
- [3] UNFCCC Conference of the Parties (COP), "Report of the Conference of the Parties on its sixteenth session, held in Cancun from 29 November to 10 December 2010. Addendum. Part two: Action taken by the Conference of the Parties at its sixteenth session," United Nations Office at Geneva, Geneva, 2010.
- [4] K. Warner, K. van der Geest and S. Kreft, "Pushed to the limit: Evidence of climate change-related loss and damage when people face constraints and limits to

- adaptation. Report No. 11," United Nations University Institute of Environment and Human Security (UNU-EHS), Bonn, 2013.
- [5] K. Warner, K. van der Geest, S. Kreft, S. Huq, S. Harmeling, K. Kusters and A. de Sherbinin, "Evidence from the frontlines of climate change: Loss and damage to communities despite coping and adaptation," United Nations University, Bonn, 2012.
- [6] Actionaid, Care International, WWF, "Tackling the climate reality: A framework for establishing an international mechanism to address loss and damage at COP19," 2013. [Online]. Available: <http://awsassets.panda.org/downloads/tacklingtheclimateresality.pdf>.
- [7] ActionAid, CARE, WWF, "TACKLING THE LIMITS TO ADAPTATION: An international framework to address 'loss and damage' from climate change impacts," ActionAid, Johannesburg, 2012.
- [8] ActionAid, "Loss and damage from climate change: the cost for poor people in developing countries," ActionAid, Johannesburg, 2010.
- [9] K. Dow and F. Berkhout, "Climate Change, Limits to Adaptation and the 'Loss and Damage' Debate," 2014. [Online]. Available: <http://www.e-ir.info/2014/03/13/climate-change-limits-to-adaptation-and-the-loss-and-damage-debate/>. [Accessed 15 03 2014].
- [10] K. Dow and F. Berkhout, "Commentary: Limits to adaptation," *Nature Climate Change*, vol. 3, p. 305–307, 2013.
- [11] W. N. Adger, S. Dessai, M. Goulden, M. Hulme, I. Lorenzoni, D. R. Nelson, L. O. Naess, J. Wolf and A. Wreford, "Are there social limits to adaptation to climate change?," *Climatic Change*, pp. 335-354, 2009.
- [12] C. L. Morgan, "Limits to Adaptation: A Review of Limitations relevant to the project "Building Resilience to Climate Change – Coastal Southeast Asia"," International Union for Conservation of Nature (IUCN), Gland, 2011.
- [13] IPCC, "Climate Change 2014: Impacts, Adaptation, and Vulnerability. IPCC Working Group II Contribution to AR5," 2014. [Online]. Available: <https://www.ipcc.ch/report/ar5/wg2/>.
- [14] O. K. Pedersen, "Discourse Analysis," *International Center for Business and Politics. Working Paper*, no. 65, 2009.
- [15] Subsidiary Body for Implementation, "A literature review on the topics in the context of thematic area 2 of the work programme on loss and damage: a range of approaches to address loss and damage associated with the adverse effects of climate change," UNFCCC, Bonn, 2012.
- [16] M. Jørgensen and L. Phillips, *Discourse Analysis as Theory and Method*, London: SAGE Publications Ltd, 2002.
- [17] S. Hesse-Biber and P. Leavy, *The practice of qualitative research*, Thousand Oaks: Sage Publications, Inc., 2006.
- [18] M. Friman, *Historical responsibility: Assessing the past in international climate negotiations*, Linköping: Linköping Studies in Arts and Science. Thesis number 569, 2013.
- [19] T. van Dijk, "The handbook of discourse analysis," in *Handbook of Discourse Analysis*, Oxford, Blackwell, 2001, pp. 352-371.
- [20] N. Fairclough and R. Wodak, "Critical discourse analysis," in *Discourse as Social*

*Interaction: Discourse Studies: A Multidisciplinary Introduction. Vol. 2.*, London, Sage, 1997.

- [21] N. Fairclough, *Discourse and Social Change*, Cambridge: Polity Press, 1992.
- [22] R. S. Tol and R. Verheyend, "State responsibility and compensation for climate change damages—a legal and economic assessment," *Energy Policy*, vol. 32, no. 9, p. 1109–1130, 2004.
- [23] IPCC, "Managing the Risks of Extreme Events and Disasters to Advance Climate Change Adaptation. A Special Report of Working Groups I and II of the Intergovernmental Panel on Climate Change," Cambridge University Press, Cambridge, UK, and New York, NY, USA, 2012.
- [24] B. Conforti, *Diritto Internazionale*, Editoriale Scientifica: Napoli, 2002.
- [25] J. Barboza, *The Environment, Risk and Liability in International Law*, Leiden, The Netherlands, and Boston: Martinus Nijhoff, 2011.
- [26] G. Berridge and A. James, *A Dictionary of Diplomacy*, Basingstoke: Palgrave, 2001.
- [27] D. Pehar, "Use of ambiguities in Peace Agreements," in *Language and Diplomacy*. Kubalija, J. & Slavik, H (eds), Malta, DiploProjects, 2001, pp. 153-162.
- [28] Angus Stevenson, editor, *Oxford Dictionary of English (3rd edition)*, Oxford: Oxford University Press, 2010.
- [29] Nauru on behalf of The Alliance of Small Island States, "Views and information on elements of an international mechanism to address loss and damage from the adverse effects of climate change," 12 November 2013. [Online]. Available: <http://aosis.org/wp-content/uploads/2013/11/UNFCCC-Submission-Loss-and-Damage-Warsaw.pdf>.
- [30] N. Fairclough, *Analysing Discourse: Textual Analysis for Social Research*, London: Routledge, 2003.
- [31] Climate & Development Knowledge Network, "Loss and Damage in Vulnerable Countries Initiative," 2012. [Online]. Available: <http://www.lossanddamage.net/download/6525.pdf>. [Accessed 15 March 2014].
- [32] P. J. Hoffmaister, M. Talakai, P. Dampsey and A. S. Barbosa, "Warsaw International Mechanism for loss and damage: Moving from polarizing discussions towards addressing the emerging challenges faced by developing countries," 6 January 2014. [Online]. Available: <http://www.lossanddamage.net/download/7274.pdf>. [Accessed 6 February 2014].



# Advances in Climate Science

Advances in climate change

**Climate variability &  
climate change I**

# A simple explanation for climate variations in the Sahel

Giannini A.<sup>1</sup>

<sup>1</sup>IRI for Climate and Society, Columbia University - U.S.A.

\*Corresponding Author: alesall@iri.columbia.edu

## Abstract

The difference in surface temperature between the sub-tropical North Atlantic and the global tropical oceans explains past drought, partial recovery and differences among model projections of precipitation change in the Sahel.

**Keywords:** Sahel, drought, projections, adaptation

## 1. TEXT

The Sahel, the semi-arid southern edge of the Sahara desert, usually conjures images of cracked earth and malnourished children—a harsh, inhospitable environment plagued by drought, famine and, most recently, security concerns driven by the spread of terrorism.

Persistent drought onset abruptly here in the early 1970s. Scientists studying its cause initially focused on local factors (Charney 1975). They postulated that rapid population growth led to extensive agricultural practices—cultivation of marginal lands, overgrazing and wood-cutting for fuel—and that degradation turned dryland into desert, and engendered drought, which further degraded the vegetation cover. In recent years drought has been alternating with flooding, and global policy talk around desertification has been replaced by acknowledgement of re-greening, that is, an increase in vegetation cover (Herrmann et al 2005)), if localized, attributed to successful interventions, whether instigated by individuals or Non Governmental Organizations, whether supported by development aid or spontaneous (Reij et al 2009).

In parallel, in the intervening decades an alternative explanation relating the evolution of Sahelian climate to global rather than local influence, had gained ground (Folland et al 1986), with initial attempts at operational seasonal forecasting in time leading to the institutionalization of the West African Climate Outlook Forum in the late 1990s. This global influence, making the climate of the Sahel predictable on seasonal to interannual time scales, and explaining persistent drought as well as the current partial recovery, is that of the oceans, the dominant source of moisture for semi-arid regions like the Sahel.

This paper provides a simple interpretation of the influence of the oceans on the Sahel, one that for the first time makes sense of past drought, and of the current trend towards increased rainfall consistently with near- and long-term projections.

One way to arrive at such simple explanation is to seek consistency between seasonal-to-interannual prediction approaches, which detail the role of large-scale anomalies in sea surface temperature in driving shifts in the probabilities of occurrence of, say, below, normal or above-normal precipitation, and approaches germane to the theory of climate change, which relate warming to the expected thermodynamic, i.e. driven by the concomitant increase in humidity, and dynamical responses.

From the perspective of seasonal climate prediction, a fairly detailed picture has emerged from decades of studies (Rowell et al 1995; Fontaine and Janicot 1996; Ndi-

aye et al 2011; Rowell 2013) which relates anomalies in the surface temperature of all ocean basins to anomalies in Sahel rainfall. Following Folland et al (1986) and Giannini et al (2003) respectively, Palmer (1986) and Lu and Delworth (2005) demonstrated that variation in the surface temperatures of each single basin can lead to Sahel drought. Specifically, warmer Pacific and Indian Oceans, respectively on interannual and interdecadal time scales, and a cooler northern than southern Atlantic, also on interdecadal time scales, are associated with drought.

However, this level of detail, i.e. modeling Sahel rainfall as a function of Indo-Pacific warming and of the interhemispheric contrast in the Atlantic, while broadly explanatory of 20th century behavior, does not consistently predict 21st century behavior (Biasutti et al 2008). What does begin to explain the latter is the simplification attempted here, which ties the recent evolution of Sahelian climate to anthropogenic emission through their influence on sea surface temperatures. Oceans have been warming globally, due to greenhouse gases, but not uniformly, most notably in the North Atlantic, due to aerosols. Warming oceans are hypothesized to raise the bar for deep convection (Neelin et al 2003; Held et al 2005), the process that generates precipitation in the tropics. This situation would result in fewer rainy days, prolonged dry spells, and overall seasonal drought, were it not for the fact that warming oceans also provide increased moisture (Seth et al 2013). The increased moisture can trigger convection, and more intense rains. In the case of the Sahel, the global tropical sea surface temperature average provides a quantitative estimate of the former influence, while the local North Atlantic average provides an estimate of the latter. The two can evolve independently, but it is their difference that matters to prediction of Sahel rains.

Drought in the 1970s and 1980s was associated with a North Atlantic that could not keep up with global tropical ocean warming, especially noticeable in the Indian Ocean, due to the local influence of aerosols. The current trend towards recovery is consistent with reduced aerosol emissions since legislation to curb their emissions to reduce pollution. Interestingly, the current trend is marked by less frequent, but more intense rain events (Lodoun et al 2013; Salack et al 2014). Interpreting the climate of the Sahel through the lens of oceanic influence therefore provides not only a consistent explanation of past and future, but also a global context for framing adaptation to a more variable climate.

## **2. ACKNOWLEDGMENTS**

AG wishes to acknowledge the many fruitful discussions with Michela Biasutti, Ousmane Ndiaye, Seyni Salack, Tiganadaba Lodoun and David Neelin, among others.

### 3. REFERENCES

- Biasutti, M., Held, I. M., Sobel, A. H. and Giannini, A. 2008: SST forcings and Sahel rainfall variability in simulations of 20<sup>th</sup> and 21<sup>st</sup> centuries. *J. Climate*, **21**, 3471–3486.
- Charney, J. G. 1975: Dynamics of deserts and drought in the Sahel. *Q. J. Roy. Meteor. Soc.*, **101**, 193–202.
- Folland, C. K. 1986: Sahel rainfall and worldwide sea temperatures, 1901-85. *Nature*, **320**, 602–607.
- Fontaine, B. and Janicot, S. 1996: Sea surface temperature fields associated with West African rainfall anomaly types. *J. Climate*, **9**, 2935–2940.
- Giannini, A., Saravanan, R. and Chang, P. 2003: Oceanic forcing of Sahel rainfall on interannual to interdecadal time scales. *Science*, **302**, 1027–1030. doi:10.1126/science.1089357.
- Held, I. M., Delworth, T. L., Lu, J., Findell, K. and Knutson, T. R. 2005: Simulation of Sahel drought in the 20<sup>th</sup> and 21<sup>st</sup> centuries. *Proc. Nat. Acad. Sci.*, **102**, 17891–17896. doi:10.1073/pnas.0509057102.
- Herrmann, S. M., Anyamba, A. and Tucker, C. J. 2005: Recent trends in vegetation dynamics in the African Sahel and their relationship to climate. *Global Environ. Change*, **15**, 394–404.
- Lodoun, T., Giannini, A., Traoré, P. S., Somé, L., Sanon, M., M, V. and Millogo-Rasolodimby, J. 2013: Changes in the character of precipitation in Burkina Faso associated with late-20<sup>th</sup> century drought and recovery in the Sahel. *Environmental Development*, **5**, 96–108.
- Lu, J. and Delworth, T. L. 2005: Oceanic forcing of late 20<sup>th</sup> century Sahel drought. *Geophys. Res. Lett.*, **32**, L22706. doi:10.1029/2005GL023316.
- Ndiaye, O., Ward, M. and Thiaw, W. M. 2011: Predictability of seasonal Sahel rainfall using GCMs and lead-time improvements through the use of a coupled model. *J. Climate*, **24**, 1931–1949.

- Neelin, J. D., Chou, C. and Su, H. 2003: Tropical drought regions in global warming and El Niño teleconnections. *Geophys. Res. Lett.*, **30**, 2275. doi:10.1029/2003GL0018625.
- Palmer, T. N. 1986: Influence of the Atlantic, Pacific and Indian Oceans on Sahel rainfall. *Nature*, **322**, 251–253.
- Reij, C., Tappan, G. and Smale, M. 2009: Agroenvironmental transformation in the Sahel: another kind of "Green Revolution". *IFPRI Discussion Paper 00914*.
- Rowell, D. P. 2013: Simulating SST teleconnections to Africa: what is the state of the art?. *J. Climate*, **26**, 5397–5418.
- Rowell, D. P., Folland, C. K., Maskell, K. and Ward, M. N. 1995: Variability of summer rainfall over tropical North Africa (1906-92): observations and modeling. *Q. J. R. Meteorol. Soc.*, **121**, 669–704.
- Salack, S., Giannini, A., Diakhaté, M., Gaye, A. T. and Muller, B. 2014: Oceanic influence on the sub-seasonal to interannual timing and frequency of extreme dry spells over the West African Sahel. *Clim. Dyn.*, **42**, 189–201.
- Seth, A., Rauscher, S. A., Biasutti, M., Giannini, A., Camargo, S. J. and Rojas, M. 2013: CMIP5 projected changes in the annual cycle of precipitation in monsoon regions. *J. Climate*, **26**, 7328–7351.

# Projected daily precipitation characteristics change in the early 21st century in Southern Africa

Diallo I.<sup>1, 2\*</sup>, Giorgi F.<sup>1</sup> and Stordal F.<sup>3</sup>

<sup>1</sup>Earth System Physics section, the Abdus Salam International Centre for Theoretical Physics, Trieste-Italy

<sup>2</sup>Laboratoire de Physique de l'Atmosphère et de l'Océan Siméon Fongang (LPAO-SF), Ecole Supérieure Polytechnique, Université Cheikh Anta Diop (ESP-UCAD), Dakar-Sénégal.

<sup>3</sup>University of Oslo - Department of Geosciences, Oslo, Norway

\*Corresponding author: [iduallo@ictp.it](mailto:iduallo@ictp.it)

## Abstract

We discuss a present day (1990-2009) and near future (RCP 4.5, 2010-2029) simulation for the southern Africa region with the RegCM4 regional climate model (RCM,  $dx = 25$  km) driven by the CAM4 global climate model (GCM,  $dx = 1^\circ$ ). The analysis focuses on precipitation extreme indices. With a few exceptions we find that the models reproduce reasonably well the extreme climatology of precipitation over the region, with the RegCM4 improving the simulation of daily precipitation frequency and duration of dry and wet events compared to CAM4 due to its higher resolution. In the near future both models show a prevailing shift towards a hydroclimatic regime of more intense and less frequent precipitation events. The global and regional models exhibit quite different patterns of change, an indication of the importance of internal variability and process representation for the simulation of surface climate.

**Keywords:** RegCM4, Climate Change, Extremes events, Southern Africa

## 1. INTRODUCTION

The region of Southern Africa is projected to undergo substantial changes in temperature and precipitation due to greenhouse gas (GHG) induced global warming [1]. Because the economy of the region relies heavily on rain-fed agriculture, it is important to provide projections of possible changes in hydrologic regimes over the region for use in impact studies [2].

Indeed, a number of recent studies have examined the performance of regional climate models (RCMs) over the Africa region (e.g. [3]; [4]; [5]; [6], and references therein) and have shown that these models can reproduce the basic characteristics of African climate and extreme events up to the daily temporal scale, often improving the performance of global climate models (GCMs). In this paper we present an analysis of the RegCM4 simulation over Southern Africa. RegCM4 was driven by boundary conditions provided by a CAM4 simulation of present day climate (1990-2009) and near future climate conditions (2010-2029). We stress that, since we only analyze a single realization with a single RCM and GCM, this experiment is not intended to provide a comprehensive climate change scenario for impact assessment studies, but rather a sensitivity study to evaluate the behavior of the regional climate model RegCM4 when driven by CAM4 and to compare the changes across the two models in higher order statistics.

Here we focus in particular on the model performance in simulating a range of extreme event statistics, since these are the most important for impacts. We compare results from the driving and nested models to evaluate the added value obtained from the high RCM resolution. In addition, we compare near future and present day statistics as an illustration of the magnitude of changes that can be expected in such simulations, with an emphasis on how changes in extremes relate to changes in mean climate. The production of a scenario of change, which is planned for future activities, will require an ensemble of simulations that would allow us to estimate uncertainties in the projections.

In the next section we briefly describe models; experiment and analysis design and in section 3 we then discuss the model results.

## 2. MODEL DESCRIPTION, VALIDATION DATASETS AND ANALYSES MEASURES

### 2.1 Model description and simulation design.

We have performed a GCM run followed by a dynamical downscaling with a RCM. The two models were run for a continuous transient simulation spanning the 40 year period 1990-2029. The period 1990-2009 is considered as reference (RF), while the period 2010-2029 under the Representative Concentration Pathway 4.5 (RCP 4.5) climate scenario is referred to as the early future period.

The GCM used here is the National Centre for Atmospheric Research (NCAR) Community Atmospheric Model version 4 (CAM4; [7]). It was run at a horizontal resolution of  $0.9^\circ \times 1.25^\circ$  with 26 vertical layers forced by prescribed sea surface temperature (SST) from the Community Climate System Model (CCSM4). Meteorological initial and 6-hourly lateral boundary conditions (LBC) from CAM4 along with SST from the CCSM4 experiment were used to drive the (1990-2029) corresponding RegCM4 simulation.

RegCM4 [8] is the latest version of the Abdus Salam International Centre for Theoretical Physics (ICTP) RCM system RegCM. It is a primitive equation, sigma vertical coordinate model with dynamics based on the hydrostatic version of the National Centre for Atmospheric Research/Pennsylvania State University's mesoscale meteorological model version 5 (NCAR/PSU's MM5; [9]). A detailed description of the RegCM4 can be found in [8]. RegCM4 was integrated over the Southern African domain (see Fig. 1 in [10]) with a horizontal resolution of 25 km and 18 vertical levels. The model LBC and the SST are updated 4 times daily using the relaxation procedure described by [11].

### 2.2 Observation and reanalysis estimates

The validation of the simulated daily precipitation extreme indices is carried out against the satellite-based daily precipitation data at  $0.25^\circ \times 0.25^\circ$  horizontal resolution from the Tropical Rainfall Measuring Mission (TRMM VB42V47, Jan 1998- to Feb 2013; [12]; hereafter referred to as TRMM) and the One-Degree Daily (1DD) data of GPCP V1.2 (hereafter referred to as GPCP) compiled by [13]. The GPCP V1.2 dataset provides daily rainfall estimates since October 1996. The year 1990 in

the model simulation, which is considered as spin-up time for the model, is not considered in the validation analysis.

The daily extreme indices described in the following section (section 2.3) are analyzed for the whole extended austral summer rainy season, i.e. from November through March (NDJFM) during which the southern African region receives almost its total annual rainfall [14].

### 2.3 Analysis measures

The main focus of our study is on the validation and projection of extreme climate characteristics of daily precipitation for the NDJFM season. In this paper, three indicators of hydroclimatic extremes are evaluated, for precipitation, suggested by [15] and the Expert Team on Climate Change Detection and Indices (ETCCDI; <http://cccma.seos.uvic.ca/ETCCDMI/>).

The indices are:

- Frequency: defined as the number of days with precipitation  $> 1$  mm.
- Consecutive wet days (CWD): defined as the maximum number of consecutive days with precipitation  $\geq 1$  mm ( $R_{\text{day}} \geq 1$  mm).
- Consecutive dry days (CDD): defined as the maximum number of consecutive dry days, i.e. days with rainfall amount  $< 1$ mm ( $R_{\text{day}} < 1$  mm).

## 3. RESULTS AND DISCUSSION

### 3.1 Present day-climate

Fig. 1 shows the precipitation frequency (i.e. the number of days with precipitation higher than 1 mm) in NDJFM averaged over the period 1998-2009 and obtained from GPCP, TRMM, CAM4 and RegCM4, respectively. The spatial patterns of precipitation frequency are more consistent across the two observation-based products (Fig. 1a, b), with a primary maximum over the Katanga region and a secondary one over the south-eastern coastal areas. However, GPCP shows overall greater frequency values, also in this case likely due to the coarser resolution of the data.

Both CAM4 and RegCM4 reproduce the overall patterns of the frequency (Fig. 1c-d), particularly when comparing with the TRMM data. CAM4 reproduces quite well the maximum frequency over the Katanga region compared to TRMM, but

underestimates it over the eastern coastal regions and across Madagascar, where RegCM4 shows values more in line with the TRMM estimates. The most pronounced model deficiency is the overestimate of frequency by CAM4, even compared to the GPCP data, evidently as a result of too many drizzle events at the coarse model resolution. Conversely, RegCM4 shows a good agreement especially with the TRMM data. Analyzing two WRF simulations performed respectively at 90 Km and 30 Km over Africa compared with four CMIP5 models, this deficiency was already pointed out by [6], who found that the rainfall frequency is poorly simulated by GCMs specially over the Congo Basin, a result that they attributed to physical parameterization deficiencies in the models.

Fig. 2 shows the patterns of CWD (maximum number of consecutive days with rainfall intensity  $\geq 1 \text{ mm day}^{-1}$ ) while Fig. 3 shows the patterns of CDD (maximum number of consecutive days with rainfall intensity  $< 1 \text{ mm day}^{-1}$ ). Both indices are averaged for NDJFM over the period 1998-2009 and obtained from GPCP, TRMM, CAM4 and RegCM4. Observation estimates locate the maximum CWD in the Katanga region and northwest areas of Madagascar whilst maxima of CDD appear around the Kalahari and Namibia Desert. For both indices the models reproduce the spatial patterns in the observations; however we find consistently that CAM4 overestimates CWD and underestimates CDD, again a reflection of the excessively high number of light rain days in the model. Similar results were found by [16], who have used CMIP5 data and found that most CMIP5 models represent poorly the dry and wet spell duration compared to reanalysis and HAdEX2 data. The RegCM4 values are much closer to satellite observations estimates for both indices, especially when comparing with TRMM. The main deficiencies in the RegCM4 simulation, clearly tied to the model's precipitation biases, are an overestimate of CWD over the eastern coastal regions as well across Madagascar and an overestimate of CDD over the north-western coasts of the domain (northward Angola). Finally, note in Fig. 3 that the CDD patterns in both GPCP and TRMM show high values along the "dry spell corridor" identified by [17], i.e. a region of high dry spell frequency extending across Southern Africa between about  $20^{\circ}\text{S}$  and  $25^{\circ}\text{S}$ . This corridor is also somewhat evident in the precipitation frequency plots. The models, and in particular RegCM4, reproduce this feature quite well.

### 3.2 Project early future change in extreme indices

What is of greater interest for this paper is the relation of mean change to changes in higher order statistics. The NDJFM projected change in mean precipitation and number of wet day frequency are presented in Fig. 4a-d. The patterns of change in mean frequency generally follow the changes in mean precipitation. We also note, however, that the areas of increased (decreased) frequency are less (more) extended than those of mean precipitation. This implies that the models show a trend towards a regime of less frequent events under global warming conditions, which is consistent with previous findings ([18]; [19]).

The NDJFM projected changes for the early future of CWD and CDD from CAM4 and RegCM4 are presented in Fig. 5a-d. Here we find a greater agreement across the two models, in that CWD shows a prevailing decrease, while CDD shows a prevailing increase, often also in areas where the precipitation frequency increases. This is an interesting result, because it shows that under global warming conditions precipitation events tend to organize in longer sequences of dry periods separated by shorter and more intense wet periods, as suggested by [19]. Although the reason for this is still unclear, [19] hypothesized that soil-precipitation feedbacks might be a factor in this shift of hydroclimatic regime. This result is also in agreement with the results of [20] who found from an analysis of CMIP5 models under three different RCPs scenario (RCP 2.6, RCP 4.5 and RCP 8.5) that Southern Africa is one of the regions which will undergo the strongest increase in CDD, indicating a future intensification of dry conditions. Finally, note that a prevailing increase in CDD is found in the dry spell corridor identified by [17], indicating increase in drought risk there.

## 4. SUMMARY AND CONCLUSIONS

In this paper we discussed a present day (1990-2009) and near future (2010- 2029) climate simulation over the southern Africa region conducted with the RCM RegCM4 (run at 25 km grid spacing) nested within the CAM4 global atmospheric model. The main focus of the analysis was on a series of extreme indices related to precipitation for the NDJFM wet season. Two daily satellite precipitation estimates datasets were used for the evaluation of the model performance in precipitation indices, GPCP and TRMM, i.e. a coarse and a fine resolution dataset, respectively.

Overall, the two models showed a generally quite good performance in simulating the precipitation indices, however the regional model showed a substantial improvements compared to the driving GCM in the simulation of indices related to frequency and duration of dry and wet events, particularly when comparing with the TRMM high resolution observations.

The change patterns were quite different in the driving and nested model, again an indication of the importance of the internal model physics. Although the patterns of change in extreme indices generally followed those for mean precipitation, some interesting responses were found. For both models, we found a dominant increase in length of dry periods, along with a decrease in frequency of events with an increase in the length of wet periods. This result supports the hypothesis of [19] that global warming might lead to a shift of the surface hydroclimatic regime towards conditions of more intense and less frequent events.

Overall, we found a reasonably good performance of the nested CAM4-RegCM4 system over the southern Africa domain. Therefore, we plan to use this modeling system to produce ensembles of future climate projections over the region under forcing from different scenarios of increased anthropogenic GHG concentrations.

## 5. ACKNOWLEDGEMENT

This research was funded under the project SOCOCA (Socioeconomic Consequences of Climate Change in sub-equatorial Africa, <http://www.mn.uio.no/geo/english/research/projects/sococa/index.html>), sponsored by the Norwegian research Council.

## 6. REFERENCES

- [1] Giorgi F., & Bi X. (2005), *Regional changes in surface climate interannual variability for the 21st century from ensembles of global model simulations*. Geophysical Research Letter 32: L13701. doi: 10.1029/2005GL023002.
- [2] Jury M.R. (2002), *Economic impacts of climate variability in South Africa and development of resource prediction models*. Journal of Applied Meteorology 41:46–55.

- [3] Diallo I., Sylla M.B., Giorgi F., Gaye A.T., & Camara M. (2012), *Multi-model GCM-RCM ensemble based projections of temperature and precipitation over West Africa for the early 21st century*. International Journal of Geophysics Article ID 972896. doi: 10.1155/2012/972896.
- [4] Diallo I., Bain C.L., Gaye A.T., Moufouma-Okia W., Niang C., Dieng M.D.B., & Graham R. (2014) Simulation of the West African monsoon onset using the HadGEM3-RA regional climate model. *Climate Dynamics*. doi: 10.1007/s00382-014-2219-0
- [5] Diallo I., Sylla M.B., Camara M., & Gaye A.T. (2013), *Interannual variability of rainfall over the Sahel based on multiple regional climate models simulations*. Theoretical and Applied Climatology. doi: 10.1007/s00704-012-0791-y.
- [6] Crétat J., Vizy E.K., & Cook K.H. (2013), *How well are daily intense rainfall events captured by current climate models over Africa?* *Climate Dynamics*. DOI: 10.1007/s00382-013-1796-7.
- [7] Gent P.R. & Co-author (2011), *The Community Climate System Model Version 4*. *Journal of Climate*. doi: 10.1175/2011JCLI4083.1.
- [8] Giorgi F., Coppola E., Solmon F., Mariotti L., Sylla MB., & Co-authors (2012), *RegCM4: model description and preliminary tests over multiple CORDEX domains*. *Climate Research* 52: 7-29. doi: 10.3354/cr01018.
- [9] Grell G., Dudhia J., & Stauffer D.R. (1994), *A description of the fifth generation Penn State/NCAR Mesoscale Model (MM5)*. National Center for Atmospheric Research Tech Note NCAR/TN-398 + STR, NCAR, Boulder, CO.
- [10] Diallo I., Giorgi F., Sukumaran S., Stordal F., & Giuliani G. (2014), *Evaluation of RegCM4 driven by CAM4 over Southern Africa: mean climatology, interannual variability and daily extremes of wet season temperature and precipitation*. *Theoretical and Applied Climatology* (under review).
- [11] Giorgi F., Marinucci M.R., Bates G., & DeCanio G. (1993), *Development of a second generation regional climate model (RegCM2). II. Convective processes and assimilation of lateral boundary conditions*. *Monthly Weather Review* 121: 2814–2832.

- [12] Huffman G.J., Adler R.F., Bolvin D.T, Gu G. & Co-authors (2007), *The TRMM multisatellite precipitation analysis: quasi-global, multi-year, combined-sensor precipitation estimates at fine scale*. Journal of Hydrometeorology 8: 38–55.
- [13] Huffman G.J., Adler R.F., Bolvin D.T., & Gu G. (2009), *Improving the global precipitation record: GPCP Version 2.1*. Geophysical Research Letter 36:L17808. doi:10.1029/2009GL040000
- [14] Engelbrecht F.A., McGregor J.L., & Engelbrecht C.J. (2009), *Dynamics of the Conformal-Cubic Atmospheric Model projected climate-change signal over southern Africa*. International Journal of Climatology 29: 1013-1033. doi: 10.1002/joc.1742
- [15] Frich P., Alexander L.V., Della-Marta P., Gleason B., Haylock M., Klein Tank A.M.G., & Peterson T. (2002), *Observed coherent changes in climatic extremes during the second half of the twentieth century*. Climate Research 19: 1993-212.
- [16] Sillmann J., Kharin V.V., Zhang X., Zwiers F.W., & Bronaugh D. (2013a), *Climate extreme indices in the CMIP5 multimodel ensemble: Part 1. Model evaluation in the present climate*. Journal of Geophysical Research-Atmospheres 118: 1716-1733. doi:10.1002/jgrd.50203.
- [17] Usman M.T., & Reason C.J.C. 2004. *Dry spell frequencies and their variability over southern Africa*. Climate Research 26: 199-211.
- [18] Trenberth K.E., Dai A., Rasmussen R., & Parsons D. (2003), *The changing character of precipitation*. Bulletin of the American Meteorology Society 84: 1205–1217.
- [19] Giorgi F., Im E.S., Coppola E., Diffenbaugh N.S., Gao X.J., Mariotti L., & Shi Y. (2011), *Higher hydroclimatic intensity with global warming*. Journal of Climate. 5309-5324. doi: 10.1175/2011JCLI3979.1.
- [20] Sillmann J., Kharin V.V., Zwiers F.W., Zhang X., & Bronaugh D. (2013b), *Climate extreme indices in the CMIP5 multimodel ensemble: Part 2. Future climate projections*. Journal of Geophysical Research-Atmospheres 118: 2473-2493. doi: 10.1002/jgrd.50188.

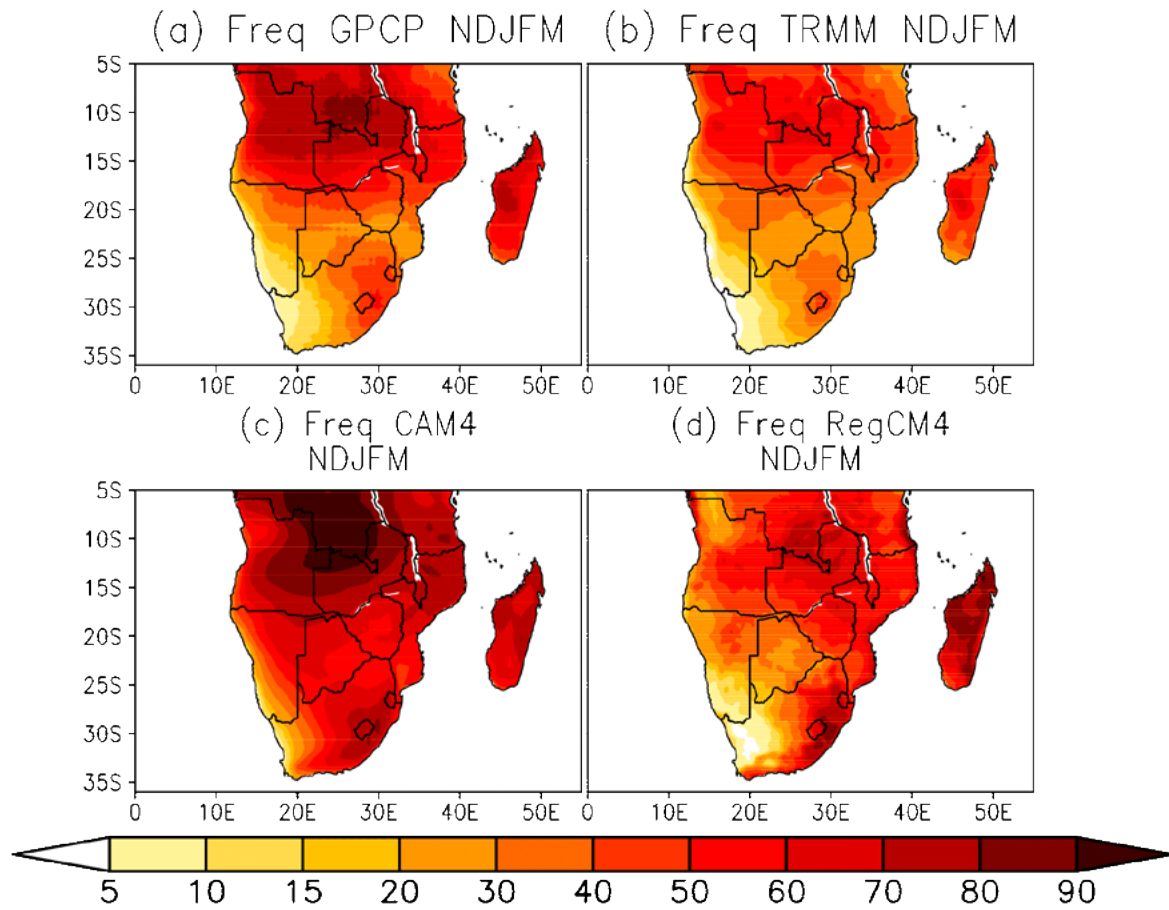


Fig. 1 Average NDJFM mean daily Frequency (in %) from (a) GPCP, (b) TRMM, (c) CAM4 and (d) RegCM4.

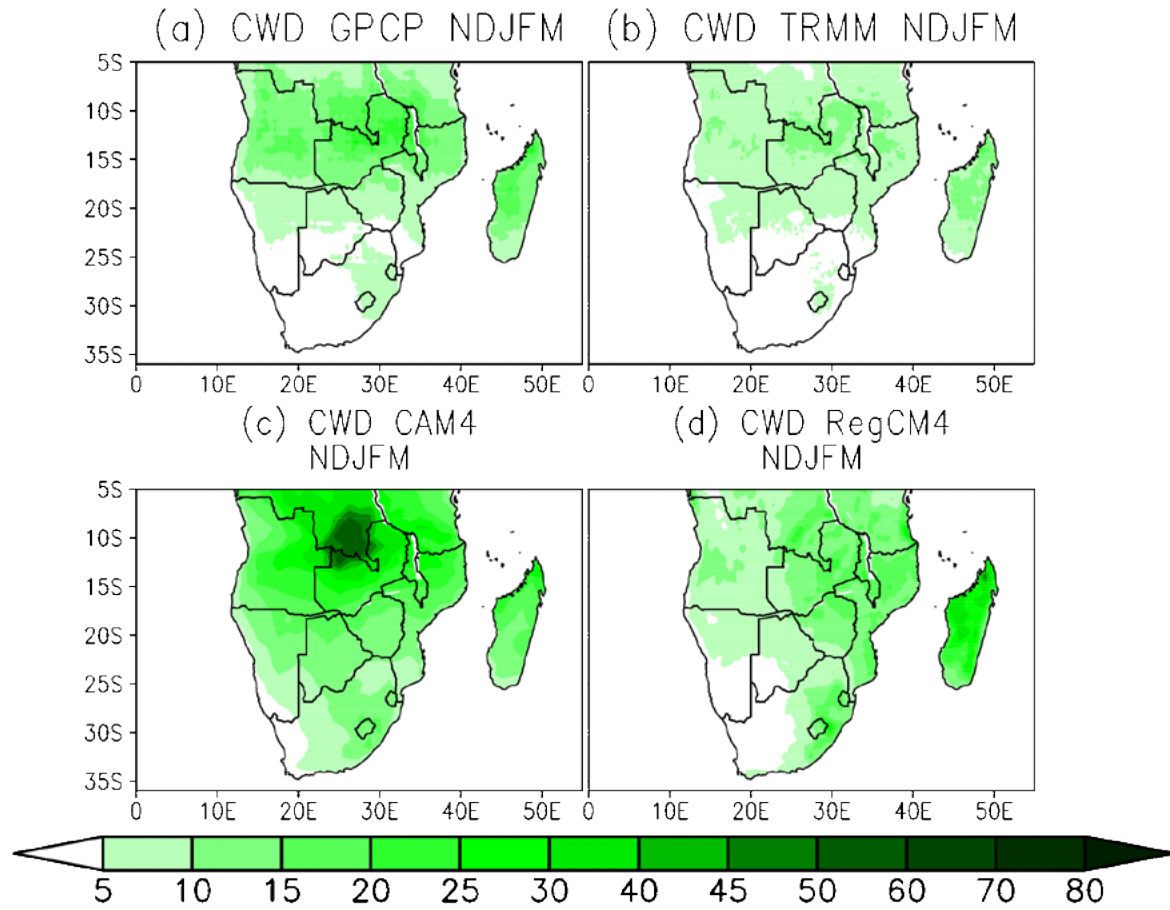


Fig. 2 Averaged NDJFM mean maximum wet spell length (CWD; in %) from: (a) GPCP, (b) TRMM, (c) CAM4, and (d) RegCM4.

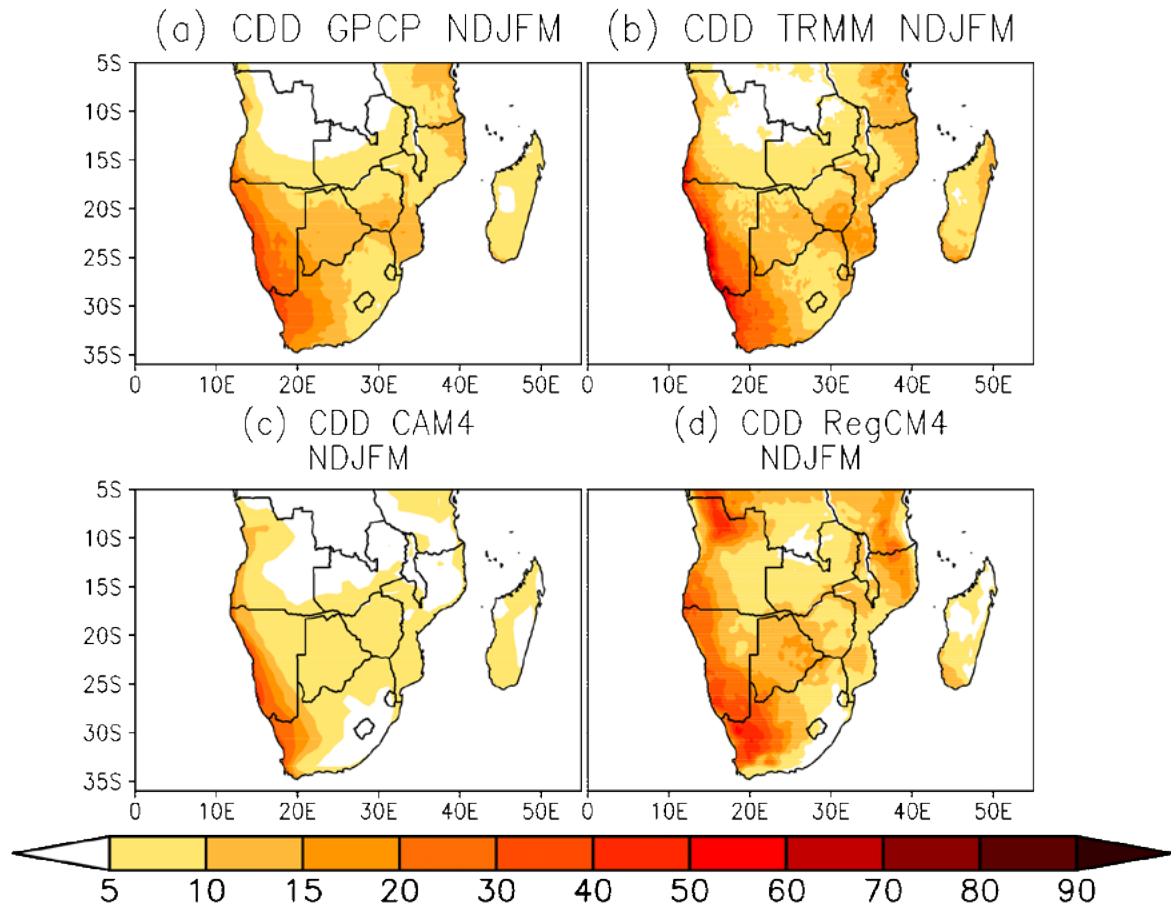


Fig. 3 Averaged NDJFM mean maximum dry spells length (CDD; in %) from (a) GPCP, (b) TRMM, (c) CAM4 and (d) RegCM4.

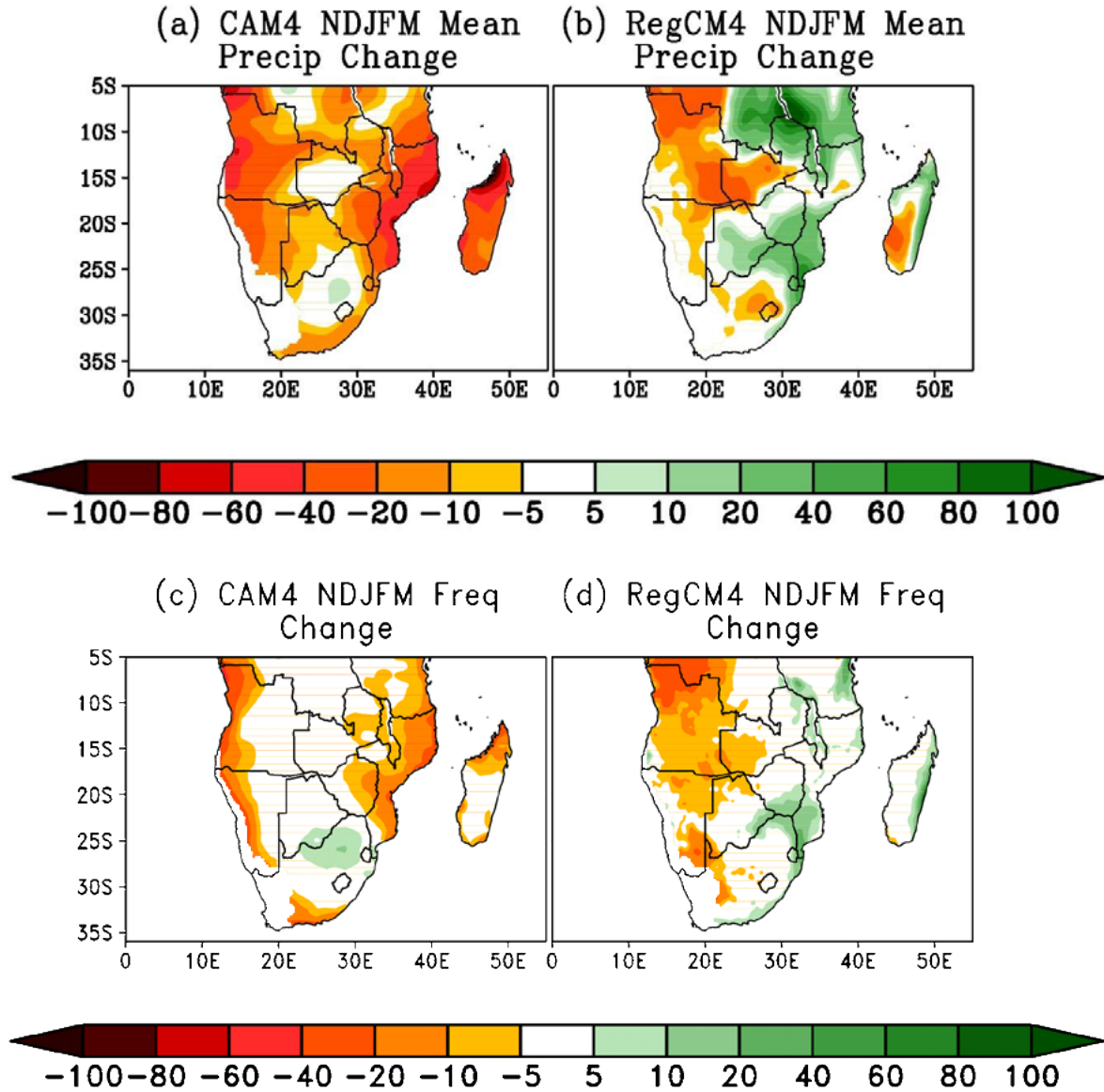


Fig. 4 Difference (RCP4.5 minus reference) in NDJFM mean daily precipitation (a, b; top panels) and mean daily frequency (c, d; bottom panels) from CAM4 (a, c) and RegCM4 (b, d) respectively. The change is expressed in percent with respect to the reference period (1990-2009).

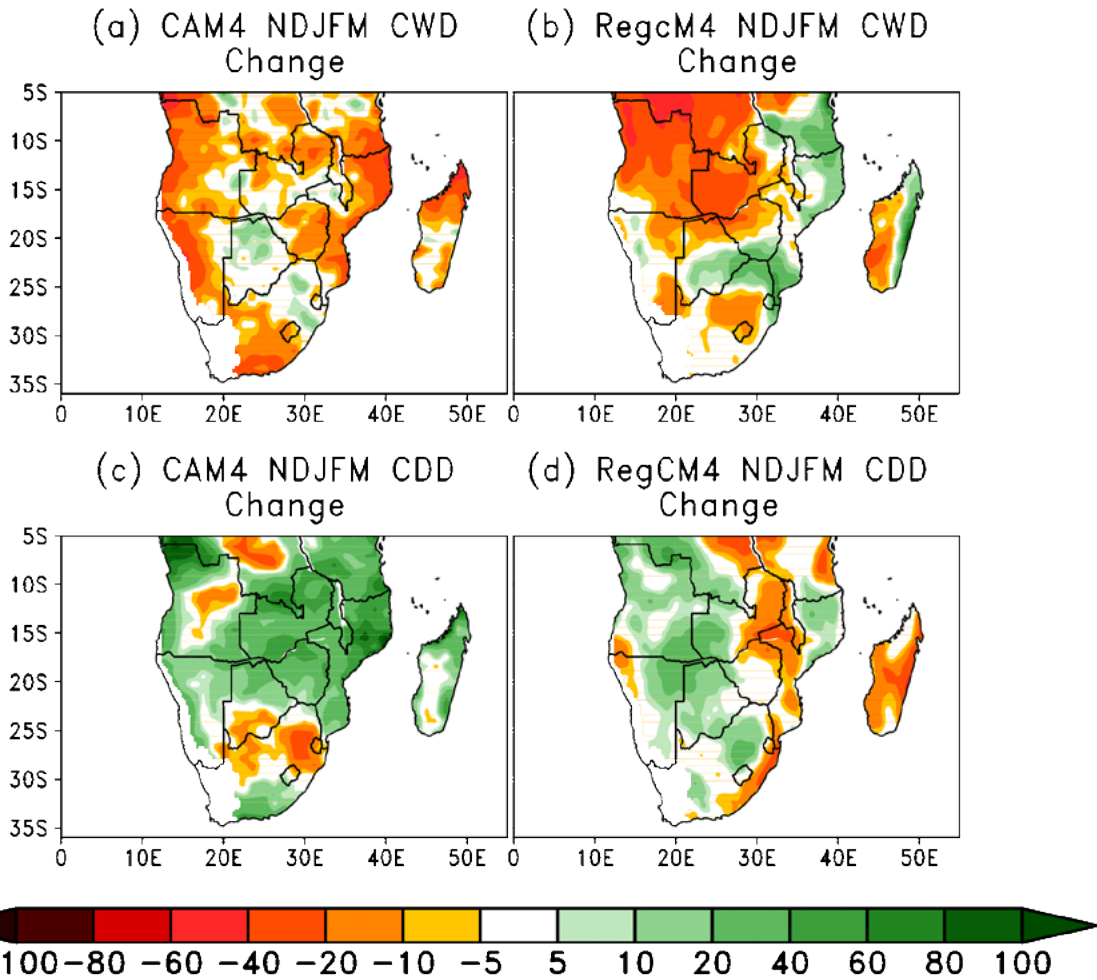


Fig. 5 Difference (RCP4.5 minus reference) in NDJFM maximum wet spells length (top panels) and maximum dry spells length (bottom panels) from CAM4 (a, c) and RegCM4 (b, d) respectively. The change is expressed in percent with respect to the reference period (1990-2009).

# Linking South Asian summer monsoon and eastern Mediterranean climate in CMIP5 simulations: performance and 21st century projections

Cherchi A.<sup>1\*</sup>, Annamalai H.<sup>2</sup>, Masina S.<sup>1</sup> and Navarra A.<sup>1</sup>

<sup>1</sup>Centro Euro-Mediterraneo sui Cambiamenti Climatici, and Istituto Nazionale di Geofisica e Vulcanologia - Italy, and <sup>2</sup>IPRC, University of Hawaii - US

\*Corresponding Author: [annalisa.cherchi@bo.ingv.it](mailto:annalisa.cherchi@bo.ingv.it)

## Abstract

Dry summers over the eastern Mediterranean are characterized by strong descent anchored by long Rossby waves, which are forced by diabatic heating associated with summer monsoon rainfall over South Asia (i.e. monsoon-desert mechanism). Our study evaluates the ability of the CMIP5 models in representing the physical processes involved in this mechanism. Despite large spatial diversity in monsoon heating, descent over the Mediterranean is coherently located and realistic in intensity. Column integrated heating over both the Bay of Bengal and Arabian Sea provides the largest descent in the eastern Mediterranean with the more realistic spatial pattern. Most models are able to capture the dominant role of horizontal temperature advection and radiative fluxes in balancing descent over the Mediterranean. The summer precipitation over South Asia is projected to increase in the 21st century. Contemporarily, over the Mediterranean the maximum of subsidence is projected to move westward, toward the center of the basin. Projected changes in mid-tropospheric meridional wind and horizontal temperature advection are consistent with the changes in subsidence, in agreement with the processes at the base of the monsoon-desert mechanism.

**Keywords:** monsoon-desert, Mediterranean, CMIP5, projections

The Mediterranean sector ( $30^{\circ}$ - $50^{\circ}$ N,  $20^{\circ}$ W- $60^{\circ}$ E) lies in a transition zone between the arid climate of North Africa and the wet climate of central Europe [1, 2]. In boreal summer (June through August) the region is characterized by descending motion, northerly surface wind, and mostly westerlies in the middle troposphere [1]. The subsidence over the eastern Mediterranean has been related to the tropical monsoon southeastward [3] through the “monsoon-desert mechanism”. In this theory, descent over the Mediterranean is a consequence of the interaction between westward propagating Rossby waves, which are generated by the diabatic heating associated with the summer monsoon rainfall in South Asia, and the mean westerly flow north of the region. Local diabatic enhancement, primarily through radiative cooling, contributes to enhancing the descent [4]. In future climate scenarios, the Mediterranean region has been identified as one of the most prominent “hot-spots”, with a large decrease in the mean precipitation during the warm season [5]. On the east, the projections of the South Asian summer monsoon indicate an increase of precipitation [6, 7, 8]. CMIP5 models’ projections provide enhancement of winter-wet and summer-dry rainfall seasonality, with a poleward shift of the Mediterranean climate zones [9].

In this study we want to verify if the coupled models participating in the Coupled Model Intercomparison Project phase 5 (CMIP5) are able to represent the teleconnection for correct reasons. Then considering the models with the better performance in the historical period, we look at the future to understand if the projected climate changes in the eastern Mediterranean could be, at least in part, ascribed to the monsoon-desert mechanism.

The Coupled Model Intercomparison Project phase 5 (CMIP5) database provides multi-century long simulations of state-of-the-art global coupled models [10]. Table 1 lists the models considered in this study. Monthly mean fields from the historical simulations for the period 1901-2004, as well as from the RCP4.5 future scenario are used. In the analysis of the historical period, the models’ results are compared with precipitation taken from the GPCP dataset [11], and other atmospheric fields taken from the ERA-40 re-analysis [12]. In the analysis of the future scenario, we considered the difference between the climatology of the end of the 21st century (i.e. 2069-2098, hereinafter 21C) and the climatology of the end of the 20th century (i.e. 1980-2004, hereinafter 20C). All the climatologies are based on boreal summer (i.e. JJA mean).

The monsoon-desert mechanism is analyzed at first in terms of omega at 500 hPa in the Mediterranean area and vertically integrated diabatic heating ( $Q_V$ ) over South Asia. Fig. 1a shows omega at 500 hPa between 20°W and 100°E averaged in 28°- 42°N and Fig. 1b shows the vertically integrated diabatic heating ( $Q_V$ ) between 60°E and the dateline averaged in 5°-25°N. Results from re-analysis shows that absolute descent occupies an extended area over the Mediterranean sector with maximum amplitude of about 2.5 hPa/hr (Fig. 1a, solid black line). Over the Mediterranean, individual models (Fig. 1a, colored marked lines) differ primarily in terms of intensity (range of maximum amplitude lies between 1.4 to 2.9 hPa/hr), but realistically reproduce longitudinal location of the maximum descent around latitudes 33°-35°N (not shown). In the monsoon region,  $Q_V$  is dominated by latent heating over deep convective areas. The longitudinal profile from reanalysis (Fig. 1b, black solid line) depicts multiple local maxima representative of deep convection over the Arabian Sea (~75°E), Bay of Bengal (90°-100°E), Southeast Asia (110°-140°E) and tropical west Pacific (~150°E). The multi-model mean (Fig. 1b, black long-dashed line) realistically captures the maxima over Bay of Bengal/Southeast Asia even though the intensity is much weaker than observed (about half of the observed intensity). The models are systematically weak in capturing the heating east of 130°E (Fig. 1b), colored lines with marks). Large spread in amplitude and longitudinal locations of  $Q_V$  maximum suggests the models' limitation in capturing important details of the monsoon [7].

Fig. 2a relates mid-tropospheric (500 hPa) summer mean omega over the eastern Mediterranean and  $Q_V$  over South Asia in terms of area averages: the scatter plot implies a quasi-linear relationship between the intensities of the diabatic heating over South Asia and that of omega over the eastern Mediterranean. Linear model solutions forced with diabatic heating that mimics the summer mean rainfall simulated by CMIP5 models suggest that the combined diabatic heating pattern over the Arabian Sea-Bay of Bengal regions exerts the largest descent over the eastern Mediterranean [13]. In response to heating centered either in the equatorial Indian Ocean or only over the Arabian Sea region, remote descent of varying intensities is simulated [13]. Given the existence of the monsoon-desert mechanism, we want to quantify the relative roles of temperature, moisture and radiative processes in shaping the descent over the eastern Mediterranean, and we apply the moist static energy (MSE) budget analysis follow-

ing [14]. The equation is:

$$\left\langle \frac{\partial m}{\partial t} \right\rangle = -\langle \mathbf{v} \cdot \nabla(c_p T) \rangle - \langle \mathbf{v} \cdot \nabla(Lq) \rangle - \left\langle \omega \frac{\partial m}{\partial p} \right\rangle + F_{rad} + LH + SH \quad (1)$$

where  $m$  is the moist static energy ( $m = c_p T + Lq + gz$ ),  $\mathbf{v}$  is the horizontal wind vector,  $c_p$  is the specific heat at constant pressure,  $T$  is temperature,  $L$  is the latent heat of evaporation,  $q$  is the specific humidity,  $\omega$  is the vertical velocity,  $F_{rad}$  represents the net column integrated radiative fluxes (as a combination of longwave and shortwave heating rates),  $LH$  and  $SH$  are surface latent and sensible heat fluxes, respectively. Angle brackets represent mass-weighted vertical integrals in the troposphere. All the terms in equation 1 are expressed in energy units ( $\text{W/m}^2$ ). The horizontal advection of dry enthalpy (i.e. second term on the right hand side of equation 1, hereinafter  $T_{adv}$ ) and the radiative fluxes ( $F_{rad}$ ) are the dominant contributors to the vertical advection of MSE (i.e. third term on the right-hand side of equation 1) over the eastern Mediterranean (not shown). If the contribution of horizontal temperature advection and radiative flux to MSE budget from reanalysis reflects “true” value (Fig. 2b, black square), then most CMIP5 models underestimate the contribution of  $T_{adv}$  while they overestimate that of  $F_{rad}$  in their respective budgets (Fig. 2b). This evidence of unrealistic contribution by adiabatic processes to the budget suggests that in some models systematic errors in diabatic processes mask the monsoon-desert mechanism.

As described in [13], the most important aspects of the “monsoon-desert” mechanism are latitudinal-longitudinal position of monsoon rainfall and associated vertical distribution of diabatic heating, descent intensity over the eastern Mediterranean, and related processes such as horizontal temperature advection and net radiative flux. For example, the scatter plots in Fig. 2 permits to estimate the models’ performance for some of them. While there are models that have realistic monsoon rainfall and vertical distribution of diabatic heating, relative contributions of  $T_{adv}$  and  $F_{rad}$  to MSE budget that determine descent intensity over the eastern Mediterranean differ considerably with those obtained from reanalysis. ERA-40 reanalysis budget terms also depend on model parameterizations, and is therefore subject to large uncertainties [15]. Within these constraints and combining the models’ performance, [13] have been able to identify few models, namely CCSM4, MIROC5, CMCC-CMS, GFDL-CM3, MPI-ESMLR, CMCC-CM and CESM1-CAM5, capable of representing the teleconnection for correct reasons. These few models are then used in the analysis of the RCP4.5 projections.

Compared to the summer mean climatology at the end of the 20th century (1980-2004), over South Asia the summer precipitation toward the end of the 21st century (2069-2098) is larger over the Indian subcontinent, in the Bay of Bengal and in the Nepal/Tibet areas, north of 25°N (Fig. 3a). Over the Arabian Sea and in the south eastern Indian Ocean there is a signature of decreased precipitation. The patterns of precipitation changes over South Asia related to anthropogenic carbon dioxide increase has been already described [6, 7]. Here we focus on the possible effects of these changes on the summer mean climate and variability over the subtropical regions in the west.

In the framework of the monsoon-desert mechanism and related processes, the regions over South Asia with the maximum increase in precipitation (i.e. Bay of Bengal and the area in the north) correspond to the regions where excitation of westward Rossby waves is favored [3, 13]. The projected changes in omega at 500 hPa indicates decrease of subsidence in the eastern part of the Mediterranean and increase in the west (Fig. 3b) implying a westward shift of subsidence. In particular, the models project a decrease of subsidence over Spain and the eastern Mediterranean/Middle East areas, but an increase in the northwestern Europe and in the central Mediterranean (Fig. 3b). Is the westward shift of the subsidence, at least in part, due to the monsoon forcing? To relate the projected changes in subsidence over the Mediterranean region to the projected changes in precipitation over South Asia, we need to investigate how the main fields and processes responsible of the monsoon-desert mechanism do change.

Descent is mostly promoted through horizontal temperature advection, and the projected changes in horizontal temperature advection (Fig. 4a) is consistent with the projected changes in subsidence (Fig. 3b). As previously discussed, the horizontal temperature advection is one of the dominant components of the MSE budget over the region in the summer mean of the 20th century climatology. In the 21C climatology and in the projected changes the relationship is maintained (not shown). In the central Mediterranean sector, the correspondence between the projected changes in subsidence and those of mid-tropospheric cross-contour flow (not shown) and horizontal temperature advection are indicative that the changes are consistent with the monsoon-desert mechanism, and are therefore associated with the projected increased

precipitation over South Asia.

To understand whether changes in the circulation or in the temperature are mostly responsible for the changes in the total horizontal temperature advection pattern we consider its decomposition as follows:

$$\langle \mathbf{v} \cdot \nabla T \rangle' = \langle \mathbf{v}' \cdot \nabla T^c \rangle + \langle \mathbf{v}^c \cdot \nabla T' \rangle + \langle \mathbf{v}' \cdot \nabla T' \rangle \quad (2)$$

where superscript  $'$  stands for the difference between 21st and 20th climatologies, and superscript  $^c$  stands for 20th century climatology. The first term on the right hand side of equation 2 represents the 20th century climatology temperature gradient advected by the projected wind anomalies, the second term is the anomalous temperature gradient advected by the 20C wind climatology and the last term represents the anomalous temperature gradient advected by the anomalous wind. The three terms are shown in Figs. 4b,c,d. In terms of intensity most of the changes are driven by the first two terms (Figs. 4b,c), while the third term (Fig. 4d) is much weaker, at least of one order. Equation 2 has a residual of the order of  $10^{-5}$ , thus negligible.

Considering the tripole structure depicted in Fig. 4a with the three maxima at  $12^\circ\text{W}$ ,  $15^\circ\text{E}$  and  $40^\circ\text{E}$ , we found that the anomalous wind advecting the climatological temperature gradient mostly provide the patterns in the west, while the climatological wind advecting the anomalous temperature gradient mostly provide the pattern changes in the east. In fact, the maximum vertically averaged changed in temperature is found in the eastern part of the domain (Fig. 4e) and the changes in the vertically averaged winds indicate also a tendency of intensification of the northerly flow and it is consistent with the previous discussion about maxima in subsidence differences (Fig. 3b). Again, the fact that the anomalous wind is mostly responsible for the changes in the horizontal temperature advection, particularly in the central Mediterranean, confirms the role of the monsoon-desert mechanism in shaping the changes.

Combining the results above we can summarize that a quasi-linear relationship exists between the intensities of diabatic heating over South Asia and descent over eastern Mediterranean, despite a large diversity in the precise location of simulated monsoon rainfall and associated  $Q_V$ . In particular, the combined diabatic heating pattern over the Arabian Sea-Bay of Bengal regions exerts the largest descent over eastern Mediterranean. CMIP5 models tend to underestimate the contribution due to adiabatic descent and to overestimate the contribution from radiative cooling, suggesting that lo-

cal diabatic enhancement in the models may play a more important role in determining the intensity of the descent. Statistical measures and budget diagnostics converge in the identification of a subset of models that are able to capture the monsoon-desert mechanism for correct reasons. In these models, the projected changes in subsidence over the Mediterranean can be related to the projected changes in rainfall over South Asia. The identification of these processes and the models' performance are favorable for the advances in climate sciences, including the understanding of these dynamical processes and their predictability.

## ACKNOWLEDGMENTS

We acknowledge the World Climate Research Programme's Working Group on Coupled Modeling, which is responsible for CMIP, and we thank the climate modeling groups (listed in Table 1 of this paper) for producing and making available their model outputs. For CMIP the U.S. Department of Energy's Program for Climate Model Diagnosis and Intercomparison provides coordinating support and led development of software infrastructure in partnership with the Global Organization for Earth System Science Portals. The financial support of the Italian Ministry of Education, University and Research, and Ministry for Environment, Land and Sea through the project GEMINA and that of INDO-MARECLIM (INCO.2011-7.3) coordination and support action are gratefully acknowledged.

## REFERENCES

- [1] Raicich F, Pinardi N, Navarra A (2003) Teleconnections between Indian monsoon and Sahel rainfall and the Mediterranean. *Int J Climatol* 23: 173–186
- [2] Giorgi F, Lionello P (2008) Climate change projections for the Mediterranean region. *Glob Planet Ch* 63: 90–104
- [3] Rodwell MJ, Hoskins BJ (1996) Monsoons and the dynamics of deserts. *Quart J Roy Meteor Soc* 122: 1385–1404
- [4] Rodwell MJ, Hoskins BJ (2001) Subtropical anticyclones and summer monsoons. *J Clim* 14: 3192–3211

- [5] Diffenbaugh NS, Giorgi F (2012) Climate change hotspots in the CMIP5 global climate model ensemble. *Clim Ch* 114: 813–822
- [6] Cherchi A, Alessandri A, Masina S, Navarra A (2011) Effects of increased CO<sub>2</sub> levels on monsoons. *Clim Dyn* 37: 83–101
- [7] Sperber K, Annamalai H, Kang IS, Kitoh A, Moise A, Turner A, Wang B, Zhou T (2012) The Asian summer monsoon: An intercomparison of CMIP5 vs CMIP3 simulations on the late 20th century. *Clim Dyn* 41: 2711–2744 DOI:10.1007/s00382-012-1607-6
- [8] Wang B, Yim SY, Lee JY, Liu J, Ha KJ (2013) Future change of Asian-Australian monsoon under RCP4.5 anthropogenic warming scenario. *Clim Dyn* DOI: 10.1007/s00382-013-1769-x
- [9] Alessandri A, De Felice M, Zeng N, Mariotti A, Pan Y, Cherchi A, Lee JY, Wang B, Ha KJ, Ruti P, Artale V (2014) Robust assessment of the expansion and retreat of Mediterranean climate in the 21st century. Submitted to *Scientific Reports*.
- [10] Taylor K, Stouffer R, Meehl G (2011) An overview of CMIP5 and the experiment design. *Bull Am Meteor Soc* 93: 485–498
- [11] Adler R and co-authors (2003) The version 2 global precipitation climatology project (GPCP) monthly precipitation analysis (1979-present). *J Hydromet* 4: 1147–1167
- [12] Uppala S and co-authors (2005) The ERA-40 re-analysis. *Quart J Roy Meteor Soc* 131: 2961–3012
- [13] Cherchi A, Annamalai H, Masina S, Navarra A (2014) South Asian summer monsoon and eastern Mediterranean climate: the monsoon-desert mechanism in CMIP5 simulations. Accepted on *J Clim*
- [14] Annamalai H (2010) Moist dynamical linkage between the equatorial Indian Ocean and the South Asian monsoon through. *J Atmos Sci* 67: 589–610
- [15] Black L, Bretherton C (2005) The relationship between wind speed and precipitation in the Pacific ITCZ. *J Clim* 18: 4317–4328

Table 1: List and basic characteristics of the CMIP5 coupled models used

Model name	Institute/Country	Exps
ACCESS1-3	CSIRO-BOM/Australia	20C
bcc-csm1-1	BCC/China	20C
CCSM4	NCAR/US	20C & RCP4.5
CESM1-CAM5	NCAR/US	20C & RCP4.5
CMCC-CM	CMCC/Italy	20C & RCP4.5
CMCC-CMS	CMCC/Italy	20C & RCP4.5
CSIRO-Mk3-6-0	CSIRO-OCCCE/Australia	20C
FGOALS-g2	LASG-CESS/China	20C
GFDL-CM3	NOAA-GFDL/US	20C & RCP4.5
GFDL-ESM2G	NOAA-GFDL/US	20C
HadCM3	MOHC/UK	20C
HadGEM2-AO	MOHC/UK	20C
inmcm4	INM/Russia	20C
IPSL-CM5A-MR	IPSL/France	20C
MIROC5	MIROC/Japan	20C & RCP4.5
MIROC-ESM	MIROC/Japan	20C
MPI-ESM-LR	MPI-M/Germany	20C & RCP4.5
NorESM1-M	NCC/Norway	20C & RCP4.5

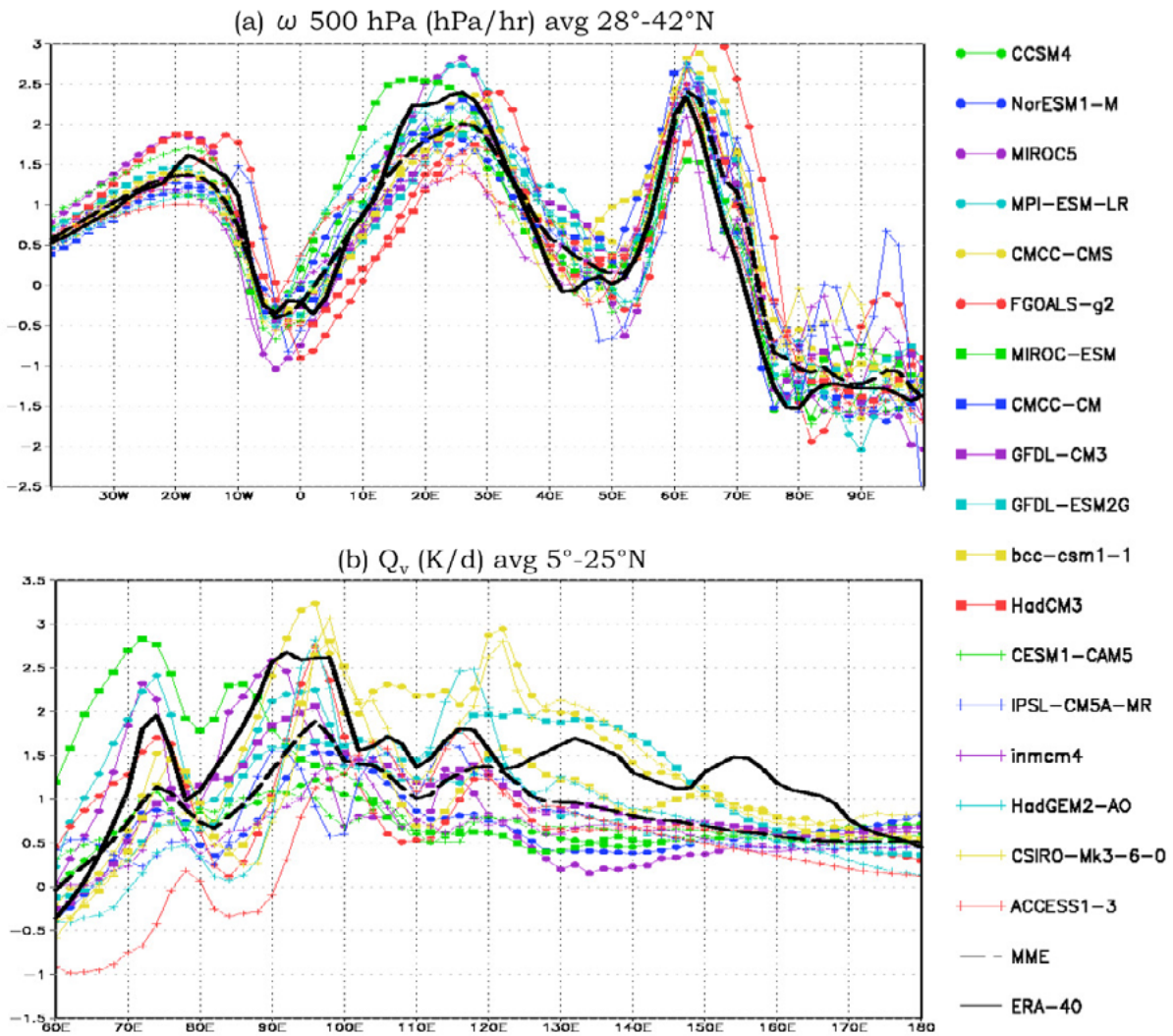


Fig. 1 JJA mean (a) omega (hPa/hr) at 500 hPa averaged in 28°-42°N and (b) mean vertically integrated diabatic heating ( $Q_v$ , K/d) averaged in 5°-25°N for ERA-40 (black solid line), individual models (colored lines with marks) and their mean (black dashed line).

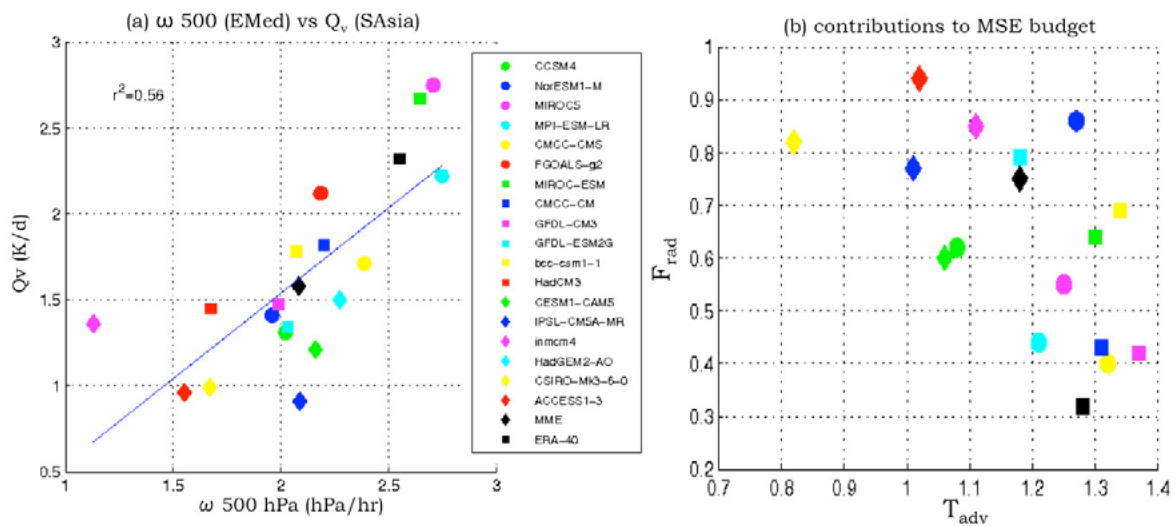


Fig. 2 Scatter plots of (a) JJA mean omega at 500 hPa ( $\omega_{500}$ ) in the eastern Mediterranean area (15 -35 E, 28 -42 N, EMed) and of vertically integrated diabatic heating ( $Q_v$ ) over south Asia (60 - 100 E, 5 -25 N) in terms of area averaged values (hPa/hr and K/d, respectively); (b)  $T_{adv}$  and  $F_{rad}$  in terms of their contribution to the vertical advection of MSE (see Equation 1) in the region 15 -35 E, 28 - 42 N. The blue solid line in panel (a) corresponds to the linear best fit, and the coefficient of determination ( $r^2$ ) is on the top-left corner of the panel.

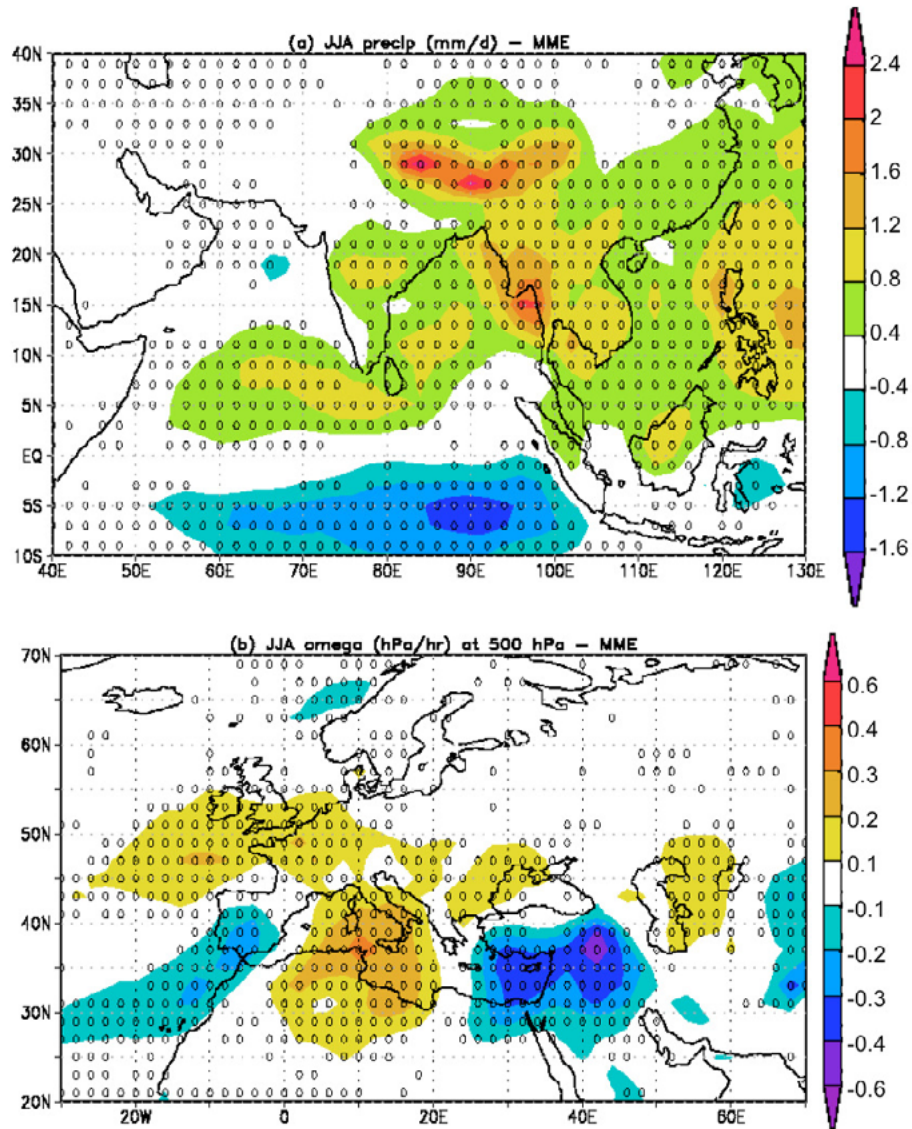


Fig. 3 Multi-model ensemble mean JJA 21C minus 20C climatologies of (a) precipitation (mm/d) and (b) omega (hPa/hr) at 500 hPa. Circle-marks indicate the grid-point where at least 2/3 of the models considered agree on the sign of the anomaly.

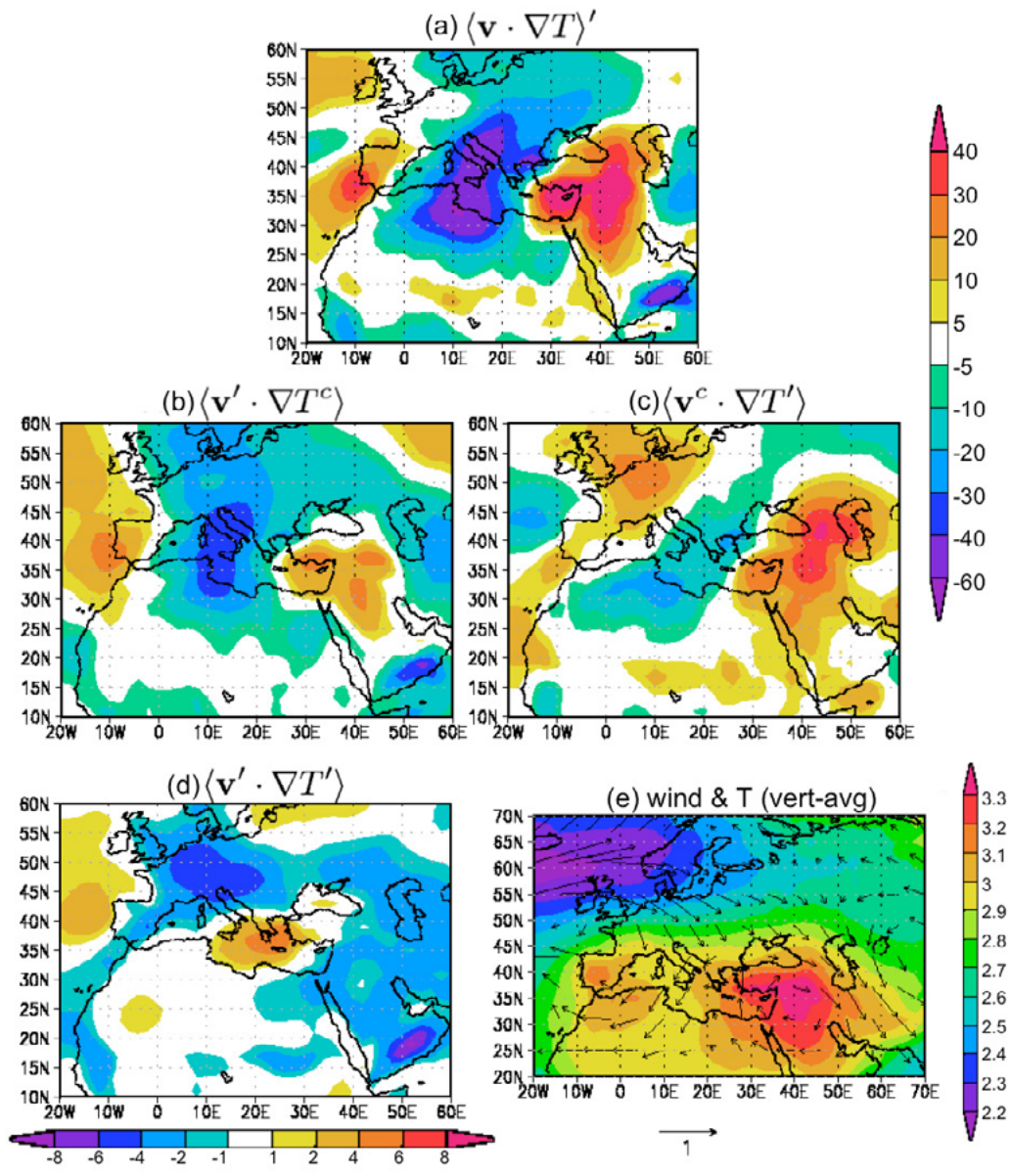


Fig. 4 Multi-model ensemble mean of JJA (a) 21C minus 20C vertically integrated horizontal temperature advection ( $W/m^2$ ) and (b,c,d) its decomposition as in equation 2. (e) is 21C minus 20C climatology of vertically averaged temperature (K, shaded) ad wind (m/s, vectors).

# A zonal view of atmospheric heat transport variability

Messori G.<sup>1,2\*</sup>, Czaja A.<sup>1</sup>

<sup>1</sup>Imperial College London - United Kingdom

<sup>2</sup>Stockholm University - Sweden

\*Corresponding Author: gabriele.messori@misu.su.se

## Abstract

The present study analyses large values (or pulses) of zonally integrated meridional atmospheric heat transport, due to transient eddies. The data used is the European Centre for Medium-Range Weather Forecasts ERA-Interim reanalysis data, at the 850mb pressure level and with daily, 0.7° latitude and longitude resolution.

The data displays a highly variable zonally integrated meridional heat transport. It is found that the large zonally integrated values do not result from a uniform increase of the transport around the whole latitude circle but, rather, that they are primarily driven by a limited number of very strong local transport events.

The existence of such pronounced variability in zonally integrated meridional heat transport can have important consequences for the energy balance of the high latitudes.

**Keywords:** heat transport, atmosphere, extreme events, reanalysis, variability

## 1. INTRODUCTION

As part of the vast body of literature dedicated to anthropogenic climate change, significant attention has been given to possible changes in meridional heat transport [e.g. 1, 2]. While there is some agreement on general trends, the transport magnitudes forecasted by models are extremely variable, for both pre-industrial and future scenarios [e.g. 2, 3]. Whether by design [e.g. 1], or due to the focus of the study [e.g. 4], the attention has often concentrated on zonally integrated, time-mean transport values.

The role of variability on sub-seasonal time-scales, and the associated modelling, has received comparatively little attention, although atmospheric heat transport has been shown to be highly sensitive to short-lived, very intense heat bursts. Swanson and Pierrehumbert [5] first highlighted the dependence of meridional atmospheric heat transport by transient motions on extreme events, by looking at three locations in the Pacific storm track. Messori and Czaja [6] generalised this conclusion by showing that, at any given location in the extra-tropical regions, only very few days every season, termed extremes, could account for over half of the net seasonal transport. Meridional heat transport by transient motions is therefore fundamentally sporadic in nature.

Both studies focussed on a local view of the transport, whereby the calculations were based on values at single data points. However, the preponderant role of the local extremes suggests that the atmospheric transport might still be characterised by a sporadic nature when a zonally integrated view is adopted. That is, the meridional transport might be modulated by strong zonal pulses, which would carry a significant amount of the net seasonal heat transport in a very short period of time. These could be due to the simultaneous occurrence of a large number of local extremes around a given latitude circle. We will refer to these hypothetical occurrences as “zonal extremes”. These zonal pulses, or extremes, could play a role in setting the mean seasonal zonally integrated transport value, much like the local extremes for single-gridbox transports. Anomalies in atmospheric heat transport magnitude and convergence can have severe impacts on the polar regions on sub-seasonal

timescales [7]. The existence of zonal extremes would therefore provide an important new perspective on the study of meridional heat transport under a changing climate.

If such extremes were indeed found to exist, the relevant questions to address would be how the local extremes relate to the zonal ones, how the frequency and intensity of zonal extremes is set to change in the future, and how this will influence the polar regions. The present paper will focus on the first of these questions, and aims to:

- i) Demonstrate that, in reanalysis data, the extremes do not exist solely in terms of local transport, but that there exist strong zonal pulses of meridional heat transport across a given latitude circle.
- ii) Show that the zonal pulses are partly driven by the synchronised occurrence of a large number of local extremes, and that this is consistent with the general features of atmospheric circulation in the mid-latitudes.

The analysis will focus on atmospheric poleward heat transport by time-dependent motions in the ERA-Interim dataset. While it is beyond the scope of the present study to extend this framework to the climate forecasts made by GCMs, it lays out the bases for an investigation on the subject. The discussion is centred on the largest zonally integrated values of meridional heat transport. It is shown that the top percentiles of the zonally integrated transport distribution are significantly different from other days and can therefore be considered as zonal extreme events. The focus is on the relationship between these zonal extremes and the local pulses.

The structure of the paper is as follows. Section 2 describes the data used and outlines the methodology. Section 3 looks at zonally integrated heat transport, with a focus on the nature and role of extreme events. A discussion of zonal versus local extremes, conclusions and scope for future research is presented in section 4.

## **2. DATA AND METHODS**

The present study utilises the European Centre for Medium-Range Weather Forecasts (ECMWF) ERA-Interim reanalysis data [8]. 0.7° latitude and longitude resolution, daily (1200 UTC) fields at 850mb are considered. The period taken into consideration spans from June 1989 to February 2011, thereby providing twenty-two

DJF (December, January and February) and twenty-two JJA (June, July and August) time series.

Transient-eddy heat transports are computed as a product of meridional velocity ( $v$ ) and moist static energy ( $H$ , hereafter also referred to as MSE) temporal anomalies between  $30^{\circ}\text{N}$  and  $89^{\circ}\text{N}$ , and  $30^{\circ}\text{S}$  and  $89^{\circ}\text{S}$ . The terminology “local event” simply refers to the transport value at a single reanalysis gridbox. When discussing local values, neither vertical nor zonal integrations are performed. On the opposite, zonally integrated values are computed by integrating each local  $v'H'$  value over the width of the gridbox it refers to. All the values around a given latitude are then summed to obtain the zonal integral of meridional heat transport. Again, no vertical integration is performed.

Taking the product  $v'H'$  for all data points and binning the values yields PDFs of local and zonally integrated transient-eddy meridional heat transport. The most likely value (MLV) of a PDF is defined as the central value of the bin with the highest frequency of events. Zonal and local extreme events are chosen as values of  $v'H'$  which exceed the 95<sup>th</sup> percentile of the respective distributions for the full hemisphere and time period considered. For further details the reader is referred to section 2 in Messori and Czaja [6].

### 3. THE ZONAL MEAN VIEW IN REANALYSIS DATA

The analysis of meridional heat transport distributions and extremes in the literature has primarily been performed on heat transport computed at single locations [e.g. 5, 6, 9]. The characteristics of the heat transport from a zonally integrated perspective have received less attention. By zonally integrated transport, what is intended here is simply the sum of all single grid box transport values around a given latitude circle, integrated over grid box width (see section 2 for further details).

As first step, we verify whether the top percentiles of the zonally integrated meridional heat transport PDFs in the ERA-Interim reanalysis data play any relevant role relative to the net seasonal transport. In constructing the PDFs, the integral of heat transport across a given latitude circle, on a given day, is treated as a single data point. In the interest of conciseness, the resulting distributions are only shown

for Northern Hemisphere (NH) DJF and Southern Hemisphere (SH) JJA [fig. 1a and 1b, respectively].

The PDFs are significantly different from the ones obtained by Messori and Czaja [6], which were constructed by treating transport at each gridbox as a single data point. For comparison, the single-point distribution for NH DJF is shown in [fig. 2], ([fig. 1c] in Messori and Czaja [6]). It can be immediately seen that the single-point distributions have a very pronounced MLV and a thin, extended positive tail. This tail accounts for a very small fraction of the overall data, but for a significant part of the net seasonal transport. These distributions also have a large skewness (3 for NH DJF).

The zonally integrated distributions shown in [fig. 1] still have a well defined MLV and long positive tails. However, these tails account for a much larger portion of the events than was seen in the single-point distributions. Furthermore, the skewness values are below 1, and the two hemispheres present radically different pictures. The MLVs of both hemispheres lie in the smallest positive bin of the respective distributions, with a lower bound at zero. The fact that both hemispheres have exactly the same MLV is simply due to the choice of plotting both distributions over the same bins.

Concerning the differences between hemispheres, the most striking one is the bimodality of the SH PDF. By splitting the distribution into two latitude bands ( $30^{\circ}$  -  $60^{\circ}$ S and  $60^{\circ}$  -  $89^{\circ}$ S, not shown), it becomes clear that the right-hand side peak is due to the lower latitudes and the left-hand side one to the higher latitudes. This is partly due to the lower frequency of extremes at higher latitudes: the pronounced near-zero MLV of the PDF is driven by the very high latitudes, where very few 850mb extremes are seen. The PDFs for NH JJA and SH DJF share the same qualitative features as their wintertime counterparts, albeit with some quantitative differences.

As is immediately evident from a visual assessment of the PDFs, the contributions of the top 5 percentiles to the overall integrals of the zonal distributions are significantly lower than those found in Messori and Czaja [6] for the local extremes. The contributions for the zonally integrated transport are shown in table I; depending on the season and hemisphere they range from 13.3% to 16.3%. The values for both i) the overall and ii) the poleward-only transports are shown. The values displayed are simply i) the percentage contribution of the selected events to the overall integral of

the distribution and ii) the percentage contribution of the selected events to the integral of the positive-only portion of the distribution. Since almost all of the zonally integrated transport values are positive, the two contributions are almost identical.

As a point of comparison, the last column in table I shows the contributions found in Messori and Czaja [6] for local extremes relative to the single-point PDFs. Compared to these, the contributions of the zonal case may seem extremely small. However, it is instructive to compare the latter to the weight of the events above the same numerical threshold in a Gaussian distribution. To obtain these values, Gaussian profiles with the same means and standard deviations as the zonal distributions are constructed. The portions of the Gaussian distributions above the numerical thresholds corresponding to the 95<sup>th</sup> percentiles of the re-analysis distributions are then selected, and their weight relative to the full integral of the Gaussians is computed as a percentage. The resulting values are shown in the third data column of table I, and are 3 to 5 times smaller than the values found for the actual reanalysis distributions. There is therefore some basis for calling the top percentiles of the zonally integrated transport distributions “zonal extremes”.

Having established that there is reason to discuss zonal extremes, the next pertinent question to address is how these zonal events might relate to the local extremes discussed in previous studies [5, 6, 9]. We consider the following three hypotheses concerning the origins of large values of zonally integrated heat transport:

- a) They are due to synchronised local extremes at several gridpoints around a given latitude. Namely, several single-gridbox extreme events occurring on the same day, at the same latitude.
- b) They are due to a larger than average transport across all longitudes, with no significant contribution from the local extremes. That is, to a generalised increase in the transport across large stretches of the latitude circle, without necessarily implying a higher than normal frequency of extreme events at fixed locations.
- c) A combination of points a) and b) above.

Since a large portion of the meridional heat transport in the mid-latitudes is driven by baroclinically unstable waves, it would be natural for large bursts to be spread over multiple longitudes (and not single unrelated points). In fact, a synoptic or mesoscale eddy will cover several gridboxes. In addition to this, several low pressure systems,

typically associated with large heat transports, can coexist around a given latitude circle, further strengthening hypothesis a). Hypothesis c) is essentially a relaxed version of a), and is therefore also plausible following the above arguments.

At the same time, Messori and Czaja [9] found that long length scales and time periods, beyond those typically associated with baroclinic motions, play an important role in the power spectrum of meridional heat transport by transient motions. This points to the possibility that a larger than average transport across a broad range of longitudes might also contribute to the zonal extremes. Hence, it is not possible to exclude *a priori* option b).

To test hypothesis a) robustly, one can first of all consider the fraction of days with no local extremes around a given latitude circle. For non-extreme zonal days, this corresponds to between 30% and 44% of the data points, depending on the hemisphere/season combination. Here, a data point refers to meridional transport integrated over a given latitude on a given day. For extreme zonal days, the values lie between 16% and 31%. For all season-hemisphere combinations, the values for the extreme zonal days are lower than those for the non-extreme ones. The fact that a significant portion of latitudes displaying zonal extremes do not correspond to any local extremes immediately suggests that perhaps hypothesis c) is a more appropriate interpretation than hypothesis a).

To further test hypothesis a), one can investigate what happens when there are local extremes at a given latitude. To this end, it is instructive to analyse the PDFs of the number of local extremes around a full latitude circle on days corresponding to zonal extremes and on all other days, excluding days/latitudes with no local extremes. If the PDFs for the extreme zonal days were to peak at significantly larger values than those for all other days this would suggest that, when local extremes are present, zonal extremes come about because of local extremes.

Panels a) and b) in [fig. 3] show the resulting PDFs for NH DJF and SH JJA, respectively. White bars correspond to data for zonal extremes, while grey bars correspond to data for all other days. For NH DJF [fig. 3a], the zonal extremes PDF's MLV and mean are both larger than the non-extreme PDF's ones by a factor of approximately three and two respectively. The distributions for SH JJA [fig. 3b], NH JJA and SH DJF (not shown) present a very similar pattern. In all four

hemisphere/season combinations, the PDFs for extreme and non-extreme zonal days are statistically different under a two-sample Kolmogorov-Smirnov test.

Hypothesis a) above would imply that the two PDFs have almost no overlap, since local extremes would be the only drivers of zonal ones. On the opposite, hypothesis b) would correspond to approximately equal PDFs for both extreme and non-extreme zonal days. Even though the distributions in [fig. 3] are statistically different, there is still considerable overlap between them. In physical terms, we therefore interpret the above results as corresponding to a background flow-driven scenario, with a contribution from the increased number of local extreme events (hypothesis c). This is in agreement with the speculations made above concerning mid-latitude baroclinic systems. The zonal heat transport is therefore characterised by a *weak synchronisation* effect, whereby zonal extremes do, in part, result from synchronised local extremes, but they have a much weaker impact on the overall transport distribution than their single-point counterparts.

#### 4. DISCUSSION AND CONCLUSIONS

The present paper examines zonally integrated meridional atmospheric heat transport due to transient eddies, focussing on low levels in the mid and high latitudes. Previous studies have already shown that the local transport is discontinuous in nature, and is very sensitive to a few extreme events every season [5, 6, 9]. Here, it is shown that a similar picture can be applied to the zonal view.

The reanalysis data indeed shows that the zonally integrated transport is modulated by large pulses, which account for a sizeable portion of the net seasonal transport. These are found to be partly due to numerous local extremes occurring simultaneously around a given latitude circle. However, the zonal events also have a significant contribution from increased transport at non-extreme locations. This suggests that scales larger than those associated with the extremes act to enhance the transport over wide areas of the latitude circle. Such inference is in agreement with the results of Messori and Czaja [9], who found that long length scales and time periods, beyond those typically associated with baroclinic motions, play an important role in the power spectra of meridional heat transport by transient motions. The importance of larger scales has also been discussed by Wen and Ronghui [10].

The percentage contributions of zonal extreme events to the net zonally integrated meridional heat transport are significantly lower than those found for local extremes in Messori and Czaja [6]. They are still, however, 3 to 5 times larger than those found for Gaussian distributions with the same means and standard deviations as the transport PDFs.

Both hemispheres display a pronounced variability on a zonally integrated level, which translates into the existence of zonally integrated transport extremes. The existence of such extremes is very significant for the energy balance of the high latitudes. The last decade has seen unprecedented sea-ice loss in the arctic basin, which has been underestimated by almost all climate models [11]. There are studies suggesting that anomalous atmospheric heat transport convergence at high latitudes, driving local long-wave forcing, could be playing a significant role in this process [7]. A more systematic analysis and modelling of the variability of zonally integrated meridional heat transport, and a study of the possible changes in variability resulting from climate change, would therefore be crucial in order to better understand the future of the polar regions.

## **5. ACKNOWLEDGMENTS**

While carrying out this work, G. Messori was funded by a bursary from the National Environment Research Council. ERA-Interim reanalysis data were obtained from the BADC ftp server at <ftp.badc.rl.ac.uk>.

## 6. REFERENCES

1. Hwang Y-T. & Frierson D.M.W. (2010), *Increasing atmospheric poleward energy transport with global warming*, Geophys. Res. Lett., No. 37: L24807, DOI: 10.1029/2010GL045440
2. Zelinka M.D. & Hartmann D.L. (2012), *Climate Feedbacks and their Implications for Poleward Energy Flux Changes in a Warming Climate*, J. Climate, No. 25, pp. 608–624.
3. Donohoe A. & Battisti D.S. (2012), *What determines meridional heat transport in climate models?*, J. Climate, No. 25, pp. 3832-3850.
4. Alexeev V.A., Langen P.L. & Bates, J.R. (2005), *Polar amplification of surface warming on an aquaplanet in “ghost forcing” experiments without sea ice feedbacks*, Clim. Dyn., No. 24.7-8, pp. 655-666.
5. Swanson K.L. & Pierrehumbert R.T. (1997), *Lower-tropospheric heat transport in the Pacific storm track*, J. Atmos. Sci., No. 54, pp. 1533–1543.
6. Messori G. & Czaja A. (2013), *On the sporadic nature of meridional heat transport by transient eddies*, Q. J. R. Meteorol. Soc., DOI: 10.1002/qj.2011
7. Graverson R.G., Mauritsen T., Drijfhout S., Tjernström M. & Mårtensson S. (2011), *Warm winds from the Pacific caused extensive Arctic sea-ice melt in summer 2007*, Clim. Dyn., No. 36.11-12, pp. 2103-2112.
8. Simmons A., Uppala S., Dee D. & Kobayashi S. (2006), *ERA-Interim: New ECMWF reanalysis products from 1989 onwards*, ECMWF Newsletter, No. 110, pp. 25–35.
9. Messori G. & Czaja A. (2014) *Some considerations on the spectral features of meridional heat transport by transient eddies*, Q. J. R. Meteorol. Soc., DOI: 10.1002/qj.2224
10. Wen C. & Ronghui H. (2002), *The propagation and transport effect of planetary waves in the Northern Hemisphere winter*, Advances in Atmospheric Sciences, No. 19.6, pp. 1113-1126.
11. Stroeve J., Holland M.M., Meier W., Scambos T. & Serreze M. (2007), *Arctic sea ice decline: Faster than forecast*, Geophysical research letters, No. 34(9).

## 7. IMAGES AND TABLES

### Contribution of extreme events to meridional atmospheric heat transport in the ERA-Interim Reanalysis

Hemisphere	Season	Zonal integration % weight			Local events % weight
		Net	Poleward-only	Gaussian Equivalent	Net
N	DJF	16.2	16.0	3.00	56.8
	JJA	15.2	15.1	3.03	61.5
S	DJF	16.3	16.3	3.31	53.3
	JJA	13.3	13.3	4.63	43.5

Tab. 1 Percentage contribution of the top five percentiles of  $v'H'$  events in DJF and JJA to net and poleward-only meridional atmospheric heat transport due to transient eddies. The data cover the 850 mb level at all latitudes from 30°N to 89°N and from 30°S to 89°S. The first three data columns refer to zonally integrated values. The last column to single-gridbox values. The zonal analysis covers the period June 1989-February 2011. The local analysis the period December 1993-August 2005. The "Gaussian Equivalent" column indicates the contribution of events above the same numerical thresholds as the zonal extremes, relative to Gaussian distributions with the same means and standard deviations as the reanalysis distributions.

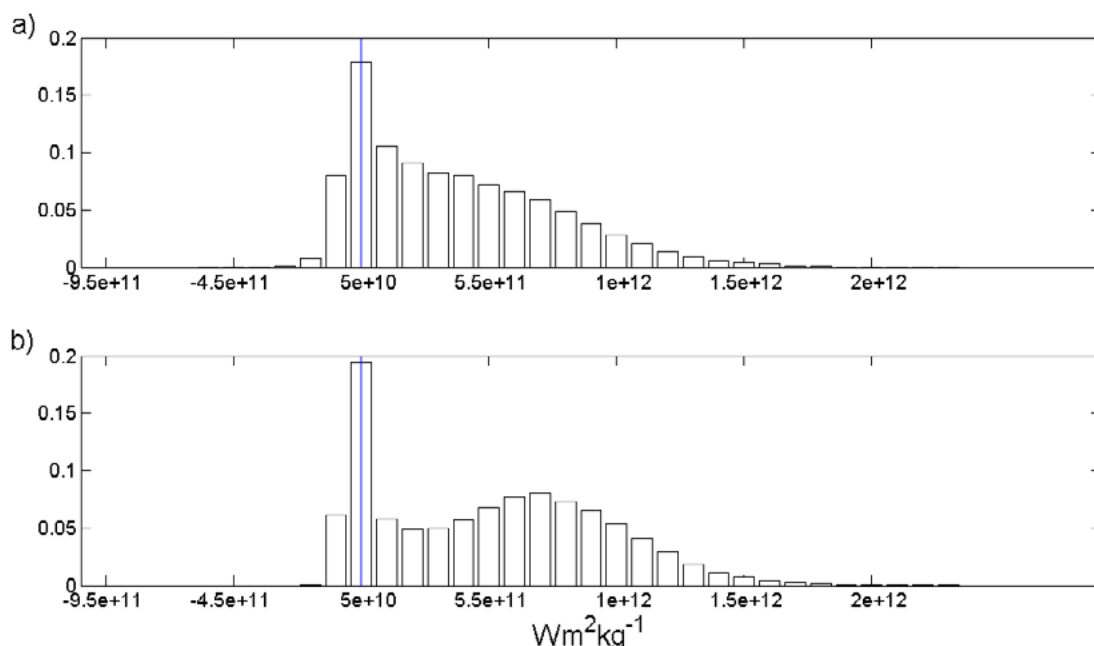


Fig. 1 PDFs of zonally integrated atmospheric heat transport due to transient eddies for a) NH DJFs and b) SH JJAs. Both PDFs are plotted over the same bins. The data cover the 850 mb fields from June 1989 to February 2011. All latitude circles between 30° and 89°N and S are taken into account. The skewnesses of the PDFs are a) 0.83 and b) 0.34. The corresponding most likely values are a)  $5.0 \times 10^{10} \text{ Wm}^2\text{kg}^{-1}$  and b)  $5.0 \times 10^{10} \text{ Wm}^2\text{kg}^{-1}$ . The vertical lines show the bins corresponding to the most likely values.

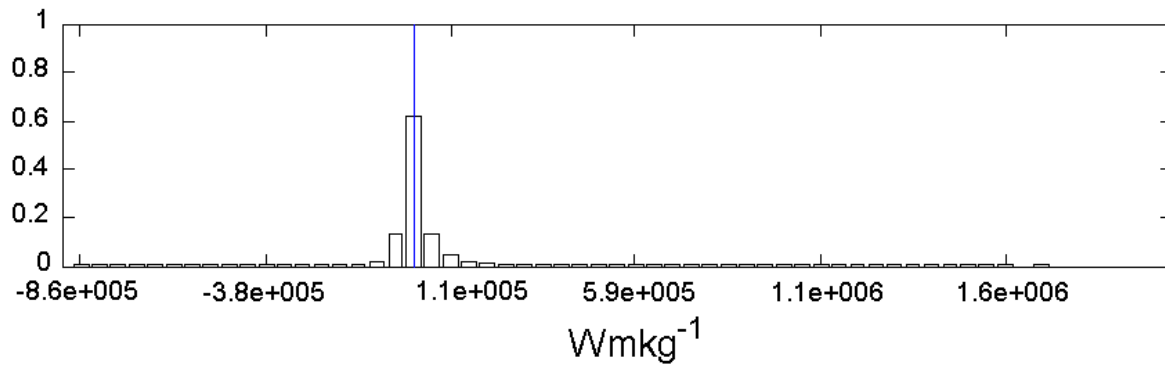


Fig. 2 PDF of atmospheric heat transport due to transient eddies. The data cover the 850 mb fields for NH DJFs, from December 1993 to February 2005. All latitudes between 30° and 89°N are taken into account. The skewness of the PDF is 3.00. The corresponding most likely value is  $9.9 \times 10^3 \text{ Wmkg}^{-1}$ . The vertical line shows the bin corresponding to the most likely value. This figure has been previously published as [fig. 1c] in Messori and Czaja [6].

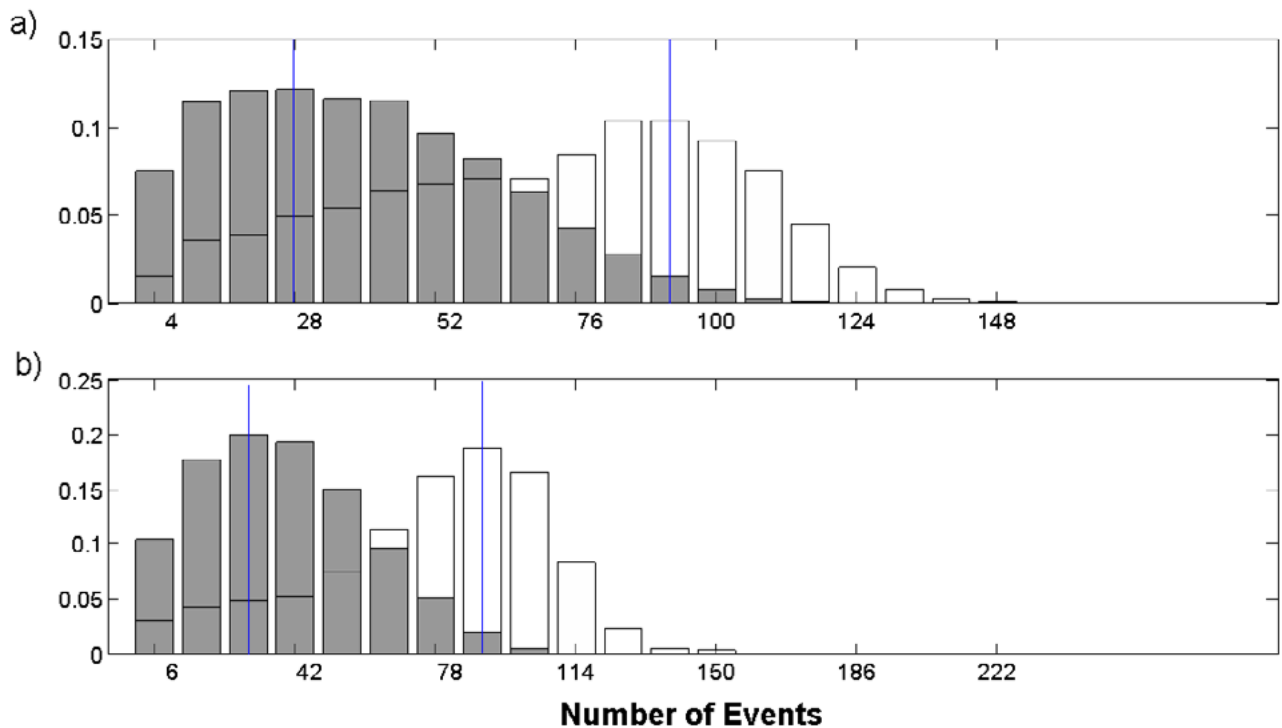


Fig. 3 PDFs of the number of local extreme events around a full latitude circle for days which are in the top 5% (white) and days which are in the bottom 95% (grey) of the distributions of the zonally integrated atmospheric heat transport due to transient eddies. The PDFs cover a) NH DJF and b) SH JJA data. The data range is the same as in figure 1. Only days/latitudes with at least one local extreme are considered. The most likely values are respectively a) 92 (extremes, in white) and 28 (non-extremes, in grey) and b) 90 and 30. The corresponding means are respectively a) 71 and 39 and b) 76 and 38. The vertical lines show the bins corresponding to the most likely values.

Advances in climate change

**Climate variability &  
climate change II**

# Turbulence Regimes deduced from the analysis of observed and modeled global ocean data

Nilsson J. A. U.<sup>1</sup>, Doos K.<sup>2</sup>, and Artale V.<sup>3</sup>

<sup>1</sup>Formerly at UTMEA-CLIM, ENEA, Rome, Italy, <sup>2</sup>Department of Meteorology/Physical Oceanography (MISU), Stockholm University, Stockholm, Sweden, and <sup>3</sup>UTMEA, ENEA, Rome, Italy

\*Corresponding Author: [vincenzo.artale@enea.it](mailto:vincenzo.artale@enea.it)

## Abstract

Following the work on Lagrangian diffusion undertaken by V. Rupolo, a large-scale tool for systematic analyses of the dispersal and turbulent properties of observed ocean currents and the subsequent separation of dynamical regimes according to the prevailing trajectories taxonomy in a certain area is presented in this study, this methodology has been extended to the analysis of model trajectories obtained by analytical computations of the particle advection equation using the Lagrangian open source software package Tracing the Water Masses of the North Atlantic and the Mediterranean (TRACMASS), and inter-comparisons have been made between the surface velocity fields from three different configurations of the global Nucleus for European Modelling of the Ocean (NEMO) ocean/sea ice general circulation model. This study aims, moreover, to shed some light on the relatively unknown turbulent properties of near-surface ocean dynamics and their representation in numerical models globally and in a number of key regions (Agulhas leakage). These results could be of interest for other studies within the field of turbulent eddy diffusion parameterization in ocean models or ocean circulation studies involving long-term coarse-grid model experiments.

**Keywords:** Global ocean circulation, Lagrangian diffusion

## 1. INTRODUCTION

Rupolo 2007a,b identified the utility of the relationship between the time scale of acceleration and that of the velocity of Lagrangian trajectories, and classified these trajectories into four homogenous classes according to their correlation and dispersion properties, this classification is better known as trajectories taxonomy. These works clearly highlights the role of ocean coherent structures in defining time scales for the diffusion of, for example, a tracer, as well as developing methods of Lagrangian analysis for identifying the average trend of ocean currents. He showed that the Lagrangian time scales could be obtained from the inverse use of Lagrangian Stochastic Models (LSMs; e.g., Veneziani et al. 2004), proposed a screening method for rationalizing the data analysis using the time-scale relationships, and successfully applied it to both drifter and Argo float observations. In the present study, his data analysis methods have been extended to study and evaluate trajectories from both surface drifters and an ocean general circulation model (OGCM) with different grid resolutions. Indeed the main scope of this study is to evaluate the representation of near-surface dynamics in non eddy-permitting ( $1^\circ$ ), eddy-permitting ( $1/4^\circ$ ), and eddy-resolving ( $1/12^\circ$ ) OGCM configurations by means of the Rupolo screening technique (Rupolo 2007a), and thereafter compare the outcome with the corresponding results from 20 years of observed drifter tracks. The manuscript is outlined as follows: section 2 provides an overview of the theoretical framework of this study, section 3 describes the drifter observations and the synthetic trajectory datasets, section 4 presents and discusses the results, and finally section 5 offers some conclusions.

## 2. METHODOLOGY

This section will serve as a summary of the theoretical considerations presented in the study by Rupolo (2007a), and these results will subsequently be applied to trajectory data in a standard Lagrangian framework (cf. LaCasce 2008). The trajectories taxonomy will be specified in order to facilitate the identification of the turbulence regimes in the vicinity of the observed and modeled drifter tracks. For more details about the theoretical background used in this papers see Nilsson et al. (2013). The “Rupolo ratio” is defined as the following acceleration and velocity timescale ratio for each trajectory:

$$\gamma_R = T_a/T_v.$$

This ratio, as proposed by Rupolo (2007a) has proven to be a powerful large-scale tool for the separation and categorization of ocean trajectories associated with different dynamical regimes. In his study, the dynamical characteristics of trajectories adhering to different intervals of the Rupolo ratio ( $0 \leq \gamma_R \leq 1$ ) were described and four dynamical classes were identified, hereafter referred to as “Rupolo classes.” The trajectories in each Rupolo class share features in terms of shape, velocity correlation properties, and the relationships between EKE and Lagrangian correlation length scales. Ocean turbulence covers a wide range of dynamical features, from large-scale low-frequency motions to small-scale high-frequency whirls, and an attempt will be made to accommodate the observed and modeled trajectories in these Rupolo classes (cf. Table 1). The Rupolo ratio can be interpreted as a geometric factor; when it is close to zero and the acceleration is not resolved, the trajectories are characterized by jagged motion, as the particles suddenly change direction, while the  $\gamma_R$  ratio is near one when the acceleration is resolved and the motion is thus much smoother.

The Class-I trajectories ( $0 \leq \gamma_R \leq 0.2$ ) are described by large-scale motions influenced by high-frequency variability in the velocity fields. The Class-II data ( $0.4 \leq \gamma_R \leq 0.8$ ), on the other hand, show intermediate flow characteristics, such as meandering around low-frequency large-scale structures (i.e., around Class-I data), though they appear to be less influenced by high-frequency motions. The low-frequency motions are typically characterized by geostrophic turbulence and are here described in terms of both Class-III and Class-IV data. The Class-IV trajectories ( $\gamma_R = 1$ ,  $\gamma_{osc.} > 1$ , where  $\gamma_{osc.}$  is the non-dimensional parameter computed by the ratio between the oscillatory and the memory time scales, Nilsson et al., 2013) are characterized by coherent structures of rapid whirls, typically trapped in eddies with determined length scales, and are often surrounded by Class-III trajectories ( $\gamma_R = 1$ ,  $\gamma_{osc.} < 1$ ) that meander between eddies of different sizes in a less energetic turbulent background field, showing only sporadic looping features. Given the fact that looping and non-looping trajectories are often found side by side (cf. Veneziani et al. 2004), an objective separation of trajectories in Rupolo classes is recommended before detailed investigations of the local near-surface ocean dynamics can be undertaken. In what

follows, we have adopted the taxonomy separation method to both observed drifter data and synthetic trajectories obtained from offline integrations of model velocity fields.

### 3. MODEL AND OBSERVATIONAL DATASETS

For the purpose of comparing two-dimensional Lagrangian trajectories from drifter observations with surface-velocity-field output from global OGCMs, an open-source Lagrangian trajectory code [Tracing the Water Masses of the North Atlantic and the Mediterranean (TRACMASS)] was set up for the different OGCM grid resolutions for subsequent integration of synthetic trajectories. Surface drifter data (Lumpkin and Pazos 2007) were collected and processed by the Atlantic Oceanographic and Meteorological Laboratory (AOML) under the Global Drifter Program, formerly World Ocean Circulation Experiment–Surface Velocity Programme (WOCE-SVP). The observed datasets are kindly made available from 1979 to the present through the Integrated Science Data Management (ISDM) system (<http://www.meds-sdmm.dfo-mpo.gc.ca/isdm-gdsi/drib-bder/svp-vcs/index-eng.asp>). In the present study, observed drifter data were gathered for a 20-yr period (January 1991–December 2010) and ordered in continuous non overlapping 64-day segments. In total, 46.136 of these were stored for analysis. The drifter positions in these trajectory segments were smoothed by a horizontal boxcar filter in order to reduce signals from inertial and sub inertial motions, which is common practice in mesoscale studies. The ocean velocity fields were obtained from fully prognostic configurations of the global Nucleus for European Modelling of the Ocean (NEMO), an ocean–sea ice general circulation model (Madec et al. 2012), and the model experiments were forced using the bulk method along with 6-hourly atmospheric fields of the so-called Drakkar Forcing Set, version 4 (DFS4). The horizontal resolution of the model configurations varies from coarse ( $1^\circ$ ; ORCA1, where ORCA stands for Oceanic Remote Chemical Analyzer) to finer eddy-permitting ( $1/4^\circ$ , ORCA025) and eddy-resolving ( $1/12^\circ$ , ORCA12) grids (cf. Table 2). Finally, the synthetic Lagrangian trajectories were calculated from the modeled Eulerian velocity fields by 64-day long integrations of the particle advection equation, starting at the observed initial positions of each observed drifter segment. Due to the fact that there was not access to 20 years of model fields for the three configurations, a seeding strategy that would yield a

reasonable global coverage of synthetic trajectories was applied for the initialization of the TRACMASS software. This technique (full seed) implied seeding in all drifter-segment start positions (collected during the period 1991–2010) on their correct days and months, but during one random model year rather than on the actually observed year. This method could be regarded as valid under the assumption that the dispersal properties of the surface trajectories would not vary crucially between one year and another.

#### 4. RESULTS AND DISCUSSION

The results to be presented here aim, in particular, to highlight the scale dependence of synthetic surface trajectories and how their dispersal properties vary with the spatial and temporal resolution of the model velocity fields from which these are computed. The quality of the model surface velocity fields were, moreover, evaluated and to some extent validated by the comparisons made between the observed and synthetic drifter tracks.

##### *4.1 Lagrangian statistics at global scale.*

Sensitivity tests were undertaken to estimate the differences in the model-derived Lagrangian statistics from a long-term period (11 years; exact seed) compared to a random year (1997 and 1999; full seed); the choice of years being dictated by the availability of the model velocity fields (cf. Table 3)

The outcome from the exact- and full-seed techniques using the ORCA025–5d model fields were compared to observations, and the estimated time scales and their corresponding variances (cf. Table 3) were found to be similar, and, moreover, showing nearly twice as large model values as those observed, in agreement with previous results due to Doos et al. (2011). Thus, it was concluded that the less costly (in terms of CPU time and storage demand) full-seed method was capable of providing reliable results and could be applied in the forthcoming Lagrangian analyses. From this first standard Lagrangian analysis, it can be deduced that higher spatial resolution increases the realism of the OGCMs in terms of global-average energy content of the flow for all frequencies and yields the best representation of the global-average absolute dispersion of the synthetic drifters (cf. Drifter absolute dispersion and the corresponding velocity autocorrelation times in Fig. 1 and velocity spectral diagrams in Fig. 2). However, with increasing spatial model resolution, more-

frequent model output would be recommended to avoid that the faster smaller scale motions be filtered by the coarse time-averaged fields. Next, it will be investigated if the synthetic trajectories are capable of describing reasonable turbulence regimes on a global scale compared to drifter observations.

#### *4.2 Global Maps of the Rupolo Ratio.*

Global-average Rupolo-ratio estimates based on observed and synthetic trajectory data are provided in Table 3 where all the model values are comparable to the observations within the given errors. However, some configurations do better than others. For example, the Rupolo ratio based on the ORCA1–5d trajectories is greatly underestimated compared to the other model configurations, this is due to the fact that the coarse-resolution model cannot resolve the mesoscale dynamics, cf. Fig 3.

In Fig. 4b this becomes particularly evident in areas that should be characterized by a high Rupolo ratio, showed  $\gamma_R$  values near 0 instead of  $\gamma_R \approx 1$ , indicating the obvious fact that the model only sees the mean flow of the meandering current system and its eddies (i.e., the acceleration of the flow is not resolved by the stochastic model).

The  $\gamma_R$  maps based on the ORCA025 datasets presented in Figs. 4b and 4c show similar features compared to the observations in Fig. 4a, with  $\gamma_R \approx 1$  (smooth flow) near the western boundary currents and the Antarctic circumpolar current in the Southern Ocean, and  $\gamma_R \approx 0$  (jagged currents) in the central parts of the global ocean sub-basins. The results from the 6-h-average output yielded distinctly separated smooth regions from adjacent quiescent areas with low  $\gamma_R$  values (even too low compared to observations), while the smooth areas in the 5-day-average velocity fields are more wide stretched, extending into the central parts of the sub-basins.

Because the ORCA12 horizontal resolution is to be regarded as eddy resolving, more mesoscale features would be expected to be present in the model output compared to the results from the coarser-grid configurations. However, the ability to create vortices could also yield increased sources of errors in the surface velocity fields, which should be taken into consideration. But in order complete this error analysis, and to exclude that the inaccuracies in the Rupolo-ratio map are not related to the time averaging of the ORCA12–5d data, a future study dealing with Lagrangian analyses of more-frequent output from this model configuration would be necessary. In summary, the spectral energy content in the ORCA12 dataset was found to be the closest to the observed values (cf. Fig. 3), compared to the ORCA1–5d and

ORCA025–5d data within the observed frequency range. However, detailed studies showed that the global-average “eddy energy” in the ORCA12–5d system was not always located in the correct regions, but rather was homogeneously distributed over the entire modeled global ocean, thus yielding an exaggerated amount of smoothly looping data in the interior of the global ocean sub-basins. The relatively realistic energy distribution of the global-average ORCA12–5d spectra could, in part, be due to the fine tuning of the model configuration, while the excess smoothness in areas that should be characterized by highly variable quiescent flow could be the product of an insufficient application of spatially varying eddy-diffusivity coefficients in the diffusion operators.

#### *4.3 Regional study: Agulhas leakage*

Separating observed and modeled trajectories in Rupolo classes as part of the Lagrangian analyses yields information of the flow characteristics that could not have been obtained by traditional methods (e.g., EKE or looper and no-looper analyses). Figure 5a) illustrates observed data while 5b-e) show the corresponding synthetic drifters crossing westward the 20°E meridional in the Agulhas retroflection area. From these results it is clear that a eddy-resolving model is needed to correctly represent the dynamics in this area. The data from ORCA1 present estimates of the mean flow of the surface currents, while the higher resolution models show more accurate trajectory features. Fig 6 presents a zoom in over the Southern Atlantic of the Rupolo ratio map, and also a specific map over the observed drifter tracks in their passage from the Indian Ocean to the southern Atlantic trough the Agulhas retroflection zone.

These data show that the modelled Agulhas leakage improve with spatial and temporal resolution, where nearly 30% of the synthetic “Indian Ocean drifters” cross both sections at 20°E and 35°S; in agreement with our observational results and those in Richardson 2007.

## **5. CONCLUSION**

When applying numerical methods for studies of ocean circulation, it is crucial to make the best trade off when it comes to choosing the size of the grid of the model configuration as well as the time-averaging window of the model output in relation to

the characteristics of the dynamical features that are to be analysed. In this study, surface velocity fields from three NEMO/ORCA grid configurations (non-eddy-permitting ORCA1, eddy-permitting ORCA025, and eddy-resolving ORCA12) have been assessed, and the influence of the output frequency on the surface dynamics in ORCA025 has been evaluated. The analyses were undertaken in a Lagrangian framework where observed drifter tracks were confronted with model trajectories sharing the same start positions, and the Lagrangian time scales were estimated through stochastic modelling.

The dispersal properties of the observations were found to be in full agreement with those presented by Rupolo (2007a), and his method for rationalising ocean trajectory data proved to be very useful for evaluating the quality of the simulated surface dynamics by comparisons with drifter data.

The results from the trajectory screening method and the subsequent scale separation of the data using the Rupolo ratio, were presented both as global-average distributions and as global turbulence maps for all model configurations. These maps can be used to identify areas where the time scales of the modelled ocean flow have been accurately resolved compared to observations. The global-average absolute dispersion improved when the model resolution was upgraded to the ORCA025 grid, and some further improvements were obtained applying the 6-h-average data compared to the 5-day model fields. Furthermore, it was found that the model output rate notably influences the velocity power spectral slope for the simulated trajectories, and the ORCA025 results gave (yet lacking generally in energy content) a more realistic slope at intermediate times when model fields were available every 6 h. Moreover, the results from the eddy-permitting ORCA025 configurations yielded reasonable global-average distributions of the simulated dynamical regimes, whereas the ORCA12–5d data showed an anomalously large amount of smooth looping trajectory data.

In conclusion, according to traditional Lagrangian analyses, the best representation of the global ocean dispersion and global-average spectral energy content would be provided by the eddy-resolving ORCA12–5d configuration, while the local characteristics of the surface turbulent flows were simulated in a more realistic manner by the ORCA-025 configurations.

## 6. REFERENCES

1. Doos, K., V. Rupolo, and L. Brodeau (2011), Dispersion of surface drifters and model-simulated trajectories. *Ocean Modell.*, 39,301–310, doi:10.1016/j.ocemod.2011.05.005.
2. LaCasce, J. (2008), Statistics from Lagrangian observations. *Prog. Oceanogr.*, 77, 1–29. 36.
3. Lumpkin, R. and M. Pazos (2007), Measuring surface currents with Surface Velocity Program drifters: The instrument, its data, and some recent results. *Lagrangian Analysis and Prediction of Coastal and Ocean Dynamics (LAPCOD)*, A. Griffa et al., Eds., Cambridge University Press, 39–67.
4. Madec, G., and Coauthors (2012), NEMOocean engine, version 3.4. Institut Pierre-Simon Laplace Note du Pole de Modelisation 27, 357 pp.
5. Nilsson J. A. U., K. Döös, P.M. Ruti, V. Artale, A. Coward, L. Brodeau, (2013), Observed and modeled global-ocean turbulence regimes as deduced from surface trajectory data, *J. of Physical Oceanography*, Vol. 43, No. 11, 2249-2269, doi: 10.1175/JPO-D-12-0193.1;
6. Richardson, P. L. (2007), Agulhas leakage into the Atlantic estimated with subsurface floats and surface drifters, *Deep Sea Res., Part I*, 54, 1361–1389.
7. Rupolo, V. (2007a), A Lagrangian-based approach for determining trajectories taxonomy and turbulence regimes. *J. Phys. Oceanogr.*,37, 1584–1609.
8. ———, (2007b), Observing turbulence regimes and Lagrangian dispersal properties in the ocean. *Lagrangian Analysis and Prediction of Coastal and Ocean Dynamics (LAPCOD)*, A. Griffa et al., Eds., Cambridge University Press, 231–274.
9. ———, B. L. Hua, A. Provenzale, and V. Artale, (1996), Lagrangian spectra at 700m in the western North Atlantic. *J. Phys. Oceanogr.*,26, 1591–1607.
10. Veneziani, M., A. Griffa, A. Reynolds, and A. Mariano (2004), Oceanic turbulence and stochastic models from subsurface Lagrangian data for the northwest Atlantic Ocean. *J. Phys. Oceanogr.*, 34, 1884–1906.

## 7. IMAGES AND TABLES

Class	$\gamma_R$	$\gamma_{osc}$	Typical features
I	$<0.2$	N/A	Low-frequency motion, high-frequency variability
II	$0.4 < \gamma_R < 0.8$	N/A	Low-frequency motion, no high-frequency variability
III	1	$<1$	High-frequency motion, meandering
IV	1	$>1$	High-frequency motion, looper

Tab.1 Rupolo-class definitions

Configuration	$\Delta y$ (60°N, 0°) (km)	$z$ levels	$L$ or $B$	$k_{visc}$	$k_{trac}$	Available periods
ORCA1	47, 111	64	$L$	$2 \times 10^4$	600	1999
ORCA025 (5 day)	14, 28	64	$B$	$-1.5 \times 10^{11}$	300	1991–2001
ORCA025 (6h)	14, 28	75	$B$	$-1.5 \times 10^{11}$	300	1997
ORCA12	3, 9	75	$B$	$-1.25 \times 10^{10}$	125	1994–99

Tab. 2 ORCA grid characteristics

Datasets	Period	$T_L$	$T_v$	$T_a$	$\gamma_R$
Drifters	1991–2010	$2.7 \pm 1.6$	$2.2 \pm 1.7$	$0.5 \pm 0.4$	$0.24 \pm 0.44$
	1991–2001*	$3.0 \pm 1.7$	$2.4 \pm 1.7$	$0.6 \pm 0.5$	$0.28 \pm 0.43$
ORCA1–5d	1999	$5.0 \pm 2.4$	$4.7 \pm 2.4$	$0.3 \pm 1.3$	$0.06 \pm 0.53$
ORCA025–5d	1991–2001*	$5.6 \pm 2.3$	$4.7 \pm 2.2$	$0.9 \pm 1.4$	$0.20 \pm 0.48$
	1997	$5.7 \pm 2.2$	$4.6 \pm 2.1$	$1.1 \pm 1.5$	$0.24 \pm 0.55$
	1999	$5.8 \pm 2.3$	$4.6 \pm 2.1$	$1.1 \pm 1.4$	$0.25 \pm 0.53$
ORCA025–6h	1997	$3.8 \pm 2.1$	$3.2 \pm 2.2$	$0.6 \pm 0.5$	$0.18 \pm 0.39$
ORCA12–5d	1997	$5.1 \pm 2.2$	$4.1 \pm 1.8$	$1.0 \pm 1.8$	$0.26 \pm 0.67$
	1999	$5.1 \pm 2.2$	$4.0 \pm 1.9$	$1.1 \pm 1.7$	$0.27 \pm 0.64$

\*The results from the ORCA025–5d exact-seed experiment during 1991–2001 are provided along with the corresponding results from the drifter data during this period.

Tab. 3 Lagrangian time scales as well as velocity and acceleration time scales (days), and Rupolo ratio (i.e.,  $\gamma_R$ ) along with the corresponding std-dev for each dataset and period. Drifter values are based on data from the period 1991–2010 and model values from full seed experiments during 1997 and 1999 (for those available).

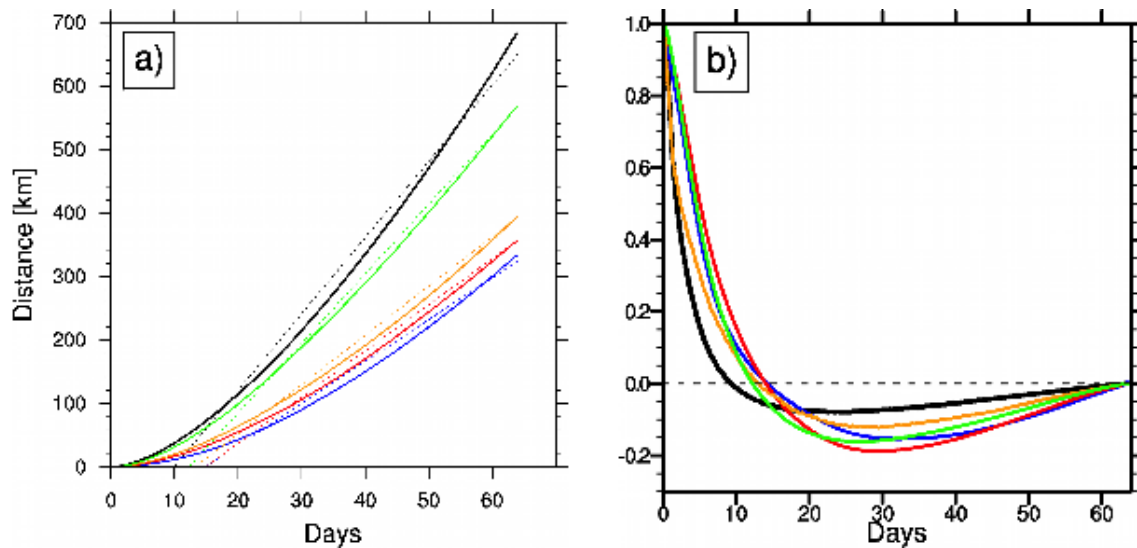


Fig. 1 (a) Global-average absolute dispersion (the corresponding dashed functions indicate the linear growth of the absolute dispersion in time for  $t > TL$ ), and (b) velocity auto-correlation time for the observed and synthetic data sets, as a function of time. Color coding: drifter (black), ORCA1-5d (blue), ORCA025-5d (red), ORCA025-6h (orange), and ORCA12-5d (green) trajectories.

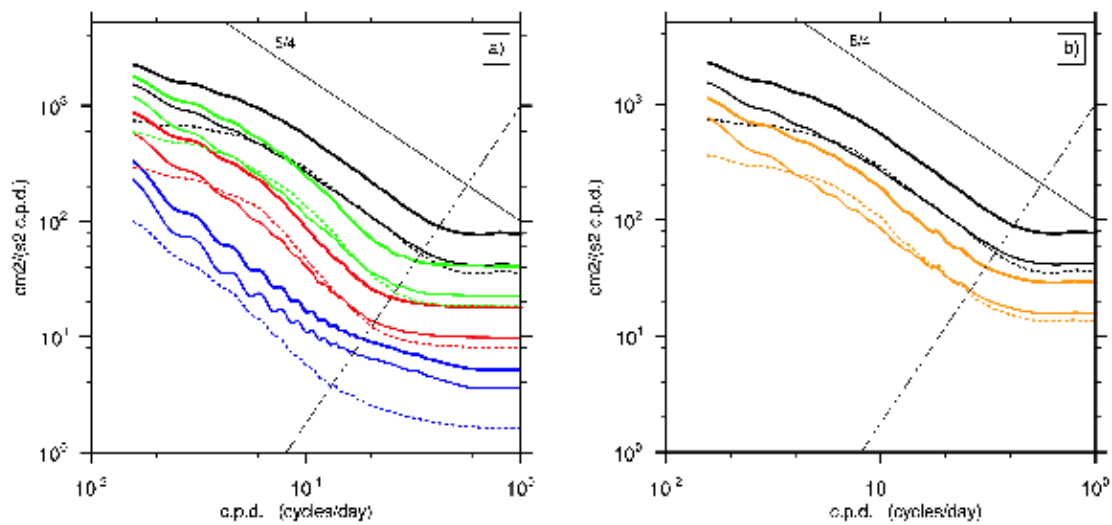


Fig.2 Power spectra for total (thick solid), zonal (thin solid), and meridional (dashed) trajectory velocities [ $cm^2 (s^2 \text{ cpd})^{-1}$ ] as a function of frequency (cpd). Color coding: drifter (black), ORCA1-5d (blue), ORCA025-5d (red), ORCA025-6h (orange), and ORCA12-5d (green) data.

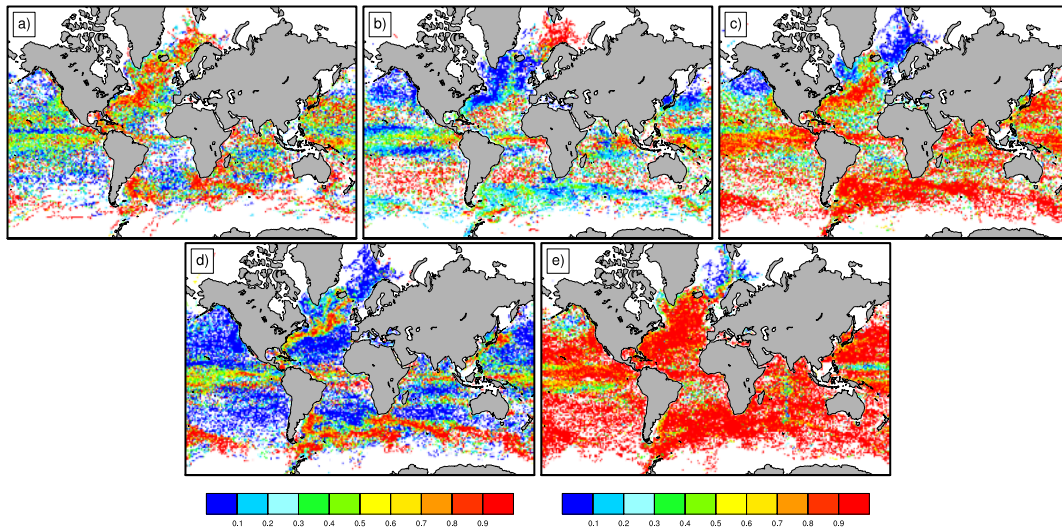


Fig.3 Rupolo ratio (binned on a  $1/4^\circ$  global grid) derived from (a) drifter observations, as well as synthetic (b) ORCA1–5d, (c) ORCA025–5d, (d) ORCA025–6h, and (e) ORCA12–5d trajectories.

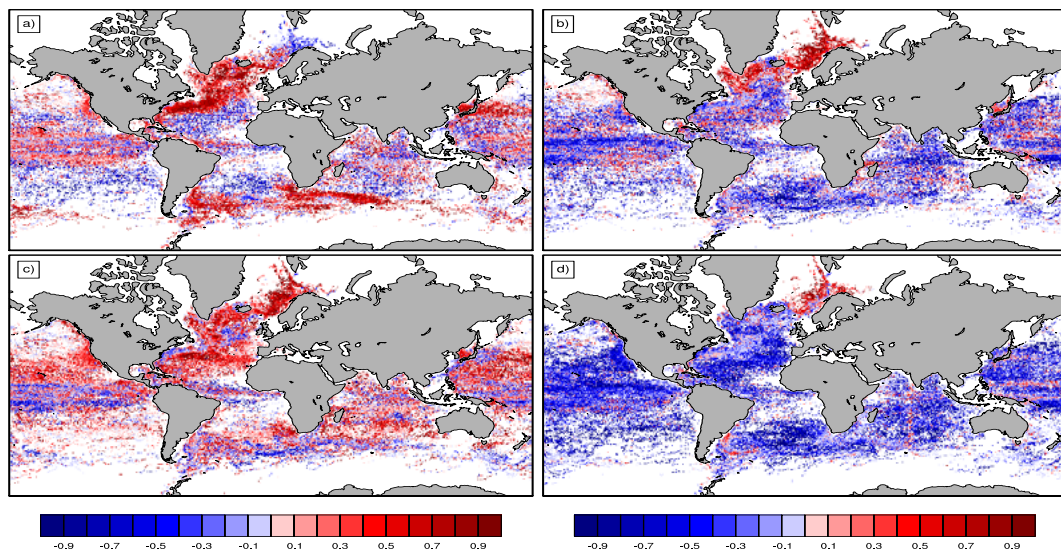


Fig. 4 Global Rupolo-ratio bias. (a) Observations:ORCA1–5d fields, (b) observations:ORCA025–5d fields, (c) observations:ORCA025–6h fields, and (d) observations:ORCA12–5d fields.

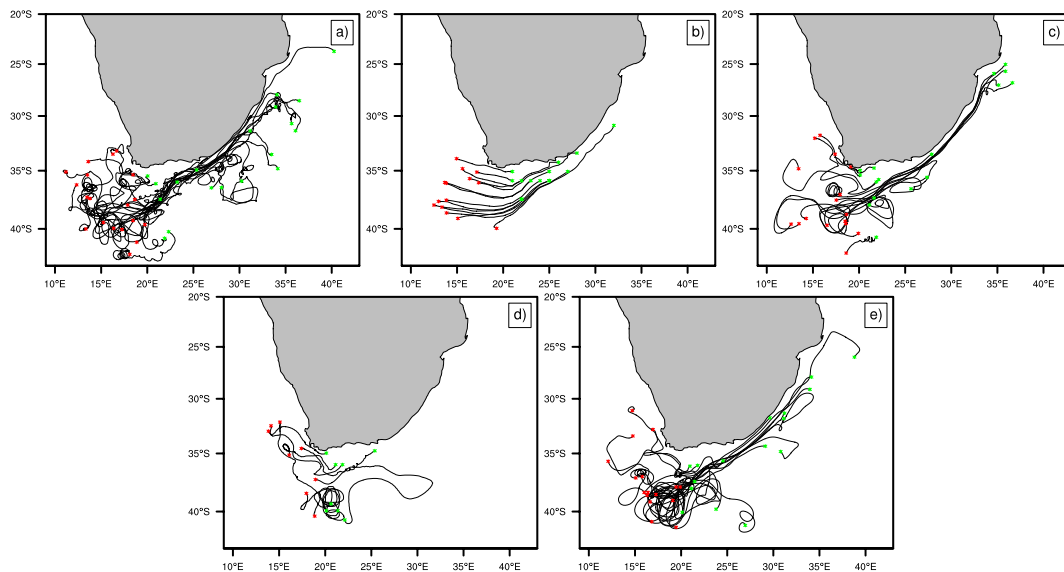


Fig.5 Observed (a), as well as synthetic (b) ORCA1–5d, (c) ORCA025–5d, (d) ORCA025–6h, and (e) ORCA12–5d westward trajectory crossings of the Cape Agulhas 20°E meridional. Green markers indicate start points and red markers end points, each segment is 64-days long.

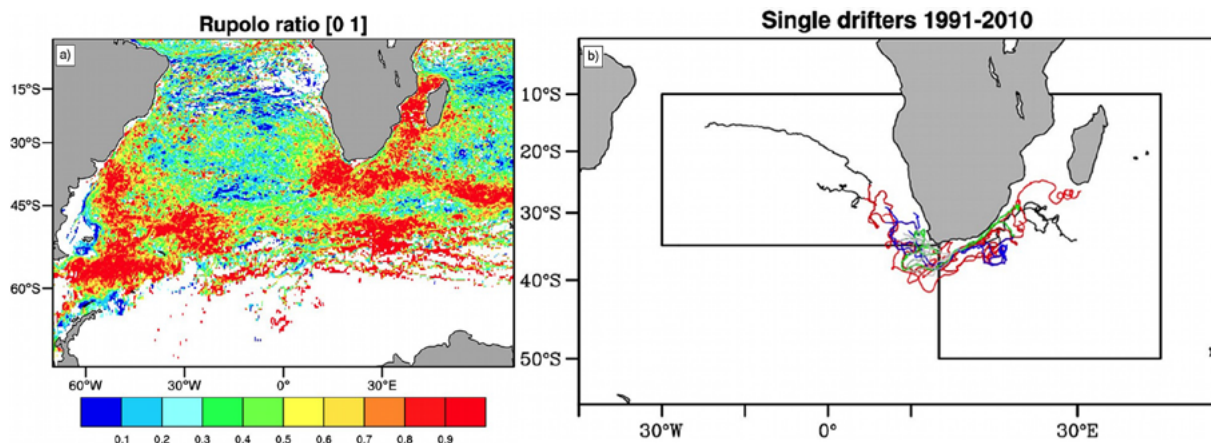


Fig.6 (a) Rupolo ratio: zoom-in over the southern Atlantic and Indian ocean (ACC), based on observations 1991-2010, showing turbulent areas (class III-IV) in the Agulhas and Malvina zones as expected; (b) Distribution of drifters observations crossing westward the 20°E, and, subsequently northward at 35°S, the segment lengths varying between 32 (light blue), 64 (green), 92 (blue), 180 (red), and 365 days (black), where all start positions are contained in the right box, and the end positions in the left box.

# Storm classification for Tyrrhenian Sea and wave conditions changes over last thirty years

Paladini de Mendoza F.\*, Melchiorri C., Marcelli M.

Laboratory of Experimental Oceanology and Marine Ecology, University of  
Tuscia Molo Vespucci, Civitavecchia, Italy

\*Corresponding author: f\_paladini@unitus.it

## Abstract

Storm waves produce the main driving force of the coastal dynamic. The changes of the energy content and recurrence of storms could modify the sedimentary balance of the beaches. In this study the storms of the Central-East Tyrrhenian Sea was classified and changes of wave conditions over the years 1978-2012 were analysed. For the first purpose, was used the methodology according with existing storm scales. For the second one, the analysis was performed by Mann-Kendall test. The parameters analysed are: average wave height, storm recurrence and energy content of storms. The classification results in five category of storms useful for coastal hazard assessment and planning purpose. The classes of storms show higher values of energy content for the 4th and 5th classes than the classification performed for NW-Mediterranean Sea. The presence of positive trend was detected in average wave height, storm recurrence and the energy content of storms. In detail, the results of the statistical analysis reveal changes of the average wave height in the months between August and December while in the other parameters the changes are restricted to the month of June. The variation on the average wave intensity and the major storminess during June could have impacted the morphodynamic of the beaches. The modifications affect the seasonal variation of the beach morphology aiding a more dissipative profile that result in a lower growth of berm during summer season with a probable impact on the beach activities.

**Keywords:** storm classification, Central-East Tyrrhenian Sea, climate change

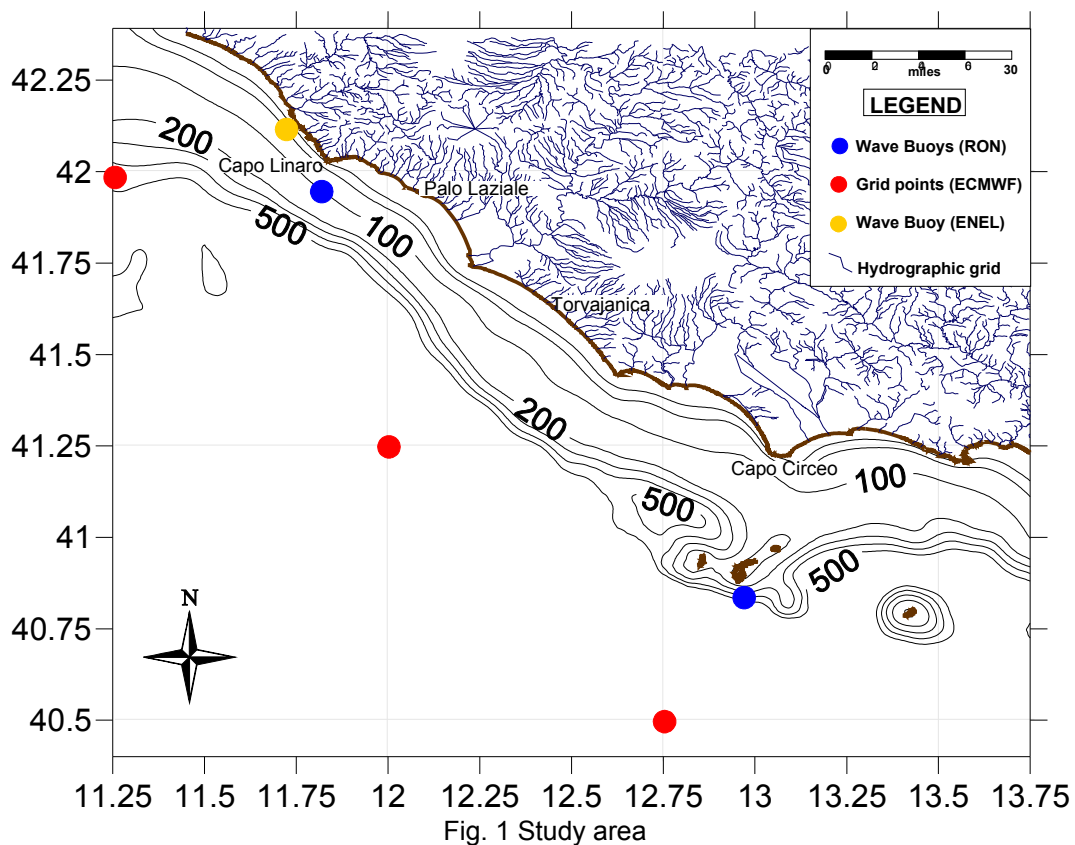
## 1. INTRODUCTION

The coastal systems represent a border area between the sea and the mainland, conditioned by processes acting on different temporal and spatial scales. Long term processes as the geological and eustatic and short term processes as seasonal and extreme storms produce a constant movement of coastal zones seaward and landward. The waves propagation from deep to shallow waters are the main driving forces of littoral dynamics and the seasonal variation of wave intensity generate, especially for sandy beaches, various morphologies of beach profiles determining a constant exchange of sediment between emerged and submerged beach. The storms are powerful events generally characterized by strong winds and huge waves able to produce in a short time a large impact on the coast like inundation and strong erosion phenomena (Katoh and Yanagishima, 1988). These events influence strongly the evolution of the coastal zones and can significantly accelerate the existing rates of shoreline (Morton and Sallenger, 2003). The amount of seasonal fluctuation depends on the number and intensity of storms during a particular year (Dewall and Richter, 1977 and Dewall, 1979) and the energy content drives a number of morphodynamic responses such as beach and dune erosion and overwash (Edelman, 1972). The classification of storms in the Mediterranean Sea was presented by Mendoza et al. (2011) for NW Mediterranean sector and based on this approach the storm scale of the Central-East Tyrrhenian Sea is presented. For this study was collected a large storm dataset that includes all wave buoy records covering the largest temporal and spatial variability of events. Furthermore, the analysis of the wave data is performed to detect changes in energy content and recurrence of storms over last thirty years. The classification of storm waves is useful for coastal hazard management, to give the critical scenarios for numerical simulations and to the coastal planning. The knowledge of the evolution of wave conditions may be useful to further clarify the role of one of the main driving force of coastal dynamics in the general erosive condition that currently affects the coasts of Latium region.

## 2. STUDY AREA AND DATA

The Latium coast is located on the eastern side of the Central Tyrrhenian Sea; the coastline is 314 Km length divided by 4 physiographic unit where the 74% is dominated by sandy beaches and 10% by coastal cliffs. Along the coast there are 7 different coastal morphotypes (Ferretti et al. 2003) where the largest is the delta cusps of Tevere river that

dominates the central portion of the coast from Torvaianica to Palo Laziale (Fig.1). The coast of Latium region is concerned since the 80's by strong erosion still in progress (Berriolo G & Sirito G., 1985; Bellotti et al. 1997) probably due to intense urbanization of the coastal zone and by the construction of dams and diversions along the rivers (Bellotti et al.,1997; La Monica et al., 1996). Furthermore, the natural factors as eustatic variations and subsidence contribute to increase the erosion trend. The information about the wave climate was retrieved by 3 wave buoys of National Wave Network (RON) and ENEL located in the south, offshore to Ponza (RON), and in the north, offshore to Capo Linaro (RON) and Torrevaldaliga (ENEL) represented in fig.1. The period of wave recording is extended not continuously from July 1989 to March 2008 for Ponza buoy, from July 2009 to February 2012 and 2013 for Capo Linaro buoy and from 1994 to 2001 for Torrevaldaliga buoy. The storm's classification proposed in this study is based on the methodology of Mendoza et al. (2011) where “real wave characteristics” are taken into account. In order to detect the long term trend of wave conditions the ERA-Interim dataset extended from 1978 to 2012 (ECMWF) was analysed. These wave data was chosen because they have 34 years of continuous data with 0.75° of spatial resolution along the study area that allow to retrieve good spatial resolution of the study area.



### 3. METHODOLOGY

In order to create the classification of storms, the criteria proposed by Mendoza et al. (2011) were used to identify the different storms that generate a significant impact on the coast in term of coastal erosion. The criteria used to identify storm are the following:

- significant wave height exceeds a threshold value of 2 m during a minimum period of 6 h
- storm involving two extreme episodes with a maximum inter-event separation of 72 h
- a period of  $H_s < 1.5$  m shorter than 6 h is considered a single two-peaked storm

Once the storms were selected, for every one was computed the energy content, the mean wave height, maximum wave height, mean direction, mean peak period and peak period associated to maximum wave height. The energy content [m<sup>2</sup>.hr] is a function of intensity and duration of phenomena and the formula is expressed by the following formulation:

$$E = \int_{t_2}^{t_1} H_s^2 dt \quad (1)$$

where  $t_1$  and  $t_2$  define the storm duration.

In order to obtain a "single storm dataset", every event recorded in every wave buoy were integrated into a dataset that taken into account the spatial variability over the study area (Mendoza et al., 2011). The categories of storms were obtained by euclidean cluster analysis and average linkage method placing a restriction on the maximum number of groups in 5 categories so as to maintain analogies with the existing scale of storms (Simpson, 1971; Saffir, 1977; Dolan and Davis, 1992; Mendoza and Jimenez, 2008). The evolution of wave climate was analysed using non-parametric test, usually exploited to find features, as environmental trend (Helsel, 1987). In particular the Mann-Kendall test (Mann, 1945; Kendall, 1975; Hirsch et al, 1982; Hirsch and Slack, 1984) is frequently used to find trend in climatological time series (Sneyers, 1998). In order to analyse the temporal evolution of wave conditions over last 30 years the parameters of monthly mean wave height, monthly energy content, monthly recurrence of storms and the sum of yearly energy content for each storm class were analysed by Mann-Kendall tests, performed trough the Computer Program USGS (Dennis et al.,2005). The variables were computed by averaging the values retrieved from three grid points of Era-Interim wave dataset (ECMWF), located respectively on the north, centre and south of Central-East side of

Tyrrhenian Sea (Fig. 1). The monthly mean wave height was obtained by LOWESS smoothing (Cleveland 1979, 1985; Chambers et al. 1983) while monthly energy content and monthly recurrence values were obtained by the monthly sum. The Seasonal Mann-Kendall test was performed on monthly data while the distribution of changes over the months along the time period was analysed by the Mann-Kendall test (Kendall, 1975).

#### 4. RESULTS

The result of cluster analysis is shown on Fig 2 where the dendrogram obtained by cluster analysis shows the different groups of storms. In table 1 is presented the energy value for each class and the related storm intensity.

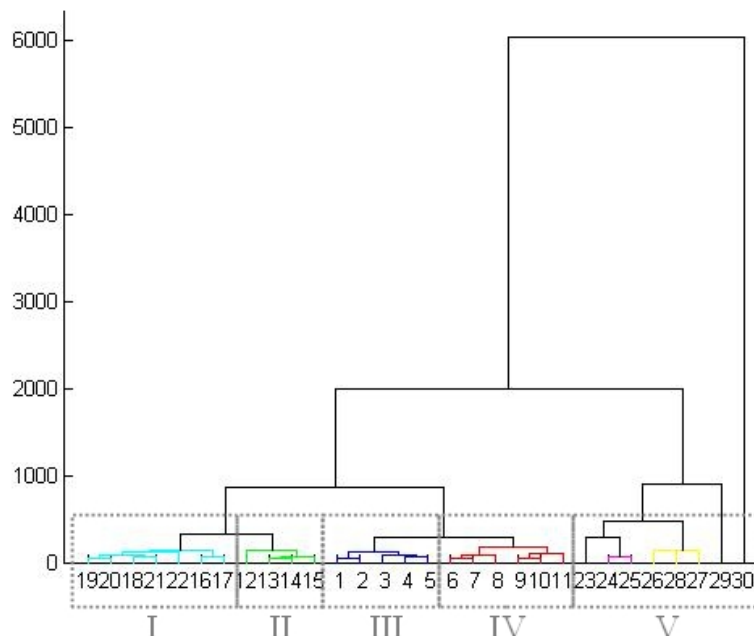


Fig. 2 Dendrogram of storm classification using cluster analysis (solid lines). Dashed lines indicated the 5 classes selected

Class	Energy content (m <sup>2</sup> hr)	Category
1	<250	weak
2	250-500	moderate
3	501-1000	significant
4	1001-2000	severe
5	>2000	extreme

Tab.1 Storm energy content for each class

The total number of storms amounts to 673 events but this value represent the integration of the different datasets. In detail, 90 events were selected by Capo Linaro buoy (RON), 119 from ENEL buoy and 464 from Ponza buoy. The largest value found on the buoy of

Ponza depends both to the record length (1989-2008) and more exposed location to storms.

The scatter plot of storm events sorted by class allow to highlight the variability in every class in terms of wave period and height.

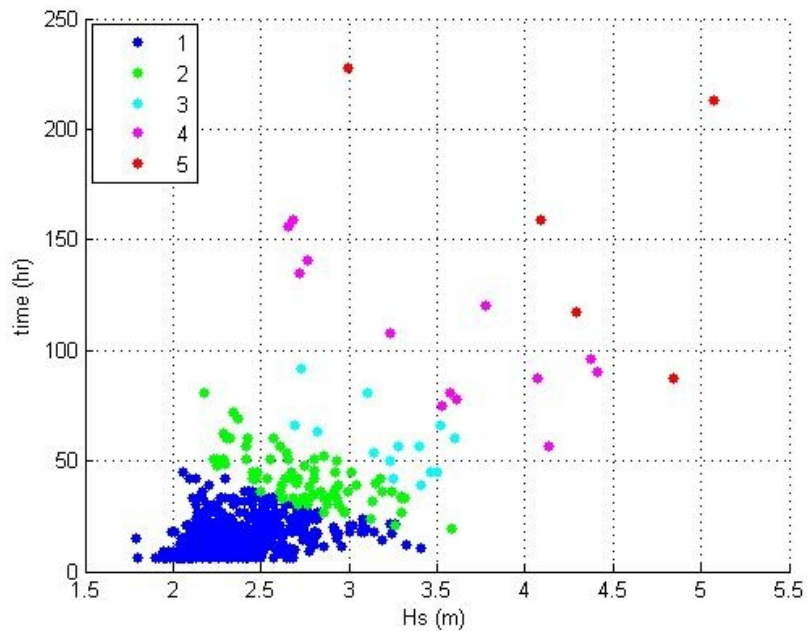


Fig. 3 Group scatter of each class in duration and intensity

The directional distribution of storms show a large sector of propagation 200° wide. Between 90° and 290°N there are two main directions from W and SW, that describe the variability observed along the study area. The largest storms come from the directional sector between 245 and 280°N.

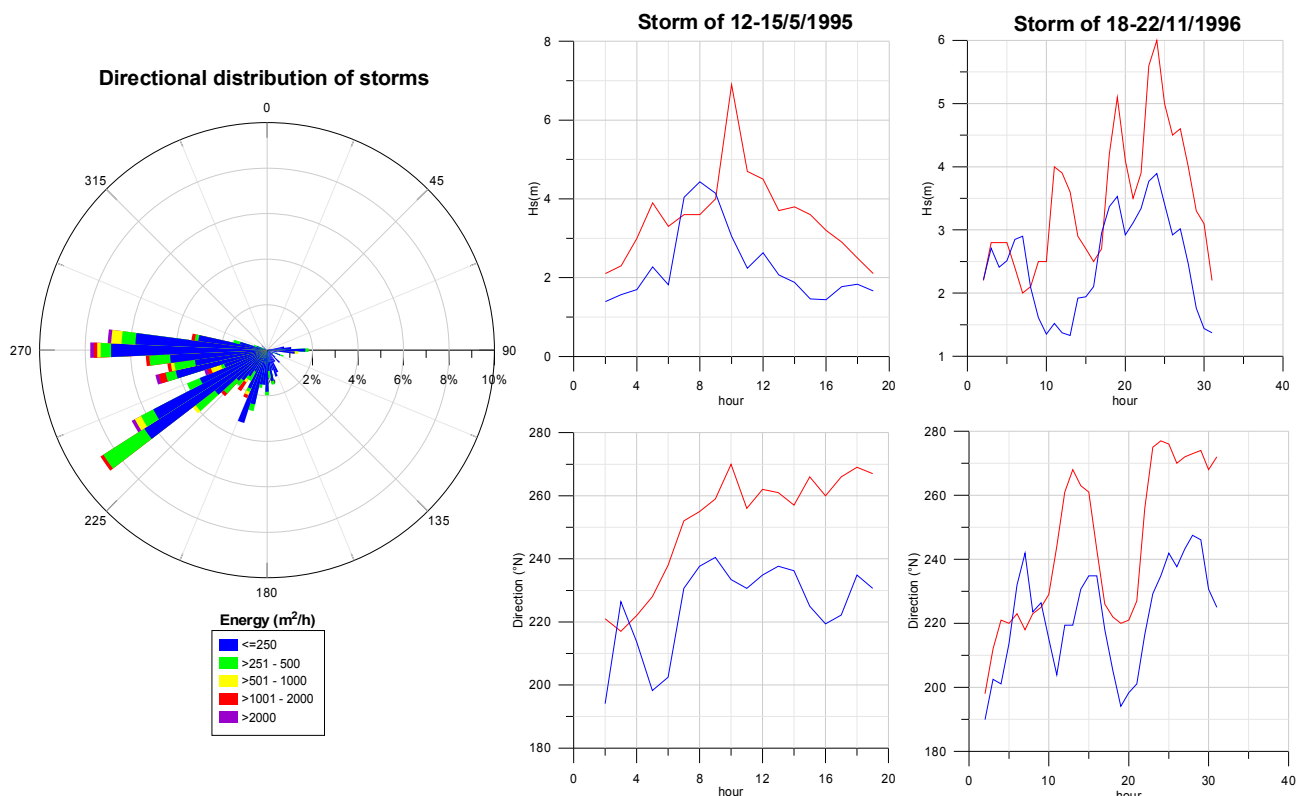


Fig. 4 Directional distribution of storms (left) and time series of two storms recorded by Ponza wave buoy (red) and Torrevaldaliga wave buoy (blue)

On the right of figure 4 is possible to see the spatial variability of intensity and direction during the same storm. In detail, the behaviour of storms shows more western waves in the southern portion than the northern portion, where the prevailing waves come from south. In addition, the wave intensity appear generally lower in the northern area than southern.

The mean value of height ( $H_s$ ), period ( $T_p$ ) and time period for every class of storm can be seen on the table 2.

Class	Mean $H_s$ (m)	Mean $T_p$ (sec)	Duration (hr)
1	2.79	8.34	15.41
2	3.71	9.43	41.82
3	4.28	9.91	50.5
4	4.61	9.96	92.46
5	6.02	11	130.5

Tab.2 Mean values for each storm class

Regarding to the temporal evolution of waves conditions the Mann-Kendall test results can be seen on the tab.2 where  $\tau$  value and  $p$ -value define, respectively, the trend and its statistical significance.

Seasonal Mann-Kendall Test		
Data	tau	p-value
Monthly Wave Height	0.184	0.00001
Monthly Storm Energy	0.06	0.0617
Monthly Storm Recurrence	0.068	0.0348
Mann-Kendall Test		
Data	tau	P-value
1 Class	0.0535	0.6672
2 Class	0.1165	0.3423
3 Class	-0.0018	1
4 Class	-0.0018	1

Tab. 3 Seasonal Mann Kendall Test and Mann Kendall test results

The monthly average wave height and the recurrence of storms, show a real positive trend while energy content of storms don't show a significant change along the time period. The results of the different classes of storms lacks of a real trend and the fifth class wasn't analysed for the few number of data. The results of the analysis performed for every months over the time period show positive trend for the monthly wave height in summer and autumn while the recurrence of storms has a significant variation in June (Fig.5).

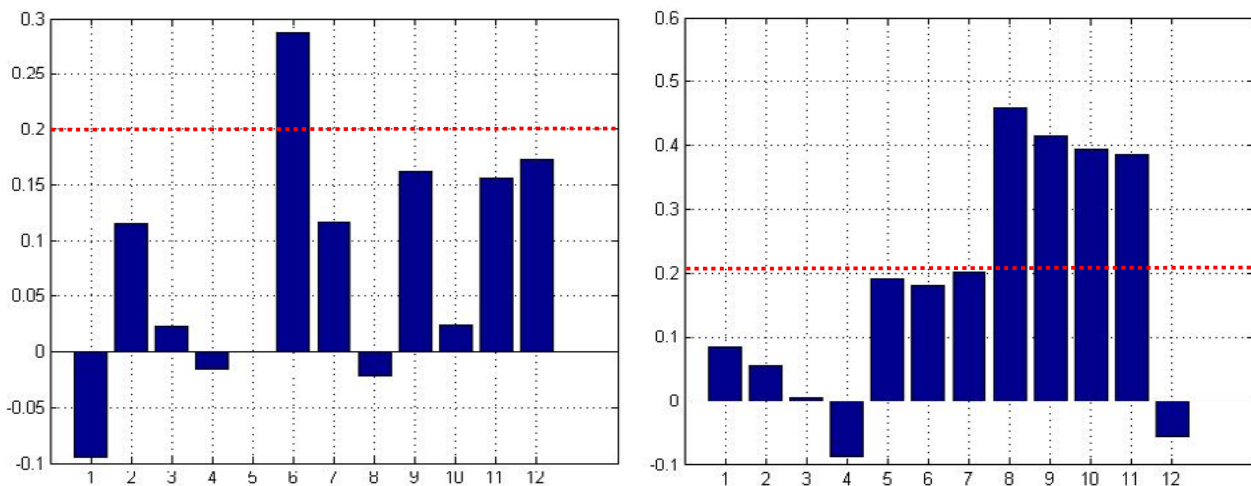


Fig. 5 Correlation tau for each month of storm recurrence (sx) and wave height (dx) over 1978-2012, dashed line represent the 95% of confidence

Regarding the monthly energy storm, the *p-value* obtained by Seasonal Kendall Test (tab.3) is very close to the threshold of null hypothesis acceptance. Thus, the monthly energy content was analysed in detail. The analysis for each month show a significant change in June (Fig.6).

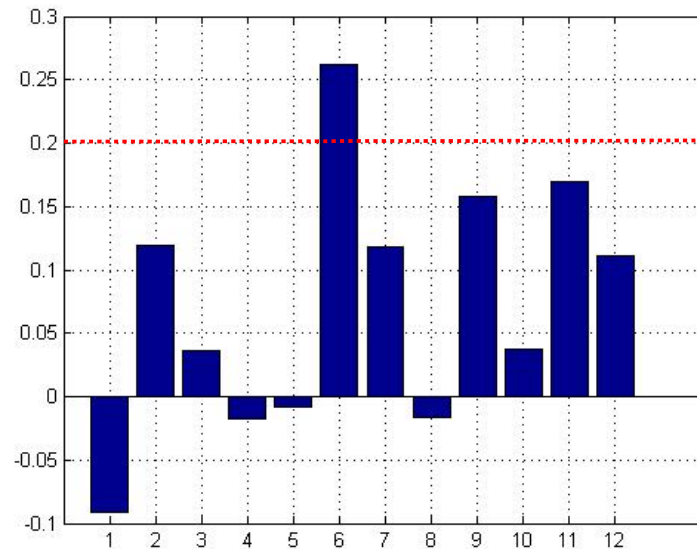


Fig. 6 Correlation tau for each month of energy content, dashed line represent the 95% of confidence

## 5. CONCLUSION

The analysis about the storms of the Central East Tyrrhenian Sea shows two main direction of waves. In detail, the behaviour of storms shows more western waves in the southern portion than the northern portion, where the prevailing waves come mainly from south. The wave intensity appear generally lower in the northern area than the southern. The observed variability is produced by the morphology of the sea basin, that affect the fetch length, and the area of generation of storms linked to the cyclogenesis areas in Mediterranean Sea (Radinovic, 1987; Trigo et al. 2002; Nissen et al. 2010). The energy content for the higher classes, obtained by Mendoza et al. (2011) for the NW-Mediterranean Sea, has larger values. The fifth class starts from a value twice as large than classification made for the Catalan coast. The statistical analysis performed on the wave conditions over last thirty years show the increase of average wave height during summer and autumn while the storms are more frequent and more intense in June. The changes observed on the wave intensity on medium term could alterate the morphology and sedimentology of sandy beaches (Hayashi et al. 2012) since the intensity of waves drives the magnitude of littoral currents. At Italian latitudes, summer is characterized by lower wave motion and beaches develop toward reflective stage that produce the growth of emerged beach. Therefore, the increase of storm's recurrence during June may have affected the seasonal dynamic of the beach profile. The increase of storminess could produce the lower growth of the berm during summer season preventing the natural recovery of the beaches. The changes observed could increase the regressive trend of the shoreline with a consequence on the beach activities.

## 6. REFERENCES

Bellotti P., Caputo C., Ciccacci S., De Rita D., Donati S., Fredi P., Funicello R., La Monica G. B., Landini B., Marra F., Milli S., Parotto M. & Pugliese F., 1997. Fundamentals for a geomorphological overview on Roma and its surroundings. *Supplementi di Geografia Fisica e Dinamica Quaternaria*, III (2), 105-121.

Berriolo G. & Siritto G., 1985. Studio Generale sul regime delle spiagge laziali e delle isole pontine. Studio Volta di Savona per conto della Regione Lazio, Cap. IV/A, pp.97-99.

Chambers, J.M., Cleveland, W.S., Kellner, B. & Tukey, P.A., 1983. *Graphical methods for Data Analysis*. Wadsworth, Belmont, California.

Cleveland, W.S., 1979. Robust locally weighted regression and smoothing scatterplots. *Journal of the American Statistical Association*, 74(368), pp. 829-836.

Cleveland W.S., 1985. *The Elements of Graphing Data*. Wadsworth, Monterey, California.

Dennis R. Helsel, David K. Mueller, & James R. Slack, 2005: Computer Program for the Kendall Family of Trend Tests, Scientific Investigations Report 2005-5275, U.S. Department of the Interior  
U.S. Geological Survey

Dewall, A. E. & Richter, J. J. 1977. Beach and Nearshore Processes in South eastern Florida; *Coastal Sediments'77*, pp 425-443.

Dewall, A. E. 1979. Beach Changes at Westhampton Beach, New York; MR 79-5, Coastal Engineering Research Center, U.S. Army Engineer Waterways Experiment Station, Vicksburg, MS.

Dolan, R. & Davis, R.: An intensity scale for Atlantic coast north-east storms, *J. Coast. Res.*, 8(4), 840-853, 1992.

- Edelman, T. 1972. Dune Erosion During Storm Conditions; Proceedings of the Thirteenth International Conference on Coastal Engineering, pp 1305-1312.
- Ferretti, O., Delbono, S., Furia S. & Barsanti M., 2003: Tipi morfo-sedimentologici dei litorali italiani, Elementi di Gestione Costiera – Parte I, ENEA, ISSN/0393-3016
- Hayashi K., Mori N., Mase H., Kuriyama Y. & Kobayashi N., 2012. Influences of climate change on beach profile; Coastal Engineering Proceedings; No 33: Proceedings of 33rd Conference on Coastal Engineering, Santander, Spain, 2012
- Helsel, D.R., 1987. Advantages of non-parametric procedures for analysis of water quality data. *Journal of Hydrological Sciences*, 32(2), pp. 179-190.
- Hirsch, R.M., Slack, J.R. & Smith, R.A., 1982. Techniques of trend analysis for monthly water quality data: *Water Resources Research* v. 18, p.107–121.
- Hirsch, R.M. & Slack, J.R., 1984, A nonparametric trend test for seasonal data with serial dependence: *Water Resources Research* v. 20, p. 727–732.
- Katoh, K. & Yanagishima, S. 1988. “Predictive Model for Daily Changes of Shoreline,” Proceedings of the Twenty-First International Conference on Coastal Engineering, American Society of Civil Engineers, Hamburg, Chapter 93, pp 1253-1264.
- Kendall, E.L., 1975. *Rank Correlation Methods*. Charles Griffin, London, fourth edition.
- La Monica G.B. & Raffi R., 1996: Morfologia e sedimentologia della spiaggia e della piattaforma continentale. In: *Il mare del Lazio*, Università “La Sapienza” di Roma, Regione Lazio Assessorato opere e reti di servizi e mobilità: 62-87
- Mann, H.B., 1945: Nonparametric tests against trend. *Econometrica*, 13:245-259.
- Mendoza, E. T. & Jimenez, J. A., 2008: Clasificación de tormentas costeras para el litoral Catalan (Mediterraneo NO), *Ing. Hidraul. Mex.*, XXIII, 2, 21–32.

Mendoza, E. T. & Jimenez, J. A., 2006: Storm-Induced Beach Erosion Potential on the Catalanian Coast, *J. Coast. Res.*, SI ,48, 81–88.

Mendoza E. T., Jimenez J. A. & Mateo J., 2011. A coastal storms intensity scale for the Catalan sea (NW Mediterranean); *Nat. Hazards Earth Syst. Sci.*, 11, 2453–2462.

Morton, R. R. & Sallenger A. H.: Morphological Impacts of Ex-treme Storms on Sandy Beaches and Barriers, *J. Coast. Res.*,19(3), 560–573, 2003.

Nissen K. M. , Leckebusch G. C. ,Pinto J. G., Renggli D., Ulbrich S. & Ulbrich U., 2010: Cyclones causing wind storms in the Mediterranean: characteristics, trends and links to large-scale patterns. *Nat. Hazards Earth Syst. Sci.*, 10, 1379–1391.

Simpson, R. A., 1971: Proposed scale for ranking hurricanes by intensity, Minutes of the Eighth NOAA, NWS Hurricane Conference, Miami.

Saffir, H., 1977: Design and construction requirements for hurricane resis-tant construction, *Am. Soc. Civil Eng.*, ASCE Preprint No. 2830, American Society of Civil Engineers, New York, 20 pp.

Sneyers R., 1998. Homogenizing time series of climatological observations. The search and adjustment for inhomogeneities. Principle of methodology and example of results. Proceedings. Second Seminar for Homogenization of Surface Climatological Data. Hungarian Meteorological Service. Budapest, Hungary.

Radinovic, D., 1987: Mediterranean cyclones and their influence on the weather and climate, WMO PSMP Rep., Ser. Num 24.

Trigo, I. F. & Davies, T. D., 2002: Meteorological conditions associated with sea surges in Venice: a 40 year climatology, *Int. J. Climatol.*, 22, 787– 803.

## Regional climate simulations with COSMO-CLM over the Mediterranean area

Bucchignani E.<sup>1,2,\*</sup>, Montesarchio M.<sup>1,2</sup> A. Zollo<sup>1,2</sup> and Mercogliano P.<sup>1,2</sup>

<sup>1</sup> Centro Euro-Mediterraneo sui Cambiamenti Climatici (C.M.C.C.) - Italy,

<sup>2</sup> Centro Italiano Ricerche Aerospaziali (C.I.R.A.) – Italy

\*Corresponding Author: e.bucchignani@cira.it

### Abstract

This study presents the results of high resolution (0.125°) climate simulations over the Mediterranean area performed with an optimized configuration of the regional model COSMO-CLM driven by ERA-Interim Reanalysis (period 1979-2011) and by the output of the global model CMCC-CM (period 1979-2100). Model results have been analysed in terms of two-meter temperature and precipitations with the aim of assessing the capabilities in reproducing the main features of the Mediterranean climate. Climate projections, under the new IPCC RCP4.5 and RCP8.5 emission scenarios, show a strong warming expected in the XXI century, associated with substantial precipitation changes. Data presented in the present work have been largely adopted to perform different impact analyses in various international projects such as Perseus, Orientgate and national project (i.e. Gemina).

**Keywords:** Regional climate simulations, Mediterranean area, climate projections

## 1. INTRODUCTION

The Mediterranean area is situated between Northern Europe and African Continent (two heavily different regions, by climate terms), so its peculiar position determines a complex whole of conditions and features, that makes it a worthy subject to analyze, since border regions are very sensitive to small perturbations. The circulation is characterized by the presence of sub-basin gyres, intense mesoscale variability and a strong seasonal signal. Any minor change occurring in this circulation system (e.g. shifts in the location of mid-latitude storm tracks or subtropical high pressure cells) may trigger considerable alterations of Mediterranean climate [1]: for such reason, also increasing concentrations of greenhouse gases deserve a particular attention (e.g. [2]). Under these conditions, Mediterranean area is considered a great point of interest also defined "hot spot" for future climate change projections [3]. A considerable impact on agriculture, tourism and water resources is expected and it is important to provide high resolution climate change projections to decision makers, in order to perform adaptation/mitigation policies.

An exhaustive review of climate projections over the Mediterranean region has been presented by Giorgi and Lionello [1]: it is based on ensembles of global (PCMDI) and regional (PRUDENCE project [4]) climate simulations according with different SRES emission scenarios: they gave a collective picture of a substantial drying and warming of the Mediterranean area (precipitation decrease of about 25-30% and warming exceeding 4-5 °C), associated with increasing anticyclonic circulation over the region, which causes a northward shift of the mid –latitude storm track.

In Europe several coordinated ensembles of high resolution regional climate simulations exist: some of these are based on grid size down to 25 km and on the previous generation of emission scenarios (i.e. ENSEMBLES) [5]. The recent CORDEX project [6] and in particular the MED-CORDEX initiative [7] aims to perform climate simulations at resolution of about 12 km, considering the new RCP emission scenarios.

The main aim of this work is the development of high resolution climate projections (about 14 km) over the Mediterranean area (including also Black Sea) with the regional climate model COSMO-CLM: a control simulation, driven by ERA-Interim Reanalysis [8] has been conducted over the period 1979-2011. Moreover, two simulations driven by the global model CMCC-CM [9] have been performed over the

period 1971-2100, employing the IPCC RCP4.5 and RCP8.5 emission scenarios [10], chosen as representative of a world with less (RCP4.5) or more (RCP8.5) pronounced radiative impact.

## 2. MODEL AND DATA

COSMO-CLM [11] is the climate version of the operational non hydrostatic mesoscale weather forecast model COSMO-LM developed by the German Weather Service (DWD). A short description of the model and of the configuration used has already been reported in [12], however the main features of the model set-up are briefly recalled here: the time integration is based on a 3<sup>rd</sup> order Runge-Kutta scheme, the Tiedtke scheme is used for convection, the number of vertical levels in the atmosphere and the number of soil levels have been set equal respectively to 40 and 7.

The area of interest is shown in [Fig. 1]; the horizontal resolution adopted in this work is  $0.125^\circ$  (about 14 km). ERA-Interim Reanalysis are characterized by horizontal resolution of about 80 km, while ECHAM5 [13] (atmospherical component of CMCC-CM) by horizontal resolution of  $0.75^\circ$  (85 km), 31 vertical levels and 4 soil levels.

Model evaluation for the whole area, in terms of mean temperature and precipitation, has been performed using the E-OBS dataset vs.9 [14]: it is a European daily high resolution ( $0.25^\circ$ ) gridded dataset for the period 1950-2012 [Fig.2]. The E-OBS dataset has the disadvantage of a low station density in some areas, but it is the only observational dataset at daily resolution covering the whole Mediterranean area.

All images presented in this paper have been obtained using CLIME, a special purpose GIS software integrated in ESRI ArcGIS Desktop 10.X, developed at CMCC (ISC Division) in order to easily evaluate multiple climate features and to study climate changes over specific geographical domains with their related effects on environment, including impacts on soil.

### 3. VALIDATION

Model evaluation focuses on two-meter temperature (T2m) and total precipitation, since they represent the two most basic climate variables and the good representation of their average values is a precondition for further analyses. The period 1980-2011 has been considered for the analyses of results, since the first year of the simulations (1979) has been removed to reduce the spin-up period influenced by initial conditions. Both the hindcast simulations, respectively driven by ERA-Interim and by CMCC-CM global model have been analyzed: the first one is cited as *clm\_era\_int*, while the second one as *clm\_cmcc\_cm*. The analysis of *clm\_era\_int* allows the characterization of bias related only to the regional climate model, since “perfect” boundary conditions have been used. From the comparison with the second one, instead, the influence of the global model on the results can be quantified. Maps of seasonal biases have been obtained over the whole domain by means of an upscaling of the model output on the dataset grid, employing the natural neighbour technique, without applying any temperature-altitude corrections. Annual cycles have been obtained considering values on the native grids, without interpolations, on the seven sub-regions, shown in [Fig. 1], considering a similar subdivision as in Giorgi and Lionello [1] nominally NW (north-west area), NC (north-center), NE (north-east), ALPS (Alpine), SW (south-west), SC (south-center) and SE (south-east).

[Fig. 3] displays the annual cycle of T2m bias of *clm\_era\_int* and *clm\_cmcc\_cm* with respect to E-OBS for the seven sub-domains considered: for *clm\_era\_int*, a general warm bias in summer in all the areas is registered (up to 4° C in NE) and a cold bias in winter in almost all the sub-domains. Concerning Alps, a behavior similar to the present one has already been highlighted in [12] with a cold bias in winter over high altitude area, along with a general overestimation in summer. It is also important to highlight, as shown in Montesarchio et al [12], that a reduction of the temperature bias over Alpine region is obtained using COSMO-CLM at an higher horizontal resolution (0.0715°, about 8 km) with respect to the configuration at 0.125° (14 km). For *clm\_cmcc\_cm*, a cold bias is registered in most of the areas, with the exception of NE and SE (summer months).

[Fig.4] shows the seasonal spatial values of T2m bias (in °C) with respect to E-OBS for winter (top) and summer (bottom). The *clm\_era\_int* exhibits a general cold bias in winter (with peaks of 4°C over Alps) while in summer a general warm bias occurs,

especially in the eastern part of the domain. This last feature could be motivated by the low number of stations available on this area for the E-OBS dataset (see Figure 2). A better agreement is registered in spring and autumn (not shown), in the areas where the bias never exceeds 2°C (with the exception of the eastern part of the domain). In all the seasons, a large bias value is registered in correspondence of the highest mountain chains, such as Alps and Carpathians, especially in winter. The shortcoming of COSMO-CLM, leading to underestimation of the winter temperature at high altitudes, has already been highlighted in several works (e.g. [15]). A possible explanation of the summer positive bias is the deficiency of the model in reproducing atmospheric dynamics typical of some areas considered: in fact, many RCM and general circulation models overestimate summer temperature in semiarid regions (e.g., Iberian Peninsula, North Africa) [16]. The overestimation of summer temperatures in Eastern Europe is a common feature in previous studies and is often related to a lack of precipitation and thus drying of the soil, enhancing the sensible heat flux [17]. The *clm\_cmcc\_cm* has a more pronounced cold bias in winter, with a general underestimation up to 5°C; this high value is partially due to the bias that affects the global model output. In summer, the cold bias affecting the GCM compensates the warm bias registered in *clm\_era\_int* (eastern part of the domain) leading to a better description of temperature in this area.

[Fig. 5] displays the annual cycle of total precipitation bias of *clm\_era\_int* and *clm\_cmcc\_cm* with respect to E-OBS for the seven sub-domains considered. For *clm\_era\_int*, most of sub areas are characterized by underestimation, generally between 0 and -1 mm/day. Overestimation is registered only in winter and spring months for ALPS, NE and NC. For *clm\_cmcc\_cm*, overestimation is observed in winter and underestimation in summer.

[Fig. 6] shows the mean total precipitation bias distribution (mm/day) for both the hindcast simulations. Concerning *clm\_era\_int*, a general underestimation occurs in summer in almost the whole domain, with the exception of the southern area, where a good agreement is registered. In winter, overestimation is observed especially in the central part of the domain, with high correlation between positive bias and elevation contour lines, especially over Alps, Carpathians and Caucasus Mountains. In spring and autumn (not shown) good agreement is registered in wide areas (bias between 0.5 and -0.5 mm/day). The winter overestimation is very likely due to an

underestimation of the orographic effects: in presence of a mountainous terrain, the airflow undergoes a forced lifting, resulting in adiabatic cooling and condensation; if the resolution of the orography is not fine enough, this effect can be underestimated, ultimately resulting in overestimation of the precipitation on the lee side of the mountains. Since summer precipitation is mainly due to convection, the observed bias proves that the model resolution is not fine enough to capture phenomena such as localized convection. The *clm\_cmcc\_cm* is characterized by a strong underestimation in almost all the domain in winter, while in summer it is confined to the Alpine space, with good agreement elsewhere.

It is worth noting that the precipitation biases found can be attributed not only to the regional model but also to low qualities of the observational data set and to errors on the estimation of the precipitation registered by the stations, being often the measurement stations not at the same altitudes as the model grid points [18]. In particular, the analysis performed by Turco et al. (2013) [19] showed that E-OBS is not a suitable dataset for spatial climatology of extreme precipitation indices over the Alpine Region.

Finally, it must be underlined that maximum values of T2m and precipitation biases registered in the present simulations are slightly smaller than biases that typically affect most of state of art RCM simulations over Europe [20,21].

#### 4. CLIMATE PROJECTIONS

Two scenario simulations until 2100 have been performed, driven by the global model CMCC-CM, considering respectively the IPCC RCP4.5 and RCP8.5 emission scenarios [10] developed in the framework of the 5th Coupled Model Intercomparison project (CMIP5), which rise the radiative forcing pathway respectively to  $4.5 \text{ W/m}^2$  and  $8.5 \text{ W/m}^2$  in 2100. [Fig. 7] shows the T2m change projections for the period 2071-2100 compared to 1971-2000 for both scenarios. Considering the RCP4.5 scenario, a general increase of temperature is projected in all seasons. The increase is more pronounced in DJF, while in JJA the North-East part of the domain is characterized by negligible variations. MAM (not shown) is also characterized by a substantial increase, while SON (not shown) by a more homogeneous warming, Considering the RCP8.5 scenario, distribution anomalies similar to those observed

for RCP4.5 are found, but with larger increases of temperature: peaks of 8° C are registered in DJF and MAM. These projections are consistent with the ones provided by the high resolution RCM ensemble for Europe (EURO-CORDEX) developed at spatial resolution of 12.5 km employing the RCP4.5 and RCP8.5 scenarios [22]: this ensemble highlights a robust and statistically significant warming in the range 1 - 4.5° C for RCP4.5 and 2.5 - 5.5° C for RCP8.5 (annual means). Climate projections for the Mediterranean region presented in [1], based on PRUDENCE simulations ensemble for the A1B emission scenario, gave also collective picture of a warming of the Mediterranean region, especially in the summer season.

Robust changes in precipitation are associated with large increase in temperature: [Fig. 8] shows the precipitation change projections for the period 2071-2100 with respect to 1971-2000 for both scenarios. For RCP4.5, in DJF precipitation reductions are projected in Italy, Greece and Turkey. In JJA, reductions are projected in north-center Europe. For RCP8.5, substantial precipitation reductions are projected in JJA over North-Center Europe. Precipitation increases are expected in DJF over France, Spain and South UK. The general precipitation reduction, along with the increase in DJF over north Italy, is in agreement with projections described in [1,23] and is due to circulation change patterns (increasing anticyclonic circulation) that will interest the whole Mediterranean region. A discrete qualitative agreement is also observed with projections described in [22].

## 5. CONCLUSIONS

In this paper, we have presented regional climate simulations for a Mediterranean area with COSMO-CLM, driven by ERA-Interim Reanalysis and by the output of the global model CMCC-CM under RCP4.5 and RCP8.5 emission scenarios. Validation has been carried out in terms of monthly averaged two-meter temperature (T2m) and precipitation, comparing model results with E-OBS observational datasets.

Results of the simulations allow for a satisfactory representation of the Mediterranean climate, being the values of bias found lower than the typical values that affect regional climate simulations [20,21].

Climate projections show a strong warming expected in the XXI century, associated with substantial precipitation changes.

## 6. ACKNOWLEDGMENTS

This paper has been developed within the framework of Work Package 6.2.2 of the GEMINA project, funded by the Italian Ministry of Education, University and Research and the Italian Ministry of Environment, Land and Sea.

## 7. REFERENCES

1. Giorgi F. & Lionello P. (2008) *Climate change projections for the Mediterranean region*, Global and Planetary change, No.63, pp.90–104.
2. Lionello P. et al. (2006) *The Mediterranean climate: an overview of the main characteristics and issues*, in Lionello P., Malanotte-Rizzoli P., Boscolo R. (Eds), Mediterranean Climate Variability, Elsevier, Amsterdam, pp. 1-26.
3. Giorgi F. (2006) *Climate change Hot-spots*, Geophysical Research Letters, No.33, L08707.
4. Christensen J. & Christensen O. (2007) *A summary of the PRUDENCE model projections of change in European climate by the end of this century*, Climatic Change, No. 81, pp. 7–30.
5. Hewitt C.D. (2005) *The ENSEMBLES Project: Providing ensemble-based predictions of climate changes and their impacts*, EGGS Newsletter, No. 13, pp. 22–25.
6. Giorgi F., Jones J., & Asrar G.R. (2009) *Addressing climate information needs at the regional level: the CORDEX framework*, WMO Bulletin, No. 58 (3), pp. 175-183.
7. Ruti P. et al. (2011) *MED-CORDEX initiative for Mediterranean Climate studies*, BAMS (in revision), available also at: [http://www.medcordex.eu/ruti\\_et\\_al\\_BAMS\\_MedCORDEX\\_11oct2011.pdf](http://www.medcordex.eu/ruti_et_al_BAMS_MedCORDEX_11oct2011.pdf)
8. Dee D. et al. (2011) *The era-interim reanalysis: configuration and performance of the data assimilation system*, Quarterly Journal of Royal Meteorological Society, No. 137, pp. 553–597. DOI: 10.1002/qj.828

9. Scoccimarro E. et al. (2011) *Effects of Tropical Cyclones on Ocean Heat Transport in a High Resolution Coupled General Circulation Model*, Journal of Climate, No. 24, pp. 4368–4384.
10. van Vuuren D.P. et al. (2011) *The representative concentration pathways: an overview*, Climatic Change, No. 109, pp. 5-31.
11. Rockel B., Will A. & Hense A. (2008) *The Regional Climate Model COSMO-CLM (CCLM)*. Meteorologische Zeitschrift. No. 17, pp. 347-348. DOI 10.1127/0941-2948/2008/0309
12. Montesarchio M., Zollo A., Bucchignani E., Mercogliano P. & Castellari S. (2014) *Performance evaluation of high-resolution regional climate simulations in the Alpine space and analysis of extreme events*, Journal of Geophysical Research, No. 119, pp. 3222–3237. DOI: 10.1002/2013JD021105
13. Roeckner E. et al. (2003) *The atmospheric general circulation model ECHAM5. Part I: Model description*, Max-Planck-Institut für Meteorologie, Hamburg, Germany, Rep. No. 349.
14. Haylock M.R., Hofstra N., Klein Tank A.M.G., Klok E.J., Jones P.D. & New M. (2008) *A European daily high-resolution gridded dataset of surface temperature and precipitation*, Journal of Geophysical Research, No. 113, D20119. DOI 10.1029/2008JD010201
15. Haslinger K., Anders I. & Hofstätter M. (2013) *Regional climate modelling over complex terrain: an evaluation study of COSMO-CLM hindcast model runs for the Greater Alpine Region*, Climate Dynamics, No. 40, pp. 511– 529.
16. Boberg F. & Christensen J.H. (2012) *Overestimation of Mediterranean summer temperature projections due to model deficiencies*, Nature Climate Change, No. 2, pp. 433–436. DOI 10.1038/nclimate1454
17. Jacob D. et al. (2007), *An intercomparison of regional climate models for Europe: Design of the experiments and model performance*, Climatic Change, No. 81, pp.31-52
18. Adam J.C. & Lettenmaier D.P. (2003) *Adjustment of global gridded precipitation for systematic bias*, Journal of Geophysical Research, 108 (D9), pp. 4257, DOI:10.1029/2002JD002499

19. Turco, M., Zollo A.L., Ronchi C., De Luigi C. & Mercogliano P. (2013) *Assessing gridded observations for daily precipitation extremes in the Alps with a focus on northwest Italy*, Nat. Hazards Earth Syst. Sci., No. 13, pp. 1457–1468.
20. Van der Linden P. & Mitchell J. (2009) *Ensembles: Climate change and its impacts: summary of research and results from the ensembles project*. Met Office Hadley Centre, No. 2, pp. 1–160.
21. Kotlarski S. et al. (2014) *Regional climate modeling on European scales: a joint standard evaluation of the EURO-CORDEX RCM ensemble*, Geosci. Model Dev. Discussion, No. 7, pp. 217-293, DOI 10.5194/gmdd-7-217-2014.
22. Jacob D. et al. (2013) *EURO-CORDEX: new high-resolution climate change projections for European impact research*, Regional Environmental Change, DOI 10.1007/s10113-013-0499-2.
23. Bucchignani E., Montesarchio M., Zollo A.L. & Mercogliano P. (2014) *Numerical simulations with COSMO-CLM over Italy: performance evaluation and climate projections for the XXI century*, Meteorologische Zeitschrift (submitted).

## 8. IMAGES AND TABLES

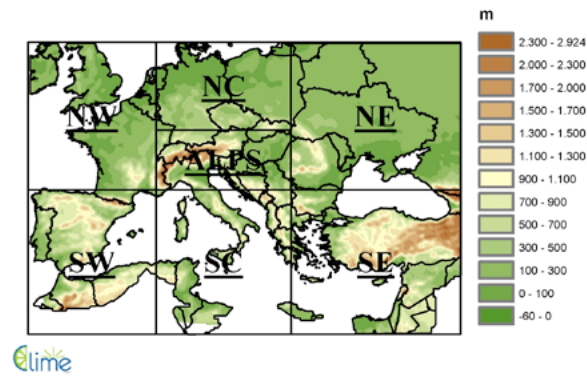


Fig. 1 Orography of the domain simulated and sub-regions considered.

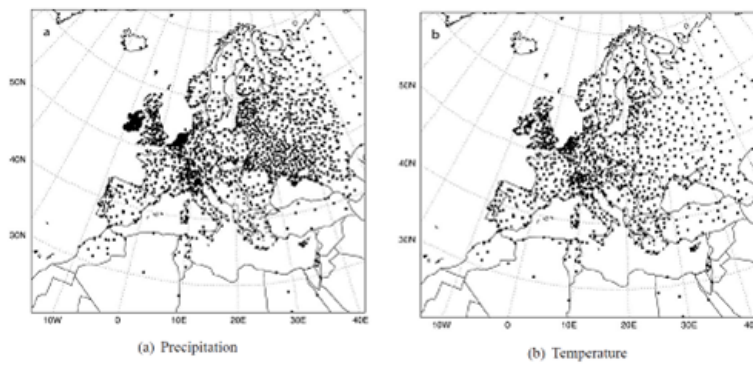


Fig. 2 E-OBS station network.

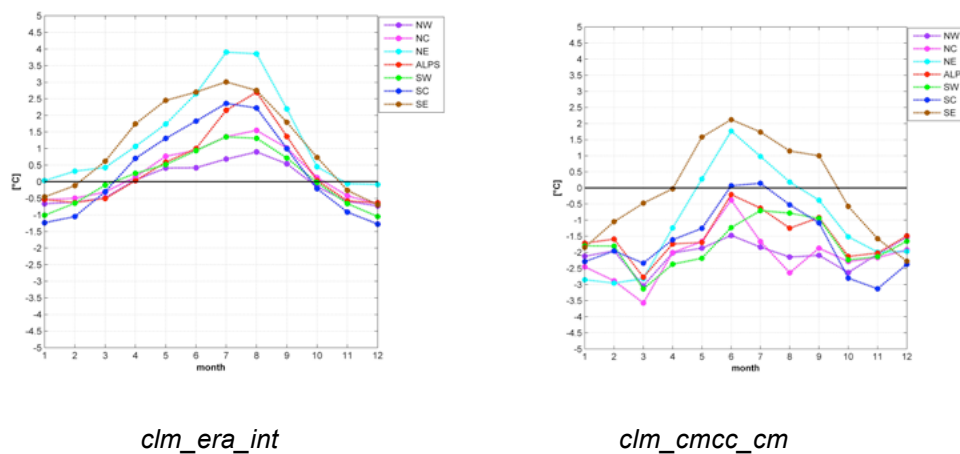


Fig. 3 Annual cycles of bias of two-meter temperature compared with E-OBS dataset for the seven sub-domains considered.

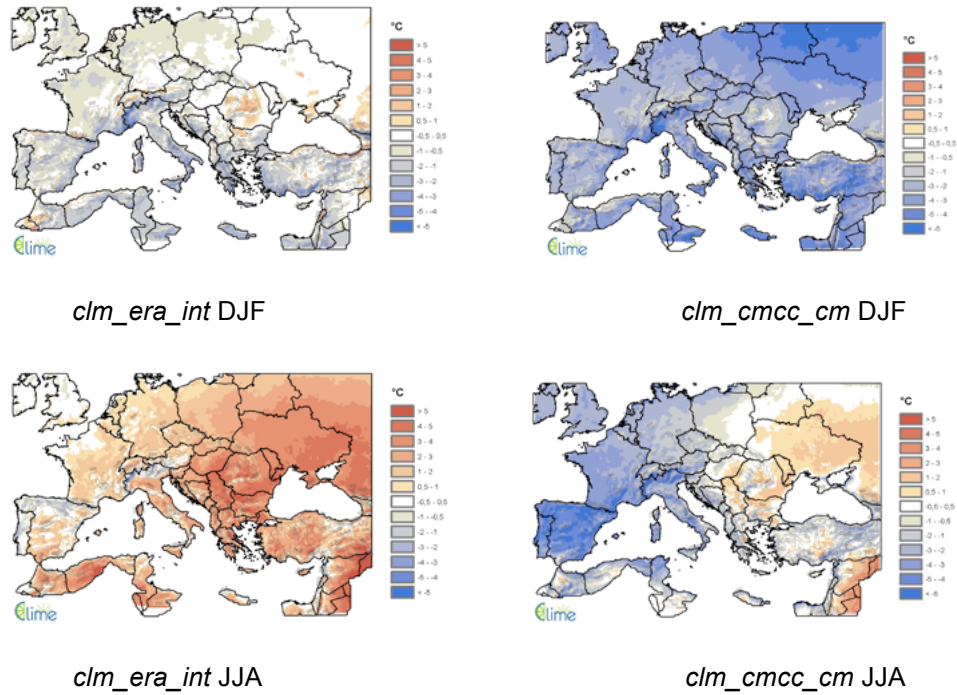


Fig. 4 Seasonal differences, in terms of 2-meter mean temperature (°C), between the output of COSMO-CLM and E-OBS dataset, for the simulation forced by ERA-Interim reanalysis (left) and the simulation forced by CMCC-CM (right).

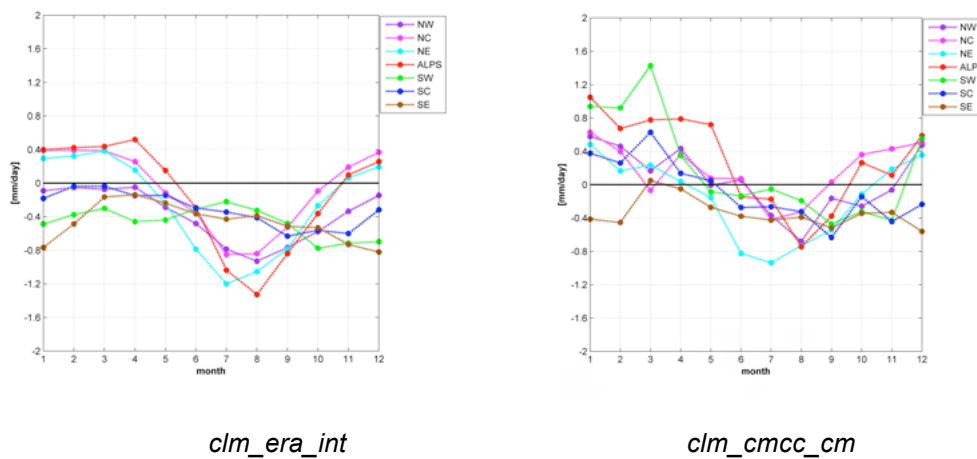


Fig. 5 Annual cycles of bias of Total precipitation compared with E-OBS dataset for the seven sub-domains considered.

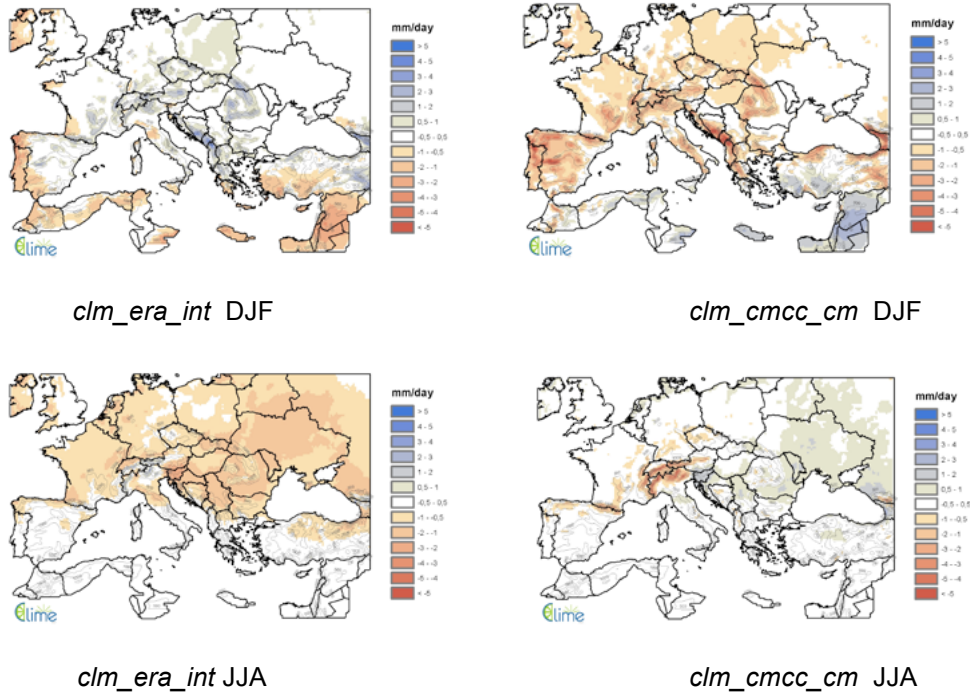


Fig. 6 Seasonal differences, in terms of daily precipitation (mm/day), between the output of COSMO-CLM and E-OBS dataset, for the simulation forced by ERA40 Reanalysis (left) and the simulation forced by CMCC-CM (right).

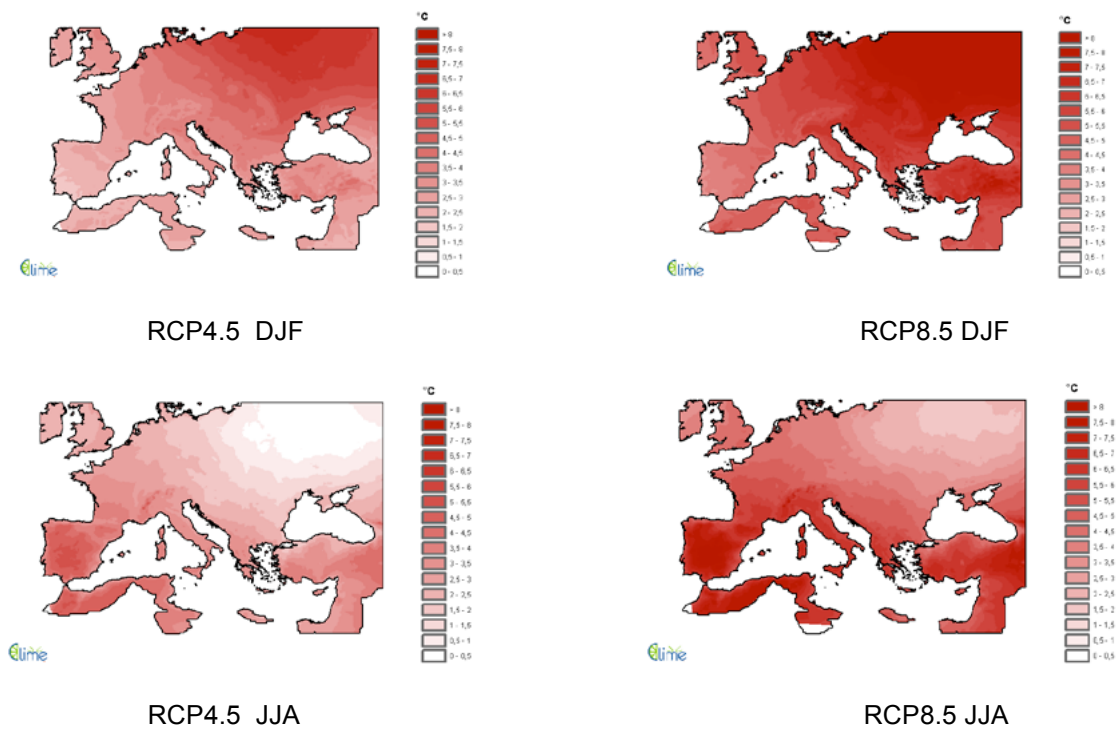


Fig. 7 Two-meter temperature (°C) climate projections for both scenarios: seasonal differences between the average value over 2071-2100 and 1971-2000.

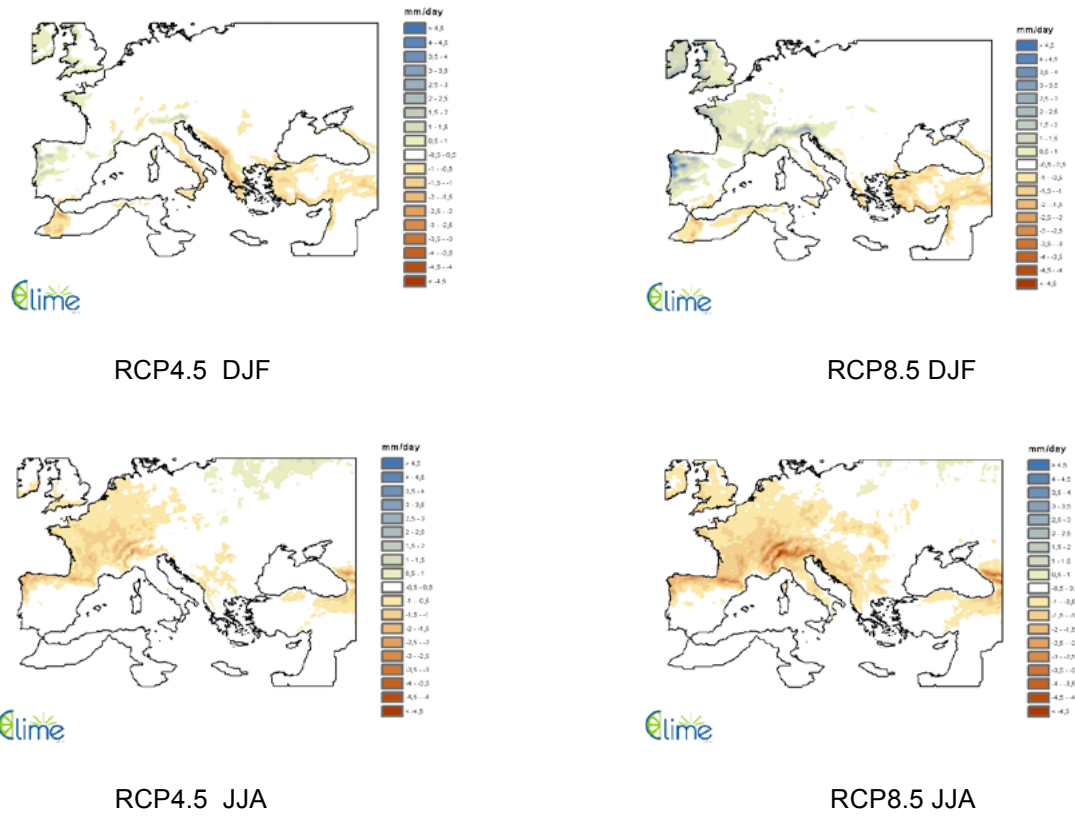


Fig. 8 Total precipitation (mm/day) climate projections: seasonal differences between the average value over 2071-2100 and 1971-2000.

# Tropical Cyclone rainfall changes in response to a warmer climate and increased CO<sub>2</sub>

Scoccimarro E.<sup>1,2\*</sup>, Villarini G.<sup>3</sup>, Gualdi S.<sup>1,2</sup>, Navarra A.<sup>1,2</sup>

<sup>1</sup>Istituto Nazionale di Geofisica e Vulcanologia, INGV - Italy, <sup>2</sup>Centro Euro-Mediterraneo sui Cambiamenti Climatici – Italy, <sup>3</sup>IIHR-Hydroscience & Engineering, The University of Iowa, Iowa City - Iowa USA

\*Corresponding Author: [enrico.scoccimarro@bo.ingv.it](mailto:enrico.scoccimarro@bo.ingv.it)

## Abstract

Possible changes in the intensity of rainfall events associated with tropical cyclones (TCs) are investigated under idealized forcing scenarios, with a special focus on landfalling storms. A new set of experiments designed within the U.S. CLIVAR Hurricane Working Group allows disentangling the relative role of changes in atmospheric carbon dioxide from that played by sea surface temperature (SST) in changing the amount of rainfall associated with TCs in a warmer world. Compared to the present day simulation, we found an increase in TC rainfall under the scenarios involving SST increases. On the other hand, in a CO<sub>2</sub> doubling-only scenario, the changes in TC rainfall are small and we found that, on average, TC rainfall tends to decrease compared to the present day climate. The results of this study highlight the contribution of landfalling TCs to the projected increase in the rainfall changes affecting the tropical coastal regions. Scenarios involving SST increases, project a TC rainfall strengthening more evident over land than over ocean. This is linked to the increased lifting effect on the landfalling TCs, induced by an increased instability of the atmospheric column along the coastal regions.

**Keywords:** tropical cyclones, rainfall, warmer climate

## 1. INTRODUCTION

Heavy rainfall and flooding associated with tropical cyclones are responsible for a large number of fatalities and economic damage worldwide (e.g., Rappaport 2000 [1]; Pielke et al. 2008 [2]; Mendelsohn et al. 2012 [3]; Peduzzi et al. 2012 [4]). Despite their large socio-economic impacts, research into heavy rainfall and flooding associated with TCs has received limited attention to date, and still represents a major challenge. Our capability to adapt to future changes in heavy rainfall and flooding associated with TCs is inextricably linked to and informed by our understanding of the sensitivity of TC rainfall to likely future forcing mechanisms.

Here we use a set of idealized high-resolution atmospheric model experiments produced as part of the U.S. CLIVAR Hurricane Working Group (US-CLIVAR HWG report [5]; Walsh et al. 2014 [6]) activity to examine TC response to idealized global-scale perturbations: the doubling of CO<sub>2</sub>, uniform 2K increases in global SST, and their combined impact.

The goal of this study is to quantify changes in the rainfall amount associated to landfalling TCs at different latitudes, as well as its dependence on different idealized climate change scenarios. A possible explanation for the more pronounced TC rainfall increase over land, when compared to the global effect, is also provided.

## 2. DATA AND METHOD

The reference data used in this study are TC tracks and precipitation. For the former, we use TC observational datasets available as 6-hourly data from the National Hurricane Center (NHC) and the U.S. Joint Typhoon Warning Center (JTWC). These datasets include the location of the center of circulation, maximum wind and minimum pressure for all the TCs during the period 1997-2006. Over the same period, the Global Precipitation Climatology Project (GPCP; Huffman et al. 2001 [7]; Bolvin et al., 2009 [8]) represents the reference data to quantify the amount of water associated with TCs. GPCP data set is obtained by combining satellite and rain gage data to provide daily global rainfall estimates with a one degree resolution.

To investigate the ability of GCMs in representing TCP and its possible changes in a warmer climate, we leverage on a set of simulations performed within the US-CLIVAR Hurricane Working Group. Here we focus on two models, one run by the

Geophysical Fluid Dynamics Laboratory (GFDL) and one by the Centro Euro-Mediterraneo sui Cambiamenti Climatici (CMCC).

Rather than running the same TC tracking algorithm on both the GFDL and CMCC models, we used the tracks provided by each modeling group. Detailed information on the ability of climate models in representing TCs can be found in Walsh et al. 2013 [9].

In this study we consider a subset of the simulations available from the US-CLIVAR Hurricane Working Group data set. More specifically, we use the following four experiments:

**CLIM:** this is a climatological run obtained by repeating the SST climatology over the period 1982-2005 for ten years. It is used to provide a baseline to contrast with the perturbation studies.

**2C:** this is a doubling CO<sub>2</sub> experiment. It is obtained by integrating the models with climatological SST (as in CLIM) but with a doubled concentration of atmospheric CO<sub>2</sub> with respect to the CLIM experiment for ten years.

**2K:** this experiment is obtained by integrating the models with climatological SST (as in CLIM) and adding a 2 K globally-uniform SST anomaly for ten years.

**2C2K:** This experiment is made by combining the 2K and 2C perturbations.

A more detailed explanation of models and simulations can be found in Scoccimarro et al. 2014 [10].

The amount of rainfall associated with a TC, both in models and observations, is computed by considering the daily precipitation in a  $10^{\circ} \times 10^{\circ}$  box around the center of the storm. According to previous studies (e.g. Lonfat et al. 2004 [11], Larson et al. 2005 [12], Kunkel et al. 2010 [13]) a  $10^{\circ} \times 10^{\circ}$  window is more than enough to include the majority of TC related precipitation in most of the cases.

### 3. RESULTS

The control simulation (CLIM) performed with the two models reproduces reasonably well the TC count at the global scale for the present climate, with a 9% underestimation for the CMCC model and a 16% overestimation for the GFDL model, compared to the reference value of 93.3 TCs/year obtained from the observation for the period 1997-2006. The CMCC model also tends to significantly underestimate the

TC count in the Atlantic basin (not shown) as confirmed by similar analyses using the coupled version of the ECHAM5 atmospheric model (Scoccimarro et al. 2011 [14]). The simulated interannual variability is slightly overestimated by both models.

In this work, we aim to assess the models' ability in simulating precipitation associated with TCs, and quantifying their relative changes for the three different idealized global forcing scenarios. To examine the TCP contribution to total precipitation, we accumulated TCP over the 10-year period - representing the present climate and we compared it to the total precipitation for the same period. Figure 1 shows the composite of rainfall during the most intense TCs for the observations (left panel) and models (middle and right panels). Models reasonably well represent TC rainfall patterns as deeply described in Villarini et al. 2014 [15].

In the observations the TC rainfall represents a large contribution to the total rainfall over the North West Pacific, North East Pacific, and North Western part of the Australian basin (figure 2, upper panel). Over these regions, the amount of precipitation contribution due to TCs is as large as about 40%, reaching a maximum of 50% in the North West Pacific. These features are captured by the simulations, despite the tendency of the CMCC model to underestimate the TCP fraction (figure 2 central panel). In terms of absolute values, the modelled TCP zonal average, normalized by TC days (hereafter TCPn) shows maximum values at about 15° in both hemispheres. Both CMCC and GFDL models are able to represent the basic aspects of the latitudinal distribution of TCPn, with the GFDL model showing a better agreement to the observations (Figure 2 lower panel).

Changes in TCPn are very similar for the two models, and show a global increase in the 2K and 2C2K experiments but not for the 2C one (Figure 3). The meridional distribution of TCPn changes (Figure 3 left panel) in the 2C case shows negative values over most of the latitudes. On the other hand, the 2K and 2C2K experiments show positive changes up to 45% when considering the average of the two models (figure 3, red and green bold lines). The positive increase is more pronounced in the 2K experiment if compared to the 2C2K one. These results are consistent with Villarini et al. 2014 [15] who found a widespread decrease in rainfall for the most intense TCs for the 2C experiment and a general increase in rainfall when SST was increased by 2K. This statement holds regardless of the distance from the center of circulation and for all the ocean basins.

Focusing on the coastal region (shaded gray area in small map shown in figure 3), the TCPn increase in 2K and 2C2K is even more pronounced (Figure 3, right panels), up to 200%. In these areas even the 2C experiment shows positive changes in most latitudes. Interestingly the TCPn increase over the coastal regions is less marked at latitudes already exposed to large amount of TCPn (i.e., between  $10^{\circ}$ - $15^{\circ}$  in the northern hemisphere and  $10^{\circ}$ - $20^{\circ}$  in the southern hemisphere) and more evident northward and equatorward these belts, leading to a more uniform distribution of TCPn with latitude in a warmer climate.

#### 4. DISCUSSION AND CONCLUSION

It is well known that atmospheric moisture content tends to increase at a rate roughly governed by the Clausius–Clapeyron equation, while the energy available to drive convection increases more slowly (e.g., Knutson and Manabe 1995 [16]; Allen and Ingram 2002 [17]; Held and Soden 2006 [18]; Meehl et al. 2007 [19]). Therefore in a warmer climate we expect an increase in the water amount associated with phenomena leading to intense precipitation (such as TCs) larger than what it is expected in moderate events (Scoccimarro et al., 2013 [20]).

Our results show that the TCP is increased in the experiments with a 2K-SST increase. On the other hand, in the simulation with doubling of atmospheric CO<sub>2</sub>, the changes in TC rainfall are small and we found that, on average, the simulated TC rainfall tends to decrease compared to the present day climate (Figure 3). Since environmental humidity was found to correlate with a larger hurricane rain field (Matyas, 2010 [21]), and because we should expect a strong relationship between changes in available precipitable water and changes in TCP, we investigated changes in the vertically integrated atmospheric water content under the different idealized warming scenarios. All the considered experiments show an increase in the water content over the tropical belt. The water content percentage increase (not shown here, see Scoccimarro et al. 2014 [10] their figure 8) is about 1% in 2C, 18% in 2K and 19% in 2C2K, suggesting that the 1% increment between 2K and 2C2K is mainly due to the higher atmospheric capability to hold moisture induced by the doubling of CO<sub>2</sub>, as shown in the 2C experiment. According to the CC, the lower-tropospheric temperature change found in the different experiments (about 0.1 K in the 2C, 2.2 K in the 2K and 2.4 K in the 2C2K) should leads to a water content increase of about 1%, 18% and 19% respectively, which is fully consistent with what obtained from the models.

Despite the increase in water content in all of the three warming experiments, the doubling of CO<sub>2</sub> tends to reduce TCP, whereas the increase of 2 K in SST tends to increase TCP. The reason should be found in the water balance at the surface: in 2K and 2C2K experiments (2Ks) we found a strong increase of the evaporation rate over the tropics (Figure 4, left panel, green and red lines respectively) due to the increase in saturated water vapour pressure at the surface. The 2K-increase in SST leads to a net increase of the evaporation rate (E). This can be easily explained considering that E is proportional to the difference between saturated water vapour at the surface ( $e_s$ ) and water vapour pressure of the lower tropospheric layers ( $e_a$ ), and that  $e_s$  depends on surface temperature following an exponential law, whereas  $e_a$  follows the same law, scaled by a factor (less than 1) represented by the relative humidity. Therefore an increase in temperature has different impacts on  $e_s$  and  $e_a$ . The doubling of CO<sub>2</sub>, on the other hand, tends to reduce E (Figure 4, blue line) independently of the boundary conditions. The doubling of CO<sub>2</sub> in forced experiments (prescribed SST) induces a weakening effect on E, since the increase in the lower tropospheric temperature leads to an increase in  $e_a$ , associated with no changes in  $e_s$  due to the fixed temperature forcing at the surface. This effect results in an increase of the atmospheric static stability in the 2C experiment.

The CO<sub>2</sub> doubling tends to slow down the global hydrological cycle by about 2% (see Table 2 in Scoccimarro et al. 2014 [10]). This is also evident in the meridional distribution of evaporation and precipitation changes (blue lines in Figure 4 left and right panels, respectively) during the TC season. The 2 K SST increase induces an acceleration of the hydrological cycle of the order of 6-7% that is reduced to 4-5% if associated with the CO<sub>2</sub> doubling (Figure 4). The changes found in the hydrological cycle are strongly influenced by the TC precipitation: a 4% / 6% (2C2K / 2K) increase in the average precipitation corresponds to an increase of about 20% / 30% in TC related precipitation.

In summary, the precipitation associated with TCs results in an increase in the experiments with a 2 K-SST increase and to a decrease when atmospheric CO<sub>2</sub> is doubled. This is consistent with the water balance at the surface, as a 2 K-increase in SST leads to a net increase of the evaporation rate, while doubling the atmospheric CO<sub>2</sub> has the opposite effect.

As already mentioned, TCPn increase projected in all of the considered 2 K-SST warming scenarios is more pronounced over land than what is expected considering also the TC path over the ocean (Figure 3). It is well known that during landfall, the TC precipitation tends to increase. This is due, in some cases, to the lifting effect induced by orographic features (Huang et al. 2009 [22]). In our 2 K-SST warming experiment the more pronounced increase of the precipitation over land might be related to an additional lifting effect on the TC, when landfall happens. Keeping in mind the possibility of an induced lifting effect source, we examined how humidity of the air is projected to change in the considered 2 K-SST experiments. The specific humidity over the coastal regions in the CLIM experiment is hundred times smaller than what is found over the entire domain including its ocean portion (Figure 5, lower left panel compared to upper left panel). In the 2C experiment, no significant differences are found in the specific humidity over land (Figure 5, upper right panel). On the other hand, the two experiments implying 2 K-SST warming, show substantial changes in the meridional distribution of the specific humidity: in the first levels of the atmospheric column (between the surface and 300 hPa) there are positive changes, over most of the tropical latitudes (Figure 5 central and lower right panels): the specific humidity increase is up to 40% the CLIM value. The more pronounced increase in TCPn over land in 2 K-SST experiments is consistent with such specific humidity increase in the lower levels of the atmospheric column: TC at landfall are projected to encounter a less stable atmospheric column, since the air at the lower levels is wetter. A more unstable atmospheric column, induced by the availability of more moist air at low levels, leads to increased updrafts, thus to an increased condensation into droplets.

## 5. ACKNOWLEDGMENTS

This work was carried out as part of a Hurricane and Climate Working Group activity supported by the U.S. CLIVAR. We acknowledge the support provided by Naomi Henderson, who downloaded and organized the data at the Lamont data library. The research leading to these results has received funding from the Italian Ministry of Education, University and Research and the Italian Ministry of Environment, Land and Sea under the GEMINA project (Enrico Scoccimarro). Moreover this material is based in part upon work supported by the National Science Foundation under Grant No. AGS-1262099 (Gabriele Villarini).

## 6. REFERENCES

1. Rappaport, E. N. (2000): *Loss of life in the United States associated with recent tropical cyclones*. Bull. Amer. Meteor. Soc., 81, 2065–2074. Dollinger J. M. (2003), *Entrepreneurship-Strategies and Resources*, Prentice Hall.]
2. Pielke, R.A., J. Gratz, C.W. Landsea, D. Collins, M.A. Saunders, and R. Musulin (2008), *Normalized hurricane damage in the United States: 1900-2005*. Nat. Hazards Rev., 9(1), 29–42.
3. Mendelsohn, R., K. Emanuel, S. Chonabayashi, and L. Bakkensen (2012), *The impact of climate change on global tropical cyclone damage*. Nat. Clim. Change, 2, 205-209.
4. Peduzzi, P., B. Chatenou, H. Dao, A. De Bono, C. Herold, J. Kossin, F. Mouton, and O. Nordbeck, (2012), *Global trends in tropical cyclone risk*. Nat. Climate Change, 2, 289–294.
5. U.S. CLIVAR Hurricane Workshop, June 5-7, 2013, Geophysical Fluid Dynamics Laboratory, Princeton, NJ.
6. Walsh et al. (2014), *Hurricanes and climate: the U.S. CLIVAR working group on hurricanes*. Bulletin of the American Meteorological Society, in preparation.
7. Huffman, G.J., R.F. Adler, M. Morrissey, D.T. Bolvin, S. Curtis, R. Joyce, B. McGavock, and J. Susskind (2001), *Global precipitation at onedegree daily resolution from multi-satellite observation*. J. Hydrometeorol., 2, 36–50.
8. Bolvin, D. T., R. F. Adler, G. J. Huffman, E. J. Nelkin, and J. P. Poutiainen, (2009), *Comparison of GPCP monthly and daily precipitation estimates with high-latitude gauge observations*. J. Appl. Meteor. Climatol., 48, 1843–1857.
9. Walsh, K. J. E., S. Lavender, E. Scoccimarro and H. Murakami (2013), *Resolution dependence of tropical cyclone formation in CMIP3 and finer resolution models*. Clim. Dynam., 40, 585–599, doi: 10.1007/s00382-012-1298-z.
10. Scoccimarro E., S. Gualdi, G. Villarini, G. Vecchi, M. Zhao, K. Walsh, A. Navarra (2014), *Intense precipitation events associated with landfalling*

- tropical cyclones in response to a warmer climate and increased CO<sub>2</sub>*. Journal of Climate, Vol. 27, No. 12., 4642-4654, doi: 10.1175/JCLI-D-14-00065.1
11. Lonfat, M., Frank D. Marks, Shuyi S. Chen (2004), *Precipitation Distribution in Tropical Cyclones Using the Tropical Rainfall Measuring Mission (TRMM) Microwave Imager: A Global Perspective*. Mon. Weather Rev., 132, 1645–1660.
  12. Larson, J., Y. Zhou, R. W. Higgins (2005), *Characteristics of Landfalling Tropical Cyclones in the United States and Mexico: Climatology and Interannual Variability*. J. Climate, 18, 1247–1262.
  13. Kunkel, K. E., D. Easterling, D. A. R. Kristovich, B. Gleason, L. Stoecker, and R. Smith (2010): *Recent increases in U.S. heavy precipitation associated with tropical cyclones*. Geophys. Res. Lett., 37, L24706.
  14. Scoccimarro, E., S. Gualdi, A. Bellucci, A. Sanna, P. G. Fogli, E. Manzini, M. Vichi, P. Oddo, and A. Navarra (2011), *Effects of tropical cyclones on ocean heat transport in a high resolution coupled general circulation model*. J. Climate, 24, 4368–4384, doi:10.1175/2011JCLI4104.1.
  15. Villarini G., D.A. Lavers, E. Scoccimarro, M. Zhao, M.F. Wehner, G. Vecchi, T. Knutson (2014), *Sensitivity of Tropical Cyclone Rainfall to Idealized Global Scale Forcings*. Journal of Climate, Vol. 27, No. 12., doi: 10.1175/JCLI-D-13-00780.1.
  16. Knutson, T. R., and S. Manabe (1995), *Time-mean response over the tropical Pacific to increased CO<sub>2</sub> in a coupled ocean– atmosphere model*. J. Climate, 8, 2181–2199.
  17. Allen, M. R., and W. J. Gram (2002), *Constraints on future changes in climate and the hydrologic cycle*. Nature, 419, 224–232.
  18. Held, I. M. and B.J. Soden (2006), *Robust responses of the hydrological cycle to global warming*. J. Climate 19, 5686–5699.
  19. Meehl, G. A. and Coauthors (2007), *Global climate projections*. *Climate Change 2007: The Physical Science Basis*, S. Solomon et al., Eds., Cambridge University Press, 747–845.

20. Scoccimarro E., S. Gualdi, A. Bellucci, M. Zampieri, A. Navarra (2013), Heavy precipitation events in a warmer climate: results from CMIP5 models. *J. Climate*, DOI: 10.1175/JCLI-D-12-00850.1.
21. Matyas, C.J., (2010), *Associations between the size of hurricane rain fields at landfall and their surrounding environments*, *Meteorol. Atmos. Phys.*, 106, 3-4, pp 135-148.
22. Huang, Hsiao-Ling, Ming-Jen Yang, Chung-Hsiung Sui (2014), *Water Budget and Precipitation Efficiency of Typhoon Morakot (2009)*. *J. Atmos. Sci.*, 71, 112–129.

## 7. IMAGES AND TABLES

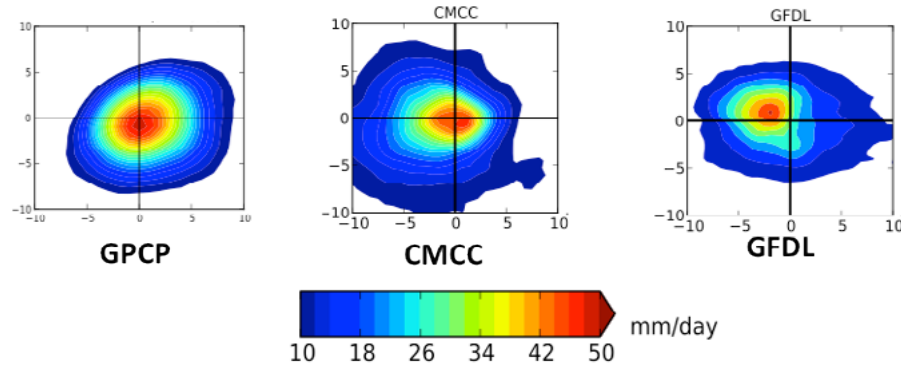


Fig. 1 Composite mean observed (GPCP, left panel) and modeled (CMCC/GFDL central/right panels) daily rainfall rate patterns associated to the 10% most intense TCs. The units are mm/day, and the x and y axes correspond to degrees from the TC center.

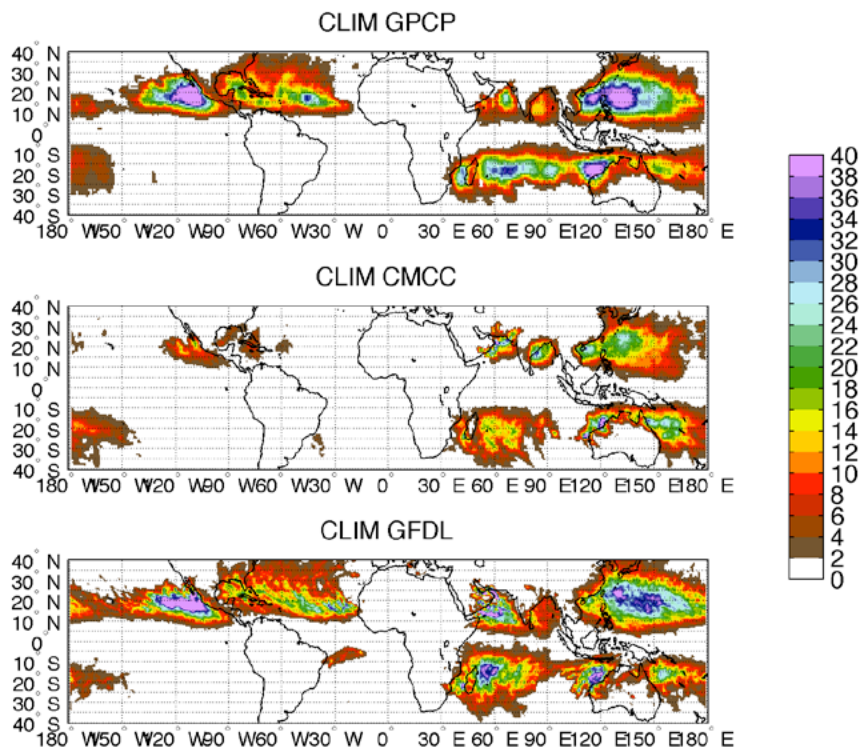


Fig. 2 Percentage of water associated with TCs in the control simulation CLIM with respect to the total annual precipitation. The accumulation is performed by taking a  $10^{\circ} \times 10^{\circ}$  window centered on the center of circulation. The upper panel refers to the observations, while the central and lower panels to the CMCC and GFDL models, respectively. Units are [%].

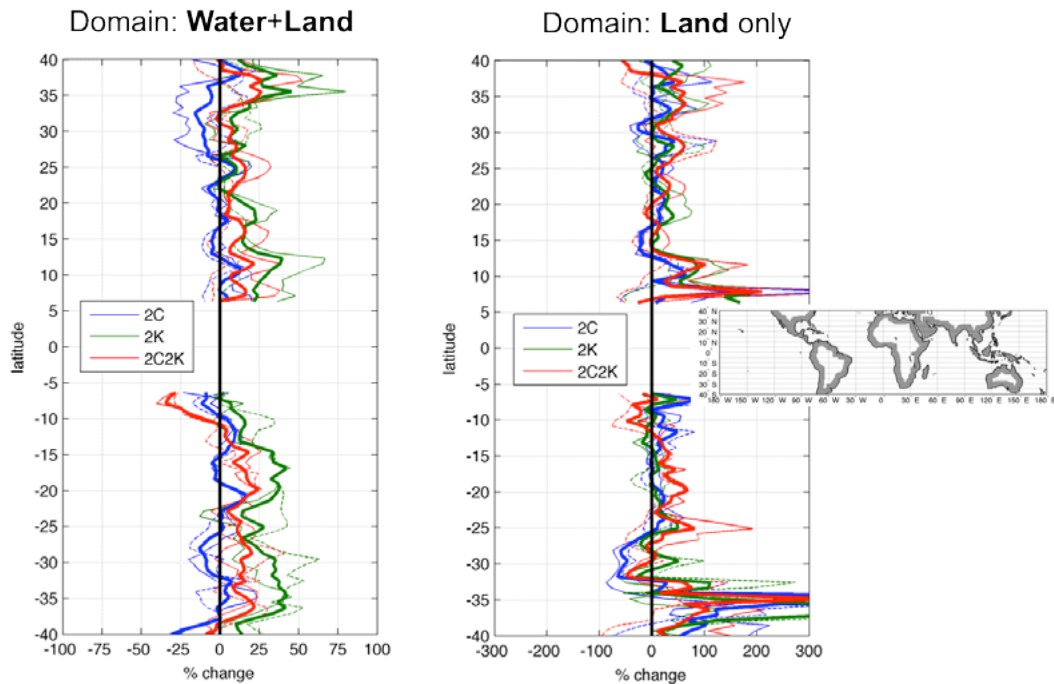


Fig. 3 Changes in TC related precipitation amount in the 2C (blue), 2K (green) and 2C2K (red) experiments as a function of latitude. Results are shown with respect to the CLIM experiment. Solid thin lines represent CMCC results. Dashed thin lines represent GFDL results. The solid thick lines represent the average of the two models. Units are [%]. Left panel refers to the entire TC track. Right panel refers to TC track over land only (the gray region represented in the small map).

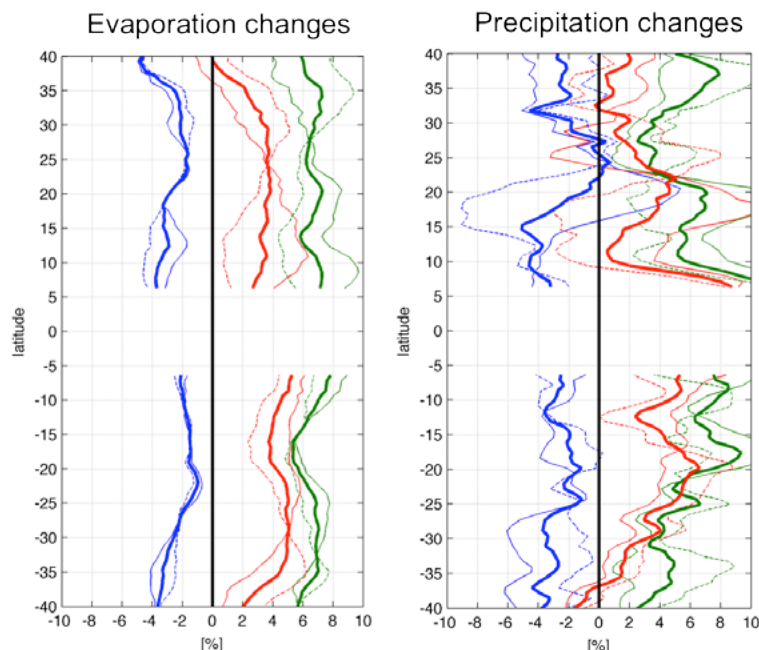


Fig. 4 Changes in evaporation (left panel) and precipitation (right panel) in 2C (blue), 2K (green) and 2C2K (red) experiments as a function of latitude with respect to the CLIM experiment. Solid thin lines represent CMCC results. Dashed thin lines represent GFDL results. Solid thick lines represent averaged values. Northern hemisphere values are computed over June-November and Southern hemisphere values over December-May.

Hemisphere values are computed over December-May. Units are [mm/d] (left panel) and [%] (right panel).

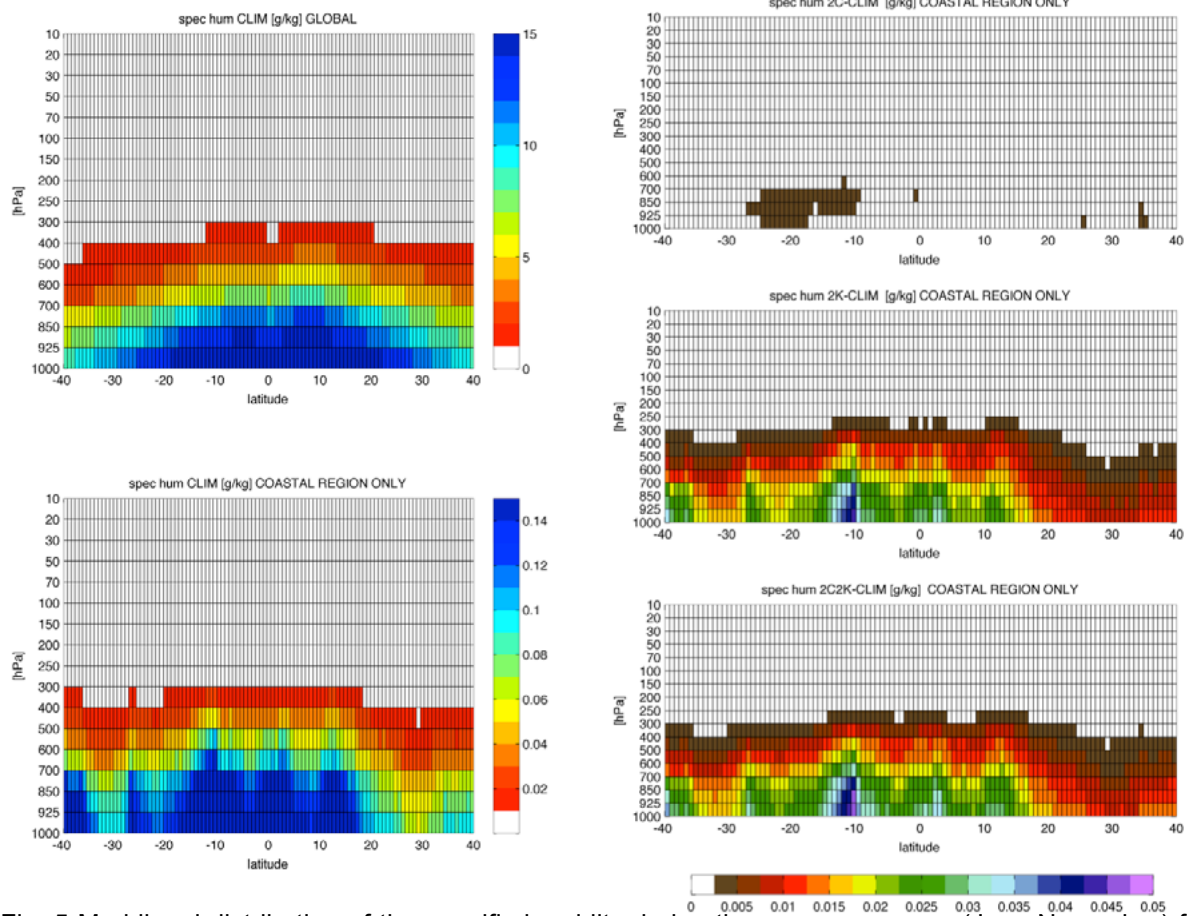


Fig. 5 Meridional distribution of the specific humidity during the summer season (June-November) for the northern hemisphere and December-May for the southern hemisphere). Left panels represent the present climate (CLIM) modeled results over the entire global domain (upper left panel) and over coastal regions only (lower left panel). In the right panels specific humidity changes in the three different scenarios (2C / 2K / 2C2K in upper right / central right / lower right panels), are shown.

Advances in climate change

**GHG & solar variability:  
past and future**

# Influence of forcings and variability on recent global temperature behavior: A neural network analysis

Pasini A.<sup>1\*</sup>, Racca P.<sup>2,3</sup>, and Cassardo C.<sup>3,4</sup>

<sup>1</sup>CNR, Institute of Atmospheric Pollution Research, Roma - Italy, <sup>2</sup>Collegio Carlo Alberto, Torino - Italy, <sup>3</sup>University of Turin, Department of Physics, Torino - Italy, and

<sup>4</sup>Ewha Womans University, Department of Atmospheric Science and Engineering, Seoul - Korea

\*Corresponding Author: pasini@iia.cnr.it

## Abstract

Attribution studies on recent global warming by Global Climate Models clearly show the fundamental role of anthropogenic forcings in driving the temperature behavior of the last half century. Here, due to the potential benefits that can be derived by a change in the analysis viewpoint of a complex system, we adopt a completely different, non-dynamical, data-driven and fully nonlinear approach to the attribution problem. By means of neural network modeling and analyzing the last 150 years, we find that the behavior of global temperatures may be attributed basically to anthropogenic forcings rather than to natural ones and circulation patterns. Furthermore, the role of Atlantic Multidecadal Oscillation and other circulation patterns in “modulating” the global temperature curve is clarified. These results corroborate our previous knowledge from Global Climate Models and give new insight into the problem of understanding the relative contributions of external forcings and internal variability in the climate system.

**Keywords:** attribution, neural modeling, forcings, variability, global temperature

## 1. INTRODUCTION

As well known, Global Climate Models (GCMs) are the standard dynamical tools for catching the complexity of climate system and simulating its behavior [1,2]. In particular, in the framework of this virtual laboratory we are able to perform attribution experiments (for instance, by “switching off” some forcings) in order to understand which factors have mainly influenced the behavior of some variables of climatic importance, such as the global temperature. The results of these experiments clearly indicate that anthropogenic forcing (primarily greenhouse gas forcing) is the main responsible for the recent global warming [3].

Even if the main road for obtaining reliable attribution results is obviously represented by the application of GCMs to this problem, we think that it is worthwhile to explore other methods of investigation. The reason for this is threefold. i) The dynamical structure of GCMs is very complex and, at least in principle, their specific simulation results could crucially depend on our wide but however limited representation of the system in the models, and on the delicate balance of fluxes between subsystems, the relative strength of feedbacks and the different parameterization routines. Ensemble runs greatly contribute to soften these problems and a big technical work is in progress on these aspects inside the modelling community, but the perception of other parts of the scientific community and, especially, of common people often emphasizes uncertainties which (they believe) could undermine the reliability of the GCMs' results. ii) As well known, climate is a complex system and the study of other complex systems has shown that we often benefit from a change in viewpoint when analyzing them: e.g., in biology, the molecular biology approach vs. a more systemic point of view. iii) Both external forcings and internal variability influence the climate behavior. At present, probably GCMs have not yet shown a satisfying ability in simulating the behavior of some patterns – such as El Niño Southern Oscillation (ENSO) and the Pacific Decadal Oscillation (PDO) – which dominate the internal variability of global temperature, even if recent results are very promising [4].

In this framework, a neural network (NN) model is adopted for analyzing the relationships between external forcings and global temperature and for clarifying the specific role of internal variability. In particular, this allows us to compare the attribution results coming from two very distinct approaches (GCMs and NNs) and to possibly increase their reliability.

Recently, neural modeling found wide application to the topic of climate change [5]. Here we use a specific neural tool developed for handling short time series and applied to several atmospheric and climatic problems in the past [6-10].

## 2. DATA

In this paper we consider the following time series of annual data since the middle of the 19<sup>th</sup> century to 2007:

- global temperatures (T) from HadCRUT3 combined global land and marine surface temperature anomalies [11]: data available at <http://www.cru.uea.ac.uk/cru/data/>;
- total solar irradiance (TSI) [12], with background from Wang et al. [13]: data available at [www.geo-fu.berlin.de](http://www.geo-fu.berlin.de);
- cosmic ray intensity (CRI) from count rates of a polar neutron monitor [14-16]: data available at <ftp.ncdc.noaa.gov>;
- stratospheric aerosol optical thickness (SAOT) at 550 nm as compiled by Sato et al. [17], updated by [giss.nasa.gov](http://giss.nasa.gov) to 1999 and extended to 2007 with zero values: data available at <http://data.giss.nasa.gov>;
- greenhouse gases (GHGs) concentrations [18]: data available at <http://data.giss.nasa.gov>; greenhouses gases total radiative forcing (GHG-RF) has been calculated as in Ramaswamy et al. [19];
- global sulfur emissions (GSE) till 2000 from Stern [20]: data available at <http://www.sterndavidi.com/datasite.html>; in absence of reliable global estimates for the last years, the series has been extended to 2007 with constant values;
- Southern Oscillation Index (SOI), related to ENSO [21-23]: data available at [www.cru.uea.ac.uk/cru/data/soi/soi.dat](http://www.cru.uea.ac.uk/cru/data/soi/soi.dat) (since 1866);
- Pacific Decadal Oscillation (PDO) [24]: data available at <ftp.ncdc.noaa.gov/pub/data/ersst-v2/pdo.1854.latest.st> (since 1854);
- Atlantic Multidecadal Oscillation (AMO) [25]: data available at <http://www.esrl.noaa.gov/psd/data/timeseries/AMO> (since 1856).

Here, we consider TSI, CRI and SAOT as natural forcings, GHG-RF and GSE as anthropogenic forcings, and SOI, PDO and AMO as representative data of natural variability.

### 3. A NEURAL NETWORK FOR CLIMATIC ATTRIBUTION

NN modeling is the method adopted here to assess the influence of external forcings and circulation patterns on global temperature. The application of NNs in atmospheric and climate sciences is quite recent: see [26-28,5] for some reviews.

Our networks are simple feed-forward ones with one hidden layer and a single output [29-30]. More specifically, here we adopt an NN tool developed some years ago [31] for both diagnostic characterization and forecast in complex systems. In the last years it has been applied to attribution studies at global and regional scales [8-10].

The kernel of our NN tool has been extensively described elsewhere [31,6,10]. Here we just stress that a sigmoidal transfer function in the hidden layer and a linear one at the output neuron are adopted. Furthermore, learning from data is performed through an error-backpropagation training characterized by generalized Widrow–Hoff rules (endowed with gradient descent and momentum terms) for updating connection weights.

NNs are very powerful tools and, in general, they are able to find a nonlinear function that reconstructs in detail the values of targets (in our case, global temperature) starting from data about inputs (external forcings and, in case, indices of circulation) if every input–target pair is known to them, and a large number of neurons in the hidden layer are allowed. But in this case, NNs overfit data and no realistic regression law can be obtained. Thus, we have to exclude some input-target pairs from the training set on which the regression law is built and must consider a small number of hidden neurons. Only if the map derived from the training set is able to describe the relation between inputs and target on independent sets can we say that a realistic regression law has been obtained.

If the data set is not so long, as in our case, one must try to maximize the training set. To do so, we adopt a method described in [10], the so-called “extended leave-one-out procedure”: see [Fig. 1]. Here, the white squares represent the elements (input–target pairs) of our training set, the black squares represent the elements of the validation

set and the single grey square represents the test set. We stop the training when the error on the validation set begins to increase. The relative composition of training, validation and test sets change at each step of an iterative procedure of training, validation and test cycles. A “hole” in the complete set represents our test set and moves across this total set of pairs, thus permitting the estimation of all temperature values at the end of the procedure. Furthermore, the validation set is randomly chosen at every step of our procedure.

Obviously, the results of this extended leave-one-out procedure critically depend on the random choices regarding the initial weights and the elements of the validation set. For taking this fact into account and obtaining more robust results, we performed ensemble runs of our NNs, by repeating 15 times every estimation shown in [Fig. 1] with new random choices for both the weights and the elements of the validation set.

Finally, after several empirical attempts, 4 neurons were chosen for insertion in the hidden layer and 15 elements were considered for the validation set.

#### **4. NN APPLICATION AND RESULTS**

As in dynamical studies about attribution of the global temperature behavior, even in our investigation the final aim is to catch the fundamental drivers of the recent global warming. To do so, due to the nonlinear nature of the climate system and to the impossibility of applying the superposition principle, it is necessary to work out a complete model which is able to correctly reconstruct the temperature behavior and, then, one must to “flatten” the influence of some forcings during the period of investigation so that the consequences on global T could be simulated (and appreciated).

Before achieving this stage, we performed some preliminary runs of our NNs in order to understand which influence can be exercised by the various forcings on the behavior of temperature. In doing so, we built NNs with annual data of some forcings and/or circulation patterns in inputs, and considered the annual global temperature anomalies as the single output.

The first results show that NNs endowed uniquely with natural forcings in input are not able to reconstruct the increasing trend of the temperature curve, and also the interannual and decadal variability present in the observations is not correctly caught.

Furthermore, in the NN outputs a signal of the 11-year solar cycle is emphasized; however, this cycle is not present, at least with this relevance, in the temperature time series [Fig. 2]. In other runs in which we have considered also data about cosmic rays, we discovered that the contribution of the input related to CRI to the output of the networks is highly irrelevant, so that we decided to exclude CRI as inputs in all the following runs.

On the other hand, building networks endowed with GHG-RF and GSE as inputs, the results allowed us to correctly reconstruct the trend of the temperature target-curve but the NN output-curve was too smooth, with very low variability [Fig. 3].

The obvious next step was to combine natural and anthropogenic forcings in a single architecture of our networks, by considering NNs endowed with 4 inputs: GHG-RF, GSE, TSI and SAOT. The results showed a very good reconstruction of the long-term trend and some increased capability of catching the interannual variability, even as ensemble mean, at least in the last decades [Fig. 4]. In particular, the correlation coefficient  $R$  (observed temperature vs. ensemble mean) = 0.89 and the mean square error  $MSE = 0.0137 \text{ K}^2$ . Nevertheless, some underestimations and overestimations are still visible and the observed curve of temperature anomalies appears more “modulated” at decadal and multidecadal scales.

At this point, it was worthwhile to analyze in more details the reconstruction results of this last network by plotting its residuals (ensemble mean – observed T anomalies). This was done in [Fig. 5], where a non-random nature of the errors of the NN model is evident. Could this be due to the absence of information about natural variability in our model?

An interesting numerical experiment can be performed by training a NN model endowed with data about SOI, PDO and AMO indices to reconstruct the series of residuals. This has been done and the fundamental result is shown in [Fig. 6]. In this brief contribution we do not enter into statistical details, but, in any case, it is clear that the consideration of these indices allows us to “attribute” the errors of our model built on external forcings to the lack of information about natural variability. As a further information, it is worthwhile to note that other runs (whose results are not shown here for lack of space), in which one circulation index is pruned at a time, show that, without AMO data, the residuals are not well reconstructed.

If now we add the reconstructions performed by the ensemble means of the last two networks, we obtain the interesting result presented in [Fig. 7], where  $R = 0.94$  and  $MSE = 0.0078 \text{ K}^2$ . Now the temperature curve appears to be well reconstructed, both in its trend and interannual, decadal and multidecadal variability.

Till now we considered as separated the influences of external forcings and natural variability, due to their (at least conceptually) different actions on the climate system. However, our data-driven model could perform better if they are included on the same level as inputs to the networks. Thus, we trained a further ensemble of NNs endowed with 7 inputs: GHG-RF, GSE, TSI, SAOT, SOI, PDO and AMO. The fundamental result is shown in [Fig. 8]. Here  $R = 0.95$  and  $MSE = 0.0066 \text{ K}^2$ , and the NN performance is even better than in the previous case, where we adopted a linear sum of the influences of forcings and variability. This obviously states the power of this fully nonlinear method.

At this stage, we have obtained a NN ensemble of models that correctly catches the behavior of the global temperatures in the last 150 years and, in particular, reconstructs the recent global warming of the last decades.

As happens for GCMs, when we have validated models, numerical experiments can be performed on these models by switching off or flatten some external forcing on the climate system, in order to understand to which influence the phenomenon of recent global warming can be attributed. Now we have validated NN models and we would like to follow the same strategy used in GCMs for attribution studies.

To do so, first we saved the structure of our validated 7-input networks (fundamentally the values of their weights) for each annual target in the ensemble runs. Then we propagated the signal from inputs to output when the inputs of GHG-RF and GSE were fixed to the values of the year 1866. In this way we were able to analyze a simulated situation in which the anthropogenic forcings did not act as drivers of changes in temperature. The results are very clearly depicted in [Fig. 9]. In this situation our NN models see no warming, but just natural variability. In particular, an approximated 60-year cycle is clearly visible, contrarily to the output of GCMs in attribution studies, which appears more smooth and not “modulated” (see, for instance, [3]).

## 5. CONCLUSIONS AND PROSPECTS

In this paper, an investigation of the attribution problem related to the recent global warming has been performed by means of a data-driven and fully nonlinear method.

Even if the technique used here is completely independent by dynamical modeling, we found results resembling those obtained by GCMs in the same framework. The very similar outcomes of these two kinds of models lead us to look at them with more confidence and vouch for their robustness and reliability.

In our opinion, the last result depicted in [Fig. 9] is particularly impressive, because corroborates the attribution results obtained by GCMs (which see in the anthropogenic forcings the main drivers of the recent global warming) by means of a completely independent approach and technique, and, at the same time, gives a deeper insight in the influence of natural variability on temperature behavior.

Just this evidence of the influence of variability in modulating the temperature curve at several time scales can suggest a further application of NN modeling: the decadal or multidecadal forecast of temperature behavior starting from emission scenarios and natural cycles of variability.

## 7. REFERENCES

1. Flato G. *et al.* (2013), Evaluation of Climate Models. In *Climate Change 2013: The Physical Science Basis* (eds. T.F. Stocker *et al.*), Cambridge University Press, Cambridge, UK, and New York, NY, USA, pp. 741-866.
2. Pasini A. (2005), *From Observations to Simulations. A conceptual Introduction to Weather and Climate Modelling*, World Scientific, Singapore.
3. Bindoff N.L. *et al.* (2013), Detection and Attribution of Climate Change: from Global to Regional. In *Climate Change 2013: The Physical Science Basis* (eds. T.F. Stocker *et al.*), Cambridge University Press, Cambridge, UK, and New York, NY, USA, pp. 867-952.
4. Stoner A.M.K., Hayohe K. & Wuebbles D.J. (2009), *Assessing general circulation models simulations of atmospheric teleconnections patterns*, Journal of Climate, No. 22, pp. 4348-4372.

5. Pasini A. (2009), Neural network modeling in climate change studies. In *Artificial Intelligence Methods in the Environmental Sciences* (eds. S.E. Haupt, A. Pasini & C. Marzban), Springer, New York, NY, USA, pp. 235-254.
6. Pasini A., Pelino V. & Potestà S. (2001), *A neural network model for visibility nowcasting from surface observations: Results and sensitivity to physical input variables*, Journal of Geophysical Research, No. 106, pp. 14951-14959 (2001).
7. Pasini A. & Ameli F. (2003), *Radon short range forecasting through time series preprocessing and neural network modeling*, Geophysical Research Letters, No. 30, 1386, doi:10.1029/2002GL016726.
8. Pasini A., Lorè M. & Ameli F. (2006), *Neural network modelling for the analysis of forcings/temperatures relationships at different scales in the climate system*, Ecological Modelling, No. 191, pp. 58-67.
9. Pasini A. & Langone R. (2012), *Influence of circulation patterns on temperature behavior at the regional scale: A case study investigated via neural network modeling*, Journal of Climate, No. 25, pp. 2123-2128.
10. Pasini A. & Modugno G. (2013), *Climatic attribution at the regional scale: a case study on the role of circulation patterns and external forcings*, Atmospheric Science Letters, No. 14, pp. 301-305.
11. Brohan P., Kennedy J.J., Harris I., Tett S.F.B. & Jones P.D. (2006), *Uncertainty estimates in regional and global observed temperature changes: A new dataset from 1850*, Journal of Geophysical Research, No. 111, D12106, doi:10.1029/2005JD006548.
12. Lean J.L. & Rind D.H. (2008), *How natural and anthropogenic influences alter global and regional surface temperatures: 1889 to 2006*, Geophysical Research Letters, No. 35, L18701, doi:10.1029/2008GL034864.
13. Wang Y.-M., Lean J.L. & Sheeley Jr N.R. (2005), *Modeling the Sun's magnetic field and irradiance since 1713*, Astrophysical Journal, No. **625**, pp. 522-538.
14. Usoskin I.G., Mursula K., Solanki S.K., Schüssler M. & Kovaltsov G.A. (2002), *A physical reconstruction of cosmic ray intensity since 1610*. Journal of Geophysical Research, No. 107, 1374, doi:10.1029/2002JA009343.

15. Usoskin I.G., Alanko-Huotari K., Kovaltsov G.A. & Mursula K. (2005), *Heliospheric modulation of cosmic rays: Monthly reconstruction for 1951-2004*. Journal of Geophysical Research, No. 110, A12108, doi:10.1029/2005JA011250.
16. Alanko-Huotari K., Mursula K., Usoskin I.G. & Kovaltsov G.A. (2006), *Global heliospheric parameters and cosmic-ray modulation: An empirical relation for the last decades*. Solar Physics, No. 238, pp. 391-404.
17. Sato M., Hansen J.E., McCormick M.P. & Pollack J. (1993), *Stratospheric aerosol optical depths (1850-1990)*, Journal of Geophysical Research, No. 98, pp. 22987-22994.
18. Hansen J. et al. (2007), *Climate simulations for 1880-2003 with GISS modelE*, Climate Dynamics, No. 29, pp. 661-696.
19. Ramaswamy V. et al. (2001), Radiative forcing of climate change. In *Climate Change 2001: The Scientific Basis*, (eds. J.T. Houghton et al.) Cambridge University Press, Cambridge, pp. 349-416.
20. Stern D.I. (2005), *Global sulfur emissions from 1850 to 2000*, Chemosphere, No. 58, pp.163-175.
21. Ropelewski C.F. & Jones P.D. (1987), *An extension of the Tahiti-Darwin Southern Oscillation Index*, Monthly Weather Review, No. 115, pp. 2161-2165.
22. Allan R.J., Nicholls N., Jones P.D. & Butterworth I.J. (1991), *A further extension of the Tahiti-Darwin SOI, early SOI results and Darwin pressure*, Journal of Climate, No. 4, pp. 743-749.
23. Können G.P., Jones P.D., Kaltofen M.H. & Allan R.J. (1998), *Pre-1866 extensions of the Southern Oscillation Index using early Indonesian and Tahitian meteorological readings*, Journal of Climate, No. 11, pp. 2325-2339.
24. Smith T.M. & Reynolds R.W. (2004), *Improved extended reconstruction of SST (1854-1997)*, Journal of Climate, No. 17, pp. 2466-2477.
25. Enfield D.B., Mestas-Nunez A.M. & Trimble P.J. (2001), *The Atlantic Multidecadal Oscillation and its relationship to rainfall and river flows in the continental U.S.*, Geophysical Research Letters, No. 28, pp. 2077-2080.

26. Krasnopolsky V.M. (2007), *Neural network emulations for complex multidimensional geophysical mappings: Applications of neural network techniques to atmospheric and oceanic satellite retrievals and numerical modeling*, *Reviews of Geophysics*, No. 45: RG3009, doi:10.1029/2006RG000200.
27. Haupt S.E, Pasini A. & Marzban C. (eds.) (2009), *Artificial Intelligence Methods in the Environmental Sciences*, Springer, New York, NY, USA.
28. Hsieh W.W. (2009), *Machine Learning Methods in the Environmental Sciences: Neural Networks and Kernels*, Cambridge University Press, Cambridge, UK.
29. Hertz J., Krogh A. & Palmer R.G. (1991), *Introduction to the Theory of Neural Computation*, Addison-Wesley, New York, NY, USA.
30. Bishop C.M. (1995), *Neural Networks for Pattern Recognition*, Oxford University Press, Oxford, UK.
31. Pasini A. & Potestà S. (1995), *Short-range visibility forecast by means of neural-network modelling: A case study*, *Nuovo Cimento C*, No. 18, pp. 505-516.

## 8. FIGURES

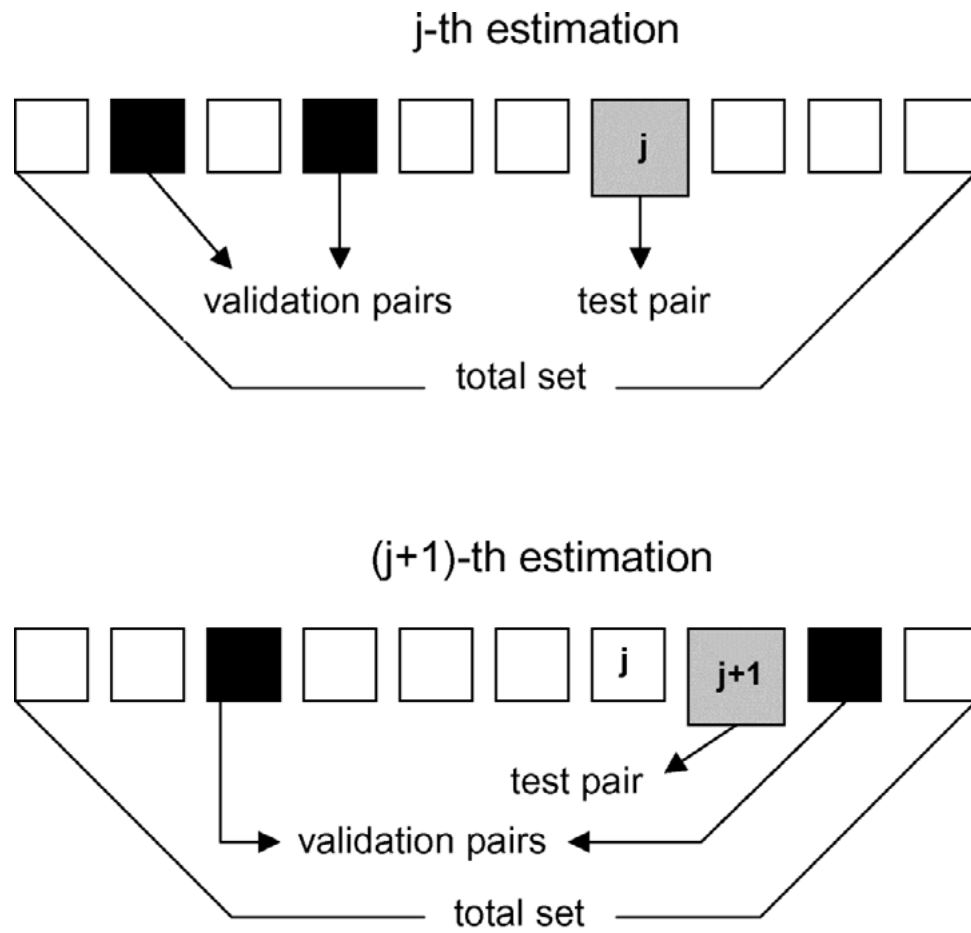


Fig. 1 Sketch of the generalized leave-one-out procedure adopted in this paper.

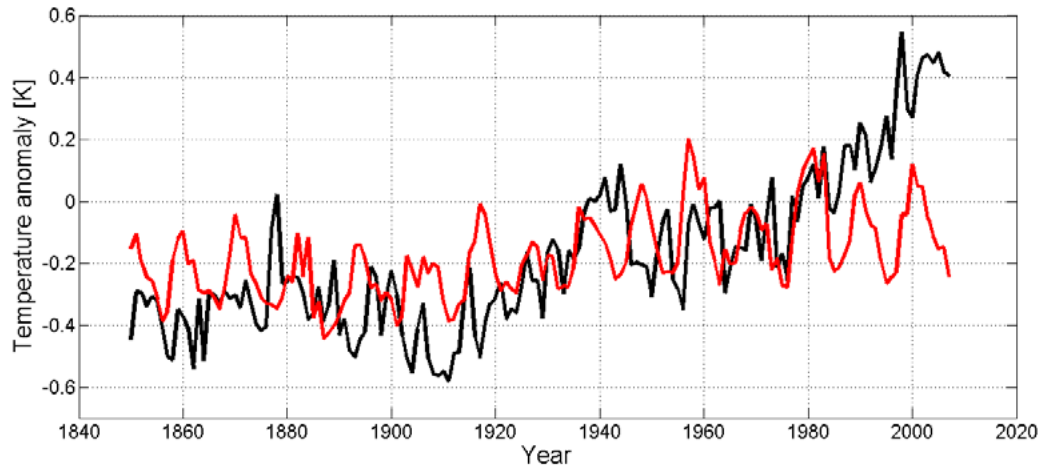


Fig. 2 Output of a single NN run when just natural forcings (TSI and SAOT) are considered as inputs. Black line: observed temperature anomalies, red line: NN output.

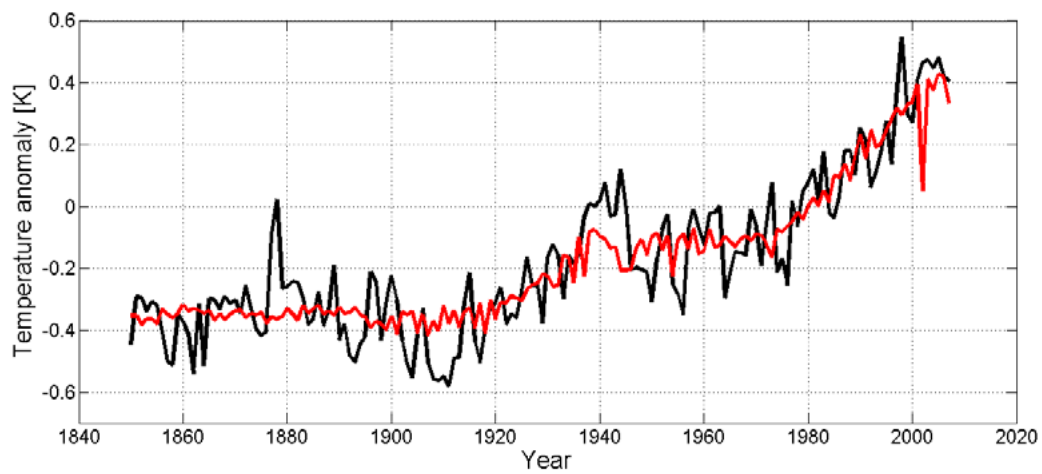


Fig. 3 Output of a single NN run when just anthropogenic forcings (GHG-RF and GSE) are considered as inputs. Black line: observed temperature anomalies, red line: NN output.

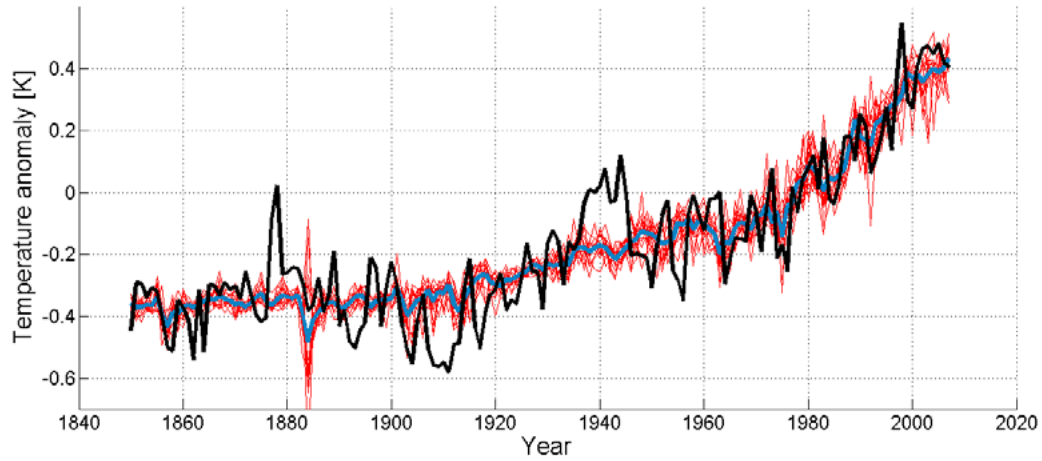


Fig. 4 Results of networks endowed with natural and anthropogenic forcings as inputs. Black line: observed temperature anomalies, red lines: NN outputs of single runs, blue line: ensemble mean.

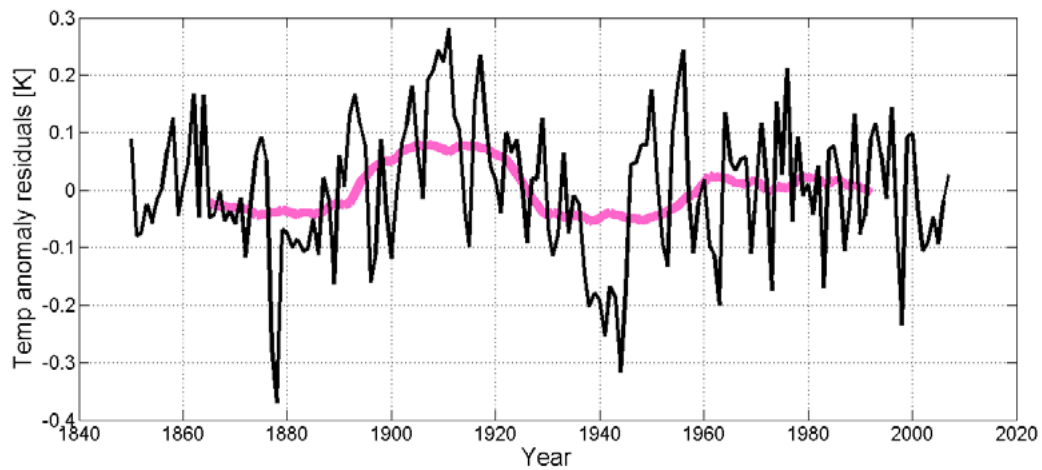


Fig. 5 The residuals show a “multidecadal variability” in the score of the NN model endowed with natural + anthropogenic forcings as inputs. Black line: residuals (ensemble mean – observed temperature anomalies), magenta line: 31-year moving average.

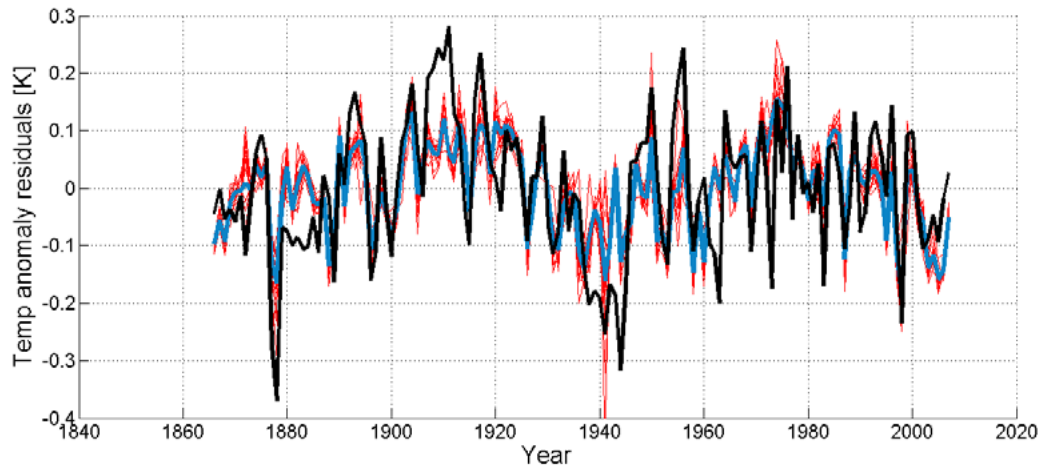


Fig. 6 Reconstruction of the residuals by NNs endowed with data about SOI, PDO and AMO indices as inputs. Black line: residuals, red lines: NN outputs of single runs, blue line: ensemble mean.

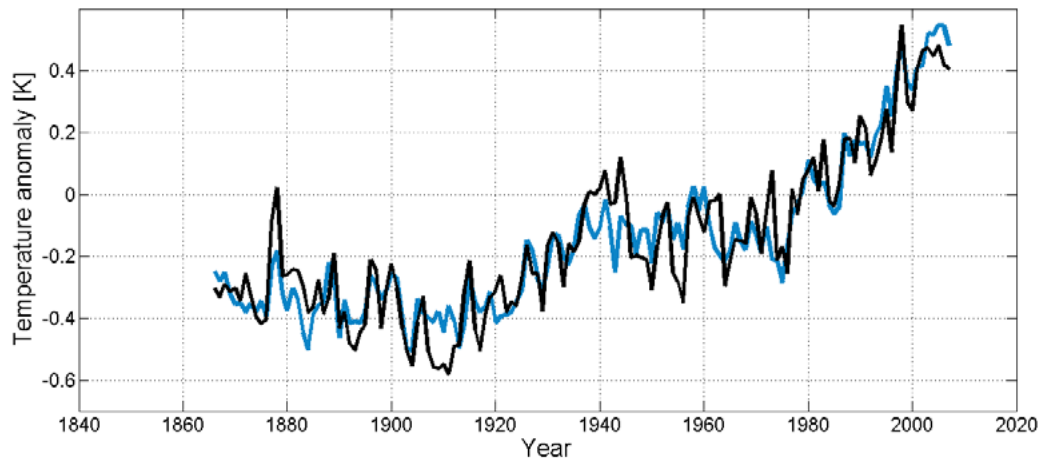


Fig. 7 Reconstruction of the global T as sum of ensemble results of the runs of Fig. 4 and Fig. 6. Black line: observed temperature anomalies, blue line: sum of the ensemble means.

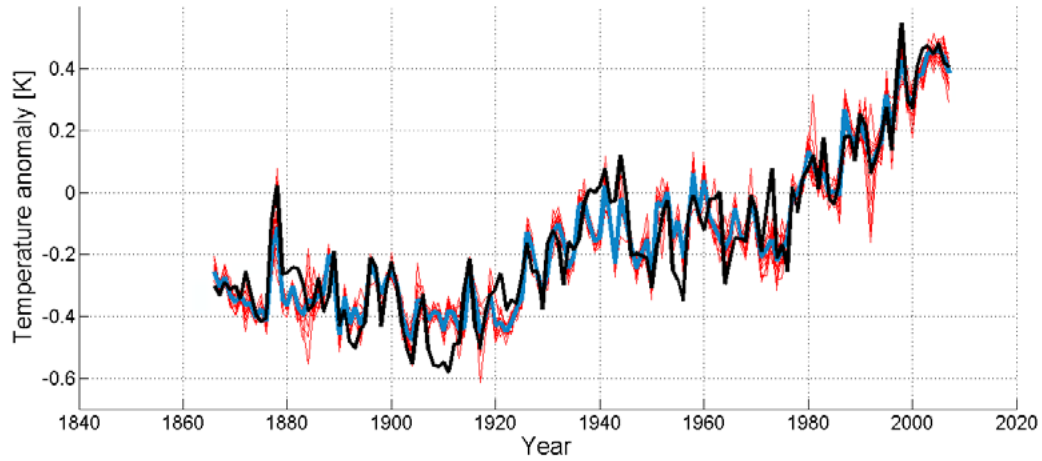


Fig. 8 Results of networks endowed with external (natural and anthropogenic) forcings and indices of natural variability as inputs. Black line: observed temperature anomalies, red lines: NN outputs of single runs, blue line: ensemble mean.

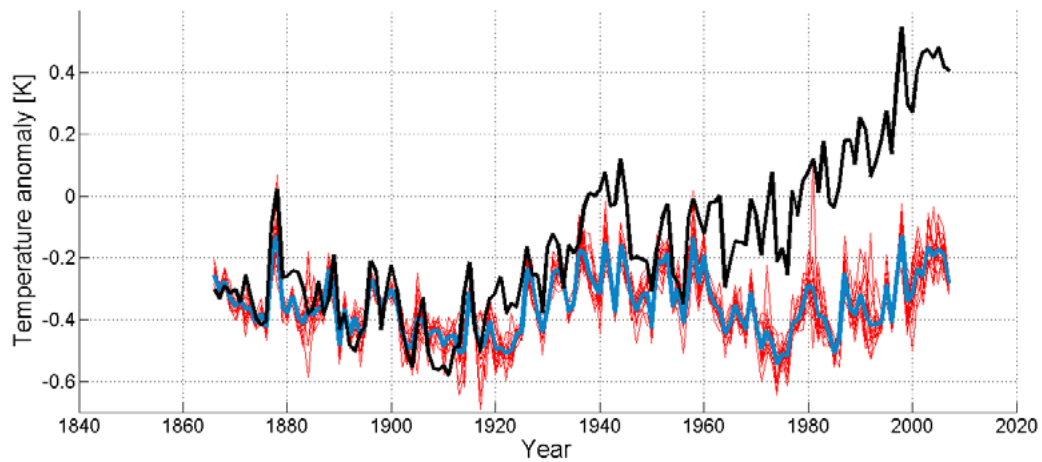


Fig. 9 Effect of NN simulations in which the anthropogenic forcings are kept fixed at the values of 1866. Black line: observed temperature anomalies, red lines: NN outputs of single runs, blue line: ensemble mean. No recent global warming, just natural variability!

# Impact of greenhouse gases and insolation on the threshold of glacial inception

Colleoni F.<sup>1,\*</sup>, Masina S.<sup>1,2</sup>

<sup>1</sup>Centro Euro-Mediterraneo sui Cambiamenti Climatici - Italy, <sup>2</sup>Istituto Nazionale di Geofisica e Vulcanologia, Sezione di Bologna - Italy

\*Corresponding Author: [florence.colleoni@cmcc.it](mailto:florence.colleoni@cmcc.it)

## Abstract

Before the so-called Mid-Brunhes Event (MBE, 430 kyrs BP), the proxy records show that the intensity of the interglacials was less important than for the last past five interglacials. Pre-MBE interglacials are characterized by low sea-level, particularly low CO<sub>2</sub> concentrations and cold Antarctic temperatures, whereas post-MBE interglacials present opposite characteristics. In the present contribution, we model two glacial inceptions, one representative of pre-MBE interglacials (Marine Isotope Stage 7, MIS) and one representative of post-MBE interglacials (MIS 5) to show that low CO<sub>2</sub> concentrations directly impact on the glacial inception processes. Results show that MIS 7 climate is more favorable to glacial inception than MIS 5 climate. As a consequence, the glacial inception during MIS 7 could have started before than that of MIS 5. Moreover, results suggest that MIS 7 climate is more favorable to an extensive glaciation over Eurasia, while MIS 5 climate is more favorable to larger North American ice sheets. Based on those results and on the combination of summer insolation and CO<sub>2</sub>, we propose that some of the pre-MBE interglacials but not all, could have led to an extensive glaciation over Eurasia.

**Keywords:** MIS 7 glacial inception, Mid-Brunhes Event, climate modeling, ice sheet modeling

## 1. INTRODUCTION

Over the last five million years, the Earth's climate experienced two major transitions. The first one occurred at the end of the Pliocene,  $\approx 3.3$  to 2.7 Myrs ago [9] [22], when the ice sheets started to develop over the Northern Hemisphere. The second one occurred roughly one million years ago when the frequency of the glacial/interglacial cycles evolved from 40 kyrs to 100 kyrs [18]. During the last decades, the analysis of ice cores and marine sediment records revealed that another threshold in global climate occurred towards 430 kyrs BP, the so-called "Mid-Brunhes Event" (MBE) [12]. The proxy records show that the intensity of the interglacials that occurred before this event was less important than for the last past five interglacials. Pre-MBE interglacials are characterized by low sea-level, probably large Northern Hemisphere ice sheets [10], particularly low CO<sub>2</sub> concentrations [20] and no CO<sub>2</sub> overshoots [30]. In particular, while pre-MBE CO<sub>2</sub> concentration dropped below 240 ppm, for post-MBE interglacials, CO<sub>2</sub> concentration did not drop below 260 ppm. Therefore, the glacial inception that followed the pre-MBE and post-MBE might reflect this difference.

[Figure 1 about here.]

In the present study, we use a coupled Atmosphere-Ocean General Circulation Model and an ice-sheet model to simulate the climate and the Northern Hemisphere ice-sheet distribution representative of a pre-MBE and a post-MBE glacial inception. We chose to simulate MIS 7 glacial inception period at 239 kyrs BP (interglacial), 236 kyrs BP and 229 kyrs BP (glacial inception). By many aspects, MIS 7 is representative of pre-MBE interglacial, with low sea-level, low CO<sub>2</sub>, and low Antarctic temperatures (Figure 1). Simulating this time period is therefore useful to understand the impact of low greenhouse gases (GHGs) in glacial inception [31]. In addition, in order to better stress the impact of low GHGs on the inception processes, we simulate the mean climate state and ice-sheet distribution of MIS 5, representative of a post-MBE interglacial. Time slices are computed at 125 kyrs BP (interglacial), 122 kyrs BP and 115 kyrs BP (glacial inception).

The impact of external forcing and of GHGs, on the high-latitudes climate has been extensively investigated in the context of glaciations and glacial inceptions. Several studies, e.g. [16] and [3], suggest that the timing and the amplitude of glacial inception

is affected by the degree of synchronicity between insolation minimum and the drop in GHGs. [3] further show that, while a decrease in high-latitude summer insolation is sufficient to trigger glacial inception over North America, a drop in atmospheric CO<sub>2</sub> is necessary to trigger a long-lasting glaciation over Eurasia. Finally, another modeling study shows that, for CO<sub>2</sub> values ranging from 260 to 290 ppm (typical post-MBE glacial inception - interglacial values) and a range of orbital parameters close to those of the last five glacial inceptions, the impact of CO<sub>2</sub> on perennial snow is more or less similar to that of orbital parameters [31]. However, this study does not explore the impact of GHGs lower than 260 ppm, therefore missing the effect that the particularly low pre-MBE GHGs might have on the timing and the intensity of glacial inception.

## 2. METHODS

We use the CESM 1.0.5 which consists in a fully coupled atmosphere-ocean-sea-ice-land model [8]. The atmospheric component CAM has 26 vertical levels and an horizontal grid resolution of 96x48 (T31) shared with the land component (CLM). The ocean component (POP, displaced pole located over Greenland) has 60 vertical levels and a nominal 3° horizontal resolution in common with the sea-ice component (CICE). Since the CESM 1.0.5 does not include a fully-coupled Ice-sheet Model (ISM), we force the stand-alone GRISLI ISM [24] using the mean climate states computed from our experiments (Table 1).

GRISLI is a 3D-thermo-mechanical ice sheet - ice stream - ice shelf model, able to simulate both grounded and floating ice. The grounded part uses the shallow ice approximation (SIA) [11] whereas ice shelves and ice streams are simulated following the shallow shelf approximation (SSA) [21]. For more details about the physics, the reader may refer to [26] and [24]. Mass balance is computed using the Positive Degree-Day semi-empirical method [23]. Temperature are corrected for elevation changes during runtime using lapse rates set to 5°C/km and 4°C/km for mean annual and summer temperatures respectively following [3]. Precipitation is corrected along with temperature corrections assuming that atmospheric vapor content decreases exponentially with increasing elevation [4].

## 2.1 Settings

In total, nine experiments are carried out, all differing in orbital parameters and GHGs concentrations. MIS 5 interglacial simulation K125 is spin up to 125 kyrs BP time period and is used after 400 years of integration to branch the two experiments K122 and K115 set up with 122 kyrs BP and 115 kyrs BP orbital parameters and GHGs values, respectively (Table 1). Similarly, MIS 7 interglacial simulation K239 is spin up to 239 kyrs BP time period and used to initialize the two runs K236 and K229 set up using 236 kyrs BP and 229 kyrs BP orbital and GHGs values, respectively (Table 1). In order to isolate the effect of the low MIS 7 GHGs, three additional simulations, accounting for MIS 7 orbital parameters but MIS 5 GHG values are carried out, all branched on K239 spin-up experiment, namely K239\_GHG, K236\_GHG and K229\_GHG. These nine simulations have been regrouped in three different sets to increase readability in the following sections: MIS5<sub>FULL</sub> accounting for MIS 5 orbital parameters and GHG; MIS7<sub>FULL</sub> accounting for MIS 7 orbital forcing and GHG; MIS7\_GHG accounting for MIS 7 orbital parameters and MIS 5 GHG. Those sets are defined such that the comparison between MIS7<sub>FULL</sub> and MIS7\_GHG shows the impact of GHG, the comparison between MIS7\_GHG and MIS5<sub>FULL</sub> shows the impact of orbital parameters and the comparison between MIS7<sub>FULL</sub> and MIS5<sub>FULL</sub> gives the impact of GHG combined with orbital parameters. The detailed settings are summarized in Table 1.

[Table 1 about here.]

The ice-sheet experiments have been designed on a 40 km regular rectangular grid from  $\approx 47^\circ\text{N}$  to the North Pole. Non uniform geothermal heat fluxes are prescribed after [28]. Since we do not have any precise informations about dimensions of the Greenland ice sheet for the periods we are modeling, we initialize our experiments with present-day Greenland ice sheet topography. Two steady-state spin-up of 150 kyrs are performed using K239 and K125 climate forcing from which, two transient ice-sheets simulations are carried out, from 239 kyrs BP to 229 kyrs BP and from 125 kyrs BP to 115 kyrs BP, forced by each of the simulated climate of MIS7<sub>FULL</sub> and MIS5<sub>FULL</sub> sets (Table 1). Furthermore, climate was linearly interpolated between each climate time slice by using an index representative of the climate evolution from [14] (see [6] for more details).

### 3. RESULTS

On one hand, due to the lower eccentricity combined to a slightly different perihelion date, MIS 7 time period is generally colder than MIS 5 over Northern Hemisphere (Table 1). On another hand, the low obliquity combined to the low eccentricity contributes to reduce the seasonal contrast during MIS 7 compared to MIS 5 [6]. In addition, MIS 7 GHGs concentrations are by far lower than during MIS 5, which combined to insolation, induces a mean annual cooling over the Northern Hemisphere of 1°C to 3°C with respect to MIS 5 (Figure 2a to 2c). The strongest negative temperature anomaly between  $MIS7_{FULL}$  and  $MIS5_{FULL}$  experiments is simulated over the Arctic Ocean. In  $MIS7_{FULL}$  experiments, sea-ice cover is thicker than in  $MIS5_{FULL}$  (not shown). In addition, a perennial snow cover accumulates on top of it, which increases the local albedo and therefore decrease local temperature with respect to  $MIS5_{FULL}$ . Note that in the two glacial inception simulations K229 and K115, this temperature anomaly over the Arctic is reduced compared to the other simulations (Figure 2c). This is because from an orbital point of view, K229 and K115 are highly similar, leading to a comparable sea-ice thickness and extent in this area (not shown). However K229 is still colder than K115 due to the low GHGs concentration, which further cool the climate (Table 1).

Our climate simulations show that the perennial snow cover, indicative of glacial inception, is by far more extensive in  $MIS7_{FULL}$ , at least more than three times larger than in  $MIS5_{FULL}$  over Eurasia and about 50 % larger over North America (not shown, see [5]). Similarly to [6] we force the GRISLI ice sheet model [24] using the climate of  $MIS7_{FULL}$  and  $MIS5_{FULL}$ . Following [6], results show that glacial inception over North America and Eurasia is more important during MIS 7 than during MIS 5 in terms of volume and extent (Figure 2d to 2i).

[Figure 2 about here.]

As expected from the two interglacial simulations K125 and K239, no ice accumulates over North America and Eurasia (Figure 2d and 2g). However, Greenland ice thickness greatly differs between the two simulations. In K125, Greenland ice volume decreases, especially over the southern part, leading to an initial ice volume over the Northern Hemisphere of about -1.5 m Sea Level Equivalent (SLE) relative to present-day. This is in line with the paleo sea-level reconstructions (Figure 1). On the contrary,

in K239, Greenland thickens, leading to a Northern Hemisphere ice volume of +1.5 m relative to present-day, which slightly underestimates paleo reconstructions (Figure 1). In K236, the extent of the ice cover is already larger over both North America and Eurasia than in K122 (Figure 2e and 2h). Note that some ice also accumulates over the Bering Strait. It has been shown that the existence of an ice sheet large enough over Eurasia could significantly affect the regional circulation by reducing the moisture advection that usually reaches Eastern Siberian topographic highs, therefore stopping an ice cap from developing in this area [15]. However, the CESM simulations do not account for changes in topography caused by ice sheet growth and the circulation patterns remain similar in Eastern Siberia for all the ice-sheet simulations regardless of the period. Therefore, some ice accumulates over the Bering Strait in our ice experiments.

Similarly to K236 and K122, in the case of the glacial inceptions, the ice sheets are larger and bigger in K229 than in K115 (Figure 2f and 2i). In K229, the ice thickness over Eurasia reaches 1800 meters and exhibits a well-developed ice shelf over the Barent Sea (Figure 2f). Some ice also accumulates over the Eastern Siberian shelf while, in K115, this area remains ice free (Figure 2i). Over the Cascadian mountain range, an ice cap of about 2000 meters thick accumulates in K229 while it remains twice thin in K115. The Eurasian ice sheet is about three times larger for all the MIS7<sub>FULL</sub> experiments (except for K239) compared to MIS5<sub>FULL</sub> experiments (Figure 2). The Eurasian ice volume reaches 6.24 m SLE at K229, with a volume 5 times larger at K229 than in K236 (Figure 2e and 2f). In K115, the Eurasian ice sheet volume is of about 1.98 m SLE only and the volume in K115 is by about 4 times larger than in K122. Over North America, ice volume is about two times larger in MIS7<sub>FULL</sub> experiments than in MIS5<sub>FULL</sub> ones. The ice volume reaches 12.78 m SLE in K229, with a volume about 3 times larger than in K236, while it reaches 6.43 m SLE in K115 with a volume more than 4 times larger than in K122.

[Figure 3 about here.]

From those results, it appears that MIS7<sub>FULL</sub> ice sheets are much larger than in MIS5<sub>FULL</sub>, especially at the glacial inception. Another remarkable result is that the ice covered area is highly similar in K236 and in K115, but there is still a notable difference in ice volume between these two simulations (Figure 2e and 2i). This indicates that the glacial inception might start slightly before during MIS 7 than during MIS 5 over the

Northern Hemisphere. The last point is about the difference in the growth of Eurasian and North American ice sheets. The rate of growth of the North American ice sheet is lower in MIS7<sub>FULL</sub> experiments than in MIS5<sub>FULL</sub> ones. On the contrary, the growth of Eurasian ice sheet is faster in MIS7<sub>FULL</sub> experiments than in MIS5<sub>FULL</sub> simulations. This suggests that climate similar to MIS 5, with warm interglacial and high GHGs concentrations, are more favorable to ice accumulation over North America, whereas climate similar to MIS 7, with cold interglacial and low GHGs concentrations, are more favorable to inception over Eurasia [3].

To demonstrate that GHGs are responsible for this difference, we separated the effect of GHGs from that of orbital parameters, by comparing MIS7<sub>FULL</sub> to MIS7\_GHG and MIS7\_GHG to MIS5<sub>FULL</sub> (Table 1). The comparison shows that at least two thirds of the mean annual temperature anomaly between the two time periods is explained by the low MIS 7 GHGs concentrations over both North America and Eurasia (Figure 3). Therefore we can conclude that climates representative of pre-MBE interglacials are more favorable to glacial inception over Northern Hemisphere.

#### 4. CONCLUSIONS

We simulated the climates and ice-sheet distributions representative of pre-MBE (MIS 7) and post-MBE (MIS 5) glacial inceptions to understand the impact of low GHGs concentrations on the glacial inception processes. Results show that:

1. MIS 7 climate is more favorable to an extensive glacial inception over Northern Hemisphere than MIS 5.
2. The Eurasian ice sheet grows faster under MIS 7 climate conditions, while the North American ice sheets grows faster under MIS 5 climate conditions.
3. MIS 7 climate conditions bring forward glacial inception with respect to MIS 5 climate.

However, this is the synergy between orbital parameters and GHGs that results in extensive glacial inceptions. To understand if based on those criterias, other pre-MBE interglacials could have led to extensive Eurasian ice sheets, we compared the drop in summer insolation preceding the glacial inception for all the pre-MBE interglacials.

If we consider MIS 7 as a reference of extensive glacial inception, all pre-MBE interglacials present a peak interglacial summer insolation comparable to MIS 7, except MIS 15 (Figure 3). MIS 15 also has a slightly higher CO<sub>2</sub> concentrations and Antarctic temperatures than the other pre-MBE interglacials. Based on our results and on those observations we propose that MIS 19, MIS 17 and MIS 13 could have been more favorable to an extensive glaciation over Eurasia. This could be a characteristic of pre-MBE interglacials in general. This fact is supported by [2] who shows that after the Mid-Bruhnes Event, the North American ice sheets becomes bigger and the Eurasian one smaller.

## 5. ACKNOWLEDGMENTS

We gratefully acknowledge the support of Italian Ministry of Education, University and Research and Ministry for Environment, Land and Sea through the project GEMINA. We address a special thanks to members of the Past Interglacials (PIGS) working group of the Past Global Changes (PAGES) project for their support and feedbacks.

## 6. REFERENCES

- [1] A. Berger. Long-term variations of daily insolation and quaternary climatic changes. *J. Atmos. Sci.*, 35(12):2362–2367, 1978.
- [2] R. Bintanja, R. S.W. van de Wal, and J. Oerlemans. Modelled atmospheric temperatures and global sea levels over the past million years. *Nature*, 437:126–128, 2005.
- [3] S. Bonelli, S. Charbit, M. Kageyama, M.-N. Woillez, G. Ramstein, C. Dumas, and A. Quiquet. Investigating the evolution of major Northern Hemisphere ice sheets during the last glacial-interglacial cycle. *Clim. Past*, 5:1013–1053, 2009.
- [4] S. Charbit, C. Ritz, and G. Ramstein. Simulations of Northern Hemisphere ice-sheet retreat: sensitivity to physical mechanisms involved during the Last Deglaciation. *Quaternary Sci. Rev.*, 23:245–263, 2002.

- [5] F. Colleoni, S. Masina, A. Cherchi, and D. Iovino. Impact of orbitals and greenhouse gas on the climate of MIS 7 and MIS 5 glacial inception. *J. Climate*, submitted.
- [6] F. Colleoni, S. Masina, A. Cherchi, A. Navarra, C. Ritz, V. Peyaud, and B. Otto-Bliesner. Modeling Northern Hemisphere ice-sheet distribution during MIS 5 and MIS 7 glacial inception. *Clim. Past*, 10(1):269–291, 2014.
- [7] A. Dutton, E. Bard, F. Antonioli, T.M. Esat, Lambeck K., and McCulloch M.T. Phasing and amplitude of sea-level and climate change during the penultimate interglacial. *Nat. Geosci.*, 2:355 – 359, 2009.
- [8] P. R. Gent, G. Danabasoglu, L. J. Donner, M. M. Holland, E. C. Hunke, S. R. Jayne, D. M. Lawrence, R. B. Neale, P. J. Rasch, M. Vertenstein, P. H. Worley, Z-L. Yang, and M. Zhang. The Community Climate System Model Version 4. *J. Climate*, 24:4973–4991, 2011.
- [9] G.H. Haug, A. Ganopolski, D.M. Sigman, A. Rosell-Mele, G. Swann, R. Tiedemann, S.L. Jaccard, J. Bollmann, M.A. Maslin, M.J. Leng, et al. North Pacific seasonality and the glaciation of North America 2.7 million years ago. *Nature*, 433(7028):821–825, 2005.
- [10] J.P. Helmke, H.A. Bauch, and H. Erlenkeuser. Development of glacial and interglacial conditions in the Nordic seas between 1.5 and 0.35 Ma. *Quaternary Sci, Rev.*, 22(15):1717–1728, 2003.
- [11] K. Hutter. *Theoretical glaciology: material science of ice and the mechanics of glaciers and ice sheets*. Reidel Publishing Company, Dordrecht, The Netherlands, 1983.
- [12] J.H.F. Jansen, A. Kuijpers, and S.R. Troelstra. A mid-Brunhes climatic event: Long-term changes in global atmosphere and ocean circulation. *Science*, 232(4750):619–622, 1986.
- [13] J. Jouzel, V. Masson-Delmotte, O. Cattani, G. Dreyfus, S. Falourd, G. Hoffmann, B. Minster, J. Nouet, J.M. Barnola, J. Chappellaz, H. Fischer, J.C. Gallet, S. Johnsen, M. Leuenberger, L. Loulergue, D. Luethi, H. Oerter, F. Par-

- renin, G. Raisbeck, D. Raynaud, A. Schilt, J. Schwander, E. Selmo, R. Souchez, R. Spahni, B. Stauffer, J.P. Steffensen, B. Stenni, T.F. Stocker, J.L. Tison, M. Werner, and E.W. Wolff. Orbital and Millennial Antarctic Climate Variability over the Past 800,000 Years. *Science*, 317:793–797, 2007.
- [14] N. Kirchner, R. Greve, A.P. Stroeven, and J. Heyman. Paleoglaciological reconstructions for the Tibetan Plateau during the last glacial cycle: evaluating numerical ice sheet simulations driven by GCM-ensembles. *Quaternary Sci. Rev.*, 30(1):248–267, 2011.
- [15] G. Krinner, B. Diekmann, F. Colleoni, and G. Stauch. Global, regional and local scale factors determining glaciation extent in Eastern Siberia over the last 140,000 years. *Quaternary Sci. Rev.*, 30:821–831, 2011.
- [16] C. Kubatzki, M. Claussen, R. Calov, and A. Ganopolski. Sensitivity of the last glacial inception to initial and surface conditions. *Clim. Dynam.*, 27:333–344, 2006.
- [17] L.E. Lisiecki and M.E. Raymo. A Pliocene-Pleistocene stack of 57 globally distributed benthic  $\delta^{18}\text{O}$  records. *Paleoceanography*, 20:PA1003, 2005.
- [18] L.E. Lisiecki and M.E. Raymo. Plio-Pleistocene climate evolution: trends and transitions in glacial cycle dynamics. *Quaternary Sci. Rev.*, 26:56–69, 2007.
- [19] L. Loulergue, A. Schilt, R. Spahni, V. Masson-Delmotte, T. Blunier, B. Lemieux, J.-M. Barnola, D. Raynaud, T.F. Stocker, and J. Chappellaz. Orbital and millennial-scale features of atmospheric  $\text{CH}_4$  over the past 800,000 years. *Nature*, 453:383–386, 2008.
- [20] D. Luthi, M. Le Floch, B. Bereiter, T. Blunier, J.M. Barnola, U. Siegenthaler, D. Raynaud, J. Jouzel, H. Fischer, K. Kawamura, and T.F. Stocker. High-resolution carbon dioxide concentration record 650,000-800,000 years before present. *Nature*, 453:379–382, 2008.
- [21] D.R. MacAyeal. Large-Scale Ice Flow Over a Viscous Basal Sediment: Theory and Application to Ice Stream B, Antarctica. *J. Geophys. Res.*, 94:4071–4087, 1989.

- [22] M. Mudelsee and M. E. Raymo. Slow dynamics of the Northern Hemisphere glaciations. *Paleoceanography*, 20:PA4022, 2005.
- [23] N. Reeh. Parameterization of Melt Rate and Surface Temperature on the Greenland Ice Sheet. *Polarforschung*, 5913:113–128, 1991.
- [24] C. Ritz, V. Rommalaere, and C. Dumas. Modeling the evolution of Antarctic ice sheet over the last 420,000 years: Implications for altitude changes in the Vostok region. *J. Geophys. Res.*, 106:31943–31964, 2001.
- [25] E.J. Rohling, K. Grant, M. Bolshaw, A.P. Roberts, M. Siddall, C.H. Hemleben, and M. Kucera. Antarctic temperature and global sea level closely coupled over the past five glacial cycles. *Nat. Geosci.*, 2(7):500–504, 2009.
- [26] V. Rommelaere and C. Ritz. A thermomechanical model of ice-shelf flow. *Ann. Glaciol.*, 23:13–20, 1996.
- [27] A. Schilt, M. Baumgartner, T. Blunier, J. Schwander, R. Spahni, H. Fischer, and T.F. Stocker. Glacial-Interglacial and Millennial Scale Variations in the Atmospheric Nitrous Oxide Concentration during the last 800,000 Years. *Quaternary Sci. Rev.*, 29:182–192, 2010.
- [28] N.M. Shapiro and M.H. Ritzwoller. Inferring surface heat flux distributions guided by a global seismic model: particular application to Antarctica. *Earth Planet. Sci. Lett.*, 223:213–214, 2004.
- [29] M. Siddall, E. Bard, E.J. Rohling, and C. Hemleben. Sea-level reversal during Termination II. *Geology*, 34(10):817–820, 2006.
- [30] P.C. Tzedakis, D. Raynaud, J.F. McManus, A. Berger, V. Brovkin, and T. Kiefer. Interglacial diversity. *Nat. Geosci.*, 2(11):751–755, 2009.
- [31] G. Vettoretti and W.R. Peltier. Sensitivity of glacial inception to orbital and greenhouse gas climate forcing. *Quaternary Sci. Rev.*, 23:499–519, 2004.

## 7. IMAGES AND TABLES

Tab. 1 Climate experiments settings. Three sets of simulations were carried out: MIS5 and MIS7 correspond to experiments forced using the proper orbital parameters and greenhouse gas concentrations from MIS 5 and MIS 7 periods respectively; MIS7\_GHG experiments were forced using MIS 7 orbital parameters but MIS 5 GHG values. GHG were retrieved from EPICA Dome C, East Antarctica and come from [20] for the CO<sub>2</sub>, [19] for the CH<sub>4</sub> and [27] for the NO<sub>2</sub> records. Orbital parameters are calculated according to [1]. For the Pre-industrial control experiment CTR1850, orbitals were set to 1990 while the greenhouse gas were set at their pre-industrial values (1850). Finally, K115 and K122 experiments were initialized from the 400th model year of K125 while K229 and K236 simulations were initialized from the 400th model year of K239.

Set	ID (%)	Ecc. date	Peri. (°)	Obl. (ppm)	CO <sub>2</sub> (ppb)	CH <sub>4</sub> (ppb)	NO <sub>2</sub>	Spin-up (model years)	Length
	<b>CTR1850</b>	0.017	Jan. 4	23.44	284	791	275	Pre-ind	700
MIS5 <sub>FULL</sub>	<b>K115</b>	0.042	Jan. 14	22.44	262	472	251	K125 branch	300
	<b>K122</b>	0.041	Sept. 12	23.33	274	607	257	K125 branch	300
	<b>K125</b>	0.040	Jul. 23	23.80	276	640	263	-	700
MIS7 <sub>FULL</sub>	<b>K229</b>	0.043	Feb. 3	22.22	224	493	256	K239 branch	300
	<b>K236</b>	0.038	Oct. 2	22.23	241	481	267	K239 branch	300
	<b>K239</b>	0.036	July. 12	22.70	245	565	267	239k	700
MIS7_GHG	<b>K229_GHG</b>	K229	K229	K229	262	472	251	K239 branch	300
	<b>K236_GHG</b>	K236	K236	K236	274	607	257	K239 branch	300
	<b>K239_GHG</b>	K239	K239	K239	276	640	263	-	700

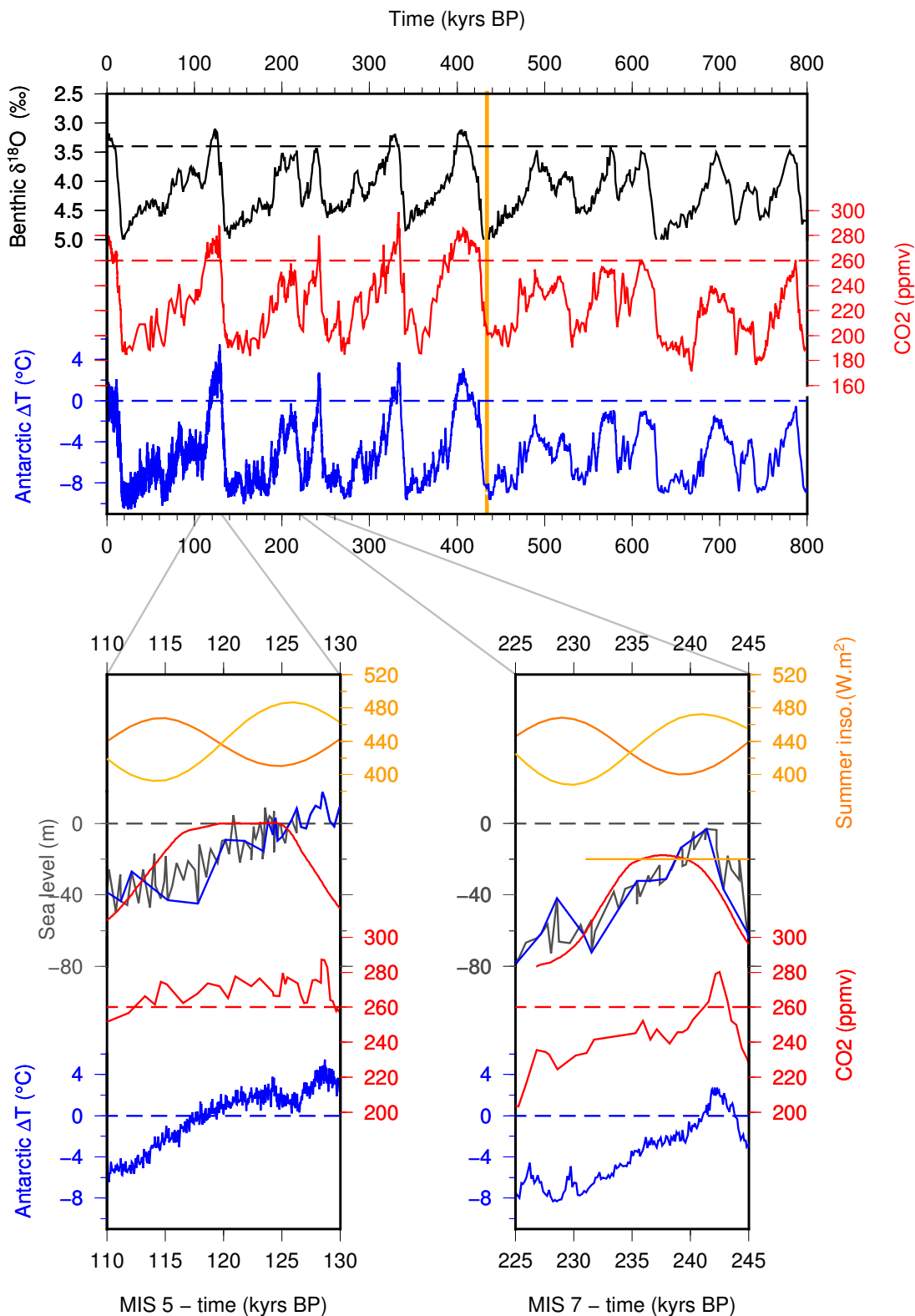


Fig. 1 Global climate context of the last eight glacial cycles. Top frame: benthic  $\delta^{18}\text{O}$  stack from [17], atmospheric  $\text{CO}_2$  (ppmv) concentration from EPICA Dome C, East Antarctica [20], temperature anomaly ( $^{\circ}\text{C}$ ) relatively to present-day [13]. The vertical orange bar indicates the Mid-Brunhes Event (MBE) after [12]. Dashed lines stress the pre-MBE and post-MBE interglacial difference in terms of benthic  $\delta^{18}\text{O}$ ,  $\text{CO}_2$  and Antarctic temperature as highlighted in [30]; b. and c. close-up of MIS 5 (left panel) and MIS 7 (right panel) interglacials illustrated by different external forcing and climate proxies. From top to bottom: summer insolation at  $65^{\circ}\text{N}$  (light orange) and  $70^{\circ}\text{S}$  (dark orange) [1] ( $\text{W}\cdot\text{m}^{-2}$ ); sea level reconstructions (m) from [25] (grey), [29] (blue), [2] (red) and constraint on global mean sea level from Argentola Cave, Italy [7] (orange); atmospheric  $\text{CO}_2$  (ppmv) concentration from EPICA Dome C, East Antarctica [20]; EPICA Dome C, East Antarctica, temperature anomaly ( $^{\circ}\text{C}$ ) relatively to present-day [13].

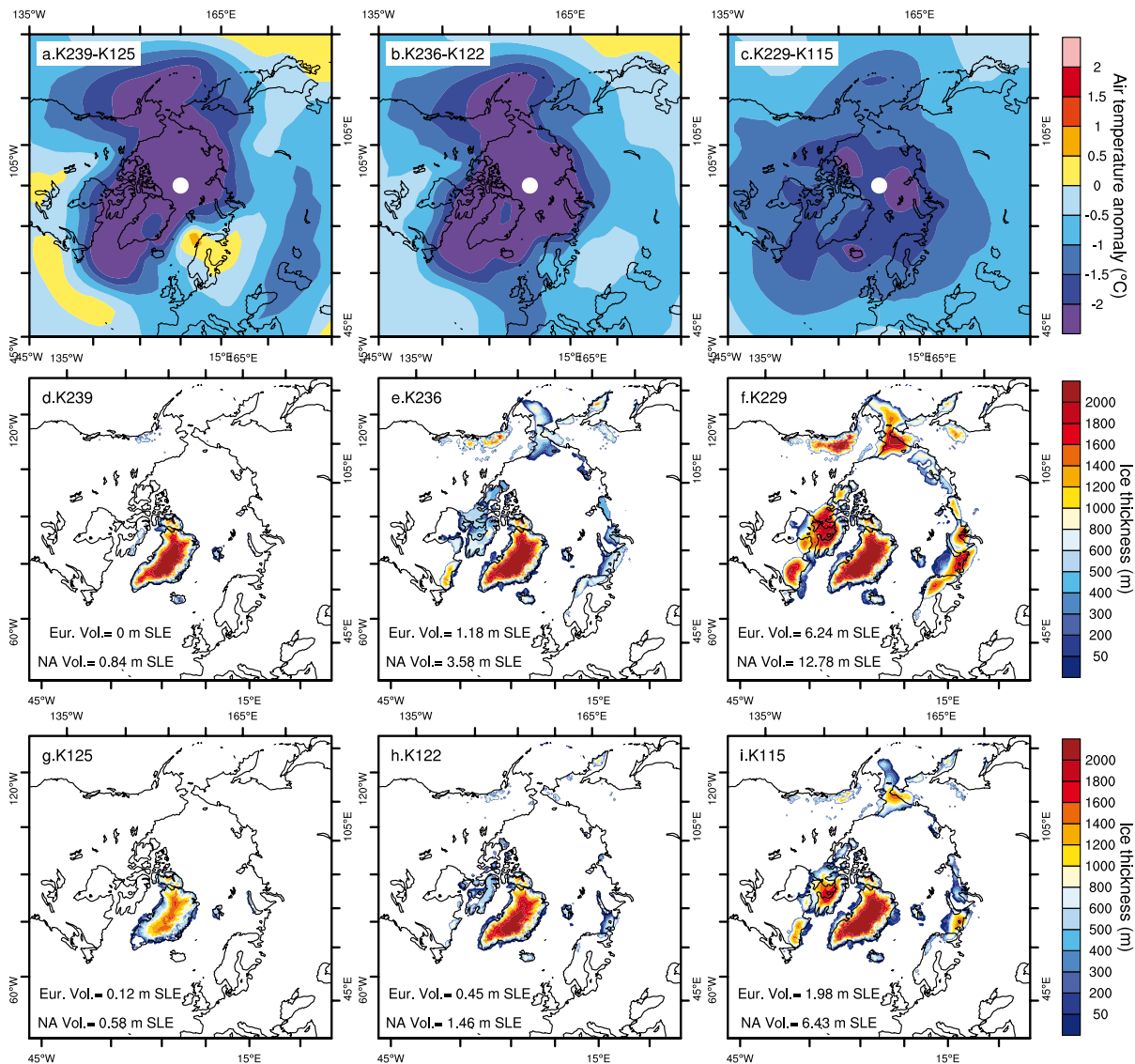


Fig. 2 Mean annual temperature difference ( $^{\circ}\text{C}$ ) between  $\text{MIS7}_{\text{FULL}}$  and  $\text{MIS5}_{\text{FULL}}$  experiments over the Northern Hemisphere (a. to c.); Northern Hemisphere MIS 7 ice thickness (meters) for each time slice of  $\text{MIS7}_{\text{FULL}}$  (d. to f.); Northern Hemisphere MIS 5 ice thickness (meters) for each time slice of  $\text{MIS5}_{\text{FULL}}$  (g. to i.). Total simulated meter sea-level equivalent (m SLE) ice volume is indicated on each frame for North America (NA, excluding Greenland) and Eurasia (Eur). Note that the ice cap growing over the Bering Strait has not been accounted for in volume calculations.

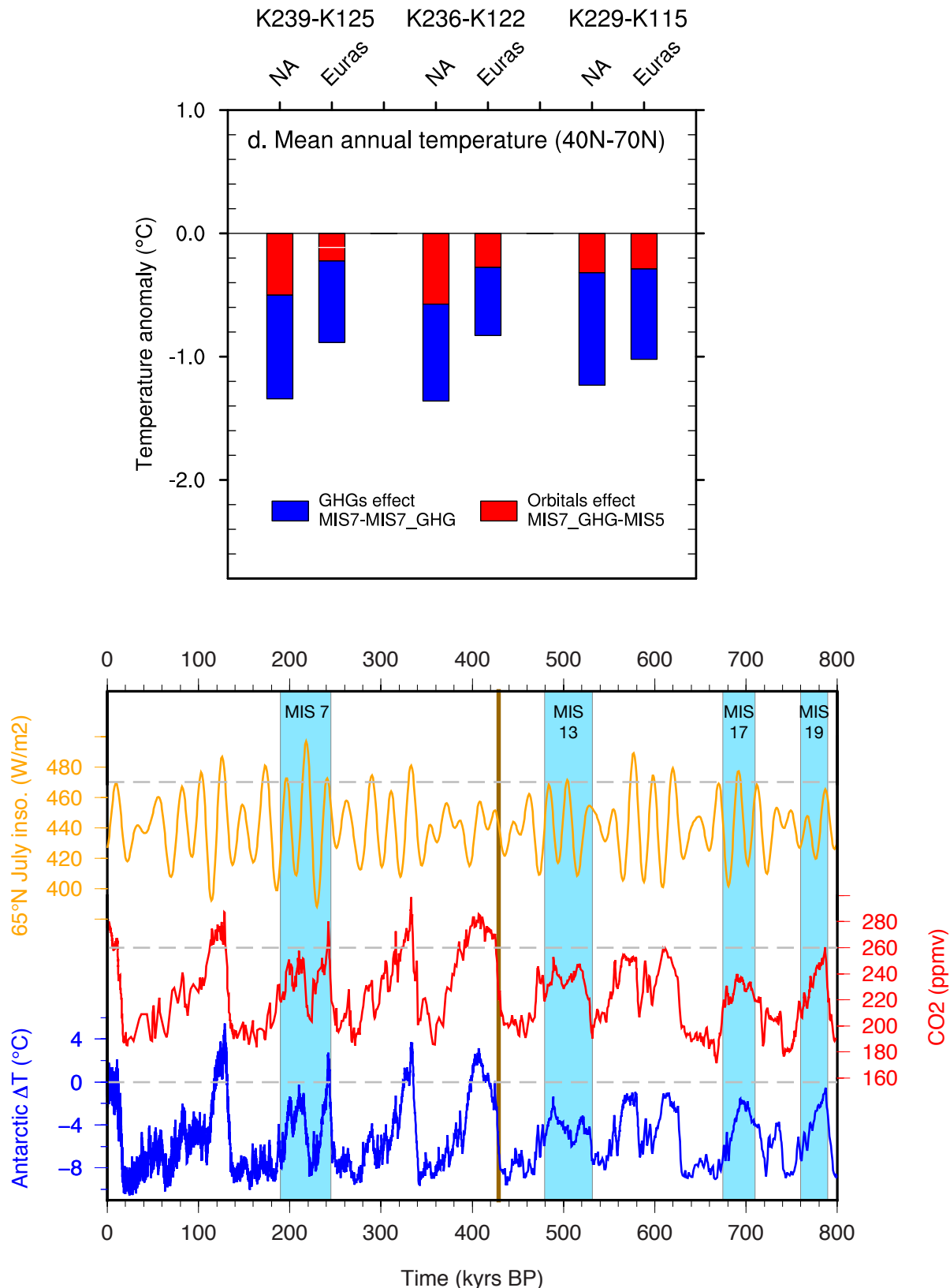


Fig. 3 Top frame: mean annual air temperature anomaly between MIS7<sub>FULL</sub> and MIS5<sub>FULL</sub> experiments (see Figure 2a. to c.) divided in contribution of GHG (blue, MIS7<sub>FULL</sub>-MIS7\_GHG experiments) and orbital parameters (red, MIS7\_GHG - MIS5<sub>FULL</sub> experiments). Temperature has been averaged over Eurasia and North America over the latitudinal band 40°N - 90°N. Bottom frame: summer insolation at 65°N (light orange) [1] (W·m<sup>-2</sup>); atmospheric CO<sub>2</sub> (ppmv) concentration from EPICA Dome C, East Antarctica [20]; EPICA Dome C, East Antarctica, temperature anomaly (°C) relative to present-day [13]. Vertical brown bar corresponds to the Mid-Bruhnes Event. Vertical blue boxes indicate the interglacials favorable to an extensive glaciation over Eurasia.

# Past and future solar radiation variability and change over Sicily

Manara V.\*<sup>1</sup>, Brunetti M.<sup>2</sup>, Maugeri M.<sup>1,2</sup>, Pasotti L.<sup>3</sup>, Simolo C.<sup>2</sup>

<sup>1</sup>Università degli Studi di Milano Dip. di Fisica, Milano, <sup>2</sup>CNR ISAC, Bologna

<sup>3</sup>SIAS- Regione Sicilia, Catania

\*Corresponding Author: veronica.manara@unimi.it

## Abstract

We estimate Sicily global radiation 1961-2000 monthly climatologies from already available climatologies (2002-2011) and from a regional sunshine duration anomaly record (1936-2013). We compare these climatologies with corresponding climatologies from 4 RCM-GCM combinations and present correcting factors introduced in order to make the model outputs representative of the observational data. Then, we apply the same correcting factors to future model simulations in order to produce monthly climatologies for the 2001-2050 and 2051-2100 period.

**Keywords:** global radiation, sunshine duration, past and future climatologies, Sicily

## 1. INTRODUCTION

High-resolution datasets of monthly climatological normals (i.e. high-resolution climatologies) have proved to be increasingly important in the recent past, and they are likely to become even more important in the future. They are used in a variety of models and decision support tools in a wide spectrum of fields such as, just to cite a few, energy, agriculture, engineering, hydrology, ecology and natural resource conservation [1], [2]. One of the most important variables for many possible applications (e.g. energy production and agriculture) is solar radiation.

In this context, we set up a methodology for estimating high-resolution solar radiation climatologies from these records. This methodology has been presented in SISC 2013 [3] and it has been applied to a network of 41 Sicily stations of the SIAS network [3]. It consists of the following steps that have to be run on a monthly basis:

- calculating global radiation normals for all station sites;
- estimating, for all station sites, the bias due to shading and adjusting the normal values in order to make them representative of un-shaded sites;
- calculating clearness index normals from these shading-bias-adjusted global radiation normals and decomposing global radiation normals into the direct and diffuse components;
- projecting global radiation normals and the direct and diffuse components onto a high-resolution regular grid, considering flat ground;
- evaluating atmospheric turbidity over the same grid by means of the direct component of global radiation normals;
- calculating normal values for the direct, diffuse and reflected components of global radiation for any grid-cell, taking into account its slope and aspect (i.e. slope orientation) and considering shading from the cell itself and from the neighbouring cells.

In this paper we present a methodology which allows to estimate from the 2002-2011 results, climatologies for any other period of the 1936-2013 interval and which allows to estimate future scenario climatologies too.

## 2. TEMPORAL EVOLUTION OF SOLAR RADIATION OVER SICILY IN THE 1936-2013 PERIOD

### 2.1 Introduction

Temporal variability of solar radiation in the last decades is discussed in a number of recent papers [4]. The results suggest a widespread reduction of solar radiation between the 1960s and the early 1980s and a tendency toward an opposite trend starting from the 1980s. The first phenomenon is known as “global dimming”, the second as “global brightening” [4], [5].

In this context we studied the temporal evolution of solar radiation in the last decades over Italy. Specifically we studied sunshine duration: it is defined as the length of time in which direct solar radiation on a plane normal to it is above a certain threshold, usually taken at  $120 \text{ Wm}^{-2}$ . Sunshine duration, which is usually measured with an uncertainty of  $\pm 0.1\text{h}$  and a resolution of  $0.1\text{h}$ , is directly correlated with solar radiation through Angström's law [6]. A very important advantage of sunshine duration records is that they cover usually a much longer period than global radiation records.

### 2.2 Data

We collected sunshine duration data not only for Sicily, but for the entire Italian territory. The sunshine duration records were recovered from three main data sources: the paper archive of CRA-CMA (<http://cma.entecra.it/homePage.htm>) that is the former Italian Central Office for Meteorology (24 records), the database of Italian Air Force synoptic stations (47 records) and the Italian National agrometeorological database (BDAN, 59 records). Beside the records we recovered from these data sources, we considered also two records (Modena and Trieste) from university observatories, one record (Pontremoli) from an observatory managed by a volunteer joining the Italian Society for Meteorology and one record (Varese) from a meteorological observatory managed by a local association.

For some sites we set up composite records, merging data of the same station from different sources. In particular 18 of the BDAN records were used to update the records provided by Italian Air Force. Moreover, for eight records we merged data from different sites. They concern stations at short distances and belonging to areas with homogeneous geographical features.

The final data set encompasses 104 sunshine duration daily records covering the entire Italian territory. It refers to the 1936-2013 period. The spatial distribution of the stations is rather uniform, with the only exception of the Alpine area, which is covered only by 3 stations. The station coverage is rather low also in the Apennine area. 11 of the stations are in Sicily.

Data availability versus time is rather inhomogeneous. The best data coverage concerns 1958-1964, 1971-1977 and 1982-2013, whereas 1965-1970 and 1978-1981 have lower data availability. The period with the most critical situation in terms of data availability corresponds to the first 14 years (1936-1949).

### **2.3 Data pre-processing**

Before data analysis, the records were pre-processed in order to get quality checked and homogenised gridded records.

#### **2.3.1 Quality check and calculation of monthly records**

All daily records were checked in order to identify and correct gross errors. A further check concerned the position of the stations: all coordinates were checked for consistency (i.e. elevation was checked in relation to position) by means of Google Earth mapping tool. Moreover, we verified the consistency of the coordinates with the information from stations metadata.

All records were expressed in hours and tenths of hour, corresponding to a time resolution of six minutes. They were then converted into relative sunshine duration (i.e. the ratio between measured and eso-atmospheric sunshine duration) records and corresponding monthly average records were calculated only when the fraction of missing data did not exceed 10%.

#### **2.3.2 Data homogenization**

We subjected all our monthly records to the relative homogeneity Craddock test [7]. When a break was identified, the portion of the series that precedes it was corrected, leaving the most recent portion of the series unchanged in order to allow an easy updating of the record when new data become available.

Applying the homogenization procedure to the database, only 34 out of 104 records resulted homogeneous, whereas the remaining 70 were homogenized. A total number of 116 breaks was found.

### **2.3.3 Gap filling and calculation of monthly anomaly records**

After homogenisation, we filled the gaps in the monthly records. Specifically, each missing datum was estimated by means of the closest record – in terms of distance and elevation difference – among those with available data within the same geographical region. The selection of the record to use for the estimation of the missing datum was performed considering only the records fulfilling two conditions: distance within 500 km from the record under analysis and availability of at least 10 monthly values in commune with it in the month of the break. If no records fulfilled these conditions, the missing datum was not estimated.

After gap filling, only the 95 records for which at least 90% of the data were available in the 1984-2013 period were considered. These records were then transformed into anomaly records, with respect to the monthly normals of this period.

### **2.3.4 Gridding and calculating Sicily average sunshine duration record**

Starting from the 95 gap-filled anomaly records, we generated a gridded version of monthly sunshine duration anomalies. This gridded version has the advantage of balancing the contribution of areas with a higher number of stations with those that have a lower station coverage. We used a grid with 1-degree resolution both in latitude and longitude, following the technique described by [8]: it is based on Inverse Distance Weighting approach (distance and elevation difference), with the addition of angular term weight introduced in order to take into account the anisotropy in stations' spatial distribution.

The grid was constructed from 7 to 19 degree E and from 37 to 47 degree N, selecting 68 points covering the Italian territory. The gridded records in most cases cover the entire 1936-2013 period and there are only a few grid points with some missing data, especially in the first ten years. 10 of the grid-points concern Sicily.

The gridded records can be used to calculate national and regional records simply by averaging all corresponding grid-point anomaly records belonging to the region of interest. Here we present the Sicily record which has been obtained averaging all Sicily grid point records. [Fig. 1] shows these grid-points, together with the stations that we used to calculate the Sicily grid-point records.

## 2.4 The Sicily sunshine duration record

The average Sicily seasonal and annual sunshine duration regional records are shown in [Fig. 2], together with a 3-year standard deviation Gaussian low-pass filter working on 11-year windows. The figure gives evidence of a clear brightening phase starting at about the mid of the 1980s, whereas the dimming phase of the 1960s and 1970s is less evident.

A paper on the temporal evolution of sunshine duration over Italy will be submitted to a scientific journal within short time. In this paper, a more complete analysis of the records will be presented, including the comparison with sunshine duration records of other datasets and other areas and with records of other proxy variables of solar radiation such as cloudiness and daily temperature range.

## 3. ESTIMATION OF GLOBAL RADIATION CLIMATOLOGIES FOR ANY PERIOD OF THE 1936-2013 INTERVAL

### 3.1 Angström's law

The dataset used to obtain the results presented in [3] and in section 2 includes both global radiation and sunshine duration records. In particular, the 2002-2011 spatial patterns are based on global radiation data, whereas the temporal evolution in the 1936-2013 period is based on sunshine duration data.

Sunshine duration and global radiation are linked by Angström's equation. It links the clearness index ( $K_T$  i.e. the ratio between the global radiation received by a surface ( $H_T$ ) and the exo-atmospheric radiation received by the same surface ( $H_0$ )) to the relative sunshine duration (i.e. the ratio between the number of sun hours measured by a sunshine recorder ( $S$ ) and the solar day length from sunrise to sunset ( $S_0$ )) by means of the following linear relation:

$$K_T = a \frac{S}{S_0} + b \quad (1)$$

with coefficients  $a$  and  $b$  depending on the considered month. A detailed discussion on this relation is reported in [9] and [10], which report also  $a$  and  $b$  coefficients

obtained by means of about 30 Italian station with both global radiation and sunshine long-term records.

### 3.2 From the 2002-2011 climatologies to other reference periods

We used Angström's equation to estimate the clearness index normal values corresponding to any period of the 1936-2013 interval from the 2002-2011 ones. This estimation is rather easy. In fact, considering a fixed month and a given station, we get from relation (1):

$$\overline{K_{T_{A-B}}} - b = a \frac{\overline{S_{A-B}}}{S_0} \quad (2)$$

where the over bar denotes a temporal average and A-B denotes the corresponding time period.

Writing the same equation for period 2002-2011, dividing equation (2) for the corresponding 2002-2011 equation and rearranging the terms, we get:

$$\overline{K_{T_{A-B}}} = \overline{K_{T_{2002-2011}}} \frac{\overline{S_{A-B}}}{\overline{S_{2002-2011}}} + b \left( 1 - \frac{\overline{S_{A-B}}}{\overline{S_{2002-2011}}} \right) \quad (3)$$

If we now divide the sunshine duration averages in equation (3) for the corresponding averages in the 1984-2013 period, we have simply to calculate the average of the sunshine duration anomaly record over period A-B. It is therefore simply necessary to project the sunshine duration anomaly records (see section 2) over the SIAS stations. This projection was performed with the same technique we used for the projection of the sunshine duration anomaly records onto a regular grid (see section 2.3.4).

This procedure allowed estimating the clearness index normal values for the 41 SIAS stations over any period of the 1936-2013 interval. Here we obviously used the shading-bias-adjusted value presented in [3].

Once we estimated the clearness index monthly normals over period A-B for all 41 SIAS stations, the corresponding climatologies could simply be obtained applying to them all the procedure presented in [3]. Actually, we used a slightly different approach projecting the station clearness index normals onto the grid-points of 4

RCM combinations before applying the procedure presented in [3]. In this way, the climatologies we get from the observational data are easier to compare with the results from the RCMs and they can be better used to adjust model results.

## **4. GLOBAL RADIATION SCENARIOS FOR THE XXI<sup>th</sup> CENTURY**

### **4.1 Regional Climate Models**

Thanks to the robust high-resolution past reconstruction of global radiation for Sicily, it was possible to evaluate the ability of some ENSEMBLES Regional Climate Models (RCMs) in reproducing global radiation in this region. In particular, we evaluated whether the spatial distribution and the range of the model outputs resulted in agreement with the observational data.

Four RCM-GCM combinations were taken into account: KNMI-ECHAM5, SMHI-ECHAM5, SMHI-BCM and SMHI-Had. We considered the historical run of the models forced by GCM and their future projections under the A1B scenario.

[Fig. 3] shows the 78 grid-points we considered for RCMs scenarios. We underline that, in order to allow an easier comparison between model and observational data, we projected the SIAS stations' clearness index normals on these grid-points before estimating the climatologies for the 1961-2000 period.

### **4.2 Comparison of observed and modelled global radiation**

In order to compare global radiation from the RCMs with observed global radiation, we calculated the clearness index monthly normal values from the model records for the 1961-2000 period and compared them with the corresponding observational normals. The results of this comparison are reported in [Fig. 4a-e] that shows the ratios between the model and the observational normals for March, June, September and December. These comparisons shows that the model outputs have to be adjusted in order to be representative of the real data.

### **4.3 Adjustment of the RCM clearness index normals and estimated future solar radiation climatologies**

The ratios between the modelled and the observed clearness index normals in the 1961-2000 period have been used to adjust the future climate simulations. More precisely, for each model grid-point, the clearness index monthly normals calculated

from the model data for the periods 2001-2050 and 2051-2100 have simply been multiplied for the ratio between the clearness index normals of the observed and modelled data in the 1961-2000 period.

Once these adjusted clearness index normals were available for each model grid-point, the global radiation climatologies were estimated applying the procedure outlined in [3].

In order to better give evidence of the time evolution of global radiation for the model projections, we show maps [Fig. 5a-e] with the ratios between the 2001-2050 and the 1961-2000 climatologies and the ratios between the 2051-2100 and the 1961-2000 climatologies for March, June, September and December. The trend pattern is not well defined, with results depending on the considered month and model. Moreover, the variations from one period to the other are always within the variability of 30-year climatologies (e.g. 1951-1980 and 1984-2013 period) derived from the observed data.

## **5. CONCLUSION**

A methodology which allows obtaining Sicily solar radiation climatologies for any period of the 1936-2013 interval has been set up. The clearness index normal values of the 1961-2000 period have been used to validate and adjust the outputs of 4 RCM-GCM combinations. The adjusted scenario clearness index normals have been used to produce 2001-2050 and 2051-2100 climatologies. These climatologies do not give evidence of well defined global radiation trends. In the future we plan to extend these studies to a wide range of RCMs-GCM models and a paper on global radiation scenario will be prepared.

## **6. ACKNOWLEDGMENTS**

This study has been carried out in the framework of the EU project ECLISE (265240).

## 7. REFERENCES

1. Daly C., Gibson W.P., Taylor G.H., Johnson G.L. & Pasteris P.A. (2002), *A knowledge-based approach to the statistical mapping of climate*, *Climate Res.*, 22, 99–113.
2. Daly C. (2006), *Guidelines for assessing the suitability of spatial climate data sets*, *Int. J. Climatol.*, 26, 707–721.
3. Manara V., Brunetti M., Maugeri M., Pasotti L., Simolo C., Spinoni J. (2013), *Sicily monthly high-resolution solar radiation climatologies*, PROCEEDINGS of climate change and its implications on eco system and society, SISC, 22-23 September 2013, Lecce, Italy, 198-209.
4. Wild M. (2009), *Global dimming and brightening: A review*, *J. Geophys. Res.*, 114, D00D16, doi: 10.1029/2008JD011470.
5. Wild M. (2012), *Enlightening global dimming and brightening*, *Bulletin of the American Meteorological Society* 93, 27-37.
6. Angström A. (1924): *Solar and terrestrial radiation*, *Q. J. R. Meteorol. Soc.*, 50, 121-125.
7. Craddock JM. (1979), *Methods of comparing annual rainfall records for climatic purposes*, *Weather* 34, 332–346.
8. Sanchez-Lorenzo A., Brunetti M., Calbò J., Martin-Vide (2007): *Recent spatial and tempo rally variability and trends of sunshine duration over the Iberian Peninsula from a homogenized data set*, *Journal of Geophysical Research*, 112, D20115, doi: 10.1029/2007JD008677.
9. Spinoni J. (2010), *1961–90 High-Resolution temperature, precipitation, and solar radiation climatologies for Italy*, Ph.D. thesis, Milan University, available at: [http://air.unimi.it/bitstream/2434/155260/2/phd\\_unimi\\_R07883\\_1.pdf](http://air.unimi.it/bitstream/2434/155260/2/phd_unimi_R07883_1.pdf).
10. Spinoni J., Brunetti M., Maugeri M. & Simolo C. (2012): *1961-1990 monthly high-resolution solar radiation climatologies for Italy*, *Adv. Sci. Res.*, 8, 19-21, available at: [www.adv-sci-res.net/8/19/2012](http://www.adv-sci-res.net/8/19/2012).

## 8. IMAGES AND TABLES

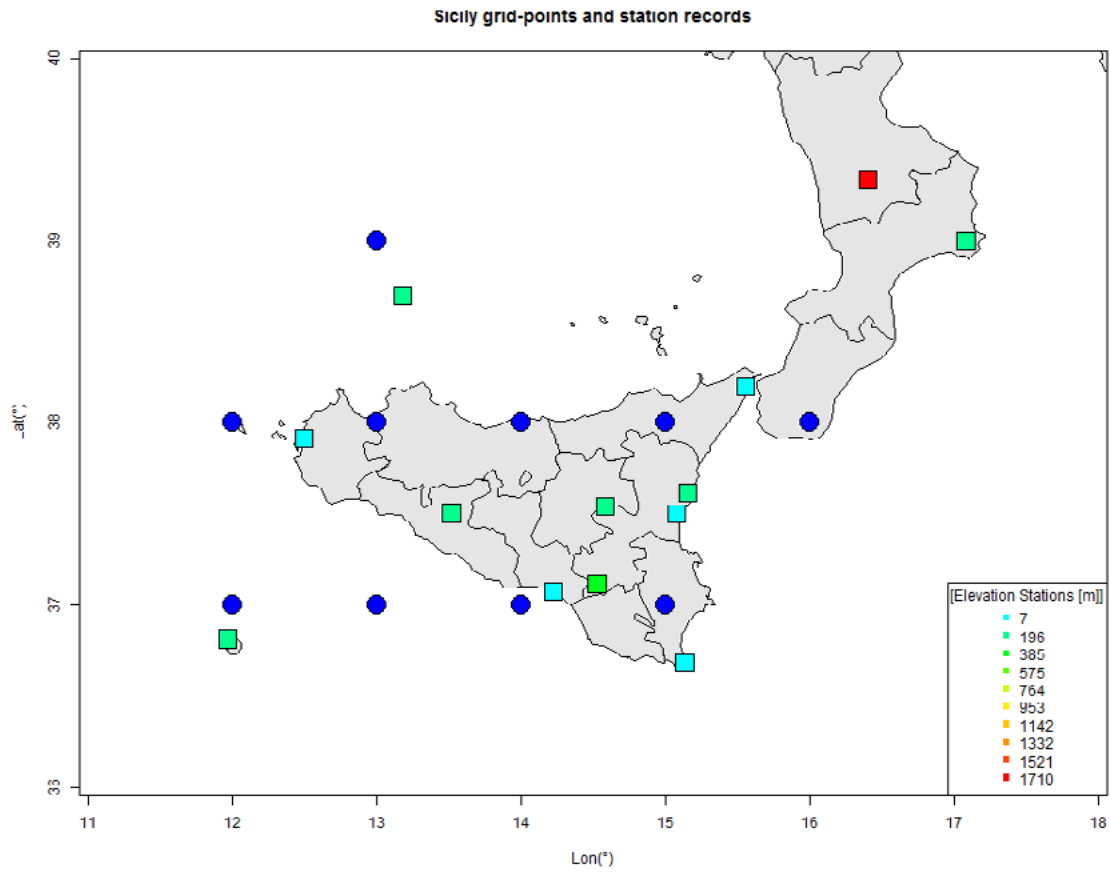


Fig. 1 Sicily grid-points (blue points) and station records (other color squares) we used to calculate the grid-point series.

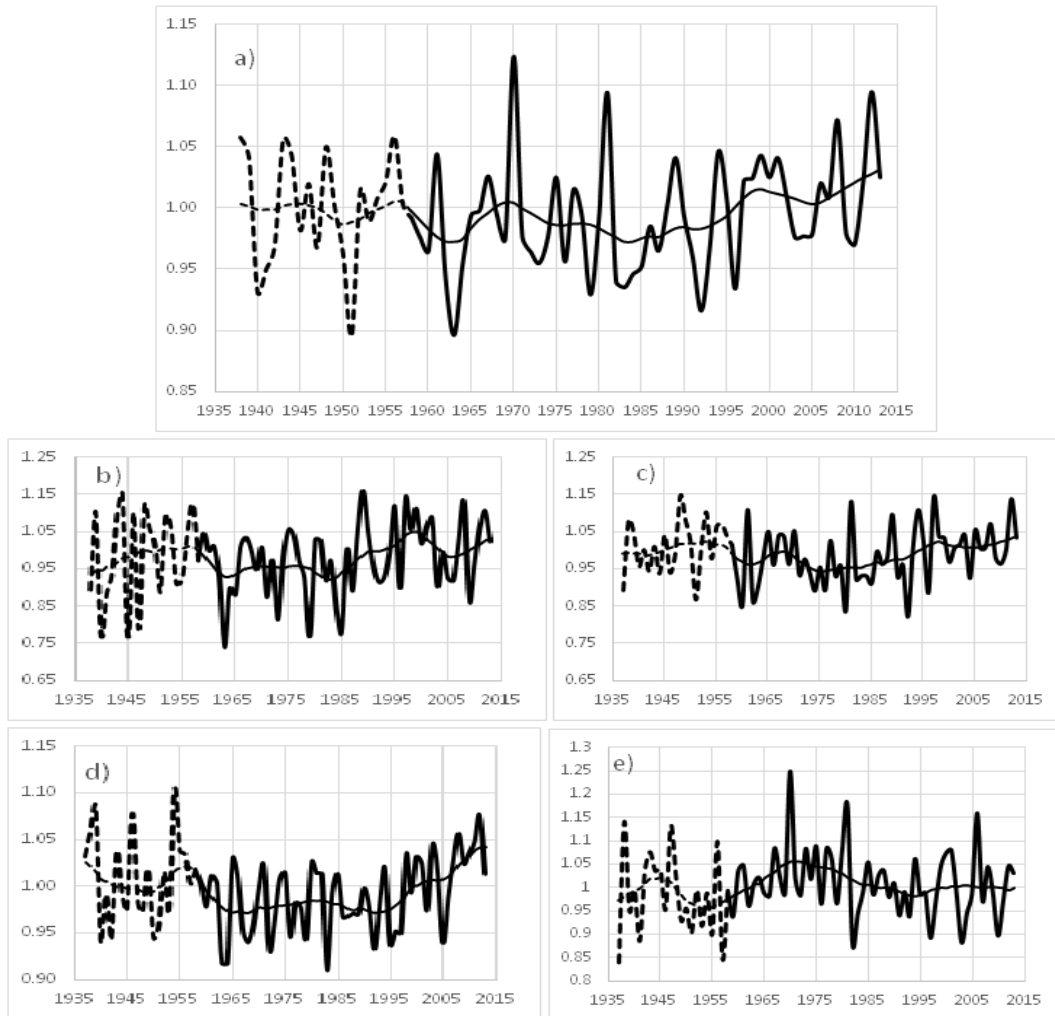


Fig. 2 Average Sicily sunshine duration (thin line), plotted together with an 11-y window - 3-y standard deviation Gaussian low-pass filter (thick line) for (a) year; (b) winter; (c) spring; (d) summer; (e) autumn. The series are expressed as relative deviations from the 1984-2013 means. Dashed lines are used prior to 1958 owing to the lower number of records for this initial period.

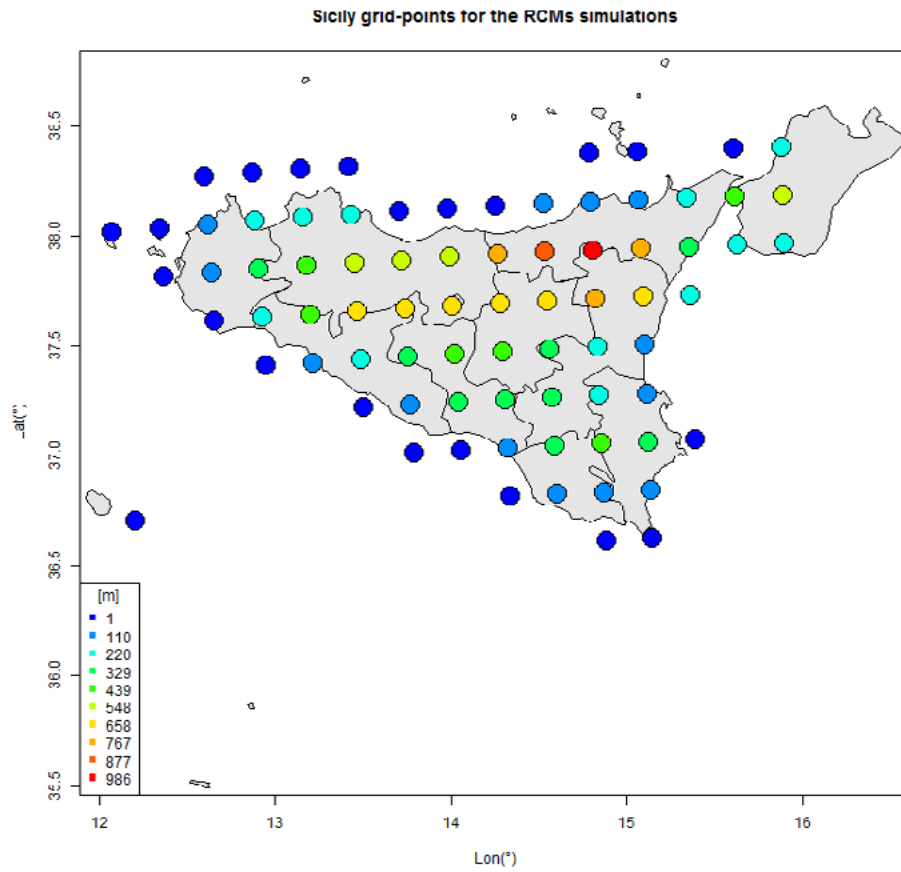


Fig. 3 Sicily grid-points for the RCMs simulations. The colors indicate the elevation of the model grid-points.

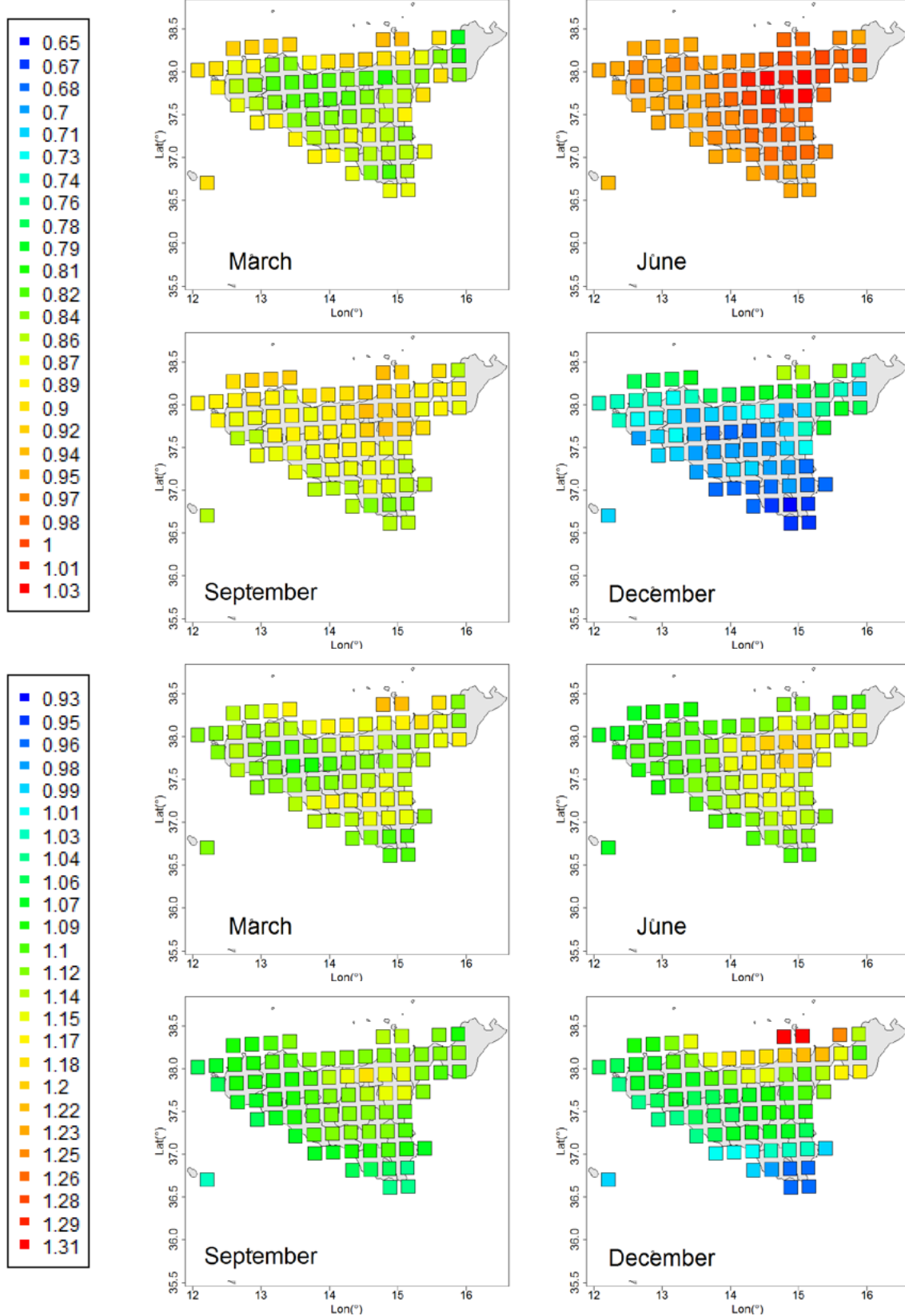


Fig. 4a-b Ratios between model and observational normals for the 1961-2000 period: March, June, September and December. Upper graphs KNMI-ECHAM5; lower graphs SMHI-ECHAM5 model.

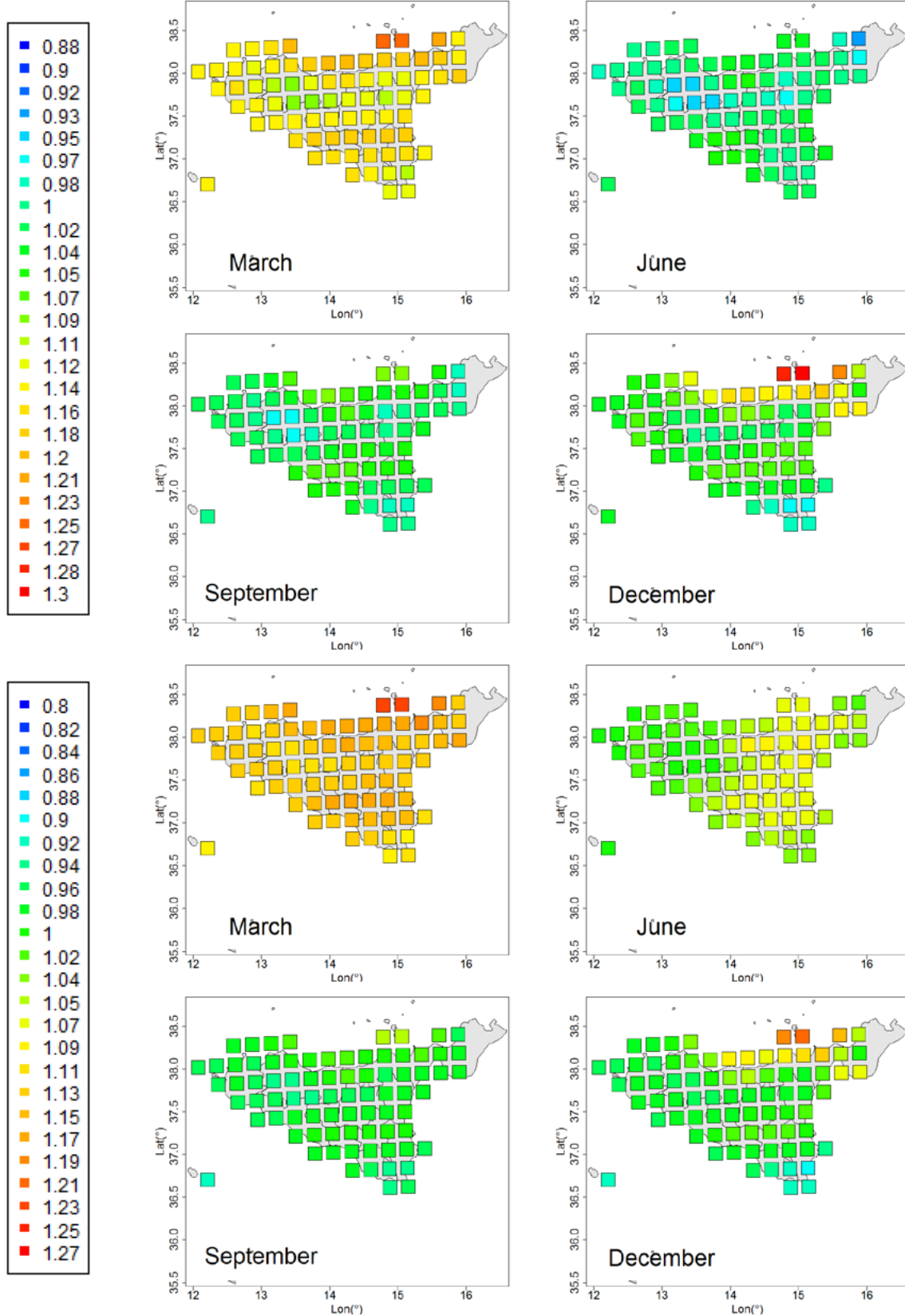


Fig. 4c-d Ratios between model and observational normals for the 1961-2000 period: March, June, September and December. Upper graphs SMHI-BCM; lower graphs SMHI-Had model

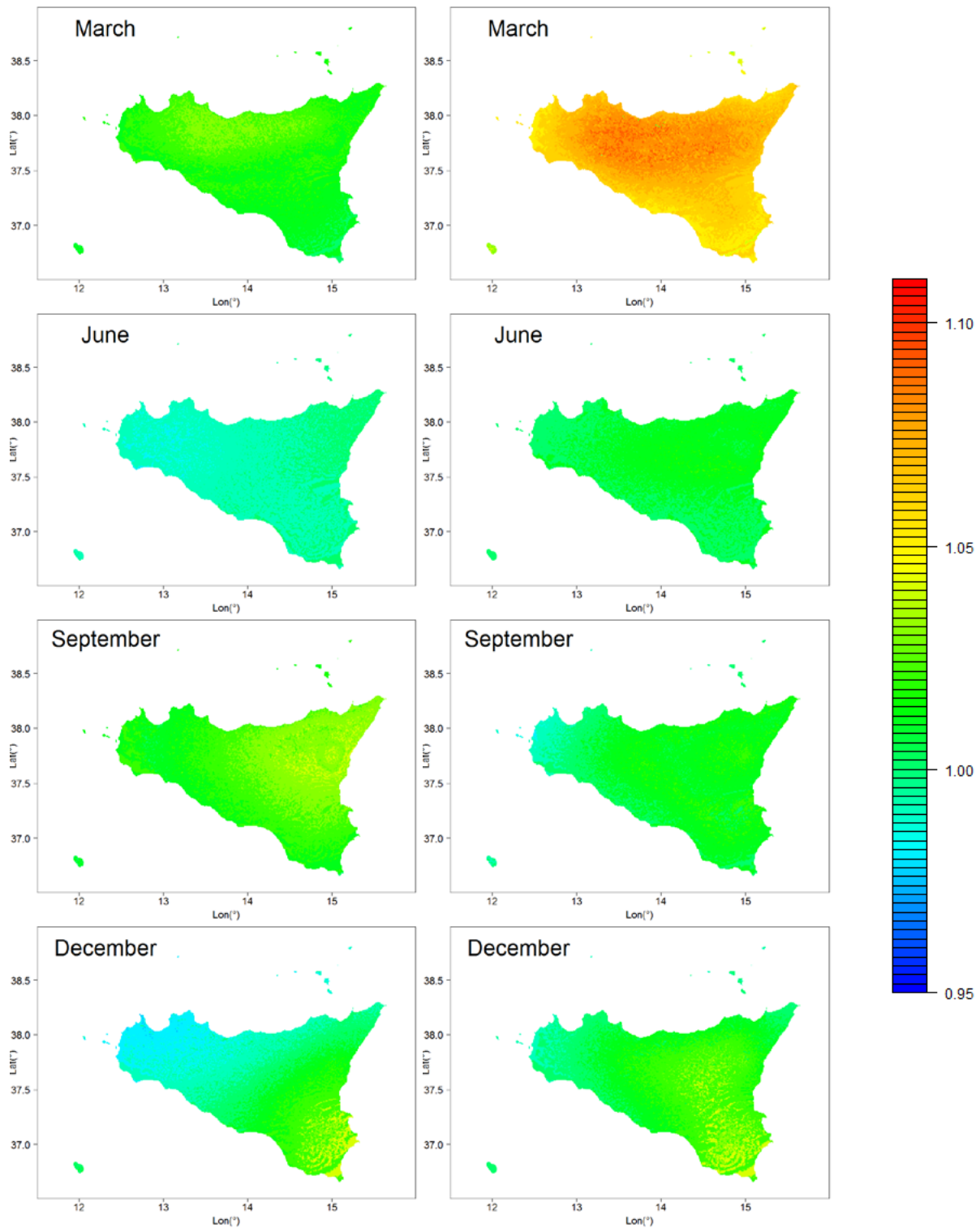


Fig. 5a Ratios between the 2001-2050 and the 1961-2000 climatologies (left column) and ratios between the 2051-2100 and the 1961-2000 climatologies (right column) for March, June, September and December for the KNMI-ECHAM5 model.

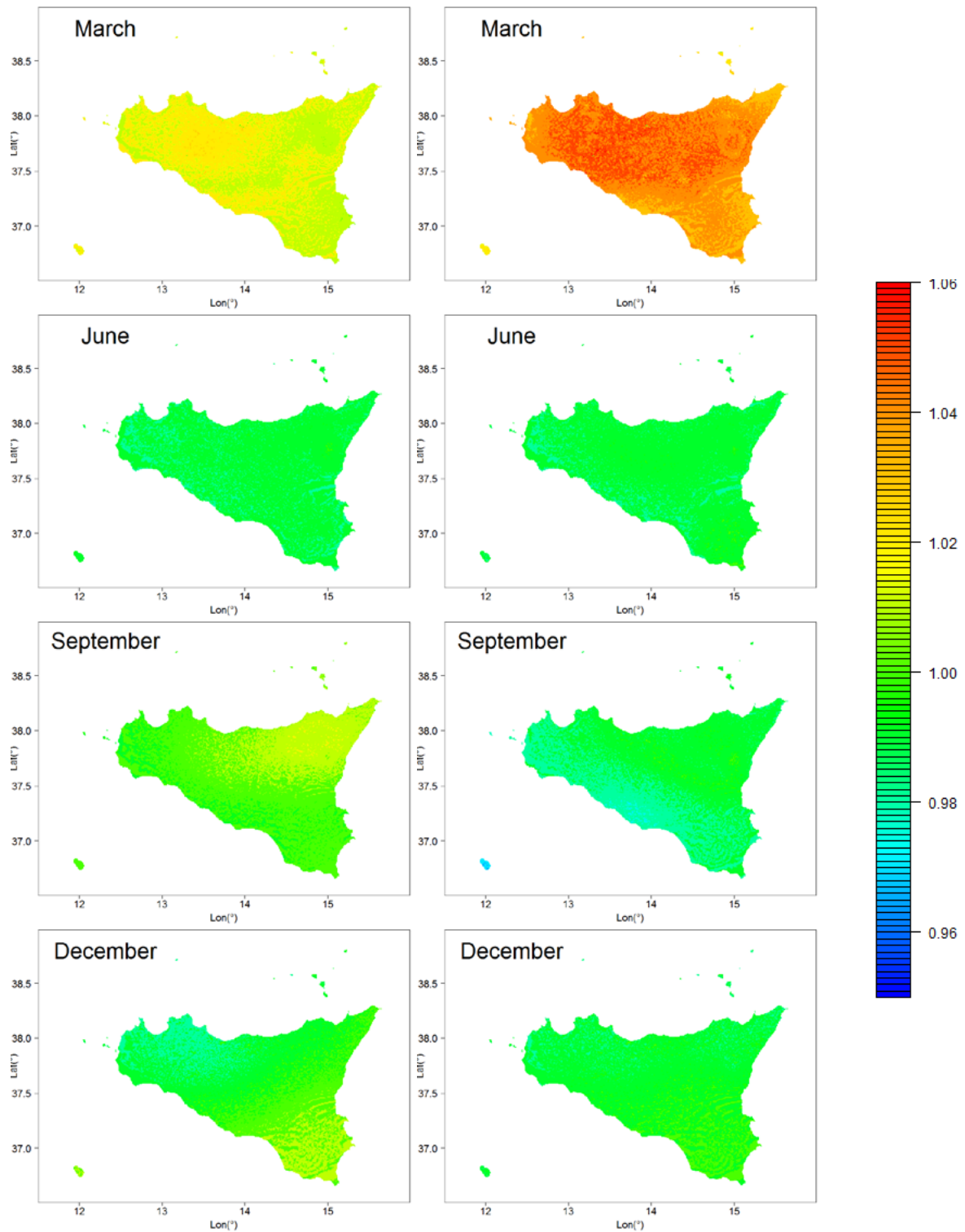


Fig. 5b Ratios between the 2001-2050 and the 1961-2000 climatologies (left column) and ratios between the 2051-2100 and the 1961-2000 climatologies (right column) for March, June, September and December for the SHMI-ECHAM5 model.

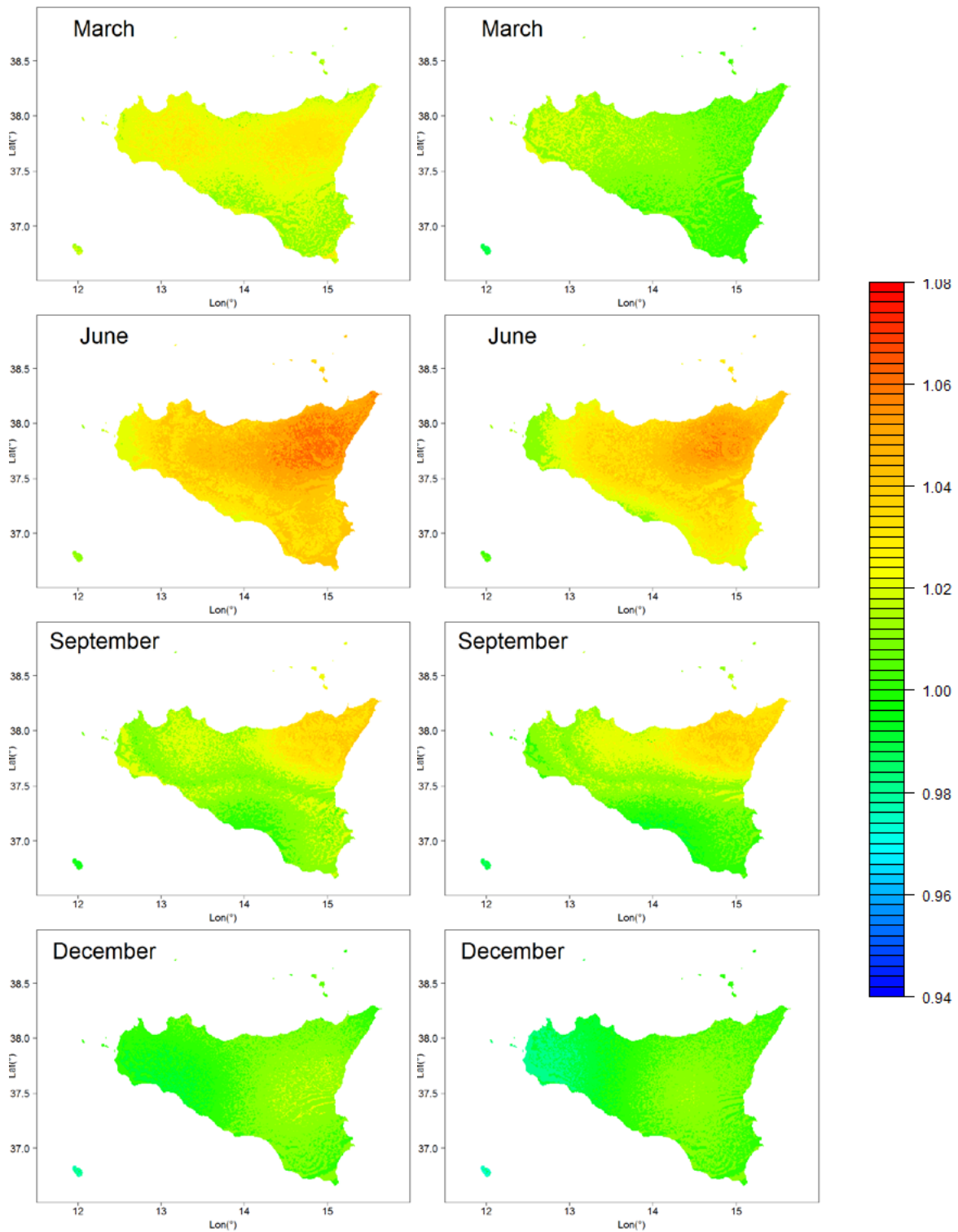


Fig. 5c Ratios between the 2001-2050 and the 1961-2000 climatologies (left column) and ratios between the 2051-2100 and the 1961-2000 climatologies (right column) for March, June, September and December for the SHMI-BCM model.

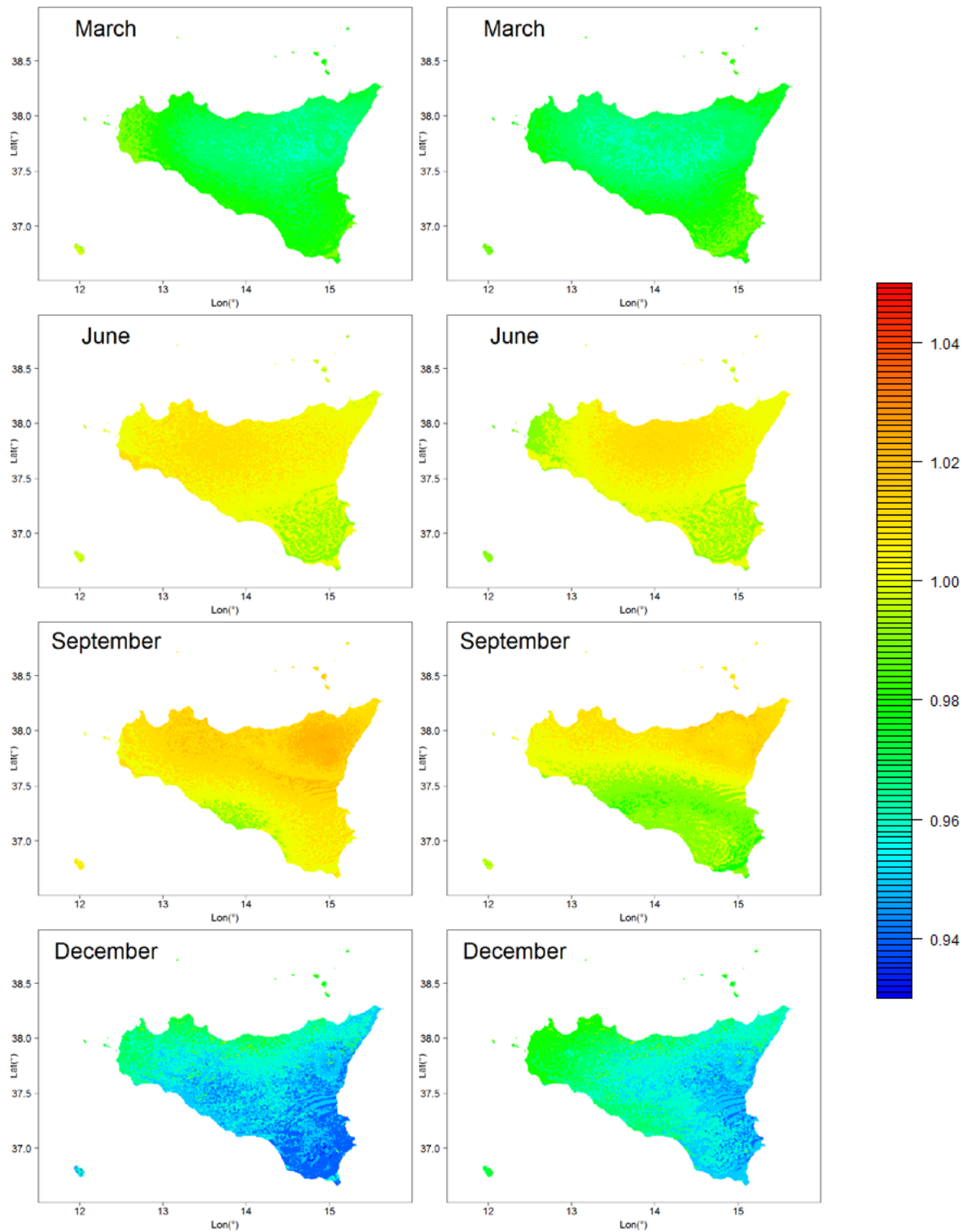


Fig. 5d Ratios between the 2001-2050 and the 1961-2000 climatologies (left column) and ratios between the 2051-2100 and the 1961-2000 climatologies (right column) for March, June, September and December for the SHMI-Had model.

## Top down emission estimates of radiatively active F-gases vs bottom up inventories

Graziosi F., Furlani F. , Giostra U., Arduini J., Lo Vullo E. and Maione M.\*

University of Urbino “Carlo Bo” Dep. of Basic Sciences and Foundations, Italy

\*Corresponding Author: [michela.maione@uniurb.it](mailto:michela.maione@uniurb.it)

### Abstract

Fluorinated gases (F-gases) are strong greenhouse gases included in the United Nations Framework Convention on Climate Change (UNFCCC) Kyoto Protocol. Parties to the Protocol are required to submit to UNFCCC their annual emission inventories. Such emissions are normally assessed through “bottom-up” methods aggregating various local statistics. Since emissions as measured by their accumulation in the atmosphere can significantly disagree with reported bottom - up emissions a ‘Good Practice’ for a correct estimation of emissions a verification through independent methods such as inverse modelling is needed. We present regional emission estimates of F-gases derived through a combination of situ long-term high frequency observations and a Bayesian inversion method. The estimates provided by this analysis are relevant for constraining the atmospheric budget of these gases on a regional scale, also improving the accuracy of their emissions quantification on a global scale. The comparison of our estimates with bottom-up inventories revealed not negligible discrepancies, thus showing the effectiveness of this approach as a verification tool for declared emissions.

**Keywords:** fluorinated gases, Kyoto Protocol, mmission estimates, atmospheric observations, inventories

## 1. INTRODUCTION

The fluorinated gases (F-gases) are organofluorine compounds, that include the hydrofluorocarbons (HFCs), man made chemicals containing, beside carbon, fluorine and hydrogen atoms. They are widely used as refrigerant fluids, foam blowing agents, fire extinguishers and solvents, after having been introduced as replacements for ozone depleting gases such as the chlorofluorocarbons (CFCs) and hydrochlorofluorocarbons (HCFCs), whose production and consumption are regulated under the Montreal Protocol on Substances that Destroy the Ozone Layer. HFCs, are not harmful towards the ozone layer, however they strong greenhouse gases being able to absorb the long wave radiation emitted by the earth surface in that region of the electromagnetic spectrum known as the “atmospheric window” where the most abundant greenhouse gases do not have any absorption band. For this reason, the HFCs are included in the United Nations Framework Convention on Climate Change (UNFCCC) Kyoto Protocol basket. Under the Protocol, countries' actual emissions have to be monitored and Parties are required to submit to UNFCCC their annual emission inventories. Such emissions are normally assessed through “bottom-up” methods aggregating various local statistics. However, these emissions, as measured by their accumulation in the atmosphere, can significantly disagree with reported bottom - up emissions [1]. The Intergovernmental Panel on Climate Change (IPCC) recommends in its ‘Good Practice’ manual [2] for estimating emissions that nations undertake verification studies, including atmospheric verification, consisting in a combination of long term high-frequency atmospheric observations with various modelling techniques. Among these, inverse modelling has proved to be not only a qualified independent tool for checking the reliability of inventories, but also a better method of establishing inventories.

Here we present regional emission estimates of F-gases derived through a combination of situ long-term high frequency observations and a Bayesian inversion method. The estimates provided by this analysis are relevant for constraining the atmospheric budget of these gases on a regional scale, also improving the accuracy of their emissions quantification on a global scale.

## 2. METHOD

In situ long-term high frequency observations of F-gases are conducted at the WMO-GAW (World Meteorological Organisation, Global Atmospheric Watch) Global Station of Monte Cimone (CMN) since 2001. Air samples are analysed every two hours, using a Gas Chromatographic-Mass Spectrometric (GC-MS) system equipped with a sampling and pre-concentration unit, providing high quality observation of ca 40 species [3]. Atmospheric data from CMN and from other European stations that are part of the AGAGE (Advanced Global Atmospheric Gases Experiment) network (Mace Head, Ireland and Jungfraujoch, Switzerland) are used in combination with the Lagrangian dispersion model FLEXPART [4] and an analytical inversion method [5]. FLEXPART is a stochastic model with detailed treatment of turbulence and convection and uses meteorological analyses from the European Centre for Medium-Range Weather Forecasts (ECMWF). We use the ECMWF analyses at  $1^\circ \times 1^\circ$  resolution and FLEXPART is run backward in time from the measurement stations at three-hourly intervals, using 40000 particles for each backward run. The FLEXPART output is an emission sensitivity, also called source receptor relationship (SRR). The SRR in a particular grid cell, expressed in units  $\text{s kg}^{-1}$ , is proportional to the particle residence time in that cell and expresses the simulated mixing ratio at the receptor that a source of unit strength ( $1 \text{ kg s}^{-1}$ ) in the cell would produce for a given air sample. Multiplying the footprint emission sensitivity (i.e. the emission sensitivity in the lowest model layer) with the emission flux taken from an appropriate emission inventory gives the simulated mixing ratio at the receptor, which can be compared with a coincident measurement. The FLEXPART output can be ingested directly by the inversion algorithm: the basic idea is to find an a posteriori emission distribution leading to the best fit between the measurements and the model results while keeping the solution within the given error bounds of the a priori emissions. The “best” agreement is measured as the sum of the squared errors, inversely weighted with the uncertainty variances. We also identify “outliers” in the model-simulated mixing ratios and assign them large uncertainties to prevent the solution being strongly influenced by large measurement and/or model errors.

## 3. RESULTS

We present the case study of HFC-152a, a refrigerant with a 100-year GWP of 140. We used as a priori emissions given by the Emissions Database for Global

Atmospheric Research (EDGAR), which provides global past and present day anthropogenic emissions of greenhouse gases and air pollutants by country and on spatial grid. For this study, we used the version 4.2 (v42\_HFC-152a\_2008\_IPCC\_2\_3.txt), with a spatial resolution of  $0.1 \times 0.1^\circ$  lat long. Emissions are then grouped in  $0.5 \times 0.5^\circ$  lat long grid cells.

A comparison between the a priori HFC-152a fluxes for 2008 and the a posteriori fluxes obtained with the inversion for the same year, is reported in [Fig. 1].

We have also compared our results with annual emission inventories submitted to UNFCCC by the various countries and our results showed that:

- i) Emissions estimated through the inversion for the various countries are constantly higher with respect to what countries have declared to UNFCCC;
- ii) With respect to the EDGAR inventories, the emission estimates through the inversion are generally lower, with the exception of Italy and Spain;
- iii) On the whole, the estimated European geographic domain emissions are lower than the emissions reported by EDGAR. However EDGAR estimates are much closer to the inversion results than the UNFCCC data [Fig. 2]

#### **4. CONCLUSIONS**

We used a combination of long term, high-frequency atmospheric measurements with a Bayesian inversion method to estimate European emissions of F-gases included in the Kyoto basket and we compared our estimates with emissions reported by the various countries to the UNFCCC. The comparison of our estimates with bottom-up inventories revealed not negligible discrepancies, thus showing the effectiveness of this approach as a verification tool for declared emissions.

#### **5. ACKNOWLEDGMENTS**

Scripps Institution of Oceanography and the SIO2005 scale are gratefully acknowledged, as well as the science teams of the AGAGE consortium. The InGOS EU FP7 Infrastructure project (grant agreement n° 284274) supported the observation activity. The University Consortium CINFAI (Consorzio Interuniversitario Nazionale per la Fisica delle Atmosfere e delle Idrosfere) supported F. Graziosi grant (RITMARE

Flagship Project). The "O. Vittori" station is supported by the National Research Council of Italy and the Italian Ministry of Education, University and Research, through the Project of National Interest "Nextdata".

## 6. REFERENCES

1. Nisbet, E. & Weiss, R. (2010) *Top-down versus bottom-up*, Science, No 328, pp. 1241-1243.
2. Annex 2 (Verification) to the IPCC Good Practice Guidance and Uncertainty Management in National Greenhouse Gas Inventories (2001).
3. Maione M., Giostra U., Arduini J., Furlani F., Graziosi F., Lo Vullo E. Bonasoni P. (2013), *Ten years of continuous observations of stratospheric ozone depleting gases at Monte Cimone (Italy) - Comments on the effectiveness of the Montreal Protocol from a regional perspective*, The Science of the Total Environment, No. 445–446, pp.155–164.
4. Stohl A., Hittenberger M., and Wotawa G. (1998), *Validation of the Lagrangian particle dispersion model FLEXPART against large scale tracer experiment data*, Atmospheric Environment, No 32, pp.4245–4264.
5. Stohl A., Seibert P., Arduini J., Eckhardt S., Fraser P., Grealley B. R., Lunder C., Maione M., Mühle J., O'Doherty S., Prinn R. G., Reimann S., Saito T., Schmidbauer N., Simmonds P. G., Vollmer M. K., Weiss R. F., and Yokouchi Y. (2009), *An analytical inversion method for determining regional and global emissions of greenhouse gases: Sensitivity studies and application to halocarbons*, Atmospheric Chemistry and Physics, No 9, pp.1597-1620.

## 6. IMAGES AND TABLES

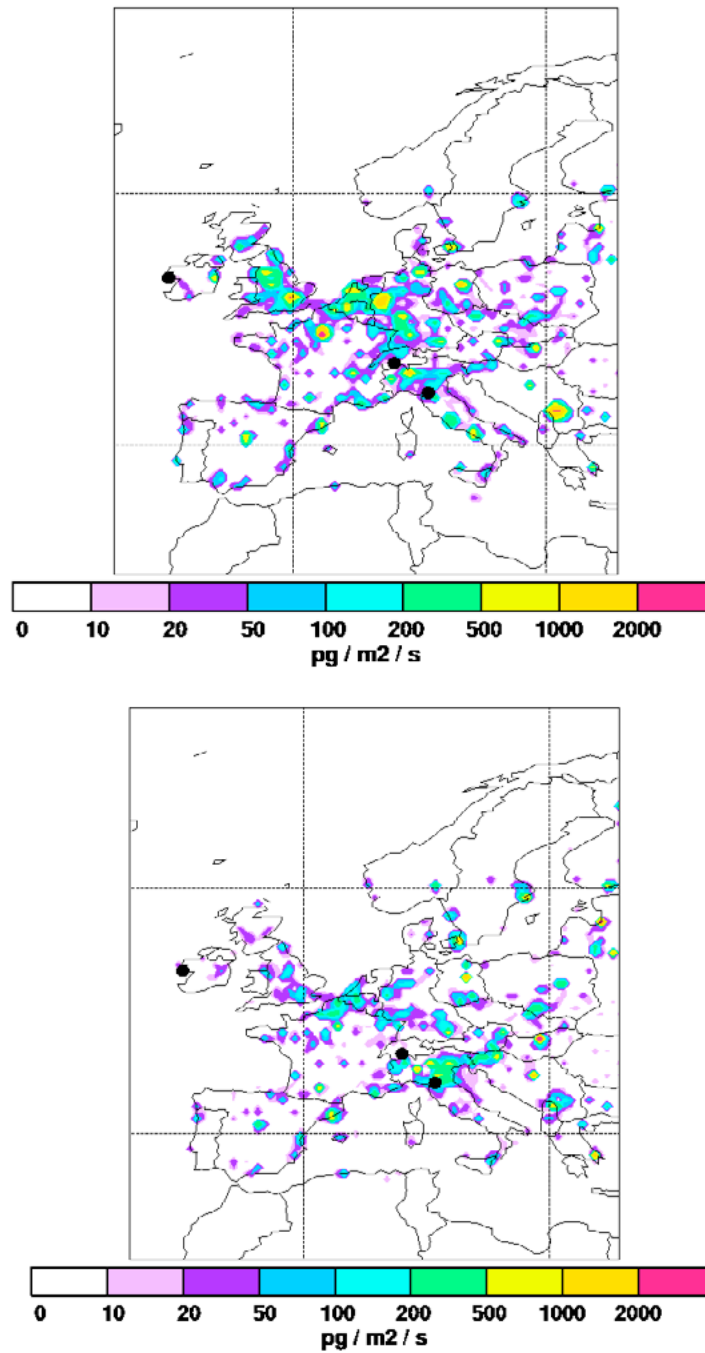


Fig. 1 A priori (top) and a posteriori (bottom) HFC-152 fluxes (in  $\text{pg} / \text{m}^2 / \text{s}$ ) from the European Geographic domain in 2008

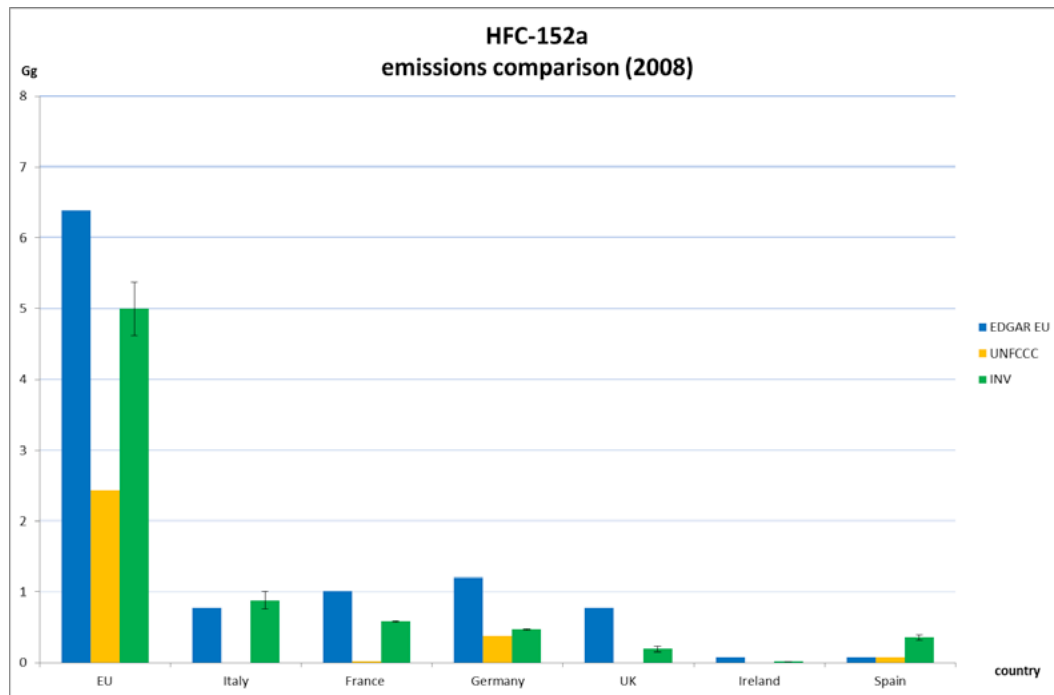


Fig. 2 Comparison of top down HFC-152 emissions estimates (in Gg) from the European geographic domain and from selected European Countries (green bars) with emissions reported to UNFCCC (Yellow bars) and emission in the EDGAR inventory (blue bars)

Advances in climate change

**Climate data:  
management & analysis**

## Preliminary comparison study of two independent precipitation network in Piedmont

Acquaotta F.<sup>1\*</sup>, Fratianni S.<sup>1</sup>, and Venema V.<sup>2</sup>

<sup>1</sup>Dipartimento di Scienze della Terra, Università di Torino, Torino - Italy,

<sup>2</sup>Meteorological Institute, University of Bonn, Bonn – Germany

\*Corresponding Author: [fiorella.acquaotta@unito.it](mailto:fiorella.acquaotta@unito.it)

### Abstract

Long historical climate records typically contain inhomogeneities. Parallel measurements are ideal to study such non-climatic changes. In this study we will analyze the transition from conventional precipitation observations to automatic weather stations. The dataset comes from two independent climate networks in the region of Piedmont, Italy. From this dataset we could identify 20 pairs of stations with up to 17 years of overlap. This is a valuable dataset because it allows us to study an ensemble of independently managed pairs of standard-quality stations. The main systematic differences was found in the number of weak rainy events. The automatic weather stations report more events. On average they report 7 events more per year. While for the heavy and extreme precipitation, in some cases, we have identified great differences between the two series that can falsify the behavior of the variables.

**Keywords:** daily precipitation, parallel measurement, inhomogeneity

## 1. INTRODUCTION

Climate change is one of the great environmental concerns facing mankind in the twenty first century. The major changes are likely to occur in the global hydrological and energy balance. The greatest threat to humans will be manifested locally via changes in regional extreme weather and climate events. The society is particularly vulnerable to change in frequency and intensity of extreme events such as heavy precipitation, droughts and heat waves [11, 12].

Long term climate datasets are essential to study climate change. More specifically, long series of rainfall are essential for various hydrological applications related to water resource planning, power production, irrigation, flood control, forecasting and validation of remotely sensed data from space platforms. However, these applications require high quality long series. The observations need to be recorded, transmitted, digitized, quality controlled and then examined by an expert familiar with the instruments and the climatology [13].

Italy has a leading role in the development of meteorological observations. This interest in meteorology over the last three centuries has produced a wealth of observational data of enormous value.

This long legacy, however, also means that the Italian networks have experienced many technological, economical and organizational changes, which may affect the homogeneity of the record [4,15]. Consequently, studies on non-climatic changes are necessary to be able to reliably interpret the climatic changes [14]. For precipitation gauge measurements inhomogeneities can be caused by changes in the instruments, in the position or changes in the surrounding environment [2,5].

It is necessary to apply a homogenization procedure to detect and correct non-climatic changes. [18].

These homogenization corrections allow the quantification of the climatic changes in the mean value of precipitation and in some indices of rain [7, 10, 12]. These studies found significant increasing trends in the mean annual precipitation and in the average precipitation intensity, in particular in winter. The extreme weather and climate events that have a deep impact on society are studied less because they require high-quality daily series. The most direct way to study non-climatic biases in daily data relies on parallel measurements with multiple measurement set-ups.

In this study we have analyzed the recent transition to automatic precipitation measurements in Piedmont, Italy.

An important feature of our study is that it is based on 20 pairs of nearby high-quality stations. This enables us to study the variability of the inhomogeneity from station to station and in particular to understand as the discontinuities occur on the precipitation events classified as weak, moderate or extreme.

## 2. METHODOLOGY

In this study we have analyzed the difference between the precipitation events recorded by two independent networks present in the Piedmont region, North-Western Italy, during 17 years, from 1986 to 2003 [1]. Then we have evaluated the effects of the differences on the climate analysis.

The first network considered is the Hydrographic Mareographic Italian Service (SIMN) which was founded in 1913. In the closing year, 2002, the SIMN in Piedmont handled only 142 meteorological stations in total.

Most of the rainfall stations of SIMN have used a tipping bucket rain gauge with a calibrated mouth (1000 cm<sup>2</sup>). The height of the mouth was typically 2 m. The stations of SIMN require the presence of an operator for collecting the measurements. The registration of the rain gauge was done on a paper roll, which needed to be collected weekly and read for the manual transcription of the values [Fig. 1].

A new meteorological network managed by Agency for Environmental Protection Piedmont (ARPA) was build up in Piedmont starting 1986. In the first year ARPA had 42 stations. Now it is extended to 400 automatic stations with a density of 1 rain gauge per 70 km<sup>2</sup> [8].

The instrument used by ARPA is a rain gauge with a calibrated mouth (1000 cm<sup>2</sup>) and a tipping bucket. The height of the mouth is 1.5 m. The data are subjected to an immediate quality control, during which a flag is attached to every value and the data is directly transmitted to the database [Fig. 1].



Fig. 1 (left) Photos of rain gauge used by SIMN to measurement the rain; (right) Photo of rain gauge utilizing by ARPA Piedmont.

In 2002, a national law has forced the unification of the meteorological networks owned by the SIMN with those of the ARPA. Because the ARPA network was more modern, ARPA has decided to discontinue the SIMN stations after unification for reasons of technological innovation and cost-effectiveness.

In Piedmont there are therefore rain series from two different meteorological networks; the SIMN network, with data collected from 01/01/1913 to 31/12/2002 and the ARPA network of automatic stations, that providing information since 1986. This gives us an overlapping period of up to 17 years to study the influence of this transition in detail.

We have selected locations with pairs of stations according to several criteria. First of all, they need to have an overlapping period greater than 5 years [19].

A further selection criterions are the difference in elevation and the distance between two stations. This selection has been based on the results of the work already done [9, 6], in which a spatial consistency check, depending on the elevation difference, less than 200 m, and distance below 20 km, is estimated.

We have selected only 20 pairs of meteorological stations with a long overlap period and a good continuity in the recorded of daily precipitation data [Tab. 1].

Successively we have analyzed if these pairs of stations have recorded the same precipitation events or an instrument overestimates or underestimates a particular rain event. An accurate statistical analysis to identify if the two series have the same

statistical characteristics, same distribution, same mean, median, variance and so on, have been conducted [5, 6, 7].

<b>Location</b>	<b>SIMN elevation</b>	<b>ARPA elevation</b>	<b>Difference elevation</b>	<b>Distance</b>	<b>Period</b>
Ala di Stura	1006	1006	0	70	1993–2003
Bardonecchia	1250	1353	103	800	1991–2003
Boves	590	575	15	1240	1988–2003
Bra	290	285	5	15	1993–2003
Carcoforo	1150	1290	140	2500	1997–2003
Casale M.to	113	118	5	20	1988–2000
Ceresole Reale	2260	2304	44	920	1996–2003
Cumiana	289	327	38	2800	1988–2003
Lanzo T.se	540	580	40	2200	1989–1999
Locana - L.Valsoera	2410	2365	45	250	1987–2003
Luserna S. Giovanni	478	475	3	760	1988–2003
Mondovi	440	422	18	390	1993–2003
Oropa	1180	1186	6	5	1991–2002
Piedicavallo	1050	1040	10	180	1996–2003
Salbeltrand	1031	1010	21	1250	1991–2002
Susa	510	520	10	820	1991–2003
Torino	270	240	30	850	1990–2003
Valprato Soana	1550	1555	5	465	1993–1999
Varallo Sesia	453	470	17	2040	1989–2003
Vercelli	135	132	3	1360	1994–2003

Tab. 1 The 20 selected locations for the compared the SIMN precipitation series and ARPA precipitation series: elevation [m a.s.l.], difference of elevation [m], distance [m] and period of overlap.

We have calculated for every month and for every location the precipitation class using the percentiles calculated for each station on the reference period, from 1961 to 1990. We have divided the rain event in five principles class (weak, moderate, heavy, very heavy and extreme) [Tab. 2]. The heavy and extreme precipitation class were calculated exactly as the RClimdex software created by the Expert Team (ET) on Climate Change Detection and Indices (ETCCDI). RClimdex is one of the more utilized package by the scientific community to calculate the climate indices [3, 13].

For each one, we have calculated the number of events and the amount of rain and then we have compared the results between the pairs of the meteorological stations.

For every year and for each class we have calculated the difference of the number of events and the ratio of cumulate rain.

Class	Range
weak rain (w_r)	$R < 50\text{th}$
mean rain (m_r)	$50\text{th} \leq R < 80\text{th}$
heavy rain (h_r)	$80\text{th} \leq R \leq 95\text{th}$

very heavy rain (R95p)	R95p = Rclimdex; R>95p
extremely rain (R99p)	R99p =Rclimdex; R>99p

Tab 2: Five precipitation class and their range

### 3 RESULTS

The first result of the comparison study on precipitation class highlight two difference behavior for precipitation events classified as weak and moderate and events catalogued as heavy, very heavy and extreme. For the weak or moderate precipitation the major difference is estimated in the number of events. Averagely the automatic stations (ARPA) report 7 events more per year for the weak rains and more 3 events per year for the mean rains [Tab. 3]. For the cumulate precipitation these two class does not highlight great difference. The ratio is near to 1 and averagely the ARPA stations record more 3% of annual rain of weak events and more 4% for mean rain events [Tab. 3 and Fig. 2].

Class	Difference number of events	ST_DEV diff	Ratio cumulate precipitation	ST_DEV ratio
w_r	7	23	1.01	0.06
m_r	3	18	1.01	0.08
h_r	-6	13	0.97	0.06
R95p	-4	13	0.92	0.19
R99p	-2	2	0.86	0.14

Tab. 3 The mean annual values of difference of number of events and the mean annual ratio and their standard deviation between the pairs of stations calculated for every precipitation class. The difference is calculated as ARPA events - SIMN events while for the ratio ARPA amount /SIMN amount.

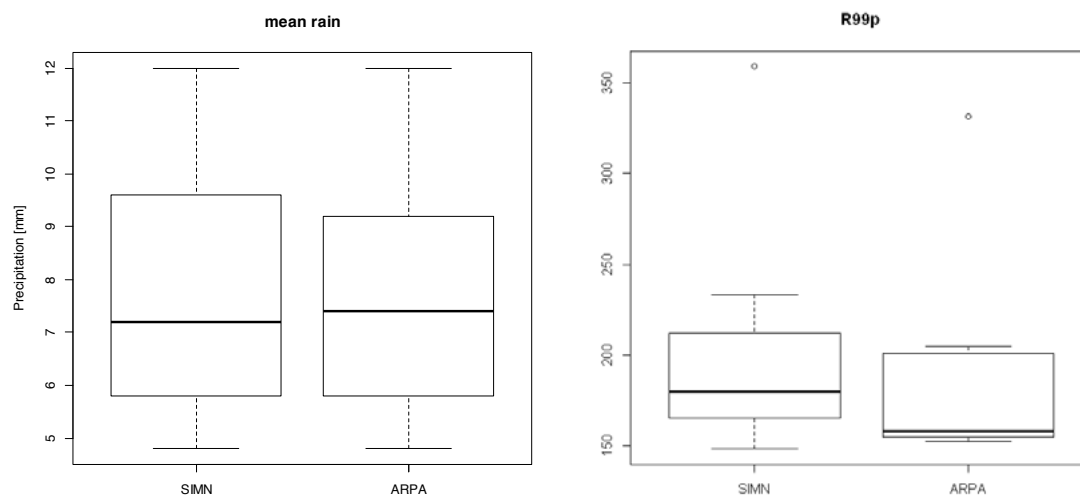


Fig. 2 left box plot of the mean rain recorded by the two meteorological stations of Torino from 1990 to 2002; right box plot of the extremely rain recorded by the two meteorological stations of Oropa from 1990 to 2002.

For the heavy, very heavy and extreme class of precipitation the SIMN stations record a greater number of events and a greater amount of rains respect to ARPA stations [Tab 3]. For the number of events the major differences are highlighted in the heavy rains with averagely more 6 events per year in the SIMN stations while for the ratio in the extreme rains. For the extreme class the SIMN station record averagely more 24% of amount precipitation per year [Fig 1 and Fig 3].

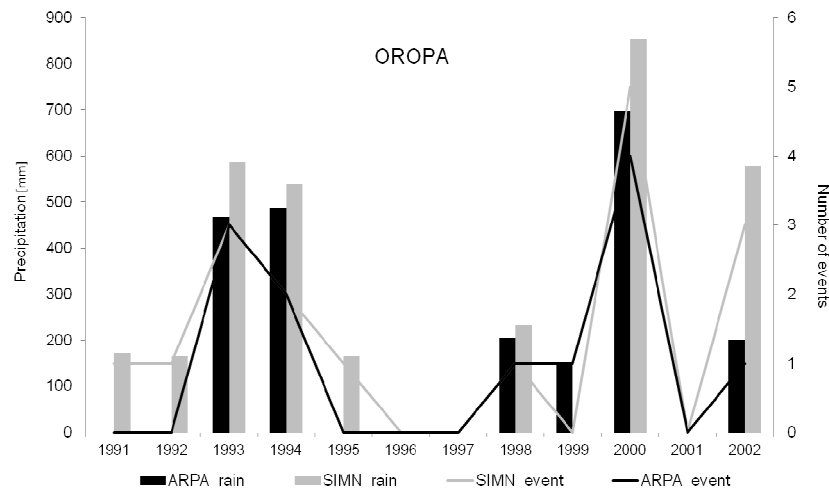


Fig. 3 Amount of extreme precipitation and number of extreme events recorded in the ARPA station, black, and in the SIMN station, grey, for Oropa.

#### 4 CONCLUSIONS

We have studied an important non-climatic change in the precipitation record of the Piedmont region. This region has many long daily precipitation series. The meteorological observations have been recorded continuously since 1913.

In 2002 the observational network was replaced by a new automatic network. In 20 locations the transition from the old to the new network has allowed for a period of overlapping measurements for up to 17 years. The overlapping period provides a unique dataset with independently measured parallel observations.

The two networks, SIMN and ARPA, have shown important differences in the measurements of the precipitation.

For the weak and mean precipitation the major difference is estimated in the number of events. The ARPA stations record a greater number of these rainy events and this divergence can alter the real behaviour of some climate indices for example the dry or wet periods.

For the heavy, very heavy and extreme precipitation we have identified great differences between the two series. The SIMN stations record a greater number of events and a consequently a greater amount of rain. These divergences can falsify the behavior of the variables.

The present study has clearly highlighted the importance of analyzing parallel measurements for the study of non climatic changes in the climate record to identify the real variation of the meteorological variable.

Finally, further analyses will be conducted on other manual and automatic stations, in order to quantify the inhomogeneities at regional scale. This is especially important in case of precipitation, where statistical relative homogenization is hampered by low cross-correlations between stations. The differences were found to vary highly from location to location, emphasizing the importance of studying ensembles of parallel measurements over studying single pairs of observations.

## 5. REFERENCES

1. Acquaotta F., Fratianni, S. (2013). *Analysis on Long Precipitation Series in Piedmont (North-West Italy)*. American Journal of Climate Change No. 2, pp. 14-24. doi: 10.4236/ajcc.2013.21002.
2. Acquaotta F., Fratianni, S., Cassardo, C., and Cremonini, R. (2009). *On the continuity and climatic variability of meteorological stations in Torino. Asti. Vercelli and Oropa*. Meteorology and Atmospheric Physics No. 103, pp. 279-287. doi: 10.1007/s00703-008-0333-4.
3. Acquaotta F., Fratianni S. and Garzena G. (2014). *Temperature changes in the North-Western Italian Alps from 1961 to 2010*. Theoretical and Applied Climatology in review.
4. Aguilar E., Auer I., Brunet M., Peterson T.C., and Wieringa J. (2003). *Guidelines on climate metadata and homogenization*. World Meteorological

*Organization*, WMO-TD No. 1186, WCDMP No. 53, Geneva, Switzerland, pp. 55.

5. Aguilar E., Peterson TC., Ramírez Obando P. et al. (2005). *Changes in precipitation and temperature extremes in Central America and Northern South America, 1961-2003*. Journal of Geophysical Research, 110 doi: 10.1029/2005JD006119.
6. Biancotti A., Destefanis E., Fratianni S. and Masciocco L. (2005). *On precipitation and hydrology of Susa Valley (Western Alps)*. Geogr. Fis. Dinam. Quat., suppl. VII, 51-58, IT ISSN 1724-4757.
7. Burauskaite-Harju A., Grimvail A. and von Bromssen C. (2012). *A test for network-wide trends in rainfall extremes*. Int. J. Climatol. 32: 86–94, doi: 10.1002/joc.2263.
8. Cagnazzi B., Cremonini R., De Luigi C., Loglisci N., Paesano G., Ronchi C., Pelosini R., Poncino S., Bari A. and Cesare M. R. (2007). *Piemonte Il Piemonte nel Cambiamento climatico osservazioni passate, impatti presenti e strategie future*. ARPA Piemonte, 155 p., ISBN 978-88-7479-066-1.
9. Isotta F., Frei C., Weilguni V., Perčec Tadić M., Lassègues P., Rudolf B., Pavan V., Cac-ciamani C., Antolini G., Ratto S.M., Munari M., Micheletti S., Bonati V., Lussana C., Ronchi C., Panettieri E., Marigo G., Vertačnik G. (2013). *The climate of daily precipitation in the Alps: development and analysis of a high-resolution grid dataset from pan-Alpine rain-gauge data*. Int. J. Climatol., DOI: 10.1002/joc.3794.
10. Lenderink G., Meijgaard E. and Selten F. (2009). *Intense coastal precipitation in the Netherlands in response to high sea surface temperature analysis of the event of August 2006 from the perspective of changing climate*. Climate Dynamics 32: 19-33, doi: 10.1175/s00382-008-0366-x.
11. Moberg A, Jones P., Lister D., Walther A., Brunet M., Jacobeit J., Alexander L., Della-Marta P., Luterbacher J., Yiou P., Chen D., Klein Tank A., Saladié O., Sigró J., Aguilar E., Alexandersson H., Almarza C., Auer I., Barriendos M., Begert M., Bergström H., Böhm R., Butler C., Caesar J., Drebs A., Founda D., Gerstengarbe F., Micela G., Maugeri M., Österle H., Pandzic K., Petrakis M., Srnec L., Tolasz R., Tuomenvirta H., Werner P., Linderholm H., Philipp A.,

- Wanner H., Xoplaki E. (2006). *Indices for daily temperature and precipitation extremes in Europe analyzed for the period 1901-2000*. Journal of Geophysical Research No.111: D22106. doi: 0.1029/2006JD007103.
12. Klein Tank A. and Konnen G. (2003). *Trends in indices of daily temperature and precipitation extreme in Europe, 1946-99*. Journal of Climate, No.16, pp. 3665-3680.
  13. Mekis E. and Vincent L. (2011). *An overview of the second generation adjusted daily precipitation dataset for trend analysis in Canada*. Atmosphere-Ocean.No. 2, pp. 163-177.
  14. Parker D.E. (1994). *Effects of changing exposure of thermometers at land stations*. Int. J. Climatol. 14: 1-31.
  15. Peterson, T. C., Easterling, D. R., Karl, T. R., Groisman, P., Nicholls, N., Plummer, N., Torok, S., Auer, I., Boehm, R., Gullett, D., Vincent, L., Heino, R., Tuomenvirta, H., Mestre, O., Szentimrey, T., Salingeri, J., Førland, E. J., Hanssen-Bauer, I., Alexandersson, H., Jones, P., and Parker, D. (1998). *Homogeneity adjustments of in situ atmospheric climate data: A review*. Int. J. Climatol. 18: 1493–1517.
  16. Peterson, T.C., (2005): *Climate Change Indices*. WMO Bulletin, 54 (2), 83-86.
  17. Sevruk B., Ondras M. and Chvila B. (2009). *The WMO precipitation measurement intercomparisons*. Atmospheric Research, No. 92, pp. 376-380.
  18. Venema V., Mestre O., Aguilar E., Auer I., Guijarro J.A., Domonkos P., Vertacnik G., Szentimrey T., Stepanek P., Zahradnicek P., Viarre J., Müller-Westermeier G., Lakatos. M., Williams C.N., Menne M.J., Lindau R., Rasol D., Rustemeier E., Kolokythas K., Marinova T., Andresen L., Acquavotta F., Fratianni S., Cheval S., Klancar M., Brunetti M., Gruber C., Prohom Duran M., Likso T., Esteban P., Brandsma T. (2012). *Benchmarking homogenization algorithms for monthly data*. Climate of the Past, No. 8, pp. 89-115, doi: 10.5194/cp-8-89-2012.
  19. Vincent L. and Mekis E. (2009). *Discontinuities due to joining precipitation station observations in Canada*. Journal of Applied Meteorology and Climatology **48**: 156-166, doi: 10.1175/2008JAMC2031.1.

## Clime: analysing climate data in GIS environment

Cattaneo L.<sup>1\*</sup>, Rillo V.<sup>1</sup> and Mercogliano P.<sup>1,2</sup>

<sup>1</sup>CMCC (Euro-Mediterranean Center on Climate Change), Italy,

<sup>2</sup>CIRA (Italian Aerospace Research Centre), Via Maiorise, 81043 Capua (CE), Italy

\*Corresponding Author: luigi.cattaneo@cmcc.it

### Abstract

*Clime software*, an ArcGIS Desktop 10.0 add-in, developed at CMCC, has been designed as an interactive platform allowing users to easily evaluate multiple climate features, analyze climate changes over specific geographical domains and also to support the study of the impacts related to climate change. Its main processes include the elaboration of different statistical functions percentiles, trends test and evaluation of extreme indices with a flexible system of temporal and spatial filtering. The results can be also displayed through spatially referenced maps, temporal and statistic plots (time series, seasonal cycles, PDFs, scatter plots, Taylor diagrams) or using Excel tables. Furthermore, it features bias correction techniques for climate model results. *Clime* has already been used for different national and international projects, for realization of maps and post processing analysis in international publications.

**Keywords:** software, GIS platform, extremes, climate change, post-processing, impacts

## 1. INTRODUCTION

ISC-Capua division had several collaboration experiences with impact communities, among these the European projects IS-ENES (VII FP –Infrastructure 2008) [4], SafeLand (VII FP –Environment 2008) [5] and ORIENTGATE (South East Europe Transnational Cooperation Programme 2012) [10] which led to develop different research activities about climate, climate changes and their potential impacts. In particular, the performed analysis are mainly based on the use of numerical simulations of the present and future climate, obtained using the regional climate model (RCM) COSMO-CLM [1] currently adopted at CMCC [2,6]. ISC-Capua also collaborates with different local national institutions interested in the evaluation of the effect of climate change on hydrological dynamics, such as river basin authorities in the Campania region, ARPA Emilia Romagna and ARPA Calabria. Hence *Clime*, a Geographic Information System (G.I.S.) developed add-in tool, is the result of such close partnerships: it features a graphical interface allowing users to easily manage climate data and evaluate their reliability over any geographical entity of interest, by accepting multiple sources of different formats, like observational datasets, gridded or point stations, and/or numerical model outputs, and using them as inputs for hydrologic and slope stability numerical models.

*Clime* has been implemented as an extension for *ESRI ArcGIS Desktop* and is launched from a plugin user interface (bar anchored to the main toolbar), allowing users to take full advantage of the ArcGIS functionalities (e.g. block functions for interpolation, algebra on raster, reference systems transformations): as a result, this combined array of processes is expected to cover all the steps concerning the phases of validation and post processing. Finally, analysis of results can be visualized in a variety of formats and standards with any assignment of classifications, histograms, and labels. One of the most innovative feature of *Clime* is related to managing the import of long time series of simulated high resolution climate data and to validate them through comparisons with time series collected from weather stations, radar and satellite data.

Requirements about comparison of large amounts of data, along with processes for data homogenization through automated and generalized procedures, equipped with interfaces to link them into the operating chain are addressed by the software.

## 2. SOFTWARE ARCHITECTURE

Clime is an ArcGIS Desktop 10.X plugin developed using ArcObjects (ArcGIS development environment) and written in C# language.

It presents a toolbar [Fig. 1] equipped with function buttons, each one related to a distinctive feature of the software (spatial interpolation, bias correction, data import and export and elaboration and visualization tools) allowing users to easily select the desired functionality. The system is interfaced to a geodatabase containing all the regional climate data and observational dataset available at CMCC ISC Capua division, reported in a format suitable by a GIS platform. Currently, there are more than 40 observed and simulated dataset, for a total of 5 TeraBytes managed by *CLIME*. These data are collected, preprocessed and stored in the geodatabase and, then, available for further elaborations without any other pre-processing activity.

Moreover, it can access to all the ArcGIS features and store climate and observed data in a set of layers. Moreover, the usage of C# language allows executing computations in a faster way. The execution speed is a key requirement of this product so that it can handle and elaborate large amounts of data for validation procedures.

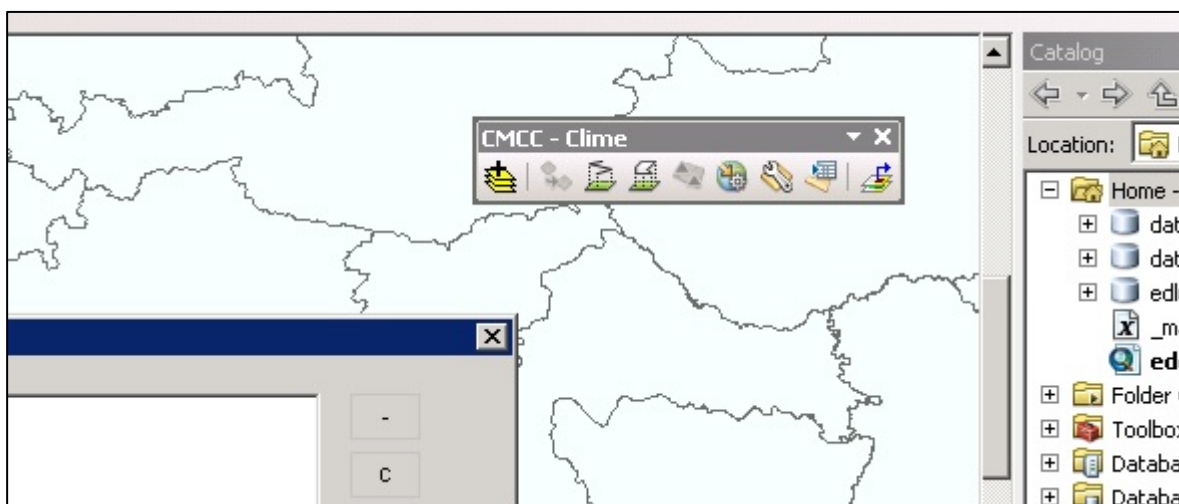


Fig. 1 *Clime* Toolbar in *ArcMap* environment

### 3. GENERAL STRUCTURE AND PROCESSING CYCLE

*Clime* can operate on several kinds of climate datasets available under different formats recognizing the original format and properly converting them for the import in the database. This step, introduces a process for the proper processing of spurious and null data. The most commonly managed files are in NetCDF (Network Common Data Form), XLS, ASCII-R and CSV formats, containing values distributed on a regular and time-invariant grid for model data or spread on an erratic cluster of points (for station data). After the conversion, such files are imported in a selected database, which could also be located in a remote unit [Fig. 2].

Such pre-processing phase is carried out by *Clime Data Manager*, a database interface which allows importing new data and editing existing ones. After that, the requested process is handled by the main software.

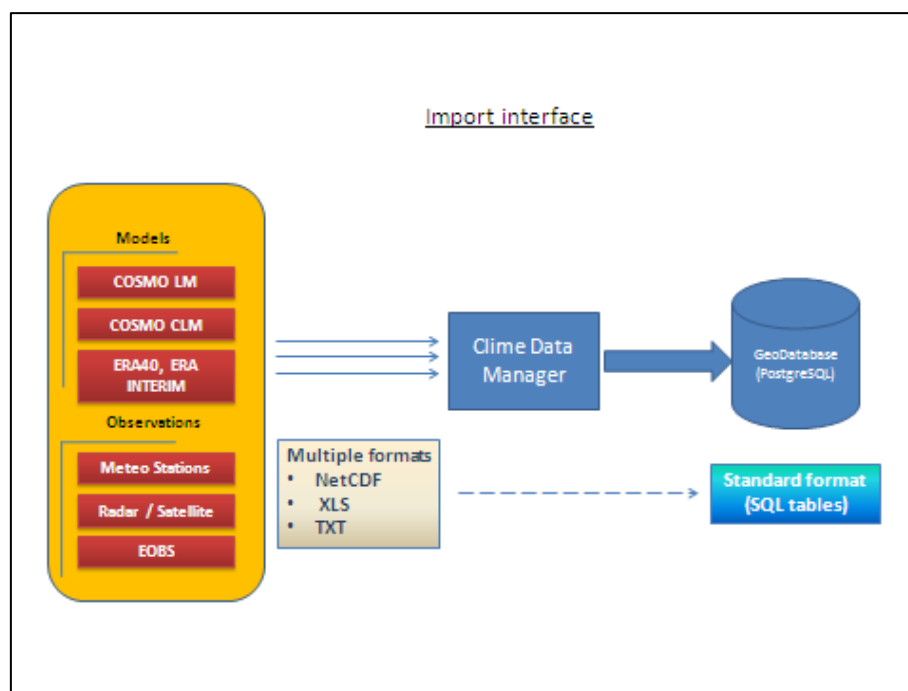


Fig. 2 *Clime* data import flow chart

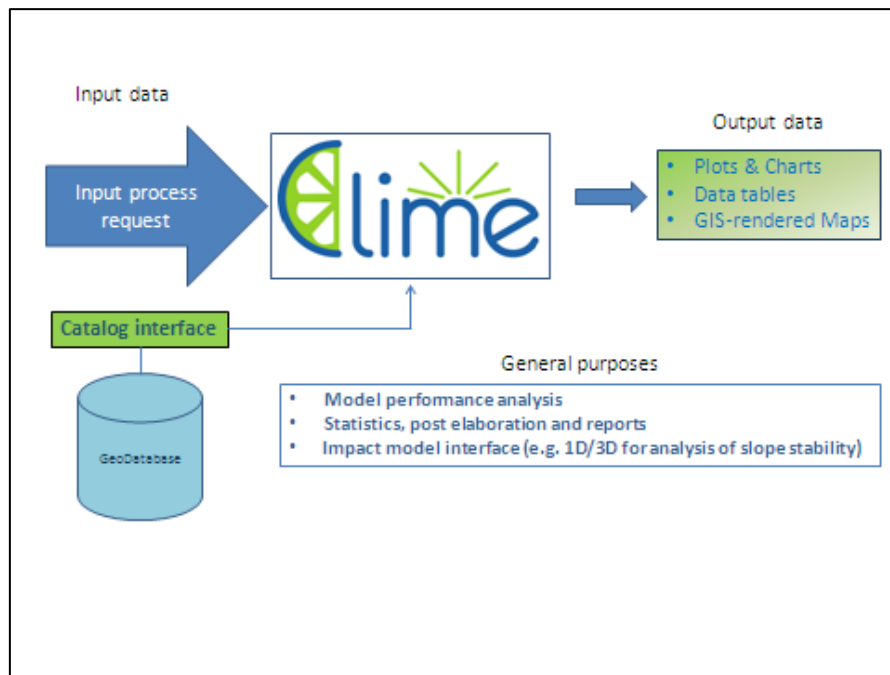


Fig. 3 *Clime* Data process

Once that all atmospheric variables of interest are stored (e.g. 2-meter temperature, precipitation) into *Clime* databases, they are selectable through a catalog interface and ready to be processed [Fig. 3] according to user needs. In fact, such catalog interface reports all the data available, allowing the user to visualize and easily select the information of interest. In this way, data stored in the database and reported as layers, are visualized in a list showing the different features (e.g. name, category, grid resolution, and time aggregation). There is no restriction on the number of layers, but it is worth noting that selection is limited to data sharing a common period and the same time aggregation (day, month, etc.). One object is always labeled as *Reference Layer*: in case of processes requiring two operators (mostly for comparing purposes), it is constantly assumed as one of the inputs, while the other always changes. Otherwise, algorithms are repeated for each selected single layer.

After selection of layer, the user can choose the space domain from a list of reference areas (provinces, regions and other sub areas of Italy, foreign countries and continents) and a time period (with season filter, if desired) [Fig. 4]. Then, a tab-arranged menu explains which operations could be run (*plots* or *elaborations*). Outputs vary according user's selections: if *plots* is selected, a plot chart is reported;

on the other hand if *elaboration* is selected, it is possible to visualize a map represented as a layer/raster object in the GIS environment. In the following, a more detailed description of *Clime* outputs is reported.

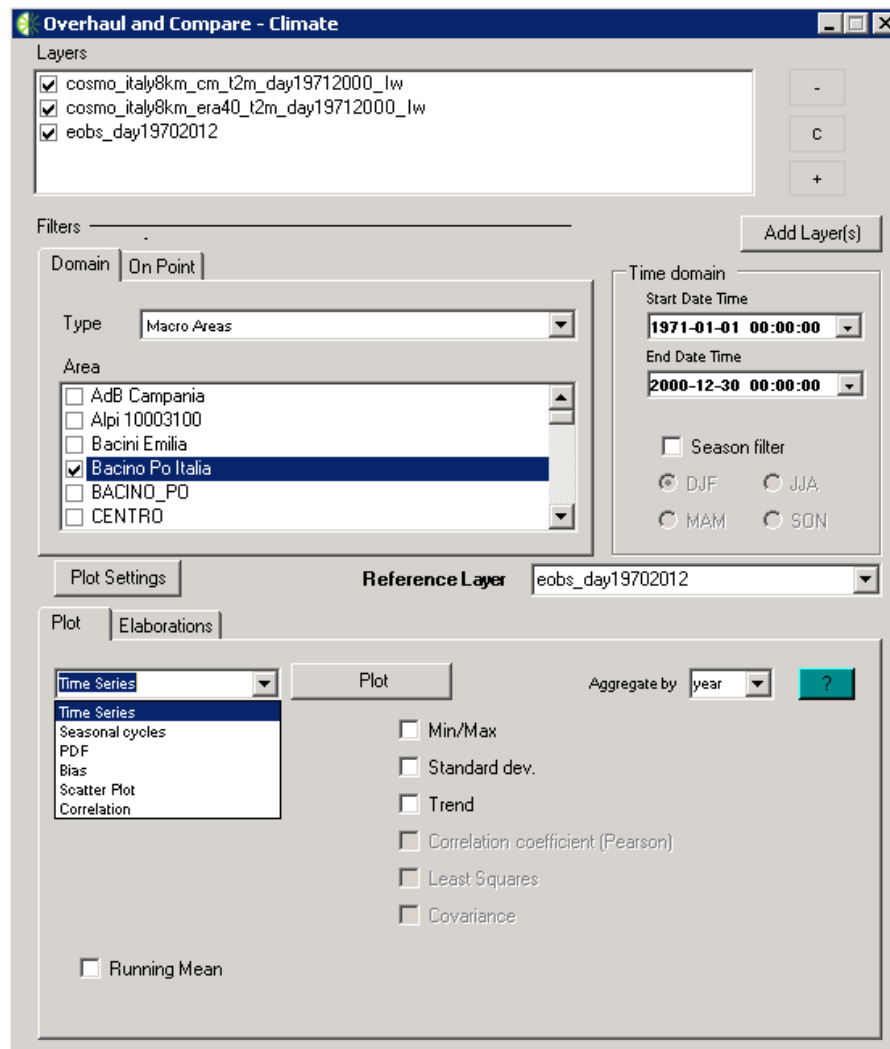


Fig. 4 the window called “Overhaul & compare” permits, in the upper part, to select the layers and variables that have to be processed. In the central part the geographical domains from a list of references areas (mostly countries and continents and cities), the time domain while at the bottom the other features of the analysis can be selected

Selecting tab *Plot*, it is possible to run different data analysis of every input layer, averaged over the selected domain [Fig.5]. *Clime* reports charts displaying the temporal evolution of a variable (time series, seasonal cycles) and, optionally, the extreme values (max/min), standard deviations and trends (obtained with *least square* method), providing the overall behaviour about data considered. Moreover, it allows to estimate the correlation among datasets of different nature and the bias among datasets related to the same variable

Otherwise, PDF (Probability Distribution Function) function can be derived counting the occurrences within every bin interval, and then normalizing on the total number of values (discrete approach). Bin resolution is selectable, as well as total range of values, but the latter could also be automatically detected.

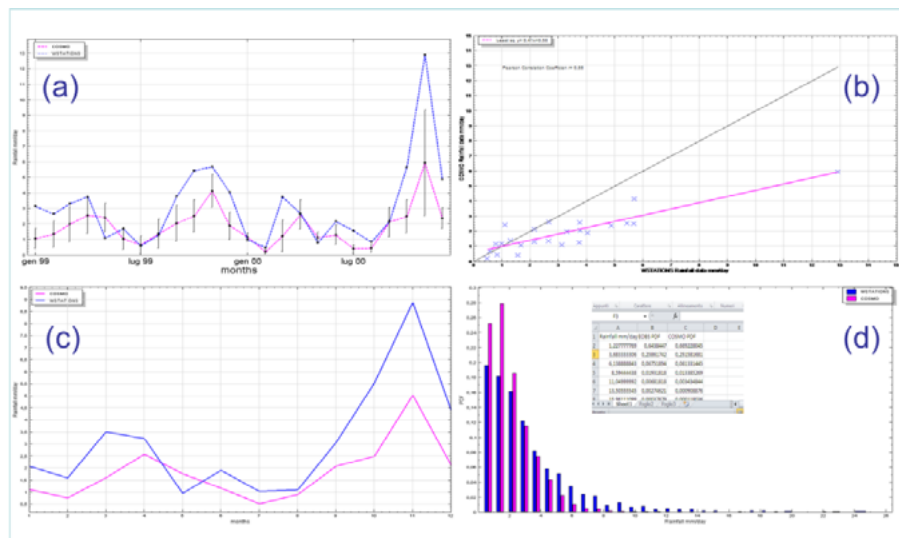


Fig. 5 Examples of plots generated through *Clime* software : (a) time series, (b) scatter plot, (c) seasonal cycle, (d) PDF.

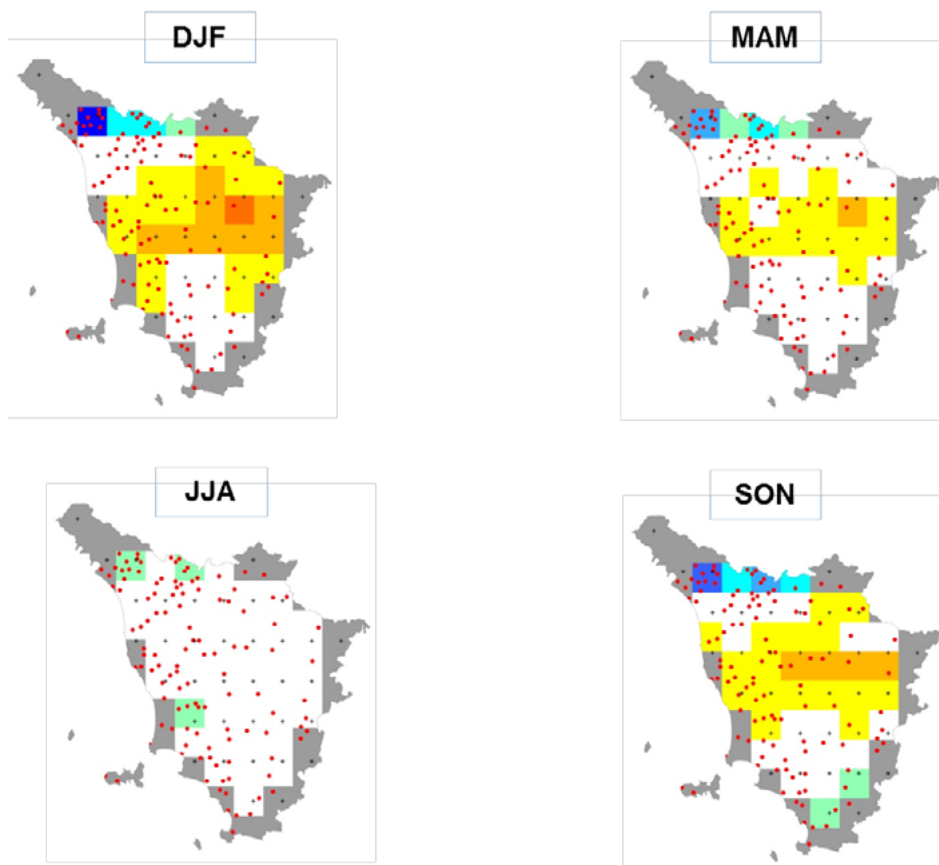


Fig.6: An example of maps generated through *Clime* software: Precipitation seasonal differences (E-OBS gridded station vs A.R.P.A. Toscana *in situ* stations) over the time period 1972-2000

A different set of operation is available when the analysis concerns data comparing and validation processes. *Scatter Plot* is implemented in order to compare two layers (for instance, a modeled series and an observational dataset). The feature *Verification Measures*, available for rainfall data, is conceived to compare observations with the corresponding forecasted values: going ahead with a dichotomous (yes–no) prediction, each value is compared in order to verify if it is equal or greater than a determined threshold (respectively 1,2,5,10 mm/day)-. Final results are represented through statistical indices (PC, BIAS, POD, FAR, PSI) [12]. The *Errors* functionality traces a synthetic behavior after comparing test layers with a reference one. A way of displaying results is a table showing bias, average errors and correlation factors over the selected time scale. In Fig. 5 and in Fig. 6 some outputs of *Clime* functionality are reported.

Moreover, in order to resume differences and/or bias between two or more datasets, the Taylor Diagrams can be produced [Fig. 7], reporting and summarizing multiple factors in a single plot, showing variances, root mean errors and correlations in a single plot [7].

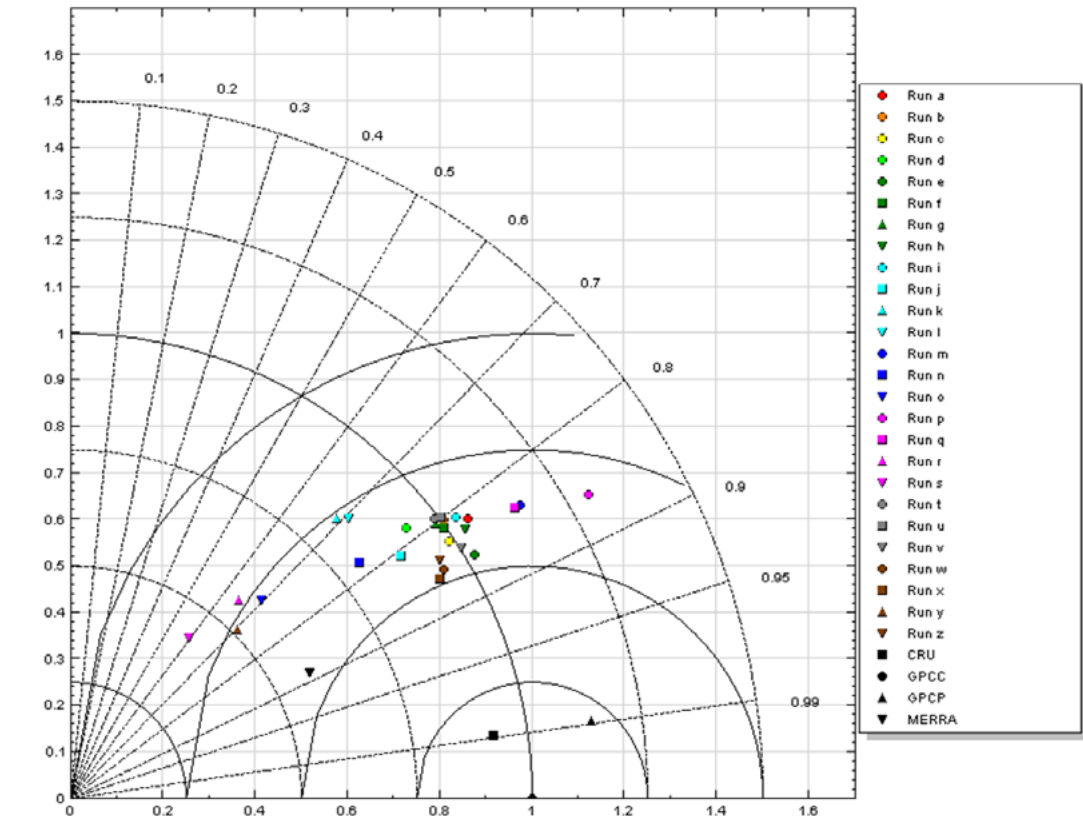


Fig. 7  $\sigma$ -normalised Taylor Diagram evaluated from different temperature datasets.

Selecting *Elaborations* tab, the visualization of maps in a GIS environment is enabled, reporting the model and observational datasets. In fact, the presence of geographic references allows *Clime* to evaluate features and statistics, such as space varying functions, and to represent them through maps placed inside a specified area. The base output is a grid point of the model or station data (the position of points is given by their geographic reference), which can be turned into raster after an interpolation process: in this way, the original object is approximated to an homogenous layer composed by square cells of the same size, each one characterized by a single value. The default interpolation algorithm is Natural Neighbour, anyway, other algorithms are available (e.g. IDW, Spline). The analysis of the occurrence of extreme events is carried out by evaluating percentiles related to a selected period: for this purpose, a basic set of ETCCDI extreme indices for temperature and rainfall is included; some examples are reported in the Fig.8 [11]. A dedicated section provides a large choice of operators and conditions, making it a valuable tool to define custom indices, which may possibly fit any request from the

user and produce an all-round complete documentation about selected dataset. For validation processes, it is possible to directly display “difference maps” – either expressed with simple or percentage values – obtained by comparing test datasets with any desired reference: typical examples are the bias between modeled and observed data, or anomalies obtained by comparing future with past periods. Examples of bias maps taken from literature [8] [9], are shown in Fig. 6-9-10. Seasonal analyses (DJF, MAM, JJA, and SON) are also possible.

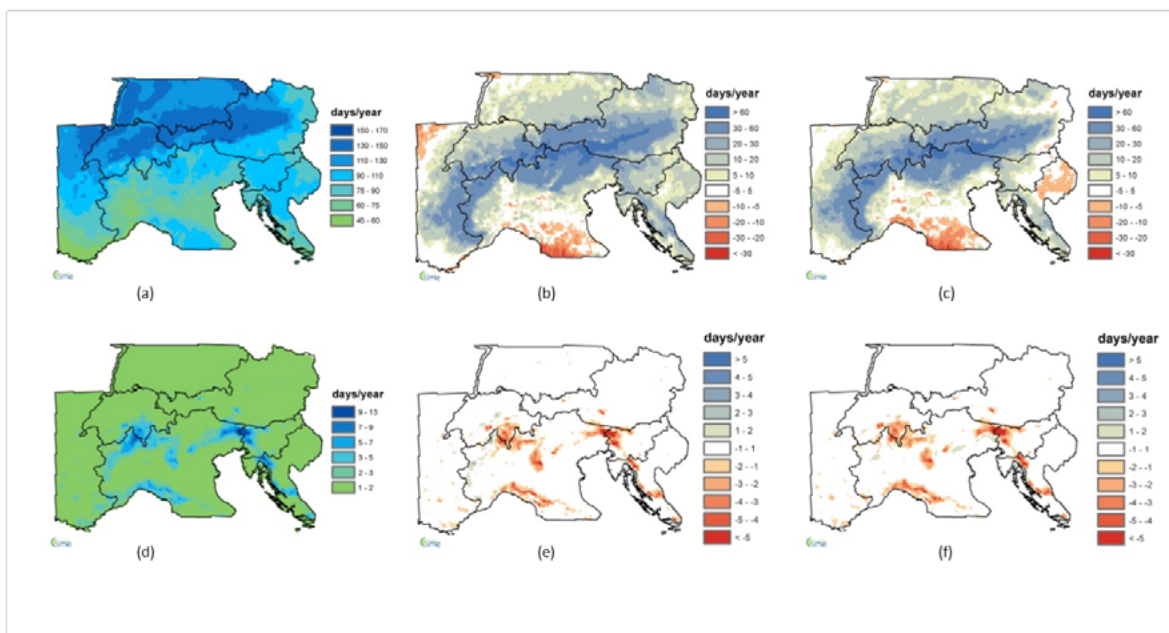


Fig 8. Example of indices: (a) number of weak precipitation days (d/yr) provided by EURO4M-APGD data, bias of weak precipitation days of (b) COSMO-CLM0.0715° and (c) COSMO-CLM 0.125° versus EURO4M-APGD data. (d) number of intense precipitation days (d/yr) provided by EURO4M-APGD data, bias of intense precipitation days of (e) COSMO-CLM 0.0715° and (f) COSMO-CLM 0.125° versus EURO4M-APGD data.

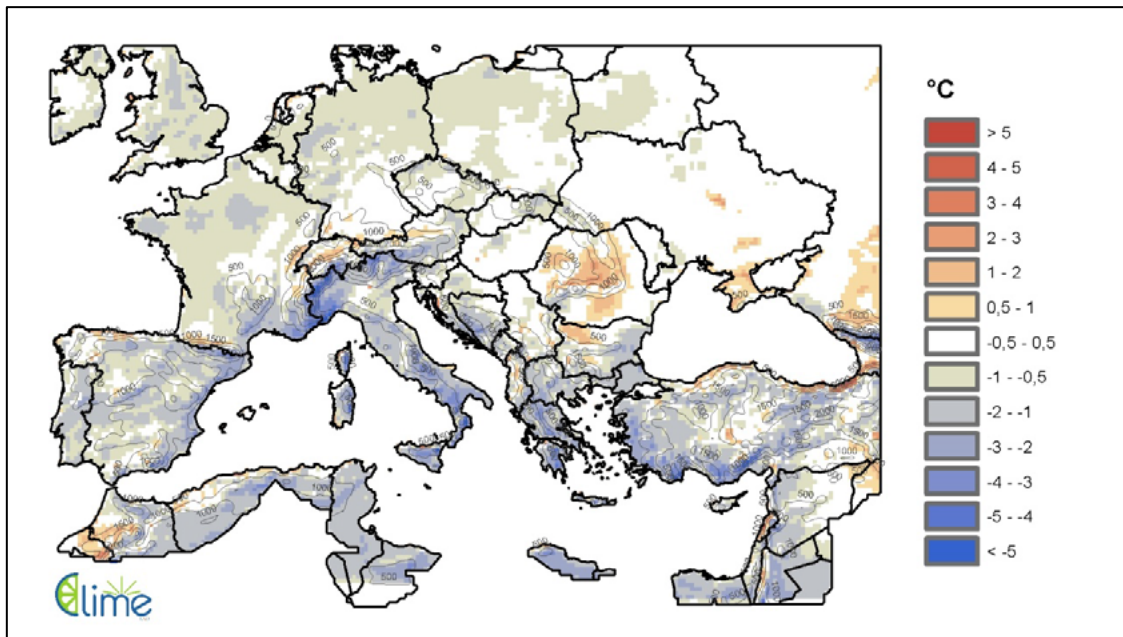


Fig. 9 Alpine area. An example of map: bias of Cosmo CLM output against E-OBS dataset over the European domain.

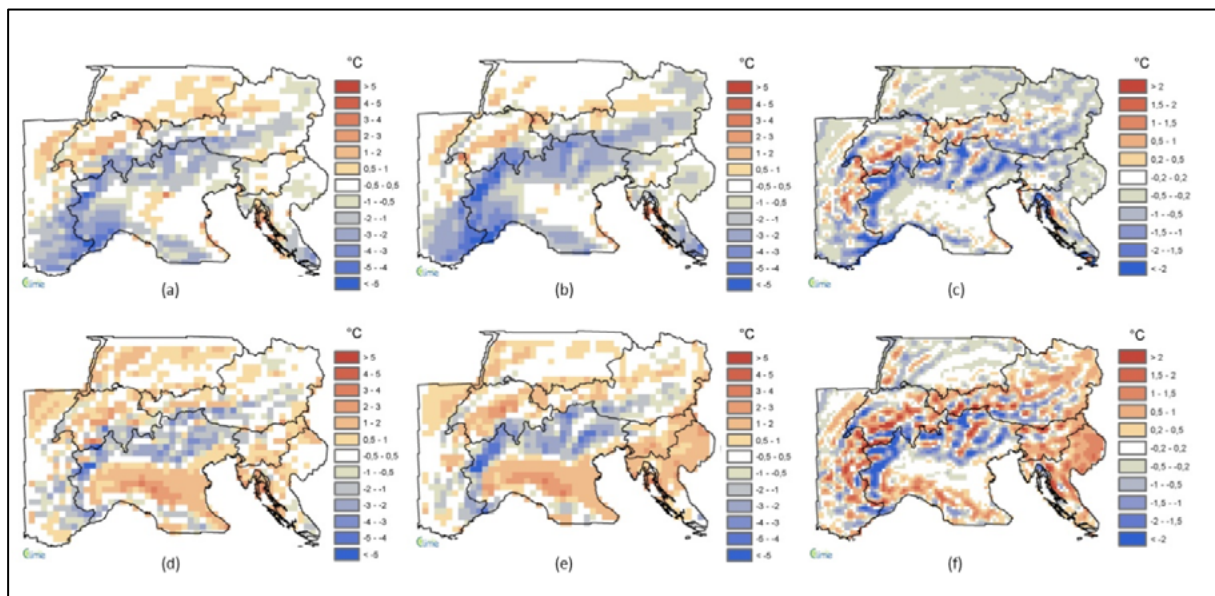


Fig. 10 Alpine area. Two-meter mean temperature bias distribution of COSMO-CLM 0.0715° versus E-OBS ((a): DJF and (d): JJA), COSMO-CLM 0.125° versus E-OBS ((b): DJF and (e): JJA), and COSMO-CLM 0.125° versus COSMO-CLM 0.0715° ((c): DJF and (f): JJA).

## 4. DATA EDITING: BIAS CORRECTION

*Clime* allows creating to provide a climate data bias corrected. Currently, it only supports *linear scaling* [7] approach, using observed data gridded or point stations. An example of application is reported in the figure 11.

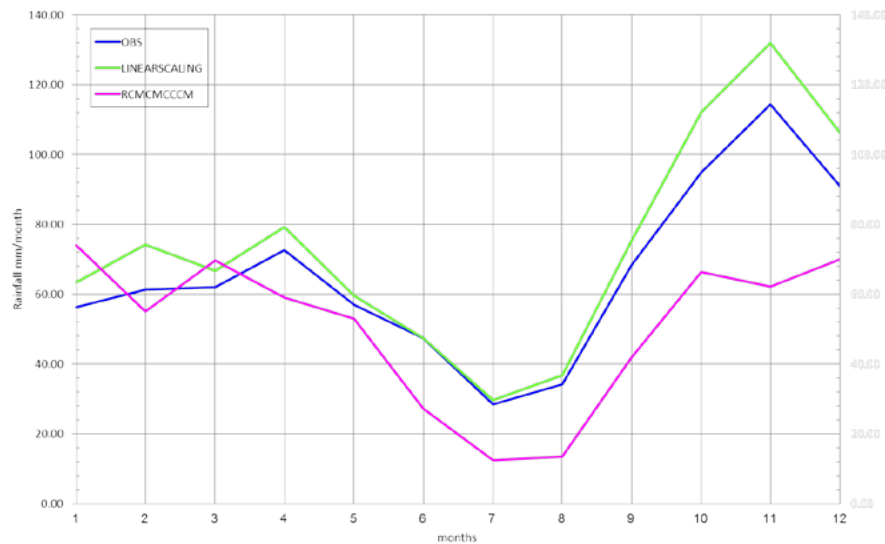


Fig 11. An example of application of bias correction technique (BCT) on Orvieto case-history comparing mean monthly cumulative precipitation values observed (blue), estimated by RCM analysis (pink) and adopting for such analysis a linear scaling BCT (green).

In order to perform such processes, *Clime* uses *R* libraries and functions [13], able to quickly perform many computations in an easy way; this configuration also allows to rapidly obtaining new tools and features by linking pre-generated *R* scripts to the default environment. It is also scheduled the implementation of “quantile mapping” [14] algorithms by the same interface.

## 5. CONCLUSIONS

The main purpose of *Clime* software is to serve impact communities and climate researchers and act as an easy and comfortable interface in order to perform a wide range of processes and operations with any kind of data gathered through outputs of numerical models and observations, thus providing a substantial contribution during post-processing and validation phases. In fact it provides a wide range of outputs (maps, graphs, diagrams, tables) reporting statistical analysis and comparisons

carried out on modeled and observational datasets. Such functionalities are accessible through an user-friendly interface allowing users to easily select, analyze and visualize the wide range of available datasets on area of interest (provinces, regions, countries, etc.) and for a selected period. Future developments may include the definition and implementation of additional tools, and multiple versions of the software, unlocking it from a single defined graphical environment and eventually bringing to the creation of portings on UNIX-like platforms, properly integrated with Open Source GIS software.

## 6. ACKNOWLEDGEMENTS

*Clime* has been developed in the frame of projects NEXTData (WP 2.5), GEMINA (WP A.2.2-A.2.17) and ORIENTGATE (WP 3-5) at CMCC-ISC Capua, with every single division member having an active role in software developing and/or testing phase. A special thanks also to A.R.P.A Emilia Romagna, A.R.P.A Toscana, A.R.P.A Campania, A.R.P.A Piemonte, A.R.P.A Veneto, A.R.P.A Calabria and Provincia di Bolzano e Trento for providing their data for the present research activity.

## 7. REFERENCES

1. Montesarchio M., Zollo A., Bucchignani E., Mercogliano P. & Castellari S. (2014) Performance evaluation of high-resolution regional climate simulations in the Alpine space and analysis of extreme events, *Journal of Geophysical Research*, No. 119, pp. 3222–3237. DOI: 10.1002/2013JD021105
2. Rockel B., Will A. & Hense A. (2008) The Regional Climate Model COSMO-CLM (CCLM). *Meteorologische Zeitschrift*. No. 17, pp. 347-348. DOI 10.1127/0941-2948/2008/0309
3. Michalakes, J., Dudhia J., Gill D., Henderson T., Klemp, Skamarock W. and Wang W. (2004) The Weather Research and Forecast Model: Software Architecture and Performance, in proceedings of the 11th ECMWF Workshop on the Use of High Performance Computing In Meteorology, pp. 25-29, October 2004, Reading U.K. Ed. George Mozdzynski.

4. Déandreis C, Braconnot P., Pagé C, Bärring L, Bucchignani E, Som de Cerff W, Hutjes R, Joussaume S, Mares C, Planton S, Plieger M. (2014) Towards a dedicated impact portal to bridge the gap between the impact and climate communities : lessons from use cases, Climatic Change (in press).
5. <http://www.safeland-fp7.eu/Pages/SafeLand.aspx>
6. L. Comegna, L. Picarelli, E. Bucchignani, P. Mercogliano (2013) Potential effects of incoming climate changes on the behaviour of slow active landslides in clay, Landslides, No. 10, pp. 373-391, DOI: 10.1007/s10346-012-0339-3
7. M. Turco, A. Zollo, G. Rianna, L. Cattaneo, R. Vezzoli, P. Mercogliano (2013) Post-processing methods for COSMO-CLM precipitation over Italy, CMCC RP0171,
8. Montesarchio, M., Mercogliano, P. (2013) A simulation over the Mediterranean area with COSMO-CLM: assessment of the performances, Tech.rep.RP0184, CMCC, 2013
9. M. Montesarchio, A. L. Zollo, E. Bucchignani, P. Mercogliano, S. Castellari (2014) - Performance evaluation of high-resolution regional climate simulations in the Alpine space and analysis of extreme events J. Geophys. Res. Atmos., 119, 3222–3237, doi:10.1002/2013JD021105
10. <http://www.orientgateproject.org>
11. [http://etccdi.pacificclimate.org/list\\_27\\_indices.shtml](http://etccdi.pacificclimate.org/list_27_indices.shtml)
12. S. Moszkowicz, K. Osrodka, V. Poli, P.P. Alberoni, D. B. Giaiotti, A. Gimona, F. Stel RISK-Advanced Weather forecast system to Advise on Risk Events and management, Report for WP-Action 1.10
13. <http://www.r-project.org/>
14. Gudmundsson, L.; Bremnes, J. B.; Haugen, J. E. & Engen Skaugen, T. (2012) Technical Note: Downscaling RCM precipitation to the station scale using statistical transformations - a comparison of methods. Hydrology and Earth System Sciences, 2012, 9, 6185-6201, doi: 10.5194/hessd-9-6185-2012

# The Ophidia framework: toward big data analytics for climate change

Fiore S.<sup>1\*</sup>, D'Anca A.<sup>1</sup>, Elia D.<sup>1</sup>, Palazzo C.<sup>1</sup>, Mariello A.<sup>1</sup>,  
Nassisi P.<sup>1</sup>, and Aloisio G.<sup>1,2</sup>

<sup>1</sup> Centro Euro-Mediterraneo sui Cambiamenti Climatici, Italy

<sup>2</sup> University of Salento, Italy

\*Corresponding Author: [sandro.fiore@cmcc.it](mailto:sandro.fiore@cmcc.it)

## Abstract

The large volume, velocity, and variety of data are key challenges in the climate change domain to enable scientific discovery. Novel approaches in the *big data and extreme computing* landscape are strongly needed to address data analytics at peta-exascale. This paper introduces Ophidia, a big data analytics research effort aiming at supporting the access, analysis, and mining of scientific ( $n$ -dimensional array based) data at large scale. This framework provides a common way to run analytics tasks applied to big datasets on large clusters.

**Keywords:** multidimensional data, big data, data analytics, scientific workflow

## 1. INTRODUCTION

Data-intensive computing plays a major role in the climate change scientific discovery path toward exascale [1-5]. The n-dimensionality of scientific datasets requires tools that support specific data types (e.g. arrays) and primitives (e.g. slicing, dicing, pivoting, drill-down, roll-up) to properly enable data access, analysis, and visualization [6]. With regard to general-purpose analytics (OLAP) systems [7], climate change data has a higher computing demand, which definitely leads to the need of having efficient parallel/distributed solutions to meet the (near) real-time analytics requirements. Conversely, domain-specific software and libraries in this domain (e.g. NCO, CDO) strongly meet scientific user requirements, by providing comprehensive and specific sets of operators. However, most of them fail to address data analytics needs at large scale since they (i) exploit a client-side approach, (ii) are mainly sequential, (iii) are strongly tied to the NetCDF data format, and (iv) rely on disk-based workflows. Solutions like ParCAT [8] are mainly a toolkit, whereas Ophidia is rather a framework with multiple server-interfaces interoperable with grid/cloud and WS-based services and environments. Finally, with regard to well-known big data frameworks like Hadoop [9], Ophidia is designed to provide a native support for scientific data management in terms of array data types and primitives, scientific data formats and numerical libraries, in-memory workflow support, metadata and provenance management.

## 2. THE CURRENT WORKFLOW FOR SCIENTIFIC DISCOVERY

The current workflow exploited by climate scientists in the context of the CMIP5 experiment [10] is based on the sequence of steps “*search, locate, download, and analyze*”. This workflow will not be feasible at peta-exascale and will fail for several reasons like: (i) ever-larger scientific datasets, (ii) time- and resource- consuming data downloads, and (iii) increased problem size and complexity requiring bigger computing facilities. At large scale, scientific discovery will strongly need to rely on data-intensive facilities (not available today) close to data storage, parallel I/O systems and server-side analysis capabilities. Such an approach will move the analysis (and complexity) from the user’s desktop to the data centers and accordingly will change the infrastructure focus from data sharing to data analysis.

### 3. THE OPHIDIA PROJECT

A recent effort in the big data area is Ophidia [11-13], a research project focusing on scientific data analysis challenges in the climate change domain. It provides a framework for parallel (server-side) I/O and data analysis, a dimension-independent storage model and a hierarchical storage organization to partition and distribute multidimensional scientific datasets. The Ophidia storage model does not rely on the NetCDF file format. More specifically, it exploits a cross-domain *key-value* approach able to manage  $n$ -dimensional data cubes. To address scalability and enable parallelism, from a physical point of view, a data cube in Ophidia is horizontally split into several chunks (called *fragments*) that are distributed across multiple I/O nodes. Each I/O node hosts a set of I/O servers optimized to manage  $n$ -dimensional arrays. Each I/O server, in turn, manages a set of databases consisting of one or more fragments. As it can be easily argued, tuning the levels in this hierarchy can also affect performance. For a specific data cube, the higher the product of the four levels is, the smaller the size of each fragment will be.

#### 3.1 ARRAY BASED PRIMITIVES

As mentioned before, the Ophidia framework addresses the analysis of  $n$ -dimensional arrays. This is achieved through a set of primitives included into the system as plugins (dynamic libraries). So far, about 100 primitives have been implemented. Multiple core functions of well-known numerical libraries (e.g. GSL, PETSc) and tools (e.g. CDO) have been included into new Ophidia primitives. Among others, the available array-based functions allow to perform data sub-setting, data aggregation (i.e. max, min, avg), array concatenation, algebraic expressions, and predicate evaluation. It is important to note that multiple plugins can be nested to implement a single more complex array-based task.

Bit-oriented plugins have also been implemented to manage binary data cubes. Compression routines, based on zlib, xz, lzo libraries, are also available as array-based primitives.

### 3.2 DATA AND METADATA OPERATORS

The Ophidia analytics platform provides several MPI-based parallel operators to manipulate (as a whole) the entire set of fragments associated to a data cube. Some relevant examples include: datacube sub-setting (slicing and dicing), datacube aggregation, array-based primitives at the datacube level, datacube duplication, datacube pivoting, and NetCDF file import and export.

Along with *data* operators, the framework provides a comprehensive set of *metadata* operators. Metadata represents a valuable source of information for data discovery and data description. From this point of view, in a data-intensive context, it will be important to: (i) provide server-side metadata management capabilities, (ii) describe a dataset with provenance metadata information in terms of applied data analytics primitives (to help reproduce analyses and products), (iii) enrich this information with descriptive metadata and links to cross-related digital objects, that could be indexed as well, to improve the data search and discovery process, (iv) build new community-oriented tools to enrich metadata and provide, at the same time, a way to move this process towards much more open, multi-level and collaborative forms.

### 3.3 FRAMEWORK EXPLOITATION

The entire Ophidia software stack has been deployed at CMCC on 24-nodes (16-cores/node) of the Athena HPC cluster. Preliminary experimental results have been published in [13]. A comprehensive benchmark and test cases are being defined with climate scientists to extensively test all of the features provided by the system.

The most relevant data analytics use cases implemented in national and international projects target fire danger prevention (OFIDIA), sea situational awareness (TESSA), interactions between climate change and biodiversity (EUBrazilCC), climate indicators and remote data analysis (CLIP-C), large scale data analytics on CMIP5 data in NetCDF format, Climate and Forecast (CF) convention compliant (ExArch).

## 4. CONCLUSIONS

Data-intensive computing plays a major role in the climate change scientific discovery path toward exascale. In the 2020 timeframe the scientific community should take the

chance to exploit revolutionary strategies for large-scale scientific data analytics. There are strong scientific and real-time big data analysis requirements to be addressed, and big datasets to be managed, compared and visualized. *Evolutionary* approaches may require less short-term effort but are unlikely to succeed in all cases and at large scales. On the contrary, *revolutionary* approaches would require a from-scratch design and long-term implementation strategy that could definitely target and address large-scale data-intensive issues and requirements. In such a landscape, Ophidia is a novel (“revolutionary”) research effort at CMCC tackling big data challenges for eScience. It provides a parallel I/O & analytics framework, in-memory workflow support, and a large set of operators and primitives to address large scale scientific discovery in the climate change domain.

## 5. REFERENCES

1. Dongarra J., Beckman P., et al. (2011), *The International Exascale Software Project roadmap*, International J. High Performance Computing Apps. 25, no. 1, 3-60, ISSN 1094-3420 doi: 10.1177/1094342010391989.
2. Aloisio G., Fiore S. (2009), *Towards exascale distributed data management*, International J. of High Performance Computing Apps. 23, no. 4, 398-400, doi: 10.1177/1094342009347702.
3. Fiore S., Aloisio G. (2011), *Special section: Data management for eScience*, Future Generation Computer System 27(3): 290-291.
4. Chen J., Choudhary A., Feldman S., Hendrickson B., Johnson C.R., Mount R., Sarkar V., White V., Williams D. (2013), *Synergistic Challenges in Data-Intensive Science and Exascale Computing*, DOE ASCAC Data Subcommittee Report, Department of Energy Office of Science.
5. Gray J., Liu D. T., Nieto-Santisteban M., Szalay A., DeWitt D. J., Heber G. (2005), *Scientific data management in the coming decade*, SIGMOD Rec. 34, 4, pp. 34-41. <http://doi.acm.org/10.1145/1107499.1107503>.
6. Williams D., Doutriaux C., Patchett J., Williams S., Shipman G., Miller R., Steed C., Krishnan H., Silva C., Chaudhary A., Bremer P., Pugmire D., Bethel W., Childs H., Prabhat M., Geveci B., Bauer A., Pletzer A., Poco J., Ellqvist T., Santos E., Potter G., Smith B., Maxwell T., Kindig D., Koop D. (2013), *The Ultra-scale Visualization Climate Data Analysis Tools (UV-CDAT): Data*

- Analysis and Visualization for Geoscience Data*, Computer , vol.PP, no.99, pp.1,1, 0. doi: 10.1109/MC.2013.119.
7. Han J., Kamber M. (2005), *Data mining: Concepts and Techniques*, Morgan Kaufmann Publishers.
  8. B. Smith, D. M. Ricciuto, P. E. Thornton, G. M. Shipman, C. A. Steed, D. N. Williams, M. Wehner, "ParCAT: Parallel Climate Analysis Toolkit", ICCS2013, pp. 2367-2375.
  9. Hadoop - <http://hadoop.apache.org/>
  10. Taylor K.E., Stouffer R. J., Meehl G. A. (2012), *An overview of CMIP5 and the experiment design*, Bulletin of the American Meteorological Society 93, no. 4, 485-498 (2012), doi:10.1175/BAMS-D-11-00094.1  
<http://journals.ametsoc.org/doi/abs/10.1175/BAMS-D-11-00094.1>.
  11. Fiore S., D'Anca A., Palazzo C., Foster I., Williams D. N., Aloisio G. (2013), *Ophidia: toward big data analytics for eScience*, Proceedings of the International Conference on Computational Science 2013, Procedia Elsevier, Barcelona, June 5-7, 2013, pp. 567-576.
  12. Aloisio G., Fiore S., Foster I., Williams D. (2013), *Scientific big data analytics challenges at large scale*, Big Data and Extreme-scale Computing (BDEC), April 30 to May 01, Charleston, South Carolina, USA.
  13. Fiore S., Palazzo C., D'Anca A., Foster I., Williams D. N., Aloisio G. (2013), *A big data analytics framework for scientific data management*, Workshop on Big Data and Science: Infrastructure and Services, IEEE International Conference on BigData 2013, October 6-9, 2013, Santa Clara, USA, pp.1-8.

# Levels and particle size distribution of water-soluble organic compounds in the Antarctic particulate matter

Zangrando R.<sup>1\*</sup>, Barbaro E.<sup>1</sup>, Vecchiato M.<sup>3,1</sup>, Kehrwald N.<sup>2</sup>,  
Gambaro A.<sup>1,2</sup>, Barbante C.<sup>1</sup>

<sup>1</sup>Istituto per la Dinamica dei Processi Ambientali-CNR - Italy, <sup>2</sup>Università Cà Foscari di Venezia, Dipartimento di Scienze Ambientali Informatica e Statistica - Italy,

<sup>3</sup>Università degli studi di Siena, Dipartimento Scienze fisiche, della Terra e dell'ambiente - Italy

\*Corresponding Author: roberta.zangrando@idpa.cnr.it

## Abstract

The organic fraction is an important part of particulate matter in the atmosphere, and Water Soluble Organic Compounds (WSOC) constitute between 40 and 60% of organic carbon. WSOC have great environmental importance, as they can reduce the surface tension of aqueous solutions by influencing the hygroscopicity of the aerosol and consequently the particles' ability to act as cloud condensation nuclei (CCN), with consequences on the optical properties of the aerosol, the air quality, and climate.

In the aerosol samples, we determined the levels and particle size distribution of the following compounds: levoglucosan and methoxyphenols (vanillic acid, isovanillic acid, homovanillic acid, syringic acid, coniferil aldehyde, ferulic acid, syringaldehyde, p-coumaric acid, vanillin), as biomass burning markers and 36 amino acids as indicators of primary production.

**Keywords:** biomass burning, amino acids, Antarctica

## 1. TEXT

Antarctica represents a perfect laboratory to study the environmental processes such as those regarding atmospheric aerosols. Our scientific activity had the purpose of obtaining further information about the formation, chemical composition and transport processes of aerosols. The study was conducted over 5 campaigns, two of which at the Mario Zucchelli Station (MZS) (29 November 2010-18 January 2011 and 3 November 2004-10 January 2005), two at Concordia Station (Dome C) (19 December 2012- 28 January 2012 and 7 December 2012-26 January 2013), and one during an oceanographic cruise on the Ross Sea (13 January -19 February 2012).

The Arctic aerosol samples were collected using a high volume sampler PM10 TE-6070, equipped with a 5-stage cascade impactor Model TE-235. The 6 aerosol fractions collected ranged between  $10.0 \mu\text{m}$  and  $< 0.49 \mu\text{m}$  at the Antarctic bases of MZS and Dome C. During the oceanographic cruise, atmospheric particulate matter (Total Suspended Particles, TSP) was collected using a TE5000 High Volume Air sampler (both samplers are produced by Tisch Environmental Inc., Cleves, OH).

The mean amino acids concentration detected at the Italian coastal base was  $11 \text{ pmol m}^{-3}$ . The main components were fine fractions, establishing a local marine source. Once produced on the sea surface, marine aerosols undergo an ageing process, due to various phenomena such as coagulation/condensation, or photochemical transformations. This was demonstrated by using the samples collected on the Antarctic plateau, where the background values of amino acids ( $0.7$  and  $0.8 \text{ pmol m}^{-3}$ ) were determined, and concentration enrichment in the coarse particles was observed. Another important source of amino acids in marine aerosols is the presence of biological material, demonstrated by means of a sampling cruise on the R/V *Italica* on the Southern Ocean.

Levoglucosan (LG) and phenolic compounds (PCs) were determined. As they reached the Antarctic plateau, they were observed in aerosol in accumulation mode (median concentration for LG  $6.4 \text{ pg m}^{-3}$  and  $4.1 \text{ pg m}^{-3}$ , PCs  $15.0 \text{ pg m}^{-3}$  and  $7.3 \text{ pg m}^{-3}$  respectively). Aged aerosols, while reaching the coastal site through katabatic circulation, age even further. LG mass was distributed on a larger particulate matter, while PCs were observed in fine particles (LG  $24.8 \text{ pg m}^{-3}$ , PCs  $34.0 \text{ pg m}^{-3}$ ). The LG/PCs ratios calculated for Antarctic aerosols were lower than those calculated for aerosols influenced by biomass burning areas, and acid/aldehyde ratios were lower

in coastal sites than inland. All these clues indicated that PCs behave differently from levoglucosan and that PC could be affected by a local source in Antarctica. LG and PC atmospheric concentration determined during the oceanographic cruise were  $37.6 \text{ pg m}^{-3}$  and  $58.5 \text{ pg m}^{-3}$  respectively.

## **2. ACKNOWLEDGMENTS**

This work was financially supported by the Italian Programma Nazionale di Ricerche in Antartide (PNRA) through the project “Studio delle sorgenti e dei processi di trasferimento dell’aerosol atmosferico antartico” (2009/A2.11). The research was also funded by the National Research Council of Italy (CNR) and by the Early Human Impact ERC Advance Grant from the European Commission’s VII Framework Programme, grant number 267696.

Advances in climate change

**Data analysis &  
modelling over Italy**

# Extreme events in a new climate regime over Italy

Faggian P.

<sup>1</sup>Ricerca sul Sistema Elettrico (RSE Spa), Milano

paola.faggian@rse-web.it

## Abstract

Climate change projections have been elaborated from seven regional climate change simulations provided by the ENSEMBLES Project, with an horizontal resolution of 25 km and driven by the SRES A1B scenario forcing. Temperature, precipitation and wind outputs at different time scale (daily, monthly, seasonal and annual) have been analysed with focus over Italy. At first a model validation have been performed at seasonal scale, comparing temperature and precipitation values provided by ENSEMBLES simulations with EOBS gridded data-set (for the period 1961-2013), and ENSEMBLES wind intensities with ERA-Interim data (for the period 1981-2000). Then climate change projections for the twenty-year period 2031-2050 have been elaborated considering as reference period the years 1986-2005, according the new AR5 base period, aware that the last 5 years (2001-2005) ENSEMBLES simulations have been forced by SRES A1B emission scenario.

Beyond changes in mean values, some projections about the risk of extreme events (heat waves, drought, heavy precipitation events) have been investigated because of its impact on societal activity and, in particular, on energy demand.

A significant warming is projected, above all in the summer season with a greater occurrence of extremely high temperature events. Precipitation and wind change signals are of more difficult interpretation but it is found a likely precipitation decrease during the summer season especially in the Southern of Italy, and an increasing of extreme precipitation events localized mostly over coastal areas. No significant signals of strong wind changes have been detected in this study, but some results show the risk for an increasing number of strong storms events over different sub-regions depending on the season.

**Keywords:** ensemble projections, extreme events

## 1. INTRODUCTION

Both gradual climate changes and extreme weather events may represent severe risks for energetic infrastructure vulnerability, with remarkable social and economic consequences. For these reasons there is a great interest for investigations on climatic incremental changes (as temperature increase) and extreme events (such as flooding and storm) projected for the future.

Annual mean temperatures over Mediterranean is likely to increase more than the global mean with the largest warming in summer ([1]); annual precipitation is very likely to decrease in most of the Mediterranean area (whereas increasing is projected over the most of Northern Europe), with a very likely decreasing of annual number of precipitation days and increasing of risk of summer drought ([2], [3]). Mediterranean Region results very sensitive to climate changes and has been identified as one of the most prominent “Hot-Spots” in the future climate projections ([4]).

The purpose of this paper is to analyse climate changes, in particular changes in extreme events, for the forthcoming decades over Italy on the basis of ENSEMBLES results.

## 2. DATASETS AND METHODOLOGY

Future climate change scenarios have been elaborated on the basis of seven ENSEMBLES Regional Climate Models (RCMs, Tab.1, <http://www.ensembles-eu.org>), under the emission scenario A1B [5], whose performances resulted satisfactory in comparison with: gridded E-OBS data (<http://eca.knmi.nl/dailydata>, [6]) regarding temperature and precipitation seasonal values in the period 1961-2013; ERA-Interim Reanalysis ([http://data-portal.ecmwf.int/data/d/interim\\_daily/](http://data-portal.ecmwf.int/data/d/interim_daily/), [7]) about seasonal wind intensities in the period 1981-2000. The seven RCM simulations selected well represent the observed patterns and well capture the seasonal cycles, even if there are some biases above all over mountain regions ([8]).

In this study climate change projections for the twenty-year period 2031-2050 (FUT) are given relative to the 1986-2005 average (REF). The results inferred from an ensemble mean of these models (labelled ENSEMBLE in the following figures) are discussed to describe the mean changes. Analysing some percentile values (10<sup>th</sup> percentile and 90<sup>th</sup> percentile) and the frequency of days with precipitation intensities

and wind speeds greater than some threshold values, some information about the probability of extreme event occurrences is provided.

### 3. RESULTS

Despite a range of responses from the models (Figures 1-2), some significant changes can be inferred regarding the Italian Region. In accordance with the AR5 results, there is high confidence that temperatures will continue to increase throughout the next decades, above all during summer season, with an increase of about  $1.5\div 2^{\circ}\text{C}$  [Figure 3]. The precipitation regimes will change depending on the season and on the area considered. The results highlight a remarkable reduction of precipitation during summer season (of about 20%), whereas in the other season the projected changes show spatial variability with some signals of increasing precipitation: in autumn over most part of the Peninsula, in winter on Alpine Region and during spring over southern coastal area ([8]).

These mean changes can exacerbate some climatic conditions of great interest nowadays because of their potential impacts on population wealth and/or different sectors (energy, agriculture, tourism,..). In particular, a warming of  $1.5\div 2^{\circ}\text{C}$  during winter season over Alpine Region represents a serious risk for snow cover reduction and an hazard for substantial Alpine glacier melting; an increasing temperature of about  $2^{\circ}\text{C}$  during summer season over most of Italy, concomitant with a reduction of precipitation of about 20%, highlights an upcoming risk for summer heat wave and drought events.

These results are confirmed also by the analysis of two indexes: the 10<sup>th</sup> percentile values for minimum temperature (left diagram of Figure 4) and the 90<sup>th</sup> percentile values for maximum temperature (right diagram of Figure 4). These changes and the increasing number of hot days ([8]) can potentially increase the peak in energy demand in the summer season with implications for the need for additional energy capacity and increased stress on water resources.

Also climatic changes projected for spring and autumn seasons have to be considered with great attention, as it is recognized an increasing risk for extreme events such as floods and storms ([9], [10]). This conclusion has been inferred also by analyzing some percentile maps for precipitation and wind fields ([8]). This has

been confirmed by computing, in the reference and future scenarios, the days characterized by precipitation intensities and wind speeds greater than some threshold values and then implementing a probabilistic approach considering the anomalies between FUT and REF periods described by the seven regional models.

Precipitations/wind regimes are characterized by fields with high spatial-temporal variability. As ENSEMBLES models have a spatial resolution of 25 km and daily step, these simulations are insufficient to capture properly the features of extreme events (as heavy precipitations or strong winds), especially over a complex topography like Italian Region. Nevertheless they can give some information about areas characterized by an high frequency of moderate weather events and, therefore, they can define the areas more likely vulnerable with respect to severe weather events.

With this assumption model simulations have been investigated by selecting weather events with precipitation/wind values above some threshold values, fixed lower than the typical ones used to classify heavy precipitation (typically heavy rain 7.6 mm per hour, strong wind 15m/s), but high enough to select significant weather events.

For each model the occurrences of precipitation days have been estimated selecting in each grid point the events with precipitation value greater than 20 mm/day; then the sum of such occurrences has been counted at seasonal scale over the whole analysis domain. After processing the REF and FUT scenarios, the anomalies fields have been computed by difference between the FUT and REF mean values. Then for each  $i$ th model the anomaly values  $A_{FUT}$  (%) have been computed according the formula:

$$A_{FUT} = 100 \cdot (N_{FUT} - N_{REF}) / N_{REF}$$

where  $N_{FUT}$  and  $N_{REF}$  are respectively the number of events occurred in the periods FUT and REF according the model  $i$ .

To identify the areas more likely interested by significant weather events, the following probabilistic approach have been applied: for each grid-point the occurrence anomalies have been classified in two types according their sign. Then positive and negative anomalies have been added and normalized respect to the number of models considered (seven in this case), computing the two values  $S_p$  e  $S_n$ , respectively. Such values, ranging from 0 to 1, describe the area in which most of the models agree in projecting an increase/decrease of the weather events if the

values are greater than 0.5; conversely they indicate the areas where there is uncertainty about the trend.

Only in the case in which at least 4 model over 7 provide the same trend (Sp or Sn larger than 0.55), the projected change has been elaborated using only the information of these sub-set of coherent models.

Finally, for each grid-point, the mean value of event in the REF period  $\langle N_{REF} \rangle$ , and mean percent anomaly value in the FUT scenario  $\langle A_{FUT} \rangle$  have been computed to provide an anomaly field in term of days directly.

Figure 5 indicates the changes about the occurrence of precipitation days projected over Italy, selected with a threshold value 20 mm/day. The results indicate some likely vulnerable areas: the Central-North Italy in winter, the Eastern coastal sites in spring and most of the peninsular regions during autumn.

An analogous investigation has been computed considering windy days selected with a threshold value of 5 m/s. Figure 6 represents the spatial pattern of windy day changes: in this case the Central-North Italy is interested by a likely increasing of the occurrence of windy events during winter and spring months, whereas in the other season the projections give a general decreasing of such events .

With the aim to investigate changes in storm frequency, the days characterized by the simultaneous occurrence of wind speeds greater than 5 m/s and precipitations greater than 10 mm/day have been computed in the future scenario relative to the reference one, with the assumption that areas identified by most models as more likely interested by an increase of storm events delineate the more vulnerable areas. A visual inspection of Figure 7 let have some information about the probability in the occurrence of severe events. The projections give an increasing risk over: several Italian areas in the winter season; Adriatic coastal areas and Ionic regions in spring; northwestern Italy, Liguria and Toscana regions in autumn.

#### 4. CONCLUSIONS

Future climate projections of temperature, precipitation and wind over Italy have been elaborated using seven transient regional climate model runs provided by ENSEMBLES data set and using as reference observational datasets EOBS and Era-Interim archives. The analysis indicates a significant warming and drying of Italy

especially in the warm season, with an upcoming risk for heat wave and drought events. It should not be neglected the signal of increasing temperature even in winter, because the warming of 1.5-2 °C could have serious impacts of Alpine glacier.

Quantifying the risk or probability of an extreme weather events over Italy is particularly challenging. A probabilistic approach has been implemented to have some information about the sub-region more likely vulnerable with respect to severe weather events. The results highlight an increasing risk over several Italian areas in the winter season; Adriatic coastal areas and Ionic regions in spring; Liguria and Toscana regions in autumn.

## 5. ACKNOWLEDGMENTS

This work has been financed by the Research Fund for the Italian Electrical System under the Contract Agreement between RSE SpA and the Italian Ministry of Economic Development - General Directorate for Nuclear Energy, Renewable Energy and Energy Efficiency, stipulated on July 29, 2009, in compliance with the Decree of November 11, 2012.

We acknowledge the ENSEMBLES data from the EU-FP6 Integrated Project ENSEMBLES (<http://ensembles-eu.metoffice.com>) and the E-OBS data providers in the ECA&D project (<http://www.ecad.eu>).

## 6. REFERENCES

1. EEA Report No 12/2012. "Climate change, impacts and vulnerability in Europe 2012".
2. Christensen H.J., Christensen O.B., 2007: "A summary of PRUDENCE model projections of change in European climate by the end of this century". *Climatic Change*, 81, 7-30, DOI 10.1007/s10584-006-9210-7.
3. Faggian P., F. Giorgi, 2009: "An analysis of global model projections over Italy, with particular attention to the Italian Greater Alpine Region (GAR)". *Climatic Change*. 96, 239-258.
4. Giorgi F. 2006: "Climate Change Hot –spots". *Geophys. Res. Lett.* 33, L08707.

5. Nakicenovic N., and Coauthors, 2000: *Special report on emissions scenarios: a special report of Working Group III in the Intergovernmental Panel on Climate Change*. Cambridge University Press, p 600.
6. Haylock, M.R., N. Hofstra, A.M.G. Klein Tank, E.J. Klok, P.D. Jones, M. New. 2008: "A European daily high-resolution gridded dataset of surface temperature and precipitation". *J. Geophys. Res (Atmospheres)*, **113**, D20119, doi:10.1029/2008JD10201"
7. Simmons, A. J., and A. Hollingsworth, 2002: Some aspects of the improvement of skill of numerical weather prediction. *Quart. J. Roy. Meteor. Soc.*, **128**, 647–677.
8. Faggian P. , 2014 :“Climate change projections for Mediterranean region with focus over Italy. *Climatic Change* (submitted)
9. Nikulin G., Kjellström E., Hansson U., STRANDBERG G., ULLERSTIG A., 2011: “Evaluation and future projections of temperature, precipitation and wind extremes over Europe in an ensemble of regional climate simulations”. *Tellus*, **63A**, 41–55
10. Cacciamani C. 2013: “Eventi estremi, entità e ricorrenza”. *Ecoscienza*,**5**, 26-27

## 7. IMAGES AND TABLES

Institute	Driving GCM	RCM	Simulation	Acronym
CNRM <sup>(1)</sup>	ARPEGE_RM5.1	Aladin	CNRM-RM5.1_ARPEGE	C&A
ETHZ <sup>(2)</sup>	HadCM3Q0	CLM	ETHZ-CLM_HadCM3Q0	E&H
ICTP <sup>(3)</sup>	ECHAM5-r3	ICTP-REGCM3	ICTP-REGCM3_ECHAM5	I&E
KNMI <sup>(4)</sup>	ECHAM5-r3	RACMO	KNMI-RACMO2_ECHAM5	K&E
HC <sup>(5)</sup>	HadCM3Q0	HadRM3Q0	METO-HC_HadCM3Q0	M&H
SMHI <sup>(6)</sup>	ECHAM5-r3	RCA	SMHIRCA_ECHAM5	S&E
SMHI	BCM	RCA	SMHIRCA_BCM	S&B

(1) **Météo-France (CNRM)**

(2) **Swiss Institute of Technology (ETHZ)**

(3) **The Royal Netherlands Meteorological Institute (KNMI)**

(4) **The Abdus- Salam International Centre for Theoretical Physics (ICTP)**

(5) **UK Met Office, Hadley Centre for Climate Prediction and Research (HC)**

(6) **Swedish Meteorological and Hydrological Institute (SMHI)**

Tab. 1 Regional Climate Models considered in this study provided by ENSEMBLES Archive: horizontal resolution 25 km, emission forcing scenario SRES A1B [6]. The Global Circulation Model (GCM) driving each regional simulation is specified

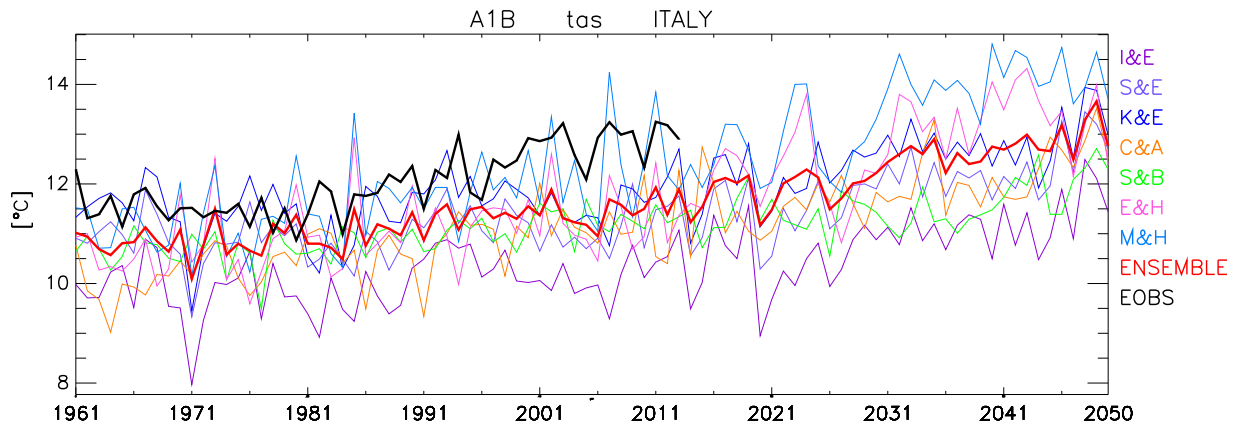


Fig. 1 Annual values of mean surface temperature over Italy described by EOBS (thick black line), ENSEMBLE mean (thick red line) and by the models (thin coloured lines)

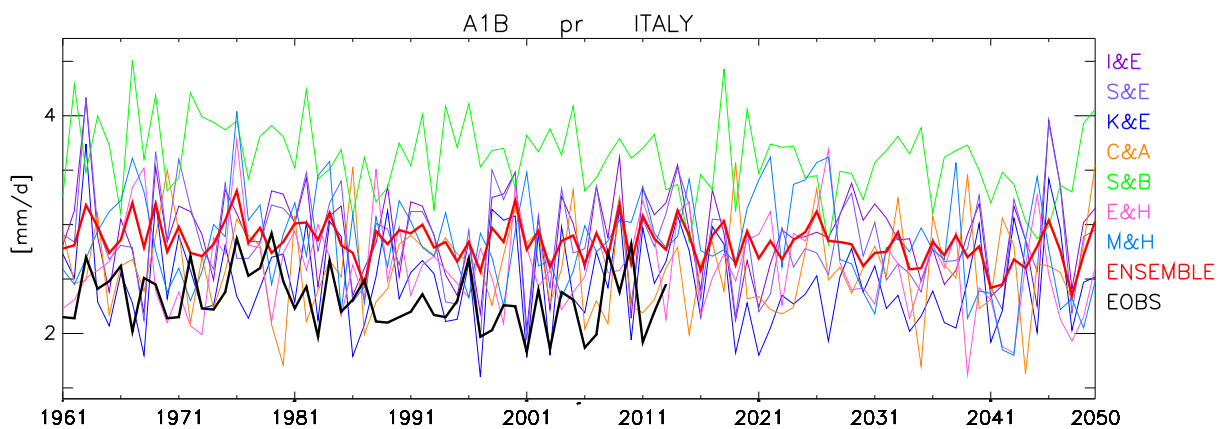


Fig. 2 Like Fig.1 but for precipitation

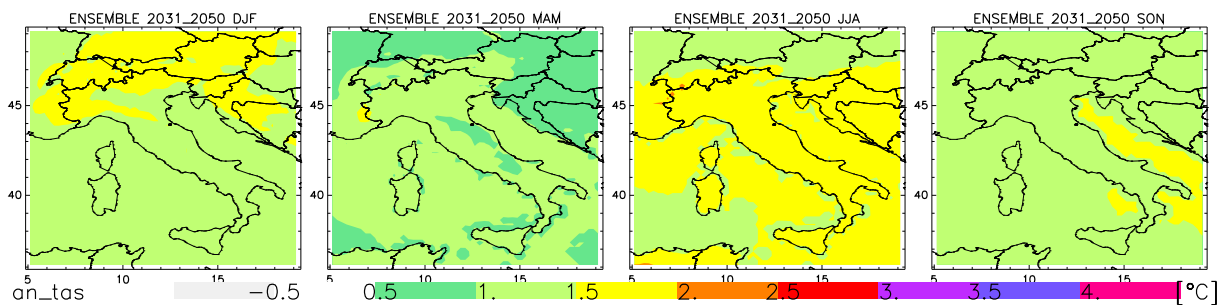


Fig. 3 Seasonal surface air temperature anomalies projected by 2031-2050, relative to 1986-2005 scenario, ordered from left to right for winter (DJF), spring (MAM), summer (JJA) and autumn (SON)

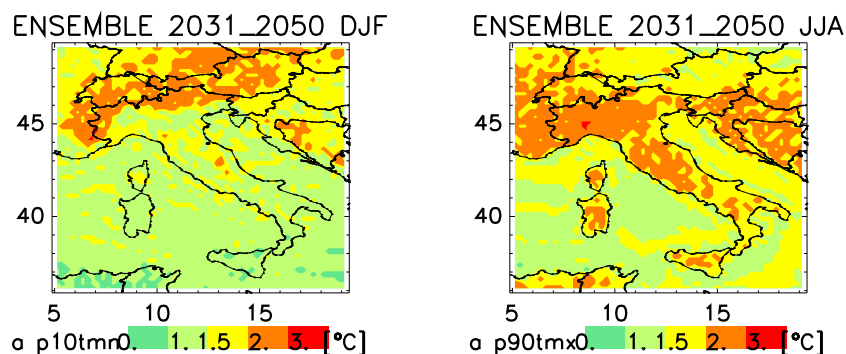


Fig. 4 Winter mean anomalies for 10th percentile of minimum temperature (left diagram) and Summer mean anomalies of 90th percentile for maximum temperature (right diagram)

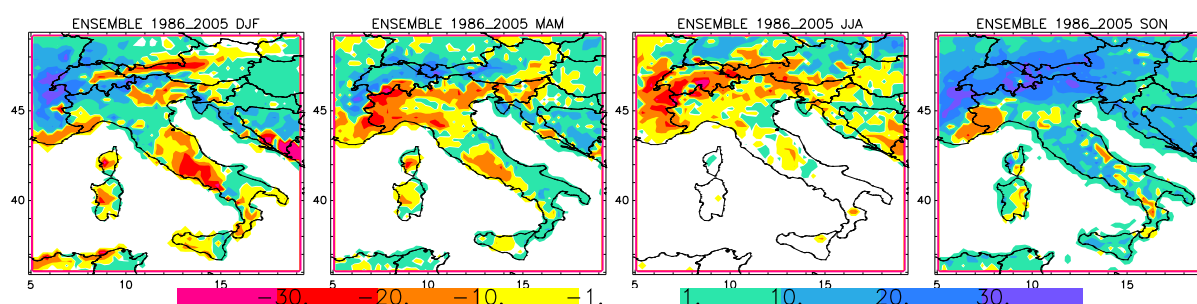


Fig. 5 Changes in the number of events with daily precipitation > 20mm/d projected by 2031-2050, relative to 1986-2005 scenario, inferred by seven ENSEMBLES models

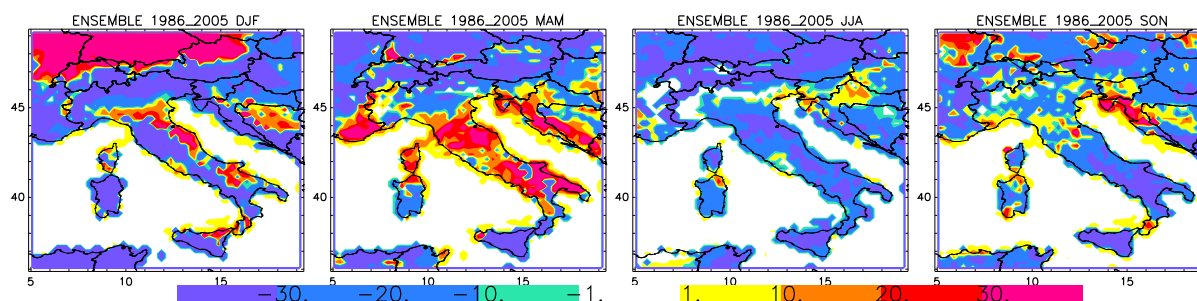


Fig. 6 Changes in the number of windy events with daily speed > 5m/s projected by 2031-2050 relative to 1986-2005 scenario, inferred by seven ENSEMBLES models

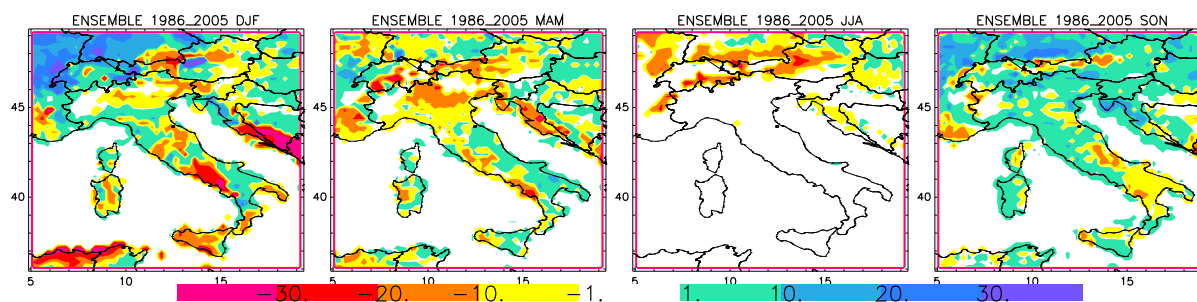


Fig. 7 Changes in the number of meteorological events with daily precipitation > 10mm/d and daily speed > 5m/s projected by 2031-2050 relative to 1986-2005 scenario, inferred by seven ENSEMBLES models

# Evaluating the effects of changes in observational sites position and surrounding urbanisation on the historical temperature time series of the city of Trento in the Alps

Giovannini L.<sup>1\*</sup>, Zardi D.<sup>1</sup>, and de Franceschi M.<sup>1,2</sup>

<sup>1</sup>Atmospheric Physics Group, Department of Civil, Environmental and Mechanical Engineering, University of Trento – Italy, <sup>2</sup>Diocese of Bolzano-Bressanone - Italy

\*Corresponding Author: [lorenzo.giovannini@unitn.it](mailto:lorenzo.giovannini@unitn.it)

## Abstract

Two datasets resulting from a long-term field campaign and from numerical simulations with the WRF model, coupled with an urban parameterisation scheme, were analysed to gain information supporting the reconstruction of the temperature time series of the city of Trento in the Alps, dating back to 1816. This project is challenging, due to various relocations of the observational sites and the increasing effects of urbanisation.

Identical temperature sensors were placed at the historical observational sites of the city, to detect systematic differences between these places under various seasonal patterns and weather conditions. However, since differences measured nowadays may not be representative of those occurring in the past, numerical simulations were also run with the WRF model, using a historical land use, to integrate the experimental dataset. Furthermore, results from the numerical simulations were analysed to estimate the increasing effects of urbanization on the time series.

**Keywords:** Temperature time series, Urbanisation effects, WRF model.

## 1. TEXT

Regular observations of air temperature in Trento, a medium-sized city on the Adige Valley floor, in the Italian part of the Alps [Fig. 1], date back to 1816. However measurements were collected at different sites from that time, as shown in Fig. 2. The changes in the position of the observational sites introduced inhomogeneities in the time series, not only due to the different degree of urbanisation between the sites, but also due to topographic effects, since observations were collected at different altitudes on the slopes of the valley.

In order to obtain reliable information supporting the reconstruction of the historical time series, a field campaign was carried out aiming at evaluating temperature differences between the principal sites where observations were performed. Of course it is clear that temperature differences detected nowadays may be different from those occurring in the past. Nevertheless the analysis of the results of the field measurements provides important information about typical microclimatic differences between parts of the city with different degrees of urbanisation and altitude. However, to overcome this issue, the information obtained from the field campaign was integrated with the results from numerical simulations with the Weather Research and Forecasting (WRF) model [1], coupled with an advanced urban parameterization scheme. Simulations reproducing the present situation on selected representative days of different weather conditions and seasons were first validated against measurements from the above field campaign, in order to test the ability of the model to reproduce the thermal field in the urban area. Then, simulations were performed with identical initial and boundary meteorological conditions, but with historical land use and no anthropogenic heat releases, to reproduce climatic conditions in Trento in the late 19<sup>th</sup>-early 20<sup>th</sup> century. The results from the “historical” simulations were analysed with a twofold aim. On one hand, as described above, these simulations allowed the results of the field campaigns to be integrated, to get a clearer understanding of the effects of changes in the position of the observational sites. The modelled temperature differences between these locations were assumed to be representative of those occurring in the past, when the observational sites moved [Fig. 2]. On the other hand, the comparison between the “present” and the “historical” simulations allowed us to estimate the effect of the increasing urbanisation and the

subsequent stronger intensity of the UHI on the time series, similarly to Van Weverberg et al. [2].

*a) The field campaign*

The field campaign was carried out from August 2009 to November 2010 in the city of Trento to monitor systematic temperature differences between the sites where historical measurements were performed. Identical thermohygrometers (Onset Inc. Mod. HOBO H8 Pro) were placed in most of the historical observational sites in Trento and were set up so as to take measurements every 5 minutes. Two sensors were placed close to the city centre, one at the ex-Imperial Royal Gymnasium (now Liceo Classico “Giovanni Prati”, PRA) and one at the ex-Sericultural Institute (now location of the Department of Economics and Management, ECO). One sensor was placed at San Bernardino Convent (BER), just above the valley floor, on the eastern valley slope [Fig. 1]. Finally two sensors were placed at Laste, on the eastern slope of the valley, one in the same Stevenson shelter where measurements were carried out in the past (LASST), and one close to the sensor currently used by the local Meteorological Office (Meteotrentino), on the roof of the building (LASRO). No measurements could be performed, due to lack of authorization, in two of the historical sites: Casa Wolkenstein (CWO), in the city centre close to PRA and ECO, and San Giorgio (SGI), on the western slope.

To evaluate whether temperature differences between the five sensors change according to weather conditions, data were divided into three weather classes. These classes were derived from global solar radiation measurements at the Molino Vittoria station, located close to the city centre on top of a tower above the mean roof level [Fig. 1] [3,4,5]. The idea behind this choice consists in assuming solar radiation is a proxy of weather conditions. In particular, the data were divided as follows:

- Sunny days:  $S > 2/3 S_{\max,m}$ ;
- Partly cloudy days:  $1/3 S_{\max,m} < S \leq 2/3 S_{\max,m}$ ;
- Cloudy days:  $S \leq 1/3 S_{\max,m}$ ;

where  $S$  is the daily global solar radiation observed on each day to be classified and  $S_{\max,m}$  is the maximum daily global solar radiation observed in that month.

From Tab. 1, showing the average seasonal temperature contrasts between each sensor and LASRO for the three weather classes, it can be seen that temperatures registered by ECO and PRA, the two sensors close to the city centre, are between 1.1°C and 1.7°C higher than at LASRO, with stronger differences in spring and summer than in fall and winter. The temperature contrasts between BER and LASRO also follow a similar behaviour, but with smaller differences (~1°C in summertime, ~0.5°C in wintertime). Since LASRO is located about 110 m above the valley floor and 70 m above BER, these temperature contrasts result from a combination of urbanisation and topographic effects. The smaller temperature differences in wintertime are caused by the fact that in the cold season ground-based thermal inversions develop more frequently in the Adige Valley and, as a consequence, the mean lapse rate is lower [3]. Temperature differences between the sites in the city centre and LASRO display a rather small variability with respect to weather types. Nevertheless slightly larger temperature differences tend to occur under cloudy conditions than on sunny days, probably due to the higher frequency of ground-based thermal inversions on clear-sky days. On the other hand temperature differences between BER and LASRO are considerably affected by weather conditions: in all seasons they are significantly smaller on sunny days than in cloudy conditions, when temperature at BER is quite similar to that observed in the city centre. It can be noticed that temperature contrasts between the two sensors in the city centre, located in areas with a similar urban morphology, are very small in all weather conditions and in all seasons, despite the siting differences. The same behaviour is found between the two sensors at Laste. This result suggests that, on average, at these locations microclimatic effects connected with peculiarities of the experimental set-up and of the local surroundings of the sensors do not play a significant role.

*b) Numerical simulations: set-up*

In order to obtain a WRF-modelled exemplar day for each weather situation, one sunny and one cloudy representative day for each season were selected for being simulated. The candidates were chosen so as to be representative of the average temperature differences between the observational sites, as presented above. Indeed on the selected days, the average values of the temperature differences

between the sites are very similar to those presented in Tab. 1. It was decided not to take into account partly cloudy days, since they generally present simply intermediate behaviours between sunny and cloudy situations.

The set-up of the WRF model in the present paper closely follows the settings adopted in a previous work, investigating the alterations induced by the urban area of Trento on local atmospheric processes [5]. Each simulation lasts 30 h and starts at 1800 UTC of the previous day; the first 6 h, being spuriously affected by the initialisation, are not considered for the analysis. The horizontal domain used for the simulations is composed of five two-way nested domains with 100x100, 91x91, 91x100, 91x100, and 73x73 cells, and grid spacing of 40.5, 13.5, 4.5, 1.5, and 0.5 km respectively. For the vertical resolution, 42 levels are used, with higher resolutions near the ground (first full eta level at ~15 m above ground level and 9 levels in the first 1000 m). The initial and boundary conditions are supplied by the 6-hourly National Centers for Environmental Prediction (NCEP) Final Operational Global Analysis data on 1-degree grids. Physical settings are similar to those used in [5]. In particular the BEP model [6] is adopted as the urban parameterisation scheme.

As outlined above, simulations reproducing both present and historic climatic conditions in Trento were performed. The present land use was provided by the Corine dataset (<http://www.eea.europa.eu>), reclassified into the 20 Modis classes (+3 special classes for urban land use), in order to fit the WRF look-up tables. In the historical simulations it was decided to use the land use of the early 20<sup>th</sup> century, because the two longest time series (San Bernardino and Laste), which have been presumably more affected by the progressive urbanisation, started in that period. The historical land use was estimated from the available images dating back to the beginning of the 20<sup>th</sup> century, and in particular from Fig. 1b.

### *c) Present simulations*

First, results from the present simulations were validated against the observations from the field measurements, highlighting that the model is able to reproduce reasonably well the thermal field in the urban area of Trento. Fig. 3 shows the comparison between simulated temperatures and observations at PRA. It can be seen that temperature is quite well predicted by the model on all the days, even

though in some situations errors up to 2-3°C are present. Similar results were found at the other sites monitored in the field campaign (not shown here).

The model is able to correctly capture also the main features of the temperature differences between the observational sites. Temperatures simulated at ECO and PRA, in the city centre, are very similar and higher than at the other observational sites, while the lowest temperatures are simulated at Laste. In most cases the mean absolute error (MAE) of the temperature differences between the sites is of the order of 0.5°C (Tab. 2). Moreover the mean errors (ME) are generally small, indicating that overestimations and underestimations balance. However in some cases larger errors are present, considering both the MAEs and the MEs. MAEs are generally larger on sunny days, when the diurnal variability, mostly determined by microclimatic effects, is larger: the model, calculating a spatially-averaged thermal field, cannot capture the microclimatic features characterising each location. Moreover, Fig. 4, showing the modelled and observed temperature differences between the sites on the 8 days analysed, shows that the model poorly reproduces the temperature difference variability connected with seasonality and weather conditions. For example, in contrast to observations, the simulated temperature differences between the sites analysed and LASRO are larger in winter than in the other seasons. Therefore the model does not simulate correctly the seasonal changes in the mean lapse rate. Moreover it does not capture the large variability associated with weather conditions in the temperature differences between BER and LASRO: actually it simulates nearly constant temperature contrasts on all the days analysed. These limitations must be carefully considered when using model results to infer temperature shifts due to the changes in the position of the observational sites.

The modelled diurnal cycles of the urban heat island (UHI) were also tested against observations, to evaluate how the model simulates urban-rural temperature contrasts. This validation is important to assess whether the model can be used to estimate the effects of progressive urbanisation on the time series. Here UHI intensity is calculated as the temperature difference between PRA, in the city centre, and Roncafort weather station, permanently operated by the local Meteorological Office (Metetrentino) and located just outside the urban area toward north, on the floor of the Adige Valley [Fig. 1]. Comparisons in Fig. 5 highlight that during sunny days the model captures the major features of the diurnal cycle, characterised by

stronger intensities at night than during daytime. However the model does not see the development of an urban cool island in the morning. Furthermore the model is able to capture the different behaviour of urban-rural temperature differences occurring during cloudy days, characterised by nearly constant values throughout the day, and by smaller nocturnal intensities than on sunny days. However, the model generally overestimates the intensity of the UHI, especially in winter, as can be clearly appreciated from the statistics in Tab. 3. On average, the UHI intensity is overestimated by ~60%: this overestimation should be carefully taken into account when using model results to infer the effects of progressive urbanisation on the time series.

#### *d) Historical simulations*

Historical simulations were first analysed to evaluate how temperature contrasts between the observational sites have changed from the present simulations: this comparison is presented in Tab 4. From this Table it can be inferred that temperature differences between ECO and PRA do not change between the present and the historical simulations. Moreover, the contrasts between BER and the locations in the city centre also remain rather similar: on average they are only 0.1°C smaller in the historical simulations than in the present ones. Therefore the model results suggest that the average temperature differences found in the field measurements can be assumed as representative of those occurring between these observational sites in the past. On the other hand, according to the model results, the temperature contrasts between LASRO and the other stations were larger in the past than nowadays, probably because the surrounding urbanisation increased more significantly around this site [Fig. 1].

The average temperature differences between present and historical simulations at BER and LASRO, i.e. an estimate of the effects of the increased urbanisation, are shown in Tab. 5. Larger differences are found at LASRO, where, as stated above, the most significant urbanisation changes have occurred in the last century. At BER, temperature differences between the two simulations are quite similar on cloudy and sunny days, with an average difference of 0.8°C, whereas at LASRO urbanisation effects are larger in sunny conditions (~1.7°C) than on cloudy days (~1.1°C), as on average the UHI is stronger on sunny days. However, as seen above, it is likely that

these differences are overestimated, especially on the cloudy winter day, given the overestimation of the model in reproducing urbanisation effects.

#### *e) Conclusions*

Two datasets resulting from a long-term field campaign and from numerical simulations with the WRF model, coupled with an urban parameterisation scheme, were analysed to gain information supporting the reconstruction of the temperature time series of the city, dating back to 1816.

Results from the field campaign revealed the temperature differences existing nowadays between the places where observations composing the time series were performed. On average, no temperature differences were detected between the two sensors close to the city centre. On the other hand it was found that the average temperature contrasts between the sensors on the valley floor and on the slope significantly depend on the season and on the weather conditions. These temperature differences result from a combination of urbanisation and topographic effects [3], as the observational sites were located at different altitudes. Topographic effects can be assumed to be the same as in the 19<sup>th</sup> century, whereas the present urbanisation is very different from the past. As a consequence, the results of the field campaign cannot be directly used to correct the time series. Therefore, to integrate the experimental measurements, simulations with the WRF model were performed, using both present and historical land use datasets. Simulations with the present land use on selected days, taken as representative of different weather and seasonal conditions, were first validated against the results of the field campaign. It was found that the model is able to reproduce reasonably well the average characteristics of the thermal field inside the urban area of Trento, including the main features of the thermal differences between the observational sites. However the model is not able to capture the variability of the temperature differences between the sites connected with seasonality and weather conditions. Urban-rural thermal contrasts are also reproduced quite well, in particular the different behaviour between sunny and cloudy days, even though on average the intensity of the UHI is overestimated. In particular the development of an urban cool island during daytime is not captured by the model.

Results from the historical simulations were then analysed to obtain information aimed at correcting the time series. It was found that the average temperature differences between the sites more embedded in the urban area are not significantly different from the present runs, probably because urbanisation grew similarly around them in the last century. Therefore temperature differences measured in the field campaign between these sites can be assumed as representative also of the shifts in the time series involving these observational sites. On the other hand the temperature contrasts between Laste, on the eastern slope, and the other sites were larger in the past, as the surroundings of this weather station have changed more: it was actually in the open countryside at the beginning of the last century, while it is now surrounded by a suburban area.

Finally, changes in urbanisation effects at the two sites, Laste and San Bernardino, where measurements were continuously performed in the last century, were estimated by comparing the results of present and historical simulations. Significant differences were found at both sites, but were larger at Laste, where major urbanisation changes occurred in the last century. As expected, the differences found at this site are larger during sunny days, when urbanisation effects are stronger. The warming due to urbanisation estimated in this work is not distant from the results obtained with a similar methodology by Van Weverberg et al. [2] in Brussels. However it is likely that in the present work urbanisation effects are overestimated by the model, considering the overestimation of the UHI intensity.

## 2. REFERENCES

1. Skamarock W.C., Klemp J.B., Dudhia J., Gill D.O., Barker D.M., Duda M.G., Huang X.-Y., Wang W., Powers J.G. (2008), *A description of the advanced research WRF version 3*, NCAR Technical Note TN-475+STR.
2. Van Weverberg K., De Ridder K., Van Rompaey A. (2008), *Modeling the contribution of the Brussels heat island to a long temperature time series*, Journal of Applied Meteorology and Climatology, No. 47, pp. 976-990.
3. Giovannini L., Zardi D., de Franceschi M. (2011), *Analysis of the urban thermal fingerprint of the city of Trento in the Alps*, Journal of Applied Meteorology and Climatology, No. 50, pp. 1145-1162.

4. Giovannini L., Zardi D., de Franceschi M. (2013), *Characterization of the thermal structure inside an urban canyon: field measurements and validation of a simple model*, Journal of Applied Meteorology and Climatology, No. 52, pp. 64-81.
5. Giovannini L., Zardi D., de Franceschi M., Chen F. (2014), *Numerical simulations of boundary-layer processes and urban-induced alterations in an Alpine valley*, International Journal of Climatology, No. 34 (4), pp. 1111-1131.
6. Martilli A., Clappier A., Rotach M.W. (2002), *An urban surface exchange parameterisation for mesoscale models*, Boundary-Layer Meteorology, No. 104, pp. 261-304.
7. Giovannini L., Zardi D., de Franceschi M. (2014), *Effects of changes in observational sites position and surrounding urbanisation on the temperature time series of the city of Trento*, Urban Climate.

### 3. IMAGES AND TABLES

		ECO-LASRO	PRA-LASRO	BER-LASRO	LASST-LASRO
WINTER	S	1.33	1.29	0.24	-0.17
	PC	1.27	1.22	0.50	-0.14
	C	1.39	1.31	0.92	-0.07
SPRING	S	1.43	1.47	0.51	0.12
	PC	1.67	1.56	1.07	0.19
	C	1.63	1.49	1.16	0.12
SUMMER	S	1.47	1.47	0.84	0.16
	PC	1.63	1.46	1.18	0.19
	C	1.56	1.35	1.46	0.22
FALL	S	1.11	1.14	0.27	0.04
	PC	1.16	1.12	0.58	0.11
	C	1.43	1.31	1.07	0.09

Tab. 1 Average seasonal temperature differences between each sensor used in the field campaign and LASRO for sunny (S), partly cloudy (PC) and cloudy (C) conditions. Table from [7].

Date	Category	ECO-LASRO		PRA-LASRO		BER-LASRO		ECO-BER		PRA-BER		ECO-PRA	
		MAE	ME	MAE	ME	MAE	ME	MAE	ME	MAE	ME	MAE	ME
15 Jan 2010	WS	0.40	0.06	0.50	0.49	0.84	0.84	0.79	-0.79	0.35	-0.35	0.44	-0.44
12 Jan 2010	WC	0.16	-0.03	0.23	0.23	0.20	-0.17	0.17	0.14	0.40	0.40	0.26	-0.26
19 Apr 2010	SpS	0.49	-0.02	0.40	0.19	0.69	0.61	0.68	-0.63	0.42	-0.42	0.52	-0.20
02 May 2010	SpC	0.85	-0.85	0.54	-0.53	0.58	-0.58	0.36	-0.26	0.27	0.05	0.32	-0.31
25 Jun 2010	SuS	0.95	-0.39	0.50	-0.26	0.59	-0.22	0.58	-0.17	0.52	-0.05	0.60	-0.12
03 Aug 2009	SuC	0.76	-0.76	0.40	-0.25	0.68	-0.64	0.59	-0.12	0.66	0.39	0.51	-0.51
02 Oct 2009	FS	0.72	-0.42	0.40	-0.40	0.43	0.06	0.48	-0.48	0.55	-0.46	0.41	-0.02
16 Nov 2009	FC	0.27	-0.14	0.25	0.11	0.25	-0.01	0.22	-0.12	0.19	0.12	0.25	-0.25
TOT		0.57	-0.32	0.40	-0.05	0.53	-0.01	0.48	-0.30	0.42	-0.04	0.41	-0.26

Tab. 2 Mean absolute errors (MAE, °C) on an hourly basis and mean errors (ME, °C) for the temperature differences ECO-LASRO, PRA-LASRO, BER-LASRO, ECO-BER, PRA-BER, and ECO-PRA for the present simulation compared with measurements in the 8 days analysed. WS = Winter Sunny, WC = Winter Cloudy, SpS = Spring Sunny, SpC = Spring Cloudy, SuS = Summer Sunny, SuC = Summer Cloudy, FS = Fall Sunny, FC = Fall Cloudy. Table from [7].

Date	Category	UHI obs. [°C]	UHI model [°C]	MAE [°C]	ME [°C]
15 Jan 2010	WS	1.76	2.60	1.10	0.84
12 Jan 2010	WC	1.09	2.60	1.52	1.52
19 Apr 2010	SpS	1.44	2.19	1.13	0.74
02 May 2010	SpC	0.73	0.93	0.51	0.20
25 Jun 2010	SuS	1.36	2.22	1.46	0.87
03 Aug 2009	SuC	1.27	1.27	0.74	0.00
02 Oct 2009	FS	1.05	1.82	1.07	0.76
16 Nov 2009	FC	0.91	1.66	0.75	0.75
TOT		1.20	1.91	1.03	0.71

Tab. 3 Average observed and modelled intensity of the UHI, mean absolute errors (MAE) on an hourly basis and mean errors (ME) for the present simulations compared with observations in the 8 days analysed. UHI intensity is calculated as the temperature difference between PRA and Roncafort [Fig. 1]. Table from [7].

Date	Category	ECO-LASRO		PRA-LASRO		BER-LASRO	
		PRE	HIS	PRE	HIS	PRE	HIS
15 Jan 2010	WS	1.49	2.13	1.70	2.31	1.06	1.84
12 Jan 2010	WC	1.63	1.31	1.79	1.49	1.08	0.98
19 Apr 2010	SpS	1.19	1.61	1.32	1.74	0.86	1.45
02 May 2010	SpC	1.08	1.12	1.13	1.21	0.74	0.94
25 Jun 2010	SuS	1.34	2.14	1.41	2.34	0.86	1.92
03 Aug 2009	SuC	1.12	1.56	1.23	1.69	0.81	1.31
02 Oct 2009	FS	0.93	2.14	0.99	2.19	0.68	1.93
16 Nov 2009	FC	1.11	1.41	1.27	1.51	0.84	1.17
TOT		1.24	1.68	1.35	1.81	0.87	1.44

Tab. 4 Average temperature differences (°C) between the sites analysed and LASRO in the present (PRE) and historical (HIS) simulations. Table from [7].

Date	Category	BER PRE-HIS	LASRO PRE-HIS
15 Jan 2010	WS	1.12	1.90
12 Jan 2010	WC	1.78	1.68
19 Apr 2010	SpS	0.58	1.16
02 May 2010	SpC	0.46	0.66
25 Jun 2010	SuS	0.86	1.91
03 Aug 2009	SuC	0.42	0.92
02 Oct 2009	FS	0.42	1.67
16 Nov 2009	FC	0.77	1.09
TOT		0.80	1.37

Tab. 5 Average temperature differences (°C) at BER and LASRO between the present (PRE) and historical (HIS) simulations. Table from [7].

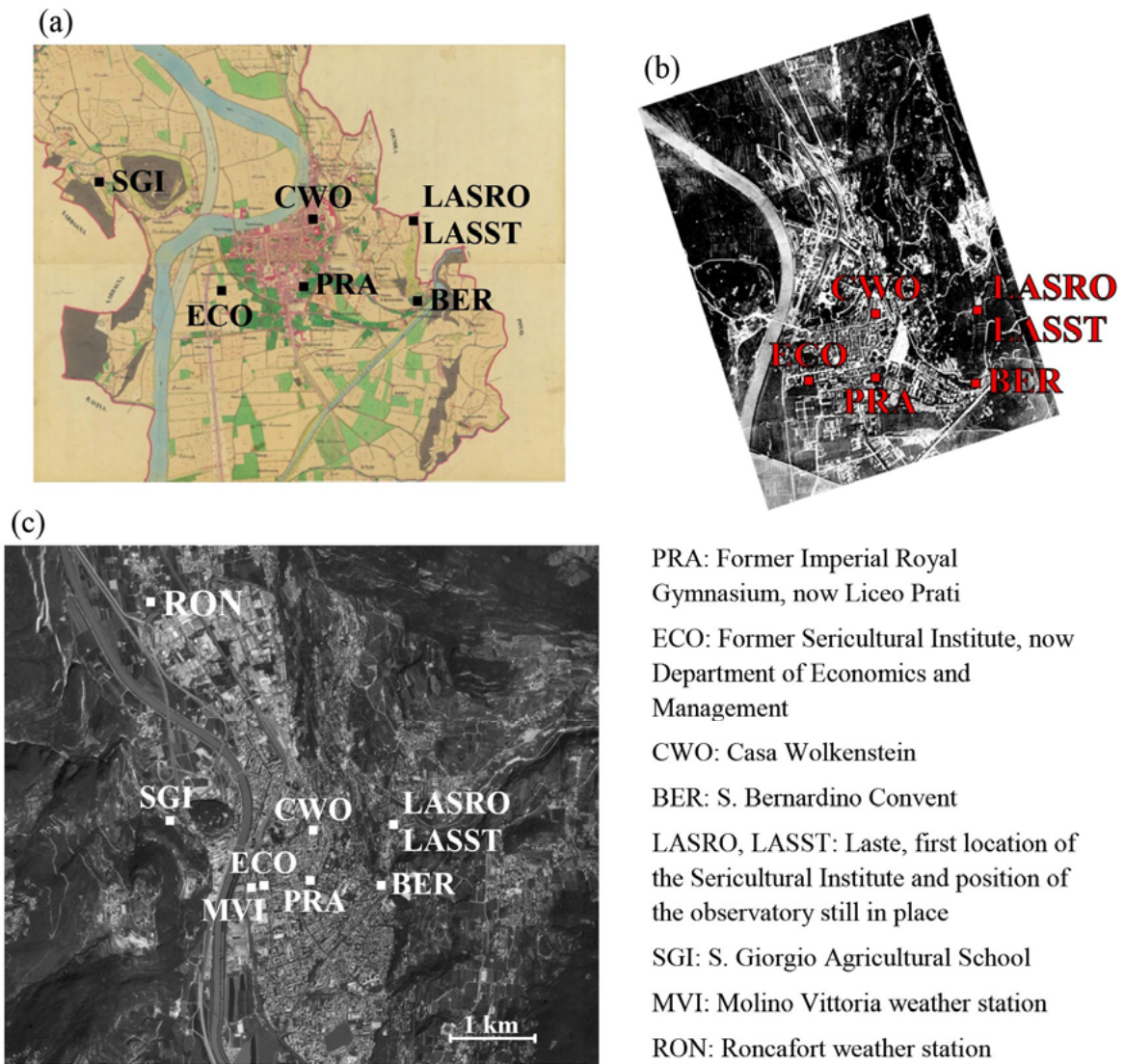


Fig. 1 The urban area of Trento in (a) mid XIX century (Austrian land register), (b) 1919, and (c) nowadays (aerial photo), along with location of historical observational sites in Trento and weather stations analysed in this work. Figure from [7].

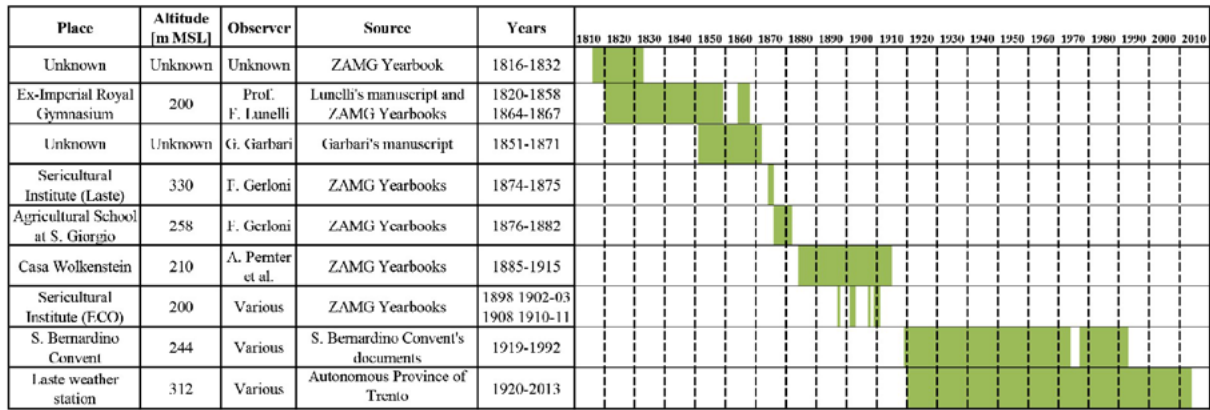


Fig. 2 GANTT of the observations composing the temperature time series of Trento. Figure from [7].

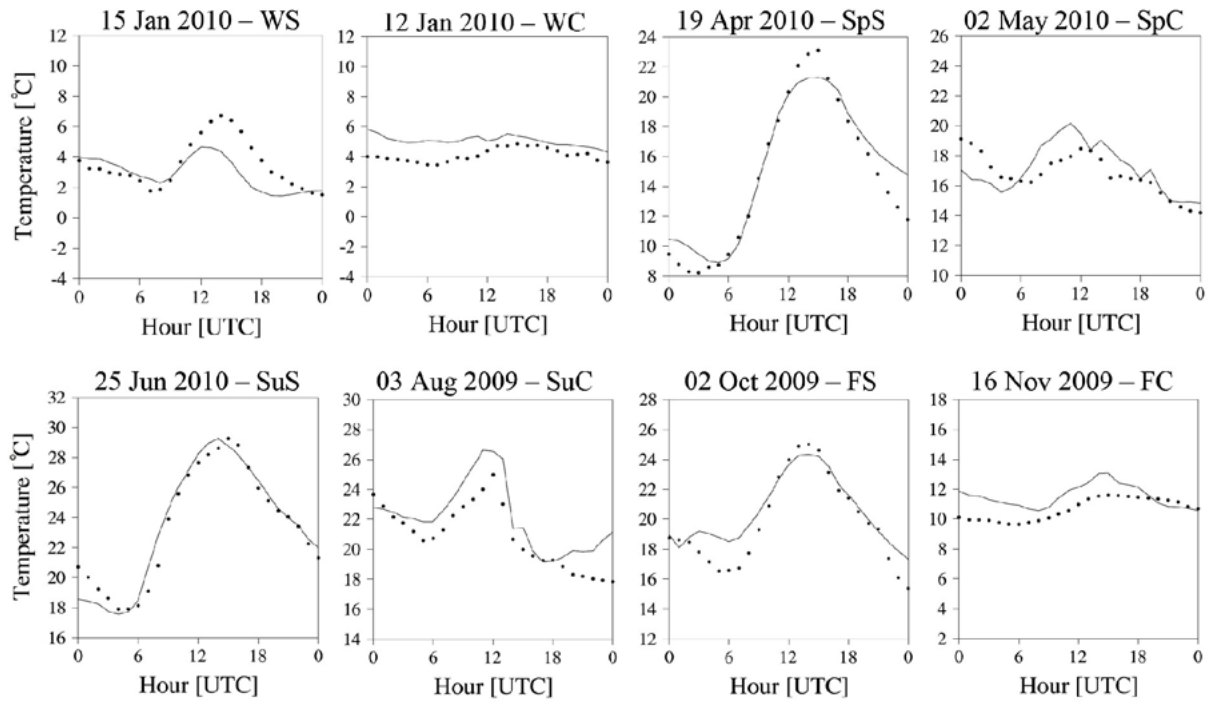


Fig. 3 Diurnal cycles of temperature as observed (dots) and simulated by the present simulations (solid line) at PRA in the 8 days analysed. Figure from [7].

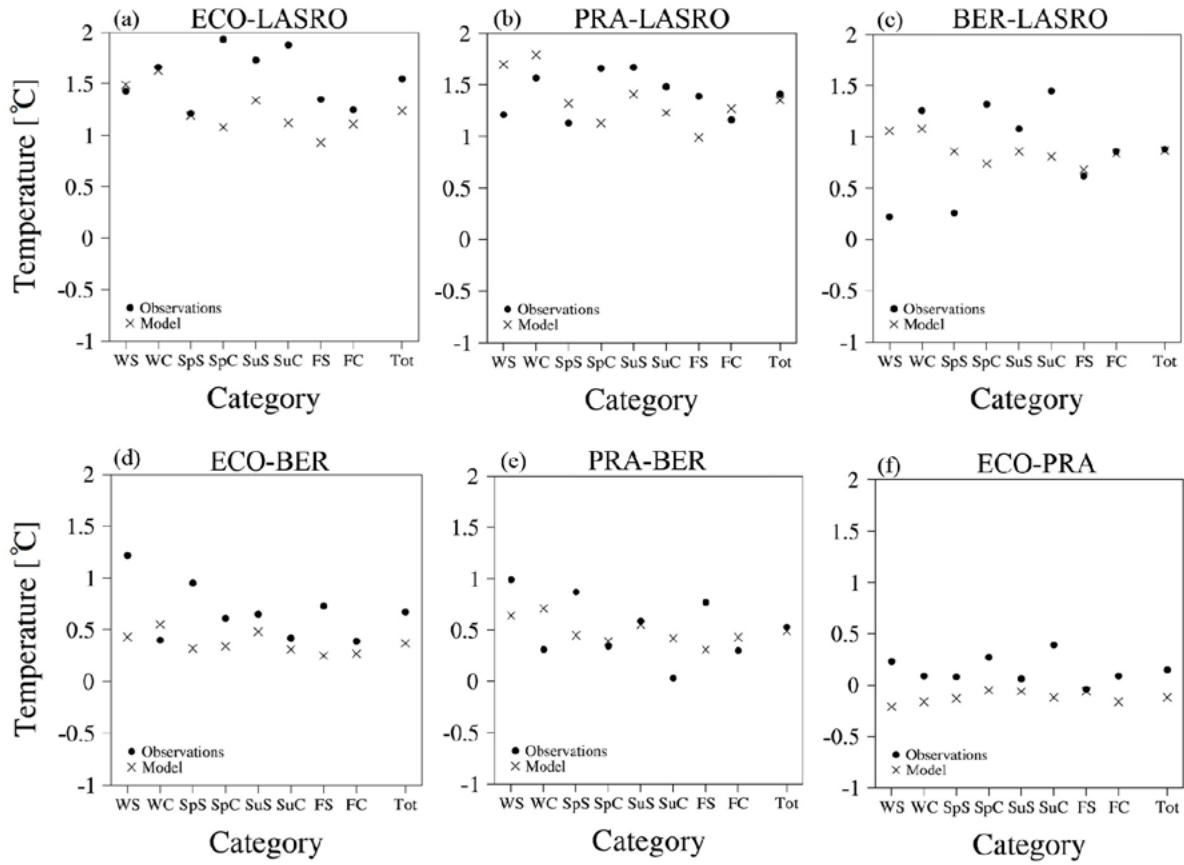


Fig. 4 Comparison of the average temperature differences (a) ECO-LASRO, (b) PRA-LASRO, (c) BER-LASRO, (d) ECO-BER, (e) PRA-BER, and (f) ECO-PRA, observed (dots) and simulated by the present simulations (crosses) in the 8 days analysed. Figure from [7].

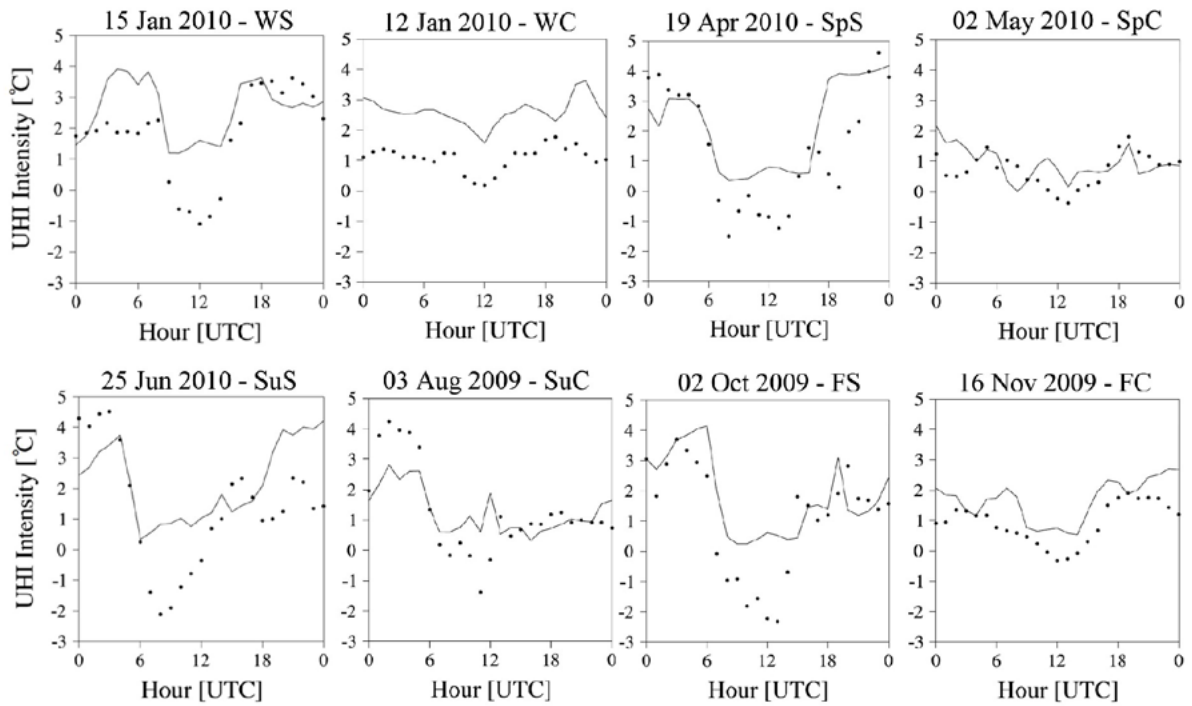


Fig. 5 Diurnal cycles of UHI intensity, calculated as the temperature difference between PRA and Roncafort weather station (see Fig. 1), as observed (dots) and simulated by the present simulations (solid line) in the 8 days analysed. Figure from [7].

# High resolution hindcast simulations over Italy with COSMO-CLM model

Montesarchio M.<sup>1,2\*</sup>, Mercogliano P.<sup>1,2</sup> and Bucchignani E.<sup>1,2</sup>

<sup>1</sup>Centro Euro-Mediterraneo sui Cambiamenti Climatici (CMCC) - Italy,

<sup>2</sup>Centro Italiano Ricerche Aerospaziali (CIRA) - Italy

\*Corresponding Author: m.montesarchio@cira.it

## Abstract

In this work, a reconstruction of the past Italian climate of Italy has been obtained with the regional climate model COSMO-CLM. Two hindcast simulations have been performed: the first one is driven by ERA-Interim Reanalysis (covering the time period 1979-2005), whereas the second one has been forced by the global climate model CMCC-MED (considering the timeframe 1950-2005). Model performance evaluation has been assessed comparing results with the E-OBS dataset. In order to characterize the uncertainty of the two simulations performed, the average values of 2-meter mean temperature and total precipitation have been analyzed over seven climate subregions defined according with the Köppen-Geiger classification.

**Keywords:** Regional climate modeling, Italian peninsula, past climate, performance evaluation

## 1. INTRODUCTION

The effects of changes on climate variables are felt regionally through water demand, ecosystems and agriculture. In this view, several studies have been conducted over Mediterranean region [e.g. 1, 2, 3] in order to estimate, through the usage of Regional Climate Models (RCMs), climate change projections over this very particular area, identified as one of the most vulnerable zone to climate change [1]. In order to obtain useful information on future climate projections, it is firstly fundamental to assess the RCMs capabilities in reproducing past climate of a specific area of interest. To this aim, considerable works have been conducted over Europe: in the frame of PRUDENCE [4] and ENSEMBLES [5] projects, several RCMs have been evaluated and compared to available observations, revealing a warm bias in the extreme seasons and a tendency to cold biases in the transition ones; furthermore, all the RCMs exhibit a tendency to over-predict precipitation. Recently, within the WCRP Coordinated Regional Downscaling Experiment (CORDEX) project [6], a high resolution RCM ensemble for Europe (EURO-CORDEX) has been completed at spatial resolution of 0.11°; performances of individual models in representing the basic spatio-temporal patterns of the European climate for the period 1989–2008 have been evaluated against E-OBS dataset in [7], confirming the ability of RCMs to capture the basic climatic features.

Italy is characterized by different climate conditions, being influenced mainly by Mediterranean Sea and by the presence of Apennines and Alps, the highest mountainous European chain. Following the Köppen-Geiger classification [8], three main climate categories are identified in Italy (see [Fig. 1 (a)]): 1) warm temperate climate (with dry and hot summer, *Csa*; dry and warm summer, *Csb*; fully humid with hot summer, *Cfa*; fully humid, with warm summer, *Cfb*), characterized by minimum temperatures in the range between -3°C and +18°C; 2) snow climate (fully humid, with warm summer, *Dfb*; fully humid, with cool summer and cold winter, *Dfc*), characterized by minimum temperatures less than or equal to -3°C; 3) polar climate (tundra climate, *ET*), characterized by maximum temperature lower than +10°C, both in the Alpine region.

Due to this high climate variability, the usage of a high resolution RCM can be a useful tool to represent the Italian climate [9]. In this framework, the added value of

using finer scale to represent the climate at local scale has been already assessed in several studies. For example, in [10] a comparison between two simulations over Alpine region at  $0.125^\circ$  (about 14km) and  $0.0715^\circ$  (about 8km) has been performed: results show that precipitation and temperature are better represented when the finest scale is adopted over this area with very complex topography, characterized by particular climate features. Furthermore, RCMs allow also to obtain a detailed reconstruction of climate variables in a not recent past, which can be used for several applications and also to facilitate impact studies and adaptation strategies [11].

In this work, two simulations at  $0.0715^\circ$  (about 8km) of spatial resolution have been carried out over the Italian peninsula with the RCM COSMO-CLM [12]: the first one, covering the period 1979-2005 is driven by ERA-Interim Reanalysis [13], while the second one, covering the period 1950-2005 is driven by the output of the global model CMCC-MED [14]. Model performances have been evaluated analyzing average surface temperature and precipitation values and comparing the results with E-OBS gridded dataset. The principal aim is, then, to provide a reconstruction of the average features of the past climate over Italy and to characterize the uncertainty of the two simulations analyzed.

## 2. MODEL AND OBSERVATIONS

COSMO-CLM is the climate version of COSMO model [15], developed by the CLM Community. Its non-hydrostatic formulation allows a better representation of convective phenomena and subgrid scale physical processes. The model can be used for simulations on time scales up to centuries and spatial resolutions between 1 and 50 km. A detailed description of COSMO-CLM model, its main characteristics and the optimized configuration adopted in this study is reported in [10].

The simulations have been performed over the area shown in [Fig. 1(b)] at  $0.0715^\circ$  of horizontal resolution (about 8km). As regards the forcing data, ECHAM5 [16] (the atmospheric component of CMCC-MED) and ERA-Interim Reanalysis have a horizontal resolution of  $0.75^\circ$  (about 85km) and  $0.703125^\circ$  (about 79km) respectively.

Model results have been compared with the E-OBS dataset vs.9 [17]: it is a European daily high resolution ( $0.25^\circ \times 0.25^\circ$ ) gridded dataset for several variables,

including temperature (mean, minimum and maximum) and precipitation, for the period 1950-2012. It is widely used for evaluation of regional climate simulations over Europe. However, it is important to point out that it is affected by a number of potential uncertainties [18]. In particular, over Italy the number of stations from which the dataset has been obtained through interpolation technique is very low, especially for the southern regions (detailed information about the E-OBS station network is available in [17]).

All images presented in this paper have been obtained using CLIME, a special purpose GIS software integrated in ESRI ArcGIS Desktop 10.X, developed at CMCC (ISC Division) in the frame of Project GEMINA in order to easily evaluate multiple climate features and to study climate changes over specific geographical domains (more details are available at <http://www.cmcc.it/it/servizi-climatici/clime-the-gis-software-developed-by-cmcc-isc-division-2>).

### 3. MODEL PERFORMANCES

In this section, model performances in simulating 2-meter temperature (T2m) and precipitation are evaluated. The analyses reported hereinafter have been carried out over two different time periods, according with the whole timeframe of the two simulations: the CMCC-MED driven simulation, cited as `clm_cmccmed`, has been analyzed over 1951-2005; the ERA-Interim driven simulation, cited as `clm_eraint`, has been evaluated over 1980-2005. In both cases, the first year (1950 and 1979 respectively) has been neglected to reduce spin-up effects due to the initial conditions.

[Fig. 2] and [Fig. 3] show seasonal bias distribution of `clm_cmccmed` with respect to the E-OBS data over the whole Italian peninsula, respectively for temperature and precipitation. To this aim, an upscaling of model output on the dataset grid has been performed using the natural neighbor technique. Furthermore, for the evaluation of temperature bias, a height correction has been carried out (according with several literature works, e.g [7,19]), using the E-OBS orography as reference and applying a constant lapse rate of 0.0065 K/m. [Fig. 2] shows a tendency of the `clm_cmccmed` to underestimate the T2m in all seasons, more evident in winter and in correspondence of the mountainous chains, with a cold bias even higher than  $-4^{\circ}\text{C}$ . It might be partially ascribed to the global forcing data, since most Atmosphere-Ocean General Circulation Models (AOGCMs) are characterized by a general temperature

underestimation [20]; in particular, in the report [21] performances of the CMCC-MED model have been evaluated and compared with other state-of-the-art global coupled models, confirming a general tendency to underestimate the T2m, especially in winter over the Alpine region, although the temperature spatial pattern is well reproduced. In summer, `clm_cmccmed` simulation shows a better agreement over Alpine arc and Apennines, but with a slight warm bias (always lower than 2°C) over Po valley and along the eastern coast of Italy.

Concerning precipitation ([Fig. 3]), an overestimation occurs over the Alpine region in all seasons, especially in spring when peaks of 5 mm/day are reached in western Alps. It is partially ascribed to an underestimation of E-OBS precipitation caused by hydrometeor deflections [22]. Po valley is characterized by a very good agreement with observations (bias never exceeding 0.5 mm/day in absolute value), with the exception of autumn, when a general underestimation occurs in the whole central Italy. Finally, in southernmost regions, a general overestimation occurs in winter and spring, whereas in summer and autumn precipitation is generally well represented, with a bias lower than 1 mm/day.

A comparison between `clm_eraint` and observations (results not shown here, reported in [23]) reveals a general better agreement for temperature and precipitation values in all seasons with the exception of summer months, characterized by strong dry and warm biases (reaching peaks of 3mm/day and 3°C over Po Valley). This tendency to overestimate summer temperature is probably due to the underestimation of latent heat fluxes, that leads to overestimate sensible heat fluxes [24].

It is important to highlight that the `clm_eraint` simulation is affected by a lower bias compared to other literature works, carried out at coarser resolution, confirming the important role of using a finer scale, even if the bias pattern is anyway similar. For example, evaluation of regional climate simulations driven by ERA-Interim Reanalysis over EURO-CORDEX domain [7] reveals that most of models are affected by a temperature underestimation in winter months (in some cases up to -5K) and a summer overestimation (between 2 and 3K) over Italian domain; in addition, a general summer underestimation of precipitation in center Italy and a winter overestimation (higher on the Alps) is recorded.

Performance evaluation in terms of annual cycle, PDFs and trend analysis have also been carried out (without interpolation of model output on the observations grid) considering the seven climate subregions individuated for Italy by Köppen-Geiger classification (Cfa, Cfb, Csa, Csb, Dfb, Dfc and ET hereinafter).

[Fig. 4(a)] and [Fig. 4(b)] show the bias of annual cycle of T2m and precipitation respectively. The `clm_cmccmed` simulation generally underestimates the temperature in the Italian peninsula (as already highlighted in [Fig. 2]). Only in June and July a very slight overestimation (lower than  $0.5^{\circ}\text{C}$ ) occurs in Csa and Cfa, corresponding to coastal areas. Dfb subregion is affected by the highest bias (with a peak of  $4^{\circ}\text{C}$ ), but it can be partially ascribed to the low number of observation stations: only four E-OBS grid points are present in this area. For precipitation, instead, subregions corresponding to the temperate climate (Cfa, Cfb, Csa and Csb) show a very good agreement with the E-OBS dataset (error lower than  $1.8\text{ mm/day}$ ), whereas the areas corresponding to snow and polar climates reveal a strong overestimation of precipitation values, especially in spring, reaching also  $4\text{ mm/day}$  of differences (also in this case confirming the results shown in [Fig. 3]).

[Tab. 1] and [Tab. 2] report three synthetic errors for the two simulations with respect to the observations: BIAS (COSMO-CLM minus E-OBS), MAE (Mean Absolute Error) and RMSE (Root Mean Square Error). For each index, the 95% bootstrap confidence intervals are provided, calculated using the bias corrected and accelerated percentile method [25], considering 10000 resamples. They confirm the good agreement of `clm_eraint` simulation in reproducing the two variables studied, especially when temperate regions are considered. The highest peaks of bias are always reached in Dfb subregions (excepted when the precipitation of `clm_cmccmed` is considered) but, as already explained, in this area results are strongly influenced by the low number of observation stations. It is worth noting that confidence intervals are small for all the T2m indices in all the subregions (for both simulations) whereas, when precipitation is considered, the confidence interval of synthetic indices computed for Dfb, Dfc and ET subregions are slightly higher with respect to the temperate regions.

For precipitation, also the PDFs of daily values have been analyzed, considering only precipitation greater than  $0.1\text{ mm/day}$  (in [Fig. 5] the results for only two subregions, ET and Csa, are shown). A strong overestimation of drizzle precipitation

(0.1–1mm) is observed (slightly higher for the `clm_eraint` simulation than the `clm_cmccmed` one), more accentuate in temperate regions, and a general underestimation of moderate precipitation. Heavy precipitation is, instead, well reproduced, especially when the `clm_eraint` simulation is considered. Several studies have already highlighted this tendency to overestimate low precipitation rates (e.g [26]), although they show an overestimation of heavy precipitation not identified in our work.

The time series of variables under study for the seven subregions are displayed in [Fig. 6] and [Fig. 7]. For `clm_cmccmed`, the 5-yr running mean have also been considered. As regards the T2m, a general good agreement between `clm_eraint` and the observational dataset is found, especially for the subregions characterized by warm temperate climate (Cfa, Cfb, Csa and Csb subregions), whereas in snow and polar climates subregions a temperature underestimation occurs, with a strong cold bias over the Dfb subregion (as already described, in this case results are influenced by the difference between the number of modeled and E-OBS grid points). The `clm_cmccmed`, instead, is characterized by a stronger underestimation in all the subregions considered. Furthermore, a strong difference in terms of trend between this simulation and the observations is evident. Indeed, a negative trend is found applying the Mann-Kendall non parametric test [Tab. 3], stronger when the period 1980-2005 is taken into account. On the other hand, the `clm_eraint` simulation has the same trend sign of the E-OBS, although also in this case it is underestimated in the warm temperate regions, whereas a very good agreement with the observations occurs over high altitude areas. However, only observations show significant trend values in all the subregions, at a confidence level of 95% (with the exception of the Dfb one for the period 1980-2005), whereas modeled values are significant only in some areas.

The positive temperature trends found with E-OBS and `clm_eraint` are in agreement with analysis reported in [27], where time series of minimum and maximum temperatures (obtained from several Italian stations for the period 1865- 1996) are characterized by a positive trend, more pronounced in southern Italy. Also in [28] authors assessed a temperature increase in the timeframe 1920-1993, when especially the last years gave the highest contribution (indeed, also E-OBS data confirm that the trend value is higher when a more recent timeframe is considered).

Precipitation time series ([Fig. 7]), as already shown in [Fig. 4(b)] reveal a very good agreement between observed and simulated values when the warm temperate climate regions are considered, but a strong wet bias occurs over Alpine region (higher for `clm_cmccmed`). However, it is worth noting that precipitation results are influenced by the E-OBS systematic undercatchment of rain gauges [29,30] that lead to an underestimation of the precipitation amount. Analysis of trend values [Tab. 4] reveals that, considering the timeframe 1951-2005, only observations are characterized by a significant trend (at a confidence level of 95%), and only for Csb and Dfb subregions. When the more recent timeframe is taken into account, a good agreement between both simulations and E-OBS data is found, showing a general, in some cases very slight, precipitation decrease (with the exception of Dfc subregion, where only observations reveal an increase of precipitation amount). This general decreasing precipitation trend has already been found in [31,32]: in these works, authors analyzed daily precipitation records for several subareas of Italian peninsula, considering the timeframe 1951-1996 and 1921-1998 respectively; they recorded a general tendency to a reduction of precipitation, even though in most cases trends were not significant (as in the present analysis).

#### 4. CONCLUSIONS

In this study, a reconstruction of the past Italian climate of Italy with the regional climate model COSMO-CLM has been performed. Model capabilities in reproducing the past Italian climate have been assessed in “perfect” and “sub-optimal” boundary conditions by using as forcing ERA-Interim Reanalysis and the output of the global model CMCC-MED respectively. Averaged values of 2-meter mean temperature and precipitation have been evaluated, comparing the model results with E-OBS observational dataset.

Results show a satisfactory agreement of the ERA-Interim driven simulation, whereas the simulation forced by the global model is characterized by worse performances. It is important to highlight that:

1. trend analysis for the ERA-Interim simulation is consistent with results found in other literature studies (i.e. a temperature increase and a slight precipitation decrease); however a quantitative comparison with reference works is not applicable, since period and observations considered are different;

2. bias assessment has been evaluated over homogeneous areas individuated following the Köppen-Geiger classification: in some case, these subregions are very small, leading to a more stringent test of the model performances;

3. the strong differences between `clm_eraint` e `clm_cmccmed` results confirm the strong dependence of the results provided by a dynamical downscaling from the quality of the data provided by the AOGCMs adopted.

In order to overcome the not negligible bias affecting global model driven simulation, bias correction techniques must be applied [33,34] to reduce this significant bias, especially when the regional model output is used as input for impact studies [35].

The present analysis has been focused only on average climate properties, rather than on variability or extremes; in a successive work, the performed simulations will be analyzed also in order to investigate the capabilities of COSMO-CLM in reproducing climate extreme values over Italy.

## 5. ACKNOWLEDGMENTS

This paper has been developed within the framework of Work Package A.2.2 of the GEMINA project, funded by the Italian Ministry of Education, University and Research and the Italian Ministry of Environment, Land and Sea. The authors thank dr. Alessandra Lucia Zollo (CIRA-CMCC) for the support provided for the analysis of the results.

## 6. REFERENCES

1. Giorgi F. and Lionello P. (2008), *Climate change projections for the Mediterranean region*, Global and Planetary Change, 63(2), 90-104.
2. Ulbrich, U., et al., 2006. The Mediterranean climate change under global warming. In: Lionello P., Malanotte-Rizzoli P., Boscolo R. (Eds.), *Mediterranean Climate Variability*. Elsevier, Amsterdam, pp. 398–415.
3. Sànchez E., Gallardo C., Gaertner M.A., Arribas A. and Castro M. (2004), *Future climate extreme events in the Mediterranean simulated by a regional climate model: a first approach*, Global and Planetary Change, 44(1), 163-180.

4. Jacob D., Bärring L., Christensen O.B., Christensen J.H., de Castro M., Déqué M., Giorgi F., Hagemann S., Hirschi, M., Jones R., Kjellström E., Geert L., Rockel B., Sánchez E., Schär C., Seneviratne S.I., Somot S., van Ulden A., van den Hurk B. (2007), *An inter-comparison of regional climate models for Europe: model performance in present-day climate*. *Climatic Change*, 81(1), 31-52
5. Van der Linden P. and Mitchell J. (2009), *Ensembles: Climate change and its impacts: Summary of research and results from the ensembles project*. Met Office Hadley Centre 2, 1–160.
6. Giorgi F., Jones C. and Asrar G.R. (2009), *Addressing climate information needs at the regional level: the CORDEX framework.*, World Meteorological Organization (WMO) Bulletin, 58(3), 175-183.
7. Kotlarski S., Keuler K., Christensen O.B., Colette A., Déqué M., Gobiet A., Goergen K., Jacob D., Lüthi D., van Meijgaard E., Nikulin G., Schär C., Teichmann C., Vautard R., Warrach-Sagi K. and Wulfmeyer V. (2014), *Regional climate modeling on European scales: a joint standard evaluation of the EURO-CORDEX RCM ensemble*, *Geoscientific Model Development Discussions*, 7(1),217-293.
8. Kottek M., Grieser J., Beck C., Rudolf B. and Rubel F. (2006), *World Map of the Köppen-Geiger climate classification updated*, *Meteorologische Zeitschrift*, 15(3), 259-263.
9. Coppola E. and Giorgi F. (2010), *An assessment of temperature and precipitation change projections over Italy from recent global and regional climate model simulations*, *International Journal of Climatology*, 30(1), 11-32.
10. Montesarchio M., Zollo A.L., Bucchignani E., Mercogliano P. and Castellari S. (2014), *Performance evaluation of high-resolution regional climate simulations in the Alpine space and analysis of extreme events*, *Journal of Geophysical Research*, 119 (6), 3222–3237. DOI: 10.1002/2013JD021105.
11. Rummukainen M. (2010), *State-of-the-art with regional climate models*. *WIREs Climate Change*, 1, 82–96. doi: 10.1002/wcc.8

12. Rockel B., Will A. and Hense A. (2008), *The Regional Climate Model COSMO-CLM (CCLM)*. Meteorologische Zeitschrift, 17(4), 347-348. DOI 10.1127/0941-2948/2008/0309.

13. Dee D.P., Uppala S.M., Simmons A.J., Berrisford P., Poli P., Kobayashi S., Andrae U., Balmaseda M.A., Balsamo G., Bauer P., Bechtold P., Beljaars A.C.M., van de Berg L., Bidlot J., Bormann N., Delsol C., Dragani R., Fuentes M., Geer A.J., Haimberger L., Healy S.B., Hersbach H., Hólm E.V., Isaksen L., Kållberg P., Köhler M., Matricardi M., McNally A.P., Monge-Sanz B.M., Morcrette J.J., Park B.-K., Peubey C., de Rosnay P., Tavolato C., Thépaut J.-N. and Vitart F. (2011), *The ERA-Interim reanalysis: Configuration and performance of the data assimilation system*, Quarterly Journal of the Royal Meteorological Society, 137(656), 553-597.

14. Gualdi S., Somot S., Li L., Artale V., Adani M., Bellucci A., Braun A., Calmanti S., Carillo A., Dell'Aquila A., Déqué M., Dubois C., Elizalde A., Harzallah A., Jacob D., L'Hévéder B., May W., Oddo P., Ruti P., Sanna A., Sannino G., Scoccimarro E., Sevault F., Navarra A. (2012), *The CIRCE simulations: a new set of regional climate change projections performed with a realistic representation of the Mediterranean Sea*. Bulletin of the American Meteorological Society, 10.1175/BAMS-D-11-00136.1.

15. Steppeler J., Doms G., Schättler U., Bitzer H.W., Gassmann A., Damrath U. and Gregoric G. (2003), *Meso-gamma scale forecasts using the non-hydrostatic model LM*. Meteorology and Atmospheric Physics, 82 (1-4), 75-96.

16. Roeckner E., Bäuml G., Bonaventura L., Brokopf R., Esch M., Giorgetta M., Hagemann S., Kirchner I., Kornblueh L., Manzini E., Rhodin A., Schlese U., Schulzweida U. and Tompkins A. (2003), *The atmospheric general circulation model ECHAM5. Part I: Model description*, Max Planck Institute for Meteorology, Hamburg, Germany, Rep. No. 349.

17. Haylock M.R., Hofstra N., Klein Tank A.M.G., Klok E.J., Jones P.D. and New M. (2008), *A European daily high-resolution gridded dataset of surface temperature and precipitation*, Journal of Geophysical Research, 113(D20), DOI 10.1029/2008JD010201

18. Hofstra N., Haylock M., New M. and Jones P.D. (2009), *Testing E-OBS European high-resolution gridded data set of daily precipitation and surface temperature*, Journal of Geophysical Research, 114(D21101), doi:10.1029/2009JD011799.

19. Jaeger E.B., Anders I., Lüthi D., Rockel B., Schär C. and Seneviratne S.I. (2008), *Analysis of ERA40-driven CLM simulations for Europe*, Meteorologische Zeitschrift, 17(4), 349-367.

20. Macadam I., Pitman A.J., Whetton P. H. and Abramowitz G. (2010), *Ranking climate models by performance using actual values and anomalies: Implications for climate change impact assessments*. Geophysical research letters, 37(16).

21. TRUST project (2010) Report describing the method and including the spatially resolved temporal trends of relevant climate parameters. Deliverable 4.1, available at <http://www.lifetrust.it/>

22. Frei C., Christensen J.H., Déqué M., Jacob D., Jones R. G. Vidale P.L.(2003), *Daily precipitation statistics in regional climate models: Evaluation and intercomparison for the European Alps*, Journal of Geophysical Research: Atmospheres (1984-2012), 108(D3)

23. Bucchignani E., Mercogliano P., Manzi M.P., Montesarchio M., Rillo V. (2013), RP0183 - *Assessment of ERA-Interim driven simulation over Italy with COSMO-CLM* - CMCC Research Paper

24. Bellprat O., Kotlarski S., Lüthi D. and C. Schär (2012), *Objective calibration of regional climate models*, Journal of Geophysical Research: Atmospheres, 117, D23115, doi:10.1029/2012JD018262.

25. DiCiccio T. J. and Efron B. (1996) *Bootstrap confidence intervals*. Statistical Science, 11(3), 189--228.

26. Gutowski Jr W.J., Decker S.G., Donavon R.A., Pan Z., Arritt R.W. and Takle E.S. (2003) *Temporal-spatial scales of observed and simulated precipitation in central US climate*. Journal of Climate, 16(22), 3841-3847.

27. Brunetti M., Buffoni L., Maugeri M. and Nanni T. (2000), *Trends of minimum and maximum daily temperatures in Italy from 1865 to 1996*, Theoretical and Applied Climatology, 66(1-2), 49-60.

28. Maugeri M. and Nanni T. (1998) *Surface air temperature variations in Italy: recent trends and an update to 1993*. Theoretical and applied climatology. 61(3-4), 191-196

29. Kotlarski S., Bosshard T., Lüthi D., Pall P. and Schär C. (2012), *Elevation gradients of European climate change in the regional climate model COSMO-CLM*. Climatic change, 112(2), 189-215.

30. Turco M., Zollo A.L., Ronchi C., De Luigi C. and Mercogliano P. (2013), *Assessing gridded observations for daily precipitation extremes in the Alps with a focus on northwest Italy*, Natural Hazards and Earth System Science, 13(6), 1457-1468.

31. Brunetti M., Colacino M., Maugeri M. and Nanni T. (2001), *Trends in the daily intensity of precipitation in Italy from 1951 to 1996*, International Journal of Climatology, 21(3), 299-316.

32. Brunetti M., Maugeri M. and Nanni T. (2001), *Changes in total precipitation, rainy days and extreme events in northeastern Italy*, International Journal of Climatology, 21(7), 861-871.

33. Lafon T., Dadson S., Buys G. and Prudhomme C. (2013), *Bias correction of daily precipitation simulated by a regional climate model: a comparison of methods*. International Journal of Climatology, 33(6), 1367-1381.

34. Zollo A.L., Rianna G., Mercogliano P., Tommasi P. and Comegna L. (2014) - *Validation of a Simulation Chain to Assess Climate Change Impact on Precipitation Induced* – Landslide Science for a Safer Geoenvironment pp 287-292 - Proceedings of World Landslide Forum 3, 2-6 June 2014, Beijing.

35. Teutschbein C. and Seibert Jan (2012), *Bias correction of regional climate model simulations for hydrological climate-change impact studies: Review and evaluation of different methods*, Journal of Hydrology, 456,12-29

## 7. IMAGES AND TABLES

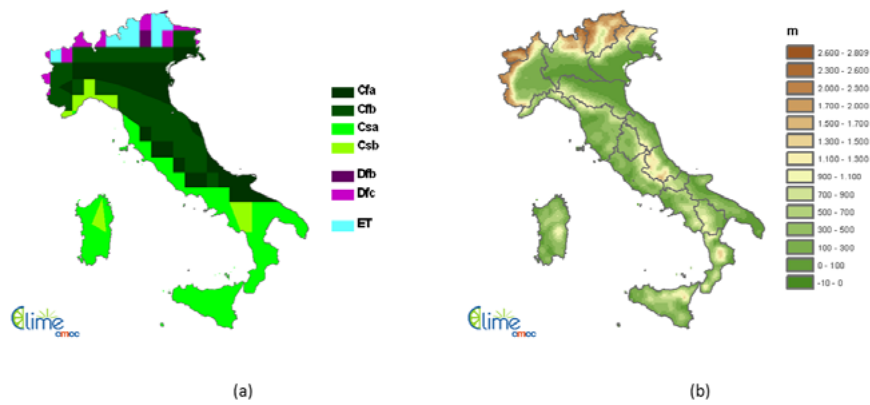


Fig. 1 Köppen-Geiger classification of Italian climate (a) and orography of COSMO-CLM at 0.0715° of resolution for Italian peninsula.

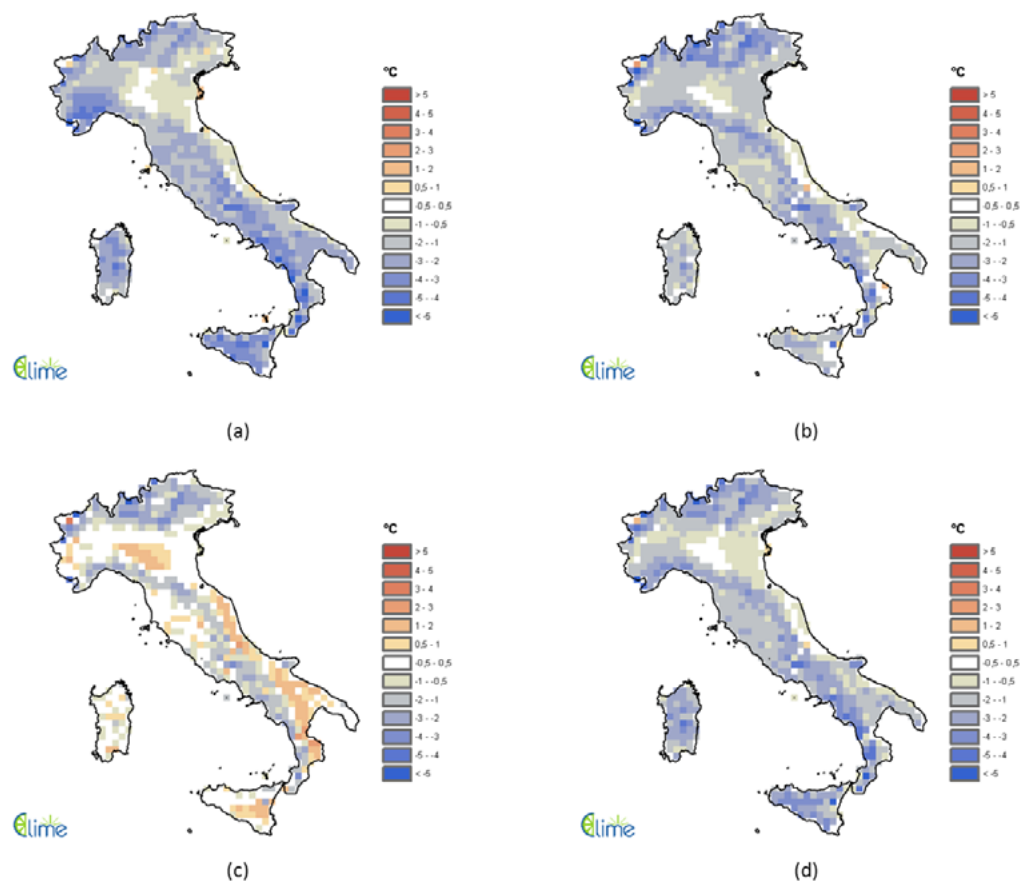


Fig. 2 2-meter mean temperature bias distribution (°C) of clm\_cmccmed with respect to E-OBS: DJF (a), MAM (b), JJA (c) and SON (d) seasons.

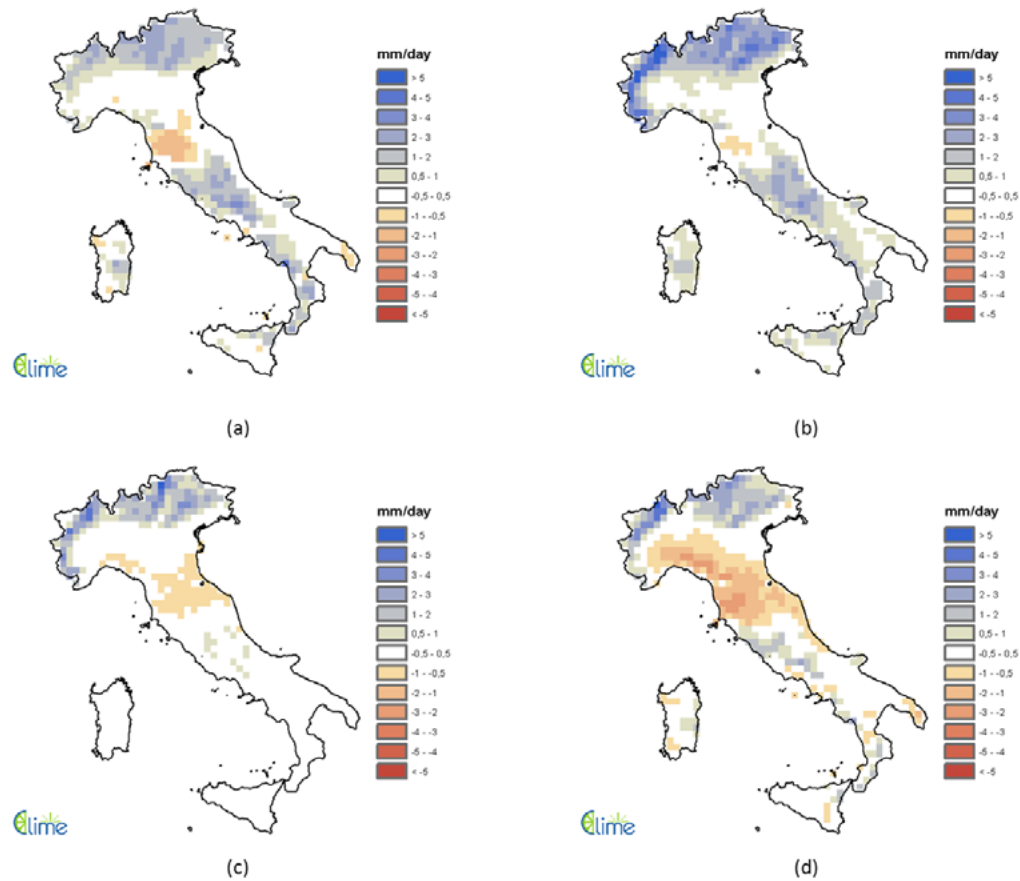


Fig. 3 Precipitation bias distribution (mm/day) of clm\_cmccmed with respect to E-OBS: DJF (a), MAM (b), JJA (c) and SON (d) seasons.

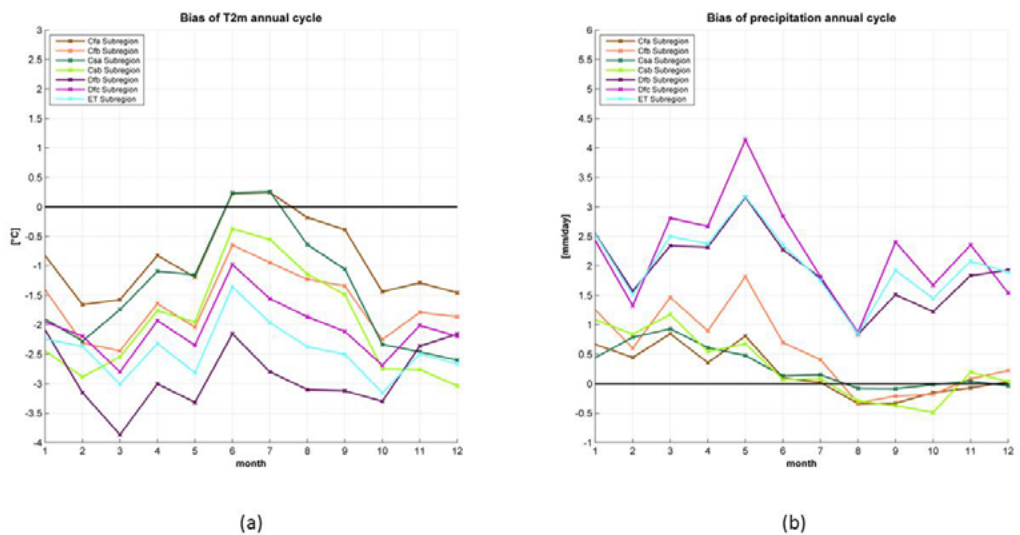


Fig. 4 Bias of annual cycle of clm\_cmccmed with respect to E-OBS, for the seven climate subregions, in terms of 2-meter temperature (a) and precipitation (b).

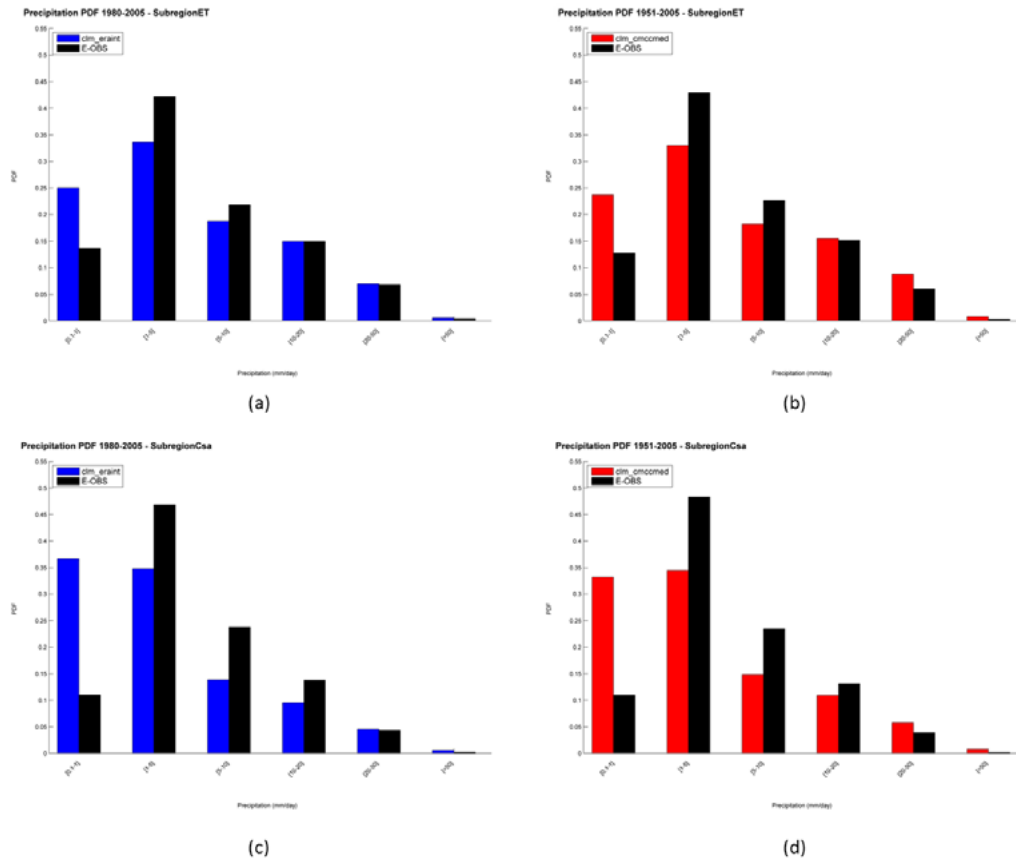


Fig. 5 PDFs of daily precipitation of clm\_eraint (left panels) and clm\_cmccmed (right panels) with respect to E-OBS, for ET (upper panels) and Csa (bottom panels) subregions.

		Cfa	Cfb	Csa	Csb	Dfb	Dfc	ET
TEMPERATURE	E-OBS (°C)	13.55	11.37	15.34	13.04	7.93	4.61	3.19
	BIAS (°C)	0.27	-0.55	-0.20	-0.92	-1.77	-0.83	-1.30
		(0.15; 0.37)	(-0.63; -0.47)	(-0.31; -0.08)	(-1.05; -0.80)	(-1.84; -1.71)	(-0.89; -0.78)	(-1.37; -1.25)
	MAE (°C)	0.82	0.73	0.91	1.15	1.78	0.85	1.31
		(0.76; 0.89)	(0.67; 0.79)	(0.85; 0.98)	(1.05; 1.25)	(1.71; 1.84)	(0.80; 0.90)	(1.25; 1.37)
RMSE (°C)	1.02	0.90	1.07	1.46	1.87	0.98	1.42	
	(0.95; 1.10)	(0.84; 0.96)	(1.01; 1.14)	(1.36; 1.57)	(1.81; 1.93)	(0.93; 1.03)	(1.35; 1.48)	
PRECIPITATION	E-OBS (mm/day)	1.76	2.60	1.44	2.02	1.80	3.30	2.66
	BIAS (mm/day)	-0.06	0.03	-0.13	-0.26	1.47	1.09	1.26
		(-0.12; 0.00)	(-0.07; 0.13)	(-0.19; -0.08)	(-0.35; -0.18)	(1.33; 1.61)	(0.95; 1.24)	(1.13; 1.39)
	MAE (mm/day)	0.41	0.69	0.36	0.58	1.57	1.28	1.35
		(0.37; 0.45)	(0.63; 0.76)	(0.32; 0.40)	(0.52; 0.65)	(1.45; 1.70)	(1.16; 1.42)	(1.24; 1.47)
RMSE (mm/day)	0.54	0.91	0.51	0.81	1.92	1.73	1.71	
	(0.49; 0.61)	(0.83; 1.01)	(0.46; 0.57)	(0.73; 0.92)	(1.79; 2.06)	(1.59; 1.91)	(1.59; 1.84)	

Tab. 1 Average value of T2m (°C) and precipitation (mm/day) of E-OBS dataset over the seven climate subregions and synthetic errors of clm\_eraint with respect to E-OBS (with 95% bootstrap confidence level in brackets). The timeframe considered is 1980-2005.

		Cfa	Cfb	Csa	Csb	Dfb	Dfc	ET
TEMPERATURE	E-OBS (°C)	13.24	11.07	15.06	12.66	7.53	4.31	2.85
	BIAS (°C)	-0.86	-1.66	-1.40	-1.97	-2.87	-2.05	-2.44
		(-1.03;-0.7)	(-1.83;-1.49)	(-1.55;-1.23)	(-2.14;-1.81)	(-3.04;-2.69)	(-2.23;-1.88)	(-2.62;-2.25)
	MAE (°C)	1.88	2.22	2.03	2.43	3.13	2.53	2.84
		(1.77;2)	(2.1;2.35)	(1.92;2.14)	(2.31;2.56)	(2.98;3.28)	(2.4;2.67)	(2.69;2.99)
RMSE (°C)	2.37	2.75	2.51	2.97	3.67	3.10	3.42	
	(2.25;2.51)	(2.61;2.91)	(2.39;2.64)	(2.83;3.12)	(3.53;3.84)	(2.96;3.27)	(3.27;3.59)	
PRECIPITATION	E-OBS (mm/day)	1.84	2.73	1.47	2.20	1.97	3.27	2.70
	BIAS (mm/day)	0.20	0.56	0.28	0.30	1.94	2.24	2.03
		(0.1;0.3)	(0.41;0.71)	(0.19;0.37)	(0.16;0.43)	(1.77;2.12)	(2.05;2.44)	(1.87;2.2)
	MAE (mm/day)	0.36	0.66	0.36	0.51	1.95	2.24	2.03
		(0.3;0.43)	(0.55;0.78)	(0.3;0.43)	(0.42;0.59)	(1.77;2.12)	(2.05;2.44)	(1.87;2.19)
RMSE (mm/day)	0.44	0.79	0.44	0.60	2.06	2.36	2.12	
	(0.37;0.52)	(0.69;0.91)	(0.37;0.53)	(0.52;0.69)	(1.89;2.23)	(2.17;2.58)	(1.97;2.28)	

Tab. 2 Average value of T2m (°C) and precipitation (mm/day) of E-OBS dataset over the seven climate subregions and synthetic errors of clm\_cmccmed with respect to E-OBS (with 95% bootstrap confidence level in brackets). The timeframe considered is 1951-2005.

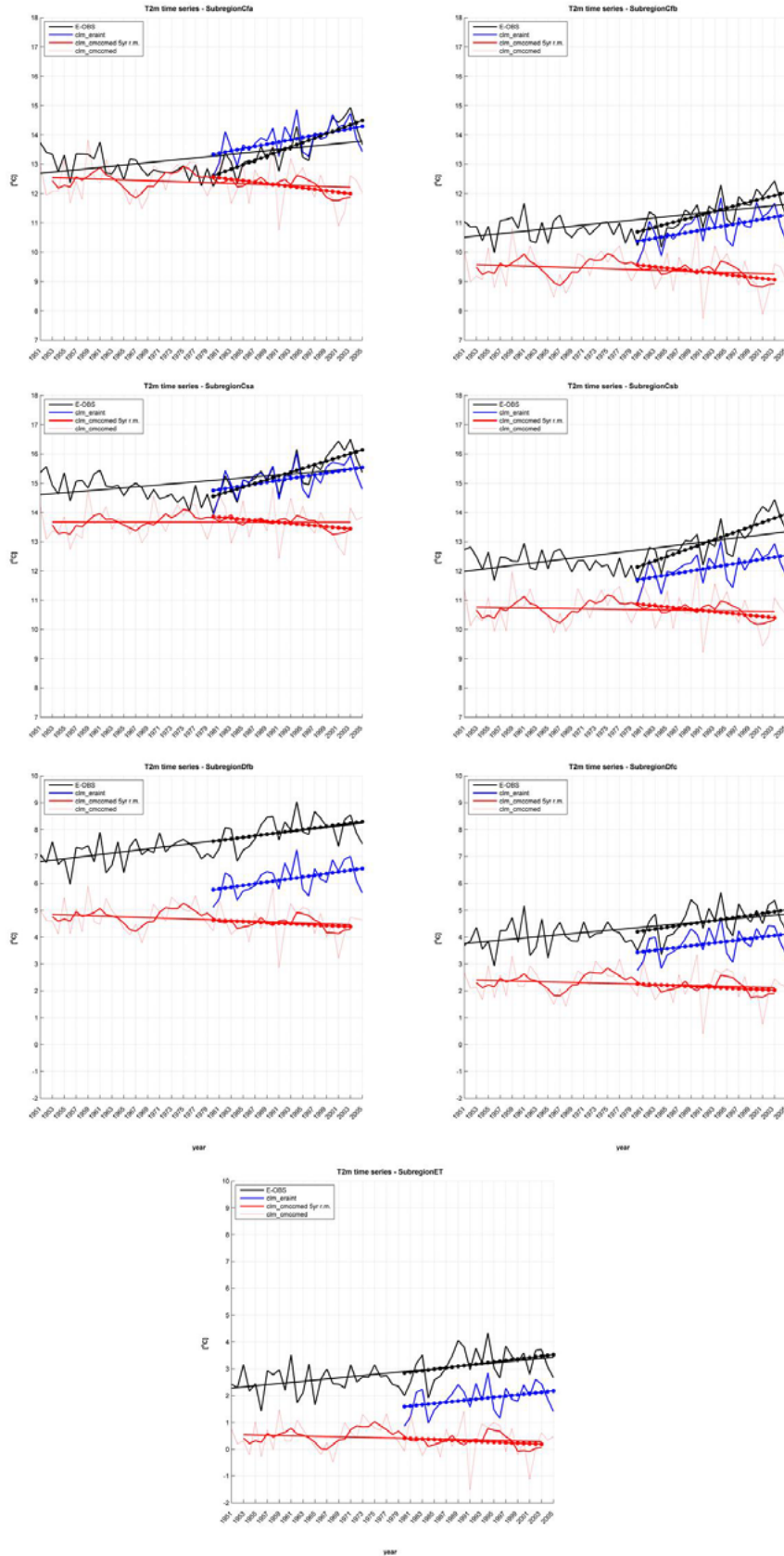


Fig. 6 2-meter mean temperature time series (°C) of clm\_cmccmed, clm\_eraint and E-OBS for the seven climate subregions. Trend dashed lines with circle symbols refer to the period 1980-2005.

	°C/yr (*10 <sup>-2</sup> )						
	Cfa	Cfb	Csa	Csb	Dfb	Dfc	ET
<b>E-OBS (1951-2005)</b>	2.0*	2.1*	1.7*	2.5*	2.7*	2.0*	2.1*
<b>clm_cmccmed (1951-2005)</b>	-0.7*	-0.6*	0.0	-0.3	-0.8*	-0.6*	-0.5
<b>clm_eraint (1980-2005)</b>	3.8*	3.6*	3.2*	3.4*	3.1*	2.7	2.3
<b>E-OBS (1980-2005)</b>	7.6*	5.4*	6.3*	7.3*	2.9	3.2*	2.7
<b>clm_cmccmed (1980-2005)</b>	-2.5*	-2.2*	-1.8*	-2.0*	-1.0	-1.0	-1.0

Tab. 3 2-meter mean temperature trends (°C /year) of clm\_cmccmed, clm\_eraint and E-OBS for the seven climate subregions (\* stand for significant, at a confidence level of 95%).

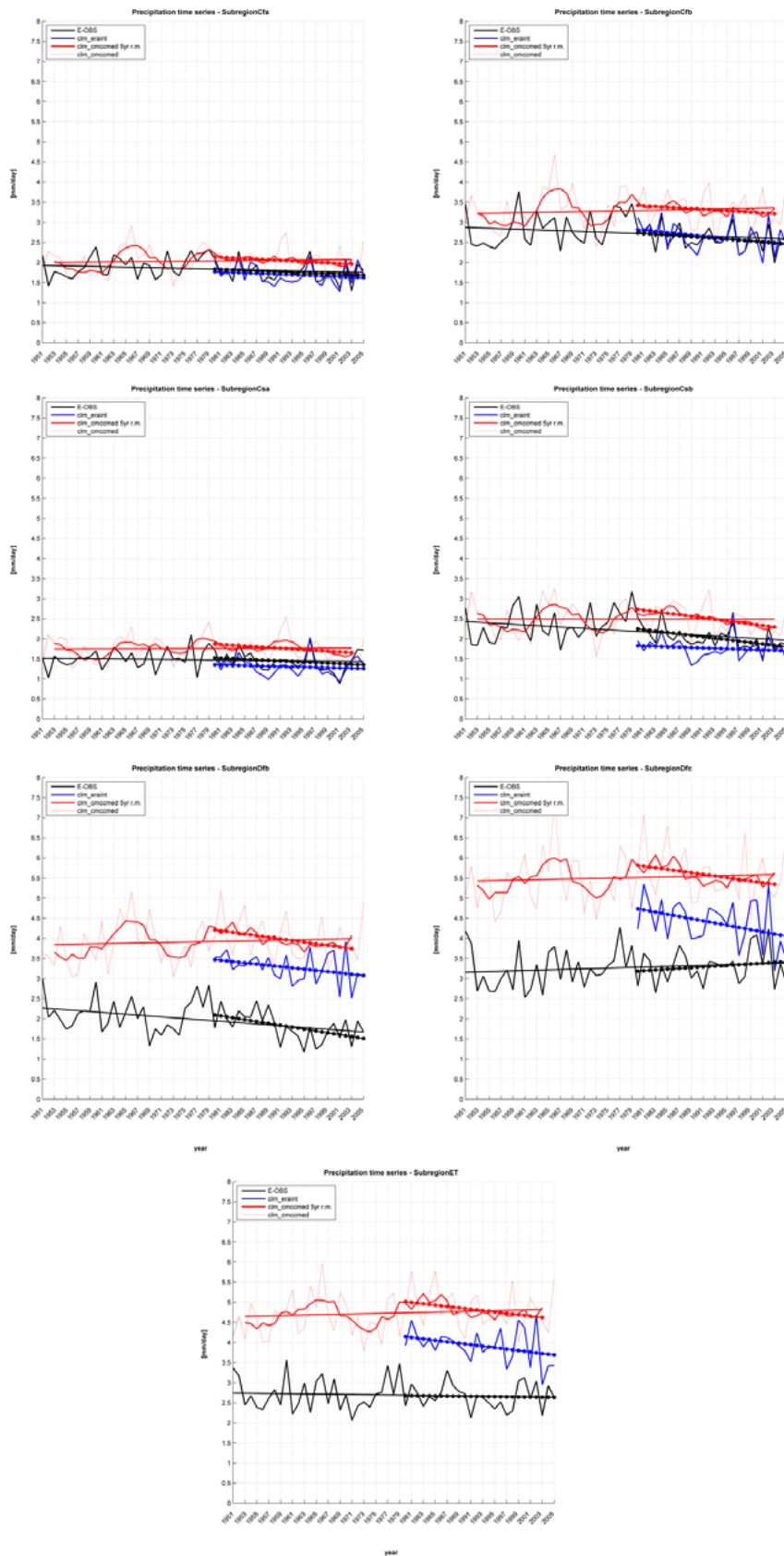


Fig. 7 Precipitation time series (mm/day) of clm\_cmccmed, clm\_eraint and E-OBS for the seven climate subregions. Trend dashed lines with circle symbols refer to the period 1980-2005.

	mm day <sup>-1</sup> / yr (*10 <sup>-2</sup> )						
	Cfa	Cfb	Csa	Csb	Dfb	Dfc	ET
<b>E-OBS (1951-2005)</b>	-0.3	-0.5	-0.1	-0.9*	-1.1*	0.4	-0.2
<b>clm_cmccmed (1951-2005)</b>	0.1	0.3	0.0	0.0	0.3	0.3	0.3
<b>clm_eraint (1980-2005)</b>	-0.6	-1.5	-0.4	-0.5	-1.6	-2.7	-1.8
<b>E-OBS (1980-2005)</b>	-0.6	-1.0	-0.7	-1.8*	-2.3*	0.9	-0.2
<b>clm_cmccmed (1980-2005)</b>	-0.8*	-0.9*	-0.9*	-1.9*	-2.0*	-2.1*	-1.7*

Tab. 4 Precipitation trends (mm day<sup>-1</sup>/year) of clm\_cmccmed, clm\_eraint and E-OBS for the seven climate subregions (\* stand for significant, at a confidence level of 95%).

# Carbon flux and climate change effects on Capo Caccia karst ecosystem (Sardinia, Italy)

Sanna L.<sup>1\*</sup>, Arca A.<sup>1</sup>, Ventura A.<sup>1</sup>, Zara P.<sup>1</sup> and Duce P.<sup>1</sup>

<sup>1</sup>Institute of Biometeorology, National Research Council - Italy

\*Corresponding Author: [sanna@ibimet.cnr.it](mailto:sanna@ibimet.cnr.it)

## Abstract

The assessment of carbon sequestration or release in the terrestrial ecosystems is crucial for understanding carbon cycling processes. Since carbon dioxide plays a key role in karst processes, it has to be taken into consideration when studying gas exchanges among atmosphere, biosphere, and geosphere. Even though karst areas have been recently used to determine the contributions of multiple carbon sink (dissolution) or source (deposition), geological processes have not been sufficiently addressed yet in global carbon cycle model. After a short summary on cave microclimatology, its atmosphere dynamic and subsurface-atmosphere-biosphere gas exchanges, this work illustrates Eddy Covariance tower and cave micrometeorological data with the purpose of assessing the correlation between meteorological variables and carbon dioxide concentration in the shrubland karst ecosystem of Capo Caccia (North-West Sardinia, Italy). The preliminary results show that the ecosystem physiological features depend not only on surface and soil environmental conditions but also on environmental forcing related to underground voids.

**Keywords:** abiotic carbon dioxide, cave atmosphere, karst ecosystem, net ecosystem carbon balance, subsurface-atmosphere-biosphere gas exchange

## 1. INTRODUCTION

Many branches of science used caves as a powerful research tool, and recognize the importance of these ecosystems from a multidisciplinary perspective [1]. Karst areas are currently strategic zones for research related to global change because caves are subject to change, often largely, in response to external environmental conditions but can also detect inertial fluctuations of the climate system [2].

Even better than most surface environments, karst systems are natural laboratories for reconstructing past climate and predict the future, since erosion that other proxies have suffered on the surface has been attenuated in the subsurface. Moreover, the medium-long term monitoring programs of cave microclimate have clearly showed the role of underground karst environment in the dynamics of subsurface-atmosphere-biosphere gas exchanges. In fact, cave atmosphere is directly connected to the surface through cave entrances and dense network of small fractures of carbonate rocks. Therefore, cave, soil and vegetation cover should be considered components of a unique ecosystem.

Although the cave environments appear to be stable and their modifications occur slowly [3], the impact of climate change on karst systems in the coming decades may help climate and environmental scientists to better predict future scenarios and large-scale events through the study of the intrinsic characteristics of these environments, even though their minor modifications. To this end, it is essential to control air temperature, relative humidity, barometric pressure and CO<sub>2</sub> content as a tracer gas (as well as other potential, i.e. Radon <sup>222</sup>Rn), in order to characterize the daily and/or seasonal variations in underground CO<sub>2</sub> compared to the outside atmosphere.

Understanding the role of the karst in the global carbon cycle is still unclear. Recent monitoring studies revealed that the concentration of CO<sub>2</sub> in cave atmosphere showed a certain degree of seasonality [4], [5], [6], [7], [8], [9].

In addition to the biotic component tied to the decomposition of organic matter, recent studies showed that only a fraction of the abnormal amount of CO<sub>2</sub> present in the caves of desert or semi-arid areas is linked to this phenomenon. In addition, they suggested an abiotic mechanism related to the processes of dissolution-precipitation of calcite and underground ventilation, and coincident with the seasonal reversal of the underground air masses flow [10].

As carbon dioxide is one of the most important greenhouse gases responsible for global warming, the aim of this work is to describe the case of Capo Caccia (North-West Sardinia, Italy) as an example of the study carbon flux on a shrubland karst ecosystem.

## 2. CAVE ATMOSPHERE

Cave environments are characterized by the lack of light, high humidity and a relatively constant air temperature similar to the annual average surface values. The study of climatic variations inside cavities (cave microclimatology) is complex since the range of parameters variation are very limited, especially in the case of temperature and relative humidity. The underground atmosphere can be considered stable and changes can only be detected using sophisticated measuring instruments.

The absence of radiation in the underground environment makes daily cycles just does not exist, except those determined by the influence of the contact with the edaphic cover and, in particular, circadian biological activity of soil. Instead, in caves can be observed other seasonal and annual cycles with small-scale periodicity (reflecting surface records), although the result is a slow response to environmental changes in the outer atmosphere.

The basic cave micro-environmental control consists in the continuous monitoring of a number of key parameters of the hypogean air [11]:

Temperature tends to stabilize at values equal to the local average annual external values, due to the large heat capacity of the rocks that damps the variations of the incoming fluids (air and water), even a few meters from your entry in the karst. Cave microclimate system is a low-pass filter that reduces amplitude of temperature fluctuations.

Relative humidity. It is a measure of the water content in the gaseous state depending on the air temperature. In general, the relative humidity of the cave atmosphere is almost always close to 100% (that means cave air is saturated), except in specific cases of extreme aridity. The saturation of water vapor in the cave atmosphere can be caused by the presence of underground waters (rivers and pools). When the humidity reaches saturation, every small variation of these

conditions can lead to condensation or evaporation of water vapor, with an important role in the evolution and development of speleothems.

Ventilation. Air circulation inside the caves follows a seasonal pattern showing a change in the direction of movement of air masses, which is a factor to be taken into account in evaluating carbon flux, especially at a small spatial scale. Air enters the caves from the outside and is renewed very slowly through the multiple fractures of the karst system. Cave ventilation and gases exchange by diffusion of the underground atmosphere within its surrounding environment (mainly soil and host rocks) regulate the levels of CO<sub>2</sub> in the air and therefore influence the processes of degassing and saturation of the drip waters. A karst system can behave as a reservoir or a natural source of CO<sub>2</sub> at yearly-seasonal scale.

Carbon dioxide in cave atmosphere can derive from disaggregation of organic matter and its further motion, but it can originate directly by the karst process. Dissolution of calcium carbonate (CaCO<sub>3</sub>) by carbonic acid consumes two molecules of bicarbonate, one coming from atmosphere or soil CO<sub>2</sub> and one further from the carbonate minerals. Nucleation of CaCO<sub>3</sub> during speleothem deposition releases CO<sub>2</sub> to the atmosphere. These two processes are thought to be balanced over long time and global scales, resulting in zero net flux of atmospheric CO<sub>2</sub>, but recent work proposed that they can impact local carbon cycling at short term scale as sinks and sources for atmospheric CO<sub>2</sub> in certain areas [12].

### 3. KARST-SURFACE GAS EXCHANGES

The stability of the karst systems and the degree of energy exchange with the outside atmosphere are controlled primarily by the difference in cave/surface temperature and relative humidity that can act filling or emptying the pores system of the soil, that operates as an insulating double membrane between the microenvironment confined inside the cavity and the outside atmosphere [13], [14].

A simple model of the aerodynamics in a karst system establishes that the major mechanisms and factors involved are:

The thermal convection: the temperature difference between the cave environment and the outside atmosphere causes the activation of the vertical currents whose direction depends on the surface temperature (inside caves temperature is relatively

constant). For example, during the winter cave air is relatively warm compared with the surface air so that there is an air flow outward cave [Fig. 1]. The flow is the more intense the larger is the underground void, and increases with the temperature gradient.

Barometric pressure does not produce too obvious effects in underground air circulation but in large rooms of some caves can induce very intense episodic responses to balance the internal pressure of the cavity with the external atmosphere. Furthermore in many karst system it is the only way to replace the in-cave air and the only source of the energy flow.

Wind swings: the surface wind can lead to a small increase in pressure, pushing the mass of air contained in a cave and causing an oscillatory movement, very intense and at a very low frequency (tens of seconds). When these variations occur, the air flow creates a new depression, followed by a reversal of the movement. This particular phenomenon, which can be treated as an infrasound, occurs at the entrance of the great karst systems and is caused by the inertia of large volumes of air mass.



Fig. 1 Cave air flowing upward is often visible at the karst system entrance during very cold nights (Photo by Riccardo De Luca).

It is worth to highlight that the emissions from geological sources in karst terrains are masked at annual scale by large amounts of CO<sub>2</sub> exchanged between the soil and atmosphere due to biological activity, including elevated anthropogenic emissions.

The correct net ecosystem carbon balance is hard to assess because, to date, the source/sink of CO<sub>2</sub> from underground karst environments has not been considered in the calculation of the current balance of CO<sub>2</sub> in the atmosphere. This is particularly important in view of the fact that approximately 10% of the rocky outcrops worldwide are limestones and dolomites and carbonate materials which represent the largest carbon surface at planetary scale.

Another quantitative data that highlights the importance of karst cavities in the dynamics of atmospheric CO<sub>2</sub> is the concentration of this gas in the hypogean atmosphere, which average values are around 10 times higher than the mean atmospheric concentration (390 ppm, approximately).

#### **4. CAPO CACCIA KARST ECOSYSTEM**

Capo Caccia karst area is located on the North-West coast of Sardinia. The climate is semi-arid with an annual mean temperature and precipitation of 15.9 °C and 588 mm, respectively, and summer drought conditions [15]. A Mediterranean maquis, constituted by sclerophyll species with a maximum height of 2.5 m over a very thin soil, covers the outcropping Mesozoic carbonate rocks. In this area, epigean and hypogean karst features are widespread and, in conjunction with the intricate fracture network related to Tertiary geodynamic, give rise to an interconnection between external and underground atmosphere. High levels of CO<sub>2</sub> have been detected in cave air [16] and also into the aquifer [17].

In this natural ecosystem, carbon flux is measured continuously using an eddy covariance tower placed over the vegetation at 3.5 m above the soil. It consists of a 3D sonic anemometer and an open-path IRGA instrument. Spot measurements inside the caves have been performed by a portable NDIR sensor (Zenith AZ7755, range 0-10000 ppm - accuracy ±50 ppm).

Net ecosystem exchanges measured at Capo Caccia karst area by Eddy Covariance tower showed a clear seasonal pattern with CO<sub>2</sub> uptake by vegetation prevailing during spring and fall depending on water availability and temperature conditions. The ecosystem is generally a sink of carbon also showing daily and seasonal variations. The carbon flux in this ecosystem does not only respond to physiological features of its vegetation but reflects environmental forcing related to atmospheric

variables and gas exchanges with soils and underground voids, where static CO<sub>2</sub> concentration reaches value of >10,000 ppm. Unusual peaks of this gas are detected by Eddy Covariance tower and seem to be related to karst emission when the temperature falls.

In winter, and, in general, when external air temperature is below the annual mean value, cave air density results lower than external. Therefore, cave air can flow upward and outside while cold external air cannot enter into underground system. This ventilation moves cave air masses, rich in carbon dioxide, in the surrounding atmosphere. The CO<sub>2</sub> seasonality tends to covary with temperature, which influences both the production of CO<sub>2</sub> in soils and the cave ventilation [Fig. 2].

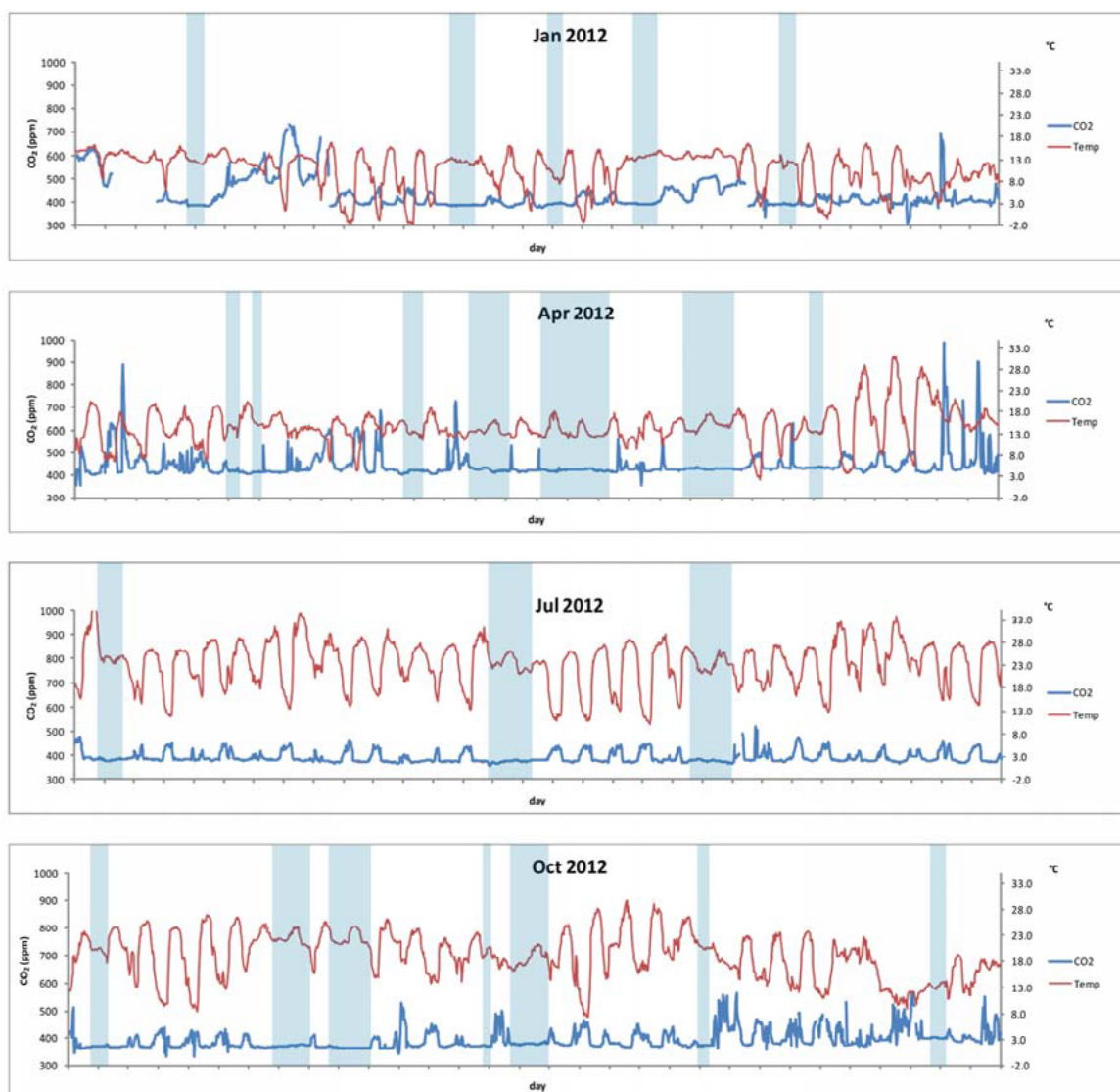


Fig. 2 Inverse correlation between atmospheric CO<sub>2</sub> molar fraction and temperature patterns in winter (January), spring (April), summer (July) and autumn (October) during 2012. The daily CO<sub>2</sub> release is inhibited when the external temperature standstills over its annual average (blue areas).

The climate change and its variations can amplify the effects of this process. In fact, the temperature rising induces an increase of CO<sub>2</sub> production in the soils and then in the vadose zone leading to a higher partial pressure of carbon dioxide (pCO<sub>2</sub>) at the top of phreatic zone. The increased CO<sub>2</sub> concentration dissolved in the water enhances carbonate dissolution. The gas is stored in the water until supersaturation determines speleothem formation. Each molecule of CaCO<sub>3</sub> is produced, two of CO<sub>2</sub> are degassed. The same ventilation, triggered by temperature gradient between outside-cave atmospheres, induces carbonate precipitation by evaporation [Fig. 3].

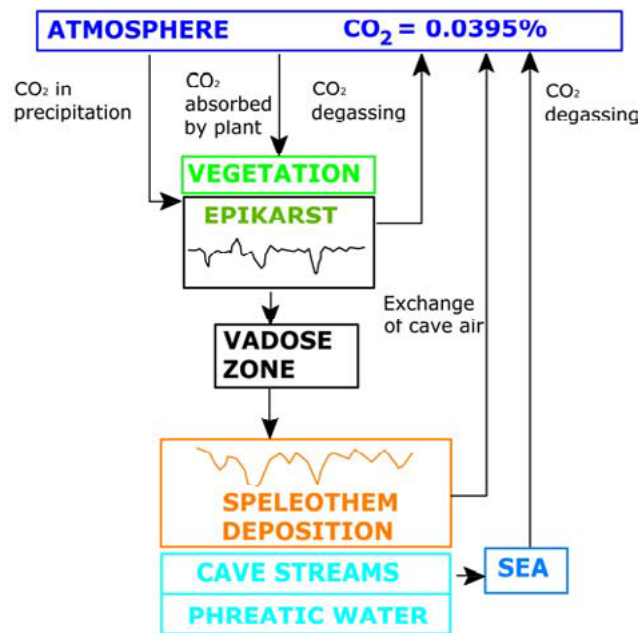


Fig. 3 Flow sheet for the movements of carbon dioxide through Capo Caccia karst ecosystem.

Moreover, it is worth to note that daily CO<sub>2</sub> cycles are not related to specific wind directions. On the contrary, the detected CO<sub>2</sub> molar fraction values are lower during windy days (average 30'-values above 2.5-3.0 m s<sup>-1</sup>) due to the effect of air masses mixing [Fig. 4].

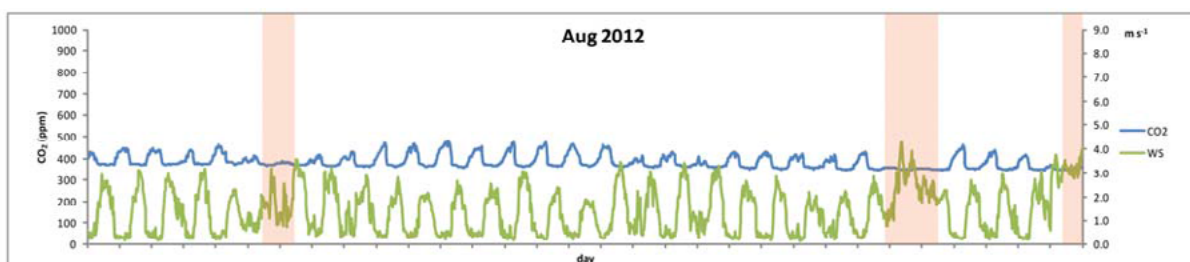


Fig. 4 Daily CO<sub>2</sub> molar fraction and wind speed patterns at Capo Caccia in August 2012. The orange areas highlight the absence of CO<sub>2</sub> peaks during the atmospheric and underground air mixing events.

## 5. CONCLUSIONS

Several researches conducted in various karst areas of the world have been shown that the detailed study of the cave micrometeorology is a high-resolution tool for better understanding global change processes. Caves are characterized by the absence of light and environmental conditions largely different from the outside temperature, humidity, partial pressure of carbon dioxide, etc. However, the physical processes occurring inside the caves are closely related to the external environment and this influences the microclimate of the karst systems. It has been shown that the thermal inertia of the host rock results in a mismatch between the climatic variations in the underground voids and the external environment [18]. In a first approximation, a cave can be considered as a insulated environment in terms of air temperature and water flow system. The study of the gradient of microclimate within a karst system reflects the responses to fluctuations in the external state [19]. Experimental data of Tarhule-Lips and Ford [20] present both short- and long-term responses to climate change. In this context, the cave micrometeorological models can be interpreted as the fluid dynamics inside the caves that affects their development and interacts with the surface atmosphere and vegetation cover [21].

Understanding the underground micrometeorology is a critical goal, in particular when the investigation focuses on the impacts of climate changes, caused by the temperature difference between inside and outside air, on the cave environment. The exchange of air between the cave exterior and interior increases with the temperature difference, accelerating the corrosion which leads to carbon dioxide sink during warm periods [22], [23]. The increase in global temperature and CO<sub>2</sub> concentration in the air can induce the increasing of condensation and corrosion on cave walls and speleothems [24]. For example, studies made in the karstic systems of gypsiferous area of Bologna (Italy) where speleothems precipitation is not influence by host rock, showed that carbonate concretions are correlated with atmospheric CO<sub>2</sub> variations experienced in the area [25], and this can have socio-economic impacts on tourist caves management. Micrometeorological data collected in Capo Caccia karst ecosystem show a strong daily correlation between the release of carbon dioxide from the karst system and outside air temperature. The carbon source behavior is inhibited when the external temperature standstills over its annual average. This result indicates that the study of atmosphere-biosphere-geosphere

interactions could allow a detailed analysis of the vulnerability of different areas to future changes in temperature and/or humidity. Indicators for assessing the impacts of global change could be useful in formulating a hypothesis and in helping define and predict both the effects of climate change and their socio-economic impacts and in turn to assess the potential anthropic impacts on underground systems. This could give rise the opportunity for a more precise spatial-temporal characterization of cave-surface atmosphere gases exchange, which is an important factor in determining the processes associated with climate change.

The integrative knowledge of biological/geological origin of subterranean carbon dioxide storage together with the understanding of mechanisms associated with degassing or ventilation processes will allow a more accurate estimation of carbon balances at regional spatial scales for ecosystems that insist on karst areas [26].

## 6. ACKNOWLEDGEMENTS

This study was conducted under the research project “*An integrated system for quantifying the net exchange of CO<sub>2</sub> and evaluating mitigation strategies at urban and landscape level*”, funded by the Regional Administration of Sardinia, Regional Law n. 7, 7 August 2007. Many thanks to Giovanni Badino for his comments and to Riccardo De Luca for providing his photography.

## 7. REFERENCES

1. Wilkens H., Culver D.C. & Humphreys A. (2000), *Subterranean ecosystems*, Elsevier, pp. 791.
2. Badino G. (2010), *Underground meteorology – “What’s the weather underground?”*, Acta Carsologica, No. 30(3), pp. 427-448.
3. Badino G. (2004), *Cave temperatures and global climatic change*, International Journal of Speleology, No. 33(1-4), pp. 103-114.
4. Baldini J.U.L., Baldini L.M., McDermott F. & Clipson N. (2006), *Carbon dioxide sources, sinks, and spatial variability in shallow temperate zone caves: evidence from Ballynamintra Cave, Ireland*, Journal of Cave Karst Studies, No. 68, pp. 4-11.

5. Badino G. (2009), *The legend of carbon dioxide heaviness*, Journal of Cave and Karst Studies, No. 71(1), pp. 100-107.
6. Fernández-Cortés A., Sanchez-Moral S., Cuezva S., Cañaveras J.C. & Abella R. (2009), *Annual and transient signatures of gas exchange and transport in the Castañar de Ibor cave (Spain)*, International Journal of Speleology, No. 38(2), pp. 153-162.
7. Ginés A., Hernández J., Ginés J. & Pol A. (1987), *Observaciones sobre la concentración de dióxido de carbono en la atmósfera de la Cova de les Rodes (Pollença, Mallorca)*, Endins, No. 13, pp. 27-38.
8. Liñán C., Vadillo I. & Carrasco F. (2008), *Carbon dioxide concentration in air within the Nerja Cave (Malaga, Andalusia, Spain)*, International Journal of Speleology, No 37(2), pp. 99-106.
9. Madonia P., Bellanca A., Di Pietro R. & Mirabello L. (2012), *The role of near-surface cavities in the carbon dioxide cycle of karst areas: evidence from the Carburangeli Cave Natural Reserve (Italy)*, Environmental Earth Science, No. 67, pp. 2423-2439.
10. Serrano-Ortiz P., Roland M., Sanchez-Moral S., Janssens I.A., Domingo F., Goddérís Y. & Kowalski A.S. (2010), *Hidden, abiotic CO<sub>2</sub> flows and gaseous reservoirs in the terrestrial carbon cycle: Review and perspectives*, Agricultural and Forest Meteorology, No. 150, pp. 321–329.
11. Badino G. (1995), *Fisica del Clima Sotterraneo*, Memorie Istituto Italiano di Speleologia, No. 7, pp. 136.
12. White W.B. (2013), *Carbon fluxes in karst aquifers: sources, sinks, and the effect of storm flow*, Acta Carsologica, No. 42 (2-3), pp. 177-186.
13. Cuezva S. (2008), *Dinámica microambiental de un medio kárstico somero (Cueva de Altamira, Cantabria): microclima, geomicrobiología y mecanismos de interacción cavidad/exterior*, Doctoral Thesis, Universidad Complutense de Madrid.
14. Fernández-Cortés A., Sanchez-Moral S., Cuezva S., Benavente D. & Abella R. (2009), *Characterization of tracer gas fluctuations in a “low energy” cave*

- (Castañar de Ibor, Spain) using techniques of entropy of curves, International Journal of Climatology, DOI: 10.1002/joc.2057.
- 15.Spano D., Duce P., Sirca C., Zara P., Marras S. & Pisanu S. (2006), *Energy and CO<sub>2</sub> exchanges of a Mediterranean shrubland ecosystem*, Proceedings of the 27th Conference on Agricultural and Forest Meteorology of the American Meteorological Society, San Diego, California.
  - 16.Mucedda M. (1998), *Grotte e pozzi della Nurra di Sassari*, Bollettino del Gruppo Speleologico Sassarese, No. 7, pp. 10-26.
  - 17.Ghiglieri G., Oggiano G., Fidelibus M.D., Alemayehu T., Barbieri G. & Vernier A. (2009), *Hydrogeology of the Nurra Region, Sardinia (Italy): basement-cover influences on groundwater occurrence and hydrogeochemistry*, Journal, No. 7, pp. 447-466.
  - 18.Badino G. (2004), *Clouds in cave*, Speleogenesis and Evolution of Karst Aquifers, No. 2(2), pp. 1-8.
  - 19.Taboroši D., Hirakawa K. & Sawagaki T. (2005), *Carbonate precipitation along a microclimatic gradient in a Thailand cave - Continuum of calcareous tufa and speleothems*, Journal of Cave and Karst Studies, No. 67(1), pp. 69-87.
  - 20.Tarhule-Lips R.F.A. & Derek F.C.,(1998), *Condensation Corrosion in Caves on Cayman Brac and Isla de Mona*, Journal of Cave and Karst Studies, No. 60(2), pp. 84-95.
  - 21.Shindo S. (2005), *Micrometeorological modeling of an idealized cave and application to Carlsbad Cavern, NM*, Master of Science thesis – Socorro University, New Mexico, pp. 244.
  - 22.Schmekal A.A. & de Freitas C.R. (2001), *Condensation in Glow-worm Cave, Waitomo, New Zealand: management guidelines*, Doc Science Internal Series, No. 15, pp. 5-12.
  - 23.Russell M.J. & MacLean V.L. (2008), *Management issues in a Tasmanian tourist cave: Potential microclimatic impacts of cave modifications*, Journal of Environmental Management, No. 87, pp. 474-483.
  - 24.de Freitas C.R. & Schmekal A.A. (2005), *Prediction of condensation in caves*, Speleogenesis and Evolution of Karst Aquifers, No. 3(2), pp. 9.

25. Shopov Y.Y., Stoykova D. & Forti P. (2009), *Luminescence of speleothems in Italian gypsum caves: preliminary report*, In: Gypsum Karst Areas in the World: their protection and tourist development, Memorie Istituto Italiano di Speleologia, No. 16, pp. 87-90.
26. Pérez-Priego O., Serrano-Ortiz P., Sánchez-Canete E.P., Domingo F. & Kowalski A.S. (2013), *Isolating the effect of subterranean ventilation on CO<sub>2</sub> emissions from drylands to the atmosphere*, Agricultural and Forest Meteorology, No. 180, pp. 194-202.

Advances in climate change

**Poster Session**

# Global scale energy budget variations in the outputs of the ERA-20CM experiment

Lembo V.<sup>1,2\*</sup>, and Lionello P.<sup>1,2</sup>

<sup>1</sup>University of Salento, Lecce - Italy, and <sup>2</sup>CMCC - Italy

\*Corresponding Author: [valerio.lembo@unisalento.it](mailto:valerio.lembo@unisalento.it)

## Abstract

In this contribution the outputs of the ERA-20CM experiment have been considered. This is a 10-member ensemble integration of the ECMWF atmospheric model covering the 1900-2009 period, driven at the lower boundary conditions by 10 realizations of SST fields, with CMIP5 recommended atmospheric composition and solar irradiance. The 20th century global mean surface temperature increase has occurred throughout two distinct phases, characterized by an evidently different behavior. The analysis considers atmospheric, surface and top-of-atmosphere (TOA) variations in the components of the energy budget within these two warming phases. Differences in the meridional distributions of some components are shown. Shortwave (SW) atmospheric absorption increases in both periods. The longwave (LW) components behave differently in the two phases. Particularly the TOA Outgoing LW radiation (OLR), increases during the first phase, decreases during the second, the LW net budget for the atmosphere increases during the first phase, is stable during the second. Therefore in last decades a coherent pattern emerges in which the system absorbs more energy than it emits, diverging from equilibrium. In particular the atmospheric layer decreases its energy deficit, ingesting more energy because of SW absorption increase in NH, and LW emission decrease in SH.

**Keywords:** atmospheric energy budget, climate change, model outputs

## 1. INTRODUCTION

Being the Earth system a thermal engine, although quite inefficient, it is straightforward that understanding the variability of the energy exchanges within the atmosphere is a prerequisite for understanding the climate change. This is even more evident, if such an interest is focused on addressing the accountability of anthropogenic emissions, and defining strategies and policies of mitigation and adaptation to this change.

A valid proxy for climate change investigation is still the surface air temperature (SAT), not only because of the wide availability of data, but also because of its relatively wide decorrelation interval, as noticed by Hansen, and Lebedeff, 1987 [1]. It is evident that global mean SATs have recently increased at an unprecedented ratio in the last three decades (Hansen, et al., 2010 [2]). Nonetheless historical and paleoclimate reconstructions suggest that a certain variability in such a proxy has always occurred. The question is to what extent such a *natural* variability is responsible for the recent warming.

Thanks to the efforts of hundreds of scientists involved in the development of the IPCC assessment reports, whose latest edition has been published in 2013 (Stocker, et al., 2013 [6]), it is nowadays clear that human activities impacts on climate are mainly effected by means of dramatic changes in the atmospheric composition. Particularly emissions of so-called *greenhouse gases* (GHG) have a deep impact on the way atmosphere and surface interact with incoming radiation, affecting their absorption, emission and scattering capability, directly or indirectly. The Earth is indeed a highly non-linear complex stochastic system, in which a wide number of forcings and feedbacks act, some of them not yet clearly explained.

In this contribution, the components of the energy budget within the atmosphere are analyzed and discussed, making use of the outputs of a 10-member ensemble simulation of an Atmospheric General Circulation Model (ACGM), ingesting prescribed Sea Surface Temperatures (SST) and atmospheric gases composition over the last century. It is well known that two warming phases can be distinguished in this period, one during the first half of the century, the other one, as mentioned, in the last decades. Assuming that relatively small changes in gases composition have occurred during the first half of the century, compared to last decades (see, for instance,

<https://www.ncdc.noaa.gov/indicators/>), a comparison between changes in the energy budget during the two phases of warming can provide precious hints on the way the GHG anthropogenic forcing acts, and vice versa how natural variability modulates the warming.

The paper is structured as follows: in Section 2 the model and the outputs that are used for the analysis are described, and the statistical tools for the assessment of results consistency are briefly discussed. In Section 3 some outstanding results emerging from direct retrieval of model outputs are discussed, and the energy budget for the TOA and the atmospheric layer are computed and described. In Section 4 results are put together, in order to set up a coherent pattern of the changes in the energy budget.

## 2. DATA AND METHODS

The ERA-20CM experiment (Hersbach, et al., 2013 [3]) is considered, 10-member integration of the Integrated Forecast Model (IFS), the atmospheric model developed by the European Center for Medium-range Weather Forecasts (ECMWF), over the 1900-2010 period. The model ingests 10 possible realizations of the SST and Sea-Ice Concentration (SIC) fields, according to the HadISST2.0 datasets (Kennedy, et al., 2013 [4], Titchner, et al., 2013 [8]), and the Coupled Model Intercomparison Project Phase 5 (CMIP5) prescriptions for the radiation scheme, including GHG, ozone, tropospheric aerosols and solar irradiance (Taylor, et al., 2012 [7]). The IFS release is the Cy37r3 at a T63 spectral resolution. It has 91 levels in the vertical, from 10m above the surface to 1 Pa. It is noticeable that the model is not coupled, so the ocean acts as infinite source of energy, and the energy fluxes from the atmosphere to the surface do not affect the ocean conditions. Hersbach, et al. [3] show that the global scale SAT time series simulated by the model ensemble show indeed a very good agreement with observations, particularly at inter-annual and decadal timescale. In general, it is assumed that the model can describe with a reasonable confidence some peculiar statistical features of the climate system.

The components of the energy budget here considered are:

- Top net SW radiation (TSR)

- Top net LW radiation (OLR)
- Surface net SW radiation (SSR)
- Surface net LW radiation (STR)
- Surface sensible heat vertical flux (SSHF)
- Surface latent heat flux (SLHF)

The net budgets are considered at the TOA and for the atmospheric layer, between the surface and the TOA. Moreover the LW and SW net budget by the atmosphere are separately retrieved.

The changes in the zonal mean energy budget are analyzed at a decadal timescale, in order to remove possible adjustments of the system to transient equilibrium states. Having computed the ensemble mean of the 10 members, yearly averages of monthly means are considered, the two warming phases (conventionally defined as 1906-1949 and 1940-2009) are studied by means of the differences between the first (1906-1915, and 1940-1949) and the last (1940-1949, and 2000-2009) decadal averages. In order to provide as a complete picture as possible of these variations, meridional sections are shown. A Mann-Whitney test at a 0.02 confidence level is performed, in order to test the significance of such differences against the internal variability of the decades, and the uppermost 95th and lowermost 5th percentile are empirically computed.

### 3. RESULTS

ERA-20CM global mean surface temperature time series are plotted in [Fig.1]. Land surface air temperatures (LSAT) and sea surface air temperatures (SSAT) at 2 metres height are separately considered and compared (respectively in red and blue), showing each member of the ensemble, in order to evidence the emergence of the land-sea contrast in the last decades of the integration period. The contrast reaches in the last decade roughly  $0.25 K$ , starting from the early 1990s.

[Figure 1 about here.]

As a reference, the meridional distribution of the surface warming occurred in the two periods is shown in [Fig.1]. The main difference between the two periods is in the

warming of Northern hemisphere middle and high latitudes. An outstanding peak is reached, amounting to  $1.5\text{ K}$ , while elsewhere the warming ranges between  $0.3$  and  $0.4\text{ K}$  in both periods. This is the well-known *Arctic amplification* mechanism (Serreze, and Francis, 2006 [5]). It is a typical positive feedback involving GHG and the sea-ice albedo, and it can be explained as follows: GHG direct radiative forcing warms lower troposphere temperature at all latitudes, causing a reduction of the sea ice extent at the end of the warm season, and a thinner new ice sheet at the end of the cold season. The latter causes an earlier development of open water areas during the warm season, consequently more absorption of incoming SW radiation by the sea. SST temperatures are thus warmer, and act to enhance the ice-melting. Together with the presence of more open water at the end of the warm season, this turns up in warmer air temperatures during the cold season.

[Figure 2 about here.]

The net input and output of energy to the system are represented, respectively, by the TSR and the OLR. The TSR differences are shown in [Fig.2]. The TOA SW budget differences are generally positive during both periods, particularly at low latitudes. Nonetheless an outstanding peak is found over NH high latitudes. This obviously accounts for the above mentioned dramatic change in the surface albedo, due to the sea-ice melting.

[Figure 3 about here.]

On the other hand OLR differences of [Fig.3] account for an opposite behavior in the two periods. In the former period the radiation emitted by the system to outer space increases, where significant, while in the latter period OLR decreases almost everywhere, and reaches significance over most part of the SH.

[Figure 4 about here.]

The TOA radiative budget is thus the balance between the TSR and the OLR. It is fairly null in the former period, generally positive in the latter, as shown in [Fig.4]. The meridional sections account for a dramatically different behavior within the two periods. In the former, the increased net SW input shown in [Fig.2] is balanced by an almost equal increase in LW emission. In the latter a combined effect is observed, depending

on the latitude. In the SH to an almost null increase in SW input, the system responds with a significant decrease in the LW emission. In the NH, the significant increase in SW input is not balanced by an equally significant increase in LW emission, particularly in the higher latitudes. It is remarkable that during the second period, this also leads to a poleward translation of the transition latitude from a region of energy surplus to a region of energy deficit. This has important implications for the dynamics within the atmosphere, particularly for what concerns the NH.

[Figure 5 about here.]

Within the atmospheric layer, significant changes in the SW and LW budgets, i.e. the difference between the amount of SW/LW radiation entering/exiting from the TOA and the SW/LW budget at the surface, are found. SW absorption [Fig.5] is increased in both periods, particularly in the latter, with a peak at NH middle latitudes. An opposite behavior is shown, for what concerns the LW net budget [Fig.6]. This is computed as the absolute value of the difference between the LW net input from the surface, and the LW emission at TOA. It obviously act to balance the SW absorption of [Fig.5], since the LW emission to outer space is more intense than the input from the surface. It is increased during the first period, while slightly significant changes are found in the latter period.

[Figure 6 about here.]

[Figure 7 about here.]

SW and LW budget are combined with the sensible and latent heat vertical fluxes, in order to compute the overall energy budget for the atmospheric layer. On average, it is negative, because most of the energy ingested by the system is passed to the surface. Differences are shown in [Fig.7]. In the former period differences are not significant, and an irregular distribution over latitudes is found, a clear pattern of the preponderance of heat fluxes variability (not shown). In the latter period variations are smoother and mostly everywhere significant, in the sense of an overall increase, thus a reduction in the energy deficit. This has a clear explanation if one compares the SW atmospheric absorption variations of [Fig.5] with the OLR changes of [Fig.3]. In the NH the main

contribution comes from the increase of the former, while in the SH the OLR reduction plays a dominant role.

[Figure 8 about here.]

#### 4. CONCLUSIONS

It is here noticed that in the ERA-20CM simulations the Earth system is in thermodynamic equilibrium in the first part of the century, while it is not in the last decades. There is a net energy input to the system, that is a consequence of a number of internal processes modulating not only the absorption of incoming, but also the overall emission of radiation. The opposite sign of OLR differences occurring in the two phases confirms that, although the surface warming has generally the same amount, and the opacity of the atmosphere to SW radiation is similarly increased in both periods, in the last decade the positive feedback on the warming is affected by atmospheric opacity to LW radiation. The atmosphere reacts to such changes by ingesting on average more energy, in the SH because of less LW emission, in the NH because of more SW absorption.

It is evident that a substantial variation in the average energy budget of the two periods has occurred. The question is what drives these discrepancies. It is a matter of debate whether the first period warming is a signature of an early trend of climate response to the anthropogenic forcing, or it has to be ascribed to an inter-decadal oscillation in natural variability. It is indeed likely to be a superposition of the two features. The attribution of these changes is even more pressing since many have recently associated the last decade "hiatus" in the surface temperature increase to a negative phase of a hypothetical 60-70 years' period oscillation, as mentioned before similar to the ones observed in AMO or PDO variability (Trenberth, and Fasullo, 2013 [9]). Nevertheless their understanding is based on the empirical observation of recent decades, or at least the indirect reconstruction of the last millenia, where possible. Thus very little is known about the robustness of these oscillations, and the physical processes involved in that. In order to capture the anthropic impact on the energy budget, it is necessary to decompose the variations in at least two components, one accounting for trends, the

other accounting for all possible modes of natural variability.

Finally, let us remark that a careful validation of the model, in particular of its radiation scheme, is required, in order to assess the coherency of the outputs with the real past climate. Unfortunately, a comparison is feasible only with the very recent decades, while very few observations are available for the first period of warming, from 1906 to 1949. An assessment of the model performance has been accomplished by Hersbach, et al. (2013) [3]. It is found that the net balance at TOA and at the surface does not meet on average the observations. The model displays a net out-flux of energy to space, and a net in-flux at the surface, that is exactly the opposite of what one might expect in a context of global warming. Nonetheless the signs and the magnitudes of the recent trends are correctly resolved. In order to understand whether such errors are due to a bias that is constant over time, thus can be easily removed, or it is randomly distributed, it is needed to extend back in time as long as it is possible the assessment of the model.

## 5. REFERENCES

1. Hansen, J., and S. Lebedeff, (1987), *Global Trends of Surface Air-Temperature*, J. Geophys. Res., 92, 13345-13372
2. Hansen, J., R. Ruedy, M. Sato, and K. Lo, (2010), *Global surface temperature change*, Rev. Geophys., 48, RG4004, doi:10.1029/2010RG000345
3. Hersbach, H., C. Puebey, A. Simmons, P. Poli, D. Dee, and P. Berrisford, (2013), *ERA-20CM: a twentieth century atmospheric model ensemble*, ERA Report Series, 16
4. Kennedy, J. J., N. Rayner, S. Millington, and M. Saunby, (2013), *The Met-Office Hadley Center sea-ice and sea-surface temperature data set, version 2, part 1: sea-surface temperature analysis*, J. Geophys. Res., submitted for publication, doi: 10.1002/2013JD020316
5. Serreze, M. C., and J. A. Francis, (2006), *The Arctic amplification debate*, Clim. Change, 76, 241-264

6. Stocker, T.F., D. Qin, G.-K. Plattner, M. Tignor, S.K. Allen, J. Boschung, A. Nauels, Y. Xia, V. Bex and P.M. Midgley (eds.), 2013, *IPCC, 2013: Climate Change 2013: The Physical Science Basis. Contribution of Working Group I to the Fifth Assessment Report of the Intergovernmental Panel on Climate Change*, Cambridge University Press, Cambridge, United Kingdom and New York, NY, USA, 1535 pp.
7. Taylor, K., Stouffer, R., and Meehl, G., (2012), *An overview of the CMIP5 and the experiment design*, Bull. Amer. Meteor., Soc., 93, 485-498
8. Titchner, H. A., and N. Rayner, (2013), *The Met-Office Hadley Center sea-ice and sea-surface temperature data set, version 2, part 2: sea-ice*, in preparation
9. Trenberth, K. E., and J. T. Fasullo, (2013), *An apparent hiatus in global warming?*, Earth's Future, 1, 19–32, doi:10.1002/2013EF000165.

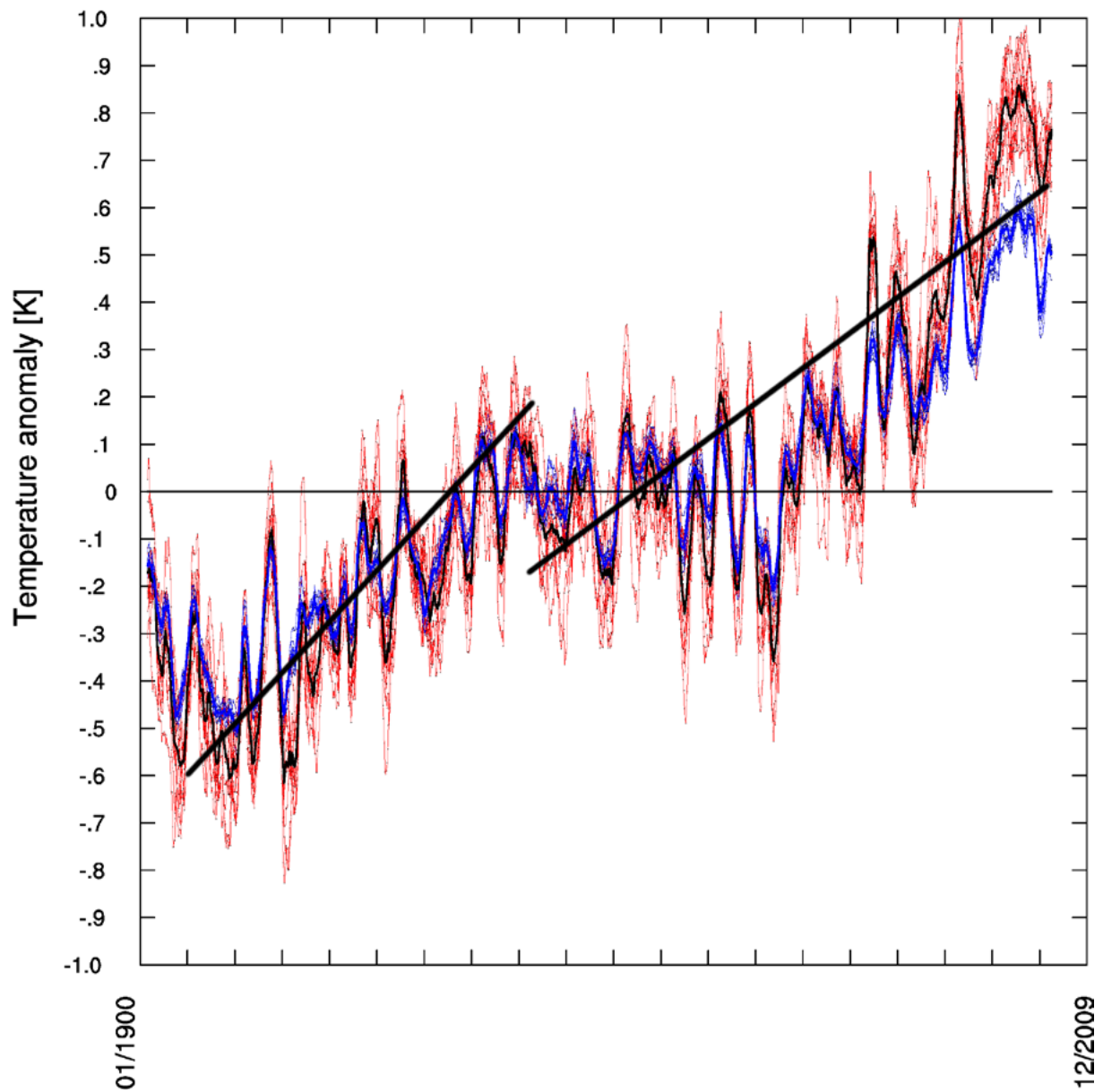


Fig. 1 SSAT (blue) and LSAT (red) time series over the 1900-2009 period, as reconstructed by each member of the ERA-20CM ensemble model. The ensemble average for LSAT is marked by a black thick line, the SSAT by a blue thick line. Records have been deseasonalized, and anomalies have been computed as the departure from the whole period ensemble mean. A 12-month running average filter has been also applied. The slope of the warming for each period is qualitatively represented by means of two bold black lines.

## Surface air temperature [K]

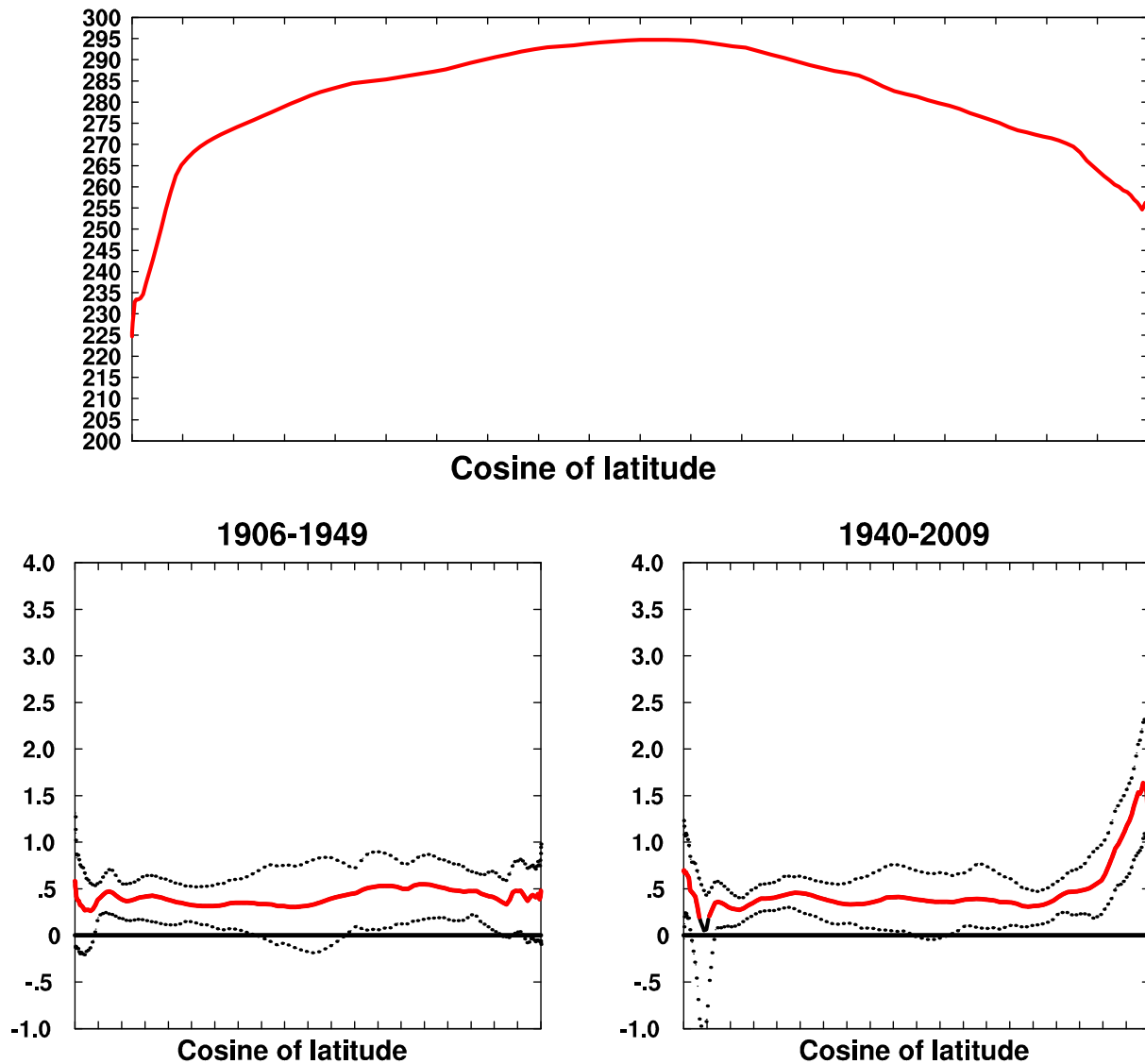


Fig. 2 Surface air temperature meridional sections. Top: meridional sections of mean decadal averages. Bottom left: meridional section of differences between 1940-1949 and 1906-1915 decadal averages. Bottom right: meridional section of differences between 2000-2009 and 1940-1949 decadal averages. Concerning the differences, the uppermost 95th and lowermost 5th percentile are shown (dotted lines). The significance of the differences is assessed by means of a Mann-Whitney test at a 98% confidence level. Significant differences are marked by thick red lines; dashed thin lines are displayed where the differences are not significant.

## Top net solar radiation [W/m<sup>2</sup>]

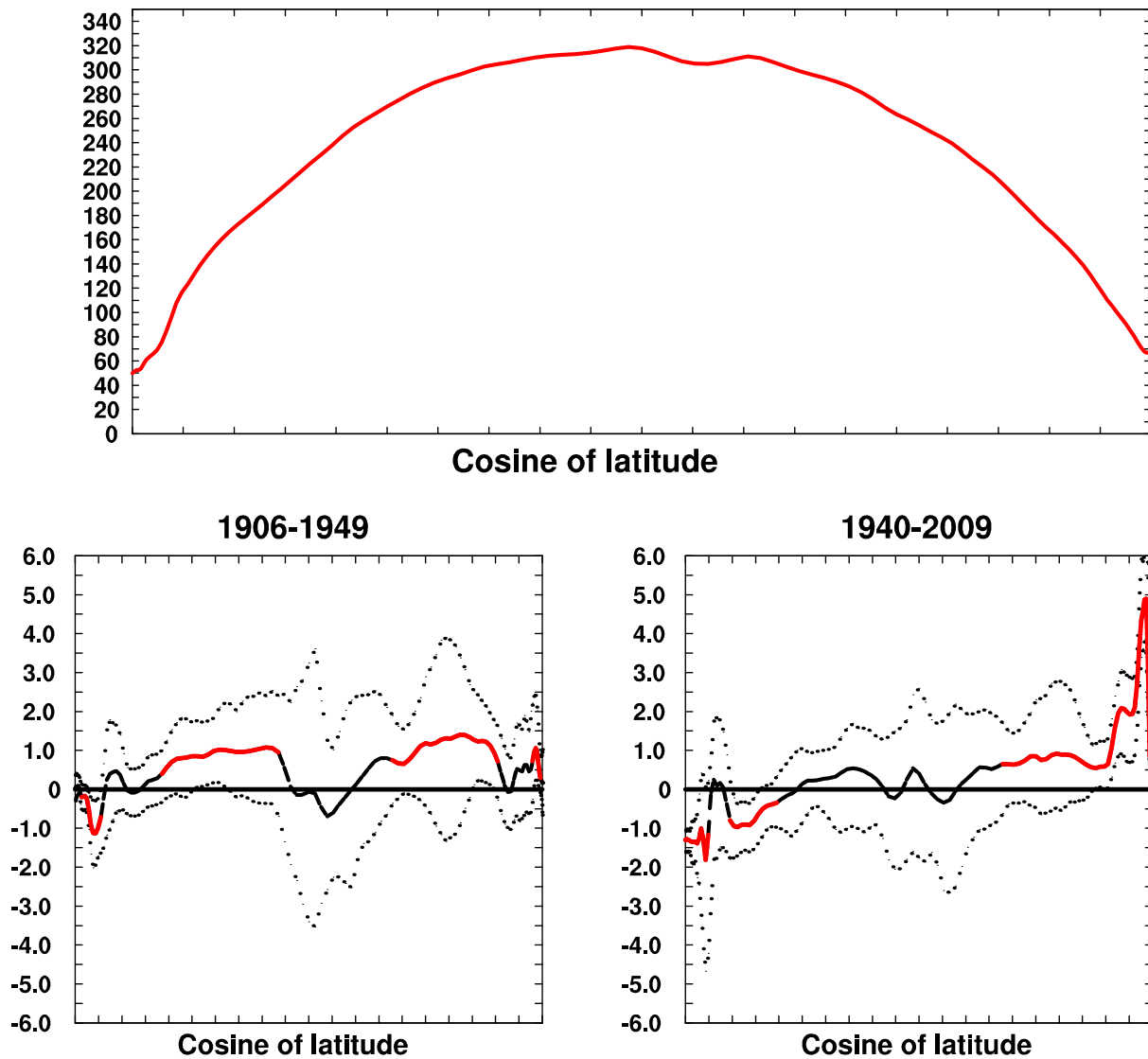


Fig. 3 Same as in [Fig.2], but for Top Net Solar Radiation (TSR). Values are in  $\frac{W}{m^2}$ , and conventionally positive downwards.

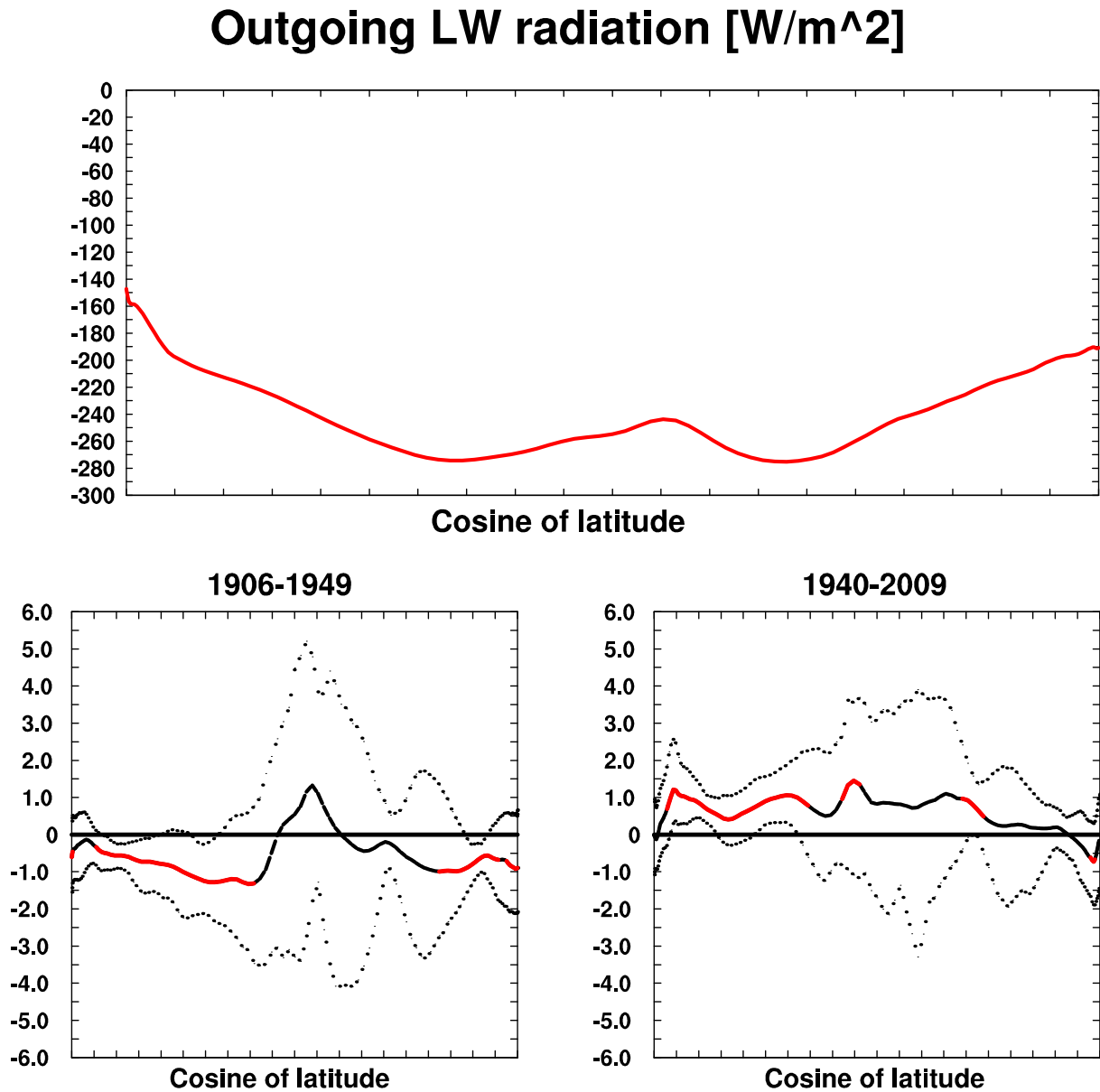


Fig. 4 Same as in [Fig.2], but for Outgoing Longwave Radiation (OLR). Values are in  $\frac{W}{m^2}$ , and conventionally positive downwards.

## TOA radiation budget [W/m<sup>2</sup>]

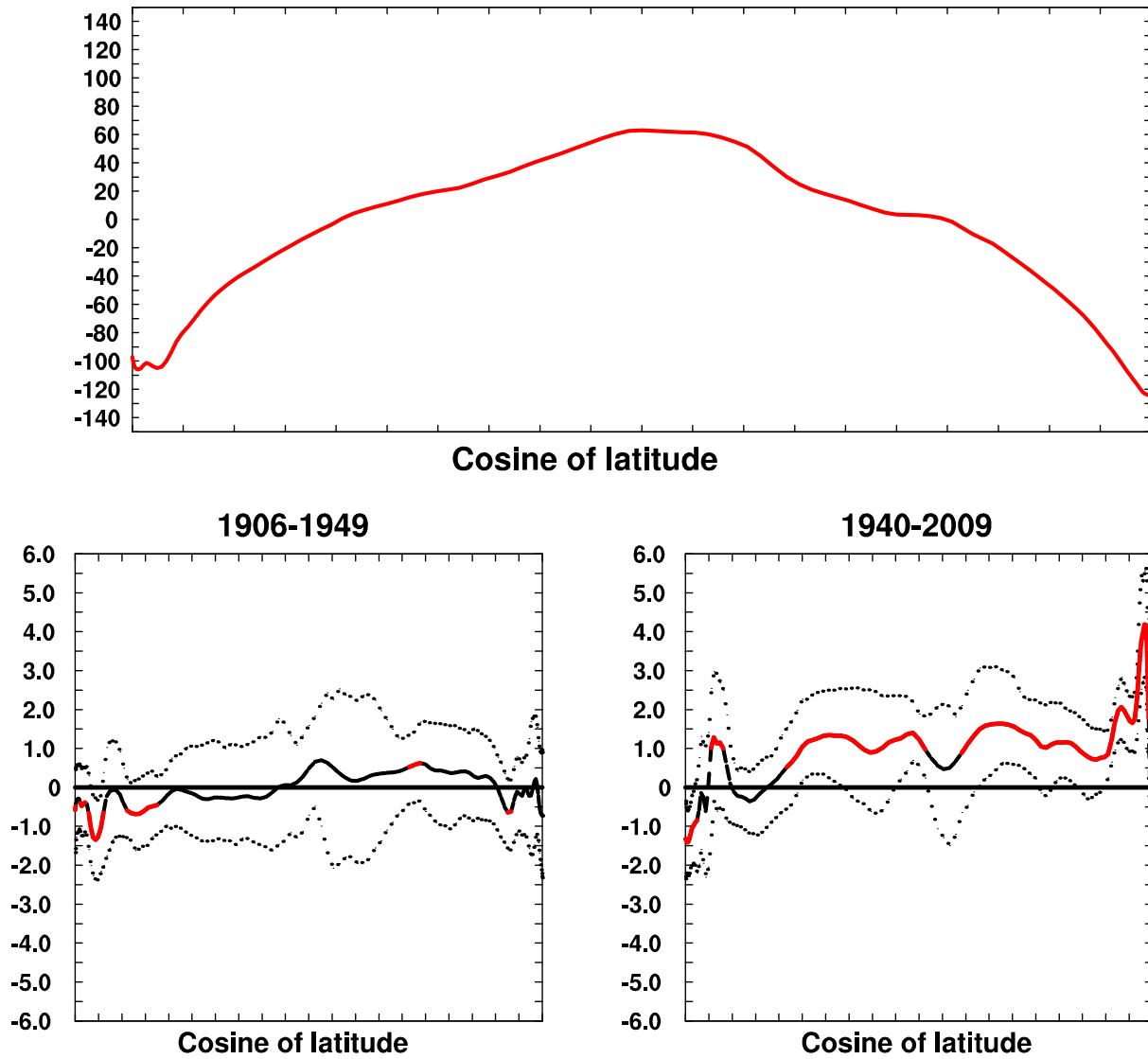


Fig. 5 Same as in [Fig.2], but for the TOA radiative budget. Values are in  $\frac{W}{m^2}$ .

## Atmospheric SW absorption [W/m<sup>2</sup>]

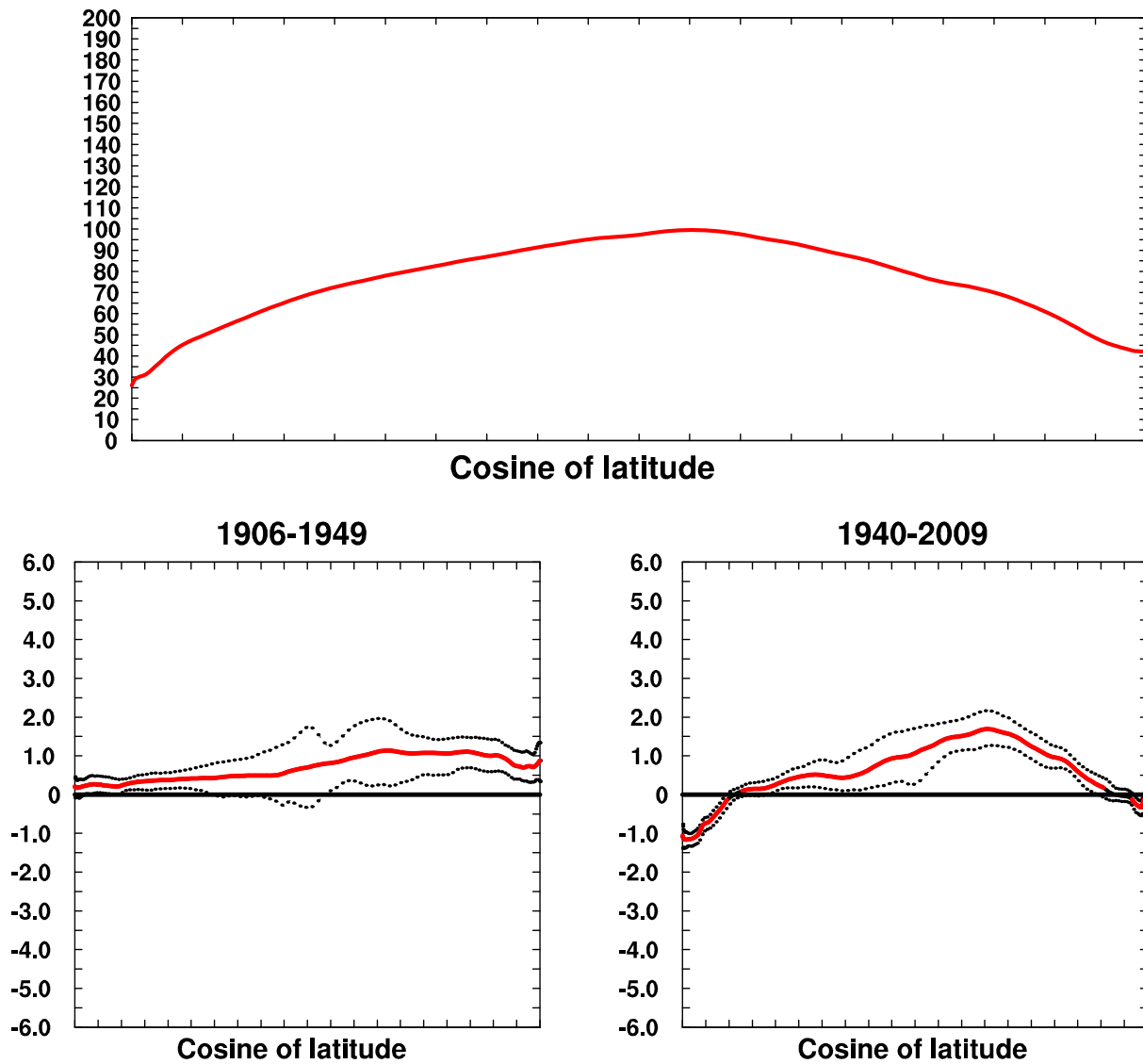


Fig. 6 Same as in [Fig.2], for SW absorption by atmosphere (TSR-SSR). Values are in  $\frac{W}{m^2}$ .

## Atmospheric LW budget [W/m<sup>2</sup>]

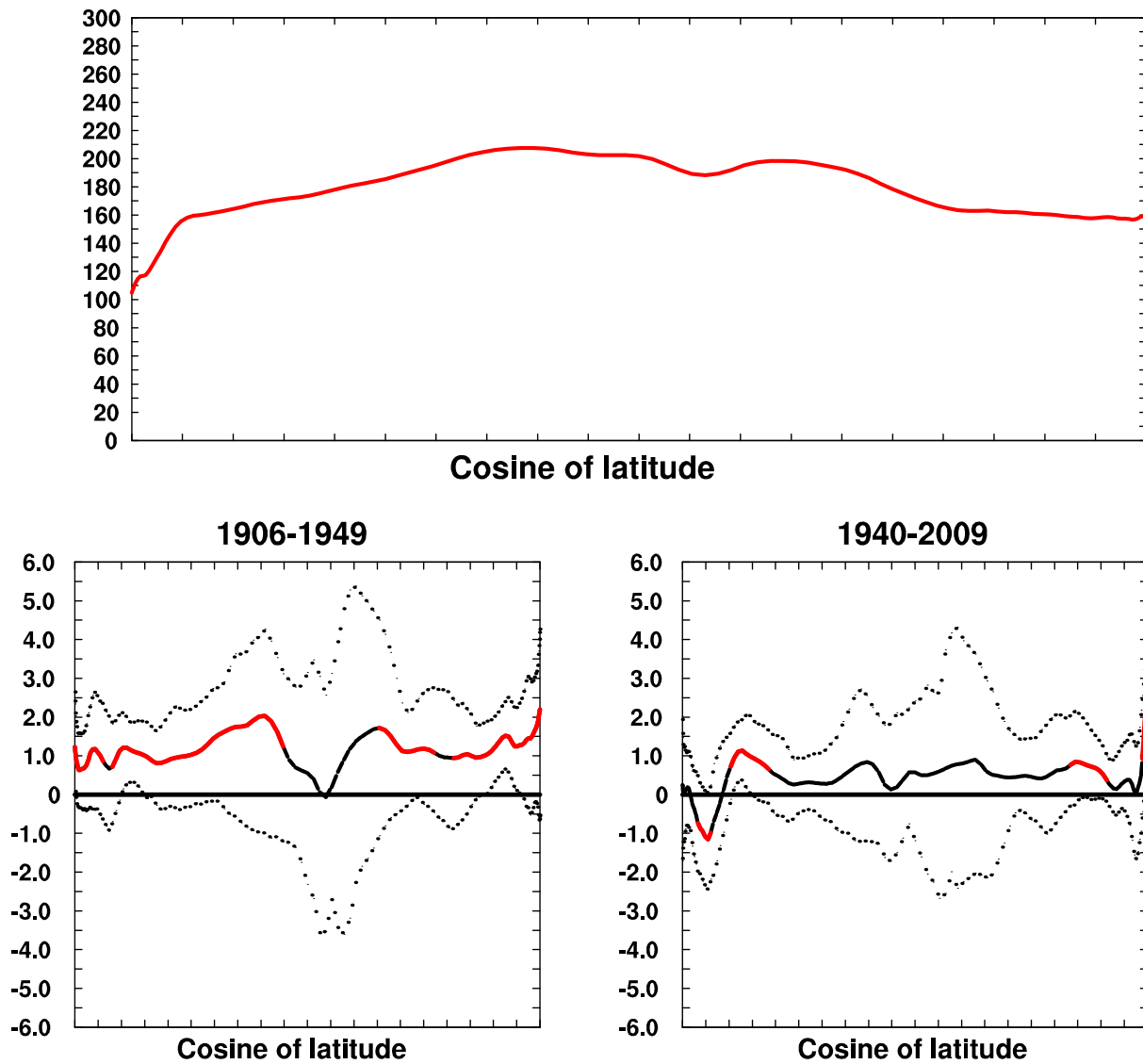


Fig. 7 Same as in [Fig.2], for LW atmospheric budget. Values are in  $\frac{W}{m^2}$ .

## Atmospheric residual budget [W/m<sup>2</sup>]

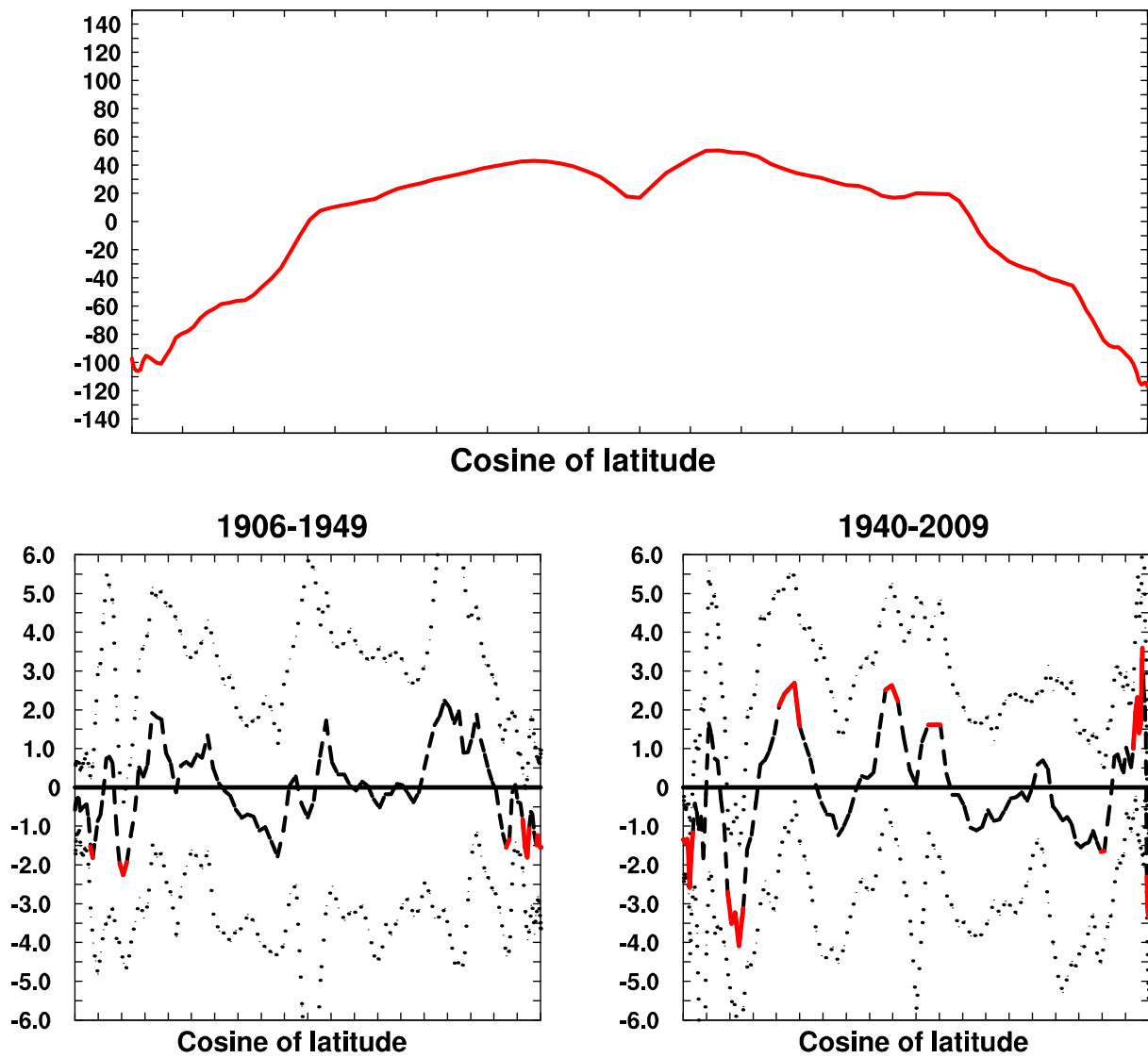


Fig. 8 Same as in [Fig.2], but for the atmospheric energy budget. Values are in  $\frac{W}{m^2}$ .

# Climate models performance optimization through Min-Apps

Italo Epicoco<sup>1,2\*</sup>, Silvia Mocavero<sup>2</sup> and Giovanni Aloisio<sup>1,2</sup>

<sup>1</sup>University of Salento, Italy <sup>2</sup>Euro-Mediterranean Center on Climate Change, Italy

\*Corresponding Author: italo.epicoco@unisalento.it

## Abstract

Modelling the climate system requires the simulation of an extremely large number of interacting and complex processes as well as their analysis at different time and spatial scales. Sophisticated numerical models are used to solve the inherently non-linear governing equations, while huge computational resources are needed to calculate billions of individual variables describing the physical processes at different scales. Indeed model simulations are required to represent both modification of the larger-scale, global, state (inside which extreme events are developing) and the fine-scale temporal and spatial structure of such events (storms, cyclones, intense precipitation, etc.). Several efforts are needed to analyze and understand the computational performance of a coupled climate application and to design new numerical approaches at exascale. The traditional parallel domain decomposition approach will not be enough to efficiently exploit the exascale architectures. The development of mini-applications can be a viable solution to introduce new numerical methods, new algorithms and to drive the hardware development following a co-design approach.

**Keywords:** mini-applications, performance analysis, climate modelling

## 1. COMPUTATIONAL ISSUES

Today, one of the main issues for the high performance computing is the exploitation of the new emerging architectures executing legacy applications, such as climate models, designed and developed 30 years ago. They have to be re-designed at different levels, starting from the new physical phenomena to be modeled at high resolution, through the choice of alternative numerical methods and unstructured grids preserving the accuracy, up to a co-design process involving mathematicians, climate scientists, computational scientists and technology providers.

The starting point of the process is the analysis of both the state of the art and the main scalability bottlenecks of the stand-alone and coupled models [1,2]. The climate applications and namely the oceanic models are generally based on the Navier-Stokes equations, solved by finite difference methods on structured grids, executed in parallel by using a spatial domain decomposition. The new architectures allow increasing the spatial resolution of climate models. However, we have to consider that, for climate models, the key problem is related to the sequential nature of the time-stepping algorithm used to solve the involved partial differential equations. Indeed, simply reducing the mesh spacing increases the time for solution, due to the Courant-Friedrichs-Lewy condition, even with perfect weak scaling. The wall-clock time of a simulation also includes a factor related to the increasing of the time resolution, preventing the algorithm to be cost-optimal. Some time-parallelization techniques [3] have been developed in order to overcome this limit. Moreover, the parallelization is often performed by the message-passing paradigm. If the models are executed on massive parallel architectures, the ratio between the communication and the computational load of each task can become very high. New parallel programming languages [4] allow to better exploit the shared memory and then to reduce the communication weight. Also at algorithmic level, the efforts aim at the development of new communication-avoiding [5] and communication/computation-overlapping algorithms.

The improvement of both spatial and time resolution causes the increasing of the data read/written by the application making the I/O a bottleneck for the scalability. The parallelization of the I/O operations is needed to overcome the limit of the intrinsic sequential operations. However, on some architecture, also the management of a huge quantity

of data produced by a single simulation could be a problem. For example executing the NEMO [6] oceanic model on 16K cores of an IBM's BlueGene machine and taking into account that each process performs I/O on different files, the filesystem management becomes a very complex operation.

## 2. MINI-APPLICATIONS FOR CLIMATE

The real climate applications, used for the production of scientific data, are typically large, complicated and the outcome of a coupled set of different model components. As a result, they tend to be challenging to port on new computer platforms and require skilled computer scientists to do so. Although the climate applications benchmarking on new platforms is essential as part of the design and implementation of a new computer system, the scope of this benchmarking is necessarily limited by the complexity of the software product. The characteristics that impact on performance should be understood to better evaluate the performance portability on different architectures and drive the design of new computers. Furthermore, it is often the case that there are multiple ways to design and implement the algorithms used in an application, and the choice can have a dramatic impact on application performance. To address these needs, two important properties of many climate models can be considered: (i) although a model may have one million or more source lines of code, performance is often dominated by a very small subset of lines included in a single or few computational kernels; (ii) for the remaining code, these applications often contain many physics models that are mathematically distinct but have very similar performance characteristics [7]. Mini-applications as lighter versions of complex HPC applications attract growing interest as a flexible test bed to facilitate software development. They aim to project how more complex applications will interact with future computing hardware and are highly valuable to system designers and architects as long as they represent the behaviour of the complete workload with sufficient fidelity. They should capture a code's essential features in terms of core data structures, algorithms and parallel constructs while demonstrating state-of-the-art implementations relying on modern programming paradigms. Two ways to build them can be considered: (i) to start from the real application and applying the needed changes or (ii) to write a new code breaking a specific barrier to extreme scale, constructing the mini-application around it. Both approaches, evolu-

tionary vs. revolutionary are valuable but not interchangeable. The need to maintain mini-applications up-to-date with the major evolution of the reference code is critical for their long term usability [8].

The development process of a mini-application has to start from the identification of the bottlenecks and the computational characteristics of the target climate model. The computational kernels can be extracted and a stand-alone application will be developed around them preserving the computational characteristics, the data structure and the communication pattern of the original model.

## 2.1 THE NEMO TEST CASE

As an example, we can consider the NEMO oceanic model use case. At very high resolution, one of the most computationally intensive kernel is represented by the advection tendency term of a tracer (salinity or temperature). The advection term is the divergence of the advective fluxes and it implicitly requires the use of the continuity equation. It is of paramount importance to design the discrete analogue of the advection tendency so that it is consistent with the continuity equation in order to enforce the conservation properties of the continuous equations. The key difference among the advection schemes available in NEMO is the choice made in space and time interpolation to define the value of the tracer at the velocity points. In the Monotone Upstream Scheme for Conservative Laws (MUSCL), the tracer at velocity points is evaluated assuming a linear tracer variation between two T-points. The time stepping is performed using a forward scheme, this means that the tracer field estimated in the previous step is used to evaluate the tracer at the current step. From the computational point of view, the kernel includes the evaluation of the advective term for each of the element of the domain and the data exchanges between neighbours following a 5-points stencil communication pattern. The mini-application built around this kernel will allow to evaluate the performance portability of the NEMO model on several platforms and to estimate the computational performances achievable by the introduction of an OpenMP-MPI hybrid parallelization [9] as well as to evaluate how the new parallel architectures based on accelerators (GPU, MIC) can suite for the execution of oceanic models. As an example, the nodes of Cray's XE6 machine have hardware support for 32 threads while the nodes of IBM's BlueGene/Q have hardware support

for 64 threads. Increasingly, high-end machines are being equipped with accelerators such as GPUs or Intel's Xeon Phi. These devices have many, lightweight cores and writing efficient software for them can be complex. Figure [1] shows the execution of

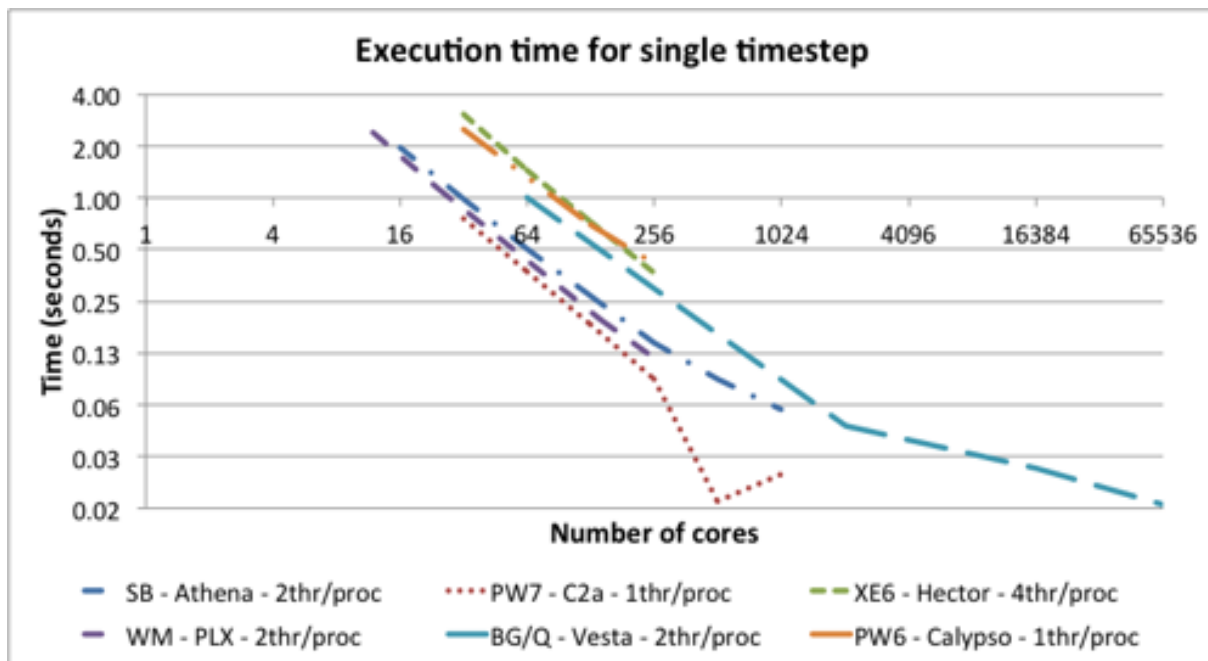


Fig. 1 Tracer Advection mini-application used to compare different architectures.

the MUSCL mini-application to compare different parallel architectures and to evaluate how many core architectures can be exploited through the hybrid parallelization. The MUSCL kernel parallelisation has been evaluated on different architectures: the IBM iDataPlex based on SandyBridge processor (Athena) located at CMCC, Italy; the IBM cluster based on Power6 processor (Calypso) located at CMCC, Italy; the IBM cluster based on Power7 processor (C2A) located at ECMWF; the Cray's XE6 machine (Hector) located at STFC, UK; the IBM iDataPlex based on Westmere processors (PLX) located at Cineca, Italy; a IBM BluGene/Q (Vesta) located at ALCF, USA. The results highlight the differences on the exploitation of multithreaded parallelisation for different computing architectures. In particular, the Power processor family does not provide any advantage on multithreaded parallelisation. The Cray XE6 can be fully exploited using 4 threads for each MPI process. For the other architectures, 2 threads for each MPI process is the best balance between threads and processes.

Another computationally intensive kernel for NEMO is represented by the successive over relaxation (SOR), a variant of the iterative Gauss-Seidel method for solving a linear system of equations  $Ax = b$ . An enhanced parallel version of the algorithm has

been developed by acting on the size of the overlap region to reduce the frequency of communications and an analytical performance model of the SOR that can be used for establishing the optimal size of the overlap region has been designed [10]

### 3. CONCLUSION

The mini application here presented is an initial contribution towards what is already recognised as a relevant effort to foster a co-design approach in the development of models optimisation. The advection schemas, described in the paper, has been used for testing the computational behaviour of multithreading and hybrid parallelization on the current parallel architectures. The main purpose of the mini applications is indeed to handle simpler code but significantly representing the real application for testing new numerical schemas, new parallel paradigms or new computing architectures. As next steps we plan to use this mini application to evaluate how the new Xeon Phi processor is suitable for ocean models and how the improvement of vectorisation level could reduce the time to solution.

### 4. REFERENCES

1. I. Epicoco, S. Mocavero, and G. Aloisio, *The NEMO Oceanic Model: Computational Performance Analysis and Optimization*, High Performance Computing and Communications (HPCC), 2011 IEEE 13th International Conference pp.382,388, 2-4 Sept. 2011 doi: 10.1109/HPCC.2011.56
2. I. Epicoco, S. Mocavero, and G. Aloisio, *A Performance Evaluation Method for Climate Coupled Models*, Procedia Computer Science, Volume 4, 2011, Pages 1526-1534, ISSN 1877-0509, <http://dx.doi.org/10.1016/j.procs.2011.04.165>
3. J. Lions, Y. Maday, and G. Turinici. *A "parareal" in time discretization of PDE's*, C.R. Acad.Sci. Paris, Serie I, 332:661-668, 2001
4. K. A. Yelick, *Performance Advantages of Partitioned Global Address Space Languages*, PVM/MPI, 2006.

5. J. Demmel, *Communication-Avoiding Algorithms for Linear Algebra and Beyond*, 2013 IEEE 27th International Symposium on Parallel & Distributed Processing, 2013.
6. G. Madec and the NEMO team (2008), *NEMO ocean engine*, Note du Pole de modélisation, No. 27, Institut Pierre-Simon Laplace (IPSL), France, ISSN: 1288-1619
7. M. A. Heroux, D. W. Doerfler et al., *Improving Performance via Mini-applications*, SANDIA REPORT SAND2009-5574, 2009.
8. P. Ricoux et al., *EESI2 First Intermediate Reports*, EESI2 project reports - <http://www.eesi-project.eu/pages/menu/deliverables.php>
9. I. Epicoco, S. Mocavero and G. Aloisio, *Hybrid Strategies for the NEMO Ocean Model on Multi-core Processors*, EASC2013: Solving Software Challenges for Exascale, 9-11 April 2013, Edinburgh, Scotland, UK
10. I. Epicoco, S. Mocavero and G. Aloisio, *The performance model for a parallel SOR algorithm using the red-black scheme*, Int. J. of High Performance Systems Architecture, 2012 Vol.4, No.2, pp.101 - 109

## 5. IMAGES AND TABLES

Fig. 1 Tracer Advection mini-application used to compare different architectures

# The response of the mean meridional circulation to global warming and its relationship with precipitation distribution

D'Agostino R.<sup>1,2,\*</sup>, P. Lionello<sup>1,2</sup>

<sup>1</sup>University of Salento, Italy

<sup>2</sup>CMCC, Euro-Mediterranean Centre on Climate Change

\*Corresponding author: roberta.dagostino@unisalento.it

## Abstract

Modifications in the Mean Meridional Circulation (MMC) have important implications for meridional heat transport and for the distribution of precipitation. This work discusses the response of the MMC to global warming in terms of strengthening/weakening and widening/narrowing of the Hadley Cells. The analysis is based on the ERA-20CM ensemble, which describes the response of the atmospheric circulation to the variability of the Sea Surface Temperature (SST) and changes of atmospheric composition. The meridional mass stream function is computed for the warmest and coldest decade of the 20<sup>th</sup> century and the variations of the Hadley Cells are analyzed. Results show that in both hemispheres the Hadley cells are significant stronger in the warmest than in the coldest decade. The intensification of the Hadley Circulation determines more precipitation in the Tropics and less in Subtropics. Moreover, the poleward shift of the Ferrel Cells displaces precipitation poleward both in Northern and Southern Hemispheres.

**Keywords:** Mean Meridional Circulation, ERA-20CM, total precipitation, global warming.

## 1. INTRODUCTION

The Mean Meridional Circulation (MMC) plays an essential role in the transport of heat and moisture from the equator to high latitudes [3] and its changes have large impacts on global and regional climate [5].

Many previous studies show the strengthening of the Hadley Cell (HC) in both hemispheres [17,15,8,10,16], the widening of the tropical belt [22,12,9,13] the poleward shift of the subtropical edges [6,20,27] across reanalyses, observations and simulations and attributed it to global warming. Mitas and Clements [15] showed an upward tendency of strengthening of the HC over last several decades through two major reanalyses project (NCEP/NCAR and ERA-40). This upward trend cannot be attributed to increasing ENSO frequency, since it persists even when the ENSO signal has been removed by regressing on the Niño 3.4 Index. Liu et al. [10] found a substantial multidecadal variability in strength of the HC based on 20CRv.2 data, with a significant upward trend ( $0.61 \times 10^{10}$  Kg/s) and a significant increasing trend ( $0.91 \times 10^{10}$  Kg/s) in Northern and Southern Hemispheres (NH and SH) HC, respectively. The analysis of the annual cycle of intensity, extent and width of the HC conducted by Nguyen et al. [16] across 31-yr period (1979-2009) from all existent reanalyses reveals a good agreement among the dataset, in which they showed an expansion of the HC in both hemispheres and a slight tendency toward intensification.

About the widening of the tropical belt, Liu et al. [10] found that the HC shrunk by  $^{\circ}$  in latitude from 1870s to the mid-1920s, followed by two major expansion periods (from the mid-1920s to the mid-1940s, and from the late 1970s to the present) which are in accordance with two major warming periods (1925-1944 and 1978-present). They suggested that HC has a long-period oscillation and it might have not yet completed a single cycle since 1871, although there is no guarantee that the behavior of the width of the HC has to be cyclical. To further confirm the identified secular variability, they performed the spectral analysis on the time series of the width of the HC, and it exhibits a clear secular peak indicative of century-scale variability. Moreover, some studies showed that the HC is also dominated by ocean-atmosphere variability associated with ENSO on interannual time-scale [17,18]. The analysis made by Nguyen et al. [16] on reanalyses, proved that during warm/El-Niño events the Southern and Northern Hemisphere HC (SH and NH, respectively) tend to be less extensive and more intense. The opposite behavior is seen during cool/La-

Niña events. In the study of Nguyen et al. [16], the intensification associated with contraction has been linked to an increase in meridional temperature gradient, which result in an intensification of the thermally driven HC [19]. The expansion might be caused by a reduction in baroclinicity in the subtropics driven by an intense in (dry) static stability and/or by an increase in the phase speed of upper-tropospheric baroclinic waves [12]. However, the effect of the El-Niño/La-Niña events are rarely studied separately from the Global Warming. Lu et al. [12] have proposed a comparison between the effect of the global warming and the El-Niño forcing on the zonal mean atmospheric circulation examining the model simulations conducted for the Fourth Assessment Report (AR4) of the Intergovernmental Panel on Climate Change (IPCC). They found that the HCs response to global warming in somewhat opposite fashion to the El-Niño teleconnection pattern. Their analysis is consistent with the one made by Seager et al. [21] in which during El-Niño event, the tropical atmosphere warms at all longitudes, and subtropical jets in both hemispheres strengthen on their equatorial flank and shift toward the equator. Poleward of the tropical warming there are latitudinal belts of marked cooling, extending from the surface to the tropopause in both hemispheres. The HC intensifies and contracts equatorward. On the contrary, the atmospheric response to global warming is characterized by a poleward expansion of the Hadley circulation [14], a poleward shift in eddy-driven jets [11] and mid-latitude storm-tracks [25] and a weakening of the tropical atmospheric circulation [23,14].

Our analysis focuses on trend in the MMC and on the differences in the zonal mean Hadley Circulation between “warm” and “cold” surface temperature conditions. Therefore, we have used the ensemble of 10-model integrations of the ERA-20CM, an atmospheric global circulation model performed by ECMWF throughout the 20<sup>th</sup> Century. In this model, the climate variability is represented by 10 different realizations of the Sea Surface Temperatures and forcing terms (solar forcing, greenhouse gases, ozone and aerosols) follow CMIP5 recommendations. Moreover this study shows that changes of the MMC are consistent with those of the meridional distribution of the precipitation.

## 2. DATA AND METHODS

This study is based on the ERA-20CM experiment that has been performed at ECMWF. ERA-20CM is an ensemble mean of ten atmospheric model integrations from 1900 to 2009. This ensemble has T159 horizontal resolution, which corresponds about 125 Km in grid-point space, 91 levels in the vertical from the surface up to 1 Pa. Here, we choose 1.5 horizontal regular resolution for  $\bar{v}$  field and 17 pressure levels (1000, 925, 850, 700, 600, 500, 400, 300, 250, 200, 150, 100, 70, 50, 30, 20, 10). We use also the total precipitation field. In this ensemble, SSTs and sea-ice cover are prescribed using an ensemble of realizations (HadISST2), recently produced by Met Office Hadley Center within ERA-CLIM project, whose differences reflect uncertainties in the available observational sources. Forcing terms in the model radiation scheme follow CMIP5 recommendations. These terms include solar forcing, greenhouse gases, ozone and aerosols. Both the ocean-surface and radiative forcing incorporate a proper long-term evolution of climate trends in the 20<sup>th</sup> Century and the occurrence of major events, such as El-Niño-Southern Oscillations and volcanic eruptions. No atmospheric observations are assimilated. For this reason, ERA-20CM is not able to reproduce the actual evolution of the synoptic systems. This ensemble is, however, meant to provide a statistical estimate of the climate evolution and provide a good description of the low-frequency variability of the atmosphere for the 20<sup>th</sup> Century [4].

The MMC is studied computing the monthly Mean Mass Streamfunction [17] which is defined as:

$$\psi = \frac{2\pi a \cos \phi}{g} \int_0^p [\bar{v}] dp \quad (1)$$

where  $\bar{v}$  is the zonally-time averaged meridional component of the wind,  $a$  is the radius of the Earth,  $g$  is gravity,  $\phi$  is latitude and  $p$  is pressure level. The  $\psi$  at given latitude and pressure level is equal to the rate at which mass is transported meridionally between that pressure level and the top of the atmosphere. To ensure vertical-mean mass balance, the  $[\hat{v}]$  fields are corrected by subtracting their mass-weighted vertical mean value:

$$[\hat{v}] \equiv \int_0^{p_0} [\bar{v}] dp/p_0 \quad (2)$$

According to this definition  $\psi$  is positive (negative) in the NH and SH HC and the strength of the circulation is given by the maximum (minimum) value of  $\psi$  over the entire extension of the cell.

In this way positive values of  $\psi$  correspond to clockwise rotation, while negative values of  $\psi$  correspond to counter-clockwise rotation. Using maximum/minimum values of  $\psi$  we can make time series for the strength for NH and SH HC.

Global warming is studied by comparing the "warm" decade with the "cold" decade, selecting the decade 2000-2009 in the first case and 1900-1909 in the second. Temporal subsets are been chosen analyzing the 12-months running mean global surface temperature time series (Fig.1) computed by the ensemble-mean (10 integration members) of the ERA-20CM surface temperature field. In this way, we describe how the MMC responded to warm and cold conditions. Further the difference between the selected two decades provides an estimate of the trend.

### 3. RESULTS

Our investigation about the trend in the annual mean of  $\psi$  reveals that both Hadley cells have strengthened. The intensification in the warmest with respect to the coldest decade is  $1.8 \times 10^9$  Kg/s in the NH and  $-3.5 \times 10^9$  in the SH. Both changes are significant at the >90% significance level. The cells appear to have changed their shape. In both hemispheres, they are higher and wider in the warmest than in the coldest decade. Further in the SH, the HC has shifted poleward, while in the NH, the HC has slightly shifted equatorward. Moreover the Ferrel Cells (FCs) in both hemispheres are wider and shifted poleward (Fig. 2).

The difference between 2000-2009 and 1900-1909 in the annual mean meridional precipitation distribution (Fig. 3) indicates a significant (98% confidence level) increase of the total precipitation around Tropics and a slight decrease in the Subtropics in order of  $0.4 \text{ mm/day}$  and  $-0.2 \text{ mm/day}$  respectively. This result might be connected to strengthening of the HCs. The poleward shift and the increase of the precipitation over higher latitudes in order of  $0.1 \text{ mm/day}$  in the SH and  $0.2$  in the NH, is consistent with poleward shift of the Ferrel Cell in both hemispheres and

also with the poleward shift of the mid-latitude storm-tracks projected in those studies about the global warming [3, 25].

The difference between the “warm” and “cold” decade in the annual cycle of the MMC (Fig. 4) shows an asymmetric change in the two hemispheres. The SH HC becomes higher, wider, stronger and poleward shifted almost across the entire year, while the NH HC becomes wider in late summer and narrower and slightly stronger in winter. Instead, the FCs in both hemispheres are generally poleward shifted in the warmest with respect to the coldest decade.

#### **4. CONCLUSIONS**

The analysis on the response of the MMC to global warming made with the climate model ERA-20CM data reveals a significant increase in strength of the Hadley Circulation. This is in agreement with previous studies based on reanalyses and observations [1,10,12,15]. Further, simulations show a significant increase of the total precipitation in the Tropics and in the Subtropics, which is consistent with the strengthening of the Hadley Circulation. About the extension of the Hadley Circulation, there is a tendency of the Southern Hemisphere cell to be wider and poleward shifted in the warmest than in the coldest decade while the Northern Hemisphere cell boundaries do not show any discernable trend. Meanwhile, the Ferrel Cells in both hemispheres appear to be shifted poleward and it might be the cause of the analyzed poleward shift of the total precipitation to higher latitudes. Some studies suggest also an expansion of the Hadley Circulation associated to increase in the concentration of the green-house gases: this is based on the postulation that the extent of the Hadley Circulation is determined by the latitude of the baroclinic instability, and under global warming conditions, the subtropical static stability increases due to an established consequence of moist thermodynamics which pushes the baroclinic instability zone poleward, and consequently causes the outer boundary of the Hadley Cell to extend poleward [14]. Here, our analysis shows that only the Southern Hemisphere Hadley Circulation is expanded poleward in accordance with surface warming of the last decade and with the increase of the green-house gases condition.

## 5. REFERENCES

1. Chen J., Carlson B. E., and Del Genio A. D. Evidence for strengthening of the tropical general circulation in the 1990s. *Science*, 295(5556):838-841, 2002.
2. Diaz H. F. and Bradley R. S. *The Hadley Circulation: present, past and future*, volume 21. Springer, 2004.
3. Giorgi F. and Lionello P. Climate change projections for the Mediterranean region. *Global and Planetary Change*, 63(2):90-104, 2008.
4. Hersbach H., Peubey C., Simmons A., Poli P., Dee D. and Berrisford P. ERA-20CM: a twentieth century atmospheric model ensemble. ERA Report Series No. 16, 2013.
5. Holton J. R. and Hakim G. J. *An introduction to dynamic meteorology*. Academic press, 2012.
6. Hu Y. and Fu Q. Observed poleward expansion of the Hadley circulation since 1979. *Atmospheric Chemistry and Physics*, 7(19):5229-5236, 2007.
7. Hu Y., Tao L., and Liu J. Poleward expansion of the Hadley circulation in CMIP5 simulations. *Advances in Atmospheric Sciences*, 30:790-795, 2013.
8. Hu Y. and Zhou C. Decadal changes in the Hadley circulation. *Advances in Geosciences*, Volume 16: Atmospheric Science (AS), 16-61, 2010.
9. Johanson C. M. and Fu Q. Hadley cell widening: Model simulations versus observations. *Journal of Climate*, 22(10), 2009.
10. Liu J., Song M., Hu Y., and Ren X. Changes in the strength and width of the Hadley circulation since 1871. *Climate of the Past Discussions*, 8(2), 2012.
11. Lorenz D. J. and DeWeaver E. T. Tropopause height and zonal wind response to global warming in the IPCC scenario integrations. *Journal of Geophysical Research: Atmospheres* (1984-2012), 112 (D10), 2007.
12. Lu J., Chen G., and Frierson D. M.W. Response of the zonal mean atmospheric circulation to El-Niño versus global warming. *Journal of Climate*, 21(22), 2008.
13. Lu J., Deser C., and Reichler T. Cause of the widening of the tropical belt since 1958. *Geophysical Research Letters*, 36(3), 2009.
14. Lu J., Vecchi G. A., and Reichler T. Expansion of the Hadley cell under global warming. *Geophysical Research Letters*, 34(6), 2007.
15. Mitas C. M. and Clement A. Has the Hadley cell been strengthening in recent decades? *Geophysical Research Letters*, 32(3), 2005.

16. Nguyen H., Evans A., Lucas C., Smith I., and Timbal B. The Hadley circulation in reanalyses: Climatology, variability, and change. *Journal of Climate*, 26(10), 2013.
17. Oort A. H. and Yenger J. J.. Observed interannual variability in the Hadley circulation and its connection to ENSO. *Journal of Climate*, 9(11):2751-2767, 1996.
18. Quan X. W., Diaz H. F., and Hoerling M. P. Changes in the tropical Hadley cell since 1950. *The Hadley Circulation: Present, Past, and Future*, pages 85-120, 2004.
19. Reichler T. Changes in the atmospheric circulation as indicator of climate change. *Climate Change: Observed Impacts on Planet Earth*, pages 145-164, 2009.
20. Scheff J. and Frierson D. M.W. Robust future precipitation declines in CMIP5 largely reflect the poleward expansion of model subtropical dry zones. *Geophysical Research Letters*, 39(18), 2012.
21. Seager R., Harnik N., Kushnir Y., Robinson W., and Miller J. Mechanisms of hemispherically symmetric climate variability. *Journal of Climate*, 16(18), 2003.
22. Seidel D. J., Fu Q., Randel W. J., and Reichler T. J. Widening of the tropical belt in a changing climate. *Nature geoscience*, 1(1):21-24, 2007.
23. Vecchi G. A. and Soden B. J. Global warming and the weakening of the tropical circulation. *Journal of Climate*, 20(17), 2007.
24. Wielicki B. A., Wong T., Allan R. P., Slingo A., Kiehl J. T., Soden B. J., Gordon C.T., Miller A. J., Yang S., Randall D. A., et al. Evidence for large decadal variability in the tropical mean radiative energy budget. *Science*, 295(5556):84-844, 2002.
25. Yin J. H.. A consistent poleward shift of the storm tracks in simulations of 21<sup>st</sup> century climate. *Geophysical Research Letters*, 32(18), 2005.

## 6. IMAGES AND TABLES

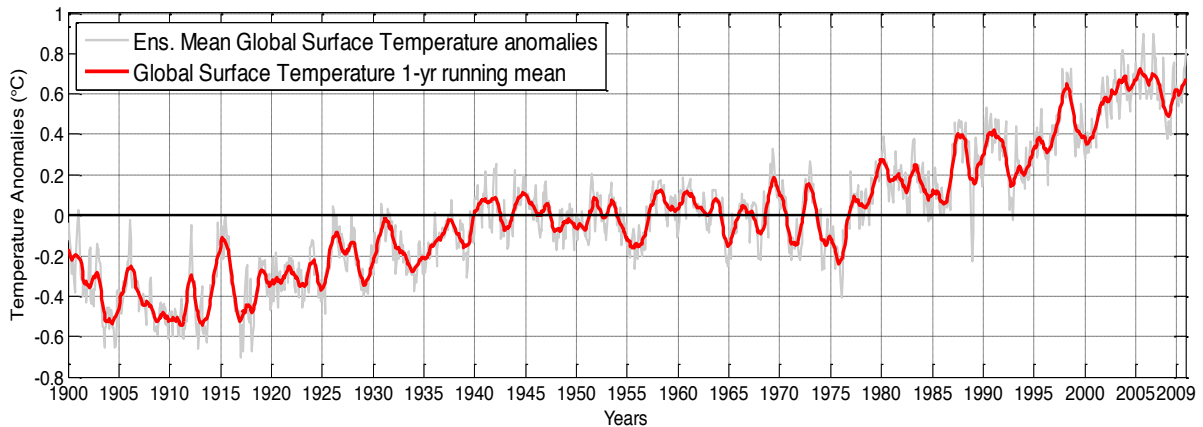


Fig. 1 Time series of the ensemble mean ERA-20CM global surface monthly temperature from 1900 to 2009 (grey line) and its annual average value (red bold line).

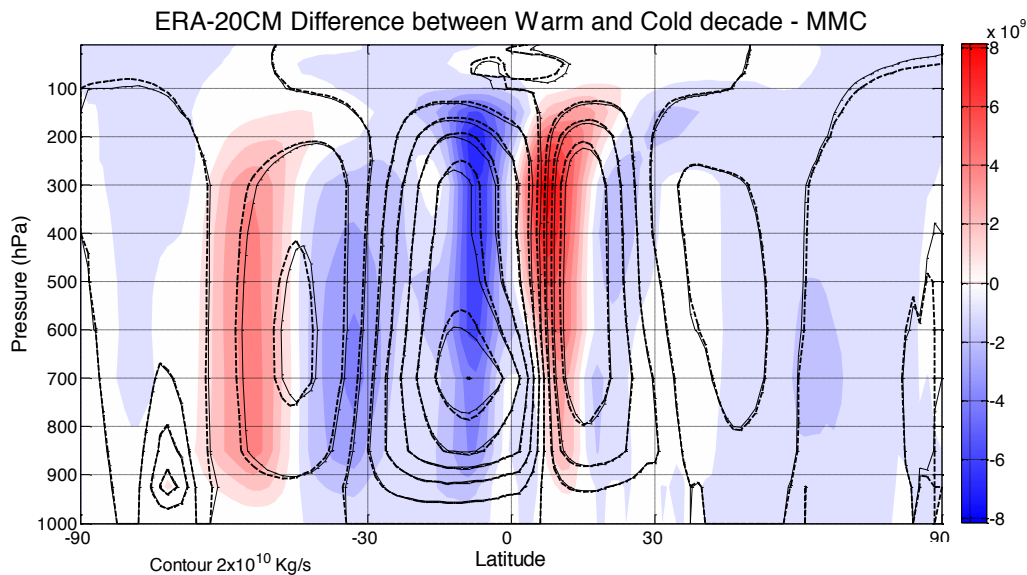


Fig. 2 Annual mean meridional Mass Stream Function ( $\psi$ , contour interval  $2 \times 10^{10}$  Kg/s), 2000-2009 (black dashed lines) and 1900-1909 (black solid lines) composites. In the Southern Hemisphere (SH)  $\psi$  is positive in the FC and negative in the HC. In the Northern Hemisphere (NH), the opposite. Colored contours show the difference between warm and cold decade ( $10^9$  Kg/s).

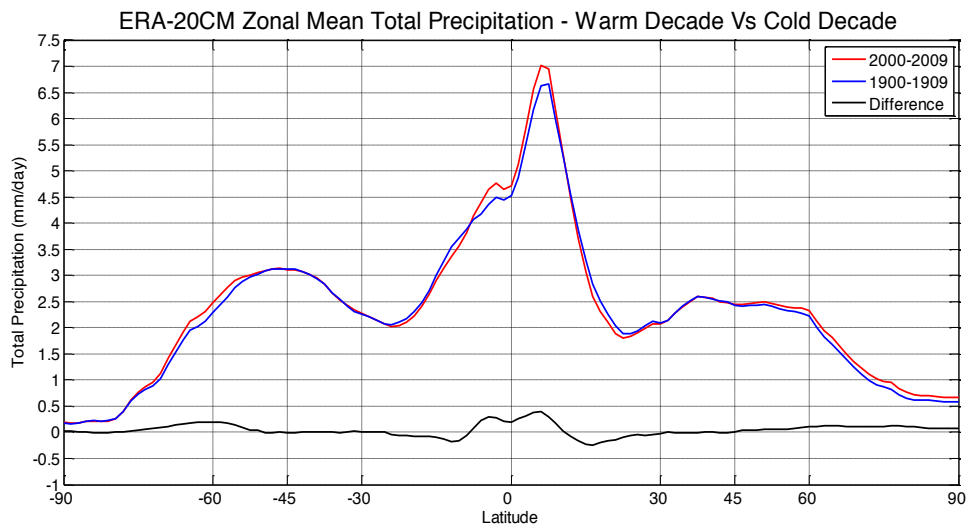


Fig. 3 Meridional distribution of the annual mean total precipitation mm/day. The red line refers to the warmest decade and the blue line to the coldest decade. The black line is the difference between blue and red line.

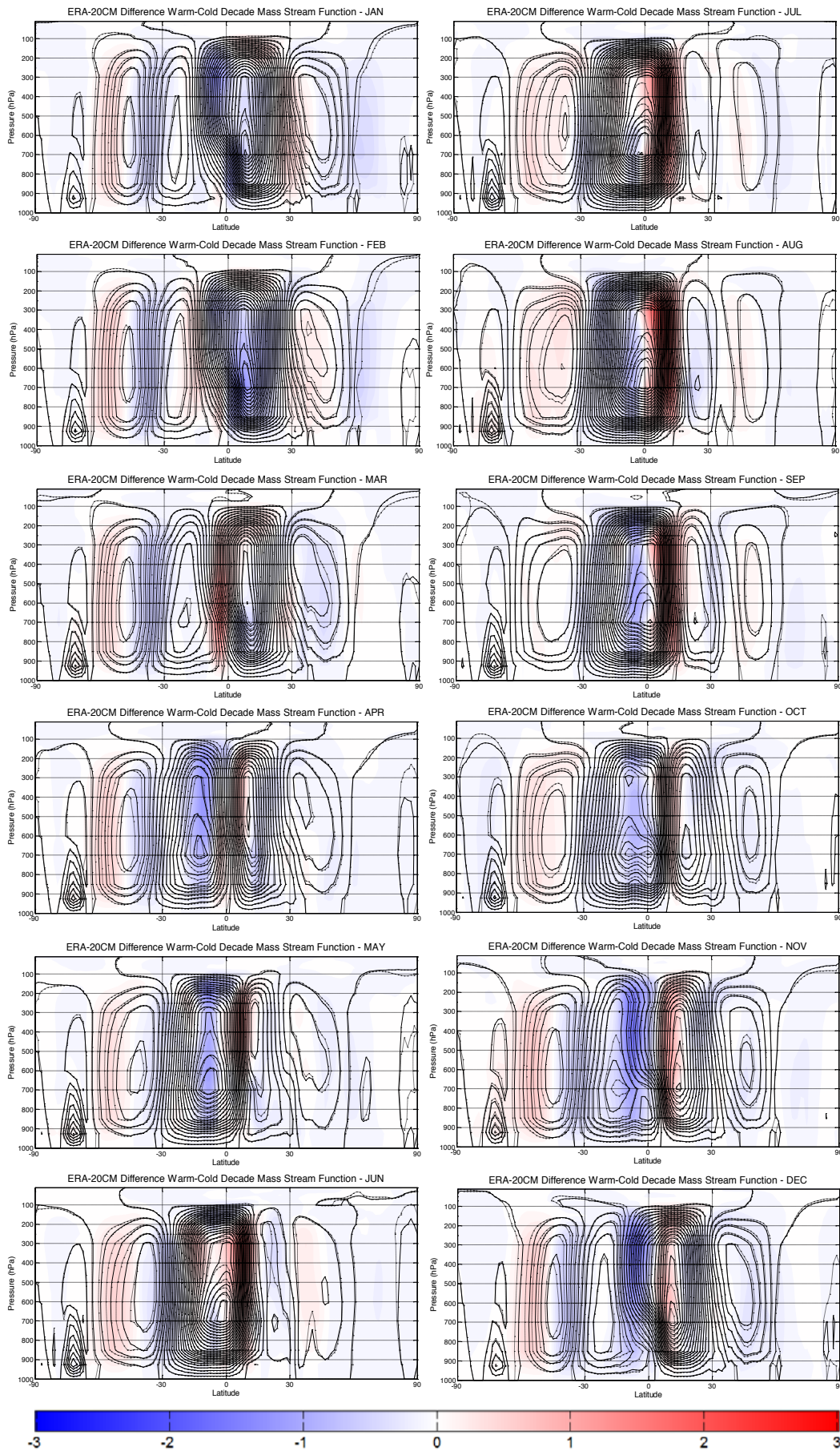


Figure 4: . Annual cycle of the meridional Mass Stream Function ( $\psi$ , contour interval  $10^{10}$  Kg/s), 2000-2009 (black dashed lines) and 1900-1909 (black solid lines) composites. In the Southern Hemisphere (SH)  $\psi$  is positive in the FC and negative in the HC. In the Northern Hemisphere (NH), the opposite. Colored contours show the difference between warm and cold decade ( $10^{10}$  Kg/s).

# Downscaled temperature scenarios for five sites in the Basilicata region

Pasini A., Attanasio A., and Giusto M.

CNR, Institute of Atmospheric Pollution Research, Rome - Italy

\*Corresponding Author: pasini@iia.cnr.it

## Abstract

At present, in the Mediterranean region, future scenarios of temperatures from outputs of many Regional Climate Models are very “convergent” and their projections can be considered reliable at this regional scale. In this framework, an open problem is to obtain more local scenarios. In this paper we address this topic by downscaling the outputs of a Regional Climate Model (referred to Basilicata) on five sites, representative of the various climatic zones of this Italian region. This has been done by application of a neural network model. Preliminary results of future local scenarios for mean temperatures and extremes are presented here.

**Keywords:** climatic scenarios, temperature projections, downscaling, neural modeling, Basilicata

## 1. INTRODUCTION

Global Climate Models (GCMs) are the standard tools for reconstructing past climate and predicting future scenarios at large scale. As well known, their results can be refined by Regional Climate Models (RCMs), which supply us with more detailed information at regional scale [1].

At present, many RCMs show their ability to reconstruct past temperatures in a satisfactory manner in the Mediterranean basin. Furthermore, their runs on future scenarios show very similar outputs in this region, for both trends and spatial patterns of warming: see, for instance, [2]. In this framework, in which future scenarios of temperatures can be considered reliable at this regional scale, an open problem is to obtain more local scenarios.

Of course, dynamical approaches to downscaling at quasi-local scale are performed by furtherly increasing the spatial resolution of RCMs or by use of nested high-resolution models for limited zones. Here we adopted a statistical downscaling method – the neural network (NN) modeling – which is able to achieve site projections. We applied NNs as tools which can successfully post-process the outputs of a RCM. In doing so, we obtained future local scenarios for mean temperatures and extremes in five sites, which well represent the various climatic zones of the Basilicata region.

In the next section the observational data and the RCM outputs, on which this study is based, are briefly presented and described. In section 3 the NN model is introduced. In section 4 our results are presented and discussed. Finally, brief conclusions are drawn in section 5.

## 2. DATA

Daily temperature time series from 18 observatories in the Basilicata region, spanning the period 1951–2010, were analysed in a recent study [3] and a homogenized dataset has been obtained from this investigation. The original dataset was provided by the National Hydrographic Service (Servizio Idrografico Italiano). Thermometers used in the Italian observation network are approved and normalized by the National Hydrographic Service, which provides the instruments and guarantees their uniformity.

Here we consider the temperature records of five of these stations: Potenza, Matera, Metaponto, Maratea and Melfi [Fig. 1]. Basilicata shows three main climatic regions, as depicted in [Fig. 1]: a mountain zone, a hilly area and a coastal one. The climatic characteristic features of these zones are well represented in our dataset by data of Potenza, Matera and Metaponto, respectively. Furthermore, in order to give some insight into the local climate of the short Tyrrhenian coastline, the station of Maratea was also considered. Finally, due to the importance of the Vulture area from an economic and environmental point of view, the station of Melfi has been chosen for our investigation, too.

As far as the RCM output data to be downscaled are concerned, we chose the scenario results obtained from 1950 to 2100 by the RegCM3 model [4] for the A1B “balanced” emissions scenario [5]. At present, the RegCM3 model is widely considered as one of the best available RCMs. Its performances are very satisfying on the Mediterranean region and it is endowed with a horizontal resolution of about 25 km. For our study we analyze the surface variables supplied by this model at a 3-hour time-scale for 36 grid points which cover the Basilicata region. The choice of the specific variables considered as inputs of our networks will be discussed in section 4.

### 3. NEURAL NETWORK MODELING

NN modeling is the method adopted here to downscale temperatures from RCM's outputs to local sites, in both the past and future scenarios. This is fundamentally due to their capability for modeling nonlinear relationships between large-scale variables/patterns and local variables of fundamental importance, like temperature and precipitation.

The application of NNs in atmospheric and climate sciences is quite recent: see [6-9] for some reviews. Downscaling of temperature and precipitation has been performed in several investigations by means of NNs: see, for instance, [10] for a pioneering attempt and [9] for a short review of more recent studies. In the majority of applications, the downscaling performances of the NN models showed better results than those coming from linear methods.

Here we adopt an NN tool developed some years ago [11] for both diagnostic characterization and forecast in complex systems. In the last years it has been also

applied to climatic studies at global and regional scales [12-14]. For a description of its main features see [15] and references therein.

#### 4. NN APPLICATION AND RESULTS

The RegCM3 outputs supplied us with data about 27 variables at the surface. The first elaboration consisted in averaging their 3-hour values to daily means. Then we decided to consider just the grid points closest to our 5 stations for the downscaling activity. Finally, for each station and the corresponding grid point, we calculated the linear correlation coefficient  $R$  and the correlation ratio  $R_{nl}$  (a nonlinear generalization of  $R$ , see [16] for its definition) for each model variable vs. observed  $T$ .

In doing so, we chose the model variables which are more linearly and nonlinearly correlated with the daily temperatures as inputs of our networks, i.e. temperature, west and south components of the wind, mean intensity of the wind, humidity and incident solar energy flux. Thus we built networks endowed with 6 inputs (model variables) and one output (predicted temperature) to be compared with observed temperature, which is our target, in the training phase. As far as the hidden layers are concerned, we chose to perform ensemble runs with a different number of neurons, from 2 to 10, in a single hidden layer. The best performant network on the validation set was chosen for supplying us with the final outputs.

In order to validate our neural network method of downscaling, some runs have been performed for reconstructing past temperatures at our stations. In doing so, due to the quite short time series available, we adopted a technique recently developed (see [14]), the so-called extended leave-one-out method of training-validation-test. This allowed us to obtain reconstructions for the whole observed period.

The results, annually averaged, are shown in [Fig. 2] for the station of Potenza. The runs on the other stations gave very similar outcomes. It is clear that the main advantage of our downscaling technique is the large reduction of the bias: the RegCM3 model outputs are colder than observations (about  $3^{\circ}\text{C}$ ), while the NN bias is very close to zero. In this framework, in which scenarios runs of the RegCM3 model are used, interannual variability is obviously not well reconstructed, but this is fully understandable.

Furthermore, the improvement of performances is statistically significant, even in comparison with the results coming from the application of a linear model to the downscaling activity. In fact, even if we consider not only the best performant networks, but an ensemble of 30 NNs with different random choices for the initial weights and the validation set, the Mean Square Error (MSE) – targets vs. outputs – of both the RegCM3 and the linear model are higher than the right extreme of the MSE spread for the NN ensemble runs [Fig. 3].

As a next step, we tried to obtain downscaled scenarios in the future. In doing so, we needed a trained and validated network (i.e., with fixed weights) to which we might furnish data about RegCM3 future scenarios as inputs in order to obtain output values (our NN projections). Thus we had to apply a more standard training-validation-test approach on past values, by considering the period 1951-2000 as training set, 2001-2007 as validation set and 2008-2010 as test set. After ensemble runs with different initial random weights, for each station the best performant network on the test set has been chosen and future scenarios were obtained.

An example of these projection results is shown in [Fig. 4] for the station of Matera. In particular, a trend of about 0.030 K/year is predicted for the period 2011-2100 both in Matera and Metaponto. The NN runs on the other stations show an increase of about 0.026-0.027 K/year. The original RegCM3 outputs gave a trend which is substantially equal for all the sites of the Basilicata region and is estimated to be about 0.043 K/year. Thus, our downscaling activity shows a lesser increase of temperature along the region: this could be partially due to the fact that the networks have been trained and validated on a colder climate. In any case, the NN model allows us to distinguish different trends of warming in distinct sites of Basilicata.

Obviously, in this scenario framework, projected annual values have no significance. So, it is perhaps more instructive to plot temperature estimated densities on 30-years intervals [Fig.5]. In this way the warming can be easily caught in significant climatic periods.

As well known, together with future outputs about the mean trend of T, an important climatic information can be related to the extreme values of temperature. For this reason, we performed NN runs for reconstructing maximum temperatures ( $T_{\max}$ ) and minimum temperatures ( $T_{\min}$ ) in the past and then obtaining future scenarios of these variables, with the aim of achieving information about cold and warm periods. Once

obtained these results (not shown in this short paper), we analyzed the warm extremes by calculating the number of days of the year for which  $T_{\min} > 20$  °C (the so-called “tropical nights”) and those for which  $T_{\max} > 30$  °C (we call them “hot days”). The cold extremes were analyzed by means of an index which counts the number of days in which  $T_{\max} < 0$  °C (the so-called “frost days”).

Examples of our results are presented in [Figs. 6-8]. In every site we can appreciate a strong increase of both hot days and tropical nights. At the same time our model sees a substantial decrease of the frost days, which almost disappear in the last 20 years of this century at all sites considered here.

More specifically, the strongest trend in hot days has been predicted in Maratea (0.68 #days/year) and the weakest one in Matera and Metaponto (0.55 #days/year). The most pronounced increase in tropical nights has been predicted in Metaponto (0.86 #nights/year), the less important one in Potenza (0.55 #nights/year). Here, in particular, we note that the variance of the time series of projections [Fig. 7] increases with time, so that our model predict not only an increase in minimum temperature, but also an increase in its variability.

## 5. CONCLUSIONS

The approach adopted here is quite preliminary and further development is surely required to our investigation in order to obtain reliable scenarios at local scale. For instance, this approach does not take the possible changes in the use of soil into consideration, while this could be crucial for better determining local climate in the future. Furthermore, just RCM’s output variables at the surface has been considered, when probably also information about circulation in the atmosphere could be relevant for our problem.

Nevertheless, our results clearly show that our downscaling method is able to discern different behaviors of mean temperature and, especially, of extreme indices at distinct sites in the Basilicata region. For instance, it is worthwhile to note that the increasing trend in tropical nights is stronger in coastal areas and weaker in the mountain zone, here represented by Potenza.

In short, our NN model has shown its validity and found transfer functions from the regional scale to the local scale that allowed us to appreciate quite distinct climatic evolutions in different zones of a small Italian region.

## 6. ACKNOWLEDGMENT

F. Giorgi, E. Coppola and G. Giuliani (ICTP, Trieste, Italy) are kindly acknowledged for having supplied us with data from outputs of the runs of the RegCM3 model.

## 7. REFERENCES

1. Flato G. *et al.* (2013), Evaluation of Climate Models. In *Climate Change 2013: The Physical Science Basis* (eds. T.F. Stocker *et al.*), Cambridge University Press, Cambridge, UK, and New York, NY, USA, pp. 741-866.
2. Coppola E., Giorgi F., Rauscher S.A. & Piani C. (2010), *Model weighting based on mesoscale structures in precipitation and temperature in an ensemble of regional climate models*, Climate Research, No. 44, pp. 121-134.
3. Piccarreta M., Lazzari M. & Pasini A. (2014), *Trends in daily temperature extremes over the Basilicata Region (southern Italy) from 1951 to 2010 in a Mediterranean climatic context*, International Journal of Climatology (published online as early view), doi: 10.1002/joc.4101.
4. Pal J.S. *et al.* (2007), *The ICTP RegCM3 and RegCNET: regional climate modeling for the developing world*. Bulletin of the American Meteorological Society, No. 88, pp.1395-1409.
5. IPCC (2000), *Emissions scenarios*, IPCC special report.
6. Krasnopolsky, V.M. (2007), *Neural network emulations for complex multidimensional geophysical mappings: Applications of neural network techniques to atmospheric and oceanic satellite retrievals and numerical modeling*, Reviews of Geophysics, No. 45: RG3009, doi:10.1029/2006RG000200.
7. Haupt S.E, Pasini A. & Marzban C. (eds.) (2009), *Artificial Intelligence Methods in the Environmental Sciences*, Springer, New York, NY, USA.

8. Hsieh W.W. (2009), *Machine Learning Methods in the Environmental Sciences: Neural Networks and Kernels*, Cambridge University Press, Cambridge, UK.
9. Pasini A. (2009), Neural network modeling in climate change studies. In *Artificial Intelligence Methods in the Environmental Sciences* (eds. S.E. Haupt, A. Pasini & C. Marzban), Springer, New York, NY, USA, pp. 235-254.
10. Trigo R.M. & Palutikof J.P. (1999), *Simulation of daily temperatures for climate change scenarios over Portugal: a neural network model approach*, *Climate Research*, No. 13, pp. 45-59.
11. Pasini A. & Potestà S. (1995), *Short-range visibility forecast by means of neural-network modelling: A case study*, *Nuovo Cimento C*, No. 18, pp. 505-516.
12. Pasini A., Lorè M. & Ameli F. (2006), *Neural network modelling for the analysis of forcings/temperatures relationships at different scales in the climate system*, *Ecological Modelling*, No. 191, pp. 58-67.
13. Pasini A. & Langone R. (2012), *Influence of circulation patterns on temperature behavior at the regional scale: A case study investigated via neural network modeling*, *Journal of Climate*, No. 25, pp. 2123-2128.
14. Pasini A. & Modugno G. (2013), *Climatic attribution at the regional scale: a case study on the role of circulation patterns and external forcings*, *Atmospheric Science Letters*, No. 14, pp. 301-305.
15. Pasini A., Racca P. & Cassardo C. (2014), Influence of forcings and variability on recent global temperature behavior: A neural network analysis. In *Proceedings of the 2nd SISC Conference*, Venezia, Italy.
16. Marzban C., Mitchell E.D. & Stumpf G.J. (1999), *On the notion of "best predictors": An application to tornado prediction*. *Weather & Forecasting*. No. 14, pp. 1007-1016.

## 8. FIGURES

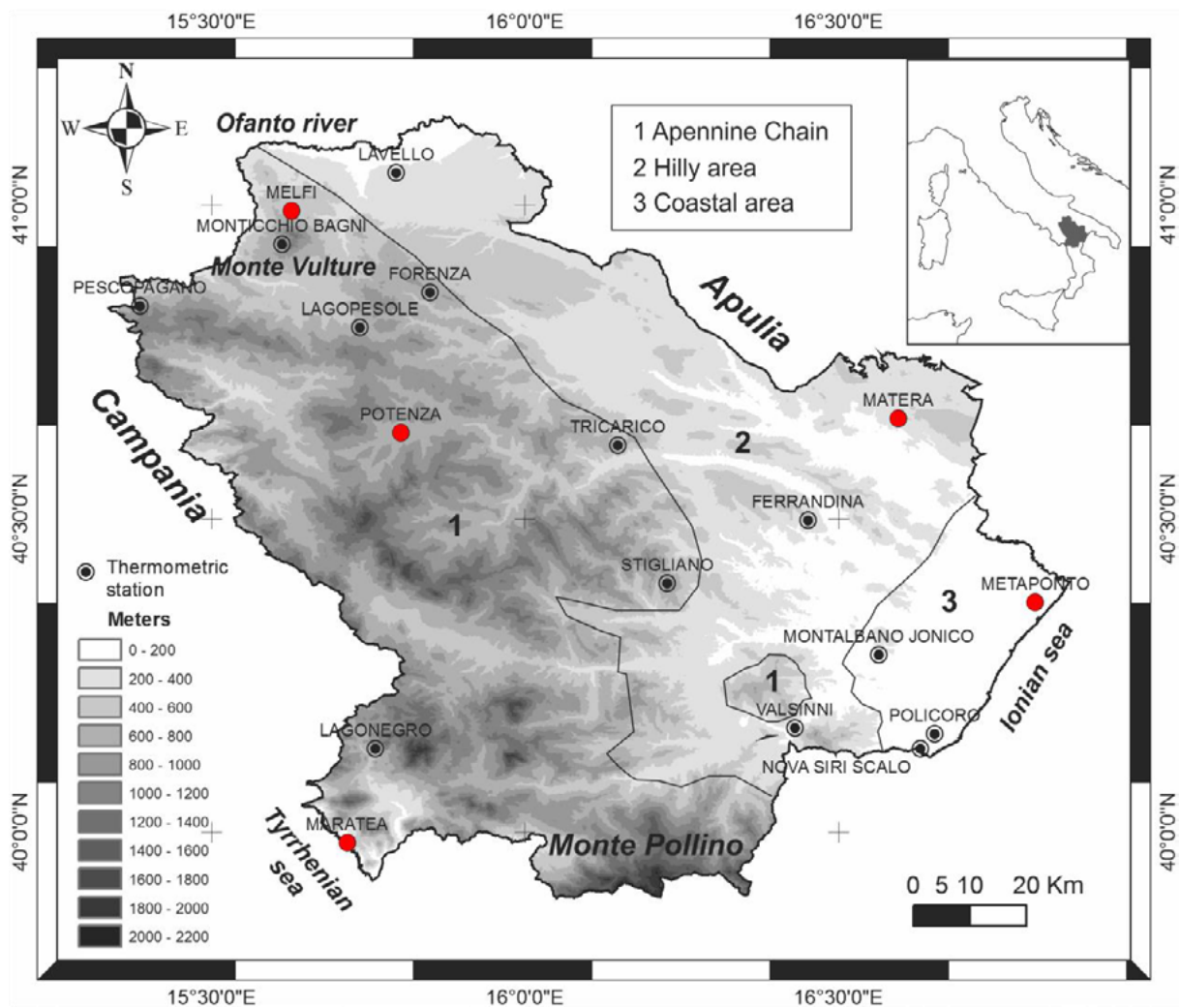


Fig. 1. The Basilicata region. Its three climatic zones are visible. The stations considered by the present study are shown (red circles); black circles identify the other stations of our original dataset.

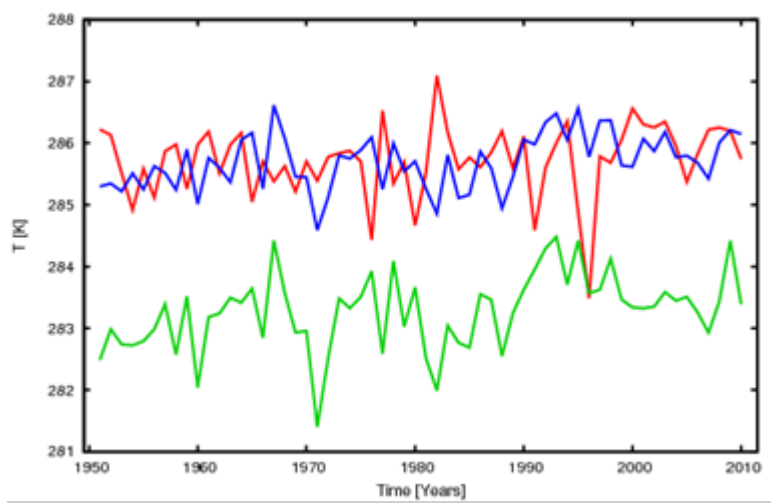


Fig. 2 Annual averaged values of mean temperature at Potenza site. Red line: observed temperatures, green line: reconstruction by RegCM3, blue line: reconstruction by NN model.

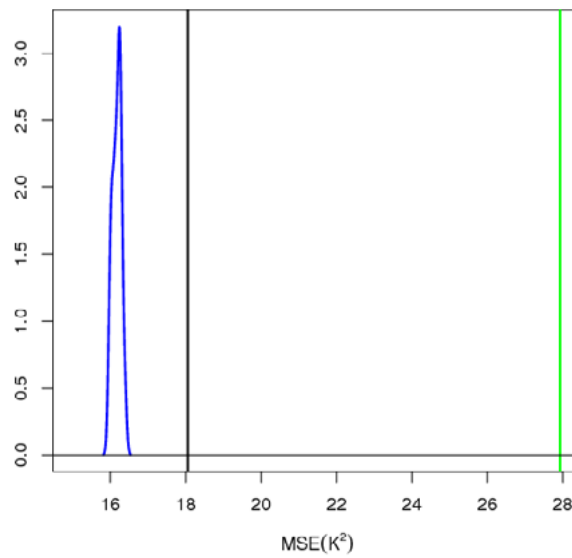


Fig. 3 Errors in reconstructing temperatures at Potenza site. Blue line: spread from the outputs of the NN ensemble runs, black line: linear model, green line: RegCM3.

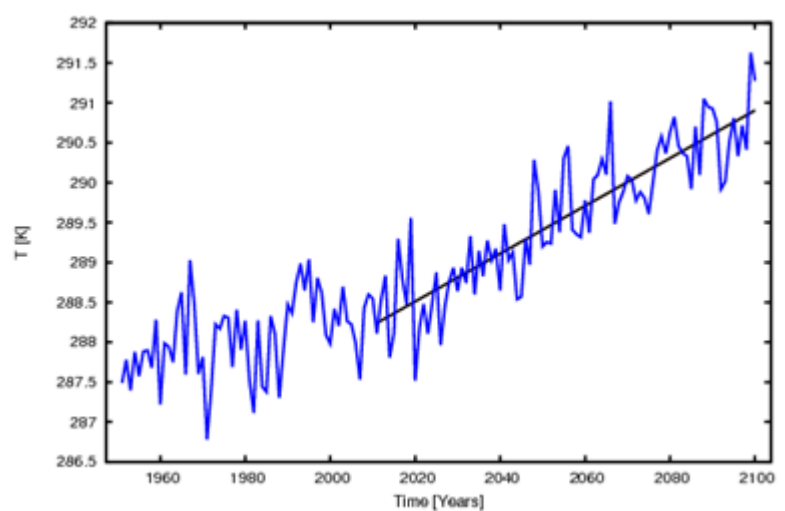


Fig. 4 Results of the NN model for annual mean temperatures at Matera site: reconstructed till 2010 and predicted from 2011 to 2100. The black line shows the trend on the predicted values.

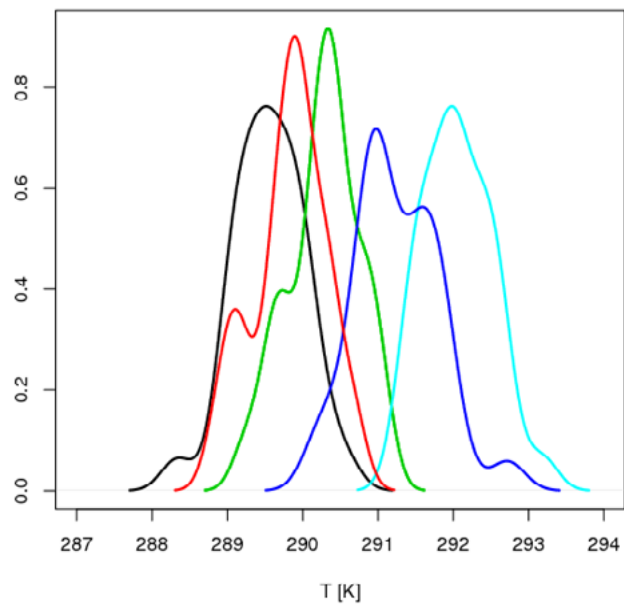


Fig. 5 Results of the NN model for density functions of annual mean temperatures over 30-year time intervals at Metaponto site. Black line: 1951-1980, red line: 1981-2010, green line: 2011-2040, blue line: 2041-2070, light blue line: 2071-2100.

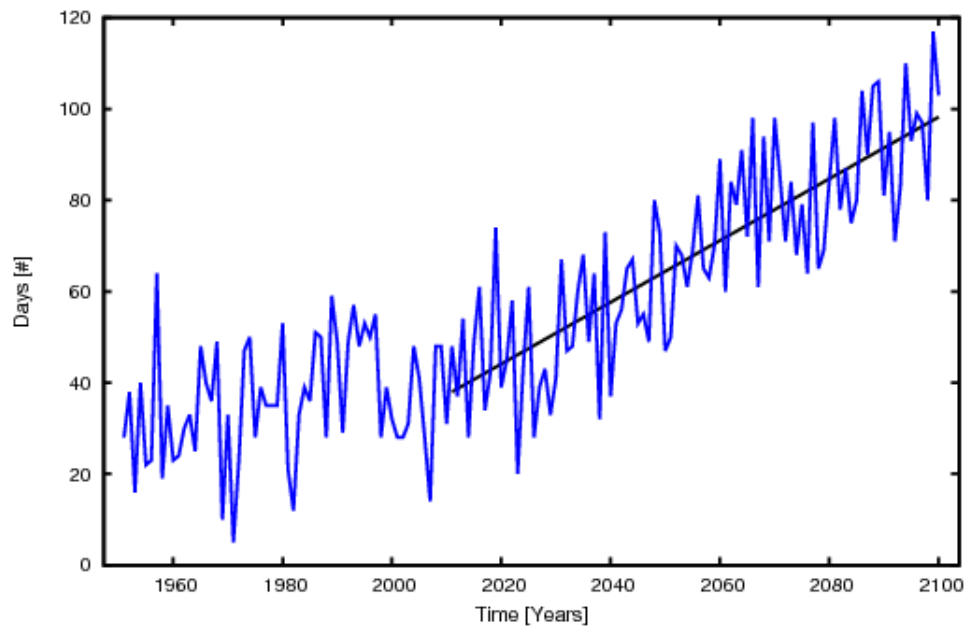


Fig. 6 Results of the NN model for the number of hot days in Maratea: reconstructed till 2010 and predicted from 2011 to 2100. The black line shows the trend on the predicted values.

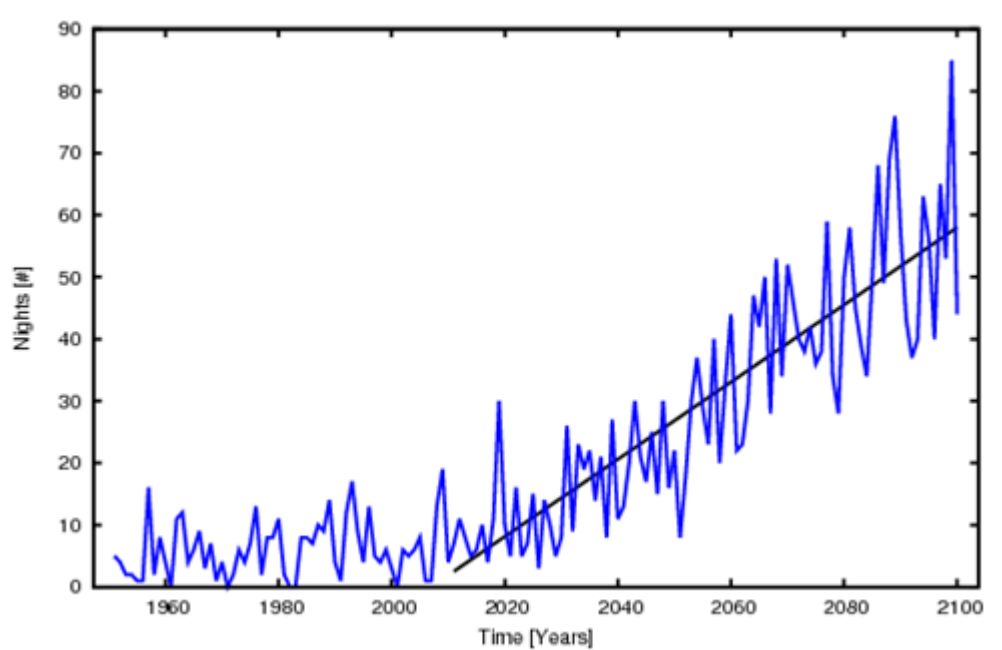


Fig. 7 Results of the NN model for the number of tropical nights in Melfi: reconstructed till 2010 and predicted from 2011 to 2100. The black line shows the trend on the predicted values.

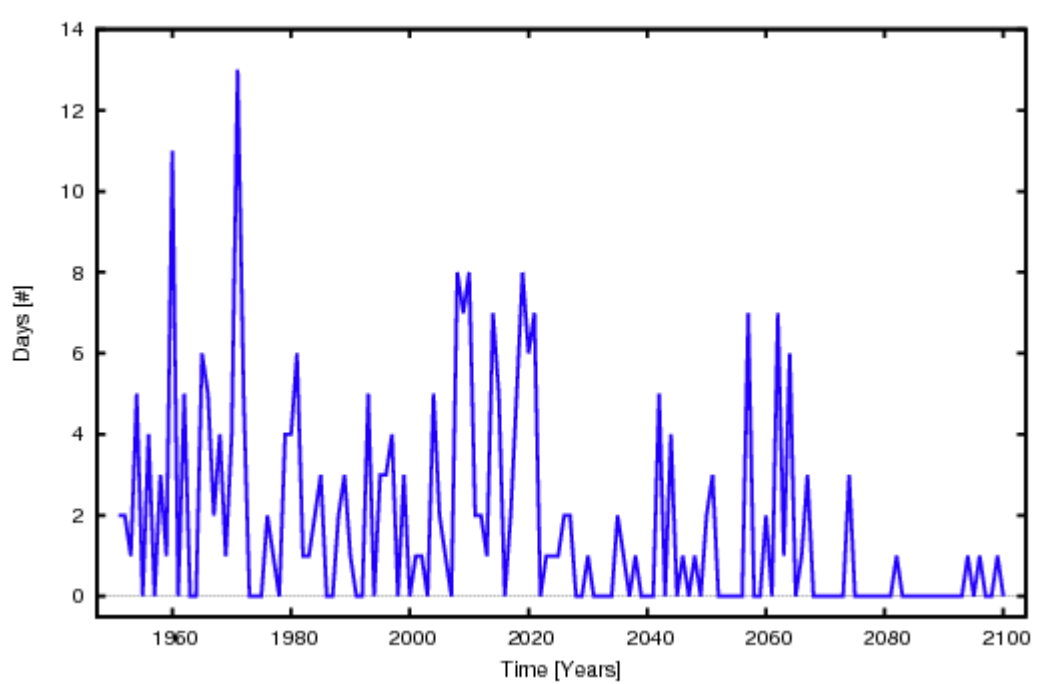


Fig. 8 Results of the NN model for the number of frost days in Potenza: reconstructed till 2010 and predicted from 2011 to 2100.

# An Uncertainty Monster: Advances In Addressing Model Uncertainty

Mistry M.<sup>1</sup>

Department of Economics, Università Ca'Foscari, Venezia - Italy

malcolm.mistry@unive.it

## Abstract

The uncertainties in climate projections; beginning from our lack of complete understanding of all participating processes, is further compounded by the limited skills of General Circulation Models (GCMs) in simulating the state of the climate system. And even if a hypothetical methodology existed to narrow down (or completely eliminate) these two sources of uncertainty, another source that would remain difficult to address is the scenario uncertainty, i.e. uncertainty in the future emission and subsequent concentrations of greenhouse gases (GHGs). Whereas techniques exist to represent model skill, no such known and universally accepted measure exists to represent uncertainty in deterministic terms. The methodology adopted by the Inter-Governmental Panel on Climate Change (IPCC) in addressing uncertainties in GCMs in their recent assessment reports (AR4 and AR5) is examined in this paper. A literature review of IPCC's referred studies show that in spite of a certain degree of uncertainty that remains in our understanding of the climate system, the modelling community has come a long way through in addressing the uncertainties in GCMs. The scope for narrowing future uncertainties in climate science remains; and advancement in techniques to quantify uncertainty although encouraging, are both crucial and urgent.

**Keywords:** uncertainty, GCM, climate prediction

## 1. AN UNCERTAINTY DILEMMA

Uncertainties in how our planet's climate system will evolve in the coming decades have been one of the biggest dilemmas faced by the scientific community in recent years. For a decision maker using a range of climate projections as the basis of future policy formulation, inherent uncertainties in model projections provide one of the biggest headaches. The uncertainties are not only limited to models projecting climate change, but also to the models investigating various impacts; such as impacts of climate change, economic and social paradigm [1].

The subject of uncertainty in climate science has not surfaced recently. In fact, beginning from the early days of computer modelling in the 1950s when the first computer models were developed for generating weather forecasts [2], researchers have been aware of the so called "known unknowns"<sup>1</sup>. Study by Lorenz [3] was perhaps the first of its kind to highlight a fundamental limitation in our ability to represent the planet's dynamic and non-linear climate system numerically. Since then, technology has grown in leaps and bounds with an exponential rise in the computing capacity of today's generation of earth system models –ESM- [2], better data assimilation with the dawn of satellite era and an improved parameterization of earth system processes. Yet, the plethora of uncertainties has not necessary abated at the same rate [4]. It is therefore understandable when the modelling community is often questioned about their own projections on different spatial and temporal scales. However, before proceeding further, it is important to understand the anatomy of uncertainties in the climate system.

## 2. ORIGINS OF UNCERTAINTIES IN CLIMATE PROJECTIONS

Prediction of a climate<sup>2</sup> system is inundated mainly by three distinctive sources [Fig. 1]. Natural oscillations (fluctuations) in the absence of an external forcing on the

---

<sup>1</sup> Known Unknowns: A term coined to refer to a system plagued with inherent uncertainties (unknowns) that cannot be quantified correctly, but whose implications are nevertheless understood (known). Also referred to as 'Recognized Ignorance' [7].

<sup>2</sup> A distinction is being made here from 'Weather system' which is the evolution of the state of the atmosphere-oceans, upto a few days, weeks or months. On the contrary, while discussing prediction of climate system, it is understood to be on at least annual timescales.

system exist in the physical state of the atmosphere and oceans. This is broadly categorized as ‘Internal’ or ‘State’ variability<sup>3</sup> of a climate system and an understanding of the same is the first building block for a climate modeller [5].

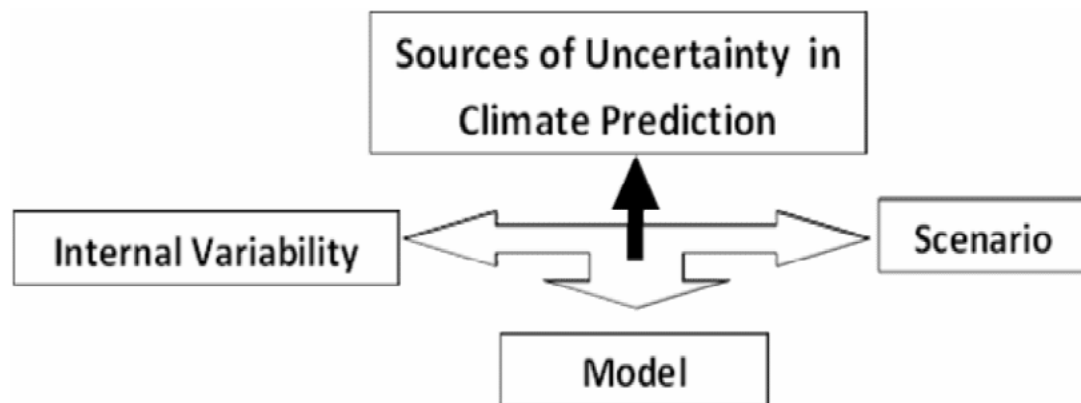


Fig.1 Different components of uncertainties<sup>4</sup> in climate predictions

The second is the uncertainty arising out of numerical models. Different GCMs simulate a different response to the same forcing. To put it simply, running ten different GCMs with the same sets of initial conditions can give us ten diverging projections of how climate system would evolve. This is commonly known as ‘model’ or ‘response’ uncertainty.

It may be tempting to pause and consider if the two sources of uncertainties are sufficient to be resolved in order to abate the total prediction uncertainty. Any such attempt would be futile because a third source of uncertainty that is perhaps the most difficult to address is the uncertainty in future emissions of greenhouse gases (GHGs). This ‘scenario’ uncertainty emanates from the uncertainty of how the human activities would result in the emission trajectories of GHGs, and subsequently the radiative forcing (i.e. warming potential of GHGs).

<sup>3</sup> Some common examples of internal variability/oscillations include El Nino Southern Oscillation (ENSO) and North Atlantic Oscillation (NAO).

<sup>4</sup> The directional arrows signify the coupling and (to a certain extent) the complex interaction of the three sources in quantifying the subsequent uncertainty in the projections of future climate. The complexity is further compounded due to the variation in the relative importance of each uncertainty with temporal and spatial scales [5]. For a complete discussion on other different ways of expressing uncertainty in climate science, see references [6,7]

### 3. ANATOMY OF UNCERTAINTY IN GCMs

At the very heart of GCMs, there are hundreds of lines of complex numerical codes (equations) that attempt to represent the various non-linear feedbacks and processes in the earth's climate system. Coupled GCMs<sup>5</sup> form the foundation for many other complex models (e.g. land use, carbon cycle).

Having discussed the overall encapsulation of uncertainties in climate predictions in earlier section, attention can now be focused on 'model' uncertainty. To keep the discussion within the bounds of uncertainties in GCMs, emphasis is laid on global models that simulate pure climate parameters such as temperature and precipitation. True, other models such as those examining the impacts of climate at regional scale are often inundated by their own (often wider) range of uncertainties. However, GCMs form the overall capsule for a wide number of other models and thus, addressing uncertainties in GCMs is of paramount importance before any sub-class models can be examined for uncertainties on small scale regional processes.

Uncertainties in GCMs are broadly characterized by five factors<sup>6</sup> [Fig. 2].

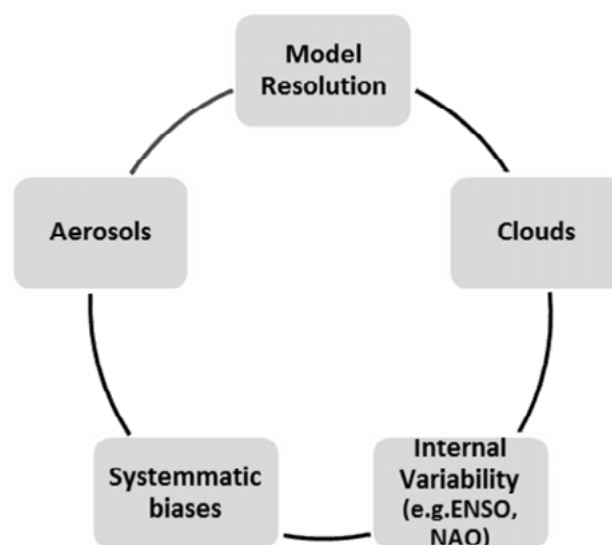


Fig. 2 Sources of uncertainties in GCMs

<sup>5</sup> Coupled GCMs: Models that couple the dynamics of atmosphere and oceans; i.e. instead of prescribing parameters such as sea surface temperature to the Atmosphere-only model, all such processes are modeled to interact and exchange information with each other.

<sup>6</sup> The uncertainties in GCMs can indeed be polymorphic (e.g. see [6,7]). The one represented here is a simple conceptual framework.

It may be worthwhile to mention that a crucial source of uncertainty in a Model (i.e. 'Initial Condition') can have significant and exponentially fast divergence of forecasts in a few days [3]. This so called 'perturbation effect' indeed hampers our ability to model weather events accurately. However, when referring to the evolution of the climate system in GCMs on much longer timescales, boundary conditions are considered more relevant and dominant [6].

#### 4. QUANTIFYING MODEL UNCERTAINTY: PROGRESS IN RECENT YEARS

How to present the overall uncertainties in model projections has remained a modeller's predicament [6]. Whereas methods exist to represent skills in GCMs, no such universally acceptable method exists in measuring uncertainty [8]. Since existing formal methods to quantify uncertainties in projections are complex, a commonly used technique to represent both uncertainties arising due to initial condition and model physics is 'ensembles'. The first-order estimate of the total uncertainty envelope dispersion is given by the Multi-Model Multi Ensemble (MMME)<sup>7</sup>. This technique is widely accepted to represent all possible outcomes of a prediction simulation [8, 9]. However, the interdependence (or independence) of different GCMs used in a MMME simulation plays a crucial role in understanding how uncertainty is interpreted [10].

The studies contributing to the previous two IPCC ARs (AR4 and AR5) have shown a sense of urgency and recognition amongst researchers and policy makers to formulate a meaningful and acceptable methodology of representing uncertainty in climate science [11]. Although the methods addressing uncertainty arising from different sources may not be robust and universally applicable to each of them, guidance on uncertainty and confidence issued by IPCC in AR4 for lead authors was a first important step<sup>8</sup>.

---

<sup>7</sup> A combination of projections derived from running different GCMs, with different sets of initial and boundary conditions. The wide range of projection envelope thus generated by these simulations, are considered to capture all aspects of uncertainty [6].

<sup>8</sup> The latest comprehensive guidance note on uncertainty in IPCC AR5, which is a follow up from the previous AR4 recommendations, can be found at <http://www.ipcc.ch/pdf/supporting-material/uncertainty-guidance-note.pdf>

Uncertainty in GCMs is usually represented in terms of the equilibrium climate sensitivity<sup>9</sup> (ECS). A discussion of the methodology adopted in the evaluation of the GCMs since IPCC AR4 (2007) is summarized in Tab. 1. It must be emphasised here that the analyses is not meant to focus on gauging the superiority of an individual methodology over another. Instead, the aim is to understand the progress made in individual methodologies and implementation of new techniques not previously known or utilized.

Methodology	Description	Application
Multi-Model Ensemble (MME)	Perhaps the most popular approach implemented since the late 1990s (with the exponential rise in computing capacity)	Uncertainties, both structural as well as internal variability in climate are represented by the spread of ensembles simulation [6].
Perturbed Parameter Ensemble <sup>10</sup> (PPE)	Unlike MME, PPE are intended to examine the uncertainty arising out of a single GCM and can be examined at a much finer scale.	PPE permits other techniques (e.g. statistical) to determine what component of model physics drives the uncertainty spread
Statistical Methods (SM)	Includes simple arithmetic mean of results from models in MME simulation (unweighted multi-model mean). More complex methods such as weighted means, Bayesian methods etc. also exist.	SM help to evaluate how well individual models fare in objective <sup>11</sup> of the simulation and thus give a realistic interpretation of the ensemble convergence or dispersion (i.e. uncertainty)

Tab. 1: Overview of methodologies in addressing uncertainties in GCMs, adapted from IPCC AR5 [12]

In a remarkable departure from the earlier approach adopted by IPCC in their earlier ARs, there has been a strong emphasis and applications of quantitative statistical

<sup>9</sup> ECS indicates the change in global mean surface air temperature (after typically a century), as a result of doubling of CO<sub>2</sub> concentration in the atmosphere, keeping all other external factors constant and after the climate has reached a new statistical equilibrium.

<sup>10</sup> Also known as Perturbed Physics Ensemble

<sup>11</sup> GCMs in MME often inherit components from other GCMs and are hence interdependent to a certain extent [13].

measures -known as performance metrics- [12]. In evaluating the overall model results, one notable improvement has been the use of cluster analysis. This has been adapted with an aim to identify redundancy of multiple performance metrics [12]. The improvements made in the methodologies listed in Tab.1 are summarized below in Tab. 2.

Methodology	Improvements (since IPCC AR4)
MME	Inter-dependence (i.e. sharing of model components) reduces the actual truly independent model ensembles. Detailed analyses of classifications of GCMs dependency initiated in recent years [14]
PPE	Structural uncertainty is not explored in this method and this has been identified as an important drawback. Efforts to address the limitations of this technique are on-going [12]
SM	Further complex methods (such as ‘Rank Histogram’, ‘Bayesian Paradigm’, ‘Bootstrapped Plausibility’) have been introduced in recent years <sup>12</sup>

Tab. 2: Improvements in methodologies addressing uncertainties in GCMs [12]

## 5. CONCLUSIONS

As addressed in this study, the scientific community has made considerable progress in addressing model uncertainties. A systematic practice has been to pour more models in simulation runs and thus represent the projections in the form of MMEs. Are we justified in devoting more resources to simply run an increasing number of GCMs in the hope of estimating all aspects of uncertainty? Or is there a need to divert the same resources to improve the existing model parameterizations and resolutions? After all, both these alternatives can pose substantial burden on computing resources [15]. And for both these exercises, further understanding of the complex climate feedback processes, with possibly finer scale observational data would be added burden.

<sup>12</sup> A comprehensive discussion of these methods would be outside the scope of this paper and readers are recommended to refer to readings [9,11,13]

A number of studies examining the benefits of using models for future climate predictions have widely considered GCMs to be the best viable option [1] in climate science. At the same time, few recent studies (e.g. [4]) argue that climate models have reached their so called “current limit” and thus, the policy makers worldwide should stop waiting for further certainty or persuasion, but instead consider focusing on appropriate mitigation and adaptation policies. While this may sound as a logical argument, it omits a fundamental view on the cost of coping actions (adaptation) and implementing long term policies of mitigation. This has somewhat been nicely captured by Weitzman, who argues that great uncertainty does not necessarily favour mitigation or adaptation, but instead investments in research aimed at decreasing the uncertainty itself should form the basis on an optimal strategy [16]. The difficult issue is to determine how much and how soon is future research capable of abating the uncertainty in GCMs.

In spite of impressive leaps have been made in the last three decades in encompassing more earth system processes in GCMs [2], one domain in particular that the modeling community still lags behind is in their ability to represent the extreme events realistically under past climate runs [6]. Extreme events (such as floods, heat waves etc.) can have significant impacts on society and are often more detrimental than the change in the mean state of the climate itself. Although occurring at shorter timescales thereby falling more under the domain of numerical weather prediction (NWP), its’ complex interaction and possible amplification within the climate system necessitates a closer look in GCMs. Existing approach for examining extreme events that may require further focus and investment include downscaling GCM simulations to regional scales, using both dynamical and statistical techniques. Representation of finer scale geography (e.g. mountains and rivers) and possible improvements in model physics are some avenues of narrowing the uncertainty. On the regional scale, the nonlinearities are thought to play a more dominant role [17]. Forecasting the same may thus be extremely cumbersome.

Eventually, we may never completely address model uncertainty. Chaos and unpredictability, and determinism of the state of the system within may perhaps remain a legacy of Lorenz [3]. But that shouldn’t be a justification to abandon the efforts to improvise further. One can gain optimism from the days of Charney, Fjortoft and VonNeumann (1950) whose first numerical weather forecasts were far from

perfect, and which took 24-hours to actually generate a 24-hour regional forecast [2]. And yet, we are now generating global simulations for decades, by churning equations in super-computers in just a couple of months.

## 6. ACKNOWLEDGMENTS

I am grateful to Dr. Jaroslaw Mysiak for valuable discussion on the subject of uncertainty as part of the course '*Analysis and Modelling of Uncertainty*' (Phd on Science and Management of Climate Change, III term, 29<sup>th</sup> Session, Department of Economics, Università Ca'Foscari, Venezia – Italy)

## 7. REFERENCES

1. Shackley S., Young P., Parkinson S. and Wynne B. (1998), *Uncertainty, Complexity and Concepts of Good Science: Are GCMs the Best Tools?*, Climatic Change, No. 38, pp. 159-205
2. Weart S. (2010), *The development of general circulation models of climate*, Studies in History and Philosophy of Modern Physics, No. 41, pp. 208-217
3. Lorenz E.N. (1963), *Deterministic Nonperiodic Flow*, Journal of the Atmospheric Sciences, No. 20, pp. 130-141
4. Maslin M. (2013), *Cascading uncertainty in climate change models and its implications for policy*, The Geographic Journal, No. 179, pp. 264-271
5. Hawkins E. and Sutton R. (2009), *The Potential to Narrow Uncertainty in Regional Climate Predictions*, Bulletin of American Meteorological Society No 90, pp. 1095-1107
6. Tebaldi C. and Knutti R. (2007), *The use of the multi-model ensemble in probabilistic climate projections.*, Philos. Trans. of the Royal Society - A. Math. Phys. Eng. Sci. No. 365, pp. 2053-75
7. Curry J.A. and Webster P.J. (2011), *Climate Science and the Uncertainty Monster*, Bulletin of American Meteorological Society, No. 92, pp. 1667–1682
8. Hargreaves J.C. (2010), *Skill and uncertainty in climate models*, Wiley Interdiscip. Rev. Climate Change, No. 1, pp. 556–564

9. Pirtle Z., Meyer R. and Hamilton A. (2010), *What does it mean when climate models agree? A case for assessing independence among general circulation models*, Environment Science Policy, No. 13, pp. 351–361
10. Knutti R., Masson D. and Gettelman A.(2013), *Climate model genealogy: Generation CMIP5 and how we got there*, Geophys. Res. Letters, No. 40, pp. 1194–1199
11. Katz R.W, Craigmile P.F, Guttorp P., Haran M., Sansó B. and Stein M.L.(2013), *Uncertainty analysis in climate change assessments*, Nature Climate Change, No. 3, pp. 769–771
12. Flato G., Marotzke J., Abiodun B., Braconnot P., Chou S.C., Collins W., Cox P., Driouech F., Emori S., Eyring V., Forest C., Gleckler P., Guilyardi E., Jakob C., Kattsov V., Reason C. and Rummukainen M. (2013), *Evaluation of Climate Models*, Climate Change: The Physical Science Basis. Contribution of Working Group I to the Fifth Assessment Report of the Intergovernmental Panel on Climate Change [Stocker, T.F., D. Qin, G.-K. Plattner, M. Tignor, S.K. Allen, J. Boschung, A. Nauels, Y. Xia, V. Bex and P.M. Midgley (eds.)]. Cambridge University Press, Cambridge, United Kingdom and New York, NY, USA. pp. 753-756
13. Knutti R. and Sedláček J. (2012), *Robustness and uncertainties in the new CMIP5 climate model projections*, Nature Climate Change, No. 3, pp. 369–373
14. Pennell C. and Reichler T. (2011), *On the Effective Number of Climate Models*, Journal of Climate, No. 24, pp. 2358–2367
15. Shukla J., Hagedorn R., Hoskins B., Kinter J., Marotzke J., Miller M., Palmer T.N. and Slingo J. (2009), *Revolution In Climate Prediction Is Both Necessary And Possible*, A Declaration at the World Modelling Summit for Climate Prediction, Bulletin of American Meteorological Society, pp. 175-178.
16. Weitzman M.L. (2009), *On Modeling and Interpreting the Economics of Catastrophic Climate Change*, Review of Economics and Statistics. No. 91, pp. 1–19
17. Rind R. (1999), *Complexity and Climate*, Science, No. 284, pp. 105–107



# Vulnerability, Risk Assessment and Adaptation to Climate Change

Vulnerability, Risk Assessment and  
Adaptation to Climate Change

**Economic value of  
adaptation strategies**

# Climate change impacts and market driven adaptation: The costs of inaction including market rigidities

Bosello F.<sup>1,2,3\*</sup> and Parrado R.<sup>1,2</sup>

<sup>1</sup> Euro-Mediterranean Center on Climate Change - Italy,

<sup>2</sup>Fondazione Eni Enrico Mattei, Italy and <sup>3</sup>University of Milan – Italy

\*Corresponding Author: francesco.bosello@feem.it

## Abstract

In this paper we address one specific criticism that can be raised against the economic climate change impact assessments conducted with CGE models: that of overly optimistic assumptions on the ability of markets to react to climate change shocks (market driven adaptation). These models usually assume frictionless and instantaneous adjustment to a new equilibrium. First, we run a standard climate change impact assessment with a recursive-dynamic CGE model using updated estimates of climate change impacts. Then, we perform the same exercise, but restricting the elasticity of input substitution in the production function, the substitution of domestic and imported inputs, and finally sectoral workforce mobility. These frictions increase the cost of climate change from the 0.6% to the 7.8% of world GDP. This suggests a further caution in handling the impact assessment stemming from CGE models as climate change losses can be high also in a moderately warming world. It also points to the need for careful sensitivity analyses on model parameterization, a basic practice not yet widespread when using CGE models. More on the positive ground, it also shows that CGE models are not “structurally unable” to highlight relevant losses from climate change and remain useful and credible investigation tools.

**Keywords:** climate change costs, adaptation, computable general equilibrium models

## 1. INTRODUCTION AND BACKGROUND

To manage the complexity of economic assessments of climate change impacts, since its beginning, climate change research saw an increasing development and application of integrated assessment models (IAMs). One of their major feature is to describe in a controlled environment the “climate-change issue” in its entirety, i.e. connecting the climatic, the environmental and the social components.

Two broad approaches can be identified in the economic quantification of climate change damages. One, makes ample use of reduced-form climate change damage functions (CCDFs). Basically, a more or less sophisticated functional form translates temperature increases into GDP losses [29, 31, 30, 36, 27, 20, 10, 21, 33]. Parameterization of these functions derives from the impact literature or from expert opinions. A different approach, standard in impact assessments conducted with Computable General Equilibrium (CGE) models, consists in translating climate changes pressures into changes in quantity/quality of factors of production and/or in agents' preferences driving demand and supply behavior in the models. GDP losses (climate change costs) are thus the direct outcome of the simulation [42, 17, 18, 7, 8, 9, 19, 1, 16].

The assessments performed with CGE models tend to fall somewhat in the lower end of cost estimates. For instance according to [15] the highest welfare loss in the EU for a quite high 5.4°C increase in temperature is -1.25% experienced by the Southern EU region; according to [1], for a 4°C warming, the highest GDP loser in the EU is the Iberic peninsula with its -0.5%. [25] and [37] report higher, but still moderate losses. The former highlights a world GDP contraction of the 1.9% for a 4°C temperature increase and the latter of the 1.8% for a temperature increase of roughly 2.5°C.

A heated debate surrounds these estimates and many authors suggest that they are likely to underestimate climate change costs. Namely: key features of climate change and dynamics are still uncertain and/or not well captured by IAMs. For instance, relatively small changes in climate sensitivity can greatly change the cost estimates from these models [2, 3]. In this vein, a higher emphasis on seasonal and extreme-weather short-term effects lead Hanemann [22] to quadruple Nordhaus [30] damage estimates for the US in response to a 2.5°C warming. Quantitative modeling frameworks are also ill suited to measure important social phenomena like conflicts,

mass migrations, disruption of knowledge, learning and social capital potentially triggered by climate change [3, 39]. IAMs emphasize impacts on GDP, which even disregarding its deficiency as a welfare measure, captures flow and tend to overlook stock losses [39]. Risk and irreversibility associated to high damage low probability events is usually left out of the analysis [46, 47, 48, 2]. Finally, IAMs tend to be overly optimistic in describing timing and scale of adaptation processes, disregarding the fact that, while adapting, agents may not use perfect information and for technological, economic, psychological and cultural characteristics may resist to some changes [35]. This last critique is particularly relevant to CGE models. They have been increasingly applied to climate change impact assessment, among other reason, to capture market adjustments triggered by price signals. But these adjustments typically take place instantaneously and without frictions.

A possible conclusion is that IAMs should be used just to assess smooth climatic changes and in the range of 2°C, 3°C warming [39].

In this paper we present a simple exercise to show that similar reasoning can be applied (even though with less dramatic consequences) to a 2°C warming world introducing limits in the ability of the world economic system to autonomously react to climate change shocks. We demonstrate that these frictions increase the cost of climate change impacts from the 0.6% to the 7.8% of world GDP. This also shows that, even though all the criticisms above mentioned can be raised to CGE models, they are not unable, by construction, to produce high climate change costs.

## **2. THE ICES CGE MODEL AND BENCHMARK**

ICES is a recursive-dynamic computable general equilibrium (CGE) model based on the GTAP 8 database [28]. ICES simulation period is 2007-2050 resolved in one-year time steps, with 2007 as the calibration year. Compared to the standard GTAP database and model, in addition to the dynamic in capital stock, it includes renewable energy production. Different versions of the ICES model have been extensively used in past exercises to economically assess many kinds of climate change impacts for

different climatic scenarios and regional aggregations [5, 6, 7, 8, 19, 9].<sup>1</sup> For the sake of the present analysis, the world economic system has been specified into 25 regions and 19 representative industries [Tab. 1].

<b>Regional detail</b>				
<b>Europe</b>	<b>Africa/Middle East</b>	<b>Americas</b>	<b>Asia</b>	<b>Oceania</b>
North Europe	North Africa	USA	Japan	Australia
North_EU15	Sub-Saharan Africa	Canada	South Korea	New Zealand
Med_EU15	South Africa	Rest of LACA	South Asia	
Med_EU12	Middle East	Brazil	India	
East_EU12		Mexico	China	
Rest of Europe			East Asia	
Russia				
Rest of FSU				
<b>Sectoral detail</b>				
<b>Sectors</b>			<b>Energy sectors</b>	
Agriculture			Coal	
Forestry			Oil	
Fishing			Gas	
<i>Energy sectors (see right column) →</i>			NuclearFuel	
Energy Intensive industries			Oil_Pcts	
Other industries			Ely_Nuclear	
Transport			Ely_Biomass	
Market Services			Ely_Hydro	
Public Services			Ely_Solar	
			Ely_Wind	
			Ely_Other	

Tab. 1 Regional and sectoral detail of the ICES model applied in this study

The social-economic reference for the analysis is the SSP2 – “Middle of the Road or Dynamics as Usual” scenario of the Shared Social Economic Pathways [32]. This scenario assumes a socio economic development in line with that of recent decades, with reductions in resource and energy intensity at historic rates and a slowly decreasing fossil fuel dependency. Quantitatively, the ICES reference baseline assumes [Fig. 1]:

- GDP and population growths as those reported for the SSP2 in the “OECD version”.<sup>2</sup>
- Labour force growth the same as that of population.

<sup>1</sup> A more detailed description of the core of the model can be found in [34] and in the ICES website at <http://www.feem-web.it/ices/>.

<sup>2</sup> The SSPs database is available at: <https://secure.iiasa.ac.at/web-apps/ene/SspDb/>.

- Fossil fuel prices growth trends of the 25%, 73% and 18% for coal, oil and gas respectively within the period 2007 to 2050.<sup>3</sup>
- Energy efficiency yearly increases between 0.28% and 0.56% in developed countries and 0.63 % in developing countries.<sup>4</sup>

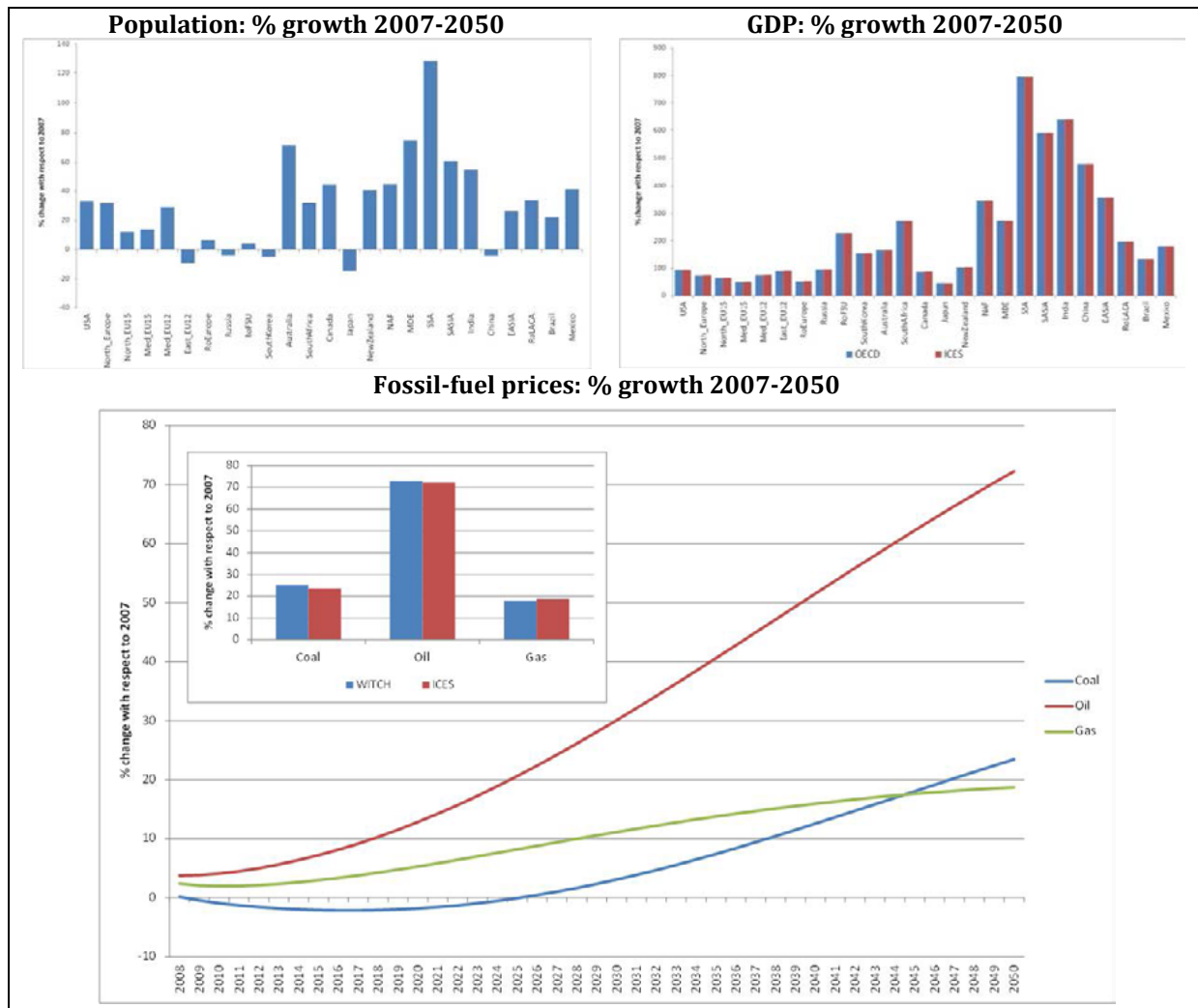


Fig. 1 Population, GDP and fossil-fuel prices trends for the ICES baseline

<sup>3</sup> These price trends are derived from simulations performed with the WITCH integrated assessment dynamic optimization model [11] applied to the SSP2. WITCH, among other features, offers a detailed description of the energy system and therefore an endogenous energy price formation.

<sup>4</sup> We set these average growth rates for energy efficiency based on information from IEA (23, 24). For 2011 the World Energy Outlook 2011 shows an annual average reduction of energy intensity about 1.3% and almost 1.5 % for OECD and Non-OECD countries in the period 1985-2009. In the following edition of the WEO 2012, the annual average percentage change of world energy intensity is reported to be only -0.5% for the period 2000-2010. Accordingly, we impose higher growth rates of energy efficiency for developing countries (0.63%) and lower rates for developed countries (between 0.28% and 0.56%).

### 3. ECONOMIC ASSESSMENT OF CLIMATE CHANGE IMPACTS

This exercise considers an extended set of climate change impacts. They refer to the consequences of changes in sea level, in fish stock productivity, in land productivity, in tourism flows, in energy demand, in health status and in ecosystem services. Source information are bottom-up partial-equilibrium exercises performed within the framework of recently concluded and ongoing EU Sixth and Seventh Framework Program (FP6 and FP7) research projects: ClimateCost, SESAME and Global-IQ. The impact literature and the methodology applied by dynamic optimization hard linked integrated assessment models supported the computations of impacts on health and ecosystem services. Tab. 2 provides a summary of the impacts considered and sources.

Impacts are computed for temperature increases consistent with the Representative Concentration Pathways (RCPs) 8.5, and 6.0 [44]

#	CC Impact	Source	Project	Time frame	Scenarios / Reduced form	
					AR5	SRES
1	Sea level Rise	DIVA model [43]	ClimateCost	2001-2100		A1B
2	Fisheries	[12]	SESAME	2000-2060		A1
3	Agriculture	PIK – LPJmL model ISIP-MIP runs	GLOBAL-IQ	2007-2100	RCP8.5 RCP6.0	
4	Ecosystem	[45, 26]		2000-2060	<b>Reduced form</b>	
5	Tourism	[40, 4]	ClimateCost	2005-2100		A1, B2
6	Energy demand	POLES – [13, 14]	ClimateCost	2000-2050		A1
7	Health	[40, 41]	-	2008-2060	<b>Reduced form</b>	

Tab. 2 Summary of climate change impacts

Fig. 2 reports the data computation for 2050 referring to the RCP 8.5 and 6.0 (respectively associated to a temperature increase of 1.6°C and 2.2°C)

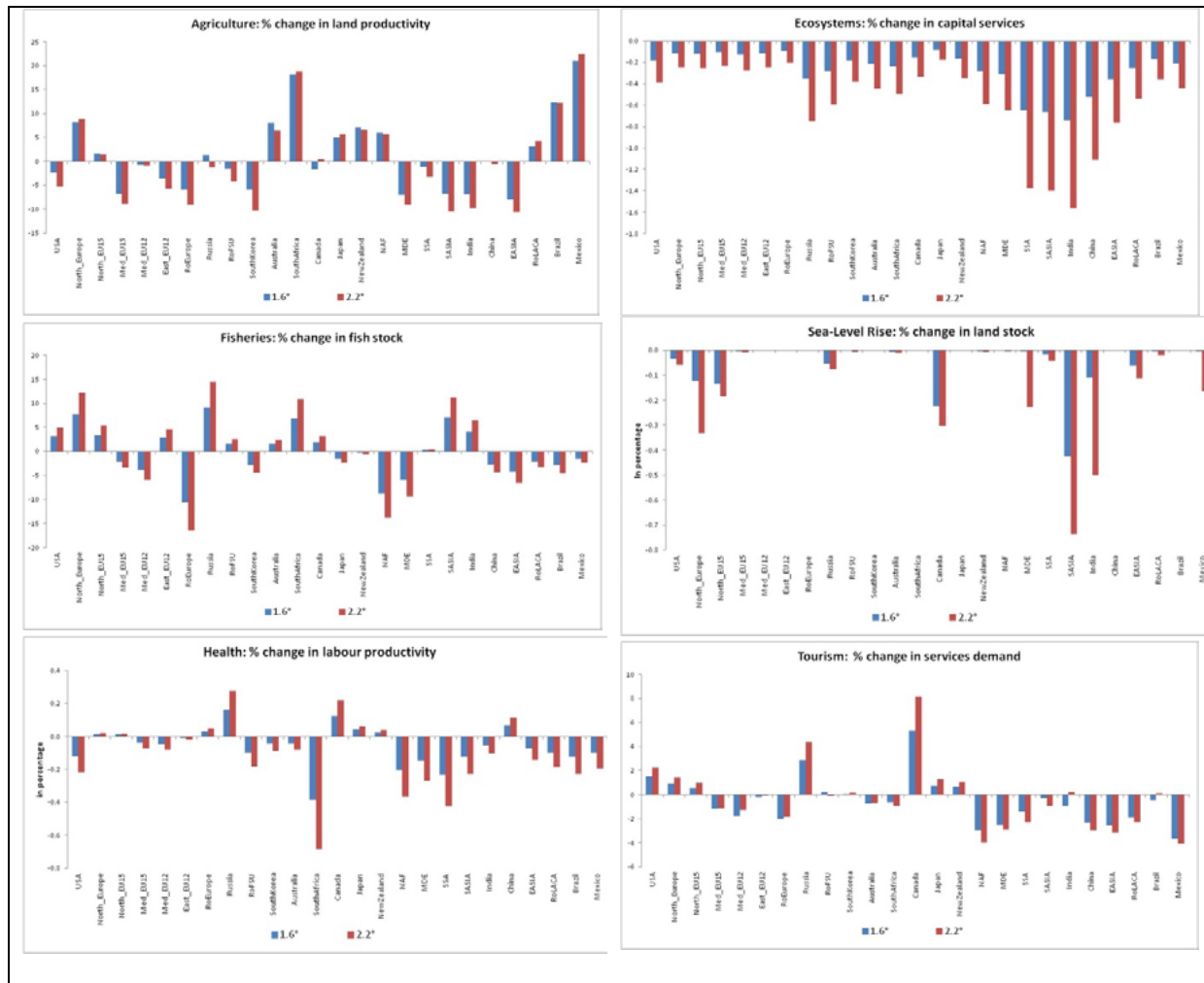


Fig. 2 Direct impacts of climate change, inputs to the ICES CGE model (ref. year 2050)

### Including climate change impacts in the CGE model

Once the impacts have been quantified, they need to be translated into a format compatible with that of the ICES model. Accordingly, into changes of those factors driving demand and supply patterns inside the model.

In what follows we briefly discuss the procedures adopted to implement each of the impacts considered inside the ICES model and summarized in Tab. 3.

Land losses to sea-level rise have been modelled as percent decreases in the stock of productive land and capital by region. Both modifications concern land and capital stocks, which are exogenous to the model and therefore can be

straightforwardly implemented. As information on capital losses are not readily available, in the ICES simulations it is assumed that they exactly match land losses.<sup>5</sup>

Changes in potential fish catches have been modelled as per cent reductions in the natural resource stock (primary factor of production) available to the countries' fishing sectors.

<b><i>Supply- side impacts</i></b>
Impacts on land quantity (land loss due to sea level rise)
Impacts on capital stock (assumed to be equal in % to land loss due to sea level rise)
Impacts on fisheries (changes in fish stock available to the fishing industry)
Impacts on land productivity (Yield changes due to temperature changes)
Impacts on ecosystem services (assumed to reduce capital stock according to the willingness to pay to avoid the impacts due to an increase in temperature)
Impact on labour productivity (changes in morbidity and mortality – health effect of climate change)
<b><i>Demand-side impacts</i></b>
Impacts on energy demand (change in households energy consumption patterns for heating and cooling purposes)
Impacts on recreational services demand (change in tourism flows induced by changes in climatic conditions)
Impacts on health care expenditure

Tab. 3 Climate-change impacts modelled in ICES

Changes in crops' yields have been modelled through exogenous changes in land productivity. Due to the nature of source data, land productivity varies by region, but is uniform across all crop types present in ICES.

Impacts on ecosystems have been modelled as a loss of physical capital stock. In ICES the capital stock does not enter directly in the production function, rather capital services do. Nonetheless in the model there is a one on one relation between capital stock and capital services as any change in the former implies an equal change in the latter. The assumption made thus, is that ecosystems offer a set of support services to the production activity which are all embedded in capital services. When ecosystem deteriorates, its production support services deteriorates and thus (through deterioration of the capital stock) capital services deteriorate.

Changes in tourists' flows have been modelled as changes in (re-scaled) households' demand addressing the market services sector, which includes recreational services. In addition, changes in monetary flows due to variations in tourism demand are simulated through a direct correction of the regional income of each region.

<sup>5</sup> We could have avoided including capital losses, however they are an important part of sea-level rise costs therefore we prefer to have a rough even though arbitrary estimation of this component rather than none. We are not including displacement costs.

Changes in regional households' demand for oil, gas and electricity have been modelled as changes in households' demand for the output of the respective industries.

Changes in labour productivity are also considered as the channel to account for health impacts. Lower mortality translates in an increased labour productivity which is one on one proportional to the change in the total population. The underlying assumption is that health impacts affect active population, disregarding the age characteristic of cardiovascular and respiratory diseases. This information is complemented with health expenditures as percentage of GDP.

#### 4. CLIMATE CHANGE IMPACTS IN A CONTEXT OF FULL MARKET ADAPTATION

Results refer to the economic effects of all the impacts above mentioned when they are jointly imposed over the model baseline. Fig. 3 reports climate change impacts on world GDP. In 2050 total costs remain small even in RCP 8.5 reporting the higher CO<sub>2</sub> concentrations. In that year, temperature increase is just slightly larger than 2°C, impacts are still manageable and roughly amount to the 0.64% of GDP.

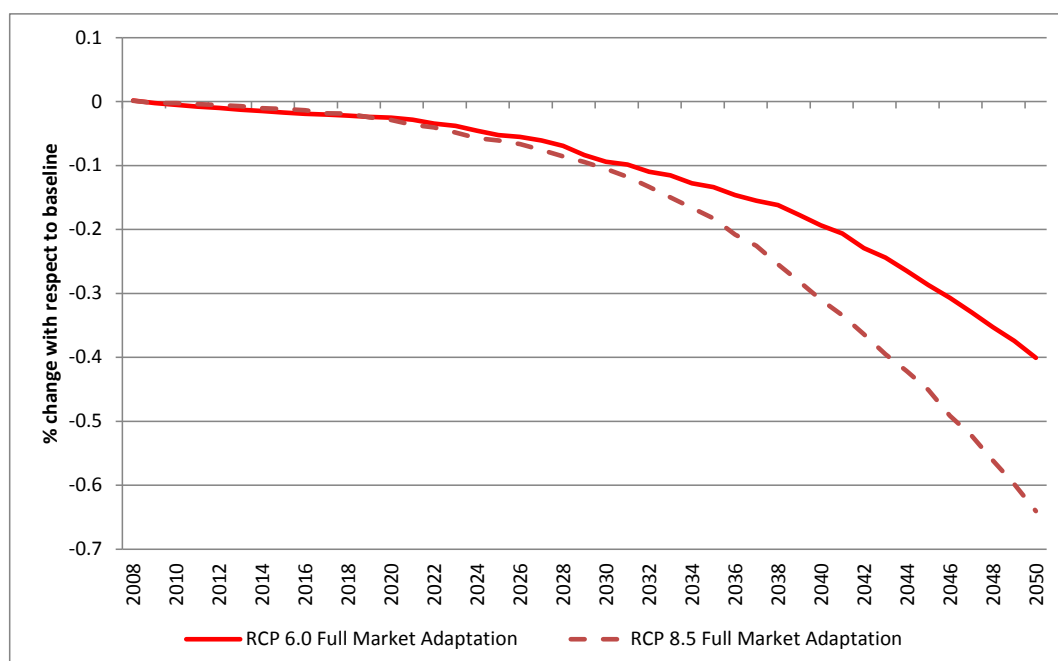


Fig. 3 Climate change impacts on world GDP

This aggregate figure however hides important regional asymmetries that are revealed by Fig. 4. A clear message is that developing countries are more vulnerable to climate change impacts than the developed world, with regions like South Asia and India losing more than 4% of their GDP, and Eastern Asia and Sub Saharan Africa losing roughly 2% of their GDP in 2050 in the RCP 8.5 scenario. This result is standard to and well established in the literature.

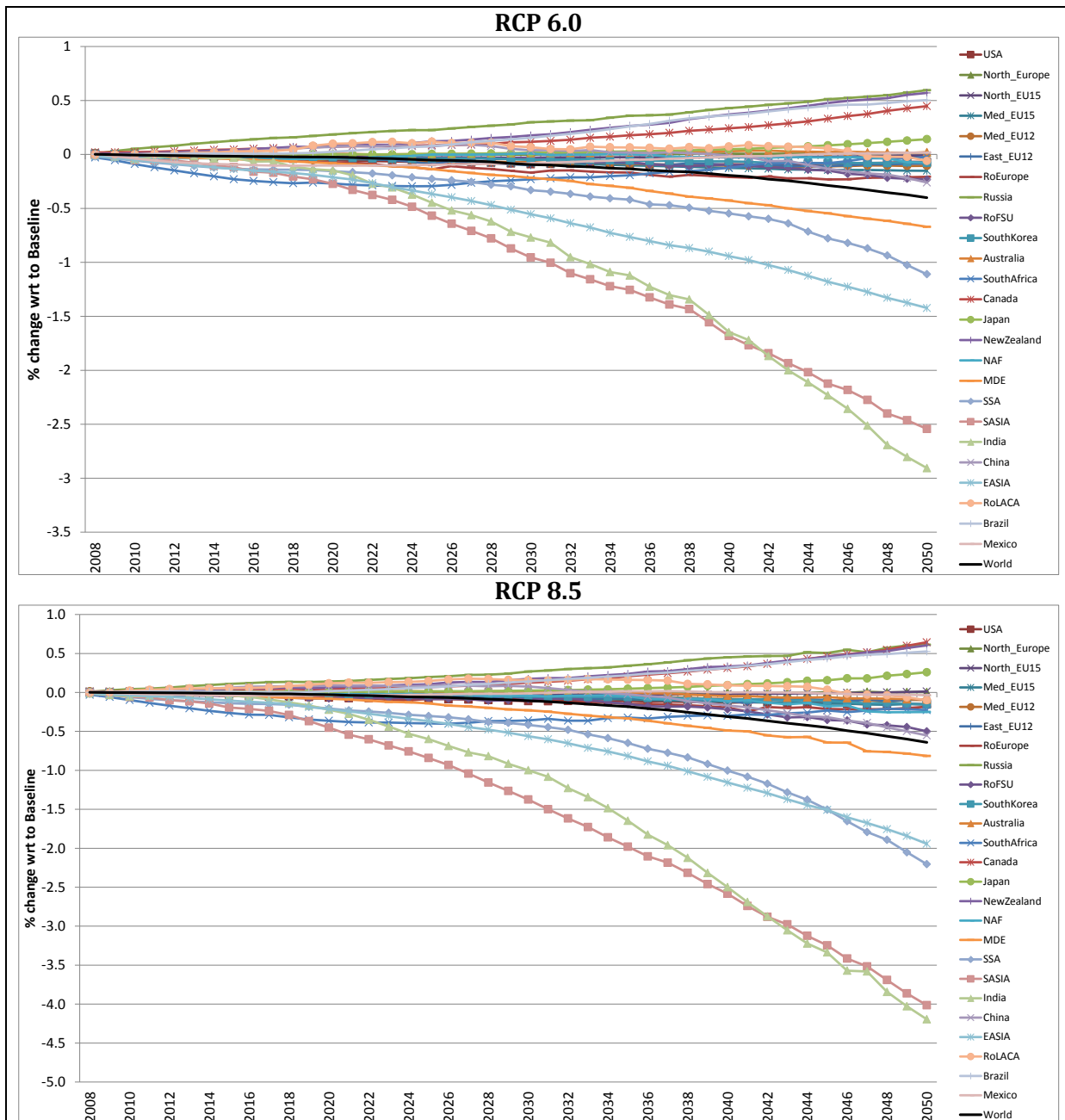


Fig. 4 Climate change impacts on regional GDP (RCP 6.0 top; RCP 8.5 bottom)

Taken as it is, it clearly conveys the following implications: climate change is of concern just in the longer term; it can be a relevant issue for developing and much less for developed countries; albeit important, it is basically a distributional/equity issue rather than a “scale” issue. In fact, all the caveats and limitations introduced in section 1 should be considered for a correct interpretation of the results. Structural to the CGE approach is the inability to consider non market losses, as these models typically record marked transactions only; stock losses, as they are based on GDP and more generally on flow values; frictionless and instantaneous adjustment to a new equilibrium after a shock, implying an overly optimistic view of market adjustments, or differently said of market-driven adaptation.

In the next section we deal expressly with this last assumption.

## 5. INTRODUCING RIGIDITIES IN MARKET-DRIVEN ADAPTATION

As standard in CGE models, ICES production functions are specified via a series of nested CES functions as shown in Fig. 5. Final output is the result of the combination of a Value Added-Energy composite with other intermediate inputs in a Leontief technology production function. The value added nest is a particularly important node of the production function. It governs the substitutability across primary factors, among which the capital-energy composite, in order to produce the final output. The key parameter is the elasticity of substitution  $\sigma_{VA}$ . Furthermore, intermediate inputs can be produced domestically or imported. Domestic and foreign inputs are not perfect substitutes according to the so-called “Armington” assumption, which accounts for - amongst others - product heterogeneity. Armington elasticities  $\sigma_{Arm-D}$ , and  $\sigma_{Arm-I}$  specify substitutability. In general, inputs grouped together are more easily substitutable among themselves than with other elements outside the nest.

Sectoral mobility of primary input within a region, can be perfect or sluggish. In the standard ICES version labour and capital, are perfectly mobile across sectors within a region and accordingly there is just one wage economy-wide.

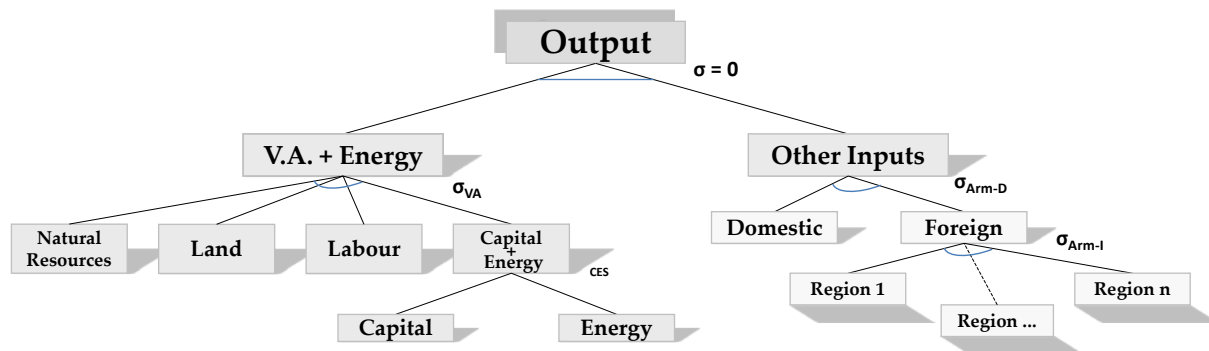


Fig. 5 A reduced representation of the production functions in ICES

We model a more difficult market-driven adaptation working on these three different “stages” of the production activity. Very simply, we reduce by  $\frac{1}{4}$  the degree of substitutability between primary factors; between domestic and imported intermediates;<sup>6</sup> we reduce the labour mobility across sectors transforming labour into a sluggish factor of production. In the first two cases it is sufficient to reduce the relevant elasticities  $\sigma_{VA}$ ,  $\sigma_{Arm-D}$  and  $\sigma_{Arm-I}$  to the 75% of their original value. In the third case we impose that labour force cannot move across sectors. In a final experiment, we combine all these three rigidities in a worst-case scenario. The climate change impacts are those calculated for the RCP 8.5. The aim of this exercise is to explicit the role of market-driven adaptation in impact smoothing, and to investigate what the consequences could be if it were more difficult than that assumed by the model. In this context for instance the possibility to move freely and instantaneously labour force from a shrinking to an expanding sector seems particularly unrealistic. But also the degree of substitutability between primary factors, albeit derived from calibration procedures or econometric estimations, presents a variability whose effects are important to investigate.

## 6. RESULTS

The impact assessment of section 4 could be regarded as the cost of inaction given that there is no planned adaptation, but with full market adaptation.

<sup>6</sup> In this case we want to simulate a more difficult international trade in inputs rather than a more difficult technological substitutability.

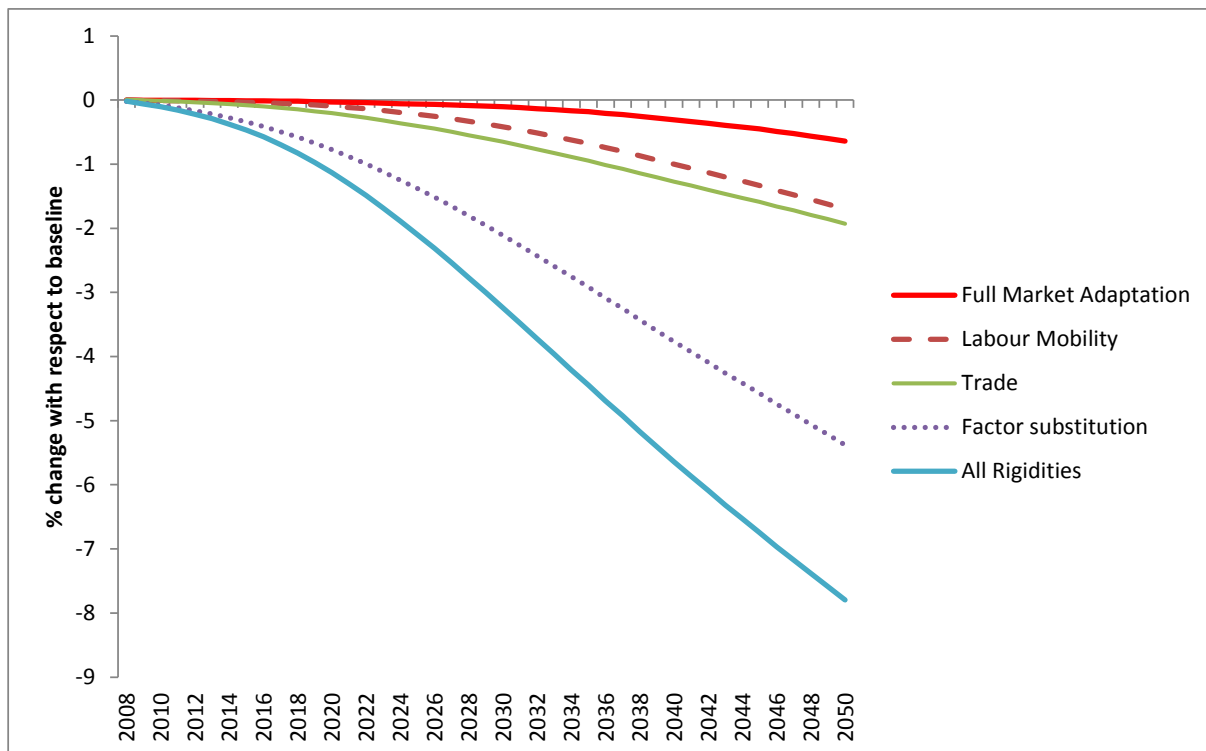


Fig. 6 Climate change impacts on GWP with market rigidities for RCP 8.5 scenario

The inclusion of rigidities in the impact assessment reveals an increase of the costs of climate change as shown in Fig. 6. Gross World Product (GWP) losses rise from roughly 0.5% to almost 8%. The stronger driver of these peaking costs is the lower degree of substitution across primary factors, pushing alone losses to more than 5% of GWP in 2050. Facing a reduced ability to recombine primary factors intensifies the initial negative impact on the supply side of the economy. For instance the reduced land productivity can only partly be compensated by using more of the remaining primary factors as in the full market adaptation case. Limiting the model's flexibility related to labour mobility and international trade increases inaction costs to 1.7% and 1.9% of GWP in 2050 respectively.

A quick inspection of the regional detail (Fig. 7) confirms the asymmetric distribution of negative impacts which are much higher in developing countries with Sub Saharan Africa, South Asia, India, North Africa and China showing losses higher than 14% of GDP. Developed countries are much less adversely affected: the USA and the EU lose roughly the 2% of GDP and Southern Europe the 4%. Nonetheless impacts are far from negligible, and all the potentially positive economic effect of climate change with full market adaptation disappeared.

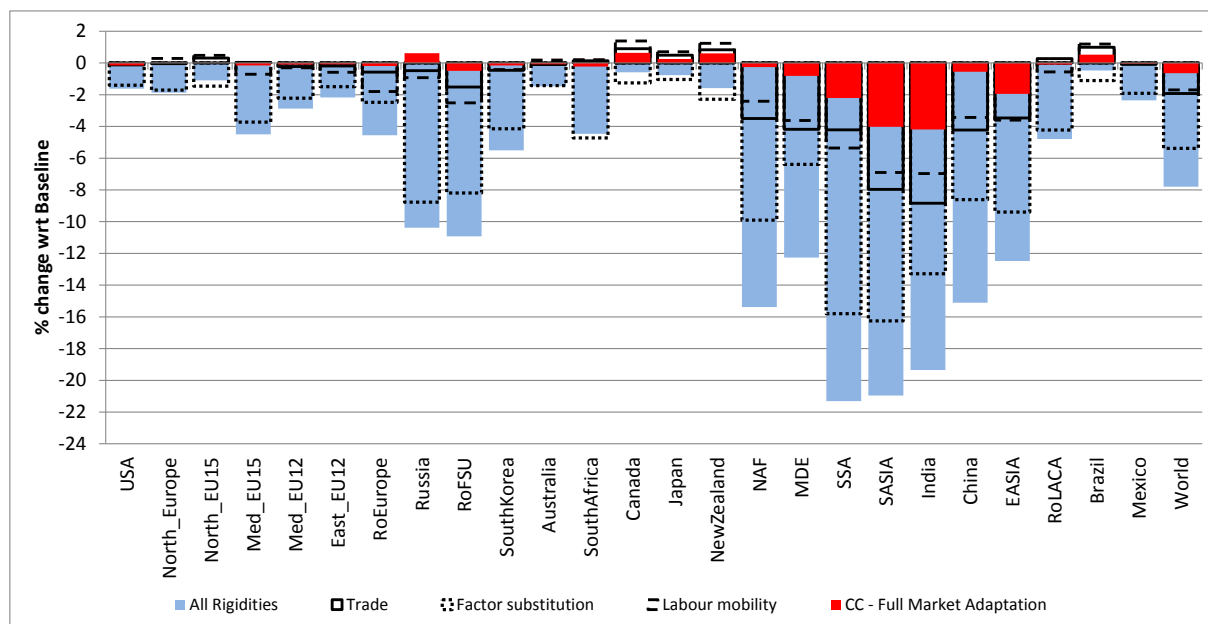


Fig. 7 Climate change impacts on regional GDP with market rigidities for RCP 8.5 scenario

All in all, relatively minor deviations from the basic parameterization of the model concerning input substitutability/intersectoral mobility, are able to increase impacts by more than an order of magnitude. This without the need to invoke catastrophic events, risk, irreversibility, non-use value losses which naturally exist and should be accounted for.

## 7. CONCLUSIONS

Albeit useful investigation tools, IAMs still suffer from major limitations especially when they provide costs assessments of the potential impacts deriving from climate change. Key features of climate change and dynamics are still uncertain and accordingly not well captured by IAMs. Assessments performed with IAMs assume perfect information and the absence of frictions to adaptation such as technological, economic, and cultural barriers that might increase final costs.

In this paper we address this criticism particularly relevant to economic climate change impact assessments conducted with CGE models. These indeed usually assumes frictionless and instantaneous adjustment to a new equilibrium after a

shock affecting relative prices. We first run a standard climate change impact assessment exercise with a recursive-dynamic CGE model using updated estimates of climate change impacts (RCP 6.0 and 8.5 in 2050). Then we performed the same exercise, but restricting the elasticity of input substitution in the production function, the substitution of domestic and imported inputs, and finally sectoral workforce mobility. We demonstrate that these frictions increase the cost of climate change from the 0.6% to the 7.8% of world GDP. The most important driver of cost increases is the elasticity of input substitution followed by labor mobility and by restrictions in domestic and imported input substitution.

This suggests a further caution in handling the impact assessment stemming from CGE models as climate change losses can be very high also in a moderately warming world imposing relatively minor changes in model parameterization. It also points to the need of conducting careful sensitivity analyses on model parameterization. This basic practice is not yet that widespread at least when CGE models are used. More on the positive ground, it also shows that CGE models are not “structurally unable” to highlight relevant losses from climate change and that they can remain useful and credible investigation tools.

## **8. ACKNOWLEDGMENTS**

We are highly indebted with many people and institutions who shared the results of their research and made the related data available for inclusion in the present report.

In particular:

We thank Sally Brown Robert Nicholls, Athanasios Vafeidis and Jochen Hinkel who generated sea-level rise impacts as part of the EU Seventh Framework Programme project ClimateCost and the Met Office who elaborated climate change scenarios for sea-level rise within the same project.

We thank Silvana Mima who provided data on climate change impacts on energy demand elaborated during the EU Seventh Framework Programme project ClimateCost.

We thank Franziska Piontek who provided data on climate change impacts on crop yields elaborated during the EU Seventh Framework Programme project Global IQ.

We thank Richard Tol who provided data on climate change impacts on tourism elaborated during the EU Seventh Framework Programme project ClimateCost as well as his elaborations on climate change impacts on mortality and morbidity.

Nevertheless please consider that the values reported in this document are our elaborations based on these data and accordingly ours is the only responsibility for any mistake or imprecision.

Finally the present paper has been produced as part of the research conducted under the framework of the FP7: "Impacts Quantification of global changes (Gobal-IQ)" research project (Grant agreement no: 266992), whose financial support is gratefully acknowledged.

## 9. REFERENCES

- 1 Aaheim, A., Amundsen, H., Dokken, T., Ericson, T., Wei, T. (2009), "A macroeconomic assessment of impacts and adaptation to climate change in Europe", CICERO Report 2009.06
- 2 Ackerman F. and Stanton E.A, (2012), "Climate Risk and Carbon Prices: Revising the Social Cost of Carbon", Economics: The Open-Access, Open-Assessment E-Journal, Vol. 6, 2012-10.
- 3 Anthoff, D. and R.S.J. Tol (2013), "The Uncertainty about the Social Cost of Carbon: A Decomposition Analysis Using FUND." Climatic Change, 117(3), 515-30
- 4 Bigano A., Hamilton J.M. and Tol R.S.J. (2007), "The Impact of Climate Change on Domestic and International Tourism: A Simulation Study", Integrated Assessment Journal 7, 25-49.
- 5 Bosello, F., Zhang, J., (2006), Gli effetti del cambiamento climatico in agricoltura. Questione Agraria 1–2006, 97–124.
- 6 Bosello, F., Roson, R. and R.S.J. Tol (2006), " Economy wide estimates of the implications of climate change: human health" Ecological Economics, 58, 579-591

- 7 Bosello, F., Roson, R., Tol, R.S.J., (2007), Economy wide estimates of the implications of climate change: sea level rise. *Environmental and Resource Economics* 37, 549–571.
- 8 Bosello, F., Roson, R., Tol, R.S.J., (2008), Economy wide estimates of the implications of climate change: human health - a rejoinder. *Ecological Economics* 66, 14–15.
- 9 Bosello, F., Nicholls, R.J., Richards, J., Roson, R. and R.S.J. Tol (2012), “Economic impacts of climate change in Europe: sea-level rise”, *Climatic Change*, 112, pp. 63-81.
- 10 Bosetti, V., Carraro, C., Galeotti, M. (2006), “The dynamics of carbon and energy intensity in a model of endogenous technical change”, *The Energy Journal*, Endogenous Technological Change and the Economics of Atmospheric Stabilisation, pp. 191–206 (special issue).
- 11 Bosetti, V., E. De Cian, A. Sgobbi and M.Tavoni (2009). “The 2008 WITCH Model: New Model Features and Baseline”, FEEM Note di Lavoro N. 85.2009.
- 12 Cheung, W. W. L., Lam V. W. Y., Sarmiento J.L., Kearney K, Watson , R., Zeller, DI R K and D. Pauly (2010), “Large-scale redistribution of maximum fisheries catch potential in the global ocean under climate change”, *Global Change Biology* 16, 24–35, doi: 10.1111/j.1365-2486.2009.01995.x
- 13 Criqui P., (2001), POLES: Prospective Outlook on Long-term Energy Systems, Institut d’Economie et de Politique de l’Energie, available on line at: [http://webu2.upmf-grenoble.fr/iepe/textes/POLES8p\\_01.pdf](http://webu2.upmf-grenoble.fr/iepe/textes/POLES8p_01.pdf)
- 14 Criqui P., Mima S. and Menanteau P. (2009), Trajectories of new energy technologies in carbon constraint cases with the POLES Model, IARU International Scientific Congress on Climate Change, p. 16.
- 15 Ciscar, J.C. , Iglesias, A., Feyen, L., Goodess, C.M., Szabó, L., Christensen, O.B., Nicholls, R., Amelung, B., Watkiss, P., Bosello, F., Dankers, R., Garrote, L., Hunt, A., Horrocks, L., Moneo, M., Moreno, A., Pye, S., Quiroga, S., van Regemorter, D., Richards, J., Roson, R., Soria, A., (2009), “Climate change impacts in Europe Final report of the PESETA research project”, JRC Scientific and Technical Reports. EUR 24093.

- 16 Ciscar, J.-., A. Iglesias, L. Feyen, L. Szabó, D. Van Regemorter, B. Amelung, R. Nicholls, P. Watkiss, O.B. Christensen, R. Dankers, L. Garrote, C.M. Goodess, A. Hunt, A. Moreno, J. Richards, and A. Soria, (2011), "Physical and economic consequences of climate change in Europe". Proceedings of the National Academy of Sciences of the United States of America, 108(7), pp. 2678-2683.
- 17 Darwin, R. F. and R. S. J. Tol (2001), "Estimates of the Economic Effects of Sea Level Rise", Environmental and Resource Economics, 19, pp. 113–129.
- 18 Deke, O., K.G. Hooss, C. Kasten, G. Klepper, and K. Springer, (2001), "Economic Impact of Climate Change: Simulations with a Regionalized Climate-Economy Model", Kiel Institute of World Economics, 2001: 1065.
- 19 Eboli F., Parrado R. and Roson R. (2010), "Climate Change Feedback on Economic Growth: Explorations with a Dynamic General Equilibrium Model", Environment and Development Economics, 15 (5), pp. 515 -533
- 20 Edenhofer, O., Bauer, N., Kriegler, E., (2005), "The impact of technological change on climate protection and welfare: insights from the model MIND", Ecological Economics 54, pp. 277–292.
- 21 Gerlagh, R. (2007), "Measuring the value of induced technological change", Energy Policy, 35, pp. 5287–5297.
- 22 Hanemann, M., (2008), What is the economic cost of climate change?, No 1071, CUDARE Working Paper Series, University of California at Berkeley, Department of Agricultural and Resource Economics and Policy.
- 23 IEA (International Energy Agency), (2011) "World Energy Outlook - 2011", Paris.
- 24 IEA (International Energy Agency), (2012) "World Energy Outlook - 2012", Paris.
- 25 McCallum, S., Dworak, T., Prutsch, A., Kent, N., Mysiak, J., Bosello, F., Klostermann, J., Dlugolecki, A., Williams, E., König, M., Leitner, M., Miller, K., Harley, M., Smithers, R., Berglund, M., Glas, N., Romanovska, L., van de Sandt, K., Bachschmidt, R., Völler, S., Horrocks, L. (2013): Support to the development of the EU Strategy for Adaptation to Climate Change:

Background report to the Impact Assessment, Part I – Problem definition, policy context and assessment of policy options. Environment Agency Austria, Vienna.

- 26 Manne, A., Mendelsohn, r., Richels, R., (1995), MERGE A Model for evaluating regional and global effects of GHG reduction policies, Energy Policy, Vol. 23 No. 1 pp. 17-34.
- 27 Manne, A. and R. Richels, (2004), “MERGE an Integrated Assessment Model for Global Climate Change”, on line documentation on the MERGE model, available at: <http://www.stanford.edu/group/MERGE/GERAD1.pdf>
- 28 Narayanan, G., B., Aguiar A., and McDougall, R., (Eds) (2012), Global Trade, Assistance, and Production: The GTAP 8 Data Base, Center for Global Trade Analysis, Purdue University.
- 29 Nordhaus, W.D., (1991), To Slow or Not to Slow: The Economics of The Greenhouse Effect, The Economic Journal, Vol. 101, No. 407 (Jul., 1991), pp. 920-937.
- 30 Nordhaus, W.D. and J. Boyer (2000) Warming the World: Economic Models of Global Warming, MIT Press, Cambridge, MA.
- 31 Nordhaus, W.D. and Z. Yang. (1996), “A Regional Dynamic General-Equilibrium Model of Alternative Climate-Change Strategies.” American Economic Review 86(4), pp 741–765.
- 32 O’Neill B.C., Kriegler E., Riahi K., Ebi K.L., Hallegatte S., Carter T.R., Mathur R., van Vuuren D., (2014), A new scenario framework for climate change research: the concept of shared socio-economic pathways. Climatic Change, 122:387-400.
- 33 Ortiz, R.A., Golub, A, Lugovoy, O, Markandya, A. and J. Wang (2011), “DICER: a tool for analyzing climate policies”, Energy Economics. 33. S41-S49
- 34 Parrado, R., and De Cian, E., (2013), Technology spillovers embodied in international trade: Intertemporal, regional and sectoral effects in a global CGE framework, Energy Economics 41.

- 35 Patt, A.G., van Vuuren, D., Berkhout F., Aaheim, A., Hof, A.F., Isaac, M., Mechler, R. (2010), "Adaptation in integrated assessment modeling: where do we stand?", *Climatic Change*, 99:383–402
- 36 Popp, D. (2004), "ENTICE: endogenous technological change in the DICE model of global warming", *Journal of Environmental Economics and Management* 48, pp 742–768.
- 37 Roson R. and Van der Mensbruegghe (2010), "Climate, Trade and Development", background paper for Round Table 1 on The Impact of Climate Change on Trade Patterns, at the "business-government-academic conference Climate Change, Trade and Competitiveness: Issues for the WTO". Geneva, 16th, 17th and 18th June, 2010.
- 38 Stern, N. (2013), "The Structure of Economic Modelling of the Potential Impacts of Climate Change: Grafting Gross Underestimation of Risk onto Already Narrow Science Models", *Journal of Economic Literature* 51(3), 838-859.
- 39 Tol, R.S.J. (2002a), 'New Estimates of the Damage Costs of Climate Change, Part I: Benchmark Estimates', *Environmental and Resource Economics*, 21 (1), 47-73.
- 40 Tol, R.S.J. (2002b), 'New Estimates of the Damage Costs of Climate Change, Part II: Dynamic Estimates', *Environmental and Resource Economics*, 21 (1), 135-160.
- 41 Tsigas, M.E., Frisvold, G.B. and B. Kuhn (1997), 'Global Climate Change in Agriculture' in *Global Trade Analysis: Modeling and Applications*. Thomas W. Hertel, editor, Cambridge University Press
- 42 Vafeidis A.T., Nicholls R.J., McFadden L., Tol R.S.J., Hinkel J., Spencer T., Grashoff P.S., Boot G. and Klein R.J.T., (2008), "A new global coastal database for impact and vulnerability analysis to sea-level rise", *Journal of Coastal Research*, 24 (4):917-924
- 43 Van Vuuren et al. (2012), "A proposal for a new scenario framework to support research and assessment in different climate research communities", *Global Environmental Change*, Volume 22, Issue 1, February 2012, Pages 21–35

- 44 Warren et al. (2006), "Spotlighting impacts functions in integrated assessment", WP 91, Tyndall Centre for Climate Change Research.
- 45 Weitzman, M. L. (2007), "A Review of the Stern Review on the Economics of Climate Change", *Journal of Economic Literature* 45(3), pp. 703-724
- 46 Weitzman, M. (2009), "Additive Damages, Fat-Tailed Climate Dynamics, and Uncertain Discounting." *Economics: The Open-Access, Open-Assessment E-Journal*, Vol. 3, 2009-39. <http://www.economics-ejournal.org/economics/journalarticles/2009-39>
- 47 Weitzman, M. (2010), "What is the "Damages Function" for Global Warming - and What Difference Might It Make?" *Climate Change Economics*, 1(1), pp. 57-69

# **Adapting natural capital: cost-benefit challenges and indicative net present values**

**Dominic Moran\*, Anita Wreford, Eileen Wall**

\*Corresponding Author: dominic.moran@sruc.ac.uk

## **Abstract**

We generate net present values for adaptation measures applicable across categories of natural resources identified as priority areas for early anticipatory adaptation action. Categories include agriculture, forestry, habitats and water as well as assets characterised by specific vulnerabilities, or irreversibility, and whose management is often private yet underpins a range of public goods. We focus on measures that either require long lead times, or are low/no-regrets. A focus on the latter arguably obviates some concerns about the numerous and interacting climate uncertainties sometimes cited as handicapping adaptation action. The analysis responds to a demonstrable policy requirement for guidance on early action and clarity on data gaps hindering the use of current scientific information in policy appraisal. We highlight some sector-specific cost-benefit assumptions, and find high returns in relation to peatland restoration, livestock disease surveillance, animal production, and some soil management measures.

**Keywords:** climate change adaptation, natural capital, cost-benefit analysis

## 1. INTRODUCTION

Despite the need for better guidance on climate change adaptation planning, public policy continues to struggle with the appraisal of adaptation measures<sup>1</sup>. Part of Government's role to address relevant information failures arguably includes demonstrating evidence of which adaptation measures will yield relatively greater social rates of return earlier than others. Such information would help to delineate public and private roles and incentives while defining an efficient adaptation agenda. But faced by numerous and interacting scientific uncertainties<sup>2,3</sup> underpinning climate impact scenarios, implementation of adaptation options remains limited. Rather than focusing on reducing the uncertainties around impacts, a middle ground in the science versus policy led discourse<sup>4,5</sup> is reflected by some consensus on the need for robust, cost-effective investment approaches that are typically either flexible/reversible, no- or low-regrets, have built-in safety margins, reduced decision time horizons, or a combination of the above<sup>6</sup>. That is, the focus should be on robust actions yielding net benefits irrespective of the climate outcome or particular unit values for valuing non-market impacts. This means that they can be low or no-cost or otherwise be privately profitable, or, more likely, provide benefits in the current climate as well as under possible future climates. If some actions are worthwhile irrespective of the climate outcome and across a range of unit values, then, it is argued, part of the scientific ambiguity associated with climate change impacts is obviated in the context of economic appraisal. Despite this observation, there is a lack of evidence attempting any appraisal of such measures. Moreover we would add that although the identification of options with no or low-regrets is desirable, it is insufficient to solve the public choice problem when there are many competing cost-effective investment options.

This paper draws on analysis developed to inform a statutory duty of the Adaptation Sub-Committee (ASC) of the UK Committee on Climate Change (CCC) to identify the preparedness of the key goods and services provided by England's ecosystems for climate change, including the type and level of adaptive action that should be implemented over specific time horizons. We apply cost-benefit analysis (CBA) to

categories of adaptations using benefits transfer to estimate market and non-market benefits associated with impact scenarios. Drawing on the National Climate Change Risk Assessment<sup>7</sup>, the ASC identified the management of natural resources as a priority area for early adaptation action. Such resources are highly sensitive to weather and climate and some management decisions may have either long lead-times or are long-lasting with potentially irreversible consequences, such as the permanent loss of important habitats and ecosystems, which support biodiversity and the productive capacity of agriculture. As public goods, responsibility lies predominantly though not entirely within the domain of government; this overlapping responsibility in some cases truncating investment time horizons and obscuring private incentives. The ASC was particularly interested in low or no-regrets adaptation options, as well as those that require early action.

## 2. ADAPTING NATURAL CAPITAL

The definition of a country's natural assets or capital base can broadly include renewable and non-renewable resources that contribute to national productive capacity and wellbeing UK NEA<sup>8</sup>. We narrowed a long-list of potential adaptation options to focus on a smaller set that meets either the robustness criteria (specifically no-low regrets or win/win measures), or have a long lead-time, requiring action now, anticipating impacts later in the century. Adaptations considered here can either be categorised as 'adaptive management' involving incremental adjustments to existing systems or more fundamental or transformative 'land-use change'. Table 1 summarises the adaptations considered and indicates whether they involve adaptive management or land-use change. The table also indicates whether the analytical approach to estimating adaptation benefits was science-first 'predict then act', or policy-first (vulnerability/risk-based)<sup>4</sup>. The analytical distinction is the extent to which the appraisal is explicit in deriving impacts using downscaled climate data working through a biophysical model, relative to a more *ad hoc* investment appraisal based on benefits assessment where a climate projection is less informative relative to the presence of other ancillary benefits. The analysis used the UKCP09 low (P10) and high (P90) emissions scenarios<sup>9</sup>.

Tab. 1 Adaptations considered, by sector, type ( land-use change or adaptive management) and approach (either policy-first or science-first)

<b>Sector</b>	<b>Adaptations considered</b>	<b>Adaptation type</b>	<b>Approach</b>
Peatland	Peatland restoration measures (such as re-seeding of bare peat with sphagnum, blocking drains/gullies to raise water levels) and the cessation of activities causing degradation (such as heather burning, over-grazing and peat cutting)	Land-use change	Policy first
Coastal managed realignment	Coastal defences and counterfactuals of managed retreat involving impacts to land and buildings and the creation of ecosystems	Land-use change	Policy first
Biodiversity and protected areas	Adapting a range of habitat types in different locations – the complexity of these interactions means there is not a simple set of adaptation measures for which costs and benefits can be assessed	Land-use change	Policy first
Crop disease	Increased disease surveillance, changes in sowing dates, new fungicide developments, disease resistant seed, precision agriculture, expert advice and breeding resistant cultivars	Adaptive management	Science first
Livestock disease	Increased surveillance programme	Adaptive management	Policy first

Intensive livestock transportation	Interventions combatting heat and water stress in broiler transport, such as increased ventilation and mechanical cooling	Adaptive management	Science first
Dairy system losses	Increased labour required to move animals in and out of shelter to address heat stress	Adaptive management	Science first
Water management	Water storage in on-farm reservoirs	Adaptive management	Policy first
Soil management	Soil drainage, cover crops, shallow ploughing, spring cultivation, contour ploughing and dealing with compacted soils	Adaptive management	Science first
Forestry	Restocking with varieties projected to have higher yields in the latter half of this century, and developing new species or subspecies more likely to be suited to the new climate	Adaptive management	Science first

Table 2 shows indicative Net Present Values (NPV) for each sector, calculated from scenarios that identified public and private investment costs for sector-relevant adaptations and benefits in terms of anticipated impacts avoided, estimated over a period of 90 years. Benefit estimates included market and non-market values and, where relevant, ancillary or co- benefits and costs, such as impacts to water quality, biodiversity and carbon emissions. NPVs were calculated using a discount rate of 3.5% for the first 30 years and 3% to the end of the century, and where possible aimed to reflect the magnitude of returns to adaptation investments in each category at a national scale.

Prioritising options based on the magnitude of their NPVs indicates that peatland restoration, animal disease surveillance, animal production and some soil management options offer highest NPVs. Aside from peatlands, impacts in these sectors have been valued using market values, reflecting the largely private incidence of the impacts in the first instance.

A range of analytical challenges in each sector means that ranges are provided to reflect uncertainty in some key values. For some sectors e.g. peatlands and managed realignment of flood defences this reflects the site-specific nature of key variables in cost and benefit calculations.

Tab. 2 NPV values by sector

<b>Sector adaptation</b>	<b>NPV (£m)(2012, to end of century, using discount rate of 3.5% for first 30 years and 3% for remainder of century)</b>	<b>Comments</b>
Peatland	1840	English uplands only, so conservative estimates. But significant heterogeneity across sites in terms of initial conditions, potential for benefits and costs of restoration – aggregate figures are thus illustrative only
Coastal managed realignment	Central estimate 92; Low 24 - High 161  (Range due to central, low and high estimates for	England; assuming early implementation of shoreline management plans (SMPs) resulting in

	non-market benefits including carbon)	the creation of 6,200 ha inundated habitat area following the realignment of 310 km of coastline defences
Protected areas	37	For the South East Region of England
Crop disease	1.1-12	A range of 8 different adaptation options - covering wheat at the national level
Animal disease (exotic incursions)	1280 (median value)	National (England) level. Potential benefit is very assumption specific; see supplementary material for a full range of values.
Livestock?? Transport	36	National level
Animal Production and System losses/impacts	0.82 – 3279	National level
Soil management	-122 – 1744	A range of 6 different adaptation options – covering a range of crops
Water	1 – 21	Covers a range of on farm water storage capacities
Forestry	222 – 470	National level

Peatlands cover around 10 % of the UK, but most are degraded to some extent and thus contribute less to various ecosystem services than would otherwise be the

case. Climate change is anticipated to worsen their condition unless they are restored to a more resilient, functional state<sup>10,11,12</sup>. The benefits of restoration as a proactive adaptation response derive from the potential recovery of some ecosystem service flows<sup>10,13</sup>. For example healthy peatland may assist in the retention and movement of threatened species and biodiversity, and possibly offset and/or delay the need for downstream flood control and water treatment by lessening the effect of extreme rainfall events on peak flow rates and water contamination. Moreover, since functioning peatlands act as net carbon sinks but degrading peatlands act as net sources, restoration offers significant potential emission savings.

The extent to which restoration will be able to achieve desired effects and at what cost will vary significantly by location, initial baseline conditions, current land use and anticipated climate change. The costs of restoration – which include capital works, on-going management & monitoring plus income foregone - are themselves poorly reported and highly context-specific<sup>14,15</sup>.

Nevertheless, using a plausible range of values for sensitivity analysis of different combinations of key parameters allows exploration of the conditions under which restoration may be worthwhile<sup>15,16</sup>. Using DECC carbon prices<sup>17</sup> and indicative values for other non-carbon, non-market benefits<sup>18</sup> our analysis suggests that restoration is worthwhile in most, but not all cases.

Figure 1 summarises how the NPV of restoration is generally positive even under a scenario of no further climate change, under which degradation continues at current rate, and more so under P10 and P90 change scenarios, under which degradation accelerates. Negative NPVs are associated with both high cost sites (e.g. difficult to access, high-value current land use) where even significant gains may not be sufficient to outweigh expensive restoration and low cost sites where modest degradation offers only limited gains that may not be sufficient to offset even (e.g.) modest monitoring and opportunity costs. In such cases, better information on site-specific costs and non-carbon benefits could still show restoration as worthwhile, but some sites may indeed not merit restoration efforts.

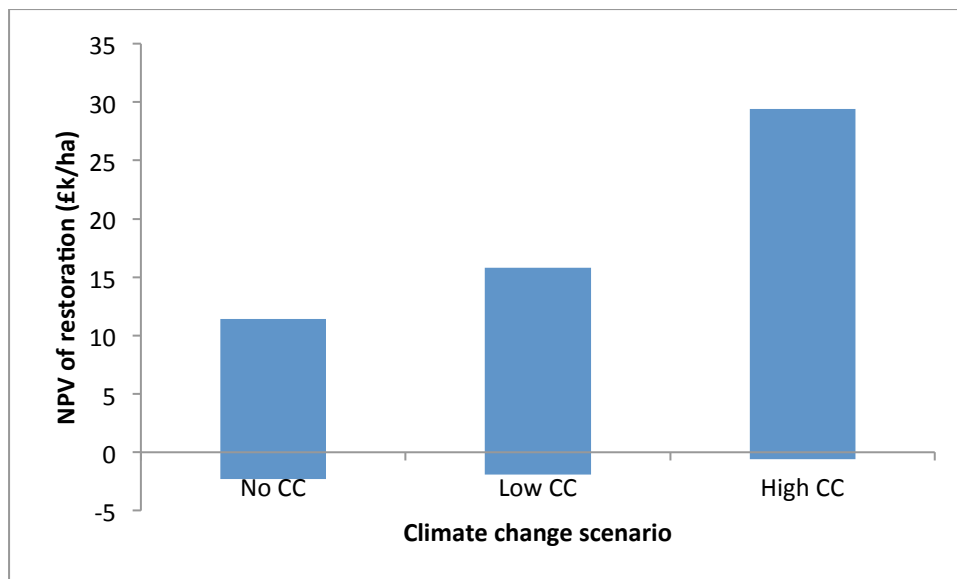


Fig. 1 illustrative range of NPV estimates for restoration under different climate change scenarios

Although the analysis shows considerable variation in NPVs, combining mid-range values with ASC (2013) estimates of the extent degraded peatlands in the uplands of England alone generates an aggregate NPV approaching £2bn. Given that this neglects more extensive upland areas in Scotland and any lowland peats, and the timeframe considered disregards the long-term durability of functioning peatlands<sup>19</sup>, this is a conservative estimate.

Similar uncertainties are addressed in the context of adapting to predicted sea level rise and impacts on coastal defence structures.

CBA can be usefully applied to coastal adaptation involving managed realignment (MR), as also demonstrated by Turner et al.<sup>20</sup> and Luisetti et al.<sup>21</sup>. MR has been identified as a potential no-regrets response and refers to deliberately breaching existing sea defences to create or restore areas of intertidal habitat helping to dissipate wave energy, and reducing pressure on adjacent artificial coastal defence structures. The retreat may imply the creation of a new defence line further inland, or making use of areas of higher ground that can serve as a natural flood defence. Current strategic plans aim to realign approximately 10% of England's coastline by 2030, rising to nearly 15% by 2060. While there is an opportunity cost associated with the loss of valuable agricultural land, the 2030 target can be achieved without the loss of a single built property. An early realisation of the 10% MR target is therefore likely to be efficient (NPV>0) relative to maintaining current defences, so-

called holding the line. This applies even assuming increasing opportunity cost due to agricultural activity becoming more profitable towards the end of the century.

Nevertheless, estimated NPVs generalise across a number of site-specific conditions. This may have implications on the overall efficiency, particularly if MR schemes eventually affect residential and commercial property. A crucial factor is the ratio of habitat area created to the length of realigned coastline. Local MR schemes are more likely to be beneficial if this ratio is large. Variation around the mean ratio (used in the analysis) is large, and therefore some MR schemes may not pass the cost-benefit test. Equally, both costs and benefits are highly site-specific. Based on past observations, capital requirements per ha of inundated habitat created via MR schemes can vary substantially between £620/ha and £273,000/ha<sup>22</sup>. Annual maintenance costs have been suggested to be as high as £104/m<sup>23</sup> defence, but have been reported in past studies to be as low as £8/m<sup>20,21</sup>. Benefits of many ecosystem services provided via MR are spatially explicit. This includes recreational and amenity benefits, which depend on the proximity of the MR site to beneficiaries and the availability of substitute coastal habitat areas, and impacts on local fisheries due to newly created saltmarshes acting as fish nurseries.

The analysis indicates the magnitude of expected NPVs relative to other adaptation options at a national level. But actual implementation should be aggregated from detailed site-specific cost-benefit information of local MR sites. Such information would facilitate targeting those with the greatest NPVs, after taking broader considerations regarding flood risk and protection of strategically relevant areas and infrastructure into account.

Other sectors present a more certain picture of nationwide impacts linked to climate scenarios working through known biophysical models. For example, animal (poultry, pigs and beef and dairy cattle) production and transportation system losses are expressed in terms of mortality and lower productivity related to heat stress. The impact on key performance parameters for livestock under alternative Livestock Temperature Humidity Index (THI) conditions is well-studied in some livestock species<sup>24</sup> and is used on the basis of modelling the climate impacts and impact valuation. The THI combines the effects of temperature and humidity into one value and offers a relatively robust link to production losses. Reliable data on both housed

and transported livestock numbers allows estimates to be scaled nationally. The analysis can rely on known plant and vehicle modifications for cost estimates while market prices of the final product provide an initial estimate of the value of impacts. If necessary, estimates of the non-market value of animal welfare are also available, although the analysis shows that positive NPVs can be generated without adding these benefits.

A national estimate can also be derived to inform adaptation to animal disease outbreaks, which are expected to increase under climate change<sup>25</sup>. Uncertainties also surround the effects of climate change on animal disease but (with existing evidence???) returns to improved disease surveillance and detection can be estimated with reference to costs associated with previous disease outbreaks (e.g. foot and mouth) matched with trends observed in climate driven diseases (e.g. bluetongue). In the illustrative analysis these are compared to the cost of a 50% increase in surveillance effort, to facilitate control and management of such disease incursions. The potential decreases in outbreak costs for a given increase in surveillance level are highly variable, due to e.g. sensitivity/specificity of testing technologies and implementation of post testing control strategies. The results of a sensitivity analysis indicate that there is potential for economic benefit for the majority of possible parameter values (figure 1) making it a low-regrets adaptation, despite the uncertainty. Modelling studies based on past outbreaks also indicate that the actual net benefit would be in the upper part of figure 1<sup>26</sup>.

In addition to improved surveillance, other options are available to mitigate the threat of increased disease outbreaks, including investment in improved diagnostics tools and control strategies. Although we know the likely direction of return for such low-regrets adaptations (i.e. improvements in surveillance, diagnostics, and control will decrease the costs of disease outbreaks), quantitative analysis remains difficult due to current knowledge gaps.

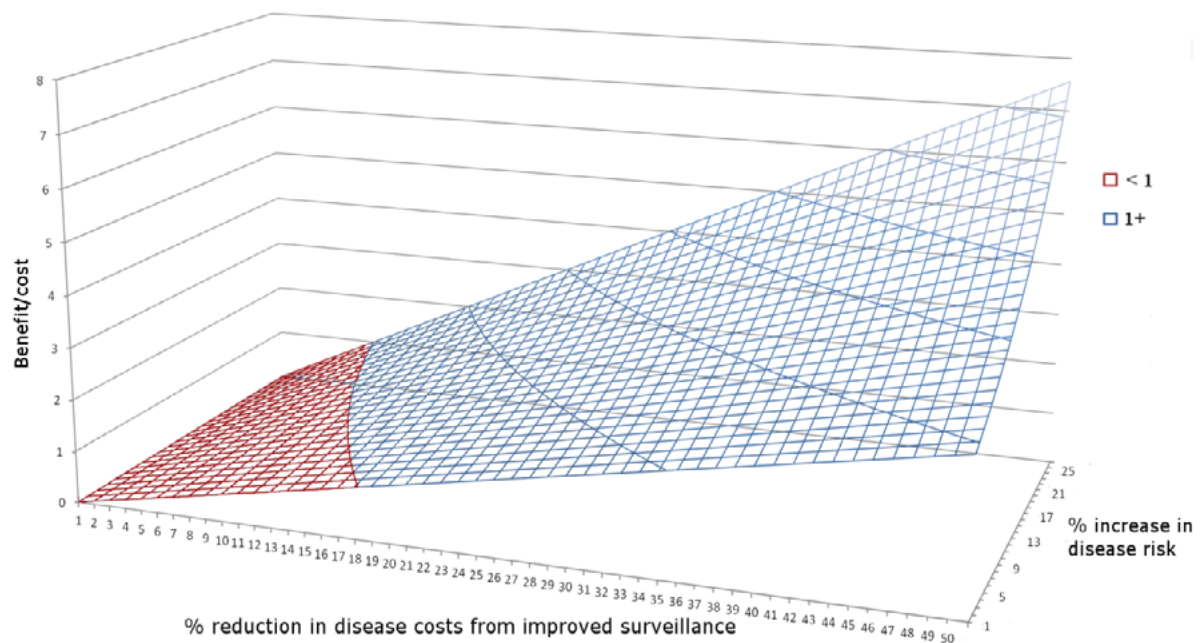


Fig. 11 Overall benefit/cost of improved surveillance (based on NPV) from 2013-2100, for varying degrees of increased risk of disease outbreaks under climate change, and varying levels of reduction in disease costs for a 50% increase in surveillance investment.

Analysis for other no-regrets measures revealed several noteworthy data challenges and some analytical anomalies. Soil management measures aimed at maintaining productive capacity in agriculture. Measures included land management for water retention generated large NPVs, due to the wide applicability, but also negative values associated when high costs were associated with some low-yielding cover crops. Overall analysis revealed the need for more evidence on the relationships between climate change and yield, soil health, and in particular soil organic matter.

Water adaptation involved on farm reservoir investments that can be appraised from a private or social perspective. Investments look less attractive from a private perspective comparing the highest value water use (irrigated potato crops) with installation costs over a short time horizon typically taken by private investors (i.e. maximum 20 years). They look more attractive with a longer time horizon and using a social opportunity cost metric to value water; in this case, the recreational or biodiversity value or willingness to pay (WTP) for water left in stream. A key assumption here is the assumed WTP value and how this is likely to increase through time with increasing scarcity.

Non-market valuation is also central to the estimated value of protected areas, while longer time horizons affect the analysis of forestry measurements and investments in plant and animal genetic resources.

### **3. CONCLUDING COMMENTS**

This paper provides some indicators of the relative returns to adapting England's natural environment to climate change. Relative to other sectors natural capital is a challenging category of assets for adaptation appraisal with scientific uncertainties about vulnerabilities, biological responses and spatial and temporal heterogeneity of costs and benefits. The UK institutional context has accelerated consideration of adaptation needs and highlights the challenges of adaptation planning using CBA. In this context our analysis highlights a variety of challenges to interpret the science of climate impacts, the overlapping nature of public and private costs and benefits and the role of non-market valuation. While these complicate the application of CBA, a focus on no-regrets measures arguably circumvents some of these problems and offers policy messages relevant to build resilience sector under uncertainty. The analysis highlights data gaps and priority areas for further research, and does not obviate the use of complementary criteria for robust evaluation.

## Methods

Conventional economic appraisal of the return on an investment employs cost-benefit analysis (CBA), to compare an outlay (cost) and a resulting flow of returns (benefits) that typically accrue over time. Costs and benefits are compared at each time period and the net result collapsed to a present value equivalent through a process of discounting to calculate a net present value (NPV), more formally expressed:

$$NPV = \sum_{t=0}^N \frac{R_t}{(1+i)^t}$$

Where  $i$  = discount rate,  $N$  = total number of time periods,  $t$  = time period, and  $R$  = net cash flow (or benefits minus costs at each point in time). The choice of a discount rate depends on the investment perspective. Private investors normally look to use a rate that compares with market rates of return on alternative investment options. Public investors (i.e. governments) have other delivery criteria such as the need to generate public goods (e.g. flood control, education defence), which normally have a less tangible and longer term return. In the UK, public discount rates are normally prescribed in the Treasury Green Book; currently a rate of 3.5% for the first 30 years, and 3% for the remainder of the century. This adjustment acknowledges the need to allow for longer term returns. The NPV of a project indicates the extent to which the option represents a good investment opportunity. Values greater than zero suggest the option makes a return on outlay greater than investing at the rate of discount. Competing project options can be ranked from highest to lowest return on this basis.

The extension of CBA into the environmental domain generates considerable debate about the theory and ethics of how we value environmental goods and how the discounting process implicitly treats future preferences. These concerns are in fact central to competing definitions of sustainable development and competing viewpoints can be reflected in the adjustments made to net benefit flows and or the discount rate or time horizon.

CBA becomes even more challenging in the context of climate change. The valuation of environmental benefits represents a difficulty and so does the deep uncertainty about projected impacts as the starting point to determine benefits of adaptation. Figure 2 summarises how benefits are considered, relative to both the costs of not adapting and to the cost of adaptation itself and any residual impact costs.

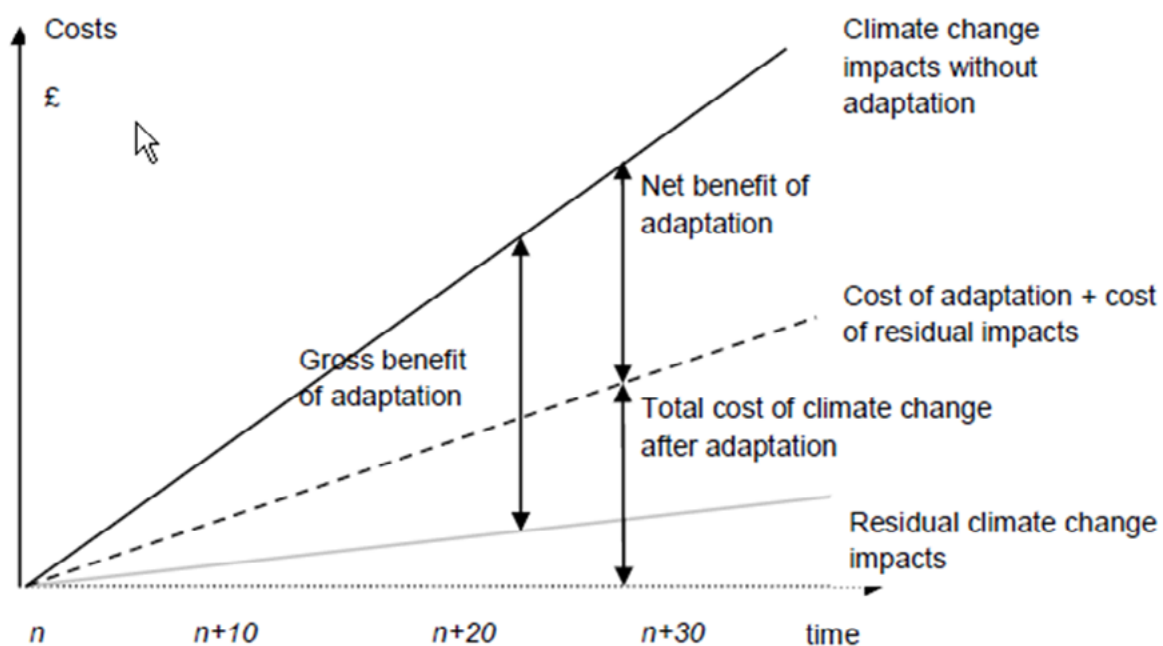


Fig. 2 impacts, adaptation and residual impacts (ref to be added)

As we attempt to demonstrate in this study, many of the objections to CBA can arguably be addressed using sensitivity analysis to identify how key parameters affect the results. The process highlights key gaps and debate often reduces to issues around the clarity of such assumptions and key switching values.

More recent evolutions of financial investment appraisal have led to the development of alternative appraisal methods beyond CBA, so-called robust methods<sup>27,28,29</sup> that meet their adaptation purpose across a variety of plausible futures as they are designed to be less sensitive to uncertainty about the future.

Generally, robust approaches do not assume a single climate change projection but

integrate a wide range of climate scenarios through different mechanisms. Such mechanisms include flexibility in timing or technology in the adaptation options as in Real Option Analysis that has been primarily applied to adaptation in flood risk<sup>30,31,32</sup>. Robust Decision Making focuses on finding the least vulnerable strategy across climate change scenarios<sup>33,34</sup>, while Portfolio Analysis allows an explicit trade-off between the return and the uncertainty of the return of alternative combinations of adaptation options under alternative climate change projections applied for example in conservation management<sup>35,36</sup>.

The list of methods can be extended further but so far case studies applying these robust methods are rare: application is still in its early days and while robust methods can help in choosing an appropriate adaptation strategy under deep uncertainty, they come at a cost. Often these methods are data and technology-intense, requiring expert knowledge, whereas the application of CBA is relatively straightforward and generic. While robust methods are likely to find more application to climate change adaptation, it remains to be seen whether they will become more prominent than CBA to inform policy.

- 
- <sup>1</sup> S. Fankhauser & R. Soare (2013) An economic approach to adaptation: illustrations from Europe, *Climatic Change* (2013) 118:367–379, DOI 10.1007/s10584-012-0655-6
- <sup>2</sup> R. N Jones (2000) Managing uncertainty in climate change projections: Issues for impact assessment. **45**(3-4).
- <sup>3</sup> S. H. Schneider (1983) CO<sub>2</sub>, Climate and Society: A Brief Overview, in *Social Science Research and Climatic Change: An Interdisciplinary Appraisal*, edited by R. S Chen, E. M Boulding, and S. H. Schneider. D.Reidel Publishing, Dordrecht, the Netherlands. pp.9-15.
- <sup>4</sup> T. R. Carter, et al., (2007) New Assessment Methods and the Characterisation of Future Conditions, in *Climate Change 2007: Impacts, Adaptation and Vulnerability. Contribution of Working Group II to the Fourth Assessment Report of the Intergovernmental Panel on Climate Change*, edited by M. L Parry, et al. (Cambridge University Press, Cambridge, UK, pp.133-171.
- <sup>5</sup> Ranger, N., Antony, M., Dietz, S., Fankhauser, S., Lopez, A. & Ruta, G. (2010). Adaptation in the UK: a decision-making process. Policy Brief. Environment Agency 2010-09.
- <sup>6</sup> Hallegatte (2009) Strategies to adapt to an uncertain climate. *Global Environmental Change*, 19 (2), 240 -247.
- <sup>7</sup> CCRA (2012) The UK Climate Change Risk Assessment 2012: Evidence Report. Defra Project Code GA0204
- <sup>8</sup> UK National Ecosystem Assessment (2011) The UK National Ecosystem Assessment: Technical Report. UNEP-WCMC, Cambridge.
- <sup>9</sup> Murphy, J, Sexton, D, Jenkins, G, Boorman, P, Booth, B, Brown, K, Clark, R, Collins, M, Harris, G, and Kendon, L (2009). UK Climate Projections science report: Climate change projections. Met Office Hadley Centre.
- <sup>10</sup> Bain, C., Bonn, A., Stoneman, R., Chapman, S., Coupar, A., Evans, M., Geary, B., Howat, M. et al. (2011) Commission of Inquiry on UK Peatlands. IUCN UK Peatland Programme, Edinburgh
- <sup>11</sup> JNCC (2011) Towards an assessment of the state of UK peatlands. Joint Nature Conservation Committee report No 445.
- <sup>12</sup> Gallego-Sala, A. & Prentice, I.C. (2012) Blanket peat biome endangered by climate change. *Nature Climate Change*. DOI: 10.1038/NCLIMATE1672
- <sup>13</sup> Artz, R.R.E., Chapman, S.J., Donnelly, D. & Matthews, R. (2012) Potential abatement from peatland restoration. Briefing Note to Scottish Government.
- <sup>14</sup> Holden, J., Walker, J., Evans, MG, Worrall, F., Davison, S. & Bonn, A. (2008) A compendium of UK peat restoration and management projects. Report to Defra, London.

- 
- <sup>15</sup> Moran et al 2013 Assessing the preparedness of England's natural resources for a changing climate: Assessing the type and level of adaptation action required to address climate risks in the 'vulnerability hotspots'.  
[http://www.theccc.org.uk/wp-content/uploads/2013/07/Final-report-SRUC-ASC\\_-4-July\\_ASC-FINAL-9-July-2013\\_clean.pdf](http://www.theccc.org.uk/wp-content/uploads/2013/07/Final-report-SRUC-ASC_-4-July_ASC-FINAL-9-July-2013_clean.pdf)
- <sup>16</sup> Moxey, A. & Moran, D. (under review) UK Peatland Restoration: Some Economic Arithmetic, Science of the Total Environment.
- <sup>17</sup> DECC 2011 A brief guide to the carbon valuation
- <sup>18</sup> Harlow, J., Clarke, S., Phillips, M. & Scott, A. (2012) Valuing land-use and management changes in the Keighley & Watersheddies catchment. Natural England Research Report No.44, Peterborough
- <sup>19</sup> Lindsay, R. (2010) Peatbogs and carbon: a critical synthesis to inform policy development in oceanic peat bog conservation and restoration in the context of climate change. Report to RSPBS, Edinburgh.
- <sup>20</sup> Turner RK, Burgess D, Hadley D, Coombes E, Jackson N (2007) A cost-benefit appraisal of coastal managed realignment policy. *Global Environmental Change* 17, 397-407.
- <sup>21</sup> Luisetti T, Turner RK, Bateman IJ, Morse-Jones S, Adams C, Fonseca L (2011) Coastal and marine ecosystem services valuation for policy and management: Managed realignment case studies in England. *Ocean and Coastal Management*, 54 (3), 212-224.
- <sup>22</sup> ABPMer database 2013
- <sup>23</sup> Royal Haskoning for EA 2013
- <sup>24</sup> St-Pierre et al. (2003),
- <sup>25</sup> Burnett et al., 2009
- <sup>26</sup> Carpenter et al., 2011.
- <sup>27</sup> Ranger, N., et al (2010)
- <sup>28</sup> Dessai, S. & van der Sluijs, J. P. (2007). Uncertainty and climate change adaptation - a scoping study. report NWS-E-2007-198, department of Science, Technology and Society. Utrecht University: Copernicus Institute.
- <sup>29</sup> Hallegatte, S., Shah, A., Lempert, R., Brown, C. & Gill, S. (2012). Investment decision making under deep uncertainty--application to climate change. The World Bank, Policy Research Working Paper Series: 6193.
- <sup>30</sup> Scandizzo, P. L. (2011). Climate Change Adaptation and Real Option Evaluation. A Case Study in Campeche, Mexico. In: BANK, R. T. T. W. (ed.).
- <sup>31</sup> Gersonius, B., Ashley, R., Pathirana, A. & Zevenbergen, C. (2013). Climate change uncertainty: building flexibility into water and flood risk infrastructure. *Climatic Change*, 116, 411-423.

---

<sup>32</sup> Woodward, M., Gouldby, B., Kapelan, Z., Khu, S. T. & Townend, I. (2011). Real Options in flood risk management decision making. *Journal of Flood Risk Management*, 4, 339.

<sup>33</sup> Lempert, R. J. & Schlesinger, M. E. (2000). Robust strategies for abating climate change - An editorial essay. *Climatic Change*, 45, 387-401.

<sup>34</sup> Lempert, R. J. & Groves, D. G. 2010. Identifying and evaluating robust adaptive policy responses to climate change for water and management agencies in the American west. *Technological forecasting & social change : an international journal*, 77, 960-974.

<sup>35</sup> Crowe, K. A. & Parker, W. H. (2008). Using portfolio theory to guide reforestation and restoration under climate change scenarios. *Climatic Change*, 89, 355-370.

<sup>36</sup> Ando, A. W. & Mallory, M. L. (2012). Optimal portfolio design to reduce climate-related conservation uncertainty in the Prairie Pothole Region. *Proceedings Of The National Academy Of Sciences Of The United States Of America*, 109, 6484-6489

# The Value of Protecting Venice from the Acqua Alta Phenomenon under Different Local Sea Level Rises

Caporin M.<sup>1</sup> and Fontini F.<sup>1</sup>

<sup>1</sup>Department of Economics and Management, University of Padua, Italy

\*Corresponding Author: fulvio.fontini@unipd.it

## Abstract

Venice (Italy) is built on several islands inside a lagoon. It undergoes a periodical flooding phenomenon, called "Acqua Alta" (AA). A system of mobile dams, called Mo.S.E., is currently under construction to protect it. When needed, several floodgates will be lifted to separate the lagoon from the Adriatic sea. AA, whose length and height has been increasing in recent years, is a random phenomenon, correlated with local sea level rise (LSLR). Several possible LSLRs can be assumed as consequences of different global warming scenarios. We investigate here the cost-benefit of Mo.S.E. under different possible LSLRs. First, we simulate the future patterns of AA for the next 50 years under alternative LSLRs. Then, we calculate the benefit of Mo.S.E., converting each avoided AA episode into an economic value (avoided cost). We show that the benefits are just at the level of the costs, when a low LSLR is assumed and increase with LSLR, provided that it does not reach a catastrophic (yet unpredictable) extreme level.

J.E.L. Classification code: Q54, D61, C22, C53.

## 1. INTRODUCTION

The city of Venice, famous worldwide, has a peculiar geographic location resulting in a periodic flooding phenomenon, known as "Acqua Alta" (AA), which threatens its preservation and interferes with people's everyday life. A system of mobile dams, called Mo.S.E. (an acronym that stands for Experimental Electromechanical Module, "Modulo Sperimentale Elettromeccanico" in Italian) is currently under construction. It is a system of mobile barriers lying on the bottom of the lagoon's inlets. When needed, they are lifted to separate the lagoon from the Adriatic Sea and stabilize the height of the water inside it.

The Mo.S.E. system has been designed to protect Venice from AA for an extremely long times scale. During this time lag it will face the consequences that global warming will induce on the Venice lagoon and the AA phenomenon. Local sea level rise (LSLR) plays, inter alia, an important role for AA. The higher a LSLR is, the higher and the more frequent flooding, and the higher the benefits of protecting Venice from the damages will be (but the interferences with harbour activities will be higher too). The benefits of Mo.S.E. can be contrasted with its costs. Mo.S.E. is a huge financial project. Its original budget, (1.6 billion euro), has been increasing manifold, the latest figure amounting to (roughly) 5.4 billion euro. The purpose of the present work is to evaluate the benefits of the Mo.S.E. net of the installation costs and the (expected) yearly operations and management costs. To do so, we first simulate the future pattern of AA for the next 50 years, replicating the observed time trend and simulating future AA under different possible scenarios for LSLR. We limit the analysis to 50 years since the economic evaluation is based on the actual technologies and knowledge, i.e., it does not take into account technological progress that can significantly alter the definition of the damage function. Then we convert these figures into an economic value by measuring the value of the avoided damage to Venice. Finally, we compare it with the reported investment costs and assess the Mo.S.E. cost-benefit.

## 2. AA AND TIDE SIMULATION

AA depends on the tide in the Venetian lagoon, which is a partially random phenomenon. It can be defined as a tide above a given threshold, conventionally set at +80

cm above the Punta della Salute tidal datum. Tides are generated by the interaction of two components: the astronomical tide and storm surge [1]. The former depends on the effect on sea level rise of a well-known set of deterministic parameters, the moon's influence and the season's changes being two of most relevant. The astronomical tide has a sinusoidal shape that can be calculated with very high precision. The storm surge depends on the interaction of some components of the upper Adriatic Sea's climatology, in particular on the winds, the barotropic pressure and the "seiches" (the oscillations of an almost closed basin, like the Adriatic Sea, after a perturbation). The interaction of storm surge and the astronomical tide determines the height of the sea level in the Venetian lagoon. Due to its nature, storm surge is a random phenomenon. Historical data show that it has had over the years an almost zero mean. The tide is thus a random variable given by the sum of a deterministic component and a stochastic component. As a result, it is possible to derive the random behavior of the tide by observing the stochastic pattern of the storm surge. Within a given day, AA, if present, is associated with a maximum daily tide level above the threshold. Clearly, the duration of AA may vary from day to day, but this element does not affect the impact of AA on economic activities since the discriminatory element is represented by the occurrence of the phenomena (and not its length). Therefore, we focus on the daily maxima, and we evaluate the Mo.S.E. system using the daily time series of Venice lagoon sea-level maxima.

By construction, even the sequence of daily maxima is composed by the sum of two components, one being the astronomical tide and the second associated with storm surge. To evaluate the performance of the Mo.S.E. system we simulate the evolution of daily maxima. To this end, we first specify a model for the daily maxima time series. Then we fit the model to data from January 1975 to December 2009, for a total of 12,784 days (sample size  $T$ ). The model we consider assumes that the daily maxima time series is given as the sum of two components, a deterministic component capturing the mean impact of the astronomical tide level on the daily maxima and a stochastic component that we can associate with the storm surge multiplied by a deterministic component exploiting the effect of the astronomical tide in the dispersion of daily maxima. The two deterministic components have a similar structure, and are given by the combination of a linear component and a set of harmonics, whose frequen-

cies are expressed in days and can be easily calibrated by looking at the periodogram of the daily maxima. The stochastic component associated with the storm surge, is modelled as an ARMA-EGARCH model.<sup>1</sup> The model parameters are estimated using a multi-step approach. First, parameters are estimated by simple linear regression methods (with robust standard errors due to the presence of heteroskedasticity in the innovations) Secondly, the ARMA-EGARCH parameters are recovered by maximum likelihood methods. Finally, given the estimated parameters, the model is used easily used to generate long-range simulations for the evolution of the daily maxima time series.

### 3. AA AND THE DAMAGE TO VENICE

The levels and frequencies of possible future AA episodes are converted into economic values by measuring the damage to the municipality of Venice due to AA. We follow the methodology proposed in [2], that considered two components for the damage function. The first one depends on the refurbishment of real estate damaged by flooding. It is assumed that refurbishment and restoration take place only once (during the time of year with no AA) on the basis of the highest episode observed in the time span. We deduce from the so-called "Frassetto" altimetry<sup>2</sup> the surface of the town involved by AA and the length of the walls of the buildings affected that need work. The cost of refurbishment (plastering) is applied to the length of walls affected by episodes of AA. We consider constant 2013 prices and assume that 50% of buildings are of special (historical) interest and/or need aspecific care; for these, the costs of refurbishment are doubled.

The second component of the damage function depends on the frequencies of the AA episodes. Two levels of AA are relevant for this component. The first one is a level of AA that is high enough to hinder everyday activities, in particular the displacement of young and elderly people and tourism activities. We follow the methodology proposed in [2] that allows us to convert the number of Mo.S.E. activations above the +120cm

---

<sup>1</sup>We follow the EGARCH model of [12]. Detailed explanations of the model are available from the authors upon request.

<sup>2</sup>See <http://www.comune.venezia.it/flex/cm/pages/ServeBLOB.php/L/IT/IDPagina/2973> [last access February 2014].

threshold into values of lost tourism expenditures and replacement costs, for elderly people requiring day-care and for baby-sitting (for school-age children who cannot attend school). The second relevant height is the activation level of the Mo.S.E. We assume a +110 cm as the reference level for the tide inside the lagoon, once the Mo.S.E. has been activated.

Every Mo.S.E. activation will have an impact on the Venice harbour activity.<sup>3</sup> When the floodgates are closed, ships will first be hosted outside the lagoon and then allowed to enter through a lock gate. Ships already at the wharfs within the lagoon will have to wait until proper navigation conditions are restored. Mo.S.E. operation will thus entail costly delays in the harbour operations. Clearly, the more frequently the floodgates are kept closed, the higher the cost will be due to the interference with harbour activity, but the lower the damage to Venice due to AA will be. We calculate an average interference cost per episode of Mo.S.E. closure as the average of the two scenarios considered in [4]. It amounts to 0.168 million euro. Finally, in the evaluation exercise, we also take into account the yearly figures for O&M costs, which amount to 13.3 million euro yr<sup>-1</sup>.

AA forecasts depend, inter alia, on the LSLR. Because of the lack of data, we do not consider the possible interaction between global warming and the meteorological components of AA (storm surge) and take into account the possible LSLRs under different scenarios, simulating their impact only through the (annual) increase in the tide's trend. We consider five possible scenarios in which the LSLR ranges from the lowest level (the historical trend, namely 2.5 mm yr<sup>-1</sup>) to an extremely high level. The historical trend scenario would exclude any increase in the LSLR due to global warming. We consider three other scenarios in which global warming plays a progressively increasing role. In particular, we first consider a low LSLR scenario, that assumes a constant yearly LSLR of 3.7 mm yr<sup>-1</sup>. Such a level corresponds to the common starting value of the global mean SLR for the four process-based projections (RCP2.6, RCP4.5, RCP6.0 and RCP8.5) considered by [3]. In those IPCC projections, such a level increases over time; thus, keeping it fixed corresponds to the adoption of an optimistic assumption about the LSLR. Second, we construct an "average IPCC" scenario, averaging the estimated rises extracted from the four process-based IPCC scenarios [3] mentioned

---

<sup>3</sup>Interferences with the activities of small tourist wharfs and other harbours located in Chioggia - mostly devoted to fishing - are not considered in our study because of lack of data.

above and assuming a linear rise throughout the period. The derived figure equals  $5.6 \text{ mm yr}^{-1}$ . Interestingly enough, such a level coincides with the lower boundary for global SLR estimates, as reported by [5]. We also consider a pessimistic (high-rise) scenario assuming a yearly LSLR that derives from the IPCC scenario that delivers the highest projections for the global mean SLR, namely, the RCP8.5. It amounts to  $7.4 \text{ mm yr}^{-1}$ . Finally, we consider a worst-case scenario that corresponds to the highest forecast in the literature from semi-empirical models [6], namely, two meter over the whole century. Such a figure, which also coincides with the upper bound of the forecast considered in [5] yields a (constant) yearly LSLR of  $20 \text{ mm yr}^{-1}$ . Table 1 summarizes the five scenarios considered.

[Table 1 about here.]

The five scenarios determine a different impact of LSLR on the AA. We conducted 10,000 simulations for each scenario. Figure 1 reports the yearly average expected number of Mo.S.E. activations for each scenario, a figure that is relevant for the second component of the damage to Venice due to AA. The left panel (Figure 1a) reports scenarios from S1 to S4, while the worst-case scenario S5 is reported in the right panel (Figure 1b). Figure 2 plots the expected average of AA events above 180 cm in each scenario, a crucial level that affects the first component of the damage function.

[Figure 1 about here.]

[Figure 2 about here.]

We note that the higher the expected LSLR, the more frequent the Mo.S.E. activations will be in each year and the higher the episodes of extreme high AA will be. In particular, we can see that the frequency of Mo.S.E. activation rises exponentially for scenarios from S1 to S4; in scenario S5, it reaches a frequency so high that Mo.S.E. will (almost always) remain closed throughout the whole year in the last decade. Obviously, such a result depends on the extremely high level of LSLR assumed in the worst-case scenario. As for the frequency of the highest tide throughout period, we can see that, even in the most conservative S1 scenario, there will be two episodes of a tide above 180 cm in 50 years. Even if such an AA is, at present, considered an

exceptionally extreme event, it is not implausible given that it has been observed once in the last 50 years and because of the continuing rise of the sea level. Clearly, such a frequency increases the higher the LSLR is, reaching an overwhelming figure of 25 episodes of AA above 180 cm in 50 years. Impressive as it might be, such a figure is not implausible, taking into account that, in the S5 scenario, there will be a one-meter rise of the sea level at the end of the period, which would imply that there would be several episodes of extremely high AA per year in the last decade.

#### 4. THE EVALUATION OF Mo.SE BENEFITS

The difference between the damages that would occur without Mo.S.E. and those that can be experienced once the Mo.S.E. is operated provides an economic measure of Mo.S.E. benefits. For each simulation of the tide level in a 50-year horizon, we evaluate the costs associated with AA episodes both with and without the Mo.S.E. To obtain comparable monetary figures, the costs are discounted at a 2% rate. Figure 3 plots the evaluation of the damages with and without Mo.S.E. for the S3 (average) scenario. The graph describes the median, the first and the third quartile and the min and the max of the simulations for the cumulated values of the first 5, 10, 25 and 50 years, with and without Mo.S.E. The dashed lines identify the Mo.S.E. total costs. All figures are in billion of euro, at constant 2013 prices.

[Figure 3 about here.]

Note that the damage increases over time as LSLR increase. Mo.S.E. functioning reduces the volatility of the estimates, since it caps the height of AA. Thus, the remaining volatility depends only on the expected numbers of its activation. We point out that, without Mo.S.E., there is an expected overall level of damages to Venice that amounts to 8.27 billion euro in 50 years. Mo.S.E. reduces it to 2.25 billion euro, thus determining an expected benefit, i.e., avoided damages, above 6 billion euro. Such a figure is above the reported costs, that amount to 5.4 billion euro. Therefore, we can expect a net positive value for Mo.S.E. in 50 years. Clearly, the value of the benefits depend on the different LSLRs assumed. Figure 4 summarizes the benefits to Venice from Mo.S.E. in the S1, S2, S3, S4 and S5 scenarios. The figures (median values) are

reported in Table 2.<sup>4</sup>

[Figure 4 about here.]

[Table 2 about here.]

We can see that damage increases over time as expected, both without and with Mo.S.E. Its functioning reduces the damages. As a result, positive benefits accrue from the use of Mo.S.E. in each scenario. The value of the benefits increases with the LSLR for the S1, S2, S3 and S4 scenarios. The median figure ranges from 5.3 billions to 6 billion. Taking into account that the reported costs are 5.4 billions of euro, we observe a positive net benefit from Mo.S.E. under scenarios S2, S3 and S4. The benefits increase with the higher LSLRs assumed in each scenario, with a slightly negative figure for the baseline (no global warming) scenario S1. Looking at the figures of the first quartile and the maximum, we note however, that in S1, (almost) half of the simulations report a net benefit higher than the cost. Therefore, even in S1, we can assess a non-negative cost-benefit analysis for Mo.S.E. The figure of the extreme S5 scenario appears contradictory at a first glance, since the median estimate of benefit from Mo.S.E. is lower than the values for the other scenarios. This can be understood looking at the values of damage reported in Table 3. Note that the damage without Mo.S.E. in S5, even if it is higher than damage in S2 and S3, is not too high and are even comparable to the damage in S4 for the first 25 years of simulations. However, damage both with and without Mo.S.E. explodes in the second half of the considered period for the S5 scenario compared to the damage under the other scenarios. This determines the reduced values of benefits compared to the other scenarios. The explanation depends on the frequency of Mo.S.E. activations under the S5 scenario compared with activations in the other scenarios (see Figure 1a and Figure 1b), which determines continuous interference with harbour activity. However, we point out that a precise estimate of AA consequences in the S5 scenario cannot be considered as reliable as the estimates under the other scenarios, since S5 assumes a LSLR that is at the border of levels that are (supposed to be) compatible with Mo.S.E. operation (and, on the other hand, even the probability of a SLR higher than the one reported in the RCP8.5 - our S4 scenario - cannot be reliably evaluated according to [3]).

---

<sup>4</sup>Descriptive statistics for the 10,000 simulations per scenario are available from the authors upon request.

## 5. CONCLUDING REMARKS

Our analysis provides a lower boundary to the value of protecting Venice for several reasons:

- limited data (only the historical part of Venice is considered).
- not all possible damages are considered (e.g., the impact of AA on shops and warehouse inventories) due to lack of data.
- no interaction between LSLR and storm surge is assumed (which could reinforce the frequency and height of AA)
- indirect costs (such as externalities), risk attitudes (which affect the option values of the investment) and strategic reactions to LSLR are not taken into account.

We have shown that the estimated benefits, which are largely higher than the original planned cost of the investment, have been greatly eroded by the increase in the budget during its construction. However, there is still a positive net benefit, whose value depends crucially on the assumed LSLR. In particular, the benefits are higher than the costs the higher the assumed LSLR, provided that it is not too extreme. If, on the contrary, there were a limited or null LSLR, the benefits of protecting Venice from AA would be entirely overtaken by the investment and O&M costs. Similarly, in the case of a catastrophic one-meter LSLR in 50 years, both AA and Mo.S.E. would interfere with everyday activities so frequently that the Mo.S.E. benefits would not balance with its costs. Our work points out the importance of correct budget planning for investments of such a large scale and highlights the negative economic impact of high LSLR and consequently the importance of a large-scale adaptation expenditure, such as the Mo.S.E. system, to minimize it. It also casts some doubt on its positive net value, should a catastrophic rise happen.

## 6. ACKNOWLEDGEMENTS

We thank Alberto Tomasin for having made available the data set of Centro Maree and jointly with Georg Umgiesser for their help on the Acqua Alta phenomenon. Clearly,

we are responsible for the contents of the article. F. F. acknowledges the research grant PRIN-MIUR 2010-11 “Climate changes in the Mediterranean area: evolutionary scenarios, mitigation policies and technological innovation”.

## 7 REFERENCES

1. Canestrelli, P., Mandich, M., Pirazzoli, P.A. and Tomasin, A. (2001). Wind, Depression and Seiches: Tidal Perturbations in Venice (1951-2000), Centro previsioni e segnalazioni maree, Comune di Venezia. Available at [http://93.62.201.235/maree/DOCUMENTI/Venti\\\_depressioni\\\_e\\\_sesse.pdf](http://93.62.201.235/maree/DOCUMENTI/Venti\_depressioni\_e\_sesse.pdf) [last access: February 2014].
2. Fontini, F., Umgiesser, G. and Vergano, L. (2010). The Role of Ambiguity in the Evaluation of the Net Benefits of the MO.S.E. System in the Venice Lagoon, *Ecological Economics*, 69, 1964–1972.
3. IPCC, (2013). *Climate Change 2013: The Physical Science Basis*. Working Group I Contribution to the Fifth Assessment Report of the Intergovernmental Panel on Climate Change, 2007. Available at <http://www.ipcc.ch/report/ar5/wg1/> [last access: February 2014].
4. Vergano, L., Umgiesser, G. and Nunes, P. A.L.D. (2010). An economic assessment of the impacts of the MOSE barriers on Venice port activities, *Transportation Research Part D*, 15, 343–349.
5. National Research Council, (2010). *Advancing the Science of Climate Change*. Washington, DC: The National Academies Press.
6. Nicholls, R. J., Marinova, N., Lowe, J. A., Brown, S., Vellinga, P., de Gusmão, D., Hinkel, J. and Tol, R. S. J., (2011). Sea-level rise and its possible impacts given a ‘beyond 4 degrees C world’ in the twenty-first century. *Philosophical Transactions of the Royal Society A*, 369, 161–181.

scenario	impact on AA	LSLR
S1	historical	2.4 mm yr <sup>-1</sup>
S2	low	3.7 mm yr <sup>-1</sup>
S3	medium	5.6 mm yr <sup>-1</sup>
S4	high	7.4 mm yr <sup>-1</sup>
S5	worst case	20 mm yr <sup>-1</sup>

Tab. 1 Assumptions on LSLR for each scenario.

*Scenario S5*

years	Damage without Mo.S..E. (A)	Damage with Mo.S..E. (B)	Mo.S.E. benefits (A-B)
5	716	205	511
10	1576	443	1133
25	4817	2154	2664
50	16746	12252	4494

*Scenario S4*

years	Damage without Mo.S..E. (A)	Damage with Mo.S..E. (B)	Mo.S.E. benefits (A-B)
5	649	197	452
10	1363	396	967
25	3848	1043	2806
50	8783	2738	6046

*Scenario S3*

years	Damage without Mo.S..E. (A)	Damage with Mo.S..E. (B)	Mo.S.E. benefits (A-B)
5	640	196	444
10	1328	393	935
25	3674	999	2675
50	8276	2255	6020

*Scenario S2*

years	Damage without Mo.S..E. (A)	Damage with Mo.S..E. (B)	Mo.S.E. benefits (A-B)
5	622	195	427
10	1292	388	904
25	3475	964	2512
50	7640	1976	5664

*Scenario S1*

years	Damage without Mo.S..E. (A)	Damage with Mo.S..E. (B)	Mo.S.E. benefits (A-B)
5	613	195	419
10	1269	386	883
25	3349	946	2403
50	7197	1871	5326

Tab. 2 Damages with and without Mo.S.E. in the S1, S2, S3, S4 and S5 scenarios, in 5, 10, 25 and 50 years.

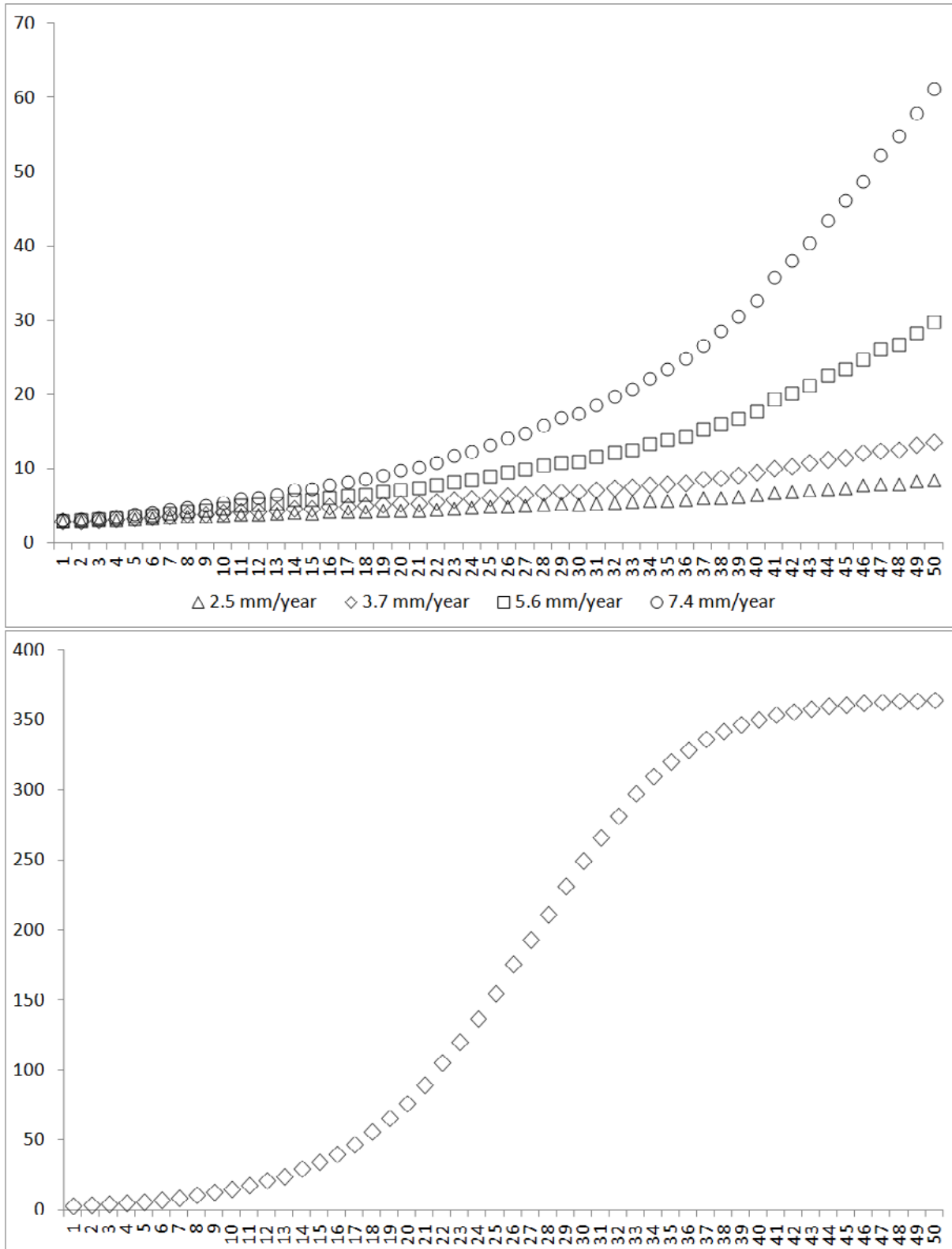


Fig. 1 Expected number of Mo.S.E. activations in S1, S2, S3, S4 (left panel) and S5 (right panel) scenarios.

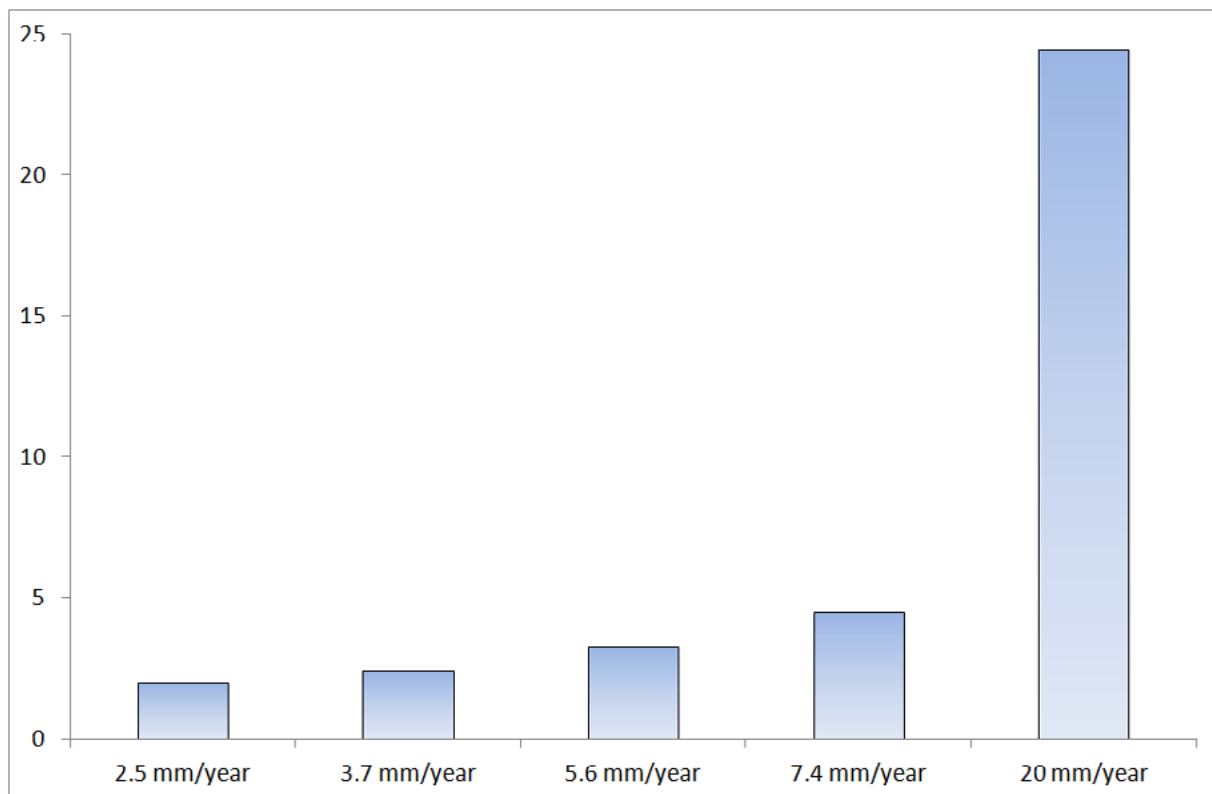


Fig. 2 Expected number of AA events above +180 cm in S1, S2, S3, S4 and S5 scenarios.

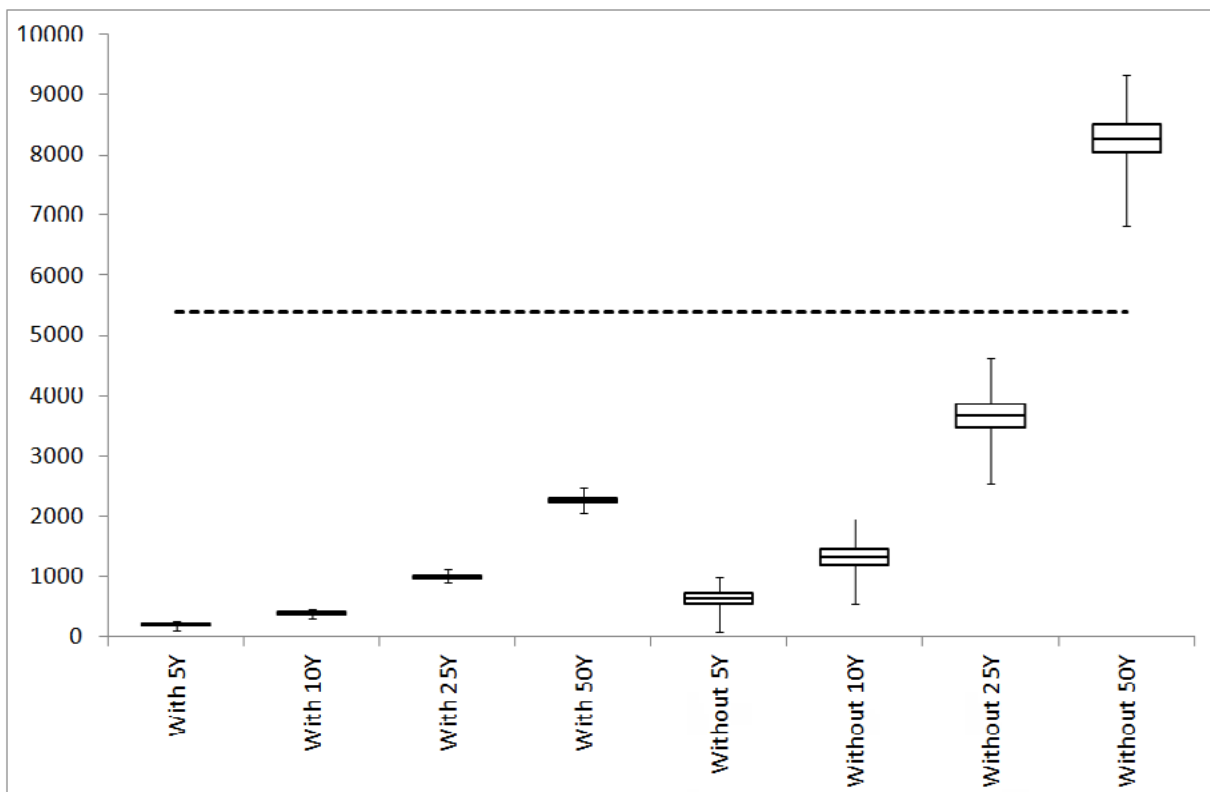


Fig. 3 Damages to Venice in the S3 scenario with and without Mo.S.E. in 5, 10, 25 and 50 years.

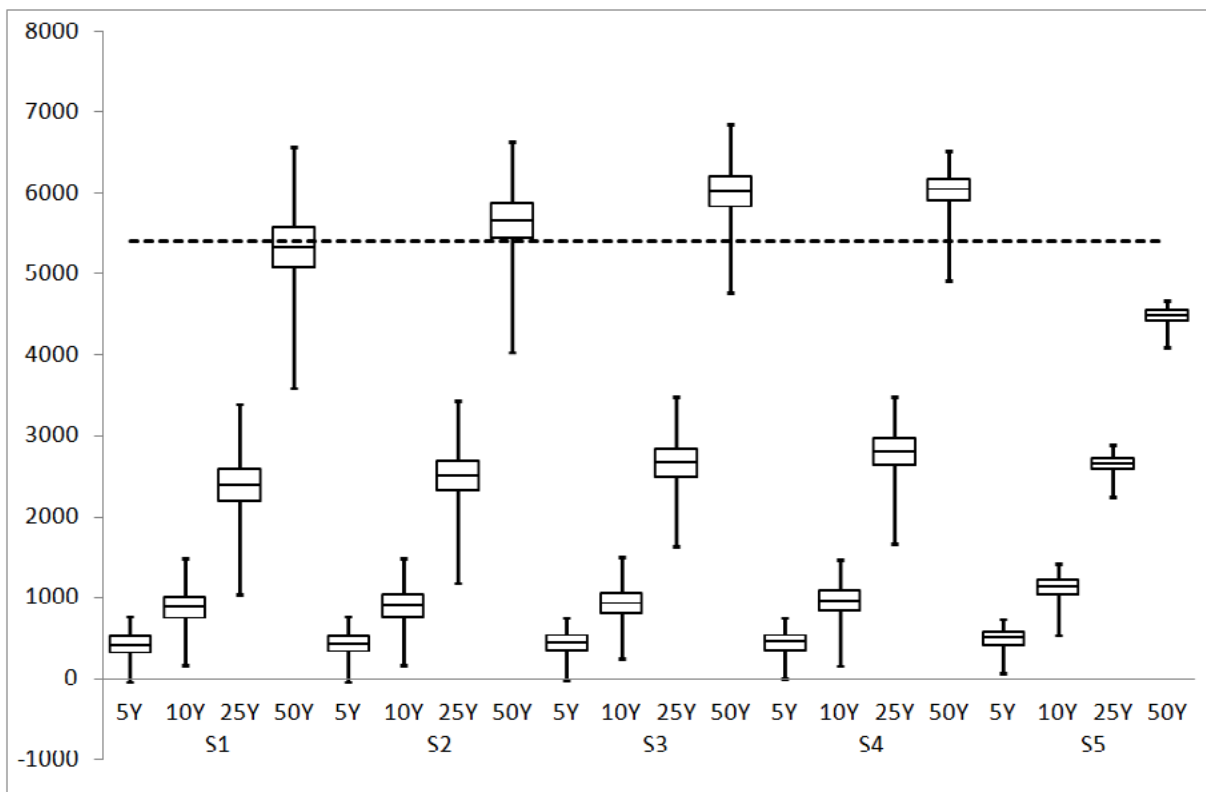


Fig. 4 Mo.S.E. benefits to Venice in the S1, S2, S3, S4 and S5 scenarios in 5, 10, 25 and 50 years.

## **A Choice Experiment application for valuing adaptation of river services to climate change**

**\*Andreopoulos D.<sup>1</sup>, Damigos D.<sup>2</sup>, Comiti F.<sup>1</sup>, Fischer C.<sup>1</sup>**

<sup>1</sup>Faculty of Science and Technology, Free University of Bozen/Bolzano, Italy

<sup>2</sup>School of Mining and Metallurgical Engineering, National Technical University of Athens, Greece

\*Corresponding author: dimitrios.andreopoulos@natec.unibz.it

### **Abstract**

Using the Choice Experiment (CE) method, this paper examined public preferences for adapting to climate change services provided from a river basin in Italy. The study design accounted for preservation of current levels of different river services since climate change projections indicate a considerable recharge loss of the Piave River the forthcoming decades. Our estimation strategy consisted in estimating a Conditional Logit (CL) model, its extended form and a Nested Logit (NL) model. Results for all models present a tendency towards the selection of an adaptation alternative showing that people are willing to pay for most of the river services. The policy implications of these results may assist to develop more robust adaptation practises for water resources.

**Keywords:** climate change, river uses, choice experiment

Vulnerability, Risk Assessment and  
Adaptation to Climate Change

**Risk assessment**

# **Developing climate risk and adaptation services in coastal zones: an integrated bottom-up approach applied in the North Adriatic coast**

**Torresan S.<sup>1,2</sup>, Sperotto A.<sup>1,2</sup>, Gallina V.<sup>1,2</sup>, Furlan E.<sup>1,2</sup>, Critto A.<sup>1,2</sup>, Marcomini A.<sup>1,2\*</sup>**

<sup>1</sup>Centro Euro-Mediterraneo sui Cambiamenti Climatici (CMCC), Impacts on Soil and Coast Division, Italy

<sup>2</sup>Department of Environmental Sciences, Informatics and Statistics, University Ca' Foscari Venice Italy

\*Corresponding Author: marcom@unive.it

## **Abstract**

Nowadays, coastal stakeholders and decision makers request an increasing amount of information on climate variability and its impacts on natural and human systems in order to incorporate climate adaptation in land and policy planning and ensure a sustainable integrated coastal zone management. In the framework of the CLIM-RUN project (Climate Local Information in the Mediterranean region: Responding to User Needs) (<http://www.climrun.eu/>), a participatory Regional Risk Assessment (RRA) methodology for the evaluation of climate-related hazards in coastal zones (i.e. pluvial flood and sea-level rise inundation risks) was applied in the North Adriatic region considering future climate change scenarios for the timeframe 2041-2050. Through the analysis of hazard, exposure, vulnerability and risk and the application of Multi-Criteria Decision Analysis (MCDA), the methodology allowed to identify and prioritize targets and sub-areas that are more likely to be affected by pluvial floods and sea-level rise impacts in the same region. From the early stages of application, the RRA followed a bottom-up approach taking into account the needs and perspectives of local stakeholders in terms of case study areas, time scenarios, spatial scale and resolution, choice of receptors, vulnerability factors and thresholds. Relevant outputs of the analysis are GIS-based maps and statistics representing tailored risk and adaptation services for local stakeholders dealing with coastal zone management.

**Keywords:** regional risk assessment, coastal zones, risk and adaptation services

## Changing meso level response to extreme climate events in Viet Nam

**Christoplos I.<sup>1\*</sup>, Le Duc N.,<sup>2</sup> Le Thi Hoa Sen,<sup>3</sup> Nguyen Thi Thanh H.,<sup>4</sup> and  
Lindegaard Salloum L.<sup>5</sup>**

<sup>1</sup> Danish Institute for International Studies - Denmark, <sup>2</sup> Centre for Climate Change Study in Central Viet Nam – Viet Nam, <sup>3</sup> Centre for Climate Change Study in Central Viet Nam – Viet Nam, <sup>4</sup> Quang Binh University – Viet Nam and <sup>5</sup> Danish Institute for International Studies - Denmark

\*Corresponding Author: [ian@glemdev.com](mailto:ian@glemdev.com)

### **Abstract**

How do extreme climate events shape local government perceptions and responses to climate change? This paper, based on three case studies from Central Viet Nam, looks at changes that have occurred over time in how local officials perceive their social contract for risk reduction, including the partial merging of pre-existing trajectories related to disaster risk management with new plans and investments in climate change adaptation. Findings indicate that extreme floods and storms are indeed critical junctures that stimulate genuine institutional change. Local officials are proud of their strengthened role in disaster response and they are eager to increase investments in infrastructure. There are signs of a recognition of the need to work with households to 'build back better'. However, the changing role of the state, growing engagement from the public, private sector and civil society, and undiminished prevalence of high-risk development models have meant that their responsibilities for responding to emerging climate change scenarios are increasingly nebulous.

**Keywords:** Disaster risk reduction, Extreme climate events, Local government, Decentralisation

## 1. INTRODUCTION

This paper presents findings on the changing nature of local government response to extreme climate events in central Viet Nam from the Climate Change and Rural Institutions research programme. It build on initial findings from field research{1}. Three such events are analysed: the 1999 flood in Thua Thien Hue Province, the 2010 flood in Quang Binh Province and recent experience with Typhoon Wutip which affected Quang Binh in September 2013. These interlinked cases document and provide a basis to chronologically analyse the changes that have been underway in meso level institutions in Central Viet Nam in relation to confronting extreme climatic events. This research has shown that local government officials interpret climate change scenarios against a backdrop of how they have experienced extreme climate events.

## 2. 1999 FLOOD IN THUA THIEN HUE

During the period of 2<sup>nd</sup> to 11<sup>th</sup> November in 1999 an extreme flood affected Thua Thien Hue Province in Central Viet Nam. Flooding was severe throughout the coastal areas, including Hue City. The level of major rivers rose to an unprecedented height. Rainfall on November 2 in Hue was the second heaviest rainfall ever recorded in the world. There were 352 fatalities. Over 25 thousand houses collapsed or were washed away; over one thousand schools collapsed, and 160,000 cattle and close to 900,000 poultry were killed{2}.

The response to the disaster was very much dominated by public institutions. Civil society, apart from the mass organisations (closely associated with the state and the Communist Party) was very weak, and structures through which local government and private firms might cooperate were not in place. Agricultural cooperatives were very weak due to the virtual collapse of the past system as part of overall structural reforms. Despite this, a large amount of the credit for restarting rice production that was provided after the flood was channelled through the cooperatives.

All informants describe the 1999 flood as being an event that contributed to major changes in both attitudes and institutions. Inadequate response revealed to all levels of government that existing agencies responsible for flood and storm control were in

urgent need of renewal and strengthening. It has been claimed that this was due to the dismantlement of collective structures as part of the reform process that had been underway over the preceding decade<sup>{3}</sup>. While there were formal (but not detailed) procedures and directives already promulgated for annual flood and storm control preparation and response prior to 1999, these responsibilities were not given high priority. This changed significantly after 1999, apparently due to the realisation of the serious threat such events posed to economic development, food security and the livelihoods of local people, as well as the understanding that the existing procedures, if properly applied, could significantly reduce these risks. Changes and strengthening of national disaster risk management structures and pressures on local government for stronger efforts are widely seen to have originated in a response to problems in response to the 1999 flood and another extreme flood in the Mekong Delta the following year. A major focus has been on investments in infrastructure such as sea and river dykes, which overwhelmingly dominates recently developed provincial climate change plans. The climate change adaptation agenda in central Viet Nam today has been profoundly shaped by the experience of events such as the 1999 floods.

### **3. 2010 FLOODS IN QUANG BINH**

In October 2010, the nearby province of Quang Binh was impacted by an extreme storm (though not as extreme as the 1999 floods in Thua Thien Hue) leading to almost total flooding of the province. The trajectories between the 1999 flood and the 2010 flood in Quang Binh are difficult to trace. In Quang Binh today there is little remembrance of the 1999 experience despite it having occurred only 150 km away. The concerns raised at national level in relation to that earlier disaster led to new formal policies which were rolled out in the interim years. However, in Quang Binh Province, the reforms that followed the 1999 floods did not have a notable impact.

When asked about changes inspired by the 2010 flood, officials particularly note that provincial and district Committees for Flood and Storm Control (CFSCs) have become more open to engaging the private sector to provide support in disaster situations. For example, procedures and regulations are now in place to ensure that

the authorities are able to temporarily requisition all fishing boats for relief, rescue and evacuation purposes in the event of a disaster. In addition, the provincial agricultural department has developed new modes of disseminating early warnings and other information about disasters, involving mass media sources such as television, newspapers and internet sites. As with Thua Thien Hue, provincial officials emphasise sea and river dykes to control such flooding as the main priorities for climate change adaptation investments.

The responsibilities of CFSC members have also changed to include more responsibility for promoting community awareness and capacity for local response. Training courses, supported by various international NGOs, on improving capacity in disaster risk management have been organised. However, at district level staff are not active in implementing community-based activities, and given that the provincial level is far from 'the community' this is highly problematic in relation to actual roll out of these reforms.

The difference in the state of preparedness between Thua Thien Hue and Quang Binh provinces points to the significance of local level discretion and innovation. Despite the 1999 floods having been relatively nearby and constituting a mega-event in a national perspective, substantial strengthening in meso-level flood and storm control practices in Quang Binh only occurred following local experience of an extreme event. This may reflect the path dependency that prevails within meso level institutions and the extent to which actual lived experience of local officials in addressing extreme events determines local practices in Viet Nam. While national policies were previously nominally enacted in both provinces and grave climate change scenarios have been disseminated by national authorities, changes in actual practice have been predicated upon a local experience which catalyses officials' engagement and level of commitment.

#### **4. 2013 WUTIP**

Starting at 16:00 on September 30 2013 Quang Binh was hit by Typhoon Wutip, an extremely intense storm with a wind speeds of between 51 and 61 metres per second. This was followed by a more modest but still significant tropical storm 16

days later, which brought heavy rains to already affected communities. Interviewees stress that Wutip was an extreme and devastating event in several respects:

- It carried with it heavy winds, which had been rare in recent years when people had become more oriented towards dealing with floods.
- The duration of the intense winds was extraordinarily long; up to eight hours as opposed to two to three, which is normal in storms of this type.
- It affected the entire province.
- It was preceded and followed by several intense tropical storms that strained coping capacities.

Wutip's impacts were very different from those of flooding such as in 2010. Impacts on households were mostly related to damaged roofs and housing more generally. The season's rice and most of the aquaculture production had already been harvested, but there were some losses due to stored rice becoming wet. Damage to winter crops, such as vegetables and maize, were severe. Many aquaculture producers incurred losses as their equipment was washed away and some already saturated bunds collapsed. The greatest economic damage in agricultural production was to perennials. Pepper plants were heavily affected and most of the province's rapidly expanding rubber sector was heavily damaged. As rubber trees take five to ten years to start producing, and most of trees were just starting to produce, many years of investment were lost. The resulting indebtedness is likely to impact on the affected households for years to come. It has been noted that the shift towards plantation production in Viet Nam carries with it risks for the rural population that are certainly different and possibly greater<sup>{4}</sup>.

Compared to past disasters, local officials emphasise far more strongly the importance of households investing in their own risk reduction in the form of raised and concrete houses. There is a recognition in Quang Binh today that dykes alone are not a sufficient solution for climate risk. The experience of losses in rubber is also leading to critical reflection over this high-risk development model. Provincial officials acknowledge having received warnings of these risks before, but had judged that the potentially high profits justified these risks. They now acknowledge that the decision to proceed despite these risks may have been wrong. The province took the unusual

step of organising a scientific conference to bring together research on how to reduce risks of wind damage to rubber.

Regarding the emergency response, in addition to the stronger local preparedness there is a new and potentially profound shift underway driven by both social and mass media. In the past the main non-governmental support reaching the area was through international aid. With declining development assistance to Viet Nam, international relief support is also diminishing. The international agencies are being replaced by what may be a larger but certainly amorphous domestic public (and to some extent private) response. This is driven by the media, for whom disasters and extreme weather events are becoming 'big news'. Triple the number of news agencies came to Quang Binh to report on Wutip as came during the 2010 flooding. Some informants mentioned that this rapidly growing interest seems to be related to more reporting on weather related disasters in other countries and also due to the multiplier effect when such news spreads through the internet, spawning demand for even more information.

The mass media reporting led to social media mobilisation. Groups of former residents of Quang Binh, students and good Samaritans came together after Wutip through Facebook, or even travelled to Quang Binh on their own to directly deliver relief. Such ephemeral organisations<sup>{5}</sup> with a strong commitment to "being there" when a disaster strikes are not new internationally but they are a new phenomenon in Viet Nam, where authorities are accustomed to having a comprehensive overview and unquestioned authority over initiatives in their areas of operation. Some private companies also came, particularly those selling building materials, but local officials note that it is difficult to judge whether their attention is due to commitments to corporate social responsibility or to opportunities to generate exorbitant profits by supplying a sudden, huge demand for building supplies. Provincial authorities intervened to stop this price gauging.

Officials note their discomfort and uncertainty about if and how they should manage these new influxes of support. They are unclear about whether this is just an inevitable new phase in the 'socialisation' process, the term used in Viet Nam for decentralisation and handover of public responsibilities to other actors; or if it constitutes a 'wild card' in relation to how they are expected to fulfil their social contract in responding to disasters. In the past officials were able to insist that

international NGOs work through meso level public institutions, but this was not possible with these new actors, some of whom did not even inform local authorities of what they were doing or who they were supporting. Those arriving generally only wanted to support the most affected households or communities they had read about on the internet (which may reflect where an individual journalist had visited, rather than actual greater need). The result was a 'mini-CNN effect' leading to very uneven distribution of aid, with some households receiving exceedingly generous support, whereas others who were slightly less affected or located in more isolated areas received nothing. Some authorities reported reducing their own level of relief assistance due to the influx from outside, which could aggravate this trend towards uneven support.

Overall, these changes in a relatively short period of three years indicate that in many respects path dependency has been overcome in Quang Binh. Changes are underway and local authorities are indeed learning from disasters. There are even some signs of a readiness to look critically at prevailing development models. However, they do not have all the answers. They recognise that the new mass- and social-media- driven relief efforts and the emergence of corporate social responsibility and Vietnamese civil society have both positive and negative implications.

## **5. CHANGES THAT CAN BE ATTRIBUTED TO THE EXPERIENCE OF EXTREME CLIMATE EVENTS**

Several major changes can be observed that can be attributed (at least partially) to these three extreme events:

*Human resource and organisational capacity*, there is clear evidence and pride in how district and commune officials, mass organisations and other entities with official responsibilities for disaster response, and in some instances recovery, are increasing their capabilities to coordinate, prepare for and carry out their work. There is general awareness that climate change scenarios suggest that disasters will become more frequent, but limited capacities to apply this knowledge in non-disaster related actions.

*Detail*, as pre-existing policies have been fleshed out, particularly with clearer delineation of responsibilities. Particular attention has been given to greater explicitness regarding rescue and evacuation. Norms for community-based disaster risk management have also been better defined. By contrast, local officials acknowledge their bafflement about the implications of broader climate change directives.

*Guidance*, as training and provision of guidelines has been expanded through pressures from central government to ensure that governmental staff are aware of their duties. Meso level officials stress that they are not just told what they should do, but also how to do it. Again, this is in clear contrast to new directives related to climate change adaptation, which are seen as vague and overambitious.

*Pre-season planning*, perhaps the activity most often stressed by interviewees in meso level institutions is the meetings that are held each year in July and August before the flooding season to take stock of lessons learnt from the previous year, to mobilise a broad array of actors and to ensure that roles are understood.

*Engagement of mass media*, since the 1999 floods there has been considerable investment in and engagement with the mass media and in sources of weather information to ensure that more and better quality information reaches the affected areas in a timely manner. Today the media no longer needs to be encouraged to write about disasters, as their interest is great. Rather than being a tool for local authorities, media organisations are increasingly setting the agenda.

*Pluralism, ephemerality and ambiguous relations*, in marked contrast to the growing formality and structure in governmental response, the emergence of new ephemeral structures for disaster response, mobilised through social media has created an ambiguous situation wherein, for the first time in recent history the roles of the state and emergent independent civil society are in flux. There has been greater openness to and involvement of the private sector, mass organisations and NGOs in disaster preparedness and community based disaster management.

*Investment*, considerable flows of resources, some coming from climate change adaptation funding, are being invested in infrastructure, human resource development, organisational development, shelter improvement and emergency supplies for relief response and evacuation.

*Decentralisation*, district and commune level officials feel empowered to make their own decisions and find the most effective ways to implement national directives. This is presumably not directly related to the experience of disasters, but is probably related more to the broader decentralisation process, which is in turn impacting on disaster risk management.

*Merging of disaster risk management and climate change adaptation*, though not clearly attributable to these extreme events, it appears likely that the legacy of these disasters and the constant reminder of these hazards have meant that climate change adaptation is understood to be largely a matter of infrastructural climate proofing, 'building back better' and disaster preparedness.

## 6. CONCLUSIONS

A social contract clearly exists in Viet Nam for disaster response, and this in turn has translated into a strong emphasis on disaster preparedness. Non-infrastructural recovery and climate-related risk reduction are not absent from the agenda, but have often received less attention for three reasons.

First, it is hard to disentangle the actions that may be needed to reduce risk and recover from disasters from the broader range of decisions that need to be made in relation to socio-economic development in general. The broader concerns related to opportunities and risks in broader development seem to take precedence over recovery and non-infrastructural risk reduction, despite some signs of increasing readiness to engage in these areas as well.

Second, despite changing perspectives after Wutip, the juggernaut of climate change adaptation investment plans has meant that the solution of infrastructure dominates risk reduction efforts, even though other factors that generate risk are starting to be recognised as having significant dimensions that cannot be addressed by infrastructure.

Third, many risks are amorphous, both in relation to their nature and the responsibilities for their response, and are therefore generally given lower priority. Interviewees recognise that climate change scenarios point towards a range of risks.

They are also increasingly aware (and concerned about) ambitious directives to respond to climate change. But they also realise that it is not self-evident who should respond to the warnings in emerging scenarios and who should implement and pay for such a response.

At district and commune levels, respondents are explicit in explaining how extreme events have constituted critical junctures that have stimulated change. Even if a bias exists towards certain types of solutions, when a new and very different problem appears, as with the winds of Wutip, local officials are attentive and they are prepared to change course. But are emerging risks related to prevailing development models enough to break more profound path dependencies? It is apparent that people are prepared to reflect over this, as evidenced by expressed concerns about how rubber is now perceived as a very risky proposition. But it is less clear whether these concerns lead to actual changes in development priorities and planning.

In focusing on the state of the social contract at meso level we have encountered a complex picture of the social contract. There is certainly a much stronger (perhaps renewed) social contract for saving lives. This is evidenced by the emphasis given in interviews to information/early warning, evacuation and dykes. The evidence is more mixed regarding whether there is a different social contract for broader household level risk reduction. In the past most households were left to manage their own recovery. Wutip shows signs suggesting that changes may be afoot. Due to the nature of losses concentrated in housing, and perhaps also due to media attention focusing on shelter needs, a social contract for supporting households to 'build back better' is gaining momentum.

In the longer term the nature of the social contract will be influenced by the shifting nature of public authority. The ways local government officials have struggled to improve their performance in disaster response illustrates concerns about declining control over market-led and urban/industrial driven development. The emergence of ephemeral domestic relief organisations is a new factor impinging on the extent of the social contract. In sum, a dynamic and complex process is underway wherein the social contract for responding to climate change is being actively renegotiated amid typhoons, directives, failed plantations, emerging corporate social responsibility and Facebook driven charity.

## 7. ACKNOWLEDGMENTS

This ongoing research programme is funded by the Danish Ministry of Foreign Affairs. The research team acknowledges the very open and constructive engagement of the provincial, district and commune level officials interviewed in the research on these case studies.

## 8. REFERENCES

1. Le Duc Ngoan, Le Thi Hoa Sen, Nguyen Thi Thanh Huong, Christoplos, I & Salloum Lindegaard, L. (2013), *Climate Change and Rural Institutions in Central Viet Nam*, DIIS Working Paper 2013:14, Danish Institute for International Studies
2. Nguyễn Ty Niên ( 2012) Nhìn lại thiên tai miền Trung sau hơn mười năm lũ lịch sử 1999. [<http://www.vncold.vn/Web/Content.aspx?distid=2916>].
3. Adger, W.N. (1999) Social vulnerability to climate change and extremes in coastal Vietnam, *World Development*, 27(2): 249-69
4. Thulstrup, A.W. (2014) Plantation livelihoods in central Vietnam: Implications for household vulnerability and community resilience, *Norsk Geografisk Tidsskrift – Norwegian Journal of Geography*, 68(1): 1-9
5. Lanzara, G. F. (1983) Ephemeral organizations in extreme environments: Emergence, strategy, extinction, *Journal of Management Studies*, 20/1 71-95

# **Assessing the impacts of climate change on marine water quality through a spatially resolved risk assessment approach: the North Adriatic sea (Italy) as case study**

**Rizzi J.<sup>1,2</sup>, Torresan S.<sup>2</sup>, Zabeo A.<sup>2</sup>, Critto A.<sup>1,2</sup>, Brigolin D.<sup>1</sup>, Carniel S.<sup>3</sup>, Pastres R.<sup>1</sup>, Marcomini A.<sup>1,2\*</sup>**

<sup>1</sup>Department of Environmental Sciences, Informatics and Statistics, University Ca' Foscari Venice, Venice, Italy. <sup>2</sup>Euro-Mediterranean Centre for Climate Change (CMCC), Impacts on Soil and Coast Division, Venice, Italy. <sup>3</sup>Institute of Marine Science - National Research Council (ISMAR-CNR), Venice, Italy

\*Corresponding Author: marcom@unive.it

## **Abstract**

Global climate change is posing additional pressures on coastal ecosystems through variations in water biogeochemical and physical parameters (e.g. primary production, pH, salinity) leading to aquatic ecosystem degradation.

In order to analyse the potential consequences of climate change on marine water quality and evaluate the related impacts, a Regional Risk Assessment (RRA) methodology was developed and applied to the marine coastal waters of the North Adriatic sea (i.e. in front of the Veneto and Friuli Venezia regions, Italy). The analysis integrate outputs from numerical models providing information about water biogeochemical and physical parameters (i.e. primary production, macronutrients, dissolved oxygen, pH, salinity and temperature) under future climate change scenarios (i.e. years 2070 and 2100) with site-specific environmental and socio-economic indicators (e.g. Evenness index, presence and extension of seagrasses).

The final outputs are GIS-based exposure, susceptibility and risk maps that support the communication of the potential consequences of climate change on water quality to decision makers and stakeholders and provide a basis for the definition of adaptation and management strategies. The paper presents the RRA methodology and some results of its application to the marine coastal waters of the Northern Adriatic sea.

**Keywords:** Climate Change, Water quality, Regional Risk Assessment, GIS, North Adriatic.

Vulnerability, Risk Assessment and  
Adaptation to Climate Change

**Adaptation policies and  
strategies**

# **Do Political Systems Matter? Differences And Similarities In Institutional Settings That Support National Adaptation Strategies Across European States**

**Venturini S.<sup>1\*</sup>, Capela Lourenço L.<sup>2</sup>, Avelar D.<sup>2</sup>, Castellari S.<sup>1-3</sup>, Leitner M.<sup>4</sup> and  
Prutsch A.<sup>4</sup>**

<sup>1</sup>Euro-Mediterranean Center on Climate Change - Italy, <sup>2</sup>Foundation of the Faculty of  
Sciences of Lisbon University - Portugal, <sup>3</sup>National Institute of Geophysics and  
Volcanology – Italy, and <sup>4</sup>Environment Agency Austria – Austria

\* Corresponding Author: sara.venturini@cmcc.it

## **Abstract**

This paper studies the influence of political systems on national adaptation policy planning in European countries, by applying a Principal Component Analysis (PCA) to the adaptation research domain. Fourteen countries are selected on the basis of a proposed definition of National Adaptation Strategy (NAS) and categorized according to their political-administrative structure. About fifty institutional settings established to respond to horizontal and vertical integration challenges of adaptation are analyzed along their main characteristics. Aggregated country data are then tested to verify the patterns and relations between the political systems and the institutional capacity. Through the PCA, some statistical correlation can be found between the political dimension and the institutional capacity, particularly about the degree of novelty of institutions dedicated to a NAS that seems to be strongly influenced. It can be stated that federal countries tend to use pre-existing institutions, mechanisms and processes, while unitary tend to create new institutions. Ultimately, however, political systems can explain only a limited part of the countries' choices in terms of adaptation governance settings, and other external or internal variables may have a stronger impact, such as financial and economic circumstances, different political conditions, cultural values, or societal expectations that must be further investigated.

**Keywords:** Adaptation, Governance, Institutions, Federalism, Europe

## 1. INTRODUCTION

European countries have developed policies for climate change adaptation based on current and future climate change risks. National Adaptation Strategies (NASs) mostly represent the first effort to coordinate the issue of adaptation at the country level.

The progress on planning and implementing adaptation in Europe has been assessed to varying degrees and scopes. The European Environment Agency (EEA) published a summary of adaptation action in the region [7] and is expected to release further analyses regarding the lessons learned [27]. Other studies consider adaptive processes and strategies in Europe, both in grey literature [22] [8] [4] [3] [17] [24] [18] [29] [30] [19] [10] [25] and scientific peer-reviewed analyses [1] [9] [26] [2].

Although the amount of literature on the assessment of NASs in Europe is considerable and increasing, some research gaps still persist in this field.

Firstly, due to the fast evolution of policy processes, the information contained in the assessments can become quickly obsolete [29].

Secondly, the issue of adaptation governance has not been satisfactorily investigated despite being a critical area. In fact, the identification, implementation and evaluation of adaptation responses is expected to primarily occur through the brokerage of institutions [1] [12] [20] [21] [28] [30] [23] [14] [15] and the discrepancy of adaptation framings across countries is deemed to echo the differences in political-administrative national systems potentially affecting both the development and the effectiveness of these strategies [22] [7] [1] [4] [16] [3] [17].

Building on the work of Bauer et al. [1] and other relevant assessments, this paper focuses on the institutional settings put in place by the European countries that have addressed “governance challenges” within their NASs, namely distinctive attributes of adaptation that make traditional ways of planning and implementing policies more complex, which requires some institutional innovations to be overcome.

The analysed adaptation challenges relate to *horizontal integration* (the need to coordinate adaptation action across different socio-economic sectors that are responsibility of different ministerial or departmental bodies but present inter-linkages and possible conflicts) and *vertical integration* (the need for a response spanning

various decision-making scales from international and European to national and sub-national administrations to provide adequate means to take action).

The main goal of this study is to investigate the influence of the different political-administrative systems of those countries on their adaptation policy processes and institutions. Ultimately, the study has the ambition to foster the transferability of knowledge on NASs in Europe.

## 2. METHOD

Initially we screened the current status of adaptation policy-making in European countries by taking stock of the information displayed on the European Climate Adaptation Platform “Climate-ADAPT” (June/July 2013).<sup>1</sup> The great heterogeneity of definitions used by each country to assess progress in terms of adaptation planning allows for a substantial degree of misinterpretation. Thus, we applied the following criteria to cross-check national information as reported in Climate-ADAPT and verify if the country could be considered having an actual NAS to be included in the analysis:

- Form-wise: the country government’s executive body must have adopted a policy document or a piece of legislation on climate change and adaptation;
- Content-wise: the document must contain a vision focusing solely or substantially on adaptation at the national level, putting forward priority adaptation options, based on the country’s available knowledge on impacts and vulnerabilities to climate change, aimed at strengthening national adaptive capacity.

Secondly, an assessment of political-administrative systems of the selected countries was performed on the basis of the classification between federal, administrative-federal and unitary states proposed by Inman [13] [Tab.1]. Inman used locally collected revenues to measure decentralization of powers, assuming that own revenues reflect a larger degree of provincial autonomy, and then ranked world countries according to their performance. Since our analysis is restricted to Europe, and the category of administrative-federal states helps dealing with the diversity of

---

<sup>1</sup> The scope of Climate-ADAPT is the EEA 32 member countries: 27 EU Member States together with Iceland, Liechtenstein, Norway, Switzerland and Turkey.

country cases found in this context, the definition was applied in a slightly broader logic.

Thirdly, we analyzed the institutional settings that support adaptation policy in all the countries that were considered to have a NAS. In particular, with respect to horizontal integration of adaptation we screened the selected NASs for inter-ministerial coordination bodies and processes such as public consultations, workshop series etc. Similarly, for vertical integration we sought for inter-governmental coordination bodies, multi-level governance processes, networks and partnerships, and monitoring and reporting schemes.

Finally, we performed a correlation test of the horizontal and vertical institutional settings identified, and evaluated them against the countries' political-administrative structure. The method used to assess the relationship between the various dimensions was the Principal Components Analysis (PCA), a data reduction technique that allows to identify patterns in data, and express them in a way to highlight their similarities and differences.

As a preliminary step to the PCA, a number of criteria were selected to cover the main dimensions of the investigation [Tab.2]. The number of existing institutions, their degree of formalization and novelty, the timing and the focus of institutional action with respect to the NAS, the mode of institutional coordination and the "transversality" of the challenge addressed by the institutions, were considered proxies of the overall institutional capacity for adaptation. The national political-administrative structure represented the political dimension. Each criterion was further specified with classes. Finally, these criteria were applied to the identified catalogue of institutional settings in order to obtain a standardized matrix of basic data [Tab.3].

Subsequently we interpreted the initial matrix of data to obtain single values for each of the selected countries in a secondary matrix [Tab.4]. To do so, we assigned a score to the classes, without implying any value judgment. Since we considered the entire set of institutions found in each country as a single data, we needed to create a new progressive set of classes to grasp the meaning of the aggregated information. The values for each criteria input in the secondary matrix were thus scores associated to the whole of the institutions per country, and only these were used to run the PCA software.

### 3. RESULTS AND DISCUSSION

#### ***Is there a common approach for defining a NAS across European countries?***

Looking at the overview of NASs across European states [Tab.5], two main ways of intending an adaptation strategy in terms of its content stand out: 1) an adaptation-focused approach, and 2) a broader climate change approach. While the first is followed by the majority of countries that have developed or are in the process of developing their adaptation policy, others (Bulgaria, Hungary, Lithuania, Greece, Czech Republic, Iceland, Liechtenstein, Sweden, Turkey) rely on a framework that includes the predominant consideration of mitigation issues. The UK government is a special case since a broad climate change act was the legal basis for an adaptation-focused implementation plan, complemented by devolved countries' adaptation strategies and plan.

Fourteen NASs are acknowledged in this analysis: Lithuania and Sweden, despite being listed as having a NAS on Climate-ADAPT, are left out since they do not fulfill the criteria proposed above related to the form and content of a NAS. The selected NASs are thus the ones that focus only or substantially (e.g. Hungary) on adaptation.

Within the set of analysed NASs, a number of differences can be found about the content, but the shortcomings are quite similar. Most NASs do not include explicit prioritization of options based on cost-benefit analyses for all fields of action, nor specific implementation provisions. The issues of monitoring adaptation action, reporting on the progress and reviewing the strategy are tackled through institutional settings in few countries, particularly those with a climate change strategy. It can be noted that where a climate change act is in place, either serving as the NAS or complementing it (e.g. Hungary, UK, and Switzerland) those arrangements are institutionalized and of mandatory nature as opposed to *ad hoc* and voluntary (Finland).

With regard to the form of a NAS, all countries refer to it as a single policy document or legal act that sets strategic priorities, separated from an eventual action or sectoral plan of implementation that is, in few cases, mandated by the NAS (e.g. UK). As such, NASs do not necessarily imply the completion of the recommended adaptation policy process as described in the Commission guidance [6].

Such inconsistency of definitions is likely to have implications on the future national and European policy in the context of the 2013 EU Adaptation Strategy. In fact, coverage and quality of NASs will be assessed by the Commission through key indicators and a scoreboard. If countries' achievements in adapting to climate change will be judged unsatisfactory, a legally binding instrument could be put forward and create obligations on adaptation for Member Countries [5].

***Can the characteristics of adaptation governance be statistically associated to the countries' political-administrative system?***

A convergent thinking towards the possibility that adaptation policy responses to climate change are affected by political-administrative structures has emerged among scholars, although it is based on general evidence [22] [4].

Dumollard and Leseur [4] noted that the role of regional and local governments has been emphasized especially in decentralized systems at the stage of drawing up and/or implementing adaptation policies, in some European countries. A study on OECD members by Mullan et al. [22] provides examples on the likely overall influence of the political systems on the scope and characteristics of national adaptation planning.

Bauer et al. [1] confirm this idea through a qualitative analysis of governance challenges, stating that especially the characteristics of vertical coordination of adaptation depend on national systems, as federal countries appear to involve regional and local governmental tiers more than unitary countries particularly in the early phases of developing a NAS.

We can preliminarily support this theory looking at our overview of the NASs and the countries' respective political-administrative systems [Fig.1]. An immediate association between the tendency towards federalism and the promptness of the countries in adopting a NAS comes out. All the federal and administrative-federal countries in Europe have been more pro-active in adaptation planning compared to the centralized states. Only three unitary countries out of eighteen (Hungary, Ireland and Malta) have adopted a NAS. This diversity in the pace of policy planning may be due to the ferment on adaptation at the local levels that has been the driver for national policies in some federal countries (e.g. in Switzerland). Also, pre-existing

regional partnerships and networks of cities largely contributed to the adaptation landscape (e.g. in Germany and Spain). However, other reasons besides the political structure may better explain this dynamic.

Through our study we wanted to *quantitatively* verify if the organization of powers determines the institutional process followed to outline and implement the adaptation policy.

From the results of the statistical analysis performed it can be confirmed that there is a correlation between the political dimension and the institutional capacity of NASs. Such correlation exists between the political system variable and all the seven criteria concerning the institutional settings, although it is valid to different degrees [Fig.2-3]. A particularly robust correlation can be seen between the political dimension and the novelty of institutions for adaptation.

### ***What are the main differences and similarities in institutional settings of NASs between federal and unitary states?***

According to the results of the PCA, countries do not follow an univocal pattern of adaptation governance according to their political-administrative systems, although separate trends can be noticed for federal and unitary states [Fig. 3].

The identified correlations between the political dimension and the institutional capacity are interpreted as follows :

- Novelty: while all unitary and administrative-federal countries tend to establish new institutions within a NAS, federal countries tend to use pre-existing institutions, perhaps already in place to meet the needs and give voice to lower governmental tiers and existing “provinces” (*high confidence*).
- Number of institutions: federal and administrative-federal countries tend to involve a higher amount of institutions to deal with the NAS while unitary countries tend to have less (*medium confidence*). These additional institutions are often public consultation processes and boards of regional/local representatives that are necessary to integrate adaptation across governance scales and thus may serve the purposes of vertical integration jointly with cross-sectoral coordination.

- Timing of action: federal countries seem to engage the institutions since the earlier phases of the NAS covering the whole process from the development to the implementation, while unitary countries mostly wait for later stages to set up appropriate institutional mechanisms (*medium confidence*). Generally speaking, pre-NAS institutions or ad hoc processes may disappear once they have fulfilled their task (e.g. preliminary consultation, drafting) while post-NAS arrangements are longer-term provisions (e.g. monitoring and review, committees for implementation).
- Coordination mode: federal states tend to have mandatory requirements for their institutional arrangements based on NAS and climate laws, while unitary states can have more voluntary modes (*low confidence*). More mandatory-like coordination modes (e.g. monitoring and review schemes) are likely to appear only once the NAS is adopted with the aim of enforcing its provisions.
- Formalization: federal countries tend to assign a high degree of institutionalization to the arrangements for the NAS compared to unitary countries. However, also administrative-federal unitary countries do although to a slightly lesser proportion (*low confidence*). There is indeed a general tendency of all governments to have more permanent institutions as opposed to temporary processes.
- Transversality: federal countries tend to have more integration between horizontal and vertical challenges in their institutional settings when compared to unitary states, but the administrative-federal countries are the ones that promote more the transversality (*low confidence*). There is an overall trend to address the two adaptation challenges jointly. Having already existing institutions in place that are suitable, federal countries may tend to optimize by integrating the challenges there, while in unitary countries new institutions are mostly created to respond to single challenges.
- Scope of action: federal and unitary countries do not seem to have a preference for institutions with focus on adaptation or those with focus on climate change (*low confidence*). There is an overall (expected) tendency towards adaptation-focused institutions.

In the course of the statistical test, four clusters of countries emerged as they share certain similarities in their institutional capacity for adaptation [Fig.4]:

- 1) France and Portugal (all);
- 2) Denmark and Finland (novelty, timing of action, scope of action, transversality);
- 3) UK, Netherlands and Germany (nr. of institutions, formalization, novelty);
- 4) Spain and Belgium (formalization, novelty, timing of action, transversality).

#### **4. CONCLUSIONS**

The data collected from literature and country reporting on NASs were elaborated and originally employed in this paper to run a factor analysis aimed at identifying the correlation among the political dimension and the institutional capacity of the selected countries. To our knowledge, the PCA method was used for the first time in the research domain of adaptation by the present paper.

A number of scientific uncertainties around the method applied must be acknowledged. The major uncertainty is associated with the basic data. To overcome this issue, the data were validated by NAS focal points who provided clarification and determined the final data matrix. Nevertheless, this validation was based on the individual scrutiny and remained at least partly subjective. Furthermore, the narrow countries sample could have been a bias to the PCA. The analysis produced conclusions that naturally needed further interpretation to ensure coherence with single cases.

As per initial hypothesis, we acknowledged that the pattern of response of any nation to climate change will be conditioned by the configuration of political-administrative systems. This study presented empirical evidence of the promptness of federal countries in adopting a NAS as opposed to a late reaction by the majority of unitary countries. Furthermore, through the PCA, some significant statistical correlation confirmed the link between the political dimension and the institutional capacity.

However, we can reasonably state that political systems only explain a limited part of the countries' choices in terms of adaptation governance settings, and other external or internal variables may have a stronger influence. The financial and economic circumstances, different political conditions (how strategies are perceived within different governments and the role with respect to other environmental / development issues), cultural values (inclination towards long-term or short-term planning), as well

as societal expectations (increased awareness due to the existence of similar strategies in neighboring countries and the push from the EU) are all drivers that need to be considered in future analyses.

While the transferability of knowledge and good practices across regions and countries is deemed essential to achieve progress on adaptation in Europe, the context-dependency of adaptation may affect the value of transferability.

In fact, one “best practice” of adaptation governance to follow cannot be identified in principle, and in practice the aim of this paper is not to provide a ranking of the institutional performances of countries based on their political-administrative system. Instead, the outcomes of this research suggest that lessons on adaptation planning should be continuously exchanged between countries that are closer in terms of governance, such as the four clusters identified in the analysis. These governments, that are now putting their NAS into operation with diverse speed and modalities, are encouraged to establish cooperation, dialogue and exchange of good practices on the aspects that have determined the success (or failure) of the institutional settings involved in the NAS implementation, in order for others at earlier stages of implementation to adjust the future phases of the process as necessary. Countries that are still developing their NAS, as Italy and all the remaining European unitary states, should first of all establish cooperation with countries belonging to the same “climate change regions” [11] to learn how to face similar and transnational expected climate change impacts through their future NAS. Finally, these countries are advised to further deepen the knowledge of the role that their national administrative and socio-economic systems can play in the development and implementation of adaptation strategies, so to address potential barriers.

## **5. ACKNOWLEDGMENTS**

This work has benefited from the support of the EU FP7 ERA-Net Project CIRCLE-2 - *Climate Impact Research & Response Coordination for a Larger Europe*. The authors took great advantage of the participation to the research activities carried out within CIRCLE-2 involving national focal points for adaptation of 23 pan-European countries and representatives of EU institutions.

The authors would like to gratefully acknowledge the support of Dr. Rob Swart (Wageningen UR) and Roger Street (UKCIP) who helped to fine-tune the research.

## 6. REFERENCES

1. Bauer, A., Feichtinger, J., & Steurer, R. (2012), *The Governance of Climate Change Adaptation in 10 OECD Countries: Challenges and Approaches*, Journal of Environmental Policy & Planning, 14(3), 279-304.
2. Biesbroek, G.R., Swart, R.J., Carter, T., Cowan, C., Henrichs, T., Mela, H., Morecroft, M.D., & Rey, D. (2010), *Europe adapts to climate change: Comparing National Adaptation Strategies*, Global Environmental Change, 20, 440–450.
3. BMVBS (German Federal Ministry of Transport, Building and Urban Development) (2010), *National strategies of European countries for climate change adaptation: A review from a spatial planning and territorial development perspective*, BMVBS-Online-Publikation, No. 21/2010.
4. Dumollard, G., & Leseur, A. (2011), *Drawing up a national climate change adaptation policy: Feedback from five European case studies*, Climate Report No. 27.
5. EC (European Commission) (2013), *An EU Strategy on adaptation to climate change*, Communication from the Commission to the European Parliament, the Council, the European Economic and Social Committee and the Committee of Regions.
6. EC (European Commission) (2013a), *Guidelines on developing adaptation strategies*, Commission Staff Working Document Accompanying the Communication *An EU Strategy on adaptation to climate change*.
7. EEA (European Environment Agency) (2013), *Adaptation in Europe: Addressing risks and opportunities from climate change in the context of socio-economic developments*, Report no. 3/2013.
8. EUROSAI-Working Group on Environmental Auditing (EUROSAI-WGEA) (2012), *Adaptation to climate change – are governments prepared? A cooperative Audit*, Joint Report.

9. Ford, J.D., Berrang-Ford, L. & Paterson, J. (2011), *A systematic review of observed climate change adaptation in developed nations*, *Climatic Change*, 106, 327–336.
10. Gagnon-Lebrun, F. & Agrawala, S. (2006), *Progress on adaptation to climate change in developed countries: An analysis of broad trends*, OECD Report ENV/EPOC/GSP(2006)1/FINAL, Paris: OECD.
11. Greiving, S., et al. (2011), *Climate change and territorial effects on regions and local economies*, Main Report - Final project report version 31/5/2011, Dortmund: ESPON & IRPUD, TU.
12. Gupta, J., Termeer, C., Klostermann, J., Meijerink, S., Van den Brink, M., Jong, P., Nootboom, S. & Bergsma, E. (2010), *The Adaptive Capacity Wheel: a method to assess the inherent characteristics of institutions to enable the adaptive capacity of society*, *Environmental Science & Policy*, 13, 459-471.
13. Inman, R.P. (2007), *Federalism's Values and the Value of Federalism*, *CESifo Economic Studies*, 53(4), 522–560.
14. IPCC (Intergovernmental Panel on Climate Change) (2007). Parry, M.L., Canziani, O.F., Palutikof, J.P., van der Linden, P.J. & Hanson, C.E. (Eds.), *Climate Change 2007: Impacts, Adaptation and Vulnerability. Contribution of Working Group II to the Fourth Assessment Report of the Intergovernmental Panel on Climate Change*, Cambridge: Cambridge University Press, 976pp.
15. Jordan, A. & O'Riordan, T. (1997), *Social Institutions and Climate Change: Applying Cultural Theory to Practice*, CSERGE Working Paper GEC 97- 15.
16. Juhola, S., Keskitalo, E.C.H. & Westerhoff, L. (2011), *Understanding the framings of climate change adaptation across multiple scales of governance in Europe*, *Environmental Politics*, 20(4), 445-463.
17. Keskitalo, E.C.H. (Eds.) (2010), *Developing adaptation policy and practice in Europe: Multi-level governance of climate change*, Berlin: Springer.
18. Massey, E. (2009). *Adaptation policy and procedures in Central & Eastern Europe*, Report nr. R-09/012, Netherlands Environmental Assessment Agency.

19. Massey, E., & Bergsma, E. (2008). *Assessing adaptation in 29 European countries*, Report W-08/20, Institute for Environmental Studies, Vrije Universiteit, Amsterdam.
20. Meadowcroft, J. (2009), *Climate change governance*, Policy Research Working Paper 4941, A paper contributing to the 2010 World Bank World Development Report.
21. Mickwitz P., Aix, F., Beck, S., Carss, D., Ferrand, N., Görg, C., Jensen, A., Kivimaa, P., Kuhlicke, C., Kuindersma, W., Máñez, M., Melanen, M., Monni, S., Pedersen, A., Reinert, H. & van Bommel, S. (2009), *Climate Policy Integration, Coherence and Governance*, PEER-Report No 2, Helsinki: Partnership for European Environmental Research.
22. Mullan, M., Kingsmill, N., Matus Kramer, A. & Agrawala, S. (2013), *National Adaptation Planning: Lessons from OECD Countries*, OECD Environment Working Papers, No. 54, OECD Publishing.
23. Paavola, J. (2008), *Science and social justice in the governance of adaptation to climate change*, *Environmental Politics*, 17(4), 644 – 659.
24. Pfenninger, S., Hanger, S., Dreyfus, M., Dubel, A., Hernandez-Mora, N., Esteve, Pl., Varlea-Ortega, C., Watkiss, P. & Patt, A. (2010, submitted to the European Commission), *Report on perceived policy needs and decision contexts*, Final draft Report, Mediation Deliverable D1.1, MEDIATION Seventh Framework Project (Methodology for Effective Decision-making on Impacts and Adaptation).
25. Perkins, B., Ojima, D. & R. Corell (2007), *A survey of climate change adaptation planning*, The H. John Heinz III Center for science, economics and the environment, Washington.
26. Preston, B., Westaway, R., & Yuen E. (2011), *Climate adaptation planning in practice: an evaluation of adaptation plans from three developed nations.*, *Mitigation and Adaptation Strategies for Global Change*, 16, 407–438.
27. Prutsch, A., McCallum, S., Leitner, M., Lexer, W., Offenthaler, I., Hildén, M., Mäkinen, K., Weiland, S., Beck, S., Castellari, S., Swart, R., Conix, I., Biesbroek, R., Capela Lourenço, T., Alves, F., Havranek, M., Street, R.B.,

- Downing, C., Ramieri, E., Iglesias, A. & Isoard, S. (2013), *Contributions to EEA assessment reports: Assessment of national adaptation policy process in 32 EEA Member. Final Work Plan*, ETC/CCA Study.
28. Schipper, E.L.F. & Burton, I. (Eds.) (2008), *The Earthscan Reader on Adaptation to Climate Change*, Earthscan Reader Series, London: Earthscan.
29. Swart, R., Biesbroek, R., Binnerup, S., Carter, T.R., Cowan, C., Henrichs, T., Loquen, S., Mela, H., Morecroft, M., Reese M. & D. Rey (2009), *Europe Adapts to Climate Change: Comparing National Adaptation Strategies* (PEER Report No 1), Helsinki: Partnership for European Environmental Research.
30. Termeer, C.J.A.M., Biesbroek, G. R. & van den Brink M.A. (2009), *Institutions for adaptation to climate change: Comparing national adaptation strategies in Europe*. Presented at ECPR APSA Panel for Toronto 2009 (September 3-6) on “Energy Policy and Global Warming: American and European Approaches”.

## 7. IMAGES AND TABLES

EEA Member Country (year of NAS adoption)	Type of political system	Nr. of independent constituents*	Political representation of constituents in central government	Allocation of overall responsibility to lower-tier governments or federal states	Adaptation policy developed in sub-national constituents
Austria (2012)	Federal	9	Yes	++++	
Belgium (2010)	Federal	3	Yes	++	√
Denmark (2008)	Adm. federal	-	No	++++	
Finland (2005)	Adm. federal	-	No	++++	
France (2007)	Adm. federal	-	No	+++	
Germany (2008)	Federal	16	Yes	++++	√
Hungary (2008)	Unitary	-	No	n.a.	
Ireland (2012)	Unitary	-	No	++	
Malta (2012)	Unitary	-	No	n.a.	
Netherlands (2007)	Adm. federal	12	No	+++	
Portugal (2010)	Adm. federal	2	No	++	√
Spain (2006)	Federal	17	Yes	++	√
Switzerland* (2012)	Federal	26	Yes	++++	√
United Kingdom (2008)	Adm. federal	4	No	++	√

\*Note / Special autonomous territories that politically are not part of the EU (overseas territories of France and the Netherlands, and Greenland for Denmark), or small independent islands (Åland Islands in Finland, Faroe Islands in Denmark) are not reported in the analysis as independent provinces

Tab. 1 Classification of countries with a NAS by political-administrative systems

(Source: based on Inman, 2007)

<b>Dimensions</b>	<b>Criteria</b>	<b>Description</b>	<b>Classes for single institutions analysis</b>	<b>Classes and scores for aggregated institutions analysis (per country)</b>
Institutional capacity	<b>Number of institutions</b>	The amount of existing specific institutions, mechanisms, procedures that address horizontal/vertical challenges in the framework of a NAS	---	<i>Actual number of institutions = x</i>
	<b>Formalization</b>	The degree of formalization of the institutional settings within a NAS	<i>Temporary Institutionalized</i>	<i>Mostly temporary = 1 An equal combination = 2 Mostly institutionalized = 3</i>
	<b>Novelty</b>	The degree of novelty of institutions according to the time of their establishment with respect to the development of the NAS	<i>Pre-existing New</i>	<i>Mostly pre-existing = 1 An equal combination = 2 Mostly new = 3</i>
	<b>Timing of action</b>	The time when the institutions initiated their action with respect to the various phases of a NAS, either pre- (ad hoc for developing the NAS) or post-NAS (for NAS implementation)	<i>Pre-NAS Whole process Post-NAS</i>	<i>Mostly Pre-NAS = 1 During the whole process / all phases covered = 2 Whole process and Post-NAS = 3 Mostly Post-NAS = 4</i>
	<b>Scope of action</b>	The main scope of the institutional action within a NAS	<i>Sectoral policy Adaptation Climate change Broader policy</i>	<i>Sectoral policy = 1 Adaptation only = 2 Equal mix of adaptation and climate change = 3 Climate change = 4 Broader policy fields = 5</i>
	<b>Coordination mode</b>	The modality of institutional coordination, from voluntary-networking-negotiation modes (e.g. informal workshops, fora, committees) to mandatory requirements (e.g. binding reporting schemes, establishment of committees mandated by law) within a NAS	<i>Voluntary Mandatory</i>	<i>Voluntary = 1 Mostly voluntary (with some mandatory) = 2 Mostly or completely mandatory = 3</i>
	<b>Transversality</b>	The overall level of integration or separation of horizontal and vertical governance challenges addressed by the institutions within a NAS	<i>Horizontal Vertical Horizontal+Vertical</i>	<i>Mostly separated = 1 Partially integrated, equal combination = 2 Mostly Integrated = 3</i>
Political dimension	<b>National structure</b>	The type of political-administrative system characterizing the country	---	<i>Unitary = 1 Administrative-federal = 2 Federal = 3</i>

Tab. 2 Framework for the analysis of institutions

Country with NAS	Institutions	Transversality	Formalization	Novelty	Timing of action	Scope of action	Coordination mode
	Special coordination bodies, mechanisms, processes within the NAS	Horizontal/ Vertical/ H+V	Temporary/ Institutionalized	Pre-existing/ New	Pre-NAS/ Whole process/ Post-NAS	Sectoral policy/ Adaptation / Climate Change / Broader policies	Voluntary/ Mandatory
<b>Austria</b>	Series of informal workshops	H+V	Temporary	New	Pre-NAS	Adaptation	Voluntary
	Consultation process (workshops with public adm. and non-gov actors)	H+V	Temporary	New	Pre-NAS	Adaptation	Voluntary
	Austrian Kyoto Forum	H+V	Institutionalized	Pre-existing	Pre-NAS	Climate change	Voluntary
	Inter-ministerial committee on climate change (IMC Climate)	H+V	Institutionalized	Pre-existing	Whole process	Climate change	Voluntary
<b>Belgium</b>	National Climate Commission (NCC)	H+V	Institutionalized	Pre-existing	Whole process	Climate change	Mandatory
	WG on Adaptation (CABAO)	H+V	Institutionalized	Pre-existing	Whole process	Adaptation	Mandatory
<b>Denmark</b>	Task Force on Climate Change Adaptation	H+V	Institutionalized	New	Whole process	Adaptation	Voluntary
<b>Finland</b>	Series of seminars during NAS development	H+V	Temporary	New	Pre-NAS	Adaptation	Voluntary
	Finnish Coordination Group for Adaptation to Climate Change	H+V	Institutionalized	New	Whole process	Adaptation	Voluntary
	Monitoring and review of the NAS	H	Temporary	New	Post-NAS	Adaptation	Voluntary
<b>France</b>	Consultation process based on Grenelle Environment Forum structure	H+V	Temporary	New	Post-NAS	Adaptation	Voluntary
	Grenelle Environment Forum (moved into the National committee for ecologic transition)	H+V	Institutionalized	New	Post-NAS	Broader policies	Mandatory
	General directorate for energy and climate within ONERC	H+V	Institutionalized	Pre-existing	Post-NAS	Broader policies	Mandatory

Country with NAS	Institutions	Transversality	Formalization	Novelty	Timing of action	Scope of action	Coordination mode
<b>Germany</b>	Preliminary Inter-ministerial WG	H	Temporary	New	Pre-NAS	Adaptation	Voluntary
	Inter-ministerial WG on adaptation	H	Institutionalized	New	Post-NAS	Adaptation	Mandatory
	Consultation procedures in specific sectors	V+H	Temporary	New	Whole process	Adaptation	Voluntary
	Standing commission on adaptation of the federal conference of the environment ministers (AFK)	V+H	Institutionalized	New	Post-NAS	Adaptation	Mandatory
	“Bund-Länder” Committee on Climate Impacts	V	Institutionalized	Pre-existing	Whole process	Adaptation	Voluntary
<b>Hungary</b>	Climate Change Commission	H	Institutionalized	Pre-existing	Post-NAS	Climate change	Voluntary
	Hungarian WG on Climate Change	H	Institutionalized	New	Post-NAS	Climate change	Voluntary
	Review of the NAS under climate change law	H+V	Institutionalized	New	Post-NAS	Climate change	Mandatory
<b>Ireland</b>	Institutional arrangements proposed under the Climate Action and Low carbon development Bill 2013	H+V	Institutionalized	New	Post-NAS	Climate change	Mandatory
<b>Malta</b>	Climate Change Committee for Adaptation (CCCA)	H	Institutionalized	New	Pre-NAS	Adaptation	Voluntary
	Public consultation process	V	Temporary	New	Pre-NAS	Adaptation	Voluntary
<b>Netherlands</b>	Steering committee and programme team of the National Programme for Spatial Adaptation to Climate Change (ARK)	H+V	Temporary	New	Pre-NAS	Adaptation	Voluntary
	Delta Commissioner	H+V	Institutionalized	New	Post-NAS	Sectoral policy	Mandatory
	Ministerial Steering group of the Deltaprogramme	H	Institutionalized	New	Post-NAS	Sectoral policy	Voluntary
	Steering committees of area-based Delta sub-programmes	V+H	Institutionalized	New	Post-NAS	Sectoral policy	Voluntary
	Ministerial drafting group of the 2013 Climate Roadmap	H	Temporary	New	Pre-NAS	Climate change	Voluntary

Country with NAS	Institutions	Transversality	Formalization	Novelty	Timing of action	Scope of action	Coordination mode
<b>Portugal</b>	Adaptation and Monitoring division within Portuguese Environment Agency (APA) Climate Department (following integration of Climate Change Commission into APA)	H	Institutionalized	New	Post-NAS	Climate change	Mandatory
	Inter-ministerial Coordination Group for the NAS	H+V	Institutionalized	New	Post-NAS	Adaptation	Mandatory
	2 Regional WGs for the autonomous regions	H+V	Institutionalized	New	Post-NAS	Climate change	Mandatory
<b>Spain</b>	Inter-ministerial Commission on Climate Change	H	Institutionalized	Pre-existing	Whole process	Climate change	Voluntary
	Spanish Coordination Commission of Climate Change Policies (CCPCC)	H+V	Institutionalized	Pre-existing	Whole process	Climate change	Mandatory
	CCPCC WG on Impacts and Adaptation	H+V	Institutionalized	New	Whole process	Adaptation	Mandatory
	National Climate Council	H+V	Institutionalized	Pre-existing	Whole process	Climate change	Voluntary
	Public consultation process	H+V	Temporary	New	Pre-NAS	Adaptation	Voluntary
<b>Switzerland</b>	Interdepartmental Committee on Climate (IDA Climate)	H	Institutionalized	Pre-existing	Whole process	Climate change	Mandatory
	IDA Climate WG 2 on adaptation	H	Institutionalized	Pre-existing	Whole process	Adaptation	Mandatory
	Monitoring	H	Institutionalized	New	Post-NAS	Adaptation	Voluntary
	Reporting scheme under CO2 Act	H+V	Institutionalized	New	Post-NAS	Adaptation	Mandatory
<b>United Kingdom</b>	Cross-UK Government Climate Adaptation Board	H	Institutionalized	New	Whole process	Adaptation	Voluntary
	Consultation on framework	V	Temporary	New	Pre-NAS	Adaptation	Voluntary
	Local Adaptation Advisory Panel (LAAP) (since 2011, used to be Local and Regional Adaptation Partnership Board)	V	Institutionalized	New	Whole process	Adaptation	Voluntary
	Climate UK network of Regional Climate Change Partnerships	V	Temporary	New	Post-NAS	Climate change	Voluntary
	Adaptation Reporting Power under the Climate Change Act 2008	H	Institutionalized	New	Post-NAS	Adaptation	Mandatory
	Monitoring and reporting scheme (Indicator "NI 188")	V	Institutionalized	New	Post-NAS	Adaptation	Mandatory
	Review of the nat. adaptation programme	H+V	Institutionalized	New	Post-NAS	Adaptation	Mandatory

Tab. 3 Institutional settings addressing horizontal and vertical coordination of adaptation within European NASs

Country with NAS	Nr. institutions	Formalization	Novelty	Timing of action	Scope of action	Coordination mode	Transversality	Political system
<b>Austria</b>	4	Equal combination	Equal combination	Pre-NAS	Adaptation + Climate Change (equal mix)	Voluntary	Integration	Federal
<b>Belgium</b>	2	Institutionalized	Pre-existing	Whole process (single institutions)	Adaptation + Climate Change (equal mix)	Mandatory	Integration	Federal
<b>Denmark</b>	1	Institutionalized	New	Whole process (single institutions)	Adaptation	Voluntary	Integration	Adm-Fed
<b>Finland</b>	3	Temporary	New	All phases covered (different institutions)	Adaptation	Mostly voluntary	Integration	Adm-Fed
<b>France</b>	3	Institutionalized	New	Post-NAS	Broader policies	Mandatory	Integration	Adm-Fed
<b>Germany</b>	5	Institutionalized	New	All phases covered (different institutions)	Adaptation	Mostly voluntary	Separation	Federal
<b>Hungary</b>	3	Institutionalized	New	Post-NAS	Climate change	Mostly voluntary	Separation	Unitary
<b>Ireland</b>	1	Institutionalized	New	Post-NAS	Climate Change	Mandatory	Integration	Unitary
<b>Malta</b>	2	Equal combination	New	Pre-NAS	Adaptation	Voluntary	Separation	Unitary
<b>Netherlands</b>	5	Institutionalized	New	Post-NAS	Sectoral policy	Mostly voluntary	Integration	Adm-Fed
<b>Portugal</b>	3	Institutionalized	New	Post-NAS	Climate change	Mandatory	Integration	Adm-Fed
<b>Spain</b>	5	Institutionalized	Pre-existing	Whole process (single institutions)	Climate change	Mostly voluntary	Integration	Federal
<b>Switzerland</b>	4	Institutionalized	Equal combination	Whole process and post-NAS	Adaptation	Mostly mandatory	Separation	Federal
<b>UK</b>	7	Institutionalized	New	Post-NAS	Adaptation	Mostly voluntary	Separation	Adm-Fed

Tab. 4 Secondary matrix with aggregated data used in the PCA

EEA Member Country	NAS reported in Climate-ADAPT	Year	Title of NAS or climate change strategy	Language (English if available)	Adopted by the government (Form-wise)	Adaptation-focused (Content-wise)	NAS according to defined analysis criteria
Austria	√	2012	<a href="#">Austrian Strategy for Adaptation to Climate Change</a>	EN	√	√	√
Belgium	√	2010	<a href="#">Belgian national climate change adaptation strategy</a>	EN	√	√	√
Bulgaria		2012	<a href="#">Third National Action Plan on Climate Change 2013-2020</a>	EN	√	Plan focuses on mitigation	No
Czech Republic		2004	<a href="#">National Programme To Abate the Climate Change Impacts in the Czech Republic</a>	EN	√	Programme focuses on mitigation	No
Cyprus							
Denmark	√	2008	<a href="#">Danish Strategy for adaptation to a changing climate</a>	EN	√	√	√
Estonia							
Finland	√	2005	<a href="#">National Adaptation Strategy</a>	EN	√	√	√
France	√	2007	<a href="#">National strategy for adaptation to climate change**</a>	FR	√	√	√
Germany	√	2008	<a href="#">German Strategy for Adaptation to Climate Change</a>	EN	√	√	√
Greece		2003	<a href="#">National Action Plan regarding Climate Change**</a>	GR	√	Plan focuses on mitigation	No
Hungary	√	2008	<a href="#">National Climate Change Strategy 2008-2025</a>	EN	√	Strategy is on both adaptation and mitigation – Comprehensive adaptation section	√

Iceland*		2007	<a href="#">Iceland's Climate Change Strategy</a>	EN	√	Strategy focuses on mitigation	No
Ireland	√	2012	<a href="#">National Climate Change Adaptation Framework</a>	EN	√	√	√
Italy							
Latvia							
Liechtenstein*		2007	<a href="#">National Climate Change Strategy for the Liechtenstein Principality</a>	DE	√	Strategy focuses on mitigation	No
Lithuania	√	2012	<a href="#">Lithuanian climate change management policy and its implementation</a>	LT EN summary	√	Strategy focuses on mitigation	No
Luxembourg							
Malta	√	2012	<a href="#">National Climate Change Adaptation Strategy</a>	EN	√	√	√
Netherlands	√	2007	<a href="#">Make room for Climate</a>	EN	√	√	√
Norway*		2008	<a href="#">Adaptation in Norway The government's efforts to adapt to climate change**</a>	NO	√	Workprogramme on adaptation – not a comprehensive strategy	No
Poland		2013	<a href="#">Strategic Plan for Adaptation to sectors and areas vulnerable to climate change by 2020, with a view to 2030**</a>	PL	Strategy document NOT yet adopted	√	No
Portugal	√	2010	<a href="#">National strategy for adaptation to climate change**</a>	PT		√	√
Romania		2011	<a href="#">Adaptation component of the National Climate Change Strategy (2012-2020)**</a>	RO	Strategy document NOT yet adopted	Strategy is on both adaptation and mitigation – comprehensive adaptation section	No
Slovakia							

Slovenia		2011	<a href="#">(Draft) National Climate Strategy – Strategy for the transition of Slovenia to a low carbon society by 2050</a>	SI EN summary	Strategy document NOT yet adopted	Strategy focuses on mitigation	No
		2008	National adaptation strategy for forestry and agriculture	SI	√	Sectoral strategy - not comprehensive	No
Spain	√	2006	<a href="#">National plan for adaptation to climate change**</a>	SP	√	√	√
Sweden	√	2009	<a href="#">Bill: An Integrated Climate and Energy Policy</a>	SE	√	Bill focuses on mitigation - country opted for integrated and coordinated cooperation for adaptation	No
				EN summary			
Switzerland*	√	2012	<a href="#">Adaptation to Climate Change in Switzerland</a>	EN	√	√	√
Turkey*		2010	<a href="#">National Climate Change Strategy 2010-2020</a>	EN	√	Strategy focuses on mitigation	No
		2010	<a href="#">Turkey's National Climate Change Adaptation Strategy and Action Plan (Draft)</a>	EN	Strategy document NOT yet adopted	√	No
United Kingdom	√	2008	<a href="#">Climate Change Act</a>	EN	√	√	√

Tab. 5 List of national strategies relevant for climate change adaptation as reported in Climate-ADAPT against the proposed definition of NAS

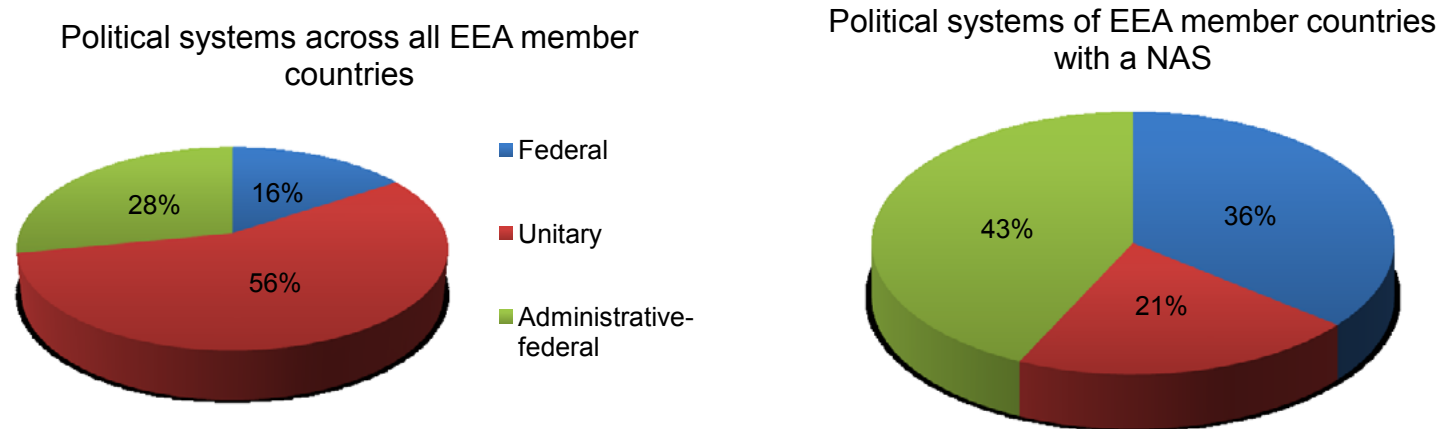


Fig. 1 Representation of different political systems across 32 EEA member countries (on the left), and across those that have adopted a national adaptation strategy (on the right)

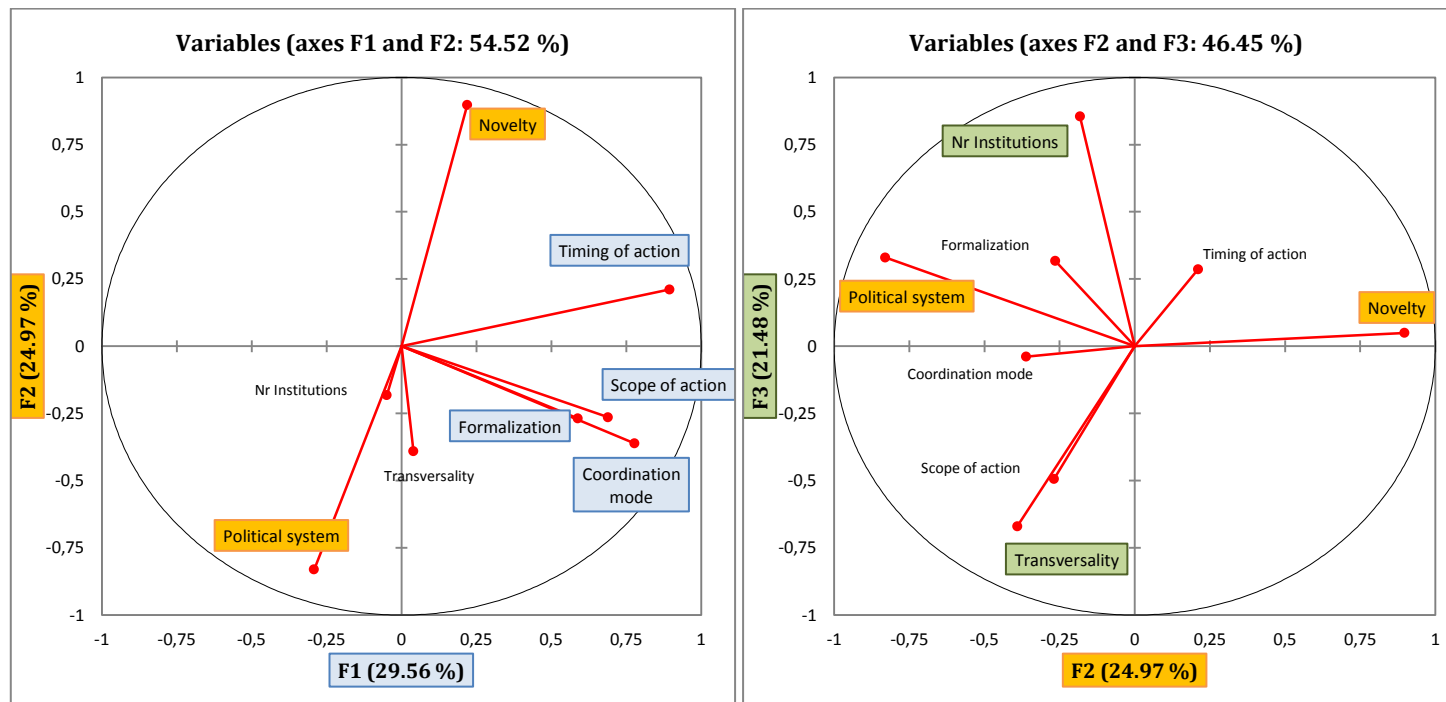


Fig. 2 Correlation between variables and factors: biplot of F1&F2 (on the left) and F2&F3 (on the right) explaining 76% of the data variability. When analysing, special attention should be given to the variables more related to each factor, signalled in each graphic with a correspondent box colour (e.g. F2 axis and the related variables “Political system” and “Novelty” are highlighted in orange). Vectors in the same quadrant and with the same length are highly positively correlated (e.g. “Formalization”, “Scope of action” and “Coordination mode”). Vectors in opposite quadrants are highly negatively correlated (e.g. “Political system” and “Novelty”)

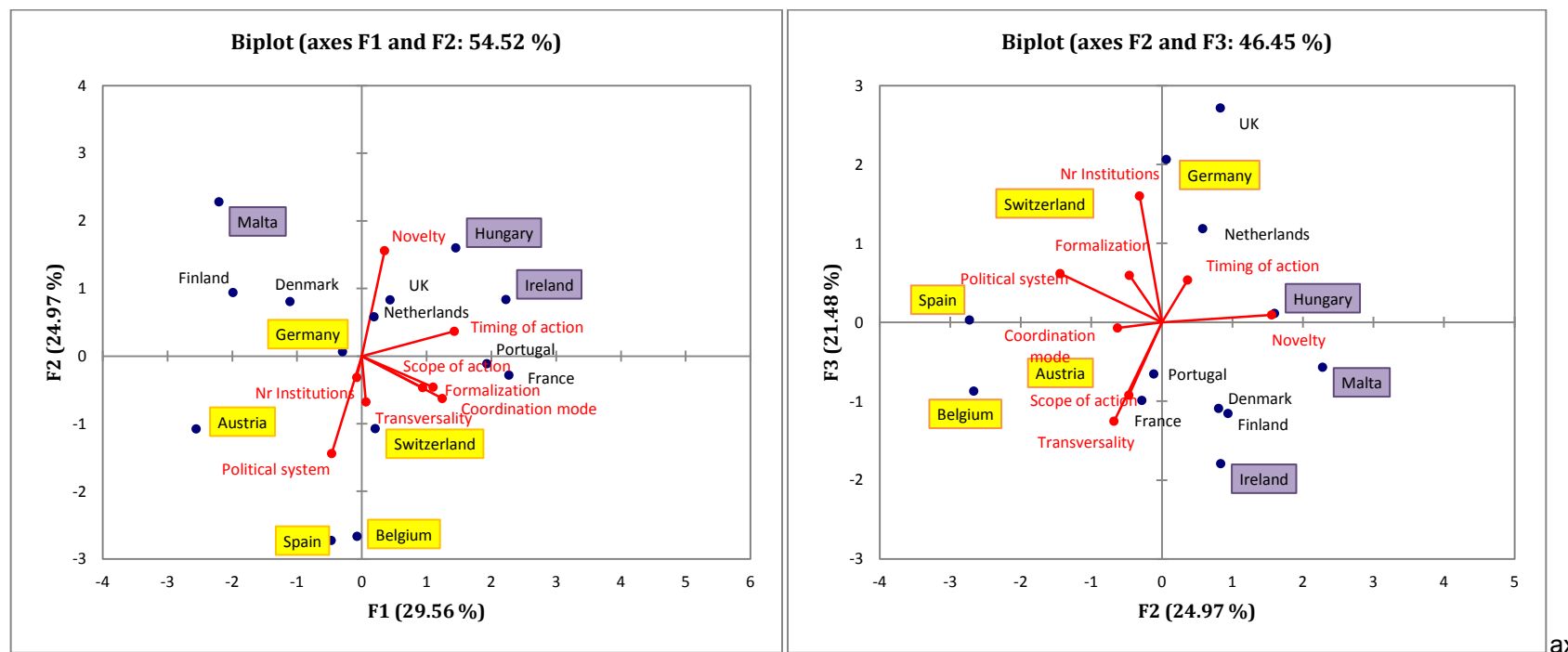


Fig. 3 Correlation among variables, country scores and factors: biplot of F1&F2 (upper box) and F2&F3 (lower box) explaining 76% of the data variability. In purple the unitary countries and in yellow the federal countries. Countries in the same variable quadrant are highly positively correlated with the characteristic (e.g. Hungary with “Novelty”: the country mostly uses new institutions), while in opposite quadrants are highly negatively correlated (e.g. Spain with “Novelty”: the country mostly uses pre-existing institutions)

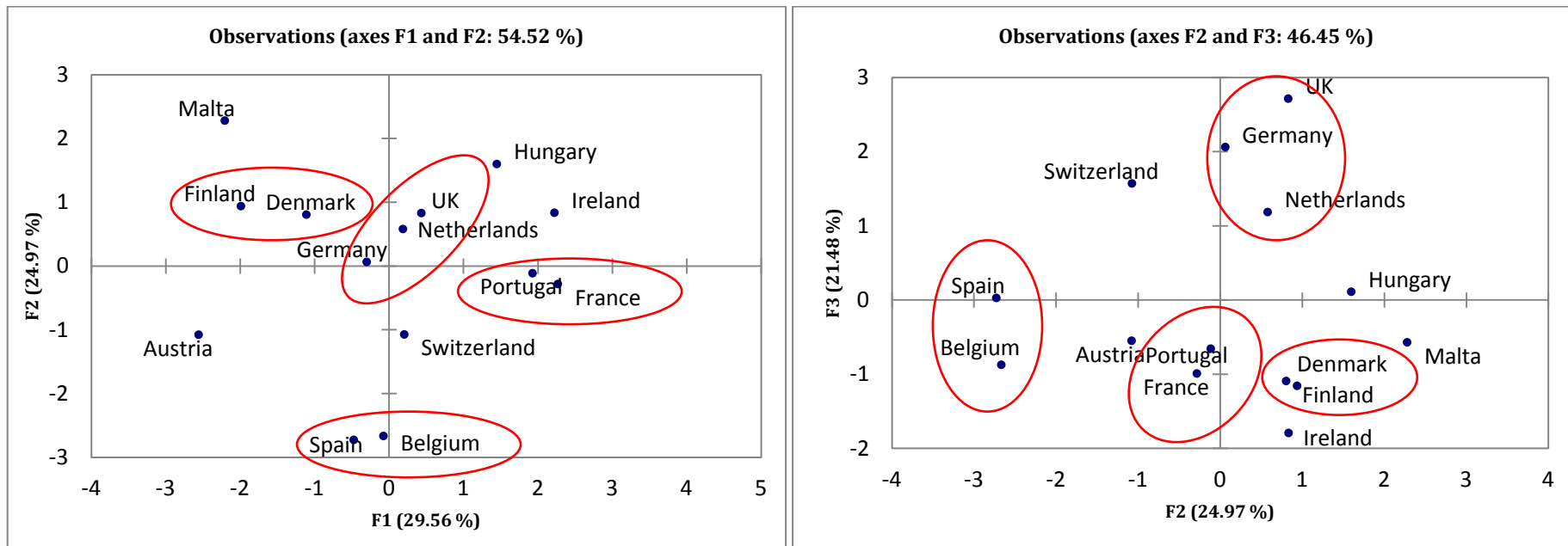


Fig. 4 Country scores similarities: biplot of F1&F2 (upper box) and F2 & F3 (lower box) explaining 76% of the data variability. The circles cluster countries with higher similarities in terms of institutional capacity

## **A national adaptation strategy to climate change in Italy: can the right stakeholders be engaged?**

**Venturini S.<sup>1</sup>, Giannini V.<sup>2</sup>, Davide M.<sup>3\*</sup> and Castellari S.<sup>4</sup>**

<sup>1</sup> Centro Euro-Mediterraneo sui Cambiamenti Climatici - Italy, <sup>2,3</sup> Centro Euro-Mediterraneo sui Cambiamenti Climatici and Fondazione Eni Enrico Mattei - Italy, and <sup>4</sup> Centro Euro-Mediterraneo sui Cambiamenti Climatici and Istituto Nazionale di Geofisica e Vulcanologia – Italy

\*Corresponding Author: [marinella.davide@feem.it](mailto:marinella.davide@feem.it)

### **Abstract**

This study aims at analyzing stakeholders' participation in the development of the Italian NAS, in order to understand their opinion about the strategy and discuss the very significant challenges of identifying and actively engaging them in a meaningful way. A first open questionnaire suggested that the majority of Italian stakeholders perceive a high degree of risk and great vulnerability related to impacts of climate change, while acknowledging a low sectoral adaptive capacity. In part, the respondents seemed to lack the necessary information over the national ongoing adaptation actions. A further round of interviews specified that the Italian NAS should have a holistic approach and coordinate sectoral action as well as exploit synergies between adaptation and mitigation. Alternatively, it could be part of a wider strategy for sustainable development. These results appeared to be in line with the 2007 "thirteen actions for sustainable adaptation" and the primary attention the Italian Ministry for Environment gave to prevention and protection from flood and landslide risks within the current NAS process. This paper recommends that the next phases of the NAS development take the form of both informative interaction and consultative participation, but be more inclusive with respect to the potentially most affected groups.

**Keywords:** Stakeholders participation, Climate Change, National adaptation strategies

## 1. INTRODUCTION

Italy, as a Mediterranean country, has already become familiar with the consequences of climate change that are posing new and augmented threats [1]. As shown by other European countries, successfully tackling negative effects of climate change requires a strategic approach to ensure that adaptation measures are taken promptly, are effective and consistent across different sectors and levels of governance [2][3]. The European Commission (EC) launched a EU Strategy on adaptation to climate change in April 2013 to top-up Member States' adaptation efforts with support for transnational coordination and possibilities of funding adaptation measures and research [4]. The EC provides guidance to the countries to further design and implement adaptation strategies [5] with a view to monitor and evaluate them and eventually strengthen European legislation.

The Italian Ministry for the Environment, Land and Sea (MATTM) began to develop a structured and collective thinking around adaptation during the process of the National Climate Change Conference held in 2007, where plans to formulate a national adaptation strategy were put forward and the earliest “13 actions for sustainable adaptation” were identified [6]. However, the Ministry formally initiated the preparation of a National Adaptation Strategy (NAS) only in July 2012. Given the intersectoral nature of adaptation policy itself, the process was envisaged to have an appropriate involvement of relevant institutions and stakeholders from the beginning.

In line with the findings of other scholars [7][8][9], we argue that stakeholder participation is a key challenge that governments face when developing and later implementing adaptation policies. The involvement of non-governmental stakeholders in the governance of adaptation is not only a matter of democracy or “social justice” [10], but also it helps to guarantee support and commitment to decisions that potentially affect stakeholders' interests at the local level [11]. Stakeholders may also enrich the process with relevant “indigenous” knowledge and experience in particular sectors [12].

Participation of stakeholders in adaptation planning processes is considered both a challenge [7] and a typical success factor [2][8][9]. According to Ebi et al. [13, pag. 37] stakeholders are “those who have interests in a particular decision, either as

individuals or as representatives of a group”, which encompasses both influencers and those affected by the final result of such a decision.

A positive sentiment is expressed by scholars with respect to the use of approaches for engaging the broader society when planning for adaptation strategies [14][8][9][3].

Main reasons that make participation so valuable include:

- Decisions under high uncertainty, as for climate change and adaptation, and scarce resources, can be more effective when recognizing multiple interests and community-based knowledge in addition to traditional science [14][15];
- A shared adaptation strategy contains more realistic options and early consideration of possible barriers and conflicts, which may result in a more straightforward implementation phase [14];
- Participation often brings intangible improvements in democracy and social justice that help build the social capital in a country [10].

The objective of this article is therefore to analyze how the challenges of participation have been faced in the Italian National Adaptation Strategy and deepen the understanding of the involved stakeholders’ opinion with regards to its objectives of and possible priority actions.

## **2. METHODOLOGY**

The development of the Italian NAS engaged various non-governmental stakeholders in three distinct moments of the process. In a first phase, a questionnaire was designed and disseminated on-line to gather the views of the stakeholders and initiate a structured dialogue with the society and the scientific community, in order to identify specific needs and obstacles to the implementation of any adaptation actions and measures. This was followed by an in-depth analysis of the results and a second more specific questionnaire. In a more advanced phase, a public consultation took place through an on-line review platform and ad hoc meetings, to obtain feedback on the elements of the draft Strategy document. A final consultation is expected at the end of the drafting process, aimed at gaining endorsement of the Strategy from society and all relevant institutions. In this context, CMCC has played the role of a “boundary organization” [3] by coordinating the work of the Technical Board,

maintaining a dialogue with the MATTM and the Inter-ministerial Advisory Group and managing the participation of the broader public. This article describes the work done by CMCC in involving non-governmental stakeholders throughout the first phase of the consultation process.

The preliminary on-line questionnaire (Q1) was designed following recent examples of consultative processes regarding climate change policies at both national and regional level as well as other documents of relevance for the Italian context. The information drawn from these led to the identification of topics to be elicited in the consultation, which included:

1. *Perceptions about climate change risks, vulnerability and adaptation;*
2. *Objectives and contents of a national adaptation strategy;*
3. *Sectoral approaches for adaptation (focus on sustainable land use and urban areas);*
4. *Needs and priorities for the implementation of a national adaptation strategy;*
5. *Opportunities and barriers to the implementation.*

The questionnaire was framed around these five sections, breaking them down into a total of 23 queries. The questionnaire was then launched using a web platform that was advertised on the MATTM and CMCC websites. It was left open to the public from October 1st to November 15th, 2012. Although it was accessible by any interested citizen, a list of selected stakeholders received an invitation from the MATTM to encourage their specific contribution. The “preferred stakeholders” were individuals or group representatives chosen if they matched at least one of the following criteria:

- Professional affiliation to one of the sectors of reference considered within the work of the Technical Board;
- Belonging to a civil society organization working on climate change adaptation;
- Belonging to a firm that is expected to develop its own climate adaptation strategy.

Several efforts were made to involve the target audience within society, which was meant to be an expert audience. Invitations were sent and these included the possibility of forwarding the questionnaire to other relevant stakeholders, thus making use of the “snowball technique”.

The questionnaire gathered 154 answers that were exported and elaborated using spread-sheet software. Based on the early elaboration of these results, the need to clarify and deepen the understanding of three main issues emerged:

1. the greatest share of the respondents came from four specific socio-economic sectors: Forestry, Biodiversity and ecosystems; Agriculture, aquaculture and fisheries; Energy;
2. views on the contents of the Strategy converged towards the issues of land protection, behavioural changes and more sustainable use of resources, being unclear what these mean for them (e.g. risk averse behaviour or environmental-friendly behaviour);
3. respondents’ preferences mostly tended towards synergies between adaptation and mitigation when they had the choice of a number of options.

This unclear feedback led to the design of the second questionnaire (Q2) addressed to stakeholders from the four most represented sectors in the Q1. In June 2013 twenty-four stakeholders were interviewed on five questions, three common ones and two specific for each sector, covering the following themes:

1. *Motivation to participate to the Q1;*
2. *Clarification about the meaning of “behavioural changes” as a modality for implementing adaptation;*
3. *View on synergies between mitigation and adaptation within the strategy;*
4. *Priority interventions within the specific sector of competence;*
5. *Possible cross-sectoral issues and synergies within the strategy.*

In this second survey, 17 stakeholders provided full responses, which were then elaborated one by one and compared to understand general similarities and differences.

### 3. RESULTS AND DISCUSSION

Overall, the participation of stakeholders is characterized by a wide heterogeneity both across professional affiliations and sectors, going beyond the list of preferred stakeholders. When analyzing the outcomes it is possible to recognize that the target group for which the original questionnaire was designed has been hit as a large share of respondents come from private sector and non-governmental institutions [Fig. 1]. Also, in the second part of the survey it becomes clear that most stakeholders are experts in their sector of affiliation [Fig. 2]. In fact, their participation is mainly motivated by their personal interest in contributing to the NAS with their expertise as they feel it is their duty to share their knowledge for such a purpose.

By analyzing the results of the initial questionnaire (Q1), it appears clear that the majority of Italian stakeholders perceive a high or extremely high degree of risk (81.8% of respondents) and great vulnerability (85.7%) related to impacts of climate change, while generally acknowledging a low adaptive capacity. Main concerns are the increase in frequency and intensity of extreme events, and the damages these can cause, mainly in relation to flooding. Other impacts of concern include decrease in snow cover, biodiversity and ecosystem services loss, soil erosion and degradation, drought, and the risk of floods and landslides. The latter is a recurrent issue, traceable throughout the questionnaire. Narrowing down the focus to the sectoral perception, the picture seems to get worse. According to 46% of the respondents, their sector has capacity to respond, but more than 85% notes a great overall vulnerability [Fig. 3].

This may signify that respondents think that there is capacity, but this capacity will not be turned into action. However, from the recent overview of adaptation action in Italy [1], we know that there is capacity and a number of initiatives on adaptation have already started, at least in some sectors, around the themes of rural development, safeguard of biodiversity, fight against desertification, health protection, and many others. Therefore, what is partly lacking is the knowledge of citizens on the existing institutional, economic, technological and cultural means to actually reduce vulnerability and the ongoing action on adaptation.

We also notice that stakeholders focused their attention on “territory” and “behavioural changes” when they are asked about the meaning of adaptation. Significantly, the risk of floods and mass movements associated to soil and land management emerges as one of the issues of concern for the Italian stakeholders (the so-called “dissesto idrogeologico” in Italian). This may be due to the resonance that these types of phenomena have had in the Italian media in recent years, as they triggered major disasters: Lunigiana and Cinque Terre (2011), Genova (2011), Vicenza (2010). Indeed, Italy has an infamous history starting with the landslide in Agrigento, and the floods in Florence and in Venice (1966), which led to the national debate for the reform of the “Legge Urbanistica Nazionale” (National Urban Law), and to the “Legge Ponte” (L. 765/1967) and the “Decreto sugli Standard Abitativi” (D.M. 1444/1968) [16][17]. More recently, in 1998, a tragic event occurred in Sarno (Campania): a series of special legislative measures for environmental protection were named after this as “Legge Sarno”. In fact, stakeholders’ alarm is real, as in Italy the risk of landslides and floods concerns pretty much all the national territory (two municipalities out of three): Calabria, Umbria and Valle d’Aosta regions are the most threatened, along with Marche and Tuscany [18].

The respondents suggest that the NAS should aim at the protection of the territory as a whole in the first place, including the monitoring and safeguarding of areas at risk. Specific priorities of the NAS should include limiting land-use change and halting soil sealing, managing water resources sustainably, and, again, reducing hazards related to floods and landslides. Also, a large share of respondents pointed out that there is the urgency to rethink energy use making the national economic system shock-averse [Fig. 4].

Furthermore, there is a shared perception that individual life-styles have to change, which is mostly intended as changing personal habits especially by reducing the unsustainable use of resources. In the free text answers of the Q1, in fact, the issue of the importance of individual life-styles “to promote climate change adaptation” emerges. From this general comment it is unclear whether stakeholders mean risk-averse behaviour (like emergency planning) or climate-friendly behaviour (like energy saving). This aspect is looked into more specifically in the second round of interviews [Tab. 1]. We find that, in short, behavioural change is intended as a broader environment-friendly and sustainable approach by all citizens.

As for the synergy between adaptation and mitigation within the NAS, this is intended as a two-fold possibility. On the one hand, contributing to design win-win strategies and to achieve co-benefits with mitigation. On the other hand, creating synergies by fostering the increase of environmental resilience, which could be achieved by assigning a larger role to local stakeholders (e.g. forest owners or tourism sector workers). For these synergies to take place, some point to top-down solutions, i.e. the MATTM should coordinate the creation of integrated plans also through the use of incentives and de-taxation; others point out bottom-up solutions, i.e. stakeholder engagement at the local scale.

However, according to some, the NAS should be an integral part of a wider strategy for sustainable development or sustainable urban growth. Moreover, it should be implemented through coordinated sectoral strategies, focusing specifically on the following sectors: energy, agriculture, and land-use planning.

Another important message that we get from stakeholders is about communication and education. The NAS should promote specific awareness-raising campaigns in schools and support climate and adaptation research in universities to form a new generation of professionals with multi-disciplinary knowledge. The NAS should ultimately enable decision-making processes and management of natural resources to be informed by the latest scientific knowledge on adaptation. Information should then be made available in the widest possible mode.

#### **4. CONCLUSIONS**

The following recommendations have been formulated with the aim to support the continuation of the participatory process and the finalization of the NAS, based on the lessons learnt.

First of all, some insights can be drawn about the success factors and barriers associated with a survey-like participatory process. Among the positive elements of the Italian participatory process, we can recognize that:

- by involving stakeholders and experts in the development of a NAS, the gap between the top-down and bottom-up approaches to adaptation can be bridged;

- using specific selection criteria leads to meeting stakeholders who can be precious in identifying adaptation options relevant to their own domain that were not considered before in the design of the NAS;
- using internet-based surveys enables widespread participation.

Among the limits, that are typical of all participatory processes, we acknowledge that:

- the most expert and influential stakeholders (e.g. NGOs, trade unions, private sector) are pre-selected, which may have represented an additional bias to the actual “openness” of the process;
- respondents may have voiced their frustration about poor environmental management in general rather than share their specific views on adaptation;
- open-ended questions are harder to interpret systematically, but relatively easier to formulate;
- in multiple-choice questions it is difficult to cover all the possible answers and some relevant options may be thus left out unintentionally; or, conversely, the inclusions of too many/certain options may prejudice the respondents choice;
- snowball methods carry bias: if the first selection of stakeholders leaves someone relevant out, they will not be found; however, it is very useful to reach a large number of experts.

We also recall that there are significant gradations of public participation ranging from forms of “non-participation” to “citizen power”. When Arnstein [19, pag. 216] stated that “the idea of citizen participation is a little like eating spinach” he meant that participation is in theory praised by everyone, however engagement is quite hard to obtain due to implicit limitations fixed by power-holders.

In the Italian NAS case, the process has been envisaged as a consultative participation mode, where the government has involved stakeholders for mutual exchange of information and expects actual contribution to shape the NAS, without having the obligation to heed their input. To best support the successful development of a NAS, on one side there is a need to insist on a more informative interaction in

the form of public meetings, awareness-raising campaigns, release of dedicated communication, establishment of a national adaptation portal, especially aimed at shedding light on the different opportunities that exist within adaptation and mitigation policies. On the other side, a higher number of consultative events, such as workshops with specific focus groups, roundtables and dialogue, should take place. This participatory process was designed in a way that allowed experts to be heard more. The next phases of the NAS development and adoption should be more inclusive and make an effort to address the potentially most affected groups in the country besides the most influential and competent ones. One good example to look at would be the process that led to the development of the National Biodiversity Strategy in Italy, that included a broad consultation aimed at gathering all the possible contributions from the relevant actors belonging to institutions, private sector and society (over 500 participants in 3 targeted workshops) [20]. Decisional participation may be postponed to the stage of designing the implementation plan of the NAS, where specialized support would be needed from stakeholders. A variety of approaches to engaging society has been realized in support of the different phases of adaptation planning across European countries. These can also provide good (and bad) practice examples.

There is clear advice from stakeholders that adaptation be framed as a component of an overarching climate change strategy, or even sustainable development strategy, along with mitigation to exploit mutual benefits. The importance of the overlaps between the two policies is recognized by the stakeholders, as they demonstrated in the single interviews. Significantly, in 2007, in the context of the first National Conference on Climate Change, the MATTM had already put forward a list of recommended actions for sustainable adaptation that largely included synergies with mitigation, such as the support to the system of incentives for energy saving in the residential sector and the definition of standards that would enable the development of green buildings [6]. Within the ongoing NAS process, mitigation aspects are being considered when identifying potential sectoral adaptation measures.

The NAS, at its current stage of formulation, also seems to be in line with the stakeholders' recommendations, as the MATTM, by the means of draft guidelines for economic planning, has emphasized the need to cope with flood and landslide risk through a comprehensive adaptation approach (MATTM, 2013). The expectation is

that the future NAS would fix the current incoherence of the action on adaptation across sectors and multiple scales of governance and thus put an end to the so-called “failure of adaptation narrative” [21].

## 5. ACKNOWLEDGMENTS

The authors gratefully made use of the results of the participatory process within the project SNAC – Elements for the development of a National Adaptation Strategy to Climate change, funded by the Italian Ministry for the Environment, Land and Sea and coordinated by the Euro-Mediterranean Center on Climate Change (CMCC).

## 6. REFERENCES

1. Medri, S., Venturini, S. & Castellari, S. (2013). Overview of Climate Change Impacts, Vulnerabilities and related Adaptation Initiatives in Italy (CMCC Research Paper nr. RP0178)
2. EEA (European Environment Agency) (2013, May). Adaptation in Europe: Addressing risks and opportunities from climate change in the context of socio-economic developments (Report no. 3/2013). Retrieved from EEA: <http://www.eea.europa.eu/publications/adaptation-in-europe>
3. Swart, R., Biesbroek, R., Binnerup, S., Carter, T.R., Cowan, C., Henrichs, T., Loquen, S., Mela, H., Morecroft, M., Reese M. & D. Rey (2009). Europe Adapts to Climate Change: Comparing National Adaptation Strategies (PEER Report No 1). Helsinki: Partnership for European Environmental Research. Retrieved from PEER: <http://www.peer.eu/publications>
4. EC (European Commission) (2013, April). An EU Strategy on adaptation to climate change. Communication from the Commission to the European Parliament, the Council, the European Economic and Social Committee and the Committee of Regions. Retrieved from DG CLIMA: [http://ec.europa.eu/clima/policies/adaptation/what/documentation\\_en.htm](http://ec.europa.eu/clima/policies/adaptation/what/documentation_en.htm)
5. EC (European Commission) (2013a, April). Guidelines on developing adaptation strategies. Commission Staff Working Document. Accompanying the document An EU Strategy on adaptation to climate change, Communication from the Commission to the European Parliament, the

Council, the European Economic and Social Committee and the Committee of Regions. Retrieved from DG CLIMA: [http://ec.europa.eu/clima/policies/adaptation/what/documentation\\_en.htm](http://ec.europa.eu/clima/policies/adaptation/what/documentation_en.htm)

6. APAT (Agenzia per la protezione dell'ambiente e per i servizi tecnici) – MATTM (Ministero dell'Ambiente e della Tutela del Territorio e del Mare) (2007). Conferenza Nazionale sui Cambiamenti Climatici 2007 - Sintesi dei lavori. [National Conference on Climate Change 2007 – Synthesis of the works]. Rome
7. Bauer, A., Feichtinger, J., & Steurer, R. (2012). The Governance of Climate Change Adaptation in 10 OECD Countries: Challenges and Approaches. *Journal of Environmental Policy & Planning*, 14(3), 279-304. doi:10.1080/1523908X.2012.707406
8. Preston, B., Westaway, R., & Yuen E. (2011). Climate adaptation planning in practice: an evaluation of adaptation plans from three developed nations. *Mitigation and Adaptation Strategies for Global Change*, 16, 407–438. doi: 10.1007/s11027-010-9270-x
9. Smith, J.B., Vogel, J.M. & Cromwell III, J.E. (2009). An architecture for government action on adaptation to climate change. An editorial comment. *Climatic Change*, 95, 53–61. doi: 10.1007/s10584-009-9623-1
10. Paavola, J. (2008). Science and social justice in the governance of adaptation to climate change. *Environmental Politics*, 17(4), 644 – 659. doi: 10.1080/09644010802193609
11. Beierle, T.C. & Cayford, J. (2002). *Democracy in practice – Public Participation in Environmental Decisions*. Washington: RFF Press Book
12. Reed, M.S. (2008). Stakeholder participation for environmental management: A literature review. *Biological Conservation* 141, 2417-2431. doi:10.1016/j.biocon.2008.07.014
13. Ebi, K.L., Lim, B. & Aguilar, Y. (2004). Scoping and Designing an Adaptation Project. In Lim, B., Spanger-Siegfried, E., Burton, I., Malone, E., Huq, S. (Eds.), *Adaptation Policy Frameworks for Climate Change: Developing*

- Strategies, Policies and Measures (pp. 35-46). Cambridge: Cambridge University Press
14. de Bruin, K., Dellink, R.B., Ruijs, A., Bolwidt, L., van Buuren, A., Graveland, J., de Groot, R.A., Kuikman, P.J., Reinhard, S., Roetter, R.P., Tassone, V.C., Verhagen & A., van Ierland, E.C. (2009). Adapting to climate change in the Netherlands: an inventory of climate adaptation options and ranking of alternatives. *Climatic Change*, 95, 23–45. doi: 10.1007/s10584-009-9576-4
15. Brunner, R.D., Steelman, T.A., Coe-Juell L. et al (2005). *Adaptive governance: integrating science, policy and decision making*. New York: Columbia University Press
16. Astengo, G. (1966). Urbanistica. In *Enciclopedia Universale dell'Arte*, vol. XIV, Sansoni: Venezia
17. Salzano, E. (1988). *Fondamenti di urbanistica*, Laterza
18. Legambiente (2011). *Ecosistema Rischio 2011. Monitoraggio sulle attività delle amministrazioni comunali per la mitigazione del rischio idrogeologico (Dossier)*. Retrieved from Legambiente: [http://www.legambiente.it/sites/default/files/docs/dossier\\_ecosistemarischio2011.pdf](http://www.legambiente.it/sites/default/files/docs/dossier_ecosistemarischio2011.pdf)
19. Arnstein, S.R. (1969). A Ladder Of Citizen Participation. *Journal of the American Institute of Planners*, 35(4), 216-224. doi: 10.1080/01944366908977225
20. MATTM (Ministero dell'Ambiente e della Tutela del Territorio e del Mare) (2010). *Italian National Biodiversity Strategy*. Roma: MATTM
21. Juhola, S., Keskitalo, E.C.H. & Westerhoff, L. (2011). Understanding the framings of climate change adaptation across multiple scales of governance in Europe. *Environmental Politics*, 20(4), 445-463. doi: 10.1080/09644016.2011.589571

## 7. IMAGES AND TABLES

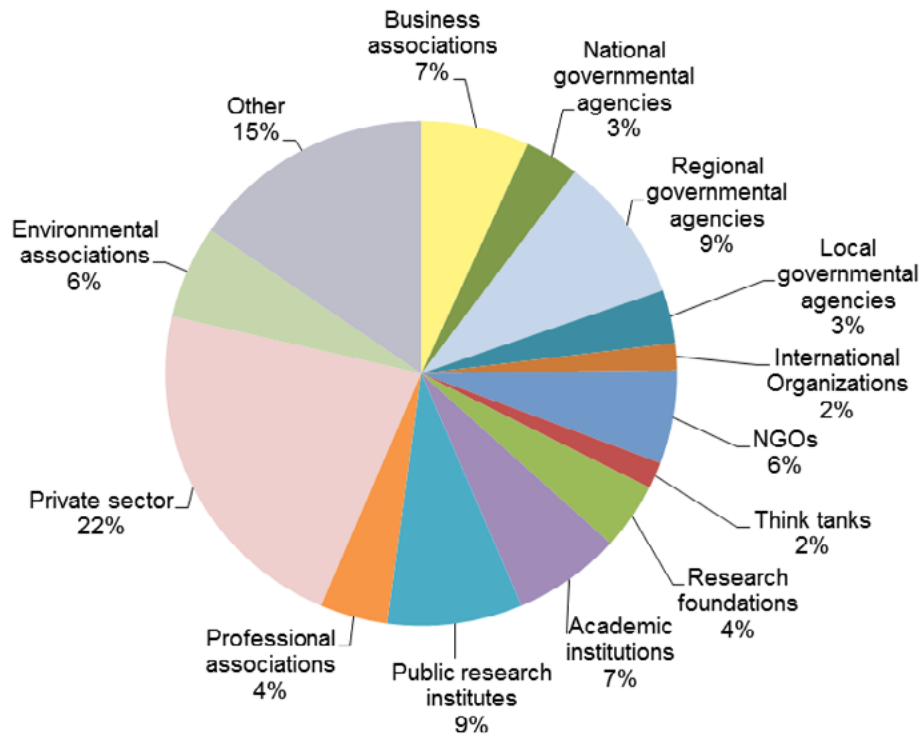


Fig. 1 Stakeholder participation in the on-line questionnaire (Q1) by professional affiliation.

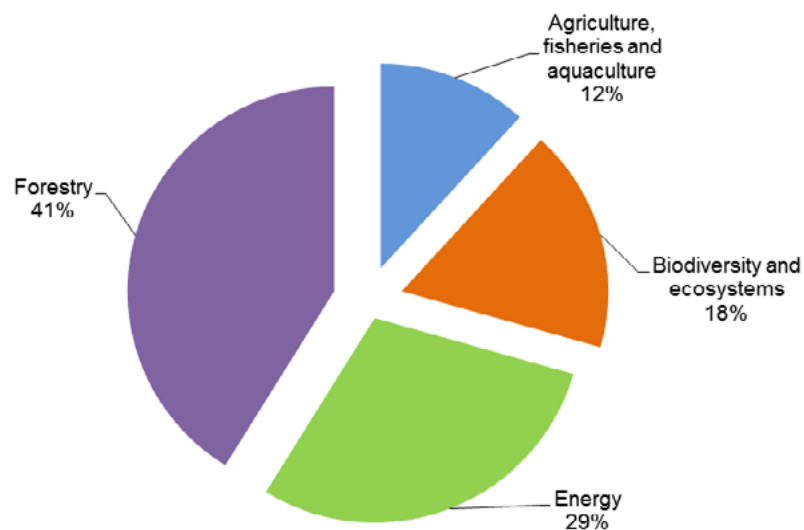


Fig. 2 Stakeholder participation in the interviews (Q2) by sector.

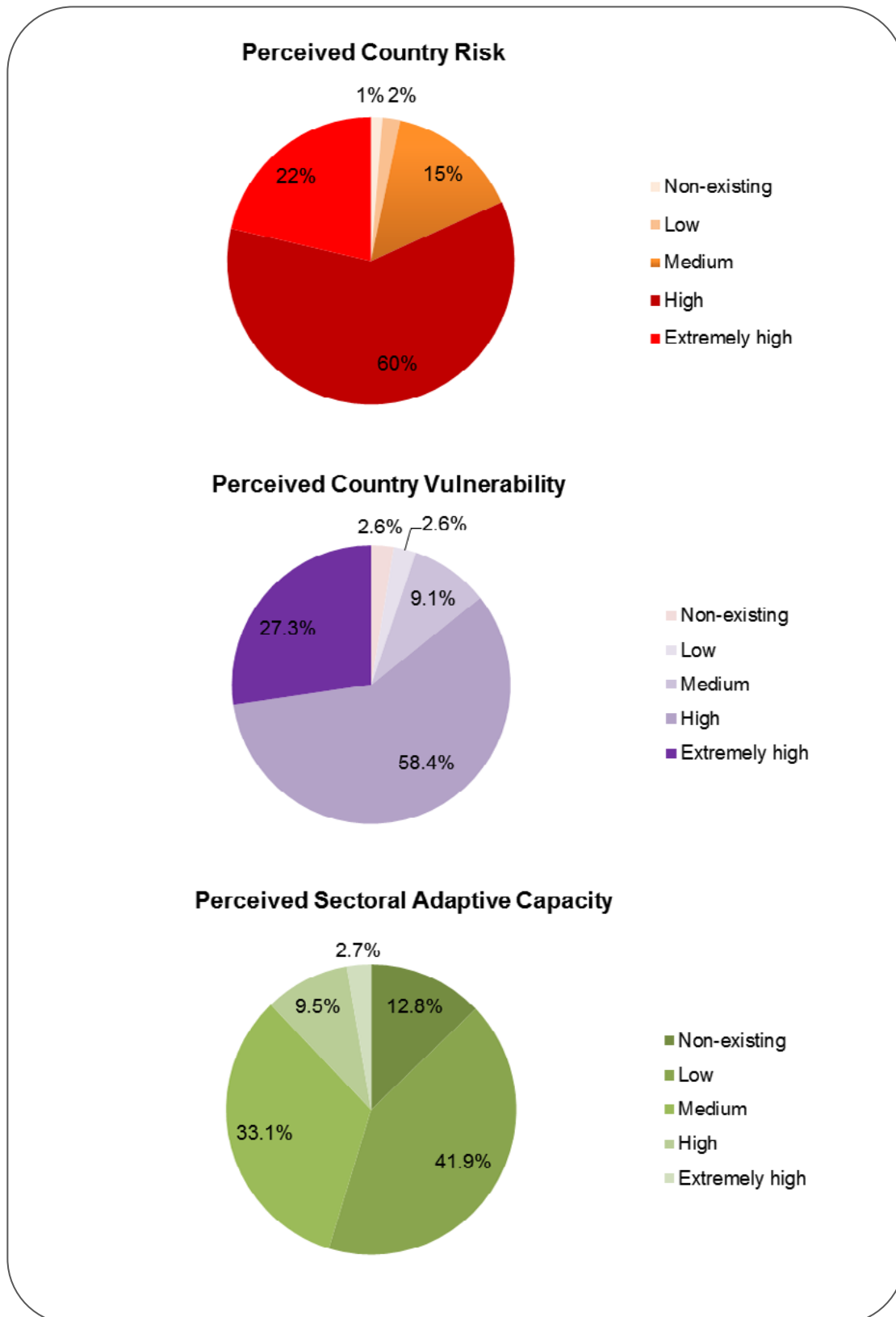


Fig. 3 Climate change risk, vulnerability and adaptive capacity in Italy as perceived by the respondents to the on-line questionnaire (Q1).



	<ul style="list-style-type: none"><li>– forest owners should receive incentives (e.g. from electricity bill) if they have management plan to extract biomass for energy production;</li><li>– promote sustainable forest management practices to: create synergies between adaptation and mitigation, integrate research on impacts of climate change; provide ecosystem services, produce biomass, to increase resilience and adaptation capacity of forests;</li><li>– learn from tradition of common forest tenure, use it to foster ownership and forest preservation.</li></ul>
--	--

Tab. 1 Priorities for the NAS design for the four considered sectors (Q2)

## **A methodological approach for stakeholder engagement at regional level in Climate Change Adaptation Policies**

**Terradez Mas J.<sup>1</sup>, Rossetto M.<sup>2</sup>, Frascini F.<sup>1</sup>, Lapi M.<sup>1</sup> and Ballarin Denti A.<sup>1,3</sup>**

<sup>1</sup>Fondazione Lombardia per l'Ambiente - Italy, <sup>2</sup>Politecnico di Milano - Italy, and

<sup>3</sup>Univesità Cattolica del Sacro Cuore – Italy

\*Corresponding Author: [juan.terradez@flanet.org](mailto:juan.terradez@flanet.org)

### **Abstract**

This paper explores how communities can begin planning for climate change adaptation. We provide a methodological contribution to emerging debates on the role of stakeholder engagement, by exposing an overview of the Lombardy Region engagement framework in the planning for adaptation. The results suggested that providing meaningful information and ensuring effective key stakeholder participation at a very early step of the adaptation strategy can enhance building capacity of decision-makers in developing adaptation plans to climate change at sub-national level (regional and local level).

**Keywords:** climate change, adaptation strategy, stakeholder engagement, subnational governance, Lombardy

## 1. INTRODUCTION

Adaptation is a multidisciplinary and intersectoral matter, and no longer simply a challenge to be addressed by people engaged in the environmental sector [1]. Involving community stakeholders in adaptation planning is crucial to ensure effective adaptation strategies and leads to better results for many reasons. Firstly, community members possess important local knowledge of the unique social, environmental and economic conditions of an area [2]. Secondly, working with stakeholders in an early step can help to set the direction and to oversee the implementation of the adaptation strategy, and may encourage future resources allocation and support for implementation of adaptation measures [3]. Third, an early engagement of managing authorities in the definition of the adaptation strategy is the most effective way to enhance a successful mainstreaming of adaptation into existing policies at each level of governance.

### 1.1 The Lombardy Region: toward the definition of the Regional Adaptation Strategy

In the last years, the authorities of Lombardy Region (North of Italy) have become increasingly aware about the complexity of climate change implications and hence of the importance of including climate change adaptation in their policy agenda. In 2012, the Lombardy Regional Authority issued a preparatory study on climate change adaptation – the Guidelines for a Regional Climate Change Adaptation Strategy (GRCCAS) – [4] to endorse the regional administration in the planning and coordination of climate change adaptation across sectoral departments. Within the GRCCAS, a Climate Change Impact and Vulnerability Assessment (CCIVA) was carried out [5], which provided a preliminary description of the potential impacts and vulnerabilities to climate change of a list of key sectors. During the implementation of the Guidelines, it also emerged that the proper engagement and commitment of all sectoral authorities, decision-makers and other stakeholders was a crucial aspect to ensure an efficient adaptation planning process at the regional level. After the success of the GRCCAS [6], the Lombardy Regional Authority decided to go further with the adaptation policy by commissioning the elaboration of a Regional Adaptation Strategy (RAS), whose completion is expected in December 2014. In particular, a group of researcher and scientists, coordinated by Lombardy Foundation for the

Environment referred hereafter to as ‘Research Team’, was identified as the leading group in charge of the definition and writing of the RAS. A ‘Regional coordination leader’ was also identified among the employees of the Lombardy Regional Authority as the leading politicians of the adaptation process. The process of elaboration is being guided by the step-by step implementation framework [Fig.1] identified and arranged during the participatory process carried out for the definition of the GRCCAS. The implementation of effective public processes was identified as a key requirement to build awareness and capacity on climate change, and support planning and decision-making in the definition of the RAS. The methodological framework employed to effective engagement of stakeholder is described in the methods section.

## **2. METHODS**

To engage stakeholders in the definition process of the RAS, the Research Team defined and implemented a methodological approach consisting of the following steps:

- I. Stakeholders mapping
- II. Online questionnaire
- III. Plenary workshop
- IV. Intersectoral workshops

### **2.1 Stakeholder mapping**

As a first step of the engagement process, the Research Team carried out a ‘Stakeholder Mapping’ in order to identify the full range of relevant groups and individuals potentially interested in the definition of the RAS. In particular, the Research Team identified a group of Regional Strategic Stakeholders, namely representatives of each key sector departments of the regional administration (a couple at least from D.G. Agriculture, D.G. Trade, tourism and services, D.G. Infrastructures and mobility, D.G. Civil protection, police and security, D.G. Health, D.G. Systems and landscape; D.G. Sport and youth activities; D.G. Land and urban management), representatives of Regional technical bodies (Regional Agency for

Environmental Protection, Energy Efficiency in Building Certification Body, Agency for Agriculture and Forest Services and civil protection among others) and other relevant regional research organizations. The overall people involved as stakeholders were forty-four; twenty nine of them were officials and leaders from the above listed D.G., while the remaining fifteen people were components of the Regional technical bodies. Due to time and resources limitation, the Research Team decided together with the Regional coordination leader to not yet involve the general public in this step of the definition of the RAS.

## **2.2 Online questionnaire**

Once the Regional Strategic Stakeholders were identified, an online questionnaire [7] was prepared to promptly involve them in the joint definition of the RAS's priorities [Fig.2]. In particular, participants were asked to express their opinion about the selection of the main vulnerable regional sectors to focus on [Fig.3]. In addition, respondents were asked to express their personal view about the main potential barriers for the adaptation process in the Region [Fig.4]. Other relevant strategic information concerning perception of climate change risks, impacts and vulnerabilities were also gathered. The total number of respondents was forty-four, 54 % of which were components of the regional administration, and the remaining 46% were representatives of the main Regional technical bodies and universities.

## **2.3 Plenary workshop**

The results of the questionnaires, along with a road map of the definition process of the RAS and the methodological framework for the stakeholder engagement, were presented to the group of Regional Strategic Stakeholders during a plenary workshop conducted by the Research Team and introduced by the Regional coordination leader. From the discussion on the questionnaire results, an agreement on the contents and key regional sectors of the RAS was achieved. Specifically, the following 8 key sectors were selected as considered more vulnerable to climate change in the Lombardy Region, namely human health and air quality, soil defense, urban planning and natural hazard management, water resources, tourism, agriculture, forest and biodiversity and energy. In addition, during the plenary

workshop, the Research Team aimed to stress the participants about the importance of their active participation to the definition of the RAS in order to maximize the agreement on the adaptation objectives and selected measures of the strategy. Another main aspect highlighted during the plenary workshop was the importance of the 'mainstreaming approach' in the adaptation to climate change, that is, the incorporation of the adaptation objectives and measures in the 'main stream' activities of regional policies, rather than being addressed in separate initiatives [8]. Given that the results of the survey pointed out a misperception of participants about the meaning of 'mainstreaming', a careful explanation of this concept was provided to the participants. The whole duration of the plenary workshop was about one hour and thirty minutes, and participants expressed positive responses and strong willing to collaborate farther in the following steps.

## **2.4 Intersectoral workshops**

After the plenary workshop and once key sector were selected, Research Team started with the more crucial part of the engagement process. Specifically a number of intersectoral and operative workshops with representatives of the key sectors were conducted. The aims of the intersectoral workshops were i) to share with the stakeholders the relevant scientific information on climate change in a face to face and comprehensive way; ii) to present the evidence and projections of the main climate change impacts; iii) to evaluate, discuss and prioritize the sectorial objectives for adaptation and to initiate the jointly definition of specific adaptation measures by sectors, taking into account also the potentialities and weakness of current and future sectorial policies. Instead of conducting 8 separate workshops, one for each key sector, four intersectoral workshops were held by jointly involving in the same workshop those with common crosscutting issues and/or greater potential conflicts of interest. In particular, the following intersectoral workshops were organized: one involving sectors with shared competences on water management at regional level, namely agriculture, water resources and energy; one involving representatives from the sectors of tourism and forest and biodiversity, given the interlink existing between natural services and tourism resources attractiveness; one involving the urban planning and natural hazard sectors; and one involving human health and air quality. According to the above-mentioned objectives, the workshops were divided into four

thematic sections, namely i) climate change evidences and projections; ii) identification of climate change impacts and vulnerabilities; iii) definition of priorities and outline of specific adaptation options; while the first two parts were mainly informative, the third and fourth parts were more proactive, and were intended to actively involve the stakeholders on the prioritization of the adaptation objectives and on the relevance of the proposed adaptation measures. The exercise was implemented in an open, non-hierarchical and non-political manner, in order to maximize the productivity of the discussion. Each workshop lasted about two hours and levels of participation were from satisfactory to acceptable depending on sectors. In the following paragraphs the four steps are described in details.

#### ***2.4.1 Climate change evidences and projections***

The Research Team and the Regional coordinator leader recognized the need of informing stakeholders on the more recent and sound scientific evidences on climate change. An overview of historical climate trends, information about regional climate variability and future climate projections, concerning the main climate variables (namely precipitation, annual and seasonal temperatures, climate extremes) was prepared. The challenge was to present the overview in short time in way comprehensive to a range of participants from different backgrounds. The Research Team explained in a simple and clear manner the differences between climate normal (temperature and precipitation conditions usually averaged over the period 1961–1990), climate change (occurred changed in the climatic conditions in the last few decades), and climate projection (projected shifts in climate over long periods concerning two future time periods: 2020-2050; 2070-2100). It was also clarified the role of climate variability induced by climate change (relates to changes in temperatures and precipitation ranging from months to multi-decadal oscillations) and the inherent uncertainties of future climate projections (especially concerning extreme climate events such as drought and heat wave). Scientific information was explained by means of diagrams [Fig.5] and regional maps [Fig.6]. The whole duration of this section was no more than twenty-five minutes plus time for questions and discussion.

### **2.4.2 Identification of regional climate change impacts and vulnerabilities**

In this stage, a facilitator member of the Research Team and expert on the topic presented a synoptic view of the main impacts and vulnerabilities of each key sector in a precise way but easily understandable way, in order to improve iterative learning [9]. The Research Team gathers information on climate change impacts from the CCIVA and subsequent integration of an extensive grey and scientific literature review and own data elaboration. The Research Team tried to make use of most recent available datasets and models existing at regional scale. Information was presented in two forms. On the one hand, graphs, charts, maps and diagrams regarding present and projected impacts of climate change were illustrated to the participants through a power point presentation [Fig.7]. On the other hand, a review of quantitative data concerning past trends and future projections of each identified impact was provided to participants in a document form in order to facilitate consultation [Fig.8]. The whole duration of this step, including time allocated for discussion, was no more than twenty-five minutes.

### **2.4.3 Definition of priorities and outline of the specific adaptation options**

It is widely recognized the importance of consulting and involving stakeholders in the prioritization processes of any adaptation strategy [9]. This may ensure that priorities are not established by individual opinions but are obtained by shared judgments. In order to ensure involvement in this participatory step of the strategy, the Research Team designed and implemented an ad hoc consultation exercise. The core goal of this training was to jointly evaluate and prioritize a set of impact-specific adaptation objectives by sector. Additionally, the Research Team aimed at sharing a list of specific adaptation measures by impact, obtained from an intensive review of existing national and regional adaptation strategies within the EU, customized to the specific regional context to fit with the specific adaptation objectives [Fig.9]. A list of adaptation objectives was conceived taking in mind the overall objective of maximizing the resilience and adaptive capacity of society, economy and environment of Lombardy region. Operatively, participants were asked to express their opinion by assigning weights to each adaptation objective concerning two different dimensions. The first dimension referred to the 'relative importance of climate change impact' for each specific objective proposed. Participants were asked

to rank from 1 (very low importance) to 5 (very high importance), the relevance of each impact presented in the sectoral-specific list. It was specified that judgment criteria should arise from participant's personal expertise, complemented by information from the qualitative and quantitative CCIVA provided in both document and presentation format during the workshop. The second dimension referred to the 'need for actions' to fulfill each adaptation objective. In this case, participants were asked to rank from 1 (very reduced need) to 5 (very high need) the degree of need of adaptation actions in each adaptation objective, depending whether adaptation objectives had already been addressed by regional policies or whether they had not yet been addressed with sufficient robustness. In this case, judgment criteria for the weighting of the 'need for actions' should arise from participant's management experience and personal knowledge, complemented by the results of a comparative analysis of regional policies from the adaptation objectives viewpoint [Fig.10]. The results of this analysis was provided and illustrated by an expert of the Research Team during the workshops in order to facilitate the identification of the already implemented adaptation measures and of the opportunities to implement new ones, with the aim of enhancing the effectiveness of mainstreaming adaptation into current sectoral policies and plans. To facilitate the weighting process, a document with detailed instructions on the prioritization exercise was provided to each participant. Finally, the weights assigned for each dimension by all participants were averaged to obtain a ranking from 1(very low priority) to 5 (very high priority) of each adaptation objectives priority. Additionally, researchers provided also a wide range of adaptation measures for each adaptation objective [Fig.9]. Measures were structured in three different typologies of adaptation options, namely soft or non-structural (i.e. policy incentives such as land-use control or information dissemination), grey (i.e. physical interventions or construction measures) and green infrastructure (i.e. using the functions and services provided by ecosystems to achieve more cost-effective and sometimes more feasible adaptation solutions).

### 3. RESULTS

**Building capacity:** The involvement of the stakeholders and the organization of the workshops were designed based on lessons learned from the definition of the regional Guidelines. This allowed us to better identify the potential barriers to the adaptation process, the impact that need to be evaluated more accurately and the new sectoral vulnerabilities not yet considered at regional level. The series of workshop undertaken with stakeholders –along with the provided information on climate change and relative impacts –served as an important capacity building factor. The active participation of experts with important local knowledge and their operational involvement in the planning and definition of the adaptation strategy were important processes that contribute to build effective political capacity and competencies to strengthen the resilience of Lombardy region to climate change.

**Awareness:** Dissemination and effective communication of relevant information during the engagement process of the RAS has enabled the regional government to realize the real dimension of dealing with present and future climate change challenges. The climate information helped workshop attendees to grasp what the major trends in the region are, what types of changes in Lombardy region climate are expected and how significant these projected changes are in the context of historical variability and past trends. Having a climate information expert in attendance to present the data and answer the multitude of participant questions was very helpful.

**Commitment:** The first major challenge to ensuring commitment during the elaboration of the RAS was to make understand how the process of adaptation works and how it can improve resilience. Since adaptation is a multidisciplinary issue that cuts across policies and service areas, political backing and managerial commitment were crucial to ensure horizontal and vertical coordination in the different steps of the RAS. During the whole process, periodic meetings, briefings, updates about the results and findings and continuous information sharing, consolidated the commitment and confidence between the Research Team, the relevant decision-makers, the regional technicians and the executive leader in charge of the horizontal coordination. A proper mutual assistance and coordination among key regional stakeholders in an early step helps to secure allocation of resources and efforts to implement adaptation actions in the future.

**Engagement:** Key issues to enhance engagement of stakeholders were i) to guarantee an adequate perception of the identified climate change impacts at regional level; and ii) to contribute in the joint definition and prioritization of the adaptation objectives as part of the consensus building process. This makes stakeholders aware of being part of an iterative process in which adaptation decisions are taken by consensus. The participatory and reproducible framework for the definition of the RAS, the use of decision-making tools (such as questionnaires, weighting process) and the joint analysis of the proposed adaptation measures may further help to ensure further engagement.

#### 4. DISCUSSION AND CONCLUSIONS

Planned adaptations is crucial in increasing the resilience of cities and regions to the effects of climate change and in enabling socioeconomic sectors to develop in a way that ensures their long-term sustainability in the face of a changing climate. Successfully integrating climate change adaptation considerations into the already existing policies at regional level implies commitment of all sectorial authorities and to be aware about the urgent need of dealing with climate challenges to decision makers and stakeholders. In very general terms, engagement improves the likely outcomes of decision-making, and so enhances the benefits of an adaptation strategy in terms of preparedness of socio-economic systems to affront climate challenges, and so resilience.

Those benefits are namely:

- Facilitating clear and fluid communication and exchange of information in a comprehensive way, with all parties involved developing a more thorough understanding of adaptation issues, potential solutions and alternative adaptation perspectives;
- Improving the effectiveness of decision-making processes, by gaining better insight into potential equitable outcomes, solutions to conflicts, and effective adaptation planning;
- Strengthening the resources of involved groups, by increasing awareness, confidence, skills and co-operation in the definition of measures for making “climate proofing” regional policies;

- Improving the socio-economic sustainability of any adaptation initiatives, by increasing the quality and consensus degree of decisions and their acceptance amongst all stakeholders.

The more meaningful information and effective stakeholder participation at regional level are implemented at a very early step of the adaptation strategy definition, the more the building capacity of decision-making and planning on climate change will be, and hence the more the resistance of the socio-economic and natural systems against climate change implications.

## 5. ACKNOWLEDGMENTS

Insert your acknowledgments here; do not place them on the first page of your paper or as a footnote.

## 6. REFERENCES

1. Sheppard, S. R., Shaw, A., Flanders, D., Burch, S., Wiek, A., Carmichael, J., (2011). *Future visioning of local climate change: a framework for community engagement and planning with scenarios and visualisation*. *Futures*, 43(4), 400-412.
2. Ribeiro, M. M., AEA, C. L., Dworak, T., IVM, E. M., WUR, R. S., AEA, M. B., & Laaser, C. (2009). *Design of guidelines for the elaboration of Regional Climate Change Adaptations Strategies*. Ecologic Institute, Vienna.
3. COM (2013). *An EU Strategy on adaptation to climate change*. Communication from the commission to the European parliament, the council, the European economic and social committee and the committee of the regions, Brussels, 16.4.2013.
4. Terradez Mas, J.M., Rossetto, M. De Leo, G.A., Palencia Rocamora, R., (2012). *Linee Guida per un Piano di Adattamento ai Cambiamenti Climatici in Lombardia*. Fondazione Lombardia per l'Ambiente. [http://www.reti.regione.lombardia.it/shared/ccurl/778/935/Linee%20guida%20PACC%20Lombardia\\_Abstract.pdf](http://www.reti.regione.lombardia.it/shared/ccurl/778/935/Linee%20guida%20PACC%20Lombardia_Abstract.pdf)
5. Terradez Mas J., Rossetto M., Ballarin Denti A., Lapi M., De Leo G. A. (2013). *Guidelines for the implementation of the Regional Adaptation Strategy in*

*Lombardy (RAS)*. SISC first annual conference, climate policy and economic assessments, Lecce.

6. McGuinn J., Stokenberga L., White O., Baker J. (2013). *Climate change adaptation practice across the EU: Understanding the challenges and ways forward in the context of multi-level governance*. <http://bookshop.europa.eu/en/climate-change-adaptation-practice-across-the-eu-pbML0113690/>
7. Fondazione Lombardia per l'Ambiente (2013). Questionario ONLINE per la Strategia Regionale di Adattamento al Cambiamento Climatico (SRACc) della Lombardia. <https://docs.google.com/forms/d/1-U2g9Ch9mKcCQvH6UUcEHbIhClcvvSUFtVUoPB91JI8/viewform>
8. Few R., Brown K., and Tompkins E.L.(2006). *Public participation and climate change adaptation*. Tyndall Centre for Climate Change Research Working Paper 95.
9. Tschakert P. and Dietrich K. A. (2010). *Anticipatory Learning for Climate Change Adaptation and Resilience*. *Ecology & Society*, 15(2).
10. Pahl-Wostl, C. (2009). *A conceptual framework for analysing adaptive capacity and multi-level learning processes in resource governance regimes*. *Global Environmental Change*, 19(3), 354-365.

## 7. IMAGES AND TABLES

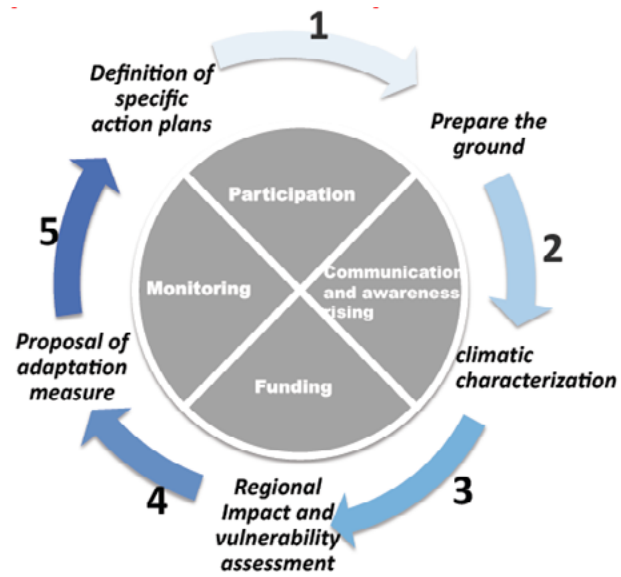


Fig. 1 step-by step implementation framework defined in the Guidelines for the elaboration of the Regional Climate Change Adaptation Strategy of the Lombardy region. Source: Adapted from Ribeiro et al. 2009.

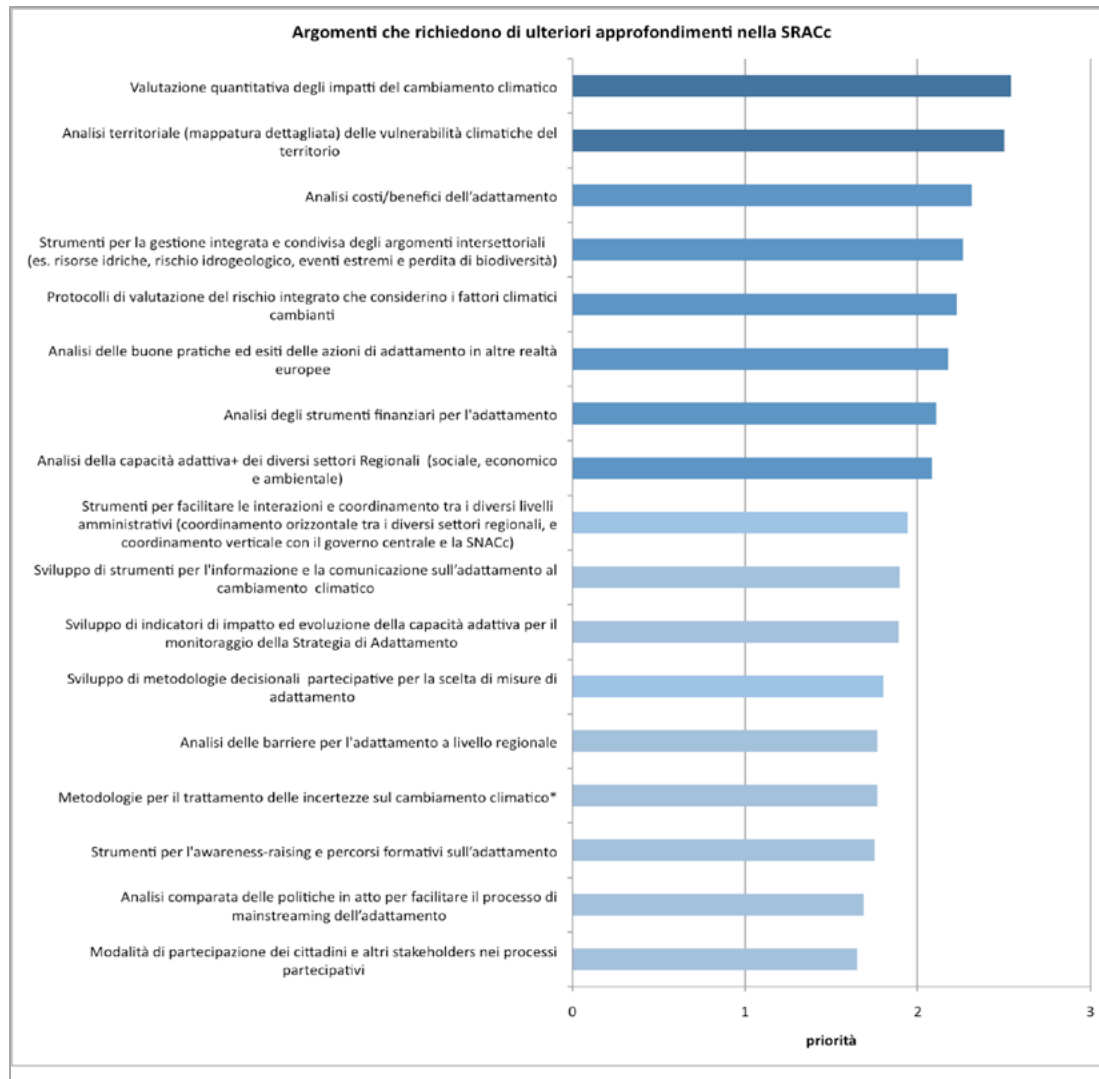


Fig. 2 Statement of respondents about priority arguments to deal in depth within the Lombardy RAS.

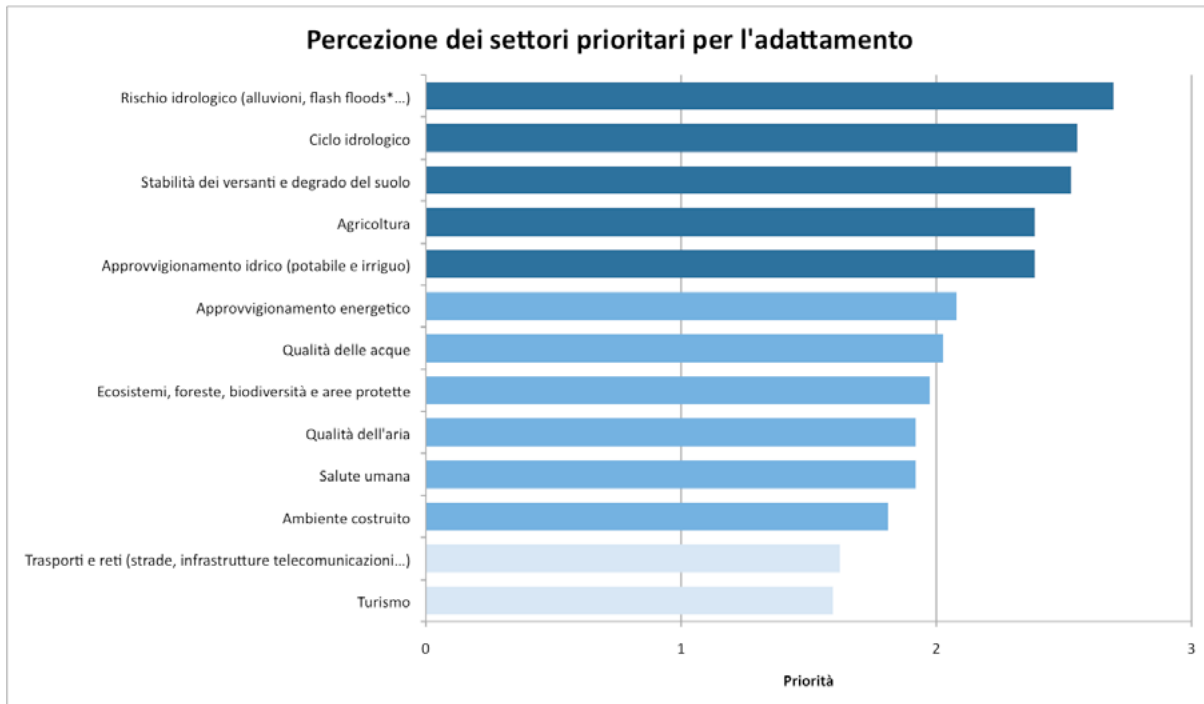


Fig. 3 Statement of respondents about the level of priority of regional sectors to focus on in the RAS.

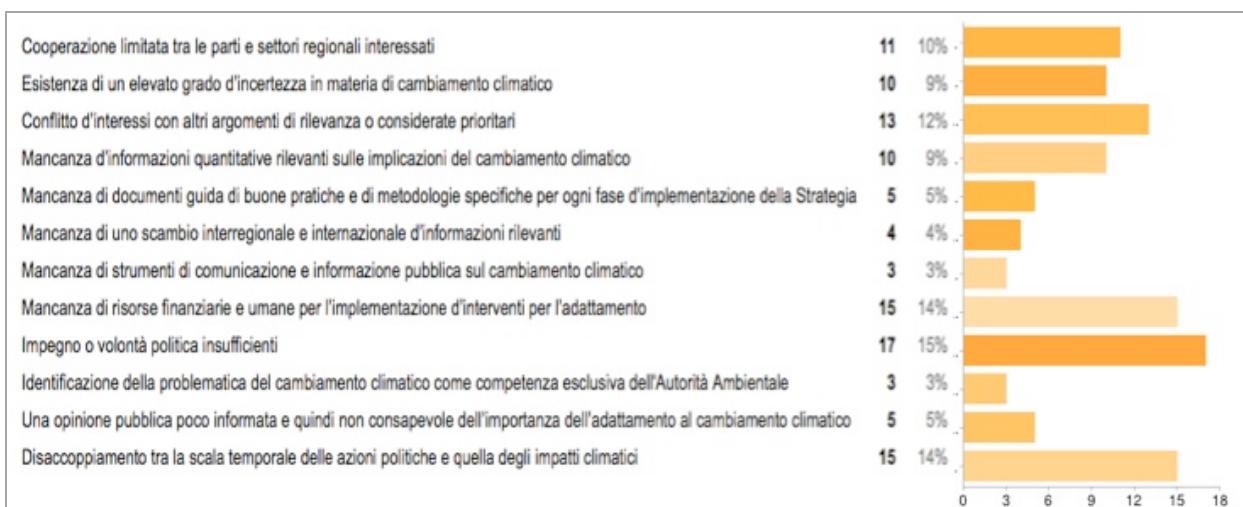


Fig. 4 Respondent's perception about the most persistent adaptation barriers in Lombardy.

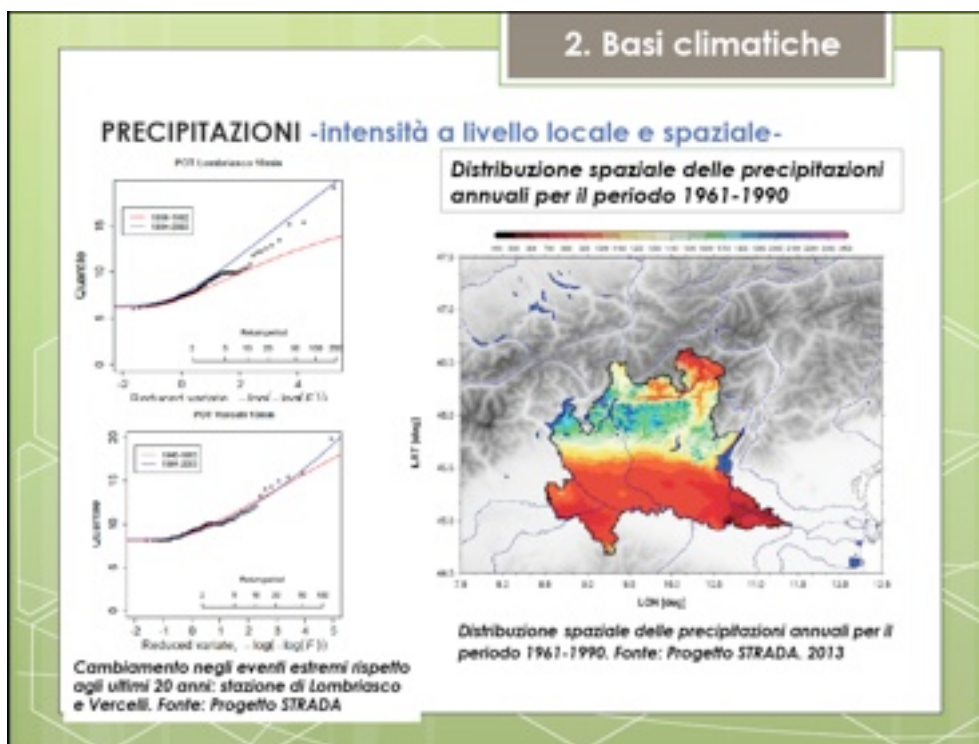


Fig.5 Example of climatic information presented during the workshops. Left: evolution of intense precipitation events during the period 1984-2003 compared with 1958-1982 in two weather stations of the Lombardy territory. Right: map of the rainfalls intensity in the Lombardy territory during the 1961-1990 time period. Source: with data from STRADA Project, 2013.

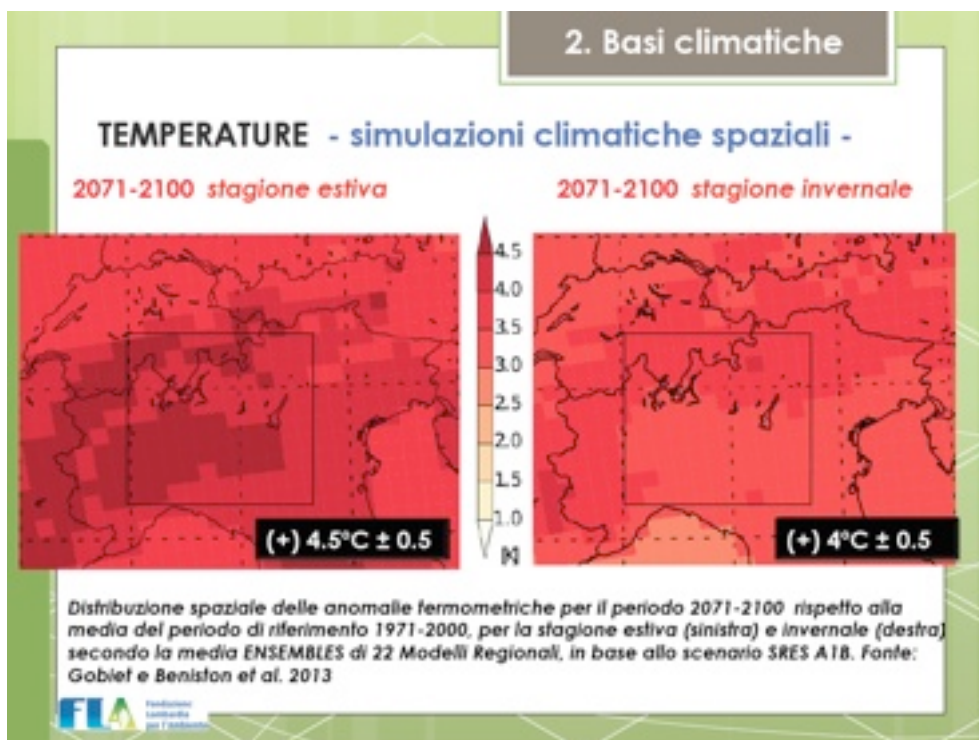


Fig. 6 Spatial distribution of the projected thermometric anomalies for the period 2071-2100 compared to mean temperature of the reference period 1971-2000, for the summer season (left) and winter

(right) according to the mean of 22 ENSEMBLES regional models, using the SRES A1B emission scenario. Source: with data from Gobiet and Beniston et al. 2013.

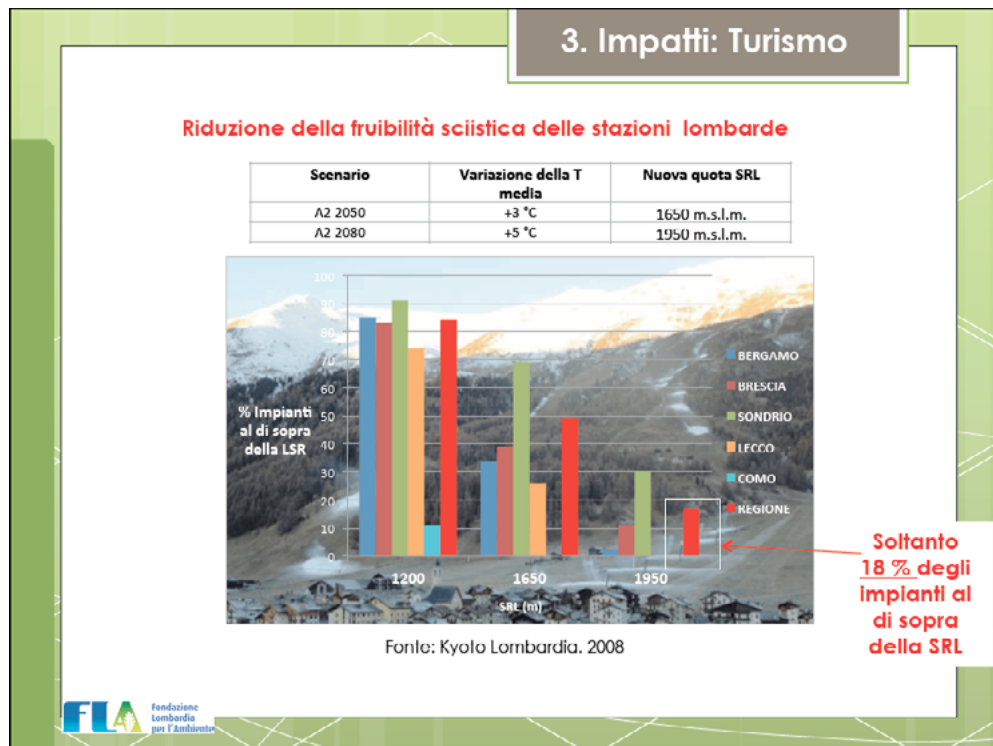


Fig. 7 Projected impact of climate change on the winter tourism sector in Lombardy: projected percentage of skiing areas below the snow line (Snow Reliability Line) by provinces under two different future scenarios of global warming. Source: with data from Kyoto Lombardia Project. 2008.

## Ecosistemi, foreste, biodiversità e aree protette

Tabella 1. Ricognizione dei dati bibliografici disponibili sugli impatti del cambiamento climatico negli ecosistemi, le foreste, la biodiversità e le aree protette lombarde

IMPATTI				
<i>Ecosistemi, foreste, biodiversità e aree protette</i>	Indicatore	Variazione	Periodi	Fonte
<b>i. Modifiche nella fenologia e interazioni tra le specie</b>	Anticipo medio della data di arrivo di 117 uccelli migratori	(+) 0.2 ± 0.15 giorni /anno	1958-2008	[1]
	Anticipo nella data degli eventi riproduttivi degli anfibi	(+) 2 ± 1 settimane /decennio	1980-2008	[2]
	Incremento delle discordanze trofiche tra lepidotteri e le loro piante ospiti	(-) 50 % ± 20 di aree a concordanza trofica	2080	[3]
<b>ii. Cambiamento nella distribuzione e composizione delle popolazioni e dei biotopi, e incremento del rischio di estinzioni</b>	Spostamento medio della distribuzione geografica delle specie europee	(+) 17 km verso nord o (+) 11 m verso quote superiori / decennio	1950-2005	[4]
	Incremento della ricchezza specifica di piante nell'orizzonte alpino superiore e subnivale	(+) 10 %; (+) 9%	2001-2006	[5]
	Risalita delle specie vegetali alpine	(+) 23.9 m/decennio	1954-2005	[6]
	Riduzione dell'areale di distribuzione di 15 specie vegetali alpine	(-) 47 ± 3 %	2070-2100	[17]
	Riduzione del bioma boreale e bioma alpino	(-) 25% (-) 14%	2071-2100	[11] [12]
	Riduzione dell'areale di distribuzione delle farfalle europee	previsto per l' 80% delle specie	2070-2100	[7]
	Riduzione delle aree di vocazionalità faunistica	(-) camoscio (-) stambecco (-) gallo forcello	2020-2080	[8]

Fig. 8 Example of document-form provided to participants during the workshop, containing results of quantitative data concerning past trends and future projections of each identified impact. Source: own elaboration by an extensive peer review.

Nome/cognome: \_\_\_\_\_  
 Email: \_\_\_\_\_

**Risorse idriche: Obiettivi settoriali per l'adattamento e proposta di misure di adattamento**

 **FIA** Fondazione Lombardia per l'Ambiente

Ciclo idrologico e qualità delle acque		Obiettivi strategici per l'adattamento		Proposta di misure di adattamento <sup>1</sup>	
Impatti	Importanza relativa dell'impatto	Obiettivi	Necessità d'intervento	Proposta	
	Importanza (1-5)		Necessità (1-5)		
1-Alterazione delle caratteristiche fisico-chimiche e biologiche delle acque superficiali e sotterranee (Qualità)		<p><b>1.1</b> Ampliare e rinforzare le reti di misurazione, monitoraggio e sorveglianza delle risorse idriche superficiali e sotterranee</p> <p><b>1.2</b> Incrementare la resilienza dei corpi idrici alle implicazioni del mutamento del clima per assicurare la continuità dei servizi ecosistemici da loro forniti</p> <p><b>1.3</b> Garantire il buono stato ecologico e di qualità delle risorse idriche regionali anche in considerazione al mutamento del clima</p> <p><b>1.4</b> Approfondire le conoscenze sulle implicazioni del cambiamento climatico nella qualità delle acque</p>		<p><b>Soft o non strutturali:</b></p> <ol style="list-style-type: none"> <li>Potenziare ed estendere gli attuali strumenti e reti di monitoraggio e il controllo della qualità delle risorse idriche lombarde (identificare i gap esistenti nell'attuale rete di monitoraggio costituita da 260 punti di prelievo e misura, relativi a 175 corpi idrici superficiali)<sup>(1.1, 2.1, 2.2, 3.3)</sup></li> <li>Intensificare il controllo dell'evoluzione del grado di diluizione degli inquinanti nelle acque sotterranee durante i periodi a maggiore rischio (es: periodi siccitosi prolungati)<sup>(1.1, 1.2, 1.3, 2.3, 3.1)</sup></li> <li>Rinforzare la prevenzione dei casi di penuria, fioriture algali e peggioramento eccessivo della qualità dei corpi idrici in considerazione all'incremento di eventi climatici estremi (es: intensificare il monitoraggio dell'influenza degli scarichi termici nelle acque superficiali)<sup>(1.1, 1.3)</sup></li> <li>Minimizzare i disturbi associati alla captazione e al rilascio di acque dalle centrali idroelettriche e termoelettriche<sup>(1.3, 2.1, 2.2, 2.3)</sup></li> <li>Ampliare la caratterizzazione dettagliata delle acque del territorio regionale e concretamente completare la cartografia dettagliata (e informatizzata) del reticolo irriguo minore<sup>(1.1, 2.1, 2.2, 3.3, 4.4)</sup></li> <li>Migliorare la comprensione dei fattori di controllo del clima e dei feedback del suolo<sup>(1.1, 2.1, 2.3, 4.4)</sup></li> <li>Introdurre le considerazioni sulla variabilità climatica futura nei sistemi di monitoraggio attuali: Introdurre i fattori della variabilità climatica nella definizione dell'Indice Sintetico di Invaso per i corsi d'acqua Montani della Lombardia (previsto nel PTUA, 2006), per valutarne la portata e lo sfruttamento da parte dell'uomo<sup>(1.1, 1.3, 2.1, 2.2, 3.1, 4.3)</sup></li> </ol> <p><b>Grey o strutturali:</b></p> <ol style="list-style-type: none"> <li>Estendere gli interventi volti a ridurre la vulnerabilità delle acque rispetto alle attività antropiche in previsione della possibile intensificazione dei fattori climatici connessi (es: misura 121 del Programma di Sviluppo Rurale 2007-2013 che prevede la realizzazione di coperture delle vasche di stoccaggio degli effluenti di allevamento, per il contenimento degli inquinanti azotati)<sup>(1.3, 3.1)</sup></li> </ol> <p><b>Green o basate su un approccio ecosistemico:</b></p> <ol style="list-style-type: none"> <li>Miglioramento dell'ecologia e delle caratteristiche chimico-fisiche delle acque superficiali e sotterranee<sup>(1.2, 1.3)</sup></li> <li>Consolidare le misure di conservazione e ripristino dell'integrità ecologica delle aree riparie e delle zone di transizione boscate dei fiumi in difesa del loro ruolo nella modulazione e regolazione dei processi e delle</li> </ol>	

<sup>1</sup> I superindici localizzati alla fine di ogni proposta di misura di adattamento fanno riferimento agli **obiettivi strategici** per i quali la misura in questione si prevede abbia delle **sinergie positive per il raggiungimento di tali obiettivi**.

Fig. 9 Example of document provided to workshop participants, containing the relevant information for the consultation process. From left to right columns contain 1) the list of relevant impacts per sector, 2) the list of adaptation objectives per impact and 3) the proposed adaptation measures.

Source: own elaboration.



# Adapting to Climate Change: Bologna as Resilient City

Pelizzaro P.<sup>1</sup>

<sup>1</sup>Head of the International Cooperation Unit at Kyoto Club (Italy)

\*Corresponding Author: [p.pelizzaro@kyotoclub.org](mailto:p.pelizzaro@kyotoclub.org)

## Abstract

Looking at the increasing awareness that global temperatures will raise, a mentality "Climate-smart" must be adopted by all levels of decision-making. "Climate-smart" is a term that originated in agriculture, to describe those interventions in the agricultural sector that are able to increase the resilience of adaptive capacity to climate change and at the same time reduce emissions of greenhouse gases. A mentality "Climate-smart" incorporates the analysis of climate change taking place in the definition of strategies and operational decision-making processes. This approach involves the search for synergies between climate change mitigation and adaptation, wherever is possible.

**Keywords:** adaptation, climate change, memory, mitigation, resilience

## 1. BACKGROUND

In the last decade, the international community has taken the knowledge that our planet will face serious consequences due to climate change, whether attributable to natural causes, and the action of man. While there is a broad consensus on how fast and how our climate is changing, there is an increasing perception of the impact and this can be seen by the shift of the debate about how society should adapt. Growing awareness promoted by the political and economic institutions for adaptation is controversial in some areas of environmentalism, in fact for some senior figures is interpreted as a tacit admission that efforts to mitigate greenhouse gas emissions are no longer sufficient. However it should be remembered how, less efficient mitigation measures will require more pronounced adaptation actions to be undertaken. Therefore this suggests that policies for mitigation and adaptation must be addressed in concert, by exploiting all possible synergies. The Global Risk Report 2013 confirmed the integration of the two policies recently, published by the World Economic Forum (WEF), a reference document for global investors on the main risks that may afflict their investment portfolio. In the 2013s report, one of the main risks identified is the "failure of the system to adapt to climate change." More then this, if you combine the Global Risk Report with the WEF report "The Green Investment Report. The ways and means to unlock private finance for green growth", which indicates an increase in public investment world of 36 billion dollars / year to trigger private investment by enough to contain the critical threshold of 2 ° C global warming, we understand how mitigation and adaptation goes together. Both WEF reports reflect what suggested in 2012 by the EU Climate Change Expert Group, which indicates an increase in the costs of climate change impacts, equivalent to 5% up to 20% of the GDP (or higher) in the long run, parallel with the current trend of increase in global temperature. The European Environment Agency (EEA) has recently published the "Climate change, impacts and vulnerability in Europe 2012" reports, where the evidence of the impacts is well identified. In all European regions have been observed an increase in average temperatures combined with a decrease in rainfall in the southern regions and increased precipitation in Northern Europe. The Greenland ice sheet, sea ice and many glaciers are melting all over Europe, the snowpack has decreased and most of the permafrost soils have warmed. These extreme weather events have generated local urban phenomena such as heat

waves, floods and droughts causing a consequent increase in costs in terms of human lives and infrastructure. While these scenarios show that more elements are needed to understand the role of climate change, the growth of human activity in areas at risk could be a key factor. The Agency predicts that extreme weather events will become more intense and frequent, helping to accentuate the vulnerability of such a situation. The recent weather and climate events have shown clearly and unequivocally the high economic and social costs of such disasters, that are expecting to be even worst in the near future. Estimated losses in 2011 alone, for the floods in Thailand amounted to U.S. \$ 30 billion, Hurricane Katrina resulted in damage to the U.S. economy \$ 125 billion. It should be remembered that in 2003 the heat wave that struck Europe caused 35 thousand victims, while the 2011 drought that hit the Horn of Africa has resulted in tens of thousands of victims and threatened the survival of 9.5 million people .As stated by Jacqueline McGlade, Executive Director of the European Environment Agency: "Climate change is a reality all over the world, and the extent and speed of change is becoming more evident. This means that every part of the economy, including households, needs to adapt and reduce emissions". However, it should be pointed out that some regions of the world will be less capable of adapting to climate change than others because of economic disparities and the effects of these changes could deepen these inequalities. The consequences, however, has to be considered not only at the global level, in fact in the report of the EEA is emphasized that a different adaptive capacity because of economic inequalities, there might be even within the EU borders. In order to reconcile the challenge of building climate resilience in a situation of great economic stress, it is therefore necessary to re-evaluate current policies and national strategies. For example, in many countries, national insurance systems and housing policies continue to encourage urbanization of coastal areas prone to flooding or high landslide risk, rather than avoid the risks. Decide to continue with these policies may be the cause of the creation of pockets of vulnerability to climate risks. A 2007 OECD report analyzes 136 port cities around the world, and highlights how the population exposed to coastal flooding could triple by 2070 and this was due to the combined effects of climate change and urbanization. Another interesting fact that comes from the EU project Corinne tells us that between 1990 and 2006 the area of artificial soil of the European Union has grown from 176,000 to 192,000 km <sup>2</sup> (1), this is an area like half Germany. In the past sixteen years the consumption of fertile soil was then

equal to 970 km<sup>2</sup> per year, or 265 acres per day. That is to say, it is an area as large as the historical center of Milan (2). If you were to continue business as usual by 2050 would add other 43,000 km<sup>2</sup> of ground cemented, an extension equivalent to the entire Denmark.

## 2. OUTLINE OF THE WORK

As for the energy, this approach has been well described in the position paper of the Alliance to Save Energy "Energy Efficiency: A Tool for Climate Change Adaptation. An Alliance to Save Energy White Paper " (February 2012), according to American scholars energy efficiency is the first tool to mitigate the changes taking place, through the reduction of fossil fuel consumption, but at the same time measures for energy demand management are also able to address some of the vulnerabilities of the energy sector in relation to the impacts of changing climate. For example, we should consider as win-win solution: (1) The distribution of energy efficient technologies in end-use efficiency and production services, transmission and distribution can help to counteract the increase in demand and at the same time reduce the production of power in a context of higher temperatures; (2) Demand response programs and efficiency programs aimed at the management of energy peak load, that can help to counteract the increase in peak demand due to increased use of air conditioning and to address the uncertainties in the production and consumption of electricity and heating, due to extreme weather conditions , and so far, avoiding the need for construction of new energy facilities; (3) The manufacturers can design buildings "future proof", ensuring long life characteristics such as orientation and insulation and installing fixtures appropriate for the climate conditions; (4) cities can reduce the environment temperature , and make buildings more energy efficient , with cool roofs or green, (5) the construction of distributed generation, particularly efficient combined production of heat and electricity (CHP) , able to ensure the supply of electricity to large consumers or micro grid because they are less prone to outages due to extreme weather conditions , (6) efficiency programs in water management can address climate impacts on water resources and reduce the consumption of energy for pumping and water treatment. Energy efficiency, energy savings and demand reduction programs offer consumers and relatively inexpensive technologies to utilities and programs that allow a reduction in demand and the amount of climate-altering gases emitted.

### **3. METHODS**

The importance to look at adaptation has become fundamental to tackling climate change with an integrated approach, as repeatedly stressed by the Working Group II of the IPCC, which since long time stressed the concept that mitigation and adaptation should be complementary components of a strategy to response to global warming. Develop an adequate adaptive capacity has become therefore a priority for European policy on climate. The European Commission White Paper "Adapting to climate change: Towards a European framework for action", has traced the path to the definition of the European Strategy for Adaptation which was published last April. The Strategy will provide a leading role of governments but calls for a strong commitment of the local government and companies, since the impact of the changes are highly local. While some national governments are struggling to make binding commitments, many cities have taken the first steps, creating networks such as the ICLEI Initiative Resilient Cities and the EU Adaptation Strategies for Cities Climate (CITIES ADAPT), to share best practices and to promote bottom-up initiatives. The impacts of climate change will be different in every urban context, and therefore new approaches to local urban planning should include these factors in an appropriate manner.

### **4. RESULTS**

A "local tailor made" global response and a mix of real politics it is now necessary for the city to quickly adapt to climate change. The first step of the project BlueAP Bologna Resilient City - led by the Municipality of Bologna - is heading in this direction and proposes the definition of the adaptation plan by 2015. The Plan will be based on an analysis of vulnerability and territorial adaptive capacity - Local Climate Profile - made by ARPA Emilia Romagna. The measures to be implemented will then be identified and shared with the citizens and businesses through a participatory process - implemented by Kyoto Club and Ambiente Italia - which aims to engage the community and to improve the existing resilient capacity, starting the collection of memories and the ancient tradition of Bologna. For responding to the complex future risks a link with what has already been implemented by Bologna Municipality in the definition of its Sustainable Energy Action Plan - Covenant of Mayors and the Metropolitan Strategic Plan will be take in consideration. This integrated approach

show how the Administration is adopting a "Climate-Smart" strategy in future planning.

## **5. CONCLUDING REMARKS**

But the fact remains that today we are facing enormous socio-economic challenges that require immediate attention, with the availability of limited public resources - in particular to finance efforts to prevent the long-term effects of climate change, which, in turn, could seriously affect the global economy. We find ourselves in front of a negative feedback loop daunting. The logic of risk management tells us that countries should invest today for the protection of critical infrastructures and centers of economic activity for two main reasons: (1) estimates of future climate-related losses and damage are on the increase and these annual measures may (2) create new jobs to boost economic growth in the shortest possible time. The real problem is that investment in strategic infrastructure is easier to list than to do; in spite of the benefits you can have both in the short and long term. Thus, a new approach, which is based on a meeting of minds in various professions, sectors and geographical areas, and the ability to act decisively in the face of considerable uncertainty about what the best plan of action, could tell. Continuing to hesitate to act today, we will continue to add burdens to the future generations.

## 6. ACKNOWLEDGMENTS

The present work benefited from the input of Lorenzo Bono, Project Manager at Ambiente Italia, Lucio Botarelli ARPA Emilia Romagna, Chiara Caranti Municipality of Bologna, Giovanni Fini Municipality of Bologna and Raffaella Gueze Municipality of Bologna who provided valuable comments/ideas/assistance to the writing/undertaking of the research summarized here.

## 7. REFERENCES

1. Agrawal, A., and M. Lemos. 2007. A Greener Revolution in Making? Environmental Governance in the 21st Century." *Environment* 49(5): 36-45
2. Agrawal, A. (2008) The Role of Local Institutions in Adaptation to Climate Change. Prepared for the Social Dimensions of Climate Change, Social Development Department. Washington, DC: World Bank. March 5-6.
3. EEA (European Environmental Agency) Environmental Indicators: Typology and Overview, Technical Report, Copenhagen: EEA, 1999.
4. Figueira, J., and B. Roy, Determining the weights of criteria in the ELECTRE type methods with a revised Simos' procedure, *European Journal of Operational Research*, 139(2), 317-326, 2002.
5. Giupponi, C., Decision Support Systems for implementing the European Water Framework Directive: The MULINO approach, *Environmental Modelling & Software*, 22(2), 248-258, 2007.
6. Giupponi, C., A. Sgobbi, J. Mysiak, R. Camera, and A. Fassio, NetSyMoD - An Integrated Approach for Water Resources Management. In: Meire, P., M. Coenen, C. Lombardo, M. Robba, and R. Sacile, (ed.), *Integrated Water Management*, 69-93, Netherlands: Springer, 2008.
7. Intergovernmental Panel on Climate Change (IPCC) 2007a: Climate Change 2007: The Physical Science Basis. Contribution of Working Group I to the Fourth Assessment Report of the Intergovernmental Panel on Climate Change Solomon, S., D. Qin, M. Manning, Z. Chen, M. Marquis, K.B. Averyt, M. Tignor and H.L. Miller (eds.). New York: Cambridge University Press.
8. Intergovernmental Panel on Climate Change (IPCC) 2007b: Climate Change 2007: Impacts, Adaptation and Vulnerability. Contribution of Working Group II

to the Fourth Assessment Report of the Intergovernmental Panel on Climate Change. M.L. Parry, O.F. Canziani, J.P. Palutikof, P.J. van der Linden and C.E. Hanson, Eds. Cambridge: Cambridge University Press.

9. IPCC (2012): Managing the Risks of Extreme Events and Disasters to Advance Climate Change Adaptation. A Special Report of Working Groups I and II of the Intergovernmental Panel on Climate Change [Field, C.B., et al (eds.)]. Cambridge University Press, Cambridge, UK, and New York, NY, USA. 582 pp.
10. Janssen, M.A., M.L. Schoon, W. Ke, and K. Borner. 2006. Scholarly networks on resilience, vulnerability, and adaptation within the human dimensions of global change program. *Global Environmental Change* 16: 240-52.
11. Kates, R. 2000. Cautionary tales: Adaptation and the global poor, *Climatic Change* 45 (2000) (1), pp. 5–17.
12. Kaylen, M. S., J.W. Wade, and D.B. Frank. 1992. Stochastic trend, weather and us corn yield variability. *Applied Economics* 24 (5): 513–18.
13. World Bank (2011). *Conflict, Security and Development: World Development Report 2011*. Washington D.C., USA.
14. World Bank (2007). *CDD in the Context of Conflict-Affected Countries: Challenges and Opportunities*. Report. No. 36425-GLB. Washington D.C., USA.

**Vulnerability, Risk Assessment and  
Adaptation to Climate Change**

**Water management**

## **Experience in water modelling in agriculture considering climate and policy change**

**Bazzani G. M.<sup>1</sup>, Mannini P.<sup>2</sup> and Genovesi R.<sup>2</sup>**

<sup>1</sup>National Research Council - IBIMET, Bologna, Italy

<sup>2</sup>Consorzio Canale Emiliano Romagnolo - CER, Bologna, Italy

\*Corresponding Author: [g.bazzani@ibimet.cnr.it](mailto:g.bazzani@ibimet.cnr.it)

### **Abstract**

Tools and models are commonly used all over the world to support water managers and decision makers in their activities. In the Po Valley in Northern Italy water is a strategic resource since it impacts on both the quality and the quantity of crop production. Over recent years, the variability in water availability has increased dramatically due to the effects of climate change and water is becoming scarce, especially in dry summers when a higher demand from other sectors competes with agricultural use. The implementation of the Water Framework Directive by the Regional Authority, has imposed strict environmental rules and has forced Irrigation Boards to prepare Water Conservation to reduce consumption and improve water quality. This task requires the analysis and comprehension of the interaction of agriculture and water in a context characterized by climate change, the contemporary reform of water and agricultural policies and by market globalisation. The paper presents the Trebbia irrigation district experience, in the Po valley in Italy, where a pilot project is currently set up. The results show that a participative use of well-tailored tools can support the identification of management and planning measures necessary to implement balanced solutions preserving environmental and economic sustainability.

**Keywords:** climate change, water, agriculture, decision support, economic analysis

## **1. TOOLS TO SUPPORT WATER USE IN AGRICULTURE UNDER CLIMATE AND POLICY CHANGE**

Water is a resource which simultaneously serves economic, social and environmental objectives. The availability of the resource, even if renewable, is not infinite and the provision of good quality water is increasingly becoming a limiting factor. In many regions the conflict among competing uses (e.g., civil, agricultural, and industrial) and environmental protection has grown to such an extent that it requires a prompt response [5]. The 2000/60/EC Directive known as the Water Framework Directive (WFD) establishes a framework for common action in the field of water policy in Europe and has as its main goal to raise all water quality to a “good status” by 2015) [17]. It recommends the consideration of economic principles, e.g., the polluter pays, cost recovery for water services and the inclusion of environmental and resource costs economic and it calls for the application of economic approaches and tools for achieving its environmental objectives in the most effective manner.

Climate change makes this task more demanding and complex [18, 20]. Temperature and rain have changed impressively in recent years, more in the distribution than in quantity, with an alternance of dry and wet periods and often extreme events have broken the normal course of the seasons.

Previous studies have shown that the impact on agriculture will probably be severe, especially in the Mediterranean region where irrigated agriculture, though covering only 20-25% of the total cultivated surface, accounts for about 50% of total agricultural production and 60-80% of the total water demand [4, 10, 11]. The Common Agricultural Policy (CAP) reform has recognized the centrality of water issues in agricultural policy and introduced several measures to make a better use of the resource [15].

The present situation, characterized by climate change, the contemporary reform of water and agricultural policy and by market globalisation, represents a moment of discontinuity with the past [26]. Higher environmental risk and price variability put at risk agricultural profitability which is responding by trying to adapt to the new conditions and this has an important impact on water demand, traditional irrigated crops are disappearing, others are emerging. In this context a feasible way to ascertain the effects of many interlinked changes is to adopt integrated models to analyse possible future states. While uncertainty can never be eliminated, models

can explore it by generating information which decision-makers and the public can use to make better-informed decisions. Information represents a strategic resource which need to be fully exploited. Many data are in fact available but up to now have not been adequately connected including: land use, crop irrigation requirements under different climatic and geographic conditions, available water from different sources and economic data on cost and benefit and labour impact.

Tools and models are commonly used all over the world to support water managers and decision makers in their activities[8, 25], over the last two decades much effort has been expended in order to develop new integrated tools [2, 19, 21, 22, 27], but in Italy, as far as concerns water use in agriculture, only GIS tools seem to be used, while integrated tools still receive little attention. Many barriers exist between research, where tools are created, and the real world where most decisions are taken on the basis of consolidated experience and habits, and tools are generally perceived as expensive, time consuming and unnecessary if not completely useless [12].

## **2. THE TREBBIA IRRIGATION DISTRICT CASE STUDY**

In the Po Valley in Northern Italy water is a strategic resource since both the quality and quantity of crop production are highly dependent on its availability. The irrigation season starts in April and ends in September, but is highly concentrated in June and July, in contrast with rain distribution which is generally low in that part of the year. Most farmers have autonomous access to water at the farm level through wells and pumps directly from the aquifer, but most of them also have access to surface water provided by the local “Consorzio di bonifica ed irrigazione” (Irrigation and Reclamation Board - IRB), a public body with legal rights to the resource derived from rivers [24].

Over recent years, the variability in water availability has increased dramatically due to the effects of climate change and water is becoming scarce, especially in dry summers when a higher demand from other sectors competes with agricultural use. The implementation of the WFD by the Regional Authority, has imposed the respect of the Safe Minimum Standard (SMS) in the rivers and has forced IRBs to prepare Water Conservation Plans (WCP) in accordance with Water Blueprint recommendations to reduce consumption and improve water quality [16].

In this context the Institute of Biometereology (IBIMET) of the Italian National Research Council and the Board for “Canale Emiliano Romagnolo” (CER), a research and training institute active in the Po Basin, started a research activity to analyse water use in various irrigation districts, to identify key issues and existing problems and to set up operative tools and models to assess in quantitative terms feasible solutions to be implemented in the WCP [6, 7, 8].

Different tools have been implemented to support farmers and irrigation boards in water planning and management both at the basin and farm scale considering climate and policy change and different economic conditions. The models are based on mathematical programming techniques implemented in GAMS [28] and have been run as a simulation tools adopting a scenario approach to deal with uncertainty [23]. All the DS can be easily updated, since data are kept separate from the modelling structure; extended to address new issues thanks to the modular approach adopted; applied in other contexts in a short time and at low cost whenever similar problems and data exist.

The Trebbia irrigation district, which includes the plain forming part of the Piacenza Province in the region of Emilia Romagna (Fig. 1, left), is taken as reference.

[Fig. 1 The Trebbia River irrigation district]

In this area, covering nearly 180 km<sup>2</sup>, water used to be abundant and farmers have developed an irrigated agriculture specialized in the production of tomatoes and other vegetables for industrial processing and livestock based on maize and alfalfa cultivation. Over 11000 hectares, nearly two-thirds of the c.18000 hectares of cultivated land are irrigated.

The Piacenza Irrigation and Reclamation Board (PIRB) on average withdraws from the Trebbia River 4000 l/s. In the past, in dry years this amount could be increased up to 6000 l/s. The Board adopts a Geographical Information System (GIS) tool to support the management activity which fully describes the irrigation network (Fig. 1, top right) and land use. Fig. 1, bottom right, shows in grey the distribution of the area irrigated at the cadastral level. The irrigation district is divided into two sub-basins, one to the east/right and one to the west/left of the Trebbia River which flows between them.

The water derived from River Trebbia by the Irrigation Board by period and location is a key variable. This quantity is an input for the farmers who would like to have an abundant access to the resource, but which is instead constrained to a quantity fixed by law. The withdrawal volume is reduced by distribution losses in the network which in many cases have been estimated to be as high as 70%, since many channels are old and operate under poor conditions, and on average are assumed equal to 50% of the pumped volume as stated in a previous study conducted by the Emilia Romagna Environmental Agency (ARPA)[3].

This unsatisfactory situation, from an agricultural point of view, is further deteriorating since the requirement to respect the SMS in the river could in future reduce the quantity available to the irrigation board. This possibility is made more concrete by higher competing uses coming from the urban sector, and climate change which in certain years creates conditions which make it difficult to respect the environmental goal which is the first priority by law.

Estimating the effects of policy measures as requested by the WFD requires the identification of the causal links between the proposed measure and impacts on human activities and the environment. A conceptual framework to address this issue can be found in the DPSIR (Driving force–Pressure–State–Impact–Response) approach proposed by the European Environment Agency [14] for the description of environmental pathways. A conceptual model addressing water use in agriculture linking the macro and the micro levels has been set up to facilitate interdisciplinary dialogue and the definition of a common vision among stakeholders, before adopting and implementing any specific quantitative models [9]. The main outcome of this first phase can be summarized as follow.

- Agriculture is recognized as a multifunctional activity to be assessed within a multi-criteria framework. In the present context relevant dimensions are: the economic dimension quantified by farm income; the social dimension measured by employment; the environmental dimension identified by water inflow and outflow by source.
- The following key issues should be further investigated:
- assessing water demand by period considering different climatic and economic conditions and comparing them to water supply;

- investigating the surface/deep water relationship;
- analysing available water management options at the basin scale considering allocation (space) and scheduling (time);
- assessing the impact on representative farms of different scenarios considering variations in water availability and the cost of irrigation services.

In order to investigate these aspects two different tools have been implemented: an integrated irrigation district model on the macro scale and different bio-economic farm models on the micro scale [7].

In Emilia Romagna Region the CER since 1985 supports farmers in irrigation practices through a sophisticated alerting system integrating computer simulation, WEB and mobile telephone with in-field assistance. An ad hoc service called IRRINET is employed which yields an average 20% reduction in water consumption.

At farm level another tool called DSIRR is adopted. The tool is a scenario manager for bio-economic models which analyze the conjoint choice of crop mix, irrigation level, technology and employment as an optimization problem. Inputs and outputs including externalities are expressed in physical terms, this implies the possibility of measuring and evaluating the effects of different sources of change on environment as well as on socio-economic dimensions, and requires the integration of agronomic and economic data and models. Optimal irrigation requirements for full production over a reference surface of one hectare are provided by the CER for homogeneous areas and different climatic conditions (dry, average, wet year) considering the overall irrigation season, from April to September, using ten-day periods. These parameters, diversified by crop and period, type of soil and irrigation technique, are calculated by the CER through the IRRINET software which entails making water balance calculations on the basis of real data related to farming practices. The CER also provides data on production losses due to missing irrigation. Such values vary throughout the season and depend on the production phase of the crop. They are calculated with a methodology which adapts the FAO approach to local conditions [1, 13].

The approach allows further levels of analysis, among them: changes in soil and irrigation management practices, changes in the use of farm input and natural

resources, and how agri-environmental measures and environmental regulation may constrain actions taken by farmers.

### **3. APPLICATION OF THE SUANBI TOOL IN THE TREBBIA IRRIGATION DISTRICT**

At the irrigation district level a different tool (SUANBI - water use simulator in irrigation districts) has been implemented integrating various data: land use at cadastral level, crop irrigation requirements and water derived from the river. The irrigation network is linked to the cadastral units to calculate water balances, including farmers' provision from the aquifer, over ten-day periods. Economic data quantify the cost and benefit of the agricultural activity.

A first group of applications analyse the impact of management options under different policy and climate scenarios.

The PIRB has three pumping stations, two furnish the right sub-basin, one the left. Water withdrawals from the Trebbia River in the period 2004-11 average nearly 35 M m<sup>3</sup>. In the period a decreasing trend can be observed.

Unitary irrigation requirements show a great variability in the observed period due to the impact of changing climatic condition. The volume for the entire irrigation season on average goes from about 1600 m<sup>3</sup>/ha for string-beans and sugar-beet up to over 4200 m<sup>3</sup>/ha for mixed greens.

Land use represents a basic data in the analysis. The 2011 situation is taken as an example. The database comprises 48,654 observations, each identifying a plot on a cadastral basis, for a total surface area of nearly 22350 ha of which 17876 (about 80%) is cultivated land. Rain-fed cultivations cover 6532 ha, 36.5% of the total; winter cereals alone represent 85% of this group. Irrigated crops extend over 11354 ha (63.5%); two crops alone cover 2/3 of this surface: maize and industrial tomatoes (respectively 38% and 30%), while an additional 25% is cultivated with alfalfa and mixed greens which, along with part of the maize, is used for animal feed.

The joint consideration of land uses, the unitary irrigation requirements, PIRB withdrawal from the Trebbia River and water allocation in the network, has led to the estimation of the total irrigation requirements by channel and sub-basin and to an

estimate of the missing volume to full irrigation, which is assumed to be pumped from the aquifer by the farmers. Tab. 1 summarizes the results by month, but the model quantifies these values over the full irrigation season considering a ten-day periodization.

[Tab. 1 Water balance]

Over the season only 13.16 M m<sup>3</sup> of the 30.468 M m<sup>3</sup> derived by the PIRB are used by the farmers for irrigation since 17.309 M m<sup>3</sup>, 56.8% of the pumped volume, is lost in the network, most of it infiltrating into the soil. This high loss value is mainly due to the fact that no materials are used for the interior lining over 90% of the network and channels must be completely filled in order to permit water pumping at the farm level. The consideration of periods offers a richer picture which supports water management. Variability is clear, even if supply is always lower than the irrigation requirement (42% on average), it reaches a minimum in August when less than 17% of the demand is covered by the PIRB (Fig. 2). The relevance of the aquifer for the irrigation balance is high, and in the figure the gap between the requirement and the supply is shown.

At the territorial level it emerges that while the PIRB on average allocates 76% of the total distributed volume to the right sub-basin (see figure 1) and only 24% to the left, water requirements show an opposite distribution: about 44% for the right and 56% for the left. Simulation clarifies that reallocation among sub-basins and different scheduling could have important positive environmental effects by lowering the existing high consumption from the aquifer with no economic impact on the farmers.

The joint consideration of economic data including production, output prices, subsidies, variable costs with water requirements permits a water productivity index to be estimated for the entire irrigation season. This index varies from 18 Euro-cent/m<sup>3</sup> for sugar-beet up to over 1 Euro for industrial vegetables (Tab. 2).

[Tab.2 Crop indicators]

Given the diversity existing within the irrigation basin separate analyses have considered distinct areas with homogeneous characteristics. As an example the Villano area, located in the southern part of the right sub-basin is presented. The chosen period is the third decade of June 2011; in that decade important crops such as maize and industrial tomatoes are in the critical vegetative phase when water

scarcity is particularly critical. For this reason this period is a good example with which to analyse the impact of reductions in water availability for the Irrigation Board, which could be introduced in the near future due to the implementation of the SMS.

The total irrigated surface covers 416.26 hectares, nearly 50% being cultivated with industrial tomatoes while maize covers an additional 34% (Tab. 3). The total irrigation requirement in the decade is 166186 m<sup>3</sup>, nearly 400 m<sup>3</sup>/ha. In the area another 136.23 hectares are cultivated with irrigable crops which do not require irrigation in that period. Unitary production and losses due to missing irrigation are reported in the final two columns. Ten channels, with a total length of 24.61 km provide water to the area.

[Tab.3 Villano irrigated crops in the third decade of June]

Water allocation is analysed under two scenarios: the first reproduces the existing institutional framework where farmers have equal rights to water; the second seeks the efficient allocation which minimizes the economic damage due to production losses but violates the equity criteria.

To provide 166186 m<sup>3</sup> at the farm level, at least 317794 m<sup>3</sup> needs to be withdrawal from the river, since network losses in the considered channels are 42%. A parametric analysis with a progressive reduction of 5% of this initial quantity has been conducted. The results are presented in Fig. 3, where the horizontal axis shows water quantity in cubic metres, the left axis is the total damage in Euro, and the right axis is unitary damage in Euro per hectare.

[Fig. 3 Economic impact of a reduction of PIRB water supply in the third decade of June 2011 in the Villano area]

In the case of equal rights to access water, increasing water scarcity has a constant impact on damage as the unitary damage line, represented with a dotted line and square indices, shows by being parallel to the horizontal axis at 765 €/ha. In fact due to equal rights to access water all plots reduce the available quantity in the same percentage; the aggregate effect is the straight continuous line with square indices representing the total damage. This is clearly an inefficient solution since water productivity is different among crops as the index reported in Tab. 3 shows.

Optimal water allocation from an economically efficient point of view can be calculated by removing the water rights constraint and maximizing the aggregate

agricultural income. The results for this scenario are plotted as the two lines with circular indices, dotted for the unitary damage and continuous for the total damage. Both lines show a non-linear trend which depends on the different water productivity of the crops in that period, as well as from the location of the plots, since network losses to provide water are considered. Irrigation is in fact suspended on the cultivation in the following order: mixed greens, maize, industrial tomatoes and lastly industrial vegetables, starting from the parts of the sub-district more distant from the pumping station and served by inefficient channels. When scarcity is low, unitary damage is limited to 432 €/ha since only mixed greens cultivation suffers production losses. This value increases up to 766 €/ha when all crops suffer water scarcity.

Other criteria can be considered in water allocation and each of them leads to different results; for instance, maximizing irrigation network efficiency, which is relevant for environmental considerations, stops irrigation in the area served by channels with higher losses and in the ones more distant from the pumping station, since losses increase with the distance covered in the network. Separate analyses have estimated the equivalent values in other periods and areas and additional variability exists among the years.

#### **4. COMMENTS AND CONCLUSIONS**

The Trebbia Basin case study shows that a better use of available information can support easy to implement but effective measures, such as water reallocation among sub-basins and a different scheduling. These measures have positive environmental effects by lowering the pressure on the aquifer, with no impact on the economic sustainability of the agricultural sector but require the adoption of compensative measures when farmers' water rights are changed and/or a redesigned of the tariff scheme.

Reductions of the existing PIRB rights to withdraw from the Trebbia River are foreseen as possible in the near future. This environmental policy measure, which should be adopted to protect surface water, would induce, as a primary effect, a reduction of the PIRB supply to farmers, which in turn would have not only an economic impact, but different environmental consequences. Low water in the irrigation network would reduce infiltrations, which currently represent over 40% of

the total circulating volume, but also would induce a substitution effect at farm level. In normal years farmers would be pressed to pump more water from the aquifer to maintain full irrigation to the cultivated crops. In dry years the situation could be drastically different since the aquifer may not represent an accessible source and so water scarcity would emerge. In this case the analysis of the integrated water-production systems in a scenario approach by comparing alternative institutional frameworks can provide useful information to decision makers; the quantified lower efficiency of the existing allocation, based on equal farmers' rights to water, with respect to the economically efficient allocation can be used to start a reallocation process where introducing compensation could reduce the negative impact of water scarcity while still respecting equity issues.

In a similar fashion the tools favour the identification of set of measures capable of providing balanced solutions preserving water and agriculture activity as the Blue Print recommends.

## **5. ACKNOWLEDGMENTS**

We thanks the Consorzio di Bonifica e di Irrigazione di Piacenza for the valuable collaboration.

## **6. REFERENCES**

1. Allen, R.G, et al. (2006), "Crop Evapotranspiration - Guidelines for computing crop water requirements", Irrigation and Drainage Series, No. 56, FAO, Roma.
2. Argent, R. M. (2004), "An overview of model integration for environmental applications-components, frameworks and semantics", Environmental Modelling and Software, Vol. 9, pp. 219-234.
3. ARPA (2006), "Studio del bacino idrografico del fiume Trebbia per la gestione sostenibile delle risorse idriche", Regione Emilia Romagna, Bologna.
4. Bartolini, F., Bazzani, G.M., Gallerani, V., Raggi, M. and Viaggi D. (2007), "The impact of water and agricultural policy scenarios on irrigated

farming systems in Italy: An analysis based on farm multi-attribute linear programming models”, *Agricultural Systems*, Vol. 93, pp. 90-114.

5. Bates, B.C., Kundzewicz, Z.W., Wu, S. and Palutikof, J.P., Eds. (2008), “Climate Change and Water. Technical Paper of the Intergovernmental Panel on Climate Change”, IPCC Secretariat, Geneva, 210 pp.
6. Bazzani, G.M. (2005) “A decision support for an integrated multi-scale analysis of irrigation: DSIRR”, *Journal of Environmental Management*, Vol. 77, pp. 301-314.
7. Bazzani, G.M. (2005), “An integrated decision support system for irrigation and water policy design: DSIRR”, *Environmental Modelling and Software*, Vol. 20, 153-163.
8. Bazzani, G.M. (2011), “Review of model-based tools with regard to the interaction of water management and agriculture”, in *Decision Support for Water Framework Directive Implementation Volume 3*, Vanrolleghem, P.A. (Eds.), IWA Publishing; ISBN-10: 1843393271.
9. Bazzani, G.M. (2013), “Tools and models to support water management in agriculture under policy and climate change. The Trebbia irrigation district experience”, IAERE Annual Conference, 8-9 February 2013, Ferrara (I), in print.
10. Bazzani, G.M., Di Pasquale, S., Gallerani V., Viaggi D. (2004), “Irrigated agriculture in Italy and water regulation under the European Union Water Framework Directive”, *Water Resour. Res.*, Vol. 40, W07S04, doi:10.1029/2003WR002201.
11. Berbel, J., Gutierrez, C, Eds. (2005), “Sustainability of European Irrigated Agriculture under Water Framework Directive and Agenda 2000”. EUR 21220. Luxembourg: Office for Official Publications of the European Communities. ISBN 92-894-8005-X.
12. Borowski, I., Hare, M. (2007) “Exploring the Gap Between Water Managers and Researchers: Difficulties of Model-Based Tools to Support Practical Water Management”, *Water Resources Management*, Vol. 21:7, pp. 1049-1074.

13. Doorenbos and Kassam (1979), "Yield response to water, Irrigation and Drainage Series, No. 33", FAO, Roma.
14. European Environment Agency (1999), "Environmental indicators: Typology and overview", Technical report No 25/1999, 7 September.
15. European Commission (2010), "The CAP towards 2020, Meeting the food, natural resources and territorial challenges of the future", Communication from the Commission to the European Parliament, the Council, the European Economic and Social Committee and the Committee of the Regions, 672 final Brussels, 18.11.2010.
16. European Commission (2012), "A Blueprint to Safeguard Europe's Water Resources", Communication from the Commission to the European Parliament, the Council, the European Economic and Social Committee and the Committee of the Regions, 673 final, Brussels, 14.11.2012.
17. European Union (2000), "Directive 2000/60/EC of the European Parliament and of the Council establishing a framework for the community action in the field of water policy". Official Journal (OJ L 327), 22 December.
18. Global Water Partnership (2000), "Integrated water resources management", Paper 4, Technical Advisory Committee.
19. Heinz, I., M. Pulido-Velasquez, Lund, J.R. and Andreu, J. (2007) "Hydro-economic Modeling in River Basin Management: Implications and Applications for the European Water Framework Directive", Springer Netherlands, ISSN 0920-4741 (Print) pp. 1573-1650.
20. IPCC (2007), "Fourth Assessment Report: Climate Change (AR4)", Pachauri, R.K. and Reisinger, A. (Eds.), Geneva, Switzerland. pp 104.
21. Jakeman, A.J., Letcher, R.A. (2003), "Integrated assessment and modelling: features, principles and examples for catchment management", Environmental Modelling and Software, Vol. 18, pp. 491-501.
22. Kundzewicz, Z.W., Hattermann, F. and Krysanova V. (2010), "Model-supported implementation of the Water Framework Directive", Water, 21, April, pp. 25-26.

23. Leenhardt, D., Therond O., Cordier M.O., Gascuel-Oudoux C., Reynaud A., Durand P., Bergez J., Moreau, P. (2012), "A generic framework for scenario exercises using models applied to water-resource management", *Environmental Modelling and Software*, Vol. 37, pp. 125-133.
24. Massarutto, A. (2001), "Water Institutions and Management in Italy", Working Paper No. 01-01-eco. Università degli Studi di Udine, Dipartimento di Scienze Economiche.
25. McKinney, D.C., Cai, X., Rosegrant, M.W., Ringler, C., Scott, C.A. (1999), "Modeling Water Resources Management at the Basin Level: Review and Future Directions", International Water Management Institute, Colombo, Sri Lanka.
26. Mejias, P., Varela-Ortega, C. and Flichman, G. (2004), "Integrating agricultural policies and water policies under water supply and climate uncertainty", *Water Resour. Res.*, Vol. 40, W07S03, doi:10.1029/2003WR002877.
27. Parker, P., Letcher, R., Jakeman, A., Beck, M.B., Harris, G., Argent, R.M., Hare, M., Pahl-Wostl, C., et. al. (2002), "Progress in integrated assessment and modelling", *Environmental Modelling and Software*, Vol. 17, pp. 209-217.
28. Rosenthal, R. E. (2012), "GAMS A User's Guide", December, GAMS Development Corporation, Washington, DC, US.

## 7. FIGURES AND TABLES

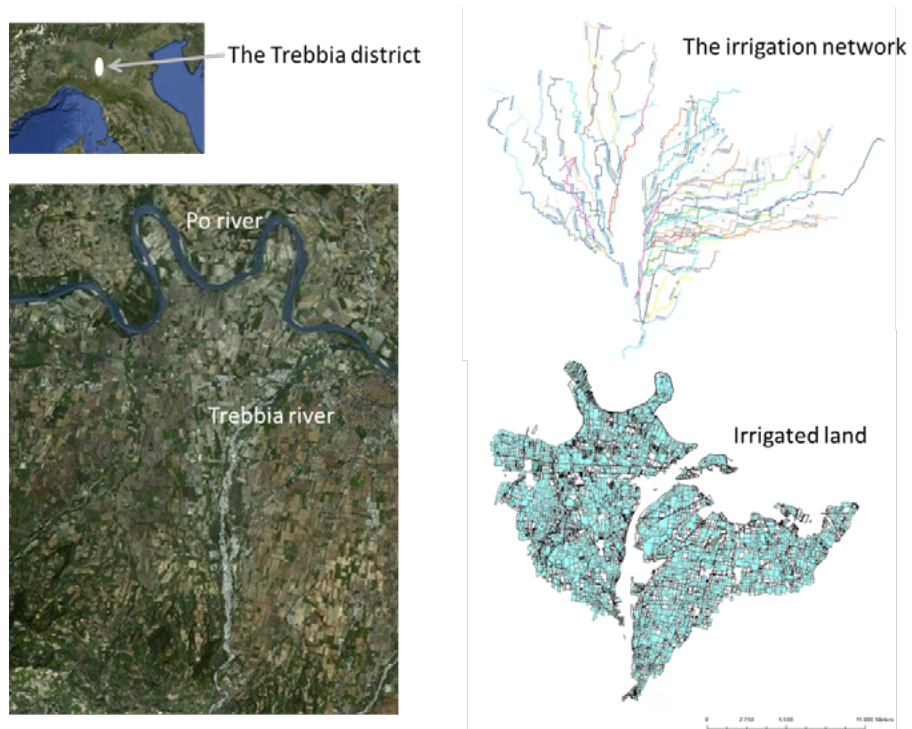


Fig.1 The Trebbia River irrigation district

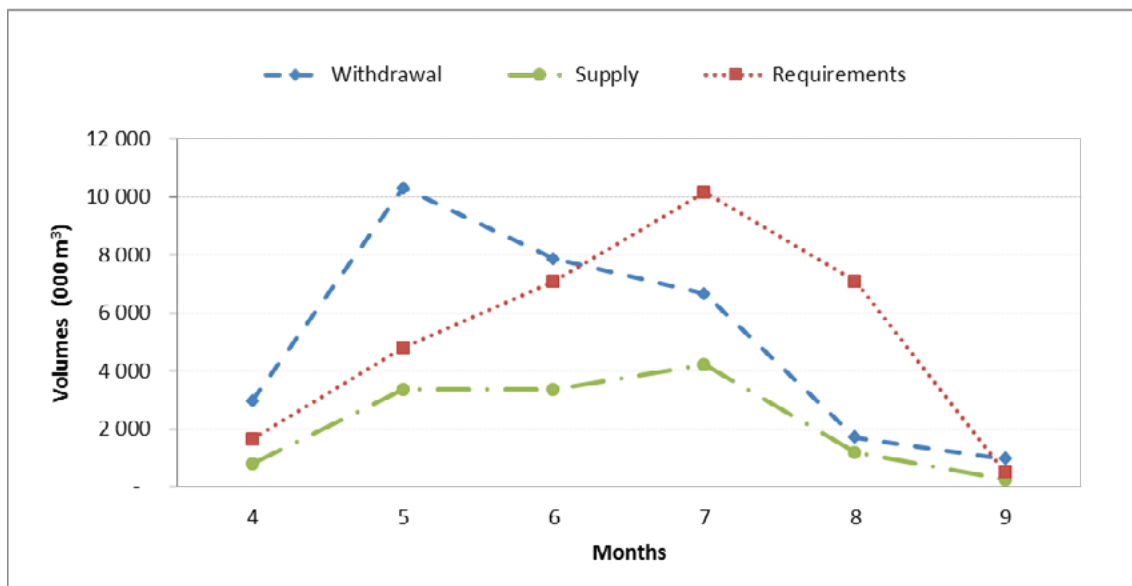


Fig. 2 Withdrawals from the Trebbia River and irrigation requirements

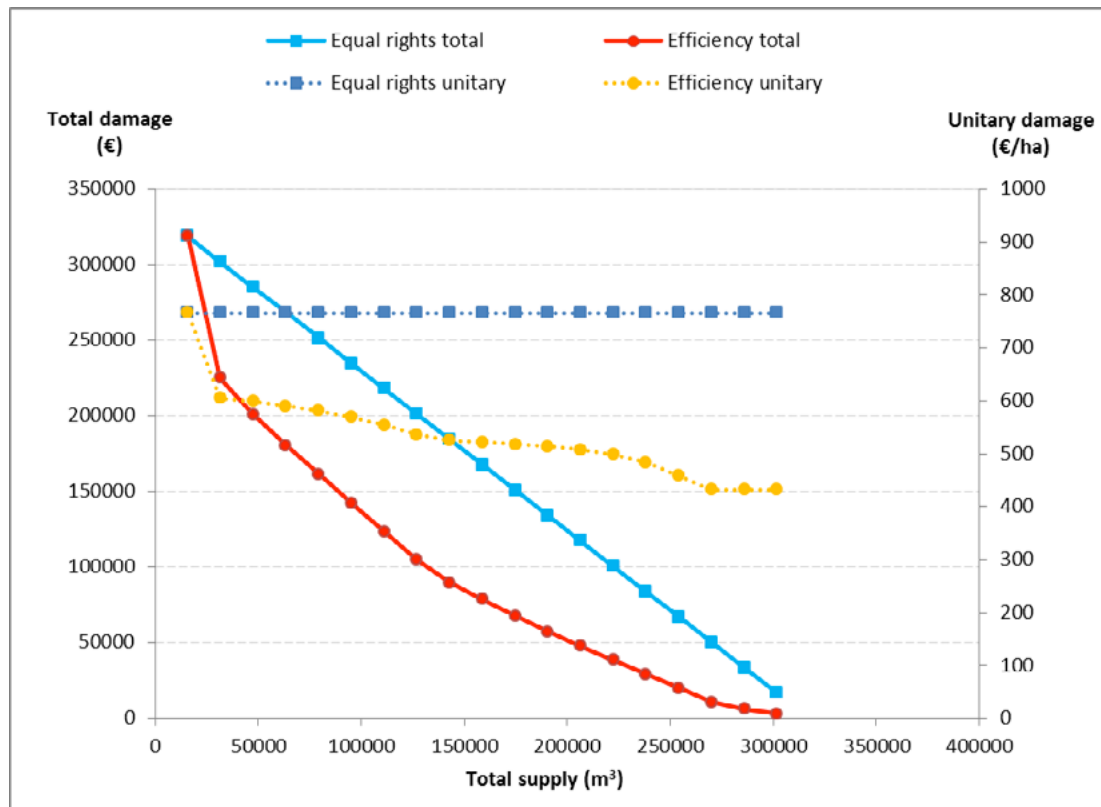


Fig. 3 Economic impact of a reduction of PIRB water supply in the third decade of June in the Villano area

Description	Unit	Total	Months					
			4	5	6	7	8	9
Unitary irr. requirements	000 m <sup>3</sup> /ha	2.753	0.144	0.423	0.624	0.894	0.625	0.044
Irrigation requirements	000 m <sup>3</sup>	31257	1635	4798	7082	10151	7096	495
PIRB withdrawals	000 m <sup>3</sup>	30468	2957	10313	7874	6664	1695	966
Network infiltration	000 m <sup>3</sup>	15927	2059	6476	4132	2155	425	681
Network evaporation	000 m <sup>3</sup>	838	108	341	217	113	22	36
Network other losses	000 m <sup>3</sup>	544	-	134	160	178	62	10
Total network losses	000 m <sup>3</sup>	17309	2167	6950	4509	2447	509	726
Deep water supply	000 m <sup>3</sup>	18097	844	1435	3717	5935	5910	255
PIRB supply	000 m <sup>3</sup>	13160	790	3363	3364	4217	1186	240

Tab.1 Water balance by month

Crop	Unit	Maize	Soya	Sugar beet	Industrial tomatoes	Industrial vegetables	Alfalfa	Mixed greens
Irrigated	ha	4368	178	164	3407	399	1698	962
Irr. requirement	m <sup>3</sup> /ha	2960	1810	1590	2340	1330	2000	4440
Production	q/ha	137	60	550	704	70	230	184
Gross margin	€/ha	685	510	281	1571	1350	1580	1477
Water productivity	€/m <sup>3</sup>	0.23	0.28	0.18	0.67	1.02	0.79	0.33

Tab.2 Crop indicators

	Surface ha	Unitary irr. req. m <sup>3</sup> /ha	Total irr. req. m <sup>3</sup>	Unitary production q/ha	Unitary losses q/ha
Maize	142.74	525.14	74960	137.2	44.0
Industrial tomatoes	203.77	320.28	65265	704.0	137.3
Industrial vegetables	27.99	259.29	7242	70.0	14.0
Mixed green	41.75	448.32	18719	183.0	36.0
Total irrigated	416.26	399.29	166186		
Irrigable not irrigated	136.23				
Total irrigable	552.49				

Tab.3 The situation in the third decade of June in the Villano sub-basin

# Water security issue in the Caribbean Windward Islands

Amadio M.<sup>1</sup>

<sup>1</sup>Euro-Mediterranean Centre on Climate Change – Venice, Italy

\*Corresponding Author: [mattia.amadio@feem.it](mailto:mattia.amadio@feem.it)

## Abstract

Water security in Small Island Developing States (SIDS) has historically been a challenging goal due to their small geographic extension, isolation and limited water storage capacity. SIDS are highly exposed to both prolonged periods of deficient precipitation and intense storm events, resulting respectively in periods of water scarcity and flood events. Their economies, relying mostly on tourism, have low resilience to external shocks and high vulnerability to natural hazards. Climate change may pose additional strains to their economic and social development due to alteration of precipitation regimes and increase in extreme meteorological events. This paper concerns the issue of present and long-term freshwater security in the Windward Caribbean island states. A framework is developed to relate key drivers and stressors to both natural freshwater availability and national demand. Then, historical trends about freshwater supply and observed climate are summarized and compared with projections from a regional climate scenarios; national water demand records are collected and related to main economic activities, such tourism and agriculture. Based on the analysis of present status and projected scenarios, evidence of key vulnerabilities in water security are discussed to inform the climate adaptation strategies.

Keywords: Water Security SIDS Caribbean Islands

## 1. INTRODUCTION

SIDS are a group of island-based countries spread between the Caribbean Sea and the Atlantic, the Indian and the Pacific Oceans. They are recognized as some of the most beautiful places on Earth, with atolls of white sand beaches, mountain ranges covered in cloud forest, historic ports and towns, and agricultural landscapes. However, their distinguishing features also bring some intrinsic issues. They are *small*, since the available land surface is physically very limited. Small is also the population, below 200 thousand residents, comparable to that of a medium-sized town, and little are the available natural resources in comparison to neighboring landlocked countries. Tourism income, within their small economies, often accounts for up to 50 per cent of the total GDP [1]. Being *islands*, most of their population and activities are located near the coastline, which is exposed for its whole perimeter to hurricanes and storm surges. Lastly, as they are on a *developing* track, they are trying to improve their infrastructures to achieve a better quality of life, but there are some specific challenges to tackle. Among them, water security is among the most important ones. Freshwater availability and quality has been a major issue on many small islands, but especially the south-eastern Caribbean sub-region is quoted to be very water scarce [2]. A country is classified as “water scarce” if available water resources are insufficient to satisfy long-term average requirements [3]. Some Caribbean SIDS are already quoted as very scarce, like Barbados, St. Kitts, Antigua and Barbuda [4]. However, IPCC [5] highlights a lack of both reliable records of climatic observation and properly developed regional projections. Moreover, this region shows a strong inter-seasonal and inter-annual variability in terms of water availability due to cyclic meteorological phenomena, such as ENSO, which hinders the identification of a climatic trend.

## 2. THE WINDWARD ISLANDS

The Windward Islands consist of a small group of countries located in the south-eastern part of the Caribbean region, known as Lesser Antilles. Two countries are included as case study for this study, St. Lucia (SLA) and St. Vincent and Grenadines (SVG), shown in figure 1. The main islands of Saint Lucia and Saint Vincent share similar characteristics: they are volcanic islands consisting of a central high plateau, usually the wettest area, dropping to the sea through undulated plains

or steep cliffs. River basins can be very different on the same island, smooth or very rugged. Due to their and geographical proximity, they share similar climate conditions and are thus prone to similar vulnerabilities. They are not the most water-stressed islands [6] as almost the whole population is reported to have access to the resource [5,6,7], yet their water management systems are not capable of ensuring water security throughout year [10]. The Grenadines, an archipelago of over 30 islands, represent a much smaller and sensible reality. Both countries have nascent water management legislation and planning, though they lack sufficient human and financial capabilities to implement the most efficient and effective solutions. The absence of a comprehensive sewage disposal system (only 5 per cent of population served in the southern Caribbean) is also a major problem [11], contributing to pollution and deterioration of water quality. Water leakage is another critical factor: average non-revenue water (NRW), which is treated water “lost” between the production plant and the customers, peaks 50 per cent in this region. This loss can happen due to real leaks, or non-paid withdrawals. Tourism is a critical sector for both countries, accounting for about half of their national GDP. But as tourism increases [12], so does the demand for freshwater and the pressure for pollution control and maintenance of water security. Agriculture is diffused in both main islands, even though its economic importance is declining.

Effective water management aimed at water security requires an analysis of both supply and demand patterns of a country and the climatic and non-climatic drivers that determine them [13], though the amount of rainfall over the island is the first limiting factor of availability. The availability of freshwater in these countries can change due to effect of different stressors:

- Altered precipitation, runoff and recharge patterns and rates leading to increased drought periods frequency, intensity and duration.
- Increase in sea level, erosion of coastal systems and salinization of aquifers.
- Increase in storms frequency and intensity, with tidal extremes and storm surges causing inundation and disruption of water infrastructures.
- Increase in deforestation rate, amplifying soil erosion and reducing infiltration.
- Issues in the management and distribution of the resource (leakages, pollution).
- Increased demand due to socio-economic factors, such as population growth, tourism trends, agricultural activities.

Figure 2 provides a framework relating climatic and non-climatic drivers and stressors as affecting freshwater supply and quality or freshwater demand.

### 3. CURRENT STATUS OF WATER AVAILABILITY

Water availability in SIDS depends on an a unique and sensitive hydrological system [14] which is strongly influenced by island geomorphology, soil and vegetation, climate variability and human activity, including withdrawal of water and pollution [15]. Both SLA and SVG main islands consists of submerged volcanic mountains (figure 3), characterized by impervious rock and steep slopes, leading to high levels of surface run-off. Local population traditionally relied on rainfall as a source of water, though their small size and the lack of important natural surface water reservoirs, such as big rivers and lakes, does not help for abundant long-term rainwater capture. However, both main islands have perennial streams due to low rock permeability, while the low-lying Grenadines islands rarely have surface water [15]. Few groundwater resources infiltrates in the fractured basaltic rock, but their importance for human use is marginal due to quality issues and abstraction costs [16].

The Grenadines, due to their small size and low elevation, cannot collect enough rainfall to feed permanent rivers and streams, and their calciferous nature does not support water retention [17]. The geometry of their aquifers typically shapes as an unconfined fresh-water lens which floats on the underlying saline water [18]. There is no distinct border between saltwater and freshwater, but rather a mixed transition zone of brackish water. Water lenses may be 20 meters deep on some high islands, while in low islands such as coral atolls they hardly reach 20 cm. The combined effect of sea level rise and over-withdrawal from shallow groundwater resources has already caused saline intrusion in some very small islands, which led to the depletion of the resource [15].

Water supply in SLA and SVG main islands is produced by several Water Supply Systems located in different watersheds and distributed to the population via an integrated network of river intakes, treatment plants, and transmission pipelines [19]. Raw water is taken from the source uphill to the treatment plants where it is then treated in filtration plants followed by disinfection. In SLA and SVG the entire population has access to acceptable quality drinking water, mostly through house and yard connections. In SVG production of water increased in the last decade by 13

per cent to an average daily production of 25 thousand cubic meters. Dalaway plant provides with 41% of freshwater production (figure 4). SLA produces an average of 63 thousand cubic meters per day from 20 treatment plants.

Natural disasters impacts water infrastructures and cause interruption of the distribution network, but land use change has also a role. In such high islands with moderate or steep slopes, the removal of trees for agriculture, firewood and mining cause erosion and faster rainfall runoff, resulting in loss of soil, high water turbidity, and sediment loads in water treatment plants [14]. As an example of this, the John Compton dam in Saint Lucia have been designed to hold 3 million cubic meters to serve the near capital of Castries, but it actually holds just 1.5: debris and silt have filled half of its capacity after recent disaster events (Hurricane Tomas, Christmas Storm) caused heavy runoff and landslides [20]. This significantly reduces the capacity for long term water storage. Furthermore, these countries depend on revenues from tourism, which are also strongly susceptible to natural disasters. In fact, the direct damage to the network is often followed by an indirect economic impact caused by loss of touristic presences during and after an emergency.

#### **4. PROJECTED CHANGE IN WATER AVAILABILITY**

Climate change literature is limited by a lack of reliable data and observations regarding past climate trends in this region [21]. Observational records for the Caribbean [22] report a 30-years warming trends ranging from 0.24°C to 0.5°C per decade and a decline in rainfall for the 1971 to 2004 period. However, seasonal effect coupled with climate variability may lead up to a 40 per cent reduction in water supply during the dry season [8,26]. The IPCC [24] states that nearly all climate change scenarios indicate with very high confidence that water resource availability of SIDS are likely to be seriously compromised in terms of both quantity and quality. Downscaled projections of SRES A2 and B2 climate scenarios produced by PRECIS-RCM for 2071-2099 suggest a warming between 1 and 5°C and small reductions in rainfall in the eastern Caribbean, even though with some uncertainties. With the exception of the northern latitudes, most of the Caribbean can be up to 25 per cent drier in the annual mean by 2080 under both A2 and B2 scenarios. The decrease ranges from 25–50 per cent and is largest over the Lesser Antilles and the south-central Caribbean basin. There is no unambiguous agreement that climate change

will cause an increase in extreme weather events on SIDS. In general, an increase in the intensity and duration of tropical storms has been identified, though they are strongly dependent from ENSO inter-annual variability, which limits the evaluation of these trends [22]. The AR5 [25] reconfirms with high confidence the high level of vulnerability of water security in SIDS due to multiple stressors, both climate and non-climate, though baseline monitoring of island systems and further downscaling of climate-model projections would heighten confidence in projecting impacts.

## 5. NATIONAL WATER DEMAND

*NWD* includes all sources of consumption in the island, though only a share of it can be quantified. Demand from households is the largest among all demand sectors in both island, and it is slowly growing despite the population trend being now almost flat after a strong growth after 1960. Per capita consumption is about 136 liters per day, on average (equal to 50 m<sup>3</sup>/year). However, during the dry season consumption is limited to 46 liter per day in water scarce area. In SVG few residential areas show notable increase in the use of water, while commercial consumes display a slight decrease in the last years. In most of the areas, average daily production covers the needs of the domestic and commercial activities (figure 5), although daily averages cannot represent seasonal changes. In the Grenadines, estimated water consumption is smaller: 91 liters per capita per day during the wet season, 63 liters during the dry season [26].

Water availability is sufficient for all sectors in SLA and SVG; however, stream flow of rivers is reducing due to competition for the resource. For example, in SVG water was redirected from a river in Richmond to be able to meet the demands of the Cumberland hydroelectric plant, which provides between 14 and 26 per cent of the country electricity supply [27]; as a result, this river remains dry for most of the year preventing any water related activity in that area.

Water rates are differentiated on the basis of customer category and overall consumption, with domestic price being the lowest (2.5-5.5 \$/m<sup>3</sup>), followed by commercial and industrial activities (7.3 \$), hotels and residences (8 \$), and ships (14.6 \$) (WASCO rates in September 2013). Figure 6 provides monthly freshwater demand statistics for Saint Lucia. The change in consumption is relatively small, and does not relate to any critical period of the year.

Tourism is a major employer in these countries, accounting for half of their GDP. SLA has approximately a 5,000-room capacity, mostly located in the north of the island. SVG has approximately 1,600-room capacity, growing to cope with increasing demand. However, the tourism industry is very sensitive to external drivers. For example, after 9/11 2001, visitors and cruise ships declined so much that several hotels declared bankruptcy, including the Hyatt. In the last years, the tourism industry fully recovered, reaching 350,000 annual presences in SLA and 230,000 in SVG. As in fig. 6, hotels and ships together account for about 20% of total freshwater consumption in SLA. It is estimated that per capita water consumption by tourists is about four times higher compared to local households [11]. Assuring water security to this sector is identified as a major problem, especially during the dry season which coincides with the cruise ships arrivals. To avoid dependency on the public water provision system, several hotels are installing water-saving devices and desalination plants [19].

Agriculture is mostly rain-fed. Because of this, it does not impact the supply from the distribution network. Once the first item of GDP, nowadays it contributes by just 5 per cent. Banana production is the most important, occupying 48 per cent of the cultivated land. Other important crops include coconut, cocoa, vegetables and herbs. SVG introduced mini sprinklers to improve irrigation efficiency, but most of the system was lost during Hurricane Tomas in 2010 and the 2011 April floods [28]. In SLA, only 10 per cent of crops are irrigated, using low efficiency techniques. Agricultural fields are predominately located in the middle to the upper part of watersheds. FAO [9] registered some worrisome observations about slash and burn, herbicide application and mechanization in SLA, together with an unwise choice of rotation crops and planting on steep slopes and river banks. Encroachment is occurring at higher elevations due to the scarcity of agricultural land, contributing to reduction in forest areas. Forests are of great importance as tree vegetated soils reduce runoff and lower the risk of erosion and sedimentation. The elimination of the forest cover leads to soil erosion, reduction in groundwater filtration and increased transportation of sediments. Global Forest Watch [29] reports that, from 2000 to 2011, about 530 Ha of forest have been lost in SLA, and 256 Ha in SVG.

## 6. LONG TERM SCENARIO OF WATER AVAILABILITY

The comparison between yearly or daily average freshwater production and consumption does not evidence overall strong insufficient natural availability of freshwater in SLA and SVG main islands. In the last twenty years water production increased proportionally to demand, which is driven mostly by households consumption: from 1993 to 2000, the number of customers (households, commercial and institution) more than doubled in SVG, while freshwater production increased by c.a. 40 per cent.

Figure 7 compares yearly water production and consumption from 1995 to 2010 for SVG. The blue area is the difference between production and consumption, or non-revenue water. It ranges between 40 and 50 percent of total production. Yearly averages do not allow to take in account seasonal variability, but they highlight that overall water production is more than sufficient to cope with actual demand in both countries. The problem is more related to the efficiency of the distribution and storage network, which is far from optimal. Moreover, natural hazards such tropical storms often compromise its functionality. Demand does not show remarkable seasonal effect (figure 6), but it is increasing as the countries are developing. Even though population is projected to decrease in four over five SSP scenarios [30], this may not necessary translate into decrease of water demand, as per capita consumption is also growing. National GDP, on the other side, increases steadily under all SSPs. Considering the average trend, we could expect a slow steady increase in GDP, which may translate into better provision for water management and infrastructures. However, the economic stability of these countries is dependent on the tourism sector, which is very sensitive to external drivers and suffers from natural disaster events. Currently, entire districts are exposed to interruption of network during such events. Water management in agriculture is also poor, lacking water storage practices and irrigation systems. This makes the entire sector vulnerable to dry spell periods. Meteorological events and natural water availability are inherently variable and sensible to climatic drivers. On the long term there are evidence that total annual rainfall will slightly decrease and dry periods may become longer, as much as rain season may become shorter and more intense, putting water security at risk. Both sea level rise and tropical storms pose additional worries to the security of coastal infrastructures, especially in the low-lying Grenadines.

## 7. CONCLUSION

Both climate and tourism are strong drivers influencing the development process in Caribbean SIDS, and both are sensible to external effects. Reliability of water supply during dry periods and after disastrous events is a critical problem on many islands at present, and it will likely worsen in the future. Smaller islets of the Grenadines already suffers from the reduction of water scarcity throughout the year. Projected change in availability coupled with change in demand suggest that pressure over the resource will increase. Tourism pressure will likely be part of the increase, but still as a minor share of total national consumption, while it strongly contribute to the national GDP as well as to the water service billings. On the other side, distribution issues and agricultural management depend on the policy and its regulatory enforcement and should be addressed as no-regret measures. The implementation of an integrated national water security plan to reduce vulnerability and to cope with increasing variability and growing demand is a priority for both countries.

## 8. ACKNOWLEDGMENTS

This paper has been produced with the financial assistance of the European Union under the CASCADE Action (Climate change adaptation strategies for water resources and human livelihoods in the coastal zones of Small Island Developing States, Grant contract id number FED/2011/281-147) implemented by the ACP Caribbean & Pacific Research Programme for Sustainable Development, 10th European Development Fund.

## 9. REFERENCES

- [1] UN-OHRLLS, "The impact of climate change on the development prospects of the least developed countries and small island developing states," 2009.
- [2] FAO, "Review of world water resources by country," 2003.
- [3] European Environment Agency, "European waters: current status and future challenges," vol. ', no. 'Place of Publication'. 2012.
- [4] UNEP, "Caribbean Environment Outlook," Nairobi, Kenya, 2005.
- [5] IPCC, *Climate change and water*. 2008.

- [6] CEHI, "Water and climate change in the Caribbean," no. October, 2002.
- [7] World Bank, "St. Lucia indicators and data," 2012. [Online]. Available: <http://data.worldbank.org/country/st-lucia>. [Accessed: 29-May-2014].
- [8] World Bank, "St. Vincent and the Grenadines indicators and data," 2012. [Online]. Available: <http://data.worldbank.org/country/st-vincent-and-the-grenadines>. [Accessed: 29-May-2014].
- [9] FAO, "Baseline Study on Existing Sustainable Practices , Models and Technologies used by farmers in Barbados and six countries of the Organization of Eastern Caribbean States ( OECS )," no. February, 2012.
- [10] A. Cashman, L. Nurse, and C. John, "Climate Change in the Caribbean: The Water Management Implications," *The Journal of Environment & Development*, vol. 19, no. 1, pp. 42–67, Nov. 2009.
- [11] UNEP, *Climate Change in the Caribbean and the Challenge of Adaptation*. 2008.
- [12] UN, "The economics of Climate Change in the Caribbean," 2011.
- [13] C. Sadoff and M. Muller, *Water Management , Water Security and Climate Change Adaptation : Early Impacts and Essential Responses*, no. 14. 2009.
- [14] A. C. Falkland, E. Custodio, D. Arenas, and L. Simler, *Hydrology and water resources of small islands: a practical guide*. 1991.
- [15] A. Falkland, "Tropical Island Hydrology and Water Resources," *Hydrology and Water Management in the Humid Tropics*, 2012.
- [16] Government of Saint Lucia, "National Issues Paper on Climate Change and the Water Sector in Saint Lucia," no. April, 2009.
- [17] L. Culzac-Wilson, "Report to the Regional Consultation on SIDS Specific Issues," 2003. [Online]. Available: [http://www.pnuma.org/sids\\_ing/documents/National Reports/St. Vincent National Report.pdf](http://www.pnuma.org/sids_ing/documents/National Reports/St. Vincent National Report.pdf). [Accessed: 16-Mar-2014].
- [18] A. W. Herbert and J. W. Lloyd, "Approaches to modelling saline intrusion for assessment of small island water resources," *Quarterly Journal of Engineering Geology and Hydrogeology*, vol. 33, no. 1, pp. 77–86, Feb. 2000.
- [19] C. Springer, "Cost pricing for water production and water protection services in Saint Lucia," 2005. [Online]. Available: <http://pubs.iied.org/pdfs/G00312.pdf>. [Accessed: 16-Mar-2014].
- [20] S. Sukhnandan, "Desilting and rehabilitation study to be undertaken on John Compton dam," 2014. [Online]. Available:

<http://www.stlucianewsonline.com/desilting-rehabilitation-study-to-be-undertaken-on-john-compton-dam/>. [Accessed: 29-May-2014].

- [21] S. H. Bricker, "Impacts of climate change on small island hydrogeology - a literature review," 2009.
- [22] N. Mimura, L. Nurse, R. McLean, J. Agard, L. Briguglio, P. Lefale, R. Payet, and G. Sem, "Climate Change 2007: Impacts, Adaptation and Vulnerability. Contribution of Working Group II to the Fourth Assessment Report of the Intergovernmental Panel on Climate Change," *Change*, vol. 90, no. 5, pp. 687–716, 2007.
- [23] A. Cashman, "Water Security and Services in The Caribbean Water Security and Services in The Caribbean," no. March, 2013.
- [24] B. Bates, Z. W. Kundzewicz, S. Wu, and J. Palutikof, "Climate Change and Water. Technical Paper of the Intergovernmental Panel on Climate Change," 2008.
- [25] L. Nurse and R. McLean, "AR5 WG2 Ch29: Small Islands," 2014.
- [26] ECLAC, "An assessment of the economic impact of climate change on the water sector in Saint Vincent and the Grenadines," no. October, 2011.
- [27] M. C. Simpson, D. Scott, M. Harrison, R. Sim, N. Silver, E. O’Keeffe, S. Harrison, M. Taylor, G. Lizcano, M. Ruddy, H. Stager, J. Oldham, M. Wilson, M. New, J. Clarke, O. J. Day, N. Fields, J. Georges, R. Waithe, and P. McSharry, "Quantification and Magnitude of Losses and Damages Resulting from the Impacts of Climate Change: Modelling the Transformational Impacts and Costs of Sea Level Rise in the Caribbean (Full Document)," Barbados, West Indies, 2010.
- [28] ECLAC, "Macro socio-economic and environmental assessment of the damage and losses caused by Hurricane Tomas," 2011.
- [29] Google, "Global Forest Watch," 2011.
- [30] R. H. Moss, J. A. Edmonds, K. A. Hibbard, M. R. Manning, S. K. Rose, D. P. van Vuuren, T. R. Carter, S. Emori, M. Kainuma, T. Kram, G. A. Meehl, J. F. B. Mitchell, N. Nakicenovic, K. Riahi, S. J. Smith, R. J. Stouffer, A. M. Thomson, J. P. Weyant, and T. J. Wilbanks, "The next generation of scenarios for climate change research and assessment.," *Nature*, vol. 463, no. 7282, pp. 747–56, Feb. 2010.

## 10. FIGURES

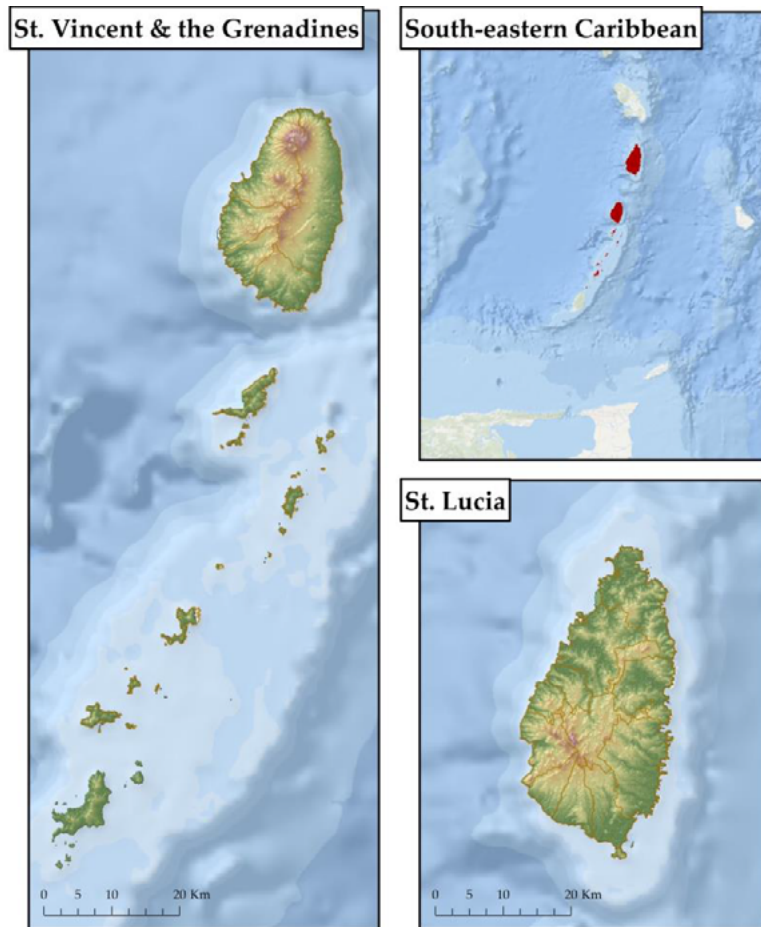


Fig. 1 Case study countries in the Caribbean sub-region.

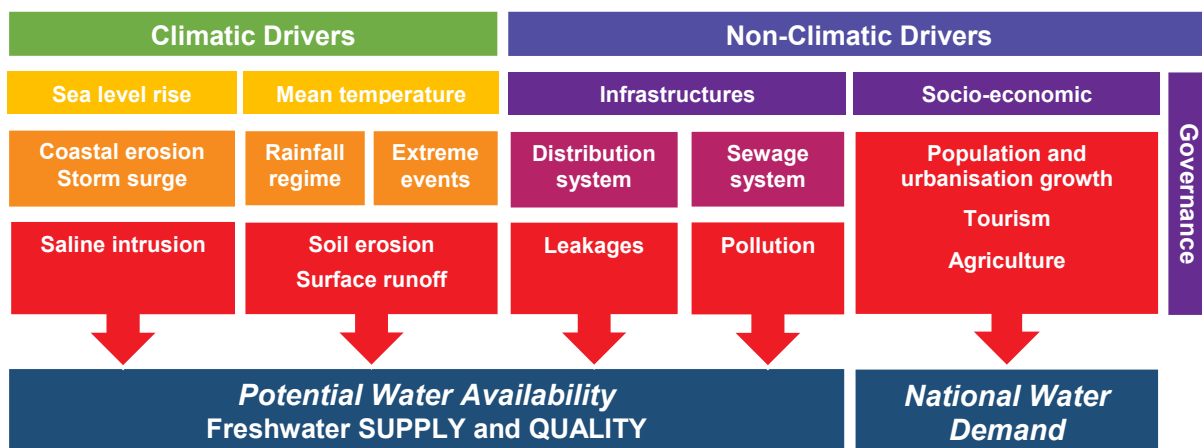


Fig. 2 conceptual framework linking climate change, water resource availability and socio-economic demand in the Caribbean sub-region. Colour red indicates the stressors or hazards influenced by climatic or non-climatic drivers.

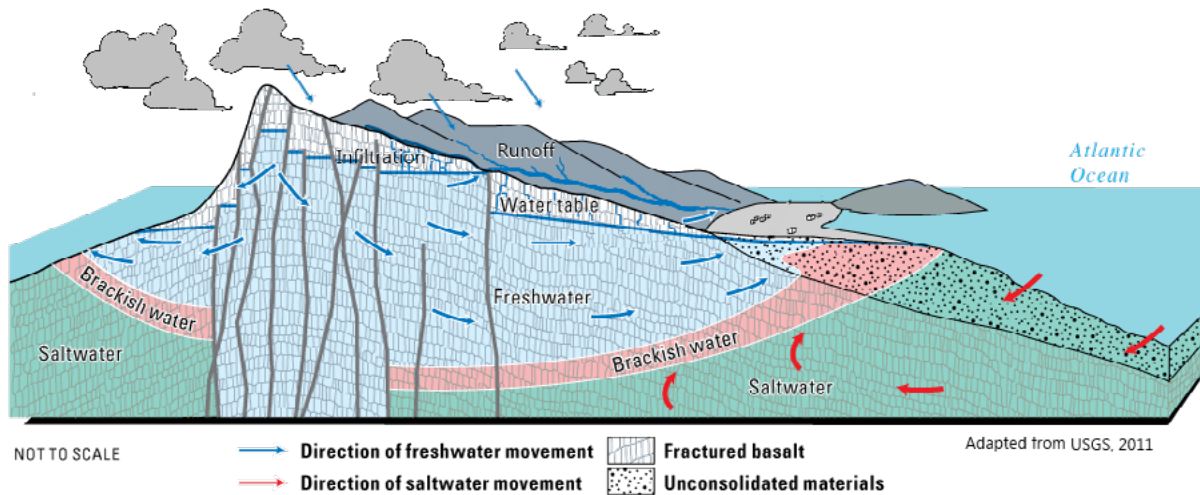


Fig. 3 generalized conceptual model of volcanic island hydrologic processes.

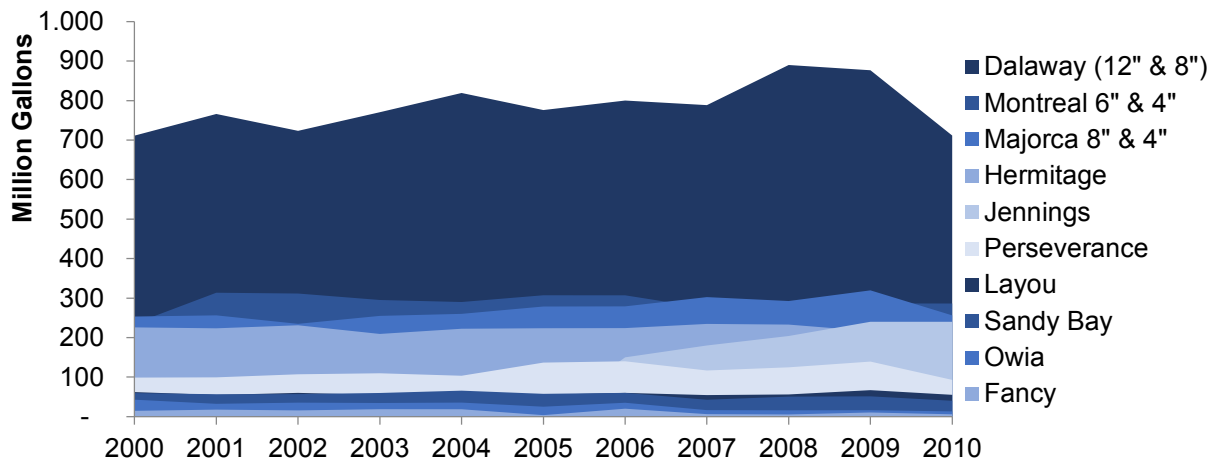


Fig. 4 yearly water production (million gallons) in Saint Vincent and the Grenadines, from the ten biggest production plants (from Dalaway) to smaller ones. Source: St Vincent central water and sewerage authority.

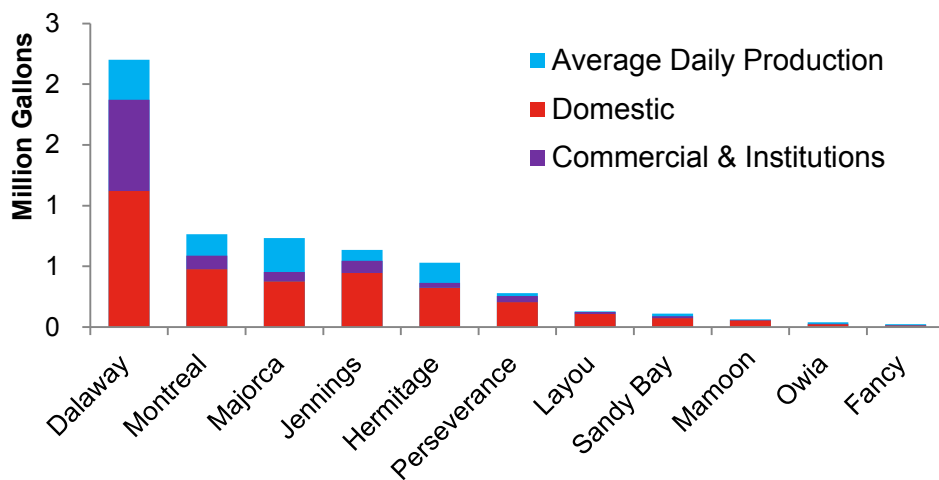


Fig. 5 Average daily water consumption in million gallons for 2000-2011 in Saint Vincent from households and commercial plus government institution compared to total production per each water system. Source: St Vincent central water and sewerage authority.

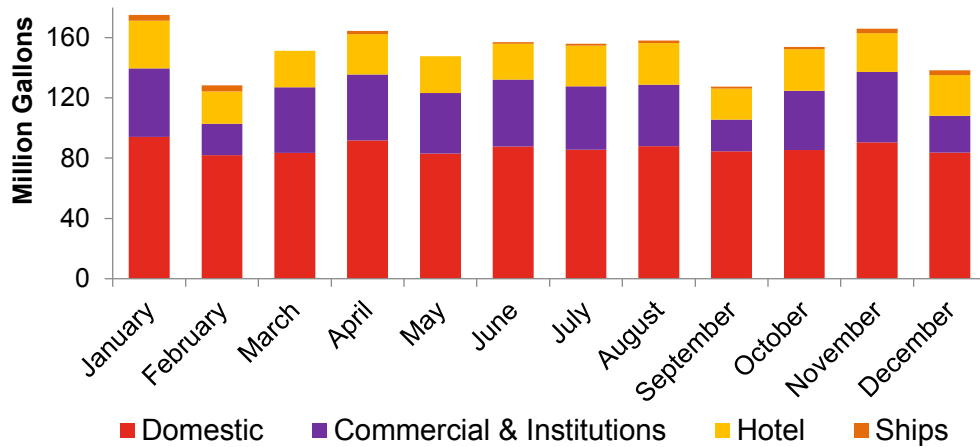


Fig. 6 Monthly water consumption in million gallons for 2012 in Saint Lucia from households and commercial plus government institution. Hotels and ships show relatively small consumptions. The monthly total consumption highlights little season effect (STD 12%). Source: St Lucia central water authority, 2012.

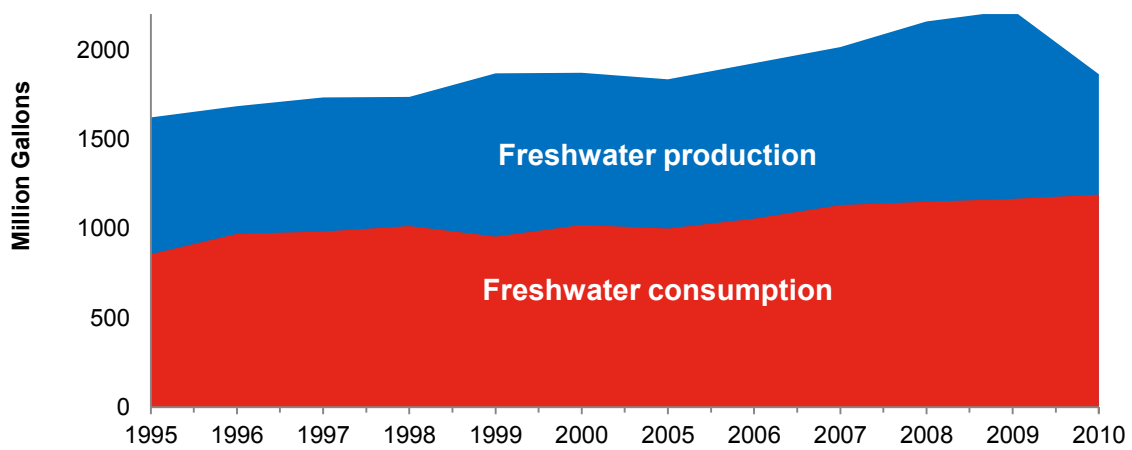


Fig. 7 SVG water production/consumption trends from 1995 to 2010

# **The Water Abstraction Licence Regime In Italy:**

## **A Case For Reform?**

**Santato S.<sup>1,2\*</sup> and Mysiak J.<sup>1,2</sup>**

<sup>1</sup>Euro-Mediterranean Center on Climate Change - Italy

<sup>2</sup>Fondazione Eni Enrico Mattei - Italy

\*Corresponding Author: [silvia.santato@feem.it](mailto:silvia.santato@feem.it)

### **Abstract**

The contemporary water abstraction licence (WAL) regime in Italy is no longer flexible enough to cope with the challenges posed by human-induced climate and global environmental changes. To cope with mounting water stress risk, the reformed WAL policy policies should i) foster sustainable levels of water withdrawals, ii) relate the water abstraction entitlements to medium- to long-term natural availability, and iii) foster efficient use of water resource and re-allocation of entitlements. The fundamentals of the WAL regime in Italy remained essentially unchanged since the 1930s. The sole noteworthy change was the decentralization of the regulatory competences from the state to the regional authorities in the late 1990s. As a result, the WAL administrative frameworks nowadays vary across the Regions. The main differences lie in the concession-free entitlements, the administrative practices, and the levels of water concession fees. In this paper we review the WAL regimes across the Regions in the Po River Basin District (PRBD), and outline the principles of a reform that promote water security.

**Keywords:** water abstractions licence regime, Po River Basin District, water security

## 1. INTRODUCTION

The European Water Framework Directive (WFD, Directive 2000/60/EC,[1]) recognised water scarcity and droughts as threats which may undo the efforts to achieve good ecological status of the Community water bodies. Yet drought mitigation is but the last among the aims underpinned in the Article 1 of the Directive, and the one which is least substantiated. The issues of water scarcity and droughts have been further addressed in the EC Communication on water scarcity and droughts [2] which identified a more efficient water allocation among the seven European concerted actions. More recently, the EU Water Policy Review [3], [4] identified some but insufficient progress in drought management in Europe, and the application of economic principles (e.g. cost recovery, water pricing). It encouraged, cautiously, use of market mechanism (e.g. water right trading scheme) where this represent a value-added improvement [3]. The European Parliament (EP) recommended on several occasions a targeted European policy on water scarcity and droughts [5]. Efficient water use is also a cornerstone of the EU Resource Efficiency Flagship initiative as a part of the Europe 2020 Strategy. The late 2000s economic and financial crisis revealed the high exposure of the EU to economic shocks, including that of extreme weather and climate related hazards, exacerbated by fiscal and 'other macro-economic imbalances' [6]. The Union's Internal Security Strategy (ISS), adopted in 2010 to 'increase Europe's resilience to crises and disasters', targets risks posed by natural and man-made hazards along with organised crime, terrorism and cybercrime, and management of EU external borders.

The effects of human induced climate change are believed to become particularly pronounced in the Southern Europe, notably Italy (e.g. Ciscar et al., 2014). The European Climate Adaptation Strategy [8] recognises that the risk posed to water security [9] will make out the bulk of the expected most likely impacts. Improved efficiency of water allocation and use, coherent application of water pricing and cost recovery principle, and better planning for drought spells, likely to be amplified by climate change throughout Europe are widely accepted as the most effective ways of adapting to climate variability and change. Notwithstanding the European efforts, wide-reaching effects of droughts, and water scarcity, on regional economies and social wellbeing are not known in sufficient detail [10]. The inattention to causes and

impacts of water stress precludes water policy reform and efficient water re-allocation [11].

In light of changing patterns of water availability and demand, some EU Member States have started a reform of water licence abstraction (WAL) regimes. In the UK, the reform was recommended in the Cave Report [11] and supported by the analysis of the Water Service Regulation Authority (OFWAT) and the Environmental Agency (EA). Announced in the Natural Environment White Paper [12] and further substantiated in the Department for Environment Food & Rural Affairs [13], [14], the reform entails smooth transition to a new regimes, without compensation for the losses incurred, by 2020s. The scope of the reform is to install tradable licensing regime capable to respond to current and future challenges. In Spain, with the reform of the Water Law in 1999 [15], introduced for the first time the lease contracts (*contratos de cesion*) and the exchange centres (*centros de intercambio*), which made possible the temporary transfer of water rights including a pecuniary compensation [16].

In Italy, the WAL regime in Italy is convoluted and substandard and reflects the tortuous interplay of water institutions in Italy [17]. An abstraction licence is required under the Royal Decree (R.D.) n° 1775 of 1933 for the abstraction of surface waters (such as from rivers, streams and canals) and ground water. Since then the regime evolved through the process of institutional decentralisation which started with the creation of the Regions ('72, '78), and continued towards the progressive empowerment of the Regions [18] that have gained full competence over the WAL matter. As a result, the WAL vary across Regions in terms of legislative and organisational frameworks. The present system gives the licence holder the right to abstract a specified quantity of water from a specific source and for a specific purpose. Although the concession awarding practise is similar across the regions, there are differences in terms of who is entitled to withdraw water without concession, which entities manage the administrative application, and how much is paid for the withdrawn water. Importantly, the licences are specified in *absolute* terms and are not transferable. Moreover, the licence terms are not compatible with a long term water resources availability, considering the ongoing climate change and population growth. Because the human induced climate change will likely result in lower average annual water availability and greater intra- and inter-annual variability

[19], the *National Climate Adaptation Strategy* for the PRBD suggested a revision of the WAL regimes [20]. Analysing the PRBD case study, we will detail recommendations on priorities for a national water abstraction reform, in line with international best practices on water abstraction reform [21], [22].

## 2. WATER MANAGEMENT ISSUES IN THE PO RIVER BASIN DISTRICT

Water demand in the Po River Basin District (PRBD) has increased over the last decades and the volume of authorized water abstraction entitlements exceed the average water availability [23]. The problems become more pronounced during the irregular periods of drought spells. A major part (42%) of the PRBD consists of low altitude floodplains, in which some 38% of the national GDP is generated. Irrigated agriculture is the largest consumptive water use in the basin (~80 per cent of water withdrawals) [24]. During the spring and the summer of 2003, a severe and persistent drought afflicted Southern Europe, including the PRBD. The Po river reached its absolute minimum at the closing section in Pontelagoscuro: -6.99 m or 270 m<sup>3</sup>/s compared to an average of 1400 m<sup>3</sup>/s. In 2006 and 2007, the Northern Italy experienced another anomaly in terms of precipitation. Scarce precipitation led to rainfall deficit of 200 mm by the end of 2006 and 30% by April 2007. In 2007 rivers discharges were lower than in 2003, marking a decline of one fourth compared to historical minimum values. Since 2003, the state of (national) emergency (SoE) under the law 224/1992 has been declared three times (2003, 2006, 2007) for a total duration of 21 months [25].

The Drought Steering Committee (DSC) was initiated and presided by the Po River Basin Authority (PRBA) in May 2003 amidst a severe water crisis posing a threat to domestic water supply in lower part of the district and sufficient volume for irrigation throughout the district. The cooperative decision of the DSC was sanctioned by signing a Memorandum of Interest (MoU, in Italian *Protocollo d'Intesa*) which laid down the commitments of irrigators to reduce water withdrawal by 25 to 50 per cent, and utilities to release more water of the impounded water in the Alpine reservoirs and large regulated lakes. Moreover, the DSC sanctioned a close monitoring of the evolving drought conditions. Since 2003, the DSC conveyed every time when the persistent drought conditions threatened to strain the Italy's most important economic regions [26]. Importantly, the DSC played an important role during the drought in

2007, although institutionalised through the decree of the Commissioner Delegate for the management of the state of emergency (SoE). Notwithstanding, the droughts are still predominately managed by resorting to emergency instruments [27]. A priority for a WAL reform have been identified as the main framework to planning and programming activities with a long-term water security perspective in order to move from an emergency to a proactive and ordinary approach to drought.

### 3. NORMATIVE REGIMES ACROSS THE PRBD

Among the first normative acts to govern the WAL, the R.D. 1775/1933 distinguished between the small and large volume abstraction permits [Table 1].

Use	Small volume abstractions	Large volume abstractions
Hydroelectricity [HE] generation	< 3000 kW of average generating year capacity	> 3000 kW of average generating year capacity
Irrigation	< 1000 l/s or < 500 ha	> 1000 l/s or > 500 ha
Others	< 100 l/s	> 100 l/s

Tab. 1 Abstraction differentiation depending on quantity of water withdrawn and type of use (R.D. 1775/1933)

For both small volume (SV) and large volume (LV) permits, the R.D. 1775 entrusted the management of the WAL to the Public Works Office<sup>1</sup> (PWO). With the Legislative Decree (D.Lgs.) 112/1998, the authorities over the WAL were shifted from the State to the Regional governments. Where not otherwise specified, the provisions of the R.D. 1775/1933<sup>2</sup> still apply. The five Regions comprised either entirely or for a substantial part of their territory in the PRBD introduced to some extent different WAL regimes in terms of administrative application and the delegated responsibilities. Piedmont, Emilia-Romagna and Lombardy have adopted apposite pieces of regional legislations for WLA over the period 2000-2006: first Emilia Romagna (L.r.<sup>3</sup> 41/2001), followed by Piedmont (L.r. 10R/2003) and Lombardy (Regional Regulation 02/2006). Valle d'Aosta, a region enjoying high administrative autonomy, applies a law which dates back to 1950s (L.r. 04/1956). Veneto governs the WAL through sporadically updated regulations.

<sup>1</sup> The Public Work Office (in Italian: *Genio Civile*) is a regional peripheral authority on a provincial basis, which ensures all the functions relating to the execution of public works.

<sup>2</sup> *Testo unico delle disposizioni di legge sulle acque e impianti elettrici.*

<sup>3</sup> L.r. – regional law (in Italian *legge regionale*).

The regional authorities have the faculty to enforce additional limits and obligations, the permit holders have to comply with, for safeguarding of environmental integrity and quality, and to contribute to the objectives of the Water Protection Plans (WPP - *Piano di tutela delle acque*). Typically, the Regions issue WAL for LV abstractions and specify water concession fees for all types of uses. The WAL for SV abstractions are issued by lower administrative authorities which are also in charge for the conduction of the preliminary assessment of the environmental compatibility of the new entitlements.

In Valle d'Aosta, given the small extent, the regional public water management office is responsible for both SV and LV abstractions licences. The Provinces of Piedmont and Lombardy carry out the preliminary assessment both for SV and LV WAL. While the competences vested in regional and provincial authorities are essentially the same in Piedmont e Lombardy, in Veneto the lower authorities for all uses but hydropower is the PWO (different from provinces but comparable in extent and subordinate to the Regional authorities). In Emilia – Romagna, the WAL are administered by the (four) Technical River Basin Services (TRBS).

The R.D. 1775 established that anyone, including the owners of land property, regardless whether natural or juridical person, can withdraw water from natural water bodies only if authorised and in possession of water concession permit. An exception to this general rule was granted to the landowner or tenants entitled to abstract and use groundwater<sup>4</sup> for domestic use. This use is exempt from the obligation to declare the withdrawal and hence the payment of the water concession fee. This exception is limited to domestic water supply and sanitation, watering of gardens and orchards, and/or water use by livestock. Under the current regimes the abstractions that are exempt from permits and fees are subordinated to limits that vary across the PRBD regions. In Piedmont, the flow rate must not exceed 2 l/sec and 5000 m<sup>3</sup>/year, while in Lombardy it is limited to 1 l/s and 1,500 m<sup>3</sup>/year. Veneto allows the water withdrawal for domestic use in areas not served by aqueduct and limited to 0.1 l/s. In Emilia – Romagna and Valle d'Aosta withdrawal limits are not specified.

---

<sup>4</sup> Licenses for abstractions have been required for surface waters since the end of the XIX century, while groundwater use (GU) has remained more or less free until 1994. After Galli Law, the previous free GU has been converted into an abstraction license for a limited and renewable period of time [20].



Fig. 1 The boundaries of the authorities in charge of issuing the water abstraction licences (WAL) within the Po River Basin District (PRBD). [The shown extent to the PRBD corresponds to the recently proposed modification].

The Galli Law (GL) 36/1994 obliged owners to declare their existence and characteristics in order to make an overall census possible. Importantly, the GL also sets a hierarchy between various uses of water, giving priority to human consumption above other uses.

The administrative procedures, both for SV and LV WAL are rather similar across the Regions and the permits are issued upon the preliminary impact assessment [Fig. 2].

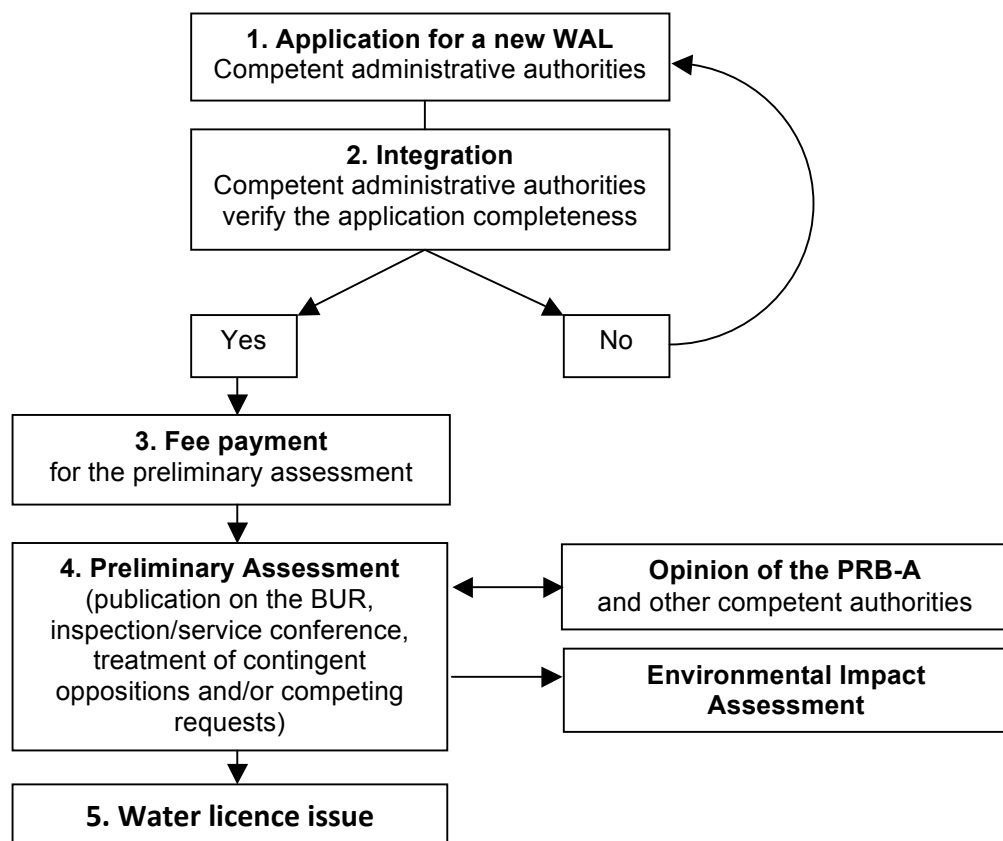


Fig.2 Administrative phases for LV and SV WAL across Regions comprised in the PRBD.

The preliminary assessment typically include the opinion of the Po River Basin Authority (PRBA), a fee collected from the applicant, publication of the water concession application in the official regional bulletin (BUR, *bollettino ufficiale regionale*), an inspection or a services conference (*conferenza dei servizi*) and, finally, the treatment of contingent oppositions and/or competing requests. The Environmental Impact Assessment (EIA) is based on the water concession flow rate and considers the environmental impacts to protected natural area (SPAs –special protection areas, SACs – special areas of conservation, etc). Only if the EIA is positive, the water concession application is accepted. The legislation of Piedmont refers to three scenarios considering positive or negative environmental effects with or without the water abstraction and propose different compensation measures in case of negative impacts. Lombardy introduce and describe the different EIA stages including the responsible authorities for each of them.

The predominant water uses among Regions are defined by R.D. 1775/1933: civil, drinkable use, irrigation, energetic, industrial use, health and sanitation. The WAL for irrigation have a duration of 40 years and other uses 30 years where not specified by law [Table 2].

Water uses	Piedmont	Lombardy	Veneto	Emilia-Romagna	Valle d'Aosta
Irrigation	40	40	40	40	no limitation
Potable	30	30	-	30	no limitation
Civil	30	-	-	-	99
Industrial	15	15	-	-	99
Fish farming	30	40	-	40	99
Energy	30	30	-	40	99
Sanitation	-	30	-	40	99
Zootecnic	30	30	-	-	99
Others	30	30	-	-	-

Tab. 2 Terms of water uses by Regions comprised in the PRBD.

The permits are typically specified in ‘modules’ [Table 3] consisting of 100 l/s flow, except for industrial use specified as three cubic meters per second, if not specified otherwise.

Region	Potable		Irrigation			Industrial		Hydropower
		<i>no return</i>	<i>with return</i>	<i>not metered</i>	<i>no return</i>	<i>with return</i>		
Lombardy	€/mod	€/mod	€/mod	€/ha	€/mod	€/mod*	€/Kw	
Piedmont	l/s	l/s	l/s	€/ha	l/s	l/s	€/Kw	
Emilia-Romagna	€/mod	€/mod	€/mod	€/ha	€/mod	€/mod	€/Kw	
Valle d'Aosta	€/mod	€/mod	€/mod	€/ha	€/mod	€/mod	€/Kw	
Veneto	€/mod	€/mod	€/mod	€/ha	€/mod	€/mod	€/Kw	

Tab. 3 The water concession units (as in 2013) for the major water uses across the PRBD regions.  
 Legend: \* from 2008 the WCF for industrial water uses in Lombardy are specified according to the volume withdrawn of 100 l/s.

The application for the WAL renewal must be submitted before the license expires, subject to regional regulation and substantial variation of water withdrawal, otherwise it follows a new WAL procedure [Figure 2]. Besides that the renewal is rejected for reasons connected to public interests. Piedmont regulation states that the renewal application has to be submitted at least 1 year before the licence expired. Differently, Lombardy accept the application for a renewal if submitted no later than 6 months before the licence expires.

The applications can be declined as a result of the following omissions or negligence: i) the (intended) water use differ from that granted; ii) the user does not respect the conditions and requirements associated with the license; iii) failure to pay the abstraction charge for two consecutive years; iiiii) end of term of the concession e) sub-licensing to third parties. In particular, the legislations of Piedmont and Lombardy consider also the following cases i) no abstraction for 3 consecutive years, ii) an inadequate release of the environmental flow (EF), and iii) a failure to install the flow rate meter, mandatory for all new water licenses (Lombardy Piedmont and Emilia - Romagna) as required by the “Environmental Code” (Delegated Legislative Decree no. 152/2006).

The transferable water permits (TWP) are not addressed in the decrees and statutes of regional authorities. The WAL cannot be sold (i.e. transferable water permits), neither entirely nor in part, without consent of the responsible authority. This doesn't mean that TWP between sub-basins and/or across jurisdictions does not occur.

Indeed, the water exchange (abstraction and emission) between different water bodies is not regulated beyond the ordinary abstraction licenses.

#### 4. WATER ABSTRACTION FEES

For each permitted water abstraction a water concession fees (WCF) is due [Table 4].

Region	Potable		Irrigation		Industrial		Hydropower
	<i>no return</i>	<i>with return</i>	<i>with return</i>	<i>not metered</i>	<i>no return</i>	<i>with return</i>	
	[€/m <sup>3</sup> /s]	[€/m <sup>3</sup> /s]	[€/m <sup>3</sup> /s]	[€/ha]	[€/m <sup>3</sup> /s]	[€/m <sup>3</sup> /s]	[€/Kw]
Lombardy	22.177	52.040	26.010	0,52	179.958*	362.769*	15** [30**]
Piedmont	21.890	52.000	52.000	1,14	164.280	164.280	28
Emilia-Romagna	20.130	47.470	47.470	0,43	155.042	155.042	14
Valle d'Aosta	19.309	45.310	45.310	0,41	70.802	141.605	16
Veneto	41.822	98.142	49.071	0,89	322.394	322.394	29

Tab. 4: The water concession fees (as in 2013) for the major water uses across the PRBD regions.  
 Legend: \* the WCF for industrial water uses in Lombardy are specified according to the volume withdrawn (more and less than 3 m<sup>3</sup>/s); \*\* WCF for hydropower generation is specified for small and large volume withdrawal.

The WCF vary substantially across the PRBD. Over the past decades, the real value of the WCF declined since the applied inflation rate used for the update of the tariffs falls far below the real inflation rate.

In addition, the WCF are calculated based on the permitted and not the actually withdrawn volumes of water. Besides the WCF, water users pay supplementary abstraction fees for riverine communities (*sovracanone per gli enti rivieraschi*) and supplementary abstraction fees mountainous basins (*sovracanone per bacini imbriferi montani*) benefit specific (*and often disadvantaged*) communities.

## 5. CONCLUSION

A more flexible water abstraction license (WAL) regime in the PRBD and elsewhere in Italy is warranted due to altering pattern of water availability and amplified climate variability [20], as well as a mean of implementing new requirements of environmental flow. The new regime should be built upon experiences gained from elsewhere [28]–[30]. First, the new regime should specify the entitlements as shares of harvestable water resources. Second, the entitlements should specify both the volume that can be withdrawn and the rate of return flow, so as not to harm the entitlements of downstream users. Third, a single publicly accessible register of all water entitlements across the PRBD should be introduced. Fourth, the river basin (district) authority should play a major role in controlling the environmental compatibility of the intended withdrawals. This holds true especially for the large volume abstraction. Fifth, the water concession fees across the PRBD should reflect the value of intended water use(s), water ‘scarcity’ value, and the environmental costs of the water withdrawal. All charges should be based on actual volumes of water withdrawn. Sixth, the potential efficiency gained through making the water entitlements transferable should be analysed in depth. The ample existing infrastructure favours the transfer of entitlements as it does the physical water transfers. Seventh, the length for which the WAL will be released depends on whether or not the final scope will be to foster fully fledged tradable permit scheme. In the latter case the WAL should be released if not in perpetuity for a time frame sufficiently long to favour long term investments and sustain innovation incentives. In the former case the WAL should be issued for a time frame that permits regular ‘back-end’ adaptation to changing pattern of precipitation and river flow.

The above principles will help to overcome the institutional ‘maze’ which characterise the current WAL regime, while introducing a flexible regimes of water allocation utterly based on the harvestable water resources beyond the water flow needed to preserve environmental integrity of river and riverine ecosystems. The sequential reform driven by public consultation and debate is more likely to succeed in overcoming the barriers to change the current historically settled regime.

## 6. ACKNOWLEDGMENTS

This paper has been produced with the financial assistance of the European Union under the ORIENTGATE project (A structured network for integration of climate knowledge into policy and territorial planning, Grant number SEE/C/0001/2.2/X ).

## 7. REFERENCES

- [1] EC, Water Framework Directive 2000/60/EC. 2000.
- [2] EC, “Communication from the Commission to the European Parliament and the Council Addressing the challenge of water scarcity and droughts in the European Union. COM(2007) 414 final.” 2007.
- [3] EC, A Blueprint to Safeguard Europe’s Water Resources. Communication from the Commission to the European Parliament, the Council, the European Economic and Social Committee and the Committee of the Regions. COM(2012) 673 final. 2012.
- [4] P. Strosser, T. Dworak, P. G. A. Delvaux, M. Berglund, G. Schmidt, J. Mysiak, M. Kossida, I. Iacovides, and V. Ashton, Gap Analysis of the Water Scarcity and Droughts Policy in the EU. European Commission Directorate General Environment, Final report Tender ENV.D.1/SER/2010/0049, 2012.
- [5] EP, “Report on ‘Towards a stronger European disaster response: the role of civil protection and humanitarian assistance’ (2011/2023 INI)) A7-0283/2011.”2011.
- [6] EC, “Communication from the Commission to the European Parliament, the Council, the European Economic and Social Committee and the Committee of the Regions: Reinforcing economic policy coordination. COM(2010) 250 final.” 2010.
- [7] J.-C. Ciscar, L. Feyen, A. Soria, C. Lavalle, F. Raes, M. Perry, F. Nemry, H. Demirel, M. Rozsai, A. Dosio, M. Donatelli, S. Srivastava, Amit Kumar Fumagalli, Davide Niemeyer, Stefan Shrestha, P. Ciaian, M. Himics, S. Van Doorslaer, Benjamin Barrios, N. Ibáñez, G. Forzieri, R. Rojas, A. Bianchi, P. Dowling, A. Camia, G. Libertà, D. San-Miguel-Ayanz, Jesús de Rigo, G. Caudullo, J.-I. Barredo, D. Paci, B. Pycroft, Jonathan Saveyn, T. Van Regemorter, Denise Revesz, T. Vandyck, Z. Vrontisi, I. Baranzelli, Claudia Vandecasteele, F. Batista e Silva, and D. Ibarreta, “Climate Impacts in Europe - The JRC PESETA II Project. Published in: EUR – Scientific and Technical Research , Vol. 26586, (2014):” 2014.

- [8] EC, "Communication from the Commission to the European Parliament, the Council, the European Economic and Social Committee and the Committee of the Regions An EU Strategy on Adaptation to climate COM(2013) 216 final change." 2013.
- [9] OECD, "Water Security for Better Lives," Organisation for Economic Co-operation and Development, Paris (France), Report, Sep. 2013.
- [10] W2A, "Synthesis report. ERA-net initiative, 2nd Joint Call for Research on IWRM." 2013.
- [11] C. Report, "Independent Review of Competition and Innovation in Water Markets: Final report." .
- [12] HM Government, "The Natural Choice: securing the value of nature." 2011.
- [13] DEFRA, "Water for life. Market reform proposals. Department for Environment, Food and Rural Affairs." 2011.
- [14] DEFRA, "Water for life. Department for Environment, Food and Rural Affairs." 2011.
- [15] "BOE, Ley 46/1999 de 13 de diciembre, de modificación de la Ley 29/1985, de 2 de agosto, de Aguas. 1999." .
- [16] C. D. Pérez-Blanco, "Economic Instruments for Water Management in Spanish Mediterranean Basins. University of Alcalá, Alcalá de Henares." 2013.
- [17] OECD, "OECD Environmental Performance Reviews: Italy 2013." Publishing. <http://dx.doi.org/10.1787/9789264186378-en>, 2013.
- [18] A. Gorla and N. Lugaresi, "The Evolution of the National Water Regime in Italy." 2002.
- [19] E. Coppola and F. Giorgi, "An assessment of temperature and precipitation change projections over Italy from recent global and regional climate model simulations." 2010.
- [20] J. Mysiak, L. Carrera, F. Puma, S. Pecora, F. Farinosi, A. Amadio, E., Calliari E., Santato S., Cappuccini, D. Balzarolo, C. Alessandrini, C. Vezzani, and M. De Salvo, "Distretto Idrografico Padano," in *Strategia Nazionale per l'adattamento ai cambiamenti climatici*, S. Castellari, Ed. 2013.
- [21] M. Young, "Towards a generic framework for the abstraction and utilisation of water in England and Wales." UCL Environment Institute: Visiting Fellowship Report 2012, 2012.
- [22] L. Carrera, J. Mysiak, and J. Crimi, "Droughts in Northern Italy: Taken by Surprise, Again. Review of Environment, Energy, Economics." 2013.

- [23] AdB, “Sintesi dell’analisi economica sull’utilizzo idrico. Elaborato 6, Piano di Gestione. Autorità di Bacino del Fiume Po.” 2010.
- [24] AdB, “Caratteristiche del bacino del fiume Po e primo esame dell’impatto ambientale delle attività umane sulle risorse idriche. Autorità di Bacino del Fiume Po.” 2006.
- [25] J. Mysiak, L. Carrera, and A. Massarutto, “Sicurezza idrica nel contesto dei cambiamenti climatici,” in *Qualità dell’ambiente urbano, IX Rapporto, Focus su Acque e ambiente urbano*, ISPRA, Ed. L’istituto Superiore per la protezione e la ricerca ambientale, 2013, pp. 113–120.
- [26] E. Calliari, “Ordinary and extraordinary tools for managing drought. The 2003 and 2006/2007 events in the Po river basin.” 2011.
- [27] M. V. Civita, “Ground water in the Southern Member States of the European Union: an assessment of current knowledge and future prospects - Country report for Italy, European Academies – Science Advisory Council.” 2011.
- [28] J. Mysiak, M. Vollaro, C. M. Gómez, M. S. Andersen, P. Defrance, P. A. G. Delvaux, C. Green, T. Dworak, M. Davide, G. Delacámara, E. Ibáñez, A. Kis, A. Maziotis, M. Lago, S. McCarthy, M. Molinos Senante, C. P. Pérez-Blanco, M. Rodríguez, G. Ungvári, D. Viaggi, and C. Viavattene, “EPI-WATER Synthesis report.” Report of the EPI-WATER project, 2013.
- [29] M. Young, “Environmental Effectiveness and Economic Efficiency of Water Use in Agriculture,” in *OECD Studies on Water*, Paris (France): Organisation for Economic Co-operation and Development, 2010, pp. 1–33.
- [30] M. Young, “The role of the Unbundling water rights in Australia’s Southern Connected Murray Darling Basin.” Report of the EPI-WATER project, 2011.

Vulnerability, Risk Assessment and  
Adaptation to Climate Change

**Poster session**

# **Forest management in water protection areas under climate change**

**Dirnböck T.<sup>1\*</sup>, Kobler H.<sup>1</sup>, Gerhard E.<sup>2</sup> and Siegel H.<sup>2</sup>**

<sup>1</sup>Federal Environment Agency - Austria, <sup>2</sup>Federal Ministry of Agriculture, Forestry,  
Environment and Water Management - Austria

\*Corresponding Author: [thomas.dirnboeck@umweltbundesamt.at](mailto:thomas.dirnboeck@umweltbundesamt.at)

## **Abstract**

During the 19th century until today temperature has risen by almost 2°C in the European Alps. In the Northern Limestone Alps in Upper Austria, a further increase of up to 5 °C is predicted until 2100, with highest increase in the summer. Drier summer and wetter winter and early springs are expected. The Northern Limestone Alps are characterized by shallow soils which are vulnerable to nutrient loss and erosion once a forest is damaged. Since many settlements in the region depend on a high quality of water coming from forested headwaters, forest functions such as water retention and filtering of pollutants have to be maintained and even restored where necessary. Forest management affects water quality in many ways. The dominant Norway Spruce management has led to even-aged, often monoculture forests. The common management of Spruce forests is done with clearcuts or shelterwood-cuts potentially causing water pollution. With regard to pollutants such as nitrate, expected climate change will, during sensitive periods such as when trees are young, enhance the negative effects of these management interventions to water quality. Adaptation towards continuous forest cover management is indispensable in water protection areas.

**Keywords:** forest ecosystem, nitrate, water pollution, karst

## 1. THE STUDY, RESULTS AND CONCLUSIONS

Nearly 22 % (about 18.000 km<sup>2</sup>) of Austria's total area consists of calcareous rocks. About 15 % of the whole territory is karstified. Karst catchments provide half of the water supply for the Austrian population. Due to a short residence time of part of the karst water in the system, in particular in limestone karst aquifers, the filtering and transformation capacity of vegetation and soil are of ultimate importance for the quality of karst spring water. Large karst areas are located in the Northern Limestone Alps, where in the montane and subalpine life belt forests are the dominating land cover. Forest management and climate change directly or indirectly affect forest dynamics and thereby exert impacts on water supply, both in terms of quality and quantity.

A forest ecosystem model [1] was applied with data from a long-term ecosystem research site in the "Kalkalpen" national park (LTER Zöbelboden, N 47°50'30", E 90 14°26'30") in order to study effects of climate change and management on runoff dynamic and water quality. The model was calibrated and validated with long-term forest growth (aboveground biomass from inventories), soil (soil hydraulic parameters, C and N content, texture, etc.) and soil water measurements (Nitrate concentration in lysimeter samples). Future climate projections were derived for A1B-, A2- and B2-scenarios for three time slices: 2025-2035, 2045-2055 and 2085-2095. We used existing downscaling scenarios for Austria reclip:century ([http://reclip.ait.ac.at/reclip\\_century/](http://reclip.ait.ac.at/reclip_century/)) together with the weather generator ClimGen [2]. The latter was calibrated with long-term meteorological data measured at the site. In order to account for the sensitivity of the models to climate inputs 5 ClimGen climate series were derived for each the 3 scenarios, the 3 time slices plus a baseline for comparison (years 1995-2005). Three forest management options were defined and implemented into the model: low (spruce-beech management, single tree harvest), medium (spruce shelterwood management, natural regeneration) and high intervention (spruce clearcut management, planting). In total 150 model runs were performed for a full rotation period of 120 years: (5 x (3 scenarios x 3 time slices) + 5 baseline runs) x 3 management options.

Climate change in the Northern Limestone Alps will exert warmer temperatures, particularly during summer and a precipitation change, which is rather uncertain however, may increase in winter and decrease in summer. These climatic changes

will have both positive and negative effects to nitrate loss from managed forests. Peak nitrate concentrations and leaching during clearcut and thinning increased under all scenarios. Also during understory reinitiation in clearcut and shelterwood systems nitrate concentrations in the seepage as well as leaching were higher as compared to the current climate (Fig. 1). That is due to a retarded tree development resulting from increasing water stress in summer. Nitrogen is therefore less efficiently taken up by planted young trees, transpiration is lower and higher infiltration enhances the transport of nitrate below the rooting zone and subsequently into the groundwater. With increasing age of the forest nitrogen uptake did weaken again and nitrate concentration in the seepage and leaching were increasing. The reason for that is forest growth. At the altitude of almost 1000 m a.s.l. a warmer climate will be beneficiary for the growth of adult Norway spruce trees. Hence, tree growth during the old age period outweighed the biomass accumulation which was achievable under current climate. As a consequence, more nitrogen had been retained in the system and nitrate leaching was lowered during this phase (Fig. 1). The study exemplifies the need to include all relevant ecosystem processes in climate impact assessment.

The best management for optimizing water protection, which is particularly important in water protection areas, is therefore a mixed forest which includes a wider range of naturally occurring tree species, the prevention of clear-cut phases, single tree, group selection cuts or a continuous forest cover. Particularly in the light of expected climate changes effects to forests, an adaptation towards such a management is indispensable.

## 2. ACKNOWLEDGMENTS

The study was supported by the ETZ SEE Project Orientgate

## 3. REFERENCES

1. Haas E., Klatt S., Fröhlich A., Kraft P., Werner C., Kiese R., Grote R., Breuer L., & Butterbach-Bahl K. (2013), *LandscapeDNDC: a process model for simulation of biosphere–atmosphere–hydrosphere exchange processes at site and regional scale*. *Landscape Ecology*, 28, pp. 615-636.

2. Stöckle C.O., Campbell G.S. & Nelson R. (1999), *ClimGen Manual*. Biological Systems Engineering Department, Washington State University, Pullman, WA.

## 4. IMAGES AND TABLES

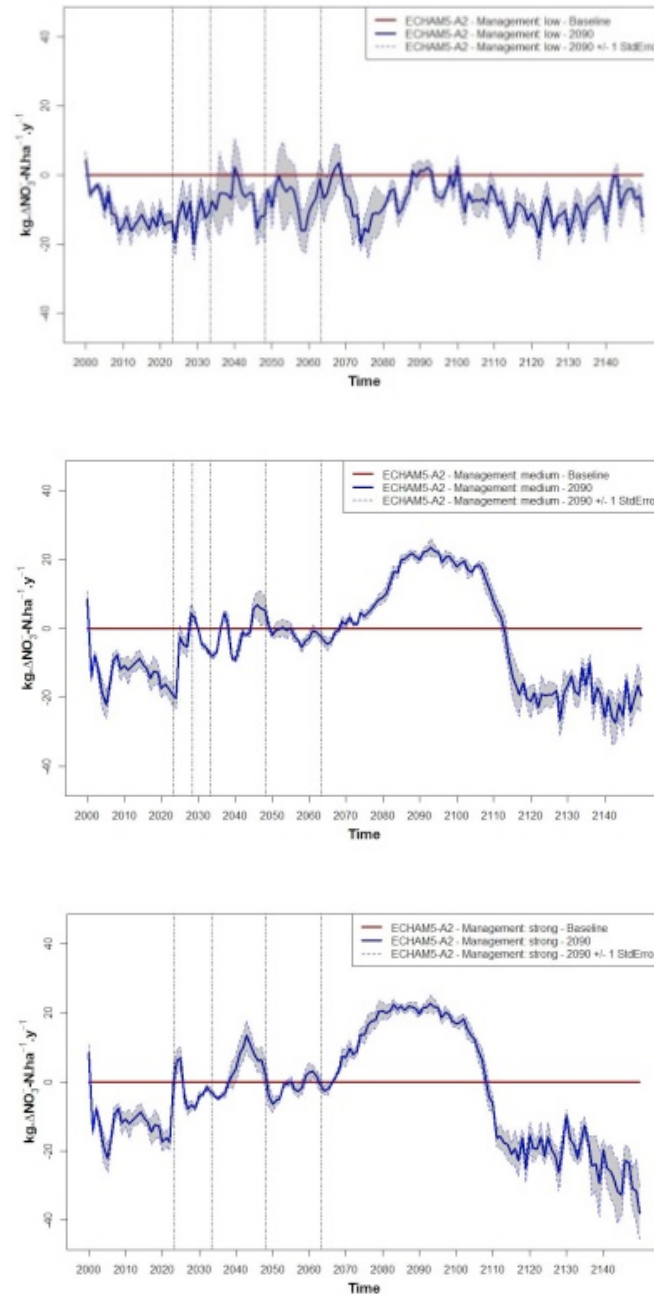


Fig. 1 Climate effects to nitrate leaching in managed Norway Spruce forests. Deviations in nitrate leaching with the seepage water under an ECHAM5-A2 Scenario (blue line with variation in grey shade) as compared to the current climate (horizontal red line at zero). Upper to lower: continuous forest cover management, shelterwood-cut management (dashed lines indicate the 50% cut, 100 % cut and 3 thinnings), clearcut management (dashed lines indicate 100 % cut and 3 thinnings).

# **Risk assessment on coastal environments under climate change: Southern Brazil**

**Germani Y. F.<sup>1</sup>, Figueiredo S.A.<sup>2\*</sup>, and Calliari L.J.<sup>3</sup>**

<sup>1, 2\*, 3</sup> Universidade do Rio Grande, Instituto de Oceanografia - Brazil

\*Corresponding Author: saletteoc@gmail.com

## **Abstract**

Considering future scenarios of global climate change, coastal regions around the world will become more vulnerable to erosion and flooding. Rio Grande do Sul coastline, in the southern Brazilian coast exemplifies an area which may be under very high risk in the future. Due to its intrinsic large scale morphodynamical setting: a low lying coastal gradient combined with a high degree of exposure to ocean dynamics, places several ecosystems associated with it at risk. In order to determine the possible loss of habitats in case of a rise of mean sea level in the long term (2100), coastal environments were classified and the percentage loss for each habitat was calculated considering three projected coastline positions. Regarding the results obtained by calculations, all habitats presented some loss, even when considering the best case scenario. Coastal vulnerability index (CVI) values calculated for the study area were 14.4 and 51.0, for the current coastal setting and for year 2100, respectively. The results indicate that a region currently characterized as moderately vulnerable, could become highly vulnerable due to the rising of mean sea level as projected. Thus, the information obtained here is crucial to properly plan land use and adaptation of this coastal region under the current scenario for global climate change, as well as to assist future studies on habitat management.

**Keywords:** climate change, coastal vulnerability, sea level rise

# **An Online Platform for Supporting the Analysis of Water Adaptation Measures in the Alps**

**Bojovic D.<sup>1,2</sup>, Giupponi C.<sup>1,2</sup>, Klug H.<sup>3</sup>, Morper-Busch L.<sup>3</sup>,  
Cojocaru G.<sup>4</sup>, Schörghofer R.<sup>3</sup>**

<sup>1</sup>Ca' Foscari University of Venice, Department of Economics – Italy,  
<sup>2</sup>Euro-Mediterranean Centre on Climate Change, Climate Change Impacts and  
Policy Division – Italy, <sup>3</sup>University of Salzburg, Interfaculty Department of  
Geoinformatics (Z\_GIS) – Austria and <sup>4</sup> TIAMASG Foundation – Romania

\*Corresponding Author: dragana.bojovic@cmcc.it

## **Abstract**

The Alps are an important water resource for the central Europe. Climate change may result in the reduced water availability in all the regions dependent on this supply. Different initiatives emphasised importance of the inclusion of a broader group of stakeholders in discussions over water management in the Alps. This paper presents an eParticipation approach that combines spatial and multicriteria decision-support tools in supporting collaboration on the analysis of alternative adaptation measures and finding suitable solutions. The interactive map allows participants to focus on a particular area of the Alps facing water scarcity problem, while a decision-support component allows finding a compromise solution for diverse interests presented by stakeholders. The physical space is not a barrier for participating in this online platform. This aspect, together with its multilingual interface, makes the platform available for participants from all over the cross-border Alpine space. Then again, the exercise allows geographical characterisations of the adaptation preferences among different geographical units within this area. The initial results are obtained from the professionals from the field. In the future, this platform could be used to inform decision-makers on the adaptation habits and preferences of a broader group of stakeholders from the Alps.

**Keywords:** Alps, water scarcity, adaptation measures, online participatory tools, interactive maps

# **Statistical Downscaling Method Applied for a Future Climate Profile at Local Level - Bologna Case Study as Resilient City**

**Tomozeiu R.\*, Botarelli L., Cacciamani C.**

ARPA Emilia-Romagna, Servizio Idro-Meteo-Clima

\*Corresponding Author: [rtomozeiu@arpa.emr.it](mailto:rtomozeiu@arpa.emr.it)

## **Abstract**

A detailed framework of present and future climate changes at local level represents an important tool in the study of impacts as well as in the construction of adaptation and mitigation strategies. One objective of 2011 Life+ project BLUE AP for the adaptation plan of the city of Bologna, is to produce information about climate changes, risks and vulnerability in the city and to define local measures in order to make it more resilient. Minimum, maximum temperature, total amount of precipitation, heat wave duration index, frost days and consecutive number of dry days are the main climatic indices analyzed. Future climate scenarios of these indices are then constructed at local level, over the period 2021-2050 and 2070-2099. A statistical downscaling technique, applied to the ENSEMBLES-Stream1 global climate simulations (A1B scenario) has been developed in order to reach this objective. The observed climate profile reveals significant positive trends in temperature and a slightly decrease in precipitation. As regards future scenario, the magnitude of projected changes in temperature at Bologna is around 2.5°C in the first period and 5.5°C in the second period,. The results emphasize also a significant change in seasonal precipitation especially to the end of century.

**Keywords:** temperature, precipitation, projections, statistical downscaling

## 1. TEXT

### 1.1 Introduction

The project BLUE AP –“*Bologna Local Urban Environment Adaptation Plan for a Resilient City*” leads by the Municipality of Bologna, Kyoto Club, ARPA Emilia-Romagna and Ambiente Italia aims at the definition of an adaptation plan by 2015. The IPCC report 2007 underlined that adaptation is referred to: “adjustment in natural or human systems in response to actual or expected climatic stimuli or their effects, which moderates harm or exploits beneficial opportunities. Various types of adaptation can be distinguished, including anticipatory, autonomous and planned adaptation (IPCC, AR4, WGII, 2007). This means that adaptation consists of making systems or territories less vulnerable to climate change, via measures to reduce its effective impacts, or by improving the response capacities of companies and the environment. Thus, adaptation should be defined according to the vulnerability of the territory and, in particular according to geographic factors, infrastructures and the vulnerabilities specific to local stakeholders. This is a sensitive work due to the fact that there many uncertainties to solve, for example some of them are linked with uncertainties in climate projections or emission scenarios. Thus, a detailed local climate profile, especially over future, in the framework of a multi-model approach it is required in orde to better define an adaptation plan at local level. This is the main aim of the present work, namely the construction of the local climate profile for Bologna city, the results being the baseline for the definition of the adaptation measures planned to be done in the BLUEAP project.

### 1.2 Methods and data

The best tools made available by the climate community, in order to evaluate the future climate projections over different spatial and temporal scale, are the coupled global climate models (AOGCMs). The spatial resolution of the global models has been improved in the last time arriving to 100km. Unfortunately, this resolution is not sufficient for the impact studies, such as an increase of resolution is requested in order to study the impact of climate changes at local scale. The dynamical and statistical downscaling methods are used in order to reach this objective. The statistical downscaling technique presents the advantage that is not expensive in terms of computational time and the climate signal could be constructed at the

station requested by the end-users. One major problem for all tools mentioned before is to quantify and reduce the uncertainties that appear in modeling processes. Particular attention has been paid on this problem and many projects have been focused on this issue. One of this is the Ensembles project (<http://www.ensembles-eu.org/>), where it was recommended to use a range of models over the same area and construction of an ensemble mean (EM).

In the present work, the climate change projections at Bologna are obtained through the statistical downscaling model (SD) developed by ARPA-SIMC. The statistical downscaling technique (SD) is based on the assumption that the local climate is determined by large-scale fields variability (predictors) linked to the local features (predictands). The model is in fact a multivariate regression based on canonical correlation analysis applied at seasonal level (CCAReg model). Through the canonical correlation analyses (CCA) is detected the link between “large scale fields”, that are actually best represented by GCMs ( for example mean sea level pressure, geopotential height at 500 hPa, temperature at 850hpa), and “local fields” (minimum, maximum temperature or total amount of precipitation). The most important patterns provided by CCA (von Storch, 1995) are then used in the multivariate regression scheme (CCAReg).The model is constructed over the observed period, namely 1958-1978 and 1996-2002, and validated over the period 1979-1995. This kind of approach is known as Perfect-Prognostic (Wilks 2006). The validation of the model is done in terms of BIAS, RMSE, and correlation coefficient. Once the most skilfull SD is selected for each season and predictand, this is then applied to the predictors simulated by Ensembles- GCM experiments, in order to evaluate the local future scenarios. The SDs scheme here proposed use as predictors a selection of fields as mean sea level pressure (MSLP), 500hPa geopotential height (Z500) and temperature at 850 hPa (T850), already tested in previous works over Northern-Italy and different other Italian regions (Tomozeiu et al., 2013, Villani et al., 2011).

The data used in the construction of the model includes:

- daily minimum, maximum temperature and precipitation measured over 25 stations from Emilia-Romagna region over the period 1958-2002. The selection of station has been done such as to catch the spatial variability of climate over the region. The data set includes also the historical station of Bologna, data that covers the period 1951-

2011. The station was initially placed in via della Zecca, (25/06/1934 to 31/12/1953), then has been moved to Piazza VIII Agosto (height 51m., latitude 44°29'36" and longitude 01°06'25"). These data have been used in order to compute mean and extreme events of temperature and precipitation at seasonal scale;

-large scale fields (mean sea level pressure, geopotential height and temperature at 850 hPa) from ERA40 reanalysis that covers the period 1958-2002. These data have been used in the set-up of the statistical downscaling model;

-large scale fields from the following global climate: IPSL, METOHC, MPIMET, INGV-CMCC e FUB(2 runs). The data covers the period of: control run, 2021-2050, 2071-2099, runs done in the framework of ; A1B emission scenario.

The following climatic indices had been selected, computed and analyzed at seasonal and annual level, in order to construct present and future climate profile for Bologna city:

- seasonal and annual minimum (Tmin) and maximum temperature (Tmax);
- the 90th percentile of maximum temperature (Txq90);
- the 10th percentile of minimum temperature (Tnq10);
- the number of frost days, defined as the number of days when the minimum temperature is under 0°C (Fd)
- the number of ice days, defined as the number of days when the minimum and maximum temperature are under 0°C (Txice)
- heat wave duration (HWD), defined as the maximum number of consecutive days with maximum temperature greater than 90th percentile. This index has been computed for each season and particular attention has been paid on summer.
- seasonal and annual amount of precipitation (prec);
- the number of days with precipitation greater than 90th percentile;
- the number of consecutive dry days, defined as the maximum number of consecutive days without precipitation (pxcdd).

The above indices were selected such as to describe the intensity and the frequency of extreme events over observed period. Trend analysis have been performed for each index, season and the significance of trends has been tested through statistical test (Kendall-Tau test). The results have been included in the description of the observed local climate profile of Bologna.

### 1.3 Results

#### *The variability of observed temperature and precipitation*

The analysis of annual minimum and maximum temperature registered at Bologna emphasizes a positive trend over the period 1951-2011, more intense in the maximum (0.3°C/decade) than in the minimum (0.2°C/decade). The signal of warming became more intense after 1990, when a peak of 2.5°C of anomaly had been registered. The positive trend of temperature has been detected also at seasonal level, more intense during summer and especially after 1990 when peaks up to 4°C of anomalies had been registered [Fig.1]. A similar tendency of increase has been detected analyzing the extreme of temperature. For example, 10th percentile of minimum and 90th percentile of maximum temperature exhibits positive and significant trends for each season and at annual level. In addition, a significant negative trend has been identified for the winter frost days, while positive trend has been detected in the summer heat waves [Fig.2].

The quantity of precipitation registered at Bologna shows a slightly negative trend during winter, spring, and summer and a positive trend during autumn, over the period 1951-2011. As regards seasonal extreme of precipitations, it has been noted that the dry days index presents a positive trend over 1951-2011 period, more intense during summer, while a slightly positive trend has been detected in the frequency of days with intense precipitation in all seasons (except on spring).

#### *Climate change scenarios at Bologna over the periods 2021-2050 e 2071-2099*

Climate change scenarios of seasonal minimum and maximum temperature obtained through statistical downscaling technique applied to the 6GCMs experiments, estimate a possible increasing in both minimum and maximum temperature at Bologna, in all seasons and over both periods: 2021-2050 and 2071-2099 with respect to 1961-1990.

Figure 3 presents like an example the PDFs of winter T<sub>min</sub> changes projected at Bologna over the period 2021-2050 (Ensemble Mean). As could be noted an increase of temperature around 1.2°C is projected for winter minimum temperature, that connects also to a shift of whole distribution to “warm” values. A similar signal of changes has been obtained for the other seasons, with the peak of increasing during

summer when the projected changes is around 2.5 °C, over the period 2021-2050 with respect to 1961-1990 period.

The warming becomes more pronounced going to the end of the century, namely to the period 2071-2099, when the projected increasing in minimum and maximum temperature (central value of the probability distribution function) during winter, spring and autumn is between 3-4°C and around 5.5°C during summer season[Fig.4]. As in the case of first period, a shift of the distribution to the “right” is also obtained over 2071-2099.

The analysis performed on extreme temperature reveals important future changes. An increase in seasonal 10th percentile of minimum temperature of 1.5°C in the first period and 3.5°C in the second period, has been projected by the statistical scheme. It is important to underlies that as concerns the 10th percentile of minimum temperature, the projected changes over the period 2071-2099 could connect to a values of percentile close to 1°C with respect to - 2.7°C that characterized the 1961-1990 period, so a future change not only of the magnitude of 10th minimum temperature but also of the sign. This could connect also to a decrease in the number of frost days. In fact, the scenarios constructed for the number of frost days emphasis a decrease during winter, spring and autumn, more pronounced at the end of the century. As regards summer extremes temperature, the projections shows important changes also in 90th percentile of maximum temperature, with an increase especially at the end of the century when the index could reach 40°C with respect to 33.7°C of the present climate (1961-1990). This is associated also with an increase in the number of heat waves, namely the maximum number of consecutive days with maximum temperature greater than 33.7°C. Figure 5 p presents an example of climate scenarios of seasonal heat wave at Bologna, over future. As could be noted the index shows significant signal of changes to the end of period.

The statistical downscaling techniques developed for the seasonal precipitation and applied to each GCM reveals in generally a decrease of precipitation over both periods 2021-2050 and 2071-2099. During the first period, the projected decrease is around -5% during winter (not significant from the statistical point of view) and around -15% in the other seasons[ Fig. 6]. The signal is more pronounced at the end of the century and especially during summer (-30%). As regards extreme of precipitation, the projections show a possible increase in the maximum number of consecutive dry

days ,especially during winter spring and summer, and an increase in the summer intense precipitation.

#### 1.4 Conclusions

The results of present and future climate variability at Bologna could be summarised as follows:

- positive and significant trends of seasonal minimum and maximum temperature over the period 1951-2011 (around 0.3°C/decade) have been detected. During the analyzed period, an increase in the heat wave duration, especially during summer, and a decrease in winter frost and ice days has been founded. These signals became more intense after 1990, when strong and positive anomalies in temperature have been recorded ( for example summer 2003, winter 2007-2008)
- as concerns observed precipitation, the signal of trend is different from season to season. A slightly decrease have been observed during winter, spring and summer, while a slightly increase has been noted during autumn. The observed consecutive dry days shows an increase during summer season, when it was noted also an increase in the frequency of the number of intense precipitation.
- the future scenarios constructed through the statistical downscaling scheme applied to 6GCMs show a possible increase in the minimum and maximum temperature, up to 2°C over the period 2021-2050 with respect to 1961-1990. The increase is more pronounced to the end of the century, and especially during summer , when the anomalies could reach 5.5°C respect to present climate. This will lead to a possible increase in the heat wave duration. As regards precipitation, a reduction of the amount has been projected during all seasons, more intense to the end of century and especially during summer season (reduction around 30% ).

As could be noted, significant changes are projected to occur in the climate of Bologna city and these could have important impacts in different sectors of activities and on the society. The above results of local climate profile, that underlines some risks and vulnerability of the city, represents the baseline of the measures to be

defined and implemented over Bologna city in the framework of BLUE AP Life+ project.

## 2. ACKNOWLEDGMENTS

The ENSEMBLES data used in this work was funded by the EU FP6 IP Ensembles (Contract nr 505539) whose support is gratefully acknowledged. The results have been obtained in the framework of BLUE AP Life+ project (<http://www.blueap.eu/>).

## 3. REFERENCES

1. IPCC- Intergovernmental Panel on Climate Change 2007a. Climate Change 2007: Synthesis Report. Contribution of Working Groups I, II and III to the Fourth Assessment Report of the Intergovernmental Panel on Climate Change [Core Writing Team, Pachauri R.K and Reisinger A.ed.]. IPCC, Geneva, Switzerland, 104 pp
2. Tomozeiu, R., Agrillo, G., Cacciamani, C., Pavan, V. (2013), Statistically downscaled climate change projections of surface temperature over Northern Italy for the periods 2021-2050 and 2071-2099, Nat. Hazard, DOI 10.1007/s11069-013-0552-y
3. Villani G, Tomei F, Tomozeiu R, Marletto V (2011) Climate scenarios and their impacts on irrigated agriculture in Emilia –Romagna, Italy, Italian J of Agrom, Anno XVI, no.1, Aprile 2011, Patron Editore, Bologna, pag. 5-16
4. Von Storch H (1995), Spatial Patterns: EOFs and CCA. In: von Storch H, Navarra A (eds) Analysis of climate variability. Application of statistical techniques. Springer pp 227–258

#### 4. IMAGES AND TABLES

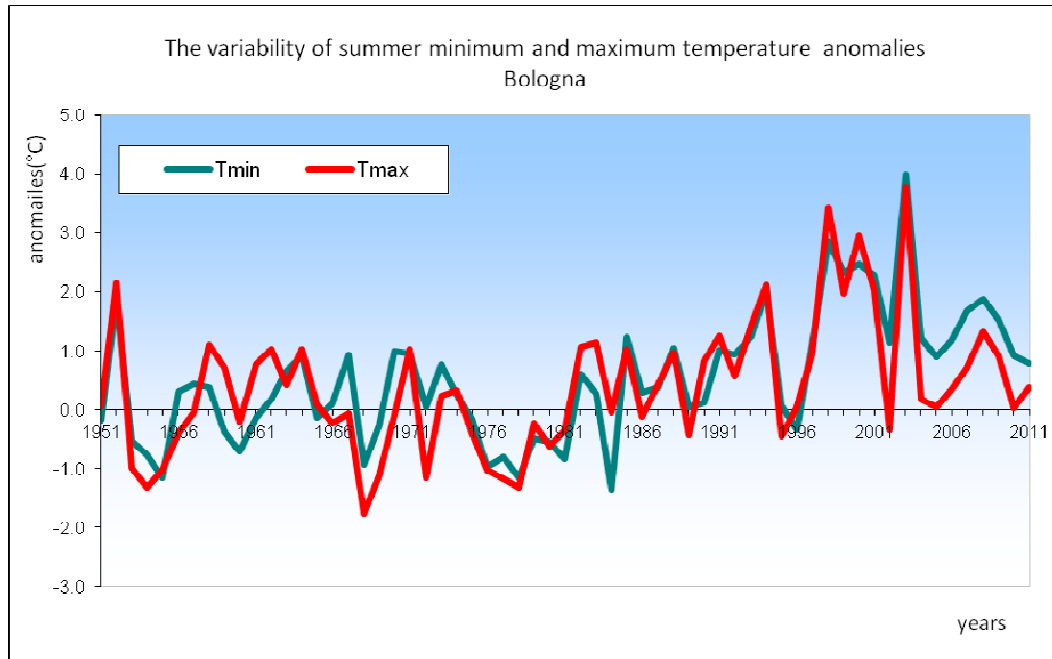


Fig. 1 The temporal variability of summer minimum and maximum temperature anomalies – Bologna

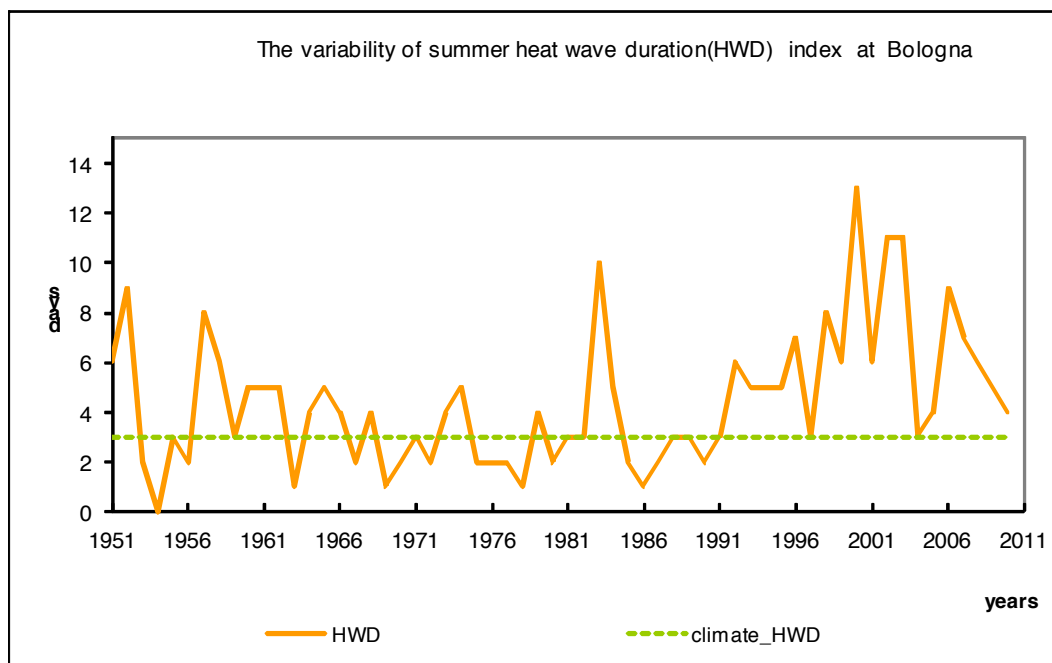


Fig. 2 The evolution of the time series of heat wave duration (continuous line) and the climatic value of the index (dashed line)

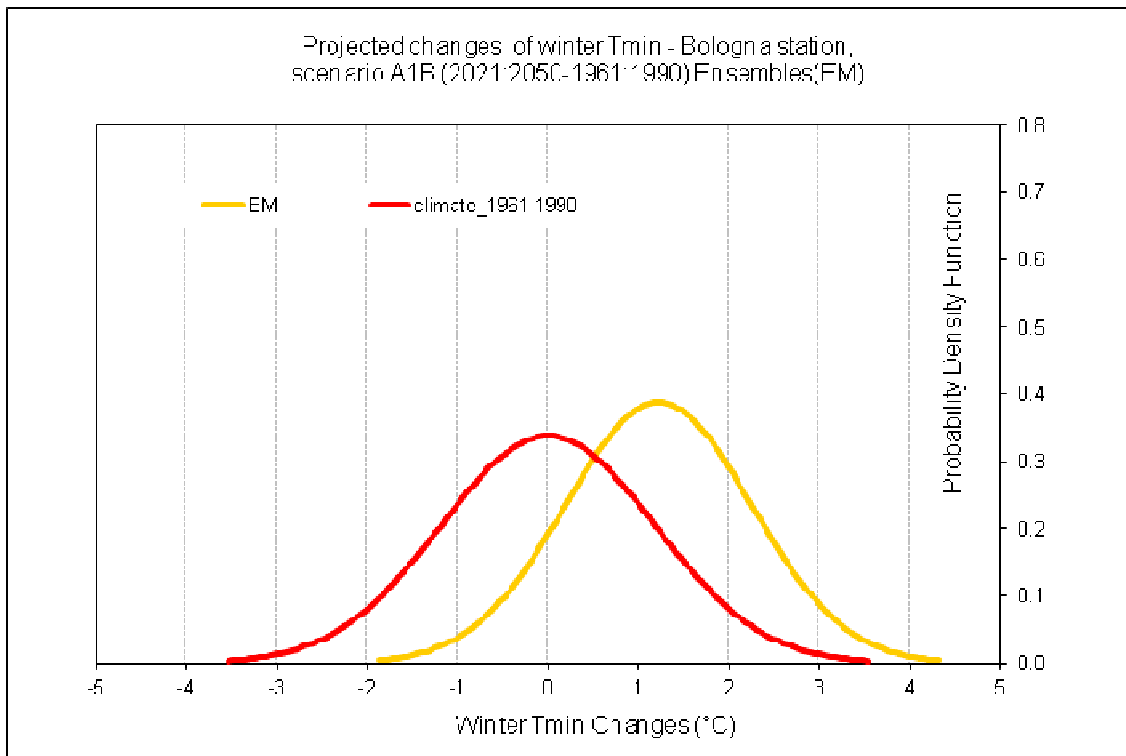


Fig. 3 Climate change projections of winter minimum temperature-Bologna (Ensemble-Mean), 2021-2050 with respect to 1961-1990.

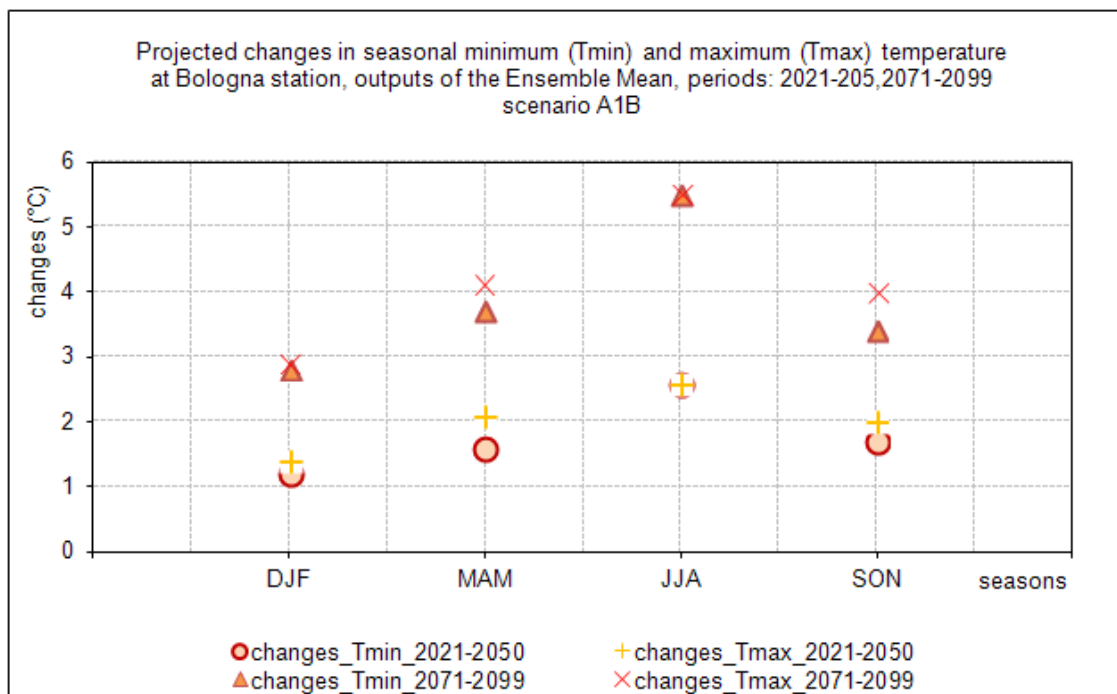


Fig. 4 Projected changes of seasonal temperature-Bologna

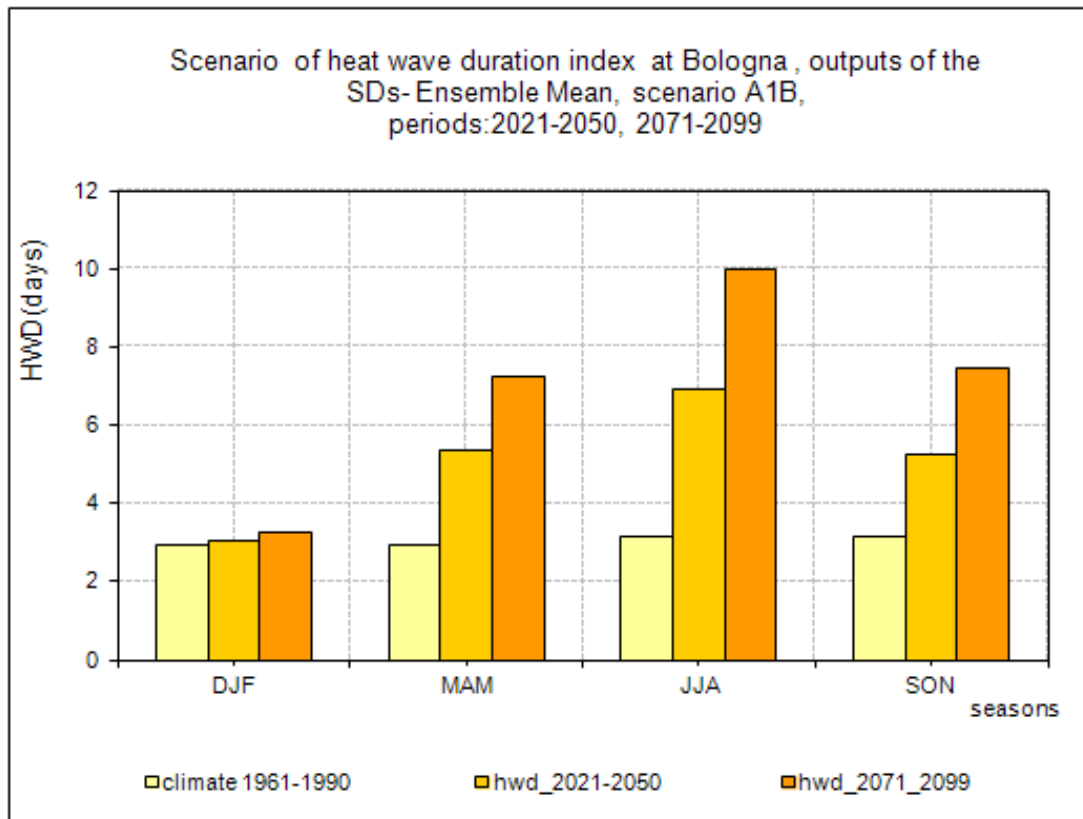


Fig. 5 Observed and projected seasonal heat waves at Bologna

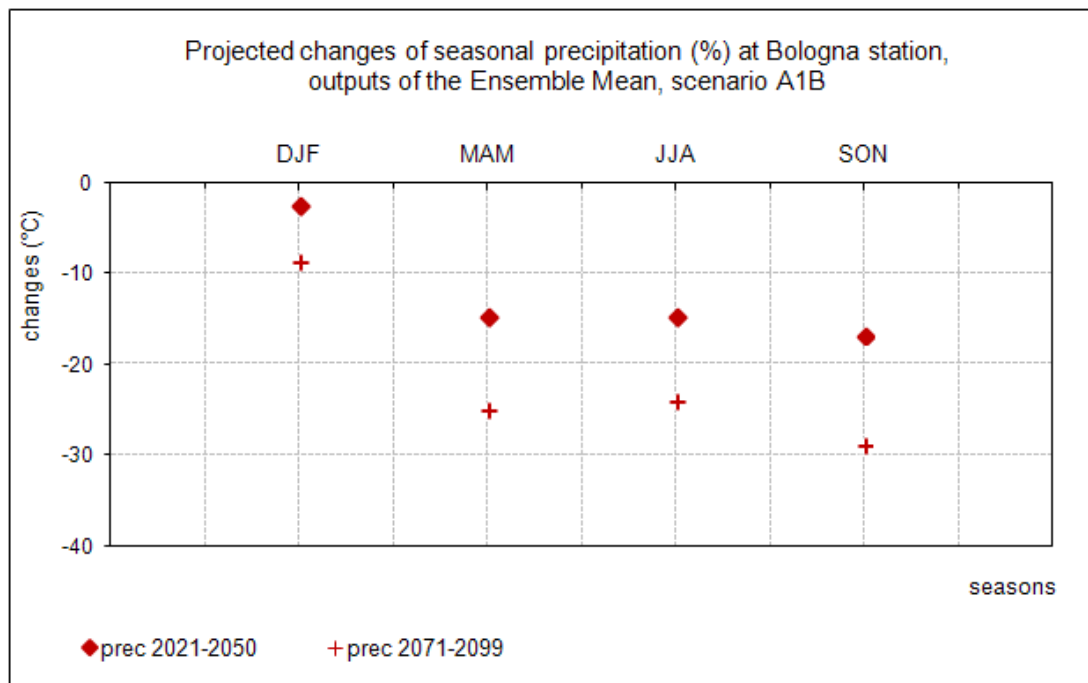


Fig. 6 Scenario of seasonal precipitation obtained through statistical downscaling technique applied to 6GCMs (Ensemble Mean) at Bologna, over the periods 2021-2050 e 2071-2099.

# Impacts & Implications of Climate Change

Impacts & Implications of  
Climate Change

**Methods for assessment/  
quantification of climate  
change impacts**

## Fire In Ice And Sediments: Looking For Early Human Impacts

Zennaro P.<sup>1,2\*</sup>, Kehrwald N.<sup>1</sup>, Kirchgeorg T.<sup>1</sup>, Zangrando R.<sup>2</sup>, Battistel D.<sup>1</sup>, Schüpbach S.<sup>1,3</sup>, Gambaro G.<sup>1,2</sup>, Barbante C.<sup>1,2,4</sup>

<sup>1</sup>Ca' Foscari University of Venice, Department of Environmental Science, Informatics and Statistics, Venice, Italy, <sup>2</sup>Institute for the Dynamics of Environmental Processes, IDPA-CNR, Venice, Italy, <sup>3</sup>Climate and Environmental Physics, Physics Institute and Oeschger Centre for Climate Change Research, University of Bern, Bern, Switzerland, <sup>4</sup>Centro B. Segre, Accademia Nazionale dei Lincei, Rome, Italy

\*Corresponding Author: piero@unive.it

### Abstract

Pre-industrial fire-history records provide baseline estimates of biomass burning at local to global scales, but there remains a need for fire proxies that span millennia in order to understand the role of humans and fire in the climate system. We present two European projects, which aim to quantify temporal and geographical changes of fire activity. In the Past4Future project we use the specific biomarker levoglucosan to produce the first high-resolution reconstruction of boreal fire activity over the past 120,000 years, by analysing the NEEM ice core (77.49 N; 51.2° W, 2480 m a.s.l.). Changes in biomass burning tracers coincide with temperature changes over the past 2000 years except during periods of extreme droughts, when precipitation changes are the dominant factor. North America is a primary source of biomass burning aerosols due to its relative proximity to the NEEM camp. During major fire events, however, links with levoglucosan peaks and regional drought reconstructions suggest that Siberia is also an important source of pyrogenic aerosols to Greenland. In the Early Human Impact project we aim to assess geographical and temporal variation of fire activity, by analysing environmental archives places in regions which correspond with the centers of the origin of agriculture, in order to assess the possibility of anthropogenic influences on the environment and on the climate system through deforestation.

**Keywords:** levoglucosan, Early Human Impact, ice cores, sediment cores, biomass burning

## 1. INTRODUCTION

Fire is a key Earth system process and has a crucial role in the behavior and extent of ecosystems<sup>1-3</sup>. Fire affects regional and global biogeochemical cycles, ecosystems, land-surface properties, the carbon cycle, atmospheric chemistry, aerosols and human activities<sup>4-6</sup>. Fire affects the climate system by releasing carbon<sup>6</sup> that would otherwise be stored in woody vegetation<sup>2</sup>. Biomass burning emits up to 50% as much CO<sub>2</sub> as fossil fuel combustion, thereby affecting the climate system<sup>6</sup>.

Fire influences the climate system, but in turn fire variations are influenced by climate<sup>7,8</sup>. Biomass burning is highest at intermediate moisture levels<sup>9</sup>, with climatic conditions that are wet enough to allow biomass to grow, but dry enough to allow combustion<sup>10</sup>. Increased temperatures and atmospheric CO<sub>2</sub> permit greater plant productivity and could result in greater fuel availability and hence increased fire activity<sup>11,12</sup>. Human activities have also influenced biomass burning trends over the past millennia<sup>6,11,13,14</sup> through deforestation and agricultural practices<sup>15</sup>. The observable impact of humans on fire regimes differs by geographic region<sup>8,14,16</sup> but over the course of the 20<sup>th</sup> century human activity began to influence the global fire regime more than natural causes<sup>11,17</sup>.

## 2. THE PROJECTS

### 2.1 *The Past4Future Project*

Many indicators or proxies of past fire activity exist including altered products of plant combustion (e.g. charcoal, black carbon), partially combusted biological material (e.g. fire scars in tree rings), or chemical markers directly produced and volatilized during vegetation combustion (e.g. resin acids, polycyclic aromatic hydrocarbons)<sup>3</sup>.

Monosaccharide anhydrides are one of the few fire proxies that have specific sources<sup>18,19</sup>. Levoglucosan (1,6-anhydro- $\beta$ -D-glucopyranose) is a monosaccharide anhydride released only during the pyrolysis of cellulose and thus is a specific molecular marker for vegetation combustion<sup>18,19</sup>. Levoglucosan is injected into the atmosphere in convective smoke plumes, deposited on glacier surfaces through wet and dry deposition, and preserved in the snow and ice<sup>18,20-22</sup>. Although levoglucosan is oxidized by OH radicals in the gas phase<sup>23</sup> and in atmospheric water droplets<sup>24</sup>, its high concentration in biomass emissions means that levoglucosan remains a strong potential tracer for fire activity even across remote distances<sup>20,25-27</sup>.

Ice cores from polar regions are widely used to reconstruct detailed climate records over the past hundreds of thousands of years, and thus are powerful tools in paleoclimate research. The North Greenland Eemian Ice Drilling Project (NEEM) provides an ice core from northwest Greenland extending back through the last interglacial, the Eemian (Fig. 1). The NEEM ice core was drilled from 2008 to 2012 and reached a depth of 2540 m.

In the Past4Future project, we determined levoglucosan fluxes throughout the Greenland NEEM ice core (Fig. 1) to reconstruct changes of fire activity during the past 120,000 yrs. We compare our results with Northern Hemisphere fire records, climate conditions obtained from historical records and paleoarchives to identify sources of and controls on fire emissions registered in NEEM and to assess potential anthropogenic contributions.

## **2.2 The Early Human Impact Project (EHI)**

Holocene fire variations are influenced by climate and by human activities<sup>8,11</sup>. Fire ignitions are caused by natural sources such as lightning but human activities, including household fires and agricultural practices are increasingly altering global fire activity<sup>15</sup>. A fundamental paleoclimate question is when humans began to significantly alter fire regimes and, in turn, the climate system. Anthropogenic aerosols may have altered the global carbon cycle and the climate system for thousands years, through the release of greenhouse gasses from deforestation and early agricultural activities<sup>28</sup>. A wide array of

archeological, cultural, historical and geologic evidence points to anthropogenic changes resulting from early agriculture in Eurasia, including widespread forest clearance 7000 years ago.

The EHI Project incorporates continuous ice and lake core climate records which correspond with centers of the origin of agriculture or from remote polar sites. Charcoal records deposited both in non-polar ice and sediment cores provide estimates of biomass burning at local scales and are powerful tools to reconstruct fire history and to infer local anthropogenic impacts<sup>7</sup>. The Global Charcoal Database (GCD) compiles individual and local charcoal records from terrestrial and marine sediment cores, and creates regional to global syntheses from the collection of hundreds of sediment cores<sup>11,29</sup>. However, human influences on biomass burning across continental to global scales are relatively unknown.

In the EHI Project, our approach acknowledges the weaknesses inherent in most fire proxies (local reconstructions, geographical sampling gaps) used in environmental archive studies and remedies this by integrating the results from multiple fire (i.e. charcoal, levoglucosan, mannosan, galactosan) and “anthropogenic” proxies (i.e. coprostanol) to identify the robust variations in past biomass burning during the Holocene. As levoglucosan can be transported hundreds to thousands of kilometers<sup>30</sup>, these ice core records complement GCD reconstructions that record combustion within tens of km of the sampling sites, and provide fire activity data for regions where charcoal records do not exist.

The combination of ice and sediment cores are the only scientific approach to fire history that provides data across all possible time scales and types of information on fire, yet this combination has never been utilized. As both levoglucosan and climate parameters are measured from the same depth and time within the ice or sediment matrix, the multi-proxy nature of ice and lake cores presents the perfect material to investigate the links between fires and climate change. We aim to integrate proxy records from seven

continents to provide an interdisciplinary synthesis of the interactions between past fires, human activity, and climate change.

### 3. METHODS

Our levoglucosan dataset consists of more than 1300 samples from the NEEM ice core, where each sample is a 1.10 m inner core section collected after being melted within the continuous flow analysis<sup>31</sup> system at the NEEM camp. Frozen samples for levoglucosan determination were transported from the field to Ca' Foscari University of Venice where they were stored in a -20 °C cold room until analysis. We slightly modified the analytical procedure for determining levoglucosan in ice core samples<sup>32</sup> using liquid chromatography / negative ion electrospray ionization - tandem mass spectrometry (HPLC/(-)ESI-MS/MS) at picogram per milliliter concentration<sup>18</sup>. This analytical method has the advantage of allowing the direct determination of levoglucosan by introducing the melted sample and <sup>13</sup>C<sub>6</sub> labeled internal standard into the HPLC instrument. Preanalytical procedures (analyte extraction and purification) are avoided and sample contamination minimized. Long-term fire activity was extracted from the levoglucosan flux profile by analyzing smoothed data, using a LOWESS smoothing tricube function<sup>32</sup>, or, after dividing the levoglucosan profile in 500- and 1000- yr windows, calculating the mean fluxes for each interval.

The analytical method for analyses of biomass burning molecular markers in archived in lake sediments is based on high performance anion exchange chromatography–mass spectrometry, which allows separation and analysis of levoglucosan and its isomers, mannosan and galactosan<sup>33</sup>. Wet sediment samples were freeze-dried, milled and homogenized before being spiked with the internal standard containing <sup>13</sup>C<sub>6</sub> labeled levoglucosan and extracted using pressurized solvent extraction<sup>33</sup>. The mass spectrometer utilized an electrospray ionization source in negative ionization mode.

### 4. RESULTS

#### 4.1 Past4Future project

##### 4.1.1 Source of NEEM fire products: Fuel Loads and Circulation Patterns

Earth's boreal forests cover 9-12 million km<sup>2</sup> (Fig. 1), extending across Scandinavia, Russia and North America, representing approximately 10% of Earth land cover and one third of the total global forested area<sup>34</sup>. Boreal forests form a green belt just below the Arctic Circle interrupted only by the Pacific and Atlantic Oceans, and thus form a major fuel source for fire emissions reaching the Greenland ice sheet. Russian forests alone represent ~25% of global terrestrial biomass<sup>34</sup>.

Back-trajectory and model analyses suggest that North American and Siberian forests are the dominant sources of pyrogenic aerosols transported to the NEEM location<sup>35</sup>. However, Siberian forests may be an essential aspect of boreal fire reconstructions that have not yet been appropriately evaluated. The isotopic composition of dust in the NGRIP, Greenland ice core indicates an Asian origin of particulate matter reaching Greenland<sup>36-38</sup>. These dust studies argue that North America and North Africa are not potential dust sources and demonstrate the influence of Asian sources on material transported to the Greenland ice sheet. Increased wind speeds result in greater dust concentrations and larger particles in ice cores<sup>39,40</sup>. Stronger winds may be expected to also increase levoglucosan concentrations in ice, as the increased wind strength could transport air plumes and biomass burning products more efficiently. However, the lack of correlation between Ca<sup>2+</sup>, dust and levoglucosan suggests that levoglucosan variability is not dominated by changes in transport or in changes in wind strength.

The correspondence of the major NEEM levoglucosan peaks with periods of extreme droughts in northern central Asia further suggests that Asia may be an important fire source during major fire events while North America may be a more important source for background fire activity. The Ushkovsky<sup>41</sup> and Belukha<sup>42</sup> ice cores both contain up to multi-decadal periods of increased fire activity that are similar to peaks in the NEEM ice core suggesting that these sites may receive a contribution from Siberian fire activity (Fig. 1). Asia has generally been ignored as a biomass burning aerosol source for Greenland due in part to the days required for air mass travel time compared to the aerosol atmospheric lifetimes. Contributions from central Asia are important sources during decadal scale droughts<sup>32</sup>.

#### 4.1.2 *Past 2 millennia: Variability in decadal to centennial fire activity*

Relative maxima in the levoglucosan profile are evident between 1000-1300 CE and 1500-1700 CE, and with a lesser extent around 500 CE and 100 CE, while the lowest fire activity is evident around 700 - 900 CE and with a lesser extent around 1300-1500 and 1700-1800 CE (Fig. 2A). The levoglucosan profile correlates with the high latitude northern hemisphere HLNH > 55° GCD composite curve, supporting our results. The HLNH > 55° GCD and levoglucosan data differ near 1600 CE when the HLNH > 55° GCD demonstrates a modest increase in fire activity, while the smoothed NEEM levoglucosan strongly peaks (Fig. 2B). We infer that this maximum in fire activity is due to increased Eurasian boreal forest fires, which are likely underrepresented in the GCD, reflecting the bias in the geographical distribution of GCD sites. Over 50 high latitude North American sites exist yet Siberia only has less than 10 lake cores > 60° N which span a distance of over 7000 km.

Comparisons of the levoglucosan profile with a high-latitude northern hemisphere terrestrial temperature anomaly record<sup>43</sup> suggests a strong correspondence between temperature and fire activity observed in the deep NEEM ice core, except during the levoglucosan maximum centered around 1600 CE (Fig. 2E). Fire activity inferred from the deep NEEM ice core is consistent with the Medieval Warm Period (1000-1300 CE)<sup>44,45</sup> and the Little Ice Age (1580 and 1880 CE)<sup>46</sup> climatic conditions, with high values between the 11<sup>th</sup> and 13<sup>th</sup> century and with low decadal-scale levoglucosan concentrations in the 18<sup>th</sup> century.

Ice core, tree-ring proxy records and archival evidences document extensive north-central Asian droughts concurrent with the strongest centennial-scale levoglucosan concentrations during the 16<sup>th</sup> and 17<sup>th</sup> centuries. The Siberian Belukha ice core identifies a period of exceptionally high forest-fire activity between 1600-1680 CE, following a drought period during 1540-1600 CE, which is coincident with the NEEM levoglucosan centennial scale maximum (1500-1700 CE, Fig. 2A), the highest of the past two millennia. Two central and northern Asian droughts (1587 and 1639 CE) were

the most extreme of the past 5 centuries<sup>47</sup>, and covered much of central Asia<sup>48</sup>. The 1587 CE drought resulted in the desiccation of Lake Taihu (the third largest freshwater lake in China) and the even more spatially extensive 1639 CE drought event resulted in no outflow of the Yellow River<sup>47</sup>.

North American droughts affected fire activity archived in the NEEM ice cores. Elevated aridity and megadroughts during the MWP (900-1300 CE), coincident with levoglucosan peaks, affected large areas of North America and were more prolonged than any 20<sup>th</sup> century droughts<sup>49,50</sup>. Dry conditions during the 16<sup>th</sup> century were also inferred in the Canadian Prairie Provinces<sup>51</sup> and in western North America<sup>50</sup>.

Temperature appears to be the main control on boreal fire activity on centennial time scales, except during dry periods when levoglucosan peaks and boreal fires are mainly influenced by precipitation changes on multi-decadal or shorter timescales<sup>32</sup>. We conclude that the 1500-1700 CE maximum in fire activity is due to increased boreal forest fires, caused by extensive dry conditions in the Asian region. This evidence suggests that climate variability has influenced boreal forest fires more than anthropogenic activity over the past.

## **4.2 Preliminary results from the Early Human Impact project**

### *4.2.1 Fire activity inferred from mountain and polar ice cores*

We are currently analysing ice cores from Antarctica (EPICA Dome C and Talos Dome), Tanzania (Kilimanjaro), the Caucasus (Elbrus), the Tibetan Plateau (Muztagh), Italy (Ortles) and multiple short ice cores and snow samples collected from polar locations. Teams of researchers including from the University of Venice, the Russian and Chinese Academy of Sciences and the Ohio State University are working together to analyse both the past fire histories in conjunction with climate parameters including past temperature, accumulation and atmospheric chemistry.

EPICA Dome C is the longest temporal ice core in the world, extending back 800,000 years or eight glacial-interglacial cycles. Under the auspices of the EHI project we are

investigating levoglucosan concentrations in both the Holocene and Eemian sections of the core in order to provide a comparison with the Arctic NEEM core. Unlike Greenland that is surrounded by the largest continental landmasses in the world, Antarctica is completely surrounded by ocean. The closest possible biomass burning sources to the Dome C site are Patagonia, southern Africa, Australia and New Zealand. Unlike NEEM, where large continental ice sheets significantly covered the majority of potential biomass burning source regions, no continental-scale ice sheets covered Antarctic source regions during the last glacial. Therefore, the distance between the Antarctic ice core sites and the biomass burning source regions remained the same over glacial-interglacial cycles.

EPICA Dome C is located in an extremely low accumulation site in central East Antarctica, resulting in the long temporal resolution of the core. Both this low accumulation (i.e. less potential for wet deposition) and the long transport distances result in mean levoglucosan concentrations that are up to 10 times lower than NEEM Holocene concentrations and up to 50 times lower than Tibetan Plateau concentrations or Kilimanjaro concentrations. Initial results from the EPICA Dome C ice core suggest that Australia and New Zealand are the main biomass burning sources for the Holocene. In order to test this hypothesis we are investigating the coastal Taylor Dome ice core as a comparison with EPICA Dome C. Both Australia and New Zealand have some of the most extreme changes in fire activity in the world<sup>14,52</sup>, where the arrival of the Maori and Europeans substantially changed the existing fire regimes, but the long-range effects of these biomass burning changes are still unknown.

#### *4.2.2 Sediment sampling and analyses*

Sediment cores record local changes in fire activity, and can be synthesized into regional to global compilations. The arrival and dispersal of the Maori in New Zealand significantly changed an ecosystem that contained no humans and rarely burned into a human-settled, cleared landscape<sup>14</sup>. This change from natural fire activity to a century of extensive deforestation presents an ideal case study for determining fire histories. We compare our methods for examining levoglucosan in sediment cores<sup>33</sup> with established

charcoal methods. Charcoal provides an idea of net burning, while the relative ratios of monosaccharide anhydrides (levoglucosan/mannosan and levoglucosan/[mannosan+galactosan]) may help determine changes in the primary burned vegetation. Levoglucosan, mannosan and galactosan concentrations correlate significantly with macroscopic charcoal concentration<sup>33</sup>. This correlation between a well-known marker and fire history with the novel technique of examining levoglucosan, mannosan and galactosan in sediment cores demonstrates the feasibility of using monosaccharide anhydrides in sediment cores as a fire and burned vegetation marker.

Reconstructions of anthropogenic activities and their impact on the environment by means of biomass burning proxy can be improved by the analysis of faecal sterol biomarkers. The presence of human fecal sterols (5 $\beta$ -coprostanol and 5 $\beta$ -epicoprostanol) indicate that people were active in the local area, while other fecal sterols indicate the presence of domesticated sheep and cattle (5 $\beta$ -stigmastanol and 5 $\beta$ -epistigmastanol)<sup>53</sup>. Compiling biomass burning information together with markers indicating the presence of humans and grazing animals can help to distinguish paleofires from natural to anthropogenic and provide insight into humans influenced local fire regimes through agricultural and pastoral practices

At University of Venice, researcher are developing novel analytical methods based on gas chromatography-mass spectrometry (GC-MS) for the determination of a number of faecal sterols of interest, such as cholesterol, coprostanol, sitosterol and stigmastanol, extracted from lake sediments. In addition, more information can be obtained from the relative amount of these indicators, as they are distinctive for human (coprostanol+cholesterol), grazing animals (stigmastanol), poultry (sitosterol+cholesterol). After validation, the method will be applied to lacustrine sediments such as the Lake Trasimeno, Italy core.

## 5. CONCLUSION

Biomass burning is a major source of greenhouse gases and influences regional to global climate. We present a fire activity reconstruction based on levoglucosan

signatures in the NEEM ice core, which demonstrates a quantifiable alteration of the climate system by fire in the Northern Hemisphere. The correlation between our innovative NEEM levoglucosan results and established existing charcoal analyses demonstrates that ice core levoglucosan records are a viable method for reconstructing past fire history.

During the past two millennia, fire activity strongly follow the temperature trend. North America is likely the main source due to the proximity to the NEEM location. However, on shorter time scale, increases in boreal fire activity coincide with the most extensive central and northern Asian droughts of the past two millennia. Regional droughts, in fact, result in large amounts of available deadwood as fuel resulting in intense fires capable of generating deep convection<sup>54-57</sup>.

The Elbrus, Muztagh and Ortles ice cores are new climate records that were drilled within the past three years, and are currently being analyzed to find anthropogenic influences on fire signature along these ice cores. EPICA Dome C, Talos Dome, and Kilimanjaro have already been analysed for suites of climate information and the fire histories will provide a bonus-added paleorecord extracted from the archive ice.

## **6. ACKNOWLEDGMENTS**

NEEM is directed and organized by the Center of Ice and Climate at the Niels Bohr Institute and US NSF, Office of Polar Programs. The research leading to these results has received funding from the European Union's Seventh Framework programme (FP7/2007-2013) under grant agreement no. 243908, "Past4Future. Climate change - Learning from the past climate", and is Past4Future contribution no. 75. The research leading to these results has received funding from the European Union's Seventh Framework programme ("Ideas" Specific Programme, ERC Advanced Grant) under grant agreement no 267696 "EARLYhumanIMPACT". This is EarlyHumanImpact contribution no. 11. We acknowledge the substantial efforts of the NEEM logistics, drilling, and science trench teams for their substantial efforts during the collection of the NEEM-2011-S1 core, as well as the entire DRI ice core analytical team for their efforts in

analyzing the core. Financial support of the Swiss National Science Foundation is acknowledged (Simon Schüpbach). We thank PAGES (Past Global Changes) for supporting the paleofire studies development. We also acknowledge Elga (High Wycombe, U.K.) for providing ultrapure water.

## 6. REFERENCES

- 1 Bond, W. J. & Keeley, J. E. Fire as a global 'herbivore': the ecology and evolution of flammable ecosystems. *Trends Ecol. Evol.* **20**, 387-394, doi:10.1016/j.tree.2005.04.025 (2005).
- 2 Bond, W. J., Woodward, F. I. & Midgley, G. F. The global distribution of ecosystems in a world without fire. *New Phytol.* **165**, 525-537, doi:10.1111/j.1469-8137.2004.01252.x (2005).
- 3 Conedera, M. *et al.* Reconstructing past fire regimes: methods, applications, and relevance to fire management and conservation. *Quat. Sci. Rev.* **28**, 555-576, doi:10.1016/j.quascirev.2008.11.005 (2009).
- 4 Keywood, M. *et al.* Fire in the Air: Biomass Burning Impacts in a Changing Climate. *Critical Reviews in Environmental Science and Technology* **43**, 40-83, doi:10.1080/10643389.2011.604248 (2013).
- 5 Andreae, M. O. & Merlet, P. Emission of trace gases and aerosols from biomass burning. *Glob. Biogeochem. Cycle* **15**, 955-966, doi:10.1029/2000gb001382 (2001).
- 6 Bowman, D. *et al.* Fire in the Earth System. *Science* **324**, 481-484, doi:10.1126/science.1163886 (2009).
- 7 Marlon, J. R. *et al.* Global biomass burning: a synthesis and review of Holocene paleofire records and their controls. *Quat. Sci. Rev.* **65**, 5-25, doi:10.1016/j.quascirev.2012.11.029 (2013).
- 8 Power, M. J. *et al.* Changes in fire regimes since the Last Glacial Maximum: an assessment based on a global synthesis and analysis of charcoal data. *Clim. Dyn.* **30**, 887-907, doi:10.1007/s00382-007-0334-x (2008).
- 9 Daniau, A. L. *et al.* Predictability of biomass burning in response to climate changes. *Glob. Biogeochem. Cycle* **26**, GB4007, doi:10.1029/2011GB004249 (2012).
- 10 Pyne, S. J. The fires this time, and next. *Science* **294**, 1005-1006, doi:10.1126/science.1064989 (2001).
- 11 Marlon, J. R. *et al.* Climate and human influences on global biomass burning over the past two millennia. *Nat. Geosci.* **1**, 697-702, doi:10.1038/ngeo313 (2008).
- 12 Daniau, A. L., Harrison, S. P. & Bartlein, P. J. Fire regimes during the Last Glacial. *Quat. Sci. Rev.* **29**, 2918-2930, doi:10.1016/j.quascirev.2009.11.008 (2010).
- 13 Kaplan, J. O. *et al.* Holocene carbon emissions as a result of anthropogenic land cover change. *Holocene* **21**, 775-791, doi:10.1177/0959683610386983 (2011).
- 14 McWethy, D. B., Whitlock, C., Wilmshurst, J. M., McGlone, M. S. & Li, X. Rapid deforestation of South Islands, New Zealand, by early Polynesian fires. *Holocene* **19**, 883-897, doi:10.1177/0959683609336563 (2009).
- 15 FAO. *Fire management: Global assessment 2006*. (Food and Agriculture Organization of the United Nations, 2007).
- 16 Marlon, J. R. *et al.* Long-term perspective on wildfires in the western USA. *Proc. Natl. Acad. Sci. U. S. A.* **109**, E535-E543, doi:10.1073/pnas.1112839109 (2012).
- 17 Pechony, O. & Shindell, D. T. Driving forces of global wildfires over the past millennium and the forthcoming century. *Proc. Natl. Acad. Sci. U. S. A.* **107**, 19167-19170, doi:10.1073/pnas.1003669107 (2010).

- 18 Gambaro, A., Zangrando, R., Gabrielli, P., Barbante, C. & Cescon, P. Direct determination of levoglucosan at the picogram per milliliter level in Antarctic ice by high-performance liquid chromatography/electrospray ionization triple quadrupole mass spectrometry. *Anal. Chem.* **80**, 1649-1655, doi:10.1021/ac701655x (2008).
- 19 Simoneit, B. R. T. Biomass burning - A review of organic tracers for smoke from incomplete combustion. *Appl. Geochem.* **17**, 129-162 (2002).
- 20 Kehrwald, N. *et al.* Levoglucosan as a specific marker of fire events in Greenland snow. *Tellus Ser. B-Chem. Phys. Meteorol.* **64**, 18196, doi:10.3402/tellusb.v64i0.18196 (2012).
- 21 McConnell, J. R. *et al.* 20th-century industrial black carbon emissions altered arctic climate forcing. *Science* **317**, 1381-1384, doi:10.1126/science.1144856 (2007).
- 22 Fuhrer, K. & Legrand, M. Continental biogenic species in the Greenland Ice Core Project ice core: Tracing back the biomass history of the North American continent. *J. Geophys. Res.-Oceans* **102**, 26735-26745 (1997).
- 23 Hennigan, C. J., Sullivan, A. P., Collett, J. L. & Robinson, A. L. Levoglucosan stability in biomass burning particles exposed to hydroxyl radicals. *Geophys. Res. Lett.* **37**, doi:L09806, 10.1029/2010gl043088 (2010).
- 24 Hoffmann, D., Tilgner, A., Iinuma, Y. & Herrmann, H. Atmospheric Stability of Levoglucosan: A Detailed Laboratory and Modeling Study. *Environ. Sci. Technol.* **44**, 694-699, doi:10.1021/es902476f (2010).
- 25 Fraser, M. P. & Lakshmanan, K. Using levoglucosan as a molecular marker for the long-range transport of biomass combustion aerosols. *Environ. Sci. Technol.* **34**, 4560-4564, doi:10.1021/es991229l (2000).
- 26 Holmes, B. J. & Petrucci, G. A. Water-soluble oligomer formation from acid-catalyzed reactions of levoglucosan in proxies of atmospheric aqueous aerosols. *Environ. Sci. Technol.* **40**, 4983-4989, doi:10.1021/es060646c (2006).
- 27 Holmes, B. J. & Petrucci, G. A. Oligomerization of levoglucosan by Fenton chemistry in proxies of biomass burning aerosols. *J. Atmos. Chem.* **58**, 151-166, doi:10.1007/s10874-007-9084-8 (2007).
- 28 Ruddiman, W. F. The anthropogenic greenhouse era began thousands of years ago. *Clim. Change* **61**, 261-293 (2003).
- 29 Power, M. J., Marlon, J. R., Bartlein, P. J. & Harrison, S. P. Fire history and the Global Charcoal Database: A new tool for hypothesis testing and data exploration. *Paleogeogr. Paleoclimatol. Paleoecol.* **291**, 52-59, doi:10.1016/j.palaeo.2009.09.014 (2010).
- 30 Mochida, M., Kawamura, K., Fu, P. Q. & Takemura, T. Seasonal variation of levoglucosan in aerosols over the western North Pacific and its assessment as a biomass-burning tracer. *Atmos. Environ.* **44**, 3511-3518, doi:10.1016/j.atmosenv.2010.06.017 (2010).
- 31 Kaufmann, P. R. *et al.* An Improved Continuous Flow Analysis System for High-Resolution Field Measurements on Ice Cores. *Environ. Sci. Technol.* **42**, 8044-8050, doi:10.1021/es8007722 (2008).
- 32 Zennaro, P. *et al.* Fire in ice: two millennia of Northern Hemisphere fire history from the Greenland NEEM ice core. *Clim. Past Discuss.* **10**, 809-857, doi:10.5194/cpd-10-809-2014 (2014).

- 33 Kirchgeorg, T., Schüpbach, S., Kehrwald, N., McWethy, D. B. & Barbante, C. Method for the determination of specific molecular markers of biomass burning in lake sediments. *Org. Geochem.* **71**, 1-6, doi:<http://dx.doi.org/10.1016/j.orggeochem.2014.02.014> (2014).
- 34 Zhang, Y. H., Wooster, M. J., Tutubalina, O. & Perry, G. L. W. Monthly burned area and forest fire carbon emission estimates for the Russian Federation from SPOT VGT. *Remote Sens. Environ.* **87**, 1-15, doi:10.1016/s0034-4257(03)00141-x (2003).
- 35 Kahl, J. D. W. *et al.* Air mass trajectories to Summit, Greenland: A 44-year climatology and some episodic events. *J. Geophys. Res.-Oceans* **102**, 26861-26875, doi:10.1029/97jc00296 (1997).
- 36 Bory, A. J. M., Biscaye, P. E., Piotrowski, A. M. & Steffensen, J. P. Regional variability of ice core dust composition and provenance in Greenland. *Geochem. Geophys. Geosyst.* **4**, **1107**, doi:10.1029/2003gc000627 (2003).
- 37 Bory, A. J. M., Biscaye, P. E., Svensson, A. & Grousset, F. E. Seasonal variability in the origin of recent atmospheric mineral dust at NorthGRIP, Greenland. *Earth Planet. Sci. Lett.* **196**, 123-134, doi:10.1016/s0012-821x(01)00609-4 (2002).
- 38 Lupker, M., Aciego, S. M., Bourdon, B., Schwander, J. & Stocker, T. F. Isotopic tracing (Sr, Nd, U and Hf) of continental and marine aerosols in an 18th century section of the Dye-3 ice core (Greenland). *Earth Planet. Sci. Lett.* **295**, 277-286, doi:10.1016/j.epsl.2010.04.010 (2010).
- 39 Ruth, U., Wagenbach, D., Steffensen, J. P. & Bigler, M. Continuous record of microparticle concentration and size distribution in the central Greenland NGRIP ice core during the last glacial period. *J. Geophys. Res.-Atmos.* **108**, doi:10.1029/2002jd002376 (2003).
- 40 Fischer, H., Siggaard-Andersen, M. L., Ruth, U., Rothlisberger, R. & Wolff, E. Glacial/interglacial changes in mineral dust and sea-salt records in polar ice cores: Sources, transport, and deposition. *Rev. Geophys.* **45**, RG1002, doi:10.1029/2005rg000192 (2007).
- 41 Kawamura, K., Izawa, Y., Mochida, M. & Shiraiwa, T. Ice core records of biomass burning tracers (levoglucosan and dehydroabietic, vanillic and p-hydroxybenzoic acids) and total organic carbon for past 300 years in the Kamchatka Peninsula, Northeast Asia. *Geochim. Cosmochim. Acta* **99**, 317 - 329, doi:10.1016/j.gca.2012.08.006 (2012).
- 42 Eichler, A. *et al.* An ice-core based history of Siberian forest fires since AD 1250. *Quat. Sci. Rev.* **30**, 1027-1034, doi:10.1016/j.quascirev.2011.02.007 (2011).
- 43 Mann, M. E. *et al.* Proxy-based reconstructions of hemispheric and global surface temperature variations over the past two millennia. *Proc. Natl. Acad. Sci. U. S. A.* **105**, 13252-13257, doi:10.1073/pnas.0805721105 (2008).
- 44 Crowley, T. J. & Lowery, T. S. How warm was the medieval warm period? *Ambio* **29**, 51-54, doi:10.1639/0044-7447(2000)029[0051:hwwtmw]2.0.co;2 (2000).
- 45 Hiller, A., Boettger, T. & Kremenetski, C. Mediaeval climatic warming recorded by radiocarbon dated alpine tree-line shift on the Kola Peninsula, Russia. *Holocene* **11**, 491-497, doi:10.1191/095968301678302931 (2001).

- 46 Pages 2k. Continental-scale temperature variability during the past two millennia. *Nat. Geosci.* **6**, 339-346, doi:10.1038/ngeo1797, <http://www.nature.com/ngeo/journal/v6/n5/abs/ngeo1797.html> - [supplementary-information](#) (2013).
- 47 Shen, C., Wang, W.-C., Hao, Z. & Gong, W. Exceptional drought events over eastern China during the last five centuries. *Clim. Change* **85**, 453-471, doi:10.1007/s10584-007-9283-y (2007).
- 48 Fang, K. Y. *et al.* Spatial drought reconstructions for central High Asia based on tree rings. *Clim. Dyn.* **35**, 941-951, doi:10.1007/s00382-009-0739-9 (2010).
- 49 Cook, E. R., Woodhouse, C. A., Eakin, C. M., Meko, D. M. & Stahle, D. W. Long-term aridity changes in the western United States. *Science* **306**, 1015-1018, doi:10.1126/science.1102586 (2004).
- 50 Stahle, D. W. *et al.* Tree-ring data document 16th century megadrought over North America. *Eos, Transactions American Geophysical Union* **81**, 121-125, doi:10.1029/00eo00076 (2000).
- 51 St. George, S. S. *et al.* The Tree-Ring Record of Drought on the Canadian Prairies. *J. Clim.* **22**, 689-710, doi:10.1175/2008jcli2441.1 (2009).
- 52 Mooney, S. D., Harrison, S. P., Bartlein, P. J. & Stevenson, J. The prehistory of fire in Australasia. *Flammable Australia: Fire Regimes, Biodiversity and Ecosystems in a Changing World*, 3-25 (2012).
- 53 D'Anjou, R. M., Bradley, R. S., Balascio, N. L. & Finkelstein, D. B. Climate impacts on human settlement and agricultural activities in northern Norway revealed through sediment biogeochemistry. *Proc. Natl. Acad. Sci. U. S. A.* **109**, 20332-20337, doi:10.1073/pnas.1212730109 (2012).
- 54 van Mantgem, P. J. *et al.* Widespread Increase of Tree Mortality Rates in the Western United States. *Science* **323**, 521-524, doi:10.1126/science.1165000 (2009).
- 55 Westerling, A. L., Hidalgo, H. G., Cayan, D. R. & Swetnam, T. W. Warming and earlier spring increase western US forest wildfire activity. *Science* **313**, 940-943, doi:10.1126/science.1128834 (2006).
- 56 Trentmann, J. *et al.* Modeling of biomass smoke injection into the lower stratosphere by a large forest fire (Part I): reference simulation. *Atmos. Chem. Phys.* **6**, 5247-5260 (2006).
- 57 Hodzic, A. *et al.* Wildfire particulate matter in Europe during summer 2003: meso-scale modeling of smoke emissions, transport and radiative effects. *Atmos. Chem. Phys.* **7**, 4043-4064 (2007).
- 58 Alhenius, H. (Joint Research Centre, European Commission. <http://www-gem.jrc.it/glc2000> 2003).
- 59 Sapart, C. J. *et al.* Natural and anthropogenic variations in methane sources during the past two millennia. *Nature* **490**, 85-88, doi:<http://www.nature.com/nature/journal/v490/n7418/abs/nature11461.html> - [supplementary-information](#) (2012).

## 7. FIGURE AND TABLE

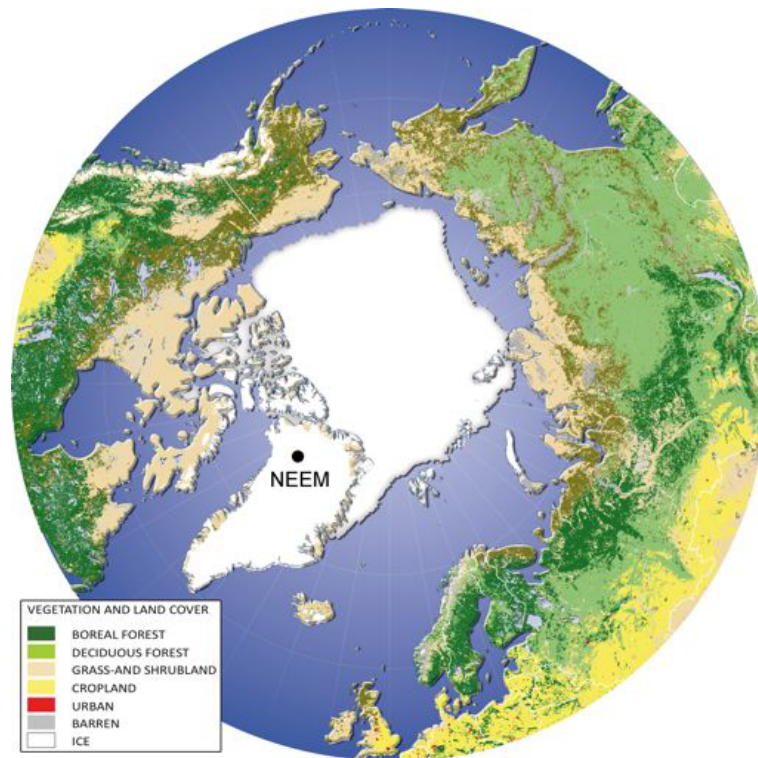


Fig. 1 NEEM camp position and representation of boreal vegetation and land cover between 50° and 90° N. Modified from the European Commission Global Land Cover 2000 database and based on the work of cartographer Hugo Alhenius UNEP/GRIP-Arendal <sup>58</sup>.

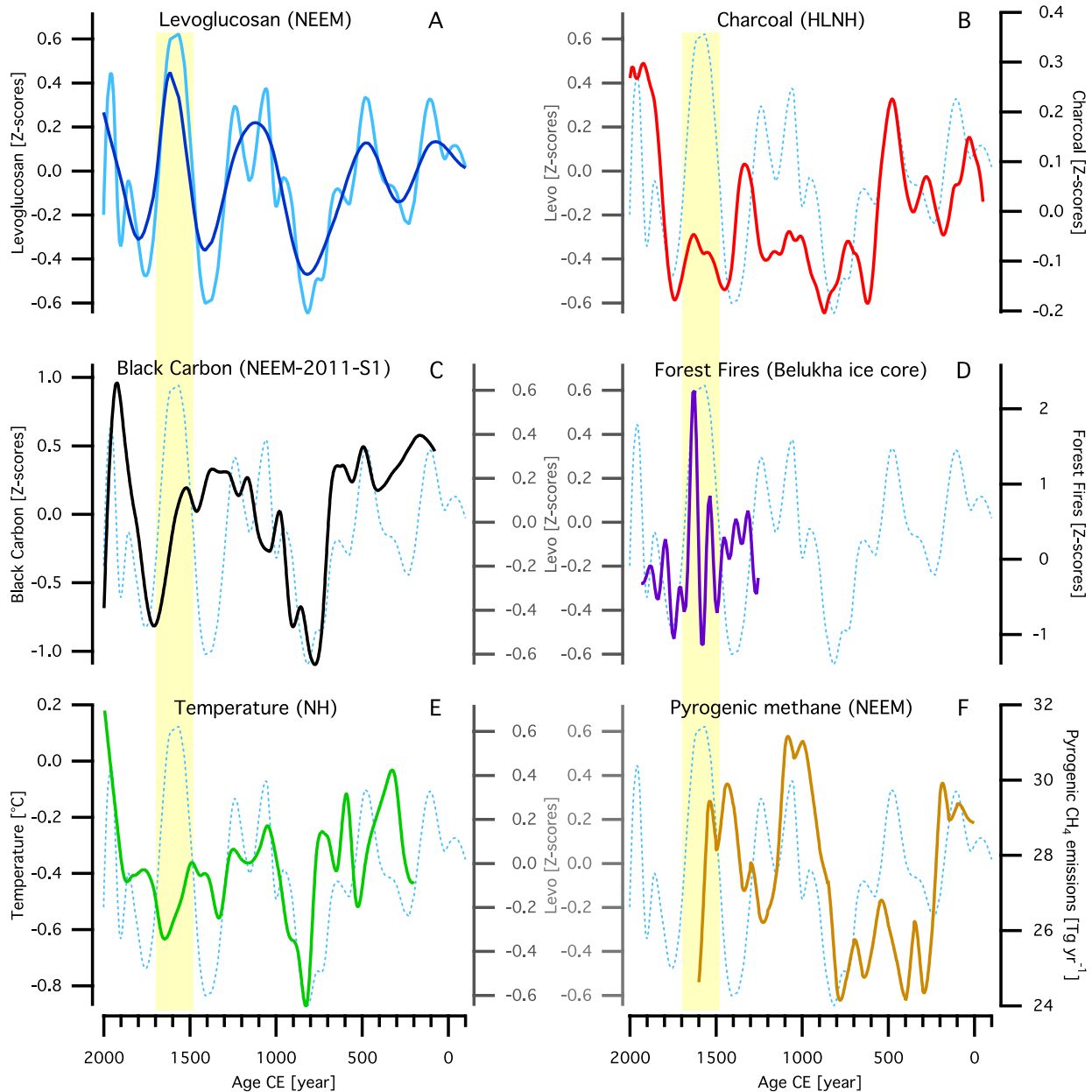


Fig. 2 LOWESS smoothing with SPAN parameter ( $f$ ) 0.1 (light blue) and 0.2 (dark blue) of levoglucosan Z-scores without peaks above the threshold  $3rd\_Q + 1.5 \times IR$  (A); High Latitude (above  $55^\circ N$ ) Northern Hemisphere (HLNH) Z-scores of charcoal influx (200-yr LOWESS smoothing) as reported in Marlon, et al.<sup>11</sup> (red) and smoothed levoglucosan with  $f = 0.1$  as in A (dashed line) (B); LOWESS smoothing with  $f = 0.1$  of Black Carbon Z-scores without peaks above the threshold  $3rd\_Q + 1.5 \times IR$  (black) and smoothed levoglucosan (dashed line)(C); Siberian forest fire reconstruction<sup>42</sup> (purple) and smoothed levoglucosan (dashed line) (D); LOWESS smoothing with  $f = 0.1$  of Northern Hemisphere land temperature<sup>43</sup> and smoothed levoglucosan (dashed line) (E); pyrogenic  $CH_4$  emissions inferred from the deep NEEM core<sup>59</sup> (light brown) and smoothed levoglucosan (dashed line) (F). The yellow vertical bar indicates the period of strongest fire activity<sup>32</sup>.

# **Could Temperature Affect the Geo-speciation of Trace Elements in sediments? LATECC Project (LAgoon, TEMperature and Chemical Contamination) in the Venice Lagoon**

**Corami F.<sup>1,2\*</sup>, Turetta C.<sup>2</sup>, Ros V.<sup>2</sup>, Polo F.<sup>1</sup>, Piazza R.<sup>1</sup>, Cescon P.<sup>2</sup>, Barbante C.<sup>1,2</sup>**

<sup>1</sup>DAIS, University Ca' Foscari, Venezia- Italy, <sup>2</sup>CNR-IDPA, Institute of Dynamics and Environmental Processes, Venezia - ITALY

\*Corresponding Author: [fabiana.corami@unive.it](mailto:fabiana.corami@unive.it)

## **Abstract**

The global impact of climate change affects urban and industrialized areas as well as remote areas (oceans and Polar Regions). A knowledge of the effects of climate change on inorganic and organic pollutants is essential, since researchers and decision makers need to cooperate closely in order to draft guidelines for management strategies. The LATECC Project (LAgoon, TEMperature and Chemical Contamination) in the Venice Lagoon aims to study the possible relation among the temperature increase due to the global climate change, the re-suspension and subsequent turbidity increase in waters, and the possible increased bioaccessibility of trace elements such as arsenic (As) cadmium (Cd), lead (Pb), etc. In order to mimic what may happen in the environment, some mesocosms (water, sediments and biota) were set up. The total concentration of trace elements in sediments and in particulate matter was assessed at the start and at the end of the experiment. Sediments were also analyzed by a Sequential Extraction Procedure (SEP, modified Tessier method) in order to assess the concentration of five different fractions: the bioaccessible fraction, the fraction bound to carbonates, the one bound to oxi-hydroxides of iron and manganese, the one bound to sulfides and to organic matter, and the residual fraction.

**Keywords:** Venice Lagoon, trace elements, climate change

## 1. AIMS OF THE PROJECT

To manage the environment and to plan actions against global climate changes, scientific researchers and decision makers need to join forces. In addition to the crucial environmental issues of the Polar Regions, global climate changes also influence industrial and urban areas. According to a study by the University of Southampton (UK)[1], the Venice Lagoon is affected by the urban heat island effect; the sea surface temperature (SST) is increasing around ten times faster than the global average of 0.13 degrees per decade. The aim of the LATECC project is to assess the possible effects of global climate change on the chemical contamination of the Venice Lagoon.

The increase of temperature may directly affect water acidification; these two phenomena may concurrently threaten the survival of Mollusca and other organisms with calcareous shell or calcareous exoskeleton. Despite being euryecious, even the organisms in transition environments (e.g., estuaries, lagoons) may be influenced by these two phenomena. In addition, the impact would be not only environmental, but also social and economic, in consideration of the activities in the lagoon nurseries.

Furthermore, the temperature increase and the water acidification may be related to the increase of the average sea level, which may consequently affect the lagoon hydrodynamic regime, the sediment re-suspension, the nutrient load and the load of inorganic and organic pollutants. Thus, not only the temperature increase and the water acidification, but also additional stressors could influence the survival of biota in the lagoon.

To mimic what might happen in the lagoon, in this study a first set of mesocosms was prepared and studied under different experimental conditions. A second set of mesocosms was prepared for the exposition experiment, in order to assess the effects on the biota. This paper presents the results of the first set of mesocosms.

## 2. MATERIALS AN METHODS

The mesocosms were set up to study the effects of temperature increase and of sediment re-suspension on the bioaccessibility and bioavailability of trace metals. The experimental work was designed in a timely manner by choosing the temperature range to study, on the basis of the collected bibliography, of the IPCC<sup>1</sup> data and of the

---

<sup>1</sup> IPCC International Panel on Climate Change

three-monthly reports by ARPAV<sup>2</sup>. Samples of water and sediments were collected during the summer of 2012, at two different sites of the Venice Lagoon, which were chosen on the basis of previous studies carried out in the lagoon. The sites were Sacca Sessola, in the central part of the lagoon, and Cona Marsh, in the northern part of the lagoon.

The water temperature of the Venice Lagoon tends to vary throughout the day, due to the tidal turnover and to the peculiar characteristics of the lagoon – a shallow laminar brackish system. The comparison between the average temperature of the lagoon and its probable increase of 3 °C was planned in the very first phase of the project design. However, this temperature gap could be representative of the normal fluctuations in summer temperatures, as later confirmed by the archives of ARPAV [2] and by the study of MAV<sup>3</sup> [3]. Furthermore, according to the ARPAV data for 2011, the temperature during spring and summer was relatively high [4]. Thus, the temperature gap chosen for the experiments was +5 °C above the average temperature observed in the water, sampled in summer 2012 in Sacca Sessola and in Cona Marsh. This temperature gap should allow: a) to take into account a possible effect of the urban heat island and b) to observe any changes in response to an actual increase in the temperature of the water.

Physical data (e.g., pH, oxygen saturation, etc.) were collected at each site at the time of sampling. In every mesocosm, the ratio between the water column and the sediments, together with the effect of tidal movements and of wave movements were simulated. The water and sediments sampled at each site were analyzed before the experiment (*ex- ante* characterization). For each site, four different mesocosms were set up:

- 1) Ambient temperature and continuous stirring
- 2) Ambient temperature and randomized stirring
- 3) Increased temperature and continuous stirring
- 4) Increased temperature and randomized stirring.

Each experiment had a short - average duration (48 hours) and was replicated twice.

---

<sup>2</sup> ARPAV Agency for the Prevention and Protection of the Environment in Veneto

<sup>3</sup> MAV Magistrato alle acque di Venezia Magistrate of the Waters of Venezia

The geo-speciation was studied in sediments by a harmonized SEP [Fig. 1] (harmonized and optimized Tessier method [5, 6]) and the five surnatants obtained were analyzed by ICP-MS. After acid mineralization, the total concentration of trace elements (e.g., As, Cd, Cu, Pb, Zn, etc.) was analyzed in the samples of sediments and of particulate matter by ICP-MS<sup>4</sup>. To minimize any possible source of contamination, the vessels and the bottles for sampling, for sample pre-treatment, for the setting up of the mesocosms and for the analysis of the samples were thoroughly washed. Procedures to minimize any source of contamination were used in every analytical step.

### 3. DISCUSSIONS AND CONCLUSIONS

The precision of measurement was  $\leq 5\%$  (RSD %). The data of total concentration and of the five fractions of the geospeciation showed a  $\text{RSD}\% \leq 10\%$ . For a few trace elements in some of the fractions analyzed, the instrumental signal of the sample was  $\leq \text{LOQ}$  (the instrumental signal of the procedural blank  $\pm 10$  times the standard deviation of the procedural blank).

The total concentration of major elements and trace elements in the sediments of Cona Marsh and of Sacca Sessola is shown [Figg. 2, 3, 4, 5, and 6].

The total concentration of trace elements in the particulate matter [Figg. 7, 8, 9 10, 11] and in the sediments of the two sites showed the same trend. Where the total concentration of a single trace element in the sediments, exposed to different temperatures and different stirring conditions, decreased, the total concentration in the particulate matter of the same element increased, and vice versa. Some other trace elements, such as Cd, did not show any sensible variation of the total concentration in both matrices.

The Geospeciation, by a harmonized and optimized sequential extraction procedure (SEP) [5, 6], was studied on the sediments of Cona Marsh and of Sacca Sessola, at different temperatures and with variable stirring conditions. The Geospeciation study could be a very useful tool for Ecological Risk Assessment (ERA). The five surnatants obtained were analyzed by ICP-MS Quadrupole (with collision cell technology). The

---

<sup>4</sup> ICP-MS Ion Coupled Plasma Mass Spectrometry

different trace elements were distributed among the five fractions, in relation with their characteristics and those typical of the sediments [Figg. 12, 13, 14, 15, 16].

According to the results, the increase of the temperature might affect the total concentration of trace elements differently in the two sites studied. Even the five fractions assessed by SEP might be influenced diversely by the rising in temperature in the two sites studied.

Despite its low total concentration in sediments, Cd may pose a risk for the environment both at Cona Marsh and at Sacca Sessola. Furthermore, the total concentration of trace elements, especially Cu, in particulate matter may represent an ecological risk for the two sites studied. The study of Geospeciation highlights the potential risk, expressed by the results of the total concentration of trace elements. The sum of the five fractions corresponds to the total concentration of the element (RSD%  $\leq 10$  %.)

The sediment's re-suspension and the temperature increase may affect the distribution in the five different fractions, assessed by SEP. The bioaccessible fraction and the one bound to carbonates could increase, as well as the fraction bound to oxy-hydroxides of Fe and Mn and the one bound to organic matter and sulfides. Hence, the less accessible fractions of some trace elements might become accessible and bioavailable for the uptake by biota, and toxic effects might potentially increase.

The increase of the atmospheric carbon dioxide may directly influence the marine and coastal environments, as well as the estuarine areas and the lagoons, because of the acidification of the oceans and of the seas by carbon dioxide uptake [7, 8 and 9]. This increase indirectly affects the rising global temperature, which in turn may contribute to the rise of the temperature in surface waters. The latter rise of temperature may enhance the oxidation of major and trace elements and thus affect their redox equilibria and their solubility. Therefore the increase of carbon dioxide is correlated not only to the rising global temperature but also to the pH, precipitation rate, river inputs and coastal upwelling [10].

The influence on the redox equilibria may be significant in transition environments, where hypoxic conditions, if not even anoxic conditions, are often observed in the sediments, due to the bacterial metabolic activity and the biomass load [11]. In these conditions, several trace elements are usually bound to sulfides and therefore are not

accessible and bioavailable, since sulfides precipitate. Therefore, any change of the redox equilibria may enhance the solubility of these complexes and hence increase the fluxes of trace elements from the sediments towards the water column; the concentration of trace elements in the particulate matter would be enriched, significantly increasing the risk for the environment and biota.

In addition to the factors mentioned above, the role of sediment re-suspension is also relevant. Sediments may be naturally re-suspended by the river's inputs, streams and tidal movements, but the intense traffic of touristic and commercial boats may deeply affect sediment re-suspension. In relation to the characteristics of estuarine and transition environments, the concentration of trace elements in the particulate matter is considerably influenced by re-suspension. Hence, the risk for the environment and for the biota caused by the sediment re-suspension may be very high, as shown by the data collected in this study. An enrichment of the concentrations of trace elements in the particulate matter is in fact observed.

The data of the geospeciation show how changes in oxygen content may influence the redox potential and affect the bioaccessibility of trace elements. In the sediments of both sites, following the re-suspension, the concentration of the elements increased in more bioaccessible fractions and diminished in less bioaccessible fractions.

Furthermore, in relation to the urban heat effect and temperature rise above the global average, the data collected suggest that the increase in temperature affects the solubility of trace elements, as noted in the literature [10, 11].

Although the mechanisms that relate the causes to the effects were not investigated in depth, the methodological aims of the project were achieved. An understanding of the potential effects of global climate change on the concentration of trace elements requires an integrated and multidisciplinary approach, which allows the synergy of various scientific disciplines. Estuarine environments and transition environments, and hence lagoon environments such as the Venice Lagoon, may represent a relevant source of trace elements and other pollutants, which can be toxic and hazardous to the environment, biota and human health. Therefore, the study of the effects on the concentration of trace elements should be supported by knowledge not only on global climate change, but also on local and regional climate changes.

#### 4. ACKNOWLEDGMENTS

This study has been carried out with the financial support of the Region of Veneto in the framework of the CoRiLa research projects. Authors wish to thank Dott. Caterina Dabalà for their contribution to the project arrangement.

#### 5. REFERENCES

1. [https://www.southampton.ac.uk/mediacentre/news/2012/sep/12\\_169.shtml](https://www.southampton.ac.uk/mediacentre/news/2012/sep/12_169.shtml)
2. <http://www.arpa.veneto.it/temi-ambientali/acqua/file-e-allegati/documenti/acque-marino-costiere/rapporti-di-fine-campagna-di-monitoraggio-acque-marino-costiere>
3. Samanet, rete di monitoraggio delle acque, 2011, MAV, Magistrato alle Acque, Ministero delle Infrastrutture e dei trasporti
4. [http://www.arpa.veneto.it/temi-ambientali/acqua/file-e-allegati/documenti/acque-marino-costiere/rapporti-di-fine-campagna-di-monitoraggio-acque-marino-costiere/Rapporto%202%20trim\\_2011.pdf](http://www.arpa.veneto.it/temi-ambientali/acqua/file-e-allegati/documenti/acque-marino-costiere/rapporti-di-fine-campagna-di-monitoraggio-acque-marino-costiere/Rapporto%202%20trim_2011.pdf)
5. Corami F., Cairns W. R., Rigo C., Vecchiato M, Piazza R., Cescon P. "Remediation and Bioremediation of Dredged Polluted Sediments of the Venice Lagoon, Italy: An Environmental-friendly approach". INTERNATIONAL CONGRESS "THE CENTENARY" 100th Anniversary of the Italian Chemical Society, Padova, August 31-September 4, 2009
6. Corami F., W. R. L. Cairns, C. Turetta, C. Rigo, C. Barbante, G. Capodaglio, P. Cescon. Speciation Analysis of Trace Elements in the Waters and in the Sediments of the Venice Lagoon. XIX Congresso dell'Associazione Italiana di Oceanologia e Limnologia. 22-25 Settembre 2009. Venezia, Isola di S. Servolo.
7. Caldeira K, Wickett ME (2003) Anthropogenic carbon and ocean pH. *Nature* 425:365
8. Doney SC, Balch WM, Fabry VJ, Feely RA (2009) Ocean acidification: a critical emerging problem for the ocean sciences. *Oceanography* 22:16–25
9. Doney SC, Fabry VJ, Feely RA, Kleypas JA (2009) Ocean acidification: the other CO<sub>2</sub> problem. *Annu Rev Mar Sci* 1:169–192

10. Hoffmann, Breitbarth, Boyd, Hunter (2012) Influence of ocean warming and acidification on trace metal biogeochemistry. Vol. 470: 191–205 MARINE ECOLOGY PROGRESS SERIES.
11. Vanessa N.L. Wonga, Scott G. Johnston, Edward D. Burton, Richard T. Bush, Leigh A. Sullivan , Peter G. Slavich, 2013. Seawater-induced mobilization of trace metals from mackinawite-rich estuarine sediments. Water Research 47, 821 -832.

## 6. IMAGES AND TABLES

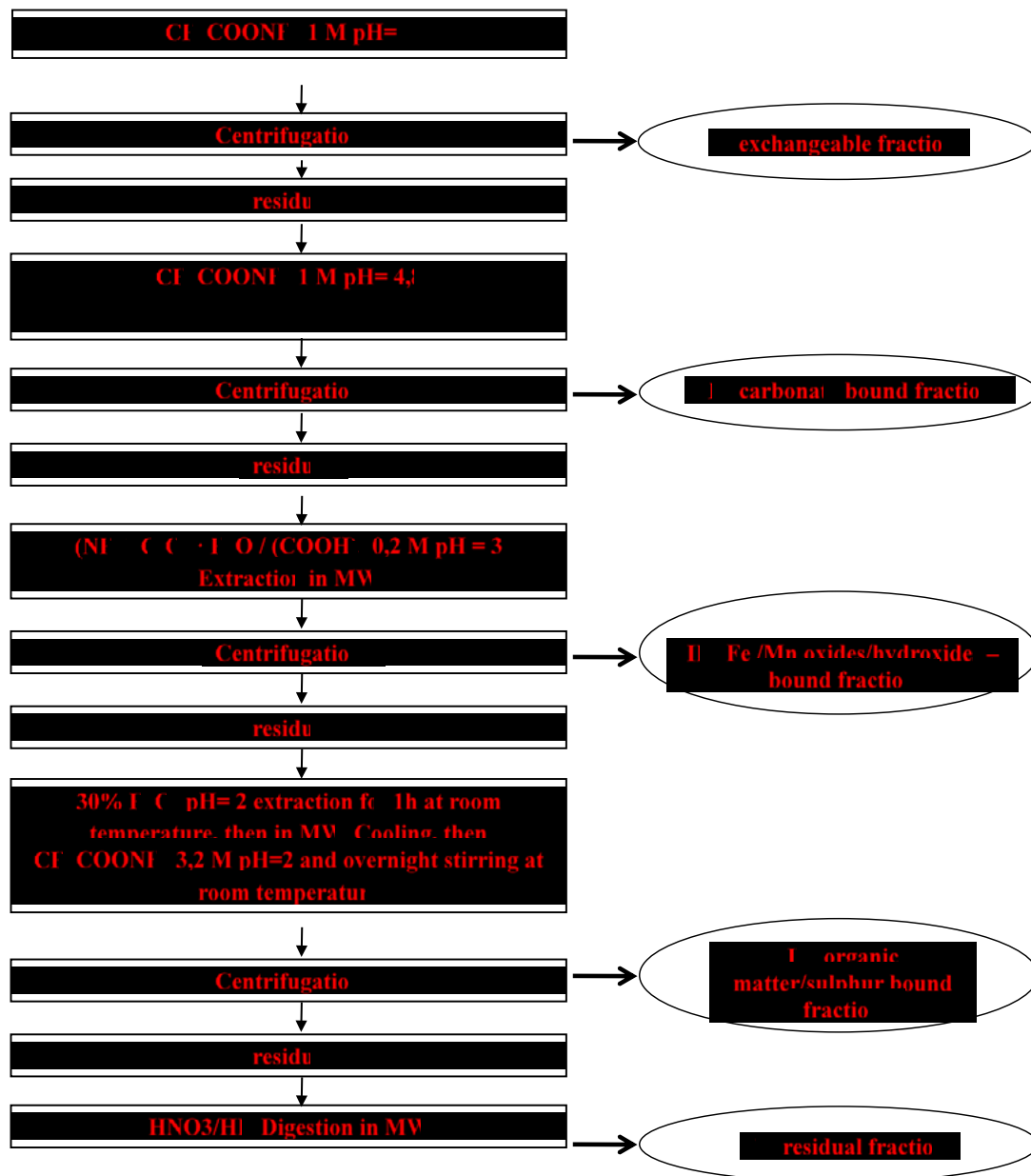


Fig. 1 Harmonized and optimized Tessier sequential extraction procedure (SEP).

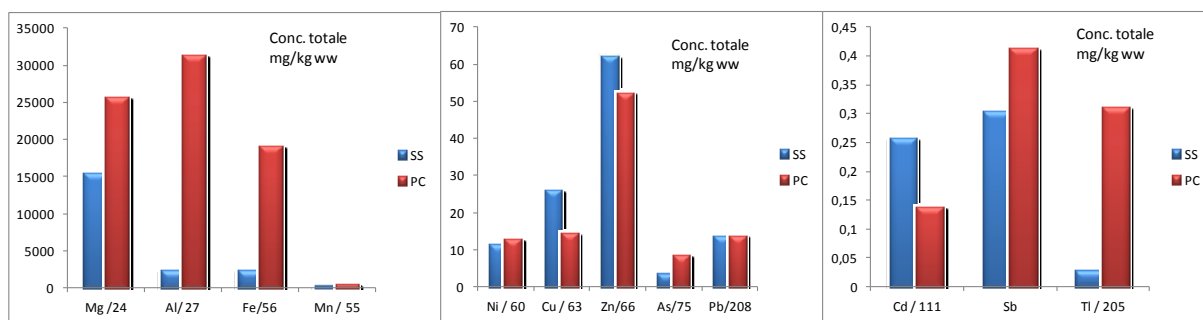


Fig. 2 Ex-ante characterization of the sediments of Cona Marsh and of Sacca Sessola, total concentration (mg/kg ww) of major and trace elements

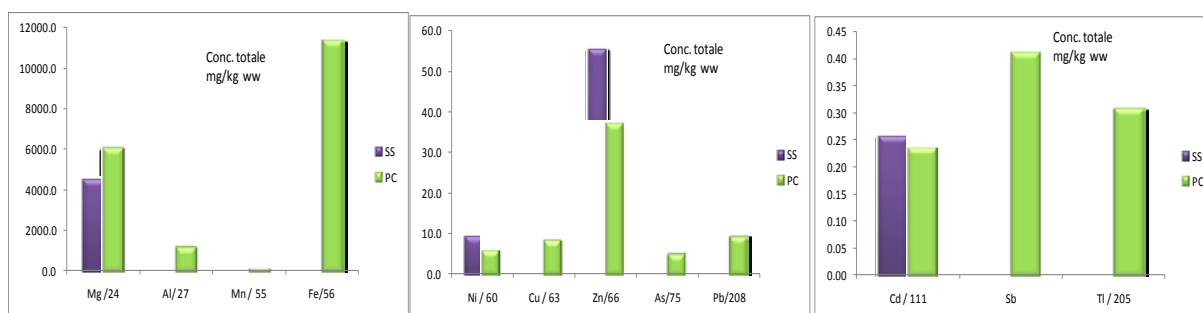


Fig. 3 Mesocosms at ambient temperature with continuous stirring, total concentration (mg/kg ww) of major and trace elements in the sediments of Cona Marsh and of Sacca Sessola.

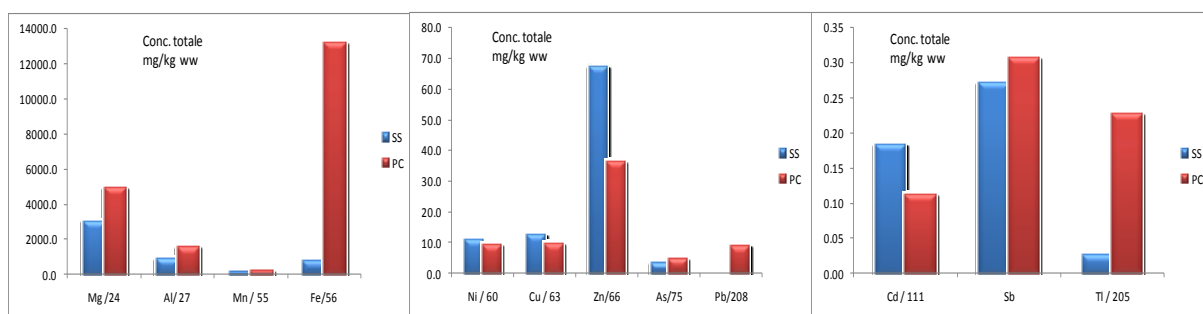


Fig. 4 Mesocosms at ambient temperature with randomized stirring, total concentration (mg/kg ww) of major and trace elements in the sediments of Cona Marsh and of Sacca Sessola.

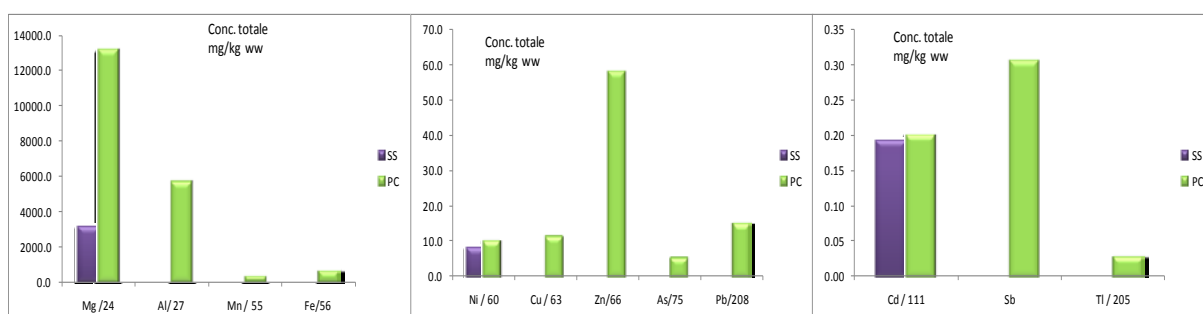


Fig. 5 Mesocosms at increased temperature with continuous stirring, total concentration (mg/kg ww) of major and trace elements in the sediments of Cona Marsh and of Sacca Sessola.

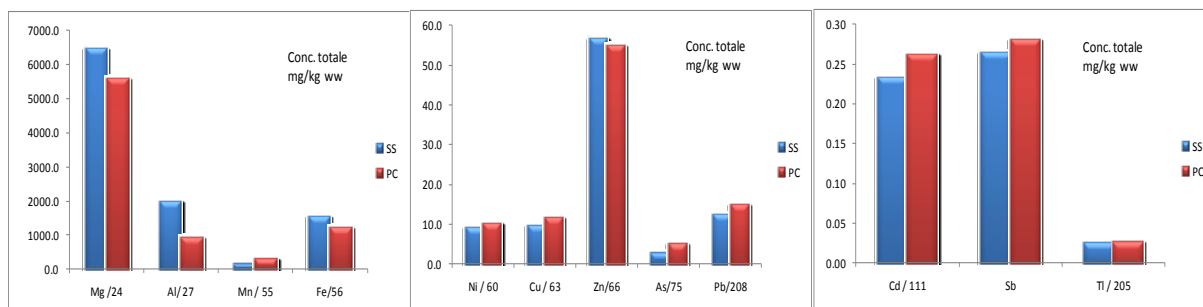


Fig. 6 Mesocosms at increased temperature with randomized stirring, total concentration (mg/kg ww) of major and trace elements in the sediments of Cona Marsh and of Sacca Sessola.

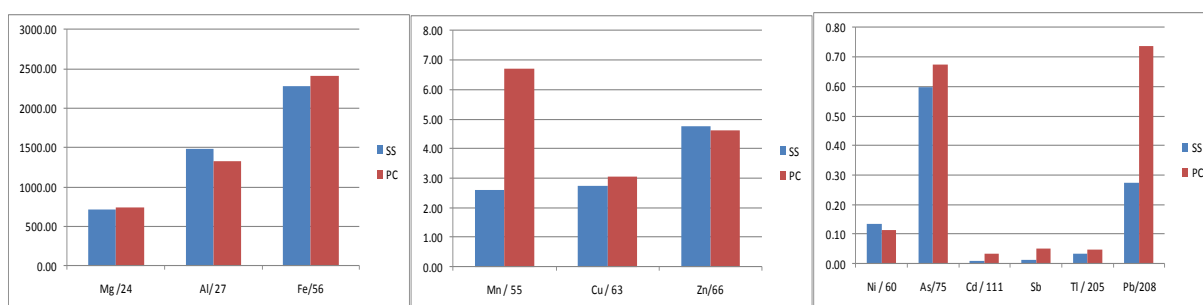


Fig. 7 Ex-ante characterization of the particulate matter of Cona Marsh and of Sacca Sessola, total concentration (mg/kg ww) of major and trace elements

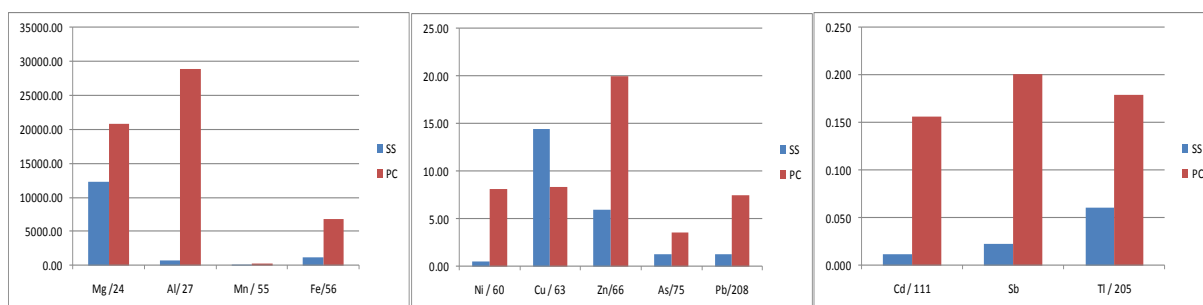


Fig. 8 Mesocosms at ambient temperature with continuous stirring, total concentration (mg/kg ww) of major and trace elements in the particulate matter of Cona Marsh and of Sacca Sessola.

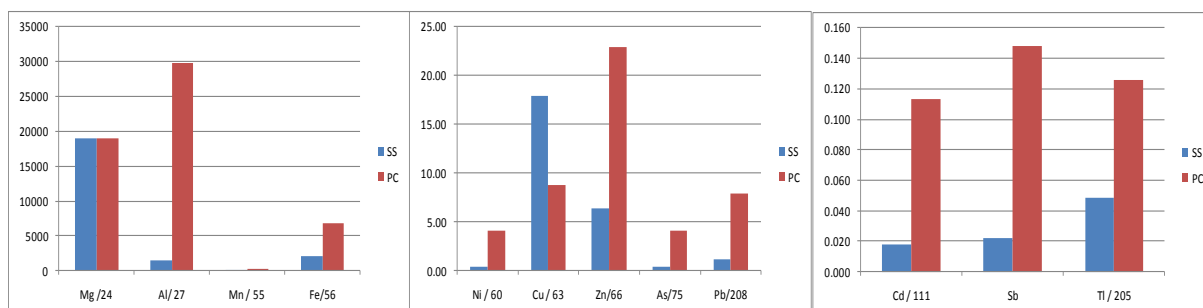


Fig. 9 Mesocosms at ambient temperature with randomized stirring, total concentration (mg/kg ww) of major and trace elements in the particulate matter of Cona Marsh and of Sacca Sessola.

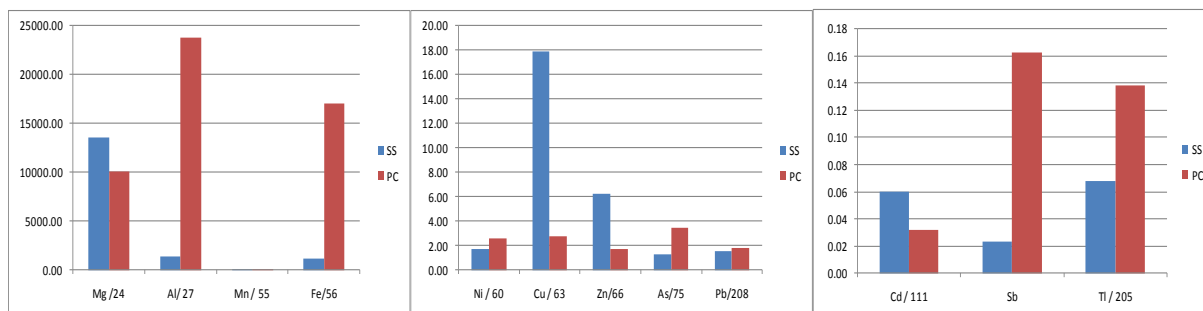


Fig. 10 Mesocosms at increased temperature with continuous stirring, total concentration (mg/kg ww) of major and trace elements in the particulate matter of Cona Marsh and of Sacca Sessola.

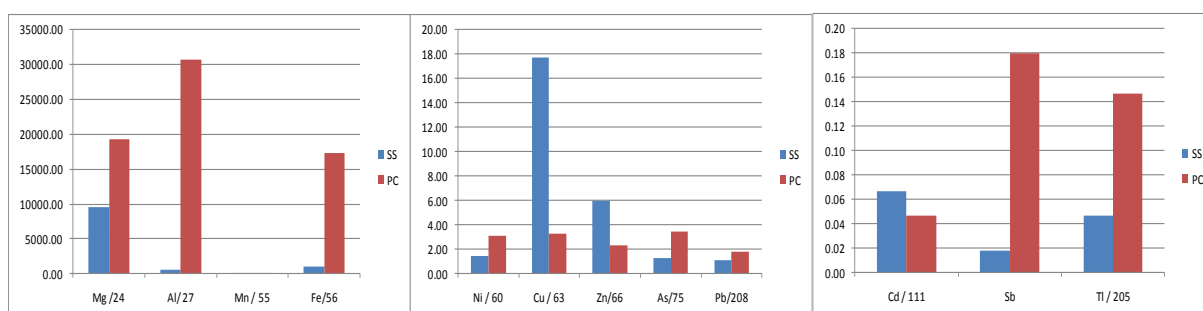


Fig. 11 Mesocosms at increased temperature with randomized stirring, total concentration (mg/kg ww) of major and trace elements in the particulate matter of Cona Marsh and of Sacca Sessola.

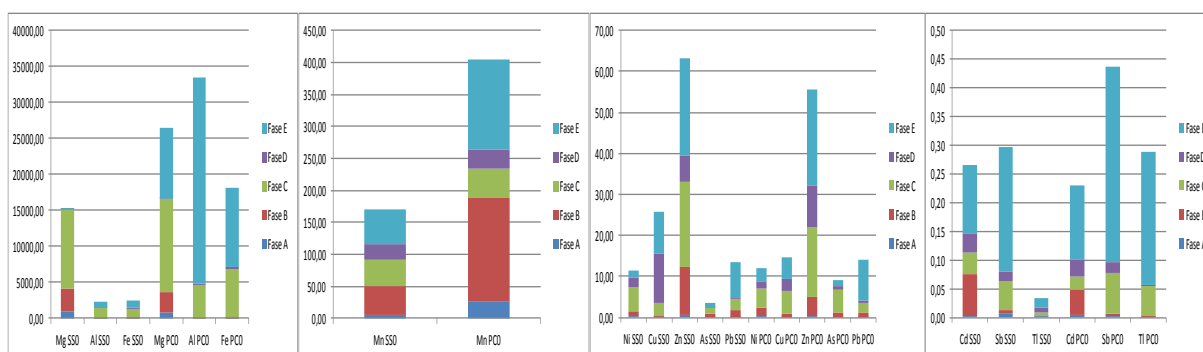


Fig. 12 Ex-ante SEP in sediments of Cona Marsh and of Sacca Sessola, major and trace elements (mg/kg ww)

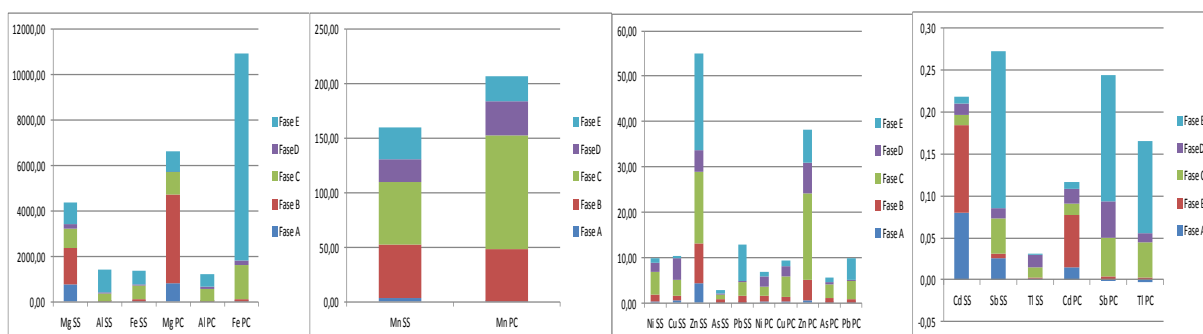


Fig. 13 Ex-post SEP in sediments of Cona Marsh and of Sacca Sessola, major and trace elements (mg/kg ww), ambient temperature and continuous stirring

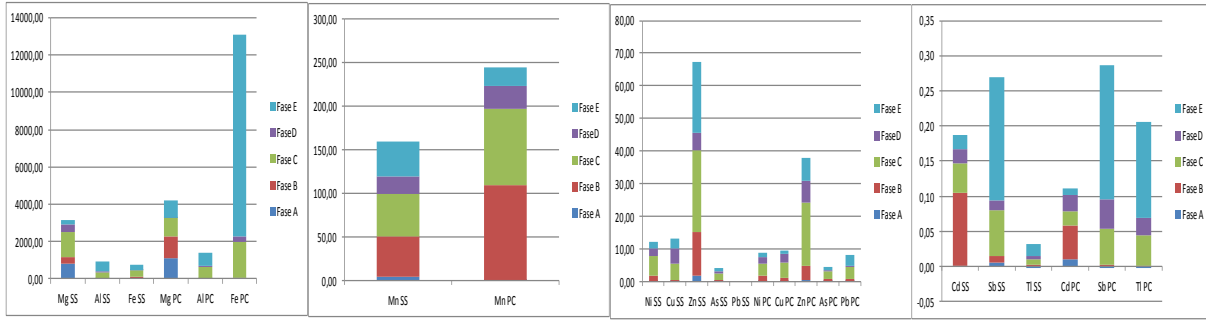


Fig. 14 Ex-post SEP in sediments of Cona Marsh and of Sacca Sessola, major and trace elements (mg/kg ww), ambient temperature and randomized stirring

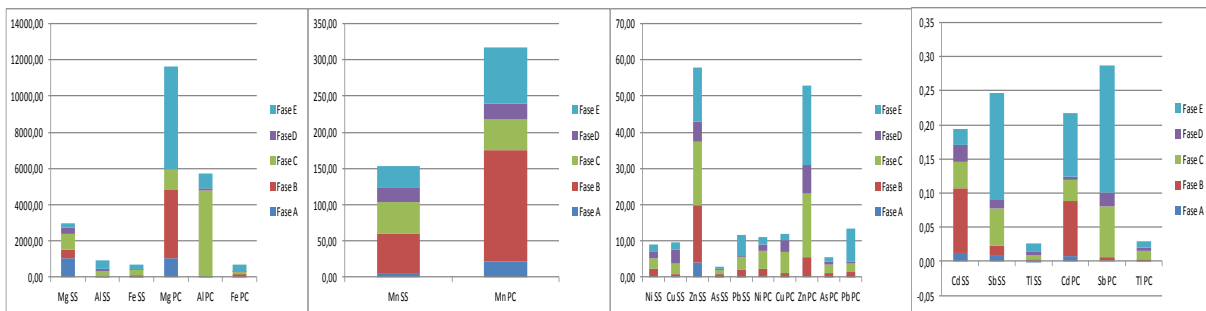


Fig. 15 Ex-post SEP in sediments of Cona Marsh and of Sacca Sessola, major and trace elements (mg/kg ww), increased temperature and continuous stirring

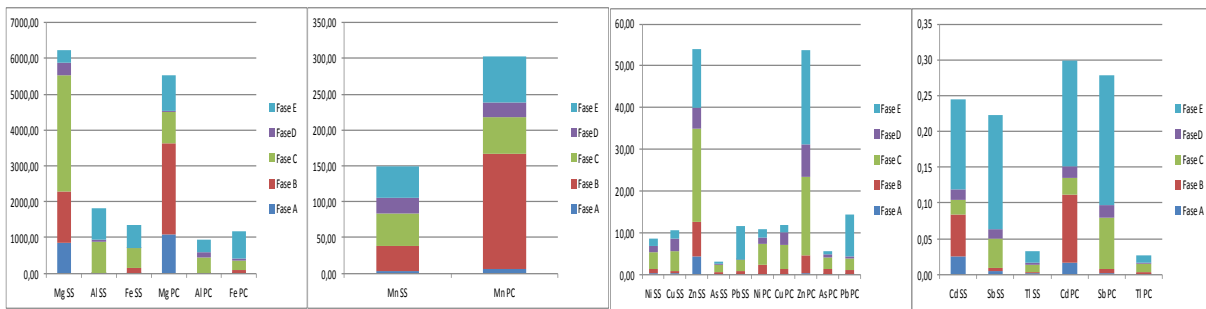


Fig. 16 Ex-post SEP in sediments of Cona Marsh and of Sacca Sessola, major and trace elements (mg/kg ww), increased temperature and randomized stirring

## **The impacts of a changing climate human environment**

**Ruggeri, G.C.**

Lega Navale Italiana, Sezione di Roma / Editrice Incontri Nautici, Roma / Rivista  
Marittima, Roma

### **Abstract**

The analysis of the effects of human activities has been carried out according to the impact of economically important sectors (agriculture, forestry, energy, transports, a.s.o.), as well as in relation to the impact on human health and on natural systems ( soils, water and biodiversity). The analysis of the effects of a changing climate is based on some environmental scenarios which express some hypothesis of future situations, coherent and integrated. The latter are not necessarily forecasts; rather they depict a choice of conditions or very likely future developments. Those scenarios have been used to identify the effects on the economic sectors that are the object of the study, rather than the effects due to the increase of the concentration of the green house gases which have effects on the climate. In the sequel, the impact of a doubling concentration of the carbon dioxide (CO<sub>2</sub>) and of the other green house gases on some of the primary sectors of the social activities (agriculture, energy, forestry, fresh water availability, transports, environmental global security), will be described. The resulting digits of the mathematical models are sometime referred to geopolitical regions or to the whole globe.

**Keywords:** scenarios, activities, models, economic sectors

## 1. AGRICULTURE

The impact of an increase of the greenhouse effect on the agriculture is ambiguous. The range of the consequences depends upon the adaptability of the operators, upon the markets' reactions and on the related politics. Together with the costs related to the sea level increasing, the effects of the climatic changes on the agriculture are perhaps the most studied. The major part of the research is focused on the productivity or on the aspects of the production and does not encompass the impact related to price changes, even if the latter is a critical for the evaluation of resulting damages. High CO<sub>2</sub> levels can lead to greater carbon amounts stored in the greenery. The greater roots' growth could entail a major carbon stowage within the soil, with significant consequences in the total carbon's budget (natural). For the time being, it is still opened the question if in this tradeoff process the monitoring factor could be the carbon or the nitrogen. The costs' assessments which concern the agriculture sector are indicated in the Table I and include the costs' effects, but do not take into consideration the managerial responses and the fertilization's effects due to the carbon dioxide. The welfare changes (weighed as variations in the manufacturers' / end users' surplus) can occur in two ways: (1) Through a change in the agricultural production due to different climatic conditions; (2) Through a variation of the global prices. The welfare's effects (as GNP percentages) are indeed indicated in the Table I. As one can notice, the results are markedly negative for the whole globe regions, with the peculiarity that the discrepancies between two scenarios are significant, notably for China, where one changes over a 5% loss to a 1% benefit. A little variance can be noticed for Russia. In general, the majority of the Global Circulation Models (GCMs) supply negative products. Among such models, in particular, three are used, which are called "*Balance Models*" (they suppose a balance situation about the introduction of CO<sub>2</sub> in the atmosphere); the impact of the climatic change on the production of wheat, rice and soy is computed for sixty sites located in eighteen countries, taking into account three reaction – adaptation attitudes related to the farmers' behavior, that is: (1) *no adaptation*; (2) *minor adaptation*; (3) *maximum adaptation*. The Table II contains nine world regions. The harvest's changes are evaluated for every country and, successively, they are inserted in a *World Food Model* called *Basic Linked System*, which generates the impact

factors on the productive levels, on the prices and on the amount of population exposed to starvation hazard. The changes in the harvest type are very powerful adaptation forms, but – as frequently happens in those circumstances – one doesn't have a deep knowledge of the process control. The harvesting practices which encompass the crop rotation, the farming practices and the nutritional elements' management practices are a very efficient weapon in the fight against the negative effects of the climate change. The scenarios that depict such changes during the final period of the global warming, due to the CO<sub>2</sub> doubling, show a negative effect on the global corn and cereal productions, even if one takes into account of the direct benefits of the carbon dioxide, of the farmers' adaptations and of the future production's technology improvements. The only scenario which shows an increase in the global corn and cereal productions entails wide and expensive changes in the agricultural system, e.g., the installation of vast irrigation systems. Furthermore, climate change was found to increase the disparities in corn / cereal productions between developed and developing nations. Where, indeed, production in the developed world benefited from climatic change, production in the developing nations (Brazil, Russia, India, China – BRIC and Mexico, Indonesia, South Korea, Turkey - MIST), will decline. The number of humans at starvation risk is estimated at 640 millions, that is to say, about 6% of the total population in the year 2060. It is estimated that the prices' increase due to the climate influence on the production reduction will range between 24 ÷ 145%. These increments in prices affect the number of people at risk of hunger. The number of individuals exposed to starvation – risk will increase by 1% for every 2 ÷ 2,5 % of price increase. People at risk of hunger increase by 10% to almost 60% in the scenario tested: this will lead to an estimated increase of 60 – 350 million people in such conditions by 2060. A good level of farm activities adaptation in the agriculture is not sufficient to prevent such negative effect (Rosenzweig /Parry, 1994). In the GCM scenarios (GISS = Global Institute for Space Studies; GFDL = Geophysical Fluid Dynamics Laboratory; UKMO = General Circulation Models of the U.K. Meteorological Office) used, the individuals at risk show to grow from 10% to 60%, depending upon the various scenarios. Many works on this subject (Nordhaus, Titus, Fankhauser, Tol), have estimated the damage costs in agriculture, in the U.S., due to climate variations. These scientists have presented damage costs of 1.0 billion dollars. The latest estimates of Tol (1996) are 10.6

billion dollars in OCSE – A and with the 15.2 billion dollars of Cline (1992), this scientist have illustrated the highest damage costs for agriculture in the OCSE – A. The results are indicated in the Table III, where the latest assessment of Tol (1996) summarises the latest regional impact. For the OCSE –E, OCSE – P, UE&fSU and S&SEA there are some benefits to obtain from agriculture.

## 2. FORESTRY

Many forests of the globe are part of the last world ecosystems which are relatively undisturbed from the human influence. Particularly in the tropics, they host the major part of the globe biodiversities. They condition the surface temperatures, the evapotranspiration, the soils' ruggedness, the clouds' development and the rainfalls. The size with which the climate variations affect those areas depend upon various factors, such as, e.g., the kind and the trees' age, the forests' possibility to migrate and the quality of their management. For this reasons, the impact of the global warming on them is ambiguous. The IPCC deems that even if the primary productivity may grow, the biomass may decrease. The regional impact will be affected by what forests' areas can migrate towards the north. Some researchers (Sedjo, Solomon) estimate that as a consequence of the CO<sub>2</sub> doubling, the global forest area may decrease by 6%. The forests of the temperate and northern emisphere areas will decrease to a greater percentage (about 16%), whereas the tropical forests will increase by 9%. Table IV shows the assessments for the globe's areas. Estimating future vegetation redistribution was based on developing predictive models. One group of models was designed to correlate the geography of climate with the geography of vegetation types. Successively, the future asset of climate was used as a basis for redesign the geography of the vegetation types. Once the new distributions of vegetation types had been defined, the carbon they could store was calculated, assuming that their current carbon densities could be supported in their future distributions. A second group of models accounted mechanistically for processes which determine the growth, shifting density and carbon uptake of vegetation during chronic climate change. These processes include the rapid dieback, reproduction, and slow regrowth of forests, all processes which induce lags in vegetation response to rapid climate change. Although these

processes could not be treated mechanistically in the correlative models described above the process effects in the correlative models had been approximated using values consistent with known biotic change rates. According to the World Research Institute, 40% of the all the forests is tropical and within the OCSE, in the ex – URSS and China there are no tropical forests. This means that in five world's regions (UE, US, China, ex – URSS and OCSE) the forest areas will decrease by 9,6%. From the international point of view, the forests' transfer towards the tropics away from the temperate and north emisphere areas, makes it possible to deem that the major part of the DCs will experience a loss of forest areas relatively minor than the ones located at medium – high latitudes. The Table IV deal with the present and future global forest areas, according to different scenarios produced by various mathematical models.

### 3. ENERGY

Two types of energy utilization are most dependent on climate variations; they are: (a) *The spaces' heating and the air conditioning in the residential and the commercial buildings;* (b): *agriculture applications, such as pumping in for irrigation and drying of the harvest;* (c): *hydropower.* Currently, hydropower accounts for close to 16% of the world's total power supply and is the world's most dominant (86%) source of renewable electrical Energy. The key resource for hydropower generation is runoff which is dependent on precipitation. The future global climate thus poses some risk for the hydropower generation sector. The crucial question and challenge then is what will be the impact of climate change on global hydropower generation and what are the resulting regional variations in hydropower generation potential ? Changes in energy's demand due to the climate variations will concern the energy amount that will have to be provided to satisfy energy services. Renewable energy (RE) and farming are a winning combination. Wind, solar, and biomass energy can be harvested forever, providing farmers with a long-term source of income. Climate change will have impacts on the size and geographic distribution of the technical potential for RE sources but research into the magnitude of these possible effects is nascent. Because RE sources are in many cases, dependent on the climate, global climate change will affect the RE resource base though the precise nature of these

impacts is uncertain. For hydropower the overall impacts on the global technical potential is expected to be slightly positive. However, results also indicate the possibility of substantial variations across regions and even within countries. The firms will have to adapt: (1) the amount of new investments necessary to satisfy the peak electricity and gas demand in the nets; (2) The investments' composition which could better satisfy, according to cost – effectiveness criteria, the temporary models of energy demand. In relation to the assumption that the warming will be of 2,5°C, the Environmental Protection Agency (EPA, USA), deems that there will be an average increase of electricity demand of 3,2%, with a CO<sub>2</sub> doubling. In this estimate we can take into account the regional differences; however, we can say that a mix of the US climate could be representative - on this occasion – at least for the OCSE countries, for the EU and to a lesser extent for China and the rest of the world. The climate precise effects on energy demand greatly depend upon the locality at study. According to a study carried out by the Japan Architecture Society, the temperatures will lead to reduction in the energy demand at Sapporo (43° N), while in Tokyo (36°N), the reduction of energy demand during the winter will be balanced by the increasing of the summer demand, due to air conditioning. In the UK, it is foreseen that the peak demand for heating fuels will diminish to a lesser extent with respect to the yearly request. In Italy, where an increasing of the average temperatures and humidity is in process, markedly over the centre – south, a similar situation has been noticed, in which, in front of a diminished winter energy demand, an increase of electricity demand for the summer's air conditioning is observed. The climatic changes can produce a transition from winter peak's demand to major summer's peak regimes. The expenses for the cooling of the places are an adaptation of the defense measures, very similar to the ones for the sea level increasing. They consist in two parts: defense costs, plus the ones related to the thermal discomforts not yet corrected.

#### **4. WATER AVAILABILITY**

The water availability is an essential component of welfare and of national productivity. The major part of the global agriculture production, of the global energy production, of the municipal and industrial needs, of the hydro pollution and of the

domestic internal shipping, depends upon the natural water surface outfits and on the underground reservoirs. The hydrological impacts are one of the most important aspects of the climatic changes. The variations of the frequency, amount and duration of the hydrological parameters influence the availability of the hydro resources. The water supply will be mostly influenced by the changes in the rainfall models and, over the coastal areas, through the seepage of salt water in the fresh water reservoirs (water salinization). The climatic changes will also increase the demand for water. A Danish study (Rijsberman), estimates, e. g., the salinization damage, for the Netherlands, to about 6 millions dollars yearly. Regardless from the natural underground water reservoirs, its amount available during a certain period and in a certain area, is given by the difference between the rainfall amount and the water amount that evaporates and perspires from the soils (evapotranspiration), in that period. The estimates foreseen, globally, indicate a rainfalls' increase between the 7% and 15% and an increase of the evapotranspiration between the 5% and 10%. The center – south Italy could record more evapotranspiration than the rainfalls, with diminished water reservoirs. Table V shows the results of a combined computation between climatic effects on the water availability and population increase, based on a IPCC 1992 scenario and on the results of three transient GCMs runs.

## 5. TRANSPORTS

Transports' requirements are strictly linked to the urbanization's human systems. The agriculture production nature and places variations, of the population growth rate in different regions, of the volume and types of fossil fuels used in the tourism and in the leisure travels could have deep effects on the present transport nets performances and could require new requirements for the creation of new structures. Even if it is globally recognized that the climatic changes can produce significant population and economic activities redistributions and economic activities, markedly agriculture, detailed studies on such phenomena are missing. While the temperature increasing could open some globe northern regions to new tourism developments, the increasing of the sea level could induce massive forced migrations of the rivers delta settlements and of the sea – levels terrains. For this

reason, the climatic changes will have direct effects on the infrastructures and on the operations of the transport systems. They can be subdivided as follows:

- Climatic effects on infrastructures;
- Sea level increasing effects on sea coasts structures,
- Climatic effects on transport operations.

The transport sector is influenced by cold periods, snow, ice, increasing rain, snow and hail showers with respect to their average (meteorological phenomena extremization), but, in the same time, could also benefit from climatic softening, owing to the reduced winter destructive potential and, then, of the decreasing maintenance activity. In front of this, however, the frequent warm air advections could be destructive, such as the heat stress on the railways equipments. About the road transport, the combined effect of the increasing rainfalls and their intensity on the viability and roads –highways safety, e.g., in the drainage delays of water amounts greater than the ones expected in the projects; of the major frequency of the thunderstorms with heavy hail and strong gusty winds. The costs related to the climatic changes damages in the subject sector are estimated between 1 – 10% of the national GDP, all the transport types considered. In what the air transport is concerned, it is necessary to mention the possibility that the increasing temperatures on the fuel consumptions, markedly on the descent and climbing subsonic phases, on the possible waiting during the approaching phase to the airport and the surface taxiing, before the lineup and take off. The extremization of the meteorological phenomena (strong and gusty winds, heavy rainfalls, heavy thunderstorms from the supercells) could produce heavy delays and flights cancellation. Maritime traffic could be penalized by strong winds, with related major sea conditions intensity (very dangerous for the containers transport), inconveniences to the structures, to the ship load and also to related dangers with relation to the ageing of the ships, load displacement, load shedding. Particular considerations must be made for the harbor load / unload ware operations, also through containers, with relation to the temperature increasing and the extremization of the atmospheric phenomena. Probably more importantly, the transport activities are negatively affected by rainfall, and precipitation is likely to increase under 2CO<sub>2</sub> (Frankhauser, 1995). The effects of different transportation scenarios on energy consumption and quantity of pollutants released to the

environment can be easily analysed using a model developed by Barbieri *et al.* (Barbieri *et al.*, 1995).

## 6. THE ENVIRONMENTAL SECURITY IN THE GLOBAL SCENARIO

The environmental security concept has been officially introduced at the 42<sup>nd</sup> Session of the General Assembly of the United Nations, on 1987, but the environmental decline theme and the Planet resources reduction appeared in the first Report of the Rome Club (1972). On the same year, the subject has been discussed in an international convention in the framework of the U.N. Conference on human Environment, in Stockholm, from which the UNEP (United Nations Environment Programme, the voice for the environment in the United Nations System) originated. On 1980, The Palme, Brandt and Bruntland Commission focalized the global attention on the links among violent conflicts, economic development and environmental decline, giving rise to the “*sustainable development*” concept for a common future. Starting from 1970 onward, the environmental problems had been linked to the safety notion. In many nations, the environmental safety concept has got into the National political debate. Within the last years, the climatic changes had been added as independent item during the aforesaid discussions. The climate change, as environmental decline, in general, is sometime not merely considered as a freestanding problem, but a potential menace to peace and to international safety and an important factor of political instability, markedly in the areas where one has yet to do with security problems owing to social and economic changes. Nowadays one can distinguish, in general, three environmental menaces basic categories:

- *National or domestic threats;*
- *Threats caused by neighbouring populations;*
- *Threats cause by distant players.*

Climatic changes, if perceived like a threat, belong to the last category, being a global phenomenon, caused by players from the whole planet. Owing to its amplitude and to the perception which it offers as a negative event, the climatic changes process needs a collective action by sovereign States. In the

meantime, the subject nature provides to the same States the potential possibility to act as a freelancer. They indeed could take advantage from the measures and from the actions, certainly expensive, taken by other neighbouring States. This unbalanced mix of common and national interests supply the basic potential for international political tensions and conflicts. The core of the problem is in the fact that the global environment or rather the global climate, is perceived like a common good, an asset that – when made available to some player (States, population) – is automatically available to everybody. If, e.g., the air pollution could be reduced and the greenhouse effect limited, everyone could benefit, independently from the fact that one had contributed or not to such reduction. As aforementioned, owing to the potential possibility to freelance the players must confront with the “*prisoners’ dilemma*”. The individual interests do not get along with the common ones and, therefore, does not exist a guarantee that common decisions will be taken and, consequently, that the related efficient actions could be taken. In fact, unless that the individual players number is very little, or unless that some coercion or some particular reason that could make such players to act in their common interest, they will not behave in a way to satisfy the shared interests. In the peculiar case of the climatic changes, the national economic interests set, for some nations, a series of incentives to freelance, thus giving rise to an additional barrier to shared and effective common actions. An example about how the international diplomacy can contribute to achieve with success a common action for the common good protection, is the Montréal protocol (1987), refined in its contents in London (1990) and Copenhagen (1992), it regulates the global production and use of the chlorofluorocarbons (CFCs), the major reason of the ozone belt depletion, recently almost completely built up. The ozone treaty has been considered as a prominent example on how the environmental diplomacy can contribute to achieve an effective global regime. A regime sets the rules in international interaction in a way that they will be extensively supported by shared certainties and by a social monitoring which does not need a sovereign power. According to Young (1994), three group of factors contribute to create (or not) such regime: the *power*, the *knowledge* and the *interests*. The supposed power role is referred to the idea that the domineering states (in a material sense) can sometime promote, assist or induce the weaker states to adapt to contribute to the

structural formation of an international environmental regime. The climatic changes, as a subject for the building up of a regime, substantially differ from the ozone theme, markedly for the item knowledge and interests, firstly since some uncertainties still exist about the temporal framework, about the effects on the extension and the effects of the climatic changes, especially at a sub – global scale (national, regional). For this certainty's lack, an agreement does not exist on the causal effects of the CO<sub>2</sub> emissions and about the related global warming in terms of costs or tangible damages on a regional or local scale in the Planet. This hamper the sound and accurate analysis of the costs – benefits by the aforesaid individual players, which affects on the agreement's and management actions terms and conditions among the parts. Further, the CFCs production affected only a minor part of the though powerful economies and the chemical industries were able to shortly produce efficient alternative products, while the most important cause of the global warming (greenhouse gases, namely the use of fossil fuels) touches the heart of the economies. The interests in play (or, if you wish, the costs), with the potential measures against the climatic changes are, therefore, wider, while efficient alternative measures are still not available. Stopping the climatic changes, is not a “*only winners*” process: while some countries could obtain benefits from this halt, others could be damaged. In contrast with the “*safe global threat*” image, with related global interests shared to fight such menace, the climate change does not proves to be unfavourable for all the players. The global warming will produce “*winners*” and “*losers*”: the latter consideration will place another barrier to common shared solutions.

## 7. REFERENCES

1. Ekko C. van Ierland, Klaassen Marcel G., Nierop Tom, Wusten Herman v.d. (1996), Climate Change: Socio – Economic Impacts and Violent Conflict;
2. Dutch National Research Programme (1996), Survey of Climate Change Scenario Studies.

TAB. I

COSTS FOR THE AGRICULTURE (CO <sub>2</sub> DOUBLING – 10 <sup>9</sup> \$)		
	Welfare change extent (%GDP)	Welfare average change (10 <sup>9</sup> \$)
<b>UE</b>	-0,400 ÷ -0,019	-0,9666
<b>USA</b>	-0,310 ÷ +0,005	-0,7392
<b>EX - URSS</b>	-0,520 ÷ +0,032	-0,6185
<b>CHINA</b>	-5,480 ÷ +1,280	-0,7812
<b>OCSE</b>	- 0,316 ÷ -0,018	-2,3130
<b>Global</b>	-0,470 ÷ +0,010	-3,9141

TAB. II<sup>1</sup>

<sup>1</sup> The subdivision among OCSE A, E, and P concerns the different GNDP among the various States of the Organization. UE & US: European Union & former Soviet Union; ME: Middle East; LA: Latin America; S&SEA: South and South East Asia; CPA: Central Pacific Area; AFR: Africa.

<sup>2</sup> Scenarios used: Balance Models of the following Centres: UKMO (UK Met Office); GISS: (Goddard Institute for Space Studies); GFDL (Geophysical Fluid Dynamics Laboratory)

<sup>3</sup> Every scenario concerns the following behavior adopted by the cultivators: (1) No adaptation; (2) Minor adaptation; (3) Maximum adaptation

CHANGES IN AGRICULTURE'S PRODUCTS (CO <sub>2</sub> DOUBLING – % OF THE GROSS AGRICULTURE PRODUCT)									
Model <sup>2</sup>	UKMO			GISS			GFDL		
Scenario <sup>3</sup>	1	2	3	1	2	3	1	2	3
<b>Ocse - A</b>	-20,0	-5,0	-5,0	-5,0	+10,0	+10,0	+10,0	-5,0	+10,0
<b>Ocse - E</b>	+5,0	+5,0	+5,0	+10,0	+10,0	-5,0	+5,0	-5,0	-5,0
<b>Ocse - P</b>	+7,5	+7,5	+7,5	+7,5	+7,5	+7,5	+7,5	+7,5	+7,5
<b>UE &amp; US</b>	+7,5	+7,5	+7,5	+22,5	+22,5	+22,5	+7,5	+7,5	+7,5
<b>M - E</b>	+22,5	+22,5	+7,5	+7,5	+7,5	+7,5	+7,5	+7,5	+7,5
<b>L - A</b>	+22,5	+22,5	-8,5	-15,0	-15,0	-1,0	-10,0	-10,0	+4,0
<b>S &amp; SEA</b>	-20,0	-20,0	-10,0	-10,0	-10,0	0,0	-10,0	-10,0	0,0
<b>CPA</b>	+7,5	+7,5	+7,5	+7,5	+22,5	+22,5	+7,5	+22,5	+22,5
<b>AFR</b>	-20,0	-20,0	-20,0	+7,5	+7,5	+7,5	-15,0	-15,0	0,0

TAB. III

<b>COSTS RELATED TO THE ECONOMIC DAMAGES TO THE AGRICULTURE, DUE TO THE CLIMATE VARIATIONS (CO<sub>2</sub> DOUBLING – 10<sup>9</sup> \$)<sup>1</sup></b>														
<b>Regions<sup>2</sup></b>	1	2	3	4	5	6	7	8	9	10	11	12	13	14
<b>Agriculture</b>	10,6	-6,0	-6,1	-23,2	7,6	13,1	23,9	-3,2	11,4	-1,5	29,7	-24,7	52,9	28,2

<sup>1</sup>Impact related to a global temperature warming of +2,5°C, to a 0,04° annual rate, accompanied by a 50 cm rise in the sea level, by a 25% increase in the hurricane frequency, by an increase of winter rainfalls and by an increase of 6% of the weather disturbances in the extratropical regions.

<sup>2</sup>1= OCSE-A; 2= OCSE-B; 3=OCSE-P; 4= UE & fSU; 5= ME; 6=LA; 7= S & SEA; 8= CPA; 9= AFR; 10= OCSE; 11= nOCSE; 12= North; 13= South; 14= Global

TAB. IV

<b>DAMAGES TO THE FORESTRY SECTOR (100 Km<sup>2</sup> AND 10<sup>6</sup> US \$, 1988)</b>		
	Loss of forestry areas (100 Km <sup>2</sup> )	Forestry loss (10 <sup>6</sup> US \$)
<b>UE</b>	52	104
<b>USA</b>	282	564
<b>EX - USSR</b>	908	363
<b>CHINA</b>	121	24
<b>OCSE</b>	901	1,801
<b>GLOBAL</b>	1235	2,005
<b>Tempered Areas</b>	2169	2,284
<b>Tropical Areas</b>	-394	-279

TAB. V

<b>PRESENT AND FUTURE WATER AVAILABILITY, ACCORDING TO CLIMATIC MODELS AND POPULATION INCREASE IN SOME NATIONS</b>		
<b>NATIONS</b>	<b>PRESENT USE (m<sup>3</sup>/YEAR/PRO CAPITE)</b>	<b>AVAILABILITY IN THE 2050, ACCORDING TO A CLIMATIC MODEL (m<sup>3</sup>/YEAR/PRO CAPITE)</b>
<b>Saudi Arabia</b>	310	80
<b>Japan</b>	4430	4260
<b>Italy</b>	3958	3558
<b>Kenia</b>	640	170
<b>Mexico</b>	4270	2100
<b>Poland</b>	1470	1200
<b>Spain</b>	2850	2680
<b>Togo</b>	3400	900
<b>Vietnam</b>	5640	2630

# Assessing the economic general equilibrium effects of Sea Level Rise in the Italian Regions

Eboli F.<sup>1,2,3</sup>, and Standardi G.<sup>1, 2\*</sup>

<sup>1</sup>CMCC, Euro-Mediterranean Center on Climate Change – Italy

<sup>2</sup>FEEM – Fondazione Eni Enrico Mattei - Italy

<sup>3</sup>Università Cà Foscari - Italy

\*Corresponding Author: gabriele.standardi@feem.it

## Abstract

Economic assessment of sea level rise (SLR) through computable general equilibrium (CGE) modelling is a widespread and effective approach to quantify economic dimensions of damages and potentially come out with useful adaptation actions. One main limitation is that traditionally CGE models, relying upon economic information derived by national statistical offices, have national details. This implies a loss of important information for local and regional social planners to detect relevance of impacts and respond accordingly.

The aim of this work is to enrich the current state of the art proposing a methodology combining the top-down approach consisting of a sub-national CGE model and a bottom-up approach (based on DIVA model) to assess the economic general equilibrium effects of SLR in Italy with regional details by the end of 21st century.

Our approach considers all the economic interactions among sub-national regions and with the rest of the world. Moreover, the optimal behavior of the economic agents responds to change in prices, which, in turn, signal the productivity loss in the resource induced by the climate change impact (market-driven or autonomous adaptation).

In order to manage the uncertainty related to the integration's degree across the regional economies, we build a rigid version of the CGE model and a flexible one. This allows us to define possible ranges of general equilibrium effects.

We show that, in spite of a larger coastline in regional islands (Sicily and Sardinia), Emilia Romagna and Veneto are the most affected regions in all the scenarios analyzed. In the flexible model we can observe a reallocation of capital and labor from these regions to the landlocked regions.

**Keywords:** sea level rise, computable general equilibrium modelling

## 1. INTRODUCTION

It is very likely that in the 21st century and beyond, sea level change will have a strong regional pattern, with some places experiencing significant deviations of local and regional sea level change from the global mean change [10]. In Europe, the expected annual damage related to SLR (Sea Level Rise) would be around €11 billion by 2050 while the estimated number of affected people would amount to 55,000 each year [4].

Economic assessment of climate change impacts such as SLR is extremely important to guide the policy-makers' actions to cope with such adverse effects.

Economic impact assessment can be performed through two different methodologies: namely, bottom-up (BU) and top-down (TD). On one hand, BU approaches, such as GIS (Geographic Information System) or bio-physical models, such as DIVA (Dynamic and Interactive Vulnerability Assessment) [6], compute a climate-related physical impact at very high geographical resolution. Economic estimates relate to the direct effects, that is accounting for the change in economic-relevant land and capital stock times the unitary price of such a stock.

On the other hand, TD approaches, as CGE (Computable General Equilibrium) models, have a lower spatial resolution but an important characteristic. Even when a specific impact affects one specific region or economic sector, these models keep track of possible reactions of economic agents – households and firms – that can re-allocate their demand for commodities and productive inputs both in domestic and international markets following climate-related price signals. These are the typical economic general equilibrium effects, which can be interpreted as indirect effects.

Taking into account such interconnections among markets can lead to different outcomes than expected through adjustment mechanisms referred as market-driven adaptation. As said, one main drawback of CGE approach is the lack of spatial detail, because in general this type of model is at the country level. This requires a scientific effort to increase the resolution of CGE tool.

To this purpose, we build a sub-national CGE model considering at the same time all the 20 Italian NUTS-2 (Nomenclature of Territorial Units for Statistics) regions.

For the economic assessment of SLR we apply the procedure followed by [3], which uses the DIVA model to compute the climate physical impacts of SLR in Europe and

then inserts them into a country level CGE model to assess the economic consequences.

We do the same thing for Italy but we use a sub-national CGE model. To the best of our knowledge, no evaluation of this type has been performed so far because no CGE model exists including simultaneously all the Italian sub-national regions. This represents the strong point of our assessment. In fact, the potential to impose differentiated shocks within a country is one of the main strengths of our approach but it is also interesting to analyze to what extent the economic effects of the physical impact propagates from the coastline in the other economies within the country.

An additional development of our sub-national CGE model is the possibility for the primary inputs (capital and labor) to move within Italy after the shock. This opportunity is usually excluded in the standard CGE models where the primary factors are immobile at the country level.

The structure of the paper is as follows. Sections 2 and 3 illustrate the methodology used to build the sub-national CGE database and model. Section 4 describes the DIVA inputs feeding the CGE model. Section 5 shows results and their interpretation. Section 6 concludes and sketches some ideas for future research.

## **2. DATABASE DEVELOPMENT**

Building a full-fledged sub-national CGE model is challenging, both in terms of data requirements and modelling capacity.

Our starting point is the GTAP (Global Trade Analysis Project) 8 database [21], consisting of 57 sectors and 129 countries or groups of countries. The reference year is 2007.

Data on value added, labor and land input for the 20 Italian regions and 40 production sectors derive from ISTAT (Italian National Statistical Institute) [11][12][17]. ISTAT also reports bilateral flows in physical volume (tons) by mode of transportation (truck, rail, water and air) for the 20 Italian regions [13][14][15][16], but for a smaller number of sectors (10 agricultural/industrial sectors).

We integrate the GTAP database with the statistical information from ISTAT to extend the original database with regional details for Italy.

The major effort in building a sub-national CGE database consists in estimating the trade flows across sub-national regions. Due to the lack of data, this is usually done through a gravitational approach [7][24]. By this method, the bilateral trade flows across sub-national regions are computed as an increasing function of the regional production in the origin and destination regions and decreasing function of their geographical distance. The equation is similar to that used for the gravity force in the Newtonian physics.

We propose an alternative and innovative approach. Practically, the statistical procedure is the following. First, we split the Italian value added and primary factors for each sector in GTAP across the 20 regions using the ISTAT production dataset. Then we use the shares obtained from ISTAT transport data to distribute the sectoral GTAP Italian production, which is demanded domestically, between domestic regional use and trade flows across Italian regions. Finally, we check if the regional accounts are verified (production = demand + exports - imports). This is done by adjusting the trade flows across regions with the RAS statistical method [2][5] to make these flows consistent with the regional production data.

In our view, this represents more effectively than the gravitational approach the actual flows of commodity within a country. Combining the transport data and the economic production information in the computation of trade flows across regions is also important for three reasons: first, economic dataset has a more detailed sectoral aggregation; second, we can translate transport data from volumes (tons of carried commodities) in economic values; finally, we use all the available information in a consistent framework.

The final result of this process is a database with 148 geographical units (128 GTAP countries or groups of countries and Italy split in 20 regions) and 57 sectors.

As the focus of the analysis is Italy, the database is re-aggregated as shown in [Tab. 1]. We keep the sectoral aggregation in [Tab. 2] as simple as possible because DIVA does not provide physical inputs differentiated by sector and inserting a large number of sectors would complicate uselessly the numerical computation of the economic equilibrium and the interpretation of the results.

### 3. MODEL IMPROVEMENT

We start from the GTAP model [8]. It is a widespread CGE model used to evaluate trade and tax policy scenarios but also to carry out climate change economic impact assessment.

The economic structure of the model is neoclassical. In each country, a representative household maximizes the consumption utility function subject to a budget constraint. In each country and sector, a representative firm maximizes profits subject to a technological constraint. All the domestic markets are perfectly competitive and factors are fully employed.

The GTAP model is tailored to countries or group of countries. In order to take into account the different degrees (national and sub-national) of factors and goods mobility we need to modify the theoretical structure of GTAP.<sup>1</sup> In fact, both commodities and factors are expected to move easier within the country than between countries. This implies that additional assumptions have to be made both on factor mobility across sub-national entities and on intra and extra regional goods substitution.

As to the first point, two opposite options are available: perfect factor immobility at the regional level or perfect mobility between Italian regions. The truth is seemingly in between. At some extent, workers (and capital) can move in other sub-national regions to react to an economic shock. As to the second point, given that trade within a country is larger than trade between countries given the same distance - the so-called border effect [18] – the product substitution inside the borders should be increased.

This implies additional assumptions and a re-calibration process of some parameters in the model. Turning to the theoretical hypothesis, we use a CET (Constant Elasticity of Transformation) function to model the supply of capital and labor at the sub-national level. In the goods market we assume a different demand structure for the Italian regions with respect to countries.

The re-calibration process would require the estimation of two parameters at the sub-national level. The first one is the substitution elasticity regulating capital and labor mobility in the CET function. The second one is the Armington elasticity in the

---

<sup>1</sup> For more details about the methodology used for the model improvement refer to [22].

demand of goods faced by households and firms establishing the degree of substitution between domestic and imported product.<sup>2</sup>

Unfortunately, econometric estimations are not available for both the parameters at the sub-national level. Therefore, we use two model specifications in order to manage the uncertainty related to the model flexibility. In the first one (rigid model) workers and capital cannot move outside the Italian region they belong after a shock in the economic system. We also assume the same values of Armington elasticity for both countries and sub-national regions.

In the second specification (flexible model) we allow for imperfect mobility of capital and labor within the country (endogenous factor supply at the sub-country level) through the CET function. In addition we increase the degree of commodities substitutability at the regional level by increasing the sub-national Armington elasticities.

#### **4. DESCRIPTION OF INPUTS FROM DIVA**

Concerning the geo-physical inputs feeding our CGE model, we use the DIVA software. This tool is a worldwide model, tailored to analyze at high geographical resolution the biophysical and socio-economic consequences of SLR. It takes into account coastal erosion, coastal flooding (including rivers), wetland change and salinity intrusion into deltas and estuaries but also number of people affected and direct costs linked to SLR phenomenon [9][19][23].

DIVA allows the quantitative assessment according to the different IPCC (Intergovernmental Panel on Climate Change) SRES (Special Report Emission Scenario) [20]. However, DIVA does not capture the economic general equilibrium effects of SLR but only physical impacts and direct costs.

Our experiment consists in using the output of the DIVA model in 2100 for the six SRES under the assumption that no adaptation in terms of raising dikes, nourishing shores and beaches takes place. Here under the SRES:

---

<sup>2</sup> The Armington elasticity derives directly from [1], which introduces imperfect substitutability between homologue domestic and imported goods. This is a standard assumption in the CGE modelling.

- A1 scenario considers a rapid economic growth, a global population that peaks in mid-century and declines thereafter, convergence among countries. The A1 scenario family develops into three groups: fossil intensive (A1FI), non-fossil energy sources (A1T), or a balance across all sources (A1B).
- A2 represents a more heterogeneous world, global population increasing during all the 21st century, and slower convergence among countries.
- B1 is similar to A1 but with rapid changes in economic structures toward a service and information economy, with the introduction of clean and resource-efficient technologies.
- Finally B2 depicts continuously increasing global population at a rate lower than A2, intermediate levels of economic development, and less rapid and more diverse technological change than in the B1 and A1.

For each one of these six scenarios DIVA provides the land impacted (km<sup>2</sup>) and the number of people affected by SLR in every Italian coastal region for the period 2000-2100.

For land we have considered these impacts:

- 1) coastal erosion,
- 2) submergence,
- 3) flooding caused by SLR and associated storm surges for both sea and river floods,
- 4) change in the coastal wetland area.

For population we take the coastal floodplain population, which is the number of people that live below 1000-year storm-surge level. This indicator gives an idea of people at potential risk of flooding because of SLR.

We use these data as inputs for the CGE analysis. However, this information cannot be inserted directly into the CGE model but need some manipulation to be consistent with the CGE theoretical structure.

Therefore, we convert the above-mentioned impacts for land and population in productivity loss of land, capital, skilled labor and unskilled labor in the sub-national CGE model.

The computation of the productivity loss is the following. The ratio between the land loss in the region over the period 2007-2100 and the total surface of the region has been used as a proxy to quantify the land productivity loss in the agricultural sector and the capital productivity loss in all the sectors.<sup>3</sup> The underlying assumption is that capital is impacted at the same extent as land and the shock is uniform across sectors.<sup>4</sup>

The ratio between the increase in people at risk over the period 2007-2100 and total population in the region for the year 2007 has been used as a proxy to quantify the productivity loss of skilled and unskilled labor for all sectors in the economy, assuming that the higher the population affected, the higher the productivity loss in terms of lost working hours. The underlying hypothesis is that the shock is uniform across sectors and between skilled and unskilled labor. In addition, we are implicitly assuming that the population does not change overtime in the Italian regions.

[Tab. 3] and [Tab. 4] show the CGE % productivity losses in the last column for the SRES A1B (a very similar regional ranking can be found in the other scenarios). In [Tab. 3] the second and third column report the % regional share of coastline over the total Italian coast length and the % regional share of DIVA impact over the total Italian impact.

Interestingly, we can observe that regions which have the highest % shares of coastline length, as Sicily and Sardinia, do not present the highest % shares of DIVA impact, which instead apply to Emilia Romagna and Veneto. This suggests that the

---

<sup>3</sup> We choose 2007 as starting year to compute the impact as this is the base year in the CGE database and previous impacts of sea level rise, as well as all other climate change impacts, are already incorporated in the economic data.

<sup>4</sup> It is worth mentioning that the GTAP database consider only agricultural land. To assess damages to other sectors, we implicitly assume that the land productivity loss can be translated to capital productivity loss referring to assets lying over the non-agricultural land and agricultural land.

shape of the coastline (rocky or flat) plays a key role to determine the SLR physical effect.

A similar dynamics characterizes the SLR impact on population [Tab. 4]. Regions which have high % shares of population, as Sicily, have not high % shares of DIVA impact, as Emilia Romagna and Veneto. This is probably caused by the different coastal urbanization of the regions.

## 5. RESULTS

The SLR shocks are cumulative impacts covering the period 2007-2100. The analysis does not consider by now transitional and recursive dynamics. As a consequence, the results should be interpreted as % changes over the period 2007-2100. In a nutshell, we carry out a comparative static exercise where all the cumulative impact is concentrated in the base year 2007 and produces instantaneously the economic general equilibrium effects in 2100.

[Tab. 5] and [Tab. 6] report the % real GDP losses in the rigid and flexible model, respectively. In the last row of both Tables we can observe that the aggregate GDP losses are similar for Italy between rigid and flexible model. However, in the flexible version the GDP decreases slightly less in all the SRES. This is due to the more competitive and integrated markets which allow the economic agents to better respond to the environmental shocks. The worst and best scenarios are A2 and B1 for Italy, respectively.

[Tab. 5] shows that in the rigid specification the most affected regions are Emilia Romagna and Veneto – not surprisingly as the physical impact is the highest – because their GDP decreases in 2100 from 4.55% to 7.78% and from 2.61% to 6.58%, respectively. Regions which have no coastline, like Piedmont and Lombardy, are essentially not affected in economic terms.

The flexible specification triggers an interesting dynamic at the sub-national level [Tab. 6]. We can notice amplification effects for regions which experienced substantial losses also in the rigid model. For example the % GDP decrease ranges from 8.72 to 14.54 in Emilia-Romagna and from 4.41 to 12.06 in Veneto. On the other hand, regions which were not impacted in the rigid version start to gain. Piedmont increases the GDP from 1.71% to 3.43%, Lombardy from 1.32 to 2.61. In

the flexible model also the landlocked regions are indirectly and positively affected by SLR as the markets are more integrated. In addition they gain more in the worst Italian scenario (A2) because compensate the bigger losses of the negatively affected coastline regions.

We can better understand the economic mechanism in the flexible model by analyzing the primary factors movement [Tab. 7]. Emilia Romagna and Veneto experience an outflow of capital, skilled labor and unskilled labor while Lombardy and Piedmont an inflow of the same primary factors.

The interpretation is straightforward. The SLR impact causes a productivity loss of the primary inputs in the coastal regions. This implies a reduction in the factor demand faced by the firms because the capital and labor have become less productive. This in turn determines a dip in the factor's price. In the rigid version no opportunity is given to capital and labor to move towards regions where the factor's remuneration is higher. The flexible version makes this possibility feasible and the factors move toward landlocked regions where the wages and the capital's returns have not been negatively affected by SLR.

In addition in each region the representative household partially shifts the demand of goods towards landlocked regions as they produce at lower costs because the productivity loss does not impact the primary inputs in these regions. This tends to strengthen the movements of capital and labor from the coast to inland. The changes in the regional GDP are the natural consequence of this mechanism.

## 6. CONCLUSIONS

Economic assessment of sea level rise can be performed through different approaches, namely bottom-up and top-down. The latter category has the advantage to consider mechanism propagation through the whole economic system beyond the sector of immediate interest by sea level rise, as well as other climate change impacts. Nevertheless, one main limitation lies in the geographical characterization, traditionally at country level in worldwide models, that indeed can hidden regional differences in climate change impacts and make less efficient a correlated adaptation strategy.

We propose and present a new approach to overcome such a limitation, providing a regional assessment of sea level rise induced impacts for regional Italian economies across a number of scenarios (the IPCC SRES). In the 2007-2100 time-horizon, the worst IPCC scenario is A2 for Italy. Veneto and Emilia-Romagna are the most affected regions by SLR in terms of GDP loss across all scenarios, given the highest physical impacts.

The uncertainty in the Italian overall impact is related to the SRES rather than the version of model (rigid and flexible), even if the economic general equilibrium effects slightly improve when the markets are more integrated and competitive.

Nevertheless, the model flexibility matters for the geographical distribution of economic effects at the sub-national level. Increasing the level of integration in the Italian economy makes the GDP regional patterns more uneven, exacerbating the winner/loser dynamic between coastal and landlocked regions.

In the flexible model regions which have no coastline are positively affected by SLR as labor and capital re-allocate from the coast to inland where remunerations are higher.

Further research will include: a) extending the construction of the regionalized database for other European and Mediterranean countries; b) moving from a static to a recursive-dynamic modelling framework; c) assessing the general equilibrium effects of SLR across all the SRES scenarios described by the IPCC, including the new SSPs (Shared Socio-Economic Pathways); d) use the framework to estimate other climate impacts, such as river floods, droughts and crop productivity.

## **7. ACKNOWLEDGMENTS**

The research leading to these results has received funding from the Italian Ministry of Education, University and Research and the Italian Ministry of Environment, Land and Sea under the GEMINA project.

## 8. REFERENCES

1. Armington P. (1969), A Theory of Demand for Products Distinguished by Place of Production, IMF staff papers, No. 16(1), pp. 159-178.
2. Bacharach M. (1970), Biproportional Matrices & Input-Output Change, Number 16 in University of Cambridge Department of Applied Economics Monographs, Cambridge University Press.
3. Bosello F., Nicholls R.J., Richards J., Roson R. & Tol R.S.J. (2011), Economic impacts of climate change in Europe: sea level rise, Climatic Change, No. 112(1), pp. 63-81.
4. ClimateCost Project. (2011), Technical Policy Briefing Note, Sea Level-Rise. Available online at:  
[http://www.climatecost.cc/images/Policy\\_brief\\_2\\_Coastal\\_10\\_lowres.pdf](http://www.climatecost.cc/images/Policy_brief_2_Coastal_10_lowres.pdf)
5. Deming W.E. & Stephan F.F. (1940), On a Least-squares Adjustment of a Sampled Frequency Table when the Expected Marginal Totals are Known, Annals of Mathematical Statistics, No. 11, pp. 427-444.
6. DINAS-Coast Consortium (2006), DIVA: Version 1.0. CD-ROM. Potsdam Institute for Climate Impact Research, Potsdam.
7. Dixon P., Rimmer M. & Wittwer G. (2012), USAGE-R51, a State-level Multi-regional CGE Model of the US Economy. Available online at:  
<https://www.gtap.agecon.purdue.edu/resources/download/5933.pdf>.
8. Hertel T.W. (Ed.) (1997), Global trade analysis: Modeling and applications, Cambridge and New York: Cambridge University Press.
9. Hinkel J. & Klein R.J.T. (2009), Integrating knowledge to assess coastal vulnerability to sea-level rise, Global Environmental Change, No. 19, pp. 384-395.
10. IPCC. (2013), 5th Assessment Report, Working Group I, Chapter 13. Available online at:  
[http://www.climatechange2013.org/images/report/WG1AR5\\_Chapter13\\_FINAL.pdf](http://www.climatechange2013.org/images/report/WG1AR5_Chapter13_FINAL.pdf)
11. ISTAT. Agricoltura e Zootecnia.

Available online at: [http://agri.istat.it/sag\\_is\\_pdwout/index.jsp](http://agri.istat.it/sag_is_pdwout/index.jsp)

12. ISTAT. Conti Economici Regionali, Anni 1995-2009.

Available online at: <http://www.istat.it/it/archivio/12718>

13. ISTAT. Trasporto Aereo, 2003-2009.

Available online at: <http://www.istat.it/it/archivio/14035>

14. ISTAT. Trasporto Ferroviario, 2004-2009.

Available online at: <http://www.istat.it/it/archivio/12909>

15. ISTAT. Trasporto Marittimo, 2005-2008.

Available online at: <http://www.istat.it/it/archivio/14084>

16. ISTAT. Trasporto Merci su Strada, 2008-2009.

Available online at: <http://www.istat.it/it/archivio/34954>

17. ISTAT. Valore Aggiunto ai Prezzi di Base dell'Agricoltura per Regione, Anni 1980-2011.

Available online at: <http://www.istat.it/it/archivio/66513>

18. McCallum J. (1995), National Borders Matter: Canada-U.S. Regional Trade Patterns, *American Economic Review*, No. 85(3), pp. 615-623.

19. McFadden L., Nicholls R.J., Vafeidis A.T. & Tol R.S.J. (2007), A methodology for modelling coastal space for global assessments, *Journal of Coastal Research*, No. 23(4), pp. 911–920.

20. Nakicenovic N. & Swart R. (2000), Special report on emissions scenarios: a special report of working group III of the intergovernmental panel on climate change, Cambridge University Press, Cambridge.

21. Narayanan B., Aguiar A. & McDougall R. (2012), Global Trade, Assistance, and Production: The GTAP 8 Data Base, Center for Global Trade Analysis, Purdue University.

22. Standardi G, Bosello F. & Eboli F. (2014), A sub-national CGE model for Italy, FEEM Working Paper, 2014.04.

23. Vafeidis A.T., Nicholls R.J., McFadden L., Tol R.S.J., Spencer T., Grashoff P.S., Boot G. & Klein R.J.T. (2008), A new global coastal database for impact and vulnerability analysis to sea-level rise, *Journal of Coastal Research*, No. 24(4), pp. 917–924.
24. Wittwer G. & Horridge M. (2010). Bringing Regional Detail to a CGE Model Using CENSUS Data, *Spatial Economic Analysis*, No. 5(2), pp. 229-255.

## 9. IMAGES AND TABLES

<b>CGE geographical units</b>	
Aosta-Valley	Lazio
Piedmont	Abruzzi
Lombardy	Molise
Trentino-Alto Adige	Campania
Veneto	Apulia
Friuli-Venezia Giulia	Basilicata
Liguria	Calabria
Emilia-Romagna	Sicily
Tuscany	Sardinia
Umbria	Rest of EU-27
Marche	Rest of the World

Tab. 1 CGE Geographical aggregation.

<b>CGE Sectors</b>
Agriculture
Manufactures
Services

Tab. 2 CGE Sectoral aggregation.

<b>SRES A1B</b>	<b>% coastline length</b>	<b>% DIVA impact</b>	<b>CGE % land/capital productivity change</b>
Friuli-V. G.	4.02	2.86	-2.34
<b>Emilia-Romagna</b>	<b>2.00</b>	<b>35.53</b>	<b>-10.17</b>
Liguria	4.36	1.04	-1.24
Tuscany	7.35	9.87	-2.76
Molise	0.45	0.41	-0.60
Apulia	10.87	7.59	-2.50
Campania	5.66	3.68	-1.73
Basilicata	0.74	0.87	-0.56
Calabria	9.00	5.09	-2.15
<b>Sicily</b>	<b>18.07</b>	<b>5.93</b>	<b>-1.48</b>
Abruzzi	1.58	1.19	-0.71
Lazio	4.30	6.51	-2.43
<b>Sardinia</b>	<b>21.60</b>	<b>5.81</b>	<b>-1.55</b>
Marche	2.11	1.54	-1.06
<b>Veneto</b>	<b>7.87</b>	<b>12.06</b>	<b>-4.21</b>
Italy	100.00	100.00	-2.13

Tab. 3 SLR impacts on land and capital

SRES A1B	% population	% DIVA impact	CGE % skilled/unskilled productivity change
Friuli V. G.	2.05	3.00	-0.98
<b>Emilia Romagna</b>	<b>7.31</b>	<b>21.51</b>	<b>-1.97</b>
Liguria	2.64	0.87	-0.22
Tuscany	6.18	8.91	-0.96
Molise	0.53	0.15	-0.19
Apulia	6.82	5.37	-0.53
Campania	9.70	9.21	-0.63
Basilicata	0.97	0.25	-0.17
Calabria	3.30	2.48	-0.50
<b>Sicily</b>	<b>8.42</b>	<b>4.77</b>	<b>-0.38</b>
Abruzzi	2.20	0.56	-0.17
Lazio	9.26	14.44	-1.04
Sardinia	2.76	2.96	-0.72
Marche	2.59	0.57	-0.15
<b>Veneto</b>	<b>8.17</b>	<b>24.95</b>	<b>-2.04</b>
<b>Rest of Italy</b>	<b>27.10</b>	<b>0</b>	<b>0</b>
Italy	100.00	100.00	-0.67

Tab. 4 SLR impacts on labor

<b>SRES</b>	<b>A1B</b>	<b>A1FI</b>	<b>A1T</b>	<b>A2</b>	<b>B1</b>	<b>B2</b>
<b>Piedmont</b>	<b>0.00</b>	<b>0.00</b>	<b>0.00</b>	<b>0.01</b>	<b>0.00</b>	<b>0.00</b>
Aosta Valley	0.01	0.01	0.01	0.02	0.00	0.01
<b>Lombardy</b>	<b>-0.02</b>	<b>-0.03</b>	<b>-0.02</b>	<b>-0.03</b>	<b>-0.02</b>	<b>-0.02</b>
Trentino Alto Adige	-0.04	-0.04	-0.03	-0.06	-0.03	-0.03
<b>Veneto</b>	<b>-3.16</b>	<b>-3.70</b>	<b>-2.71</b>	<b>-6.58</b>	<b>-2.61</b>	<b>-2.64</b>
Friuli V. G.	-1.66	-2.24	-1.32	-3.31	-1.20	-1.27
Liguria	-0.80	-0.98	-0.65	-0.92	-0.62	-0.65
<b>Emilia Romagna</b>	<b>-6.23</b>	<b>-7.34</b>	<b>-4.96</b>	<b>-7.78</b>	<b>-4.55</b>	<b>-4.85</b>
Tuscany	-1.92	-2.51	-1.37	-2.39	-1.24	-1.34
Umbria	-0.03	-0.03	-0.02	-0.03	-0.02	-0.02
Marche	-0.61	-0.70	-0.51	-0.75	-0.47	-0.50
Lazio	-1.77	-2.25	-1.30	-2.24	-1.16	-1.27
Abruzzi	-0.44	-0.51	-0.38	-0.55	-0.49	-0.37
Molise	-0.41	-0.49	-0.33	-0.50	-0.31	-0.33
Campania	-1.17	-1.50	-0.76	-1.51	-0.71	-0.75
Apulia	-1.50	-1.83	-1.16	-1.81	-1.06	-1.14
Basilicata	-0.36	-0.44	-0.29	-0.45	-0.27	-0.28
Calabria	-1.41	-1.53	-1.29	-1.64	-1.24	-1.28
Sicilia	-0.90	-1.01	-0.80	-1.07	-0.77	-0.79
Sardinia	-1.12	-1.64	-0.92	-1.60	-0.87	-0.94
<b>Italy</b>	<b>-1.52</b>	<b>-1.84</b>	<b>-1.21</b>	<b>-2.18</b>	<b>-1.12</b>	<b>-1.18</b>

Tab. 5 % real GDP change in the rigid model

<b>SRES</b>	<b>A1B</b>	<b>A1FI</b>	<b>A1T</b>	<b>A2</b>	<b>B1</b>	<b>B2</b>
<b>Piedmont</b>	<b>2.32</b>	<b>2.80</b>	<b>1.84</b>	<b>3.43</b>	<b>1.71</b>	<b>1.80</b>
Aosta Valley	2.51	3.03	1.99	3.65	1.85	1.95
<b>Lombardy</b>	<b>1.80</b>	<b>2.18</b>	<b>1.42</b>	<b>2.61</b>	<b>1.32</b>	<b>1.39</b>
Trentino Alto Adige	1.51	1.86	1.17	1.85	1.07	1.14
<b>Veneto</b>	<b>-5.13</b>	<b>-5.94</b>	<b>-4.53</b>	<b>-12.06</b>	<b>-4.41</b>	<b>-4.41</b>
Friuli V. G.	-2.01	-2.94	-1.63	-5.41	-1.48	-1.56
Liguria	0.27	0.30	0.17	0.89	0.13	0.15
<b>Emilia Romagna</b>	<b>-11.93</b>	<b>-13.95</b>	<b>-9.53</b>	<b>-14.54</b>	<b>-8.72</b>	<b>-9.33</b>
Tuscany	-2.44	-3.38	-1.60	-2.70	-1.41	-1.57
Umbria	1.81	2.18	1.45	2.73	1.36	1.42
Marche	0.36	0.54	0.24	0.93	0.22	0.23
Lazio	-2.04	-2.72	-1.36	-2.19	-1.15	-1.32
Abruzzi	1.11	1.39	0.84	1.91	0.47	0.81
Molise	1.15	1.40	0.91	1.95	0.82	0.88
Campania	-0.72	-1.06	-0.18	-0.55	-0.18	-0.18
Apulia	-1.71	-2.09	-1.31	-1.66	-1.18	-1.29
Basilicata	1.05	1.26	0.84	1.69	0.78	0.82
Calabria	-1.45	-1.34	-1.53	-1.27	-1.54	-1.54
Sicilia	-0.43	-0.34	-0.52	-0.14	-0.55	-0.54
Sardinia	-0.85	-1.71	-0.74	-1.18	-0.72	-0.80
<b>Italy</b>	<b>-1.51</b>	<b>-1.83</b>	<b>-1.20</b>	<b>-2.16</b>	<b>-1.11</b>	<b>-1.17</b>

Tab. 6 % real GDP change in the flexible model

Impacts & Implications of  
Climate Change

**Hydrological risk**

## **Assessing indirect expected annual loss of flooding in Italy under current and future climate**

**Carrera L.<sup>1,2,3\*</sup>, Standardi G.<sup>1,3</sup>, Koks E.<sup>4</sup>, Feyen L.<sup>5</sup>, Mysiak J.<sup>1,3</sup>, Aerts J.<sup>4</sup>, and  
Bosello F.<sup>1,3</sup>**

<sup>1</sup> Fondazione Eni Enrico Mattei - Italy, <sup>2</sup> Ca' Foscari University of Venice - Italy, <sup>3</sup> Euro-Mediterranean Centre on Climate Change - Italy, <sup>4</sup> Institute for Environmental Studies, Vrije University of Amsterdam –Netherlands, and <sup>5</sup>Institute for Environment and Sustainability, EC Joint Research Center – Italy

\*Corresponding Author: [lorenzo.carrera@feem.it](mailto:lorenzo.carrera@feem.it)

### **Abstract**

An integrated methodology for assessing indirect expected annual loss (EAL) of fluvial flooding is developed and used to estimate current and future flood risk in Italy. The methodology combines an high resolution spatial approach with a regionally-calibrated Computable General Equilibrium (CGE) model at NUTS2 scale. Given the level of uncertainty in the behavior of disaster-affected economies, we modelled two flood impact duration scenarios. Indirect EAL is provided for each NUTS2 region and Italy as a whole. Because of the difference between direct impacts, which represent the damage to the capital stock, and indirect impacts, which represent the damage to the flows hence the wider effects of a disaster to the economy, the latter has significant policy relevance to the economic impact assessment of disasters.

**Keywords:** flood risk, CGE, spatial analysis, impact assessment

## 1. INTRODUCTION AND BACKGROUND

The observation of climate and weather events highlighted that globally extremes have changed since 1950 [1]. Anthropogenic influence affected the global water cycle since 1960, modifying precipitation patterns over land and increasing the intensity of heavy precipitation [1]. Although the frequency and intensity of extreme precipitations have great variability in location and time, it is reported that heavy precipitation events have increased in Europe [1]. Given the increasing global temperature caused by anthropogenic activities, the IPCC reports that extreme precipitation events will occur more frequently and with stronger intensity by the end of this century [1]. Growing population and capital density, unsustainable development, inappropriate land use and climate change, threaten to intensify natural hazards' risk with even more concerning consequences for the environment and societies [2]. Against this background the EEA warned that flood related losses will rise consistently in Europe [3]. According to Feyen et al. (2012), which calculated the (direct) expected annual damage (EAD) from river flooding events in Europe, current EAD of 6.4 billion Euro will increase by 2100 to 14 - 21.5 billion Euro (constant 2006 prices) [4]. Under the medium to high emission scenario A1B Rojas et al. [5] calculated that EAD will raise by the end of this century to around 97 billion Euro (constant 2006 prices undiscounted, considering both climate and socio-economic changes).

However, economic impacts of natural hazards are still poorly understood, particularly their indirect, wider and macro-economic effects. Typically estimates from EEA [3] and global disaster databases (i.e. the EM-DAT dataset managed by the Centre for Research on the Epidemiology of Disasters, the NatCatSERVICE dataset managed by Munich Reinsurance Company, and the Sigma dataset from Swiss Reinsurance Company) undervalue the full cost of disasters to societies and environment because most of the time only direct impacts are accounted for, with partial or incomplete consideration given to indirect, wider and macroeconomic effects.

Several efforts have been made to assess indirect impacts of disasters on national and regional economies [6]–[11] using different methodologies including amongst others: post event economic surveys [12]–[14], econometric models [15]–[18], input-output (I-O) models [19]–[22], computable general equilibrium (CGE) models [23]–

[27]. Different methodologies have different pros and cons. Econometric models if well specified and based upon data of a reasonable quality can indeed quantify indirect effects on national/local GDP of extreme events. However they cannot describe the systemic economic channels through which they propagates within and between the economies affected. CGE models can do so, also capturing the feedback effects from the macro-economic context on the “markets” initially concerned. Nonetheless, one important limitation of CGE models in these kind of researches is their “coarse” investigation unit, usually the country. This may allow analysis of aggregated events or trends, but makes local analyses particularly challenging. I/O models finally can reach a high analytical specificity, they can represent urban contexts as well as even smaller economic entities like natural parks, but then they are usually missing the effect on the overall economy.

Against this background, in this paper we propose the combination of a spatially based analysis with a CGE model, regionally calibrated to the Italian NUTS2 (Eurostat) regions [28]. Our regional version of the global CGE model allows to assess regional impacts maintaining the global scale of the economic system (e.g. global trading, international exports and imports, etc.).

Our aim is to couple the high resolution of spatial analysis with the systemic ability to capture economic interaction of CGE models, without pushing the CGE aggregation need too far to loose completely local specificities. We use our methodology to estimate the indirect impacts at the regional and national level of flood risk under current and future climate (2100). The outputs of the model provide an estimation of current and future indirect expected annual loss (EAL) for Italy considering two flood impact duration. In our work the EAL is defined as the integral of the damage function [4] or, for a set of events each with a probability  $P_i$  and an associated loss  $L_i$ , the sum of expected losses for a given year:  $EAL = \sum_i P_i L_i$ .

## 2. METHODOLOGY

The terminology used in the literature related to the economics of natural disasters is extremely various [6], [10], [11], [29]–[34]. Meyer [34] distinguish between direct costs, which are damages to properties in the area of the hazard, business interruption costs, which occur to business directly affected by the hazard, often referred as primary indirect damages because they are induced by the interruption of business activities, and indirect costs, which occurs inside and outside the flooded

area and are caused by direct costs and/or business interruption costs [8]. Despite the clarity of these definitions, from a more formal economic perspective the distinction between direct and indirect losses is difficult to put into practice [10] because economists tend to differentiate between stocks and flows, where stocks is the quantity at a single point time and flows are the output of stocks over time [10].

In this paper we ponder both the more formal economic definitions of Rose et al. 2004 and the ones lately reviewed by Meyer (2013). We consider the damage to properties (direct costs) as the reduction in the value of stock, and the businesses interruptions losses as the reduction of flows, which are sometimes referred as higher-order effects [10] or macro-economic impacts [35]. We do not measure business interruptions alone because of the incapacity of our economic model to isolate the interruption of businesses directly affected by the flood from the wider effects on the regional economic system. The economic model used in this work (CGE model) is able to simulate both consumer and firms optimization behavior in response to price changes. The model includes substitution, behavioral preference, elasticity of supply, and markets, therefore we consider that business interruption in affected areas can be compensated or amplified by the economic system, nevertheless this effects are absorbed by the economic system and represented in our model outputs.

#### **a. FLOOD SIMULATION DATA**

The flood simulation dataset is provided by the Joint Research Center (JRC). The construction of the dataset is well described in Feyen et al. (2012) and Rojas et al. (2013). We use the ensemble of 12 climate experiments from 4 GCMs and 7 RCMs from the ENSEMBLE (EU FP6) Project. The simulations cover the period 1961-2100. The Ensemble simulation has horizontal resolution of ca. 25km, daily temporal steps and was forced on the SRES-A1B scenario. The hydrological simulations were obtained using the LISFLOOD model, which is a spatial model where “processes like infiltration, water consumption by plants, snowmelt, freezing of soils, surface runoff and groundwater storage” are taken into account at 5km grid resolution (Rojas et al. 2013) and daily steps. This work makes use of LISFLOOD results for 5 time steps of 30 years duration (ctrl: 1961-1990; 2000: 1981-2010; 2020: 2011-2040; 2050: 2041-2070; 2080: 2071-2100) and 8 flood return periods (2, 5, 10, 20, 50, 100, 250, 500), which were derived from fitted Gumbel distributions to the maximum annual

discharge. CORINE Land Cover 2000 (EEA 2002) was used for estimating the exposed assets. CORINE has 44 land cover classes and an horizontal resolution of 100m. One third of the land cover, such as forest, wetlands and sand to name a few were not considered. The remaining were merged into 5 classes, including residential, agriculture, industry, transport and commerce. These macro land classes represent the exposed assets. In this work we do not consider for changes in urbanization and land development in the future.

## b. THE REGIONAL CGE MODEL

Our regionally-calibrated CGE model is based on GTAP 7 (Global Trade Analysis Project, reference year 2004). Comprehensive description of the model can be found in Standardi [28]. For Italy we downscaled the country based model to regional level using three panel data: (1) the GTAP 7 database (Narayanan and Walmsley, 2008) which consists of 57 sectors and 113 countries or groups of countries (2004); (2) the regional panel data of ISTAT (Italian National Statistical Institute) from the same year, which provides information on value added, labour and land for the 20 Italian regions and 40 economic sectors; (3) ISTAT bilateral flows of carried goods (in tons) by mode of transportation (truck, rail, water and air) for the 20 Italian regions. We followed a three steps procedure: (a) we matched the 40 ISTAT sectors with the 24 GTAP sectors chosen in our aggregation. We distributed the Italian value added and primary factors in GTAP across the 20 Italian regions using the shares of ISTAT for value added, labour and land. Capital was computed as the difference between value added and labour. For the sectors that use natural resources we took the sub-national share of value added in those sector as a proxy; (b) we used the shares obtained from ISTAT transport data to split the sectoral GTAP Italian production between domestic regional demand and bilateral trade flows across Italian regions; (c) we adjusted the bilateral trade flows across Italian regions to make them consistent with the ISTAT data on the economic production.

Table 1: CGE model sectors

1	Rice	13	Textile
2	Crops	14	HeavyManif
3	VegFruit	15	Light Manif
4	Oil	16	Utilities
5	Plant	17	Construction
6	Livestock	18	Trade

7	AnimFarm	19	Transport
8	Forestry	20	WaterTrans
9	Fishing	21	AirTrans
10	Hcarb	22	Communication
11	Minerals	23	Services
12	ProcFood	24	Recreational

### c. INTEGRATING THE SPATIAL ANALYSIS AND THE CGE MODEL

The impact to the productivity factors of the CGE model, i.e. land, capital and labour are derived from the elaboration of JRC's flood raster dataset over the land use map (Corine Land Cover 2000). For each time step (ctrl, 2000, 2020, 2050, 2080) and each flood return periods (2, 5, 10, 20, 50, 100, 250, 500) we calculate the total area affected over the total area of each land cover type (as defined in Table 2) at NUTS2 level. We use these percentages (affected/total) for sectorial loss of capital and labour (all sectors), and land (agriculture-related sectors only).

Table 2: association of the 43 CORINE land cover (2000) classes to the 24 GTAP economic sectors (which are further aggregated into the sectors defined in Table 1)

CORINE land cover	CGE sector	CORINE land cover	CGE sector
111 Continuous urban fabric	22 Communication	142 Sport and leisure facilities	24 Recreational
Discontinuous urban fabric	23 Services	211 Non-irrigated arable land	2 Crops
112 fabric	22 Communication	212 Permanently irrigated land	2 Crops
Industrial or commercial units	23 Services	213 Rice fields	5 Plant
121 units	24 Recreational	221 Vineyards	1 Rice
	12 ProcFood	222 Fruit trees and berry plantations	3 VegFruit
	13 Textile	223 Olive groves	3 VegFruit
	14 HeavyManif	231 Pastures	4 Oil
	15 Light Manif	Annual crops associated with permanent crops	6 Livestock
	16 Utilities	241	3 VegFruit
	18 Trade	242 Complex cultivation patterns	3 VegFruit
	22 Communication	Land principally occupied by agriculture	2 Crops
	10 Hcarb	243	3 VegFruit
	7 AnimFarm	244 Agro-forestry areas	4 Oil
122 Road and rail networks and associated land	16 Utilities	311 Broad-leaved forest	8 Forestry
	19 Transport	312 Coniferous forest	8 Forestry
	22 Communication	313 Mixed forest	8 Forestry
123 Port areas	10 Hcarb	331 Beaches, dunes, sands	24 Recreational
	16 Utilities	511 Water courses	9 Fishing
	20 WaterTrans	512 Water bodies	9 Fishing
124 Airports	21 AirTrans	521 Coastal lagoons	9 Fishing
131 Mineral extraction sites	11 Minerals		

133 Construction sites	17 Construction	522 Estuaries	9 Fishing
141 Green urban areas	24 Recreational		

The recovery period for a business is characterized by high level of uncertainty, depending on the type of business, its location, the possibility for relocating production and activities, the elevation of the water level and the duration of water staying. Given this level of uncertainty we modelled the businesses recovery period for two durations: 3 and 12 months.

#### d. INDIRECT EXPECTED ANNUAL LOSS

In our model the flood events (characterized by a specific return period) are assumed independent Bernoulli random variables, each with a probability function defined as:

$$P(E_i \text{ happening}) = p_i$$

$$P(E_i \text{ not happening}) = (1-p_i)$$

where E is flood event and p is the annual probability of occurrence (calculated as 1 divided by the return period).

If the flood does not happen the economic loss is zero. If the flood happens the expected loss E(L) for a given year is:

$$E_i(L) = p_i L_i$$

where in our model E(L) is calculated as the sum of expected direct (DL) and indirect losses (IL):

$$E_i(L) = p_i D L_i + p_i I L_i$$

For a set of events each with a probability  $p_i$  and an associated loss  $L_i$ , the overall expected loss, named Expected Annual Loss (EAL), is the sum of expected losses for a given year:

$$EAL = \sum_i p_i L_i$$

### 3. RESULTS

For a flood return period of 100 years the model provides expected loss of 15,300 million Euro (2004 value) for the period 1961-1990 (1980) and 18,000 million Euro (2004 value) for the period 2071-2100 (2080). For a 500 years return period event losses will increase from 17,800 to 20,800 million Euro [Figure 1].

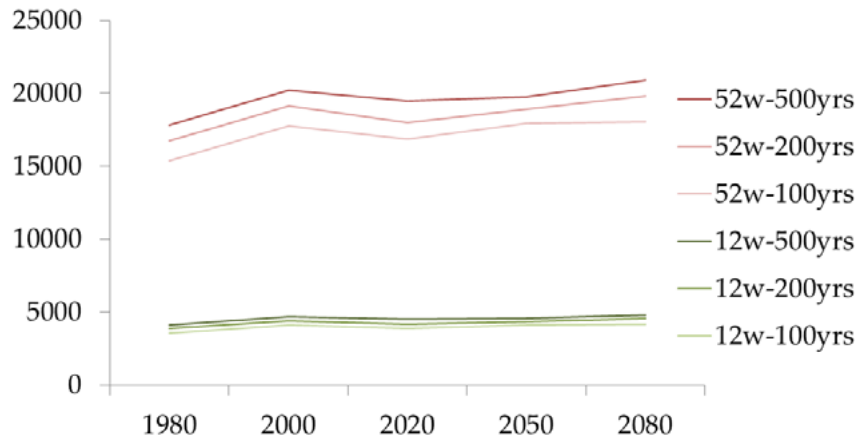


Fig. 1 expected losses (million Euro) for a flood impact duration of 3 months (12w) and 1 year (52w). Results are expressed in million Euro (constant 2004 value) for three flood return periods (100, 200, 500 yrs).

The estimated indirect EAL is described in Figure 2, which provides the indirect EAL for both 12 and 3 months impact duration on affected regions. The protection level homogeneously considered for Italy as 50 years return period. This is the cut-off level applied to the integral of the damage function. The protection level is constant in time, therefore we assume full adaptation in the future. For the 1 year impact duration, indirect EAL increases from 567 million Euro in the period 1961-1990 (CTRL) to 667 million Euro (2004 value) in the period 2071-2100 (2080). For the 3 months duration indirect EAL increases from 131 million Euro in the period 1961-1990 (CTRL) to 153 million Euro (2004 value) in the period 2071-2100 (2080).

The increases (around 17 percent for both duration) are given to climate change only because socio-economic changes are not considered.

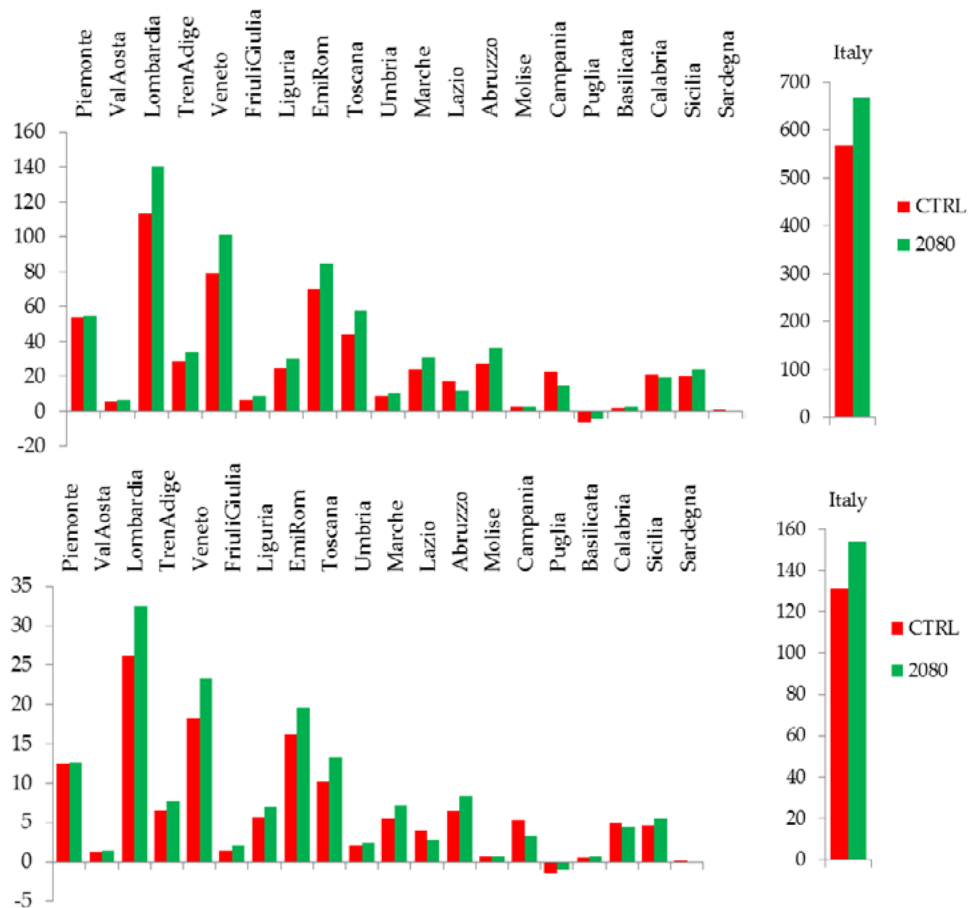


Fig. 2 indirect EAL (million Euro 2004 value) for the NUTS2 Italian regions and Italy as a whole in the periods 1961-1990 (CTRL) and 2071-2100 (2080). Top is the indirect EAL for the 1 year impact, bottom for a 3 months impact.

#### 4. CONCLUSION

This paper describes a methodology for measuring indirect EAL from flooding under current and future climate. The proposed methodology integrates high resolution spatial analysis of flood risk and land use mapping, with a regionally-calibrated version to Italy of a global CGE model. The output of the model highlights that indirect EAL will raise by the end of the century of 17 percent from our control period (1961-1990). In our model this increase is due to climate change only, without any consideration given to socio-economic development, which could raise exposure and consequent losses. Moreover we assume adaptation over time in maintaining a constant flood protection level. Hence our results shall be considered at the lower bounds of the real economic cost of flood risk in Italy.

The lack of knowledge about indirect economic impacts of flooding still undermine a proper understanding of flood risk in Italy and other parts of Europe. Our estimation

of indirect EAL is around 16 percent of the EAL provided for Italy by JRC studies [5]. This is significant part of the economic impact which shall not be further neglected in disaster's impact assessment.

## 5. ACKNOWLEDGMENTS

This work is part of the research developed by CMCC (Euro-Mediterranean Centre on Climate Change) under the GEMINA project, funded by the Italian Ministries for the Research and for the Environment, Land and Sea, and by FEEM under the European Community's Seventh Framework Programme (FP7/2007-2013) Project ENHANCE.

## 6. REFERENCES

- [1] IPCC, "Climate Change 2013: The Physical Science Basis. Summary for Policymakers," 2013.
- [2] IPCC, *Managing the Risks of Extreme Events and Disasters to Advance Climate Change Adaptation*. Cambridge: Cambridge University Press, 2012.
- [3] European Environmental Agency, "Climate change, impacts and vulnerability in Europe 2012," 2012.
- [4] L. Feyen, R. Dankers, K. Bódis, P. Salamon, and J. Barredo, "Fluvial flood risk in Europe in present and future climates," *Clim. Change*, vol. 112, no. 1, pp. 47–62, 2012.
- [5] R. Rojas, L. Feyen, and P. Watkiss, "Climate change and river floods in the European Union : Socio-economic consequences and the costs and benefits of adaptation," *Glob. Environ. Chang. - Press*, 2013.
- [6] H. C. Cochrane, "Chapter 3. Indirect Losses from Natural Disasters: Measurement and Myth," in in *Yasuhide Okuyama and Stephanie E. Chang eds. Modeling the Spatial and Economic Effects of Disasters*, New York, NY; Springer, 2004.
- [7] F. Messner, E. Penning-Rowsell, C. Green, V. Meyer, S. Tunstall, and A. van der Veen, "Evaluating flood damages: guidance and recommendations on principles and methods," 2007.
- [8] V. Przyluski and S. Hallegatte, "Indirect Costs of Natural Hazards - CONHAZ Report," 2011.
- [9] C. Green, C. Viavattene, and P. Thompson, "Guidance for assessing flood losses - CONHAZ Report," no. September, pp. 1–86, 2011.

- [10] A. Rose, “Economic Principles, Issues and Research Priorities in Hazard Loss Estimation,” in in *Okuyama, Y. and S.E. Chang (eds.) Modeling the Spatial and Economic Effects of Disasters*. New York: Springer, 2004.
- [11] Y. Okuyama, “Economic modeling for disaster impact analysis: past, present, and future,” *Econ. Syst. Res.*, vol. 19, no. 2, pp. 115–124, 2007.
- [12] C. Pfurtscheller, “Regional economic impacts of natural hazards – the case of the 2005 Alpine flood event in Tyrol ( Austria ),” *Nat. Hazards Earth Syst. Sci.*, no. 14, pp. 359–378, 2014.
- [13] C. A. Kroll, J. D. Landis, Q. Shen, and S. Stryker, “Economic impacts of the Loma Prieta earthquake: A focus on small businesses,” 1991.
- [14] D. Molinari, S. Menoni, G. T. Aronica, F. Ballio, N. Berni, C. Pandolfo, M. Stelluti, and G. Minucci, “Ex post damage assessment: an Italian experience,” *Nat. Hazards Earth Syst. Sci.*, vol. 14, no. 4, pp. 901–916, Apr. 2014.
- [15] J. M. Albala-Bertrand, “Natural disaster situations and growth: A macroeconomic model for sudden disaster impacts,” *World Dev.*, vol. 21, no. 9, pp. 1417–1434, Sep. 1993.
- [16] E. Strobl, “The Economic Growth Impact of Hurricanes: Evidence from U.S. Coastal Counties,” *Rev. Econ. Stat.*, vol. 93, no. 2, pp. 575–589, Aug. 2010.
- [17] E. Cavallo, I. D. Bank, S. Galiani, and J. Pantano, “Catastrophic Natural Disasters and Economic Growth,” pp. 1–35, 2012.
- [18] I. Noy and A. Nualsri, “What do exogenous shocks tell us about growth theories?,” Santa Cruz Inst. for International Economics, Santa Cruz, Calif., 2007.
- [19] S. Hallegatte, “An adaptive regional input-output model and its application to the assessment of the economic cost of Katrina,” *Risk Anal.*, vol. 28, no. 3, pp. 779–99, Jun. 2008.
- [20] F. Henriët, S. Hallegatte, and L. Tabourier, “Firm-network characteristics and economic robustness to natural disasters,” *J. Econ. Dyn. Control*, vol. 36, no. 1, pp. 150–167, Jan. 2012.
- [21] Y. Okuyama, G. D. Hewings, and M. Sonis, “Measuring Economic Impacts of Disasters: Interregional Input-Output Analysis Using Sequential Interindustry Model,” in in *Modeling Spatial and Economic Impacts of Disasters SE - 5*, Y. Okuyama and S. Chang, Eds. Springer Berlin Heidelberg, 2004, pp. 77–101.
- [22] Y. Okuyama, “Disaster and economic structural change: case study on the 1995 Kobe earthquake,” *Econ. Syst. Res.*, no. March, pp. 37–41, 2014.

- [23] A. Rose and S.-Y. Liao, "Modeling Regional Economic Resilience to Disasters: A Computable General Equilibrium Analysis of Water Service Disruptions\*," *J. Reg. Sci.*, vol. 45, no. 1, pp. 75–112, Feb. 2005.
- [24] M. Berrittella, A. Y. Hoekstra, K. Rehdanz, R. Roson, and R. S. J. Tol, "The economic impact of restricted water supply: a computable general equilibrium analysis," *Water Res.*, vol. 41, no. 8, pp. 1799–813, Apr. 2007.
- [25] A. Rose, J. Benavides, S. E. Chang, P. Szczesniak, and D. Lim, "The Regional Economic Impact of an Earthquake: Direct and Indirect Effects of Electricity Lifeline Disruptions," *J. Reg. Sci.*, vol. 37, no. 3, pp. 437–458, Aug. 1997.
- [26] W. Jonkhoff, "Flood risk assessment and policy in the Netherlands," in *Green Cities: new approaches to confronting climate change*, 2009, pp. 220–240.
- [27] E. A. Haddad and E. Teixeira, "Economic impacts of natural disasters in megacities: the case of floods in São Paulo, Brazil." São Paulo, p. 21, 2013.
- [28] G. Standardi, F. Bosello, and F. Eboli, "A sub-national version of the GTAP model for Italy," *Work. Pap. Fond. Eni Enrico Mattei*, vol. 2014.04, pp. 1–20, 2014.
- [29] D. J. Parker, C. H. Green, and P. M. Thompson, *Urban flood protection benefits: A project appraisal guide*. Gower technical press Aldershot, 1987.
- [30] K. Smith and R. Ward, *Floods: physical processes and human impacts*. Wiley Chichester, 1998.
- [31] B. Merz, H. Kreibich, R. Schwarze, and A. Thieken, "Review article 'Assessment of economic flood damage'," *Nat. Hazards Earth Syst. Sci.*, vol. 10, no. 8, pp. 1697–1724, Aug. 2010.
- [32] S. Balbi, C. Giupponi, M. Ursic, R. Olschewski, and J. Mysiak, "The Total Cost of Hydrological Disasters : Reviewing the Economic Valuation Methodologies and Conceptualizing a Framework for Comprehensive Cost Assessments - KULTURisk Project," Venice, 2011.
- [33] NRS, "The impacts of natural disasters: a framework for loss estimation," Washington DC, 1999.
- [34] V. Meyer, N. Becker, V. Markantonis, R. Schwarze, J. C. J. M. van den Bergh, L. M. Bouwer, P. Bubeck, P. Ciavola, E. Genovese, C. Green, S. Hallegatte, H. Kreibich, Q. Lequeux, I. Logar, E. Papyrakis, C. Pfurtscheller, J. Poussin, V. Przyluski, a. H. Thieken, and C. Viavattene, "Review article: Assessing the costs of natural hazards – state of the art and knowledge gaps," *Nat. Hazards Earth Syst. Sci.*, vol. 13, no. 5, pp. 1351–1373, May 2013.
- [35] K. Safarzyńska, R. Brouwer, and M. Hofkes, "Evolutionary modelling of the macro-economic impacts of catastrophic flood events," *Ecol. Econ.*, vol. 88, pp. 108–118, Apr. 2013.

# Climate Change Effects on Seawall Stability

Mase H.<sup>1\*</sup>, Karunarathna H.<sup>2</sup>, and Reeve D.<sup>3</sup>

<sup>1</sup>Professor - Japan, <sup>2</sup>Associate Professor - UK, and <sup>3</sup>Professor – UK

\*Corresponding Author: mase.hajime.5c@kyoto-u.ac.jp

## Abstract

Crown heights of seawalls should be designed to suppress overtopping discharges into an allowable level. Since environmental coastal forces such as sea level, waves and storm surge are non-stationary in nature, it is usually difficult to design the crown height of seawalls, especially where climate change due to global warming is surely expected to change waves and sea levels in future. This study analyses climate change effects on failure probability of seawalls by using a reliability analysis method of Level III and proposes an adaptation method to maintain the present safety level.

**Keywords:** climate change, wave overtopping, reliability analysis, failure probability

## 1. INTRODUCTION

The AR5 of IPCC [1] reported, from recent observations, analyses and projections by General Circulation Models under various scenarios, that global warming takes place at an alarming rate. Coastal disasters are expected to increase due to sea level rise and increasing storminess in wave climate. Under climate change conditions, researches on coastal defense structure design have become extremely important since the existing structures may become obsolete as the wave forces and water levels become larger.

Sea level rise has significant impacts on the coastal zone by way inundating low level areas and increasing the vulnerability of coastal regions to other physical processes (e.g., storm surges, storm waves). Ocean waves and storm surges of future climate are expected to be changed from the present, and it becomes necessary to consider the impacts of these dynamic extreme phenomena for coastal disaster prevention and reduction.

The future wave climate projections have been conducted by a few researchers (e.g. Hemer et al. [2]). These studies have shown an increase in wave height due to increased wind speeds associated with mid-latitude storms in many regions of the mid-latitude oceans. Zhang et al. [3] and Wang and Swail [4] made statistical projections of global wave height from the empirical relationships between sea-level pressure and significant wave height.

The present study investigates the failure probability of a seawall due to wave overtopping. Wave overtopping formulae given in Europe (e.g., TAW [5]) and in the USA (e.g., the Coastal Engineering Manual, CEM [6]), account for the random behavior of waves; and the effects of any non-uniformity in the cross-sections of seawalls are dealt with by employing an equivalent uniform slope. In most of the wave overtopping prediction models, input wave conditions are specified either at offshore, or at the toe of the foreshore slope, or at the toe of the structure itself. However, when a structure is built in very shallow water or on land, the wave height at its toe is not easy to define.

Mase et al. [7] proposed a wave overtopping prediction model linking wave runup and overtopping on seawalls built on land and in very shallow water. This model is used in the present study for evaluating failure probability of seawalls.

## 2. RELIABILITY ANALYSIS AND FAILURE FUNCTION RELATED TO WAVE OVERTOPPING

Reliability analysis quantifies the probability of occurrence of a particular failure mode represented by the failure function  $Z = f(X_1, \dots, X_N)$  where  $X_i$ s are the random variables with a probability density function  $f_{X_i}$  involved in the concerned problem. The equation is the mathematical basis for probabilistic analysis. The above integrations cannot be performed analytically and have to be approximated in some way: 1) Level III - Full distribution approach; 2) Level II - Semi-probabilistic approach; and 3) Level I - Limit state approach. In the present study, the Level III approach is used to estimate the failure probability of seawall due to wave overtopping.

Structural damage to seawalls can occur as a result of parapet collapse, upper surface wrecking, slope armor layer breakage, toe scouring and rear ground scouring. Any form of damage to seawalls will finally result in coastal flooding. All seawall failure modes must be identified and studied as possible risks for seawall damages. Neglect of an important failure mode will bias the estimation of the safety of the structure. Since, however, it is not generally known how to quantify such failure modes (failure functions), the present study takes up a failure mode induced by excess overtopping discharge.

The failure function due to wave overtopping is written by  $Z = q_a - q$ , where  $q_a$  is the permissible overtopping discharge ( $m^3/s/m$ ), and  $q$  the estimated discharge determined from random variables such as wave height, period, surge height and so on, by the prediction formula of Mase et al. [7]. When the value of  $Z$  is negative, the failure due to overtopping is considered to be occurred. This is carried out by the Monte Carlo method. Permissible wave overtopping discharges are determined (or given) by considering structure types, functional and structural safety, and hinterland use. For seawall's failure due to overtopping, the failure means that overtopping discharge exceeds the permissible overtopping discharge.

## 3. TARGET ANALYSIS CONDITIONS

For evaluation of climate change effects on seawall failure, a target seawall is setup considering a real scale seawall installed on the coast of Kochi Prefecture, Japan, facing the Pacific Ocean where the extreme wave height are very large.

From a report of the Coast Division of River Department, the Ministry of Land, Infrastructure and Transport, Japan (2008), the representative configuration of seawall, installed at Kochi coast, is that the crown height is T.P. (Tokyo Peil) +10 m, the front slope is 1:0.5 built on a 1/20 slope sandy beach. Taking this configuration as the basis, four different crown heights (T.P. +13.90 m, +11.95 m, +10.00 m, +8.05 m), two different the seawall slopes (1:0.5, 1:3.0), four cases of toe depth (T.P. + 5.45 m, 2.20 m, -1.05 m, -4.30 m) and 4 foreshore slopes (1/50, 1/20, 1/10) were adopted for the present study. Figure [1] summarizes the conditions of seawall and beach slope examined.

Figure [2] shows the sea level rise (SLR) trend in Japan region obtained from CMIP3 for A1B scenario (Mori et al. [8]). The mean SLR trend around Japan is slightly different from the global trend. The mean (GCM model ensemble) trend is denoted as SL-M, the large one as the mean trend plus the standard deviation, as SL-L and the small one as the mean trend minus standard deviation, as SL-S. All three different SLR trends were adopted in the present study.

The future significant wave height with 50 years return period (estimated from wave simulations from 2075 to 2100) (Shimura et al. [9]) will increase by 1.23 times compared to the present wave height offshore of Kochi Prefecture. According to future wave projection, the present design wave height of 13.0 m is multiplied by 1.23 at the 87.5 years later as shown by Line WA-M in Fig. [3]. Lines WA-L and WA-S correspond to mean value plus and minus standard deviation respectively. The linear increase in wave height was assumed since the near future wave simulation was not been carried out.

Random variables of sea level, wave height, wave period, surge height and toe depth, used in the overtopping formula, are given by specified probability density functions. The Weibull distribution is used as the offshore (design) wave height distribution. The wave period was firstly given by considering an averaged relationship between the significant wave height and period,  $T_s = 3.08H_s^{0.63}$  (modified version of Goda [10]). By using the equation, the distribution of wave period is adopted as the Gaussian distribution with the mean vale of  $T_s$  and the standard deviation of  $0.05 T_s$  for a given  $H_s$  from the Weibull distribution. For the distribution of tide, a triangle distribution with the maximum level of T.P.+0.72m, minimum level of T.P.-1.07m and mode of T.P.+0.25m was employed from observations. The surge height  $\zeta$  was related to the

wave height  $H_s$  so that the  $\zeta$  is given from the Gaussian distribution with the mean value  $\mu = 0.1 \cdot H_s$  and standard deviation of  $0.1 \cdot \mu$ .

#### 4. RESULTS

Figures [4] and [5] show examples of failure probability of seawalls in 50 years interval from the present climate to the future climate. The case shown in Fig. [4] is the seawall built in sea where beach slope is 1/20, seawall slope is 1:3, non-dimensional toe depth is 0.5. The freeboard is taken as the present design free board height. The conditions of seawall shown in Fig. [5] are the same as those installed on land at Kochi coast where beach slope is 1/20, seawall slope is 1:0.5, non-dimensional toe depth is -0.25.

It is seen from these two figures that the effect of different sea level changes of SL-L, SL-M and SL-S conditions is small compared to the effect of difference in wave height change as WA-L, WA-M and WA-S, both for seawalls built in the sea and on land.

The estimates of failure probabilities were carried out for all conditions of seawall described in Section 3, by changing the crown height, toe depth, seawall slope and foreshore slope. Figure [6] shows the result of changes of failure probability for steep slope seawall with the present freeboard after 50 years. It was found that steeper the beach slope, the larger the failure probability.

We can estimate the required values of seawall crown height, slope, toe depth and foreshore slope to keep the present failure probability at a desired future year by carrying out the reliability analysis.

#### 5. REFERENCES

1. IPCC (2014), IPCC Fifth Assessment Report (AR5), <http://www.ipcc.ch/index.htm>.
2. Hemer, M., Church, J., Swail, V. and Wang, X. (2006), Coordinated global wave climate projections, Atmosphere-Ocean Interactions, Vol. 2, 185–218.
3. Zhang, K., Douglas, B. and Leatherman, S. (2004), Global warming and coastal erosion, Climatic Change, Vol.64, No.1, 41–58.

4. Wang, X. and Swail, V. (2006), Historical and possible future changes of wave heights in Northern Hemisphere oceans, *Atmosphere-Ocean Interactions*, Vol.2, 185–218.
5. TAW (2002), Technical report wave run-up and wave overtopping at dikes, Ed. Van der Meer, J.W., Technical Advisory Committee on Flood Defense, The Netherlands, 50p.
6. U.S. Army Corps of Engineers (2002), Coastal Engineering Manual (CEM), Engineer Manual 1110-2-1100, Washington, D.C. .
7. Mase, H., Tamada, T., Yasuda, T., Hedges, T.S. and Reis, M.T. (2013), Wave runup and overtopping at seawalls built on land and in very shallow water, *Jour. Waterway, Port, Coastal, and Ocean, Eng.*, ASCE, Vol.139, No.5, pp.346-357, DOI: 10.1061/(ASCE)WW.1943-5460.0000199.
8. Mori, N., Shimura, T., Yasuda, T. and H. Mase (2013), Multi-model climate projections of ocean surface variables under different climate scenarios - future change of waves, sea level and wind, *Ocean Engineering*, Vol.71, pp.122-129, DOI: 10.1016/j.oceaneng.2013.02.016
9. Shimura, T., Mori, N., Nakajyo, S., Yasuda, T. and Mase, H. (2011), Extreme wave climate change projection at the end of 21st century, *Proc. of 6th Int. Conf. on Asian and Pacific Coasts (APAC 2011)*, pp.341-348.
10. Goda, Y. (2003), Revisiting Wilson's formulas for simplified wind-wave prediction, *J. Waterway, Port, Coastal, Ocean Eng.*, Vol.129, No.2, 93–95.

## 6. IMAGES

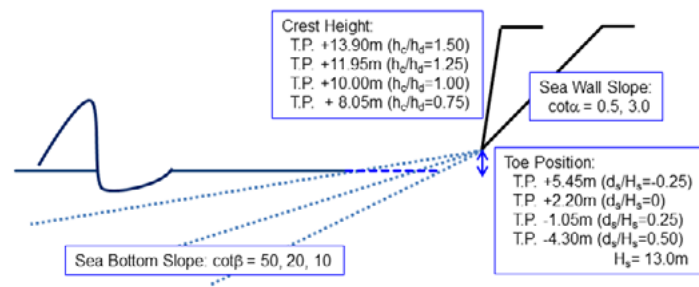


Fig. 1 Analyzed conditions of seawall and beach.

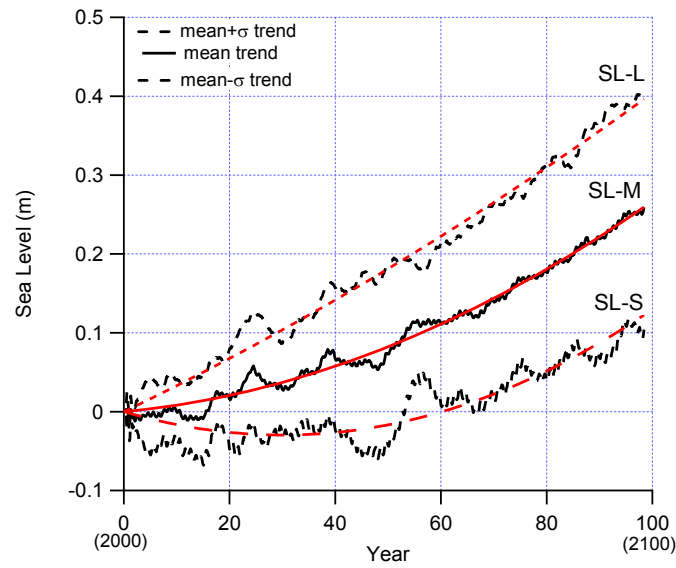


Fig. 2 Trend of sea level rise.

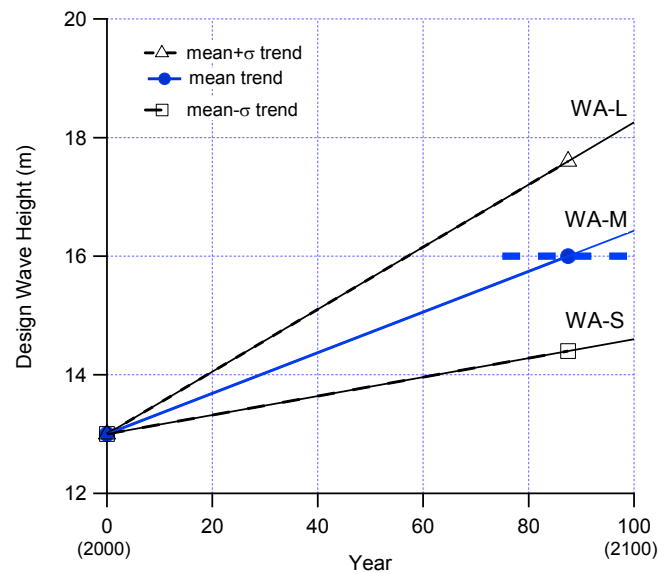


Fig. 3 Trend of wave height.

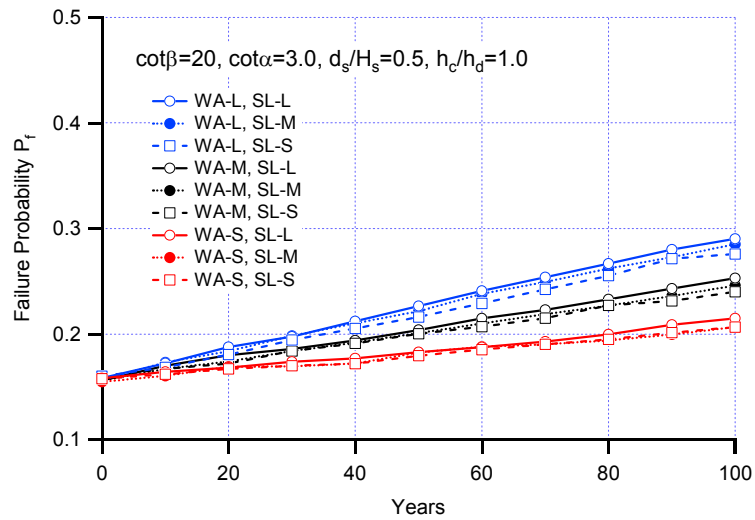


Fig. 4 Failure probability of gentle slope seawall built in sea.

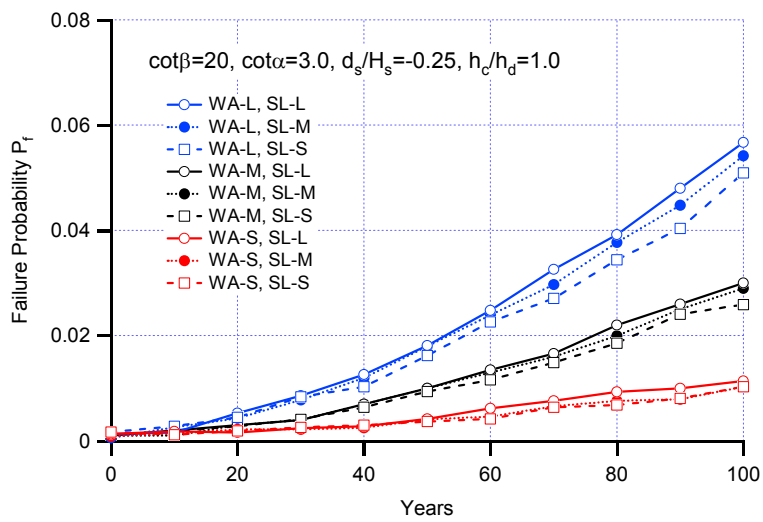


Fig. 5 Failure probability of gentle slope seawall built on land.

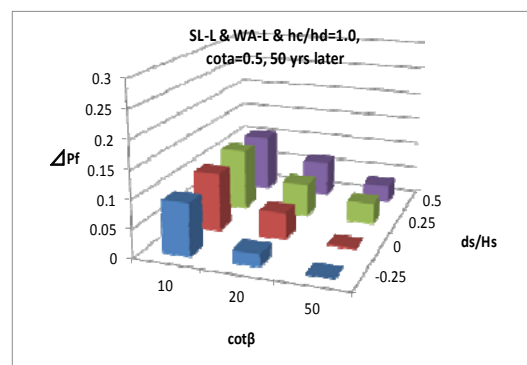


Fig. 6 Change of failure probability of steep seawall 50 years later for the present freeboard under the condition of large change of sea level rise and wave height.

## Variations in extreme values of precipitation for the next century in Central Campania

Rianna G.<sup>1\*</sup>, Guarino F.<sup>1</sup>, Mercogliano P.<sup>1,2</sup>, Cattaneo L.<sup>1</sup>, Vezzoli R.<sup>1</sup>  
Iodice L.<sup>3</sup>, Fariello L.<sup>3</sup>

<sup>1</sup> Centro Euro-Mediterraneo sui Cambiamenti Climatici (C.M.C.C.) - Capua (Italy),

<sup>2</sup> Centro Italiano Ricerche Aerospaziali (C.I.R.A.) – Capua (Italy)

<sup>3</sup> Autorità di Bacino della Campania Centrale, Napoli (Italy)

\*Corresponding Author: [guido.rianna@cmcc.it](mailto:guido.rianna@cmcc.it)

### Abstract

The Italian law 49/2010, implementing the EU Directive 2007/60/CE, states 3 steps:

- 1) identification of areas potentially affected by flooding events;
- 2) preparation of hazard maps;
- 3) elaboration of management plan for flood risk;

Moreover, this law specifically requires that the review of land use plans takes into account the effects of climate change on flood hazard. In addition, the Directive 2007/60/EC, estimating that climate change could likely induce several negative impacts, requests that the Commission reports to the European Parliament also about these ones (Article 16). To analyze and evaluate the potential effects of climate change (CC) for next century on extreme precipitations at subdaily-daily scale, typical triggers of flood events, the River Basin Authority for Central Campania and the Impact on Soil and Coasts Research division of CMCC started a collaboration whose main results are summarized in this contribution. It aims at analyzing:

- variations on seasonal scale for cumulative precipitation and mean temperature;
- performances of the climate model in reproducing the extreme values of precipitation on time scales ranging between 6 and 24 hours;
- expected changes in subdaily extreme values of precipitation on medium and long-term, under the IPCC RCP4.5 and RCP8.5 emission scenarios.

**Keywords:** regional climate simulations, flood hazard, extreme precipitation events, hydrological- geological hazard

## 1. INTRODUCTION

Climate changes (CC) could induce various effects on natural and anthropic environments, including changes in water cycles and river flows both in terms of mean values and especially, in terms of extreme values, inducing substantial variations in the occurrence of issues such as drought and floods [1].

During the last years, starting from United Nations Framework Convention on Climate Change - UNFCCC – (1992), the efforts to cope climate change effects have gradually grown up to be explicitly recalled within the national and EU directives, focusing on land protection and planning [2][3][4][5].

While the first actions were basically aimed to reduce pollutants emissions and to mitigate CC, subsequently a great effort has been devoted for devising/developing adaptation measures [6][7]. In particular, regarding Italian territory, due to its high vulnerability to hydrological and geological hazards, a proper assessment of the effects of climate change on such phenomena has become a crucial issue.

Although the most evident effects of climate change could be valued in “urban flooding” often also related to inadequate sewerage systems (usually designed for return periods equal to about 10-20 years), there are phenomena, probably less frequent, such as flash floods and hyperconcentrated flows, considered under the same term “flood” in the European Directive 2007/60/EC, that are more burdensome in terms of economic losses and casualties. For such phenomena, Italian Law 49/2010 has required that, to update the Risk Management Plans, an evaluation about the potentiality of CC to affect the geological and hydraulic hazard is carried out.

The National Law 152/2006, implementing the European Directive 2000/60/EC, has established the Authorities of River Basin District, but currently they are still in their formative stages: for this reason, the task of developing Risk Management Plans has been delegated, until now, to Basin Authorities established by previous law 183/1989.

To this aim, the tasks of Risk Management Plans concern the marking out of areas potentially affected by floods or the identification of suitable structural (e.g. embankments, detention basin, floodway) and not structural ( e.g. early warning systems) actions for mitigation of geological/hydraulic risk; however, until now, for

example, the sizing of artefacts (e.g., detention basins) followed the canonical approach based on the reference event characterized by a given return period (e.g. 20 years). Such approach appears suitable under steady state conditions while in transient conditions, such as those induced by CC, it may result in an overestimation (simply entailing increased costs) or, in the worst case, in an underestimation of volumes required to ensure the safeguard of the area.

In order to attempt to estimate how, in the next century, CC could affect rainfall patterns and then the potential risks of using steady state approaches for dimensioning mitigation works, the Basin Authority for Central Campania and Impact on Soil and Coasts Research Division of CMCC started a collaboration whose main first results are summarized in this work.

It represents a first endeavour to understand the performances of climate simulations on maximum values of sub daily rainfall (of major interest for flood events) and their estimated variations over the next century until 2100 for two different emission scenarios (i.e., IPCC RCP 4.5 and RCP 8.5) [8].

## **2. THE CLIMATE MODELING CHAIN**

The evaluation of the potential effects of CC on the precipitation pattern distribution of the Campania region over the 21<sup>st</sup> century is based on the following simulation approach: the output of a General Circulation Model (GCM) is dynamically downscaled through a Regional Climate Model (RCM) over a limited domain centred on the Italian area. More specifically, the GCM considered is CMCC-CM. It is a coupled atmosphere-ocean general circulation model developed at CMCC: the atmospheric model component is ECHAM5 [10] with a T159 horizontal resolution, while the global ocean component is OPA 8.2, in its ORCA2 global configuration, at horizontal resolution 2° x 2°. ORCA2 also includes the Louvain-La-Neuve (LIM) model for the dynamics and thermodynamics of sea-ice. In the present work, two different IPCC emission scenarios have been used to force CMCC-CM, namely RCP4.5 (medium level) and RCP8.5 (high level greenhouse gas emission). The current spatial resolution of CMCC-CM (about 80 km) is not able to capture the climate features and in particular the precipitation pattern, especially over the Italian area characterized by complex topography and coastline and the presence of

different climate regimes [11]. A more appropriate description of these features can be achieved through dynamical downscaling: the RCM considered in this work is COSMO-CLM [13][14], developed by the CLM Community ([www.clm-community.eu](http://www.clm-community.eu)), in which CMCC participates since 2008. The specific model configuration adopted, characterized by a spatial resolution of  $0.0715^\circ$  (about 8 km), has been optimized at CMCC[15].

### 3. CLIMATE NUMERICAL SIMULATIONS: VALIDATION AND PROJECTIONS

In order to assess the capabilities of the simulation chain above described to properly represent the present precipitation patterns and to characterize the model systematic errors (and then the uncertainties associated with the results) two RCM control simulations have been performed. Both simulations have been conducted over the time period 1979-2011, using a horizontal resolution of  $0.0715^\circ$  (about 8 km, time step 40 sec.): in the first one, initial and boundary conditions are provided by ERA-Interim Reanalysis [16] produced by ECMWF, in order to characterize the bias associated with the RCM; in the second one, initial and boundary conditions are provided by CMCC-CM. Comparison has been performed against different observations datasets: E-OBS [17], EURO4M-APGD (Alpine Precipitation Grid Dataset) [18] and high resolution observational datasets provided by regional Italian ARPAs (Italian Regional Agency for Environment Protection). Comparisons showed a good capability of the simulation chain to reproduce the climate over the period simulated for the different Italian subdomains considered [Fig. 1].

[Figure 1]

Figures 2 and 3 show the good capability of the model in reproducing the seasonal cycle of surface temperature and precipitation over the different considered areas, although precipitation is affected by a higher bias. More detailed analysis on the validation are reported in [19][20].

Successively, climate projections using the same simulation chain configuration, but forcing the global model according with IPCC RCP4.5 and RCP8.5 scenarios have been performed.

[Figure 2]

[Figure 3]

For what concerns the temperature, climate projections highlight a general warming expected in Italy at the end of 21<sup>st</sup> century [Fig. 4]; particularly evident for 2071-2100 time period under RCP 8.5 emission scenario when average values higher than 5°C are attained. In terms of precipitation values [Fig. 5], different variation patterns are estimated for wet and dry seasons. In the first case, in the North and Central Italy (on Tyrrhenian coast), an increase of cumulative values is assessed reaching +60% in the Alpine region under RCP 8.5 emission scenario while, in the Southern part and for insular areas, the decrease does not exceed 30%.

For dry seasons, a substantial decrease is detected; in particular, under RCP 8.5 emission scenario, on average, it is about equal to 50%.

More details on the results of the climate projections for Italian domain are reported in [21]. Figures and analysis performed in the present work have been obtained using CLIME, a special purpose GIS software integrated in ESRI ArcGIS Desktop 10.X, developed at CMCC (ISC Division) in order to easily evaluate multiple climate features and to study climate changes over specific geographical domains with their related effects on environment, including impacts on soil.

[Figure 4]

[Figure 5]

#### **4. CLIMATE SCENARIOS FOR MAXIMA AND CUMULATED PRECIPITATION OVER THE AUTHORITY OF THE CENTRAL BASIN OF CAMPANIA AREA**

Although the main issue of this research concerns the assessment of the possible changes in maximum values of sub-daily precipitation induced by climate change, it is interesting to set this analysis in a broader framework and previously investigate the variations of cumulated precipitation and average temperature at seasonal scale on the Basin of Central Campania domain for 21<sup>st</sup> century.

To this aim, only grid points entirely falling within the domain have been taken into account, avoiding any data interpolation. Furthermore, two time horizons are evaluated: short (2021-2050) and long (2071-2100) compared to the control period 1981-2010 under the two mentioned emission scenarios.

In Figure 6, seasonal cumulative precipitation anomalies are displayed (2021- 2050 vs 1981-2010 (a) and 2071- 2100 vs 1981-2010 (b)) under the emission scenario RCP 4.5; two different behaviours for dry (MAM-JJA) and wet (SON-DJF) seasons

are identifiable: in the first case, an overall reduction is estimated with values lower than 20% in spring and attaining more than 50% in summer; in the second case, in winter, the signal appears fluctuating with variations ranging between  $\pm 10\%$ , whereas in fall slight decreases (smaller than 10%) are recorded in the South-Eastern part of the domain where progressively increasing values (up to 30%) on the North-West are estimated for the 2071-2100 time span.

[Figure 6]

Such trends are also qualitatively confirmed by the simulation under the emission scenario RCP 8.5 [Fig.7].

[Figure 7]

In the dry period, estimated reductions in precipitation are characterized by remarkable homogeneity on the domain, reaching 40% on the short term (for both seasons) and 70% for the summer season on long term; in the wet period, however, in winter the slight decrease estimated on short-term is reversed, on the entire area, in the following time span with general precipitation increments higher than 20%; in autumn, the presence of two areas with opposite behaviour is confirmed: an area (South-East) characterized by a reduction in precipitation values (from about 10% for 2021-2050 to about 20% for the next period) and another (North-West) where, however, estimated increases are smaller than those estimated for the RCP 4.5 scenario.

In addition, in Table 1 the expected changes of seasonal mean temperature on the two time periods and the two emission scenarios are reported.

[Table 1]

Climate signals in terms of temperature appears unambiguous, providing an increase of temperature for all seasons which depends on the time horizon and on the "severity" of the emission scenario (up to more than 5° C, for the simulation performed under RCP 8.5 on the interval 2071-2100).

As regards the estimation of future evolutions of the maximum precipitation at sub daily scale for Italian peninsula, at our knowledge a limited number of researches has been carried out [22]. This is basically due to the current constraints of climate simulations and simultaneous lack of reliable datasets (for length and temporal resolution) adequate for the validation phase. Concerning the first aspect, nowadays, the usual spatial resolutions of climate models (also if dynamically downscaled

through RCMs) are not able to properly simulate some physical dynamics, such as convection and diurnal cycles significant for reproducing sub daily atmospheric pattern while they achieve satisfactory performances on daily scale [23][24]; for the same reason, their performances related to representation of extremes values are often significantly worse than those related to mean values [25][26].

In order to assess the ability of the adopted simulation to reproduce the extreme precipitation values on sub daily scale, for period 1981-2010, the annual maximum values reported in the Hydrological Yearbooks (until 2000) and data retrieved by Regional Civil Protection relating to all the stations including within the Basin Authority are used; since the climate simulation results are stored with a time step of 6 hours, only the three reference durations, 6, 12 and 24 hours, are considered.

A comparison between simulated values and observations, in terms of average values on the control period, returns a significant underestimation, slightly under 40% for maximum at 6 hours and slightly more than 30% for the 12 and 24 hours. However, from a detailed analysis of available observed series, for several weather stations, gaps even more than 60% are detected and thus it could partially affect the reliability of the estimated values. If the analysis is carried out by comparing, on the considered areas, the simulated values with data retrieved from meteorological stations (for which, 20 years of observations are available, at least ) the error, still relevant, drops to 33% on 6 hours and between 25 and 29% for 12 and 24 hours.

It is worth noting that a part of the underestimation is due to the temporal resolution of the maximum values available for the simulations equal to 6 hours (then with four values per day), while the maximum observed is computed on moving windows.

After assessing the magnitude of the simulation error, subsequent analyses are aimed to investigate two further issues:

- a) the significant error is, at least, characterized by time invariance;
- b) the climate simulation on the control period, excluding the error on the average value, is able to identify the pattern of spatial variation over the area.

Regarding a), although the current simulation error does not allow the use of the model results as absolute values, however, verifying on the control period that bias can be assumed as time invariant and so that the current constraints of the climate modelling affect the estimates in a comparable way, regardless of the investigated period, variations of the maximum values in sub-daily scale between future and control time period could be estimated, at least, in terms of percentage anomaly. In

this case, a first attempt to evaluate “bias time invariance” have been carried out estimating mean errors for the two subsets 1981-1995 and 1996-2010, and for sets formed by odd and even years; in both cases, the error does not undergo substantial variations, ranging between  $\pm 3\%$ .

Regarding b), in Figure 8 for maximum yearly values over 24 hours averaged on control period, a comparison is carried out between simulated (a) and observed (b) data produced as ratio between the local value and the average value over the entire area.

Thereby, values higher than 1 indicate an area in which maximum values are greater than the average value on the entire area, while the opposite occurs for values less than 1.

[Figure 8]

The model reproduces quite well the spatial patterns providing values greater than the average value in the internal and south-east part and lower values in the other parts of the domain; moreover, deviations from mean values are reproduced in an appropriate way (the same considerations apply also to the maximum values at higher temporal resolution, with slightly worst performances).

In Figure 9, projected anomalies for maximum sub daily precipitation values are shown, respectively for the emission scenario RCP 4.5 and RCP 8.5, comparing 2021-2050 vs 1981-2010; differences between the two scenarios seem very limited: for both and for all investigated time scales, two areas characterized by homogeneous behaviour are identified: an area in the north-west where mild to moderate increases in maximum values are estimated, a central area, extending from the inland areas up to the coastal areas, where, on the contrary, signal increases are not detected and with limited areas where a slight reduction (less than 10%) of the maximum values is simulated. A wider area characterized by null variations/weak decrease is estimated for RCP 8.5 scenario: it is limited in the southern part by a further inner area where, again, slight increases in the maximum values are simulated. In general terms, the climate signal is clearly assumed growing especially in the northern part of the domain, currently characterized by mean maximum precipitation values [Fig. 8] lower than the average values for the area.

[Figure 9]

In Figure 10, corresponding values for the period 2071-2100 are reported. The above identified positive anomalies (with increased magnitude) and spatial patterns of

variation persist for both emission scenarios. Concerning the magnitude of the changes, under the RCP 4.5 scenario, in the two areas previously identified as the most affected by increases, changes take comparable size (about 20% compared to the reference period), while for the emission scenario RCP 8.5, in the northern area evaluated changes, on average, could attain values about equal to +50% compared to the reference period.

[Figure 10]

In order to provide information about the frequencies of heavy rainfall events, Figure 11 reports, on seasonal scale, the relative frequency (in %) of the areal average rainfall (higher than 0.1 mm) on 6 hours for the control period and the thirty years ranging from 2071 to 2100 under emission scenarios RCP4.5 and RCP8.5; furthermore, "proportion dry" is indicated. According to the approach described in [27], precipitation values have been normalized with respect to the mean simulated value in the control period, in order to avoid taking into account absolute values affected by significant uncertainties.

Only relative frequency values higher than 0.05% are considered, while adopting a logarithmic scale allows a better view for intense events characterized by low probability of occurrence.

For both scenarios, in all seasons, an increase of proportion dry is estimated, with increases about equal to 10% for the spring season, and values up to 98% for the summer season in RCP 8.5; such result is physically consistent with the increase in estimated temperature [Tab.1] with subsequent increase in atmospheric water retention capacity; for the same reason, the expected increase is greater for the RCP 8.5 scenario characterized by a major increase in the "radiation" forcing and in atmospheric temperature. In the same way, similar considerations may, partly, explain the increase in frequency of the heaviest precipitation events, shifting the tail of the distribution for both scenarios compared to the control period. Similarly, for less intense events, (e.g. lower than the mean value of the control period), both scenarios return a reduction in frequency (such reductions are in part masked by the adoption of a logarithmic scale). Again, such assumption appears to be function of the severity of the considered emission scenario. Remarkable is the increase in the range of variability (increase of maximum values) and their weight (increase in the frequency of occurrence) during the autumn and summer season, while during wet season it is less evident.

[Figure 11]

## 5. CONCLUSIONS

The study represents a first attempt for the Italian territory to estimate the performances of the modelling chain implemented at CMCC (the global model CMCC-CM and the regional model COSMO-CLM) for the representation of the extreme values of precipitation on the scale from daily to 6 hours. After a quantification of the uncertainties related to the use of different climate numerical models, the possible future changes of such values under two climate change emission scenarios in the short and long term have been evaluated. Considering the current uncertainties in climate models previously reported, the results shown can be used, essentially, to understand what might be the "direction" and the "relative magnitude" of the expected changes in the distribution of the maximum values on the area where assumed emission scenarios prove to be consistent with the actual emissions pollutants, but, currently, they do not allow more quantitative estimates.

## 6. ACKNOWLEDGEMENTS

This paper has been developed within the framework of Work Package 6.2.17 of the GEMINA project, funded by the Italian Ministry of Education, University and Research and the Italian Ministry of Environment, Land and Sea. A particular acknowledgment to the Campania Civil Protection Department for providing their observational datasets.

## 7. REFERENCES

1. IPCC, 2012: *Managing the Risks of Extreme Events and Disasters to Advance Climate Change Adaptation*. A Special Report of Working Groups I and II of the Intergovernmental Panel on Climate Change [Field, C.B., V. Barros, T.F. Stocker, D. Qin, D.J. Dokken, K.L. Ebi, M.D. Mastrandrea, K.J. Mach, G.-K. Plattner, S.K. Allen, M. Tignor, and P.M. Midgley (eds.)]. Cambridge University Press, Cambridge, UK, and New York, NY, USA, 582 pp.
2. EC (2004), *Communication from the Commission to the European Parliament, the Council, the European Economic and Social Committee and*

*the Committee of the Regions on flood risk management — flood prevention, protection and mitigation”* (COM(2004) 472 final of 12 July 2004).

3. EEA (2010), *“Mapping the impacts of natural hazards and technological accidents in Europe”* – European Environment Agency (EEA), Report 13/2010, Office for Official Publications of the European Communities, Luxembourg.
4. EEA (2010), *“The European environment – state and outlook 2010: Synthesis”* – European Environment Agency (EEA), Report 1/2010, Office for Official Publications of the European Communities, Luxembourg.
5. EEA (2009), *“Report on good practice measures for climate change adaptation in river basin management plans”* – European Environment Agency (EEA), EEA/ADS/06/001 - Water, Office for Official Publications of the European Communities, Luxembourg.
6. European Commission (2009), *Adapting to Climate Change: Towards a European Framework for Action*. White Paper. COM(2009) 147 final. European Commission, 2009. <http://eur-lex.europa.eu/LexUriServ/LexUriServ.do?uri=COM:2009:0147:FIN:EN:PDF>
7. MATTM (Ministero dell’Ambiente e della Tutela del Territorio e del Mare) (2013), *Linee strategiche per l’adattamento ai cambiamenti climatici, la gestione sostenibile e la messa in sicurezza del territorio. Bozza di delibera del CIPE* (Draft documentation for the Inter-ministerial Committee for Economic Planning).  
  
(Ministry of Environment and Protection of Land and Sea (2013), *Strategic guidelines for adaptation to climate change, sustainable management and the safety of the area. draft CIPE resolution.*)
8. Moss, R. H., and Coauthors (2010), *The next generation of scenarios for climate change research and assessment* – Nature, 463, 747-756
9. Scoccimaro, E., S. Gualdi, A. Bellucci, A. Sanna, P. Fogli, E. Manzini, M. Vichi, P. Oddo, A. Navarra (2011), *Effects of Tropical Cyclones on Ocean Heat Transport in a High Resolution Coupled General Circulation Model* – Journal of Climate 24, 4368–4384.

10. Roeckner, E., G. Bauml, L. Bonaventura, R. Brokopf, M. Esch, M. Giorgetta, S. Hagemann, I. Kirckner, L. Kornblueh, E. Manzini, A. Rhodin, U. Schlese, U. Schulzweida, A. Tompkins (2003), *The atmospheric general circulation model ECHAM5. Part I: Model description* – Max-Planck-Institut für Meteorologie, Hamburg, Germany, Rep. No. 349.
11. Mariotti A. (2010), *Recent changes in Mediterranean water cycle: a pathway toward long-term regional hydroclimatic change?* – J of Climate, Vol. 23, No. 6.: 1513–1525. doi: 10.1175/2009JCLI3251.1
12. Feser, F., B. Rockel, H. von Storch, J. Winterfeldt, M. Zahn (2011), *Regional Climate Models Add Value to Global Model Data: A Review and Selected Examples*. Bull. Amer. Meteor. Soc., 92, 1181–1192. doi: <http://dx.doi.org/10.1175/2011BAMS3061.1>
13. Rockel, B., A. Will, A. Hense (2008), *The regional climate model cosmo-clm (cclm)* – Meteorologische Zeitschrift 17(4), 347–348.
14. Steppeler, J., G. Doms, U. Schättler, H. W. Bitzer, A. Gassmann, U. Damrath, and G. Gregoric (2003), *Meso-gamma scale forecasts using the nonhydrostatic model* - LM. Meteor. Atmos. Phys., 82, 75–96.
15. Montesarchio M., Mercogliano P. et al. (2012), *RP0143 - A sensitivity study with the RCM COSMO CLM over the north and center Italy* - CMCC Research paper
16. Dee, D. P., Uppala, S. M., Simmons, A. J., Berrisford, P., Poli, P., Kobayashi, S., Andrae, U., Balmaseda, M. A., Balsamo, G., Bauer, P., Bechtold, P., Beljaars, A. C. M., van de Berg, L., Bidlot, J., Bormann, N., Delsol, C., Dragani, R., Fuentes, M., Geer, A. J., Haimberger, L., Healy, S. B., Hersbach, H., Hólm, E. V., Isaksen, L., Kållberg, P., Köhler, M., Matricardi, M., McNally, A. P., Monge-Sanz, B. M., Morcrette, J.-J., Park, B.-K., Peubey, C., de Rosnay, P., Tavolato, C., Thépaut, J.-N. and Vitart, F. (2011), *The ERA-Interim reanalysis: configuration and performance of the data assimilation system*. Q.J.R. Meteorol. Soc., 137: 553–597. doi:10.1002/qj.828.
17. M. R. Haylock, N. Hofstra, A. M. G. Klein Tank, E. J. Klok, P. D. Jones, and M. New. (2008). *European daily high-resolution gridded dataset of surface*

- temperature and precipitation* – Journal of Geophysical Research, vol. 113, d20119, doi:10.1029/2008JD010201.
18. Isotta, F. A., Frei, C., Weilguni, V., Percec Tadic, M., Lassegues, P., Rudolf, B., Pavan, V., Cacciamani, C., Antolini, G., Ratto, S. M., Munari, M., Micheletti, S., Bonati, V., Lussana, C., Ronchi, C., Panettieri, E., Gianni, M. and Vertacnik, G., *The climate of daily precipitation in the Alps: development and analysis of a high-resolution grid dataset from pan-Alpine raingauge data*, Int. J. Climatol., 34, 1657–1675, doi:10.1002/joc.3794, 2013.
19. Zollo A.L., Montesarchio M. et al. (2012), *RP0145 - Assessment of COSMOCLM performances in simulating the past climate of Italy* - CMCC Research Paper available on <http://www.cmcc.it/it/publications/rp0145-assessment-of-cosmoclm-performances-in-simulating-the-past-climate-of-italy>
20. Bucchignani E., Mercogliano P., Manzi M.P., Montesarchio M., Rillo V., (2013): *RP0183 - Assessment of ERA-Interim driven simulation over Italy with COSMO-CLM* – CMCC Research Paper
21. Bucchignani E., Mercogliano P., Montesarchio M., Manzi M.P., Zollo A.L. - *Performance evaluation of COSMO-CLM over Italy and climate projections for the XXI century - 2013, Climate change and its implications on ecosystem and society: Proceedings of I SISC (Società Italiana di Scienze del Clima) Conference; Lecce, 23-24 settembre 2013:78-89 ISBN 978 – 88 – 97666 – 08 – 0*
22. Lionello P. et alia (2010) *Eventi climatici estremi: tendenze attuali e clima futuro sull'Italia in "I cambiamenti climatici in Italia: evidenze, vulnerabilità e impatti"* a cura di S.Castellari e V.Artale Bononia University Press
23. Maraun, D., et al. (2010), *Precipitation downscaling under climate change: Recent developments to bridge the gap between dynamical models and the end user* – Rev. Geophys., 48, RG3003, doi:10.1029/2009RG000314.
24. Fowler, H. J., Blenkinsop, S. and Tebaldi, C. (2007), *Linking climate change modelling to impacts studies: recent advances in downscaling techniques for hydrological modelling*. – Int. J. Climatol., 27: 1547–1578. doi: 10.1002/joc.1556

25. Christensen, J. H., F. Boberg, O. B. Christensen, and P. Lucas-Picher (2008), *On the need for bias correction of regional climate change projections of temperature and precipitation* – Geophys. Res. Lett., 35, L20709, doi:10.1029/2008GL035694.
26. Maurer, E. P., Das, T., and Cayan, D. R.: *Errors in climate model daily precipitation and temperature output: time invariance and implications for bias correction*, Hydrol. Earth Syst. Sci., 17, 2147-2159, doi:10.5194/hess-17-2147-2013, 2013
27. Coppola, E. and Giorgi, F. (2010), *An assessment of temperature and precipitation change projections over Italy from recent global and regional climate model simulations.* – Int. J. Climatol., 30: 11–32. doi: 10.1002/joc.1867

## 8. IMAGES AND TABLES

	DJF	MAM	JJA	SON
RCP4.5_2021-2050	1.4	1.5	1.8	1.8
RCP8.5_2021-2050	2.1	1.8	1.9	2.1
RCP4.5_2071-2100	2.8	2.9	3.5	3.5
RCP8.5_2071-2100	5.1	4.7	6.3	5.4

Tab. 1 Expected changes (in ° C) of the average seasonal temperature for domain of the Basin of Central Campania for 2 time windows 2021-2050 and 2071-2100 for two different emission scenarios compared to the control period.



Fig. 1 Representation of the 3 sub-domain considered.

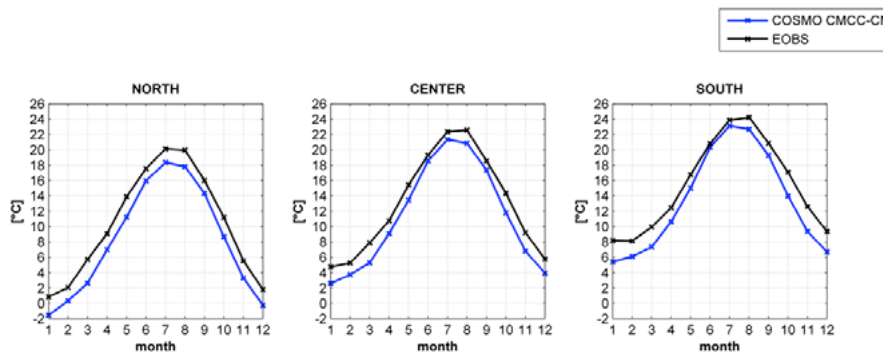


Fig. 2 seasonal cycle of the surface temperature for the three sub-areas shown in the Fig. 1.

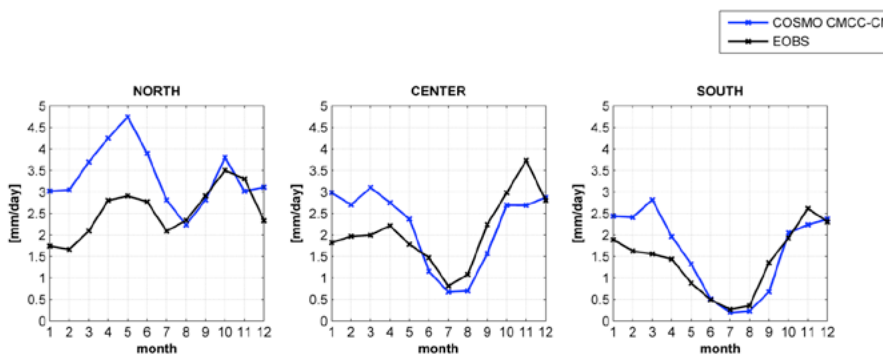


Fig. 3 seasonal cycle of the precipitation for the three sub-areas shown in the Fig. 1.

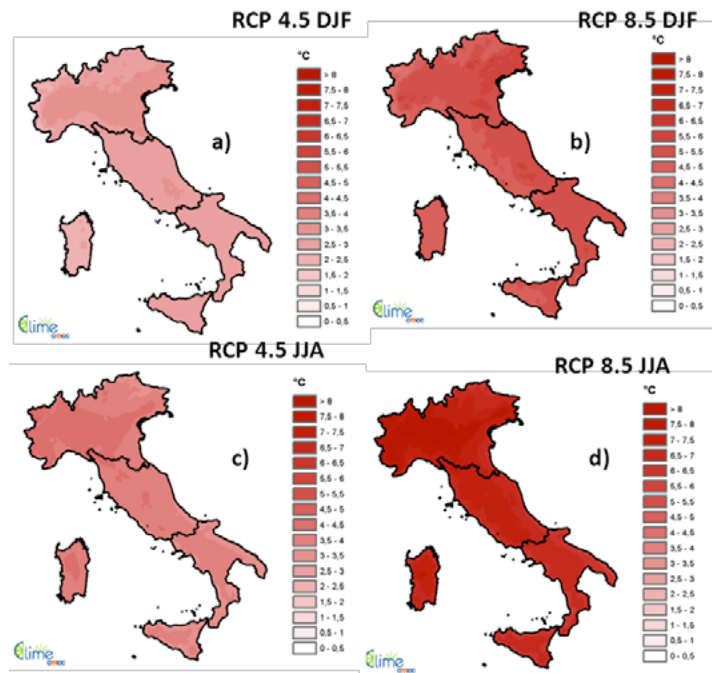


Fig. 4 Two-meter temperature (°C) climate projections for both scenarios: seasonal differences (December-January- February (DJF) [a-b] and June-July-August (JJA) [c-d]) between the average value over 2071-2100 and 1981-2010.

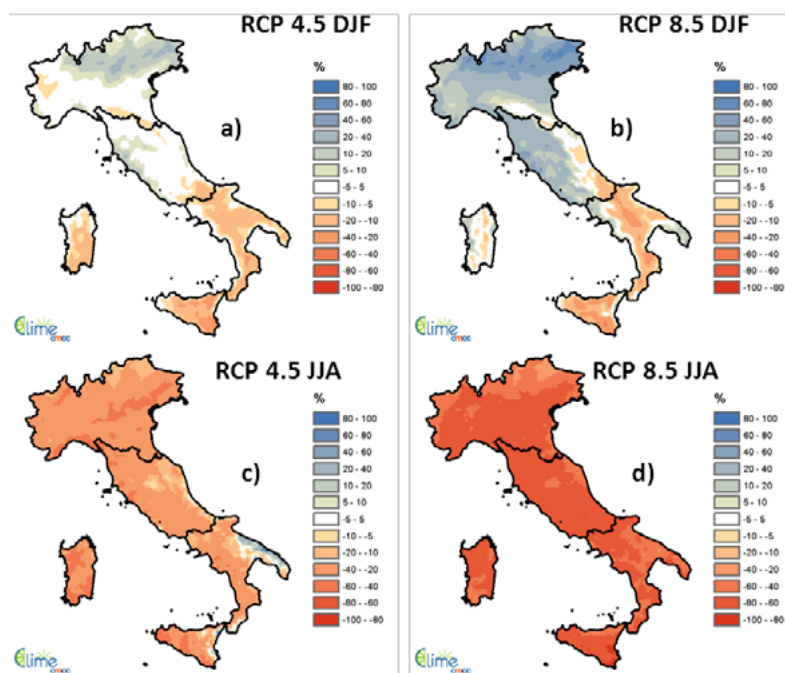


Fig. 5 Anomalies of seasonal cumulative precipitation (%) between the average value over 2071-2100 and 1971-2000 under RCP 4.5 and RCP 8.5 emission scenarios; a-b: December-January-February DJF; c-d: June-July-August JJA.

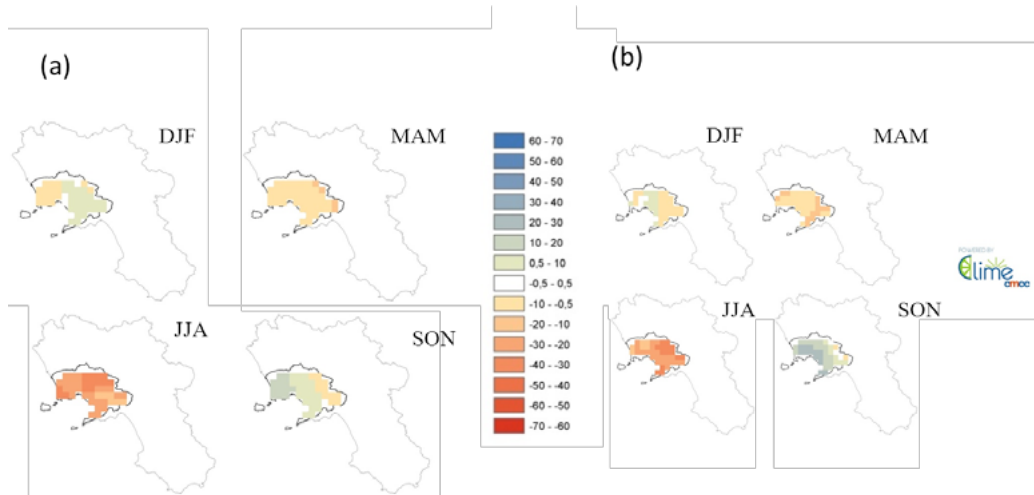


Fig. 6 Anomaly ( $\alpha$ , in %) of cumulative seasonal precipitation for the climate simulation (CMCC\_CM +CCLM), under the emission scenario RCP 4.5 for time intervals 2021-2050 (a) and 2071- 2100 (b) vs 1981-2010.

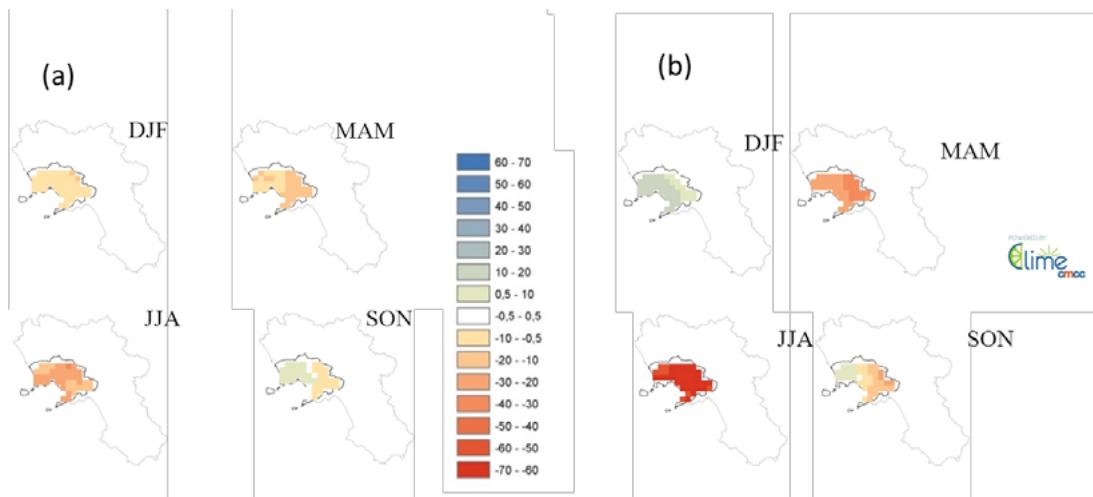


Fig. 7 Anomaly ( $\alpha$ , in %) of cumulative seasonal precipitation for the climate simulation (CMCC\_CM +CCLM), under the emission scenario RCP 8.5 for time intervals 2021-2050 (a) and 2071- 2100 (b) vs 1981-2010.

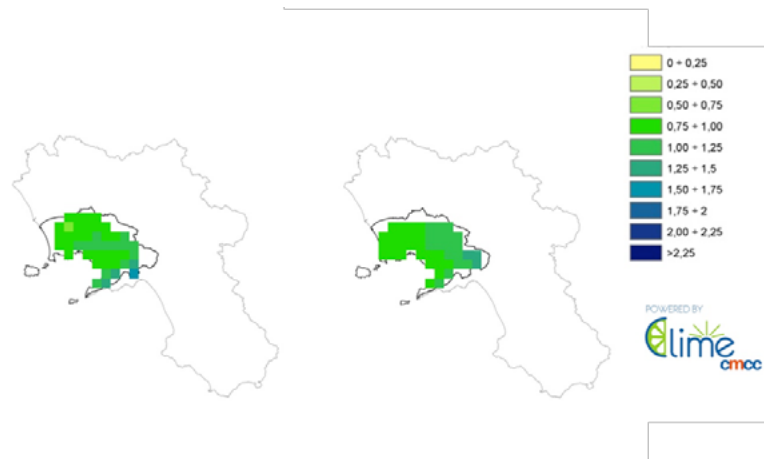


Fig. 8 Comparison of the ratio between local values and mean value for the entire area for observed data (a) and the climate simulation CMCC-CM+CCLM (b) related to averaged values of maximum rainfall over 24 h on control period.

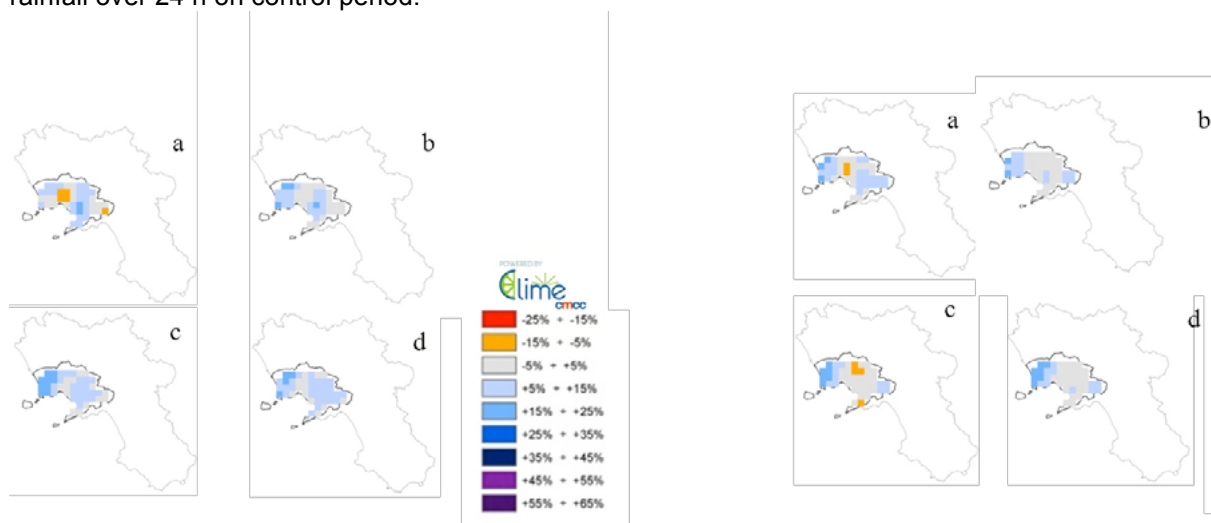


Fig. 9 Anomalies (in %) of the maximum values of precipitation at 6h (a), 12h (b), 24h (c) and daily scale (d) between 2021- 2050 and the reference period 1981-2010 for the climate simulation forced by the emission scenario RCP 4.5. (on the left) and RCP 8.5 (on the right)

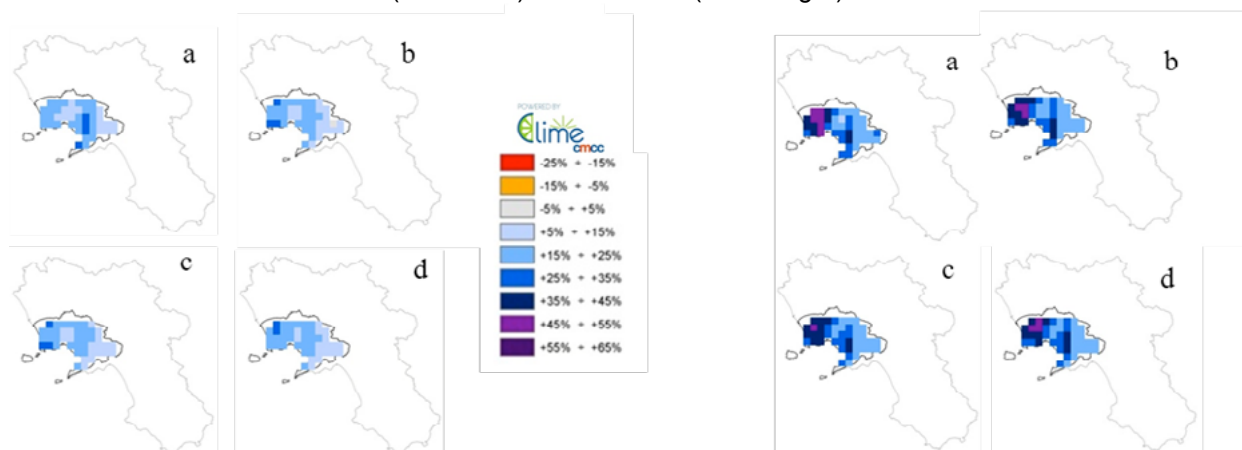


Fig. 10 Anomalies (in %) of the maximum values of precipitation at 6h (a), 12h (b), 24h (c) and daily scale (d) between 2071- 2100 and the reference period 1981- 2010 for the climate simulation forced by the emission scenario RCP 4.5. (on the left) and RCP 8.5 (on the right).

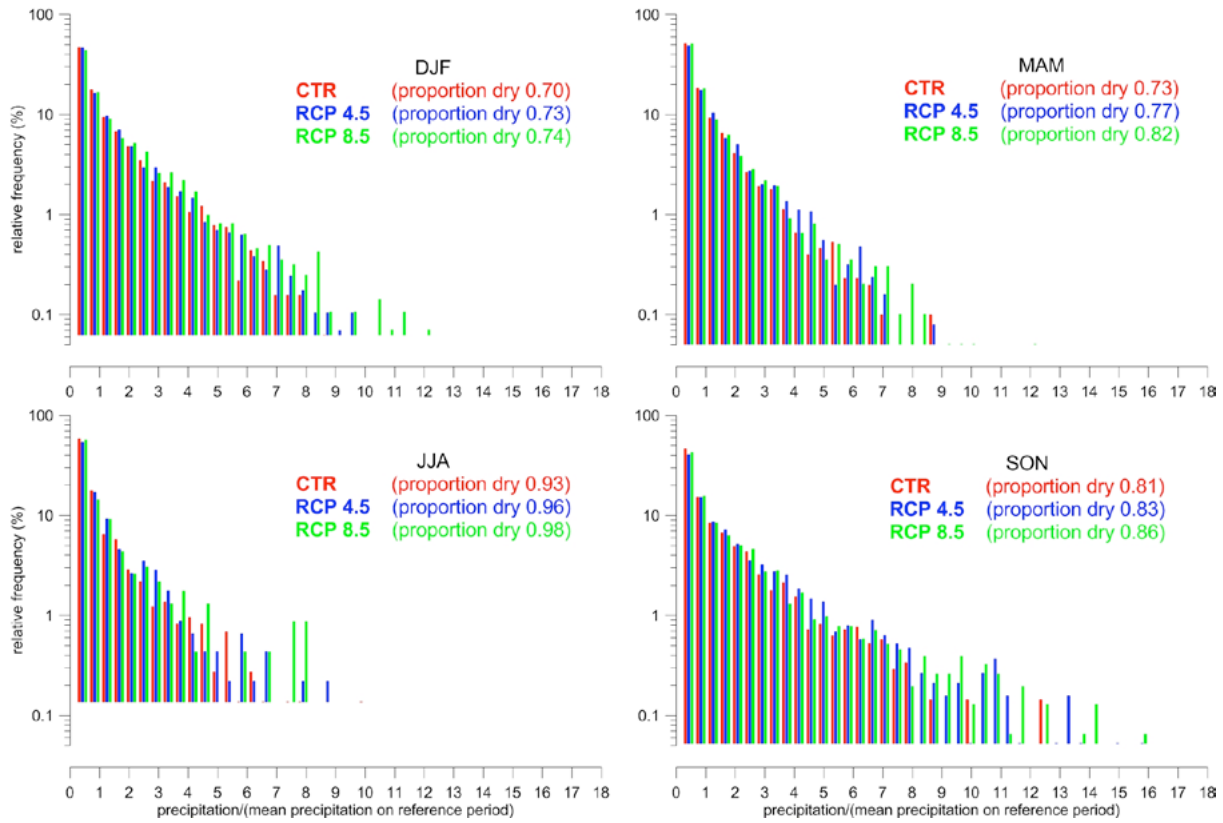


Fig. 11 Relative frequency (in %) of the average areal rainfall on 6 hours on seasonal scale, for control period (CTR) and 2071-2100 under climate scenarios RCP4.5 and RCP8.5, the probability of no precipitation for each simulation is indicated by the "proportion dry" and reported in the legend.

## **Climate Change Impacts on the flow regime of snow-dominated rivers: case study in Lebanon**

**Portoghese I.<sup>1\*</sup>, Vurro M.<sup>1</sup> Khadra R.<sup>2</sup>, Darwish T.<sup>3</sup> and Shaban A.<sup>3</sup>**

<sup>1</sup> Istituto di Ricerca sulle Acque del Consiglio Nazionale delle Ricerche, IRSA-CNR, Bari - Italy

<sup>2</sup> CIHEAM, IAM-Bari, Valenzano (BA) - Italy, and

<sup>3</sup> National Council for Scientific Research, Remote Sensing Center, Beirut - Lebanon

\*Corresponding Author: [ivan.portoghese@cnr.it](mailto:ivan.portoghese@cnr.it)

### **Abstract**

The objective of this study is to develop basin scale climate change scenarios (CCS) for a coastal watershed in Lebanon, named Nahr Ibrahim (NIW), which is representative of the snow-melt dominated area of Mount Lebanon. To this end the regional climate model PRECIS developed by Hadley Centre of U.K. was adopted as a dynamic downscaling of a global climate model (GCM) at a resolution of about 25x25 km. Daily simulations for precipitation (P), maximum and minimum temperature (Tmax, Tmin) were adopted to evaluate the impact of climate change on the water balance of the NIW in order to assess the possible future variation in water availability. To simulate the impacts on stream flow regimes, basin scale CCS were coupled with a conceptual water balance model named NIWaB that was previously developed and calibrated. Simulations allowed to assess the hydrological signature of NIW which resulted strongly influenced by a shorter snowy period and a consequent enhanced seasonality of the river flows. The results may be helpful in assessing the opportunity of a new artificial reservoir as a strategy for climate change adaptation by enabling the storage of winter and spring flows as well as the regulation of flood peaks.

**Keywords:** climate change impacts, water balance modelling, Mediterranean water resources

## 1. INTRODUCTION

Calculating water balance and diagnosing the hydrologic elements in Lebanon are still undefined due to the lack of complete series of records whether for meteorological or hydrological data. This compels applying modeling approaches in order to investigate the current status of water resources through the use of specific tools for water resources management. To this end it is necessary to implement adequate modelling approaches that allow to manage limitations in data and the complexity of hydrological processes involved due to the climatic, topographic and hydrogeological features. This trade-off between data availability and representation of physical processes is seldom available in the scientific literature, especially for case studies focusing on the Middle East region.

In the view of the changing climatic conditions the assessment of possible scenarios of future water availability and water quality is absolutely crucial for designing feasible adaptation strategies for water management in the Mediterranean region [1], [2] (Portoghese et al. 2013; Vurro et al. 2013). For the Lebanese country in particular, GCM simulations indicate higher future temperatures that will increase evapotranspiration and changes in climate patterns that might reduce rainfall [3], [4], [5], [6] (IPCC, 1996; IPCC, 1999; IPCC, 2007; Ragab and Prudhomme, 2002). Focusing on the Lebanese case study, Bou-Zeid and El-Fadel [7] adopted simulations from several GCMs to run the monthly water balance model WATBAL [8] (Star, 1999) and assessed several indicators of climate change impacts, including actual evapotranspiration, surplus, soil moisture deficit, and evapotranspiration deficit. Although limited to a couple of climate stations in the country, their compound climate scenarios adopted to develop monthly soil water balance projections provided a quantitative assessment of the likely alterations to the agricultural water needs for Lebanon and the possible adaptation measures for the water sector.

A daily water balance approach to assess climate change impacts was adopted by Hreiche et al. [9] using the MEDOR model coupled with a stochastic model of daily precipitation and temperature to generate synthetic climate scenarios. A sensitivity analysis of the stochastic model parameters on the discharge simulations was then performed and complemented with a +2°C increase in the mean temperature as a complete assessment of the potential impacts of a virtual set of climate change scenarios. The results were presented for a typical coastal watershed in Lebanon

and highlighted the impacts on the discharge regimes due to likely alterations in the snow processes.

Both reported studies are therefore based on simplified climate scenarios without considering the recent advancements of climate simulation models in describing the space-time dynamics of climate under transient emission scenarios and non-stationary conditions. Since the first high-resolution Regional Climate Model (RCM) simulations from the PRECIS system [10] (Jones et al. 2004) became available for Lebanon [11] (ELARD, 2010), a more detailed representation of the regional climate responses based realistic description of surface topography can be adopted to investigate the impacts of climate scenarios on water resources under ordinary and extreme weather conditions. Starting from the predicted precipitation decrease (-24% and -31% by midcentury and by the end of the century respectively), a significant study investigating the effects of climate change on the water resources of the eastern Mediterranean and Middle East region was presented by Chenoweth et al. [12], though with a coarse representation of the hydrology process linking precipitation to river discharge and renewable water resources of the considered countries.

In the present work we present a basin-scale synthesis of these two approaches to the assessment of climate change impacts on water resources. A semi-distributed daily conceptual water balance model is presented with particular emphasis on the snow module, the soil water balance module and groundwater storage-discharge mechanism. The model named NIWaB was developed in the Nahr Ibrahim watershed (NIW), which is situated along the Western Lebanese mountain chains [Fig. 1], and validated using discharge records and snow cover retrievals from remote sensing. The model was then forced using the PRECIS high-resolution climate simulations for the near future and the distant future.

## 2. MATERIALS AND METHODS

Lebanon, along the Eastern Mediterranean Basin, was described as the "water tower" of the Middle East, since it is characterized by several water resources both on surface and subsurface. An average precipitation of about 1000 mm/yr -with snow covering almost more than 20% of its territory - feeds 12 permanent watercourses, a

large number of springs, as well as a number of aquifers and subsurface water conduits [13]. However, the current situation does not reflect this demonstration on the existing water resources. Water shortage events occur and the inhabitants are often accusing water supply problems. This is attributed to the mismanagement in the water sector as a result of lacking in data availability and measuring instrumentations, which are required to evaluate the status quo on water resources.

One of the most representative coastal rivers in Lebanon is the NIW which flows from the 2,600 m heights of Mount Lebanon to the Mediterranean sea. NIW has a surface area of 325 km<sup>2</sup> and is characterized by one of the highest water discharge from the Lebanese rivers (~450million m<sup>3</sup>/year). The snowmelt contributes up to about half the total yearly discharge [11]. Most snowmelt water infiltrates the limestone plateau whose groundwater discharges at several springs, some of which are fed through a dense network of geological faults and lineaments extending far behind the boundaries of the NIW towards the Bekaa valley [13]. The major existing springs in NIW, the Afqa (1,200 m) and Roueiss (1,265 m) springs, are of karstic type and are characterized by abrupt seasonal changes in discharge rate [Fig. 2]. In the NIW, discharge measurement data exist at the two main spring as well as at the catchment outlet. Daily hydrological data for Afqa, Roueiss and sea outlet are available since 1967 though with lots of missing periods. Daily precipitation and temperature data exist at Qartaba station (1,150 m), located within the NIW, for the period 1965–2011 but with highly discontinuous records.

The period adopted for the development of continuous water balance simulations is limited to 11 years from 2001 to 2011 according to the concurrent and continuous daily records of snow area, discharge at the three gauge stations and at the Qartaba climate station. Other 17 climate stations surrounding the NIW are used to calibrate the linear regression between monthly temperature and precipitation with elevation. The resulting monthly gradients are then used to estimate basin scale temperature and precipitation maps [Fig. 3].

The NIWaB model allows to compute the water balance components at the daily scale. It has a semi distribute structure in which the elementary units are defined - for each of the 3 sub-basins corresponding to discharge gauge stations - according to the elevation zones mapped from the corresponding contour lines of the digital

elevation model. The NIW is divided into 26 elevation zones from 0 to 2,600 m a.s.l. and 69 elementary units with an average area of 4.5 km<sup>2</sup>.

As for the MEDOR model [14], the NIWaB is made up of three main parts: the snow cover module, the water yield module and the water transfer module. Each of these modules are daily integrated providing a semi-distributed output in mm for the considered variables while the discharge for the considered sub-basins is yielded in m<sup>3</sup>/s.

The snow cover module is actually composed of three routines: a spatialization routine for daily temperature, one for daily precipitation, and the snow cover and snowmelt module. In fact, given the high elevation gradients of mountain basin ranging from the sea level to 2,600 m and the presence of only one climate station (Qartaba) at the elevation of 1,150 m, the extrapolation of measured data to the whole NIW is necessary step. The extrapolation is based on linear gradients that were previously estimated using monthly mean values of 17 climate stations in the surrounding Mount Lebanon region [15]. Both rainfall and temperature fields are used in the snow module to reproduce the space-time variability of the snow accumulation and melting processes.

The type of precipitation (rainfall and snow) is determined in the module by a temperature threshold: when air temperature is lower than T<sub>0</sub>, precipitation turns into snow. When this temperature is higher than T<sub>1</sub>, snow starts to melt. T<sub>0</sub> and T<sub>1</sub> are estimated at 3°C and 0°C respectively. Between 0°C and 3°C, the two mechanisms are simultaneous and the snow cover evolves differently according to the intensity of precipitation and snowmelt. Local temperatures at the different elevation of the elementary units representing the basin are estimated using climatic gauging stations with a constant gradient of temperature with elevation. Snow daily accounting is made in mm of snow water equivalent (SWE).

The snowmelt mechanism is simulated using a simplified conceptual energy balance approach. The intensity of snowmelt is determined according to the snowmelt-runoff-model (SRM) [16] by the equation of the degree-day model:

$$h = \delta T \quad (1)$$

in which h is daily melt rate (mm/day) in SWE, and  $\delta$  is the degree-day coefficient (DDC) that was calibrated by Hreiche et al. [17] using local observations ( $\delta = 8$

mm/day/°C). The volume of snow as SWE is daily simulated for all elementary units of the NIW. With each time step, the theory of the degree-day applied to the snow-covered surface, allows to calculate the loss of snow volume that is available as liquid water for the hydrological processes at the basin scale. At the basin scale the snow-covered surface and the snowpack volume can be determined as an output of the snow cover module.

The water yield module allows to compute for each elementary unit of the basin the daily water stock that infiltrates as groundwater recharge or becomes available as direct runoff. Input to this module is the daily snowmelt summed to the daily rainfall. This module is composed of a potential evapotranspiration routine using the Hamon temperature-based equation and a soil water balance routine to evaluate actual evapotranspiration, soil water content and soil saturation excess that is the water yield. The actual evapotranspiration depends on the soil water content according to a widely used linear water stress function. The only parameter needed is spatially-averaged soil water holding capacity. In the performed water balance simulation this parameter is set equal to 100 mm for all elementary units. This module is quite different from the analogous developed in the MEDOR model which is based on a conceptual basin scale reservoir with characteristic capacity set by calibration of the observed annual discharge.

The water transfer module is designed to reproduce the storage-discharge processes involving the groundwater system discharging into the main springs and the river bed and is fed by the water yield module. Considering that the groundwater recharge area that contributes to the discharge of the major springs is larger than the watershed divide, an increased recharge area is evaluated by calibration of the annual water yield with the annual spring discharge. The effective areas for the Afqa and the Roueiss springs are therefore calibration parameters  $A_{adj}$ .

The transfer module is actually composed of two conceptual reservoirs having linear exits: one produces the fast drainage and the other the slow drainage. The area-adjusted water yield is then summarized by each sub-basin and divided between the two reservoirs, with the proportion being controlled by a calibrated coefficient  $R$ . For the two linear reservoirs the streamflow discharge for each sub-basin is the sum of the two exits  $Q_f$  and  $Q_s$ . The time constant of the two linear reservoirs,  $T_f$  and  $T_s$ , are one day for fast drainage while the other constant is fixed by calibration with the

observed discharge recession periods. In the corresponding eq. 2 and eq. 3, the daily water yield at the sub-basin scale  $Y(t)$  is put as inflow to the groundwater reservoir with volume  $V$ .

$$Q_f(t) = R Y(t) \quad (2)$$

$$Q_s(t) = [V(t-1) + (1-R) Y(t)] (1/T_s) \quad (3)$$

The overall parametric dimension of the NIWaB model is not minimal [Tab. 1] but the calibration of most of them is quite simple when a representative discharge record is available.

The model is implemented in Excel where all the modules described above are included in separate but interconnected spreadsheets. This structure allows for a simple and intuitive approach to the water balance modelling including an easy input of the climate forcing, post-process and graphical representation of results. Moreover, different model parameter setting can be explored and the corresponding results saved for efficient model calibration and sensitivity analysis. An example output from the NIWaB model is reported in Fig. 4.

To validate the NIWaB model both snow and discharge data were used. The MODIS-Terra snow product MOD10A2 was adopted to derive a daily retrieval for the same period [18]. Thanks to the available MODIS-derived snow area for the NIW it was possible to validate the simulated snow cover and to confirm the best fit for the DDC value of  $8\text{mm/day}/^\circ\text{C}$ .

The analysis is reported in Fig. 5 using the snow cover duration curves (SCDC) which were found a useful indicator of the space-time variability regime of the snow cover. This statistical plot was taken from the hydrological testing where the flow-duration curves (FDC) are often used to characterize the frequency of discharge values for a river cross section. The FDC plot is a cumulative curve that shows the percent of time specified discharges were equalled or exceeded during a given period. It combines in one curve the flow characteristics of a stream throughout the range of discharge, without regard to the sequence of occurrence. If the period upon which the curve is based represents the long-term flow of a stream, the curve may be used to predict the distribution of future flows for waterpower, water-supply, and pollution studies. Seeking for a practical tool to investigate the snow cover regime for

the NI watershed, the SCDC plot was adopted to validate the DDC value that provided the best fit to the MODIS snow cover data.

It is worth to remind that the snow simulation produced by the NIWaB model is the result of a precipitation dataset that was extrapolated to the entire basin using one single climate station roughly located at the centre of the basin. Nevertheless the good fit of the SCDC [Tab. 2] proves the credibility of the space-time dynamic of the snow cover that is a prerequisite for investigating the hydrological regime of snow-dominated catchments.

The validation of using daily discharge simulations and the corresponding observations was possible only for the period between November 2003 and December 2011 due to some not-recorded periods between 2001 and 2003 [Tab. 3].

The model was therefore calibrated trying to minimize the bias in the mean daily discharge and its standard deviation though accepting a certain mismatch in the frequency distribution of values. The parameters that were found more sensible to the daily discharge volume was clearly the area adjusting factor Aadj. The calibrated model was adopted to investigate the impact of climate change on the hydrological response of the NIW by forcing the water balance model with the output of the PRECIS model.

### **3. ASSESSMENT OF CLIMATE CHANGE IMPACTS ON THE HYDROLOGICAL RESPONSE OF THE NIW**

The PRECIS (Providing REgional Climates for Impacts Studies) regional climate model, developed at the Hadley Centre and based on the HadCM3 GCM, was applied in a 25 km x 25 km horizontal resolution whereby Eastern Mediterranean and Lebanon particularly are at the centre of the model domain, ensuring an optimal dynamical downscaling [11]. PRECIS is a version of the Hadley Centre's RCM HadRM3P, which is based upon the atmospheric component of the coupled atmosphere-ocean global climate model HadCM3. PRECIS simulates dynamical flow and the atmospheric sulphur cycle and includes physical parameterizations for clouds and precipitation, radiative processes, the land surface, and deep soil [10].

The driving emissions scenario adopted is A1B, assuming a world with rapid economic growth, a global population that reaches 9 billion in 2050 and then

gradually declines, and a quick spread of new and efficient technologies with a balanced emphasis on all energy sources. PRECIS was integrated from 1980 throughout the end of the 21st century and the periods considered for the present impact study are the recent past from 1980 to 2000, the present from 2001-2011, the near future from 2012 to 2032 (NF), and the distant future from 2080 to 2098 (DF).

The methodology for the assessment of potential changes in the hydrological response is based on the analysis of changes in the hydrological variables from the control simulation period corresponding to the recent past. The key meteorological variables adopted from the model's output, maximum temperature (Tmax), minimum temperature (Tmin), and precipitation (P) were evaluated using measurements of the Lebanon Meteorological Service [11] showing a good reliability of the climate model particularly for temperature.

PRECIS climate simulations for Lebanon are produced for 19 discrete grid nodes each with an average elevation estimated from the digital elevation model. For the NIW, the most representative grid node is the node D2 with an average elevation of 1,368 m which is close to the average basin elevation (1,650 m).

The adopted scenarios show a general decrease of precipitation compared to the RP for winter and spring that seems less evident for the NF than for the DF scenario [Fig. 6a]. In this latter case, in fact, precipitation is much lower than in the RP with an annual decrease of 39%. Temperature scenarios is even more unambiguous with the increase on mean annual temperature of +1.2°C in the NF and +5.90°C in the DF. The temperature scenario will be particularly impacting on the snow processes: snow cover is likely to reduce as the snow fall season (December to March) is expected to become warmer both in the NF and DF scenarios; at the same time, the start of the snowmelt season may be anticipated in February [Fig. 6b].

The results of the impact study on the NIW are presented here with specific focus on the snow and the discharge alterations. The adopted method is the relative comparison with the baseline scenario produced by coupling the PRECIS simulation for the RP (1980-2000) with the NIWaB model. To do so the PRECIS simulation for the D2 grid node is used as climate forcing therefore the simulated temperature and precipitation have been extrapolated to the entire basin using the linear regression estimated with the adopted climate record at Qartaba station.

Snow alteration in NF and DF scenarios are quite evident from the performed model experiments [Fig. 7]. Assuming daily SWE as a good indicator of the snow processes having a strong influence on the river and springs discharge regimes, the comparison between the corresponding duration curves clearly show the quantitative impact of climate alteration in the snowmelt dominated discharge. The SWE is expected to decrease moving from the NF to the DF scenarios as somehow anticipated in the previous section. By the end of the Century the annual season with active snow processes is likely to half from slightly less than 40% of the year (~140 days) to slightly less than 20% (~70 days).

A marked decrease in the discharge is therefore expected if the predicted alteration in the snow processes are confirmed. Looking at the annual discharge volumes at the sea mouth station in the NIW (Fig. 8). According to the coupled simulation of the PRECIS climate scenario with the water balance model NIWaB, the mean annual discharge with respect to the RP mean of 374 Mm<sup>3</sup> is predicted to increase slightly in the NF to 381 Mm<sup>3</sup> (+2%) while it would dramatically drop in the DF to 231 Mm<sup>3</sup> (-39%). This quantitative decrease in the basin scale water availability is of course relative to the baseline climate simulated by the PRECIS (1980-2000) and therefore cannot be considered as a prediction. Nevertheless, it is important to note that both the discharge observations (2001-2011) and the water balance simulation using the observed climate record (2003-2011) have similar annual patterns compared to the water balance simulations adopting the PRECIS climate forcing [Fig. 8].

The hydrological impact of the adopted climate scenario is also represented in terms of discharge regimes using the monthly mean values (Fig. 9). Also in this case, the expected changes in the monthly mean are compared with reference baseline. For the NF the monthly values highlight a general increase in the rainfall dominated discharge between November and January and a decrease in the snowmelt dominated discharge in April. In other words, the increase in winter temperature is responsible for a decrease in the SWE volume and its seasonal permanence in the upper basin. In the DF, this alteration in the snow process is magnified, besides a general decrease in the monthly precipitation throughout the year. The discharge between December and January is expected to increase as an effect of the reduction of snow covered areas. Moreover the month of peak discharge is anticipated to February and consequently the delay between the peak precipitation in winter and

the peak discharge in spring is minimized with the maximum of water availability in the low water-demand season with potential flood risks.

Besides giving useful information on the possible alteration of the dominant hydrological processes, this analysis can be assumed as an indirect validation of the entire modelling chain adopted. It is in fact significant that the water balance simulation adopting the climate forcing from PRECIS for the same period as that of the discharge observations shows a good fit with most of the year except for late spring and summer.

#### **4. DISCUSSION AND CONCLUSIONS**

A semi-distributed conceptual water balance model is presented here with specific capability to deal with highly dynamic snow cover that is typical of the coastal mountain chains in the Mediterranean environment. A module of the model is therefore developed to capture the space-time dynamics of the snow cover and snowmelt contribution to the daily river discharge. The model called NIWaB is a compromise between a credible representation of the basic hydrological processes involving groundwater-surface water interaction and model simplicity and usability. NIWaB has a user-friendly interface and is developed for instructive purposes of the bi-lateral research team involved.

The model is implemented in a coastal watershed of Lebanon using the climate forcing from one single climate station, thus with an uncertain reconstruction of the spatial patterns of precipitation and temperature based on the linear regression with elevation using 17 surrounding stations. After a thorough quality check, the climate forcing was reduced to only 8 years of continuous daily recording and concurrent records of daily discharge were adopted as validation set. The snow module was also validated by comparison with a MODIS snow retrieval product over the watershed area. The combined validation using the discharge records and the MODIS dataset allowed to assess the model capability in representing the dominant hydrological processes and the consequent daily discharge despite the recognized limitations in the climate forcing adopted.

The climate change scenario for the case study was extracted from a RCM simulation specifically developed for Lebanon. To simulate the impacts on stream

flow signatures, the climate scenario and the baseline simulation for the 20th Century were adopted as forcing of the NIWaB. Possible future alterations were investigated highlighting the expected impacts on the hydrological signature of the basin which resulted strongly influenced by a shorter snowy period and a consequent enhanced seasonality of the river flows. Adopting a relative change approach with respect to the baseline water balance, remarkable reduction in the mean annual water availability were found together a sensible alteration in the discharge regime.

Concerning the first point, although it is worth to remind that the intrinsic uncertainty of the adopted modelling chain can be important for the projection of future water resources, it is important to note that the mean annual discharge based on observation is 361 Mm<sup>3</sup> and the mean annual value given by the NIWaB model with the climate forcing based on observations is 367 Mm<sup>3</sup>. These values are both reasonably close to the 381 Mm<sup>3</sup> that was simulated with the NIWaB adopting the baseline climate simulation. It can be concluded therefore that the uncertainty in the future water availability is above all related to the adopted climate scenario and only limitedly to the uncertainty of the water balance model. It is therefore prudent to develop a robust assessment on the future water availability by using different climate scenarios produced with different climate models.

With regard to the discharge regime, it is to consider that according to the discharge record, the peak of water availability in the spring season corresponds to the peak water demand related to irrigation and tourism in the case study area, while the impact analysis highlighted that the delay between the peak of winter precipitation and the peak river discharge in spring is expect to reduce. In other words, the hydrological regime is likely to change from a snowmelt dominated regime to a rainfall dominated regime with clear consequences to the water availability in the dry season.

## **5. ACKNOWLEDGMENTS**

This work was developed within the Cooperative Programme of the Agreement on Scientific Cooperation between The National Research Council of Italy (CNR) and The National Council for Scientific Research of Lebanon (CNRS-L) which funded for the biennial programme 2012-2013 the research proposal for “Modelling Water Balance Using Remotely Sensed Data: Application to Ibrahim River Basin, Lebanon”.

## 6. REFERENCES

1. Portoghese, I., Bruno, E., Dumas, P., Guyennon, N., Hallegatte, S., Hourcade, J.H., Nassopoulos, H., Pisacane, G., Struglia, M.V. and Vurro, M., 2013. *Impacts of climate change on fresh water bodies: quantitative aspects*, in A. Navarra and L. Tubiana (eds.), "Regional Assessment of Climate Change in the Mediterranean", Advances in Global Change Research 50, DOI 10.1007/978-94-007-5781-3\_9, © Springer Science+Business Media Dordrecht.
2. Vurro, M., Bruno, E., and Portoghese, I., 2013. *Introduction to the impacts of climate change on fresh water bodies*, in A. Navarra and L. Tubiana (eds.), "Regional Assessment of Climate Change in the Mediterranean", Advances in Global Change Research 50, DOI 10.1007/978-94-007-5781-3\_9, © Springer Science+Business Media Dordrecht. Dollinger J. M. (2003), *Entrepreneurship-Strategies and Resources*, Prentice Hall.
3. IPCC (Intergovernmental Panel on Climate Change), Working Group I (IPCCWGI), 1996. '*IPCC workshop on regional climate change projections for impact assessment.*' Rep., Geneva.
4. IPCC (Intergovernmental Panel on Climate Change), 1999. <<http://ipcc-dcc.cru.uea.ac.uk>> (Feb. 24, 2000).
5. IPCC (Intergovernmental Panel on Climate Change), 2007. *The Physical Science Basis*. Contribution of Working Group I to the Fourth Assessment Report of the Intergovernmental Panel on Climate Change (ed. by S. Solomon, D. Qin, M. Manning, Z. Chen, M. Marquis, K. B. Averyt, M. Tignor & H. L. Miller). Cambridge University Press, Cambridge, UK and New York, NY, USA.
6. Ragab, R. and Prudhomme, C., 2002. *Climate change and water resources management in arid and semi-arid regions: prospective and challenges for the 21st century*. Biosystems Engng 81(1), 3–34.
7. Bou-Zeid, E. and El-Fadel, M., 2002, *Climate change and water resources in Lebanon and the Middle East*. Journal of Water Resources Planning and Management-Asce, 128(5), 343–355.

8. Star, M., 1999. *WATBAL: A model for estimating monthly water balance components, including soil water fluxes*. Proc., 8th Annual Report, UN ECE ICP Integrated Monitoring, 325, 31–35.
9. Hreiche, A., Najem, W., and Bocquillon, C., 2007. *Hydrological impact simulations of climate change on Lebanese coastal rivers*. Hydrological Sciences Journal 52 (6), 1119-1133.
10. Jones R.G., Noguier M., Hassell D.C., Hudson D., Wilson S.S., Jenkins G.J. And Mitchell J.F.B., 2004. *Generating high resolution climate change scenarios using PRECIS*, Met Office Hadley Centre, Exeter, UK, 40 pp.
11. ELARD (Earth Link and Advanced Resources Development S.A.R.L.), 2010. *Vulnerability, adaptation and mitigation chapters of Lebanon's second national communication: Climate risks, vulnerability and adaptation assessment (Final Report)*, submitted to the United Nations Development Programme and the Lebanese Ministry of Environment.
12. Chenoweth, J., Hadjinicolaou, P., Bruggeman, A., Lelieveld, J., Levin, Z., Lange, M.A., Xoplaki, E. and Hadjikakou, M., 2011. *Impact of climate change on the water resources of the eastern Mediterranean and Middle East region: Modeled 21st century changes and implications*, Water Resour. Res., 47, W06506, doi:10.1029/2010WR010269.
13. Shaban, A., and Darwich, T., 2011. *The role of sinkholes in groundwater recharge in mountain crests of Lebanon*. Environmental Hydrology Journal, Vol. 19. Paper 9.
14. Hreiche, A., Bocquillon, C., Najem, W., Servat E., and Dezetter, A., 2003. *Calage d'un modèle conceptuel pluie-débit journalier à partir de bilans annuels*. In: Hydrology of Mediterranean and Semiarid Regions (ed. by E. Servat, W. Najem, C. Leduc & A. Shakeel) (Proc. Montpellier Symp., April 2003), 87–93. IAHS Publ. 278. IAHS Press, Wallingford, UK.
15. Saqallah, S., 2013. *Modeling Climate Change Impact on the Water Balance of a Coastal Watershed in Lebanon*, Master of Science thesis dissertation in "Land and Water Resources Management: Irrigated Agriculture", CIHEAM - Mediterranean Agronomic Institute of Bari, academic year 2012-2013.

16. Martinec, J., Rango, A., and Roberts, R. T., 2008. *Snowmelt Runoff Model (SRM) User's Manual*, 19-39. New Mexico: New Mexico State University Press.
17. Hreiche, A., Bocquillon C. and Najem W., 2006. *River flow simulation within ungauged catchments in Lebanon using a semi-distributed rainfall–runoff model*. In: Summit on Environmental Modelling and Software (Proc. iEMS Third Biennial Meeting) (ed. by A. Voinov, A. Jakeman & A. Rizzoli). International Environmental Modelling and Software Society, Burlington, USA.
18. Darwish, T., Shaban, A, Portoghese, I., Khadra R., Saqlah, S., Drapeau, L., Gascoin, S., Amacha, N., 2012. *Using remotely sensed data to induce snow cover dynamics and water productivity for sustainable water management in Ibrahim river basin, Lebanon*. 1st CIGR Inter-regional Conference on Land and Water Challenges-Bari (Italy), 10-14 September, 2013.

## 7. IMAGES AND TABLES

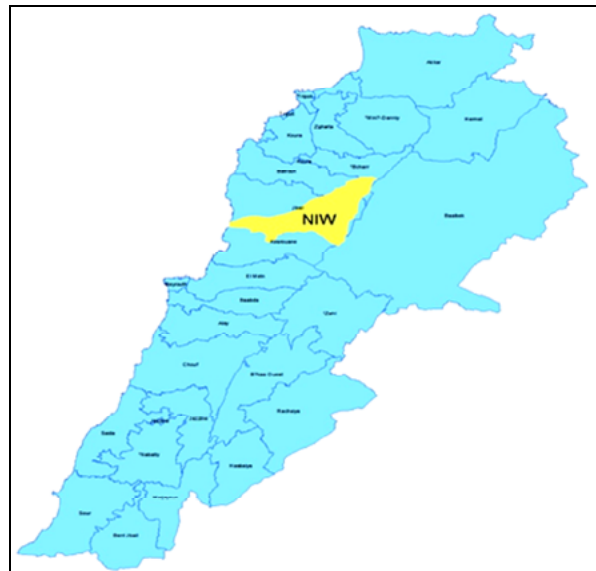


Fig. 1 Location of Nahr Ibrahim Watershed (NIW).

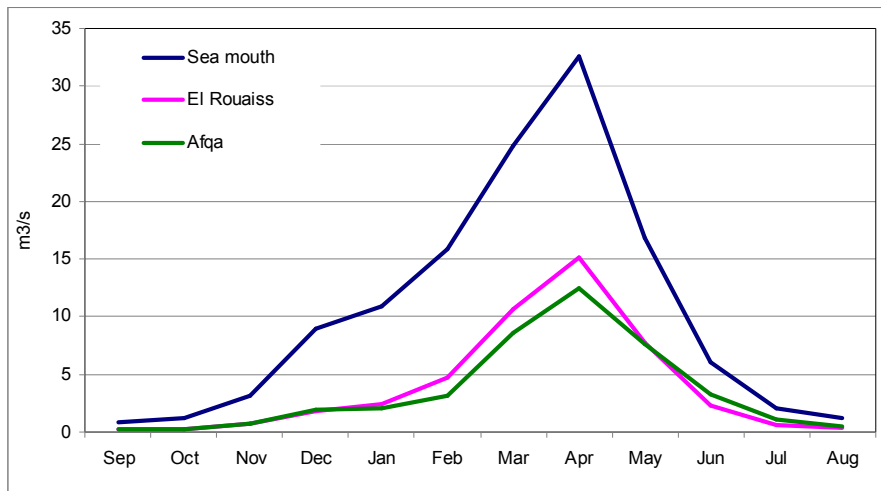


Fig. 2 Mean monthly discharge values for the period 1967-2011 at the three gauging stations in the NIW.

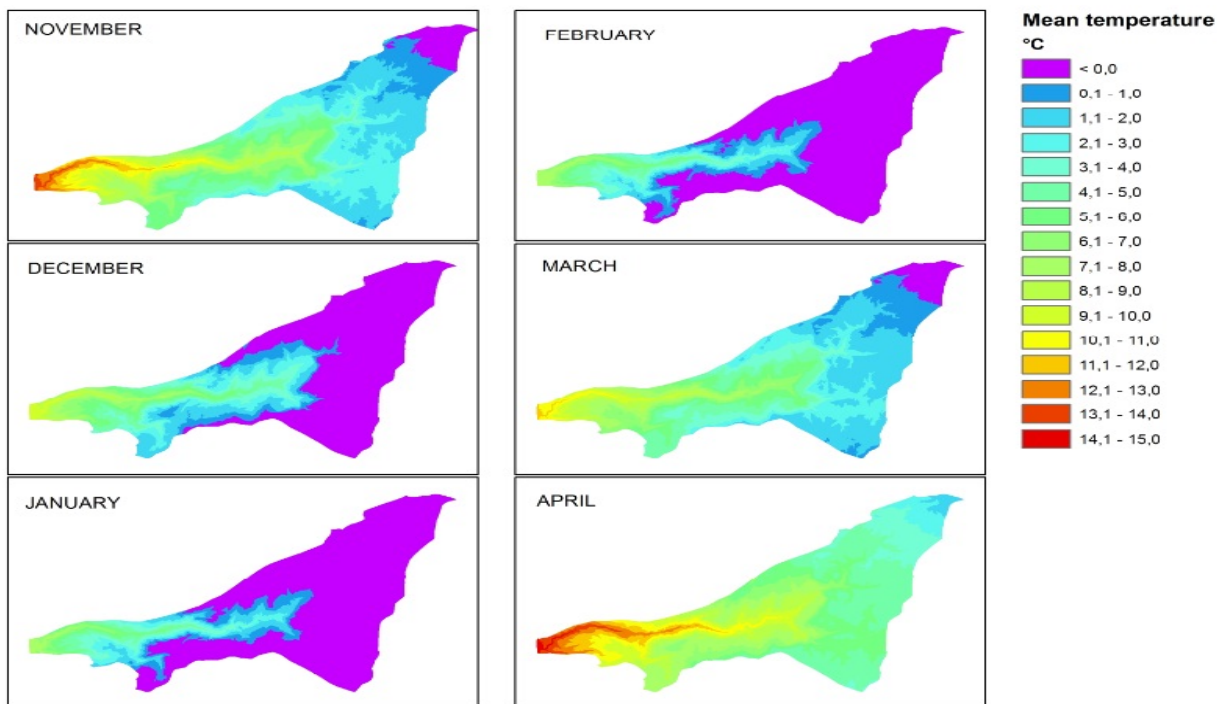


Fig. 3 Temperature maps interpolated from the mean monthly values (2001-2011) corresponding to the snow season; basin areas with temperature below 0°C represent the snow existence zone (November to March).

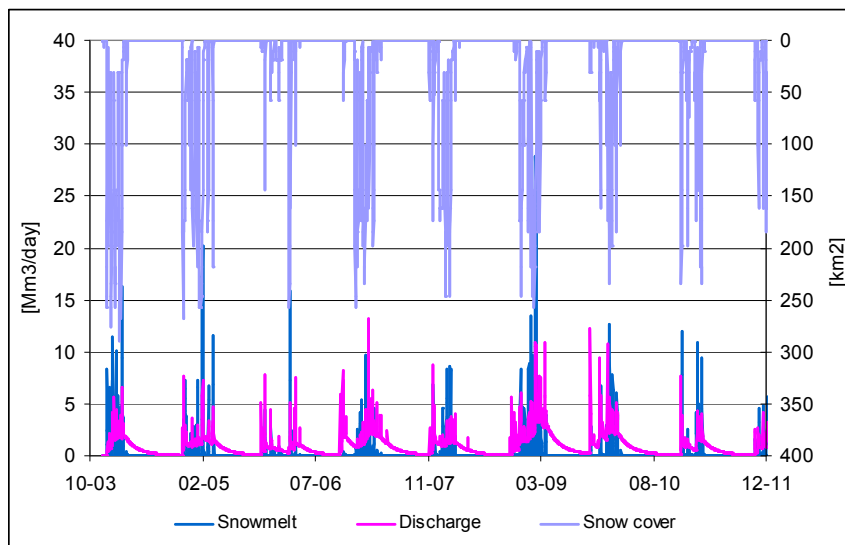


Fig. 4 Example the daily output from the NIWaB model for the period 2003-2011. The reported plot highlight the hydrological processes relating the snow cover to the river discharge.

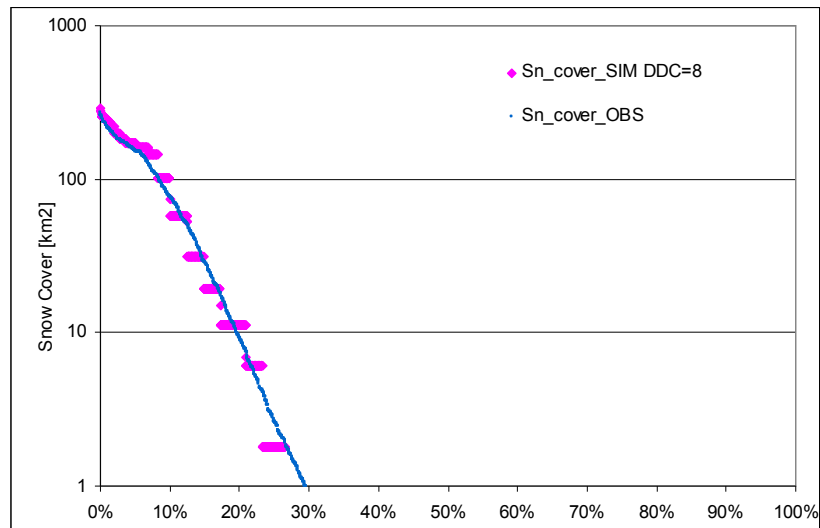


Fig. 5 Comparison between simulated snow cover and MODIS retrieval of daily snow coverage for the period 2003-2011. The figure represents the snow cover duration curve (SCDC) for a DDC value of 8 mm/day/°C.

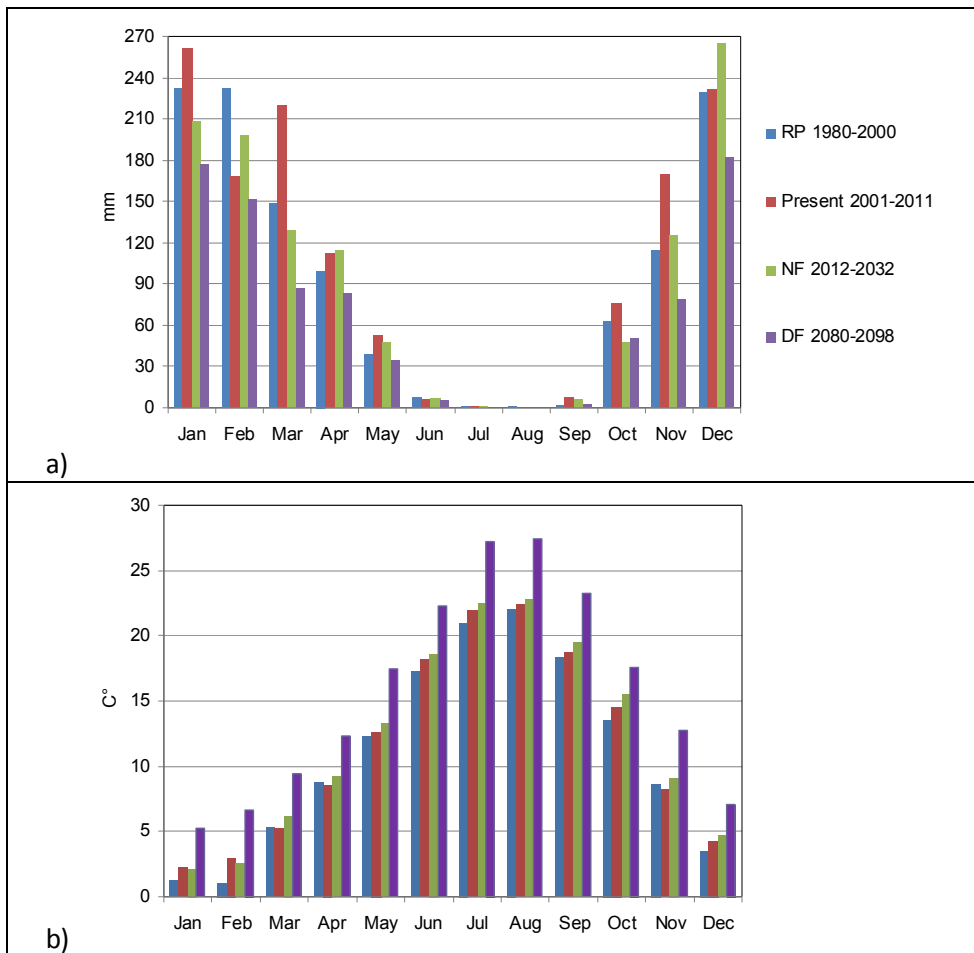


Fig. 6 Average monthly a) precipitation and b) temperature for the time intervals simulated with the PRECIS and adopted for the hydrological impact study. The values are related to the D2 grid node.

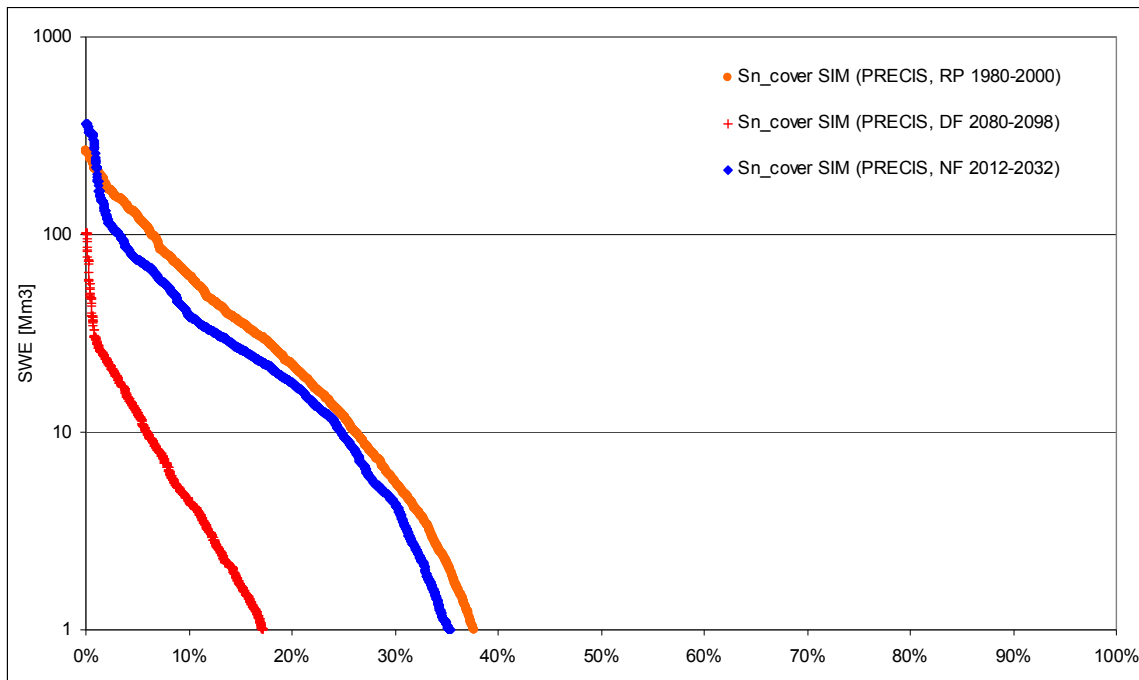


Fig. 7 Impact analysis of the PRECIS climate scenario on the SWE volume in the NIW. The analysis presents the duration curves of the SWE simulated with the NIWaB model as the snow component of the daily water balance.

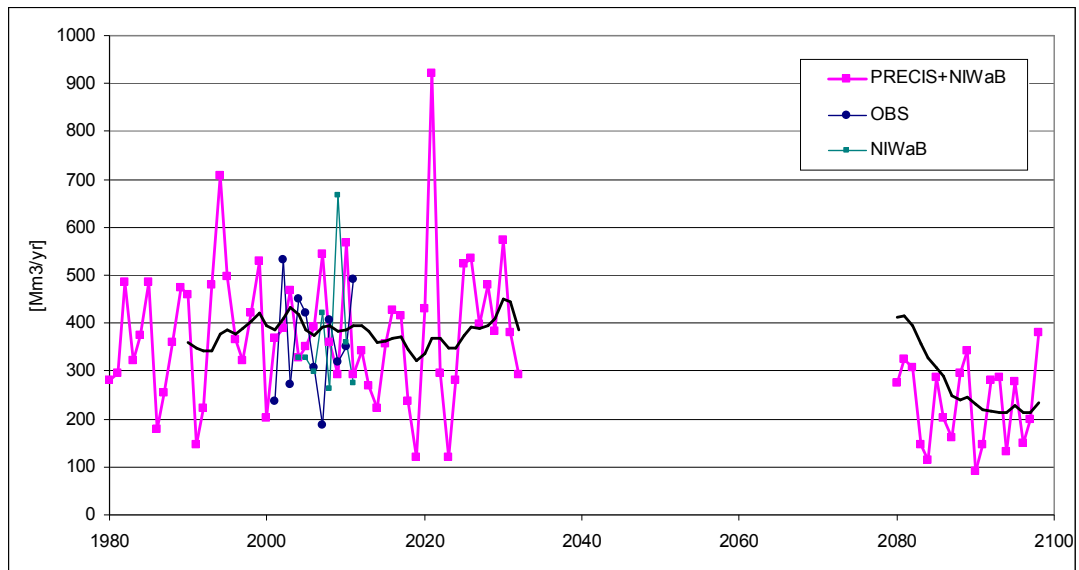


Fig. 8 Annual discharge totals at the sea mouth station simulated with the PRECIS climate scenario coupled with the NIWaB model (PRECIS+NIWaB). Annual discharge based on observations (OBS) and on the model simulation with the climate forcing based on the Qartaba station (NIWaB) are also plotted.

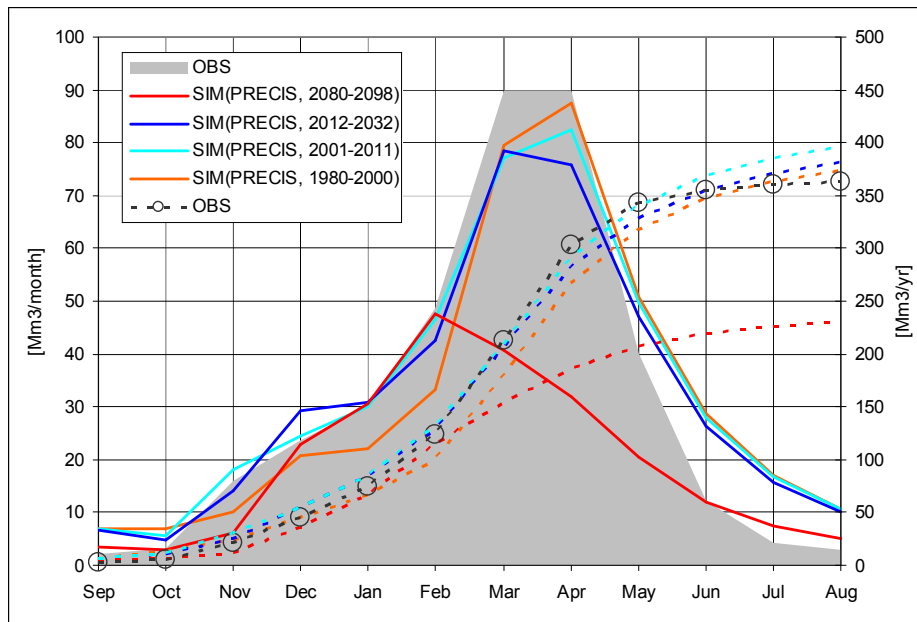


Fig. 9 Mean monthly discharge values at the sea mouth station and their cumulative sums for the 4 time intervals adopted. For the impact assessment the changes are evaluated with respect to the RP time period though the mean observed discharge values are also reported.

Table 1 Model parameters and adopted values.

Parameter	Symbol	Est. method	Afqa spring	Roueiss spring	Sea mouth
Snowmelt DDC [mm/day/°C]	$\delta$	Literature	8	8	8
Soil water holding capacity [mm]	$S_{FC}$	Lebanon soil map	100	100	100
Area adjusting factor [-]	$A_{adj}$	Calibration vs. annual discharge volumes	1.85	1.75	1.00
Fast/slow reservoir proportion [-]	R	Calibration with discharge recession	0.3	0.3	0.1
Slow reservoir time constant [days]	$T_s$	Calibration with discharge recession	45	45	120

Table 2 Basic statistics of simulated and observed daily snow cover.

Daily snow-cover (km <sup>2</sup> )	Simulated 2003-2011	Observed 2003-2011
Mean	22.4	19.3
Standard deviation	55.6	49.0
Coefficient of Variation	2.48	2.54

Table 3 Basic statistics of simulated and observed daily discharge.

Daily discharge (Mm <sup>3</sup> /day)	Simulated 2003-2011	Observed 2003-2011
Mean	0.99	0.99
Standard deviation	1.19	1.43
Coefficient of Variation	1.20	1.44

Impacts & Implications of  
Climate Change

**Impacts on energy, health  
and cultural heritage**

## **Results of the EU Project *Climate For Culture: Future Climate-induced Risks to Historic Buildings and their Interiors***

**Bertolin C.<sup>1\*</sup>, Camuffo D.<sup>1</sup>, Leissner J.<sup>2</sup>, Antretter F.<sup>2</sup>, Winkler M.<sup>2</sup>, Kotova L.<sup>3</sup>, Mikolajewicz U.<sup>3</sup>, Jacob D.<sup>3</sup>, van Schijndel A.W.M.<sup>4</sup>, Schellen, H.<sup>4</sup>, Broström T.<sup>5</sup>, Leijonhufvud G.<sup>5</sup>, Ashley-Smith J.<sup>6</sup>**

<sup>1</sup>Institute of Atmospheric Sciences and Climate – National Research Council (ISAC-CNR), Padua - Italy, <sup>2</sup>Fraunhofer Institute – Germany, <sup>3</sup>Max Planck Institute for Meteorologie – Germany, <sup>4</sup>Technical University of Eindhoven – Holland, <sup>5</sup>Uppsala University – Sweden and <sup>6</sup>JAS – United Kingdom

\*Corresponding Author: c.bertolin@isac.cnr.it

### **Abstract**

The EU funded *Climate for Culture* (CfC) Project is finalized to forecast the impact of climate change on either indoor or outdoor Cultural Heritage and advise on related risks. CfC has produced high-resolution thematic maps over Europe to highlight the expected changes and related risks for a number of key materials, building types, deterioration mechanisms for the near and far future based on two emission scenarios as developed by IPCC. The procedure to obtain a thematic map is as follows: to simulate outdoor climate change; to pass from outdoor to indoor climate change through building simulation and case studies measurements; to use damage functions and literature results to evaluate potential risk for buildings and objects; to map the above results for advice and stakeholders use. This methodology has produced 55,650 thematic maps of future climate induced risks to historic buildings and collections in their interiors. The results can be used for climate change impact assessments and for planning adaptation and mitigation measures in view of preventive conservation or other applications, e.g. human health, energy consumption, cultural tourism. This paper presents some of the main project outcomes.

**Keywords:** Climate Change, risk maps, preventive conservation, Cultural Heritage

## 1. THE CLIMATE FOR CULTURE PROJECT

Climate Change is one of the most critical global challenges of our time. This factor, coupled with the increasing demand our society makes on energy and resources, has forced sustainable development to the top of the European political agenda. Scientific research shows that the preservation of the cultural heritage of Europe is particularly vulnerable to all three of these factors. As a non-renewable resource of intrinsic importance to the European identity, it is necessary to develop more effective and efficient sustainable adaptation and mitigation strategies in order to preserve these invaluable cultural assets for the long-term future. More reliable assessments will lead to better prediction models, which in turn will enable preventive measures to be taken, thus reducing energy and the use of resources.

In the general perception, gale winds and heavy rains will likely affect outdoor monuments; museums should substantially be prepared to use more fuel for air conditioning and less for heating. The EU funded NOAH'S ARK project [1] has considered this problem for outdoor monuments and buildings and has produced a first risk atlas based on future simulations. This has provided very useful information concerning the cultural heritage at risk. However, so far nobody has a clear idea about the indoor conservation needs, i.e. if the museum collections will undergo an acceleration of the physical and chemical deterioration processes, if the risk of moulds and insect infestation will be increased or reduced and so on.

The *Climate For Culture* (CfC) project will consider not only monuments and buildings exposed to future weather injuries (e.g. precipitation, dryness, temperature, humidity, time of wetness, repeated freezing thawing or salt crystallization cycles), but the future of building interiors, collections, and various types of cultural objects and materials. CfC has connected high-resolution climate change evolution scenarios with whole building simulation models to identify the most urgent risks for specific building types and climate regions over Europe.

The CfC project has implemented high resolution regional climate model REMO with 10 km X 10 km spatial resolution [2] and it has used these results as input to assess deterioration rates and damage potentials. The innovation lies in the elaboration of a more systematically and reliable damage/risk assessment which will be deduced by

correlating the projected future climate data with whole building simulation models and damage assessment functions.

Laboratory tests, in situ measurements and investigations at cultural heritage sites throughout Europe, and computer simulations have allowed a precise assessment of the real damage impact of climate change on cultural heritage at regional scale. Sustainable (energy and resource efficient) and appropriate mitigation/adaptation strategies, have been developed and applied on the basis of these findings simultaneously.

All the above results have been incorporated into thematic maps related to the outdoor and indoor deterioration mechanisms, the risk assessment and an evaluation of the economic costs and impacts that have been forecasted until 2050 and 2100 based on two IPCC emission scenarios.

To this aim, the first step was to achieve a reliable assessment of the impact of climate change through an improvement of the prediction models, then the development of a methodology to assess the climate-induced risks on materials and building envelopes which in turn can enable preventive measures to be taken from stakeholders, thus reducing the consumption of energy and resources.

The CfC project has also considered the analysis of uncertainties deriving from combining projections of future climate, building simulations and damage functions; although the effective communication of uncertainty is a challenging task, even when full probability distributions are known.

The analysis of the uncertainties related to the project outcome include uncertainties in: risk maps, forcing conditions and the used climate model, significance of the climate change pattern, building simulation, damage functions. The above analysis is necessary to assess the confidence limits that should be related to future scenarios and that should be considered and should underlie any decision support system or any decision-making activity.

## **2. RISK ASSESSMENT**

Within the CfC project, the risk assessment process is carried out through a sequence of simulations [3]:

- Outdoor climate change simulation
- Indoor simulation to pass from outdoor to indoor climate change through building simulation and case studies measurements
- Risk assessment to using damage functions and literature results to evaluate potential risk for buildings and objects both outdoors and indoors.

This assessment method is carried out for:

- a grid of 474 European and Mediterranean locations as reported in Figure 1 [Fig.1] for each of the following items.
- three 30-year time windows i.e. for the **near future** (2021-2050), the **far future** (2071-2100) and the **recent past** (1961-1990) as reference period
- Two different moderate emission scenarios from the Intergovernmental Panel on Climate Change (IPCC) [4 and 5], respectively: **A1B Scenario** from IPCC's 4th report based on a higher CO<sub>2</sub> emission increase assumed until 2050 and a decrease afterwards. **Representative Concentration Pathway (RCP) 4.5 Scenario** based on long-term, global emissions of greenhouse gases, short-lived species, and land-use-land-cover which stabilizes radiative forcing at 4.5 watt m<sup>-2</sup> (approximately 650 ppm CO<sub>2</sub> equivalent) in the year 2100 without ever exceeding that value [4].
- 16 generic building types, each of them different in volume, window area, assemblies and moisture buffering capacity as a combination of: **Volume**: small/large building; **Area**: small/large window; **Structure**: heavy weight/light weight; **Moisture Buffering Performance (MBP)**: Low/High

## 2.1 Indoor Climate Simulation

Indoor climate and risk maps have been produced for all of the 16 generic building types as shown in Table 1 [Tab.1] through an innovative indoor simulation method based on the State Space Model (SSM). The SSM is an inverse modeling approach [6] that is applied in compiling a transfer function (TF) able to simulate the thermo-hygrometric performance of simplified building models with the characteristics of the generic buildings summarized in Table 1. Such an innovative approach allows for a

very fast simulation of indoor temperature and vapor pressure [7] for each generic building type over all the European climate locations.

The results show high accordance between the indoor simulation obtained via this combined approach and the full building simulation made using WUFI® Plus.

One of the major results obtained by the CfC Project is the use of the SSM approach to overcome the whole building simulation drawbacks as the required long elaboration run time and the extended set of detailed information.

## 2.2 Risk Simulation

Levels and fluctuations of temperature (T) and relative humidity (RH) are the main environmental drivers of risks for both building envelopes and collections taken into account in producing the CfC risk maps.

**Outdoor forcing factors** that may generate some form of damage or risk for the building exterior are related to climate changes and extreme events.

**Indoor forcing factors** that may generate some form of damage or risk for objects and/or building envelopes are related to levels and fluctuations of indoor temperature and relative humidity.

Risks are directly related to mechanisms governed by physical, chemical or biological variables, e.g. freeze-thaw cycles, crystallization-dissolution cycles, mould infestation.

The production of indoor damage/risk maps has been performed using the SSM for generic building simulation connected with the use of damage functions/tolerable ranges or risk indices collected from literature or developed within the project for various types of material/risks [8].

Damage functions and/or thresholds link the changes of the variables describing the forcing factors to a specific risk of damage. A traffic light code is used to calculate the risk for each degradation mechanism. Three risk levels are defined: **safe** (i.e. green color in the risk map legend), **attention** (i.e. orange color in the risk map legend) and **risk** (i.e. red color in the risk map legend). The level of risk is defined according to the number of events that have exceeded, or the time elapsed above, some specific risk thresholds.

The risk maps produced within CfC project can either show the risk levels for any of the three time windows (i.e. recent past, near future and far future) or the change in risk from one time window to another (i.e. difference between near future and recent past or difference between far future and recent past). The difference maps will show whether a risk is increasing or decreasing and how much per each location over Europe.

### **3. HOW TO APPLY OUTDOOR AND INDOOR DAMAGE/RISK MAPS IN PREVENTIVE CONSERVATION**

#### **3.1 Selected Materials**

Various types of materials have been used to build cultural heritage objects, buildings or sites. Within the CfC project the climate change impact on movable and immovable cultural heritage has been evaluated for mechanical, chemical and biological risks (related to T and RH environmental changes) for a number of key materials that have been commonly used in this field, or that need consideration because might be at risk under certain unfavorable circumstances:

- Stone and masonry
- Wood and veneers
- Painted wood
- Paper
- Silk
- Color photographs
- Metal

#### **3.2 Outdoor Risk Maps**

The first column in Figure 2 [Fig.2a and Fig.2b] includes some selected materials exposed to the outdoor environment (e.g. stone and masonry buildings and/or wood and metal). Each selected material is exposed to one or more risk types (e.g. mechanical, chemical and biological), given in the second column. In addition, the same example considers also other challenges for buildings: an evaluation of the

energy demand, or the risk for natural hazards (i.e. extreme events). For each material, and for each risk type, a map has been drawn to represent how the main forcing factors that contribute to the risk assessment are distributed over Europe (third column). Of course, these are only particular examples to elucidate the methodology that the final user can apply to be informed of the most critical factors (including sea level rise) that are predicted in his/her region in terms of thematic risk maps.

### 3.3 Indoor Risk Maps

Once the outdoor climate has been simulated, the produced data serve as input for the building simulation (section 2.1) and to generate the indoor climate and its future scenarios. From the knowledge of the indoor climate and the damage functions for some selected materials (section 2.2), it is possible to calculate the future risks for conservation, and map the outcome over Europe.

Some examples useful to explain the use of indoor risk maps are reported in Figure 3 [Fig.3].

## 4. SOME RESULTS AS AN EXAMPLE OF THE VARIOUS OUTCOMES

### 4.1 Outdoor Climate Maps:

Within the CfC project, four climatic zones have been individuated over Europe taking into account similar thermo-hygrometric variations (see Figure 4), the outcomes evaluation will refer to such zones [Fig.4].

The main predictions concerning the expected **temperature** differences in the near and far future with reference to the recent past, under the A1B emission scenario are reported in Figure 5a and 5b [Fig.5a and Fig.5b]. These differences are positive (i.e. greater than zero, in mathematical terms) in all the 4 climatic zones in Europe, with maximum changes in Northern Europe, inland of Northern Africa, Central Spain, Greece and Turkey. The prediction under the RCP4.5 emission scenario (Figure 5c and 5d) is similar to A1B for the near future but there is a decrease in temperature change in the respective climatic zones for the far future [Fig.5c and Fig.5d].

The expected changes in **yearly total precipitation**, in percentage terms, evaluated for the A1B emission scenario for the near and far future are visible in Figure 6 [Fig.6a and Fig. 6b]. In both periods, the predictions highlight no or small change 0-20% in Climate Zone I and II respectively Northern Europe (i.e. European Russia, Poland and Scandinavian Peninsula) and Central-Eastern Europe (i.e. Germany, Austria, Switzerland, Hungary, Czech Republic, Slovakia, and Ukraine). In Climate Zone III and IV, respectively European Atlantic Coast (i.e. Island, UK, Ireland and France) and Mediterranean regions, the prediction highlight a mixed situation with both negative and positive changes up to +50% in Egypt, Libya and Eastern Algeria and -50% in central Portugal, Morocco and Western Algeria.

#### **4.2 Outdoor Risk Maps:**

One of the outdoor climate risk features projected as future change respect to the recent past, is the tropical nights index, i.e. the number of nights in a year with daily minimum temperature  $T_{min} > 20^{\circ}\text{C}$ . This climate variable may be useful to evaluate health risks for the population as well as the potential increase in energy consumption. In the far future (Figure 7) [Fig.7], under the emission scenario A1B, the projection highlights an increase homogeneously distributed over the whole Mediterranean region with maxima of +60 days/year on the Provence (France) and the Black Sea coasts. Extreme conditions with an increase up to +110 days/year are expected on the Egyptian and Libyan coasts.

#### **4.3 Indoor Climate Maps:**

Coupled simulations of climate and buildings allow assessing the future changes in respect to the recent past (i.e. 1961-1990 period) for air temperature, relative humidity and humidity mixing ratio inside buildings. 16 buildings have been simulated changing their hygro-thermal and geometric characteristics over the different European climate zones. Figure 8 reports the future difference in indoor temperature range for the building type 1 (i.e. heavyweight, small building with small window area) respect to the recent past.

Figure 8a [Fig.8a] highlights near future changes respect to the past: higher positive ( $>0$ , in mathematical terms) increase in temperature range in Sweden and Norway,

Denmark, Holland, central Romania, Alps, Italy, former Yugoslavia and Greek coasts; a negative decrease ( $<0$ , in mathematical terms) in the rest of Europe. In the far future [Fig.8b] the projections identify two macro-areas: the first includes the Northern Europe, Germany and Poland and it highlights a decrease in indoor temperature range up to  $5^{\circ}\text{C}$ ; the second macro-area constituting the Western and Southern Europe, highlights an increase up to  $4^{\circ}\text{C}$  in indoor temperature range.

#### 4.4 Indoor Risk/Damage Maps

A number of results are related to the simulation of mechanical, biological and chemical risks concerning nine selected materials that constitute building envelopes and/or the collections preserved indoors. Figure 9 highlights the mechanical risk for marble, stone and masonry due to future change in the frequency of salt crystallization cycles per year. Looking at Figure 9a [Fig.9a], for the near future under the A1B emission scenario, mixed situations are visible in Climate Zones I and IV, respectively Northern Europe and the Mediterranean Area with changes, respect to the recent past, ranging from  $-20$  salt crystallization cycles/year in the Alps and in large part of Northern Europe, up to  $+10$  salt crystallization cycles/year in the rest of Northern Europe, Southern Mediterranean and Spanish coast. In the far future (Figure 9b [Fig.9b]), the projection shows larger changes, i.e. up to  $-40$  salt crystallization cycles/year in the Northern region (i.e. Climate Zone I) and in the Alps. A prediction of a decrease in number of salt crystallization means a lower risk of mechanical damages on masonry and stones, as opposed, an increase in frequency of salt-crystallization cycles (e.g. as in the rest of Europe with about  $+10$  salt crystallization cycles/year more) means a slight increase of risk for such materials.

#### 4.5 Energy Demand Maps

The prediction under the A1B emission scenario, related to the changes in energy demand in the near future respect to the recent past for a historic building with a strict climate control (Figure 10) [Fig.10a] highlights again two macro-areas over Europe. The first, shows a general saving of..... that can be estimated, for a building of  $500\text{ m}^3$  volume, up to  $400\text{ l oil/year}$  in Northern Europe and up to .....equivalent to  $100\text{ l oil/year}$  in central Europe; while the second macro-area shows a mixed situation with

opposite trends in energy consumption. A maximum saving of      corresponding to about 300 l oil/year is predicted for the the Alps whereas a maximum increase in consumption (i.e.      W more corresponding to an additional consumption of 300 l oil/year) is expected in central Spain and Algeria. In the Far Future (Figure 10b) [Fig.10b] the macro-area distinction persists: from one hand there will be a saving in consumption of      , (i.e. 1000 l oil/year less for a building with 500 m<sup>3</sup> volume) in Northern Region and of      i.e. 800 l oil/year if this building is located in the Alps; from the other hand, the energy consumption will double in Spain and in Northern Italy reaching a maximum of .....600 l oil/year.

If we consider, under the A1B emission scenario, the energy demand in the Near and Far Future for a modern building envelope with a modern strict climate control (Figure 11), the above identified macro-areas still persist, but the prediction is quantitatively different compared to a historic building. In the Near Future (Fig.11a) [Fig.11a], for a modern building, a maximum saving of      i.e. 60 l oil/year for a 500 m<sup>3</sup> volume is reached in Northern Europe. This saving decreases to      i.e. 10 l oil/year in central Europe. In climatic zone III and IV i.e. Western Atlantic Europe and the Mediterranean Area, the mixed situations persist: from one hand a maximum of 40 l oil/year saved in Island, Northern Scotland and Alps; from the other hand, an increase in energy consumption up to 60 l oil/year in the Western Mediterranean, Iberian Peninsula, Libya, Egypt and Northern Italy. In the Far Future (Fig.11b) [Fig.11b], Northern Europe will save double in respect to the Near Future, while in Island, Ireland and Scotland an energy saving of about 120 l oil/year will be reached. In the Alps the energy saving will modestly increase reaching 60 l oil/year, while a maximum in energy consumption is predicted for Spain, Egypt, Northern Italy; The Mediterranean and Atlantic Coasts will have an increase in consumption of about 170 l oil/year.

## 5. CONCLUSIONS

To make the results understandable about a complex matter in a simple and friendly way for specialists and non-specialist users (e.g. researchers, conservators, policy makers, stakeholders), the risk assessment process has been developed with a problem-oriented approach which considers only one variable or aspect, at a time.

The project outcomes, concerning the future changes of indoor/outdoor climate variables, the main deterioration factors, the critical frequencies distribution and/or risks for building envelopes and collections have been presented in a simplified form as thematic maps over Europe.

The total number of thematic maps produced for the various types of materials, buildings, scenarios etc. is impressive: 55,650 high-resolution maps over Europe, as reported in the Project Deliverable 5.2 and in the Project Data Base [9]. These thematic maps include detailed information concerning potential deterioration and risk factors for indoor and outdoor, movable and immovable cultural heritage. The same basic information might be useful for other health or social application fields, e.g. cultural tourism, temperature changes and increased number of tropical days or energy consumption.

In this context, climate change may have negative, neutral or positive effects, depending on specific problems, aims, solutions and use. Research results offer a timely information to prepare adaptation and mitigation strategies, or to take advantage from the positive aspects whenever possible.

In this sense, the CfC project provides an informative tool aimed to assist policy makers, conservators, architects and any type of users in their difficult task, especially in view of an efficient strategy for management and preventive conservation of the European Cultural Heritage.

## 6. ACKNOWLEDGMENTS

The Climate for Culture project has been funded by the European Union's Seventh Framework Programme for research, technological development and demonstration under grant agreement No. 226373.

## 7. REFERENCES

1. Sabbioni, C., Brimblecombe, P. and Cassar, M. 2012. *The Atlas of Climate Change impact on European Cultural Heritage*. Anthem Press, New York.
2. Jacob, D., Mikolajewicz, U, Kotova, L., et al. 2012. *Climate for Culture – WP1 Deliverable 1.2*. Internal Project Report.

3. Bertolin, C., Camuffo, D. 2013. *Climate for Culture – WP5 Deliverable 5.1*. Confidential Project Report.
4. IPCC 2014. *Climate Change 2013: The Physical Science Basis*. Intergovernmental Panel on Climate Change, Fifth Assessment Report.
5. IPCC 2007. *Fourth Assessment Report (AR4)*. Climate change 2007: Scientific basis. Available at: <http://www.ipcc.ch/>
6. Kramer, R. 2012. *From Castle To Binary Code – Inverse modeling for the prediction and characterization of Indoor climates and energy performances*. Msc-thesis. University of Technology Eindhoven.
7. Riedler, J. 2013. *Untersuchung Inverser Modellierung – Zur Bewertung der Einflüsse des Klimawandels auf Kulturgüter in Europa*. Bsc-thesis. Technischen Universität München (TUM).
8. Ashley-Smith J. et al. 2014. *Climate for Culture – WP4 Deliverable 4.2*. In print.
9. Bertolin C., Camuffo D., Antretter F., Winkler M., Kotova L., Mikolajewicz U., Jacob D., van Schijndel A.W.M., Schellen, H. Huijbregts Z., Martens M., Broström T., Leijonhufvud G., Sladek A., Mirtič M., Šijanec-Zavrl M. and Ashley-Smith J., 2014. *Climate for Culture – WP5 Deliverable 5.2*. Public Project Report. Available on request to the CfC Project coordinator.

## 8. IMAGES AND TABLES

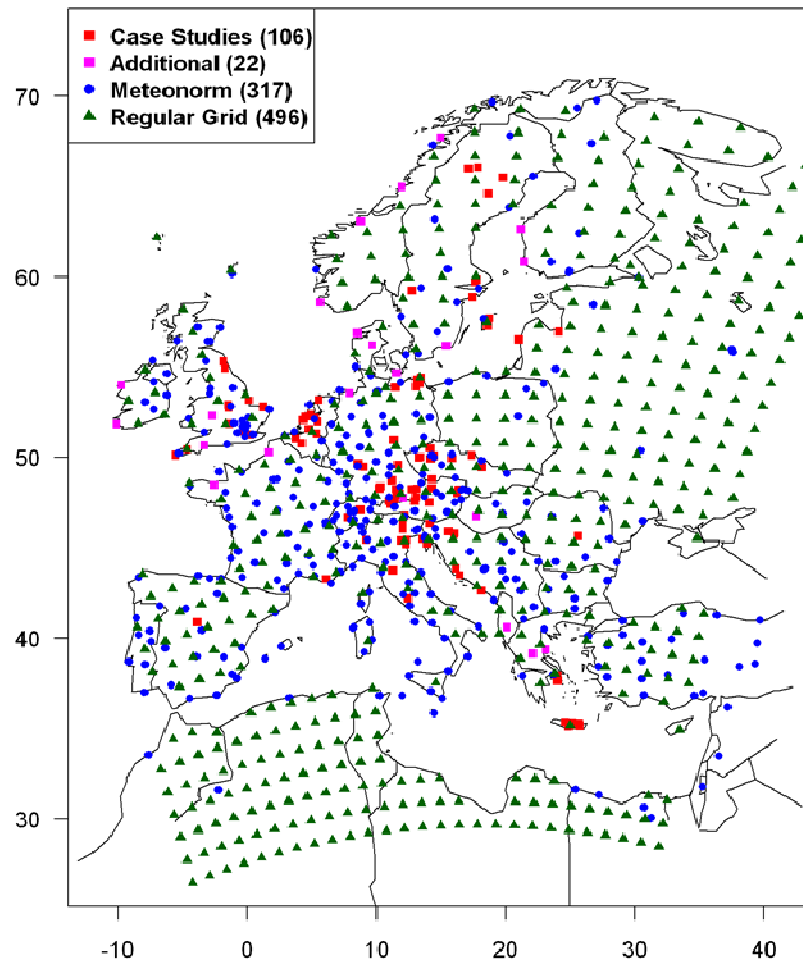


Fig. 1 Location of sites for which outdoor climate data are provided with hourly resolution for recent past, near future and far future

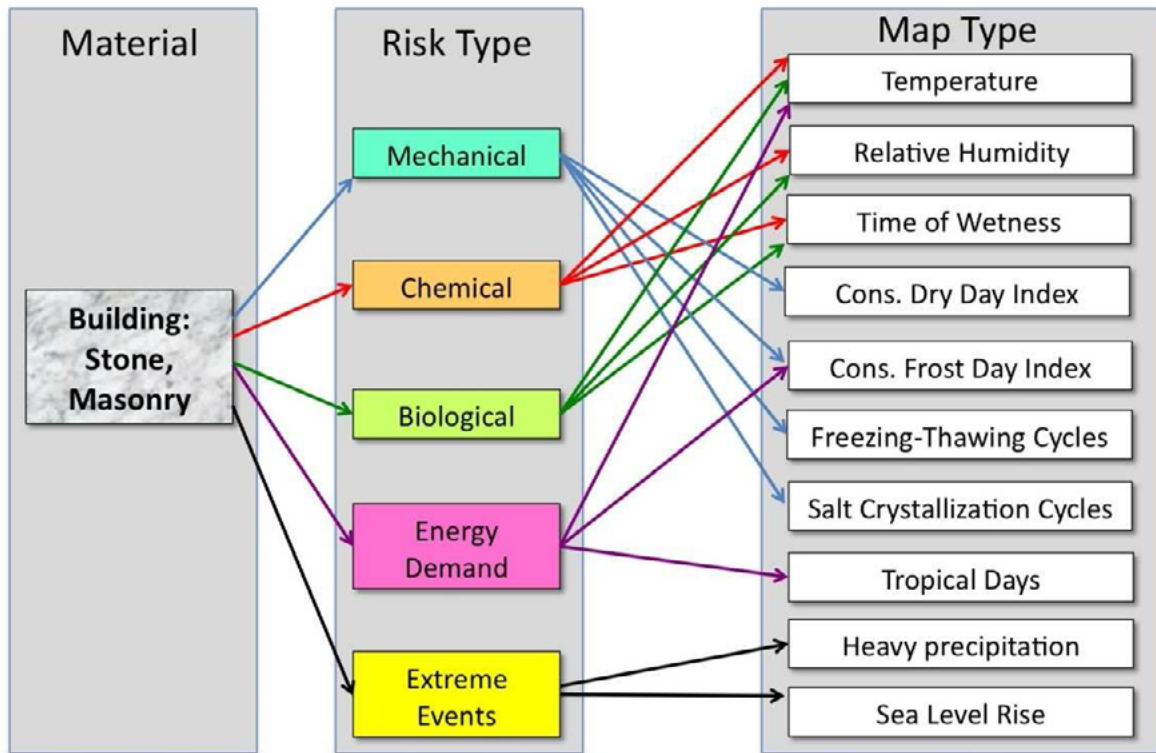


Fig. 2a An example elucidating the material oriented use of the climate risk/damage maps for a user potentially interested in stone and masonry buildings conservation outdoors.

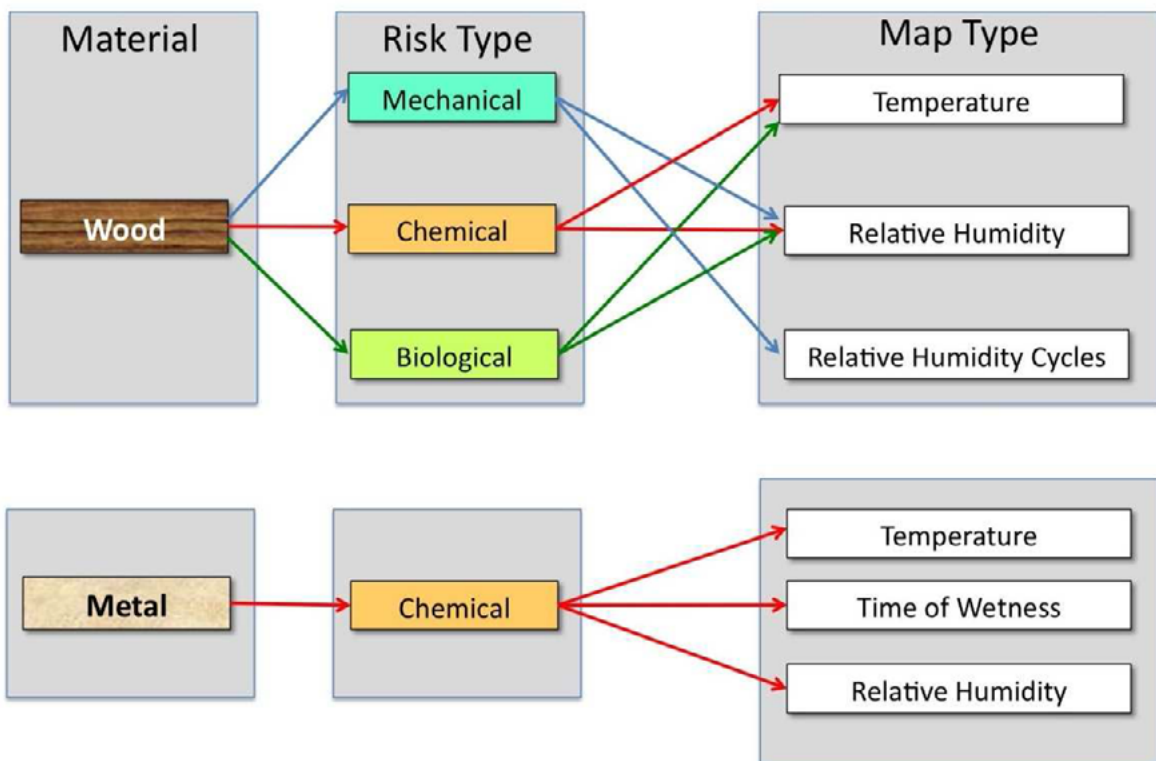


Fig. 2b An example elucidating the material oriented use of the climate risk/damage maps for a user potentially interested in wood buildings and metal conservation outdoors.

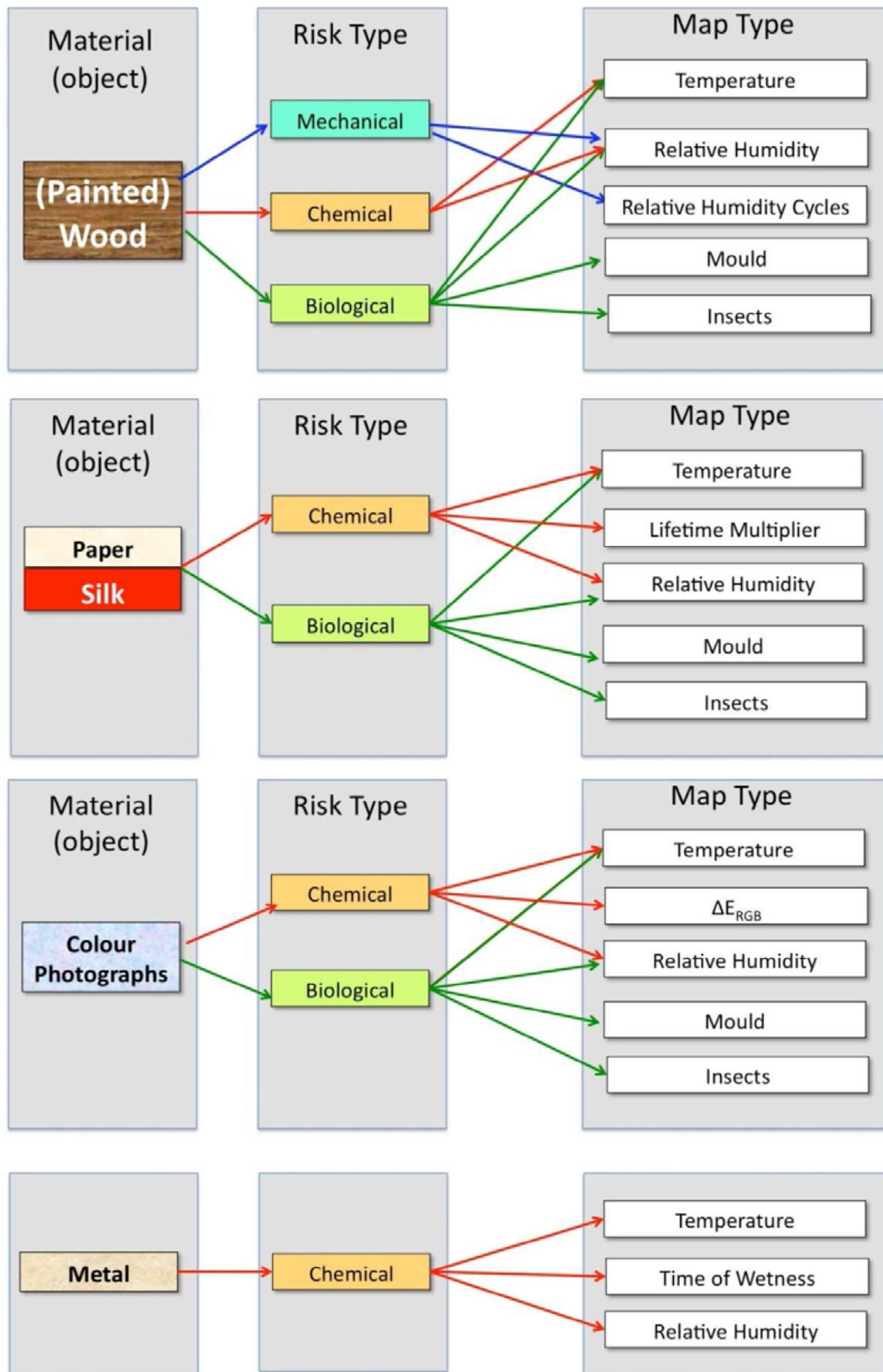


Fig. 3 An example elucidating the material oriented use of the climate risk/damage maps for a user potentially interested in indoor conservation of collection composed of several materials (e.g. painted wood, paper, silk, colour photographs and metal).

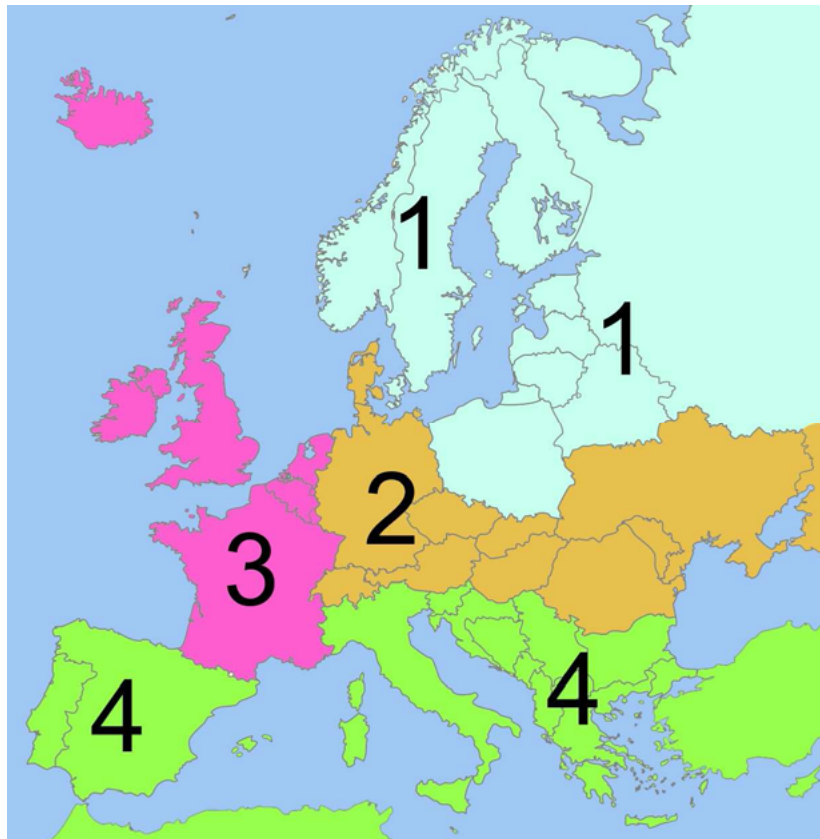


Fig. 4 Practical climate zoning for Climate for Culture outcomes evaluation

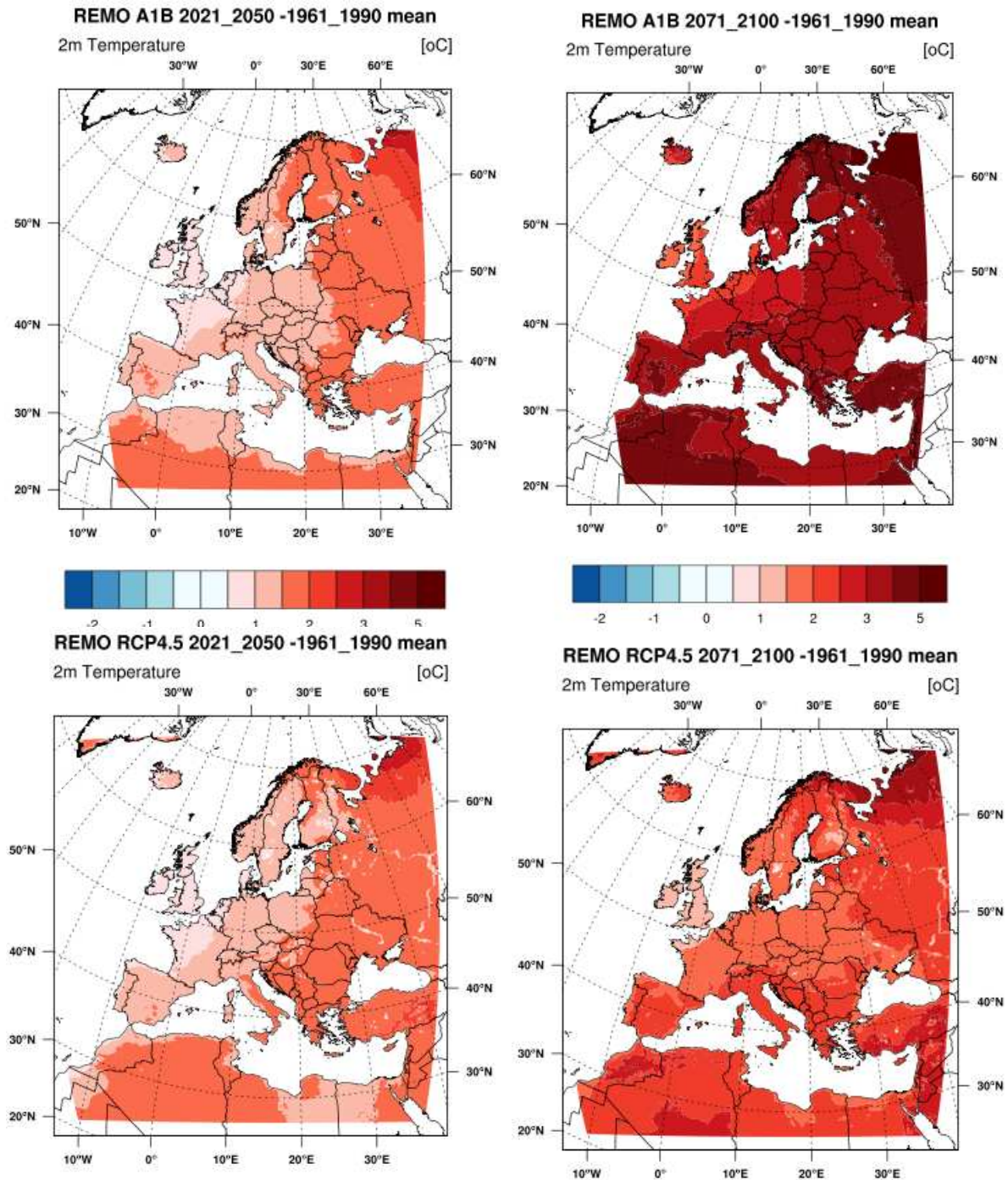


Fig. 5 Changes in air temperature at 2 m (°C) from the Recent Past to the Near Future (left side - 5a and 5c) and the same for the Far Future (right side – Fig. 5b and 5d). Simulations made under the A1B (top – Fig. 5a and 5b) and RCP 4.5 (bottom- 5c and 5d) emission scenarios.

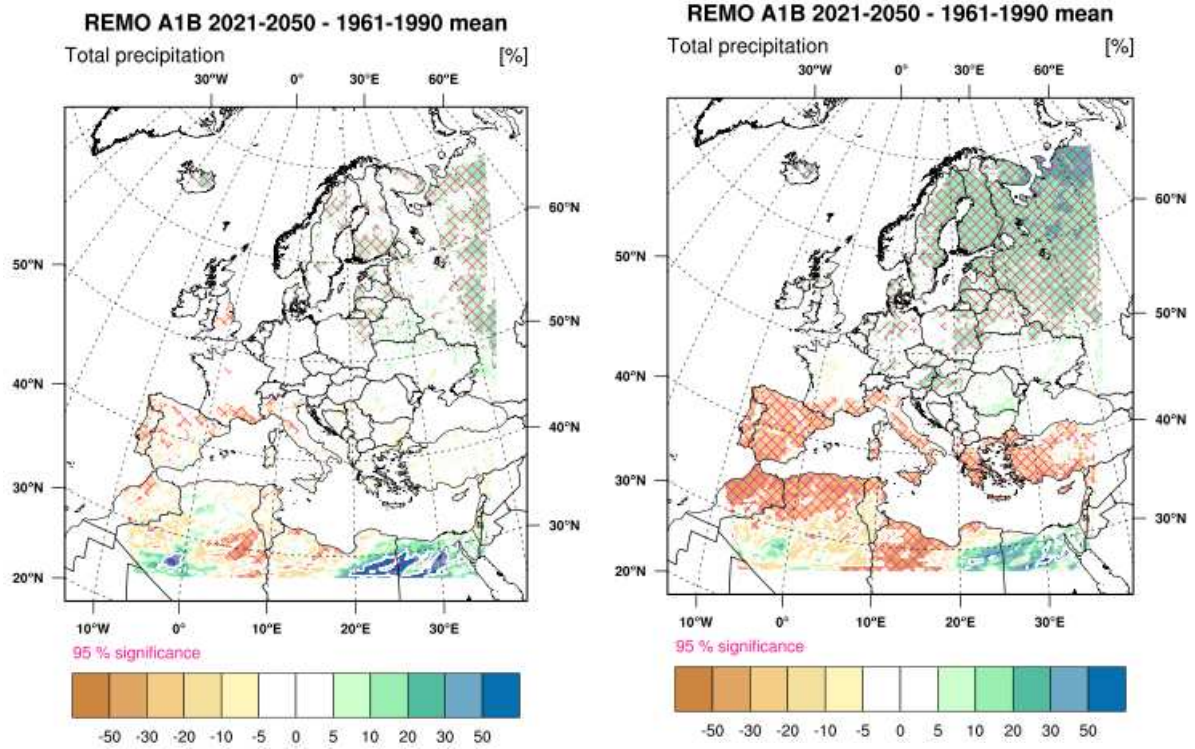


Fig. 6 Changes in yearly totals precipitation expressed in % as ratio between the Near Future and the Recent Past (Fig.6a on the left). The same but for the Far Future (Fig. 6b on the right). Simulations made under the A1B emission scenario.

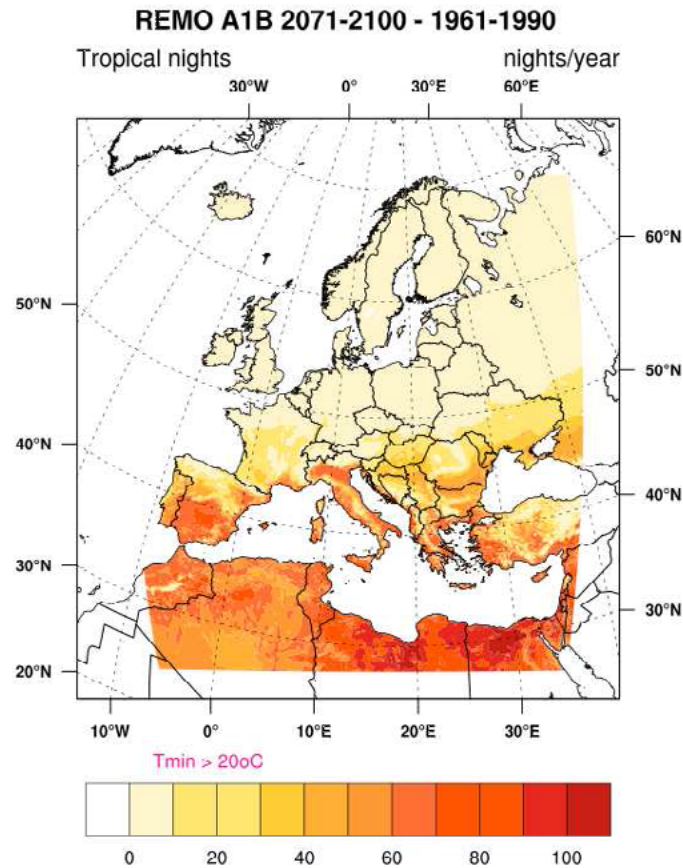


Fig. 7 Changes in number of days per year with minimum temperature exceeding 20°C calculated as a difference between the Recent Past and the Far Future. Simulations made under the A1B emission scenario.

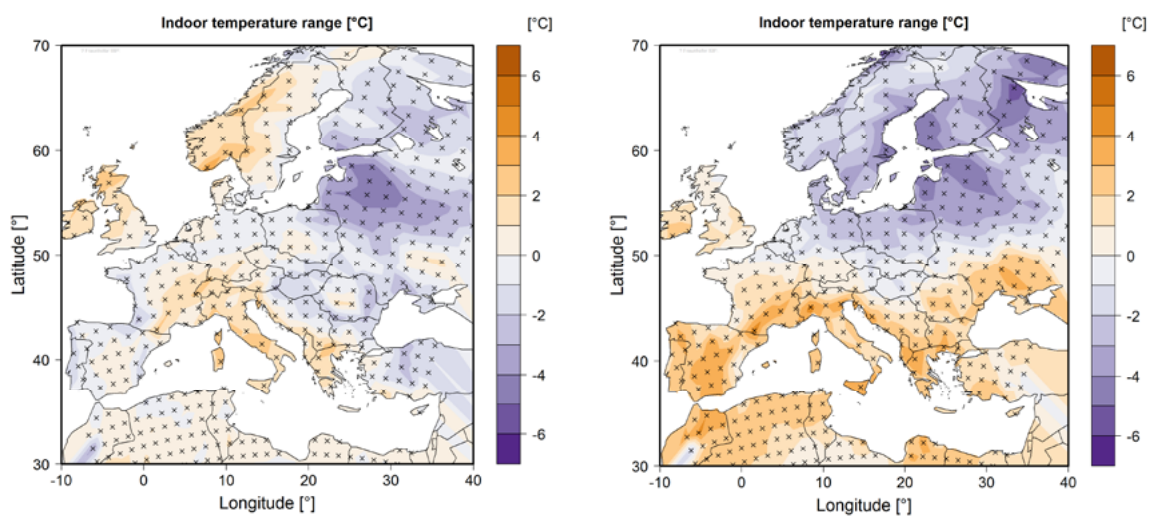


Fig. 8 Changes in yearly average of indoor air temperature range (°C) from the Recent Past to the Near Future (Fig.8a on the left side) and the same for the Far Future (Fig.8b on the right side). Simulations made under the A1B emission scenario.

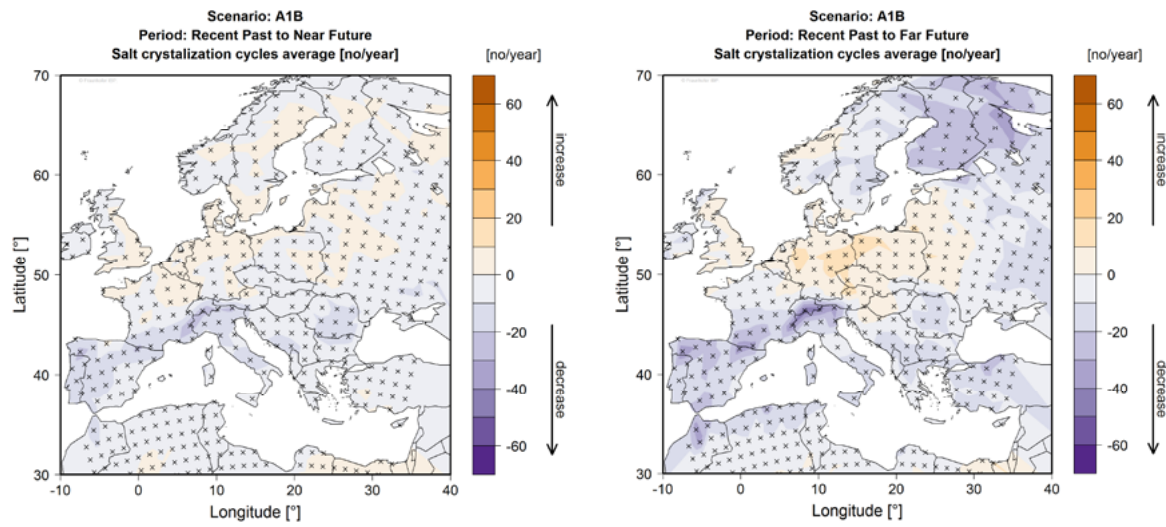


Fig. 9 Changes in yearly frequency of salt crystallization cycles from the Recent Past to the Near Future (Fig.9a on the left side) and the same for the Far Future (Fig.9b on the right side). Positive values for increasing risk; negative for decreasing.

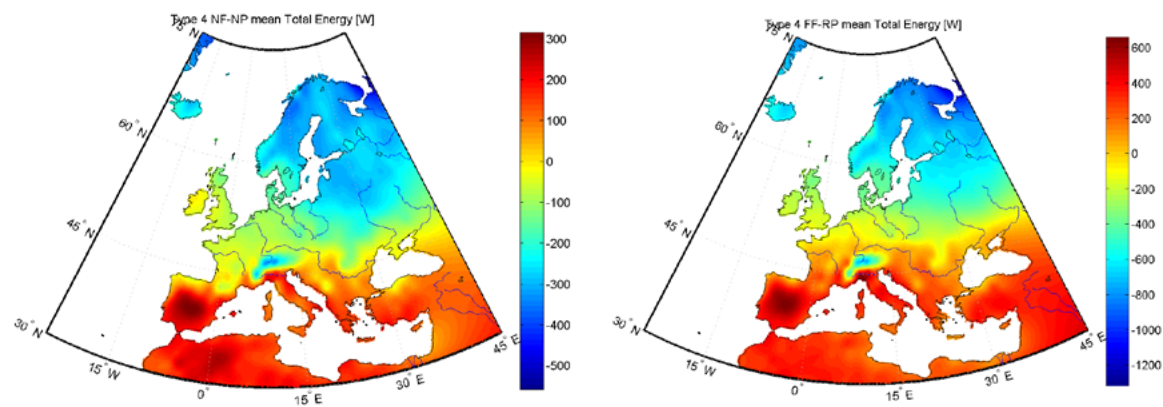


Fig. 10 Changes in energy demand (W) for a historic building with a strict climate control in the near future respect to the recent past (Fig.10a on the left) and in the far future respect to the recent past (Fig.10b on the right).

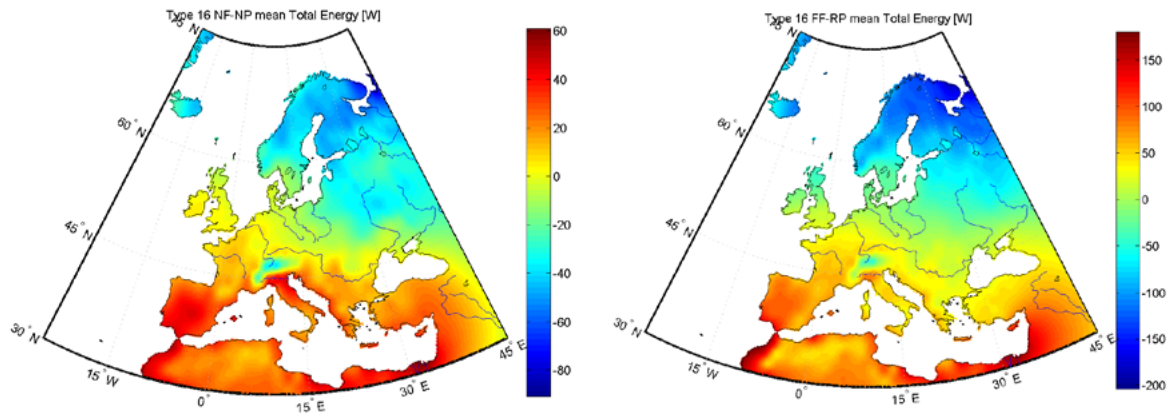


Fig. 11 Changes in energy demand (W) for a modern building envelope with a modern strict climate control in the near future respect to the recent past (Fig.11a on the left) and in the far future respect to the recent past (Fig.11b on the right).

Tab. 1 Extended nomenclature for Generic Buildings simulated within CfC Project as described in [3] - Appendix A.

	Heavyweight Building		Lightweight Building	
	Low MBP	High MBP	Low MBP	High MBP
Small Building, small window area	1	2	3	4
Small Building, large window area	5	6	7	8
Large Building, small window area	9	10	11	12
Large Building, large window area	13	14	15	16

# **Nature-based urban planning: a framework to assess the impact of green infrastructure design on ecosystem services ameliorating climate change**

**Zardo L.<sup>1\*</sup>, Geneletti D.<sup>1</sup>, Pérez-Soba M.<sup>2</sup>, Braat L.C.<sup>2</sup>,  
Van Eupen M.<sup>2</sup>, Van der Wijngaart R.<sup>2</sup>**

<sup>1</sup>University of Trento - Italy, <sup>2</sup>Alterra Research Centre, - Netherlands

\*Corresponding Author: linda.zardo@gmail.com

## **Abstract**

A well designed urban green area, coherent with the needs of the city, can foster a well-worn groove for human wellbeing. In 2013 the European Union launched, with its new Strategy for adaptation to Climate Change, a strong call for Nature-based solutions. However the application of Nature-based actions for Climate Change Adaptation in cities is still rare at European level. The main reason is the little awareness about the potential of green areas to ameliorate climate change effects. Consequently, the nature based ecosystem services in urban areas are far from being optimized. This paper presents a framework for assessing how urban green planning can enhance the delivery of ecosystem services that support climate change adaptation and improve human well-being. The framework is based on the potential capacity that different green infrastructures have for climate change adaptation depending on their physical structure and linked functions. It follows the cascade model [2] where the links between physical structure, ecosystem function and the derived benefits for human well-beings are made explicit. The framework, structured in seven steps, is applied to the urban heat island effect by analysing the influence of different green structures on climate change adaptation.

**Keywords:** climate change adaptation, urban planning, ecosystem services, Urban Heat Island, human wellbeing

## 1. INTRODUCTION

A well designed urban green area, coherent with the needs of the city, can foster a well-worn groove for human wellbeing. Nature-based actions, which imply ecosystem management and planning, have been recognized cheap, win-win and multipurpose solution by administrations and governments [5]. Scientific literature spread out in the last decade, reaching a consistent and structured state of the art in terms of definitions [8], classifications (MA, TEEB, CICES) and monetary evaluation [3; 16].

In 2013 the European Union launched its new Strategy for adaptation to Climate Change in cities which represented a strong call for Nature-based Approach application [5] and Climate Change Adaptation has been recognized as an even stronger priority than Mitigation from the last IPCC report [10]. Urban ecosystems are still a new frontier in ecosystem service research [9] because of their limited extent compared to the world's ecosystems, but talking about Climate Change Adaptation the urban environment represents the case in which the scale of the problem and the scale of possible solution do coincide. Moreover, the majority of the human beings live in cities.

At the European level, the application of Nature-based action for Climate Change Adaptation is rare and mainly represented by the creation or restoration of urban green areas [19]. Difficulties for their application come due to scarce awareness about green areas potential, thus ecosystem services provisioning is far from being optimized. There are no tools to assess and quantify effectiveness for climate change adaptation based on the impact on human wellbeing.

In particular, investigating how design can influence ecosystem services provisioning of urban green areas and how different green infrastructures represent diverse climate change adaptation potential depending on their physical structure, becomes challenging and needed.

Starting from the extended cascade model that links ecosystems to human wellbeing (see [2]), this work presents a stepwise framework for linking physical features of urban green areas to ecosystem services provisioning and impacts on Quality of Life. The goals of this study are: 1) identify key drivers for planner for optimizing green areas climate change adaptation response, making explicit the links between physical structure and derived benefits. 2) assess and quantify functioning and effects of Nature-based actions, to enable decision makers to choose between

alternatives. 3) classify urban green according to climate change adaptation potential according to Ecosystem Service provisioning. Which implies carrying the Ecosystem Service concept through the cascade model and mainstream it into the planning practice.

We present an application of the framework to the Urban Heat Island issue at European Level.

## 1.2 THE THEORETICAL FRAMEWORK

In the last decade cities are dealing with heavier and more frequent situations of urban heat island effect (UHI), flooding and water scarcity [4].

Adaptation is needed and in some places urgent. Possible approaches to adaptation can be many, but Nature-based actions save up to 50% of the cost of traditional engineeristic responses [5]. The creation, restoration and management of urban ecosystems, so green and blue areas, is the most applied action among the set of nine possible actions to adapt to climate change [19] identified by the EEA [4].

Planning can be used to make urban green deliver the right combination of Ecosystem Services (ES), in the right quantity and ratio in order to optimize the number of beneficiaries and their level of human-needs satisfaction.

No perfect green infrastructure archetype does exist: urban blue and areas are expected to provide a certain number of ES (a subset of approximately 9 of the 22 ES listed by the MA [14], but they are providing in different quantity and ratio depending on their physical features (such soil cover, tree coverage, complexity and biodiversity, ...), shape and extent.

Thus, the optimum green or blue area can only exist or be designed according to specific city and purpose, in order to optimize the supply of ES needed.

The framework here presented a stepwise process for investigating how design can influence ecosystem services provisioning of urban green areas and how different green infrastructures represent diverse climate

change adaptation potential depending on their physical structure. The paper starts from the extended cascade Model (see [2]) and translates it in into a stepwise methodology to consider ES into planning and apply the concept to both assessment and planning [Fig. 1]. There are seven components in this framework, namely:

1) Identify which are the relevant Ecosystem Services to meet the goal (e.g. climate change adaptation)

- 2) Identify the set of ecological functions providing the Ecosystem Service
- 3) Identify which physical characteristics of the ecosystem are supporting the functions
- 4) Check if there are conflicts between different uses of the physical features underlying particular ES
- 5) Assess the contribution of the different green structures for a particular ES
- 6) Investigate how shape and extent of the green and blue area influence the functioning
- 7) Highlight how the context (climatic regions, weather patterns and surroundings of a city) can influence the functioning.

The framework can be applied to the optimization of any kind of ES production (or set of ESs). To verify, assess and make consistent the framework, here an application to Climate Change adaptation is presented.

### **1.3 THE METHOD**

The application of the framework involves a multistep methodology in order to collect data from literature review and databases for fulfilling the seven components required by the process. Data analysis included also calculating and weighting data collected in order to provide synthetic information ready-to-use. Goal of data collection and analysis was to provide an order of magnitude, not specific numbers, of the impacts of actions.

#### **1.3.1 Identify which are the relevant Ecosystem Service to meet the goal**

To identify the relevant Ecosystem Services (ES) for climate change adaptation in cities, a meta-analysis was applied. A team of experts extrapolated the ES implicit in the Ecosystem-based actions for climate Change Adaptation published by the European Environmental Agency [4]. This work identified a set of ES relevant for Climate Change, divided by Climate-Change-Problem (namely, Urban Heat Island Effect, Flooding and Water Scarcity). The correspondence between the three international ES-classification systems (MA, TEEB and CICES) was analysed applying a study conducted by Maes [6] in order to bypass limitations due to terminology.

We combined the results provided by experts with the three ES classifications and 4 key-ES were determined according to the MA classification, while a set of 6 key-ES emerged from the CICES. No relevant differences between TEEB and MA were identified.

[Fig. 2] shows the correlation between Climate Change Problems and relevant ES for adaptation.

### **1.3.2 Identify the set of ecological functions providing the Ecosystem Service**

From here the work will focus on UHI and the provisioning of "local climate regulation" service. To assess the contribution of green and blue areas to urban heat island adaptation it is fundamental to identify the ecological functions through which the ES is provided.

The investigation was based on a brief literature review based on Google Scholar, using as key words: urban forests, heat island effect, green infrastructure and urban planning for climate change. According to this research, three main functions were identified:

- Shading [14; 17; 18; 1; 13; 4; 15];
- Wind sheltering [14; 18; 1; 15];
- Evapotranspiration [17; 18; 1; 4; 15].

From the literature analysed, other functions were mentioned, namely radiation reflection and heat capacity, but focusing on green and blue areas contribution to UHI mitigation, the effect of these two is negligible [11].

One more issue was represented by wind sheltering, since some sources [4; 14] cited breezes as a UHI mitigation factor. Together with "wind sheltering" function, this represents a conflict to solve.

### **1.3.3 Identify which physical characteristic of the ecosystem are supporting the functions**

"Physical features" is the terminology used in this work to define the physical components of urban ecosystems. These features are the ones enabling the ecosystem to provide the ecological functions that are relevant for UHI mitigation.

Identifying the physical features permits to understand on what planners may act to improve or better shape urban ecosystems' potential.

From the same sources used to identify the three relevant ecological functions and from the formulas applied to assess their effectiveness and working, the relevant features emerged were:

- for shading: directly linked to the presence of trees, their canopy, tree coverage, leaf area index
- for wind sheltering: directly linked to the presence of trees, their canopy, tree coverage, leaf area index, vertical complexity.
- for evapotranspiration: depending at least on two different kind of features. One directly linked to the presence of trees, their canopy, tree species and coverage, leaf area index. The other linked to soil cover and their evaporation values (or evapotranspiration, in case of crops such as grass or vegetable gardens).

So considering the information together, the features were aggregated into two categories:

- tree coverage, which is influencing the three functions. This parameter was preferred to all the others dealing with presence of trees since it is a kind of data easy to collect, compute and communicate. According to the Pareto principle, for which phenomena owe the 80% of their impact to 20% of the causes and vice-versa, to base the calculation on this information was considered enough for this stage of the work. For further and more complex version of the model, all the other information may also be computed.
- soil cover, which is influencing evapotranspiration together with the tree coverage. According to their contribution to ETA (evapotranspiration), urban ecosystems soil cover classes were organized into 5 categories. Namely, sealed, bare soil, cultivated, grass and water.

#### **1.3.4 Check if there are conflicts between physical features for the same ES**

Since the application of the theoretical framework was applied to the optimization of only on ES provisioning (local climate regulation), lots of possible conflicts were

avoided. Although presence of breeze and wind sheltering were both considered positive from the literature.

To identify this kind of conflicts and overcome them or choosing the best trade-offs. In this case, wind sheltering effect is considered positive once the statement is that the temperature of air and winds is warm [18]. Breezes are considered a positive factor if coming from cooler surroundings of the city. This leads us to consider the wind sheltering as a positive function in the computation. For taking into consideration breeze effects, we associated it with context's implications on the framework.

### **1.3.5 Assess the contribution of the different functions for the same ES**

So far the framework has been identifying the components of a Nature-based response to UHI, which is particularly useful for planner. Aim of further steps will be to assess and quantify the impacts and effects of actions.

#### **1.3.5.1 how the features deal with the function**

Focusing on shading and wind sheltering, since they depend on only one factor and their response is increasing linearly, we assigned an increasing effectiveness of these two functions according to the tree coverage values. We organized the potential response from 0 to 100%, according to a tree coverage from 0 to 100% , splitting the spectrum into 4 ranges: absence of trees, up to 30%, up to 60%, up to 100%.

Evapotranspiration depends on two factors and it was needed to assess the contribution of the two to the final ETA of the ecosystem. To do this, we used evapotranspiration values from a database collecting data from crop modelling (CGMS database from Mars Crop Yield Forecasting System (MCYFS)) for assigning values to each of the 5 classes of soil cover. We checked values for water, bare soil, grass and cultivated (computing an average values from all crops). We assumed sealed soil contribution to ETA being 0. For computing tree coverage contribution to ETA, we used data from a table published by FAO (<http://www.fao.org/docrep/x0490e/x0490e0b.htm#tabulated>) , taking into consideration Citrus and Conifers values during the summertime.

We did this computation for 6 cities (Amsterdam, Rotterdam, Madrid, Barcelona, Venice and Milan), responding to 3 different climate regions (Atlantic, Mediterranean

and Continental) , to check that even if values were different, the ranking of contribution of all factors was stable, and so it was.

#### 1.3.5.2 Aggregate the contribution on the three function into a synthetic value

To combine the three contributions of functions in one single score, representing the UHI response potential. Since these values change according to climate regions and context, we decided to keep the ratio of contribution 1/3 for each function while still dealing with general classification, for applying later adjustments according to context characteristics.

#### **1.3.6 Investigate how shape and extent of the green and blue area influence the functioning**

To complete the overall picture of ES provisioning of urban ecosystems according to their structure, physical features needed to be put together with information on shape and size of the specific area. Talking about a specific area, with a shape and a size, the provisioning contribution need to be reweighted since two different ecosystems in the same context differing on these two classes of characteristic have different behaviour in terms of provisioning.

To identify the impact of shape and extent, we based our investigation on a literature review.

Shading is not increasing in terms of effectiveness according to the size of the green area, nor wind sheltering, while evapotranspiration does [1]. So we assigned a fixed buffer of impact to shading and wind sheltering , while a more complex buffer with an inner gradient was assigned to evapotranspiration [18]. So the influence of the extent of the area to its function provisioning was organized by classifying the size in three classes: small (<1Ha), medium (1-3 Ha), large (>3 Ha).

On the contrary, shape and orientation were more affecting shading and wind sheltering, since their effect is local and dealing with wind and sun orientation. So a classification to bodies in terms of dots or ribbon was applied to this issue.

#### **1.3.7 Highlight how the context can influence the functioning**

For context analysis, experts identified three main drivers to take into account. Wind presence, cool surroundings and climate of the city. The first two are relevant to consider wind sheltering contribution, while the third for evapotranspiration. Different

behaviour of evapotranspiration were considered according to different climate regions, namely Atlantic, Continental and Mediterranean. Unlimited presence of water due to urban irrigation was assumed.

## **1.4 RESULTS AND DISCUSSION**

### **1.4.1 The green-patch typology classification**

Results from data collection and analysis, after accomplishing the first component of the framework and identifying the relevant ES to UHI, permitted to build up the green-patches typology table [Tab. 1]. This table presents on the axis the physical features (tree coverage and soil cover) and, depending on them, each patch-type presents three different scores according to its general performances in terms of shading, wind sheltering and ETA and a comprehensive one.

The table presents 20 classes of urban ecosystems and each of them is defined by a different potential contribution to UHI adaptation [Tab. 1].

### **1.4.2 Mapping benefits. A framework focused on human wellbeing**

The calculation of functions contributions enable the mapping of ES, making the provisioning spatial explicit. Thus, the values of effects of the functions and their buffers enable us to map on GIS the impact of the urban ecosystem in terms of UHI response, with gradients of contribution and potential. Overlaying this kind of map with risk maps give useful info on potential of the city and where action is needed. Combining the maps with the green-patch typology table, it can also be useful to identify easily the type of intervention needed.

From this mapping process, an inventory of city nature-based potential can be set up, classifying the urban ecosystem according to their physical characteristics and contribution to UHI mitigation. This procedure, starting from a case study, will be the first further step of this work [ Tab. 2].

### **1.4.3 context declinations of the green patch typology**

The green patch typology table is useful for identifying an order of magnitude for each type of green. This information, together with shape and extent of an area, enable to assign a UHI-response profile to a specific area, considering the areas itself in term of structure: physical features, shape and size (e.g. a park of grass,

characterized by 30% tree coverage, 3 hectares big and ribbons shape). But the same green area shows different performances in Amsterdam or Madrid, dealing with climate and surrounding situation.

Identifying the drivers of context, we choose 6 cities presenting different cases to weight and check how the general green-patch typology table is should be re-weighted. Even if the rank is stable, here the different tables are shown [Tab. 3], since this framework adopts a is no one-fit-all approach and recognize the importance of site specific considerations.

## 1.5 CONCLUSIONS

This work enable to assign a UHI response profile to each green and blue area, according to its physical characteristics and context implication. This already allow us to have an overall picture of the capital and potential of a city, to assess current situation and having tips to design a better strategy for Nature-based Climate Adaptation.

Here no aggregation is taken into consideration. Even if green and blue areas made by one single structure (one patch) do exist, a park often is made by a variety of patches and the same patch surrounded by other types of green or built capital presents different ES provisioning. More than this, according to different areas of the city (edge or core location), maybe different characteristic are providing the best performances.

Finally, considering the issue at another scale, so considering that urban ecosystems are expected to provide a variety of ES which imply different structures, an important question is if it better to find the "perfect" urban green area putting together the trade-offs or a system of different ecosystems, presenting different ES provisioning optimization, with a certain distribution.

It is evident that aggregation considerations are needed and challenging. They will be investigated and provided applying this work to a case study, starting from GIS map analysis with Quicksan (a software developed by the Alterra Research Centre for participatory decision-making), in the further steps of this research.

## 2. REFERENCES

1. Akbari et al., 1992 H. Akbari et al.; Cooling our Communities. A Guidebook on Tree Planting and Light-Colored Surfacing; EPA, Washington D.C. 20460 (1992)
2. Braat et De Groot, 2012 L.C. Braat, R.S. De Groot. The ecosystem services agenda: bridging the worlds of natural science and economics, conservation and development, and public and private policy, Ecosystem Services, Volume 1, Issue 1, Pages 4–15 (2012)
3. Costanza et al., 1997 R. Costanza et al.; The Value of the World's Ecosystem Services and Natural Capital; Nature, vol. 387, Pages 253-260 (1997)
4. EEA, 2012 European Environmental Agency; Urban adaptation to climate change in Europe. Challenges and opportunities for cities together with supportive national and European policies; EEA technical report 2/2012 (2012)
5. EU, 2013. COMMUNICATION FROM THE COMMISSION TO THE EUROPEAN PARLIAMENT, THE COUNCIL, THE EUROPEAN ECONOMIC AND SOCIAL COMMITTEE AND THE COMMITTEE OF THE REGIONS. An EU Strategy on adaptation to climate change. Brussels, 16.4.2013 COM(2013) 216 final (2013)
6. EU, 2013-b. Mapping and Assessment of Ecosystems and their Services; discussion paper; final, April 2013 (2013)
7. De Groot, 1992 R.S. De Groot. Functions of Nature: Evaluation of Nature in Environmental Planning, Management and Decision Making Wolters-Noordhoff, Groningen (1992)
8. De Groot et al., 2002 R.S. De Groot, M.A. Wilson, R.M.J. Boumans. A typology for the classification, description and valuation of ecosystem functions, goods and services, Ecological Economics, Volume 41, Issue 3, Pages 393–408 (2002)
9. Gomez and Burton, 2013 E. Gomez-Baggethun, D.N. Barton; Classifying and valuing ecosystem services for urban planning; Ecological Economics 86, Pages 235-245 (2013)
10. IPCC, 2013. IPCC; Climate Change 2013; the Fifth Assessment Report of the Intergovernmental Panel on Climate Change; Cambridge University Press, Pages 1535 (2013)
11. Lenzholzer, 2014; S. Lenzholzer (Dr. Dipl. Ing. MA (AA), Assistant professor, Wageningen University, Wageningen UR Landscape Architecture Group); oral interview; 16th June 2014 (2014)

12. MA, 2005 Millenium Ecosystem Assessment – ecosystems amd human wellbeing: synthesis. Island Press, Washington DC (2005)
13. McPhearson et al., 1997 E. G. McPhearson; Quantifying urban forest structure, function, and value: the Chicago Urban Forest Climate Project; Urban Ecosystems, 1997, 1, 49–61 (1997)
14. Oke 1988 R. T. Oke; Street Design and Urban Canopy Layer Climate; Energy and buildings 11; Pages 103-113 (1988)
15. Smith at al., 2013 P. Smith et al.; The role of ecosystems and their management in regulating climate, and soil, water and air quality; Journal of Applied Ecology 2013, 50, 812–829 (2013)
16. Stern, 2006. N. Stern; Review on the Economics of Climate Change. Executive Summary; HM Treasury; London (2006)
17. Taha et al, 1988 H. Taha et al; Residential Cooling Loads and Urban Heat Island- the effect of Albedo; Building and Environment, Vol 23, Pages 271-283 (1988)
18. Taha et al., 1991 H. Taha et al.1; Heat Island and Oasis Effects of Vegetative Canopies: Micro-Meteorological Field-Measurements; Theor. Appl. Climatol. 44, 123-138 (1991)
19. Zardo et Geneletti, 2014 Zardo L., Geneletti D., Ecosystem-based responses to climate change in cities: a review of experiences; under construction (2014)

### 3. IMAGES AND TABLES

**HOW** CAN PLANNING DO SOMETHING\_starting from the cascade model

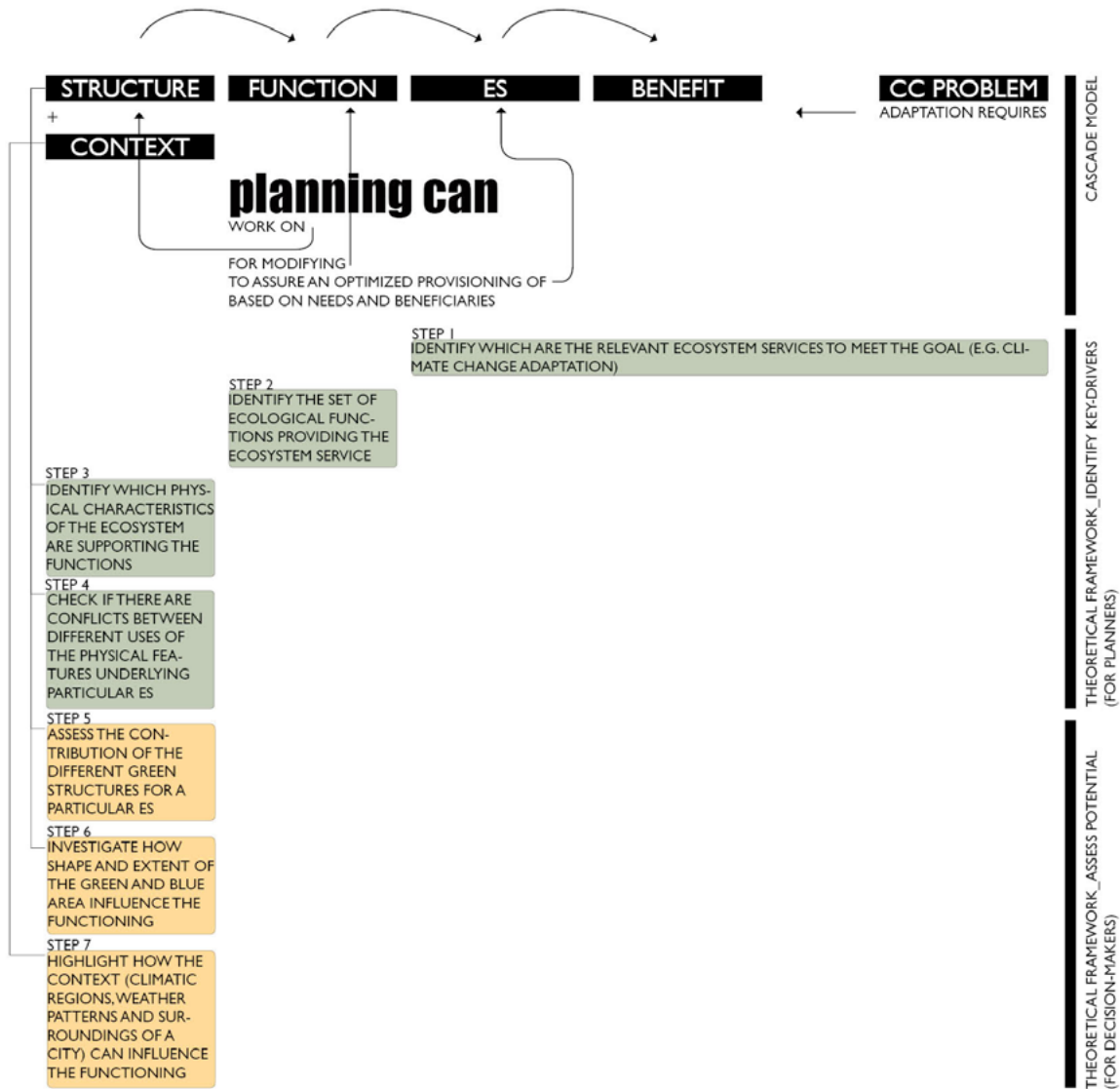


Fig. 1 The theoretical framework

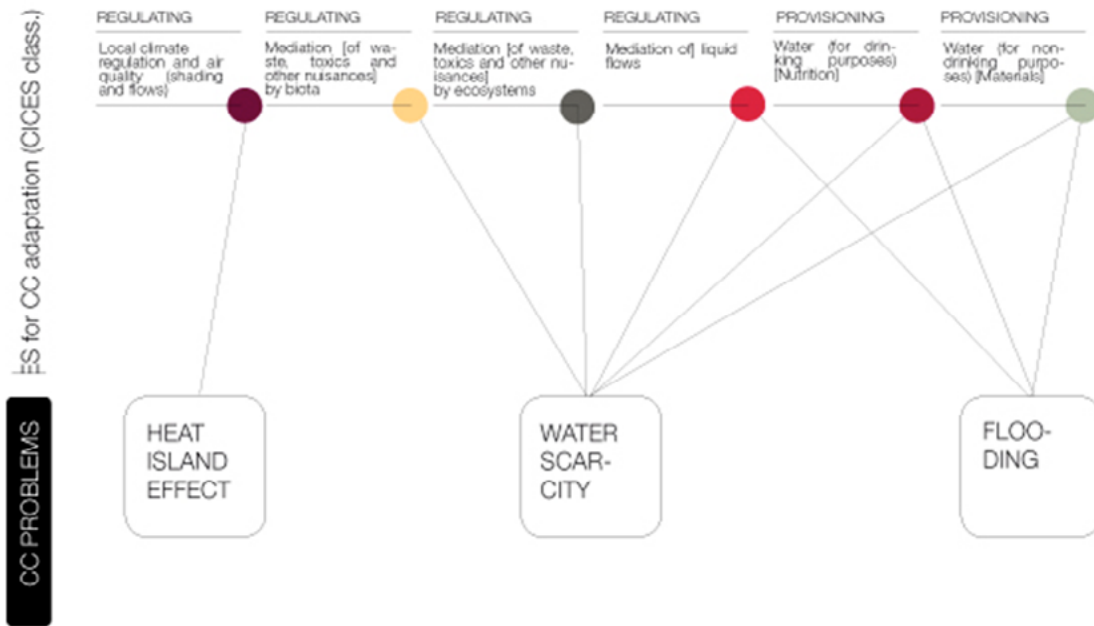
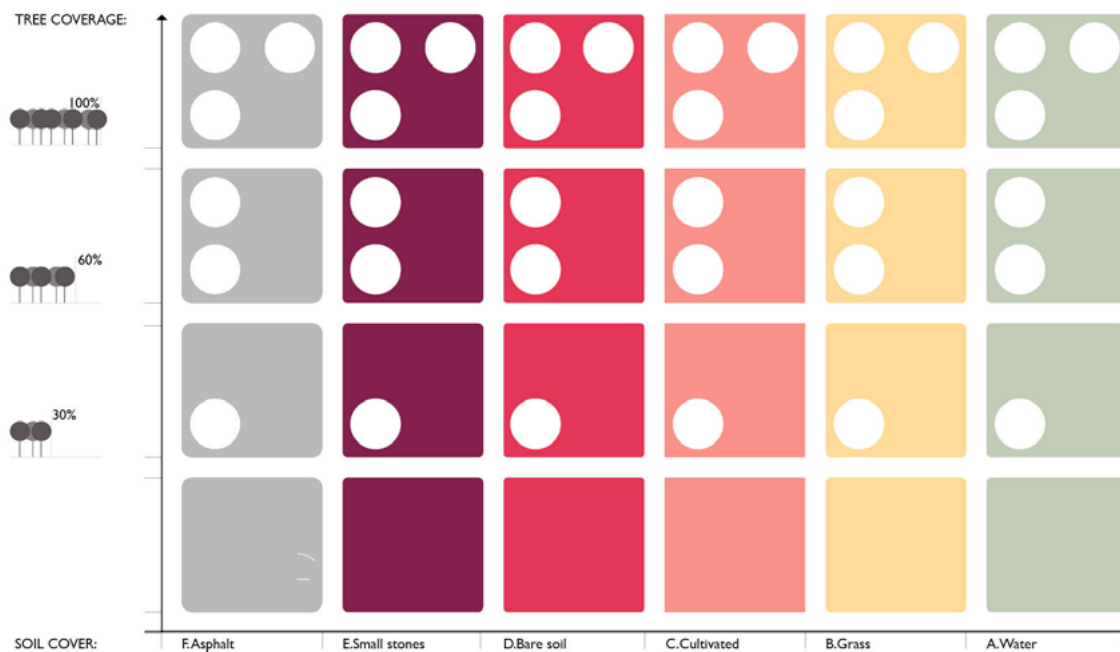


Fig. 2 Identify which are the relevant Ecosystem Service to meet the goal



Tab. 1 The green-patch typology classification (still under construction)



Tab. 2 Inventory of the natural capital of Amsterdam, classified by green-patch type and linked potential for Nature-based climate Adaptation (UHI) (still under construction)

### UNDER CONSTRUCTION

Tab. 3 “The green-patch typology classification” declinations for different contexts (Amsterdam, Rotterdam, Barcelona, Madrid, Venice, Milan)

# GLOSSARY

ECOSYSTEM-BASED ACTIONS = NATURE-BASED ACTIONS

URBAN ECOSYSTEM = URBAN GREEN INFRASTRUCTURE = URBAN GREEN (AND BLUE) AREAS: ALL NATURAL AND SEMI-NATURAL AREAS IN A CITY

URBAN GREEN PATCH: A UNIT OF URBAN GREEN (AND BLUE) AREA CHARACTERIZED BY AN HOMOGENEOUS STRUCTURE. THERE ARE NO LIMITATIONS IN TERMS OF SURFACE FOR A UNIT, BUT IT NEEDS TO PRESENT ONLY ONE STRUCTURE. AN URBAN GREEN AREA CAN BE MADE BY A UNIQUE PATCH OR A VARIETY OF THEM

(ECOLOGICAL) FUNCTIONS: THE CAPACITY OF NATURAL PROCESSES AND COMPONENTS TO PROVIDE GOODS AND SERVICES THAT SATISFY HUMAN NEEDS, DIRECTLY OR INDIRECTLY' (DE GROOT, 1992). EACH FUNCTION IS THE RESULT OF THE NATURAL PROCESSES OF THE TOTAL ECOLOGICAL SUB-SYSTEM OF WHICH IT IS A PART. ALSO REFERRED TO IN THE LITERATURE AS POTENTIAL ECOSYSTEM SERVICES, OR THE POTENTIAL SUPPLY OF SERVICES. NATURAL PROCESSES, IN TURN, ARE THE RESULT OF COMPLEX INTERACTIONS BETWEEN BIOTIC (LIVING ORGANISMS) AND ABIOTIC (CHEMICAL AND PHYSICAL) COMPONENTS OF ECOSYSTEMS THROUGH THE UNIVERSAL DRIVING FORCES OF MATTER AND ENERGY (DE GROOT ET AL., 2002)

(ECOSYSTEM/GREEN AREA) PHYSICAL FEATURES: PHYSICAL COMPONENTS OF THE URBAN GREEN AREA RELEVANT FOR ITS FUNCTIONING AND ECOSYSTEM SERVICE PROVISIONING (E.G. FOR URBAN HEAT ISLAND ADAPTATION THE PHYSICAL FEATURES ARE SOIL COVER AND TREE COVERAGE)

(ECOSYSTEM/GREEN AREA) STRUCTURES: (ECOSYSTEM/GREEN AREA) PHYSICAL FEATURES + SHAPE + EXTENT OF A SPECIFIC URBAN GREEN AREA

URBAN GREEN PATCHES TYPOLOGY TABLE: CLASSIFICATION OF URBAN GREEN PATCHES ACCORDING TO THEIR PHYSICAL FEATURES WHICH ARE CONSIDERED RELEVANT FOR THEIR FUNCTIONING (AND CONSEQUENTLY FOR THE ECOSYSTEM SERVICE PROVISIONING). THE TABLE PRESENTS 20 TYPES

ECOSYSTEM SERVICES ARE ECOLOGICAL FUNCTIONS WHICH ARE ACTUALLY USED, CONSCIOUSLY OR NOT, ON PURPOSE OR NOT, BY HUMANS. SO, INFACIT, CLIMATE REGULATION IS AN ECOLOGICAL FUNCTION OF GREEN INFRASTRUCTURE, WHICH IS ALWAYS USED, BUT THE PEOPLE BENEFITTING FROM THAT MAY DIFFER PER LOCATION

BENEFITS ARE THE RESULTS OF ECOSYSTEM SERVICES

Fig. 3 Glossary

# Future impacts of climate change on sectoral electricity demand

Enrica De Cian<sup>1\*</sup>, Ian Sue Wing<sup>2</sup>

<sup>1</sup>Fondazione Eni Enrico Mattei, Italy, <sup>2</sup>Boston University, USA

\*Corresponding Author: [enrica.decian@feem.it](mailto:enrica.decian@feem.it)

## Abstract

This paper estimate the impact on sectorial electricity demand of future changes in temperature and humidity at global scale. We use a statistical model to infer the sensitivity of sectoral electricity demand to historical variation in daily mean temperature and humidity levels. The short- and long-run response to historical variation in exposure to hot, cold, and humid days provides insight into the potential impacts of climate change on electricity use and into the adaptation responses along the intensive and extensive margin. The paper explores uncertainty in climate projections by considering the risk posed by future exposure to high and low temperature and high humidity in the decade around 2050 as projected by five Global Circulation Models (GCMs). We examine the consequences of these climatic shifts on future electricity demand by combining Representative Concentration Pathway (RCP) warming scenarios and shared socioeconomic pathways (SSPs) for population and income growth. Our results highlight the importance of another indicator of comfort, relative humidity. We also show that using short-term elasticities to infer future changes in electricity use underestimates the potential of adaptation. Especially the response to humidity occurs on the extensive margin, over a longer period of time.

**Keywords:** Electricity demand, climate change, adaptation, sectors, global.

## 1. INTRODUCTION

Energy from fossil fuels is the main source of greenhouse gas emissions, which have caused the changes in climate we are already observing [1]. Energy supply and demand are also directly exposed to changes in weather and climate conditions. Since with increasing mean temperature the energy use for heating could very likely decline whereas the energy use for cooling could increase, it is not clear whether energy will eventually decline or increase. This paper focuses on the future potential impacts of climate change on the electricity demand of four sectors, residential, agriculture, industry, and commercial and public services. Various sectors of the economy will change their electricity use both as a response to socio-economic factors as well as to the changes in the climate system. Our analysis makes an attempt to separate the contribution of these two factors.

Residential demand will likely change as hot days and nights will become more frequent [1] and significant changes can be observed especially in shoulder seasons, such as spring [2]. Other fuels are used in many countries as primary fuels for heating, such as gas or oil products, and electricity heaters are generally used as temporary solutions when the main heating system is switched off. Electricity use will likely change also in the agriculture sector. Besides responses to address heating and cooling needs, agriculture includes other activities that are electricity-intensive and that could be influenced by climate change via the water cycle, such as water lifting, pumping, and desalinization [3]. By modifying the water cycle, climate change could also indirectly affect the electricity used to collect and distribute water in the commercial and public services (e.g. water supply, collection, and treatment) both in short-run and in the long-run [4]. Together with the residential sector, commercial and public services, which includes transportation, public administration, education, health, tourism, entertainment and recreation, financial sector, can be expected to be quite responsive in terms of demand for heating and cooling needs.

as well as in industry can be expected to be sensitive to short-run and long-run meteorological fluctuations.

Prior studies looking at the impacts of climate change on energy demand have mostly focused on the residential use of electricity [5], gas, and oil products [2].

Another group of studies have examined changes in electricity demand as a mean to cope with climate change impacts on health ([6,7]). Especially on global scale, less attention has been paid to the response of electricity demand by other sectors. Moreover, existing studies have focused on temperature, both in terms of heating and cooling effects, but less attention has been paid to the role of humidity. This gap is partly due to the lack of historical data on humidity variables, which have now become available from reanalysis projects.

The short- and long-run response to historical variation in exposure to hot, cold, and humid days provides insight into the adaptation responses adopted by final users along the intensive and extensive margin. Most studies though have used fitted short-run responses to infer future potential of adapting to changes in temperature levels, underestimating the potential of adaptation, or overestimating the impacts of climate change [8]. Short-term elasticities identified using inter-annual weather variation only capture adaptation responses on the intensive margin, that is the change in electricity use given a certain stock of equipment and appliances. Ignoring changes in the stock of electricity-intensive capital stock tends to underestimate changes in future electricity consumption [9]. On macro scale, the dichotomy between intensive and extensive margin can be addressed by specifying an error correction model, which allows differentiating the short- and long-run responses to weather shock ([10], [2]). This is the approach we follow in this paper.

## **2. DATA DESCRIPTION AND EMPIRICAL MODEL**

We use data on sectoral electricity demand at country level from 1961 to 2010 from the International Energy Agency (IEA) database<sup>1</sup>. The database covers about 85 countries, depending on the sector, and it is thus an unbalanced panel. Daily gridded temperature and specific humidity data are from the NOAA 20th Century Reanalysis [11].

Relative humidity is an important metric used in weather forecasts as it is a better indicator of heat stress than specific humidity because it takes into account the evaporative cooling that occurs through perspiration of the skin. While specific humidity indicates the quantity of water vapor to unit mass of dry air (in g/kg), relative

---

<sup>1</sup> Accessed on November 2012.

humidity takes into account the effect of temperature on the holding capacity of the air. It is defined as the actual water in the air relative to the amount of water that mass of air can hold before saturation at a given temperature, and it is expressed in percentage terms. The mean daily temperature and humidity data enter the statistical model as number of days in a given temperature or humidity category (bin), in a given country, year. To match the different spatial resolution of the IEA and NOAA statistics, gridded population data<sup>2</sup> is used to spatially aggregate the annual frequencies of days in the various temperature and humidity bins to the country level while maintaining the heterogeneity within countries. More precisely, we weight the values of the climate variables in each cell with the share of population normalized with respect to the total population of a country<sup>3</sup>. Gross Domestic Product (GDP) per capita is computed using data on real Purchasing Parity Power (PPP) converted GDP and population from the Penn World Tables version 7 [12].

Table 1 summarizes the descriptive statistics of the energy and socio-economic variables for the world, tropical, and temperate regions<sup>4</sup>. The mean value of all indicators reported in Table 1 exceeds the median, pointing at the presence of few large electricity users, both in tropical and temperate regions. Industry and residential are the top user sectors. In percentage terms, the use of electricity in agriculture is relatively higher in tropical countries (17% as opposed to the 2% in temperate regions).

[Tab. 1 about here]

We estimate short- and long-run elasticities using an Error Correction Model (ECM), see Eq. (1). The dependent variable, electricity demand in the four different sectors,

---

<sup>2</sup> Center for International Earth Science Information Network - CIESIN - Columbia University, International Food Policy Research Institute - IFPRI, The World Bank, and Centro Internacional de Agricultura Tropical - CIAT. 2011. Global Rural-Urban Mapping Project, Version 1 (GRUMPv1): Population Count Grid. Palisades, NY: NASA Socioeconomic Data and Applications Center (SEDAC). <http://sedac.ciesin.columbia.edu/data/set/grump-v1-population-count>.

<sup>3</sup> It is important to mention that population data refer to the year 2005 and therefore the same weight is assumed throughout the time period considered.

<sup>4</sup> The distinction between temperate and tropical-subtropical regions is based on the climate zones as classified by Koeppen-Geiger climate zones. When more than one climatic zone appear in a country, the prevailing one is considered.

is modeled as a function of the disequilibrium deviation from the long-run relationship and of the short-run changes in the other explanatory variables:

$$\Delta \ln y_{i,t} = \alpha_i + \eta' \Delta X_{i,t} + \sum_{k=1}^K \beta_1^k \Delta T_{i,t}^k + \sum_{j=1}^J \beta_2^j \Delta RH_{i,t}^j + \gamma \left[ \ln y_{i,t-1} - \lambda' X_{i,t-1} - \sum_{k=1}^K \theta_1^k T_{i,t-1}^k - \sum_{j=1}^J \theta_2^j RH_{i,t-1}^j \right] + \varepsilon_{i,t} \quad (1)$$

Here,  $y_{i,t}$  indicates the sectoral electricity demand in country  $i$  and year  $t$ . The weather variables  $T_{i,t}^{k,m}$  and  $RH_{i,t}^{j,m}$  are annual counts of days with average temperature in interval  $k$  and relative humidity in interval  $j$ .  $X$  is a vector of socio-economic variables (real per capita gross domestic product and population) which control for the effects of potentially confounding historical demand side factors to changing climate and weather. On the right-hand side,  $\alpha_i$  is a country-specific intercept that captures the influence on electricity demand of unobserved heterogeneous time-invariant factors, the  $\Delta$  terms capture the short-run effects of inter-annual shocks, the deviation from the long-run equilibrium relationship between electricity demand and meteorology is given by the term in square brackets, and  $\varepsilon_{i,t}$  is a random disturbance term. The error-correction speed of adjustment parameter,  $\gamma$ , measures countries' average rate of adjustment toward the long-run equilibrium. The electricity demand response to weather is indicated by the vectors of short-run semi-elasticity parameters  $\beta_1$  and  $\beta_2$ , and to climate by the vectors of long-run semi-elasticity parameters  $\theta_1/-\gamma$  and  $\theta_2/-\gamma$ . Eq. (1) is estimated separately for each sector. The identification strategy relies on inter-annual variability, but the error correction model also estimates the long-run response, which is the cumulative effect during the adjustment period until the system returns to the long-run equilibrium.

### 3. ESTIMATED RESPONSE OF SECTORAL ELECTRICITY DEMAND

Table 2 shows the short-run and long-run estimated semi-elasticities of humidity and temperature bins and the elasticities of per capita GDP and population<sup>5</sup>. The nonparametric approach attempts to characterize the entire distribution of temperature and relative humidity by binning daily averages into a given number of categories. Our results indicate that the intermediate categories (between 12.5

<sup>5</sup> Complete regression results are reported in Table A1.

degree Celsius and 27.5 degree Celsius) not shown in Table 2 are not statistically significant. Only the temperature and humidity categories that are far enough from the average conditions, captured by the fixed effect term, are found to be associated with a statistically significant increase in electricity use, relative to the omitted intermediate categories.

Table 2 shows how the long-run response to a change in the frequency of hot, cold and humid days differs from the short-run sensitivity. Results are sector-specific and asymmetric on the heating (days with mean below 12.5°C) and cooling (days with mean above 17.5°C) arm. For example, an increase in the frequency of days with mean temperature between 2.5 and 10 degree Celsius raises residential electricity demand more than an increase in exposure to warm days. The reverse pattern is observed for agriculture. The industry and commercial sectors show higher electricity use only for low temperature categories, but the commercial sector is also sensitive to high humidity levels.

The error correction coefficient (the coefficient of the variable  $L.\lnely$  in Table A1, which correspond to  $\gamma$  in Eq. 1) is significant and negatively signed in all sectors considered. The commercial sector has the largest speed of adjustment, while agriculture the smallest. While all sectors adapt to changes in temperature both in the short-run and in the long-run, the response to relative humidity occurs mostly on the extensive margin, as the response to changes in humidity exposure is statistically significant only in the long-run. An increase in the frequency of humid days raises electricity use in the residential and commercial sectors. Conversely, the agriculture sector reduces the use of electricity, as higher humidity levels are correlated with higher precipitations and can be associated with less requirements for irrigation, a major source of electricity use in agriculture in some countries.

The analysis controls for the effect of real GDP per capita and population, which both drive electricity demand in all sectors. Residential and commercial electricity demand shows a higher elasticity to per capita GDP compared to industry and agriculture while agriculture electricity demand has the highest elasticity to population.

[Table 2 about here]

In the next section we use the estimated long-run semi-elasticities and elasticities to compute the future change in electricity demand around 2050 in a scenario of high warming and fast economic growth.

#### 4. FUTURE CHANGES IN ELECTRICITY SECTORAL DEMAND

Climate change impacts are assessed by combining the estimated long-run response (Table 2) with the RCP 8.5 W/m-2 climate scenario [13] simulated by an ensemble of five climate models in the CMIP5 project [14], listed in Table A2. Using each model's results, we define the change in frequency of days in a given temperature and humidity bin for all bins at the grid cell level, and weigh the change in frequencies in each cell by the normalized share of population to obtain population-weighted change in exposure. Future climate (henceforth 2050) is defined as the decadal mean in climate variable realizations between 2046 and 2055, current climate as the decadal mean between 2006 and 2015 (henceforth present)<sup>6</sup>. We compute the future baseline sectoral electricity demand by combining the estimated elasticities to real per capita GDP and population with the projections from the Shared Socio-Economic Pathways (SSP, [15], [16]). We consider the SSP5 scenario, which is characterized by fast growth in per capita income and is associated with a global emission profile that could lead to a global warming of 8.5 W/m-2.

Electricity demand will grow significantly because of population and real per capita GDP growth. Table 3, top panel, shows the baseline electricity mix as of today (current) and as projected in 2050 in the SSP5 scenario (future). Tropical countries will increase their electricity demand by 253%, as opposed to the +138% observed in temperate regions. The leading sector will be the commercial and building sector, with a growth rate of 482% and 223%, respectively. This sector will take over industry and it will account for the largest share in the future electricity use mix.

---

<sup>6</sup> An average representative year for each 10 year period was created by taking the mean of each climate variable on each day. As various models differed in their handling of leap years, the 29th of February was excluded when reported by the model. The representative year was then used for binning. This is an important distinction between binning each year and then taking the average of the "10 binned years". The latter method could include more extreme values.

The climate change-induced change in electricity demand is reported in the lower part of Table 3. Globally, electricity demand will decline when considering the multi-model mean, though the distribution of country-model realization is quite widespread and more than 50% realizations are characterized by an increase in total electricity use. The increase will be mostly driven by the higher demand in the residential and commercial sectors, mostly in tropical countries, see also Figure 1 left panel.

[Table 3 about here]

Figure 1 (left) highlights the different response of electricity use in tropical and temperate regions across the different sectors. The response of residential demand is the most different in the two areas. In tropical regions it will increase between 11 and 37%. In temperate regions it will vary between 0 and -14%. In both areas the response of electricity use in agriculture is the most uncertain across different model realizations. It could increase significantly in both regions, up to +45%.

We evaluate the bias of neglecting the role of future changes in relative humidity by computing the change in future electricity demand induced only by temperature, which is shown in Figure 1, right panel. The bias is particularly clear for agriculture and the commercial sector. When considering only the future change in exposure to hot and cold days, electricity use in the commercial sector would decline, whereas humidity can induce an increase up to about 5%. Note also that adding the effect of humidity expands the uncertainty range.

[Figure 1 about here]

Figure 2 shows the percentage change in sectoral electricity demand in the top electricity user countries along with the share of each sector in the current electricity use mix. In tropical countries (Saudi Arabia, Mexico, and Brazil) the total demand of electricity (purple line) will increase in 2050 in all climate model realizations due to the expansion observed in the residential sector (blue line). In a second group of countries including the US, Turkey, Spain, Japan, and India, the aggregate demand

of electricity always declines, but the similar aggregate pattern hides heterogeneous sectoral responses. For example, the reduction observed in India is driven by the commercial and agriculture sector, which in this country has a relatively large share (Figure 2 left panel), while the Indian residential sector increases the use of electricity, as most tropical countries. The reduction observed in the US is the result of similar patterns in the residential and commercial sector, though an increase in the residential demand cannot be excluded in some climate realizations. Increases in sectoral electricity demand could also be observed in the Turkish and Iranian agricultural sector, and in the Spanish and Iranian commercial sector.

[Figure 2 about here]

## 5. DISCUSSION

This paper contributes to the literature on climate change and energy demand by estimating the impact on sectorial electricity demand of future changes in temperature and humidity at global scale. It adds evidence on the importance of other indicator of comfort, relative humidity. Moreover, it explores the uncertainty in GCM projections by computing the impacts on electricity demand considering the exposure pattern projected by five GCMs. It shows that that the uncertainty in GCM projections can be significant and it varies by country and sector, as it can be amplified by the estimated sensitivity patterns.

Auffhammer and Mansur [8] discuss the risk of overestimating the impacts of climate change when using short-term elasticities identified from the inter-annual weather variation, as this response would only capture adaptation responses on the intensive margin. This paper confirms that short-run elasticities underestimates the ability of countries to adapt to temperature and humidity variations. Moreover, since vulnerability results from the interaction between exposure and sensitivity, using short-run elasticities would also underestimate the uncertainty range of climate change impacts.

The future baseline increase in global electricity demand will be driven by tropical countries, including major emerging economies such as India and Brazil, and we find that climate change could push the increase even more, especially in the residential and agriculture sector. The 2013 World Energy Outlook puts under the spotlight India

and Brazil as two economies where energy demand will increase faster than in other regions and where issues related to energy access and climate change impacts will deserve particular attention. Our results suggest that future warming could increase residential demand for electricity by between 5 and 18% in India. In Brazil the increase in residential electricity demand ranges between 24% and 55%. Significant changes could occur also in the commercial sector of temperate countries, whereas the smallest effects are found for the industry sector. As discussed in [5], our study finds that future climate change could thus increase the electricity bill and mitigation challenge in lower income levels, whereas the reverse could occur in higher income, temperate regions.

## 6. ACKNOWLEDGMENTS

The research leading to these results has received funding from the People Programme (Marie Curie Actions) of the European Union's Seventh Framework Programme (FP7/2007-2013) under the REA grant agreement n° 298436.

## 7. REFERENCES

1. IPCC, 2013: Summary for Policymakers. In: Climate Change 2013: The Physical Science Basis. Contribution of Working Group I to the Fifth Assessment Report of the Intergovernmental Panel on Climate Change [Stocker, T.F., D. Qin, G.-K. Plattner, M. Tignor, S.K. Allen, J. Boschung, A. Nauels, Y. Xia, V. Bex and P.M. Midgley (eds.)]. Cambridge University Press, Cambridge, United Kingdom and New York, NY, USA.
2. De Cian E., Lanzi E., Roson R., (2012). Seasonal temperature variations and energy demand. A panel cointegration analysis for climate change impact assessment. *Climatic Change* 116, 805-825 .
3. Bazilian M., et al. (2011). Considering the energy, water and food nexus: Towards an integrated modelling approach, *Energy Policy* 39, 7896–7906.
4. Howell, M. and H.H. Rogner (2014). Assessing Integrated Systems, *Nature Climate change* 4.
5. Isaac and D. van Vuuren (2009). Modeling global residential sector energy demand for heating and air conditioning in the context of climate change, *Energy Policy* 32, 507–521.
6. Barreca, A.I. (2012). Climate change, humidity, and mortality in the United States. *Journal of Environmental Economics and Management* 63, 19–34.

7. Deschênes, O., M, Greenstone (2011). Climate Change, Mortality, and Adaptation: Evidence from Annual Fluctuations in Weather in the US. *American Economic Journal: Applied Economics* 3, 152-185.
8. Auffhammer, M. E. Mansur (2012). Measuring Climatic Impacts on Energy Expenditures: A Review of the Empirical Literature. Working Paper, submitted to *Energy Economics*.
9. Sailor, D. J., A.A. Pavlova (2003). Air Conditioning Market Saturation and Long- Term Response of Residential Cooling Energy Demand to Climate Change. *Energy* 28, 941-951.
10. Masish A.M.M., Masish R. (1996). Energy consumption, real income and temporal causality: results from a multy-country study based on cointegration and error-correction modeling techniques. *Energy Economics* 18,165–183.
11. Compo, G.P. et al. (2011). The Twentieth Century Reanalysis Project. *Quarterly Journal of Royal Meteorology Society* 137, 1-28. Accessed June 2013.
12. Heston, A., Summers, R., and Atenm, B. (2013). Penn World Table Version 7.1 Center for International Comparisons of Production, Income and Prices at the University of Pennsylvania.
13. Van Vuuren, D. P. et al. (2011). The representative concentration pathways: an overview. *Climatic Change* 109, 5–31.
14. Taylor, K. E., Stouffer, R. J. and Meehl, G. A. (2012). An overview of CMIP5 and the experiment design. *Bulletin of American Meteorology Society* 93, 485–98.
15. Kriegler, E., et al. (2012). The need for and use of socio-economic scenarios for climate change analysis. *Global Environmental Change* 22, 807–822.
16. IIASA (2013), International Institute for Applied Systems Analysis (IIASA) SSP Database (Version 9 downloaded on November 3 2013) <https://secure.iiasa.ac.at/web-apps/ene/SspDb/>

## 8. IMAGES AND TABLES

World	Agriculture	Commercial	Residential	Industry	TFC	TFC per capita	Pop	Per capita GDP
Unit	Ktoe	Ktoe	Ktoe	Ktoe	Ktoe	GJ	('000)	(2005USD)
Obs	2776	3956	4389	4454	4588	4187	4187	4187
Median	66	201	301	426	902	4	11317	3673
Mean	356	1953	2227	3656	7879	10	47737	8122
Temperate	Agriculture	Commercial	Residential	Industry	TFC	TFC per capita	Pop	Per capita GDP
Obs	1785	1940	2124	2205	2242	2060	2060	2060
Median	88	675	876	1466	2997	11	10757	6921
Mean	386	3593	4029	6555	14229	16	51327	11454
Tropical	Agriculture	Commercial	Residential	Industry	TFC	TFC per capita	Pop	Per capita GDP
Obs	991	2016	2265	2249	2346	2127	2127	2127
Median	20	57	96	107	298	1	11633	1824
Mean	302	375	537	813	1811	4	44260	4894

Tab. 1 Descriptive statistics. TFC = Total Final electricity Consumption

		<b>Long-run</b>			
		Res	Agr	Comm	Ind
Per capita GDP (2005US\$)		<b>0.4391</b>	<b>0.3478</b>	<b>0.7327</b>	<b>0.3211</b>
Population		<b>1.3553</b>	<b>1.8910</b>	<b>1.5522</b>	<b>1.2257</b>
Temperature (°C)	<2.5	<b>0.0093</b>	0.0109	<b>0.0098</b>	0.0044
	2.5-5	<b>0.0096</b>	<u>0.0188</u>	<b>0.0086</b>	<b>0.0116</b>
	5-7.5	0.0065	<b>0.0195</b>	0.0089	<b>0.0104</b>
	7.5-10	<b>0.0076</b>	<b>0.0315</b>		
	10-12.5	0.0046			
	17.5-20		<b>0.0256</b>		
	25-27.5		<b>0.0096</b>		
	>27.5	<b>0.0044</b>			
Relative humidity (%)	70-90	<b>0.0054</b>	-0.0123		
	>90	<b>0.0104</b>	<u>-0.0305</u>	<u>0.0183</u>	-0.0037
		<b>Short-run</b>			
		Res	Agr	Comm	Ind
Per capita GDP (2005US\$)		<b>0.1494</b>	<b>0.2838</b>	<b>0.1862</b>	<b>0.2707</b>
Population		<b>0.6583</b>	<b>1.9180</b>	<b>1.1033</b>	0.3854
Temperature (°C)	<2.5	0.0003	-0.0001	<b>0.0008</b>	0.0004
	2.5-5	<b>0.0005</b>	0.0001	<b>0.0008</b>	<b>0.0007</b>
	5-7.5	<u>0.0004</u>	0.0000	0.0002	0.0004
	7.5-10	<b>0.0004</b>	0.0009		
	10-12.5	<b>0.0003</b>			
	17.5-20		<u>0.0011</u>		
	25-27.5		<b>0.0006</b>		
	>27.5	<b>0.0002</b>			
Relative humidity (%)	70-90	<u>0.0002</u>	-0.0006		
	>90	0.0001	<b>-0.0021</b>	0.0019	-0.0003

Tab. 2 Estimated long-run and short-run responses of electricity demand to changes in historical exposure in population-weighted meteorological variables and economic activity. Bold italic estimates are significant at the 5% level. Underlined estimates are significant at the 10% level.

Current electricity mix			Future electricity mix (SSP5)	
	Tropical	Temperate	Tropical	Temperate
Agr	0.69	0.80	2.67	1.74
Comm	1.69	11.58	9.84	37.36
Ind	3.53	19.61	8.67	37.50
Res	2.70	12.70	9.19	29.70
Total	8.61	44.69	30.37	106.30
Change from current baseline, RCP 8.5 (EJ)			Change from future baseline, RCP 8.5 (EJ)	
	Tropical	Temperate	Tropical	Temperate
Agr	0.076	0.11	0.13	0.30
	[-0.09-0.24]	[-0.19-0.35]	[-0.43-0.92]	[-0.4-0.78]
Comm	-0.033	-1.47	-0.16	-4.66
	[-0.1-0.07]	[-2.64-0.43]	[-0.51-0.46]	[-7.97-1.39]
Ind	-0.046	-0.65	-0.12	-1.10
	[-0.07--0.03]	[-1.36-0.05]	[-0.16--0.07]	[-2.45-0.26]
Res	0.739	-1.15	2.37	-2.39
	[0.36-1.08]	[-1.88--0.18]	[1.04-3.4]	[-4.01--0.13]
Total	0.735	-3.15	2.22	-7.85
	[0.38-1.18]	[-5.37--0.71]	[0.78-3.75]	[-13.52--0.32]

Tab. 3 Current and future (SSP5) baseline sectoral electricity use (top) and future change due to climate change (RCP8.5, SSP5 GDP) in 2050 according to the multi-model mean pattern of exposure. In brackets minimum and maximum values are reported.

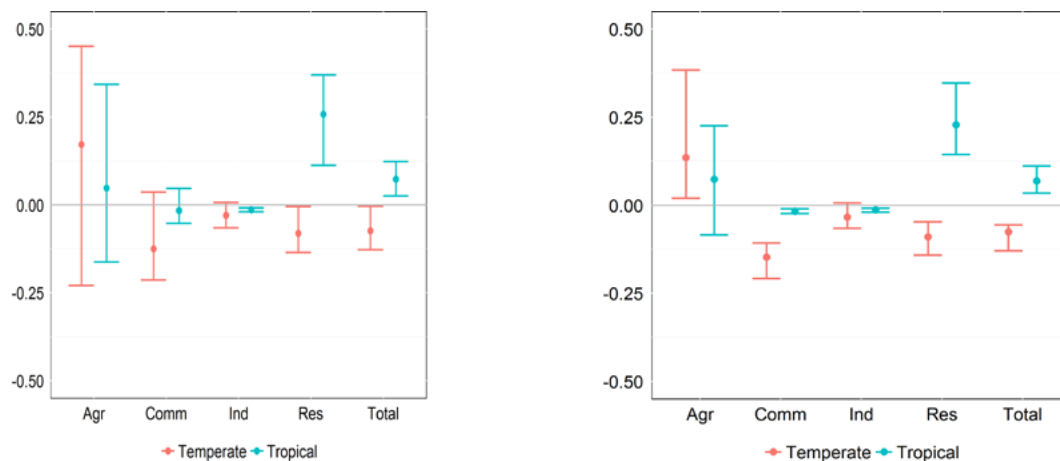


Fig. 1 Future percentage (%) change in sectoral electricity demand when accounting for future socio-economic growth, temperature and humidity changes (left) and when accounting for future socio-economic growth and temperature (right) in 2050, RCP8.5, SSP5.

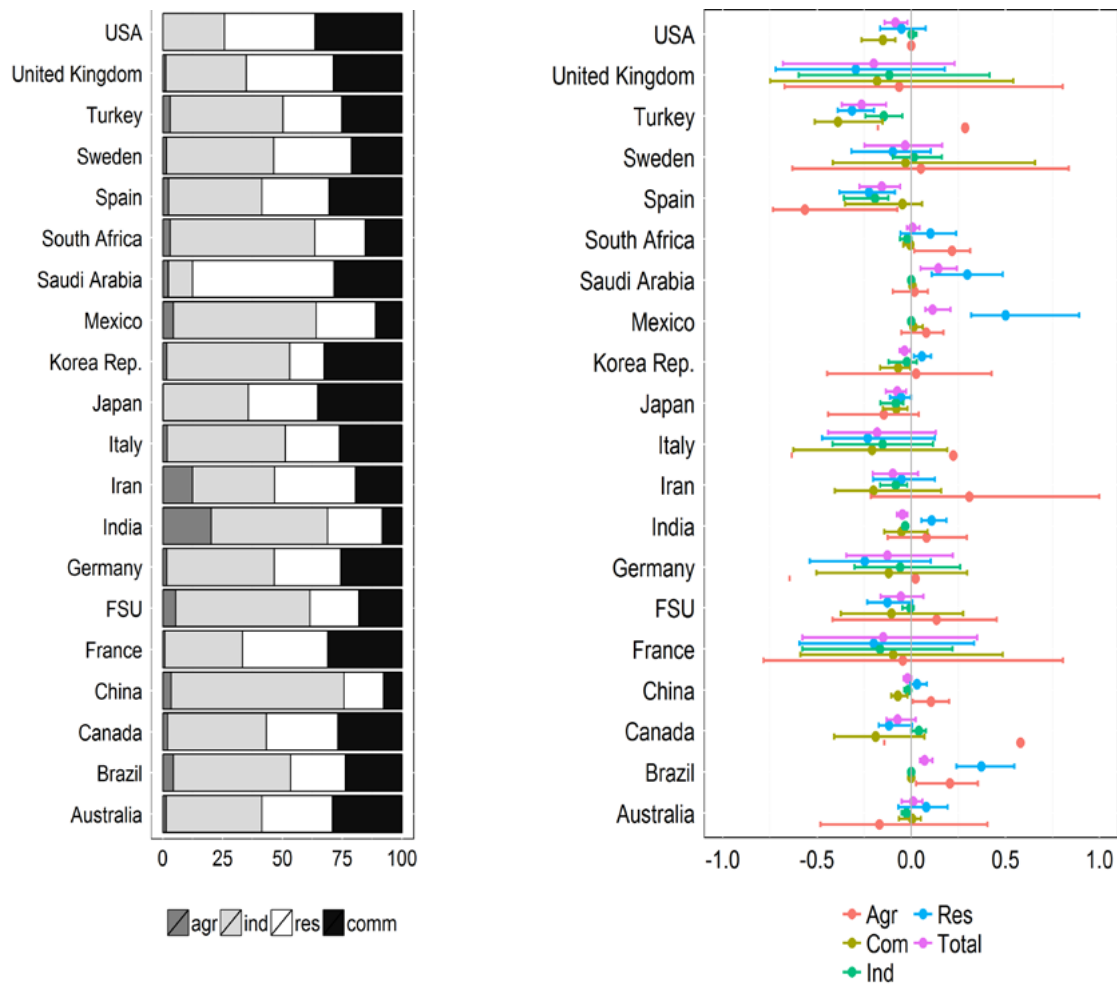


Fig. 2 Current mix of electricity demand (annual average between 2006 and 2010) and percentage change in 2050 regional future electricity demand (2046-2055) compared to present (2005-2016). Markers show the multi-model mean, ranges indicate the model minimum-maximum range. The range is limited to +/-100%. Outsiders include change in electricity use in agriculture in Italy (+232%), Canada (123%), and Turkey (147%).

## 9. Appendix

	Residential	Agriculture	Commercial	Industry
$\Delta$ .rgdppc	0.1494 (4.17)**	0.2855 (4.30)**	0.1862 (2.96)**	0.2707 (5.20)**
$\Delta$ .pop	0.6583 (8.22)**	1.9238 (2.36)*	1.1033 (11.37)**	0.3854 (0.70)
$\Delta$ .<2.5°C	0.0005 (2.39)*	0.0001 (0.14)	0.0008 (2.43)*	0.0007 (2.52)*
$\Delta$ .2.5-5°C	0.0003 (1.20)	-0.0001 (0.16)	0.0008 (3.16)**	0.0004 (1.17)
$\Delta$ .5-7p5°C	0.0004 (1.68)	-0.0000 (0.06)		0.0008 (3.71)**
$\Delta$ .7.5-10°C	0.0004 (1.99)*	0.0009 (1.43)	0.0002 (0.19)	0.0004 (1.43)
$\Delta$ .10-12.5°C	0.0003 (1.98)			
$\Delta$ .17.5-20°C		0.0013 (1.95)		
$\Delta$ .25-27.5°C		0.0018 (3.07)**		
$\Delta$ .>27.5°C	0.0002 (2.49)*	0.0013 (2.22)*		
$\Delta$ .(70-90%)	0.0002 (1.81)	-0.0007 (1.39)	0.0002 (0.56)	0.0000 (0.12)
$\Delta$ .>90%	0.0001 (0.45)	-0.0019 (2.28)*	0.0019 (1.63)	-0.0003 (0.45)
L.lnely(y)	-0.0935 (5.51)**	-0.0882 (5.46)**	-0.1471 (6.38)**	-0.1197 (3.46)**
L.rgdppc	0.0411 (3.49)**	0.0303 (2.07)*	0.1078 (4.60)**	0.0385 (2.34)*
L.pop	0.1267 (4.88)**	0.1655 (2.62)*	0.2284 (4.38)**	0.1468 (3.17)**
L.<2.5°C	0.0009 (2.84)**	0.0009 (1.09)	0.0014 (3.26)**	0.0005 (1.08)
L.2.5-5°C	0.0009 (2.88)**	0.0016 (1.87)	0.0013 (3.05)**	0.0014 (3.21)**
L.5-7p5°C	0.0006 (1.24)	0.0017 (2.14)*		0.0016 (3.17)**
L.7.5-10°C	0.0007 (2.03)*	0.0028 (2.87)**	0.0013 (1.87)	0.0012 (3.04)**
L.10-12.5°C	0.0004 (1.74)			
L.17.5-20°C		0.0023 (2.28)*		
L.25-27.5°C		0.0011 (1.47)		
L.>27.5°C	0.0004 (2.65)**	0.0003 (0.46)		
L.(70-90%)	0.0005 (2.17)*	-0.0012 (1.60)	0.0005 (1.15)	-0.0003 (0.74)
L.>90%	0.0010 (2.45)*	-0.0026 (2.03)*	0.0027 (1.66)	-0.0004 (0.50)
Constant	-1.2137 (5.02)**	-1.4622 (2.39)*	-2.4946 (4.92)**	-0.9491 (2.53)*
$R^2$	0.12	0.09	0.10	0.09
N	3,972	2,504	3,598	3,982

Table A1. Regression results, preferred specification. Fixed effect estimator with robust standard errors. T- values in brackets.

Model	Institution
CCSM4	National Center for Atmospheric Research
CNRM-CM5	Centre National de Recherches Meteorologiques / Centre Europeen de Recherche et Formation Avancees en Calcul Scientifique
CSIRO Global Climate Model Mk 3.5	CSIRO Division of Marine and Atmospheric Research - Aspendale
MIROC5	Atmosphere and Ocean Research Institute (The University of Tokyo), National Institute for Environmental Studies, and Japan Agency for Marine-Earth Science and Technology
MPI-ESM-MR	Max Planck Institute for Meteorology (MPI-M)

Table A2. Climate models used for the design of future climate change projections. All data was accessed from the <http://pcmdi9.llnl.gov/esgf-web-fe/between Jun 1st and August 31st, 2013>.

## **A preliminary approach to estimate the impact of climate change on electricity demand in Italy**

**Scapin S.<sup>1,2,3\*</sup>, Apadula F.<sup>1</sup>, Brunetti M.<sup>3</sup> and Maugeri M.<sup>2,3</sup>**

<sup>1</sup>Ricerca sul Sistema Energetico (RSE Spa), Milano – Italia, <sup>2</sup>Università degli Studi di Milano - Italia and <sup>3</sup>CNR, Istituto per le Scienze dell'Atmosfera e del Clima (ISAC), Bologna – Italia

\*Corresponding Author: [simone.scapin@rse-web.it](mailto:simone.scapin@rse-web.it)

### **Abstract**

We present a methodology to estimate cooling degree-days, heating degree-days and solar radiation records that are representative of the urbanised areas of the Italian territory. These records have recently been used within a model linking meteorological variables to the Italian aggregated electricity demand (Scapin et al., 2014): it allowed estimating the present-day dependence of the Italian electricity demand on cooling degree-days, heating degree-days and solar radiation.

We used four RCM-GCM combinations to get the evolution of Italian cooling degree-days, heating degree-days and solar radiation under A1B climate change scenario. The results give evidence of an increase of cooling degree-days of about 130% and a decreasing of heating degree-days of about 35% across the XXI<sup>st</sup> century. The global effect is a positive forcing of the electricity demand due both to the stronger increase of CDD with respect to the HDD decrease and to the much higher impact of CDD on electricity demand.

**Keywords:** electricity demand, climate change, temperature, solar radiation

## 1. INTRODUCTION

A number of recent papers have shown that temperature has a strong impact on electricity demand in many areas of the world [2,6].

A common strategy to capture, at daily resolution, the impact of temperature on electricity demand consists in using degree-days: they are proportional to the amount of heat that has to be pumped out from buildings (cooling) - or added to buildings (heating) - in order to maintain an indoor comfortable temperature. Degree-days are defined for cooling (*CDD*) as  $\max\{T - T_{S_1}, 0\}$  and for heating (*HDD*) as  $\max\{T_{S_2} - T, 0\}$ , where  $T$  is daily mean temperature and  $T_{S_1}$  and  $T_{S_2}$  are threshold values, which are usually different. There is no general agreement about threshold temperatures to be used, so they are optimized case by case.

In this context, a linear model linking the Italian daily aggregate electricity demand in the 1990-2013 period to minimum and maximum temperatures and solar radiation was developed. The model is based on the superimposition of deterministic components related to the weekly cyclical demand pattern and to long-term demand changes and on weather sensitive components. The weather sensitive components are related to cooling degree-days (*CDD*), heating degree-days (*HDD*) and solar radiation, the latter being estimated using daily temperature range as a proxy [7]. The model and the results we obtained applying it to the Italian electricity demand in the 1990-2013 period are described in a paper that was submitted to a scientific journal (Scapin et al. [9]).

In this paper, after a brief presentation of the model, we focus on the construction of *CDD*, *HDD* and solar radiation records representative of the entire Italian territory. These records were first estimated for the latest decades. Then projections for the XXI<sup>st</sup> century were obtained using 4 different combinations of RCM and GCM to downscale the A1B scenario. Finally, considering the present-day relations among meteorological variables and electricity demand, we used the *CDD*, *HDD* and solar radiation future projections to investigate the sensibility of the present-day electricity demand to climate variability and change.

## 2. TEMPERATURE DEPENDENCE OF THE ITALIAN ELECTRICITY DEMAND

The model we use in order to study the temperature dependence of the Italian daily electricity demand ( $D(t)$ ), assumes that it can be described by means of the following relation:

$$D(t) = \sum_{i=0}^3 \alpha_i t^i + \sum_{j=1}^4 \beta_j I_j(t) + \sum_{k=1}^3 \gamma_k V_k(t) + \varepsilon(t) \quad (1)$$

where:

- The first term is a third order polynomial which aims to capture the long-term temporal evolution of electricity demand, caused e.g. by the economic conjuncture, and changes in consumption habits. Higher order polynomials do not improve the model performance.
- The second term consists of dummy variables  $I_j(t)$ , introduced in order to account for the strong weekly pattern of electricity demand. In particular  $I_1(t)$  is set to 1 on Monday and 0 otherwise; in analogy,  $I_2(t)$ ,  $I_3(t)$  and  $I_4(t)$  are used to model the behaviour of Friday, Saturday and Sunday. No dummy variables are used for central weekdays (Tuesday, Wednesday, Thursday) which can be grouped together since they exhibit similar behaviour.
- The third term is the sum of three exogenous variables ( $V_k$ ), describing the influence of weather on the Italian electricity demand. In particular these variables are cooling degree-days ( $CDD$ ), heating degree-days ( $HDD$ ) and solar radiation ( $S$ ), obtained according to the procedure discussed in the next paragraph.
- The last term represents the error of the model (i.e. the difference between the actual and the estimated demand).

The coefficients  $\alpha_i$ ,  $\beta_i$  and  $\gamma_i$  of relation (1) are obtained by means of least squares regression.

We applied the model to the Italian aggregated National electricity demand of ordinary days considering twelve two-year periods, starting from 1990-1991 and ending in 2012-2013 [9]. This allowed us to get both the evolution of the electricity demand

characteristics and, at the same time, to acquire a statistically significant number of points for the regressions.

### 3. ITALY NATIONAL *CDD*, *HDD* AND SOLAR RADIATION RECORDS

#### 3.1 Construction of the model exogenous variables

The *CDD*, *HDD* and solar radiation records considered in relation (1) were obtained with a bottom-up approach: first, local *CCD*, *HDD* and solar radiation records were estimated for all Italian points of a 30-arc-second-resolution digital elevation model (GTOPO30 [11]) which are urbanised according to GLC2000 [12] land cover, then an average was computed over them. The number of GTOPO30 Italian urban grid-points is 13110 (see [Fig. 1]).

The construction of the grid-point *CCD*, *HDD* and solar radiation records will be described in the next paragraphs.

#### 3.2 Construction of grid-point temperature records

In order to compute daily *CDD*, *HDD* and solar radiation records for each Italian urbanised grid-point we first estimated the corresponding daily minimum, mean and maximum temperature records ( $T_n$ ,  $T_m$  and  $T_x$ ). For this purpose we used the technique discussed by Brunetti et al. [3,4]. The method is based on the idea that the spatio-temporal structure of temperature ( $T$ ) on a given Julian day  $j$  can be described by the superimposition of a climatological field (given by local averages for day  $j$  over a reference period) and a time-dependent anomaly field ( $A$ ).

$$T(\lambda, \theta, t) = \overline{T_j(\lambda, \theta)} + A(\lambda, \theta, t) \quad (2)$$

where  $\lambda$  and  $\theta$  are the geographical coordinates and  $t$  is time, which is here considered at daily resolution.

The climatological field of a given Julian day depends on the geographical properties of the territory (elevation, latitude, longitude, etc.) and shows considerable spatial gradients. On the contrary, the anomaly field usually exhibits strong spatial coherence;

its short-term variability is associated with weather conditions, while its long-term evolution is linked to climate change.

In order to estimate the temperature anomaly records ( $T_n$ ,  $T_m$  and  $T_x$ ) corresponding to each Italian urbanised grid-point  $A(\lambda_g, \theta_g, t)$ , we considered a network of 92 daily minimum and maximum temperature series homogenized and completed. First we transformed the data into anomalies ( $A_j(\lambda_j, \theta_j, t)$ ), taking the period 1961-1990 as a reference for the computation of daily climate normals. Then we projected the station anomalies onto the grid-points by means of the following method:

$$A(\lambda_g, \theta_g, t) = \sum_j w_j(\lambda_g, \theta_g, t) A_j(\lambda_j, \theta_j, t) \quad (3)$$

$$w_j(\lambda, \theta, t) = \alpha \exp\left(-\frac{d_j(\lambda, \theta)^2}{\tau_d^2 / \ln(2)}\right) \exp\left(-\frac{\Delta z_j(\lambda, \theta)^2}{\tau_z^2 / \ln(2)}\right) \quad (4)$$

where  $d_j(\lambda, \theta)$  and  $\Delta z_j(\lambda, \theta)$  are, respectively, the distance and the elevation difference between the position  $(\lambda_g, \theta_g)$  of the grid-point under analysis and the  $j$ -th station and  $\tau_d$  and  $\tau_z$ , - here set equal to 80 km and 400 m respectively - describe the extent to which a single observation is weighted with respect to distance and elevation: exponentials decrease by half when distance reaches  $\tau_d$  and, in analogy, when elevation difference equals  $\tau_z$ . The coefficient  $\alpha = 1/\sum_i w_i(\lambda, \theta, t)$  is a normalization term.

Once the daily temperature anomaly records ( $T_n$ ,  $T_m$  and  $T_x$ ) were available for all urbanised grid-points, the corresponding absolute value records were obtained by simply superimposing daily climate normals to the anomaly records. These grid-point normals were obtained fitting the monthly grid-point normals computed as described in Brunetti et al. [5], by means of the first two harmonics of a Fourier series.

### 3.3 Use of the effective temperature

In order to account for buildings thermal inertia we used the following effective temperature  $T^*$ , a delayed signal obtained through exponential smoothing of the temperature series:

$$T^*(t) = \beta T^*(t-1) + (1-\beta)T(t) \quad (5)$$

with time ( $t$ ) expressed in days.

The extent of smoothing is tuned by  $\beta$ . We set it equal to 0.5, in accordance with Taylor and Buizza [10]. The effective temperature index was computed for daily mean temperature only.

### 3.4 Construction of grid-point CDD and HDD records

In order to capture the non-linear response of electricity demand to temperature, we considered piecewise linear functions, namely degree-days.

Cooling degree-days are defined as:

$$CDD(t) = \max\{T(t) - T_{S_1}, 0\}$$

where  $T$  is the grid-point daily mean temperature.

In analogy, heating degree-days are defined as:

$$HDD(t) = \max\{T_{S_2} - T(t), 0\}$$

The thresholds values  $T_{S_1}$  and  $T_{S_2}$  are arbitrary, and there is no general agreement on their optimal choice. In this study we determined them by minimizing model errors, finding  $T_{S_1} = 20^\circ C$  and  $T_{S_2} = 15^\circ C$ .

### 3.5 Construction of district solar radiation records

The grid-point daily extreme temperature records ( $T_n$  and  $T_x$ ) were used to estimate grid-point global solar radiation records ( $H$ ) by means of the following formula (Hunt et al. [7]):

$$H(t) = a_0 H_0 \Delta T(t)^{0.5} + a_1 \tag{6}$$

where  $a_0$  and  $a_1$  are site-dependent empirical coefficients,  $\Delta T$  is the daily temperature range ( $T_x - T_n$ ) and  $H_0$  is the exo-atmospheric radiation on the horizontal plane, i.e. the daily integral of solar irradiance that would be observed on a horizontally oriented surface placed at the top of the atmosphere.  $H_0$  can be determined by standard computation (see e.g. Iqbal [8]), whereas  $a_0$  and  $a_1$  can be recovered from previous studies. We used for the entire Italian territory the values proposed by Abraha and Savage [1] ( $a_0 = 0.190 K^{-0.5}$ ,  $a_1 = -2.041 MJ m^{-2}$ ) for Padua (northern Italy).

In order to relate the influence of solar radiation on electricity demand we introduced the following piece-wise linear function:

$$S(t) = \max\{H_S - H(t), 0\}$$

The threshold value  $H_S=17 \text{ MJ m}^{-2}$  was selected by minimizing the model errors. Beyond this threshold the effect of an increase of solar radiation does not produce any decrease of the electricity demand.

#### **4. Impact of CDD, HDD and solar radiation on the Italian electricity demand**

The proposed methodology was applied in order to investigate the impact of CDD, HDD and solar radiation on electricity demand. The results are extensively discussed in Scapin et al. (2014). They show that relation (1) explains from 97.7% (2008-2009) to 99.4% (1996-1997) of the variance of the Italian daily demand record (ordinary days only).. Moreover, relation (1) establishes a strong contribution of cooling degree-days to the Italian electricity demand, with values peaking in summer months of the latest periods up to more than  $200 \text{ GWh day}^{-1}$  (i.e. about 23% of the corresponding average Italian electricity demand). This contribution shows a strong positive trend in the 1990-2013 period: the coefficient of the cooling degree-days term in the regression model increases from the first two-year period (1990-1991) to the last one (2012-2013) by a factor 3.5, which is much greater than the increase of the Italian total electricity demand. On the contrary, the HDD and solar radiation contributions have trends comparable to that of the electricity demand. The data of the last 3 two-year periods allow quantifying the present-day dependence of the Italian electricity demand of an ordinary day on CDD in  $24.6 \text{ GWh day}^{-1} \text{ }^\circ\text{C}^{-1}$ . For HDD and solar radiation we prefer quantifying this dependence considering the average values over the latest 6 two-year-period coefficients. The values are, respectively,  $6.6 \text{ GWh day}^{-1} \text{ }^\circ\text{C}^{-1}$  and  $2.9 \text{ GWh day}^{-1} \text{ MJ}^{-1} \text{ m}^2$ .

## 5. SCENARIOS FOR THE XXI<sup>st</sup> CENTURY

### 5.1 Regional Climate Models

Thanks to the robust high-resolution past reconstruction of temperature for Italy described in section 3), it was possible to evaluate the ability of 4 RCM–GCM combinations in reproducing temperature variability and change in this area. Specifically, four RCM-GCM combinations were considered: KNMI-ECHAM5, SMHI-ECHAM5, SMHI-BCM and SMHI-Had. We considered the historical run of the models forced by GCM and their future projections under the A1B scenario.

We first transformed the model data into anomalies with respect to the 1961-1990 normals and used these anomalies to get urbanised grid-points anomaly records by means of the procedure outlined in section 3. Then we detrended these records and compared day-to-day variability with the day-to-day variability of the corresponding observational detrended grid-point anomaly records. The comparison was performed considering the different months of the year and analysing all Italian urbanised grid-points. It allowed calculating the ratios between the standard deviations of the projected and the observational detrended records. These ratios depend both on the month of the year and on the position of the grid-point.

Figure 2 displays the grid-point ratios seasonal behaviour by means of box-plots: the central boxes correspond to the first, second and third quartiles, whereas the vertical lines indicate the absolute range covered by the ratios. Spring months show a general tendency to have a reduced variability in the model data with respect to observational data. An opposite behaviour is generally present in autumn and winter.

The spatial pattern of the ratios is shown in [Fig. 3] for March, June, September and December. The most evident result concerns some coastal areas showing a reduced variability in the model data with respect to observational data.

The ratios shown in [Fig. 2,3] were used to get the multiplicative correcting factors to adjust the scenario anomalies: they are simply the inverse of these ratios. After the correction, the monthly detrending curves were added to the records in order to obtain adjusted projected grid-point anomaly records. The anomalies were then converted into absolute values as outlined in section 3 (i.e. by means of the superimposition of the anomaly and climatology fields).

## 6. TEMPORAL EVOLUTION OF THE *CDD*, *HDD* AND SOLAR RADIATION RECORDS

The adjusted model outputs were used to calculate national CDD, HDD and solar radiation urbanised grid-point records for the 2001-2100 period, according to the procedure outlined in section 3.

We show the temporal evolution of these records in [Fig. 4]. In particular, for each 10-year interval of the 2001-2100 period we show the daily average value of the CDD record in the period May-October, the average value of the HDD record in the period November-April and the average value of the solar radiation record over the whole year. The figure also displays the curves obtained by averaging the values corresponding to the 4 RCM-GCM combinations. CDD and HDD show a clear trend, whereas solar radiation does not show a clear temporal evolution. Using least square linear interpolation and considering the average of the 4 models, the CDD trend turns out to be  $0.29 \pm 0.01$  °C/decade, whereas the HDD trend turns out to be  $-0.27 \pm 0.02$  °C.

In addition we investigated CDD and HDD yearly cycles, considering three 30-year periods of the 2011-2100 interval and investigating the monthly distributions of these variables calculated from the 4 RCM-GCM combinations. In [Fig. 5] we report these results by means of box-plots; in this case the distributions were obtained considering all model results together.

The present-day relations among meteorological variables and electricity demand we presented in section 4 and the records presented in section 6 were used to investigate the sensibility of the present-day electricity demand to climate variability and change. At this purpose, we simply run the model for the 2001-2100 period with the CDD coefficient we obtained for the 2012-2013 period and with average values of the HDD and solar radiation coefficients we get over the twelve 2-year periods of the 1990-2013 interval (these coefficients do not show significant trends in this period). The results are shown in [Fig. 6], which displays the average contribution to the Italian electricity demand of all meteorological terms of relation (1) in 10 consecutive 10-year periods of the 2001-2100 interval.

This analysis has naturally not to be considered as a future electricity demand scenario, as beside to changes in the meteorological variables, we will certainly have considerable changes in many other drivers of the electricity demand.

## 7. CONCLUSIONS

We set up a methodology to estimate cooling degree-day, heating degree-day and solar radiation records that are representative of the urbanised areas of the Italian territory. These records were used within a model linking meteorological variables to the Italian aggregated electricity demand: it allowed estimating the present-day dependence of the Italian electricity demand on cooling degree-days, heating degree-days and solar radiation.

Four RCM-GCM combinations were used to get the evolution of cooling degree-days, heating degree-days and solar radiation under A1B climate change scenario. The results give evidence of an increase of cooling degree-days of about 130% and a decreasing of heating degree-days of about 35% across the XXI<sup>st</sup> century. The global effect, considering the present-day relationship between demand and meteorological variables, is a positive forcing of the electricity demand due both to the stronger increase of *CDD* with respect to *HDD* decrease and to the much higher impact of *CDD* on the electricity demand.

## 8. ACKNOWLEDGMENTS

The present work was partly funded by the Research Fund for the Italian Electrical System under the Contract Agreement between RSE S.p.A. and the Ministry of Economic Development – General Directorate for Nuclear Energy, Renewable Energy and Energy Efficiency, stipulated on July 29, 2009 in compliance with the Decree of March 19, 2009 and partly by the EU FP7 project ECLISE. (265240).

## 9. REFERENCES

1. Abraha, M.G, Savage, M.J., 2008. Comparison of estimates of daily solar radiation from air temperature range for application in crop simulations, *Agricultural and Forest Meteorology* 148, 401 – 416.
2. Apadula, F., Bassini, A., Elli, A. Scapin, S., 2012. Relationships between meteorological variables and monthly electricity demand, *Applied Energy* 98, 346-356.

3. Brunetti, M., Lentini, G., Maugeri, M., Nanni, T., Simolo, C., Spinoni, J., 2009. Estimating local records for Northern and Central Italy from a sparse secular temperature network and from 1961-1990 climatologies. *Adv. Sci. Res.*, 3, 63-71.
4. Brunetti, M., Lentini, G., Maugeri, M., Nanni, T., Simolo, C., Spinoni, J., 2012. Projecting North Eastern Italy temperature and precipitation secular records onto a high resolution grid. *Physics and Chemistry of the Earth*, 40-41, 9-22.
5. Brunetti, M., Maugeri, M., Nanni, T., Simolo, C., and Spinoni, J., 2014. High-resolution temperature climatology for Italy: interpolation method intercomparison. *International Journal of Climatology*, 34, 1278–1296
6. Feinberg EA, Genethliou D., 2005. Load forecasting. In: Chow JH, Wu FF, Momoh JJ, et al., editors. *Applied mathematics for restructured electric power systems: optimization, control, and computational intelligence*. New York: Springer; p. 269–285.
7. Hunt, L.A., Kuchar, L., Swanton C.J., 1998. Estimation of solar radiation for use in crop modelling. *Agricultural and Forest Meteorology*, Volume 91, Issues 3–4, pp. 293–300.
8. Iqbal, M., 1983. *An introduction to solar radiation*, Academic Press.
9. Scapin. S., Apadula, F., Brunetti, M., Maugeri, M., 2014. Response of electricity demand to temperature and solar radiation in Italy, *Weather, Climate and Society*. (submitted)
10. Taylor, J. W., Buizza, R., 2003. Using weather ensemble predictions in electricity demand forecasting, *International journal of forecasting* 19, 57-70.
11. USGS (United States Geological Survey). 1996. GTOPO30 Documentation. Available at [http://eros.usgs.gov/#/Find\\_Data/Products\\_and\\_Data\\_Available/gtopo30\\_info](http://eros.usgs.gov/#/Find_Data/Products_and_Data_Available/gtopo30_info)
12. European Commission, Joint Research Centre. 2003. Global Land Cover 2000 database. Available at [http://bioval.jrc.ec.europa.eu/products/glc2000/data\\_access.php](http://bioval.jrc.ec.europa.eu/products/glc2000/data_access.php)

## 10. IMAGES AND TABLES

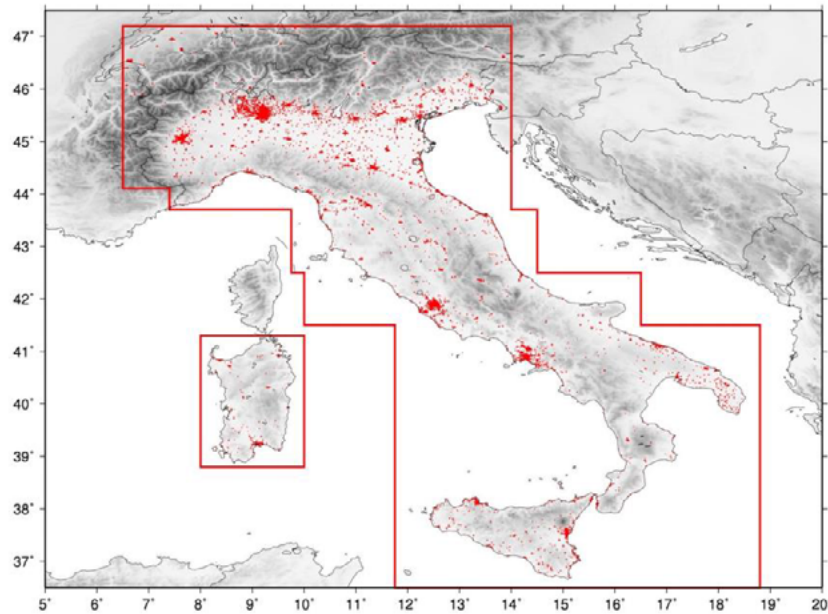


Fig. 1 Grid-points corresponding to urbanised areas according to GTOPO30 [11].

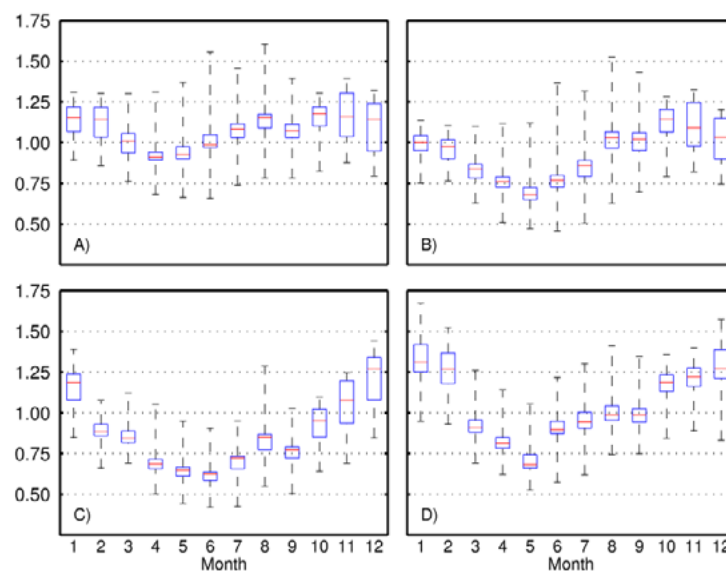


Fig. 2 Ratios between the standard deviations of the observational and projected detrended daily anomaly records. A) KNMI-ECHAM5; B) SMHI-ECHAM5; C) SMHI-BCM; D) SMHI-Had.

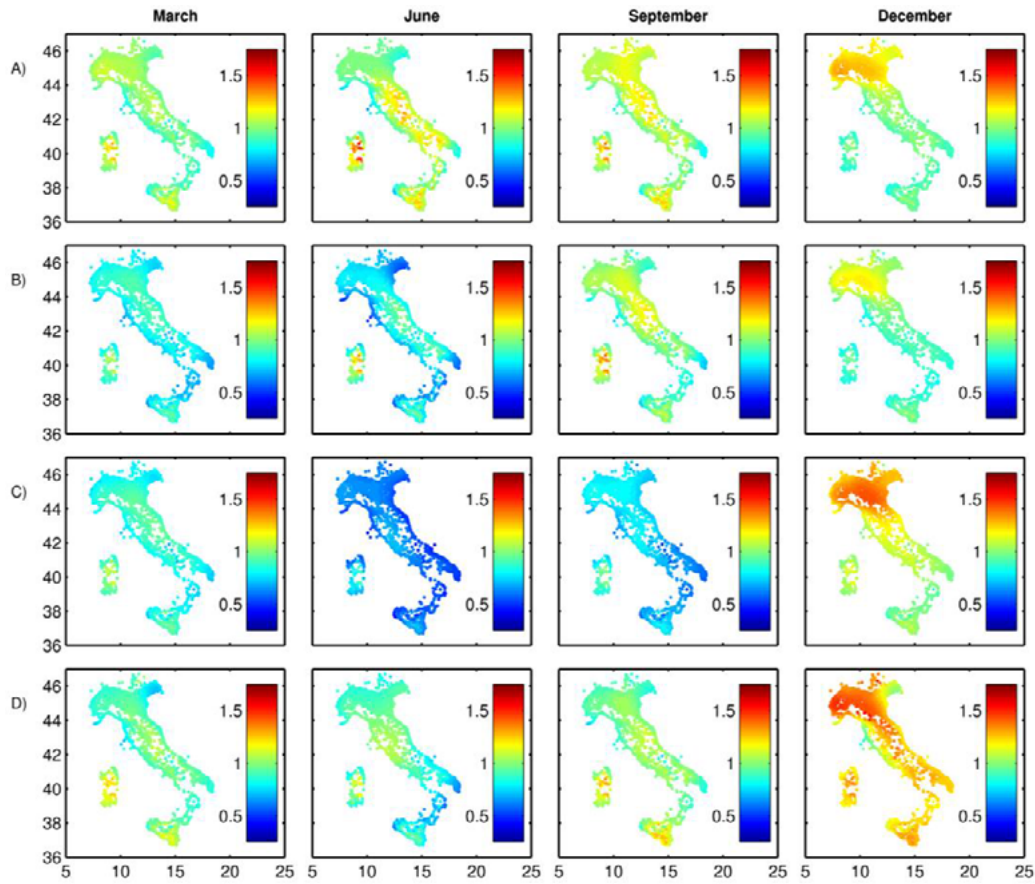


Fig. 3 Spatial distribution of the ratios between the standard deviations of the observational and projected detrended daily records for March, June, September and December. A) KNMI-ECHAM5; B) SMHI-ECHAM5; C) SMHI-BCM; D) SMHI-Had.

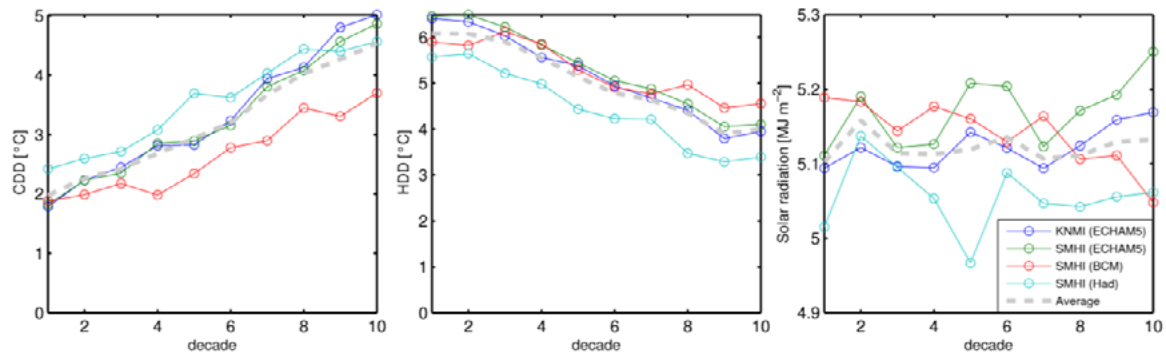


Fig. 4 10-year average CDD (May-October), HDD (November-April) and solar radiation (January-December) for the 4 RCM-GCM combinations. The figure also shows the average among the 4 model curves.

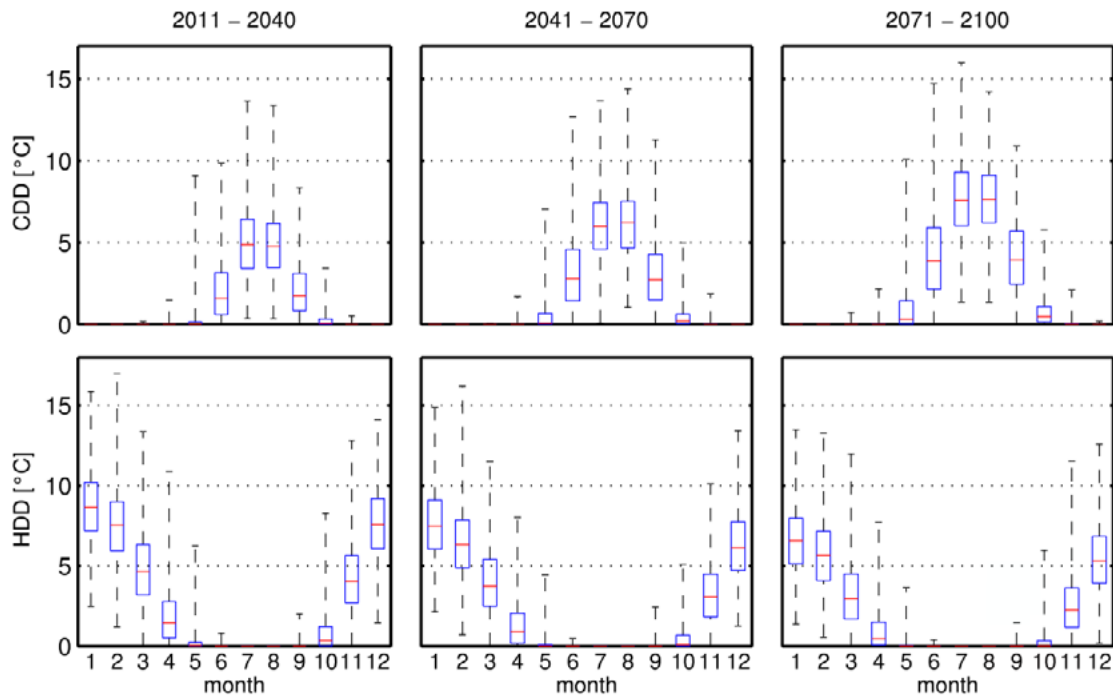


Fig. 5 CDD and HDD distributions over the months of the year, according to the RCM-GCM considered combinations, in three 30-year periods in the 2011-2100 interval.

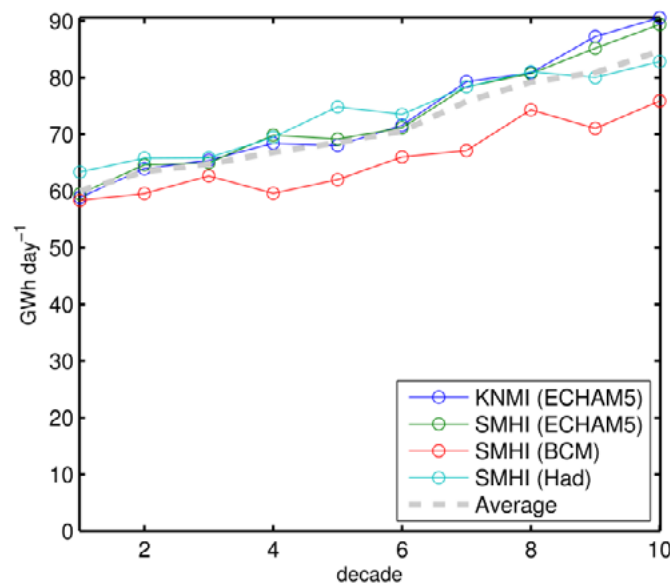


Fig. 6 Average contribution of the meteorological terms of relation (1) to the Italian electricity demand in 10 consecutive 10-year periods of the 2001-2100 interval obtained using meteorological data from the 4 RCM-GCM combinations and considering the present-day links among meteorological variables and electricity demand. Of course, this should not be considered as an energy scenario, as electricity sensibility to weather variables will certainly change in the future.

# **Impact of climate change on historic architectural surfaces of the Venetian area**

**Zendri E., Falchi L.\* , Balliana E., Izzo F. C. and Biscontin G.**

Department of Environmental Sciences, Informatics and Statistics; Venice Centre for  
Climate Studies VICCS, Ca' Foscari University of Venice – Italy

\*Corresponding Author: [laura.falchi@stud.unive.it](mailto:laura.falchi@stud.unive.it)

## **Abstract**

The impact of climate changes on the social-economic growth of Venice is, nowadays, of crucial importance for a sustainable preservation plan of Venetian Cultural Heritage. General models and data which relate climate changes and construction materials are available, but still absent are specific studies for more complex systems such as historical centres. A short description of the main degradation processes in connection to building materials and local environment, possible solutions, techniques and products for the conservation and maintenance of the architectural surfaces will be presented. This contribution hopes to animate a network of cultural heritage stakeholders devoted to promote an effective and sustainable preservation policy.

**Keywords:** Venice, architectural surfaces, degradation processes, sustainability, preventive interventions.

## **1. INTRODUCTION**

Since now, the analysis of the impact that climate change might produce on historic buildings has been quite limited, despite the many researches dealing with the damages caused by atmospheric pollution, global warming and sea level rise. In an era with declining acidic pollutants [1], climate change may play a more significant role in the decay of monuments and buildings. Published data are mainly related to construction materials rather than complex systems such as historical centres, or to general models, often far from specific cases.

In the specific case of Venice, large sums have been spent since 1970s on scientific research into what should be done to defend the city, but only in the more recent years structural interventions have been started for the protection from the effects of climate change. According to Anna Somers Cocks's opinions, the difficulty to translate the scientific knowledge and the research results into action have been mainly due to a lack of agreement about what the environmental indicators and the researches were telling us [2].

This contribution reports the 30-years experience gained by our group of Chemical Sciences for Conservation of Cultural Heritage of Ca' Foscari University, regarding the relationship between the lagoon environment, its changes and the effects on the conservation and preservation of the architectural surfaces in Venice, considering also to the current state of the art. The description of the connections and the interactions between building materials and the surrounding environments, the most important degradation factors related to climate change, the possible solutions for reducing the impact of future climate change on the architectural surfaces in Venice will be presented.

Our hope is to offer and share our experience to enhance the dialogue between disciplines and develop a better management of the Venetian architectures.

## **2. EFFECTS OF THE CLIMATE CHANGE IN VENICE**

With the global warming and the relative climate changes coastal regions have progressively become more vulnerable to intense atmospheric and hydrodynamic events [3]. No exception for Venice Lagoon, as demonstrated by several studies

implemented, in particular, after the abnormal great flood of 1966 and the consequent Campaign for the Safeguarding of Venice promoted by UNESCO [4].

The climate changes have a direct influence on different factors which might cause an acceleration in the degradation of the exposed heritage. While there is a general good knowledge and awareness regarding degradation factors in respect to cultural heritage, the quantitative relationship between pollutant concentrations, meteorological variables and stone degradation is still difficult to clear out [5].

Enhanced by the climate changes, water is without any doubt the main degradation factor for the architectural surfaces with direct and indirect actions (e.g. freeze-thawing cycles, erosion, damage salt and pollutants transport) [6]. The damages caused by water action on the architectural surfaces are worsen by the increase of relative humidity, the increase of the sea level, more frequent flooding, intense meteoric precipitations due to climate changes as well as the presence of high amount of CO<sub>2</sub> in the atmosphere [5].

In Venice in particular, more than determining completely new degradation factors, the climate changes have worsened the effects of factors already present and intrinsic in venetian environment (e.g. the capillary rise of salt solution, the erosion due to marine aerosol, etc.) and factors due to the human overexploitation of the lagoon resources, mostly for commercial aims (e.g. the air and water pollution, Porto Marghera industrial site and the harbor, the morphological variation of the lagoon due to recent and historical interventions, etc.) [7-9].

One of the evidence of climate changes in the area is the intensification of the meteoric phenomena [10]. The historical precipitation climatology of Venice was characterized in the past (1961-1990) by short rainfalls events between June and August and longer events between October and November. This situation changed showing a decrease of the total annual precipitation, the shift of the rainiest month to September in the period 1993-2009, and the intensification of heavy flash flood-events from 2006 and 2010 [10-11].

On the other side, the intensification and the prolongation of the flooding events, object of numerous studies and evidenced in particular by the data collected by Centro Maree [12], are related both to the subsidence of the lagoon (due to its

erosion, the reduced supply of sediments, further anthropogenic effects [3, 13]) and to the sea level rise.

### **3. DEGRADATION OF HISTORICAL BUILDINGS IN RELATION TO THE CLIMATE CHANGES**

Considering the impact of degradation factors on architectural surfaces in Venice, a distinction can be made between the ones mainly responsible for the degradation of the upper part of the buildings (such as meteoric precipitations, relative humidity, presence of CO<sub>2</sub>), and the ones mainly responsible for the degradation of the lower parts (such as the recrudescence of flooding phenomena).

In relation to the upper level of buildings, important degradation factors are: SO<sub>2</sub>, NO<sub>x</sub>, ozone; pH level associated to CO<sub>2</sub> concentration rate; and deposition of particulate matter pollution. The effects of pollutants and environmental parameters (e.g. rain, wind, etc.) on materials frequently result in macroscopic evidences often related to colour and textural changes, such as: black crust, whitish carbonate coatings, increase of surface roughness, etc. [14] [Tab. 1]. The sources of these degradation processes are usually well known and related to atmospheric pollution but the combined effects of these can rapidly change in relation to climate conditions. Along the last 30 years, different models have been proposed to estimate the influence of degradation parameters [1], but these general models still need to be implemented in relation to local and regional weather variations and to specific buildings.

In the case of Venice, considering the future perspective regarding the decrease of atmospheric pollutions, the contribution of sulphatation, nitration and oxidation is expected to be reduced in accordance to European environmental regulations [Fig. 2]. Data from ARPAV<sup>1</sup> shows a decrease of SO<sub>2</sub> amount and a stable situation in the Venetian area. However, for carbonate materials, the degradation processes due to pH level and acid rains are expected to play a main role due to the increase of atmospheric CO<sub>2</sub> and precipitation, even if the SO<sub>2</sub> is diminishing [1, 7]. The increase of recession of carbonate surfaces will be enhanced due also to the increase of relative humidity and time of the wetness during winter period as shown by data

---

<sup>1</sup> ARPAV is the acronym for **A**genzia **R**egionale per la **P**revenzione e **P**rotezione **A**mbientale del **V**eneto

collected in different environmental contexts (recession level expected around 30  $\mu\text{m}/\text{year}$  in the 21<sup>st</sup> century in Italy), respect to  $\mu\text{m}/\text{year}$  measured in the 90<sup>s</sup> [15].

An important role to stone degradation in Venice is also played by marine aerosol, often considered as a mere co-factor. Data collected from our research group on exposed Istria stone specimens show an average amount of deposited particulate of 230  $\text{g}/\text{m}^2\text{year}$  and a marked increase of the surface roughness [Fig. 3], parameters that indicates the presence of synergic degradation processes [16].

Rainfall represents another important degradation factor due to its increasing intensity over the years for the upper part of buildings [11-12]. Rain, in addition to its direct mechanical action on walls, is absorbed by the plaster and bricks and filters through them promoting the detachment of the finish layers and producing water infiltration within the building structures.

In the lower part of venetian buildings, the degradation can be mainly attributed to the rising damp of salt water, the sea spray and the erosion effect due to movement of water caused by waves [3, 17-19]. Rising damp together with salt crystallization affects the walls till 2.5-3 m height, with humidity content values of around 20-25% in bricks in the wet zone and a content of soluble salts around 10-15% by mass in the zone of maximum evaporation rate (the real values change according to the material, the building, the exposition, the age, etc..), causing mainly physical degradation [17] [Fig. 4, 5].

The historical building in Venice have always been designed to face the problems due to a soft soil, the presence of salt water and marine aerosol, using specific construction materials (bricks, hydraulic limes, Istria stone) and techniques (wooden foundations, curbs in Istria stone, overcooked bricks in the lower parts of the buildings) [20-21]. Nowadays, the traditional defences of venetian buildings against the rising damp are inefficient due to the high level reached by the tides and to the increased tide duration [22-23]. Emblematic of this situation is the narthex of St. Mark's Basilica (+0.74 m level on the *medio marino*), situated in one of the lowest points of Venice, which becomes more and more often a "pool", the tides with level  $\geq +80\text{cm}$  increased from an average of 43 times/year in 1983-1993 to 96 times/year in 2003-2013, and the total permanence of the tide  $\geq +70\text{ cm}$  in 1966-2013 was 8073 hours, i.e. 2.24 years [13]. This, together with the presence of stone panels with low

permeability, allows the capillary rise of water and salts to high levels damaging also the mosaics of the vaults.

Considering this situation, the choice of effective and compatible solutions in order to address the direct and indirect action of water on buildings becomes a critical point [24-25]. The solutions adopted from the 1950s-60s (i.e. the complete hydrophobization of the walls with bituminous or lead sheets, the mechanical cut of the wall, the use of chemical barriers) are nowadays obsolete considering their invasiveness and incompatibility with the historical materials. Starting from the 1980s, the use of macro-porous mortars (which allowed a fast evaporation, decreasing the level reach by the capillary rise) are still now the most compatible solutions in Venice to protect the architectural surfaces. The use of cement binders have been substituted by more compatible and traditional binders, such as natural hydraulic limes or pozzolana limes, promoted also by the results of dedicated studies that highlighted the problems of using incompatible materials with physical properties completely different from the traditional ones (e.g. excessive mechanical strengths, low water vapour permeability, source of damaging salts) [26-27]. Furthermore, the development of *ad hoc* mortars able not only to facilitate the drying of the walls thanks to high permeability to water vapour, but also to protect the wall from the intense meteoric phenomena should be enhanced.

The degradation due to the action of water can be faced, as already discussed, with passive methods, i.e. methods able to limit the damaging effects of the crystallization of salts (macroporous mortars), or with active systems, able to act directly (i.e. electro osmotic methods). However, scientific literature and information are still very limited regarding the effectiveness of the different methods against rising damp and their comparison, and scientific-based decision support tool for a conscious choice and successful use of these methods have not been developed for Venice yet.

#### **4. FINAL CONSIDERATIONS**

The data collected up to now and the models proposed for the description of future climate scenarios in Venice represent the starting point for future interventions and politics aiming to prevent the damages.

These data underlines that, in the case of Venice, the main degradation factors linked to the climate changes are: the rise of the lagoon water level, the increasing intensification of rainfall events and amount of CO<sub>2</sub>.

In order to maintain a high level of resilience, which is innate in Venice, and to face the climate changes, it is necessary to preserve and enhance the historical defenses of Venice, both the natural and the artificial ones (i.e. the morphological peculiarity of the lagoon, the particular construction techniques, the use of suitable materials) Possible solutions against the degradation factors mainly consist in physical barrier and structural interventions (as MOSE, raising the level of the paving stones, restoration of the embankment walls, maintenance of roof, etc.), that must be combined with materials and techniques suitable for the architecture restoration and conservation. However, only starting from *a posteriori* and over time evaluation of reconditioning interventions is possible to define the most suitable solutions for the specific situation in Venice in relation to the future climate changes<sup>2</sup>.

Studies and researches aimed at the investigation of the effects and of the possible solutions should be promoted and spread within a network of cultural heritage stakeholders devoted to promote effective and sustainable preservation politics, in order to support the decision making phases and an integrated economic, social and urban planning.

## 5. REFERENCES

1. Bonazza A., Messina P., Sabbioni C., Grossi C.M, Brimblecombe P. (2009), *Mapping the impact of climate change on surface recession of carbonate buildings in Europe*, Science of The Total Environment, No. 407, pp.2039-2050.
2. Fletcher C.A., Spencer T. editors (2005), *Flooding and environmental challenges for Venice and its lagoon: state of knowledge*, Cambridge University Press, Cambridge

---

<sup>2</sup> JPI Cultural Heritage – JHEP Pilot call: EMERISDA Effectiveness of methods against rising damp in buildings: European practice and perspective; <http://www.jpi-culturalheritage.eu/2014/02/projects-approved-for-funding-by-jpi-cultural-heritage-jhep-pilot-call/>

3. Seminara G., Lanzoni S., Cecconi G. (2011), *Coastal wetland at risk: learning from Venice and New Orleans*, *Ecohydrology & Hydrobiology*, No.11-3-4, pp. 183-202.
4. Biscontin G., Fassina V., Lazzarini L., Mazzon R. (1979), *Studio dell'umidità ascendente, delle caratteristiche fisiche delle murature di palazzo badoer e prove di desalinificazione in Il Mattone di Venezia: stato delle conoscenze tecnico-scientifiche*, Fondazione "Giorgio Cini", CNR, Ca' Foscari University editor, Tipo litografia Armena, Venice, pp. 305-321.
5. Watt J., Tidblad J., Kucera V., Hamilton R. editors (2009), *The effect of Air Pollution on Cultural Heritage*, Springer, New York.
6. Wendler E., Charola A.E. (2008), *Water and its Interaction with Porous Inorganic Building Materials. Proceedings of the Conference*, Hydrophobe V, Water repellent treatment of building materials, Aedificatio Publisher; Rome, pp. 57-74.
7. Biscontin G., Fassina V., Zendri E. (1990), *Il comportamento dei materiali lapidei a Venezia in relazione all'ambiente* in Zezza F., *La Conservazione dei monumenti nel bacino del Mediterraneo : influenza dell'ambiente costiero e dello spray marino sulla pietra calcarea e sul marmo*, Editore Grafo, Brescia, pp. 195-201.
8. De Zordi E. (2012), *Studio della morfologia e della composizione dei depositi su superfici lapidee in area portuale ed aeroportuale a Venezia*, Master Thesis in Scienze chimiche per la conservazione ed il restauro, Ca' Foscari University, Venice.
9. D'Alpaos L. (2010), *Fatti e misfatti di idraulica lagunare. La laguna di Venezia dalla diversione dei fiumi alle nuove opere delle bocche di porto*, Edizioni Istituto Veneto di Scienze, Lettere ed Arti, Venice.
10. ARPAV (2013), *Qualità dell'Aria Provincia di Venezia, Relazione Annuale 2012*, editors Vianello L., Pistollato S., Venezia.
11. Barbi A., Monai M., Racca R., Rossa A.M. (2012), *Recurring features of extreme autumnal rainfall events on the Veneto coastal area*, *Natural Hazards and Earth System Sciences*, No 12, pp. 2463–2477.

12. Centro previsioni e segnalazioni maree (2014), *Historic Archive of data related to tides in Venice*.  
<http://www.comune.venezia.it/flex/cm/pages/ServeBLOB.php/L/IT/IDPagina/25419#1a5487>
13. Carbognin L., Teatini P., Tomasin A., Tosi L. (2010), *Global change and relative sea level rise at Venice: what impact in term of flooding*, *Climate Dynamics*, No 35, pp. 1039–1047.
14. Maravelaki P., Biscontin G. (1999), *Origin, characteristics and morphology of weathering crusts on Istria Stone in Venice*, *Atmospheric Environment*, No 33, pp.1699-1709.
15. Maravelaki P., Biscontin G., Zendri E., Marchesini L., Repaci G. (1992), *Evaluation of deterioration processes on Istrian stone of venetian monuments*, VII<sup>th</sup> International Congress on Deterioration and Conservation of Stone, Lisboa, pp. 1093-1102.
16. Zendri E., Biscontin G., Nardini I., Riato S. (2006), *Inquinamento atmosferico e Beni Culturali. Protezione e conservazione del patrimonio culturale*, Tematiche Ambientali, Udine, pp. 1-8.
17. Biscontin G., Driussi G. (1988), *Indagini sull'umidità di risalita a Venezia*, Recuperare, PEG editrice, Milano, No 33, pp 78-83.
18. Bakolas A. (1991), *Indagine chimico fisica sull'azione dell'acqua di mare su murature storiche a Venezia*, Thesis, Ca' Foscari University.
19. Biscontin G., Zendri E., Bakolas A. (2005), *Alteration of brickwork exposed to sea tides in Venice* in Fletcher C.A., Spencer T. (2005), *Flooding and environmental challenges for Venice and its lagoon: state of knowledge*, Cambridge University Press, Cambridge, pp. 199-203.
20. Biscontin G., Izzo F.C., Rinaldi E. (2009), *Il sistema delle fondazioni lignee a Venezia*. Valutazione del comportamento chimico-fisico e microbiologico, Edizioni CORILA, Venice.
21. Biscontin G., Pelizzon Birelli M., Zendri E. (2002), *Characterization of binders employed in the manufacture of Venetian historical mortars*, *Journal of Cultural Heritage*, No. 3, pp. 31-37.

22. Centro previsioni e segnalazioni maree (2014),  
[http://93.62.201.235/maree/DOCUMENTI/Libretto\\_tascabile\\_maree\\_2014.pdf](http://93.62.201.235/maree/DOCUMENTI/Libretto_tascabile_maree_2014.pdf)
23. Camuffo D., Sturaro G. (2004), *Use of proxy-documentary and instrumental data to assess the risk factors leading to sea flooding in Venice*, Global and Planetary Change, No. 40, pp. 93-103.
24. Zendri E., Balliana E., Izzo F.C., Melchiorre M., Falchi L., Sgobbi M., Biscontin G. (2012), *The choice of parameters for the monitoring and the maintenance of architectural stone surfaces*, Euromed 2012 Progress in Cultural Heritage Preservation, Cyprus, pp. 331-336.
25. Biscontin G., Zendri E., Nardini I., Driussi G. (2007), *Consideration on the efficacy thresholds of protective polymers used in Cultural Heritage conservation*, EUROMAT 2007 - European Congress on Advanced Materials and Processes, Nurnberg.
26. Falchi L., Müller U., Fontana P., Izzo F. C., Zendri E. (2013) *Influence and effectiveness of water-repellent admixtures on pozzolana–lime mortars for restoration application*, Construction and Building Materials, No. 49, pp. 272-280.
27. Zendri E. (2004), *La protezione delle superfici architettoniche in pietra d'Istria a Venezia*, Interreg III A Phare CBC Italia-Slovenia 2000-2006: The Northern Adriatic Cultural Heritage. Experiences in protection, preservation and restoration, Mazzanti Editori, Venice, pp. 119-132

## 6. IMAGES AND TABLES

Tab. 1 Examples of composition of decay layers on Istria stone in Venice [14]. Average amount of non carbonate carbon Cnc; carbon due to oxalates Cox; sulphates, chlorides, nitrates, calcium carbonate ( $\text{CaCO}_3$ ), gypsum ( $\text{CaSO}_4 \cdot 2\text{H}_2\text{O}$ ) on Istria stone samples collected from different venetian monuments (Palazzo Ducale, Fontana Palace, Carmini School, St. Marta's Church), in points not affected by rising damp and rainfall.

Samples	Layers	Cnc	Cox	$\text{SO}_4^{2-}$	Cl <sup>-</sup>	$\text{NO}_3^-$	Gypsum <sup>a</sup>	Carbonates <sup>b</sup>
		wt%	wt%	$\text{mg g}^{-1}$	$\text{mg g}^{-1}$	$\text{mg g}^{-1}$	wt%	wt%
Dendritic black areas	A	1.84	0.22	296.33	2.11	0.89	54.77	26.88
	B	0.53	0.14	11.77	2.35	1.02	2.18	91.26
	C	0.07	0.06	8.58	1.18	0.44	1.97	94.35
Compact black areas	A	1.06	0.96	74.06	0.89	0.23	12.62	73.07
	B	0.55	0.49	5.05	0.63	0.19	0.96	91.70
	C	0.07	0.05	1.66	0.38	0.16	0.36	96.33
Grey areas	A	0.62	0.35	7.50	1.38	0.31	1.24	90.52
	B	0.39	0.25	4.61	1.00	0.20	0.65	92.41
	C	0.05	0.03	1.92	0.53	0.24	0.29	96.32
White areas	A	0.37	0.26	4.33	0.92	0.32	0.91	92.86
	B	0.15	0.12	1.09	0.35	0.12	0.25	96.47
	C	0.05	0.00	0.55	0.12	0.08	0.14	97.69

Cnc = non carbonate carbon mainly originated from atmospheric aerosol; Cox= carbon due to oxalates as related to previous treatments and/or biodeterioration; <sup>a</sup> Calculated as  $\text{CaSO}_4 \cdot 2\text{H}_2\text{O}$ ; <sup>b</sup> Calculated as  $\text{CaCO}_3$



Fig.1 Examples of black crust and white areas present in Istria stone on historical buildings in Venice

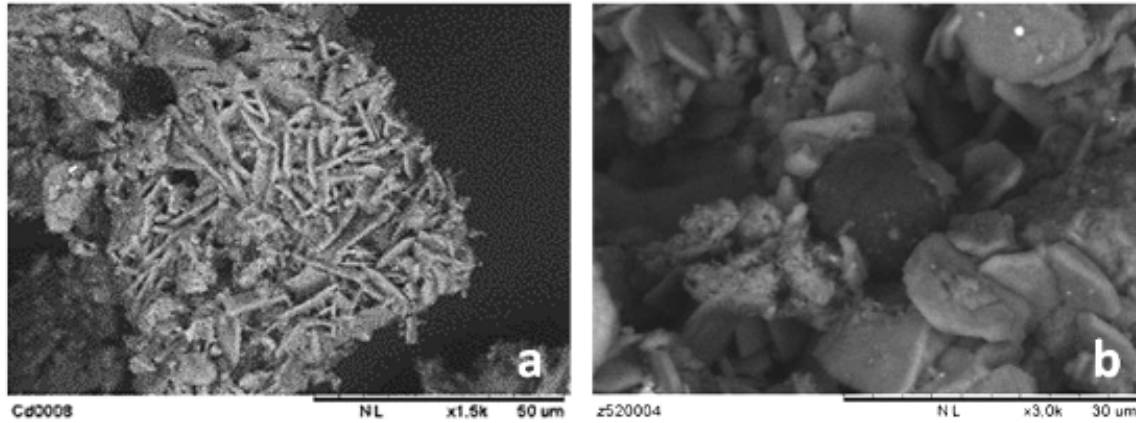


Fig. 2 SEM images of Black crusts over an Istria stone: a) presence of gypsum crystals (1500X), b) a carbon particle is visible in the center of the SEM image within gypsum crystals [8]

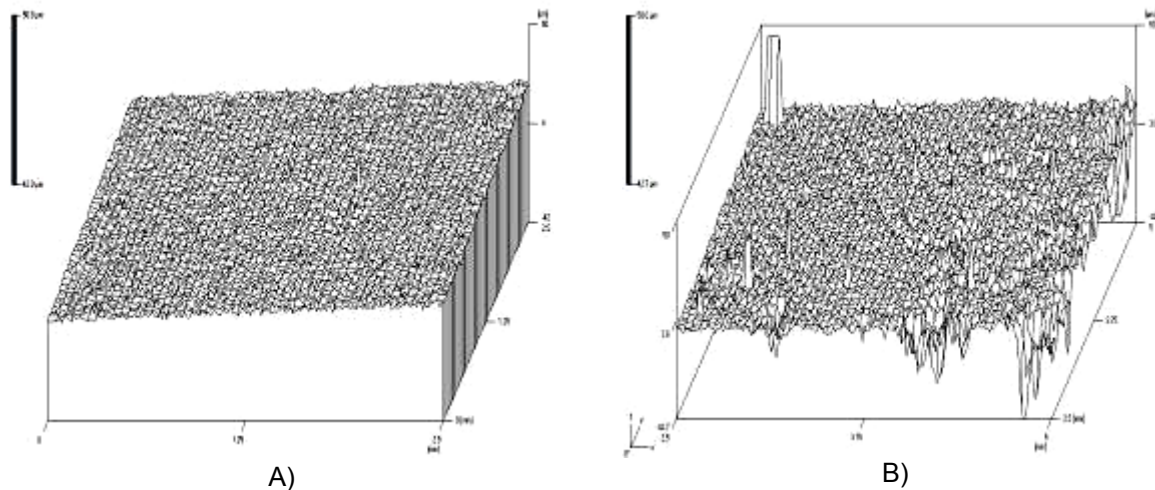


Fig. 3 Profile of the surface of Istria stone samples before (A) and after (B) the exposure to the Aerosol of Venice for 110 days. The increased roughness is due both to deposition processes of the marine aerosol and to the beginning of degradation processes which cause the erosion of the surface layer

[16]



Fig.4 Examples of degradation due to the action of rising damp and salt solutions; A) detachment of the mortar due to the crystallization of salts , B) presence of salt efflorescences over the render.

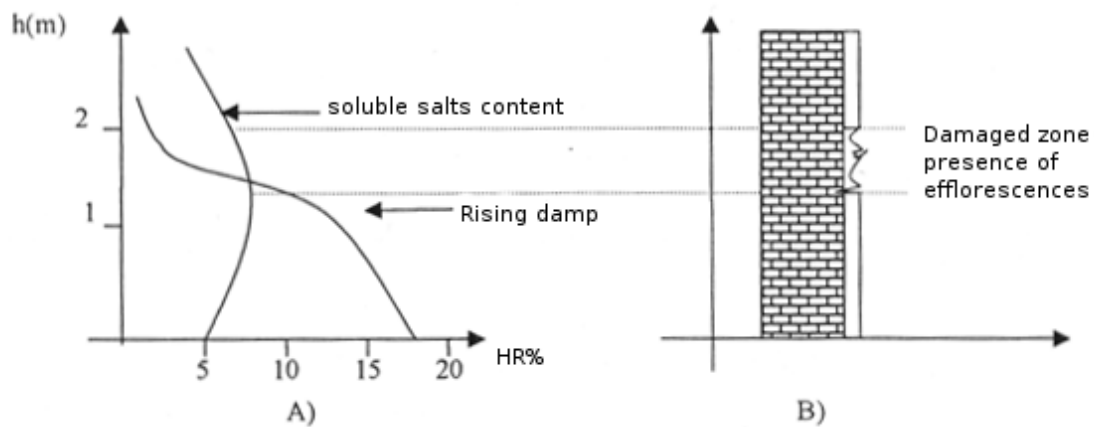


Fig.5 Distribution of relative humidity and soluble salts in Venetian brick walls: A) relative humidity HR % and distribution of soluble salts versus walls height h; B) degradation zone relative to the evaporation front. The salt solution rises up by capillary forces, when the evaporation rate overcomes the rising damp rate the solution concentrated, over saturate and precipitation of salts occurred around one meter high. The graph were built using averages of real measurements collected on several Venetian buildings [17].

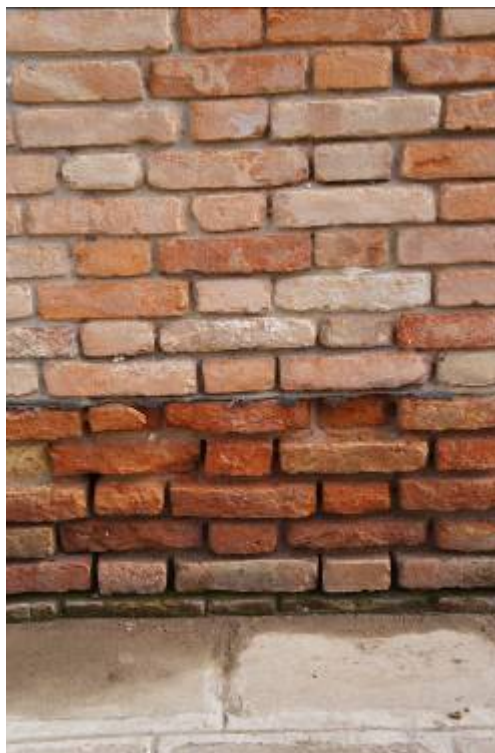


Fig. 6 Intervention of mechanical cut of the wall for reducing water rise damages.

## Impacts & Implications of Climate Change

**Impacts on ecosystems,  
food and agriculture**

## **Fires in the perspective of future changes: the contribute of CMCC to FUME Project**

**Bacciu V.<sup>1,2\*</sup>, Alcasena F.<sup>1</sup>, Arca B.<sup>3</sup>, Bosello F.<sup>1,4,5</sup>, Gualdi S.<sup>1,6</sup>, Noce S.<sup>1</sup>,  
Michetti M.<sup>1</sup>, Otrachshenko W.<sup>1</sup>, Parrado R.<sup>1,4</sup>, Salis M.<sup>2,1</sup>, Santini M.<sup>1</sup>,  
Scoccimarro E.<sup>1,7</sup>, Spano. D.<sup>2,1</sup>**

<sup>1</sup>CMCC, Euro-Mediterranean Center on Climate Change, Italy, <sup>2</sup>University of Sassari, DIPNET – Italy, <sup>3</sup>CNR, National Council of Research, IBIMET - Italy, <sup>4</sup>Fondazione Eni Enrico Mattei– Italy, <sup>5</sup>University of Milan – Italy, <sup>7</sup>INGV, Istituto Nazionale di Geofisica e Vulcanologia - Italy

\*Corresponding Author: [valentina.bacciu@cmcc.it](mailto:valentina.bacciu@cmcc.it)

### **Abstract**

According to a number of authors, the primary factors determining and shaping fire regime (climate, topography, fuel, and land use-land cover) were not stable during the last decades, significantly determining modification in fire regime and fire severity; however our understanding of how the fire driver changes affected fire regime in the past is limited. In addition to that, these changes are projected to continue, increasing fire danger and risk.

FUME project (Forest fires under climate, social and economic changes in Europe, the Mediterranean and other fire-affected areas of the world) aimed to learn from the past to understand future fire impacts. In this paper, we present and summarize the most important achievement reached by CMCC, a core partner of the project. The main findings are that: (1) fire activity significantly changed, also thank to fire management improvements; (2) future land use distribution, in not regulated, would contribute to increase fire risk; (3) this increase would be counterbalanced by projected reduction in wind speed, leading to a lower wildfire rate of spread and size; (4) the projected average yearly damage induced by Mediterranean forest fires along the 2020-2070 period ranges from \$ 5286 to \$ 7587 million.

**Keywords:** FUME project, fire regime, climate change, land use change, carbon losses

## 1. INTRODUCTION

Fire is by far the most frequent and widespread disturbance to vegetation in the world [1, 2]. This is particularly true in Mediterranean ecosystems [3, 4, 5]. In Southern Europe, every year about 45000 forest fires occur, burning approximately 0.5 million hectares of forests and other rural lands [6]. Fire occurrence varies considerably from one year to the next, which clearly indicates how much the burnt area depends on seasonal meteorological conditions [7]. On the other hand, the other driving factors (e.g., land use, vegetation) have not been stable during the last decades, mainly due to modifications in the territory caused by socioeconomic changes [8]. Looking at the future, changes in climate and socioeconomics are projected to continue, exposing to greater fire risk assets, values, and ecosystems [9].

The FUME project (Forest fires under climate, social and economic changes in Europe, the Mediterranean and other fire-affected areas of the world, FP7, 2010-2013), coordinated by the University of Castilla-La Mancha (Spain), highlighted how the understanding of fire controlling factors, and their dynamics, is of utmost importance for anticipating future fire risks. The project aims were to:

- (i) investigate and disentangle the relationships between socioeconomic, landscape and climate factors, and fires across various scales and countries during the last decades;
- (ii) translate scenarios of climate, land use and socio-economic changes to into projections of modified fire potential and risk;
- (iii) evaluate the capacity to cope with future forest fires and reduce the risk through preventive or reactive measures [10] and appraised related economic costs and policies at the European level.

This paper illustrates the most important achievement reached by CMCC (a core partner of the project) in unraveling the influence of key drivers for fire activity and regime, projecting future changes and proposing an economic assessment of future fire damages. Also, the management implications are discussed, along with major open challenges that still need to be addressed.

## 2. ANALYSING THE PAST TO PROJECT THE FUTURE

Assessing past fire regimes and changes through time due to the different key drivers required the collection and the harmonization of long-term databases to permit analysis spanning over the last thirty years and to enable comparisons among countries. After gathering information on fire, climate, land use, and socio-economic data from the EU-Med to the local scale, CMCC concurred to understand, through modeling and statistical analysis, how modifications occurred in the fire controlling factors affected fire activity, considering both behavior and regime.

Outcomes resulting from investigating the past guided projections about future fire risk and fire regime due to climate and other social and economic changes. Specifically, CMCC developed global and regional climate simulations over the FUME spatial domain (Fig. 1). In turn, climate projections were used to drive future land use change (LUC) scenarios produced also taking into account the results of the CMCC economic-energy model. LUC scenarios were then used by impact models (from vegetation to fires) to produce future fire risk scenarios.

### *2.1. Forest fire regime recent trends, changes and weather relationships*

Fire regime across the Mediterranean Basin (from EU-Med to National level down to NUTS2 scale) was described according to major fire characteristics (fire seasonality, frequency, and inter-annual variability) using fire statistics derived from different sources. The existence of significant trends and shifts in fire occurrence was also investigated. Throughout the analyzed time interval (1985-2005), summer (JJAS) resulted the main burning period, although several countries presented a secondary peak in early spring. More than the 80% of fires burned less than 10 hectares, accounting for a small portion (about 11%) of the total burned area. Fire incidence (burned area over the land area) was higher in Portugal, followed by Spain and Italy. The whole study area exhibited a general increase in the number of fires. Portugal (1989 and 1994) and Greece (2000) show an upward trend, while Italy (1994) exhibits a downward trend [11] (Fig. 2). The burned area had an opposite trend, with a generalized slight decrease throughout the period considered, significantly in Italy, Greece, and Turkey. At NUTS2 level, a significant increase in the number of fires was observed only in Attica and Peloponnese, while burned area followed a general decrease in all the study areas.

CMCC coordinated the analyses of the relationships between weather/climate conditions and fire through the application of different algorithms and methodologies at several scales, from the Euro-Mediterranean level, to national, NUT02, and local scale. At Eu-Med level, precipitation was the variable that more influenced the multiple linear regression models, while at National level, meteorological conditions, both antecedent (such as droughts) and during the fire season (such as strong wind, heat waves), seemed to have a strong influence on seasonal severity (i.e., area burned) [12]. Several results suggested the dual role of precipitation in fuel build-up and dryness [13]. Overall, in spite of the use of such a wide range of methodologies and spatial scales, the importance of similar fire season climatic factors was observed at all scales. In particular, seasonal droughts in months prior to the fire season peak, occurrence of heat waves, and strong winds during the fire season had a strong influence on fire occurrence and seasonal severity across scales [14]. A specific case study was performed for the Italian domain to investigate, with statistical techniques, the relevance of socio-economic and meteorological variables in generating fire occurrence and magnitude during 2000-2008 [15]. Italy is divided into north, center, and south, to capture local-specific characteristics in fire regimes. Results highlight the importance of railway networks, livestock presence and fuel management. Fire containment may derive from limiting illegal activities in the south.

## *2.2. Climate models and simulations*

CMCC developed global and regional climate simulations covering the period 1970-2100. These were performed using the CMCC-MED CGCM, whereas the regional ones were produced using the COSMO-CLM RCM. CMCC-MED [16,17] is a coupled atmosphere-ocean general circulation model. It focuses on the Mediterranean region and includes a very high-resolution model for the Mediterranean Sea to better represent the dynamical processes that characterize this region. The COSMO-CLM [18] is the climate version of the regional COSMO model [19], which is the operational non-hydrostatic mesoscale weather forecast model developed by the German Weather Service, further updated by the CLM-Community in order to develop also climatic applications. In the COSMO-CLM version the horizontal resolution is 14 Km, thus orography is better described with respect to the global CMCC-MED model, where there is an over-/underestimation of valley/mountain

heights resulting in errors for orographic precipitation estimation. The non-hydrostatic modeling allows providing a good description of the convective phenomena, which can redistribute significant amounts of moisture, heat and mass on small temporal and spatial scales. Furthermore, convection can cause severe precipitation events (as thunderstorm or cluster of thunderstorms). Implementing these two climate models CMCC i) provided global and regional climate simulations to be used as input in fire regime and LULC future projections; ii) defined indexes to characterize extreme events useful to determine fire development conditions [20].

### *2.3. Land use models and simulations*

Interactions between land use/cover dynamics and biophysical (including climate) to socioeconomic factors were investigated, reproduced and projected for the Mediterranean basin, comprising Southern European (EU), Middle East (ME) and North African (NA) countries bordering the Mediterranean Sea. The LUC@CMCC model [21], forced by the economic-energy model ICES@CMCC [22] provided spatially-explicit LUC scenarios as inputs to future-fire risk modelling activities in FUME. The LUC@CMCC model code, suitable for regional applications, was implemented at about 10 km resolution within two spatial sub-domains of the above defined Mediterranean basin domain: EU-Med, comprising EU countries; and EUMENA-Med, also including ME and NA countries. In the first case, the CORINE land cover dataset was used as reference to calibrate/validate the LUC@CMCC model between 1990, 2000 and 2006, respecting the CORINE class re-aggregation as agreed within FUME. In the second case, the MODIS land cover product was used considering years 2000 and 2006, requiring weaker assumptions for associating MODIS land cover categories to FUME selected land use/cover classes. In both cases, also the likely influence of restrictions in protected areas was tested.

In order to assess drivers governing land use allocation, a logistic regression (LR) analysis verified by Receiving Operating Characteristic test was applied considering between 10 and 15 explanatory factors, divided into dynamical (climatic and socio-economic) and static (like accessibility and topographic/geographic location). After the calibration/validation phase, where mainly temperature and slope demonstrated to influence land use allocation, observed and model simulated land use in 2000 matched for 84.8% of the area, considered as a good model fit. The statistical

relationships derived from the LR were thus used to drive the spatial allocation of land use in the future simulations, considering changes in the dynamical explanatory factors in terms of population density and especially climate variables, coming from above regional CMCC and two additional ENSEMBLES project simulations as bias-corrected and provided to FUME partners.

Future aggregated land use demands to drive LUC@CMCC model were developed for forestry, pasture, and agriculture using the economic-energy model ICES@CMCC based on future socio-economic trends, for EU-Med and EUMENA-Med regions. Such demands, produced for 2035 and 2050 reference years, were interpolated every 10 years up to 2070 and 2100. Results indicate that higher LUCs apply to agriculture-tree, agro-forestry and shrublands in EU-Med, and to forests in EUMENA-Med. This implies that during the period ranging from 2000 to 2100, 18.5 and 106 Mha of land in EU-Med and EUMENA-Med, respectively, should be converted into different uses.

Looking at the results of the EU-Med domain experiment (more robust thanks to the higher spatial and classification detail of CORINE dataset taken as input, and to the higher homogeneity of data across EU countries), decadal LUC simulations from 2000 to 2100 showed that, more than 10% of the territory (almost 20 Mha) could undergo changes (Fig. 3). When assuming protected area as territories preserved from changes, land modifications were reduced to 9% of the region, with about 2 Mha saved from any LUC. This confirms how land protection and regulation can favor more balanced demands and allocation of lands, avoiding overpressure and loss of natural suitability for specific uses, functions or services. Fuel spatial distribution is a key factor of these future changes: ensemble results show a future increase of land surface with medium to high fire hazard (Fig. 4). Successively, a further ensemble of simulations at local level (100 m resolution), based on combination of multiple climate change and socioeconomic projections, were performed for selected case studies (2 in Spain, 1 in France, 1 in Italy, and 1 in Greece), adapting the LUC model for local evaluations on fire hazard at finer spatial detail.

#### *2.4. Fire drivers influencing fire activity: investigation of the past and outlook of the future*

In the context of recent changes occurred in the Mediterranean area, fire activity and burned area are expected to be influenced by changes in fuel types and characteristics, in addition to climatic conditions. Two fire spread simulators based on the Rothermel's model (FARSITE [23] and FlamMap [24]) were used in different configurations with the aim to (i) calibrate wildfire models along the Mediterranean basin considering a set of historical wildfires, and then to (ii) analyze the effects through time of the main environmental factors (wind speed, wind direction, fuel moisture, land use changes, ignition locations) on wildfire likelihood and intensity [25, 26, 27]. For the predictive objective, two time periods were used to provide input data for simulations: the past conditions of land use and key factors between 1950 and 2000, and the future conditions, from the present to 2070. Spatial and temporal variations in wildfire size and burn probabilities, derived from the simulated fire perimeters, and fire intensity, derived from simulated flame length, were evaluated and associated to the key factors, analyzing the anomalies induced by both land uses, and predicted variation in fuel moisture and weather conditions.

The efficacy of wildfire simulators as tools in wildfire analysis and prediction was confirmed by the modeling activities, at different temporal and spatial scales. The results revealed that both accurate wind field data and custom fuel models are critical in predicting wildfire spread and behavior, allowing to increase the reliability of the predicted outputs.

In addition, the application of simulators in a probabilistic configuration considering past conditions of land use and other key factors highlighted significant reductions in wildfire size and increases in wildfire intensity in recent time steps in comparison with simulations performed in '60s and '70s, mainly due to land use changes and fuel dryness increase (Fig. 5). In fact, future changes in land use projected a limited but generalized increase of sclerophyllous vegetation and forests, along with a reduction in grasslands and open pastures, with an increase in fuel load and continuity. On the other hand, the projected reduction in wind speed for future scenario will result in lower wildfire rate of spread and size.

## *2.5. Economic assessment of future fire regime driven by climate-change*

CMCC social economic assessment of the direct costs implied by future fire events in the Mediterranean area is based upon area burned, direct carbon releases and change in carbon sequestered due to future fire events derived from the model SPITFIRE [28]. The economic assessment focuses on: the non use, non market cost associated to the loss of forest ecosystems; the social cost implied by damages induced by carbon emissions from forest fires; the potential value added loss consequent to the fire-induced disruption of forest areas.

Passive value losses are estimated computing the existence value per forest hectare in the different Mediterranean countries through meta analysis of the stated preference literature and value transfer methodologies. In 2070, the Mediterranean area can experience an average loss of non use value of \$ 200 million and of \$ 97 million in RCP 8.5 and 2.6 respectively. Losses are notably higher in the richer countries, accordingly in the EU Med area, and particularly in Spain, which combines high willingness to pay (high marginal passive value attached to the forest hectare) with huge amounts of burnt hectares.

Market losses are even higher. Starting from the contribution that forestry sectors provide to national value added and extracting from this an estimate of the value added generated by an hectare of forest in each Mediterranean country it turns out that the burnt area can originate a loss ranging between \$ 848 million in 2035 and \$ 2418 million in 2070 in RCP 8.5.

The social damage implied by fire-related emissions in the Mediterranean is computed using a comprehensive set of estimated of the social cost of carbon. What is evaluated is the loss of carbon sequestered by vegetation in burnt areas. All in all, the average yearly damage induced globally by Mediterranean forest fires along the 2020-2070 period amounts to \$ 7587 million in the RCP8.5 and to \$ 5286 million in RCP 2.6. This average figure hides however huge differences across social cost of carbon estimates which largely depend upon the pure rate of time preferences adopted by the different assessments.

Finally, it is shown that if additional emissions from Euro-Mediterranean forest fires had to be part of the EU emission reduction targets for 2030, policy costs would increase between 0.3 and 0.9 additional per cent points of GDP depending on the climatic model used.

### 3. POLICY AND MANAGEMENT IMPLICATIONS

In this paragraph, the management implication deriving from CMCC results in FUME project are presented:

- One of the main limitations for the analysis of long-term fire regimes was the lack of long-term comparable and harmonized historical records. Further efforts towards harmonized definitions, formats and methodologies in fire data acquisition and assemblage across countries are needed.
- Fire activity has been changing in the Euro Mediterranean countries, also thank to the law enforcement and the improvement of fire management services and monitoring systems across the analysed countries [e.g. 26]. However, fire extreme events under severe weather conditions occurred in recent years (e.g., 2007, 2009) seemed to overwhelm the fire-fighting agencies. Progress in weather forecasting, as well as long-range predictions, may be used to enhance fire danger and risk prediction and anticipate fire season dynamics.
- LUC modeling results suggest that Mediterranean future land use distribution, if not appropriately regulated, and if combined to expected climate trends, would contribute to continuously increase land vulnerability to fires. On the other hand, modeling is confirmed a valuable tool in land protection planning, including fire hazard/vulnerability reduction strategies.
- Socio-economic, climate and biophysical aspects should be all considered when assessing future fire risk scenarios. Indeed, our results showed the relevance of each standalone driver-category as well as the importance of accounting for their interconnection.
- Wildfire simulators can provide data, maps, and guidelines that can be used from tactical and strategic planning of wildfire management, to firefighter training, and even to real-time firefighting. Throughout the output of these tools, policy makers and management agencies can plan investments and activities and evaluate the responses at fine scale, even in a perspective of future climate changes and/or other changes.

- Forest fire events can entail and induce non-negligible economic losses. Moreover, the values highlighted in this research should be considered lower bound estimates of the cost involved, as for instance they do not account for impact on health and loss of human life. This calls for pro-active policy interventions at the national and local level to put in place appropriated anticipatory measures.

#### **4. ACKNOWLEDGMENTS**

This work was funded by the European Union Seventh Framework Programme (FP7/2007-2013) under Grant Agreement 243888 (FUME Project - Forest fires under climate, social and economic changes in Europe, the Mediterranean and other fire-affected areas of the world).

#### **5. REFERENCES**

- 1 Bowman DM, Balch JK, Artaxo P, Bond WJ, Carlson JM, Cochrane MA, D'Antonio CM, Defries RS, Doyle JC, Harrison SP, Johnston FH, Keeley JE, Krawchuk MA, Kull CA, Marston JB, Moritz MA, Prentice IC, Roos CI, Scott AC, Swetnam TW, van der Werf GR, Pyne SJ., 2009. Fire in the Earth system. *Science*. 2009 Apr 24;324(5926):481-4.
- 2 Krawchuk, M.A., Moritz, M.A., Parisien, M.A., Van Dorn, J., Hayhoe, K., 2009. Global Pyrogeography: the Current and Future Distribution of Wildfire. *PLoS ONE* 4(4): e5102. doi:10.1371/journal.pone.0005102)
- 3 San-Miguel, J. and Camia, A., 2009. Forest fires at a glance: Facts, figures and trend in the EU. In: *Living with wildfires: What science can tell us?* Y. Birot (ed). European Forest institute, Discussion paper 15, pp 11-18
- 4 Keeley J.E, Fotheringham C.J., Morais M., 1999. Reexamining Fire Suppression Impacts on Brushland Fire Regimes *SCIENCE* VOL 284 11 JUNE 1829-1832
- 5 van Wilgen, B.W., Forsyth, G.G., De Klerk, H., Das, S., Khuluse, S., and Schmitz, P., 2010. Fire management in Mediterranean-climate shrublands: a case study from the Cape fynbos, South Africa. *Journal of Applied Ecology* 47:631-638.

6 Camia, A., Amatulli, G. and San-Miguel-Ayanz, J. (2008) Past and future trends of forest fire danger in Europe (JRC 46533, EUR 23427 EN). European Commission, Joint Research Centre.

7 European Commission, Joint Research Centre, Institute for Environment and Sustainability 2010. Forest fire in Europe. doi:10.2788/46294

8 Moreira F., Viedma O., Arianoutsou M., Curt T., Koutsias N., Rigolot E., Barbati A., Corona P., Vaz P., Xanthopoulos G., Mouillot F. and Bilgili E. (2011) Landscape – wildfire interactions in Southern Europe: implications for landscape management, *Journal of Environmental Management*, vol. 92, 2389-2402, doi:10.1016/j.jenvman.2011.06.028

9 IPCC, 2014 Impacts, Adaptation, and Vulnerability. Volume II: Regional Aspects. Ch. 23 Europe

10 Moreno JM 2014 Introduction. In: José M. Moreno (ED), *Lesson learned and Outlook*, ISBN: 9788469597590.

11 SPANO D., CAMIA A. BACCIU V., MASALA F., DUGUY B., TRIGO R., SOUSA P., VENÄLÄINEN A., MOUILLOT F., CURT T., MORENO J.M., ZAVALA G., URBIETA I.R., KOUTSIAS N., XYSTRAKIS F. (2014). Recent trends in forest fires in Mediterranean areas and associated changes in fire regimes. In: José M. Moreno (ED), *FUME Lesson learned and Outlook*. p. 6-7, ISBN: 9788469597590.

12 Pereira M.G., Calado T.J., DaCamara C.C., and T. Calheiros, 2013. Effects of regional climate change on rural fires in Portugal. *Climate Research*, 57: 187–200.

13 Xystrakis F., Kallimanis A.S., Dimopoulos P., Halley J.M., and N. Koutsias, 2013. Precipitation dominates fire occurrence in Greece (1900–2010): its dual role in fuel build-up and dryness. *Natural Hazards and Earth System Sciences*, 1 (2): 693–720.16 Gualdi et al. 2010,

14 BACCIU V., TRIGO R., SPANO D., MASALA F., DUGUY B., PASTOR P., SOUSA P., VENÄLÄINEN A., MOUILLOT F., MORENO J.M., ZAVALA G., URBIETA I.R., KOUTSIAS N., XYSTRAKIS F., ARIANOUTSOU M., MALLINIS G., GONZÁLEZ M.E., URRUTIA R., LARA A., KAVCACI A., MIDGLEY G., GUO D., LE MAITRE D., FORSYTH G., SOUTHEY D., ARCA B., BONORA L.,

CONESE C., DA CAMARA C., PEREIRA M.G., GOUVEIA C., CAMIA A., AMATULLI G., VILAR L., SAN MIGUEL-AYANZ J., HAIRECH T., ASSALI F., MOKSSIT A., CHERKI K., ALAOUI H. (2014). Fire and weather relationships: present climate. In: José M. Moreno (ED), FUME Lesson learned and Outlook. p. 18-19, ISBN: 9788469597590.

15 Michetti M., Pinar M., (2012) Forest fires in Italy: an econometric analysis of major driving factors. CMCC Research Paper, RP052, 2012

16 Gualdi S., Scoccimarro E., Navarra A., 2008. Changes in Tropical Cyclone Activity due to Global Warming: Results from a High-Resolution Coupled General Circulation Model. *J. of Clim.*, 21, 5204-5228.

17 Scoccimarro E., S. Gualdi, A. Bellucci, A. Sanna , P.G. Fogli, E. Manzini, M. Vichi, P. Oddo, A. Navarra (2011) Effects of Tropical Cyclones on Ocean Heat Transport in a High Resolution Coupled General Circulation Model. *Journal of Climate*, doi: 10.1175/2011JCLI4104.1

18 Rockel B., Will A., Hense A., 2008. The regional Climate Model COSMO-CLM (CCLM), *Meteorologische Zeitschrift*, 17 (4): 347-348.

19 Steppeler J., Doms G., Schättler U., Bitzer H.W., Gassmann A., Damrath U., Gregoric G., 2003. Meso-gamma scale forecasts using the nonhydrostatic model LM, *Meteorol. Atmos. Phys.*, 82 75-96.

20 Sanna A., Scoccimarro E., Gualdi S., Bellucci A., Montesarchio M., Bucchignani E. (2012) Extreme events as represented by high resolution CMCC climate models at global and regional (Euro-Mediterranean) scale. In: Spano D., Bacciu V., Salis M., Sirca C. (eds.). *Modelling Fire Behaviour and Risk*, pag. 99-105. ISBN: 978-88-904409-7-7.

21 Santini M, Valentini R (2011) Predicting hot-spots of land use change in Italy by ensemble forecasting. *Regional Environmental Change*, 11(3): 483-502

22 Michetti M., Parrado R., (2012) Improving land use modelling within CGE to assess forest-based mitigation potential and costs. *FEEM Note di Lavoro*, 2012.019

23 Finney MA (2002). Fire growth using minimum travel time methods. *Canadian Journal of Forest Research* 32(8): 1420-1424

24 Finney MA (2006). An overview of FlamMap fire modeling capabilities. In: Fuels management—how to measure success: conference proceedings. 2006 March 28-30; Portland, Oregon. Proceedings RMRS-P-41. Fort Collins, CO: U.S. Department of Agriculture, Forest Service, Rocky Mountain Research Station: 213-220.

25 Arca B., Pellizzaro G., Duce P., Salis M., Bacciu V., Spano D., Ager A., Scoccimarro E. (2012) Potential changes in fire probability and severity under climate change scenarios in Mediterranean areas- In: Spano D., Bacciu V., Salis M., Sirca C. (eds.). Modelling Fire Behaviour and Risk, pag. 92-98. ISBN: 978-88-904409-7-7.

26 Salis M, Alcasena F., Ager A.A., Casula F., Arca B., Bacciu V., and Spano D. (2013) Analyzing changes in wildfire likelihood and intensity in Mediterranean areas: a case study from central Sardinia, Italy. Proceedings of the SISC 2013

27 Salis M, Ager AA, Finney MA, Arca B, Spano D (2014) Analyzing spatiotemporal changes in wildfire regimes and exposure across a Mediterranean fire-prone area. Natural Hazards 71(3): 1389-1418. ISSN: 0921-030X

28 Thonicke, K, Spessa, A., Prentice, I.C., Harrison, S.P., Dong5, L. and C. Carmona-Moreno (2010) The influence of vegetation, fire spread and fire behaviour on biomass burning and trace gas emissions: results from a process-based model”, Biogeosciences, 7, 1991–2011

29 ARCA B., SALIS M., BENOIT J., DUGUY B., ALCASENA F., KOUTSIAS N., MALLINIS G., ZAVALA G., URBIETA I.R., CURT T, SPANO D. (2014). Assessing changes in fire hazard in Mediterranean landscapes by fire modelling. In: Josè M. Moreno (ED), Forest fires under climate, social and economic changes in Europe, the Mediterranean and other fire-affected areas of the world. p. 24-25, ISBN: 9788469597590.

## 6. IMAGES AND TABLES



Fig. 1 The FUME spatial domain

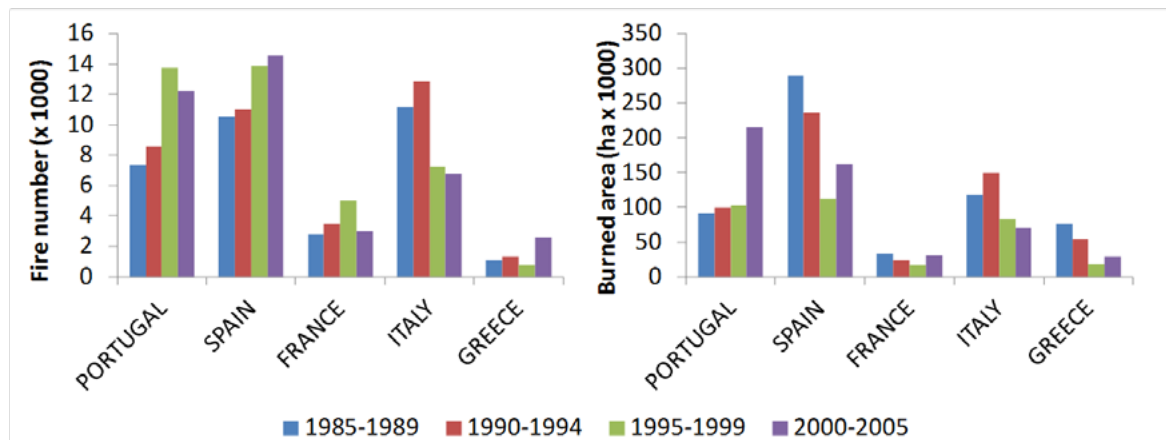


Fig. 2 Evolution of average fire number and area burned by time steps (1985-1989, 1990-1994, 1995-1999, 2000-2005) in FUME EU-Med study areas (modified from 11)

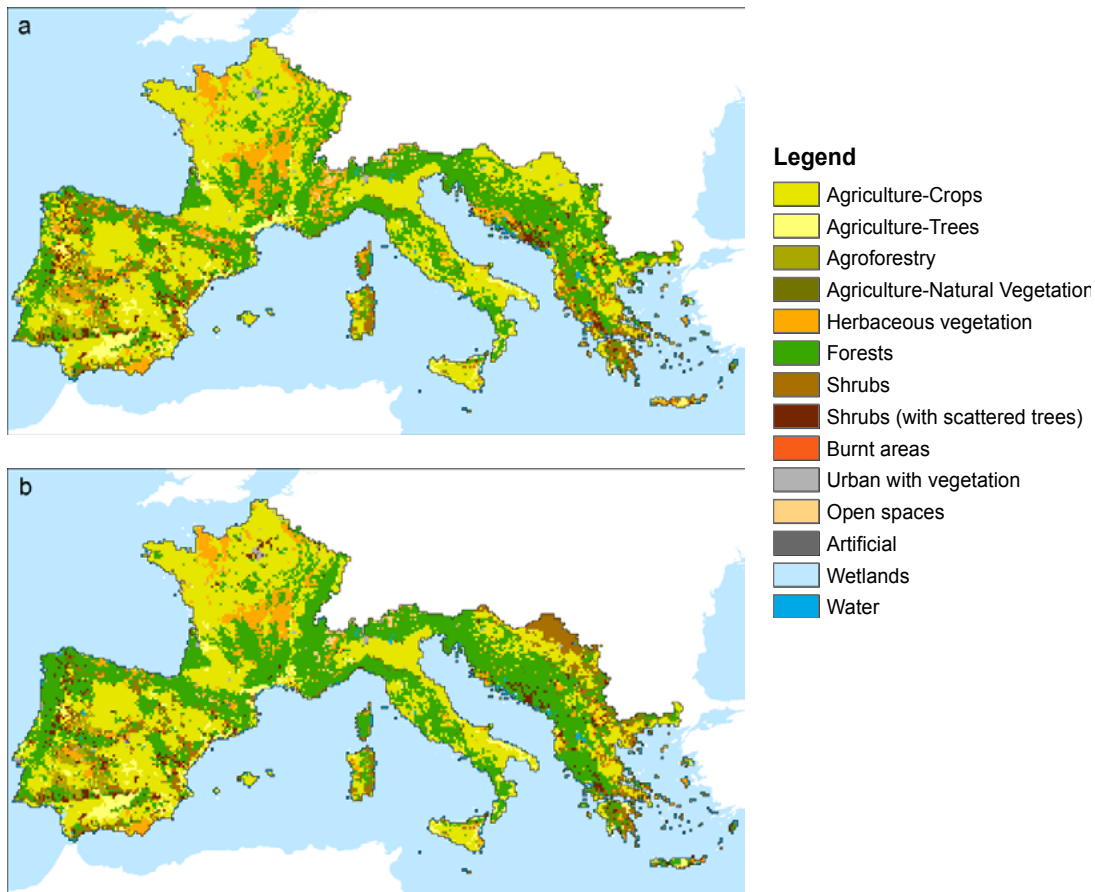


Fig. 3 EU-Med scale maps show simulated changes in land use distribution from year 2000 (a) to 2100 (b).

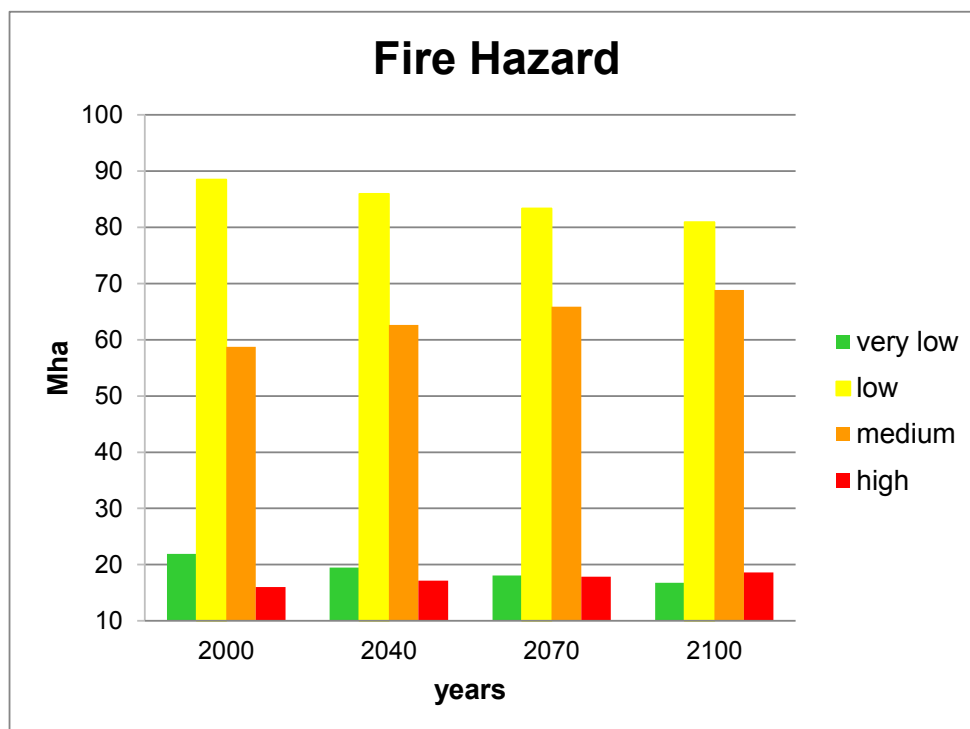


Fig. 4 Spatial distribution in surface (Mha) of fire hazard classes based on LUC classification and projections. The base year 2000 is compared with three future periods in the short (2040), medium (2070) and long (2100) term.

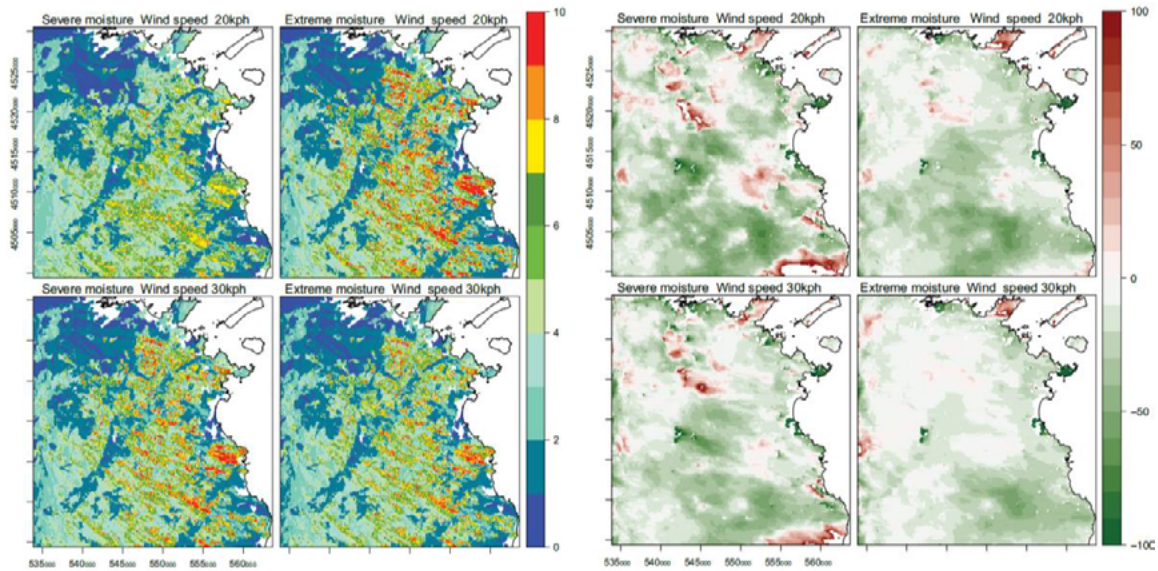


Fig. 5 On the left, maps of the North Sardinia (Italy) study area showing FlamMap flame length (m) estimates using different scenarios of fuel moisture and wind speed; the fuel model map was derived from 1977 land cover and land use data. On the right, temporal variation (%) of FlamMap burn probabilities calculated between 1977 and 2000 using different scenarios of fuel moisture and wind speed. The burn probability is the chance that a pixel will burn considering one ignition in the whole study area (from 29)

# Vulnerability of the Northern Adriatic Sea Fishery to Climate Change

Caccin A.<sup>1\*</sup>, Anelli Monti M.<sup>1</sup>, and Pranovi F.<sup>1</sup>

<sup>1</sup>CEMAS, *Center for Estuarine and Coastal Marine Sciences*, Dipartimento di Scienze Ambientali, Informatica e Statistica, Università Ca'Foscari, Venezia - Italy

\*Corresponding Author: [alberto.caccin@unive.it](mailto:alberto.caccin@unive.it)

## Abstract

Within the context of marine environments, nekton assemblages are recognised to provide several kinds of ecosystem services, both fundamental and demand-derived. They contribute, indeed, to enhance the biodiversity, the ecological processes and finally the system resilience. They also directly support the production of goods, such as in the case of renewable resources exploited by commercial fisheries. The problem of the impacts of climate change on this component of marine ecosystems, with the related consequences on ecosystem services, becomes therefore an interesting issue. In this context, the northern Adriatic Sea, hosting several species adapted to boreal climatic conditions, can be considered a good case study. By analysing the composition of landings from fisheries in terms of thermal affinity groups, we highlighted the potential vulnerability of these activities. Catches, indeed, were shown to be mainly composed of cold and temperate affinity species, whereas the contribution of warm ones resulted very low. Given the significant negative relationships between the cold and temperate groups with the recorded variations of the thermal regime and the latest projections by the IPCC in terms of ocean temperature raise, fishing activities, both professional and recreational, can be expected to experience severe consequences.

**Keywords:** climate changes, fisheries, thermal regime, northern Adriatic Sea

## 1. INTRODUCTION

According to the latest projections by the IPCC, Ocean temperature has been raising in the last decades over most of the Globe, and it is predicted to raise further in the short as well as in the long term [1]. In particular, this general trend is expected to impact the Mediterranean Sea [2], where the nektonic communities are likely to undergo deep modifications, both in terms of structure and of distribution range [3]. Nektonic communities provide several kinds of ecosystem services, both fundamental and demand – derived [4]. Fundamental ecosystem services can be described as those that are essential for ecosystem function and resilience, such as the regulation of food web dynamics, ecosystem equilibrium and biodiversity, while demand – derived services consist, among others, in food production and recreational activities. These ecosystem services will likely be impacted by modifications in the nektonic communities. In particular, fishing activities, both professional and recreational, can be expected to experience severe consequences [4]. In this context the northern Adriatic Sea, which hosts several species adapted to boreal climatic conditions [5] and, due to its nature of semi-enclosed basin, configures as a *cul-de-sac* preventing northward migration of species [6], can prove a particularly vulnerable area.

In this paper, we attempt to characterise the vulnerability of the northern Adriatic fisheries by analysing the trends of landings in relation to the composition in terms of climatic affinity groups (cold, temperate and warm climate-related species) and studying possible correlations with thermal-regime indicators.

## 2. MATERIALS AND METHODS

In analysing fish population dynamics, a choice has to be made whether to rely on data derived from scientifically conducted trawl survey campaigns (fishery-independent data), or on catch data provided by fish markets (fishery-dependent data). While fishery-independent data can theoretically provide the most accurate information, they often suffer from limitations due to the high costs of campaigns, and can be difficult to interpret because of unplanned variations in the procedures over the years [7]. Fishery-dependent data, on the other hand, are often the only data available on a large time scale, and when used with care, they can provide the

necessary information to infer the size and status of the populations being exploited [8].

Therefore, for this work, time-series of landings, spanning from 1970 to 2013 and comprising all the commercial species were retrieved from the official statistics of Chioggia fish market. Since Chioggia hosts the biggest fishing fleet in the northern Adriatic Sea, the data can be assumed to be representative of the whole basin.

Periodical observations on the quay of Chioggia harbour allowed identifying the fishing gear on-board each vessel (the three main types of gear used locally, otter trawl, *rapido* trawl and midwater pair trawl, are easily distinguishable). By integrating the fish market data with evidence from the observations on the quay, it was possible to quantify the average catch composition for each of the three main types (or métiers) of fishing gear in terms of contribution to total landings.

To account for the different sensitivity of the species to changes in temperature, the climatic affinity of each species recorded in the time-series was assessed according to the latitude-based method proposed by Pranovi et al. [9]. Each species was categorised according to the mean distribution area in terms of latitudinal range: species with a distribution over 45°N, species within the 30°N–45°N range, and species mainly found below 30°N. This allowed the identification of three climatic affinity groups, defined as cold, temperate and warm, respectively.

Monthly average sea-surface temperature (SST) time-series for the northern Adriatic was reconstructed using values from the U.S. National Oceanographic and Atmospheric Administration (NOAA) climate prediction centre website ([www.cpc.ncep.noaa.gov](http://www.cpc.ncep.noaa.gov)). For each year a temperature curve was fitted, considering the months from February to August (usually the coldest and the warmest of the year, respectively), resulting in a sigmoid shape. For these curves, the slope of the tangent at the inflection point ( $s$ ) was calculated [Fig. 1], since this parameter can be considered a good proxy both for the annual temperature raise and for the suddenness of the transition from the cold to the warm season. Temporal trends have been analysed by plotting annual landings for each thermal affinity group against  $s$ . Statistical significance of correlations was tested through the application of generalised additive models (GAM [10]) in R v. 3.0.1 (R Core Development team; [www.r-project.org](http://www.r-project.org)). In addition, temporal trends were analysed taking into the

account the landings composition of the three main métiers, to assess their vulnerability in relation to their composition in terms of climatic affinity groups. In order to assess the presence of significant regime-shifts in the time-series of both landings (in terms of climatic affinity groups) and the  $s$  indicator the Regime Shift Detection method (STARS) was applied [11,12].

### 3. RESULTS

Total landings in the considered period showed an increasing trend with two peaks recorded at the end of '70s and at the beginning of '80s, followed by a sharp decrease at the end of '80s and a fluctuating situation in the last part of the series [Fig. 2]. This pattern was mainly driven by the midwater pair trawl landings, which substantially contributed to the total values. The otter trawl and *rapido* showed both a declining trend through the time, with the highest values recorded again at the end of '70s and at the beginning of '80s. Considering the landings composition in term of climatic affinity groups, the temperate one represented the main portion of the landings, amounting, on average, to about 57% in weight of the total landings; on the other hand, species with cold climatic preferences gave a contribution of about 41%, while the remaining 2% could be ascribed to warm climatic affinity species [Fig. 3]. Differentiating the landings based on the three métiers, it is noticeable that both otter trawl and *rapido* trawl catch mainly cold affinity species, while for the midwater pair trawl temperate species represent the most significant portion of the total landings. The temporal trends analysis highlighted the presence of a negative regime shift for both the cold and temperate affinity group, between the second half of the 80s and the first half of the 90s [Fig 4]. On the contrary, warm affinity species showed a positive regime shift in 2001.

In relation to the thermal regime analysis, the temporal trend of the  $s$  indicator showed an increase through the time, with a positive shift in the early '90s, which roughly matches the negative one highlighted for the cold and temperate affinity groups [Fig. 5].

The relationship between landings and the  $s$  indicator has been tested by modelling the correlation among the temporal trend of  $s$  and the different climatic affinity groups, using GAM. Results highlighted significant negative relationships for species

of cold affinity ( $p < 0.01$ , 15.2% deviance explained), and of temperate affinity ( $p < 0.001$ , 30.6% deviance explained); no significant relationships have been detected for the warm group.

#### 4. DISCUSSION

Long term modifications in the structure and quantity of landings in the northern Adriatic Sea have been recently discussed by Barausse et al. [13], in terms of environmental drivers and life history of the different species. In this paper, we suggest that the recorded decline in catches could be related, among other factors, to changes in the thermal regime of the area recorded during the last decades. During this period, indeed, an increase of the speed in the transition from the cold to the warm season has been pointed out, with a significant shift at the beginning of the '90s.

Globally, in relation to the composition in terms of climatic affinity groups, our results seem to confirm on one side the hypothesis that the northern Adriatic Sea represents a kind of *refugium* for cold species, but on the other they highlight the high vulnerability of the nektonic assemblage to climate change. Since the Mediterranean surface waters are expected to warm by an average of 3.1°C by the end of the 21<sup>ST</sup> century [2], a general northward shift of fish ranges is expected, leading to a decrease of the cold and temperate species and a possible replacement by thermophilic ones. In this process, semi-enclosed areas located in the northern part of the basin, such as the Adriatic Sea, might act as reservoirs, but may also become a *cul-de-sac* for those species that simply cannot migrate further north [6].

Scientific evidence about the effects of climate change on fish phenology is growing in the available literature. In particular, shifts in the breeding seasons, migration timing and larval appearance in response to warming have been described in commercially relevant freshwater and marine fishes [14-17]. Similar effects have been recently described also for fish populations in the Venice lagoon [18]. All this is expected to directly influence the recruitment and ultimately the fish abundance and biomass.

These effects could be an explanation, at least for the last part of the time series, for the negative temporal trend shown by the cold and temperate affinity species of the northern Adriatic Sea, in relation to the change of the thermal regime.

The analysis of landings composition in terms of thermal affinity groups highlighted the high vulnerability of the fishing activities to climate changes in the northern Adriatic Sea, albeit with differences among the main métiers. Catches, indeed, proved to be almost entirely composed by cold and temperate species, which are the most exposed to temperature-related effects.

While recorded negative trends are certainly influenced by several factors such as increasing fishing effort and overfishing, it can be assumed that climate plays an important role in it, as confirmed by the significant negative relationship found between cold and temperate affinity groups and the thermal regime indicator.

On the other hand, in spite of the fact that northward shifts of thermophilic species are largely demonstrated in the Adriatic Sea [19-21], they still amount to just a marginal portion of the catches, even if they are increasing through time. The warm affinity species, however, showed no significant relationships with the thermal regime modifications. Their increase in the recent years can therefore be attributed to more complex dynamics possibly involving, for example, the reduced competition with local species, instead of a direct effect of temperature. All this reflected in terms of fishing activities, since landing data seem to indicate that the positive contribution from new species is not yet able to counterbalance the losses. Thus, even if fishing activity often proved to be able to adapt to the modification in the nektonic assemblage composition by quickly turning to new exploitable resources (as shown in the case of the Manila clam in the Venice Lagoon [22]) it will still have to face an overall decrease in resources, augmenting, if possible, the overall vulnerability in relation to possible effects on the system resilience.

All the recorded modifications lead to the idea that the fish community in the northern Adriatic Sea is undergoing a deep change, with a significant decrease of native species and a gradual increase of new thermophilic ones.

Nektonic communities are recognised to provide several kinds of ecosystem services, both fundamental and demand – derived [4]. For example, fundamental services like regulation of trophic-web dynamics can be significantly altered if key,

high-biomass planktivorous species such as sardine will decrease. Moreover, many species like mullet, seabream, or sardine itself are marine migrants, which spend part of their life-cycles in estuarine habitats, linking different systems in terms of energy. All this is expected to affect ecosystem functioning, finally reducing long-term capacity to adapt [23].

All this is expected to deeply affect ecological processes going on in the northern Adriatic Sea with consequences also in terms of benefits for the human populations [24]. Considering demand-derived services, other than the described effects on commercial fisheries, recreational fishing can also experience consequences, since many prized target species, like gilt-headed seabream, mackerel and bluefin tuna, belong to the temperate affinity group.

In conclusion, by analysing the nektonic composition in terms of thermal affinity groups it was possible to describe the vulnerability to climate changes of fisheries in the northern Adriatic Sea, discussing this issue in the light of possible implication in terms of ecosystem services provisioning.

## 5. REFERENCES

1. IPCC (2013), *Climate Change 2013: The Physical Science Basis. Contribution of Working Group I to the Fifth Assessment Report of the Intergovernmental Panel on Climate Change*, Cambridge University Press.
2. Somot S., Sevault F., Déqué M. & Crépon M. (2008), *21st century climate change scenario for the Mediterranean using a coupled atmosphere–ocean regional climate model*, *Global and Planetary Change*, No. 63, pp. 112-126.
3. Albouy C., Guilhaumon F., Araújo M.B., Mouillot D. & Leprieur F. (2012), *Combining projected changes in species richness and composition reveals climate change impacts on coastal Mediterranean fish assemblages*, *Global Change Biology*, No. 18, pp. 2995-3003.
4. Holmlund C.M. & Hammer M. (1999), *Ecosystem services generated by fish populations*, *Ecological economics*, No. 29, pp. 253-268.
5. Tortonese E. (1964), *Main biogeographical features and problems of the Mediterranean fish fauna*, *Copeia*, No. 1, pp. 98-107.
6. Ben Rais Lasram F., Guilhaumon F., Albouy C., Somot S., Thuiller W. & Mouillot D. (2010), *The Mediterranean Sea as a 'cul-de-sac' for endemic fishes facing climate change*, *Global Change Biology*, No. 16, pp. 3233-3245.
7. Bishop J. (2006), *Standardizing fishery-dependent catch and effort data in complex fisheries with technology change*, *Reviews in Fish Biology and Fisheries*, No. 16, pp. 21-38.
8. Pauly D., Hilborn R. & Branch T.A. (2013), *Fisheries: Does catch reflect abundance?*, *Nature*, No. 494, pp. 303-306.
9. Pranovi F., Caccin A., Franzoi P., Malavasi S., Zucchetta M. & Torricelli P. (2013), *Vulnerability of artisanal fisheries to climate change in the Venice Lagoon*, *J Fish Biol*, No. 83, pp. 847-864.
10. Hastie T.J. & Tibshirani R.J. (1990), *Generalized additive models*, CRC Press.

11. Rodionov S.N. (2004), *A sequential algorithm for testing climate regime shifts*, Geophysical Research Letters, No. 31.
12. Rodionov S.N. (2005), *A brief overview of the regime shift detection methods*, Large-Scale Disturbances (Regime Shifts) and Recovery in Aquatic Ecosystems: Challenges for Management Toward Sustainability, pp. 17-24.
13. Barausse A., Michieli A., Riginella E., Palmeri L. & Mazzoldi C. (2011), *Long-term changes in community composition and life-history traits in a highly exploited basin (northern Adriatic Sea): the role of environment and anthropogenic pressures*, J Fish Biol, No. 79, pp. 1453-1486.
14. Genner M.J., Halliday N.C., Simpson S.D., Southward A.J., Hawkins S.J. & Sims D.W. (2010), *Temperature-driven phenological changes within a marine larval fish assemblage*, Journal of Plankton Research, No. 32, pp. 699-708.
15. Gillet C. & Quetin P. (2006), *Effect of temperature changes on the reproductive cycle of roach in Lake Geneva from 1983 to 2001*, J Fish Biol, No. 69, pp. 518-534.
16. Pilling G.M., Millner R.S., Easey M.W., Maxwell D.L. & Tidd A.N. (2007), *Phenology and North Sea cod *Gadus morhua* L.: has climate change affected otolith annulus formation and growth?*, J Fish Biol, No. 70, pp. 584-599.
17. Taylor S.G. (2008), *Climate warming causes phenological shift in Pink Salmon, *Oncorhynchus gorbuscha*, behavior at Auke Creek, Alaska*, Global Change Biology, No. 14, pp. 229-235.
18. Zucchetta M., Cipolato G., Pranovi F., Antonetti P., Torricelli P., Franzoi P. & Malavasi S. (2012), *The relationships between temperature changes and reproductive investment in a Mediterranean goby: Insights for the assessment of climate change effects*, Estuarine, Coastal and Shelf Science, No. 101, pp. 15-23.
19. Dulčić J., Dragičević B., Grgičević R. & Lipej L. (2011), *First substantiated record of Lessepsian migrant - the dusky spinefoot *Siganus luridus**

- (*Actinopterygii: Perciformes: Siganidae*) - in the Adriatic Sea, *Acta Ichthyologica et Piscatoria*, No. 41, pp. 141-143.
20. Dulčić J. & Grbec B. (2000), *Climate changes and Adriatic ichthyofauna*, *Fishery Oceanography*, No. 9, pp. 187-191.
21. Dulčić J., Pallaoro A., Dragičević B. & Stagličić-Radica N. (2010), *First record of dwarf flathead *Elates ransonnetii* (Platycephalidae) in The Adriatic Sea*, *Cybium*, No. 34, pp. 222-233.
22. Pranovi F., Da Ponte F., Raicevich S. & Giovanardi O. (2004), *A multidisciplinary study of the immediate effects of mechanical clam harvesting in the Venice Lagoon*, *ICES Journal of Marine Science: Journal du Conseil*, No. 61, pp. 43-52.
23. Staudinger M.D., Grimm N.B., Staudt A., Carter S.L., Chapin F.S., Kareiva P., Ruckelshaus M. & Stein B.A. (2012), *Impacts of Climate Change on Biodiversity, Ecosystems, and Ecosystem Services: Technical Input to the 2013 National Climate Assessment. Cooperative Report to the 2013 National Climate Assessment*.
24. Caccin A., Anelli Monti M., Libralato S. & Pranovi F. (2014), *Specie aliene termofile e funzionamento dell'ecosistema: il caso di studio dell'alto Adriatico*, *Atti del 45° Congresso della Società Italiana di Biologia Marina*, No. In press, pp. 47-50.

## 6. IMAGES

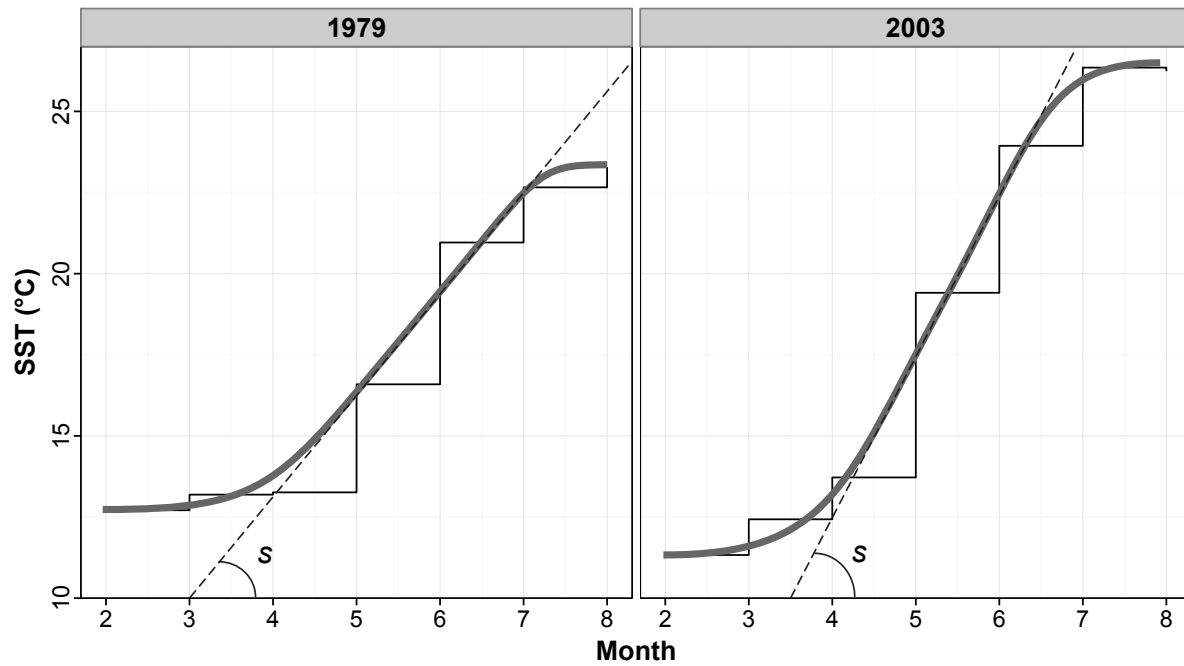


Fig. 1 SST temperatures from February to August for 1979 and 2003. The  $s$  parameter is extrapolated by fitting a sigmoid curve (grey line) to the data (black stair-step line), and then calculating the slope of the tangent to the curve (dashed line) at the inflection point. Notice that  $s$  is much higher in 2003 ( $s = 4.42$ ) than in 1979 ( $s = 2.41$ ).

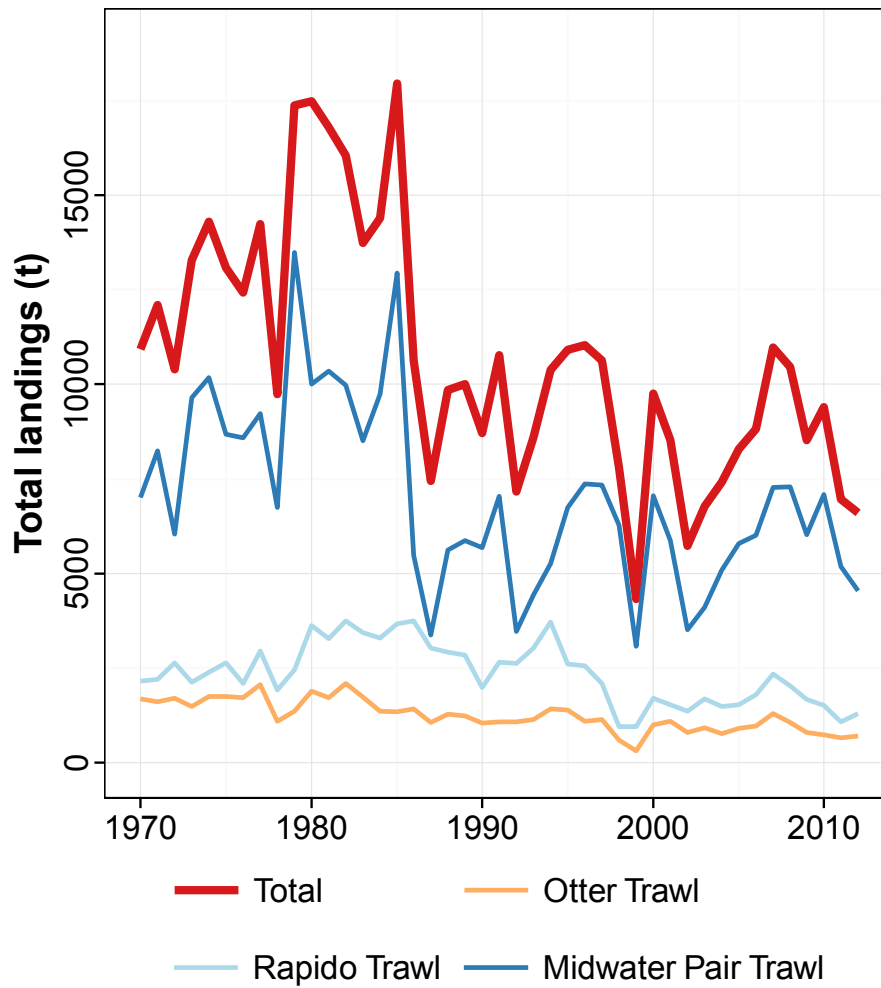


Fig. 2 Time series of landings (total and by métiers); data reconstructed using Chioggia fish market official statistics.

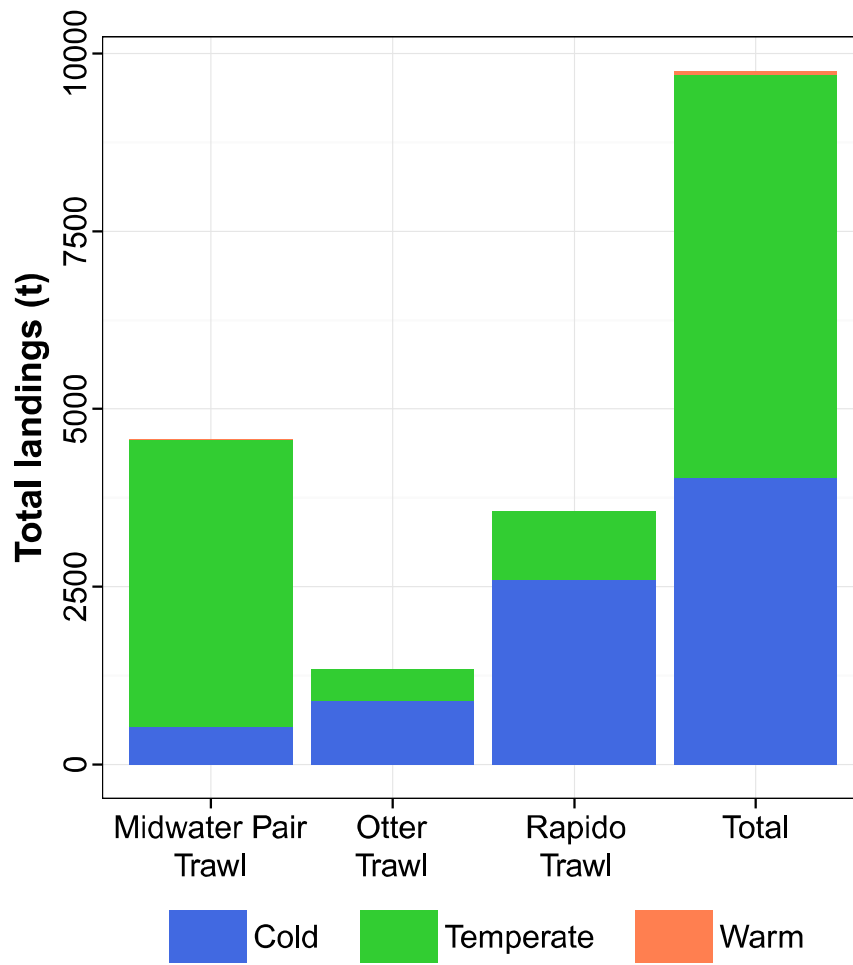


Fig. 3 Landings composition in terms of climate affinity groups (total and by métiers)

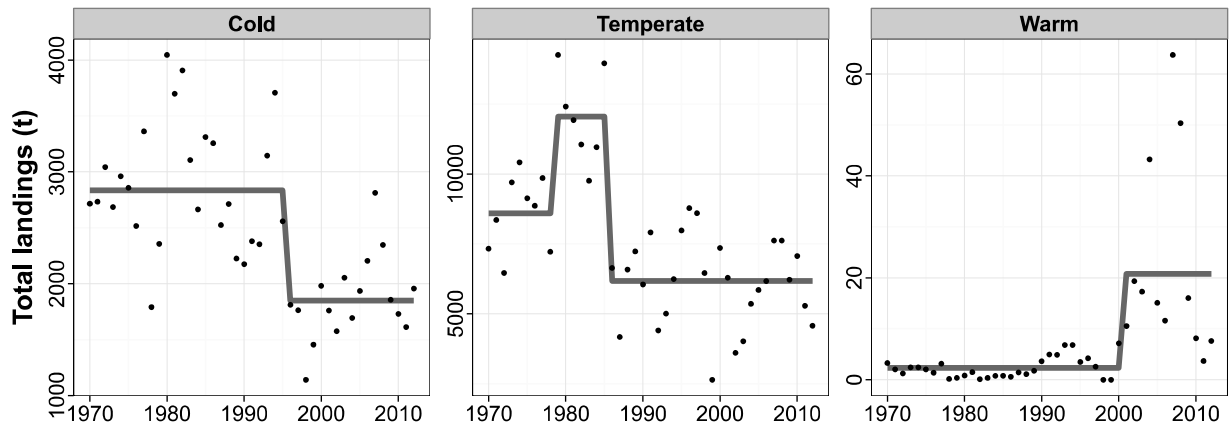


Fig. 4 Time series of landings for the three climate affinity groups; grey lines mark the regime shifts according to the STARS method

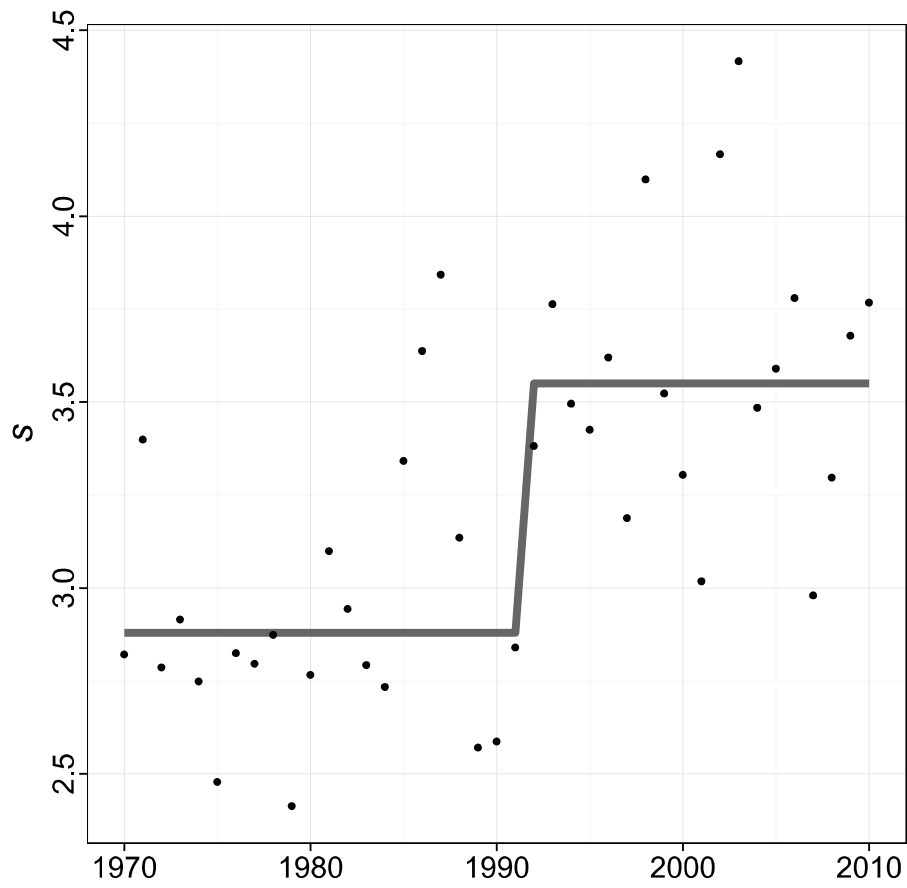


Fig. 5 Time-series of the  $s$  indicator; grey line marks the regime shift, according to the STARS method

## **Assessing multiple climate change impacts in coastal zones: the North Adriatic case study (Italy)**

**Gallina V.<sup>1,2</sup>, Torresan S.<sup>1,2</sup>, Critto A.<sup>1,2\*</sup>, Zabeo A.<sup>1,2</sup>, Sperotto A.<sup>1,2</sup>, Marcomini A.<sup>1,2</sup>**

<sup>1</sup>Centro-Euro Mediterraneo sui Cambiamenti Climatici (CMCC), Lecce, Italy,

<sup>2</sup>Department of Environmental Sciences, Informatics and Statistics,

University Ca' Foscari Venice, Venice, Italy

Corresponding Author: marcom@unive.it

### **Abstract**

The World Bank report on the main hotspots of natural hazards highlights that million people in the world are relatively highly exposed to at least two hazards, and additional impacts can be posed by climate change. Therefore, different natural and climate-related impacts should be handled in a multi-risk perspective in order to aggregate, compare and rank different kinds of impacts caused by climate change. A major challenge for climate impact research is therefore to develop new methods and tools for the aggregation of the effects expected from multiple impacts across different regions and sectors, taking into account changing climate, exposure and vulnerability. A multi-risk methodology was developed and tested at the Euro-Mediterranean Centre for Climate Change (CMCC) in order to tackle multiple climate-related hazards (e.g. sea-level rise, coastal erosion, storm surge) and sectors (e.g. natural systems, beaches, agricultural and urban areas) and support stakeholders in the definition of adaptation strategies in the North Adriatic coast. The multi-risk methodology is based on four main steps: multi-hazard, exposure, multi-vulnerability and multi-risk in which hazard metrics and physical/environmental vulnerability indicators are aggregated by means of Multi-Criteria Decision Analysis. The main results of the analysis, including GIS-based maps and statistics, will be here presented and discussed.

**Keywords:** multi-risk methodology, climate change, GIS-based maps, adaptation strategies.

# **The effects of climate change on agricultural sustainability in MENA Countries: implications for food security**

**Dhehibi B.<sup>\*1</sup>, Frija A.<sup>1</sup>, Aw-Hassan A.<sup>1</sup>**

<sup>1</sup>Social, Economics and Policy Research Program (SEPRP); International Center  
for Agricultural Research in the Dry Areas (ICARDA); Amman, Jordan

\*Corresponding Author: [b.dhehibi@cgiar.org](mailto:b.dhehibi@cgiar.org)

## **Abstract**

This paper is part of a larger study conducted by ICARDA aiming to investigate the patterns of agriculture total factor productivity (TFP) in Middle East and North African (MENA) countries during the period 1961–2011. We use output-based Tornqvist index to examine whether our estimates confirm or invalidate the results of previous studies indicating the decline of agricultural productivity in developing countries. In this paper, we only focus on the case of Tunisia, where the TFP index was calculated for the period 1961-2011 and regressed as function of disaggregated climate variables, differentiating between different regions within Tunisia. Due to limited climate data availability, the considered regression period was only from 1974 to 2006. Empirical findings showed an increasing trend in temperature, rainfall and sunshine duration while number of rain-days and relative humidity showed a decreasing trend. It was also observed that the major climate variables that strongly and negatively affected agricultural sustainability (TFP) were temperature and rainfall in the southern part of the country. The negative effects of climate change on the sustainability of agricultural sector in Tunisia requires urgent intervention by government, especially at the most critical regions as identified in this study.

**Keywords:** sustainability; food security; temperature; rainfall; MENA

Impacts & Implications of  
Climate Change

**Poster session**

# **Projecting bioclimatic trends from recent times until the end of the twenty-first century in Andalusia (south of Spain)**

**López-Tirado J.\*, Hidalgo P.J.**

Department of Environmental Biology and Public Health.  
Faculty of Experimental Sciences, University of Huelva (Spain)

\*Corresponding Author: [javier.lopez@dbasp.uhu.es](mailto:javier.lopez@dbasp.uhu.es)

## **Abstract**

Bioclimatology studies the relationship between the climate and the living beings and their communities in the Earth. It is usually known as Phytoclimatology because plants distribution determines many of the indices used in this science. In general, temperatures and rainfall values are the main key factors for the study of this science. From this values there are derived many different indices. The present work studied three bioclimatic indices for the south of Spain: Compensated Thermicity Index (CTI), Continentality Index (CI) and Ombrothermic Index (OI), in four time periods: 1971-2000, 2011-2040, 2041-2070 and 2071-2100. The main objective was to assess the trend of these indices in the context of global change. The results pointed out a generalised increment in the CTI and CI values, whereas OI values showed a drastic decreasing. In consequence, an upward migration of the bioclimatic belts could be expected. Therefore, the forecasted indices pointed out a possible negative impact on the flora and vegetation of the study area, especially in those endemisms which grow in the higher ranges in Andalusia. On the contrary, alien species could spread in the more thermic areas, possibly becoming as invasive.

**Keywords:** bioclimatology, regional change, Andalusia

## 1. TEXT

Bioclimatology or Phytoclimatology is an ecological science which studies the relationship between the climate and the living beings and their communities in the Earth [6]. Thus, climatic parameters such as temperature and rainfall are analysed taking into account the distribution of some plants and their vegetal communities. The main aim of this study is to evaluate the impact of the expected global warming in some bioclimatic parameters in Andalusia. Thus, several bioclimatic indices can be of great interest in the study of Species Distribution Modelling, and how the potential distribution of a given species could be modified in the context of global change. The final goal is to develop a methodology to predict this impact on species and ecosystems. High mountain conifers and oak trees, together with another interesting species such as wild olive, are being modelled in this area as much in present scenarios as in the future ones along the twenty-first century [3; 4].

The study area is located in the region of Andalusia (south of Spain), which comprises 87,598 km<sup>2</sup> approximately [Fig. 1]. In this area, the climate is Mediterranean, being located from 23° to 52°N & S. Its main characteristic is the existence of drought during the hottest period of the year [1]. Regarding orography, this region is composed of two ranges principally: *Sierra Morena* on one hand, located in a belt along the north, created by the Hercynian folding and characterized for having acid soils principally, rounding the highest summits 1300 m a.s.l. and, on the other hand, a more recent formation originated by the Alpine orogeny: the Baetic range, located in the east of Andalusia, where limestone is the main rock, and having the highest point in the Iberian Peninsula with 3479 m a.s.l. Between these ranges stays the depression of the Guadalquivir river that occurs in the southwest and it is narrowed towards the east. The predominant soil in this valley is marls. Its low elevation and the smooth terrain make this territory ideal for agriculture. Nowadays only remain vestigial patches of natural vegetation. Moreover, the study area shows an extreme contrast regarding rainfall, being present desert areas in the southeast, whereas other zones show the highest mean annual rainfall in the Iberian Peninsula, near the coastline, in which tropical and subtropical species persist in the actual Mediterranean climate. Raw climatic data were obtained from REDIAM (Environmental Information Network of Andalusia, Regional ministry of Environment)

as raster files and transformed into a mesh of points with 250 m resolution. This vectorial shapefile of 1,398,286 points comprised the necessary information for calculating these indices. ArcGIS 10 software (ESRI, 2010) has been used to develop this methodology. Finally, the ranges of each index were identified by means of the Worldwide Bioclimatic Classification System, Phytosociological Research Center ([www.globalbioclimatics.org](http://www.globalbioclimatics.org), last accessed May 2014), obtaining a map to each time period. The studied indices were Compensated Thermicity Index (CTI), Continentality Index (CI) and Ombrothermic Index (OI), in four time periods: 1971-2000, 2011-2040, 2041-2070 and 2071-2100.

The CI used was calculated subtracting the mean temperature of the warmest month (July) and the mean temperature of the coldest month (January). To obtain the CTI, first was calculated the Thermicity Index (TI), which follows the next equation:  $TI = (T + m + M) / 10$ , where:  $T$  is the mean annual temperature,  $m$  is the minimum mean temperature of the coldest month and  $M$  is the maximum mean temperature of the coldest month. Then, a compensation value was added as follows:  $CTI = TI + Ci$ . This compensation value was calculated according to CI [Tab. 1]. Finally, OI was the division between the sum of the mean rainfall in those months which mean temperature is over zero Celsius degrees and the sum of the monthly mean temperatures over zero Celsius degrees. In the study area, CI ranges between barely euhyperoceanic and barely subcontinental [Tab. 2] subtypes; CTI ranges between crioro-Mediterranean and upper infra-Mediterranean belts [Tab. 3] and OI ranges upper hyperarid and upper humid [Tab. 4] belts.

The resulting maps for the three indices in the four time periods studied are shown in figure 2. Taking into account these predictions, the results pointed out a generalised increment in the CI values, especially in the inland territory. On the other hand, OI values showed a drastic decreasing, therefore arid areas could spread to the detriment of the wetter ones. Finally, CTI values underwent a rise in the whole area. As a consequence, bioclimatic belts could suffer an upward migration. Thus, Oro-Mediterranean and Crioro-Mediterranean belts could be confined to the summit of the highest mountains. This trend could be reflected in the rise of the treeline in those species which grow in the high mountains of the Baetic range, such as *Pinus sylvestris* L., *P. nigra* Arnold, *A. pinsapo* Boiss. or *Quercus pyrenaica* Willd. in the main [3; 4]. On the other hand, at lower elevations could appear the Infra-

Mediterranean belt which nowadays is missing in the study area. Thus, thermophilous species could widely spread. In summary, the forecasted indices in the context of global change pointed out a possible negative impact on the flora and vegetation of the study area, a very important aspect for the conservation of those endemisms which grow in the higher ranges in Andalusia. On the contrary, alien species could spread in the more thermic areas, possibly becoming invasive. These research lines will be developed by our group using this work as a basis point in future studies. Finally, bioclimatology is an applied science that can be useful for being related to other disciplines, such as vegetation or paleoecology among others [2; 5], therefore, it is of interest the study of its traits and trends for supporting past, present and future advances in these other fields.

## 2. ACKNOWLEDGMENTS

The authors are grateful to the Regional Ministry of Economy, Innovation, Science and Employment of the Andalusian Government for supporting this study in the frame of the project entitled “Modelo espacial de distribución de las quercíneas y otras formaciones forestales de Andalucía: una herramienta para la gestión y la conservación del patrimonio natural” (Code P10-RNM-6013).

## 3. REFERENCES

1. Daget P. (1977), *Mediterranean bioclimate – General characteristics and modes of definition*, Vegetation, No. 34(1), pp. 1-20.
2. De Beaulieu J.L., Miras, Y., Andrieu-Ponel, V., Guiter, F. (2005), *Vegetation dynamics in north-western Mediterranean regions: Instability of the Mediterranean bioclimate*, Plant Biosystems, No. 139(2), pp. 114-126.
3. López-Tirado J., Hidalgo, P.J. (2013) *The potential impact of global change on the distribution of Pinus sylvestris L., P. nigra Arnold and Abies pinsapo Boiss. in the baetic range (Andalusia, Spain): a high resolution predictive model.*

Adapting to Global Change in the Mediterranean Hotspot Conference. Seville (Spain).

4. López-Tirado J., Hidalgo, P.J. (2014) *Predictive modelling of the climax oak trees (Quercus ilex subsp. ballota (Desf.) Samp., Q. suber L., Q. faginea Lam., Q. pyrenaica Willd. And Q. canariensis Willd.) and wild olive (Olea europaea L. subsp. europaea var. sylvestris (Mill.) Lehr) in Andalusia (Spain) and its potential distribution throughout the twenty-first century. 2<sup>nd</sup> International Conference of Plant Biodiversity. Marrakech (Morocco).*
5. Pons A. (1984) *Paleoecology and spatial variations in Mediterranean bioclimate*, Bulletin de la Société Botanique de France–Actualités botaniques, No. 131(2-4), pp. 77-83.
6. Rivas-Martínez S. (1988) *Bioclimatología, biogeografía y series de vegetación de Andalucía occidental*, Lagasalia, No. 15 (Extra), 91-119.

## 4. IMAGES AND TABLES

<b>CI</b>	<b>Ci</b>	<b>maximum value</b>
$lc \leq 8$	$Ci = 10 (lc - 8)$	$C0 = - 80$
$18 < lc \leq 21$	$Ci = 5 (lc - 18)$	$C1 = + 15$
$21 < lc \leq 28$	$Ci = 15 + 15 (lc - 21)$	$C2 = + 105$

Tab. 1 Calculation of the compensation value (Ci) according to the Continentality Index (CI).

<b>CI subtypes</b>	<b>Values</b>
Barely euhyperoceanic	6 – 8
Extremely euhyperoceanic	8 – 10
Barely subhyperoceanic	10 – 11
Extremely semihyperoceanic	11 – 13
Barely semihyperoceanic	13 – 14
Extremely euoceanic	14 – 16
Barely euoceanic	16 – 17
Barely semicontinental	17 – 19
Extremely semicontinental	19 – 21
Barely subcontinental	21 – 24

Tab. 2 Continentality index subtypes in the study area.

<b>CTI belts</b>	<b>Values</b>
Oro- and crioro-Mediterranean	< 120
Upper supra-Mediterranean	120 – 150
Lower supra-Mediterranean	150 – 220
Upper meso-Mediterranean	220 – 285
Lower meso-Mediterranean	285 – 350
Upper thermo-Mediterranean	350 – 400
Lower thermo-Mediterranean	400 – 450
Upper infra-Mediterranean	450 – 515

Tab. 3 Compensated thermicity index belts in the study area.

<b>Ombrotypes</b>	<b>Values</b>
Upper hyperarid	0.2 - 0.3
Lower arid	0.3 - 0.6
Upper arid	0.6 - 1.0
Lower semiarid	1.0 - 1.5
Upper semiarid	1.5 - 2.0
Lower dry	2.0 - 2.8
Upper dry	2.8 - 3.6
Lower subhumid	3.6 - 4.8
Upper subhumid	4.8 - 6.0
Lower humid	6.0 - 9.0
Upper humid	9.0 - 12.0

Tab. 4 Ombrotypes in the study area.

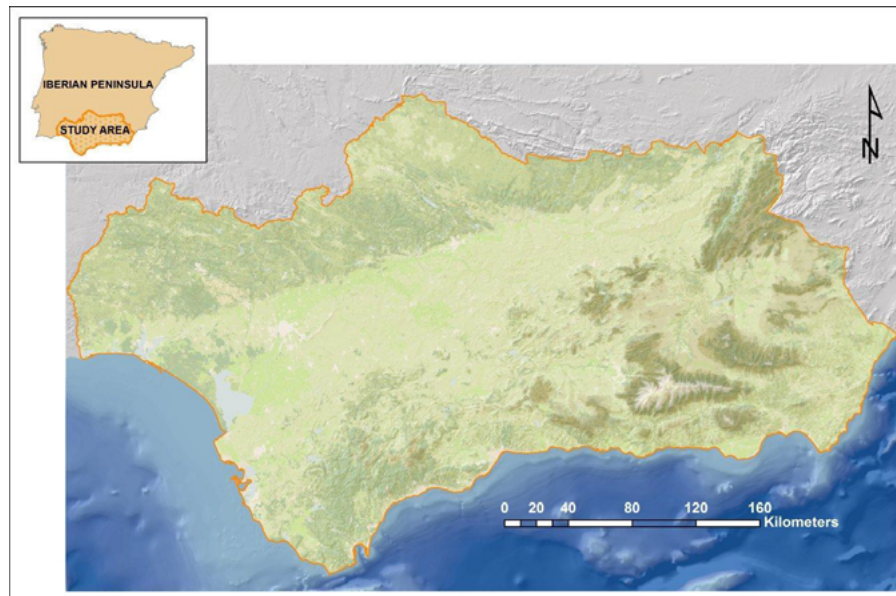


Fig. 1 Location of the study area.

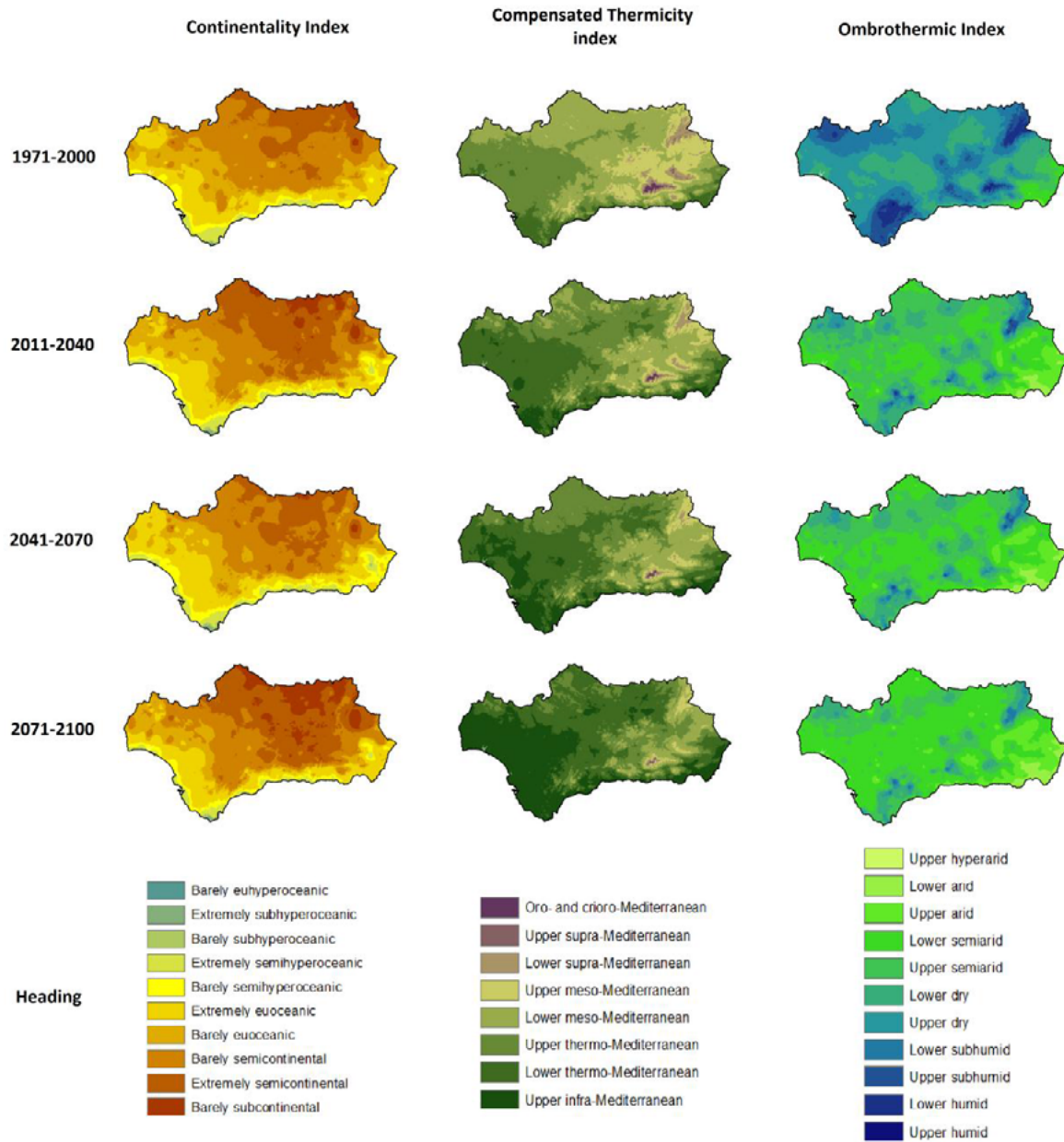


Fig. 2 Resulting maps of the three studied indices.

# Investigation on the Reference Evapotranspiration Distribution at Regional Scale by Alternative Methods to Compute the Fao Penman-Monteith Equation

Mancosu N<sup>1\*</sup>, Snyder R.L.<sup>2</sup>, and Spano D.<sup>3</sup>

<sup>1</sup>Dept. of Science for Nature and Environmental Resources (DipNET), University of Sassari, Italy, and Euro-Mediterranean Center on Climate Changes (CMCC), IAFENT Division, Sassari, Italy,

<sup>2</sup>Dept. of Land, Air and Water Resources, University of California, Davis, USA

<sup>3</sup>Dept. of Science for Nature and Environmental Resources (DipNET), University of Sassari, Italy, and Euro Mediterranean Center on Climate Change (CMCC), IAFENT Division, Sassari, Italy

\*Corresponding author: nmancosu@uniss.it

## Abstract

The goal of this study was to define procedures needed to make a standardized reference evapotranspiration ( $ET_{os}$ ) zone map using daily climate data from “Full” stations, having solar radiation, air temperature, wind speed, relative humidity, and from “Partial” stations, having only temperature data. For Partial stations, the  $ET_{os}$  was estimated either by substitution of data from nearby “Full” stations or by using a calibration factor and the Hargreaves-Samani equation estimate of reference evapotranspiration. The substitution method gave statistically better estimates of  $ET_{os}$  than the calibration method. In addition, to improve the number and distribution of  $ET_{os}$  estimates, three interpolation techniques were evaluated. Ordinary kriging provided better spatialization of  $ET_{os}$  data than the inverse distance weighting and radial basis function.

**Keywords:** Hargreaves-Samani, full and partial stations, missing weather data, interpolation models, irrigation management.

## 1. INTRODUCTION

Reference evapotranspiration ( $ET_o$ ) quantifies evaporative demand of the environment and it is used to estimate water losses from crops using the crop coefficient ( $K_c$ ) method [9; 24; 2; 29]. An accurate  $ET_o$  computation is the first step in assessing the crop water requirement (CWR), which is useful for water resources planning. Knowing the CWR helps to avoid water wastage for excessive irrigation application and yield reduction due to under-irrigation and it provides information needed for water supply assessment.

Methods to compute  $ET_o$  include empirical equations based on air temperature, or based on solar radiation. Combination methods include additional variables and they are more theoretically based on energy balance and plant physiology.

A modified Penman-Monteith (PM) equation for  $ET_o$  was adopted by the Food and Agriculture Organization of the United Nations (UN-FAO) [2]. The modified PM equation has been widely adopted as the method for computing  $ET_o$  on a worldwide basis because it is reported to be more accurate than other equations [8; 6; 17, 16; 31; 21; 13; 41; 27; 39; 5]. Later, the American Society of Civil Engineers-EWRI [1] further defined the modified PM equation and the calculation procedures for a standardized estimate of  $ET_o$ . The daily (24-hour) Standardized Reference Evapotranspiration for Short Canopies ( $ET_{os}$ ) was defined in Allen et al. [1] as the evapotranspiration from a 0.12-m tall, virtual crop surface having a fixed canopy resistance and aerodynamic resistance as an inverse function of the 2-m height wind speed. The equation for the daily  $ET_{os}$  presented in Allen et al. [1] is the same as that presented in Allen et al. [2]. Typically,  $ET_{os}$  rates are similar to the evapotranspiration of a broad expanse of 0.12-m tall, cool-season (C-3 species) grass assuming no reductions in evaporation due to stress [1].

Many weather stations lack the sensors needed to record solar radiation, wind speed, and relative humidity, which are used in the  $ET_{os}$  calculation. Procedures to estimate missing variables were provided by Allen et al. [2], and those methods are useful to estimate missing data in locations where there are no nearby stations with similar microclimates and topography. In a Mediterranean climate, difference in weather variables between nearby stations tends to be small unless the locations differ in proximity to the ocean (sea) or in local topography or elevation. Allen et al. [2] suggested substitution of data from nearby stations as a method to fill in missing

data, and other researchers [30; 18; 26; 38; 32; 22; 35] reported good results by using substitution. Alternatively, several studies have used the Hargreaves and Samani [15] equation (HS), which employs only air temperature data to estimate reference evapotranspiration. The HS equation, however, tends to fail in extreme humidity and wind conditions [33; 24; 3; 2; 37; 34; 10; 40]. Local calibration of the HS equation for wind speed or humidity has provided good estimates of reference evapotranspiration in some studies [23; 28; 14; 12; 36].

Reference evapotranspiration estimation at the field or basin scale limits the use of the information to locations near the sample point. On a regional scale, however, it is important to estimate  $ET_{os}$  for irrigation planning, crop management decisions [42], and mapping data by a geographic information system (GIS). This is a way to extend information to those locations where a direct estimation is not available.

Considering that Mediterranean basin is one of the most affected areas by climate change [20; 19], an accurate estimate of the current  $ET_{os}$  spatial distribution is useful to assess potential changes in crop water requirements. This paper reports on a study to determine the procedures to (1) assess alternative methods to estimate  $ET_{os}$  when missing meteorological variables occur, (2) compare different interpolation methods to predict the distribution of  $ET_{os}$  data at regional scale, and (3) define  $ET_{os}$  zones in a case study.

## 2. MATERIALS AND METHODS

The case study was conducted on the island of Sardinia, which is located in the center of the western Mediterranean basin (from 38°N to 41°N, and from 8°E to 10°E) and covers an area of about 24 000 km<sup>2</sup> [Fig. 1].

Daily meteorological data recorded by the weather station networks of the Specialist Regional Hydro-Weather-Climate Department (ARPAS) and the regional agency Distretto Idrografico Regionale (ID) were used. A preliminary analysis of the daily climate records was completed to identify which stations to include in the study. Stations that had more than 10% missing data were not included. Finally, 24 ARPAS network stations, having daily records from 2000 to 2004, were identified as well as 39 ID network stations for the period 2000-2002. The distribution of the 63 meteorological stations that were used in the study is shown in Fig. 2.

Following the distinction proposed by Ashraf et al. [4], weather stations were divided into sets of “partial” and “full” stations. When all variables needed for the  $ET_{os}$  equation were available, a station was deemed a “full” weather station (ARPAS network). Otherwise, it was considered a “partial” weather station (ID network).

The standardized reference equation for short canopies [2; 1] is given by:

$$ET_{os} = \frac{0.408\Delta(R_n - G) + \gamma(900/(T + 273))u_2(e_s - e_a)}{\Delta + \gamma(1 + 0.34u_2)} \quad (1)$$

and the Hargreaves and Samani [15] equation for reference evapotranspiration is expressed as:

$$ET_o = 0.0023R_a(T + 17.8)\sqrt{T_{max} - T_{min}} \quad (2)$$

In these equations,  $ET_{os}$  ( $\text{mm d}^{-1}$ ) is the daily (24-hour) Standardized Reference Evapotranspiration;  $ET_o$  ( $\text{mm d}^{-1}$ ) is the Hargreaves-Samani daily reference evapotranspiration for 0.12 m, tall grass;  $\Delta$  is the slope of the saturated vapor pressure curve ( $\text{kPa } ^\circ\text{C}^{-1}$ );  $R_n$  is the net radiation ( $\text{MJ m}^{-2} \text{d}^{-1}$ );  $G$  is the ground heat flux density at the soil surface ( $\text{MJ m}^{-2} \text{d}^{-1}$ );  $T$  ( $^\circ\text{C}$ ) is the daily mean air temperature at 1.5 to 2 m height, (i.e., the mean of maximum ( $T_{max}$ ) and minimum ( $T_{min}$ ) temperatures);  $u_2$  is the average wind speed at 2 m height ( $\text{m s}^{-1}$ ); ( $e_s - e_a$ ) is the vapor pressure deficit ( $\text{kPa}$ ), where  $e_s$  is the saturation vapor pressure at temperature  $T$  and  $e_a$  is the actual vapor pressure; and  $\gamma \approx 0.0677 \text{ kPa } ^\circ\text{C}^{-1}$  is the psychrometric constant. For daily calculations, the ground heat flux is set equal to zero (i.e.,  $G \approx 0$ ).  $R_a$  is the extraterrestrial radiation ( $\text{MJ m}^{-2}\text{d}^{-1}$ ), which is needed for both equations. For partial stations, only the  $ET_o$  was computed, and two alternative methods were used to estimate the  $ET_{os}$  from  $ET_o$ . The methods are:

**Calibration:** The calibration method uses a correction factor to estimate  $ET_{os}$  from the HS derived  $ET_o$  for a partial station. The correction factor ( $K_f$ ) equals the slope of a least squares linear regression through the origin of  $ET_{os}$  (y-axis) versus  $ET_o$  (x-axis) computed from a nearby full station. It was assumed that solar radiation, wind speed, and humidity at the partial and the nearby full station are similar. To evaluate the calibration method, ten pairs of full stations were selected from the available weather networks. Each pair of full stations was in close proximity, and it was assumed that they were in the same microclimate. One station from each pair was deemed the “training” and the other the “testing” station. The  $K_f$  was determined

using  $ET_{os}$  (Eq. 1) and  $ET_o$  (Eq. 2) calculations from the “training” station data. Then, the  $K_f$  was used to calculate  $ET_{HS} = ET_o \times K_f$ , where  $ET_{HS}$  is the calibrated  $ET_o$ , and  $ET_o$  was computed using the testing station temperature data and the HS equation. Afterward, using the observed climate data from the “testing” station, the  $ET_{os}$  was computed and compared with the  $ET_{HS}$  from the same station.

**Substitution:** Using the temperature data from a partial station and substituting solar radiation, wind speed, and humidity data from a nearby full station, one can estimate  $ET_{os}$  using the substitution data. The same set of ten pairs of full stations that were used for the calibration method was employed to evaluate the substitution method. The solar radiation, wind speed, and relative humidity data from the “training” station were substituted for the corresponding data at the “testing” stations to estimate  $ET_{SB}$  ( $ET_{os}$  using the substitution method) using Eq. 1. Then, the  $ET_{os}$  values were calculated using the observed solar radiation, wind speed, humidity, and temperature data from the “testing” station. The  $ET_{SB}$  and  $ET_{os}$  were compared.

The performance of the estimation methods was evaluated using linear regression to determine the slope ( $b$ ) and coefficient of determination ( $R^2$ ) and the root mean square error (RMSE). The monthly means of daily  $ET_{os}$  ( $\text{mm d}^{-1}$ ) from January through December (y-axis) were separately regressed against  $ET_o$ ,  $ET_{HS}$ , and  $ET_{SB}$  with the linear coefficient forced through the origin. A perfect match of  $ET_{os}$  versus the estimates should have a slope  $b=1.00$  and  $R^2=1.00$ . The performance of the testing station calculations was also evaluated using the RMSE ( $\text{mm d}^{-1}$ ) as shown in the following equations:

$$RMSE_{HS} = \sqrt{\frac{1}{n} \sum_{i=1}^n (ET_{HS} - ET_{os})^2} \quad (3)$$

$$RMSE_{SB} = \sqrt{\frac{1}{n} \sum_{i=1}^n (ET_{SB} - ET_{os})^2} \quad (4)$$

$$RMSE_o = \sqrt{\frac{1}{n} \sum_{i=1}^n (ET_o - ET_{os})^2} \quad (5)$$

where  $n$  is the number of sample pairs, and the subscripts indicate the variable being tested.

To compare the performance of the different reference evapotranspiration estimation methods (calibration, substitution, and Hargreaves-Samani) for the ten pairs of stations, the overall RMSE averages for all analyzed methods were

determined, and a double sided  $t$ -test was performed. The critical  $t$ -value ( $P \leq 0.05$ ) for 18 [ $= (10 \times 2) - 2$ ] degrees of freedom was 2.1. The hypothesis that the mean RMSE values of different methods were different was accepted when  $t$ -value was greater than critical  $t$ .

Since summer is the peak evaporation period, the mean daily full and partial station  $ET_{os}$  rate estimates for the summer months (June, July, and August) were computed and the mean data were used with GIS to map the  $ET_{os}$  zones using three spatial analysis tools [inverse distance weighting (IDW), ordinary kriging (OK), and radial basis function (RBF)] of ArcGIS 9.3 software [11].

The holdout method and k-fold techniques reported by Kohavi [25] were used for cross validation. Validation is a useful way to estimate model accuracy. For each interpolation method two cross validation techniques were applied: the holdout method and k-fold cross validation. The holdout method is the simplest kind of cross validation. The data set was randomly separated into two sets, called the training set, with 70% of data, and the testing set with the remaining 30%. To assess how much the model value estimation differed from the observed data (test set), the training set was used. The model fit a function using the training set only. Then, the function was used to predict the output values for the data in the testing set.

The k-fold cross validation is more rigorous than the holdout method. The data set, was randomly divided into  $k$  subsets, and the holdout method was repeated  $k=9$  times. Whenever a  $k$  subset was used as the test set, the other  $k-1$  subsets were collected to form a training set. Then, the average error across all nine trials was computed.

The performance of the three interpolation methods for each cross validation technique was assessed through the statistical analysis: mean absolute error (MAE), mean bias error (MBE), mean relative error (MRE), and RMSE:

$$MAE = \frac{1}{n} \sum_{j=1}^n \left| \hat{Z}_j - Z_j \right| \quad (6)$$

$$MBE = \frac{1}{n} \sum_{j=1}^n (\hat{Z}_j - Z_j) \quad (7)$$

$$MRE = \frac{1}{n} \sum_{j=1}^n \frac{\left| \hat{Z}_j - Z_j \right|}{Z_j} \quad (8)$$

$$RMSE = \sqrt{\frac{1}{n} \sum_{j=1}^n (\hat{Z}_j - Z_j)^2} \quad (9)$$

where  $n$  was the number of station points,  $Z_j$  and  $\hat{Z}_j$  were respectively observed and estimated values at the considered point  $j$  ( $j=1,2,\dots, n$ ).

### 3. RESULTS AND DISCUSSION

A preliminary analysis of data for full stations during summer months [Tab. 1] shows that the  $ET_{os}$  values ranged from 4.5 to 6.3 mm d<sup>-1</sup>, while the  $ET_o$  values ranged from 4.7 to 6.7 mm d<sup>-1</sup>. A trend analysis between the  $ET_{os}$  and  $ET_o$  calculations and wind speed was performed by dividing by the mean value of each variable to allow for a trend comparison. As shown in Fig. 3, the  $ET_{os}$  data showed a small positive relation with the wind speed, and the  $ET_o$  tends to overestimate  $ET_{os}$  when wind speeds are low (e.g., at Villa San Pietro and Decimomannu). The  $ET_o$  tends to underestimate  $ET_{os}$  in locations characterized by higher wind speeds (e.g., Sardara and Domus de Maria). The difference between the two methods is most evident in stations with the biggest differences in wind speed. There was no relationship observed between  $ET_{os}$  and either solar radiation or mean relative humidity.

Previous studies have discussed the inaccurate estimation of reference evapotranspiration using HS computations in humid, very dry, and windy regions, and calibration methods to obtain better results have been proposed. Martínez-Cob and Tejero-Juste [28] reported that under the semiarid conditions local calibration is needed for low wind speed locations. Gavilán et al. [14] also confirmed that a regional calibration of  $ET_o$  is needed for wind conditions in a semi-arid environment. The assessment of the calibration and substitution methods for ten station pairs is reported in Tab. 2. High  $R^2$  values indicate that  $ET_{os}$  is highly correlated with the  $ET_{HS}$  and  $ET_{SB}$  methods. The slopes of  $ET_{os}$  versus  $ET_{HS}$  and  $ET_{SB}$ , however, varied considerably by station pair.

The RMSE values [Tab. 3] are perhaps the best indicators of performance at estimating  $ET_{os}$ . Recall that the summer  $ET_{os}$  values range from 4.5 to 6.3 mm d<sup>-1</sup>, so RMSE values less than 0.25 mm d<sup>-1</sup> have estimated  $ET_{os}$  values that are mostly within 5% of the mean  $ET_{os}$  rates. The substitution method performed best with 7 out

of 10 stations have RMSE values less than  $0.25 \text{ mm d}^{-1}$  and none were higher than  $0.32 \text{ mm d}^{-1}$ . The calibration method did perform better than the uncalibrated HS  $ET_o$  at predicting  $ET_{os}$ . The  $t$  test analysis showed that the substitution method was significantly different (P-value = 0.03) from the calibration method, while the HS and calibration methods were not statistically different (P-value = 0.59). Therefore, the substitution method was chosen to estimate the  $ET_{os}$  for partial stations. Other studies also showed that substitution was an effective method to employ partial stations in  $ET_{os}$  estimation. For example, the use of the wind speed from a nearby station has given good results in studies by Popova et al. [32] and Sentelhas et al. [35]. Using solar radiation data from a nearby station as a substitute for missing data has shown a better performance than the application of estimation procedures when the distance between weather stations was small [30; 18; 38].

In this study, the substitution method performed well for all comparisons. This, however, may not be true in other locations where climate data from a nearby station is not representative of the station of interest. When the microclimates of paired stations are dissimilar, perhaps a subjective decision by local meteorologists is needed to decide whether or not to include the station in the data set.

The statistical analysis to test the performance of the three interpolation methods is shown in Tab. 4. The ordinary kriging showed the best performance in all statistics for the k-fold validation. In the holdout method, there is little difference between the statistics. Except for the MBE, the k-fold validation showed better results than the holdout method. Dalezios et al. [7], investigating the spatial variability of reference evapotranspiration in Greece, confirmed that the kriging technique can be successfully applied to describe the spatial variability of  $ET_o$  over large geographical regions.

Using ordinary kriging technique, the Sardinian  $ET_{os}$  map was derived (Fig. 4). The summertime mean daily  $ET_{os}$  ranges from  $4.5$  to  $6.3 \text{ mm d}^{-1}$ , so the map was separated into classes of  $0.5 \text{ mm d}^{-1}$ . The highest  $ET_{os}$  values were observed in the southwest part of the island and the lowest in the central-east mountain area and the southern coastal region.

#### 4. CONCLUSIONS

This study derived a reference evapotranspiration distribution map for Sardinia based on weather station data and use of GIS. A modified daily Penman-Monteith

equation from the UN-FAO and ASCE-EWRI was used to calculate the Standardized Reference Evapotranspiration ( $ET_{os}$ ) for all weather stations having a “full” set of required data for the calculations. For stations having only temperature data (partial stations), the Hargreaves-Samani ( $ET_o$ ) equation was used to estimate the reference evapotranspiration for a grass surface. The  $ET_{os}$  and  $ET_o$  results were different depending on the local climate, so two methods to estimate  $ET_{os}$  from the  $ET_o$  were tested. Substitution of missing solar radiation, wind speed, and humidity data from a nearby station within a similar microclimate was found to give better results than using a calibration factor that related  $ET_{os}$  and  $ET_o$ . Therefore, the substitution method was used to estimate  $ET_{os}$  at “partial” stations having only temperature data. The combination of 63 full and partial stations was sufficient to use GIS to map  $ET_{os}$  for Sardinia. Three interpolation methods were studied, and the ordinary kriging model fitted the observed data better than a radial basis function or the inverse distance weighting method. Using station data points to create a regional map simplified the zonation of  $ET_{os}$  when large scale computations were needed. Making a distinction based on  $ET_{os}$  classes allows the simulation of crop water requirements for large areas and it can potentially lead to improved irrigation management and water savings. It also provides a baseline to investigate possible impact of climate change.

## 5. ACKNOWLEDGMENTS

The authors thank the ARPAS department and the hydrographical district for weather data used in this study. This research was funded by the Ph.D. program in Agrometeorology and Ecophysiology of Agricultural and Forest Systems (Ph.D. school in Science and Biotechnology of Agricultural Systems, Forestry and Food production) of the University of Sassari in collaboration with the University of California-Davis; the European Community’s Seventh Framework Program (FP7/2007-2013) under grant agreement 244255 (WASSERMed project), and the Italian MIUR and MATTM (Gemina project) under grant agreement 232/2011.

## 6. REFERENCES

1. Allen, R.G., et al. (2005). *The ASCE standardized reference evapotranspiration equation*. Technical Committee report to the Environmental and Water

- Resources Institute of the American Society of Civil Engineers from the Task Committee on Standardization of Reference Evapotranspiration, ASCE-EWRI, Reston, VA, 192.
2. Allen, R.G., Pereira, L.S., Raes, D., and Smith, M. (1998). *Crop evapotranspiration*. Guidelines for computing crop water requirements. Irrigation and Drainage Paper 56, Food and Agriculture Organization of the United Nations, Rome.
  3. Amatya, D.M., Skaggs, R.W., and Gregory, J.D. (1995). *Comparison of methods for estimating REF-ET*. J. Irrig. Drain. Eng., 10.1061/(ASCE)0733-9437(1995)121:6(427), 427-435.
  4. Ashraf, M., Loftis, J.C., and Hubbard, K.G. (1997). *Application of geo-statistics to evaluate partial weather station networks*. Agric. Forest Meteorol., 84(3-4), 255-271.
  5. Benli, B., Bruggeman, A., Oweis, T., and Ustun, H. (2010). *Performance of Penman-Monteith FAO-56 in a semiarid highland environment*. J. Irrig. Drain. Eng., 10.1061/(ASCE)IR.1943-4774.0000249, 757-765.
  6. Chiew, F.H.S., Kamaladasa, N.N., Malano, H.M., and McMahon, T.A. (1995). *Penman-Monteith, FAO-24 reference crop evapotranspiration and class-A pan data in Australia*. Agric. Water Manage., 28(1), 9-21.
  7. Dalezios, N.R., Loukas, A., and Bampzelis, D. (2002). *Spatial variability of reference evapotranspiration in Greece*. Phys. Chem. Earth., 27(23-24), 1031-1038.
  8. De Souza, F., and Yoder, R.E. (1994). *ET estimation in the northeast of Brazil: Hargreaves or Penman-Monteith Equation?* Proc. International Winter Meeting the American Society of Agricultural Engineers, Paper No. 942545, ASAE, St. Joseph, MI.
  9. Doorenbos, J., and Pruitt, W.O. (1977). *Crop water requirements*. Irrigation and Drainage Paper No. 24, Food and Agriculture Organization of the United Nations, Rome.
  10. Droogers, P., and Allen, R.G. (2002). *Estimating reference evapotranspiration under inaccurate data conditions*. Irrig. Drain. Syst., 16(1), 33-45.

11. ESRI. (2008). *ArcGIS Desktop Ver. 9.3 program*. ESRI Inc., Redlands, CA.
12. Fooladmand, H.R., and Haghghat, M. (2007). *Spatial and temporal calibration of Hargreaves equation for calculating monthly reference evapotranspiration based on Penman-Monteith method*. *Irrig. Drain.*, 56(4), 439-449.
13. Garcia, M., Raes, D., Allen, R., and Herbas, C. (2004). *Dynamics of reference evapotranspiration in the Bolivian highlands (Altiplano)*. *Agric. Forest Meteorol.*, 125(1-2), 67-82.
14. Gavilán, P., Lorite, I.J., Tornero, S., and Berengena, J. (2006). *Regional calibration of Hargreaves equation for estimating reference ET in a semiarid environment*. *Agric. Water Manage.*, 81(3), 257-281.
15. Hargreaves, G.H., and Samani, Z.A. (1985). *Reference crop evapotranspiration from temperature*. *Appl. Eng. Agric.*, 1(2), 96-99.
16. Howell, T.A., Evett, S.R., Schneider, A.D., Dusek, D.A., and Copeland, K.S. (2000). *Irrigated fescue grass ET compared with calculated reference ET*. *Proc. 4<sup>th</sup> National Irrig. Symp.*, ASAE, Phoenix AZ, 228-242.
17. Howell, T.A., Steiner, J.L., Schneider, A.D., Evett, S.R., and Tolk, J.A. (1997). *Seasonal and maximum daily evapotranspiration of irrigated winter wheat, sorghum and corn—Southern High Plains*. *Trans. ASAE*, 40(3), 623-634.
18. Hunt, L.A., Kuchar, L., and Swanton, C.J. (1998). *Estimation of solar radiation for use in crop modeling*. *Agric. Forest Meteorol.*, 91(3-4), 293-300.
19. IPCC. (2013). *Climate Change 2013: The Physical Science Basis*. Contribution of Working Group I to the Fifth Assessment Report of the Intergovernmental Panel on Climate Change. Cambridge University Press, Cambridge, United Kingdom and New York, NY, USA, 1535 pp.
20. IPCC. (2007). *4<sup>th</sup> IPCC Assessment Rep. (AR4): Climate Change 2007*. Cambridge Univ. Press, Cambridge, U.K.
21. Itenfisu, D., Elliott, R.L., Allen, R.G., and Walter, I.A. (2003). *Comparison of reference evapotranspiration calculations as part of the ASCE standardization effort*. *J. Irrig. Drain. Eng.*, 10.1061/(ASCE)0733 -9437(2003)129:6(440), 440-448.

22. Jabloun, M. and Sahli, A. (2008). *Evaluation of FAO-56 methodology for estimating reference evapotranspiration using limited climatic data Application to Tunisia*. Agric. Water Manage., 95(6), 707-715.
23. Jensen, D.T., Hargreaves, G.H., Temesgen, B., and Allen, R.G. (1997). *Computation of ETo under non ideal conditions*. J. Irrig. Drain. Eng., 10.1061/(ASCE)0733-9437(1997)123:5(394), 394-400.
24. Jensen, M.E., Burman, R.D., and Allen, R.G. (1990). *Evapotranspiration and irrigation water requirements*. ASCE Manuals and Rep. on Engineering Practice No. 70, ASCE, New York.
25. Kohavi, R. (1995). *A study of cross-validation and bootstrap for accuracy estimation and model selection*. Proc. 14<sup>th</sup> National Joint Conf. on Artificial Intelligence (IJCAI).
26. Liu, Y., and Pereira, L.S. (2001). *Calculation methods for reference evapotranspiration with limited weather data*. J. Hydraul. Eng., 3(3), 11-17 (in Chinese).
27. Lopez-Urrea, R., Martin de Santa Olalla, F., Fabeiro, C., and Moratalla, A. (2006). *Testing evapotranspiration equations using lysimeter observations in a semiarid climate*. Agric. Water Manage., 85(1-2), 15-26.
28. Martinez-Cob, A., and Tejero-Juste, M. (2004). *A wind-based qualitative calibration of the Hargreaves ETo estimation equation in semiarid regions*. Agric. Water Manage., 64(3), 251-264.
29. Mavi, H.S., and Tupper, G.J. (2004). *Agrometeorology-principles and applications of climate studies in agriculture*. Food Products Press, New York.
30. Nonhebel, S. (1994). *Inaccuracies in weather data and their effects on crop growth simulation results*. Climate Res., 4(1), 47-60.
31. Oliveira, C.W., and Yoder, R.E. (2000). *Evaluation of daily reference evapotranspiration estimation methods for a location in the southern USA*. Paper No. 002030, ASAE, St. Joseph, MI.
32. Popova, Z., Kercheva, M., and Pereira, L.S. (2006). *Validation of the FAO methodology for computing ETo with missing climatic data application to South Bulgaria*. Irrig. Drain., 55(2), 201-215.

33. Saeed, M. (1986). *The estimation of evapotranspiration by some equations under hot and arid conditions*. Trans. ASAE. 29(2), 434-438.
34. Samani, Z. (2000). *Estimating solar radiation and evapotranspiration using minimum climatological data*. Irrig. Drain. Eng., 10.1061/(ASCE) 0733-9437(2000) 126:4(265), 265-267.
35. Sentelhas, P.C., Gillespie, T.J., and Santos, E.A. (2010). *Evaluation of FAO Penman-Monteith and alternative methods for estimating reference evapotranspiration with missing data in Southern Ontario, Canada*. Agr. Water Manage., 97(5), 635-644.
36. Tabari, H., and Talaei, P. (2011). *Local calibration of the Hargreaves and Priestley-Taylor equations for estimating reference evapotranspiration in arid and cold climates of Iran based on the Penman-Monteith model*. J. Hydrol. Eng., 10.1061/(ASCE)HE. 1943-5584.0000366, 837-845.A4014004-10
37. Temesgen, B., Allen, R.G., and Jensen, D.T. (1999). *Adjusting temperature parameters to reflect well-water conditions*. J. Irrig. Drain. Eng., 10.1061/(ASCE)0733-9437( 1999) 125:1 (26), 26-33.
38. Trnka, M., Zalud, Z., Eitzinger, J., and Dubrovsky, M. (2005). *Global solar radiation in Central European lowlands estimated by various empirical formulae*. Agric. Forest Meteorol., 131(1-2), 54-76.
39. Xing, Z., Chow, L., Meng, F.R., Rees, H.W., Stevens, L., and Monteith, J. (2008). *Validating evapotranspiration equations using Bowen Ratio in New Brunswick, Maritime Canada*. Sensors, 8(1), 412-28.
40. Xu, C.Y., and Singh, V.P. (2002). *Cross comparison of empirical equations for calculating potential evapotranspiration with data from Switzerland*. Water Resour. Manag., 16(3), 197-219.
41. Yoder, R.E., Odhiambo, L.O., and Wright, W.C. (2005). *Evaluation of methods for estimating daily reference crop evapotranspiration at a site in the humid Southeast United States*. Appl. Eng. Agric., 21(2), 197-202.
42. Zhao, C., Nan, Z., and Cheng, G. (2005). *Methods for modeling of temporal and spatial distribution of air temperature at landscape scale in the southern Qilian mountains, China*. Ecol. Model, 189(1-2), 209-220

Tab. 1 Statistical summary of Hargreaves-Samani  $ET_o$  and Standardized Reference  $ET_{os}$  computations for full stations during summer months.

Statistics	$ET_o$	$ET_{os}$
Minimum (mm d <sup>-1</sup> )	4.7	4.5
Maximum (mm d <sup>-1</sup> )	6.7	6.3
Mean (mm d <sup>-1</sup> )	5.6	5.3
Median (mm d <sup>-1</sup> )	5.8	5.3
Standard deviation	0.5	0.4
Variance	0.2	0.2
Standard error	0.1	0.1

Tab. 2 Coefficient of determination ( $R^2$ ) and slope ( $b$ ) for calibration ( $ET_{HS}$ ) and substitution ( $ET_{SB}$ ) methods in relation to reference evapotranspiration computed by use of Standardized Reference Evapotranspiration equation ( $ET_{os}$ ) for ten pairs of full stations.

Trial location	$ET_{HS}$ versus $ET_{os}$		$ET_{SB}$ versus $ET_{os}$	
	$R^2$	$b$	$R^2$	$b$
	Villa San Pietro—Decimomannu	1.00	1.02	1.00
Muravera—Dolianova	0.99	1.22	0.99	1.06
Macomer—Modolo	0.99	0.87	0.99	1.10
Dolianova—Guasila	0.99	0.92	0.99	0.96
Jerzu—Muravera	0.99	0.83	1.00	0.93
Benetutti—Nuoro	0.99	1.00	1.00	1.00
Sassari—Olmedo	0.98	1.20	0.98	1.04
Guasila—Siurgus Donigala	0.99	0.95	1.00	0.96
Olmedo—Putifigari	0.99	0.87	0.99	0.97
Aglientu—Luras	0.99	1.02	1.00	0.93

Tab. 3 Annual RMSE ( $\text{mm d}^{-1}$ ) values for Hargreaves-Samani equation ( $\text{RMSE}_o$ ), calibration ( $\text{RMSE}_{HS}$ ) and substitution ( $\text{RMSE}_{SB}$ ) methods for 10 pairs of full stations.

Trial location	$\text{RMSE}_o$	$\text{RMSE}_{HS}$	$\text{RMSE}_{SB}$
Villa San Pietro – Decimomannu	0.90	<b>0.10</b>	0.17
Muravera – Dolianova	<b>0.14</b>	0.65	0.23
Macomer – Modolo	<b>0.17</b>	0.52	0.32
Dolianova – Guasila	0.71	0.31	<b>0.22</b>
Jerzu – Muravera	0.63	0.64	<b>0.26</b>
Benetutti – Nuoro	0.53	0.12	<b>0.07</b>
Sassari - Olmedo	0.33	0.62	<b>0.24</b>
Guasila - Siurgus Donigala	0.42	0.22	<b>0.17</b>
Olmedo - Putifigari	0.43	0.55	<b>0.19</b>
Aglientu - Luras	0.22	<b>0.20</b>	0.28

Note: bold fonts depict the lowest values.

Tab. 4 Assessment of three interpolation methods as well as two cross validation techniques for reference evapotranspiration in Sardinia.

Statistical index	Model	k-fold	holdout
RMSE	IDW	0.34	0.43
	OK	<b>0.31</b>	0.41
	RBF	0.33	<b>0.40</b>
MAE	IDW	0.27	0.25
	OK	<b>0.23</b>	<b>0.24</b>
	RBF	0.25	0.25
MBE	IDW	-0.07	-0.04
	OK	<b>-0.03</b>	<b>-0.01</b>
	RBF	-0.04	-0.03
MRE	IDW	0.05	0.05
	OK	<b>0.04</b>	0.05
	RBF	0.05	0.05

Note: bold fonts depict the lowest values.



Fig. 1 Experimental site.

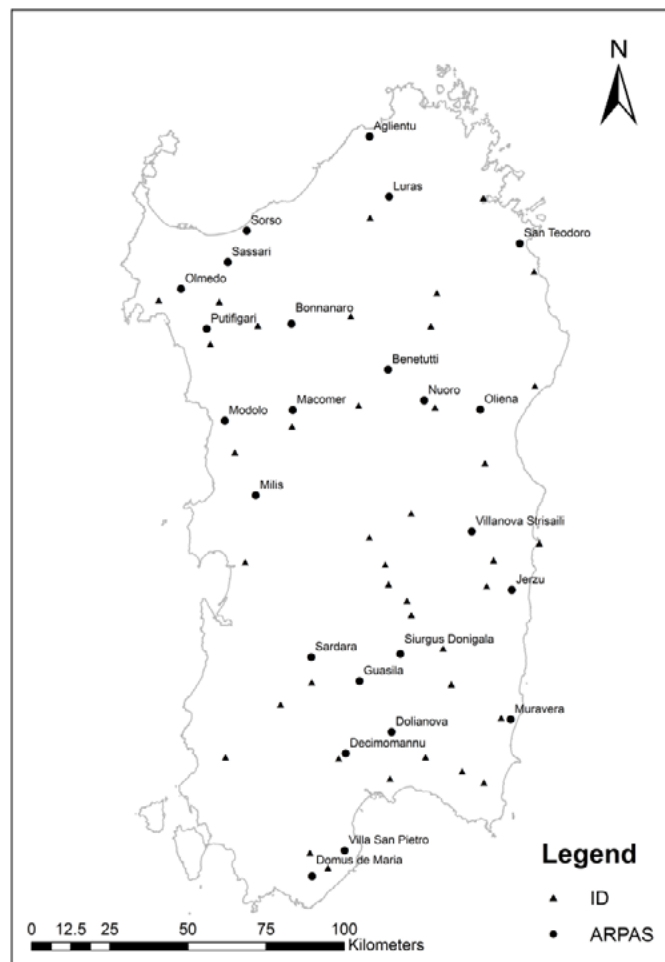


Fig. 2 Geographical location of the 63 meteorological stations used in this study; station names for the ARPAS network are shown.

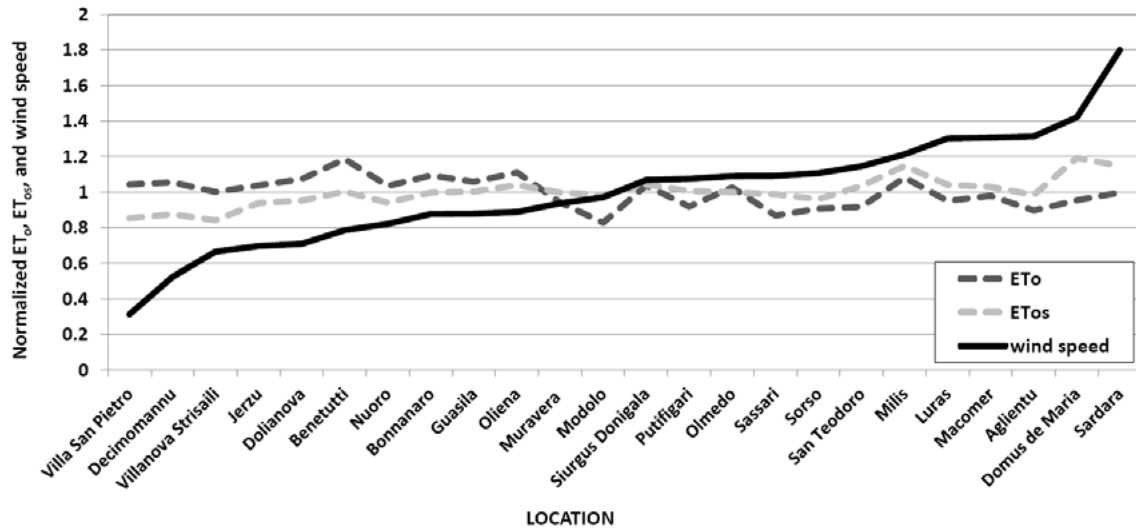


Fig. 3 Trend analysis using normalized data of mean daily reference evapotranspiration values computed with the Hargreaves-Samani equation ( $ET_0$ ) and Standardized Reference Evapotranspiration equation ( $ET_{os}$ ), and daily wind speed for full stations during summer months; data were normalized by dividing monthly values by the overall mean of each variable.

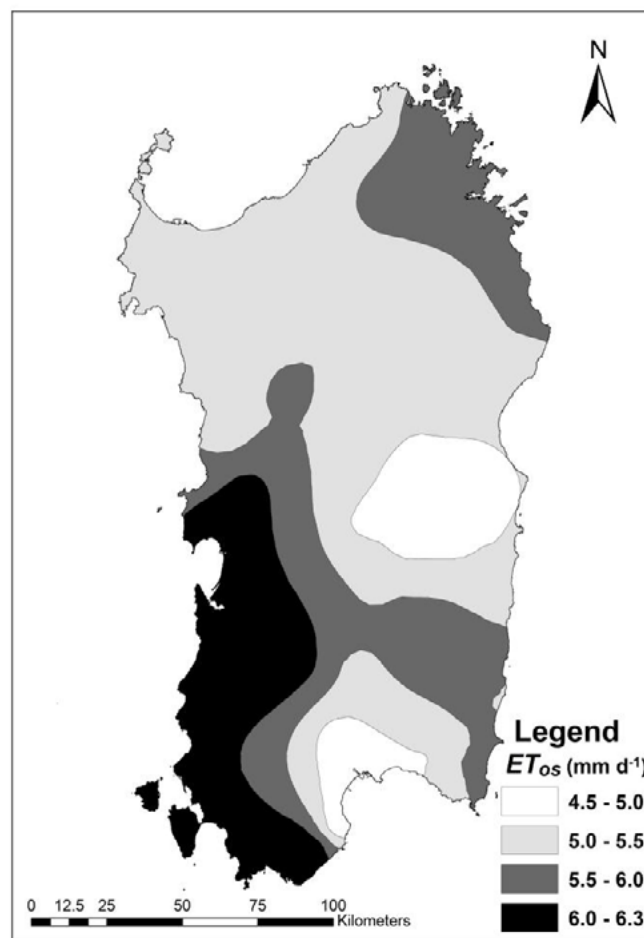


Fig. 4 Sardinian summer  $ET_{os}$  ( $mm\ d^{-1}$ ) classes map computed by ordinary kriging.

## **Spatiotemporal changes in wildfire patterns in Sardinia**

**M. Salis<sup>1,2</sup>, A.A. Ager<sup>3</sup>, B. Arca<sup>4</sup>, M.A. Finney<sup>5</sup>, O. Munoz-Lozano<sup>1</sup>, F.J. Alcasena<sup>2</sup>, V. Bacciu<sup>2</sup>, D. Spano<sup>1,2</sup>**

<sup>1</sup>University of Sassari, Department of Science for Nature and Environmental Resources (DIPNET), Via De Nicola 9, 07100, Sassari (Italy); <sup>2</sup>Euro-Mediterranean Center on Climate Changes (CMCC), IAFENT Division (Italy); <sup>3</sup>USDA Forest Service, Pacific Northwest Research Station (USA); <sup>4</sup>Rocky Mountain Research Station (USA); <sup>5</sup>National Research Council, Institute of Biometeorology (Italy)

\*Corresponding Author: [miksalis@uniss.it](mailto:miksalis@uniss.it)

### **Abstract**

We documented spatiotemporal changes in wildfire exposure and regime in Sardinia from 1980 to 2009. We explored the main contributing factors to changes in these patterns: weather, land use, ignition patterns, and suppression capability. In addition, we used simulation modeling to predict how these changes affected fire hazard and exposure for selected important human and ecological values. The combined empirical analyses and simulation modeling provided a robust approach to understanding the spatiotemporal dynamics of wildfire risk and exposure in Sardinia. From 1980-1994 to 1995-2009, our study showed 1) a strong reduction in area burned (60,000 to 20,000 ha/year) and ignitions (3,700 to 2,600 fires/year); 2) an advance of 15 days of the fire season peak; 3) an increase in spring temperatures; 4) limited changes in land use types and associated fuels. Most likely the reduction in fire activity may be due to a combination of social factors and suppression capabilities. The combined empirical analyses and simulation modeling provided a robust approach to understanding the wildfire spatiotemporal dynamics in Sardinia.

**Keywords:** fire exposure, fire regime, MTT algorithm, spatiotemporal changes, Mediterranean area

## 1. INTRODUCTION

Wildfire plays a key role in structuring vegetation and landscapes worldwide, and represents a significant threat to human values in fire-prone wildlands (1; 2). Over the past decades several studies have reported the increasing risk of mega-fires occurrence in Mediterranean Europe (3; 4; 5), together with relevant changes in fire frequency and spatial patterns (6; 7; 5). The observed shift in fire regimes and risk can have several plausible explanations, as for instance climate and land use changes, fuel buildup, fire exclusion policies, agro-pastoralism activities, and rural population ageing (8; 9; 10; 11; 12; 13; 5; 14; 15; 16; 17; 18). In this work, we examined shifts in Sardinia fire regime for the periods 1980-1994 and 1995-2009 to better understand trends in wildfire exposure on the island. A key to understanding these trends is to examine historical changes in relation to each causal factor (19; 20; 5; 15): so, we first analyzed temporal changes in the fire regime in relation to the major drivers, namely weather, land uses and fuels, fire ignitions, and suppression capacity. We then used mechanistic wildfire simulation modeling to map fine scale spatiotemporal changes in wildfire exposure on the island.

## 2. METHODS

Study area. The study area is the island of Sardinia, Italy, and has nearly 24,000 km<sup>2</sup> of land. The orography is widely hilly (Fig 1), the average elevation is about 350 m above sea level, and the largest plains are located in the western area of the island. Woodlands and forest cover 16% of the land area, and are mainly represented by *Quercus* spp.. Large expanses (30%) are covered by shrublands (Mediterranean maquis and garrigue). Urban and anthropic areas cover about 3% of the island, while herbaceous vegetation types characterize most of the remaining area (about 50%). Sardinia has a Mediterranean climate characterized by mild and rainy winters, dry and hot summers, and drought conditions from May until September (21). Annual precipitation ranges from about 500 mm in the coastlines to 1,200 mm in the mountains. Maximum temperature peaks are often higher than 30°C in the summer. The most frequent wind directions are west and northwest.

Weather. We gathered daily meteorological data from 11 weather stations from 1980 to 2009 (22; 17). Wind directions were obtained from the fire reports of the Sardinia Forest Service. Data were stratified for northern and southern provinces to obtain the

daily mean weather (Fig 1). Monthly mean values were then calculated for each study period.

Historical wildfire occurrence data. We used the historical fire database for the period 1980-2009. Sardinian wildfires typically occur between June and September (16), and our analysis focused on these four months. The fire database contains date and municipality of ignition, ignition coordinates, and fire size. Initial exploratory analysis suggested two distinct fire regimes corresponding to the periods 1980-1994 and 1995-2009.

Wildfire suppression capacity. We gathered data on the Sardinia wildfire suppression capacity between 1976 and 2009 (23; 24; <http://www.sardegnaambiente.it/>). Wildfire suppression capacity defines the available forces for the fire-fighting activities, considering the number of people involved in fire prevention and suppression, and the number of aerial means used during fire suppression and management phases. Significant data gaps existed for specific years, including the period 1977-1993, whereas we found complete and detailed information in the official reports of the Sardinian Forest Service (<http://www.sardegnaambiente.it/protezionecivile/>) for the last decade.

Land use and fuels. We analyzed the Corine Land Cover maps (CLC, 25) for the years 1990 and 2000, with the former representing land use for the first period 1980-1994, and the latter representing the second time frame 1995-2009. Eleven main land use types were identified from the CLC maps (16; 17); each land use type was assigned to a standard or custom fuel model (Table 1). The values of live and dead fuel moisture content (FMC) were set by combining literature data from Mediterranean ecosystems (26; 27; 28) with a set of field data collected in North Sardinia (29; 30; 31; 32).

Estimating fine scale wildfire exposure. We used wildfire simulation modeling to characterize fine scale changes in wildfire likelihood, intensity and exposure between the two study periods in the island (17). Specifically, we used as inputs to the simulation model 1) ignition patterns, 2) fuel maps, and 3) weather conditions of each study period. Basically, we used the minimum travel time (MTT) fire spread algorithm, as implemented in Randig, a command line version of FlamMap (33; 34). All spatial input data required for Randig (fuels, weather, and topography) were assembled in 200 m resolution grids. Wind, fuel moisture and wind speed were held

constant during the fire events simulations and reflected 97th percentile weather conditions. Wind direction was sampled in a Monte Carlo approach using historical weather. Ignition location for the simulations was determined from two ignition probability grids (IP) derived from historical ignitions (1980-1994 and 1995-2009). We simulated 100,000 fire events, randomly drawing from the frequency distribution of burn periods and wind directions. The wildfire simulations were performed at 200 m resolution consistent with the input data, and generated a burn probability (BP) and a frequency distribution of flame lengths (FL) in twenty 0.5 m classes for each pixel.

### 3. RESULTS

A slight increasing trend in annual minimum, average and maximum temperatures was observed during the period 1980-2009, but this trend was not statistically significant. Meanwhile, a decreasing trend was observed for annual precipitation, and for precipitation from May to October, but again the reductions observed were not statistically significant (17). The increase in temperatures was statistically significant in April, May and June. Dominant historical wind directions associated with the largest wildfires were from NW, W and SW, and only small differences were observed between the two periods (Table 2). Changes in land use between 1990 and 2000 (Table 1) were limited and characterized by a reduction of 49,000 ha in grassland and agricultural areas, and an increase in Mediterranean maquis vegetation of 48,000 ha. Urban areas increased nearly 11,600 ha, while pastures were reduced by an almost equivalent amount, 11,400 ha. The other vegetation types showed little or no changes between the two reference periods.

A considerable increase in the number of people involved in fire suppression activities took place after the dramatic fire season of 1983 (24; 17), though we collected discontinuous data until 1994. Fire suppression resources increased over the studied period, especially after 2000.

Sardinia experienced a significant reduction in both fire number and area burned between the two study periods. The most important decrease was observed in area burned; the annual number of ignitions also decreased (Fig 2). A seasonal shift in ignitions and area burned was observed, with the fire season peak occurring earlier in the second study period (Fig 3). The distribution of area burned by fire size class did not differ substantially between the two studied periods, and fires greater than

100 hectares, approximately 2% of the total number of fires, were responsible for about 60% of the area burned in both periods (Fig 4).

The analysis of the spatial and temporal changes in wildfire likelihood, intensity and exposure was performed using a fine scale modeling approach, which took into account the combined effects of different driving factors on wildfire behavior. The maps provided by Randig for the two periods (1980-1994 and 1995-2009) showed several variations in both mean values and 99th percentiles of burn probability (BP), fire size (FS), and conditional flame length (CFL); in addition, a different spatial arrangement of the abovementioned indicators was observed (Fig 5-7).

The maps of simulation outputs of BP showed the largest differences between the two study periods in the southwest portion of the island (Fig 5). In 1980-1994 the areas with the highest BP were located in the western coast and in the inland southeastern areas, where the main economic activity was sheep-farming (Fig 5a). In the following fifteen years, the highest BP was observed in the inland southern areas with a clear shift towards the plains (Fig 1 and 5b). BP also dropped sharply in northwestern Sardinia and a general increase was observed in several coastal areas, particularly in the province of Olbia-Tempio (Fig 1 and 5c). The potential large fire location also differed between study periods: FS maps clearly indicated which areas of Sardinia were more prone to support large fires (Fig 6). Several inland areas of eastern Sardinia showed an increase in potential FS from 1980-1994 to 1995-2009. However, other areas of Sardinia were less susceptible to large fires in the second study period than in the previous one (e.g., northwest Sardinia, Fig 6). Regarding CFL, the outputs evidenced small differences between study periods (Fig 7).

#### **4. DISCUSSION**

We documented changes in spatiotemporal regime and exposure in Sardinia wildfires from 1980 to 2009. We explored the main contributing factors to changes in these patterns; in addition, we used simulation modeling to predict how these changes affected fire exposure in the island. The combined empirical analyses and simulation modeling provided a robust approach to understanding the spatiotemporal dynamics of wildfire risk and exposure in Sardinia. Our study highlighted that Sardinia experienced a sharp reduction in wildfires, considering both fire number and area burned. This trend was clearly counter to observed weather conditions, since average, minimum and maximum temperatures increased, although only in April,

May and June these changes were statistically significant. Moreover, wind speed did not show relevant differences among the studied periods. Precipitation also showed decreasing trends from 1980 to 2009, counter to what would be expected with decreasing wildfire occurrence. Sardinia suffered a slight variation in the main land uses, mostly consisting in an increase in shrub formations and urban areas along with a reduction of agricultural lands. Considering the observed change in Sardinia fire regime, our study indicates that changes in ignition patterns and wildfire suppression capacity may be more likely to have played a major role on the observed wildfire regime changes. Besides, the reduction in burned areas might be due to a better perception of the threats related to the indiscriminate use of fire, which resulted in a reduction in fire number, together with the enhancement and strengthening of aerial and terrestrial firefighting forces as well as of tactics, coordination and organization skills.

Another specific change consisted in a variation in the temporal distribution of fire ignitions, which shifted to 15 days earlier in 1995-2009 compared to the previous fifteen years, including the peaks in both area burned and fire number. The temporal changes in fire ignitions could be a result of the reduction of fires caused by agro-pastoralism practices. Moreover, the increase in temperature in April, May and June in 1995-2009 could be responsible for the anticipation in the fire season, as Mediterranean ecosystems are strongly influenced by the moisture conditions of fine fuels and by the live/dead ratio in herbaceous fuel types (16).

The use of simulation modeling allows fine scale examination of landscape risk dynamics over time. It also permits the development of efficient guidelines and methods for mitigating risk (35, 36). Furthermore, since fire-fighting investments might be expected to decrease in the near future due to economic situation in Europe as well as in other Countries, the definition of efficient fire risk estimation and prevention approaches is a key issue for the fire management agencies. The growing incidence of wildfires in the Mediterranean region and the recent changes in fire regime and risk brought up new advances in assessing and mapping wildfire hazard, risk, and exposure. From this point of view, there is evidence that in Sardinia specific areas need to address risk mitigation activities and practices to limit the potential fire intensity and to contrast fire propagation, particularly concerning WUIs and beaches (16; 17).

## 5. ACKNOWLEDGMENTS

The authors would like to thank the Forest Service of Sardinia and the Sardinia Civil Protection for collaborating in this study. This work was partially funded by the GEMINA Project - MIUR/MATTM n. 232/2011, by the EXTREME Project (Legge Regione Sardegna 7/2007, CRP-25405), and by the Project “Modeling approach to evaluate fire risk and mitigation planning actions” (P.O.R. SARDEGNA F.S.E. 2007-2013, Asse IV Capitale umano, Linea di Attività I.3.1).

## 5. REFERENCES

1. Pyne et al (1996) Introduction to Wildland Fire (Second Edition), John Wiley and Sons, New York..
2. Pausas and Keeley (2009) A burning story: The role of fire in the history of life. *Bioscience* 59, 593-601.
3. Viegas (2004). High mortality. *Wildfire* 13, 22-26.
4. Xanthopoulos (2007) Olympic Flames. *Wildfire* 16, 10-18.
5. Moreira et al (2011) Landscape – wildfire interactions in Southern Europe: implications for landscape management. *Journal of Environmental Management* 92, 2389-2402.
6. Moreno et al (1998) Recent history of forest fires in Spain. In ‘Large Forest Fires’. (Ed Moreno JM) pp. 159-185.
7. Pausas et al (2008) Are wildfires a disaster in the Mediterranean basin? — A review. *International Journal of Wildland Fire* 17, 713–723.
8. Badia et al (2002) Causality and management of forest fires in Mediterranean environments: an example from Catalonia. *Environmental Hazards* 4, 23–32.
9. Pausas (2004) Changes in fire and climate in the eastern Iberian peninsula (Mediterranean Basin). *Climatic Change* 63, 337-350.
10. Carmona-Moreno et al (2005) Characterizing interannual variations in global fire calendar using data from Earth observing satellites. *Global Change Biology* 11, 1537-1555.

11. Camia and Amatulli (2009) Weather factors and fire danger in the Mediterranean. In Chuvieco E (Ed.) *Earth Observation of Wildland Fires in Mediterranean Ecosystems*. pp. 71-82 (Springer-Verlag: Berlin)
12. Carvalho et al (2010) The impact of spatial resolution on area burned and fire occurrence projections in Portugal under climate change. *Climatic Change* 98, 177–197.
13. Lazaro (2010) Development of prescribed burning and suppression fire in Europe. In “Best practices of fire use - Prescribed burning and suppression fire programmes in selected case-study regions in Europe” (Eds Montiel C, Krauss D eds). Research Report 24, European Forest Research Institute, pp. 17-31.
14. Pausas and Fernández-Muñoz (2012) Fire regime changes in the Western Mediterranean Basin: from fuel-limited to drought-driven fire regime. *Climatic Change* 110, 215-226.
15. Brotons et al (2013) How Fire History, Fire Suppression Practices and Climate Change Affect Wildfire Regimes in Mediterranean Landscapes. *PLoS ONE* 8(5), e62392.
16. Salis et al (2013) Assessing exposure of human and ecological values to wildfire in Sardinia, Italy. *International Journal of Wildland Fire* 22(4), 549-565.
17. Salis et al (2014) Analyzing spatiotemporal changes in wildfire regimes and exposure across a Mediterranean fire-prone area. *Natural Hazards* 71(3), 1389-1418.
18. Cardil et al (2013) Trends in adverse weather patterns and large wildland fires in Aragón (NE Spain) from 1978 to 2010. *Nat. Hazards Earth Syst. Sci.* 13, 1393-1399.
19. Brown et al (2004) The impact of twenty-first century climate change on wildland fire danger in the western United States: an applications perspective. *Climatic Change* 62, 365-388.
20. Westerling and Bryant (2008) Climate Change and Wildfire in California. *Climatic Change* 87, 231-249.
21. Chessa and Delitala (1997) Il clima della Sardegna. In (Ed A Milella) *Collana Note Tecniche di Agrometeorologia per la Sardegna*.

22. Tutiempo Network SL, 2012. Clima en Italia.  
<http://www.tutiempo.net/clima/Italia/IT.html>
23. Regione Sardegna (1976). Piano Regionale di Difesa Antincendi (Legge 1-3-1975 n.47).
24. Boni (2004) Il fenomeno degli incendi in Sardegna. In Proceedings of the Conference Incendi boschivi e rurali in Sardegna – Dall’analisi delle cause alle proposte di intervento, pag. 9-17. Cagliari, 14-15 May 2004.
25. EEA (2002) Corine land cover update 2000 – Technical guidelines. European Environment Agency, Technical Report 89. (European Environment Agency: Copenhagen).
26. Fernandes (2001) Fire spread prediction in shrub fuels in Portugal. *Forest Ecology and Management* 144, 67–74.
27. Dimitrakopoulos (2002) Mediterranean fuel models and potential fire behavior in Greece. *International Journal of Wildland Fire* 11, 127–130.
28. De Luis et al (2004) Fuel characteristics and fire behaviour in mature Mediterranean gorse shrublands. *International Journal of Wildland Fire* 13, 79–87.
29. INFC (2005) Inventario Nazionale delle Foreste e dei Serbatoi Forestali di Carbonio. Ministero delle Politiche Agricole Alimentari e Forestali, Ispettorato Generale - Corpo Forestale dello Stato. CRA - Istituto Sperimentale per l’Assestamento Forestale e per l’Alpicoltura.
30. Arca et al (2007) Evaluation of FARSITE simulator in Mediterranean maquis. *International Journal of Wildland Fire* 16, 563–572.
31. Pellizzaro et al (2007) Seasonal variations of live moisture content and ignitability in shrubs of the Mediterranean Basin. *International Journal of Wildland Fire* 16, 633–641.
32. Pellizzaro et al (2005) Influence of seasonal weather variations on fuel status for some shrubs typical of Mediterranean Basin. In ‘Proceedings 6th Fire and Forest Meteorology Symposium’ and ‘19th Interior West Fire Council Meeting’. 24–27 October 2005, Canmore, AB, Canada. P1.16.

33. Finney (2002) Fire growth using minimum travel time methods. *Canadian Journal of Forest Research* 32, 1420–1424.
34. Finney (2006) An overview of FlamMap fire modeling capabilities. In 'Fuels Management-How to Measure Success: Conference Proceedings', 28–30 March, Portland, OR. (Comp PL Andrews, BW Butler), USDA Forest Service, Rocky Mountain Research Station Proceedings RMRS-P-41, pp. 213–220.
35. Ager et al (2010b) Measuring the effect of fuel treatments on forest carbon using landscape risk analysis. *Natural Hazards and Earth Systems Science* 10, 2515-2526.
36. Ager et al (2010a) A comparison of landscape fuel treatment strategies to mitigate wildland fire risk in the urban interface and preserve old forest structure. *Forest Ecology and Management* 259, 1556-1570.

## 6. IMAGES AND TABLES

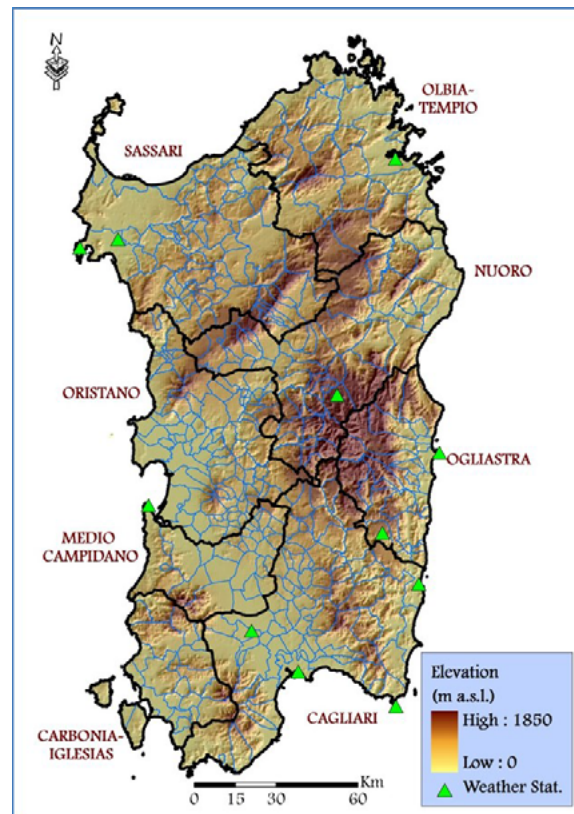


Fig. 1 Map of Sardinia showing province and municipality boundaries, and elevation. The weather stations are represented by the green triangles.

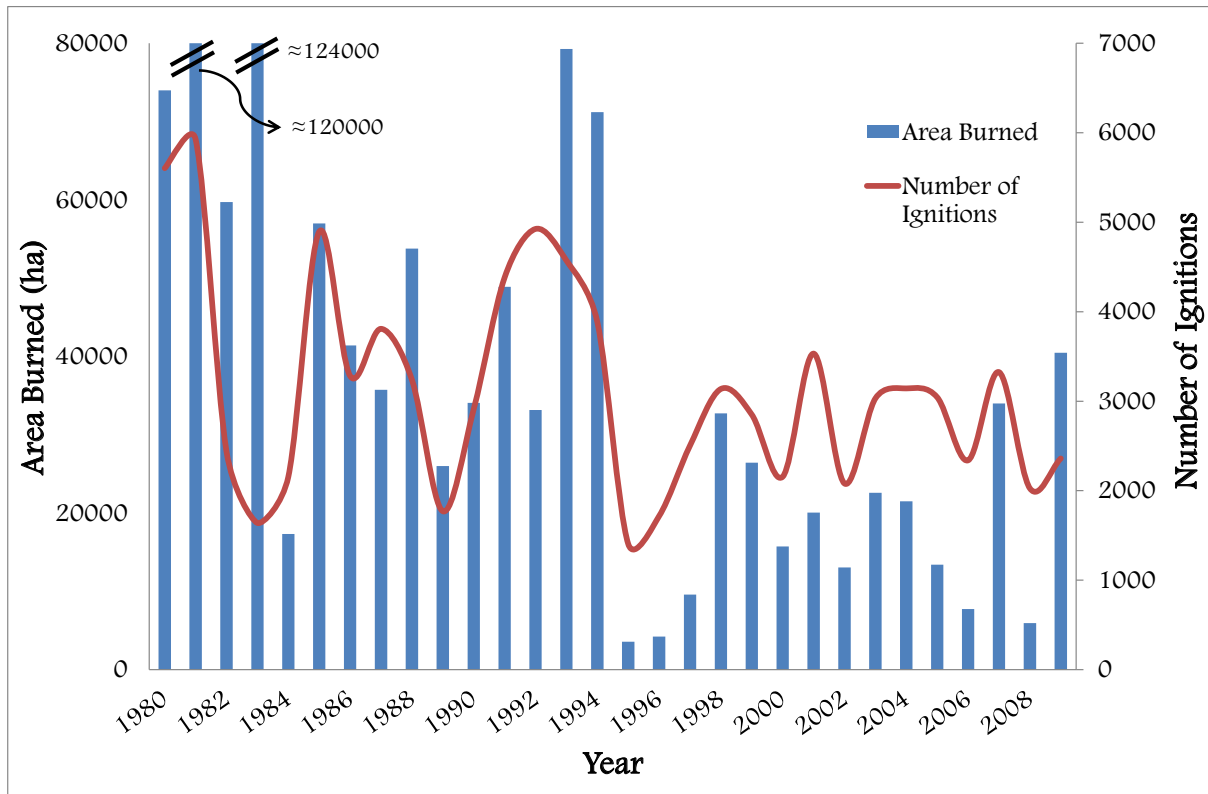


Fig. 2 Historical fire number and area burned in Sardinia (1980-2009).

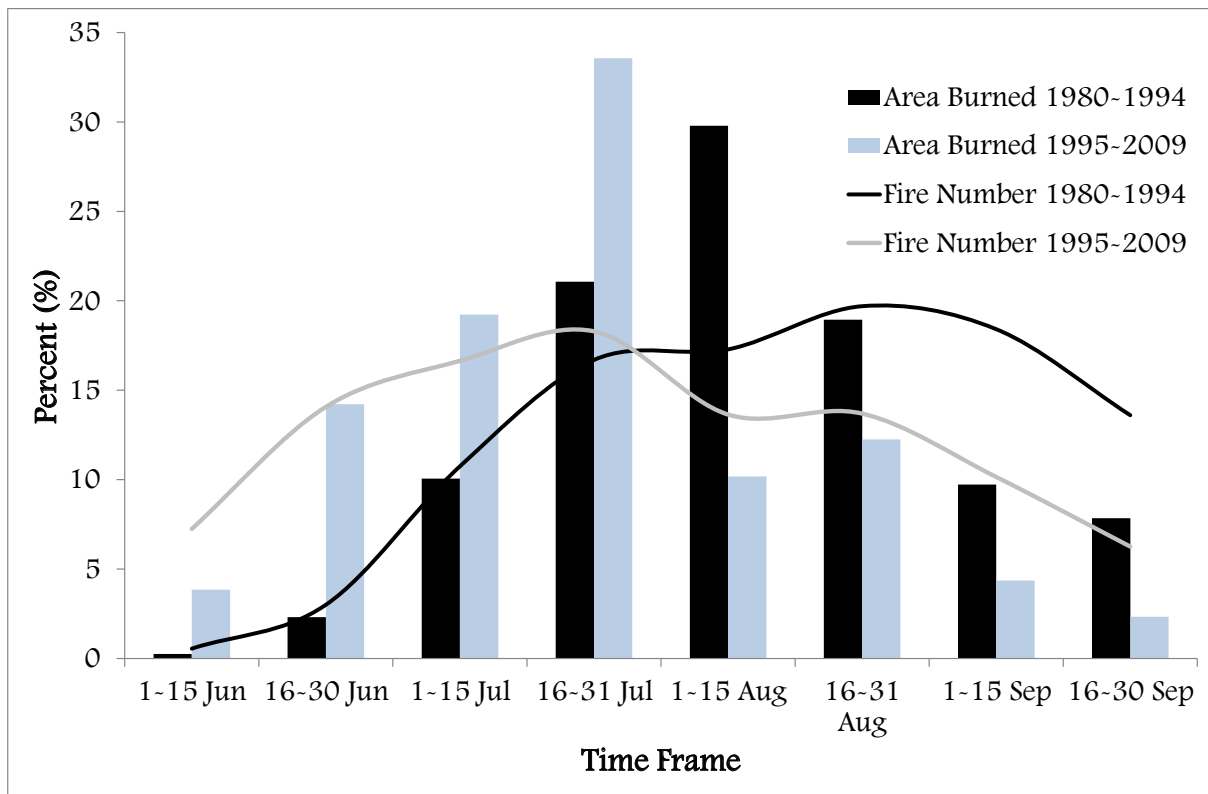


Fig. 3 Distribution of area burned and fire ignition percentage by time steps in Sardinia, for the two time frames.

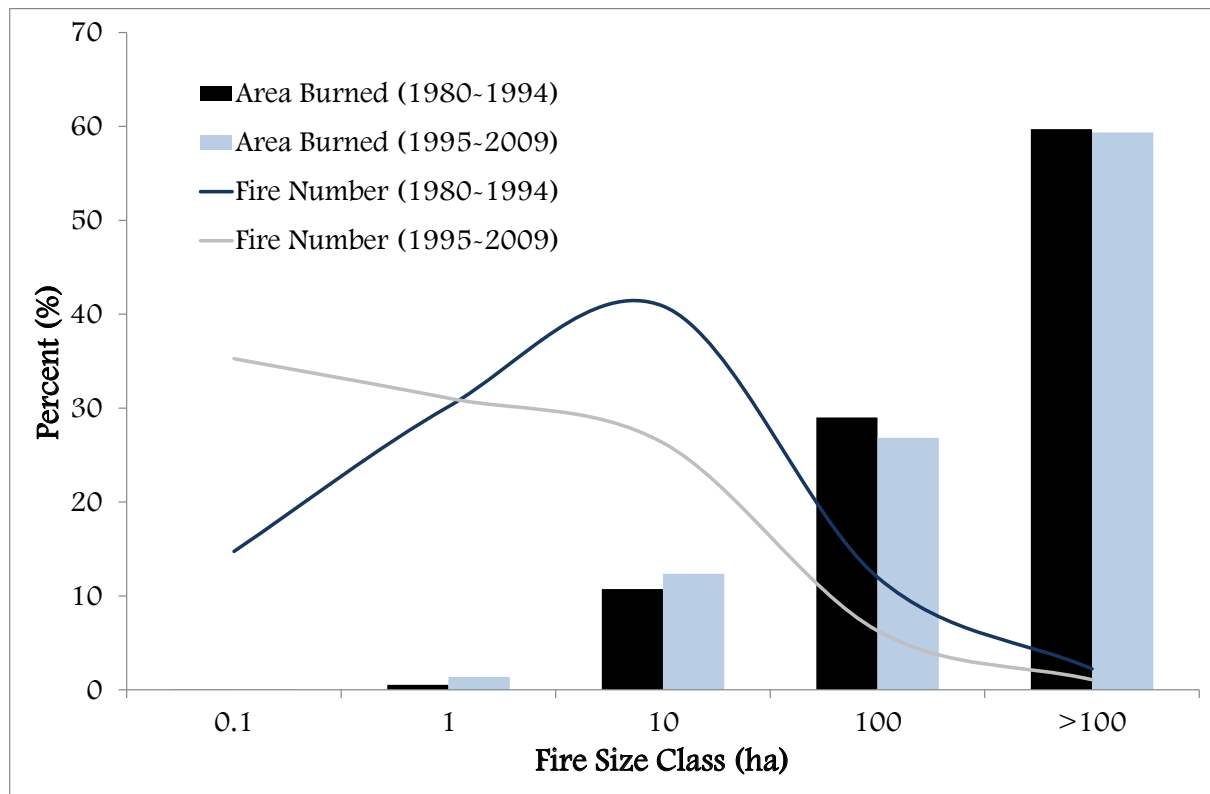


Fig. 4 Historical relationship between fire size classes and percentage of fires and area burned in Sardinia for the two time frames.

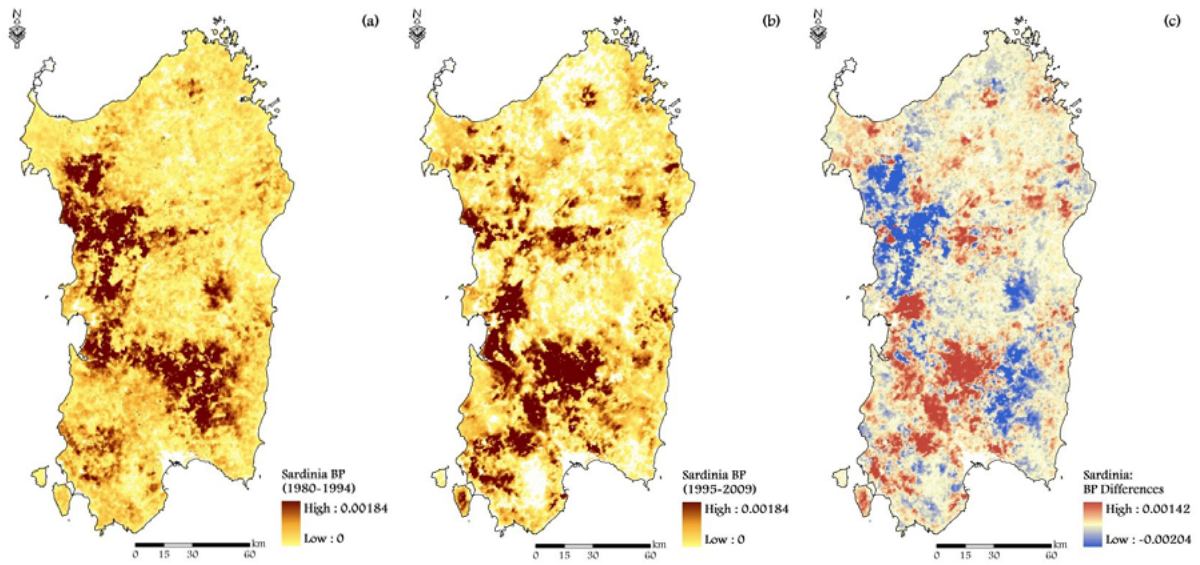


Fig. 5 Burn probability maps of Sardinia for: a) 1980- 1994, b) 1995- 2009, and c) difference between the periods.

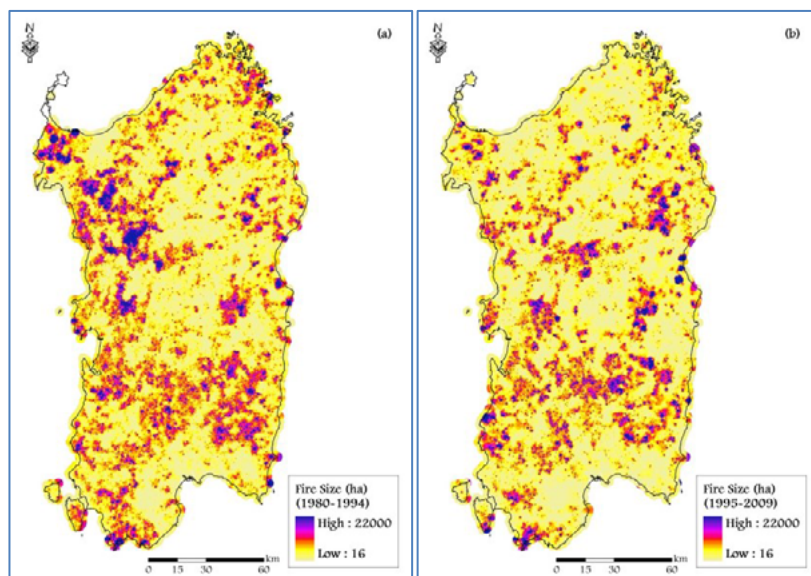


Fig. 6 Maps of potential fire size (ha) in Sardinia for the two study periods: a) 1980- 1994, and b) 1995-2009.

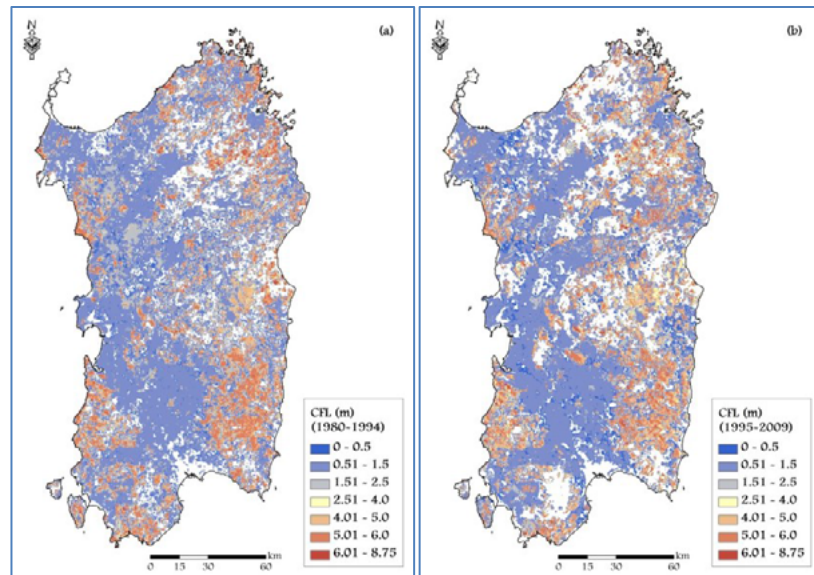


Fig. 7 Maps of simulation outputs for conditional flame length (CFL) for a) 1980-1994 and b) 1995-2009 in Sardinia.

Table 1 Vegetation types derived from CLC maps of 1990 and 2000, with the relative incidence in hectares and in percentage; the associated fuel models are also indicated.

Vegetation Type	CLC1990 – Thousand ha	CLC1990 - Incidence (%)	CLC2000 - Thousand ha	CLC2000 - Incidence (%)	Fuel Model
Broadleaf	303.0	12.6	306.6	12.7	TL3 (Scott and Burgan 2005)
Conifer	67.1	2.8	66.5	2.8	TL6 (Scott and Burgan 2005)
Broadleaf- Conifer Mix	15.3	0.6	14.7	0.6	TU1 (Scott and Burgan 2005)
Mediterranean Maquis	634.2	26.4	682.2	28.3	CM28 (Arca <i>et al.</i> 2009)
Garrigue	25.9	1.1	34.6	1.4	CM29 (Arca <i>et al.</i> 2009)
Pastures	173.8	7.2	162.4	6.8	CM27 (Arca <i>et al.</i> 2009)
Grass- Agricultural Lands	1,046.1	43.5	996.8	41.4	Mod 1 (Anderson 1982)
Tree Crops	52.2	2.2	49.6	2.1	Mod 2 (Anderson 1982)
Sands and Rocks	8.7	0.4	1.2	0.1	Mod 1 (Anderson 1982, fuel load reduced 50%)
Urban Areas	54.6	2.3	66.3	2.8	NB1 (Scott and Burgan 2005)
Water (lakes, rivers, etc.)	26.0	1.1	26.0	1.1	NB8 (Scott and Burgan 2005)

Table 2 Weather and fuel moisture parameters used in the fire simulations.

<b>Study period</b>	<b>(1980-1994)</b>	<b>(1995-2009)</b>
Variable	Value	Value
Wind Speed (km h <sup>-1</sup> )	29.0	29.0
Temperature (°C)	36.0	36.5
Rain (mm)	0	0
1hr dead FM (%)	7	7
10hr dead FM (%)	9	9
100hr dead FM (%)	11	11
Wind Direction (°)	315 (35%); 225 (22%); 270 (19%); other directions (24%)	315 (40%); 225 (24%); 270 (14%); other directions (22%)

# Using regional climate models for food-security scenarios in Africa

Calmanti S.<sup>1</sup>, Gelassie T. Y.<sup>2\*</sup>, Dell'Aquila A.

<sup>1</sup>ENEA, Italy

\*Corresponding Author: [sandro.calmanti@enea.it](mailto:sandro.calmanti@enea.it)

## Abstract

This short paper describes the preliminary results from the project IMPACT2C on the calibration of a food-security impact model and on food-security scenarios computed by using the output of 8 regional climate models driven by RCP4.5 global scenarios. The focus of the study is on Niger and Nile river basins. The question of how a rather constant and positive trend in global temperature will translate into changes in the water cycle and in the impact of drought patterns is addressed. Preliminary results from show that food security might be affected in different ways in the Nile and in the Niger basins. In particular, according to considered scenarios, the Nile basin will enjoy more stable conditions for food security whereas in the Niger basin, large fluctuations in the number of drought-affected people will be produced over time scales of decades.

**Keywords:** climate change, food-security, Africa

## 1. INTRODUCTION

Ensuring the access to sufficient food that meets the needs for an active and healthy life is an issue in many rural areas where rain-fed agriculture is a major economic resource.

The EU-FP7 project IMPACT2C, in collaboration with the African Risk Capacity (ARC) Project initiated by the African Union with technical assistance from the UN World Food Programme, has analyzed the impact of +2°C global warming on droughts and its implications on food-security in the Nile and the Niger basins.

This short paper describes the preliminary results from the project IMPACT2C on the calibration of a food-security impact model and on food-security scenarios computed by using the output of 8 regional climate models driven by RCP4.5 global scenarios.

According to a study conducted by WFP, drought accounts for an average 35% percent of all causes for humanitarian interventions in Africa. Studies on the potential impact of climate change on world food supply and security have been conducted since climate change scenarios from Global Circulation Models (GCM's) has been available [Rosenzweig and Parry, 1994]. [Soussana et al., 2010] have reviewed review all potential sources of uncertainties in crop models and highlight:

- Difficulty of calibrating to local farming practices [Brun et al. 2006]
- Dominance of environmental conditions on management and genotype.

[Parry et al., 2004] have used HadCM3 scenarios and suggested that even in a context of increased production, Africa would contribute additional risk of hunger in the 21 Century.

Aim of this work is to focus on the impact of recurring drought on food-security in Africa by adopting a methodology based on three main building blocks:

1. use of a simple crop model, already implemented in a risk assessment platform, as a proxy food production;
2. access to WFP historical records of humanitarian interventions for model calibration;
3. use of regional climate model scenarios.

The approach adopted for this study on food security in Africa is to narrow the focus on drought risk and describe a methodology for extrapolating future threats to food security by calibrating the model to a unique source of data which is the historical record of humanitarian operations conducted by WFP.

The main basis for the computation of food-security scenarios is a simple crop model, thereby following the approach of targeting only food availability (e.g. improved access to market is not considered).

The spatial resolution of state of the art climate models is of the order of a few tens to hundreds of kilometers. Therefore the spatial scale of rainfall patterns is not resolved. In tropical areas, in particular in vulnerable areas of Africa such as the Sahel, rainfall patterns tend to be organized in fine structures of the characteristic spatial scale of a few kilometers. The study of [Baron et al., 2005] warns on the use of GCM outputs with plot level crop models. Due to scale incompatibility, systematic errors as large as 50% overestimate in crop productivity can be produced at the scale of single plots. Biases can be avoided by disaggregating GCM outputs, especially rainfall, to obtain a more accurate description of weather variability at the relevant spatial and temporal scale. Observational campaigns have also shown that soil-atmosphere positive feedbacks in semi-arid climates are able to lock rainfall patterns so that wetter areas receive also more rainfall [Taylor and Lebel, 1998]. In fact, rainfall in most part of tropical Africa is mainly driven by atmospheric moist deep convection, possibly modulated by small scale orographic features. It is then unlikely that a coarse resolution model of the kind considered in this study can be effectively projected onto the specific micro-climate of any selected location, and provide useful information at the local scale. However, large scale fluctuations atmospheric circulation coexist with small scale features and represent a major driver for the latter. The international program on the African Monsoon Multidisciplinary Analysis (AMMA) has devoted substantial effort to the understanding of the mechanisms that determine the peculiar characteristics of rainfall pattern in vulnerable areas of Africa [Redelsperger et al., 2006]. The variability of the coupled ocean-atmosphere system in the Pacific (ENSO) is well known to affect rainfall patterns in Africa. Variability of the Atlantic SST has also been robustly associated to the strength of the West African Monsoon. Specific mechanisms that relate the sea surface temperature of the

global ocean to the variability of rainfall patterns in Africa have been identified in coarse resolution global climate models [Kutcharsky et al., 2009]. At the same time, it has been demonstrated that higher resolution Regional Climate Models are able to improve both the description of average rainfall [Sylla et al., 2010] and its variability (Mariotti et al., 2010) with respect to the driving global climate models. Therefore we use regional climate models from the Africa-CORDEX initiative as the source of input data for the impact model.

## 2. MODELS AND DATA

IMPACT2C, in collaboration with the African Risk Capacity (ARC) Project initiated by the African Union with technical assistance from the UN World Food Programme, has worked on the analysis of the impact of +2°C global warming on droughts and how they may affect food security in the Nile and the Niger basins.

### Africa Risk View

The ARC project as licensed IMPACT2C for using Africa RiskView (ARV), a software platform that was developed as a tool to translate satellite-based rainfall information into near real-time estimates of drought response costs, by combining models on agricultural drought with data on vulnerable populations. ARV has been combined with the output of regional climate models (RCMs) contributing to the Africa-CORDEX initiative. Africa RiskView (ARV) estimates rain-fed staple yield deviations on the basis of the Water Requirement Satisfaction Index (WRSI) approach based on the water balance model described in the FAO Technical Paper no. 56 (Allen et al., 1998; FAO56 hereinafter). The water balance calculation implemented in ARV is based on a time step of 10 days and the required input in terms of weather variables is rainfall and potential evapotranspiration. ARV uses different time spans for the crop seasons, depending on the specific area and common practices. [Tab. 1] summarizes the time span of the crop seasons adopted in ARV. [Fig. 1] shows the spatial extent of the domains defined as cropping areas in ARV during the 5 seasons reported in [Tab. 1]. Note that in East Africa and some areas of South Africa more crop seasons overlap in the same area. In those cases, the outcome of all crop seasons contribute to determine the annual number of drought affected population.

We do not consider in the present computation the impact of demographic growth and changes in society and technology. Instead, a fixed vulnerability profile is assumed for the computation of drought-affected people in future scenarios.

ARV produces two streams of output. A first intermediate output is the raw Water Requirement Satisfaction Index produced by the embedded crop model. This output is a simple indicator of crop performances and is adopted as the input of a drought impact module, which uses local vulnerability profile to compute the number of drought affected people.

To run the impact model simulations we use the climate input from the regional climate models participating to the CORDEX initiative. In particular, we use simulations from the Africa-CORDEX ensemble. The focus of IMPACT2C is on simulating the changes occurring at the time of +2°C temperature increase with respect to pre-industrial condition. We therefore use simulations of the RCP4.5 and RCP8.5 scenarios that typically reach the + 2°C threshold during the next century. The list of regional climate model simulations adopted as an input for this study is reported in [Tab. 2]

### 3. CALIBRATION

Due to the biases in the rainfall patterns produced by the climate models, the WRSI intermediate output of ARV produces an estimate of drought-affected people characterized by a model dependent bias. Most of the times, impact models use bias corrected climate input data, especially when the presence of critical threshold represent key components in the impact models. In our case, ARV offers the possibility of alternative approach to model calibration, based on the fact that relative year to year changes are used to compute the number of drought affected people. Based on this, calibration coefficients are computed for each model by using the ARV drought-affected as computed with the reference climatology.

The computation of the calibration coefficients proceeds as follows:

- Compute maximum, minimum and average historical WFP drought beneficiaries from 1996 to 2010.

- Compute ARV output of drought affected people using observational rainfall RFE from 1996 to 2010.
- Compute ARV output of drought affected people using regional climate model downscaling of the historical scenario from 1996 to 2010.
- Compute the ratio (Scaling Factor) between the corresponding maximum WFP historical record versus maximum regional climate model output.
- Use the Scaling Factors throughout the model scenario so that all scenarios based on different regional climate model downscalings are comparable.

[Fig. 2] shows an example of the comparison between un-calibrated and calibrated drought impact output of ARV for the case of the regional climate model RegCM4 driven by the global model CNRM-CM5, RCP4.5 scenario.

#### 4. RESULTS

[Fig. 3] and [Fig. 4] show the relative (%) change in drought affected people for each of the considered models, for the Nile and Niger basin, respectively. In the Nile, the food-security outlook is mostly steady with a slight tendency towards a slight improvement. In the Niger basin,

[Fig. 5] shows that, according to considered scenarios, the Nile basin will enjoy more stable conditions for food security whereas large fluctuations in the number of drought-affected people characterize the Niger basin over time scales of decades.

The main objective of IMPACT2C is to evaluate the impact of a +1.5° and a +2°C global warming with respect to the pre-industrial conditions. According to the analysis conducted during IMPACT2C, a consistently positive temperature trend is *very likely* to warm our planet above the +2°C within the next 50/60 years.

However, the question of how a rather constant and positive trend in global temperature will translate into changes in the water cycle and in the impact of drought patterns is not as easily answered.

[Fig. 6] show Relative change (percentage) in the number of drought-affected people in a +1.5°C global warming scenario. The reference historical period is 1970-2000. The +1.5°C reference is 2015-2045. [Fig. 7] the same relative changes during a +2°C

reference time frame (2030-2060) and [Fig. 8] shows again the relative changes for the period 2045-2075, when the global temperature as exceeded the +2°C threshold. By comparing the three figures we confirm that in these food-security scenarios, the paradigm of incremental impact with a well-defined trend (such as in the case of global temperature) does not always apply.

In particular, most of west Africa and the Niger basin, faces increasing threats to food-security, except for the case of Niger, where periods of increasing number of drought-affected people alternate with periods of decreasing impact on food security. Such an oscillation between positive and negative impact periods is more evident in Eastern Africa and in the Nile basin. In particular, Ethiopia seems to show increasing number of drought affected at a moderate rate. Instead, in the case of Kenya and Tanzania, and initial phase of worsening conditions for food security is followed by a period of improving conditions.

The preliminary analysis presented here can be improved in many respects, e.g. analyse more climate scenarios, use more climate models). However, the results presented in this study the kind of adaptation strategies to be envisioned will *likely* have to cope with fluctuating condition rather than with constant trends in a well-defined direction

## 5. ACKNOWLEDGMENTS

This study has been supported by the FP7-EU project no. 282746 – IMPACT2C. We acknowledge useful discussion with Joanna Syroka and Federica Carfagna from WFP and the support of Peter Hoefsloot for the development of the impact model software platform.

## 6. REFERENCES

1. Baron, C., Sultan, B., Balme, M., Sarr, B., Traore, S., Lebel, T., ... & Dingkuhn, M. (2005). From GCM grid cell to agricultural plot: scale issues affecting modelling of climate impact. *Philosophical Transactions of the Royal Society B: Biological Sciences*, 360(1463), 2095-2108.

2. Brun, F., Wallach, D., Makowski, D., & Jones, J. W. (2006). Working with dynamic crop models: Evaluation, analysis, parameterization, and applications. Elsevier.
3. Kucharski, F., Bracco, A., Yoo, J. H., Tompkins, A. M., Feudale, L., Ruti, P., & Dell'Aquila, A. (2009). A Gill-Matsuno - type mechanism explains the tropical Atlantic influence on African and Indian monsoon rainfall. *Quarterly Journal of the Royal Meteorological Society*, 135(640), 569-579.
4. Parry, M. L., Rosenzweig, C., Iglesias, A., Livermore, M., & Fischer, G. (2004). Effects of climate change on global food production under SRES emissions and socio-economic scenarios. *Global Environmental Change*, 14(1), 53-67.
5. Soussana, J. F., Graux, A. I., & Tubiello, F. N. (2010). Improving the use of modelling for projections of climate change impacts on crops and pastures. *Journal of experimental botany*, 61(8), 2217-2228.
6. Sylla, M. B., Dell'Aquila, A., Ruti, P. M., & Giorgi, F. (2010). Simulation of the intraseasonal and the interannual variability of rainfall over West Africa with RegCM3 during the monsoon period. *International Journal of Climatology*, 30(12), 1865-1883.
7. Redelsperger, J. L., Thorncroft, C. D., Diedhiou, A., Lebel, T., Parker, D. J., & Polcher, J. (2006). African Monsoon Multidisciplinary Analysis: An international research project and field campaign. *Bulletin of the American Meteorological Society*, 87(12), 1739-1746.
8. Rosenzweig, C., & Parry, M. L. (1994). Potential impact of climate change on world food supply. *Nature*, 367(6459), 133-138.
9. Taylor, C. M., & Lebel, T. (1998). Observational evidence of persistent convective-scale rainfall patterns. *Monthly Weather Review*, 126(6).

## 7. IMAGES AND TABLES

No	Seasons	Period	Length of crop season
1	East Africa one (EA1)	Feb.1 up to 20 July	Five month & 20days
2	East Africa two (EA2)	Apr.1 up to 31 Oct.	Seven month
3	East Africa three (EA3)	Sep.1 up to 20 March.	Six Month and 20 days
4	West Africa one (WA1)	Apr.1 up to 31 Oct.	Seven month
5	South Africa one (SA1)	Oct.1 up to 31 May	Seven Month

Tab. 1 Time span of african crop seasons in ARV

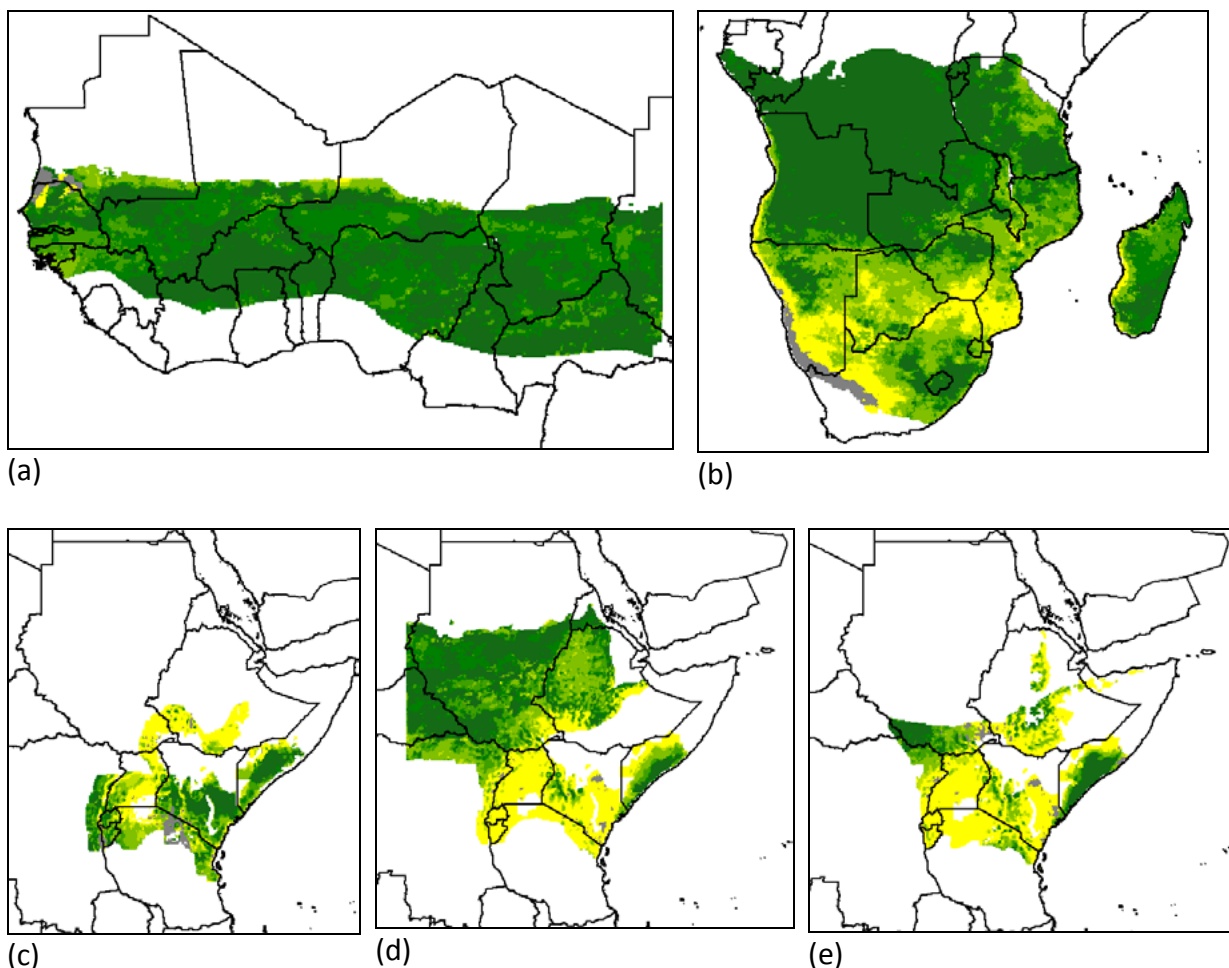


Fig. 1 Spatial coverage of the four crop seasons defined in ARV: West Africa – WA1 (a); Southern Africa – SA1 (b); Eastern Africa – EA1(c); Eastern Africa – EA2(d); Eastern Africa – EA3(e).

Scenario	GCM	RCM	+1.5°C	+2.0°C
RCP4.5	EC-EARTH	RCA4	2019-2048	2042-2071
RCP4.5	CNRM	RCA4	2021-2050	2043-2072
RCP4.5	GFDL	RCA4	2034-2063	-9999
RCP4.5	CCCma	RCA4		
RCP4.5	MIROC-ESM-CHEM	RCA4	2010-2039	2024-2053
RCP4.5	MPI-M	RCA4		
RCP4.5	NorESM1-M	RCA4	2022-2051	2053-2082
RCP4.5	CNRM	RegCM4	2021-2050	2043-2072

Tab. 2 Climate simulations adopted as input for the impact models

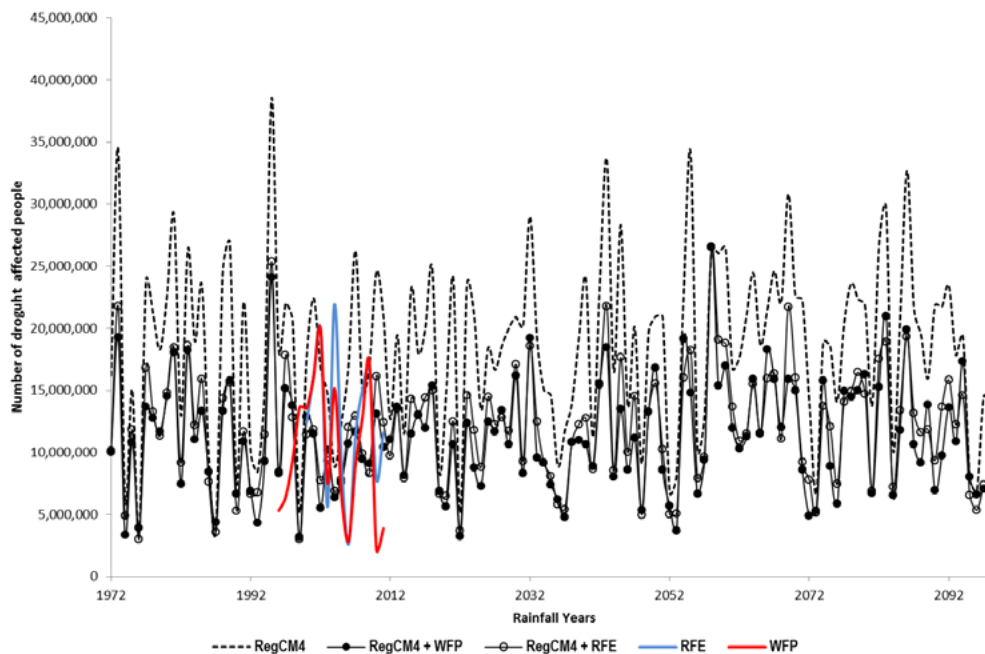


Fig. 2 comparison between un-calibrated (dotted line) and calibrated (continuous line) total drought impact in Africa as computed by ARV for the case of the regional climate model RegCM4 driven by the global model CNRM-CM5, RCP4.5 scenario. The blue line is the drought impact computed by using the NOAA/RFE dataset as climate input to ARV. The red line corresponds to the historical record of humanitarian interventions by WFP.

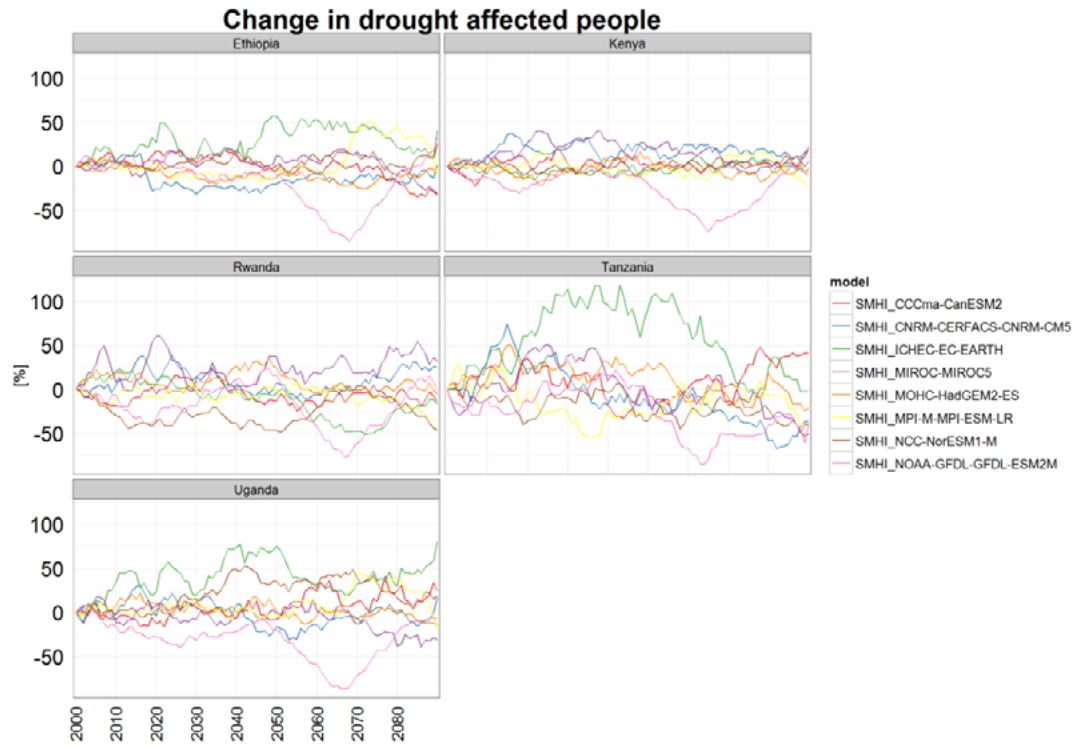


Fig. 3 Future relative change (percentage) in drought affected people for the 5 ARV countries in the Nile basins. The colors represent the WRSI output for each crop season in the area.

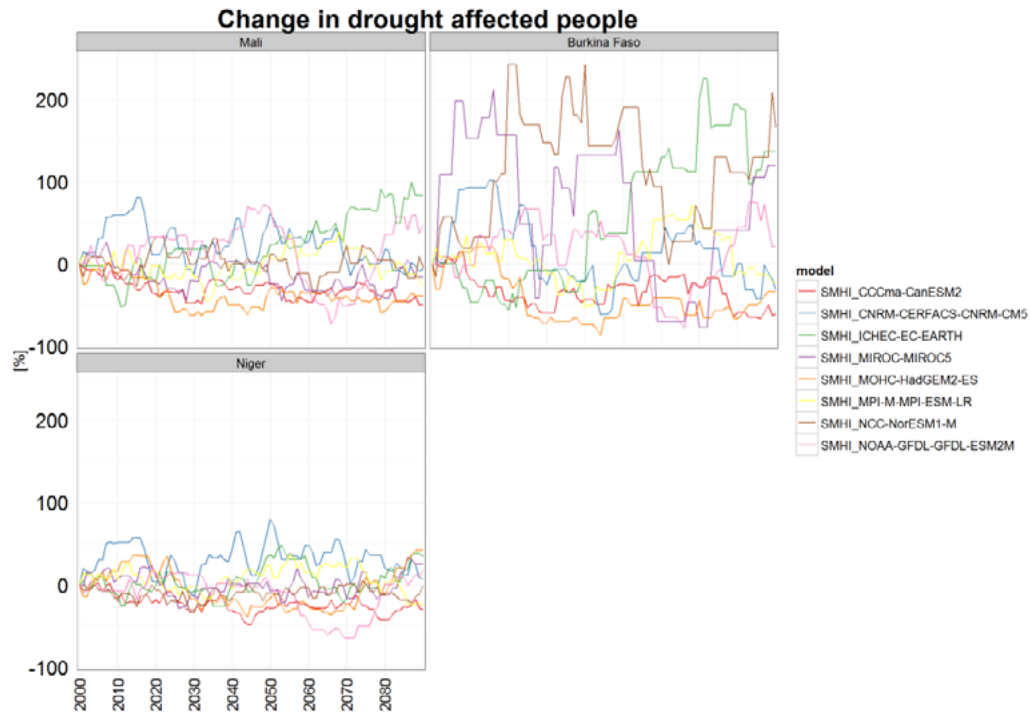


Fig. 4 Same as in Fig. 3 but for the Niger basin.

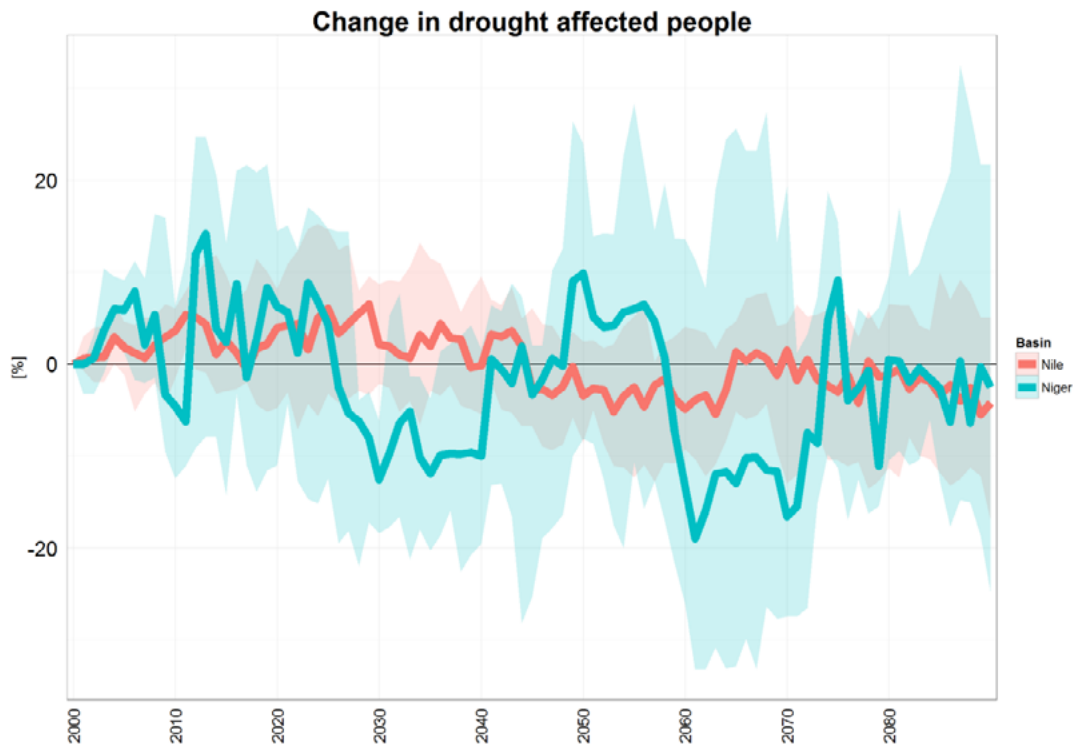


Fig. 5 Summary of the projective relative (percentage) changes in drought affected people in the Nile and Niger basins. Thick lines represent the ensemble average among the considered RCM-GCM combinations. The shaded areas represent the middle tercile of the distribution of all models.

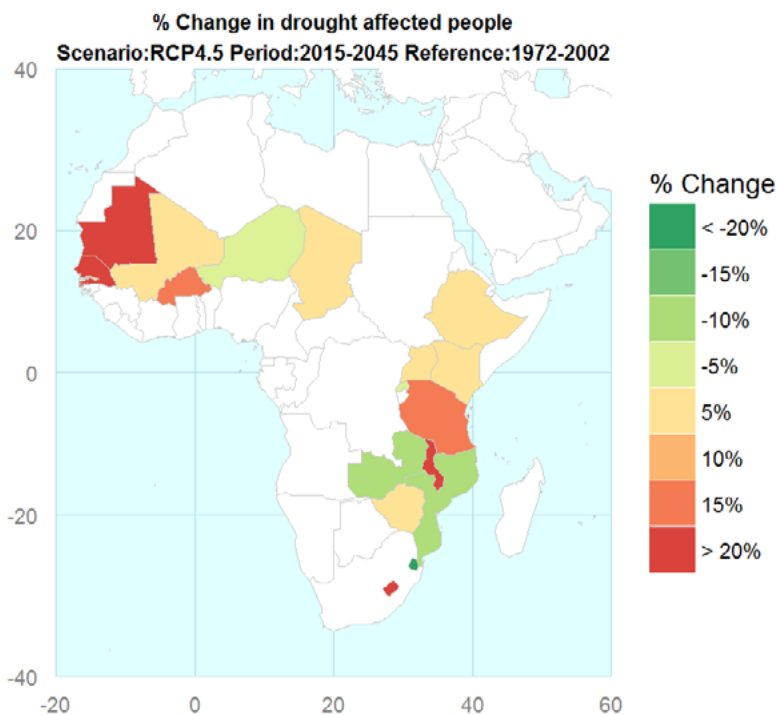


Fig. 6 Relative change (percentage) in the number of drought-affected people in a +1.5°C RCP4.5 global warming scenario. The reference historical period is 1972-2002. The +1.5°C reference is 2015-2045

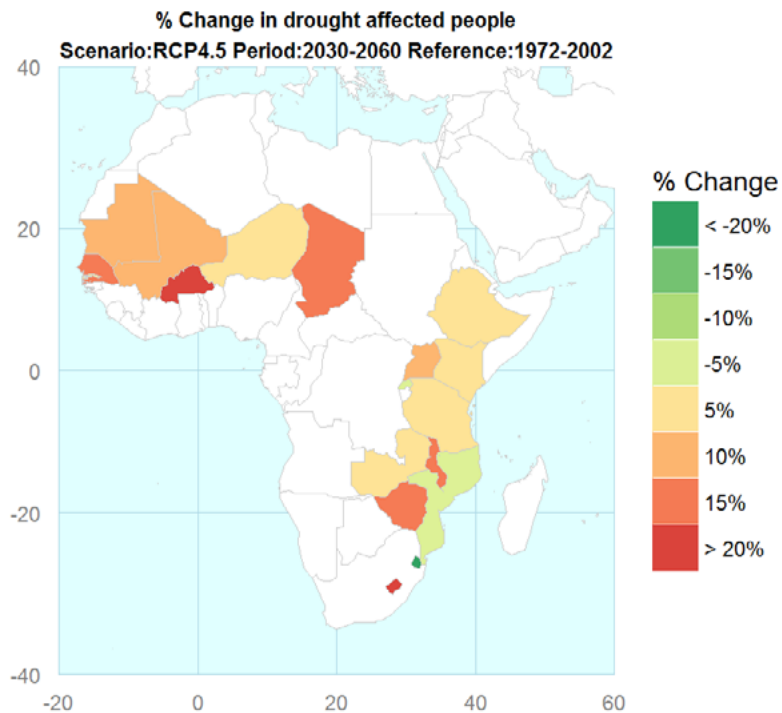


Fig. 7 Relative change (percentage) in the number of drought-affected people in a +2.0°C RCP4.5 global warming scenario. The reference historical period is 1972-2002. The +2.0°C reference is 2030-2060

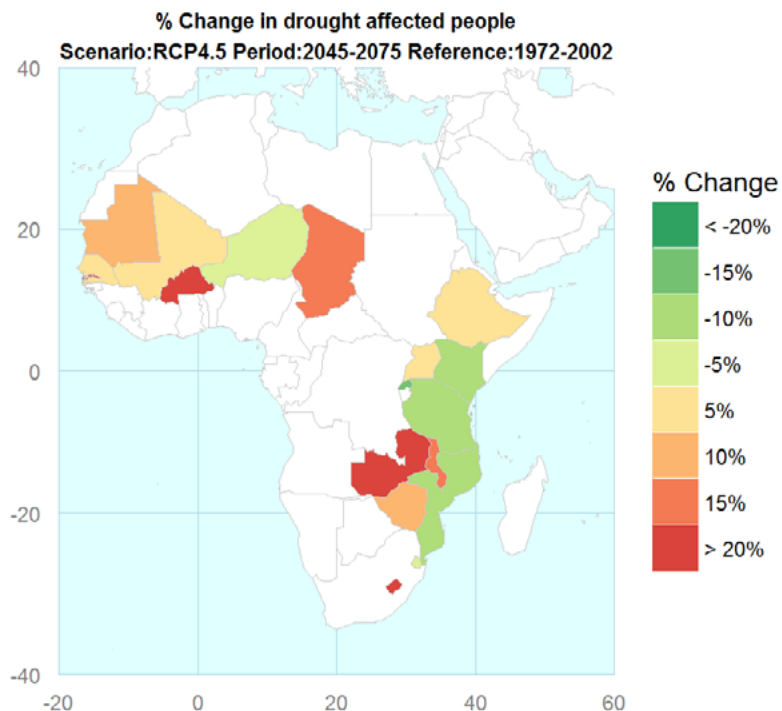


Fig. 8 Relative change (percentage) in the number of drought-affected people in RCP4.5 global warming scenario. The reference historical period is 1972-2002. The reference is 2045-2075 when global warming has exceeded the +2°C threshold.



# Author Index

## A

Acquaotta F., 424  
Adhikari B., 235  
Aerts J., 858  
Ager A. A., 1066  
Alcasena F., 1005, 1066  
Alloisio I., 78  
Aloisio G., 448, 540  
Amadio M., 745  
Ampera B., 70  
Ampri I., 70  
Anadon D. L., 106  
Andreopoulos D., 639  
Anelli Monti M., 1021  
Annamalai H., 287  
Antretter F., 923  
Apadula F., 977  
Arca A., 509, 1005  
Arca B., 1066  
Arduini J., 416  
Artale V., 313  
Ashley-Smith J., 923  
Attanasio A., 557  
Avelar D., 655  
Aw-Hassan A., 1037

## B

Bacciu V., 1005, 1066  
Ballarin Denti A., 699  
Balliana E., 991  
Barbante C., 454, 794, 812  
Barbaro E., 454  
Barron R., 106  
Battistel D., 794  
Bazzani G. M., 728  
Bertolin C., 923  
Biscontin G., 991  
Bista R., 235  
Bluffstone R., 235  
Bojovic D., 780  
Borgonovo E., 106  
Bosello F., 583, 858, 1005  
Bosetti V., 106, 191  
Botarelli L., 781  
Braat L.C., 944

Brigolin D., 653  
Broström T., 923  
Brunetti M., 397, 977  
Bucchignani E., 338, 487

## C

Cacciamani C., 781  
Caccin A., 1021  
Calliari E., 254  
Calliari L.J., 779  
Calmanti S., 1084  
Campagnolo L., 107  
Camuffo D., 923  
Capela Lourenço L., 655  
Caporin M., 623  
Carloni F.B.B.A., 3  
Carniel S., 653  
Carrara S., 108  
Carrera L., 858  
Caserini S., 35  
Cassardo C., 366  
Castellari S., 655, 682  
Cattaneo L., 434, 878  
Cervigni R., 133  
Cescon P., 812  
Chateau J., 107  
Cherchi A., 287  
Christoplos I., 642  
Cojocar G., 780  
Colleoni F., 382  
Comiti F., 639  
Corami F., 812  
Critto A., 641, 653, 1036  
Czaja A., 300

## D

D'Agostino R., 547  
D'Anca A., 448  
Damigos D., 639  
Darwish T., 897  
Davide M., 682  
De Cian E., 960  
De Franceschi M., 467  
Dell'Aquila A., 1084  
Dellink R., 107

Dhehibi B., 1037  
Diallo I., 273  
Dirnböck T., 774  
Dissanayake S.T. M., 235  
Doos K., 313  
Drouet L., 154, 191  
Duce P., 509  
Durand-Lasserre O., 107

## E

Eboli F., 838  
Elia D., 448  
Emmerling J., 11  
Epicoco I., 540

## F

Faggian P., 458  
Falchi L., 991  
Falconer A., 70  
Faria A. M. de Melo, 19  
Fariello L., 878  
Feás J., 92  
Ferreira R. Pires, 19  
Feyen L., 858  
Figueiredo S.A., 779  
Finney M. A., 1066  
Fiore S., 448  
Fischer C., 639  
Fontini F., 623  
Fraschini F., 699  
Fратиanni S., 424  
Friley P., 106  
Frisari G., 92  
Frija A., 1037  
Furlan E., 641  
Furlani F., 416

## G

Gallina V., 641, 1036  
Galluccio G., 50  
Gambaro A., 454, 794  
Gelassie T. Y., 1084  
Geneletti D., 944  
Genovesi R., 728  
Gerhard E., 774

Germani Y. F., 779  
Giannini A., 268  
Giannini V., 682  
Giorgi F., 273  
Giostra U., 416  
Giovannini L., 467  
Giupponi C., 780  
Giusto M., 557  
Glenday S., 70  
Graziosi F., 416  
Gualdi S., 352, 1005  
Guarino F., 878

## H

Henrion M., 133  
Hidalgo P.J., 1038  
Huang C.H., 210

## I

Iodice L., 878  
Izzo F. C., 991

## J

Jacob D., 923  
Jha P., 235

## K

Karunaratna H., 870  
Kehrwald N., 454, 794  
Khadra R., 897  
Kirchgeorg T., 794  
Klug H., 780  
Kobler H., 774  
Koks E., 858  
Kotova L., 923

## L

La Rovere E.L., 3  
Lapi M., 699  
Le Duc N., 642  
Le Thi Hoa Sen, 642  
Lee C.-M., 210  
Leijonhufvud G., 923  
Leissner J., 923  
Leitner M., 655  
Lembo V., 523  
Lindgaard Salloum L., 642

Lionello P., 523, 547  
Lo Vullo E., 416  
López-Tirado J., 1038  
Luintel H., 235

## M

Maione M., 416  
Manara V., 397  
Mancosu N., 1049  
Mannini P., 728  
Marangoni G., 106  
Marcelli M., 326  
Marcomini A., 641, 653, 1036  
Mariello A., 448  
Martinsson P., 235  
Mase H., 870  
Masina S., 287, 382  
Masseti E., 108  
Maugeri M., 397, 977  
McJeon C. H., 106  
Melchiorri C., 326  
Mercogliano P., 338, 434, 487, 878  
Messori G., 300  
Michetti M., 176, 1005  
Mikolajewicz U., 923  
Mistry M., 570  
Mocavero S., 540  
Montesarchio M., 338, 487  
Moran D., 604  
Morper-Busch L., 780  
Munoz-Lozano O., 1066  
Mysiak J., 759, 858

## N

Nassisi P., 448  
Navarra A. 287, 352  
Nguyen Thi Thanh H., 642  
Nilsson J. A. U., 313  
Noce S., 1005

## O

Otrachshenko W., 1005

## P

Paladini de Mendoza F., 326  
Palazzo C., 448

Parrado R., 176, 583, 1005  
Pasini A., 366, 557  
Pasotti L., 397  
Pastres R., 653  
Paudel N. S., 235  
Pelizzaro P., 719  
Pérez-Soba M., 944  
Perotto E., 35  
Piazza R., 812  
Politis S., 106  
Polo F., 812  
Portoghese I., 897  
Pozzo B., 226  
Pranovi F., 1021  
Prutsch A., 655

## R

Racca P., 366  
Reeve D., 870  
Reis Lara A., 154  
Rianna G., 878  
Rillo V., 434  
Rizzi J., 653  
Rogers, J.A., 133  
Ros V., 812  
Rosenberg A., 70  
Rossetto M., 699  
Ruggeri G.C., 825

## S

Salis M., 1005, 1066  
Sanna L., 509  
Santato S., 759  
Santini M., 1005  
Scapin S., 977  
Schellen H., 923  
Schörghofer R., 780  
Schüpbach S., 794  
Scoccimarro E., 352, 1005  
Scolieri S., 35  
Sferra F., 109  
Shaban A., 897  
Siegel H., 774  
Simolo C., 397  
Snyder R.L., 1049  
Somanathan E., 235  
Spano D., 1005, 1049, 1066  
Sperotto A., 641, 1036

Standardi G., 838, 858  
Stordal F., 273  
Su Han-Pang, 210

Zendri E., 991  
Zennaro P., 794  
Zollo A., 338

## **T**

Tavoni M., 154, 191  
Teixeira M. D. de Jesus, 19  
Terradez Mas J., 699  
Toman M., 235  
Tomozeiu R., 781  
Torresan S., 641, 653, 1036  
Turetta C., 812  
Tuwo A., 70

## **V**

Van der Wijngaart R., 944  
Van Eupen M., 944  
Van Schijndel A.W.M., 923  
Vecchiato M., 454  
Venema V., 424  
Ventura A., 509  
Venturini S., 655, 682  
Verbruggen A., 166  
Vezzoli R., 878  
Villarini G., 352  
Vurro M., 897

## **W**

Wahyudi N., 70  
Wall E., 604  
Wilkinson J., 70  
Wing I. S., 960  
Winkler M., 923  
Wreford A., 604

## **Y**

Yang C.-W., 2101

## **Z**

Zabeo A., 653, 1036  
Zangrando R., 454, 794  
Zara P., 509  
Zardi D., 467  
Zardo L., 944  
Zavala A. A., 19



**Società Italiana per le Scienze del Clima**

Isola di San Giorgio Maggiore, n. 8

I-30124, Venezia - Italia

Tel. 041.2700431 - Fax. 041.2700412

E-mail: [info@sisclima.it](mailto:info@sisclima.it)

**[www.sisclima.it](http://www.sisclima.it)**